

AD-A217 803

DTIC ACCESSION NUMBER

LEVEL

PHOTOGRAPH THIS SHEET

DTIC FILE COPY

INVENTORY

AFOSR TR 90-0052

DOCUMENT IDENTIFICATION

6 NOV 1981

DISTRIBUTION STATEMENT A

Approved for public release;
Distribution Unlimited

DISTRIBUTION STATEMENT

ACCESSION FOR

NTIS GRA&I

DTIC TAB

UNANNOUNCED

JUSTIFICATION

BY

DISTRIBUTION /

AVAILABILITY CODES

DIST

AVAIL AND/OR SPECIAL

A-1

21

DTIC
COPY
INSPECTED
5

DTIC
ELECTE
FEB 09 1990
S E D

DATE ACCESSIONED

DISTRIBUTION PRICE-\$177.00

2 East 63rd St.

New York, NY 10021

TELECON

2/9/90

CG

DATE RETURNED

00 02 06 268

DATE RECEIVED IN DTIC

REGISTERED OR CERTIFIED NO.

PHOTOGRAPH THIS SHEET AND RETURN TO DTIC-PDAC

ANNALS OF THE NEW YORK ACADEMY OF SCIENCES VOLUME 374

AD-A217 803

VESTIBULAR AND OCULOMOTOR PHYSIOLOGY:

*International Meeting
of the Bárány Society*

Editor

Bernard Cohen

ANNALS OF THE NEW YORK ACADEMY OF SCIENCES

Volume 374



EDITORIAL STAFF

Executive Editor

BILL BOLAND

Managing Editor

JOYCE M. HITCHCOCK

Associate Editor

SHEILA KATES

The New York Academy of Sciences

2 East 63rd Street

New York, New York 10021

THE NEW YORK ACADEMY OF SCIENCES (Founded in 1817)

BOARD OF GOVERNORS, 1981

HEINZ R. PAGELS, *President*
MORRIS H. SHAMOS, *President-Elect*

Honorary Life Governors

SERGE A. KORFF
I.B. LASKOWITZ

Vice-Presidents

VITTORIO CANUTO
MARIO G. SALVADORI
Secretary
PHILIP FEIGELSON

KURT SALZINGER

H. CHRISTINE REILLY
IRVING J. SELIKOFF

WALTER N. SCOTT
VIRGINIA S. SEXTON
Treasurer
ALAN J. PATRICO

Elected Governors-at-Large

ANNE M. BRISCOE
DOROTHY CUNNINGHAM

1979-1981

MICHAEL V.L. BENNETT
WILLIAM S. CAIN

1980-1982

CRAIG D. BURRELL
MURIEL FEIGELSON

1981-1983

WILLIAM T. GOLDEN
HAROLD GRAD

PETER M. LEVY
NORBERT J. ROBERTS

FRANK R. LANDSBERGER
PHILIP SIEKEVITZ

Past Presidents (Governors)

PARITHYCHERY R. SRINIVASAN
JOEL L. LEBOWITZ

SIDNEY BOROWITZ, *Presidential Advisor*

CHARLOTTE FRIEND
HERBERT J. KAYDEN

REPORT DOCUMENTATION PAGE

Form Approved
OMB No. 0704-0188

Public Reporting Burden for this collection of information is estimated to average 1 hour per response, including the time for reviewing instructions, searching existing data sources, gathering and maintaining the data needed, and completing and reviewing the collection of information. Send comments regarding this burden estimate or any other aspect of this collection of information, including suggestions for reducing the burden, to Washington Headquarters Office, Directorate for Information Operations and Reports, 1215 Jefferson Davis Highway, Suite 1204, Arlington, VA 22202-4302, and to the Office of Management and Budget, Paperwork Reduction Project (0704-0188), Washington, DC 20503.

1. AGENCY USE ONLY (Leave blank)		2. REPORT DATE Nov 6, 1981	3. REPORT TYPE AND DATES COVERED	
4. TITLE AND SUBTITLE VESTIBULAR AND OCULOMOTOR PHYSIOLOGY			5. FUNDING NUMBERS	
6. AUTHOR(S) Bernard Cohen				
7. PERFORMING ORGANIZATION NAME(S) AND ADDRESS(ES) The New York Academy of Sciences 2 East 63rd Street New York, New York 10021			8. PERFORMING ORGANIZATION REPORT NUMBER AFOSR - 80- 0277	
9. SPONSORING/MONITORING AGENCY NAME(S) AND ADDRESS(ES) AFOSR BLDG 410 BAFB DC 20332-6448			10. SPONSORING/MONITORING AGENCY REPORT NUMBER AFOSR-TR- 90-0052	
11. SUPPLEMENTARY NOTES				
12a. DISTRIBUTION/AVAILABILITY STATEMENT Unlimited			12b. DISTRIBUTION CODE	
13. ABSTRACT (Maximum 200 words)				
14. SUBJECT TERMS			15. NUMBER OF PAGES 892	
			16. PRICE CODE	
17. SECURITY CLASSIFICATION OF REPORT unclassified	18. SECURITY CLASSIFICATION OF THIS PAGE unclassified	19. SECURITY CLASSIFICATION OF ABSTRACT	20. LIMITATION OF ABSTRACT	

~~FO XOTD~~
2 Dec 81

AFOSR-80-Q277

VESTIBULAR AND
OCULOMOTOR PHYSIOLOGY:
INTERNATIONAL MEETING
OF THE BÁRÁNY SOCIETY

Approved for public release;
distribution unlimited.



AIR FORCE OFFICE OF SCIENTIFIC RESEARCH (AFSC)
NOTICE OF TRANSFER OF TECHNOLOGY

This technical information is approved and is
approved for public release under AFOSR-100-12.

Distribution Statement
MATTHEW J. FRIEDMAN
Chief, Technical Information Division

ANNALS OF THE NEW YORK ACADEMY OF SCIENCES

Volume 374

APOSR-TR. 90-0052

VESTIBULAR AND
OCULOMOTOR PHYSIOLOGY:
INTERNATIONAL MEETING
OF THE BÁRÁNY SOCIETY

Edited by Bernard Cohen



The New York Academy of Sciences
New York, New York
1981

3200-02-8207A

Copyright © 1981 by The New York Academy of Sciences. All rights reserved. Under the provisions of the United States Copyright Act of 1976, individual readers of the Annals are permitted to make fair use of the material in them for teaching or research. Permission is granted to quote from the Annals provided that the customary acknowledgment is made of the source. Material in the Annals may be republished only by permission of The Academy. Address inquiries to the Executive Editor at The New York Academy of Sciences.

Copying fees: The code at the bottom of the first page of each article in this Annal states the fee for each copy of the article made beyond the free copying permitted under Section 107 or 108 of the 1976 Copyright Act. (If no code appears, there is no fee.) This fee should be paid through the Copyright Clearance Center, Inc., Box 765, Schenectady, N.Y. 12301. For articles published prior to 1978, the copying fee is \$1.75 per article.

Library of Congress Cataloging in Publication Data

Main entry under title:

Vestibular and oculomotor physiology.

(Annals of the New York Academy of Sciences; v. 374)

Proceedings of a conference held Sept. 22-25, 1980, sponsored by the Bárány Society and the New York Academy of Sciences.

Includes index.

1. Vestibular apparatus—Congresses. 2. Eye-movements—Congresses. I. Cohen, Bernard, 1929- II. Bárány Society. III. New York Academy of Sciences. IV. Series. [DNLM:

1. Vestibular apparatus—Physiology—Congresses.

2. Vestibular nuclei—Physiology—Congresses.

3. Oculomotor muscles—Physiology—Congresses.

W1 AN626YL v. 374/WV 255 V582 1980]

Q11.N5 vol. 374 [QP471] 500s [599.01'823] 81-14230

ISBN 0-89766-137-0 AACR2

ISBN 0-89766-138-9 (pbk.)

SP

Printed in the United States of America

ISBN 0-89766-137-0 (Cloth)

ISBN 0-89766-138-9 (Paper)

ANNALS OF THE NEW YORK ACADEMY OF SCIENCES
VOLUME 374
November 6, 1981
**VESTIBULAR AND OCULOMOTOR PHYSIOLOGY:
INTERNATIONAL MEETING OF THE BÁRÁNY SOCIETY***

Editor

BERNARD COHEN

Conference Chairmen

BERNARD COHEN and KENNETH BROOKLER

Advisory Committee

ROBERT BAKER, MORRIS B. BENDER, VIANNEY DE JONG,
VOLKER HENN, STEPHEN HIGHSTEIN, HARVEY KARTEN,
THEODORE RAPHAN, JUN-ICHI SUZUKI, TAKUYA UEMURA,
LAURENCE YOUNG, and VICTOR WILSON

CONTENTS

Preface. By BERNARD COHEN	xi
Introductory Remarks. By MORRIS B. BENDER	xiii
Part I. Vestibular Receptor Mechanisms	
Otto Lowenstein, <i>Chairman</i>	
Directional Sensitivity of Individual Vertebrate Hair Cells to Controlled Deflection of Their Hair Bundles. By S. L. SHOTWELL, R. JACOBS, and A. J. HUDSPETH	1
The Function of the Endolymphatic Duct—An Experimental Study Using Ionic Lanthanum as a Tracer: A Preliminary Report. By HELGE RASK- ANDERSEN, GÖRAN BREDBERG, LEIF LYTTKENS, and GÖRAN LÖÖF	11
Eye-Muscle Geometry and Compensatory Eye Movements in Lateral- Eyed and Frontal-Eyed Animals. By JOHN I. SIMPSON and WERNER GRAF	20
Phasic Components of Frog Semicircular Canal. By YASUO HARADA and KENZO HIRATA	31
Part II. Graviception	
Fred Guedry, <i>Chairman</i>	
Physiological Mechanisms of the Nystagmus Produced by Rotations about an Earth-Horizontal Axis. By JAY M. GOLDBERG and CÉSAR FERNÁNDEZ	40
Effects of Gravity on Rotatory Nystagmus in Monkeys. By THEODORE RAPHAN, BERNARD COHEN, and VOLKER HENN	44

*This volume is the result of a conference entitled Vestibular and Oculomotor Physiology: International Meeting of the Bárány Society, held on September 22-25, 1980, by the Bárány Society and cosponsored by The New York Academy of Sciences.

Dynamic Characteristics of the Otolithic Oculomotor System. By TAKASHI TOKITA, HIDEO MIYATA, MICHIIRO MASAKI, and SADAHIDE IKEDA	56
Binocular Counterrolling in Humans with Unilateral Labyrinthectomy and in Normal Controls. By SHIRLEY G. DIAMOND and CHARLES H. MARKHAM	69
Ocular Torsion on Earth and in Weightlessness. By LAURENCE R. YOUNG, BYRON K. LICHTENBERG, ANTHONY P. ARROTT, TROY A. CRITES, CHARLES M. OMAN, and ELAZER R. EDELMAN	80

Part III. Central Vestibular Organization

Robert Baker, *Chairman*

Neuronal Interaction between Ipsilateral Medial and Lateral Vestibular Nuclei. By I. MATSUOKA, J. ITO, M. SASA, S. TAKAORI, and M. MORIMOTO	93
The Ascending Tract of Deiters' and Horizontal Gaze. By S. M. HIGHSTEIN and H. REISINE	102
Nonlinear Characteristics of Single Neurons in the Vestibular Nuclei. By JAI H. RYU, BRIAN F. MCCABE, and RICHARD W. BABIN	112
Reticulovestibular Organization Participating in Generation of Horizontal Fast Eye Movement. By S. SASAKI and H. SHIMAZU	130
Horizontal Eye Movement Signals in Second-Order Vestibular Nuclei Neurons in the Cat. By A. BERTHOZ, K. YOSHIDA, and P. P. VIDAL	144

Part IV. Central Oculomotor Organization

Morris B. Bender and Jun-Ichi Suzuki, *Chairmen*

A Transsynaptic Autoradiographic Study of the Pathways Controlling the Extraocular Eye Muscles, Using [¹²⁵ I]B-II _b Tetanus Toxin Fragment. By J. A. BÜTTNER-ENNEVER, P. GROB, K. AKERT, and B. BIZZINI	157
Some Thoughts about the Three Neurons in the Vestibular Ocular Reflex. By R. BAKER, C. EVINGER, and R. A. MCCREA	171
Cat Medial Pontine Neurons in Vestibular Nystagmus. By CHARLES H. MARKHAM, SHOZO NAKAO, and IAN S. CURTHOYS	189
Is Transmission between the Vestibular Type I Hair Cell and Its Primary Afferent Chemical? By D. A. SCHESSEL and S. M. HIGHSTEIN	210

Part V. Visual Correlates of Full-Field Motion

Masanori Morimoto and Joachim Grüsser, *Chairmen*

Organization of the Avian Accessory Optic System. By NICHOLAS C. BRECHA and H. J. KARTEN	215
Visual-Vestibular Interaction in Vestibular Neurons: Functional Pathway Organization. By WOLFGANG PRECHT	230
Neural Activity in the Nucleus Reticularis Tegmenti Pontis in the Monkey Related to Eye Movements and Visual Stimulation. By E. L. KELLER and W. F. CRANDALL	249

Visual-Vestibular Interactions in Visual Cortical Cells in the Cat. By ROBERT H. LAHUE, JR., STANISLAV REINIS, JACK P. LANDOLT, and KENNETH E. MONEY	262
--	-----

Part VI. Functional Aspects of Visual-Vestibular Processing

Laurence Young, *Chairman*

Circularvection: Psychophysics and Single-Unit Recordings in the Monkey. By U. BÜTTNER and V. HENN	274
Sigma-Movement and Sigma-Nystagmus: A New Tool to Investigate the Gaze-Pursuit System and Visual-Movement Perception in Man and Monkey. By BIRGIT ADLER, H. COLLEWIJN, G. CURIO, O.-J. GRÜSSER, M. PAUSE, URSULA SCHREITER, and L. WEISS	284
Motion Sickness Due to Vision Reversal: Its Absence in Stroboscopic Light. By G. MELVILL JONES and G. MANDL	303
Natural Retinal Image Motion: Origin and Change. By H. COLLEWIJN, A. J. MARTINS, and R. M. STEINMAN	312

Part VII. Habituation in the Vestibular System

Kurt P. Schaefer and Tauba Pasik, *Chairmen*

Vestibular Habituation in Man and Monkey during Sinusoidal Rotation. By J. JÄGER and V. HENN	330
Unilateral Habituation of Vestibulo-Ocular Responses in the Cat. By M. JEANNEROD, G. CLEMENT, J. H. COURJON, and R. SCHMID	340
Visually Induced Self-Motion Sensation Adapts Rapidly to Left-Right Reversal of Vision. By CHARLES M. OMAN and OTMAR L. BOCK	352
Patterns of Vestibular and Neck Responses and Their Interaction: A Comparison between Cat Cortical Neurons and Human Psychophysics. By T. MERGNER, L. DEECKE, and W. BECKER	361

Part VIII. Visual-Spinal-Vestibular Interactions

Victor Wilson, *Chairman*

Responses of Vestibulospinal Neurons to Neck and Macular Vestibular Inputs in the Presence or Absence of the Paleocerebellum. By R. BOYLE and O. POMPEIANO	373
Dynamics of Vestibulo-Ocular, Vestibulocollic, and Cervicocollic Reflexes. By BARRY W. PETERSON, GERARDO BILOTTO, JEFIM GOLDBERG, and VICTOR J. WILSON	395
Early Directional Influence of Visual Motion Cues on Postural Control in the Falling Monkey. By M. LACOUR, P. P. VIDAL, and C. XERRI	403
Influence of Labyrinthine Hypoactivity on Gross Motor Development of Infants. By KIMITAKA KAGA, JUN-ICHI SUZUKI, ROGER R. MARSH, and YOSHISATO TANAKA	412
Velocity Storage, Nystagmus, and Visual-Vestibular Interactions in Humans. By BERNARD COHEN, VOLKER HENN, THEODORE RAPHAN, and DEBRA DENNETT	421
Aftereffects of Vestibular and Optokinetic Stimulation and Their Interaction. By E. KOENIG and J. DICHGANS	434

Part IX. Flocculus and Visual-Vestibular Interactions

Albert Fuchs and Pedro Pasik, *Chairmen*

The Role of the Dentate Nucleus and Y-Group in the Generation of Vertical Smooth Eye Movements. By M. CARROLL CHUBB and ALBERT F. FUCHS	446
The Brain-Stem Projection to the Cerebellar Flocculus Relevant to Optokinetic Responses in Cats. By TADASHI KAWASAKI, ISAO KATO, YU SATO, and KANEMASA MIZUKOSHI	455
Visual Mossy Fiber Inputs to the Flocculus of the Monkey. By HIROHARU NODA	465
Mossy Fiber Activation of the Cerebellar Flocculus from the Visual System. By KYOJI MAEKAWA, MINORU KIMURA, and TOSHIKI TAKEDA ..	476
Input-Output Activity of the Primate Flocculus during Visual-Vestibular Interaction. By W. WAESPE, U. BÜTTNER, and V. HENN	491

Part X. Signal Processing in the Vestibulocerebellum

David A. Robinson, *Chairman*

Directional Plasticity of the Vestibulo-Ocular Reflex in the Cat. By LEX W. SCHULTHEIS and DAVID A. ROBINSON	504
The "Error" Signals Subserving Adaptive Gain Control in the Primate Vestibulo-Ocular Reflex. By F. A. MILES and S. G. LISBERGER	513
A New Neurotological Test for Detecting Cerebellar Dysfunction. By TOSHIKI YAGI, MOTOHIRO SHIMIZU, SUJI SEKINE, TOMOKAZU KAMIO, and JUN-ICHI SUZUKI	526
Further Observations on the Phenomenon of Rebound Nystagmus. By J. D. HOOD	532

Part XI. Normal and Abnormal Head-Eye Interactions

G. Melvill Jones, *Chairman*

Active Head Rotations and Eye-Head Coordination. By WOLFGANG H. ZANGEMEISTER and LAWRENCE STARK	540
Vestibular Influence upon Head-Eye Coordination. By G. R. BARNES and A. J. PROSSER	560
Disturbances of Eye-Head Coordination during Lateral Gaze in Labyrinthine Disease. By TAKUYA UEMURA, YASUKO ARAI, and CHIGA SHIMAZAKI	571
The Interaction between Accuracy of Gaze with and without Head Movements in Patients with Cerebellar Ataxia. By NATSUE SHIMIZU, MASAHIRO MIZUNO, MAKOTO NAITO, and MITSUO YOSHIDA	579
Nystagmus, Gaze Shift, and Self-Motion Perception during Sinusoidal Head and Neck Rotation. By J. M. B. V. DE JONG, W. BLES, and G. BOVENKERK	590

Part XII. Central Vestibular and Oculomotor Disorders

Johannes Dichgans, *Chairman*

Eye Movements in Patients with Wallenberg's Syndrome. By ROBERT W. BALOH, ROBERT D. YEE, and VICENTE HONRUBIA	600
---	-----

Head Nodding Associated with Idiopathic Childhood Nystagmus. By MICHAEL GRETTY and G. MICHAEL HALMAGYI	614
A Hypothetical Explanation for Periodic Alternating Nystagmus: Instability in the Optokinetic-Vestibular System. By R. JOHN LEIGH, DAVID A. ROBINSON, and DAVID S. ZEE	619
Postural Imbalance with Head Extension: Improvement by Training as a Model for Ataxia Therapy. By TH. BRANDT, S. KRAFCZYK, and I. MALSBENDEN	636
Tullio Phenomenon with Torsion of the Eyes and Subjective Tilt of the Visual Surround. By L. DEECKE, T. MERGNER, and D. PLESTER	650
Effect of Frontal-Eye-Field Lesion on Eye-Head Coordination in Squirrel Monkeys. By TOSHIAKI O-UCHI, MAKOTO IGARASHI, and TAKESHI KUBO	656

Part XIII. Auditory-Vestibular Interactions and Postural Control
Ottavio Pompeiano, *Chairman*

Acoustic-Induced Eye Movements. By K.-P. SCHAEFER, K.-J. SÜSS, and E. FIEBIG	674
Modifications of Vestibular Nystagmus Produced by Fixation of Visual and Nonvisual Targets. By R. SCHMID, D. ZAMBARBIERI, and G. MAGENES	689
Impaired Suppression of Vestibular Nystagmus by Fixation of Visual and Acoustic Targets in Neurological Patients. By E. MIRA, E. MEVIO, P. ZANOCCO, and P. CASTELNUOVO	706
A Physical Model of Human Postural Dynamics. By C. W. STOCKWELL, S. H. KOOZEKANANI, and K. BARIN	722

Part XIV. Use of Visual-Vestibular Interactions in Diagnosis
Takuya Uemura and Bernard Cohen, *Chairmen*

Dissociation of the Eyes in Saccadic Movement. By T. MIYOSHI, S. HIWATASHI, S. KISHIMOTO, and A. TAMADA	731
Different Effects Involved in the Interaction of Saccades and the Vestibulo-Ocular Reflex. By REINHART JÜRGENS, WOLFGANG BECKER, and PETER RIEGER	744
Modification of Saccade by Various Central Nervous System Dysfunctions. By YO KIMURA, ISAO KATO, YUKIO WATANABE, and KANEMASA MIZUKOSHI	755
Visual-Vestibular Interaction in Central Nervous System Disorders. By ISAO KATO, TADASHI NAKAMURA, YO KIMURA, YOSHIO KOIKE, and KANEMASA MIZUKOSHI	764
Eye-Velocity Programming in Brain-Stem Disorders. By CARSTEN WENNMO, NILS G. HENRIKSSON, ILMARI PYYKKÖ, and LUCYNA SCHALÉN	774
Compensation of Unilateral Vestibular Loss in Vestibular Neuronitis. By A. KATSARKAS and J. S. OUTERBRIDGE	784

Part XV. Additional Topics

Jan Stahle, *Chairman*

Temporal Bone Characteristics in Meniere's Disease. By JAN STAHL, HERMANN F. WILBRAND, and HELGE RASK-ANDERSEN	794
Microdisc Gel Electrophoresis in Sodium Dodecyl Sulfate of Organic Material from Rat Otoconial Complexes. By M. D. ROSS, K. G. POTE, K. E. RAREY, and L. M. VERMA	808
Ménière's Disease: Endolymphatic Sac Decompression Compared with Sham (Placebo) Decompression. By J. THOMSEN, P. BRETLAU, M. TOS, and N. J. JOHNSEN	820
Cranial Computerized Tomography in Spinocerebellar Atrophies. By D. CLAUS and J. C. ASCHOFF	831
Vestibular and Neurological Disorders in Diving Competitors. By H. KREJCOVA, L. KREJCI, J. JIROUT, B. STRACAROVA, and P. REZEK	839
Visual Suppression of Caloric Nystagmus in Brain-Stem Lesions. By SETSUKO TAKEMORI, TADASHI AIBA, and RYOICHI SHIZAWA	846
The Role of the Plantar Mechanoreceptor in Equilibrium Control. By ISAMU WATANABE and JIN OKUBO	855
Ocular Torsion in the Cat after Lesions of the Interstitial Nucleus of Cajal. By JOHN H. ANDERSON	865
Index of Contributors	873
Subject Index	875

Financial assistance was received from:

- AIR FORCE OFFICE OF SCIENTIFIC RESEARCH
- NATIONAL AERONAUTICS AND SPACE ADMINISTRATION
- NATIONAL INSTITUTE OF NEUROLOGICAL AND COMMUNICATIVE DISORDERS AND STROKE, NATIONAL INSTITUTES OF HEALTH
- PFIZER INCORPORATED

The New York Academy of Sciences believes it has a responsibility to provide an open forum for discussion of scientific questions. The positions taken by the participants in the reported conferences are their own and not necessarily those of The Academy. The Academy has no intent to influence legislation by providing such forums.

PREFACE

Bernard Cohen

*Department of Neurology
Mount Sinai School of Medicine
City University of New York
New York, New York 10029*

Rapid progress has been made in recent years toward understanding how the central nervous system processes visual and vestibular signals to produce eye movements and body postural responses. One of the most fascinating developments has been the discovery that many neurons in the central vestibular system fire in relation to the velocity of head movement, and respond to any sensory input that would be utilized in initiating or sustaining ocular nystagmus and the sense of movement. Of these extralabyrinthine inputs, that from the visual system is one of the strongest. Most cells in the rostral medial vestibular nucleus of the alert monkey can be activated by visual stimulation. Adding to the activity of central vestibular neurons are neural networks that superpose the inputs from various sensory systems, store activity, and feed it back to alter the characteristics of the vestibulo-ocular reflex (VOR), so that it more faithfully compensates for head movement. As a result, activity of vestibular nuclei neurons during head rotation at low frequencies is much different than the firing rates of receptor cells in the semicircular canals.

How activity from the visual system reaches the vestibular system is under intensive study, but subcortical visual pathways through the accessory optic system and the flocculus of the cerebellum appear to play an important role in coupling the visual and vestibular systems. In addition, many neurons in the vestibular nuclei and vestibulocerebellum have their activity modulated with rapid and slow eye movements. These are not limited to movements generated by the vestibular system but include all spontaneous and visually guided movements.

The implication is that the vestibular nuclei are much more than a simple processing station for labyrinthine activity. Rather, they appear to serve as a focal point for processing information about motion from various sensory systems and to participate in the generation of rapid and slow eye movements. Thus, there is a need to understand how specific sensory inputs converge on the vestibular nuclei, how the vestibular nuclei participate in the generation of eye and body movements, and how disorders that affect this convergence might be manifested after lesions of the central vestibular system.

Although the inputs from the semicircular canals have been studied extensively, and a new literature on visual-vestibular interactions is beginning to build, there are other important sensory interactions that require investigation before we can understand normal vestibular function. Head movements generally do not occur only in one plane around a vertical axis, exciting a single pair of semicircular canals, although this is a common laboratory and clinical test mode. Instead a rotating gravity vector is introduced during normal head movement that dynamically excites the otolith organs and contributes to the generation of compensatory eye and body movements and to the sense of motion. Little is known about the neurophysiology of dynamic otolith-canal interactions, although

work now is beginning to appear on this important topic. It probably has special bearing for understanding space motion sickness as well as clinical vertigo.

At present the diagnosis of a central vestibular disorder often is a diagnosis of exclusion, being limited to such techniques as caloric stimulation and positional testing. While useful, these tests do not test multimodal sensory interactions or the rich variety of behaviors that the vestibular system controls or elicits. Ideally, one would like to test vestibulo-ocular and vestibulospinal reflexes using signal processing techniques to determine phase and gain relationships under a variety of conditions, including those in which a "conflict" is introduced between various sensory inputs. Although the vestibular system operates over a "hard-wired" three-neuron arc, visual experience has been shown to have a powerful effect in adapting or even in reversing the vestibular-ocular reflex. Study of how and where adaptation takes place might be expected to provide insight into how vestibular disease might be treated more effectively. It should also lead to determining how similar learning and adaptation take place in other areas of the nervous system. From this approach, one would expect to develop a new pathophysiology of the vestibular system, one that would enable us to evaluate dynamic changes in the VOR and account for effects of sensory interaction, adaptation, habituation, and the ability to suppress inappropriate ocular responses. Work along these lines has come from a number of laboratories, but only through a cooperative, interdisciplinary approach can new physiologic findings be integrated into clinical testing.

These and similar considerations led to the formulation of the themes of this conference. The meeting was sponsored by the Bárány Society and the New York Academy of Sciences. The Bárány Society (named in honor of Robert Bárány) is composed of clinical and experimental scientists who have a common interest in studying the vestibular and oculomotor systems. Among others, the members include otolaryngologists, neurologists, anatomists, physiologists, psychologists, and engineers. The society exists to provide a forum where new results and common problems can be presented and discussed. The New York Academy of Sciences plays an important role in the scientific community by supporting meetings that report new findings in active and expanding fields. It was a fortuitous circumstance that brought the two together to hold this meeting.

I would like to thank Ellen Marks, Renee Wilkerson, and Erna Levine of the New York Academy of Sciences for their skilled administration and guidance of the meeting and Bill Boland and Sheila Kates for preparation of the book. Special thanks go to the National Institute of Neurological and Communicative Disorders and Stroke, which provided major support for the meeting, and to the Air Force Office of Scientific Research, the National Aeronautics and Space Administration, and the Pfizer Corporation, which provided additional funding. Without their generous contributions, the meeting would not have been possible. I am grateful to Drs. Kenneth Brookler, cochairman, Dr. Victor Wilson, Pearl Johnson, and David Borrás, who helped plan and arrange the meeting, and to members of the Advisory Committee, Drs. Robert Baker, Morris B. Bender, Vianney de Jong, Volker Henn, Stephen Highstein, Harvey Karten, Theodore Raphan, Jun-Ichi Suzuki, Takuya Uemura, Laurence Young, and Victor Wilson, who also assisted in selecting the papers. Finally, my special thanks go to the many authors who made it an interesting conference and contributed the excellent papers that form this volume. The field has made enormous strides since the first Oculomotor Symposium was held at Mount Sinai in 1961. Based on this performance, we look forward to the next 20 years with anticipation and enthusiasm.

INTRODUCTORY REMARKS

Morris B. Bender

*Department of Neurology
Mount Sinai School of Medicine
City University of New York
New York, New York 10029*

As a neurologist I find myself at home at the Bárány Society meeting. The society was founded in 1960 by Professors Nylen and Hallpike, with the aim of promoting contact between scientist and clinician so as to stimulate otoneurologic research. Bárány was the founder of neuro-otology, or—as Professor Stahle called it—otoneurology. A division in neuro-otology was established by Jones at the University of Pennsylvania in 1918. Robert Bárány, a Viennese otologist who lived during the last quarter of the nineteenth century and the first third of the twentieth century, must have been influenced by such scientists as Purkinje and Flourens, by the psychophysicist Helmholtz, by physiologists—Breuer, Ewald, and Sherrington, and by neuroanatomists, such as Meynert, Golgi, and Cajal. In May 1905, Bárány communicated his observations on caloric nystagmus to the Austrian Otologic Society. Thereafter, there was a phenomenal development of otology. Bárány became a leading aural surgeon and authority in clinical disorders of labyrinthine functions. The nystagmus produced following injection of warm or cold water into the external auditory meatus, which varied with the pathology of the internal ear, became known as Bárány's sign. Nystagmus, which has been associated almost entirely with congenital or early acquired optic defects or, in an indefinite way, with lesions of the inner ear, has become one of the most important aids in differential diagnosis for the otologist and even more so for the neurologist. In 1906 Bárány advanced a theory of vestibular nystagmus. He received the Nobel prize in medicine in 1914 for his work on the physiology and pathology of the vestibular apparatus. In his acceptance of this prize, he spoke on his discovery of new methods for functional tests of the vestibular apparatus and cerebellum. He noted that lesions of the flocculus resulted in nystagmus. Bárány also studied systematically other vestibular reactions. He provided an explanation for the vestibular phenomena occurring after rotation, which was in sharp contrast to what had been thought in previous years. Thus, he established the clinical and physiological importance of the so-called rotatory reaction. He also studied the remaining phenomena of the vestibular syndrome. Here he was concerned chiefly with developing the question of the so-called vestibular reaction movements and vertigo. Bárány's "pointing test" became an integral part of the examination methods of ear and nerve specialists. His investigations of the neural basis for nystagmus must have influenced Lorente de Nó's researches on the neuronal networks within the pontine reticular formation.

With the introduction of techniques for recording eye movements by electro-nystagmography in 1922, research in this field expanded rapidly throughout the world. By the middle of the twentieth century, various monographs and symposia on the vestibulo-ocular system were published. After the first symposium on the oculomotor system in the 1960s, research investigations and publications in neuroscience accelerated. At present it almost is impossible to follow or digest

the vast information. Anatomists, physiologists, pharmacologists, chemists, and immunologists all have contributed to an understanding of the neural basis of vestibular and oculomotor function.

It should be pointed out that the Bárány Society regularly contributed to this growth. *Inspection of today's program will disclose a variety of topics related to the vestibular and oculomotor system. Based on the content of this meeting, one might conclude that we are a society of neuroscientists. This society has grown and will continue to grow, as evidenced by the steadily increasing membership. There is a need, however, for someone to digest and synthesize the contents of these meetings, particularly the electrophysiology and minute anatomy of the various geographic boundaries of neuronal aggregates, or assemblies of neurons acting as functional units in behavior, especially the vestibular system, which participates in almost every biologic activity.*

DIRECTIONAL SENSITIVITY OF INDIVIDUAL VERTEBRATE HAIR CELLS TO CONTROLLED DEFLECTION OF THEIR HAIR BUNDLES*

S. L. Shotwell, R. Jacobs, and A. J. Hudspeth†

*Division of Biology
California Institute of Technology
Pasadena, California 91125*

INTRODUCTION

Among the most striking and consistent morphological features of vertebrate hair cells is the geometrical arrangement of their mechanosensitive organelles, the hair bundles. These structures each consist of 30-200 microvilluslike stereocilia and a single, eccentrically placed, axonemal kinocilium. Three geometrical features of hair bundles are widespread, if not universal. First, the stereocilia and kinocilium are inserted into the cellular apex in a regular, hexagonal array. Second, the lengths of stereocilia increase monotonically from one edge of the hair bundle to the other, but are approximately equal within a row of stereocilia across the hair bundle. Finally, the kinocilium is located at the edge of the hair bundle at which the longest stereocilia occur. Distortions of these features may occur; for example, the spacing of stereocilia is not absolutely uniform in some hair cells, but varies from one edge of the hair bundle to the other. Hair bundles become progressively distorted and asymmetrical as the apex of the mammalian cochlea is approached.¹ The kinocilium, although present in ontogeny, is lost from some hair cells in mammalian cochleas.² Even in these exceptional cases, however, the general pattern of arrangement of the hair bundle is evident.

A consequence of this organization is that the hair bundle possesses a plane of mirror symmetry. This plane is perpendicular to the apical surface of the hair cell and runs through the kinocilium and along the cell from the edge with the longest stereocilia to that with the shortest. It is parallel with one of the three axes of hexagonal symmetry defined by the insertions of the stereocilia and kinocilium at the hair cell's apex. Lowenstein and Wersäll suggested a coincidence of the plane of symmetry and the axis of sensitivity of hair cells;³ movement of the hair bundle's distal tip toward the kinocilium was found to produce increased firing in the eighth nerve, while oppositely directed motion inhibited firing. A similar correspondence was found during extracellular recordings of microphonic potentials in other acousticolateralis organs in which the orientation of stimulation was reasonably well known.^{4,5} Movement of the hair bundle's distal tip toward the kinocilium was shown by intracellular recordings⁶ to produce a depolarizing receptor potential, while opposite movement elicited a small hyperpolarization. The response of hair cells to stimuli directed at various angles to the plane of mirror symmetry was inferred from microphonic recordings in the lateral-line organ;⁷ for relatively small stimuli, the response declined from its

*This research was supported by National Institutes of Health Grants NS-13154 and GM-00086 and by funds from the William Randolph Hearst, Ann Peppers, and Pew Foundations.

†To whom correspondence should be addressed.

maximal value with on-axis stimulation as the cosine of the angle by which the stimulus orientation deviated from that axis.

We report here observations on the directional sensitivity of the response to hair bundle displacement. Our results confirm the cosine relationship for responses to stimuli of small amplitude and show this to be a consequence of the hair cell's general insensitivity to displacements of its hair bundle perpendicular to the plane of symmetry.

MATERIALS AND METHODS

All experiments were performed with hair cells in saccular maculi from bullfrogs (*Rana catesbeiana*) of both sexes. Organs dissected from animals 90–150 mm in snout-vent length were maintained at pH 7.2–7.3 in a saline solution containing 113 mM Na^+ , 2 mM K^+ , 4 mM Ca^{2+} , 123 mM Cl^- , 3 mM *D*-glucose, and 5 mM *N*-2-hydroxyethylpiperazine-*N'*-2-ethanesulfonic acid. The otolithic membrane overlying the hair bundles was removed by dissection, usually after loosening by mild proteolysis.⁸ Experiments were done under a Zeiss WL microscope with differential interference contrast (Nomarski) optics and at a total magnification of 800 \times . Preparations maintained at 22°C in room air yielded satisfactory responses for at least four hours.

Mechanical stimuli were usually applied directly to hair bundles by fine glass capillaries slipped over their distal ends (FIGURE 1). Ideal stimulus probes had inner diameters of 1.5–2.5 μm and encompassed the most distal 1–2 μm of the hair bundles. A few experiments were done using blunt, adhesive stimulus probes attached directly to kinocilia.⁹ This method produced generally similar results. Probes were oriented such that their tips moved in a plane parallel with the epithelium's apical surface. They were displaced with micromanipulators consisting of two perpendicularly mounted piezoelectric bimorph elements linked by balsa-wood struts.¹⁰ The axis along which a probe moved could be continuously varied through 360° by control of the fraction of the stimulus voltage applied to each of the bimorphs. Stimulus amplitudes were calibrated against an eyepiece micrometer; stroboscopic illumination was sometimes employed to sharpen the image of an oscillating stimulus probe. For amplitudes up to $\pm 4 \mu\text{m}$ and within an observational uncertainty of about $\pm 0.1 \mu\text{m}$, the stimulus amplitude was found to vary linearly with the driving voltage and to be independent of angular orientation. With the optical system employed, the angular orientations of stimuli with respect to the planes of symmetry of hair cells could be estimated to about $\pm 5^\circ$. The data presented herein were taken using static displacements and 10-Hz, triangle-waveform oscillatory stimuli.

Intracellular recordings were made with 3 M KCl-filled microelectrodes approximately 250 M Ω in resistance. The electrodes were bent¹¹ to allow their introduction under the short-working-distance, 40 \times , water-immersion objective lens. Cells from which data were analyzed had resting potentials of –45 to –60 mV that were stable for at least 10 minutes; receptor potentials elicited by saturating stimuli were 5–24 mV in peak-to-peak amplitude. Data taken from a total of 51 hair cells in 13 animals were stored with an FM tape recorder. The records shown in FIGURES 3, 4, 5, and 7 each represent averages of 8–32 consecutive responses. The sensitivities of hair cells to various stimuli were determined by plotting each receptor potential against the deflection producing it and measuring the greatest slope of the resultant curve.



FIGURE 1. Scanning electron micrograph of the apical surface of a bullfrog's saccular epithelium. The hair bundles of several hair cells are shown, one of which is engaged by a capillary-type stimulus probe about $2\ \mu\text{m}$ in internal diameter. The supporting cells between the hair cells are overlain by matted remnants of the otolithic membrane in this preparation, which was not subjected to proteolytic digestion. $\times 2300$.

In order to describe the responses of hair cells to various stimuli and to investigate the geometrical arrangement of their hair bundles, it is convenient to define a coordinate system in which stimuli occur (FIGURE 2). Because every vertebrate hair cell ordinarily possesses only one kinocilium (or its remnant after regression), a convenient and unambiguous origin for the coordinate system is the site of insertion of the kinocilium into the apical cellular surface. The x-axis of the coordinate system runs along the hair cell's apical surface in the plane of mirror symmetry of the cell; the positive x-direction (in Cartesian coordinates) or 0° (in polar coordinates) is that in which the kinocilium stands with respect to the rest of the hair bundle. This polarity convention accords with that of other investigators.⁷ The y-axis lies within the plane of the cellular apex and perpen-

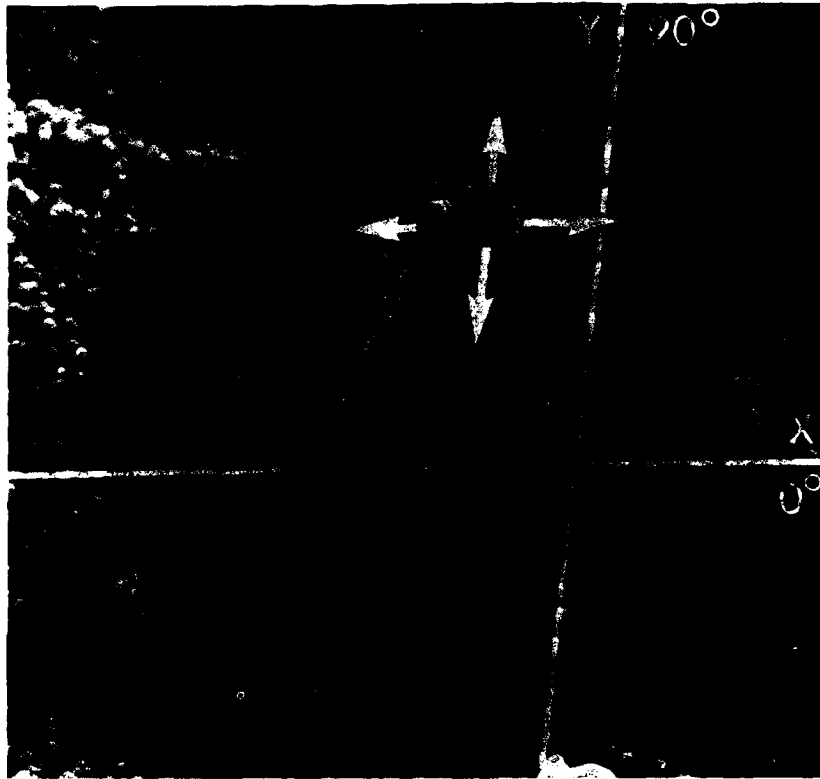


FIGURE 2. A scanning electron micrograph of the hair bundle on the apical surface of a large hair cell. Note that the stereocilia grow progressively longer from the left edge of the hair bundle to the right extreme, at which the kinocilium occurs. The superimposed lines represent the x-axis (0°), which lies at the intersection of the plane of mirror symmetry of the cell and the plane of the apical epithelial surface, and the y-axis (90°), which runs perpendicular to the x-axis and within the plane of the epithelial surface. The origin of the coordinate system is at the kinocilium's base; the z-axis runs through this origin and perpendicular to the cell's surface. Arrows emanating from the bulbous tip of the kinocilium represent positive and negative deflections parallel with the x- and y-axes. The otolithic membrane was removed from this preparation by proteolytic digestion. $\times 9000$.

dicular to the x-axis; by the standard Cartesian-to-polar transformation, the positive y-axis corresponds to 90° . The z-axis is perpendicular to the other axes, and the positive z-direction is from the base toward the apex of the hair bundle.

The distal end of the hair bundle, at which stimuli are applied, is conveniently described during experiments by the position of the kinocilium's bulbous tip. For large hair cells in the bullfrog's sacculus, the center of this bulb lies about $6.9 \mu\text{m}$ above the epithelial surface and approximately $1.2 \mu\text{m}$ in the negative x-direction. Since the stereocilia and kinocilium are rather stiff elements that pivot near their basal insertions, the tip of each process actually sweeps through an arc as the hair bundle is deflected. The amplitudes of the stimuli employed in the present study—less than $1.5 \mu\text{m}$ along any axis—involve motions of the

kinocilium through an angular range of under $\pm 12^\circ$. The height of the kinociliary bulb above the epithelial surface therefore changes by only $0.1 \mu\text{m}$, or under 2%, for the largest stimuli; the motion of the hair bundle's distal tip thus essentially lies within a plane.

Sacculi destined for histological study were dissected, mounted, and maintained as those used in electrophysiology. They were then fixed for 60 minutes at 4°C in 40 mM OsO_4 and 10 mM CaCl_2 buffered to pH 7.3 with 80 mM sodium cacodylate.⁹ After dehydration in ethanol, critical-point drying from liquid CO_2 , and gold sputter-coating, specimens were observed and photographed in a scanning electron microscope operated at 20 keV.

RESULTS

Deflection of the distal tip of a hair bundle within the hair cell's plane of mirror symmetry produces receptor potentials of a form reported previously⁶ (FIGURE 3). Motion in the positive x-direction produces a depolarization whose amplitude is graded with stimulus strength and reaches 4–20 mV. Deflection in the negative x-direction yields a graded hyperpolarization of about one-fifth this amplitude. Much of the variability in the peak amplitude of responses from cell to cell stems from damage sustained upon microelectrode penetration; hair cells studied with favorable electrodes consistently yield responses about 15 mV in peak-to-peak amplitude. Moreover, the displacement-response curve, which relates the instantaneous receptor potential with stimulus probe position, is highly consistent from cell to cell. This relationship is roughly sigmoidal, with the displacements encompassing 90% of the full response range characteristically separated by about $0.3 \mu\text{m}$.

Stimulation parallel with the y-axis, at 90° to the hair cell's plane of mirror symmetry, produces little or no receptor potential (FIGURE 3). If the hair bundle is

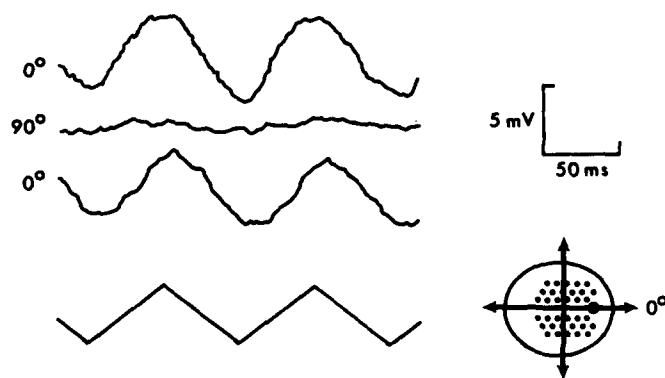


FIGURE 3. Averaged intracellular potentials from a hair cell stimulated by deflections of its hair bundle parallel with the x-axis (0°) and perpendicular to it (90°). The former yield responses that saturate in both the depolarizing and hyperpolarizing directions; the latter, no significant receptor potential. The responses have been vertically offset for clarity. A schematic representation of stimulus motion with respect to the hair bundle's orientation is shown at the lower right of this and of most subsequent figures. The peak-to-peak amplitude of the 10-Hz, triangle-waveform stimulus is $0.6 \mu\text{m}$.

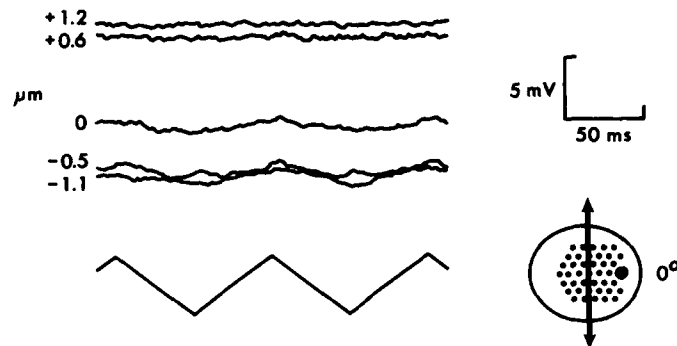


FIGURE 4. Intracellular responses from a cell whose hair bundle is moved parallel with the x-axis by the amounts indicated to the left of the responses, then held there while an oscillatory stimulus parallel with the y-axis is applied. The static deflections along the x-axis produce receptor potentials manifested by the offsets among the responses and totaling 13 mV. Movement of the hair bundle parallel with the y-axis by $\pm 0.5 \mu\text{m}$ produces little (lower traces) or no response.

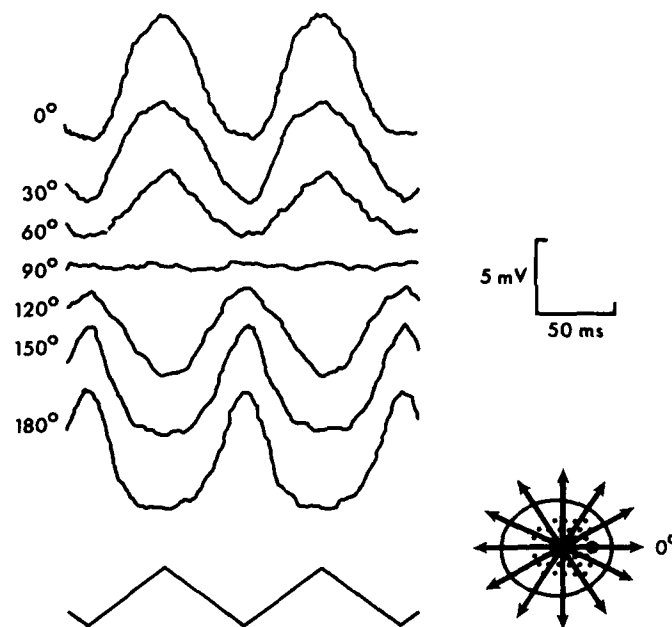


FIGURE 5. Receptor potentials elicited by $0.5\text{-}\mu\text{m}$ (peak-to-peak) stimuli directed at various angles with respect to the x-axis (0°). The traces have been vertically displaced for clarity. Note that both the peak response amplitude and the sensitivity of the cell, or greatest slope of the receptor-potential trace, decline from a maximum for stimulation parallel with the x-axis to zero at 90° to it.

pushed some distance in the positive x-direction and held there, a depolarizing receptor potential arises, then declines to a steady-state level after an adaptation process lasting a few hundred milliseconds.¹² If back-and-forth motion of the hair bundle parallel to the y-axis is now added to the sustained deflection, little additional response occurs (FIGURE 4). An analogous result ensues if a cell's hair bundle is first deflected in the negative x-direction, then stimulated parallel to the y-axis.

A small receptor potential at twice the stimulus frequency occasionally occurs in response to stimulation parallel with the y-axis (FIGURE 4, $-0.5\text{-}\mu\text{m}$ trace). This is seen frequently when a derivatized glass probe is used to move the hair bundle, but rarely when the bundle is displaced with a hollow capillary tube

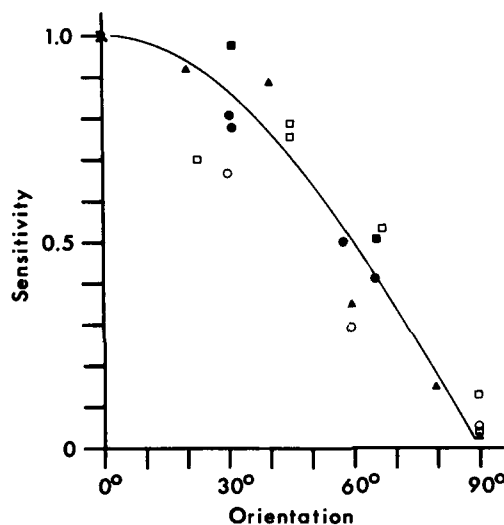


FIGURE 6. Plot of the sensitivities of hair cells to stimulation at various angles with respect to the plane of cellular mirror symmetry. For comparison among five cells (different symbols), the largest sensitivity of each cell has been normalized to unity, and other sensitivities are expressed as a fraction of this value. The continuous curve is the cosine of the angle by which stimuli differ from parallel with the cells' x-axes.

engaging the hair bundle's tip. Visual observation suggests that the hair bundle twists slightly about the vertical (z) axis when the bulbous tip of the kinocilium is pulled sideways by an adhesive probe. The component of motion along the x-axis could elicit a receptor potential, and should do so for movements in either direction, resulting in small responses at twice the stimulus frequency. Capillary stimulus probes, which apply force to a broad surface on the side of the hair bundle when driven parallel with the y-axis, presumably produce less torque than do adhesive probes, and accordingly seldom induce responses.

As the orientation of stimulus motion is varied from parallel with the x-axis to perpendicular to the x-axis, the amplitude of the receptor potential declines continuously from its maximum to essentially zero (FIGURE 5). At the same time, the sensitivity of the cell, measured as the greatest slope of the displacement-

response curve, declines from a maximum to a minimum. A plot of this slope (FIGURE 6) indicates that sensitivity decreases roughly as the cosine of the angle by which the stimulus orientation deviates from the x-axis.

The shape of the displacement-response curve is little affected by movements of the hair bundle perpendicular to the x-axis (FIGURE 7). The receptor potential

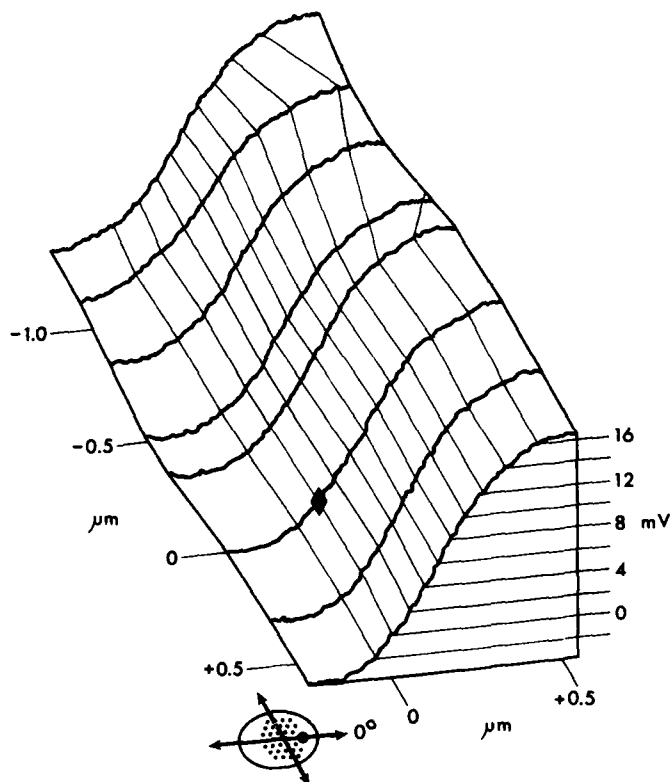


FIGURE 7. A family of displacement-response curves from a cell whose hair bundle is statically displaced by the various distances indicated parallel with the y-axis, then oscillated back and forth through $0.8 \mu\text{m}$ parallel with the x-axis. The rhomboid at the lower center of the figure represents the rest position of the kinociliary bulb before stimuli are applied. Note that the displacement-response relationships for stimulation parallel with the x-axis are similar to one another despite the fact that the distal end of the hair bundle is bent by as much as 11° to the side, parallel with the y-axis.

evoked by an oscillatory stimulus parallel with the x-axis is unaltered by additional, static displacements in either direction parallel with the y-axis.

DISCUSSION

The relationship between the displacement of the tip of a hair bundle and the cellular receptor potential is largely described by FIGURE 7. The result shown in

this figure is implicit in the data of FIGURES 4 and 5: a similar displacement-response surface is defined by appropriate combinations of static and/or oscillatory stimuli along the x- and y-axes. Within the range of amplitudes tested, stimuli parallel with the x-axis produce displacement-response curves of similar amplitudes and slopes. Stimulation parallel with the y-axis has little or no effect on the response.

The portion of the displacement-response surface near the rest position of the kinociliary bulb (rhomboid in FIGURE 7) is essentially a flat sheet of constant slope. Stimuli confined to this region would be expected to yield responses whose amplitudes scale with the cosine of the angular deviation of the stimulus from parallel with the x-axis, in agreement with a previous study on the microphonic response of a lateral-line organ.⁷ For stimuli of all sizes, even those producing saturation of the response, the greatest slope of the displacement-response curve should respect a cosine relationship with angular orientation; this prediction is supported by the data of FIGURE 6.

It should be noted that several factors act to make the apparent sensitivity of the hair cell—the slope of the displacement-response surface of FIGURE 7—less than it actually is. Since the time constant of bullfrog hair cells is about 10 mseconds in the present recording circumstances, responses to 10-Hz stimuli are significantly delayed and broadened. An adaptation process in the transduction mechanism¹² operates rapidly enough to diminish the size of responses. The coupling between stimulus probes and hair bundles is not perfect and doubtlessly exhibits some hysteresis between opposite phases of stimulation. Stimuli of saturating intensity significantly fatigue the transduction process. Finally, slow drift in the position of the stimulus probe and in the timing of the stimulating and recording apparatus acts to broaden the averaged receptor potentials displayed in the figures.

The present results demonstrate that vertebrate hair cells are not only very sensitive to displacement of their hair bundles within the plane of mirror symmetry, but also remarkably insensitive to stimulation orthogonal to this plane. The morphological feature of the hair bundle most conspicuously aligned with the cell's axis of sensitivity, the kinocilium, is not itself the source of the receptor potential.⁹ Since the individual stereocilia appear to lack any structural element of polarization along the axis of sensitivity, it seems most likely that it is the tapered array of stereocilia of differing heights that confers directional sensitivity upon the hair bundle. Whether this comes about through the mechanics by which forces are transmitted to a transducer located at the cellular apex, or by interactions among the distal ends of the tapered stereocilia themselves, remains to be determined.

ACKNOWLEDGMENT

The authors thank Dr. D. P. Corey for comments on the manuscript.

REFERENCES

1. LIM, D. J. 1980. Cochlear anatomy related to cochlear micromechanics. A review. *J. Acoust. Soc. Am.* **67**: 1886-1895.
2. LINDEMAN, H. H., H. W. ADES, G. BREDBERG & H. ENGSTRÖM. 1971. The sensory hairs and the tectorial membrane in the development of the cat's organ of Corti. *Acta Otolaryngol.* **72**: 229-242.

3. LOWENSTEIN, O. & J. WERSÄLL. 1959. A functional interpretation of the electron-microscopic structure of the sensory hairs in the cristae of the elasmobranch *Raja clavata* in terms of directional sensitivity. *Nature* **184**: 1807-1808.
4. FURUKAWA, T. & Y. ISHII. 1967. Neurophysiological studies on hearing in goldfish. *J. Neurophysiol.* **30**: 1377-1403.
5. COREY, D. P. & A. J. HUDSPETH. 1979. Response latency of vertebrate hair cells. *Biophys. J.* **26**: 499-506.
6. HUDSPETH, A. J. & D. P. COREY. 1977. Sensitivity, polarity, and conductance change in the response of vertebrate hair cells to controlled mechanical stimuli. *Proc. Nat. Acad. Sci. USA* **74**: 2407-2411.
7. FLOCK, A. 1965. Electron microscopic and electrophysiological studies on the lateral line organ. *Acta Otolaryngol. Suppl.* **199**: 1-90.
8. COREY, D. P. & A. J. HUDSPETH. 1979. Ionic basis of the receptor potential in a vertebrate hair cell. *Nature* **281**: 675-677.
9. HUDSPETH, A. J. & R. JACOBS. 1979. Stereocilia mediate transduction in vertebrate hair cells. *Proc. Nat. Acad. Sci. USA* **76**: 1506-1509.
10. COREY, D. P. & A. J. HUDSPETH. 1980. Mechanical stimulation and micromanipulation with piezoelectric bimorph elements. *J. Neurosci. Methods* **3**: 183-202.
11. HUDSPETH, A. J. & D. P. COREY. 1978. Controlled bending of high-resistance glass microelectrodes. *Am. J. Physiol.* **234**: C56-C57.
12. EATOCK, R. A., D. P. COREY & A. J. HUDSPETH. 1979. Adaptation in a vertebrate hair cell: stimulus-induced shift in the operating range. *Soc. Neurosci. Abstr.* **5**: 19.

THE FUNCTION OF THE ENDOLYMPHATIC DUCT—
AN EXPERIMENTAL STUDY USING IONIC
LANTHANUM AS A TRACER:
A PRELIMINARY REPORT*

Helge Rask-Andersen, Göran Bredberg,† Leif Lyttkens, and
Göran Lööf

*Department of Otolaryngology
University Hospital
University of Uppsala
S-750 14 Uppsala, Sweden*

INTRODUCTION

Guild's original concept of endolymph flowing from the cochlea through the reunion duct into the saccule, thence out to the endolymphatic duct and sac for reabsorption, is still supported by several recent investigations.¹⁻⁷

The mechanisms underlying this "longitudinal" flow of endolymph towards the sac and the transport across the epithelial membrane are still obscure.

We focused our interest on the narrow epithelial pathway connecting the endolymphatic sac with the rest of the membranous labyrinth, the endolymphatic duct. It is a small tubule lined by a single-layered epithelium where individual cells appear to be sealed together by fairly shallow intercellular junctions. The epithelium is encompassed by a wide zone of loose vascular tissue incorporating a lymphatic vascular network. No details of the ultrastructural anatomy of the endolymphatic duct will be given here, as they are already on record.⁸

In this investigation, we used ionic lanthanum as a tracer in order to provide morphological evidence of an intercellular (or paracellular) fluid pathway between cells lining the endolymphatic duct in the guinea pig.

The tracer was introduced into the scala media of the cochlea in small, controlled amounts. After various intervals, the endolymphatic duct and sac were investigated ultrastructurally in order to trace the lanthanum.

MATERIALS AND METHODS

Five pigmented, healthy guinea pigs (400-600 g) were anesthetized with neurolept anesthesia.⁹ The animals were mounted on rigid ear bars. The bulla and the round window were exposed through a dorsolateral approach. A glass micropipette with a beveled tip (diameter $15 \pm 3 \mu\text{m}$) was filled with a solution of 4% (0.092 M) lanthanum nitrate $[\text{La}(\text{NO}_3)_3 \cdot 6\text{H}_2\text{O}]$ in 140 mmol KCl, which gave 520 mosm, pH 4.6. At this pH, most of the lanthanum is in the form of ionic La^{3+} .

The micropipette was fitted to a 10- μl Hamilton syringe by a polyethylene tube. An Ag-AgCl electrode was inserted in the lumen of the micropipette. With a micromanipulator (Narishige), the micropipette was inserted through the round window and the basilar membrane into the scala media. The position of the tip of

*Supported by the Swedish Medical Research Council, Projects No. 3542 and 3908.

†Department of Audiology, Södersjukhuset, S-100 64 Stockholm, Sweden.

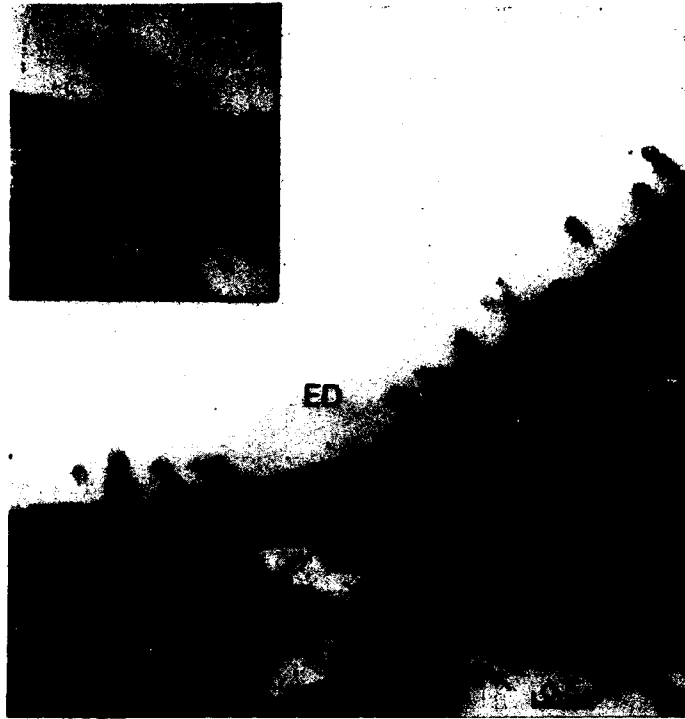


FIGURE 1. A section of the apical cytoplasm of epithelial cells in the proximal portion of the endolymphatic duct (ED) in a guinea pig 27 hours after lanthanum injection. A small deposit of electron-dense precipitate is observed at the level of the intercellular tight junction (TJ). Arrows indicate intercellular deposits of precipitate that appear to have passed the junctional complex. Inset: the junctional region at double magnification, sectioned about $0.1 \mu\text{m}$ deeper.

the micropipette was followed by monitoring the d.c. potential difference between the electrode and the neck reference electrode (Dual Electrometer F223A, W-P Instruments Inc.). The first large negative potential (-60 to -80 mV) indicated entry into the organ of Corti. Appearance of the large $+80$ to $+100$ -mV endocochlear potential proved penetration of the scala media.¹⁰

In the scala media, $1 \mu\text{l}$ of the lanthanum solution was injected during 10 minutes with a Sage syringe pump. The micropipette was withdrawn, and the skin overlying the bulla sutured. The animals were allowed to recover for 27, 41, 66, 88, and 106 hours respectively.

The animals were then anesthetized, and intraaortic perfusion performed using a solution containing 2.5% glutaraldehyde and 1% formaldehyde in 0.1 M Sørensen's phosphate buffer, pH 7.2-7.4. The temporal bones of the injected ear, with the opposite ear serving as control, were decalcified in 0.1 M Na-EDTA‡ in 2.5% glutaraldehyde for 10 days. The specimens were postfixed in 1% osmium tetroxide and stained en bloc overnight in 50% ethanol containing 2% uranyl

‡EDTA is ethylenediaminetetraacetic acid.

acetate. Epon 812 was the embedding agent. The endolymphatic duct was cross-sectioned at different levels, and thin sections analyzed in a JEOL 100-B electron microscope.

RESULTS

Electron-opaque precipitates could be observed at the level of the tight junctional complexes between epithelial cells lining the endolymphatic duct in all the injected ears.

After 27 hours, precipitates were usually seen accumulating on the membranous duct on the intercellular junctional complex (FIGURE 1). Deposits were also found in the depths of the intercellular clefts, especially where this space was narrow, whereas no precipitate was observed in the dilated regions. Intercellular precipitates were observed from the sinus portion to the mid-portion of the intraosseous duct. Intracellular deposits were also found in the epithelium and in a few of the free cells of the periductal connective tissue.

After 41 hours, intercellular deposits of precipitate appeared along the entire duct. At this stage it seemed to have reached the sac, as many of the freely floating cells showed intracytoplasmic bodies containing electron-dense material. No intercellular precipitate was discerned in any portion of the sac.

After 81 hours, every second or third intercellular space was filled throughout with precipitate (FIGURE 2). A surprising feature was the absence of dilated



FIGURE 2. Epithelial cells of the endolymphatic duct (ED) close to the proximal portion of the sac. Fixation 41 hours after lanthanum injection. Precipitate stains all intercellular spaces down to a poorly visible basement membrane.

intercellular spaces. These are normally found between epithelial cells in the distal portion of the endolymphatic duct in the guinea pig. Already after 27 hours, some collapse of the intercellular spaces apparently had occurred. In all control ears, these spaces presented the normal dilated appearance.

After 81 hours, the electron-dense substance could be localized as free particles in the periductal connective tissue (FIGURE 3). At this time, precipitate had accumulated around the periductal capillaries. A dark zone of precipitate often interdigitated the endothelial cells, as well as the pericyte and the endothelial cell (FIGURE 4). The interendothelial space was filled with electron-dense material to the level of the tight junctional elements and not infrequently beyond. Abluminal micropinocytotic vesicles of the capillaries were filled with precipitate, presumably indicating transcellular transport.

No precipitate was found between epithelial cells at the intermediate portion of the endolymphatic sac. Both epithelial cells and freely floating cells in the sac frequently displayed intracytoplasmic aggregates of precipitate (FIGURE 5). In the perisaccular tissue, no free deposits—only cellular—were observed.

No precipitate could be perceived in the utricle, common crus, or utricular duct. The basal coil of the cochlea was also sectioned near the place of injection. Apart from intrajunctional precipitate between a few cells of Reissner's membrane, no deposits could be seen in the epithelium or sensory region of the scala media. In the saccular membrane of the nonsensory region, precipitate appeared to have passed the epithelium at some points, as it could be observed locally in the subepithelial connective tissue. Some of these deposits seemingly

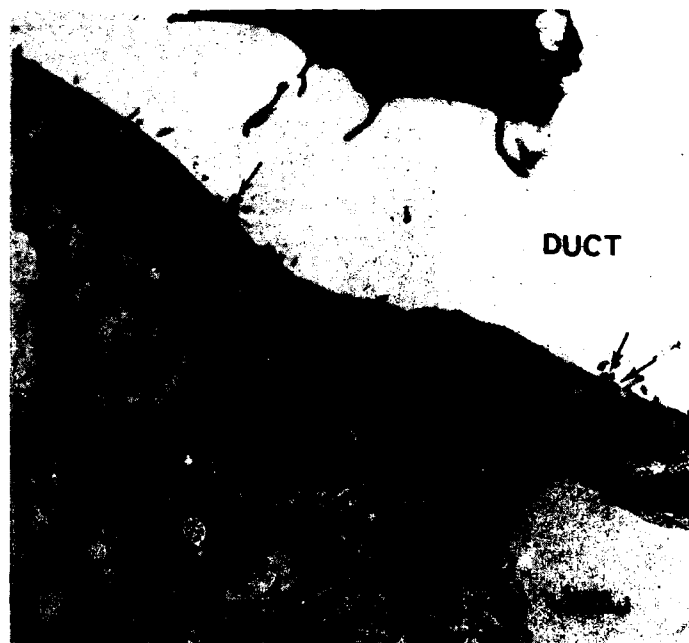


FIGURE 3. The same region as in FIGURE 2 41 hours after La^{3+} injection. Note precipitate also at the subepithelial region. Luminal cell is a macrophage.

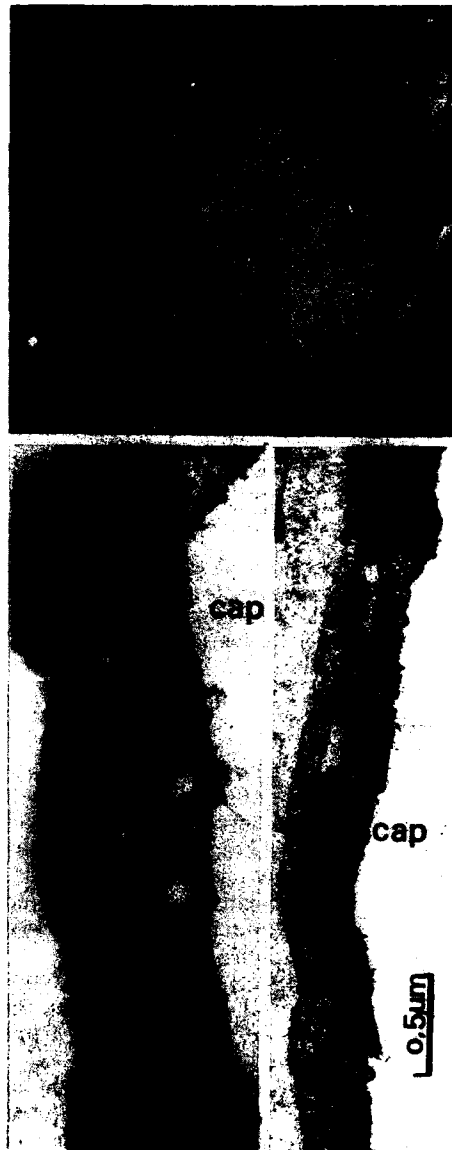


FIGURE 4. A periductal capillary (cap) close to the bony aqueduct 84 hours after La^{3+} injection. There is a dark zone of precipitate around the abluminal surface of the vessel (top). Higher magnification demonstrates precipitate between the endothelial cells and in a small pinocytotic vesicle. Note also a fine layer of dark precipitate on the luminal surface (bottom left) as well as an intercellular deposit (bottom right).

crossed the epithelium through pinocytosis, for the basal region of the epithelial cells presented pinocytotic vesicles containing characteristic electron-dense material. Moreover, the basement membrane of the epithelium here appeared more compact, possibly indicating a certain binding of the material to this structure. It should be pointed out that all areas of the membranous labyrinth have not yet been evaluated systematically and in detail.

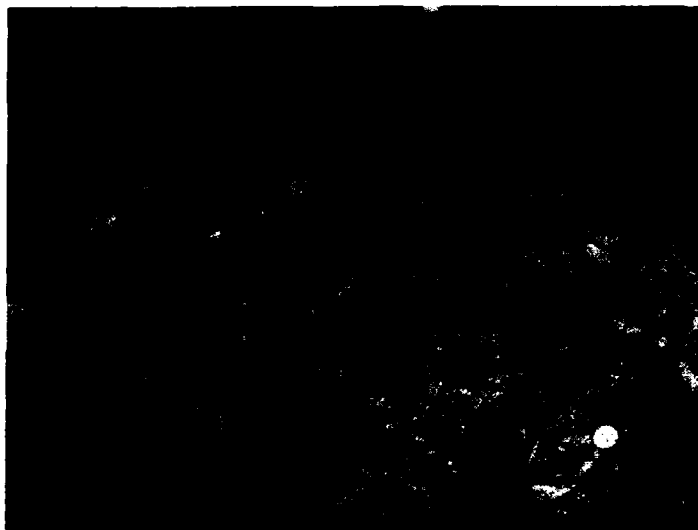


FIGURE 5. Apical cytoplasm of epithelial cells in the endolymphatic sac 106 hours after La^{3+} injection (intermediate portion). No intercellular deposits are visible, but the epithelial cells demonstrate intracellular membrane-bound structures filled with concentrated material, apparently lanthanum (arrows).

DISCUSSION

In many transporting epithelia, it has recently become apparent that the permeability that influences the movement of ions and water is largely dependent on the structural characteristics of the zonulae occludentes (or tight junctions) that seal adjacent cells. Epithelia with less developed tight junctional regions often show a higher permeability for water and ions (so-called leaky epithelia) than do epithelia with tighter junctions.^{11,12} According to Diamond and Frömter, the tight junctions may provide the main route for passive ion permeation in some epithelia.¹³

Lanthanum (La^{3+}) has been used elsewhere in the body and proved to penetrate intercellular junctions of epithelia that by physiological criteria are demonstrably "leaky," whereas those junctions of epithelia that seem "tight" remain impervious.¹⁴⁻¹⁸

Morphological studies of the epithelium of the endolymphatic duct in the guinea pig reveal a few intercellular junctional strands, suggestive of a "leaky" epithelium.⁸ However, in the endolymphatic sac, the number of junctional strands increases distally, indicating a more pronounced tightness.¹⁹

The early findings of lanthanum in the junctional complex and later in the subepithelial space of the endolymphatic duct corroborate that this epithelium is leaky.

The unexpected finding that no lanthanum appeared between cells in the endolymphatic sac may indicate greater resistance to fluid diffusion across this epithelium than in the duct.

Several tracer studies have been performed in order to study the endolymph circulation in the labyrinth, with special reference to the endolymphatic

sac.^{1,2,4-6,20,21} The tracers used (potassium ferrocyanide, ferritin, colloidal silver, trypan blue, horseradish-peroxidase) are fairly large molecules or particles, and in general the quantity injected was considerable. Rudert used ferritin and was able to trace it in the lumen of the endolymphatic sac but could not find it beyond the level of intercellular junctions.⁶ In the present study, we chose lanthanum—a small ion little larger than the sodium ion—as a tracer that had proved in several investigations to pass the level of intercellular tight junctions in a number of epithelial membranes. The volume injected in the present study was 1 μ l, which is a fraction of the total volume of the endolymphatic space. It is probable that the injection creates a certain increase in endolymphatic pressure, for which reason we protracted the injection for 10 minutes.

In future experiments, we hope to execute simultaneous measurements of the endolymphatic pressure in order to control the injection rate. A major disadvantage with lanthanum as a tracer consists of its ability to displace Ca^{2+} from its binding sites on the cellular membrane. Such a displacement may in turn lead to changes in the permeability of the membranes and the tight junctions. It is possible that lanthanum causes leakage of tight junctions via chemical interaction with the cellular membrane. This must be borne in mind when drawing conclusions on the permeability of membranes. However, Tisher and Yarger conclude that lanthanum permeability of the tight junctions in the distal and convoluted tubuli of the kidney provides morphological evidence for the existence of a paracellular shunt pathway for ion and water movement.¹⁷

Judging by morphological observations and lanthanum experiments, we suggest a model for the resorption of endolymph in guinea pigs. We hereby consider the endolymphatic duct to be involved in transepithelial transport of water and solvents, while the sac is thought to be occupied chiefly in a cellular breakdown of high molecular and particulate substances (FIGURE 6).

The concentration of K^+ in the endolymph of the cochlea and vestibule is stated at about 140 mmol/l. On the other hand, the measured concentration of K^+ in the saccus lumen of the guinea pig is about 16 mmol/l.²² The reverse situation prevails in these spaces considering the Na^+ concentration, namely, a low Na^+ concentration in the endolymph of the cochlea (2-4 mmol/l), whereas the

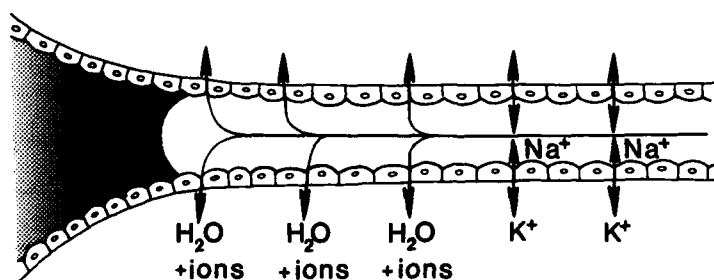


FIGURE 6. Schematic drawing demonstrating the proposed function of the endolymphatic duct in the guinea pig. Endolymph entering the duct (right) has a high content of potassium and a low content of sodium. Due to the leaky character of the epithelium, potassium and sodium are equilibrated with the ion content of the periductal extracellular tissue fluid. The surrounding lymphatics and veins create suitable conditions for reabsorption of water and ions into the vascular system. Hence, endolymph reaching the sac is extracellularlike with regard to sodium and potassium content. It is mainly composed of high molecular and particulate substances, which are phagocytosed by intrasaccular and epithelial cells.

concentration in the sac is about 150 mmol/l.²³ This shift of electrolytes is thought to occur across the epithelial sac.

The "leaky" character of the ductal epithelium would not seem to be able to resist the passive diffusion of electrolytes, as the tight junctions are shallow. Furthermore, a wide zone of loose "waterlike" subepithelial tissue surrounds the duct, and the arrangement of lymph and blood capillaries apparently anastomoses with the vein of the vestibular adqueeduct. Finally, injected lanthanum showed selective permeability of the duct but not of the epithelial sac.

We therefore consider the endolymphatic duct (and possibly the proximal sac) to be an important region for the reabsorption of water and ions and consequently also essential for the regulation of inner ear fluid homeostasis.

ACKNOWLEDGMENT

For technical help and valuable scientific discussions, the authors wish to thank Dr. Erik Persson, Department of Physiology, BMC-Center, University of Uppsala, Sweden.

REFERENCES

1. GUILD, S. R. 1927. The circulation of endolymph. *Am. J. Anat.* **39**: 57.
2. LUNDQUIST, P. G. 1965. The endolymphatic duct and sac in the guinea pig. An electron microscopic and experimental investigation. *Acta Otolaryngol. (Stockh.) Suppl.* **201**.
3. KIMURA, R. S. & H. F. SCHUKNECHT. 1965. Membranous hydrops in the inner ear of the guinea pig after obliteration of the endolymphatic sac. *Pract. Oto-Rhino-Laryngol.* **27**: 343.
4. ISHII, T., H. SILVERSTEIN & K. BALOGH, JR. 1966. Metabolic activities of the endolymphatic sac. An enzyme histochemical and autoradiographic study. *Acta Otolaryngol.* **62**: 61.
5. RUDERT, H. 1969. Experimentelle Untersuchungen zur Resorption der Endolympe im Innenohr des Meerschweinchen. I Mitteilung: Lichtmikroskopische Untersuchungen nach Injektion von Trypanblau in den Ductus cochlearis. *Arch. Klin. Exp. Ohren Nasen Kehlkopfheilkd.* **193**: 138.
6. RUDERT, H. 1969. Experimentelle Untersuchungen zur Resorption der Endolympe im Innenohr des Meerschweinchen. III Mitteilung: Elektronmikroskopische Untersuchungen zur Feinstruktur des Saccus endolymphaticus sowie zur Speicherung von Ferritin im häutigen Labyrinth. *Arch. Klin. Exp. Ohren Nasen Kehlkopfheilkd.* **193**: 201.
7. KIMURA, R. S., H. F. SCHUKNECHT, C. Y. OTA & D. D. JONES. 1980. Obliteration of the reunion duct. *Acta Otolaryngol.* **89**: 295.
8. RASK-ANDERSEN, H., G. BREDBERG & J. STAHL. 1980. Structure and function of the endolymphatic duct. In *International Symposium on Pathogenesis, Diagnosis and Treatment of Meniere's Disease*, Düsseldorf. George Thieme Verlag. Stuttgart, Federal Republic of Germany. (In press).
9. EVANS, E. F. 1979. Neuroleptanesthesia for the guinea pig. *Arch. Otolaryngol.* **105**: 185.
10. JOHNSTONE, B. M. & P. M. SELICK. 1972. The peripheral auditory apparatus. *Q. Rev. Biophys.* **5**: 1.
11. FRIEND, D. & N. GILULA. 1972. Variations in tight and gap junctions in mammalian tissues. *J. Cell Biol.* **53**: 758.
12. CLAUDE, P. & D. A. GOODENOUGH. 1973. Fracture faces of zonulae occludentes from "tight" and "leaky" epithelia. *J. Cell Biol.* **58**: 390.
13. FRÖMTER, E. & J. M. DIAMOND. 1972. Route of passive ion permeation in epithelia. *Nature London New Biol.* **235**: 9.

14. WHITTEMBURY, G. & F. A. RAWLINS. 1971. Evidence of a paracellular pathway for ion flow in the kidney proximal tubule: electron microscopic demonstration of lanthanum precipitate in the tight junction. *Pfluegers Arch.* **330**: 302.
15. MARTINEZ-PALOMO, Q., D. ERLIZ & H. BROCHO. 1971. Localization of permeability barriers in the frog skin epithelium. *J. Cell Biol.* **50**: 277.
16. MACHEN, T., D. ERLIZ & F. WOODING. 1972. Permeable junctional complexes. The movement of lanthanum across rabbit gallbladder and intestine. *J. Cell Biol.* **54**: 302.
17. TISCHER, C. & W. YARGER. 1973. Lanthanum permeability of the tight junction (zonula occludens) in the renal tubule of the rat. *Kidney Int.* **3**: 238.
18. WEIHE, E., W. HARTSCHUH, J. METZ & U. BRÜHL. 1977. The use of ionic lanthanum as a diffusion tracer and as a marker of calcium binding sites. *Cell Tissue Res.* **178**: 285.
19. BAGGER-SJÖBÄCK, D., H. RASK-ANDERSEN & P. G. LUNDQUIST. 1980. Intercellular junctions in the epithelium of the endolymphatic sac. In *International Symposium on Pathogenesis, Diagnosis and Treatment of Meniere's Disease*, Düsseldorf. George Thieme Verlag. Stuttgart, Federal Republic of Germany. (In press.)
20. ANDERSEN, H. C. 1948. Passage of trypan blue into the endolymphatic system of the labyrinth. *Acta Otolaryngol.* **36**: 273.
21. ADLINGTON, P. 1967. The ultrastructure and functions of the saccus endolymphaticus and its decompression in Meniere's disease. *J. Laryngol. Otol.* **81**: 759.
22. MIYAMOTO, H. & C. MORGENSTERN. 1979. Potassium level in the endolymphatic sac of guinea pigs in vivo. *Arch. Oto-Rhino-Laryngol.* **222**: 77.
23. SILVERSTEIN, H. 1966. Biochemical and physiological studies of the endolymphatic sac in the cat. *The Laryngoscope* **76**: 498.

EYE-MUSCLE GEOMETRY AND COMPENSATORY EYE MOVEMENTS IN LATERAL-EYED AND FRONTAL-EYED ANIMALS*

John I. Simpson and Werner Graf

*Department of Physiology and Biophysics
New York University School of Medicine
New York, New York 10016*

INTRODUCTION

Our question here has a long history and arises from the following type of observation: when a rabbit is oscillated about the naso-occipital (roll) axis, the compensatory eye movements are vertical, but when a human is oscillated about the same axis, the compensatory eye movements are torsional. What is the basis of such differences in compensatory eye movements among vertebrates with differing interocular angles? While the existence of these appropriate behavioral differences is commonly known, the origin of these differences is, currently, commonly unknown, as a search of the contemporary literature attests.^{7,15,37,43,51} This is regrettable, subsequent to arriving at our answer to the question posed above, we found that Ohm, in a rarely referenced 1919 paper, had arrived at the same answer.²⁰ The results reported here confirm and extend Ohm's lucid and accurate study, which had been "lost" to modern investigators of the vestibulo-ocular reflexes.

To answer the question of what underlies the differences in compensatory eye movements among animals with different interocular angles, one must consider the physiological relations between the vestibular labyrinth and the extraocular muscles and also the peripheral anatomy of the labyrinth and of the extraocular muscles. Högyes was the first to delve into these matters; he deduced a specific set of primary relations and pathways between the labyrinth of one side and the ipsilateral and contralateral eye muscles.²² Indeed, he came quite close to determining the actual arrangement, clarified much later by Szentágothai.⁴⁴⁻⁴⁶ In the course of his studies, Högyes also recognized the different requirements for appropriate compensatory eye movements in lateral- and frontal-eyed animals, but he did not clearly resolve the question of how the requirements are met. (Högyes' achievements in vestibular research were fully appreciated only after his main publication, originally published in Hungarian in the 1880s, appeared in German translation in 1912.)²³ Bárány accurately observed the eye movements elicited in rabbit by natural vestibular stimuli.³ However, he claimed that the actions of rabbit and human extraocular muscles were identical, and thus his description of the relations of individual vertical semicircular canals to specific eye muscles was erroneous. Why Bárány believed the actions of rabbit and human extraocular muscles to be identical is mysterious because the anatomical information about the periphery necessary to arrive at the contrary conclusion was available from his associate Rothfeld and also from Wessely.^{39,49} Bárány's viewpoint was contradicted by Ohm, who demonstrated anatomically

*Supported in part by U.S. Public Health Service Grant No. NS-13742, Deutsche Forschungsgemeinschaft Grant No. Gr-688/1, and the Irma T. Hirsch Trust.

that eye movements elicited by a given vertical extraocular muscle are different in man and rabbit.³⁵ Furthermore, Ohm was the first to conclude that the different compensatory eye movements in frontal- and lateral-eyed animals are due to differences in extraocular muscle anatomy and the resulting differences in the kinematic characteristics.

In the same year that Ohm published his work, Schilling also addressed the matter of different compensatory eye movements in animals with different orientations of the optic axis, but in his discussion of the problem, he favored the idea of a change in central neuronal connectivity, assuming that the anatomical arrangements of the extraocular muscles were similar in all species.⁴¹ In his monograph, Magnus also addressed the question of differences in compensatory eye movements in lateral- and frontal-eyed animals.³³ He proposed that during a head movement around the bitemporal axis in rabbit, only the oblique muscles are active, whereas in monkey, only the vertical recti are active. On the basis of his interpretation, he claimed that there were differences in central neural connectivity. In so doing, Magnus neglected the concept that a single muscle can produce both vertical and rotatory movements, as previously demonstrated for man by Hering and Helmholtz among others.^{19,18}

In his classical paper on the anatomical connections of the vestibulo-ocular reflexes, Szentágothai noted in frontal-eyed animals that the proportional contribution of the vertical recti and oblique muscles to producing vertical and rotatory (torsional) movement changes with the position of the eye in the orbit.⁴⁴ From this observation, he concluded that the different compensatory eye movements in animals with different positions of the optic axis in the head reflect mainly the differences in the pulling directions of identical muscles brought about by different positions of the eye in the head. But as we shall see below, the changes in pulling directions in animals with different interocular angles are also brought about by changes in the insertion points.

In summary, two types of explanations have been offered for the differences in compensatory eye movements in lateral- and frontal-eyed animals. Some investigators have proposed a change in central neuronal connectivity, with the muscular arrangements remaining constant; other investigators have proposed that the primary pattern of central connectivity of the vestibulo-ocular reflexes is preserved but that the extraocular muscles change their action. Knowing that the primary physiological relations between the vertical canals and individual extraocular muscles are the same in frontal- and lateral-eyed animals, but not knowing the work of Ohm, we set out to clarify the situation by determining the orientations of the vertical semicircular canals and the insertions and lines of action of the oblique and vertical recti muscles in different species with differing interocular angles.^{2,9-12,16,20,21,26,28,29,42,46}

METHODS

The species used experimentally in the study were pigmented and albino rabbits, albino guinea pigs, and pigmented cats. The orientations of the vertical extraocular muscles with respect to the midline were obtained in live anesthetized or dead fixed and nonfixed specimens by direct measurements *in situ* or from photographs. Measurements were referenced to the primary position of the eye using the optic axis data of Prince et al. and Hughes.^{36,25} Data on the orientation of extraocular muscles in man are readily available in the literature.^{1,18,34} Since data on the orientation of the semicircular canals in man, cat, and

guinea pig are available in the recent literature, we measured the orientation of the vertical semicircular canals only in rabbit.^{5,6,13,14} This was done by aligning a straightedge with the exposed dorsal half of the circumference of the anterior or posterior canal viewed from above and measuring the angle of the straightedge with the mid-sagittal plane. The actions of the superior extraocular muscles in rabbit were determined by photographing crossed threads placed on the cornea while a single muscle was electrically stimulated near its origin in the orbit or, in the case of the superior oblique, also activated by stimulation of the trochlear nerve at its exit from the brain stem. The initial position used in determining the actions of the superior muscles in rabbit was within five degrees of the primary position as described by Hughes.²⁴

RESULTS

Across the species investigated, the lines of action (the pulling directions) of the superior oblique and superior rectus muscles change relative to the optic axis such that the ipsilateral vertical canal to which each muscle is most nearly parallel remains the same (FIGURE 1). That canal is the one that provides the primary excitatory input to the respective muscle.^{2,9,10,16,20,21,26,28,29,42,44,45,46,48} In this paper, we will give a detailed description of the situation only in man and rabbit, representing the extreme examples of frontal- and lateral-eyed animals. Our data on the anatomical arrangements for the labyrinth and the eye muscles of rabbit agree well with those presented previously by Rothfeld and others.^{30,32,33,35,39} Several previous investigators have suggested that the vertical extraocular muscles are aligned with one or the other of the vertical canals.^{31,35,39,40} In fact, such an arrangement is not present, and is only more or less approximated depending on the species.⁸ In addition, the anterior and posterior canals of one side are not at the same angle to the midline, but the average of the two angles is close to 45 degrees.

From FIGURES 1 and 2 it is clear that the insertion points of the superior muscles on the globe are markedly different in rabbit and man. These differences have important consequences for the actions of the vertical extraocular muscles (FIGURE 3) and for understanding the organization of the vestibulo-ocular reflexes in all vertebrate species. From the primary position of the eye, contraction of the superior rectus in man causes elevation, which is commonly regarded as the primary action of this muscle, and also causes intorsion and adduction (the so-called secondary actions). Contraction of the superior oblique in man causes intorsion (the so-called primary action) and also depression and abduction (the secondary actions). (While the action of a single muscle can be described most simply by referring to its own rotational axis, we are following here the conventional practice of describing the actions of extraocular eye muscles in terms of vertical, horizontal, and torsional components.) Comparison of the extraocular muscle actions in man and rabbit reveals that the so-called primary actions remain the same (elevation for the superior rectus and intorsion for the superior oblique), but due to the different insertion points and lines of action of these muscles in rabbit as compared to man, the secondary actions about the primary position are considerably different. In rabbit, the secondary actions of the superior rectus are extorsion and abduction, and for the superior oblique, they are elevation and adduction. Evidence for differences in superior oblique action between man and rabbit can be found as early as 1823 in the experiments

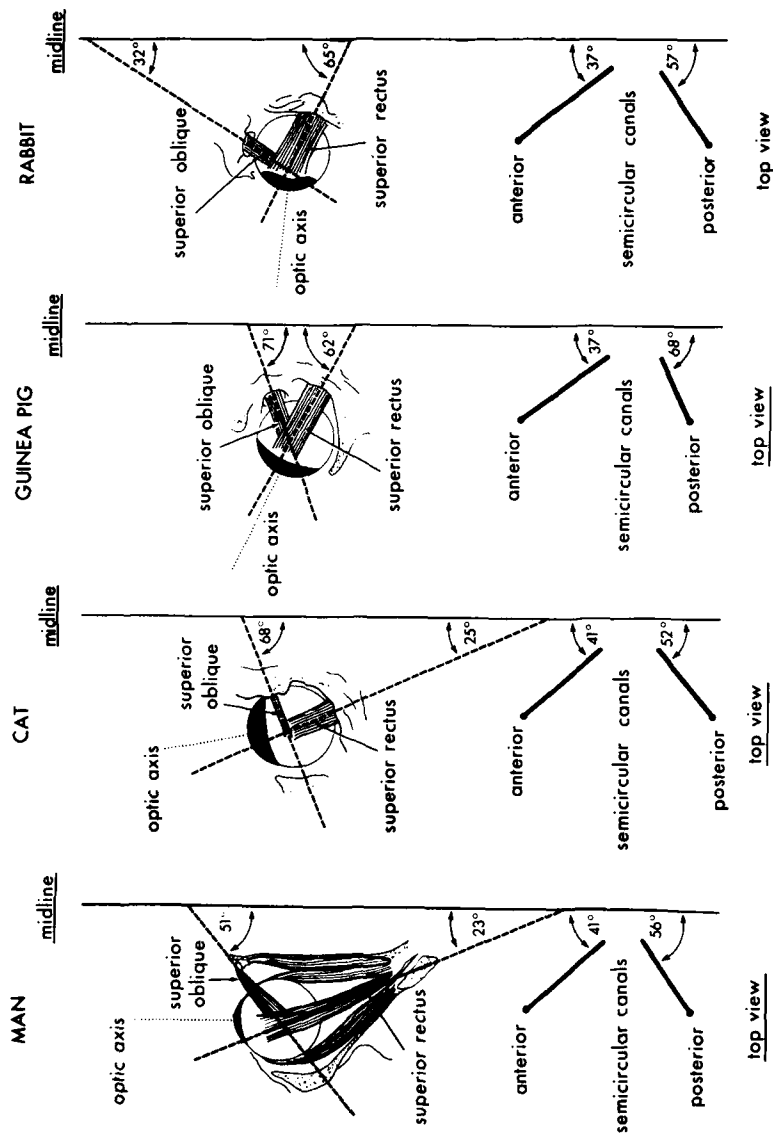


FIGURE 1. Spatial relations between the vertical semicircular canals, the optic axis, and the extraocular muscles in man, cat, guinea pig, and rabbit. In all four species, the lines of action of the superior rectus muscle and of the superior oblique muscle remain most nearly parallel to the ipsilateral semicircular canal that provides the respective primary excitatory input. A similar arrangement applies for the inferior vertical eye muscles.

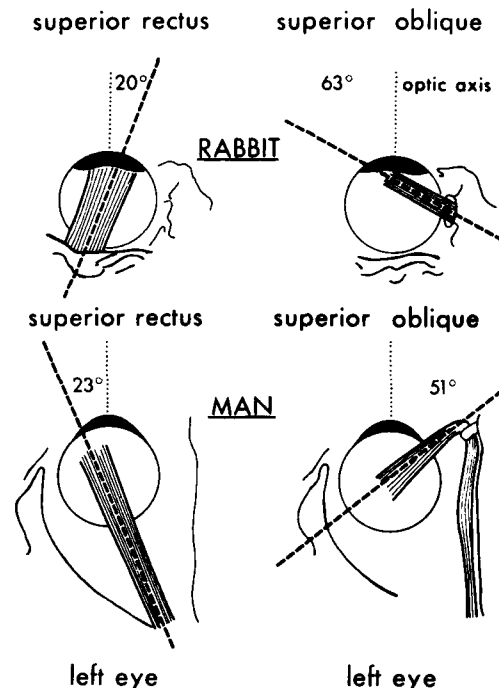


FIGURE 2. Locations of the insertion points and orientations of the lines of action of the superior vertical extraocular muscles in man and rabbit. Insertion points and lines of action of corresponding muscles in the two species have changed relative to the optic axis so that the secondary actions effect movements in opposite directions (e.g., elevation and adduction for the rabbit superior oblique; depression and abduction for the human superior oblique). The primary actions remain the same. (See also the table in FIGURE 4.)

of Bell, but since he believed that the action of this muscle was the same in rabbit and man, he offered a different interpretation of his observations.⁴

A complete synopsis of extraocular muscle actions in man and rabbit is given in FIGURE 4, which is in part a modified Hering-diagram. The different secondary actions of the vertical muscles in lateral- and frontal-eyed animals are appropriate for compensatory eye movements, as can be readily appreciated by considering rotations about the principal axes of the vertical semicircular canals. The different kinematic characteristics of the individual muscles are due to changes in insertion and line of action, as illustrated in FIGURE 2 for the superior muscles. The difference in vertical movement of the optic axis elicited by the action of the superior oblique in rabbit and man is due to the insertion of this muscle, respectively, in front of and behind the equatorial plane. Insertion in front of the equator causes elevation in rabbit, and insertion behind the equator causes depression in man. In conjunction with a change of the insertion point, a change in the line of action projected onto the horizontal plane also occurs and is responsible for the abduction-adduction differences.

DISCUSSION

Using the example of head movement about the roll axis presented in the introduction, we can illustrate the functional consequences and thus the significance of the differences in secondary actions of the vertical eye muscles of rabbit and man. In both man and rabbit, when the firing frequency of the ipsilateral (with respect to downside tilt) vertical semicircular canal nerves increases (FIGURE 5), contraction of the superior rectus and superior oblique will occur on the ipsilateral side. In man, the intorsional component of the actions of these muscles is synergistic, but the other kinematic components are antagonistic. For the contralateral eye, the extorsional components of the inferior rectus and inferior oblique cooperate in man; the other components are antagonistic. For the rabbit, a similar scenario can be run through. The fundamental difference in the case of the rabbit is that the elevation component is synergistic for the ipsilateral eye and the depression component is synergistic for the contralateral eye, resulting in the required vertical compensatory eye movements. Thus, in both species, the collective actions are appropriate for producing the different required compensatory eye movements. An analogous situation holds for pitch

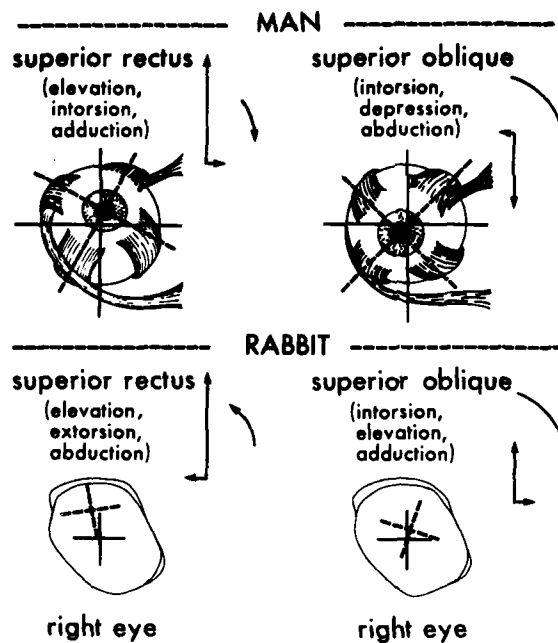


FIGURE 3. Actions of the superior vertical extraocular muscles in man and rabbit. Solid lines indicate the initial position of the eye, and dashed lines indicate the position of the eye after a contraction of the superior oblique or the superior rectus. Kinematic actions of single muscles are given in parenthesis. The first of these is the so-called primary action, the others are the so-called secondary actions. The different components of a muscular action also are depicted graphically. (Upper part of figure modified from Moses.)²⁴

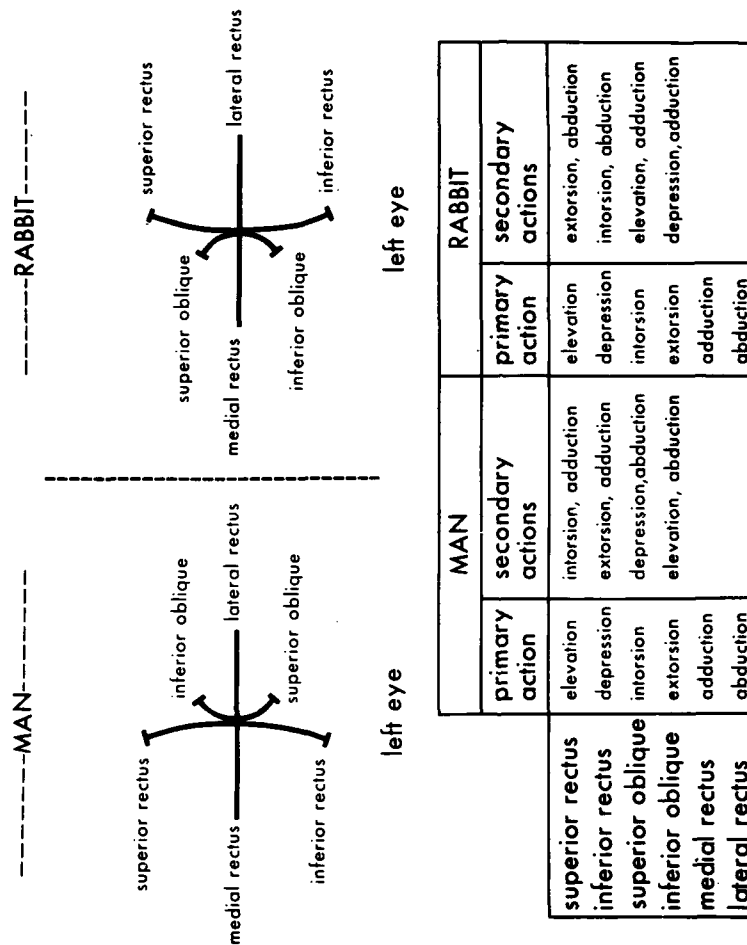


FIGURE 4. Comparison of the actions of individual extraocular muscles in man and rabbit. In the upper half of the figure, the extraocular muscle actions in man and rabbit are presented in the form of a Hering-diagram. The lines indicate the approximate relative magnitudes of the vertical, horizontal, and torsional actions of the individual muscles. The table in the lower half of the figure is a synopsis of the kinematic components and emphasizes the distinctions between what are commonly considered to be primary and secondary actions of a given muscle.

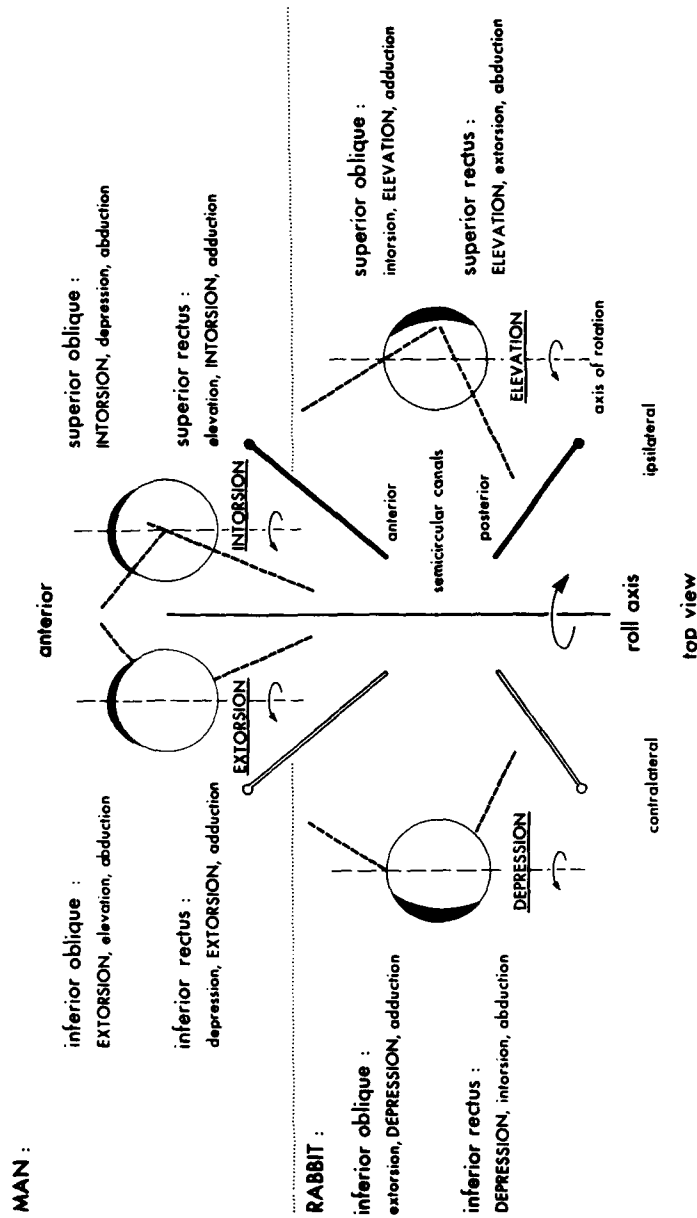


FIGURE 5. Combined muscular actions appropriate for compensatory eye movements for head tilt (right-side down) about the roll axis. During this head tilt, discharge of the anterior and posterior semicircular canal nerves on the right (ipsilateral) side increases (indicated by the filled canal symbols). In both species, increase in firing frequency of the ipsilateral anterior ampullary nerve effects activation of the ipsilateral superior rectus and the contralateral inferior oblique; excitation of the ipsilateral posterior ampullary nerve effects contraction of the ipsilateral superior oblique and the contralateral inferior rectus. These muscles are indicated by the thick dashed lines next to the eye upon which they act. Thin dashed lines indicate the axis of rotation for the compensatory eye movements. Although the compensatory eye movements are different for man and rabbit, they are effected by the same muscles connected to the same semicircular canals. This is possible because of the species differences in synergistic and antagonistic kinematic characteristics. The synergistic components are given in capital letters, while components that are in the appropriate direction to cancel each other are given in small letters.

movements of the head about the bitemporal axis when either both anterior or both posterior vertical canals are excited. Thus, the preservation of the primary relations of the three-neuron arcs of the vestibulo-ocular reflexes can be achieved by the changes in muscular organization described here. Neither rotating the entire contents of the orbit, as present in the rabbit, to the front, nor rotating just the eyeball to the front while maintaining the insertions of the muscles on the eyeball would be successful. In either case, fundamental changes in central neural connectivity would be necessary. While detailed knowledge of the relations of particular parts of the utricle and saccule to specific extraocular muscles is not available, the results of studies of frontal-eyed animals suggest that the species differences in the secondary actions of vertical eye muscles are in line with preservation of the utriculo-ocular relations found in frontal-eyed animals.^{17,43,47}

For the conceptual issue of this paper, it has not been necessary to consider other than the primary vestibulo-ocular relations, but species differences in secondary vestibulo-ocular relations may indeed exist, as already pointed out by Szentágothai.⁴⁴ Participation of all extraocular muscles during any eye movement has been demonstrated and given various interpretations.^{32,50} At least one reason for the presence of secondary vestibulo-ocular relations is apparent from comparing the geometry of the orbit and the labyrinth. Neither the vertical recti nor the obliques acting alone will produce compensatory eye movements in the planes of the vertical canals. Therefore, if stimulation of a single canal produces eye movement in the plane of that canal, activation of eye muscles in addition to that one enjoying a primary relation with the stimulated canal must occur. Presently available information on the secondary vestibulo-ocular relations in animals with different interocular angles suggests that there are species differences, but the issue is not fully resolved.^{10,26,27,29,48} The matter of secondary vestibulo-ocular relations may be addressed by using intracellular recording and staining techniques. In addition, the nonprimary connections may be predicted by first determining the coordinates of the insertions and origins of the eye muscles and of the center of rotation in different species and then using computer modeling³⁶ to determine which muscles must be activated to meet the kinematic requirements for compensatory eye movements for head movements about particular axes.

Much of the confusion about the nature of the differences in compensatory eye movements among animals with different optic axis orientations resulted from neglecting the exact arrangement of the extraocular muscles or from oversimplifying the kinematic characteristics of the extraocular muscles by considering only the so-called primary action of a given muscle. Examination of the geometry of the extraocular muscles in frontal- and lateral-eyed animals shows that there is no need for a qualitative difference in the primary vestibulo-ocular relations. The requirements for producing the different appropriate compensatory eye movements are basically fulfilled in the orbit by the changes of the insertions and lines of action of the vertical extraocular muscles, resulting in different secondary kinematic actions.

REFERENCES

1. ALPERN, M. 1969. Anatomical aspects. In *The Eye*. H. Davson, Ed. 3: 29-62. Academic Press, Inc. New York, N.Y.

2. BAKER, R., W. PRECHT & A. BERTHOZ. 1973. Synaptic connections to trochlear motoneurons determined by individual vestibular nerve branch stimulation in the cat. *Brain Res.* **64**: 402-406.
3. BÁRÁNY, R. 1917. Theoretisches zur Funktion der Bogengänge und speciell des Flocculus beim Kaninchen. *Nord. Tidskr. Oto-Rhino-Laryngol.* **2**(4): 458-507.
4. BELL, C. 1823. On the motions of the eye in illustration of the uses of the muscles and nerves of the orbit. *Philos. Trans R. Soc. London (Part 1)*: 166-186.
5. BLANKS, R. H. I., I. S. CURTHOYS & C. H. MARKHAM. 1972. Planar relationships of semicircular canals in the cat. *Am. J. Physiol.* **223**: 55-62.
6. BLANKS, R. H. I., I. S. CURTHOYS & C. H. MARKHAM. 1975. Planar relationships of the semicircular canals in man. *Acta Otolaryngol.* **80**: 185-196.
7. CARPENTER, R. H. S. 1972. *Movements of the Eyes*. Pion Limited, London, England.
8. COGAN, D. G. 1956. *Neurology of the Ocular Muscles*. Charles C. Thomas, Publishers, Springfield, Ill.
9. COHEN, B. & J.-I. SUZUKI. 1963. Eye movements induced by ampullary nerve stimulation. *Am. J. Physiol.* **204**: 347-351.
10. COHEN, B., J.-I. SUZUKI & M. B. BENDER. 1964. Eye movements from semicircular canal nerve stimulation in the cat. *Ann. Otol. Rhinol. Laryngol.* **73**: 153-169.
11. COHEN, B., K. TOKUMASU & K. GOTO. 1966. Semicircular canal nerve, eye and head movements: the effect of changes in initial eye and head position on the plane of the induced movement. *Arch. Ophthalmol.* **76**: 523-531.
12. COHEN, B. 1974. The vestibulo-ocular reflex arc. In *Handbook of Sensory Physiology*. H. H. Kornhuber, Ed. **6/1**: 477-450. Springer-Verlag, Berlin, Heidelberg & New York.
13. CURTHOYS, I. S., R. H. I. BLANKS & C. H. MARKHAM. 1975. The orientation of the semicircular canals in the guinea pig. *Acta Otolaryngol.* **80**: 197-205.
14. CURTHOYS, I. S., R. H. I. BLANKS & C. H. MARKHAM. 1977. Semicircular canal functional anatomy in cat, guinea pig and man. *Acta Otolaryngol.* **83**: 258-266.
15. DUKE-ELDER, S. & K. WYBAR. Ocular motility and strabismus. In *System of Ophthalmology*. S. Duke-Elder, Ed. **6**: 79-85. Kimpton, London, England.
16. FLUUR, E. 1959. Influences of semicircular ducts on extraocular muscles. *Acta Otolaryngol. Suppl.* **149**: 1-46.
17. FLUUR, E. & A. MELLSTRÖM. 1971. The otolith organs and their influence on oculomotor movements. *Exp. Neurol.* **30**: 139-147.
18. HELMHOLTZ, H. V. 1896. *Handbuch der physiologischen Optik*. Zweite Auflage, Voss, Hamburg & Leipzig.
19. HERING, E. 1879. Der Raumsinn und die Bewegungen des Auges. In *Handbuch der Physiologie*. L. Herman, Ed. **3/1**: 512-519. F. C. W. Vogel, Leipzig, Saxony.
20. HIGHSTEIN, S. M. 1971. Organization of the inhibitory and excitatory vestibulo-ocular reflex pathways to the third and fourth nuclei in rabbit. *Brain Res.* **32**: 218-224.
21. HIGHSTEIN, S. M. 1973. The organization of the vestibulo-oculomotor and trochlear reflex pathways in the rabbit. *Exp. Brain Res.* **17**: 285-300.
22. HÖGYES, E. 1880, 1881, 1884. Az associált szemmozgások idegmechanismusáról. *Értekezések a természettudományok köréből.* **10**(18): 1-62; **11**(1): 1-100; **14**(9): 1-84.
23. HÖGYES, A. 1912. Über den Nervenmechanismus der assoziierten Augenbewegungen. *Monatsschr. Ohrenheilkd. Laryngo-Rhinol.* **46**: 685-740, 809-841, 1027-1083, 1353-1413, 1554-1571.
24. HUGHES, A. 1971. Topographical relationships between anatomy and physiology of the rabbit visual system. *Doc. Ophthalmol.* **30**: 33-159.
25. HUGHES, A. 1977. The topography of vision in mammals of contrasting life style: comparative optics and retinal organization. In *Handbook of Sensory Physiology*. F. Crescitelli, Ed. **7/5**: 613-753. Springer-Verlag, Berlin, Heidelberg & New York.
26. ITO, M., N. NISIMARU & M. YAMAMOTO. 1973. The neural pathways mediating reflex contraction of extraocular muscles during semicircular canal stimulation in rabbits. *Brain Res.* **55**: 183-188.
27. ITO, M., N. NISIMARU & M. YAMAMOTO. 1973. The neural pathways relaying reflex inhibition from semicircular canals to extraocular muscles of rabbits. *Brain Res.* **55**: 189-193.

28. ITO, M., N. NISIMARU & M. YAMAMOTO. 1976. Pathways for the vestibulo-ocular reflex excitation arising from semicircular canals of rabbits. *Exp. Brain Res.* **24**: 257-271.
29. KIM, J. H. 1974. Studies on the functional interrelation between the vestibular canals and the extraocular muscles. *Korean J. Physiol.* **8**(2): 87-103.
30. DE KLEIJN, A. & R. MAGNUS. 1920. Tonische Labyrinthreflexe auf die Augenmuskeln. *Pfluegers Arch.* **178**: 179-192.
31. LEMERE, H. R. 1918. Oculomotor reaction to labyrinth stimulation. *J. Am. Med. Assoc.* **71**: 901-903.
32. LORENTE DE NÓ, R. 1932. The regulation of eye positions and movements induced by the labyrinth. *The Laryngoscope* **42**: 233-332.
33. MAGNUS, R. 1924. *Körperstellung*. Springer-Verlag, Berlin, Germany.
34. MOSES, R. A. 1970. *Adler's Physiology of the Eye*. 5th edit. C. V. Mosby Co. St. Louis, Mo.
35. OHM, J. 1919. Über die Beziehungen der Augenmuskeln zu den Ampullen der Bogengänge beim Menschen und Kaninchen. *Klin. Monatsbl. Augenheilkd.* **62**: 289-315.
36. PRINCE, J. H., C. D. DIESEM, I. EGLITIS & G. L. RUSKELL. 1960. *Anatomy and Histology of the Eye and Orbit in Domestic Animals*. Charles C. Thomas, Publishers, Springfield, Ill.
37. ROBERTS, T. D. M. 1978. *Neurophysiology of Postural Mechanisms*. Butterworths, London, England.
38. ROBINSON, D. A. 1975. A quantitative analysis of extraocular muscle cooperation and squint. *Invest. Ophthalmol.* **14**: 801-825.
39. ROTHFELD, J. 1913. Die Physiologie des Bogengangapparates. *Verh. Ges. Dtsch. Naturforsch. Ärzte, 85. Versammlung*, **1**: 269-322.
40. ROTHFELD, J. 1914. Das "Oto-ophthalmotrop," ein Apparat zur Demonstration der vom Ohrlabyrinth ausgelösten kompensatorischen Augenbewegungen. *Berliner Klin. Wochenschr.* **51**: 256-258.
41. SCHILLING, R. 1919. Ein Beitrag zur Funktion des Vestibularapparates. *Arch. Ohren Nasen Kehlkopfheilkd.* **104**: 120-156.
42. SUZUKI, J., B. COHEN & M. B. BENDER. 1964. Compensatory eye movements induced by vertical semicircular canal stimulation. *Exp. Neurol.* **9**: 137-160.
43. SUZUKI, J.-I., K. TOKUMASU & K. GOTO. 1969. Eye movements from single utricular nerve stimulation in the cat. *Acta Otolaryngol.* **68**: 350-362.
44. SZENTÁGOTHAJ, J. 1943. Die zentrale Innervation der Augenbewegungen. *Arch. Psychiatr. Nervenkr.* **116**: 721-760.
45. SZENTÁGOTHAJ, J. 1950. The elementary vestibulo-ocular reflex arc. *J. Neurophysiol.* **13**: 395-407.
46. SZENTÁGOTHAJ, J. 1952. Die Rolle der einzelnen Labyrinthrezeptoren bei der Orientierung von Augen und Kopf im Raume. *Akadémiai Kiadó*, Budapest, Hungary.
47. SZENTÁGOTHAJ, J. 1964. Pathways and synaptic articulation patterns connecting vestibular receptors and oculomotor nuclei. In *The Oculomotor System*. M. B. Bender, Ed.: 205-223. Harper and Row Publishers, Inc. New York, N.Y.
48. UCHINO, Y., N. HIRAI & S. WATANABE. 1978. Vestibulo-ocular reflex from the posterior canal nerve to extraocular motoneurons in the cat. *Exp. Brain Res.* **32**: 377-388.
49. WESSELY, K. 1916. Über den Einfluss der Augenbewegungen auf den Augendruck. *Arch. Augenheilkd.* **81**: 102-119.
50. WESTHEIMER, G. & S. M. BLAIR. 1972. Concerning the supranuclear organization of eye movements. *Bibl. Ophthalmol.* **82**: 28-35.
51. WILSON, V. J. & G. MELVILL JONES. 1979. *Mammalian Vestibular Physiology*. Plenum Press, New York & London.

PHASIC COMPONENTS OF FROG SEMICIRCULAR CANAL

Yasuo Harada and Kenzo Hirata

Department of Otolaryngology
School of Medicine
Hiroshima University
Hiroshima, Japan

The bidirectional responses of vestibular nerve fibers as well as their resting activity, threshold, sensitivity, and adaptation to natural stimulation have been studied. Precht, Llinas, and Clarke divided frog vestibular nerve fibers into two types according to characteristics of their frequency response to natural stimulation of the horizontal canal.¹ The first type consisted of units having short time constants to acceleration and velocity step inputs; the second type consisted of units having long time constants. Of the afferent fibers, 65% showed adaptation in frequency to prolonged steps of acceleration, whereas the remaining 35% showed no frequency decrease during prolonged stimulation.

It is well known that the frog's vestibular nerve contains efferent fibers whose cell bodies are located in the brain stem and the cerebellum. The efferent fiber system probably serves as a feedback system to the labyrinth, which on the ipsilateral side, could be partly responsible for the adaptation in frequency of some of the afferent fibers. Hence, it seemed advisable to study an isolated preparation to find out whether the end organ of the semicircular canal shows significant adaptation.

In the present research, the isolated posterior semicircular canal of frogs was stimulated with a device that induced ampullofugal currents and a controlled cupula deflection, in order to analyze in detail the function of the semicircular canal.

MATERIALS AND METHODS

The experiments were carried out in posterior semicircular canals isolated from frogs (*Rana nigromaculata*) according to the procedure suggested by Harada.² The original method was refined in order to achieve more precise control over the fluid movements in the canal. The vertical posterior semicircular canal was isolated together with its ampulla and the distal stump of the ampullar nerve. The preparation was placed in a perspex chamber filled with Tyrode solution and fastened to a micropipette filled with Tyrode solution, which was tightly inserted into the open end of the canal (FIGURE 1). The ampullar receptor was mechanically stimulated by producing fluid pulses inside the canal using an earphone connected to the preparation via a micropipette. The vibrating membrane of a magnetic earphone with good insulation covered with a thin rubber was driven by the moving coil fed by a function generator. Displacements of the vibrating membrane were related linearly to the coil voltages. The action potentials in the ampullar branch of the vestibular nerve were recorded by means of a suction electrode with an Ag-AgCl electrode. The action potentials were amplified, fed to a rectifying bridge, and integrated. They were observed on

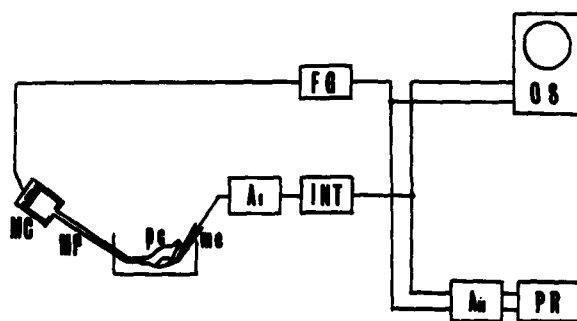


FIGURE 1. Schematic representation of the experimental setup: FG, function generator; MC, moving coil; MP, micropipette; pc, posterior semicircular canal; me, microelectrode; A_1 , amplifier; INT, integrator; A_2 , amplifier; OS, oscilloscope; PR, pen recorder.

a Braun tube oscilloscope and recorded on a pen recorder. The time constant of the integrator is 0.00265. Voltages applied to the moving coil were registered by a microammeter. Fluid flow displacement in the micropipette was measured with an ocular micrometer. Bubble displacements were related linearly to the coil voltage (FIGURE 2). Square pulses having several durations of 1 to 10 seconds and six different amplitudes were employed in the experiments. The corresponding fluid flow displacements in the micropipette were 8, 16, 32, 48, 64, and 80 μ .

RESULTS

In FIGURE 3, the original discharge of the ampullar nerve is compared with the integrated ampullar nerve activity under the same stimulus conditions. A resting discharge was maintained by low-voltage action potentials, i.e., about 50 μ V. At

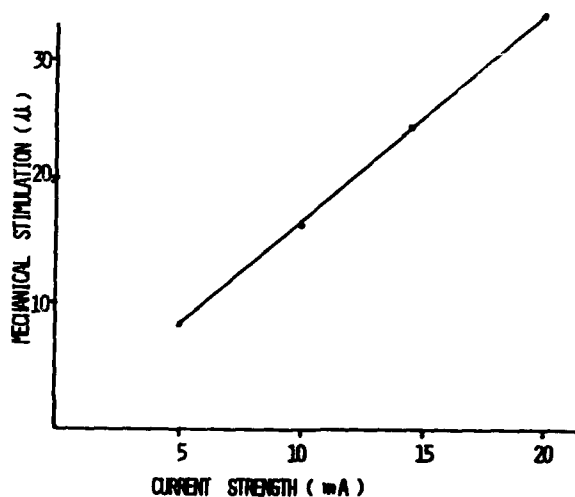


FIGURE 2. Relation between bubble displacement and coil voltage.

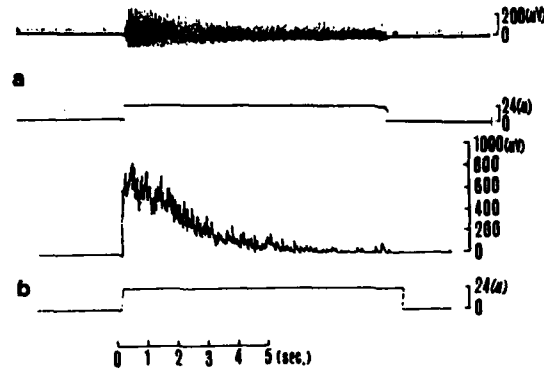


FIGURE 3. The response on ampullofugal stimulation of isolated posterior ampullar receptor. a, original discharge of the ampullar nerve; b, integrated ampullar nerve activity.

the onset of the stimulation, there was a sudden burst of action potentials of high amplitude, but these responses soon decreased. Low-amplitude action potentials lasted much longer. Although the integrated ampullar nerve activity reached the baseline (FIGURE 3), low-amplitude activity continued. This experiment shows that the integrated ampullar nerve activity reflected mainly high-amplitude action potentials.

Experiments were performed under four different stimulus conditions.

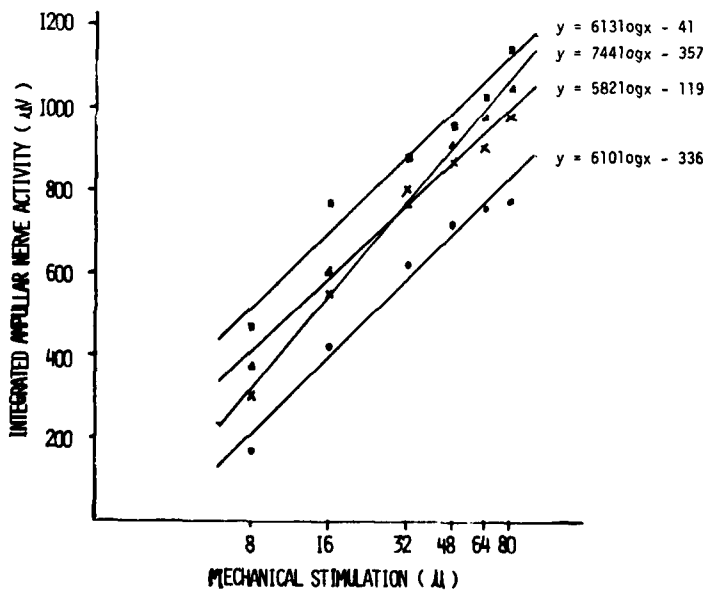


FIGURE 4. Relation between stimulus strength and maximum integration value of the ampullar nerve activity.

*Relation between Stimulus Strength and Maximum Integration Value of the
Ampullar Nerve Activity*

Four frogs were individually tested at six different rates of flow pulse (ranging from 8μ to 80μ) applied for periods of 1.5 seconds. The integrated ampullar nerve activity was recorded.

An example of this experiment is illustrated in FIGURE 4. Maximum values of the integrated ampullar nerve activity were plotted against stimulus strength on a logarithmic scale. Gradients of regression lines varied from 582 to 744; and the points where the regression line crossed the abscissa, the presumed threshold, varied from 1.2 to 4.6. Correlation coefficients ranged from 0.985 to 0.995. Maximum integration values, derived from units responsible for the action potentials of high amplitude, were proportional to the logarithm of the stimulus strength.

*Relation between Integrated Ampullar Nerve Activity and Displacement
Velocity of Mechanical Stimulation*

These experiments were performed with different gradients, but the same end voltage was applied to the moving coil. We considered the flow rate in the semicircular canal to be proportional to the gradients of the current applied to the moving coil. The tracings in FIGURE 5 illustrate the integrated ampullar nerve activity induced by a fluid flow pulse and by a $10.3\text{-}\mu/\text{second}$ fluid flow rate. In

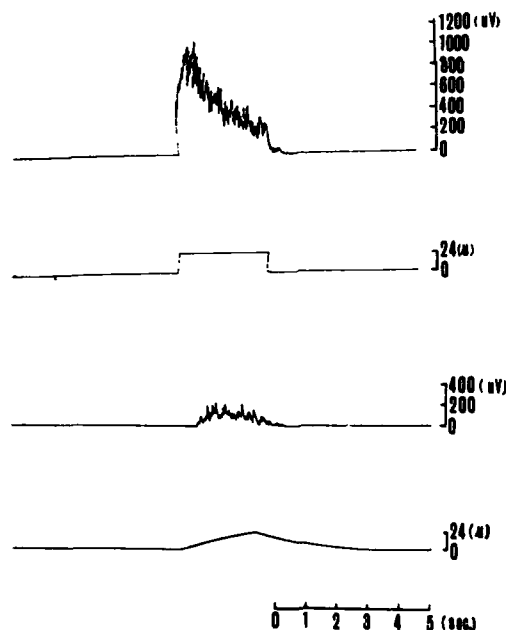


FIGURE 5. Integrated ampullar nerve activity to the fluid flow pulse and $10.3\text{-}\mu/\text{second}$ fluid flow rate.

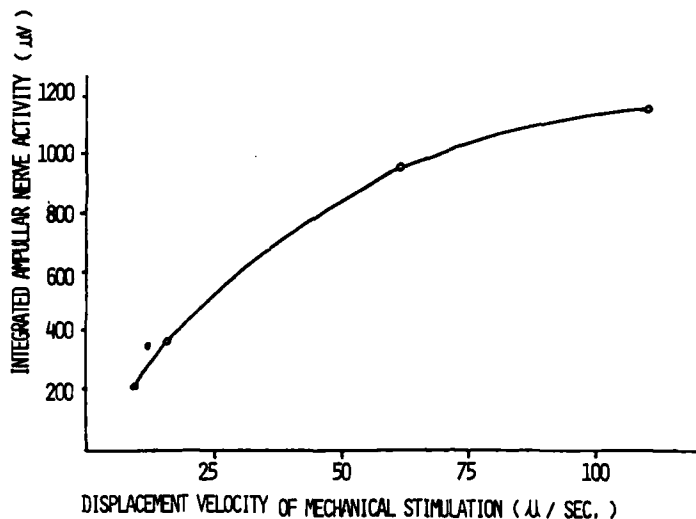


FIGURE 6. Relation between integrated ampullar nerve activity and displacement velocity of mechanical stimulation.

the upper trace, in response to a fluid flow pulse of 24μ , the integrated ampullar nerve activity value reached about $1,000 \mu V$ immediately and then exponentially decreased. In the lower trace, a $10.3\text{-}\mu/\text{second}$ flow rate caused the activity to reach a value of about $200 \mu V$ (maximum value) slowly.

In FIGURE 6, the maximum value of the integrated ampullar nerve activity is plotted against the displacement velocity of mechanical stimulation on a linear scale. The integrated ampullar nerve activity saturated at a certain displacement velocity.

Time Course of Integrated Ampullary Nerve Activity to Flow Pulse of Long Duration

A fluid flow pulse of long duration was applied to the canal to determine whether there was any adaptation in afferent fibers of the ampullar nerve. As illustrated in FIGURE 7, the integrated ampullar nerve activity reached a maximum abruptly and then declined exponentially to the baseline about 8.0 seconds after the stimulation. In addition to the stimulation procedure mentioned above, a stimulus of moderate strength (24μ) was applied to it for 1.3 seconds repeatedly at several intervals ranging from 0.4 seconds to 5.0 seconds. As illustrated in FIGURE 8, the integrated ampullar nerve activity decreased in each of the first two sets of stimulation, but did not decrease when there was a 5.0-second interval between stimuli. In FIGURE 9, the amount of response reduction differed for the different stimulation intervals, but the responses stayed constant for as long as the stimulation lasted. The shorter the intervals of the stimulation, the more rapid the response reduction. The response reduction would appear to be due to adaptation, that is, the response of the peripheral vestibular organ should not

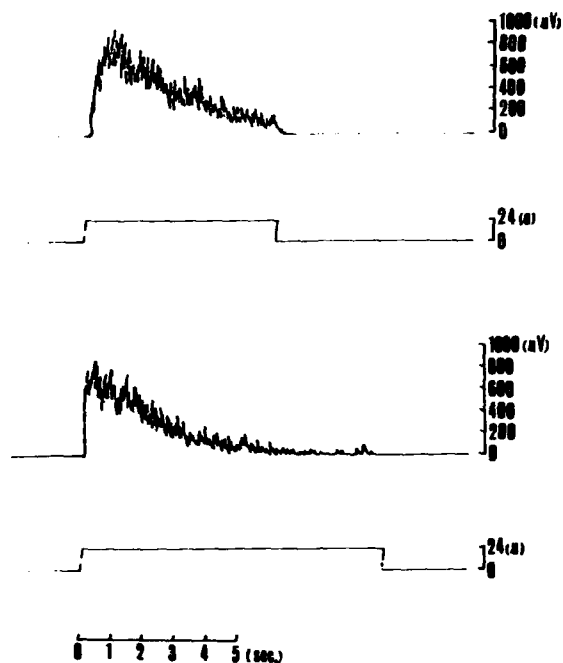


FIGURE 7. Time course of integrated ampullary nerve activity to flow pulse of long duration.

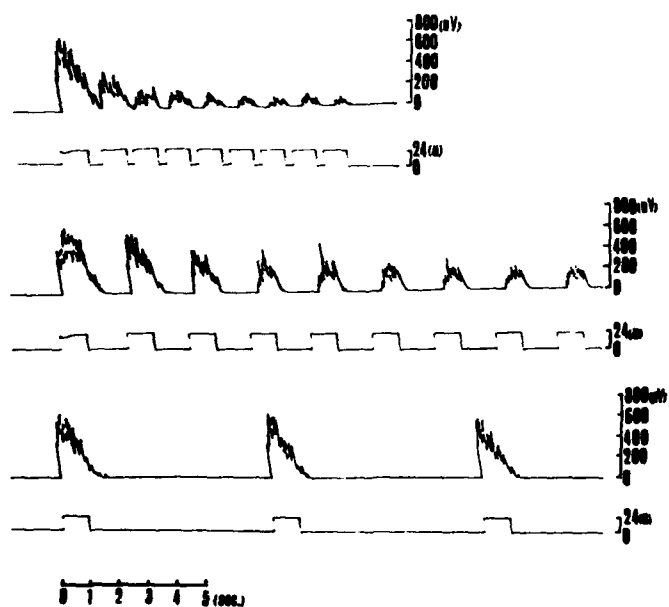


FIGURE 8. Response to repeated stimulation.

have been reduced during repeated constant stimulation if it were free from adaptation.

Superimposed Sequential Stimulation Applied at Various Times for Adaptation

In the experiment illustrated in FIGURE 10, a fluid flow pulse of 8μ was applied first. This was followed by a second short fluid flow pulse of 16μ given at four different times (1 second, 2 seconds, 3 seconds, 4 seconds). The total fluid flow pulse was 24μ . The response to the second stimulation was similar when it was applied at different times. If all of the adapting units had responded to the first stimulation, summation of superimposed stimulation should not be found in every case. From this result, we would conclude that there are adapting units with different thresholds.

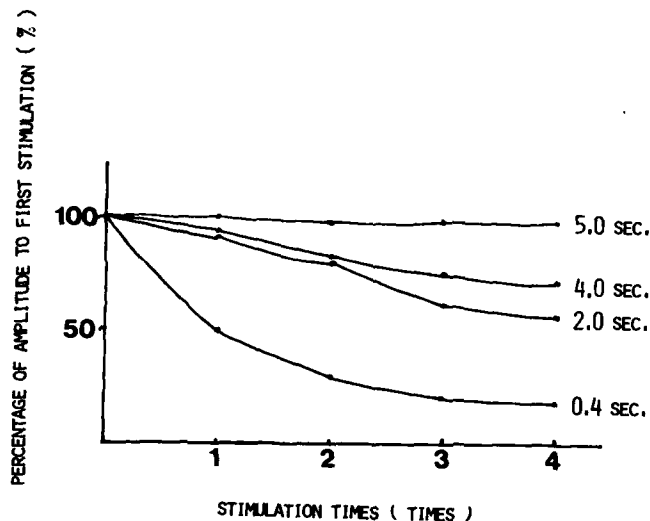


FIGURE 9. The amount of response reduction at four different intervals.

DISCUSSION

Katsuki et al. reported that the response of the single lateral-line nerve fiber of Japanese eels was linear in relation to the logarithm of the mechanical stimulation.³ Shimazu and Precht demonstrated that the constant level of maximum frequency in the cat's vestibular nuclei was proportional to the logarithm of the acceleration applied.⁴ According to the dynamic characteristics of discharge, Shimazu and Precht divided the neurons in the vestibular nuclei into two types: kinetic neurons, characterized by lack of spontaneous discharge, high threshold for frequency increase, rapid time course of frequency change, and steep gradient of acceleration-frequency relationship; and tonic neurons, showing opposite characteristics.⁴ Recordings of mass activity from the nerve of the posterior canal of the frogs by Taglietti, Valli, and Casella show that the resting discharge is maintained by low-voltage action potentials, although there are two

components, low- and high-voltage action potentials, that are recorded when the canal is excited.⁵

The phenomenon of adaptation of the sensory nerve fiber is generally believed to be an important characteristic of the end organ itself. The present experiments, done without influence of efferent nerve fibers, demonstrate that the posterior ampullary nerve shows rapid adaptation. Shimazu and Precht found no significant adaptation of vestibular neuron activity.⁴ They consider that this result is due to the experimental arrangement of rotation for producing cupula deflection. According to Lowenstein's investigation with a slowly increasing stimulating current that stimulates a slow exponential change of cupula deflection caused by a constant angular acceleration, the discharge frequency adapts only very slightly.⁶

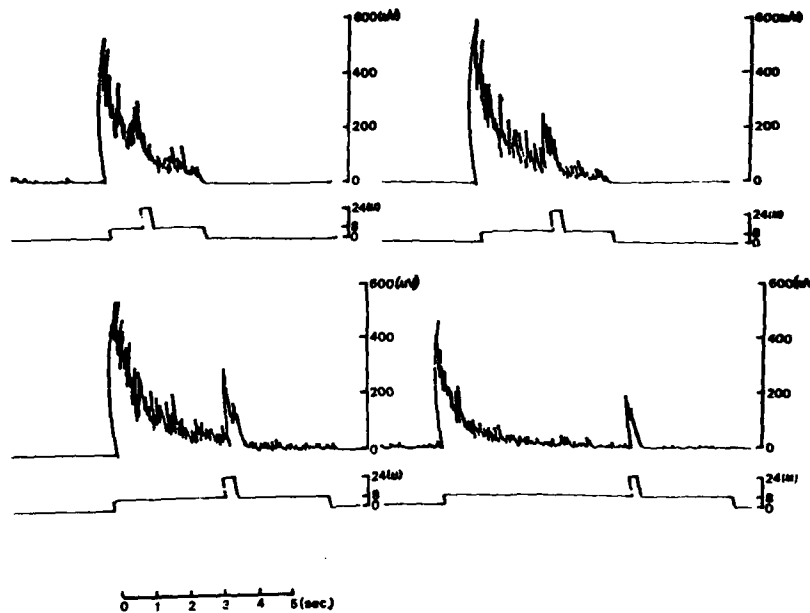


FIGURE 10. Response to two successive steps of fluid flow pulse.

On the other hand, if make-or-break currents are applied, the discharge rate shows rapid adaptation. Shimazu, Precht, and Lowenstein expected that if the cupula were to be deflected very rapidly and sustained at a constant position for a long time, the impulse discharge of the sensory organs and vestibular neurons would adapt considerably. The present procedure for producing a cupula deflection to determine whether there is any adaptation is in good agreement with their suggestions.

Since the hair cells of the crista ampullaris in the frogs are all type II, the factor responsible for the differences in dynamic properties is believed to be a difference in the encoder mechanism in the nerve fiber.¹

Nakajima and Onodera reported that marked differences in adaptation

between the slowly and rapidly adapting receptors of the crayfish were attributable to the differences in the properties of the spike-generating membrane rather than to properties of the generator potentials.⁷ Taglietti, Valli, and Casella explained that different units are subserved by fibers of different sizes: thick fibers gave rise to phasic responses, whereas thin fibers gave rise to tonic responses.⁵ The present experiments confirm that the units composing the sensory apparatus of the frog semicircular canals show phasic responses. Phasic components are more related to cupula deflection velocity than to the position of the cupula. These units display rapid adaptation, respond to fluid flow rate, and have different thresholds.

REFERENCES

1. PRECHT, W., R. LLINAS & M. CLARKE. 1971. Physiological responses of frog fibers to horizontal angular rotation. *Exp. Brain Res.* **13**: 378-407.
2. HARADA, Y. 1972. Responses from isolated individual semicircular canal ampullae in frog. *Acta Otolaryngol.* **73**: 413-417.
3. KATSUKI, Y., S. YOSHINO & J. CHEN. 1950. Action current of the single lateral line nerve fiber of fish. II. On the discharge due to stimulation. *Jpn. J. Physiol.* **1**: 179-194.
4. SHIMAZU, H. & W. PRECHT. 1965. Tonic and kinetic responses of cat's vestibular neurons to horizontal angular acceleration. *J. Neurophysiol.* **28**: 991-1013.
5. TAGLIETTI, V., P. VALLI & C. CASELLA. 1973. Discharge properties and innervation of the sensory units in the crista ampullaris. *Arch. Sci. Biol.* **57**: 73-86.
6. LOWENSTEIN, O. 1955. The effect of galvanic polarization on the impulse discharge from sense endings in the isolated labyrinth of the thornback ray. *J. Physiol. London* **127**: 104-117.
7. NAKAJIMA, S. & K. ONODERA. 1969. Membrane properties of the stretch receptor neurones of crayfish with particular reference to mechanism of sensory adaptation. *J. Physiol. London* **200**: 161-185.

PHYSIOLOGICAL MECHANISMS OF THE NYSTAGMUS PRODUCED BY ROTATIONS ABOUT AN EARTH- HORIZONTAL AXIS*

Jay M. Goldberg† and César Fernández‡

†Department of Pharmacological and Physiological Sciences

‡Department of Surgery (Otolaryngology)

University of Chicago

Chicago, Illinois 60637

The reactions to rotations about an earth-horizontal axis (EHA) were described by Guedry and by Benson and Bodin.^{1,2} Human subjects were spun in their horizontal (yaw) plane at constant speeds of 10–60°/second. EHA rotations in either direction led to a persistent unidirectional nystagmus, whose slow phase was compensatory for motion. Two components were evident in the response, a bias component responsible for the unidirectional nystagmus and a cyclic component reflected in the nystagmus being modulated as a function of instantaneous head position relative to gravity. The nystagmus appeared to be a steady-state response, since it was maintained for constant-speed rotations of several minutes duration. Postrotatory responses were short-lived or were absent. As is well known, were the same rotations applied while the subject was being spun about an earth-vertical axis (EVA), the perrotatory response would last only for 30–60 seconds and would be followed by an oppositely directed postrotatory response of comparable magnitude and duration.³ The EHA reactions were absent in labyrinthine-defective subjects, suggesting that the responses were of vestibular origin.¹ Subsequent studies of EHA nystagmus have extended these findings in several ways, of which four may be mentioned here. First, similar responses are obtained during counterrotation on a centrifuge,^{4,5} indicating that the critical physical variable is the rotation of a linear-force vector about the subject. Second, a persistent unidirectional nystagmus is also observed in experimental animals, including the rabbit, cat, and rhesus monkey.^{6–8} Third, a similar vertical nystagmus results when subjects are rotated about an EHA axis in their pitch plane, i.e., head over heels. And fourth, the horizontal EHA nystagmus changes from a unidirectional to a direction-changing nystagmus when the rotation speed is increased from 60°/second to 180°/second.⁹

The physiological basis of the unidirectional (bias) nystagmus obtained during EHA rotations is unclear. There have, in fact, been three suggestions offered as to the peripheral etiology of the bias component. Guedry thought that the bias component might reflect the dynamic pattern of activation of different groups of otolith afferents.¹ Benson and Bodin and Steer favored a semicircular-canal origin for the bias component;^{2,4} it was suggested that EHA rotations led to a maintained cupular deflection, possibly as a result of a roller-pump action. Finally, Benson and Barnes speculated that EHA rotations might lead to a steady-state d.c. response of otolith afferents that was directionally specific.⁵ Directional specificity here refers to a response whose magnitude and/or sign is altered when the rotation direction changes from clockwise to counterclockwise.

*This research was supported by National Institutes of Health Grant No. NS 01330 and by National Aeronautics and Space Administration Grant No. NGR-14-001-225.

Experimental studies have not clarified the situation. Janeke, working with the rabbit, reported that the persistent nystagmus produced by EHA yaw rotations was abolished by bilateral section of the utricular nerves combined with bilateral saccular destruction.⁶ As has been pointed out,¹⁰ Janeke's operative procedures were drastic and could have led to a general labyrinthine deterioration. Correia and Money inactivated all six semicircular canals by a plugging procedure, which reduced but did not abolish the EHA nystagmus.⁷ Correia and Money's results are difficult to interpret since plugging, while abolishing the response of canal afferents to angular accelerations, does not completely eliminate the afferents' response to linear forces.¹¹ Hence, the nystagmus observed after canal plugging could still reflect a canal activation. Electrophysiological studies have been similarly inconclusive. Benson *et al.*, recording from the vestibular nuclei in decerebrate cats, observed that rotating linear forces resulted in steady-state d.c. responses from canal-related neurons.¹⁰ The directional specificity and magnitude of the responses were appropriate to account for the bias nystagmus obtained in the same motion environment. Since nonrotating linear forces did not alter the discharge of the neurons, it was concluded that the neurons did not receive a direct otolith input. A less direct otolith input could not be excluded. Consistent with the latter possibility, Lowenstein and Compton apparently failed to find similar responses to EHA rotations in canal afferents of the isolated elasmobranch labyrinth.¹²

The present study was designed to investigate the peripheral etiology of the EHA nystagmus, especially its bias component, in the squirrel monkey. Eye-movement recordings were made with d.c. electro-oculography in alert animals to assure ourselves that squirrel monkeys, like other animals, had characteristic EHA nystagmus to both yaw and pitch rotations. Afferent responses were recorded in barbiturate-anesthetized animals. EHA rotations were obtained by placing a servo-controlled rate table on its side. The stimulus for all experiments was a velocity trapezoid with a constant-velocity plateau of 60–90 seconds.

Our eye-movement recordings show that the EHA responses in the squirrel monkey resemble those seen in other species. The similarities include (1) a persistent horizontal nystagmus during yaw rotations and a persistent vertical nystagmus during pitch rotations; (2) a unidirectional nystagmus at low rotation speeds (30°/second), which is replaced by direction-changing eye movements at higher speeds (180°/second); and (3) postrotatory responses of relatively small amplitude and duration following EHA rotations. The bias component during 30°/second rotations had a slow-phase eye velocity averaging some 15°/second. This was so for both yaw and pitch rotations.

Vestibular-nerve recordings were made from afferents innervating each of the three canals, as well as from otolith afferents presumed to innervate the utricular and saccular maculae. None of the afferents show a directionally specific d.c. response that can account for the bias component of EHA nystagmus. During EHA rotations, canal afferents show small sinusoidal responses, having peak amplitudes typically of 0–15 spikes/second. The responses are the result of the canals' sensitivity to static linear forces, which, as we have argued previously, may be artifactual in nature.¹¹ Larger sinusoidal responses with peak amplitudes of 25–75 spikes/second are recorded from otolith neurons and are consistent with the directional properties and response dynamics already described for these afferents.¹³

The bias component of EHA nystagmus requires that oculomotor centers be provided with a directionally specific d.c. input. Neither semicircular-canal nor otolith afferents give rise to such a signal. The appropriate d.c. signal apparently

has to be constructed centrally from an a.c. or sinusoidal peripheral input, most likely arising from otolith afferents. This is in line with Guedry's original suggestion.¹ It is not clear how the brain accomplishes this task. One possibility is that the generation of the bias component involves a central comparison of sequentially activated populations of otolith afferents followed by some form of a.c.-to-d.c. conversion. Regardless of specific mechanisms, we would suggest, based on the results of Benson *et al.*,¹⁰ that once the dynamic otolith signal is transformed centrally into the appropriate bias signal, the latter is relayed to canal-related neurons, where it is summed with canal inputs and then sent to oculomotor centers. The convergence of a canal signal with an otolith-related bias signal within the vestibular nuclei is consistent with the conclusion, based on the optokinetic sensitivity of canal-related neurons,¹⁴ that these neurons serve to integrate rotation-related information arising from disparate sensory channels.

The function of the bias component is obscure, since it has been observed only during prolonged rotation of a linear-force vector about the subject's head. Such a motion environment seldom, if ever, occurs during everyday life. At the outset of these experiments, we supposed that the bias component could be explained by a peculiarity in peripheral mechanics. Had this conjecture proved true, the bias component conceivably could have been dismissed as a laboratory curiosity. Our results turned out otherwise. The fact that the brain bothers to construct a directionally specific d.c. signal from an a.c. peripheral input strongly suggests that the bias component is, at the very least, a manifestation of an important vestibular function. What that function is remains to be determined.

REFERENCES

1. GUEDRY, F. E., JR. 1965. Orientation of the rotation-axis relative to gravity: its influence on nystagmus and the sensation of rotation. *Acta Otolaryngol.* **60**: 30-48.
2. BENSON, A. J. & M. D. BODIN. 1966. Interaction of linear and angular accelerations on vestibular receptors in man. *Aerosp. Med.* **37**: 144-154.
3. GUEDRY, F. E., JR. 1974. Psychophysics of vestibular sensation. In *Handbook of Sensory Physiology. Vestibular System. Part 2: Psychophysics, Applied Aspects and General Interpretations*. H. H. Kornhuber, Ed. **6/2**: 3-154. Springer-Verlag, Berlin, Federal Republic of Germany.
4. STEER, R. W., JR. 1970. Progress in vestibular modeling. I. Response of semicircular canals to constant rotation in a linear acceleration field. In *Fourth Symposium on the Role of the Vestibular Organs in Space Exploration*: 353-360. U.S. Government Printing Office, Washington, D.C.
5. BENSON, A. J. & G. R. BARNES. 1970. Responses to rotating linear acceleration vectors considered in relation to a model of the otolith organs. In *Fourth Symposium on the Role of the Vestibular Organs in Space Exploration*: 221-236. U.S. Government Printing Office, Washington, D.C.
6. JANEKE, J. B. 1968. On Nystagmus and Otoliths. A Vestibular Study of Responses as Provoked by Cephalo-Caudal Horizontal Axial Rotation. Drukkerij Cloecken Moedigh N.V. Amsterdam, the Netherlands.
7. CORREIA, M. J. & K. E. MONEY. 1970. The effect of blockage of all six semicircular canal ducts on nystagmus produced by dynamic linear acceleration in the cat. *Acta Otolaryngol.* **69**: 7-16.
8. YOUNG, L. R. & V. HENN. 1975. Nystagmus produced by pitch and yaw rotation in monkeys about non-vertical axes. *Fortschr. Zool.* **23**: 235-246.
9. CORREIA, M. J. & F. E. GUEDRY, JR. 1966. Modification of vestibular responses as a function of rate of rotation about an earth-horizontal axis. *Acta Otolaryngol.* **62**: 297-308.

10. BENSON, A. J., F. E. GUEDRY, JR & G. MELVILL JONES. 1970. Response of semicircular canal dependent units in vestibular nuclei to rotation of a linear acceleration vector without angular acceleration. *J. Physiol. London* **210**: 475-494.
11. GOLDBERG, J. M. & C. FERNÁNDEZ. 1975. Responses of peripheral vestibular neurons to angular and linear acceleration in the squirrel monkey. *Acta Otolaryngol.* **80**: 101-110.
12. LOWENSTEIN, O. & G. J. COMPTON. 1978. A comparative study of the responses of isolated first-order semicircular canal afferents to angular and linear acceleration, analysed in the time and frequency domains. *Proc. R. Soc. London Ser. B* **202**: 313-338.
13. FERNÁNDEZ, C. & J. M. GOLDBERG. 1976. Physiology of peripheral neurons innervating otolith organs of the squirrel monkey. *J. Neurophysiol.* **39**: 970-1008.
14. WAESPE, W. & V. HENN. 1977. Neuronal activity in the vestibular nuclei of the alert monkey during vestibular and optokinetic stimulation. *Exp. Brain Res.* **27**: 523-538.

EFFECTS OF GRAVITY ON ROTATORY NYSTAGMUS IN MONKEYS*

Theodore Raphan and Bernard Cohen

Department of Neurology
Mount Sinai School of Medicine
City University of New York
New York, New York 10029

Volker Henn

Faculty of Medicine
University of Zurich
CH-8091 Zurich, Switzerland

The vestibulo-ocular reflex (VOR) stabilizes gaze in response to head rotation. If a step of angular velocity is given about a vertical axis, horizontal nystagmus is induced. Initially, its slow-phase velocity is compensatory; but as rotation continues with the subject in darkness, slow-phase velocity decays to zero. Deceleration induces postrotatory nystagmus. It is essentially anticomensatory since it occurs when the subject is stationary. There are several conditions under which the compensatory response of the VOR is improved. If rotation occurs in light, optokinetic nystagmus (OKN) is induced that helps hold the velocity of the slow phases of nystagmus close to that of the stimulus. During and after deceleration, activity stored during OKN summates with the vestibularly induced postrotatory nystagmus to reduce or abolish it.¹⁻⁵

Compensatory eye velocities also can be enhanced by the introduction of a rotating gravity vector relative to the head. If subjects are rotated about an axis tilted from the vertical (off-vertical axis rotation), nystagmus is induced that lasts as long as rotation continues.⁶⁻⁹ At the end of rotation, the after-nystagmus is weaker and shorter than that after rotation about a vertical axis. While the steady-state characteristics of the nystagmus induced by off-vertical axis rotation have been examined,⁶⁻⁹ its dynamic characteristics are unknown. Moreover, there is little information about the relationship between perrotatory and postrotatory nystagmus induced by this type of stimulus. The purpose of this study was to characterize the dynamic aspects of the slow-phase velocity of nystagmus induced by off-vertical axis rotation. We wished to determine whether the velocity storage mechanism that is important for visual-vestibular interaction⁵ also plays a role in mediating nystagmus induced by rotation about an off-vertical axis.

METHODS

Twelve monkeys of various species (*Macaca mulatta*, *fascicularis*, and *nemestrina*) were used in this study. There were no basic differences between animals

*Supported by National Institutes of Health Research Grant No. NS 00294, National Eye Institute Academic Investigator Award No. EY 00157 (T.R.), and a grant from the Swiss National Foundation for Scientific Research 3.343-0.78.

in the results to be reported. Eye movements were recorded by d.c. electro-oculography (EOG) with implanted Ag-AgCl electrodes.¹⁰ The EOG was differentiated to obtain slow-phase eye velocity. Eye position, eye velocity, and stimulus parameters were recorded on paper and stored on FM magnetic tape. Eye movements to the right and up are represented in the figures by upward deflections in the EOG. The EOG was calibrated using the response to rotation at $60^\circ/\text{second}$ in light. It is assumed that the initial gain under these conditions is close to unity.^{5,11,12} The data were normalized with respect to this value. Calibrations were taken just before each trial and repeated after each period in darkness to control for gain changes in the EOG. Amphetamine sulfate (0.5 mg/kg) was given 30 minutes before testing to maintain alertness.

Eye movements were induced by optokinetic stimulation or by angular rotation about vertical or off-vertical axes. The stimulator, constructed by the

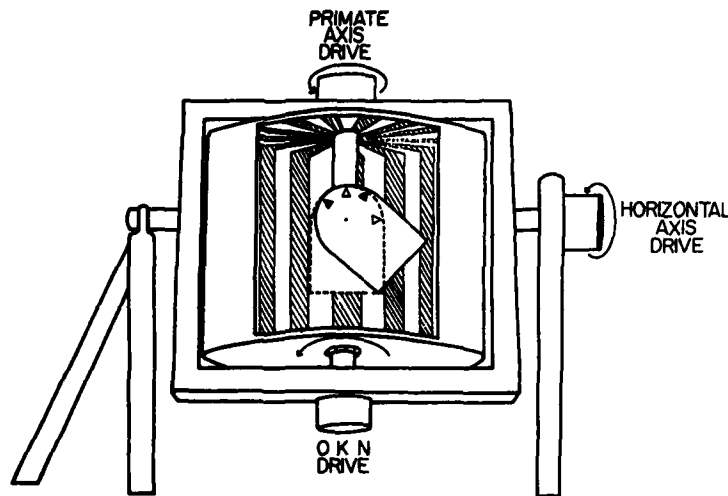


FIGURE 1. Two-axis rate table and optokinetic stimulator. See text for details.

Contraves Goertz Corporation of Pittsburgh, is shown in FIGURE 1. The monkey sits in a chair that is driven from above by a d.c. torque motor (primate axis drive). The motor is attached to a gimbal. The animal rotates within a closed aluminum OKN drum. The OKN drum is driven from below by another motor, which is also attached to the gimbal (OKN drive). Alternating 10° black and white stripes inside the drum surround the animal and fill its field of vision. The gimbal can be rotated by a motor about an earth-horizontal axis (horizontal axis drive). The animal's chair may be tilted in the primate axis from the upright position (FIGURE 1, dashed lines) to right-side-down positions (FIGURE 1, solid lines) up to 90° . The motors are controlled by a velocity servomechanism. In this study we mostly used velocity steps with an acceleration and deceleration of $2,600^\circ/\text{second per second}$ and yaw rotation at constant velocities up to $180^\circ/\text{second}$. The axis of yaw rotation (primate axis) could be tilted about the horizontal axis with an acceleration of $57^\circ/\text{second per second}$. The light inside the drum was controlled by a pulse generator and monitored by a photocell.

RESULTS

Typical slow-phase-velocity profiles induced by steps of angular velocity about an axis tilted 50° from the vertical in darkness are shown in FIGURE 2. In response to a step in stimulus velocity, slow-phase velocity rose abruptly (FIGURE 2A). The gain of the immediate response (slow-phase eye velocity/stimulus velocity) was close to unity (FIGURE 3A). This is similar to the gain of per- and postrotatory nystagmus during vertical axis rotation in darkness.⁵ This shows that off-vertical axis rotation does not affect the initial peak velocity or gain of the VOR. For stimulus velocities up to 50 - $60^\circ/\text{second}$, slow-phase velocity was maintained at a steady-state level with a gain close to one (FIGURES 2A and 3B).

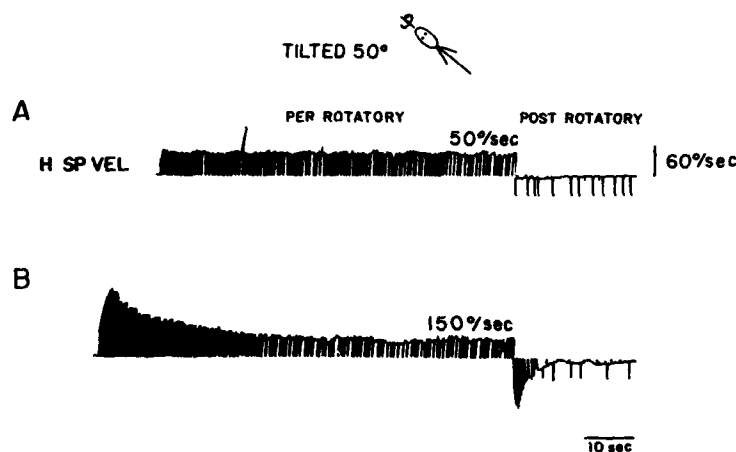


FIGURE 2. Effects of rotation in darkness about an axis tilted 50° from the vertical. **A:** Horizontal slow-phase velocity induced by rotation at $50^\circ/\text{second}$. During the perrotatory period, slow-phase eye velocity was maintained close to the velocity of stimulation. Oscillations in velocity were phase locked to the position of the head. When the animal was stopped, there was an absence of after-nystagmus. **B:** Horizontal slow-phase velocity induced by rotation at $150^\circ/\text{second}$. The peak eye velocity was similar to that recorded during rotation about a vertical axis. The postrotatory slow-phase velocity was reduced over that recorded after vertical axis rotation by the amount of the steady-state nystagmus.

For higher stimulus velocities, slow-phase eye velocity declined to a nonzero steady-state level after reaching a peak at the end of acceleration (FIGURES 2B and 3B). The dominant time constant of the decline was 15-25 seconds. The maintenance of nystagmus during rotation about an axis tilted from the vertical is different from the behavior of vestibular nystagmus during rotation about a vertical axis. In the latter instance, slow-phase velocity decays to zero as rotation continues (FIGURE 4A). Thus, off-vertical axis rotation enhances compensatory eye movements induced by the VOR during rotation in a manner similar to vision.

Superimposed on the steady-state levels were oscillations whose maximum and minimum velocities occurred at specific head positions over a wide range of

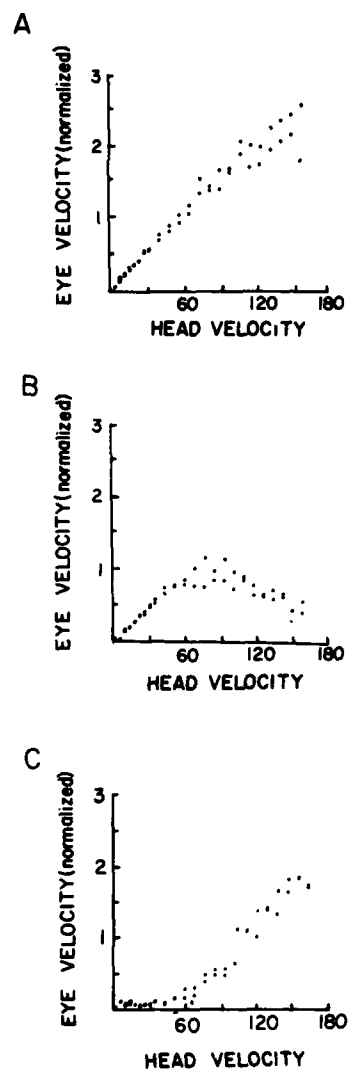


FIGURE 3. A: Peak eye velocity (ordinate) induced by steps of head velocity in darkness (abscissa) at 50° tilt. Each dot is the peak velocity of one sample of perrotatory nystagmus. It follows the same curve as the peak eye velocity vs. head velocity for rotation about a vertical axis.⁸ B: Steady-state slow-phase eye velocity recorded in darkness during rotation about an off-vertical axis (50°). Eye velocity rose linearly with head velocity to about $50\text{--}60^\circ/\text{second}$ and then declined. C: Peak velocity of postrotatory nystagmus upon stopping after off-vertical axis rotation. In all graphs, eye velocity was normalized in relation to values recorded during $60^\circ/\text{second}$ rotation in light.

stimulus velocities (FIGURE 2). When rotating to the right, the velocity was highest when the right side was down and lowest when the right side was up. The reverse occurred for rotation in the opposite direction. Thus, the frequency of the oscillations was phase-locked to the rotation. This is consistent with the results of Guedry, Benson and Bodin, and Young and Henn.^{6,7,9}

Off-vertical axis rotation also had an important effect on postrotatory nystagmus. After deceleration, the postrotatory response was approximately canceled for velocities up to 50–60°/second (FIGURES 2A and 3C). At higher stimulus velocities, the postrotatory response became progressively more prominent (FIGURE 2B), but was never as strong as the postrotatory response to rotation about a

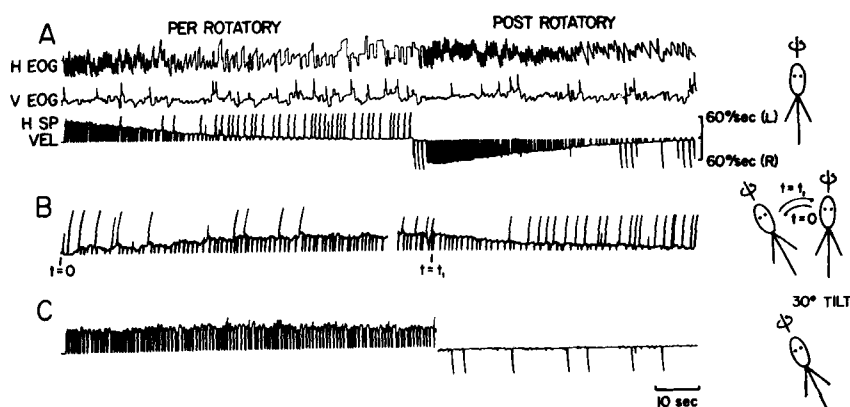


FIGURE 4. A: Nystagmus induced by a step of head velocity of 60°/second in darkness about a vertical axis. The top trace is the horizontal EOG, the second trace is the vertical EOG, and the third trace is horizontal slow-phase eye velocity. B: Slow-phase eye velocity induced by tilting the animal 30° while it was rotating in dark after the perrotatory slow-phase velocity had declined to zero. The moment of tilt is given by $t = 0$. After reaching a steady-state eye velocity, the subject was tilted back to the upright at $t = t_1$. Eye velocity declined to zero. Note that the time course of the rise and fall of slow-phase eye velocity was comparable to the time course of the per- and postrotatory nystagmus for rotation about a vertical axis (A). C: Rotation about an axis tilted 30° from the vertical at 60°/second induced sustained perrotatory nystagmus. The steady-state eye velocity was similar to that reached in B after tilting. The postrotatory response was absent when the subject was stopped in the off-vertical position. Note that the response in C is the summation of the slow-phase velocities in A and B.

vertical axis (FIGURE 4A). The difference between the postrotatory nystagmus velocity following rotation about vertical (FIGURE 3A) and off-vertical axes (FIGURE 3B) approximated the steady-state value of eye velocity achieved during off-vertical axis rotation (FIGURE 3C). This indicates that the jumps in eye velocity at the beginning and end of the responses were approximately equal. This is consistent with the interpretation that VIIIth nerve activity due to cupula deflection during and after deceleration had summated with activity stored during off-vertical rotation to reduce postrotatory eye velocity.

Storage of activity related to slow-phase eye velocity during off-vertical axis rotation was not achieved instantaneously. This was shown by the following

experiment. An animal was rotated at $60^\circ/\text{second}$ about a vertical axis in darkness until the perrotatory nystagmus had decayed to zero (FIGURE 4A). The rotation axis was tilted 30° at $t = 0$ (FIGURE 4B) as rotation continued. This induced nystagmus, which gradually built to a steady-state level. The time constant of the rise was in the range of 8-15 seconds. The steady-state slow-phase velocity achieved by tilting during rotation (FIGURE 4B) was identical to the steady-state eye velocity achieved when rotation began in the off-vertical position (FIGURE 4C). This shows that it is not necessary to have an initial step of eye velocity when rotating about an off-vertical axis for nystagmus to appear or be maintained. It also shows that the mechanism that maintains nystagmus during off-vertical axis rotation has a charging time constant in the range of 8-15 seconds.

The discharge time constant of activity stored during off-vertical rotation was determined in a similar fashion, i.e., by tilting the rotation axis back to the vertical during continuous rotation in darkness after a steady-state velocity was reached (FIGURE 4B, $t = t_1$). The discharge time constant was also in the range of 8-15 seconds. With repeated testing, habituation occurred and time constants of charge and discharge became shorter. They were smaller for large tilt angles and higher velocities of rotation. On initial testing, the rising and falling time constants of the nystagmus were similar; but over time, some animals developed an asymmetry in the rise and fall of nystagmus. Generally, the rise time was shorter than the fall time. The decay rate of nystagmus induced by rotation about an off-vertical axis after the axis of rotation was moved to the vertical (FIGURE 4B) was similar to that of postrotatory nystagmus after vertical axis rotation (FIGURE 4A). It was also comparable to the decay time constant of optokinetic after-nystagmus (OKAN).¹ This suggests that the same storage mechanism that generates nystagmus during visual and vestibular stimulation about vertical axes⁵ is utilized to store velocity information and generate continuous nystagmus during off-axis rotations.

Off-vertical axis rotation not only had an important effect on continuing perrotatory nystagmus and reducing postrotatory nystagmus, it also conditioned the dynamics of the postrotatory response. The time constant of the postrotatory response was shortened to a range of 3-6 seconds (FIGURE 2B). The final value depended somewhat on the orientation of the head with regard to gravity at the time of stopping. The response dynamics were similar to that of postrotatory nystagmus in light after rotation about a vertical axis.⁵ In both cases, the time constants were approximately equal to the dominant time constant of activity in semicircular canal afferents.¹³ This suggests that the storage mechanism was not accumulating activity during the postrotatory period after off-vertical axis rotation.

The reduced storage capability was not due to the orientation of the head during the postrotatory nystagmus. If the animal was tilted 30° but rotated about a vertical axis (FIGURE 5B), the per- and postrotatory nystagmus decayed to zero just as when the animal was upright (FIGURE 5A). Although the animal was tilted, the rotational axis was vertical and there was no rotating gravity vector relative to the head. In FIGURE 5C the animal was stopped in the same position as that of FIGURE 5B, but after off-vertical axis rotation, the time constant of the velocity decline of the postrotatory nystagmus was short. This indicates that it is the change in head position relative to gravity during the perrotatory phase that is responsible for the postrotatory effect on the storage integrator.

It was not necessary to rotate the animal about an off-vertical axis to produce enhancement of perrotatory nystagmus. Similar enhancement was obtained

when animals were rotated about a vertical axis while they were oscillated slowly in the fore-aft direction about a horizontal axis (FIGURE 6). For this purpose another turntable was used. The horizontal axis on this turntable is located above the platform. Continuous nystagmus developed when animals were oscillated in the pitch plane with a cycle time of from 6-20 seconds during constant-velocity rotation. This shows that under appropriate conditions, addition of a dynamic acceleration vector perpendicular to the axis of rotation has a similar effect as off-vertical axis rotation in sustaining perrotatory nystagmus.

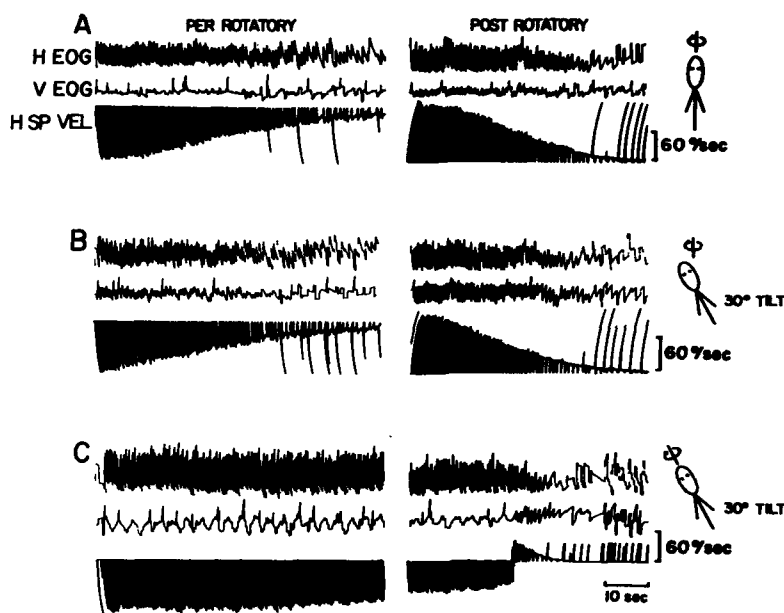


FIGURE 5. Per- and postrotatory nystagmus induced by a step in velocity of $90^\circ/\text{second}$. The upper trace is horizontal EOG, the second trace is the vertical EOG, and the third trace is slow-phase eye velocity. In A, the animal had vertical axis rotation. In B, it had vertical axis rotation but was tilted 30° . In C, the animal was rotated about an off-vertical axis tilted 30° from the vertical. It was stopped in the same right-side-down position as in B. Note the slow decline in nystagmus after vertical axis rotation and the rapid decline after off-vertical rotation.

Although tilts during perrotatory nystagmus caused nystagmus velocity to be maintained (FIGURE 6), tilts during the postrotatory phase when the animal was stationary had the opposite effect: they caused a decline in slow-phase velocity. A typical example is shown in FIGURE 7B. The animal was tilted backward 25° during postrotatory nystagmus. This caused a prompt decline in the velocity of the horizontal postrotatory nystagmus. The decline had a latency of about 1 second and occurred over a period approximately equal to the duration of the tilt. At the conclusion of the tilt, the remaining eye velocity fell at approximately the time constant of the nystagmus in the untilted condition (FIGURE 7A). The

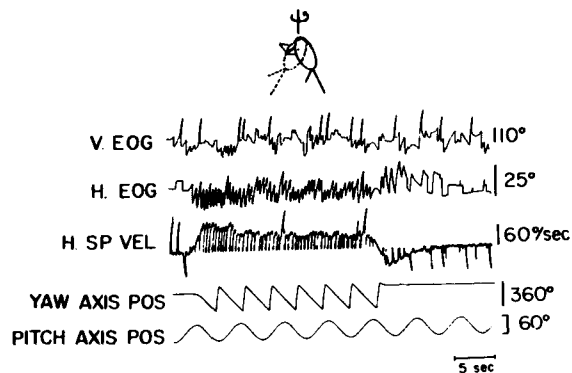


FIGURE 6. Per- and postrotatory nystagmus induced by oscillation in the fore-aft direction about a horizontal axis (pitch axis) while the animal was being rotated at constant velocity about a vertical axis in darkness. The top trace is the vertical EOG, the second trace is horizontal EOG, the third trace is horizontal slow-phase eye velocity, the fourth trace is the yaw-axis position of the table, and the fifth trace is the pitch-axis position. Note the continuous nystagmus during constant-velocity yaw-axis rotation and the shortened postrotatory nystagmus when the animal was decelerated.

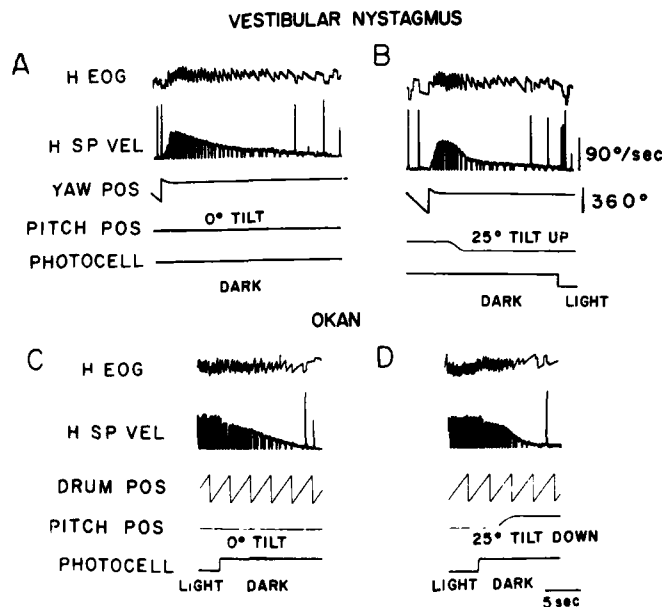


FIGURE 7. Effects of tilt out of the plane of nystagmus during postrotatory nystagmus (B) and OKAN (D). The normal responses are shown in A and C. When the animal was tilted during postrotatory nystagmus (B) or during OKAN, the decline in nystagmus was faster than in the corresponding normal responses (A, C).

discharge of nystagmus did not depend on the direction in which the animal was tilted. The change in nystagmus velocity was the same if the animal was tilted forward or back over the same angle at the same acceleration. Similar declines were seen during OKAN (FIGURE 7D and E). This shows that activity in the storage integrator was "dumped" by moving the head out of the plane of the ongoing nystagmus. It provides further support for the contention that OKN and vestibular nystagmus utilize a common storage mechanism.⁵

DISCUSSION

The persistence of nystagmus during off-vertical axis rotation indicates that the labyrinths were being continuously excited by relative motion of the head with regard to gravity. The finding that nystagmus did not disappear immediately when the animal was moved to the upright position while still rotating (FIGURE 4B) shows that stored activity induced during the off-vertical axis rotation has contributed to the production of nystagmus. Evidence of storage also was manifest in the difference between the peak velocities of the postrotatory nystagmus after off-vertical and vertical axis rotation (FIGURE 3). These findings raise the questions: Where in the labyrinth does the activity originate? How is the storage of velocity information achieved?

Canal afferents do not show maintained, direction-specific responses during constant-velocity rotation about an earth-horizontal axis.¹⁴ Therefore, it is unlikely that the signal that produces continuous nystagmus during off-vertical axis rotation originates in the semicircular canals. The otolith organs, particularly the utricle, are more likely candidates,^{6,15,16} since they would be stimulated by yaw rotation about off-vertical axes. Otolith afferents are acceleration sensitive and, due to their rapid dynamics, generate positional information about the attitude of the head with regard to gravity.¹⁷⁻²³ However, this positional information by itself would be unable to produce nystagmus without further processing to convert it into a velocity command signal.^{1,5,24,25}

Under dynamic conditions, i.e., during stimulation with a rotating acceleration vector, the activity of some utricular or saccular units can be related to head velocity. These are the irregular adapting otolith units.^{17,19} However, velocity information in these units is weak and relatively imprecise, and it is unlikely that they could be responsible for the careful matching of eye velocity to head velocity that occurs for off-vertical axis rotations up to 50-60°/second (FIGURE 3B). Moreover, if the velocity command signal depended primarily on velocity information in otolith afferents, it would imply that the precise, robust head-position signal, which is the dominant information generated by the otolith organs, is ignored. This is unlikely.

Alternatively, we would propose that the velocity command signal that produces the nystagmus is formed in the central nervous system by detecting a moving pattern that occurs as utricular afferents with different polarization vectors are excited sequentially by a rotating gravity vector. The command velocity could be generated by determining the speed of the moving pattern. Ideally this would be equal to head velocity.

The storage of activity related to the velocity command signal must also take place centrally. The response time constant of utricular afferents is about 15 mseconds.¹⁷ This is much too rapid for them to play a direct role in storing activity or canceling the postrotatory response induced by canal excitation during deceleration after off-vertical axis rotation. Instead, the velocity storage mecha-

nism that generates nystagmus during visual and vestibular stimulation^{1,5} is probably utilized as an intermediate stage in generating slow-phase eye velocity. In support of this, the time constant of decay in slow-phase velocity when the animal was moved to the vertical after rotating about a tilted axis (FIGURE 4B) was similar to the time constant of nystagmus after steps of velocity about a vertical axis (FIGURE 4A) or during OKAN.

Previous analysis has shown that both the visual system and the semicircular canals couple to the oculomotor system through the velocity storage mechanism and through direct pathways. The presence of direct pathways is indicated by rapid changes of eye velocity in response to steps of stimulus velocity. The indirect pathways that contain the storage mechanism induce slower changes in eye velocity and hold these velocities after the end of stimulation. As shown in FIGURE 3B, only slow changes in eye velocity are produced by steps of tilt. This implies that the head-velocity signal obtained from processing activity in the otolith organs couples predominantly to the integrator. There appears to be little contribution of direct pathways to generation of a sustained velocity command. There are direct pathways from the otolith organs to the oculomotor system.²⁸⁻²⁸ They probably carry positional information that functions to deviate the eyes, and do not induce sustained nystagmus. A change in eye position due to excitation of direct otolith-oculomotor pathways during horizontal and off-vertical axis rotation^{6,7,9} could be responsible for the oscillations in eye velocity during the nystagmus induced by off-vertical axis rotations.

The organization of the mechanism that reduces eye velocity when the animal was tilted during postrotatory nystagmus is not clear. Activity that causes the tilt-related changes probably couples to the integrator through the "dump" mechanism that is utilized by the visual system to suppress vestibular nystagmus and OKAN.^{1,5} One difference between visually induced and vestibularly induced dumps is that there is no rapid fall in slow-phase velocity during tilt suppression. This suggests that direct pathways responsible for rapid changes in eye velocity are not utilized during the tilt dumps. If activity that initiated the dumps arose in the otolith organs, it would be consistent with the data of FIGURE 4B, which suggest that direct otolith-oculomotor pathways do not carry an eye-velocity command signal. The finding that OKAN and vestibular nystagmus are discharged in the same way by tilts as by visual fixation further indicates that the visual and vestibular systems share a common integrator, which is utilized in visual-vestibular as well as in vestibulo-vestibular interactions.

An important question that must be answered in modeling otolith-oculomotor activation is whether there is an efference from eye velocity to the velocity command signal to form a closed-loop system, or whether the system operates in an open-loop fashion. The rise and fall times of slow-phase velocity when animals were moved to and from tilted axes during continuous rotation were approximately the same, and the gain for off-vertical axis rotation was close to unity for stimulation velocities up to 50-60°/second. This suggests that the system is operating in an open-loop fashion.

From these considerations, we would formulate the organization of nystagmus induced by steps of velocity during off-vertical axis rotation to be as follows. Initially during rotation, the semicircular canals drive the eyes in a compensatory fashion and information from the otolith organs that is centrally constituted to represent head velocity with regard to gravity is canceled. As the velocity signal from the cupula wanes, the central otolith velocity command continues to excite the velocity storage integrator. This drives the eyes for as long as rotation continues. During acceleration, the cupula is deflected in the opposite direction.

Its activity is summed with that in the storage integrator to reduce the after-response. The time constant of the storage integrator is reduced so that there is virtually no storage of activity in response to the cupula deflection at the end of rotation. The inference that the response to off-vertical axis rotation utilizes mainly the velocity storage integrator to produce slow changes in eye velocity suggests that it functions primarily to aid the VOR in generating a sustained head-velocity signal in the absence of vision.

It is of interest that a similar type of continuous excitation is produced by oscillating the head during vertical axis rotation. This type of movement induces Coriolis forces as well as forces of gravity on the otolith organs. In addition there is excitation of the vertical canals as their planes are moved into the plane of rotation while the horizontal canals are moved out of the plane of rotation. The extent to which each contributes to the generation of nystagmus is speculative. However, both off-axis rotation and oscillating the head during vertical axis rotation appear to excite the velocity storage integrator to generate continuous nystagmus. Both types of excitation elicit dynamic ocular reflexes that enhance the ocular compensatory response to head movement. These reflexes also would be of value in perceiving head movement and making postural readjustments in the absence of vision.

ACKNOWLEDGMENT

We thank Debra Dennett for assistance.

REFERENCES

1. COHEN, B., V. MATSUO & T. RAPHAN. 1977. Quantitative analysis of the velocity characteristics of optokinetic nystagmus and optokinetic after nystagmus. *J. Physiol.* **270**: 321-344.
2. MOWRER, O. H. 1934. The modification of vestibular nystagmus by means of repeated elicitation. *Comp. Psychol. Monogr.* **9**: 1-48.
3. TER BRAAK, J. W. G. 1936. Untersuchungen uber optokinetischen Nystagmus. *Arch. Neerl. Physiol.* **21**: 309-376.
4. MOWRER, O. H. 1937. The influence of vision during bodily rotation upon the duration of post-rotational vestibular nystagmus. *Acta Otolaryngol. (Stockh.)* **25**: 351-364.
5. RAPHAN, T., V. MATSUO & B. COHEN. 1979. Velocity storage in the vestibulo-ocular reflex arc (VOR). *Exp. Brain Res.* **35**: 229-248.
6. GUEDRY, F. E. 1965. Orientation of the rotation-axis relative to gravity: its influence on nystagmus and the sensation of rotation. *Acta Otolaryngol. (Stockh.)* **60**: 30-48.
7. BENSON, A. J. & M. A. BODIN. 1966. Interaction of linear and angular accelerations on vestibular receptors in man. *Aerosp. Med.* **37**: 144-154.
8. CORREIA, M. J. & F. E. GUEDRY. 1966. Modification of vestibular responses as a function of rate of rotation about an earth-horizontal axis. *Acta Otolaryngol. (Stockh.)* **62**: 297-308.
9. YOUNG, L. R. & V. HENN. 1975. Nystagmus produced by pitch and yaw rotation of monkeys. *Fortschr. Zool.* **23**: 235-246.
10. BOND, H. W. & P. HO. 1970. Solid miniature silver-silver chloride electrodes for chronic implantation. *Electroencephalogr. Clin. Neurophysiol.* **28**: 206-208.
11. SKAVENSKI, A. A. & D. A. ROBINSON. 1973. Role of abducens motoneurons in the vestibulo-ocular reflex. *J. Neurophysiol.* **36**: 724-738.
12. KELLER, E. L. 1978. Gain of the vestibulo-ocular reflex in monkey at high rotational frequencies. *Vision Res.* **18**: 311-315.

13. GOLDBERG, J. M. & C. FERNÁNDEZ. 1971. Physiology of peripheral neurons innervating semicircular canals of the squirrel monkey. I. Resting discharge and response to constant angular accelerations. *J. Neurophysiol.* **34**: 635-660.
14. GOLDBERG, J. M. & C. FERNÁNDEZ. 1981. Physiological mechanisms of the nystagmus produced by rotations about an earth-horizontal axis. *Ann. N.Y. Acad. Sci.* (This volume.)
15. GRAYBIEL, A. & E. F. MILLER. 1968. The otolith organs as a primary etiological factor in motion sickness: with a note on "off-vertical" rotation. In *Fourth Symposium on the Role of Vestibular Organs in Space Exploration*. NASA Publication No. SP-187: 53-64. National Aeronautics and Space Administration. Washington, D.C.
16. BENSON, A. J. 1974. Modification of the response to angular acceleration by linear accelerations. In *Handbook of Sensory Physiology*. H. H. Kornhuber, Ed. **6**: 281-320. Springer-Verlag. Berlin, Federal Republic of Germany.
17. FERNÁNDEZ, C. & J. M. GOLDBERG. 1975. Physiology of peripheral neurons innervating otolith organs of the squirrel monkey. III. Response dynamics. *J. Neurophysiol.* **39**: 996-1008.
18. LOWENSTEIN, O. 1936. The equilibrium function of the vertebrate labyrinth. *Biol. Rev.* **11**: 113-145.
19. LOWENSTEIN, O. & T. D. M. ROBERTS. 1949. The equilibrium function of the otolith of the thornback ray (*Raja clavata*). *J. Physiol. London* **110**: 392-415.
20. LOE, P. R., D. L. TOMKO & G. WERNER. 1973. The neural signal of angular head position in primary afferent vestibular nerve axons. *J. Physiol. London* **230**: 29-50.
21. FERNÁNDEZ, C., J. M. GOLDBERG & W. K. ABEND. 1972. Responses to static tilts of peripheral neurons innervating otolith organs of the squirrel monkey. *J. Neurophysiol.* **35**: 978-997.
22. FERNÁNDEZ, C. & J. M. GOLDBERG. 1975. Physiology of peripheral neurons innervating otolith organs of the squirrel monkey. II. Directional selectivity and force-response relations. *J. Neurophysiol.* **39**: 985-995.
23. FERNÁNDEZ, C. & J. M. GOLDBERG. 1975. Physiology of peripheral neurons innervating otolith organs of the squirrel monkey. I. Response to static tilts and to long-duration centrifugal force. *J. Neurophysiol.* **39**: 970-984.
24. ROBINSON, D. A. 1980. *Neurosci. Res. Program Bull.* **18**(4): 582-588.
25. HENN, V., B. COHEN & L. R. YOUNG, Eds. 1980. Visual-Vestibular Interaction in Motion Perception and the Generation of Nystagmus. *Neurosci. Res. Program Bull.* **18**(4).
26. SUZUKI, J. I., K. TOKUMASU & K. GOTO. 1969. Eye movements from single utricular nerve stimulation in the cat. *Acta Otolaryngol. (Stockh.)* **68**: 350-362.
27. SCHWINDT, P. C., A. RICHTER & W. PRECHT. 1973. Short latency utricular and canal input to ipsilateral abducens motoneurons. *Brain Res.* **60**: 259-262.
28. BAKER, R., W. PRECHT & A. BERTHOZ. 1973. Synaptic connections to trochlear motoneurons determined by individual nerve branch stimulation in the cat. *Brain Res.* **64**: 402-406.

DYNAMIC CHARACTERISTICS OF THE OTOLITHIC OCULOMOTOR SYSTEM

Takashi Tokita, Hideo Miyata, Michihiro Masaki,
and Sadahide Ikeda

*Department of Otorhinolaryngology
Gifu University School of Medicine
Gifu, Japan*

INTRODUCTION

The function of the human vestibulo-ocular system is expressed most distinctly by the jumbling phenomenon appearing in cases with bilateral loss of labyrinthine excitability.³ In these cases, the patients can see visual objects clearly when they themselves are at rest, but cannot recognize objects distinctly while in motion, for example, when walking or running. This indicates that the human vestibulo-ocular reflex works to perceive periodic accelerations imposed upon the head, to induce eye movements, and to maintain visual fixation on targets during motion. Therefore, examination of the ability to induce eye movements corresponding to periodic head movements at various frequencies would appear to be a promising way to examine the vestibulo-ocular system.

From this point of view, we attempted to determine a transfer function of the vestibulo-ocular system in humans. In the present investigation, a vertical eye tracking test, an up-down test, and a running test in the dark and light were carried out to obtain Bode plots of transfer functions of the opto-oculomotor, otolithoc oculomotor, and opto-otolithoc oculomotor systems.

METHODS

Vertical Eye Tracking Test

The subject was asked to follow the upward-downward movement of a light spot projected on a screen. The target movement and eye movement were simultaneously recorded by a two-channel pen-writing recorder and a magnetic tape recorder for about two minutes. The target movement was made as random as possible, with variations of $\pm 10^\circ$ of visual angle and a frequency range of 0.1 to 5 Hz.

Up-Down Test

The subject was requested to sit on an ascending-descending stool with his head and trunk fixed. A repetitive vertical displacement was given to the subject, and upward and downward head movements and vertical eye movements were recorded simultaneously for two minutes. The movement of the stool was performed pseudorandomly, with an amplitude range of ± 17 cm and a frequency range of 0.1 to 5 Hz. The head movement was recorded by tracking the movement of a light spot attached to the head, by the aid of a television camera. An

electro-oculographic technique was used to record the eye movement. The test was performed in the dark and light with the eyes open. The test in the dark was performed in a dark room. The subject wore blackout goggles, but was asked to keep his eyes open. For the test in the light, the subject was asked to fix his vision upon a spot at a distance of one meter.

Running Test

The subject was asked to run in place with the rhythm changed arbitrarily. The right-left, forward-backward, and upward-downward movements of the

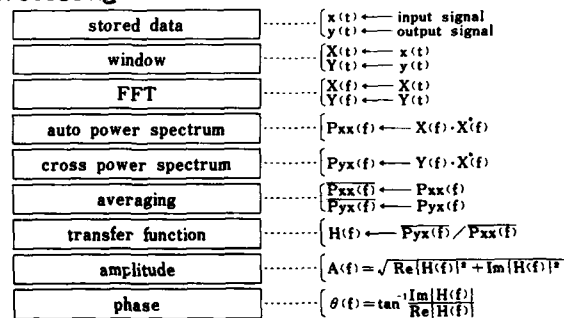
recording

- | | |
|-----------------|--|
| 1. vertical ETT | { target movement
eye movement |
| 2. up-down test | { head movement (displacement)
eye movement |
| 3. running test | { head movement (acceleration)
eye movement |

data sampling to PDP-12 computer

rate 25Hz length 102.5Hz

data processing



display

Bode plots
(gain and phase diagram) frequency range 0.1~12.5Hz

FIGURE 1. Data processing.

head and vertical movement of the eye induced by running were recorded with the aid of a five-channel telemeter. Three-dimensional head movement was recorded with three accelerometers attached to a helmet that the subject wore. The test was performed in the dark and light. The test conditions were the same as those for the up-down test.

Data Processing

From the signals recorded on the magnetic tapes, the transfer function for each system was calculated using a specially designed program with a PDP-12

computer. (See FIGURE 1.) Then the gain and phase were expressed as a Bode plot on a cathode ray tube. The Bode plot was expressed in the frequency range from 0.1 to 12.5 Hz in 0.1-Hz steps. However, the evaluation was made for a frequency range from 0.1 to 5.0 Hz, because the power of the input signal was low in any frequency range exceeding 5 Hz.

In calculating the transfer function, target displacement was used as input and eye displacement as output in the eye tracking test, and head displacement was used as input and eye displacement as output in the up-down test. The transfer function was calculated with the right-left, forward-backward, and upward-downward head acceleration as input, and eye displacement as output, in the running test.

Subjects

Ten healthy male adults and five patients with bilateral loss of labyrinthine excitability were examined.

RESULTS

Vertical Eye Tracking Test and Up-Down Test in Healthy Adults

FIGURE 2 shows records obtained from a normal subject. The upper figure is a record of the eye tracking test. In portions where frequency of target movement was low, the eye movement was in accordance with the target movement. In portions where the frequency was high, the amplitude of the eye movement was smaller than that of the target movement. The middle figure indicates a record of the up-down test in the dark. It is difficult to find any eye movement corresponding to head movement that was low in frequency. On the other hand, the higher the frequency of head movement, the more distinct the eye movement; at such times, the amplitude of the eye movement was larger than that of the head movement. The phase of head movement was almost opposite to that of eye movement. The lower figure is a record of the up-down test in the light. In portions where head movement was at low and middle frequencies, eye movement with similar amplitude appeared, but with a phase opposite that of head movement. When head movement was of high frequency, it was possible to find an eye movement with an amplitude larger than that of the head movement.

FIGURE 3 shows averaged Bode plots obtained from healthy adults in the eye tracking test and the up-down test in the dark and light. The mean and standard deviations are also given. The upper figures are averaged Bode plots of the vertical opto-oculomotor system obtained by the vertical eye tracking test. When the frequency exceeded 1 Hz, the gain decreased and the phase was prolonged. The vertical opto-oculomotor system has an innate ability to follow the target movement up to 1 Hz. The middle figures are averaged Bode plots of the otolithic oculomotor system obtained in the up-down test in the dark. The gain increased linearly at a rate of 20 dB/decade with an increase of frequency from 0.7 to 5 Hz. The phase curve was relatively flat, indicating a phase lag of 180 degrees. Thus, the otolithic oculomotor system performs a derivative control in inducing eye movement by head displacement. The lower figures show averaged Bode plots of the opto-otolithic oculomotor system obtained in the up-down test in the light.

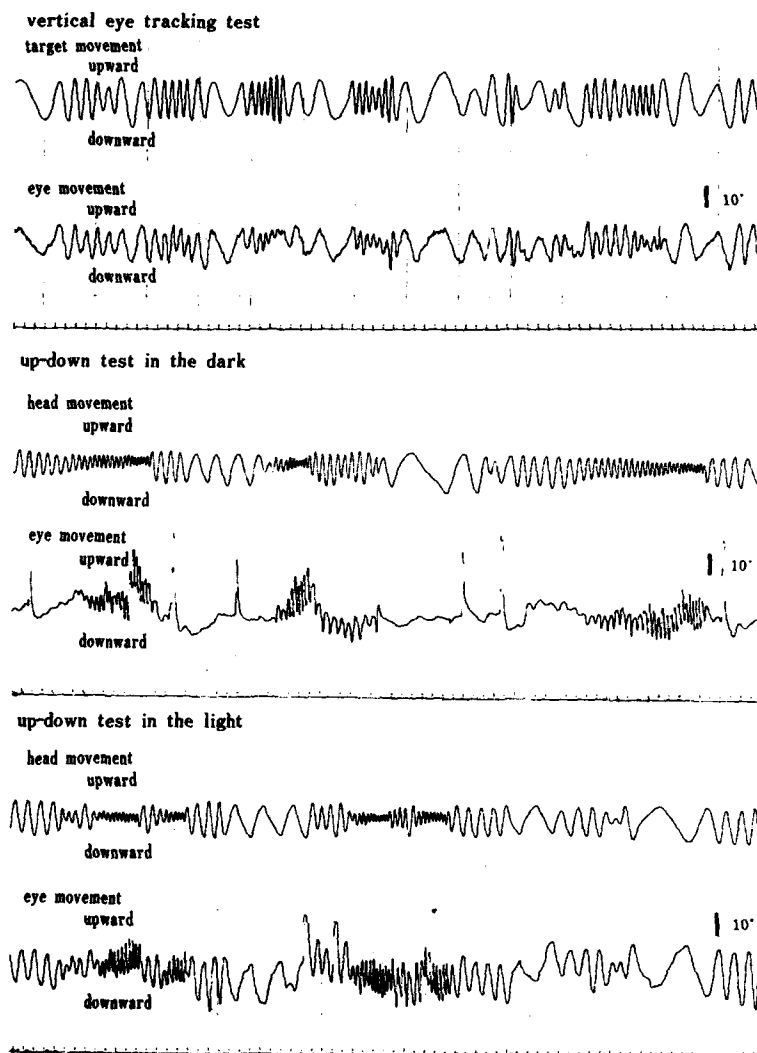


FIGURE 2. Records obtained from vertical eye tracking test (ETT) and up-down test (UDT) in a healthy adult male.

The gain and phase were relatively flat in the frequency ranges from 0.3 to 2.5 Hz. Moreover, when the frequency exceeded 2.5 Hz, the gain increased with the increase in frequency. Visual tracking capability increased to high frequency in a cooperative action of the opto-oculomotor and otolithic oculomotor systems rather than by action of the opto-oculomotor system alone. This indicates that the otolithic oculomotor system plays an important role in visual fixation during head movement whose frequency exceeds 1 Hz. Moreover, when the frequency of the

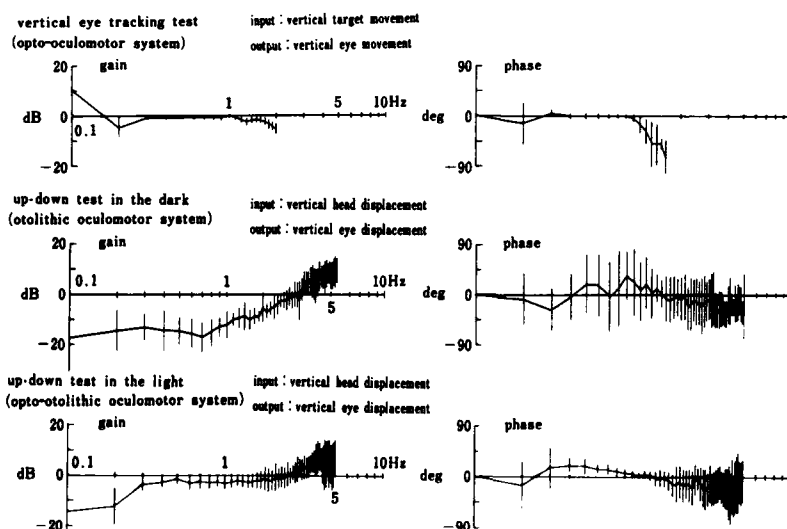


FIGURE 3. Averaged Bode plots of transfer function obtained from vertical eye tracking test and up-down test in 10 healthy adults.

head exceeds 2.5 Hz, the otolithric oculomotor reflex predominates over the opto-oculomotor reflex.

Vertical Eye Tracking Test and Up-Down Test in Patients with Bilateral Loss of Labyrinthine Excitability

FIGURE 4 shows records obtained from the test of a patient with bilateral loss of labyrinthine excitability due to streptomycin intoxication. The upper figure is a record of the eye tracking test. In portions where the frequency of the target movement was low, eye movement corresponded to target movement. The middle figure is a record of the up-down test in the dark. Eye movement corresponding to head movement was not observed. The lower figure is a record of the up-down test in the light. We note here eye movement corresponding to head movement.

FIGURE 5 shows Bode plots obtained from the tests of this same patient. As shown in the upper figures, gain and phase curves obtained by the eye tracking test are similar to those of normal subjects. The middle figures are Bode plots obtained in the up-down test in the dark. Values of the gain and phase were scattered. The frequency-dependent gain enhancement that was observed in the Bode plot in normal subjects is not observed here. The lower figure is a Bode plot obtained by the up-down test in the light. Gain values were low and scattered compared to the gain diagram obtained from action of the opto-oculomotor system alone, which is indicated in the upper figure. This result suggests that loss of the otolithric oculomotor reflex causes a disturbance in the action of the opto-oculomotor system during up-down movement.

Three of the five patients showed similar results. However, two cases showed

a periodic eye movement in the up-down test in the dark, indicating a dispersion of the gain and phase values. These two cases had suffered a loss of bilateral labyrinthine excitability for about 10 years.

Running Test in Healthy Adults

FIGURE 6 shows records obtained from running tests in the dark and light. In both records, the right-left, forward-backward, and upward-downward accelera-

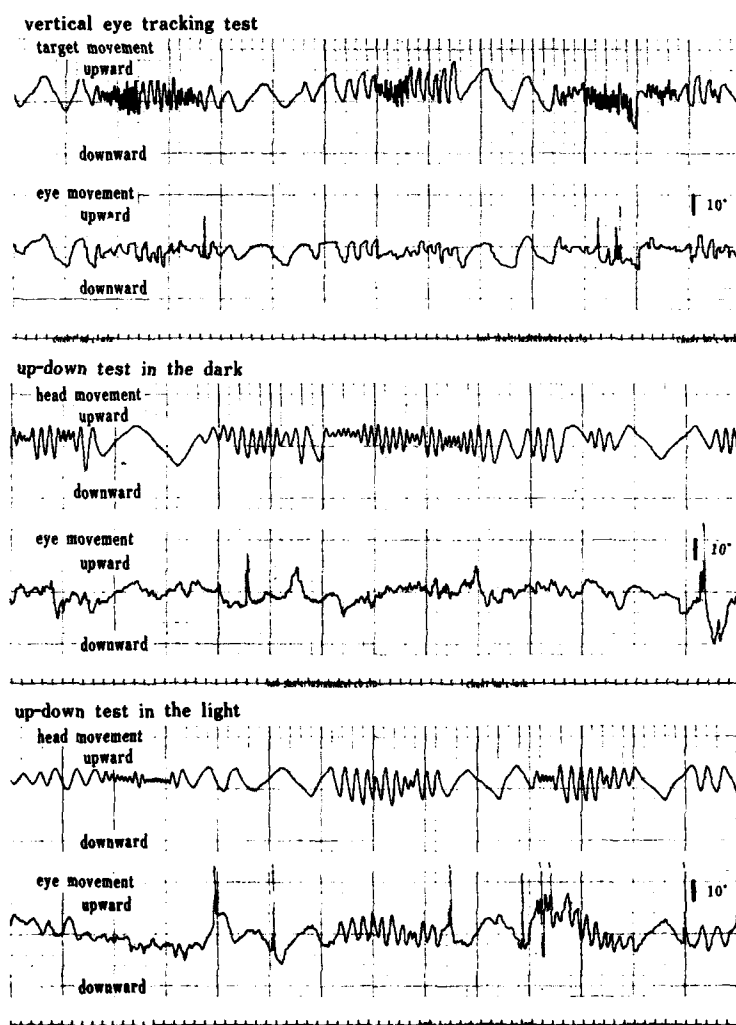


FIGURE 4. Records obtained from vertical eye tracking test and up-down test in a patient with bilateral loss of labyrinthine excitability.

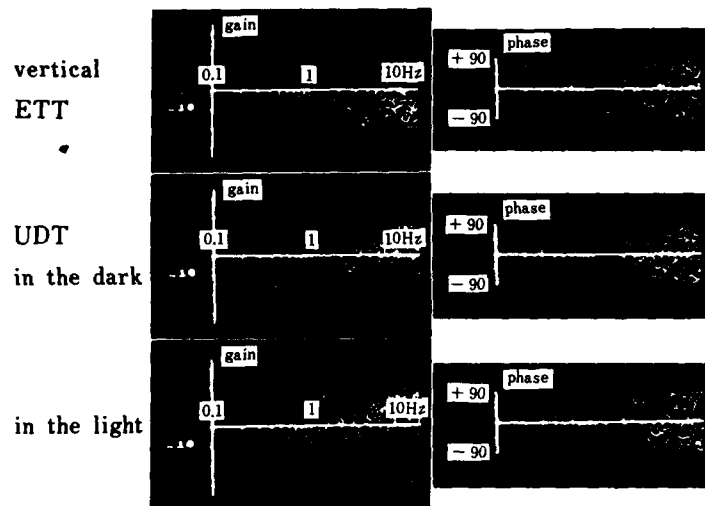


FIGURE 5. Bode plots obtained from vertical eye tracking test and up-down test in a patient with bilateral loss of labyrinthine excitability.

tions were present in the head movement. The upward-downward acceleration was the strongest and most striking. Moreover, a vertical eye movement corresponding to the vertical head movement was observed. In the portion of the head movement exhibiting a high frequency, the amplitude of the eye movement became larger than that of the head movement.

FIGURE 7 indicates average Bode plots of the transfer function obtained in the running tests in the dark and light. In addition, the averaging was done assuming that the gain at 1 Hz was 0 dB. The transfer function was calculated with the vertical head acceleration as input and the vertical eye movement as output. As shown in the upper left figure, the gain obtained by the test in the dark linearly decreased with increase of frequency from 0.3 to 3 Hz. The inclination was about 40 dB/decade in the frequency range from 0.3 to 1 Hz. It decreased in the portion where the frequency was higher than 1 Hz. The phase hovered near zero, indicating that eye displacement had the same phase as the head acceleration. This Bode plot was calculated with the head acceleration as input and the eye displacement as output. Therefore, the result indicates that eye displacement is almost in proportion to head displacement. As shown in the lower figures, the Bode plots obtained by the test in the light are similar to those of the test in the dark. However, the decrease in gain was more linear than that in the dark. The result indicates that during running in the light, eye movement is proportional to head displacement in the frequency range from 0.3 to 3 Hz. Moreover, the vertical eye movement was in proportion to the vertical head movement even when the running test was conducted in the dark. This finding indicates that in a daily, active movement such as running, the otolithic oculomotor system induces eye movement proportional to head displacement without cooperation of the opto-oculomotor system.

The transfer function was calculated with right-left and forward-backward head acceleration as input and with vertical eye movement as output (FIGURE 8). The gain was not linear, and the phase was more dispersed than in the Bode plot

obtained with the upward-downward head acceleration as input and the vertical eye movement as output. Accordingly, this shows that vertical eye movement is the main response to the vertical head acceleration.

Running Test in Patients with Bilateral Loss of Labyrinthine Excitability

FIGURE 9 indicates records of the running tests in a patient with bilateral loss of labyrinthine excitability due to streptomycin intoxication. The patient complained of the jumbling phenomenon. As shown in the upper figure, the

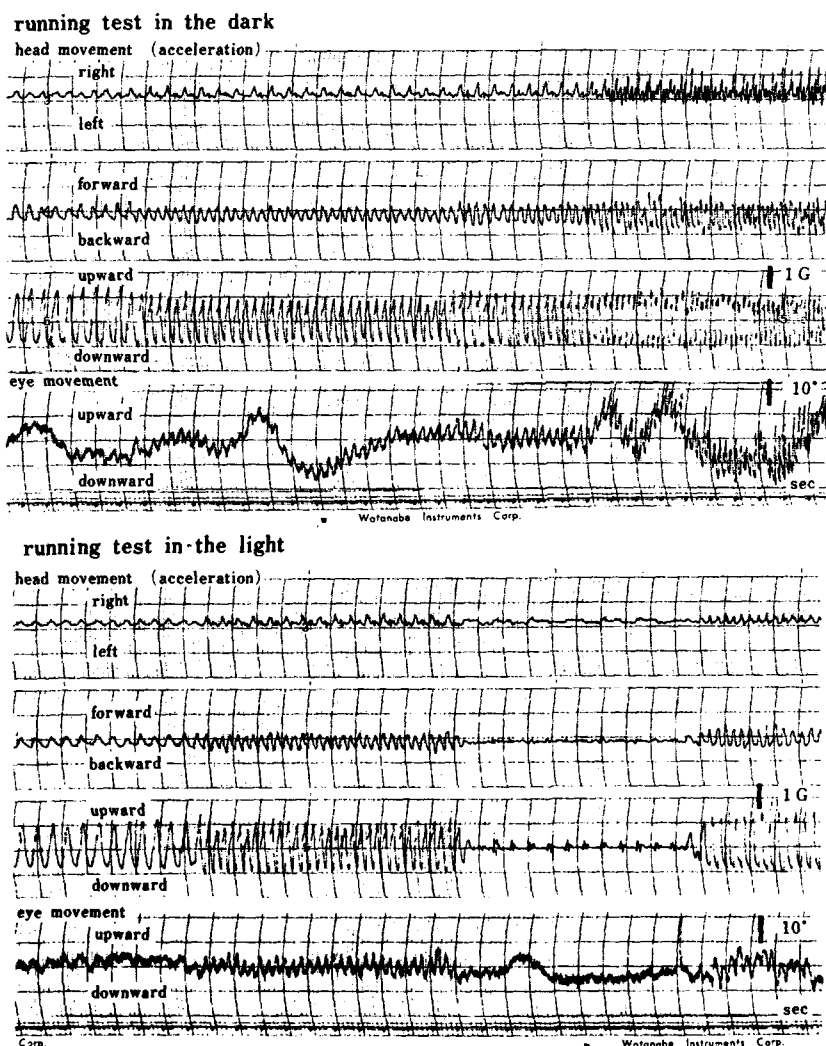


FIGURE 6. Records obtained from running test in a healthy adult male.

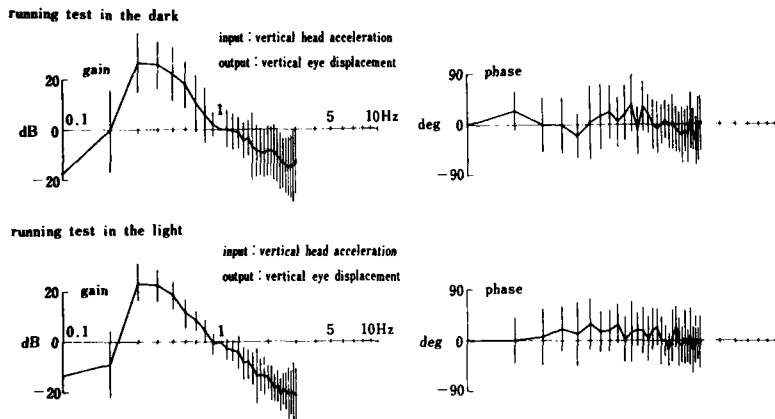


FIGURE 7. Averaged Bode plots of transfer function obtained from running test in 10 healthy adults. Input: vertical head acceleration. Output: vertical eye displacement.

record obtained from the running test in the dark indicated a rhythmic eye movement corresponding to the vertical head acceleration. In spite of loss of labyrinthine function, periodic vertical eye movement was induced. The findings were observed in all five cases with bilateral loss of labyrinthine excitability. The lower figure indicates a record of the running test in the light. Vertical eye movement corresponding to vertical head acceleration is noticed.

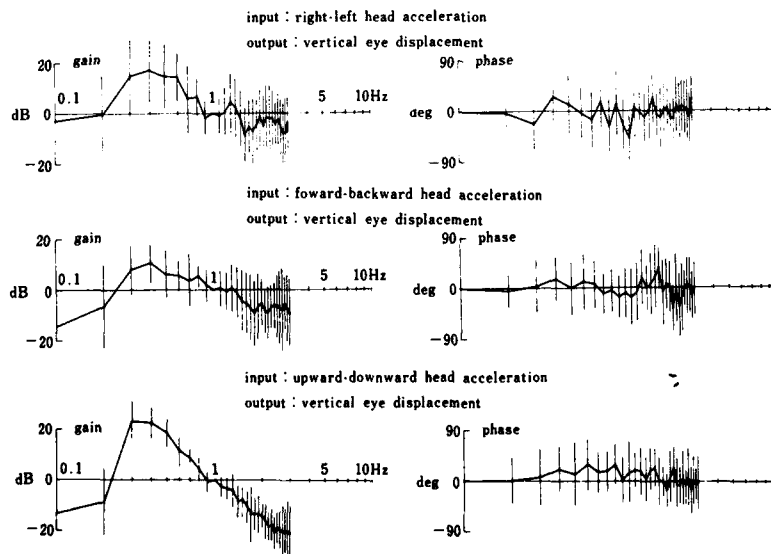


FIGURE 8. Averaged Bode plots of transfer function obtained from running test in 10 healthy adults. Input: right-left, forward-backward, upward-downward head acceleration. Output: vertical eye displacement.

FIGURE 10 shows Bode plots obtained from the case presented in FIGURE 9. The gain and phase diagrams obtained from the eye tracking test are similar to those of normal subjects. Gain and phase obtained from the running test in the dark are shown in the middle of the figure. Values of gain and phase are dispersed. The linear decrease of gain with increase of frequency, which was observed in the gain diagram of normal subjects, is not present. This finding indicates that regular eye movement corresponding to head movement is lost. Gain obtained in the running test in the light indicated a decrease with increase

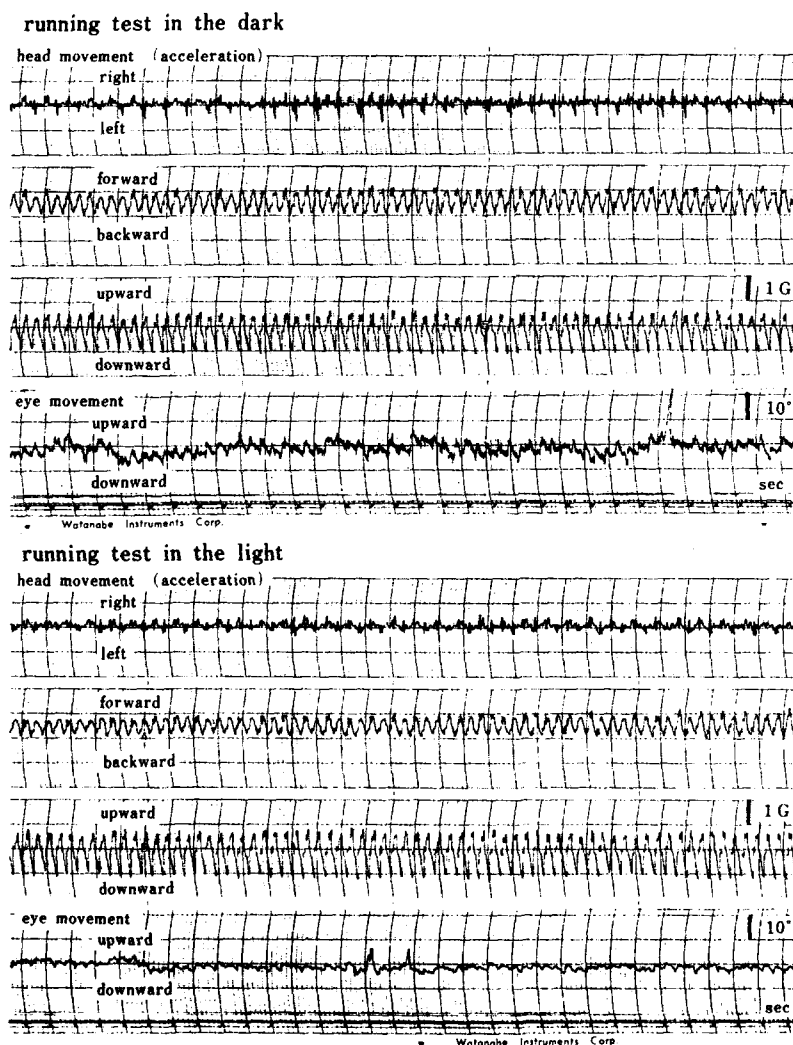


FIGURE 9. Records obtained from running test in a patient with bilateral loss of labyrinthine excitability.

of frequency. However, values of gain and phase were not well controlled. The scatter in gain was seen not only in the frequency range of more than 1 Hz, but also in the frequency range of less than 1 Hz, where the opto-oculomotor system plays a major role in visual fixation. This suggests that loss of otolithic oculomotor reflexes causes a disturbance in the functioning of the opto-oculomotor reflexes during running in the light. These are objective measures of the jumbling phenomenon.

DISCUSSION

There have been several studies of dynamic characteristics of the otolithic-oculomotor system. The mathematical model of the otolith was reported by Meiry

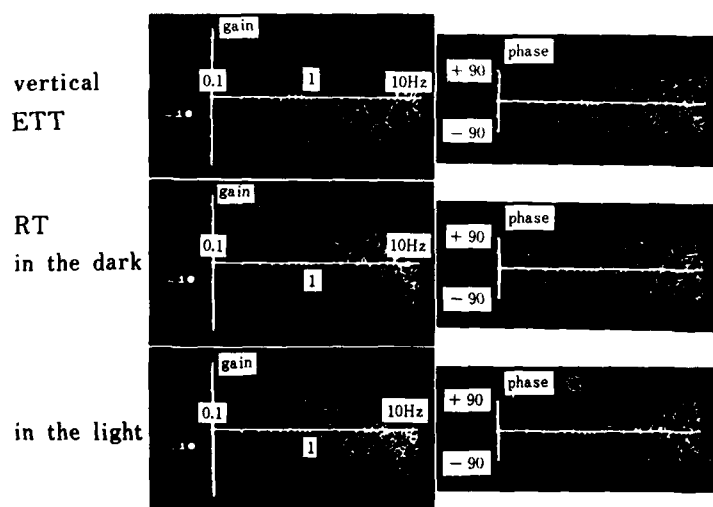


FIGURE 10. Bode plots obtained from running test in a patient with bilateral loss of labyrinthine excitability.

and Young and Meiry.^{7,11} Electrophysiological studies on the response of the peripheral otolith neurons to a sinusoidal force in squirrel monkeys were reported by Fernández and Goldberg.⁴ They indicated that units that were irregular in their sensitivity to a 1-g force showed a 20-fold frequency-dependent gain enhancement over the spectrum from 0 to 2.0 Hz. The dynamics of the otolithic system in humans were observed in counterrolling by Kellog; in the sinusoidal component of barbecue nystagmus by Benson and Bodin and Correia and Guedry; in eye movement produced by sinusoidal linear acceleration by Niven, Hixson, and Correia and Vidic *et al.*; and in subjective detection in the direction of the vertical movement by Malcolm and Melvill Jones and Melvill Jones and Young.^{1,2,5,6,8-10}

In dealing with the vertical otolithic response, Malcolm and Melvill Jones and Melvill Jones and Young reported difficulty in subjective detection of the direction of the vertical movement.^{6,8} Niven, Hixson, and Correia mentioned that

horizontal nystagmus appeared during periodic linear acceleration, and presumed that an effective stimulus might be a dynamic change of the linear acceleration component.⁹ However, they recognized no vertical nystagmus. Vidic et al. observed eye movement during a repeated vertical displacement at a periodicity of two seconds.¹⁰ They found that there was very little smooth eye movement during imagined fixation in the dark, and that a brief flash of fixed light increased the amplitude of eye movement.

These investigations suggest that any vertical otolith response would not be distinct. We have clarified the dynamic characteristics of the vertical otolith response because we observed the otolith oculomotor response in a frequency range higher than that observed by previous investigators and during an up-down movement of small amplitude that did not induce nystagmus.

Two of five patients with bilateral loss of labyrinthine excitability exhibited periodic eye movements in the up-down test in the dark, and all five cases showed a periodic eye movement in the running test in the dark. This is reflected in the scatter in the gain and phase values, and suggests that there may be factors other than the otolith oculomotor response producing the eye movements observed in the up-down and running tests. We suppose that eye movements are induced also by the cervico-ocular reflex, central programming, and inertial force.

SUMMARY

Vertical eye tracking test, up-down test, and running test in the dark and light were carried out to obtain Bode plots of transfer function of the opto-oculomotor, otolith oculomotor, and opto-otolith oculomotor systems.

1. The gain and phase of the opto-oculomotor system obtained from the vertical eye tracking test were flat in a frequency range of 0.3 to 1.0 Hz.

2. During the up-down test in the dark, the gain of the otolith oculomotor system linearly increased at the rate of 20 dB/decade with an increase of frequency from 0.7 to 5 Hz.

3. During the up-down test in the light, the gain and phase were flat in a frequency range of 0.3 to 2.5 Hz.

4. The transfer function calculated with vertical head acceleration as input and vertical eye movement as output in the running test in the dark was similar to that in the light. The gain linearly decreased at the rate of 40 dB/decade with increase of frequency from 0.3 to 3.0 Hz. During running, eye displacement is almost in proportion to the head displacement in both dark and light. In daily, active movement such as running, eye movement proportional to head displacement appears without collaborative action of the opto-oculomotor system.

5. All five patients with bilateral loss of labyrinthine excitability exhibited a similar opto-oculomotor response to that of normal subjects. Three of the five patients did not show any eye movement corresponding to head movement in the up-down test in the dark. However, two patients showed a periodic eye movement in the same test, indicating dispersion of the gain and phase values.

6. These patients exhibited a rhythmic eye movement corresponding to head movement in the running test in the dark and light. However, values of gain and phase obtained in both tests were scattered. The variations in gain obtained from the running test in the light were observed in frequency ranges above and below 1 Hz.

REFERENCES

1. BENSON, A. J. & M. A. BODIN. 1966. Interaction of linear and angular accelerations on vestibular receptors in man. *Aerosp. Med.* **37**: 144-154.
2. CORREIA, M. J. & F. E. GUEDRY, JR. 1966. Modification of vestibular responses as a function of rate of rotation about an earth-horizontal axis. *Acta Otolaryngol.* **62**: 298-308.
3. DANDY, W. E. 1941. The surgical treatment of Meniere's disease. *Surg. Gynecol. Obstet.* **72**: 421-425.
4. FERNÁNDEZ, C. & J. M. GOLDBERG. 1976. Physiology of peripheral neurons innervating otolith organs of the squirrel monkey. *J. Neurophysiol.* **39**: 996-1008.
5. KELLOC, R. S. 1965. Dynamic counterrolling of the eye in normal subjects and in persons with bilateral labyrinthine defects. In Publication No. SP-77: 195-202. National Aeronautics and Space Administration. Washington, D.C.
6. MALCOLM, R. & G. MELVILL JONES. 1974. Erroneous perception of vertical motion by humans seated in the upright position. *Acta Otolaryngol.* **77**: 274-283.
7. MEIRY, J. L. 1958. The vestibular system and human dynamic space orientation. Sc.D. Thesis. Massachusetts Institute of Technology. Cambridge, Mass.
8. MELVILL JONES, G. & L. R. YOUNG. 1978. Subjective detection of vertical acceleration, a velocity-dependent response? *Acta Otolaryngol.* **85**: 45-53.
9. NIVEN, J. I., W. C. HIXSON & M. J. CORREIA. 1966. Elicitation of horizontal nystagmus by periodic linear acceleration. *Acta Otolaryngol.* **62**: 429-441.
10. VIDIC, T. R., J. S. BARLOW, C. M. OMAN, J. R. TOLE, A. D. WEISS & L. R. YOUNG. 1976. Human eye tracking during vertical and horizontal motion. *Neurosci. Abstr.* [Revised] No. 1536: 1062.
11. YOUNG, L. R. & J. L. MEIRY. 1968. A revised dynamic otolith model. *Aerosp. Med.* **39**: 606-608.

BINOCULAR COUNTERROLLING IN HUMANS WITH UNILATERAL LABYRINTHECTOMY AND IN NORMAL CONTROLS

Shirley G. Diamond and Charles H. Markham

*Reed Neurological Research Center
University of California School of Medicine
Los Angeles, California 90024*

Ocular counterrolling (OCR) is the reflex torsion of the eyes about their visual axes in the direction opposite to the head as it is rolled about its naso-occipital axis. Considered to be mediated by the otolith receptors in the utricle,¹⁻³ OCR is an observable behavior that invites inferences on the complex functions of the inner ear. More than 75 years of effort have been devoted to the seemingly simple task of comparing OCR in persons with known unilateral lesions to that of normal persons, focusing on the amplitude of OCR under static tilt. The contradictory results of the several studies, as reviewed below, suggest that this measure is not a productive parameter in detecting unilateral otolith dysfunction.

Bárány is credited with first introducing OCR to the clinic in 1906.^{4,5} He examined the response in normals and in deaf-mutes, and felt that OCR was regulated by the semicircular canals. In 1925, Kompanejetz examined OCR in 48 deaf-mutes, tilting their heads 30° to the right and looking at both eyes "simultaneously" (actually sequentially).⁵ He separated his patients into two groups, one having some response to caloric or rotatory stimulation, and the other group having none. He found the presence and absence of OCR in both groups and therefore concluded that OCR was innervated from a point independent of the semicircular canals. He further observed that OCR may be different in the two eyes, suggesting that "in an asymmetrically injured otolith apparatus, a disturbance of the associated eye movements may occur, manifesting itself in different angles for the two eyes in counterrolling."⁵

A few years later, Kompanejetz looked at 100 normal subjects to see if both eyes performed equally.⁶ He observed that there was more OCR in the right eye when the head was inclined to the right and more in the left eye when the head was inclined to the left. He also found that both eyes showed more OCR on tilt to the right than on tilt to the left. He considered it normal to find differences of 5° in a given eye when tilted to either side, or of 3-4° between the two eyes when the head was tilted to one side. Unfortunately, this study differed in design and followed his work in the deaf-mute patients, so he was unable to make comparable observations in persons with labyrinthine defects. He wrote, "It is regrettable that up to now we have not succeeded in commanding such methods [for the otolith apparatus] as may be used for examining the functions of the semicircular canals."⁶ Today, more than 50 years later, we may say the same.

Many investigators over the years have studied OCR in a variety of experimental designs. In 1936, Gollas studied seven patients with unilateral labyrinthine and cochlear destruction.⁷ He held them at 20, 40, 60, and 90° positions on both sides and examined OCR in both eyes. He found that tipping to the side of the lesion resulted in normal OCR, but that tipping to the contralateral side produced much less OCR. He found no difference in the two eyes.

In 1963, Miller and Graybiel compared OCR in 9 normal persons to 10

subjects with bilateral defects and deafness caused by meningitis.⁸ All the deaf persons had absent caloric responses. Miller and Graybiel tilted subjects to 25, 50, and 75° on either side, held them at each position for some minutes, and photographed the right eye. They found that normal subjects had a mean maximum OCR of 4.75 to 7.75° to either side, and it was the same for both directions of tilt. In the patients, they found maximum means ranging from 0.5 to 3.0° to a side. Two of these bilaterally affected patients had no OCR in either direction; one had OCR only to right tilt. These investigators observed that significant amounts of OCR remained in several of the patients, ascribed it to residual otolith function, and stated that demarking the OCR responses in these patients from normals was difficult.

In a later work, Miller studied three patients with unilateral dysfunction from Meniere's disease and streptomycin therapy, finding that two had OCR symmetric to both sides and one had more OCR when tilted to his diseased ear.⁹ Nonetheless, Miller concluded that diagnosis of unilateral loss of otolith function as reflected in an asymmetrical OCR response to rightward or leftward tilt appeared possible. He said, "The reflex act of the eyes rolling conjugately about their lines of sight appears the most valid indicator of otolith activity."⁹ (As none of his studies looked at both eyes, the reference to conjugate activity is unclear.)

In 1971, Krejcova *et al.* looked at OCR in intact rhesus monkeys and following serial labyrinthectomies.¹⁰ They found 5-7° OCR to either side in the intact animals whether tipped to 45 or to 90°. An intact animal that had had 8° OCR when tipped to the left, had only 2° three weeks after the left labyrinth was destroyed. When tilted to the right, OCR was unchanged from the preoperative state. The right labyrinth was then destroyed; and one week later, tipping the animal to the right produced OCR of 1.5° compared to 4.5° in the intact condition. Krejcova *et al.* concluded that OCR is induced mainly by the downward utricle. They also found that OCR was not different in the presence or absence of vision.

Nelson and Cope tilted 35 normal subjects 50° to either side, looked at both eyes in separate observations, and found means of 5.4 to 6.5° in each eye to each side.¹¹ They looked at 11 patients with benign postural vertigo and found that tilt toward the side that produced the vertigo resulted in significantly less OCR than did tilt to the "good" side. These workers referred to the "persistent, static nature of OCR with sustained head tilt" but did not offer support for this assertion.¹¹ On the contrary, a figure in this paper showing 60 consecutive measures of a subject held in a stationary position reveals only five of these to be the same as the previous measurement, with the range varying 3.25°.

Nelson and House noted that earlier studies on the effect of unilateral vestibular injury had given conflicting reports of decreased OCR on tilt toward the diseased side or decreased OCR on tilt to the normal side, or no consistent asymmetry.¹² Examining magnitude of OCR in 21 patients with unilateral labyrinthectomy or total nerve section, Nelson and House looked at both eyes, one at a time.¹² They found that mean OCR of each eye for either direction was 3°, significantly different from the 6° mean of normals. They found a tendency (apparently not significant) for less OCR on tilt to the side of the lesion in 68% of the eyes measured, the reduction being greatest in the downward eye. Six patients who had had selective sections of the superior vestibular nerve (the portion believed to innervate the utricle), with preservation of the inferior vestibular nerve, showed essentially normal magnitude of OCR. Nelson and House again found a tendency to less OCR on tilt to the lesioned side. Of 17 patients with Meniere's disease or positional vertigo, 13 (76%) had less OCR on tilt to the involved side, particularly in the downward eye. Nelson and House

summarized their findings by stating that OCR activity was halved by complete loss of one labyrinth or vestibular nerve, with a slight trend to less OCR on tilt toward the injured ear.

A 1975 study by Kanzaki looked at the right eye as patients were tipped 30° to either side.¹³ Kanzaki stated that postoperative cases of acoustic neuroma (number of cases is unclear, but may be four) showed that OCR toward the diseased ear was almost absent and that in two preoperative cases of acoustic neuroma, OCR toward the normal side was greatly reduced while OCR toward the diseased side was normal. To express these findings in terms of directions of head tilt rather than directions of eye movements, one would infer that postoperative cases showed reduced OCR when tilted to the normal side and preoperative cases showed reduced OCR when tilted to the diseased side.

A later study by Kanzaki and Ouchi, examining OCR in patients who were positioned at 30 or 45°, found that in seven postoperative cases of unilateral total loss of labyrinthine function (five of these with acoustic tumors), the patients showed reduced OCR when tilted to the diseased side.¹⁴ Six preoperative cases of acoustic neuroma were also studied, and of these, two were found to have abnormal (presumably reduced) OCR when tilted to the normal side, two had abnormal OCR when tilted to the diseased side, and two had no abnormalities. As these findings are opposite to the laterality reported in the earlier Kanzaki paper,¹³ a conclusion is uncertain.

Kanzaki and Ouchi summarized OCR in 75 cases of unilateral inner ear disease and found 9 persons with abnormal or suspicious OCR when tilted to the diseased side and 11 with abnormal or suspicious OCR when tilted to the healthy side.¹⁴ This is a total of 20 cases, and presumably 55 patients showed no abnormality in OCR magnitude. These investigators concluded that judgment of pathology must be based on differences between OCR on right and left tilt rather than on magnitude alone. Values below 2° in either tilt were regarded as abnormal, and differences between the two sides of 5° at 30° tilt or 4° at 45° tilt were regarded as suspicious of otolith dysfunction. The direction of the asymmetry remained contradictory.

To summarize the past attempts to determine the principles governing OCR in cases of unilateral utricular dysfunction, one finds that these studies have focused on magnitude and asymmetry of OCR under conditions of static tilt. Attempts to correlate the side of the reduced OCR or asymmetry with side of injury have produced contradictory results. Further, a significant number of cases of known unilateral vestibular nerve section have shown neither asymmetry nor reduced magnitude. See TABLE 1 for a summary of findings.

It is clear that examining magnitude of OCR when persons are tipped and held at a given position has not proved to be a fruitful approach in detecting unilateral otolith dysfunction, despite persistent application of this method over the last 75 years. Earlier studies in our laboratory suggested that other parameters in OCR profiles while subjects are undergoing dynamic rotation, examining both eyes simultaneously, may be more sensitive delineators of pathology.¹⁵ The present study examines the profiles of OCR in both eyes of patients with unilateral labyrinthectomies and of normal controls during dynamic roll.

METHODS

Subjects were securely strapped into a large, motor-driven tilting apparatus. The centers of the pupils were aligned horizontally, the head positioned and stabilized by a bite bar. The upper part of the face was photographed with a

TABLE 1
MAGNITUDE OF OCULAR COUNTERROLLING IN PREVIOUS STUDIES OF PATIENTS WITH
UNILATERAL INNER EAR DISEASE

Investigator		Magnitude of OCR	
		Tilt to Lesioned Side	Tilt to Normal Side
Gollas (1936) ⁷		normal	reduced
Miller (1969) ⁹	2/3 patients	normal	normal
	1/3 patients	increased	normal
Krejcová et al. (1971) ¹⁰		reduced	normal
Nelson & Cope (1971) ¹¹		reduced	normal
Nelson & House (1971) ¹²		reduced	reduced
Kanzaki (1975) ¹³	preop	reduced	normal
	postop	normal	reduced
Kanzaki & Ouchi (1978) ¹⁴	preop		
	2/6 patients	normal	reduced
	2/6 patients	reduced	normal
	2/6 patients	normal	normal
	postop	reduced	normal
	9/75 patients	reduced	normal
	11/75 patients	normal	reduced
	55/75 patients	normal	normal

camera rigidly attached to the rotating device while subjects were rolled about their naso-occipital axes. The tilting apparatus and camera are described in detail elsewhere.¹⁵ Subjects were rotated at a constant velocity of 3°/second to 90° right-ear down, held steady for 30 seconds, rolled in the opposite direction to 90° left-ear down, held 30 seconds, and brought back to the upright position (trial I). Without stopping, the procedure was repeated (trial II). Acceleration and deceleration during the first and last 20° of rotation were calculated as 0.21°/second².

Subjects were instructed to fixate on the center of the camera lens, and photographs were taken at each 10° of roll, and at each 10 seconds while motionless at the 90° tilt positions. A strobe flash, triggered to fire 0.5 seconds before each photograph was taken, constricted the pupils and provided almost constant pupil size for photography.

Each eye was measured independently, using a dual projector system described earlier in which the image of the counterrolled eye was rotated until it exactly superimposed the image of the eye in the horizontal control position.¹⁵ The practical accuracy of this measurement system is 0.25°.

Six patients with unilateral vestibular nerve sections underwent testing. These were 3 men and 3 women, aged 28 to 62 years, who had had surgery performed 2 to 12 years prior to testing. Normal controls consisted of 12 persons, 7 men and 5 women, aged 23 to 59 years.

RESULTS

Examining amplitude related to head tilt, the traditional parameter of OCR, our normal subjects showed a range of 2.5–11.0° when tipped to one side, these

maxima being achieved between 30° and 90° of body tilt. The total amplitude, side to side, ranged from 7.5–21.5°. The difference in amplitude of OCR between the two directions of tilt in these subjects ranged from 0–6.5°.

In patients with unilateral vestibular nerve sections 2–12 years previous, OCR amplitude ranged from 0.5–13.8° when tipped to one side, with maxima between 20° and 90° of body tilt. Total amplitude side to side ranged from 4.5–22.3°. The difference in amplitude of OCR between the two directions of tilt in these patients ranged from 0–12.0°, with no clear correlation with the side of the lesion.

In brief, the ranges of the normal persons fell entirely within the ranges of the patients, the overlap preventing any differentiation between the two groups in terms of these criteria.

Looking at the data in terms of binocular OCR profiles during dynamic tilt, FIGURE 1 illustrates a typical pattern for D.S., a 41-year-old man. As he was tipped to 90° right-ear down, both eyes rolled smoothly and conjugately to a maximum of -6.5 and -7° at 70° of tilt. As he was brought back up through 0° to the opposite side, his OCR profile continued smooth and mostly conjugate, especially in the 20° at either side of upright. He reached a maximum of +6.5 and +7.25 at 60° left-ear down. In trial II, which was continuous with trial I, he showed essentially the same pattern.

Four characteristics were evident in profiles of this and other normal subjects:

1. Profiles were consistent from trial I to trial II. Although there was considerable variability between subjects, there was a high degree of consistency within subjects, whether examined with continuous trials or from day to day.
2. The two eyes were *conjugate* in their movements most of the time.
3. The profile was generally smooth as OCR was recorded as a function of tilt.

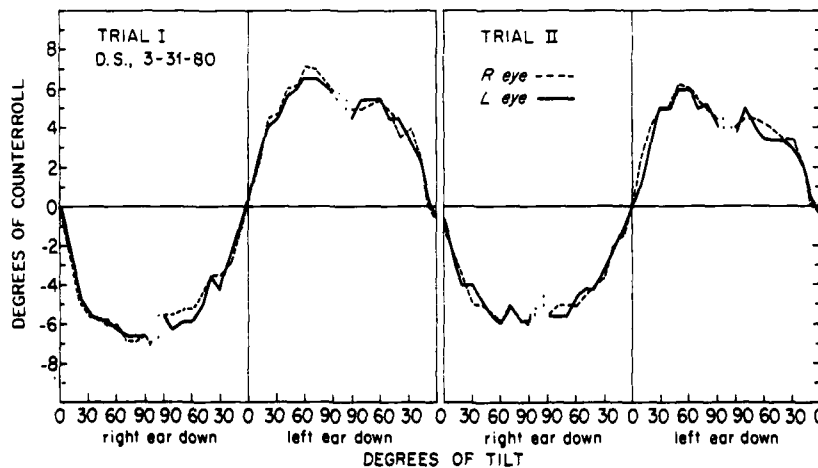


FIGURE 1. Typical normal ocular counterrolling (OCR) response to two consecutive trials, each with subject D.S. rotated at 3°/second to 90° right-ear down, held for 30 seconds, rolled in the opposite direction to 90° left-ear down, held for 30 seconds, and brought back to upright. Each eye was measured independently and is shown separately. Negative degrees of OCR on ordinate represent torsion of eyes from baseline toward the left ear, normally in response to tilting the head toward the right. Positive is the opposite.

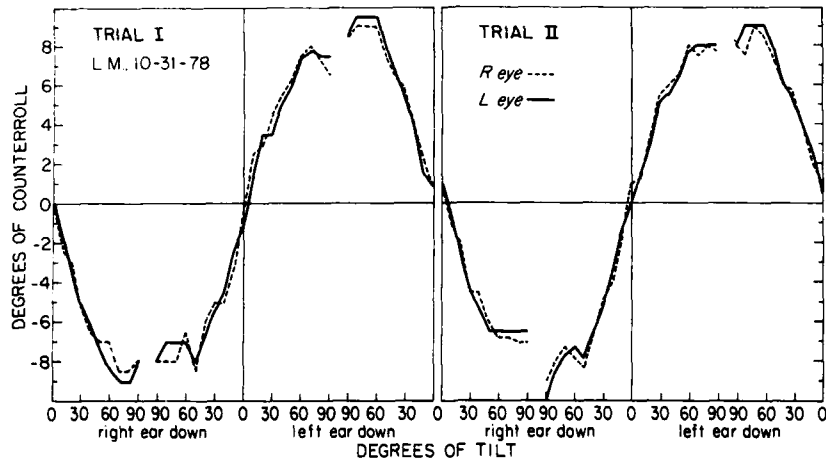


FIGURE 2. Counterrolling from subject L. M. showing characteristics of consistency, conjugate movement, smoothness, and symmetry. See text for details.

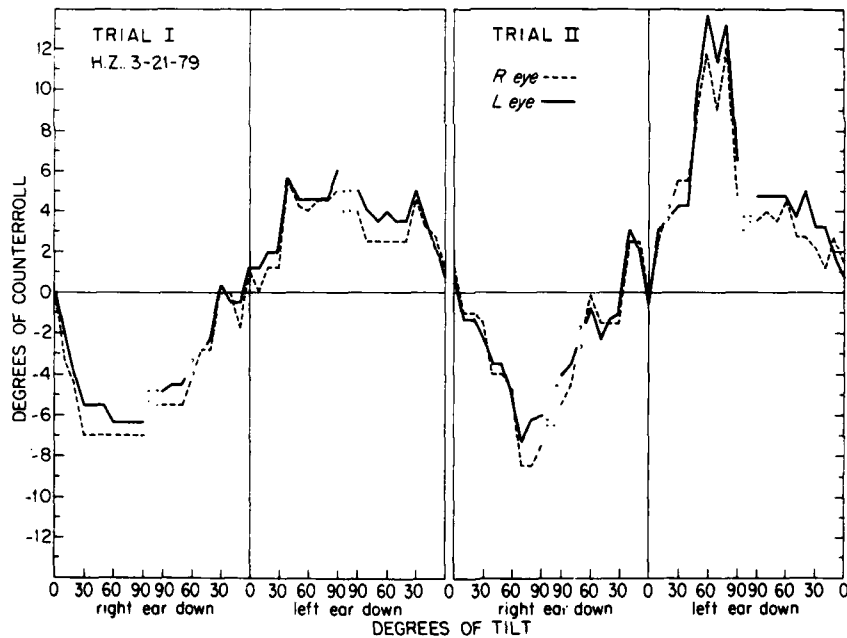


FIGURE 3. Profile of H. Z., a 58-year-old woman who underwent right superior vestibular nerve section in 1977. Note the inconsistency between trial I and trial II. Lack of smoothness and many disconjugate eye movements can be seen especially as the head is rotated from a left-ear-down to a right-ear-down position. Lack of symmetry between response to right tilt and left tilt is marked.

4. The amplitude of OCR was approximately *symmetric* with tilt to right or left side.

FIGURE 2 shows another normal profile for L.M., a 31-year-old man, in which the same characteristics were seen.

In contrast, FIGURE 3 shows the profile of H.Z., a 58-year-old woman with a right superior vestibular nerve section secondary to excision of an acoustic neuroma two years prior to testing, and demonstrates a lack of consistency from trial I to trial II. The amplitude of the left-ear-down portion in trial II was about $+14^\circ$, compared to $+6^\circ$ in trial I. The two eyes were fairly conjugate, but the profile was not smooth, particularly as she was brought back through 0° from

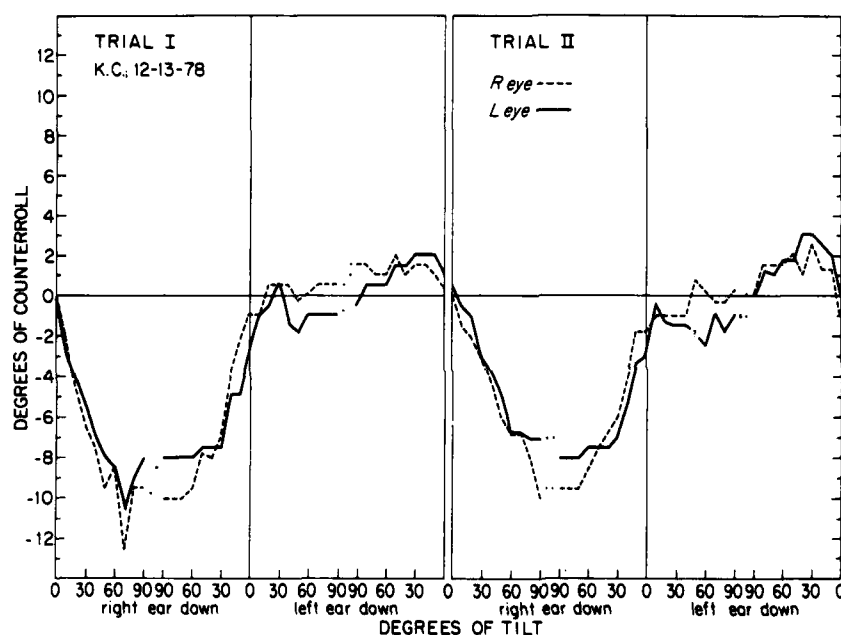


FIGURE 4. Profile of K. C., a 28-year-old woman whose right vestibular nerve was sectioned during excision of an epidermoid tumor in 1974. Her pattern demonstrates asymmetry and lack of smoothness, as well as disconjugate eye movements. Note absence of OCR to left head tilt, in contrast to H. Z. shown in FIGURE 3.

right-ear down to left-ear down. Many abrupt changes of direction in OCR were seen, especially in the left-ear-down portions. The profiles were not symmetric, with the left-ear-down portions showing less consistency, less conjugate movement, and less smoothness than did the right-ear-down portions.

FIGURE 4 shows the OCR profile of K.C., a 28-year-old woman who had had a right vestibular nerve section secondary to removal of an epidermoid tumor four years prior to testing. Although the profile was consistent from trial I to trial II, it showed considerable disconjugate movement, the two eyes as much as 3° different and moving in opposite directions, especially in the left tilts. There was a notable lack of smoothness, with several jagged peaks. Asymmetry was

dramatic, with great amplitude on right tilts and virtually no OCR on left tilt, where it barely reached baseline by the time the patient was tilted 90°. When she was brought upright from 90° left-ear down, her eyes rolled in the "wrong" direction, i.e., torsion of the eyes was in the direction of the roll of the head rather than in the opposite, or counterrolling, direction.

FIGURE 5 shows the OCR profile of D.M., a 54-year-old man who had had a right vestibular nerve section for severe vertigo two years before testing. The right tilts were consistent, smooth, and conjugate. In contrast, left tilt showed considerable lack of smoothness in the right eye in trial I. Left tilt in trial II showed inconsistency in extreme "wrong"-direction movement when the patient was rotated back to the upright position.

The OCR profile in FIGURE 6 is that of J.R., a 55-year-old man who had had an acoustic neuroma removed on the left side 12 years earlier. The superior portion of the left vestibular nerve had been sectioned, and the inferior portion preserved. His profile showed inconsistency from trial I to trial II, with the right tilt demonstrating an abrupt return to baseline by 60° and a delayed response in the comparable portion of trial II. There was a lack of smoothness in the profile on right tilt, compared to left tilt. Maximum OCR in trial I was -3° on right tilt and $+9^\circ$ on left tilt. In trial II, it was -5.5° on right tilt and $+4^\circ$ on left tilt.

The other two patients with unilateral nerve sections tested to date have shown OCR profiles similar to the ones described, i.e., displaying deficits in at least two of the criteria of consistency, conjugation, smoothness, and symmetry. In summary, the profile of OCR when the patient was tilted to the side opposite the lesion invariably was the one showing aberrant characteristics, i.e., patients with right vestibular nerve sections had OCR defects when the left ear was down, and patients with left sections showed abnormal profiles when the right ear was down.

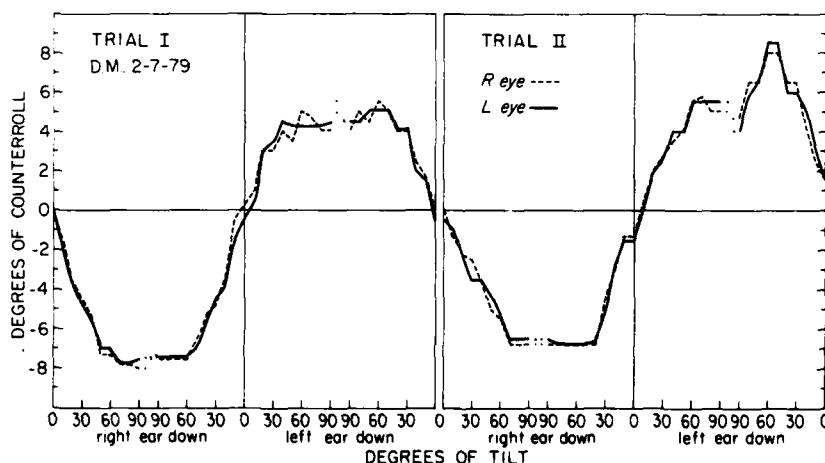


FIGURE 5. OCR profile of D. M., a 54-year-old man who had had a right vestibular nerve section in 1977. Notable is a lack of smoothness in the right eye when he was tilted to the left in trial I. Lack of consistency between trials is apparent when in trial II, eyes moved in "wrong" direction when he was brought back to upright from 90° left-ear down. OCR was normal when head was tilted to the right.

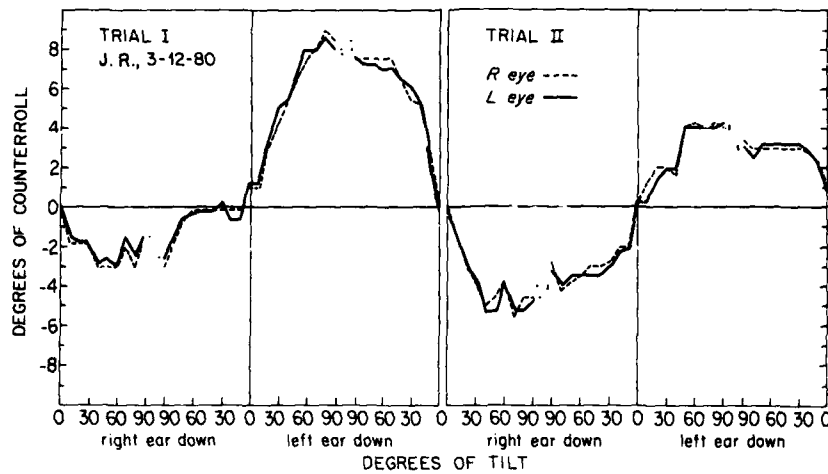


FIGURE 6. J. R., a 55-year-old man, had had his left superior vestibular nerve sectioned secondary to removal of an acoustic neuroma 12 years before testing. His OCR profile showed abnormalities mainly on right tilt, including lack of consistency from trial I to trial II (note variation in magnitude in the two trials), and lack of smoothness.

DISCUSSION

The quest for a diagnostic test of utricular dysfunction has intrigued numerous investigators for most of this century.⁵⁻¹⁴ It is perhaps premature to hope that we are now on the verge of developing a conclusive determiner of pathology and laterality in disorders of this system, yet the results of our study are promising. The behavior of the OCR mechanism under dynamic conditions—studying the pattern as a whole—suggests an avenue of investigation not previously examined. Parameters other than the ones discussed here may prove to be illuminating, and the criteria we are using at present may in time be weighted differently. The major deterrent to the volume of investigation necessary to clarify the questions still unresolved is the laborious frame-by-frame analysis that the present data-reduction system entails. We currently are investigating methods of automating the measurement of OCR, and if this is successful, a quantum increase in the number of studies may be expected.

A frequent question is the role of vision in the OCR response. The subjects studied in the present experiments fixated on the center of the rather large photographic apparatus, which rotated with the subject, was 33 cm from the face, and occupied the major portion of the visual field. Islands of peripheral vision were unobscured. Two normal subjects who had undergone several tests in the standard protocol were also tested under a hood of black velvet. This condition eliminated all peripheral visual stimuli, and the subject was tilted in complete darkness interrupted only by the strobe flashed directly in front of his face. The OCR profiles of both subjects under this condition did not differ from their profiles in the standard condition. On the basis of this result, we concluded that the role of vision was minimal at most in our studies. This finding was consistent with the results of Krejcova *et al.*¹⁰

The conflicting results of past studies, summarized in TABLE 1, are more easily

understood in light of their static nature. Similar conflicting results were obtained in our investigation when magnitude of response was examined. For example, H.Z.—with a right eighth nerve section (see FIGURE 3)—showed OCR in the left eye in trial II of -5° at 60° right tilt, and $+14^\circ$ at 60° left tilt, i.e., far more OCR when tilted to her normal side. On the other hand, K.C.—who also had a right eighth nerve section (see FIGURE 4)—had the opposite effect and showed OCR in the left eye in trial II of -6.5° at 60° right tilt, and -2.5° (i.e., less than no OCR) at 60° left tilt. Plainly, magnitude of response under static tilt is unproductive in differentiating the side of a lesion. Yet binocular OCR profiles of both these patients under dynamic conditions were abnormal when consistency, conjugation, smoothness, and symmetry were examined.

It is noteworthy that both in normal subjects and in patients, the slopes of the profiles were steepest, and therefore the sensitivity greatest, near the upright position. Further, the points at which the eyes reached their baseline positions did not materially differ in the two groups. Our finding that persons having only one utricle were similar in these respects to persons having both utricles intact leads us to speculate that the maculae of the two utricles are approximately horizontal and coplanar.

Speculating on the significance of our empirically derived criteria differentiating normal persons from patients with known unilateral lesions, we would infer that inconsistency and lack of the characteristics of conjugate movement, smoothness, and symmetry are the result of a deficiency of correcting input from a second utricle. From our findings of OCR to both directions of tilt in patients with unilateral lesions, it is apparent that each utricle influences both eyes in both directions. The observation that persons with unilateral labyrinthectomy showed the more aberrant profile when they were tilted to the intact side (with the lesioned ear up) leads us to conclude that the utricle exerts its major control to tilt to the contralateral side, i.e., the upper ear is dominant. Studies are continuing in our laboratory to refine these observations.

ACKNOWLEDGMENTS

The authors are grateful for the help of Dr. Nobuhiko Furuya and Setsuko Kashitani.

REFERENCES

1. SUZUKI, J.-I., K. TOKUMASU & K. GOTO. 1969. Eye movements from single utricular nerve stimulation in the cat. *Acta Otolaryngol.* **68**: 350-362.
2. MARKHAM, C. H., M. S. ESTES & R. H. I. BLANKS. 1973. Vestibular influences on ocular accommodation in cats. *Equilibrium Res.* **3**: 102-115.
3. BLANKS, R. H. I., J. H. ANDERSON & W. PRECHT. 1978. Response characteristics of semicircular canal and otolith systems in cat. II. Responses of trochlear motoneurons. *Exp. Brain Res.* **32**: 509-528.
4. BÄRÄNY, R. 1906. Über die vom Ohrlabyrinth ausgelöste Gegenrollung der Augen bei Normalhörenden, Ohrenkranken u. Taubstummen. *Arch. Ohrenheilkd.* **68**(1): 1.
5. KOMPANEJETZ, S. 1925. On compensatory eye movements in deaf mutes. *Acta Otolaryngol.* **7**: 323-334.
6. KOMPANEJETZ, S. 1928. Investigation on the counterrolling of the eyes in optimum head positions. *Acta Otolaryngol.* **12**: 332-350.

7. GOLLAS, E. 1936. Untersuchung der Raddrehung der Augen bei einseitigem Labyrinthausfall. *Arch. Ohren Nasen Kehlkopfheilkd.* **140**: 340-354.
8. MILLER, E. F., II & A. GRAYBIEL. 1963. A comparison of ocular counterrolling movements between normal persons and deaf subjects with bilateral labyrinthine defects. *Ann. Otol. Rhinol. Laryngol.* **72**: 885-893.
9. MILLER, E. F., II. 1969. Evaluation of Otolith Function by Means of Ocular Counterrolling Measurements. Report No. NAMI-1063. National Aeronautics and Space Administration. Washington, D.C.
10. KREJCOVA, H., S. HIGHSTEIN & B. COHEN. 1971. Labyrinthine and extralabyrinthine effects on ocular counterrolling. *Acta Otolaryngol.* **72**: 165-171.
11. NELSON, J. R. & D. COPE. 1971. The otoliths and the ocular countertorsion reflex. *Arch. Otolaryngol.* **94**: 40-50.
12. NELSON, J. R. & W. F. HOUSE. 1971. Ocular countertorsion as an indicator of otolith function: effects of unilateral vestibular lesions. *Trans. Am. Acad. Ophthalmol. Otolaryngol.* **75**: 1313-1321.
13. KANZAKI, J. 1975. New device for measurement of ocular countertorsion reflex. *Arch. Otol. Rhinol. Laryngol.* **211**: 213-215.
14. KANZAKI, J. & T. OUCHI. 1978. Measurement of ocular countertorsion reflex with fundoscopic camera in normal subjects and in patients with inner ear lesions. *Arch. Otol. Rhinol. Laryngol.* **218**: 191-201.
15. DIAMOND, S. G., C. H. MARKHAM, N. E. SIMPSON & I. S. CURTHOYS. 1979. Binocular counterrolling in humans during dynamic rotation. *Acta Otolaryngol.* **87**: 490-498.

OCULAR TORSION ON EARTH AND IN WEIGHTLESSNESS*

Laurence R. Young, Byron K. Lichtenberg,† Anthony P. Arrott,
Troy A. Crites, Charles M. Oman, and Elazer R. Edelman

Man Vehicle Laboratory
Department of Aeronautics and Astronautics
Massachusetts Institute of Technology
Cambridge, Massachusetts 02139

INTRODUCTION

Measurements of otolith function in man are difficult to obtain. Postural imbalances observed in clinical examinations may easily be the result of semicircular canal or nonvestibular disorders. Ocular torsion (OT) in response to static deviations of the head with respect to gravity, or ocular counterrolling, has long been known to reflect activity of the otolith organs, but its use in research and diagnosis has been limited to a great extent by the difficulty of its measurement.^{1,2} The current interest in problems of space motion sickness and vestibular adaptation to weightlessness places particular emphasis upon measurement of otolith function and provides the impetus for the instrumentation and research described in this paper. In order to study otolith function using measurements of OT, we improved the photographic method introduced by Miller and developed a new automatic video system using a soft-contact-lens target. The first method has been applied to analysis and consequent modeling of dynamic ocular torsion during horizontal linear acceleration on earth and during the sudden onset of linear acceleration beginning from the weightless condition. Ocular torsion also has been measured during the onset and maintenance of visually induced self-motion on earth and in weightlessness.

METHODS

Photographic Analysis

Photographic methods of measurement of ocular torsion using characteristics of the iris or of scleral blood vessels have been used by many investigators and are reviewed by Fluor.³ The technique we pursued is an extension of the photographic technique of Nelson and Cope, in which iris landmarks are identified and located.⁴ In our method, two iris landmarks located close to the outer edge of the pupil are identified, and the angle between the lines connecting them relative to the line between two head-fixed fiducial marks connected to the bite board is computed for each photograph.⁵ The OT for each photograph is the difference between this angle and the angle computed for a reference photograph. A Nikon F2 35-mm camera with a 250-frame magazine (motor drive) and a micro-Nikkor 55-mm lens is used to photograph either one or both of the eyes. A

*This work was supported in part by National Aeronautics and Space Administration Grants No. NSG 2032 and NAS 9-15343.

†Supported by a fellowship from the Fannie and John Hertz Foundation.

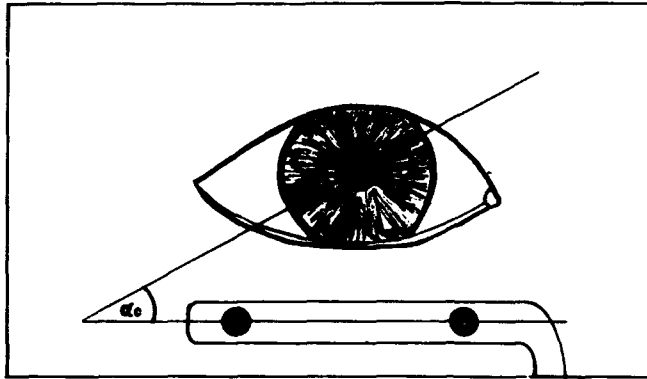


FIGURE 1. A sketch showing the method of iral-fiducial landmark angle definition. The ocular torsion (OT) was obtained by calculating α_c 's obtained during various acceleration stimuli. Two control frames were recorded prior to each acceleration profile.

reproduction ratio of 1:1.5 is used for monocular measurements, and 1:2.5 for binocular measurements. Ektachrome 200 transparency film is exposed using a ring flash and pushed one stop during developing. The transparencies, which include the fiducial marks as illustrated schematically in FIGURE 1, are projected on a Hermes Senior film analysis machine, usually used for nuclear-particle-track analysis. Coordinates of each point for multiple measurements of the two iris landmarks are determined manually four times for each frame. The standard deviation of the four sets of ocular torsion angles relative to the line between the fiducial marks is taken as a measure of the repeatability of the measurements. The grand mean of the standard deviation for all data is 0.2° in the range from 0 to 0.5° . By selecting landmarks near the edge of the iris, the effects of changes in pupil diameter are minimized, and neither drugs nor prephotograph dilation is required. Differences in measurements between individual scanners have been determined to be negligible. The processing is carried out entirely by computer from the time of the original scanning, and is illustrated schematically in FIGURE 2. Despite the partial automation, the scanning time per

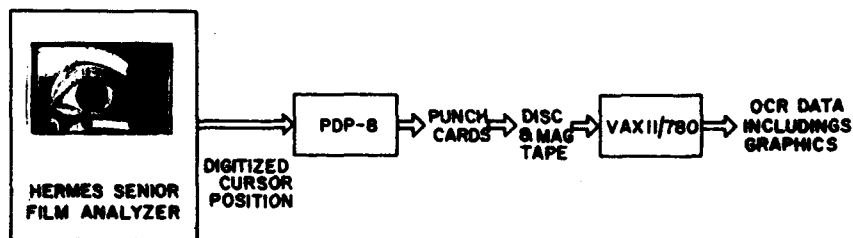


FIGURE 2. Block diagram of photographic data analysis procedures. Four manual measurements of x-y coordinates of each of two iral landmarks, and single measurements of the fiducial marks, are digitized, and punch cards produced. Landmark coordinates are averaged, tested for consistency, and converted to α_c for each frame on a VAX 11/780 computer.

frame is one to two minutes and the cost per frame is \$1.10. High-speed motion-picture photography is practical only for brief periods because of lighting limitations. The repetition rate for our technique is limited by the camera and flash to three per second. Because of these limitations, we have carried out a long-term program towards development of a fully automatic high-sampling-rate OT-measurement method as described below.

Video Measurement of OT

Automatic analysis of the orientation of the eye in torsion is feasible, and has been carried out in a preliminary fashion in a joint effort with Goodyear Corporation, using only natural features of the eye. Practical implementation of the fully automatic system involves a considerable number of further technical developments. We concentrated on a method that would involve minimal

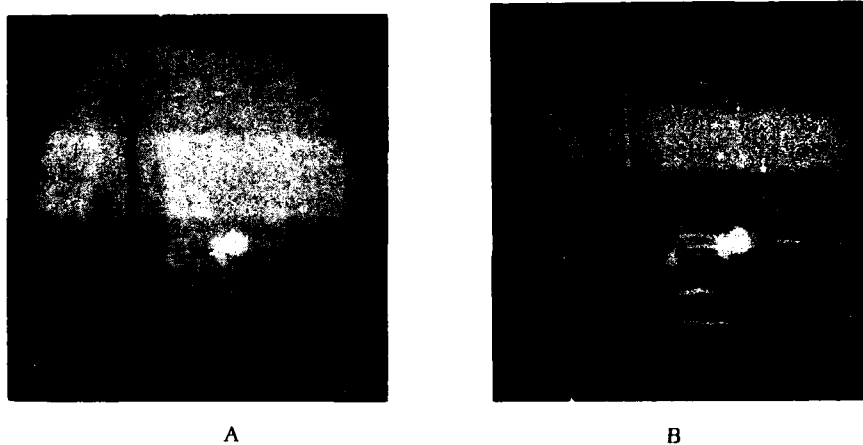


FIGURE 3. (A) Photograph of video monitor showing soft lens hair visible against "bright pupil." Dark area is iris. (B) Same as (A) with video signal processor-detected coordinates of hair highlighted.

interference with the subject and yet be achievable with current technology. The requirements for high sampling rate and electronic data analysis dictated the use of a video system. The need for artificial landmarks to be placed upon the human eye called for the development of appropriate markers in a nonslipping contact lens. A prototype video-image processing system was developed for measurements of OT at a 60-Hz sampling rate.^{6,7} The optical target tracked by the video system consists of a human hair mounted within a soft-contact-lens sandwich, located over a "bright pupil" (FIGURE 3). The soft lens is made to adhere temporarily and painlessly to the cornea by application of distilled water at 5- to 10-minute intervals, thereby changing the osmolarity of the lens. The soft-contact-lens sandwich does not move with respect to the iris during saccades,

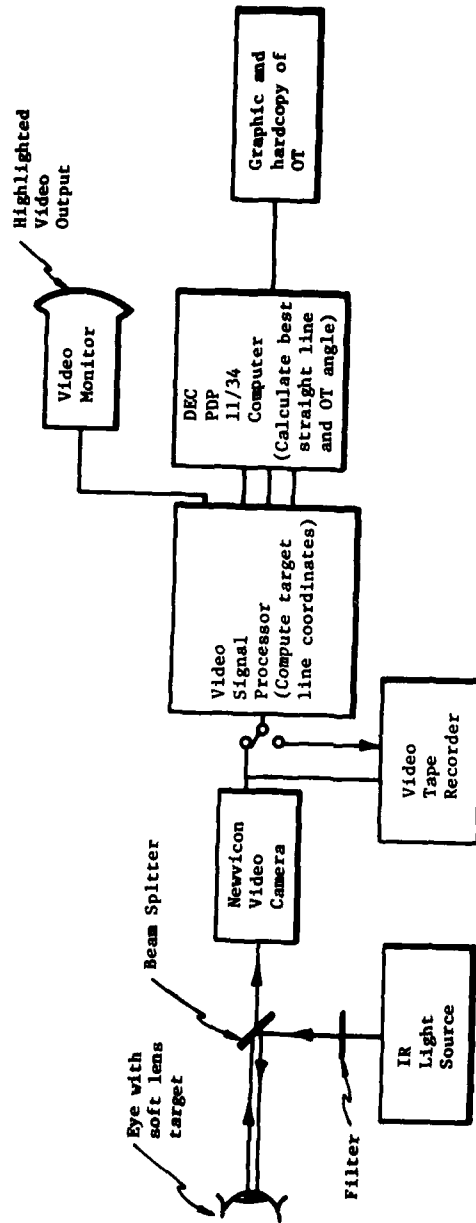


FIGURE 4. Schematic of system for video measurement of OT using soft contact lens. Video signal processor accepts input from camera or video recorder; transmits x-y coordinates of raster intersection with target image to PDP 11/34 disk memory for subsequent automatic analysis.

blinks, or long-term use. The lens is made more visible against the "bright pupil," which is illuminated by infrared light, and is viewed by a low-light-level infrared-sensitive (Newvicon) camera, as illustrated in FIGURE 4. Video output is processed to determine the x-y coordinates of the target line along each scan line. These coordinates are transmitted to a minicomputer for subsequent off-line automatic analysis. The angle between the line and the video reference is calculated for each frame. Practical resolution of the device in tracking a contact lens feature is approximately 0.1 to 0.3 degree. It has been successfully applied to monitoring of torsional nystagmus during rotatory optokinetic stimulation.

OCULAR TORSION DURING HORIZONTAL LINEAR ACCELERATION

Measurements of ocular torsion on astronauts are planned by several investigators for the forthcoming orbital flights of Spacelab on the space shuttle. Our interest in these measurements comes first of all from the relatively direct way of assessing changes in otolith function by observing its response to transient linear accelerations early and late in a space mission. Beyond that, however, is a fundamental difference between the type of otolith stimulation achievable in weightlessness and the type that can be produced by either tilting of the head or lateral horizontal acceleration on earth. As illustrated in FIGURE 5A, ocular torsion on earth, as usually defined by ocular counterrolling, results from a lateral head tilt with respect to the vertical and a compensatory rotation of the eye. The dynamic characteristics of such tilt have been investigated both by transient head rotation and by continuous rotation about an earth-horizontal axis.⁶⁻¹⁰ During lateral horizontal acceleration, as illustrated in FIGURE 5B, the net gravito-inertial vector rotates, just as for dynamic head rotation, but the semicircular canals are not stimulated either by transient angular accelerations or by the possible mechanism of a rotating linear acceleration vector.¹¹ The first step in our investigation consequently was to compare the dynamic characteristics of ocular torsion in response to linear acceleration with those reported for ocular counterroll resulting from tilt. The second step in our investigation is illustrated in FIGURE 5C, when a lateral linear acceleration is applied from a weightless exposure. The lateral component of acceleration now suddenly appears, but does not represent in any sense a rotation of the gravito-inertial vector, since this vector had zero magnitude and undefined direction prior to the initiation of the acceleration. The interpretation of the instantaneous direction of a vertical reference, any perception of tilt rather than linear acceleration, and the consequent ocular torsion during such sudden linear acceleration were all unknown prior to our investigations.

In order to investigate the responses of ocular torsion to linear acceleration, a ground-based version of the "space sled" was constructed at the Massachusetts Institute of Technology, as illustrated in FIGURE 6.⁵ The 16-foot usable track length permits step, pseudorandom, and sinusoidal acceleration stimuli up to a peak amplitude of 0.7 g and at frequencies up to 2 Hz. The equipment illustrated in FIGURE 6 was used only for lateral acceleration in the studies discussed in this paper. The head was held in a foam-lined fixation device, which normally limited head movement to 1.0° of rotation and 5 mm of translation during maximum acceleration. Ocular torsion was measured relative to the head using a bite stick with fiducial marks, and the influence of the slight ocular torsion associated with semicircular canal stimulation was subtracted from the results.

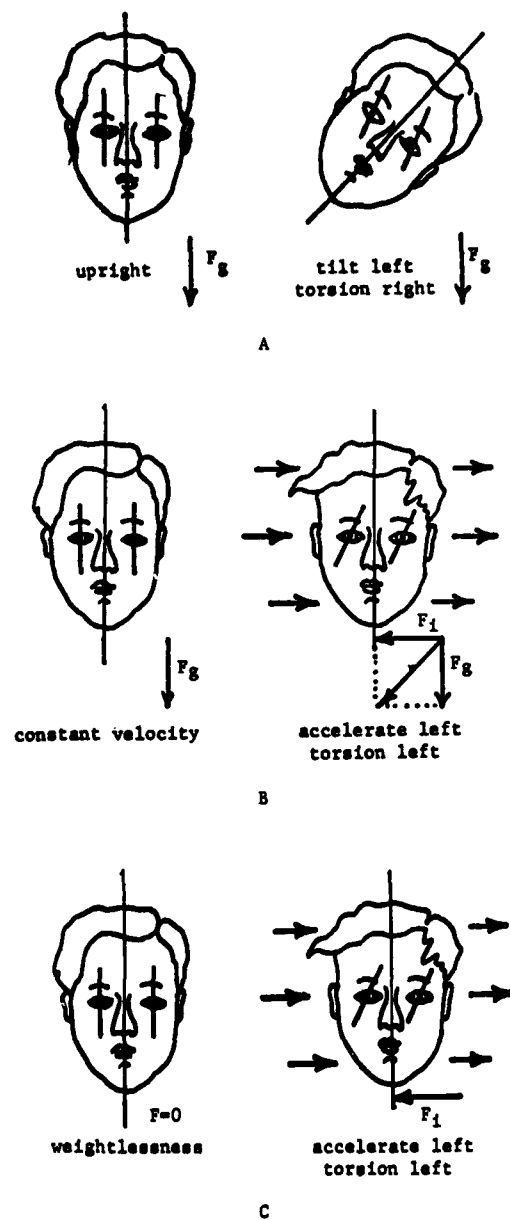


FIGURE 5. Ocular torsion resulting from three different stimulus conditions: (A) lateral head tilt in a 1-g field, F_g ; (B) lateral horizontal acceleration, in a 1-g field, produces an inertial force F_i resulting in a rotation of the gravito-inertial force vector ($\vec{g} - \vec{a}$); (C) lateral acceleration beginning from a weightless condition produces onset of inertial force F_i , but no rotation of gravito-inertial vector.

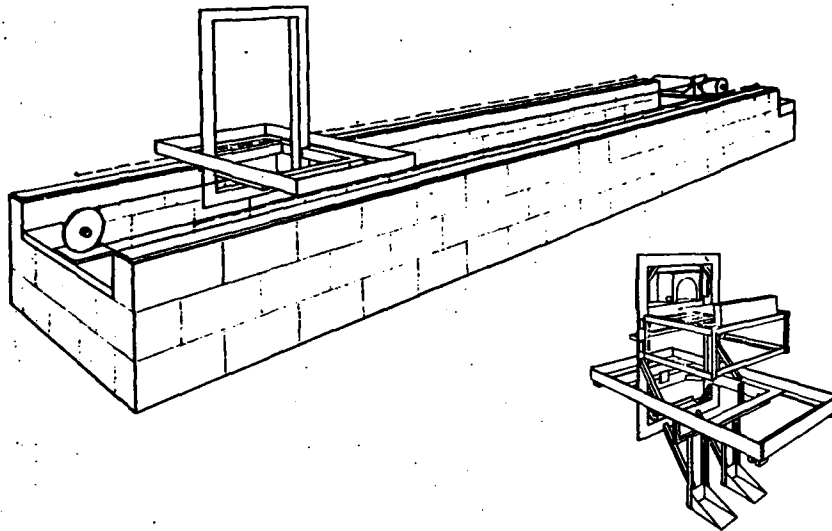


FIGURE 6. A sketch of the acceleration sled used to produce lateral acceleration stimuli.

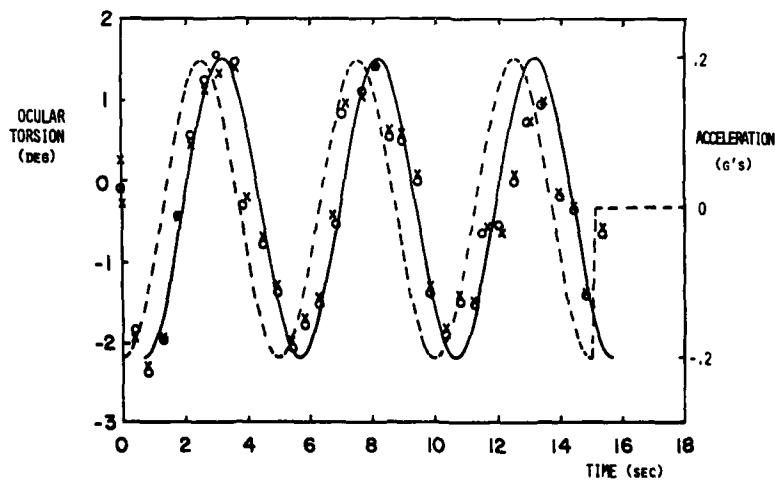


FIGURE 7. A particularly robust example of ocular torsion in response to 0.2-Hz acceleration. Dashed line indicates acceleration profile, solid line is sinusoidal fit to torsion data. The mean of four measurements on each frame is plotted for raw data (O) and for data corrected for head rotation (x). The correction factor was one-half of the head rotation added algebraically to account for semicircular-canal-induced torsion. The phase lag for this fit is 48.6° .

Testing was carried out at sinusoidal oscillations of 0.2, 0.4, and 1.0 Hz at a peak amplitude of 0.2 g. Both the sinusoidal ocular torsion results and the response to acceleration steps of various magnitudes and durations were well matched by a simple low-order linear system with a dominant time constant of 0.33 second for the seven subjects tested.¹² The transfer function is closely fit by the model derived by Hannen et al. for ocular torsion during head tilt,⁹ and consists of a pure delay ranging from 0 to 400 mseconds and a first-order lag of time constant of 0.33 second. A large response to sinusoidal oscillation at 0.2 Hz is shown in FIGURE 7, and a response to a 0.2-g step acceleration is shown in FIGURE 8. The frequency response for all subjects and the related responses for the Hannen et al. and Young-Meiry models are shown in FIGURE 9.^{9,13}

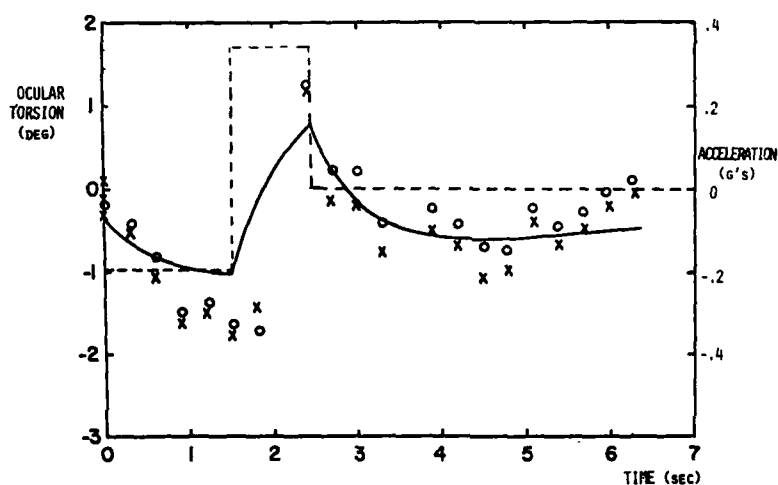


FIGURE 8. A representative OT response to a 0.2-g step acceleration for one subject. (O) and (x) as in FIGURE 7. Commanded acceleration is indicated by the broken line. The response of the Young and Meiry acceleration perception model is indicated by the solid line. The transfer function of their model, relating input acceleration to perceived acceleration, is $Y(s) = 1.5(s + 0.076)/[(s + 0.19)(s + 1.5)]$. The amplitude was scaled for a 0.3-g step acceleration on a different subject; all other parameters of the model are taken directly from Young and Meiry.¹³

OCULAR TORSION DURING ACCELERATION FROM WEIGHTLESSNESS

The ground-based acceleration tests serve as reference data for identical tests to be performed in Spacelab. Preliminary measurements in weightlessness were made during the 0-g portion of parabolic flight using the National Aeronautics and Space Administration's KC-135 aircraft. The transition from the free-fall portion of approximately 25 seconds duration to the 2-g pullout was utilized to produce lateral accelerations in our subject population. Our subjects all were oriented in a form-fitting evacuated mold, so that the onset of linear acceleration from the weightless condition appeared laterally along the y-axis in a direction associated with "right-ear down." If this orientation, as illustrated in FIGURE 10,

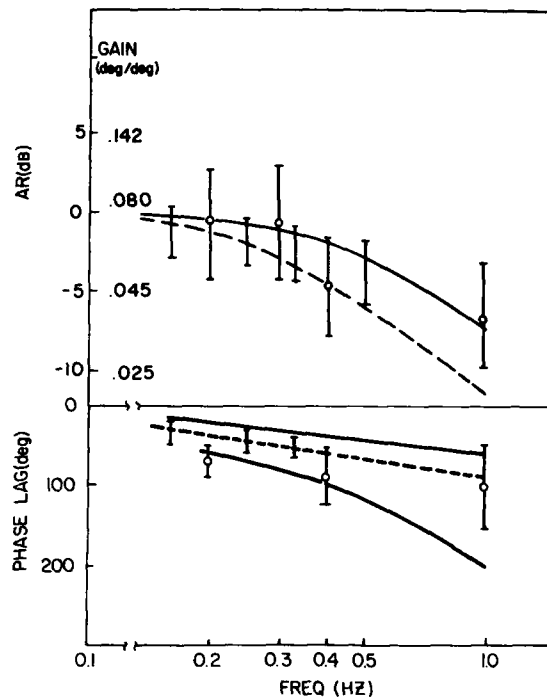


FIGURE 9. A Bode plot of human ocular torsion data. The solid vertical lines indicate the range of gain data from Kellogg (1965, two subjects undergoing constant roll rotation about a horizontal axis).¹⁰ The vertical bars with an open circle indicate the mean ± 1 standard deviation of the data of this paper (seven subjects, 0.2-0.3 g peak amplitude linear horizontal acceleration). The broken line on the gain plot is the prediction of the Young and Meiry model (see legend of FIGURE 8). The solid line is the prediction of the Hannen model. The transfer function of this model is $H(s) = (k \exp -as)/(s + 3.14)$ relating OT to lateral head tilt. Also included on the plot is an absolute gain scale (relating OT to rotation of the gravito-inertial vector) that is relevant only for the data of this paper. Zero dB for the Kellogg data and for both models is referenced to the measured gain at 0.08 Hz. Lichtenberg *et al.*'s data are referenced to match the Hannen model gain at 0.2 Hz. For the phase plot, all data are referenced to acceleration. The broken line is again the prediction of the Young and Meiry model; the solid lines indicate the predictions of the Hannen model with time delays (a) of 0 (upper line) and 400 mseconds (lower line).

had been arrived at by tilting the subject to the right-ear-down position from the upright, counterclockwise compensatory ocular torsion would appear. Since the orientation was arrived at from the weightless state, however, in the absence of any rotation of the gravito-inertial vector, the resulting ocular torsion was not self-evident. As shown clearly in FIGURE 11, a pronounced counterclockwise ocular torsion does appear in response to the lateral stimulus, just as would be the case if the head were tilted to this orientation. Since the final stress is 2 g, the total ocular torsion is larger than would be seen in a 1-g field. The sensitivity (approximately 0.07 radians or four degrees of ocular torsion per g of lateral acceleration) is about the same as that observed on earth.

OCULAR TORSION DURING ROLL VECTION: SUPINE AND IN WEIGHTLESSNESS

The final set of ocular torsion measurements taken in the course of the KC-135 flights involved measurement of ocular torsion during optokinetic stimulation about the roll axis. This type of stimulation normally results in a paradoxical sensation of sustained tilt and rotation about a horizontal axis on earth. It can produce perceptions of continuous rotation when carried out about a vertical axis with the subject supine in the laboratory. When similar tests were carried out during the brief weightless exposures during flight, onset latencies of vection were found to be reduced relative to the supine one-gravity situation, even though the latter presented no clear conflict between otolith cues and sustained rotation.^{14,15} Experiments with the creation of an artificial vertical reference by the use of tactile cues on the feet during weightlessness similarly produced an increase in latency to onset of vection. Ocular torsion measurements were made in an attempt to see whether or not the perceived rotation of the body axis, as reflected in the vection perception, contributed to the vection.^{15,16} Large individual differences among subjects were observed. For some subjects, as illustrated by the example shown in FIGURE 12, the measurements indicated that ocular torsion shifted markedly in the direction of field motion during constant optokinetic stimulation in weightlessness when the subject reported the onset of vection. The binocular measurements indicated that the two eyes moved synchronously, and torsional nystagmus was noted. However, the mean eye

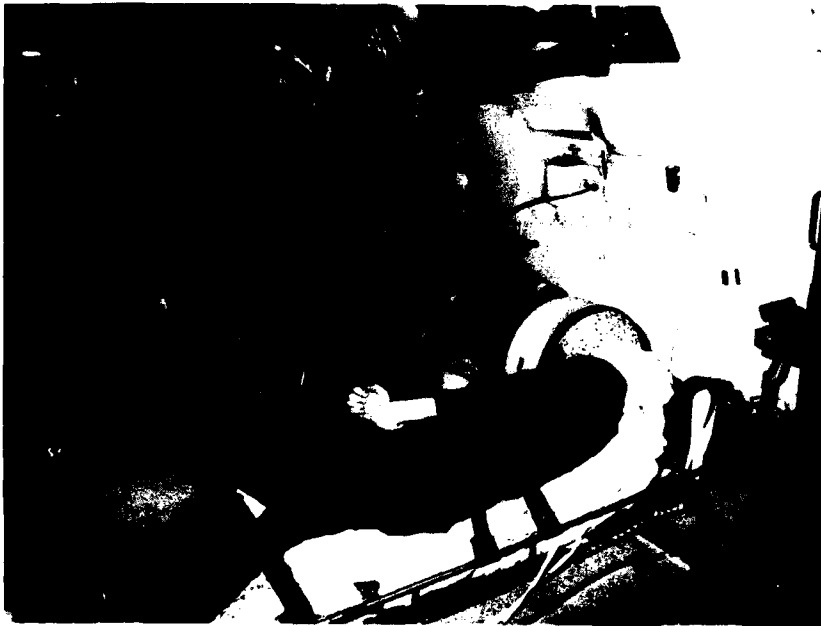


FIGURE 10. Photograph of experimental apparatus during weightless portion of parabolic flight in NASA's KC-135 aircraft. Pullout from the aircraft dive produces a 2-g acceleration directed toward the aircraft floor.

position could not be correlated to perceived motion for the population of subjects tested, and our tentative conclusion is that ocular torsion and visually induced tilt—though both stimulated by the rotating visual field and both sensitive to otolith stimulation—are essentially independent processes.^{14,15}

CONCLUSION

The availability of convenient and accurate methods for ocular torsion measurement and analysis has permitted several investigations of otolith func-

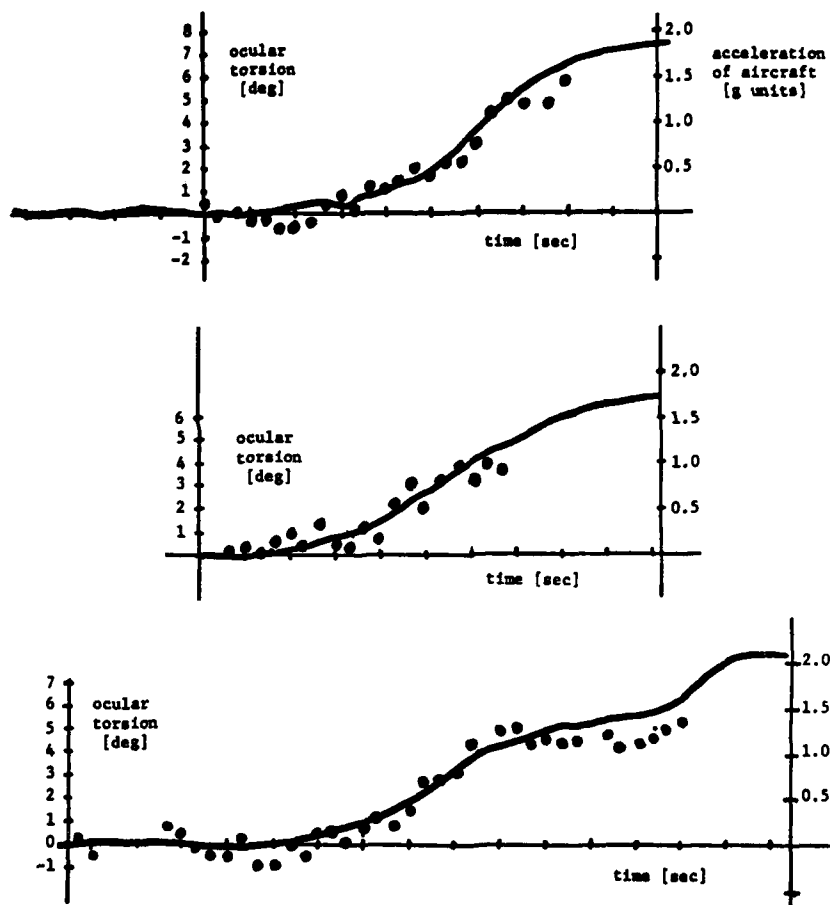


FIGURE 11. Three examples of ocular torsion (counterclockwise positive) induced by the onset of gravito-inertial force following approximately 30 seconds of weightlessness. Subjects were positioned such that the force was exerted in a lateral direction (y-axis). Solid line indicates acceleration of aircraft. Solid circles indicate angle of torsion measured in each frame of photographic data.

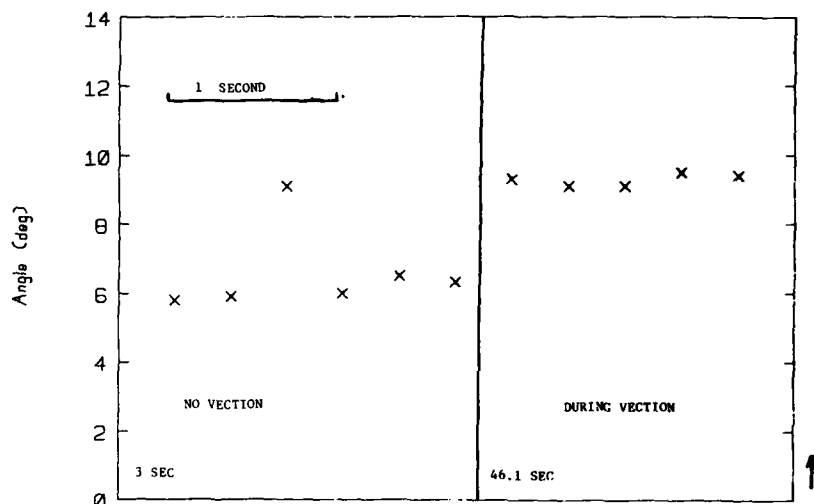


FIGURE 12. Example of ocular torsion measured during constant 30° /second clockwise optokinetic stimulation about the visual axis, subject supine in 1 g. First six measurements were taken prior to the onset of vection, last five measurements after the subject reported vection. Frame rate, 3/second. Change in OT with vection is in the clockwise direction.

tion under normal conditions, as well as in unusual acceleration environments. Further development of these techniques holds considerable promise for investigation of basic otolith physiology, otolith-semicircular canal response interaction, and diagnostic applications.

SUMMARY

Ocular torsion (OT) was measured in human subjects during horizontal linear acceleration on a sled in the laboratory and when emerging from weightlessness during parabolic flights in NASA's KC-135 aircraft. Analysis of the frequency response of OT to sinusoidal horizontal oscillation on earth shows results consistent with constant tilt rate studies and with earlier models based on perception of acceleration. Step responses of OT to lateral acceleration are compared to similar profiles from aircraft tests with no preexisting gravito-inertial force on the otoliths. The sensitivity of OT to rotating wide fields producing vection and to tactile cues is compared for earth and weightlessness. A new instrument for high bandwidth video measurement of OT using a soft-contact-lens target is described.

ACKNOWLEDGMENT

We are grateful for the collaboration of Anthony Cavallerano, O.D., of the Massachusetts Institute of Technology Medical Department in the development of the contact lens sandwich.

REFERENCES

1. MILLER, E. F. 1962. Counter-rolling of the human eyes produced by head tilt with respect to gravity. *Acta Otolaryngol.* **54**: 479-501.
2. MILLER, E. F. & A. GRAYBIEL. 1965. Otolith function as measured by ocular counterrolling. In *The Role of the Vestibular Organs in Space Exploration*: 121-132. Publication No. SP-77. National Aeronautics and Space Administration. Washington, D.C.
3. FLUUR, E. 1975. A comparison between subjective and objective recording of ocular counterrolling as a result of head tilting. *Acta Otolaryngol.* **79**: 111-114.
4. NELSON, J. R. & D. COPE. 1971. The otoliths and countertorsion reflex. *Arch. Otolaryngol.* **94**: 40-50.
5. LICHTENBERG, B. 1979. Ocular counterrolling induced in humans by horizontal accelerations. Sc.D. Thesis. Massachusetts Institute of Technology. Cambridge, Mass.
6. EDELMAN, E. R. 1979. *Video based monitoring of torsional eye movements*. S.M. Thesis. Massachusetts Institute of Technology. Cambridge, Mass.
7. EDELMAN, E. R. & C. M. OMAN. Video based monitoring system for eye movement analysis. (In preparation.)
8. PETROV, A. P. & G. M. ZENKIN. 1973. Torsional eye movements and constancy of the visual field. *Vision Res.* **13**: 3465-3477.
9. HANNEN, R. A., M. KABRISKY, C. R. REPLOGLE, V. L. HARTZLER & P. A. ROCCAFORTE. 1966. Experimental determination of a portion of the human vestibular response through measurement of eyeball counterroll. *IEEE Trans. Biomed. Eng.* **BME-13**: 65-70.
10. KELLOGG, R. S. 1965. Dynamic counterrolling of the eye in normal subjects and in persons with bilateral labyrinthine defects. In *The Role of the Vestibular Organs in Space Exploration*: 195-202. Publication No. SP-77. National Aeronautics and Space Administration. Washington, D.C.
11. BENSON, A. J. 1974. Modification of the response to angular acceleration by linear accelerations. In *Handbook of Sensory Physiology. Vestibular System*. H. H. Kornhuber, Ed. **6/2**: 281-320. Springer-Verlag. Berlin & New York.
12. LICHTENBERG, B. K., L. R. YOUNG & A. P. ARROTT. Human ocular counterrolling induced by varying linear acceleration. (In preparation.)
13. YOUNG, L. R. & J. L. MEIRY. 1968. A revised dynamic otolith model. *Aerosp. Med.* **39**: 606-608.
14. CRITES, T. A. 1980. Circularvection and ocular counterrolling in visually induced roll supine and in weightlessness. S.M. Thesis. Massachusetts Institute of Technology. Cambridge, Mass.
15. YOUNG, L. R., C. M. OMAN & T. A. CRITES. Weightlessness and tactile cues influence visually induced roll. (In preparation.)
16. FINKE, R. A. & R. HELD. 1978. State reversals of optically induced tilt and torsional eye movements. *Percept. Psychophys.* **23**: 337-340.

NEURONAL INTERACTION BETWEEN IPSILATERAL MEDIAL AND LATERAL VESTIBULAR NUCLEI*

I. Matsuoka,† J. Ito,† M. Sasa,‡ and S. Takaori‡

†Department of Otorhinolaryngology

‡Department of Pharmacology

Faculty of Medicine

Kyoto University

Kyoto 606, Japan

M. Morimoto

Faculty of Medicine

Kochi Medical School

Kochi 781-51, Japan

Peripheral afferent fibers from different end organs in the inner ear project to distinct areas of the four main vestibular nuclei: superior, lateral, medial, and descending nuclei.¹⁻⁵ The lateral vestibular nucleus (LVN) receives its main input from the utricle and a minor projection from the horizontal canal and saccule, and sends its main efferents to the spinal cord. The medial vestibular nucleus (MVN) receives input from the posterior and horizontal canals, and sends its axons to the motor nuclei of the ocular nerves through the ascending medial longitudinal fasciculus. It is well documented that the vestibular nucleus neurons also receive fibers from the cerebellum, reticular formation, and spinal cord, and the activities of these neurons are under control from the central areas.⁵⁻⁸ However, there is little information on the relationship between vestibulo-ocular and vestibulospinal reflexes. Since neurons in the vestibular nuclei (such as MVN) have long axons passing through other vestibular nuclei (such as LVN) and give off collateral branches in the vicinity of the perikaryon, Brodal has suggested that the neurons in the vestibular nuclear complex cannot be considered independent and cooperation between the neurons may take place.¹

We attempted to determine the existence of a direct influence of the MVN on the LVN neurons that receive input from the peripheral vestibular nerve. We used electrophysiological techniques and the horseradish peroxidase (HRP) retrograde transport method.

MATERIALS AND METHODS

Adult cats weighing 2.5-4.0 kg underwent surgical procedures after being anesthetized with ether. The trachea and femoral vein were cannulated, and the tympanic bulla was exposed using a ventral approach. A bipolar stainless steel electrode for stimulation of the vestibular nerve was inserted through the round window. The head of the animal was fixed in a stereotaxic instrument, and parts of the parieto-occipital skull and bony tentorium were removed to allow for insertion of electrodes. After the operation, the ether anesthesia was replaced by

*This work was supported in part by a Grant-in-Aid for Scientific Research from the Ministry of Education, Science, and Culture, Japan.

one with α -chloralose (30 mg/kg intravenous) and the cat was immobilized with gallamine triethiodide (5 mg/kg per hour, iv). All wound edges and pressure points were locally anesthetized with 8% lidocaine repeatedly throughout the experiment. Respiration was artificially sustained, and body temperature was maintained at 36.5–37.5°C with a heating pad.

A glass-insulated silver-wire microelectrode with a resistance of approximately 1 M Ω was used for extracellular recording of single neuron activity in the LVN (P, 8.0; L, 4.0; H, –3.5 to –4.5) and the MVN (P, 9.0; L, 2.5; H, –4.0), according to the brain atlas of Snider and Niemer.⁹ In the HRP experiment, a glass micropipette with a tip diameter of 1–2 μ m was attached along the recording microelectrode. The distance between the tips of electrode and micropipette was within 10 μ m. The micropipette was filled with a freshly prepared 10% solution of HRP (Toyobo, grade II) in tris-HCl buffer at pH 8.6.

A bipolar stainless-steel electrode with a tip diameter of 0.1 mm was used to stimulate the MVN and LVN. When the typical field potential composed of P, N₁, and N₂ waves (Shimazu and Precht)¹⁰ was obtained from the electrode following vestibular nerve stimulation, the electrode tip was preliminarily considered to be properly located in the MVN and LVN. A square wave pulse of 0.05 msec duration and 1–10 V was supplied to the vestibular nerve, MVN, and LVN every 1.6 seconds, unless otherwise stated. At least 10 successive responses amplified and displayed on an oscilloscope (Nihon Kohden, VC-9) were photographed with a long-recording camera. The statistical significance of the data was determined by Student's t-test.

When excitatory or inhibitory responses were obtained in the LVN neuron with MVN stimulation, HRP was iontophoretically ejected for 1–5 minutes with a positive current of 100–300 nA, using a microiontophoresis programmer (WP-I, Model 160). These procedures resulted in an extremely restricted deposit and prevented injury of nerve fibers in the LVN. The retaining current of 10–50 nA was used to cancel the passive leakage of HRP from the pipette. After the ejection of HRP, the animal was allowed to survive for 12–15 hours under deep anesthesia with supplemental administration of pentobarbital sodium (30–40 mg/kg iv). The animal was then perfused transcardially with 7% formalin solution in 0.1 M phosphate buffer at pH 7.3. The brain was removed, stored in 0.1 M phosphate buffer containing 30% sucrose for 48–72 hours, then sectioned at 40–60 μ m on a freezing microtome. The sections were treated with benzidine or tetramethylbenzidine in the presence of hydrogen peroxide, then briefly washed in 30% cold methanol and mounted on gelatin-coated glass and counterstained with neutral red.

Other details of the electrophysiological procedure were as described elsewhere.^{11,12}

RESULTS

Effects of MVN Stimulation on LVN Neurons Activated by Vestibular Nerve Stimulation

The LVN neurons were classified into two groups, mono- and polysynaptic neurons, according to the response pattern to vestibular nerve stimulation.¹³ The effects of MVN stimulation were examined on monosynaptic neurons that fired spikes superimposed on the N₁ wave of field potential. A typical example is

demonstrated in FIGURE 1A. The mean spike latency was 1.1 ± 0.1 (standard error) mseconds ($n=18$), and the spikes could not follow a high-frequency stimulation over 50 Hz (FIGURE 1A₁ and 1A₂). When the stimulus was applied to the MVN, a spike generation was also obtained in these 18 LVN neurons, monosynaptically elicited by vestibular nerve stimulation (FIGURE 1B). The mean spike latency of the neurons with MVN stimulation was 1.1 ± 0.1 mseconds, and the spike did not follow a high-frequency stimulation over 50 Hz (FIGURE 1B₁ and 1B₂).

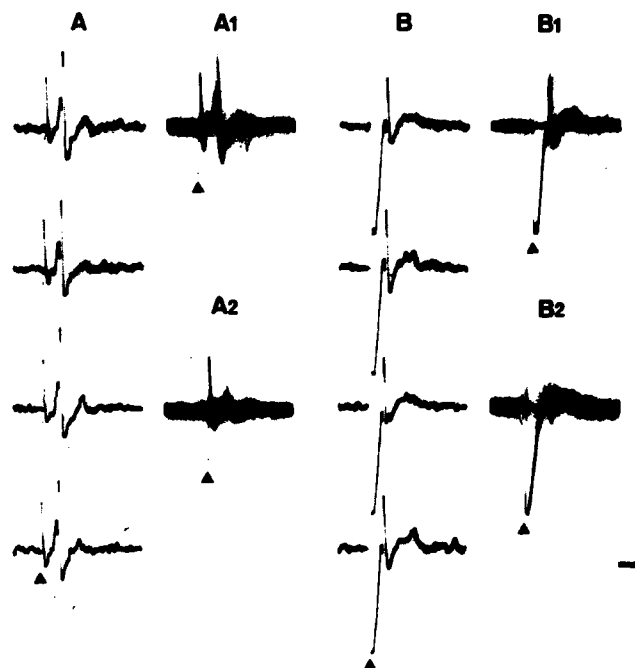


FIGURE 1. Spikes of lateral vestibular nucleus neuron elicited by stimulation of the vestibular nerve (A) and medial vestibular nucleus (B). A₁ and A₂: superimposed spikes following high-frequency stimuli of 20 Hz and 50 Hz to the vestibular nerve, respectively. B₁ and B₂: superimposed spikes following high-frequency stimuli of 20 Hz and 50 Hz to the medial vestibular nucleus, respectively. Solid triangles indicate the stimulus artifacts. Calibration: 2 mseconds, 0.2 mV.

In the other 11 LVN neurons monosynaptically activated by vestibular nerve stimulation, we found that a conditioning stimulus applied to the MVN at various intervals preceding the test stimulus to the vestibular nerve (C-T interval) significantly inhibited the spike generation with the nerve stimulation (FIGURE 2). The inhibition was prominent during 5-60 mseconds of the C-T interval (FIGURE 3). The mean spike number of 11 LVN neurons was 1.5 ± 0.2 (SE) without the MVN conditioning stimulation, while the number was significantly ($p < 0.01$) reduced to 0.6 ± 0.2 with the MVN conditioning stimulation 10 mseconds preceding the test stimulus to the vestibular nerve.



FIGURE 2. Inhibitory effect of conditioning stimulation of the medial vestibular nucleus on spike generation of the lateral vestibular nucleus neuron upon vestibular nerve stimulation. **A:** spikes without conditioning stimulation. **B and C:** spikes disappear with conditioning stimulation 5 and 10 mseconds preceding the test stimulus to the vestibular nerve, respectively. Solid triangles indicate the stimulus artifacts to the nerve. Calibration: 2 mseconds, 0.2 mV.

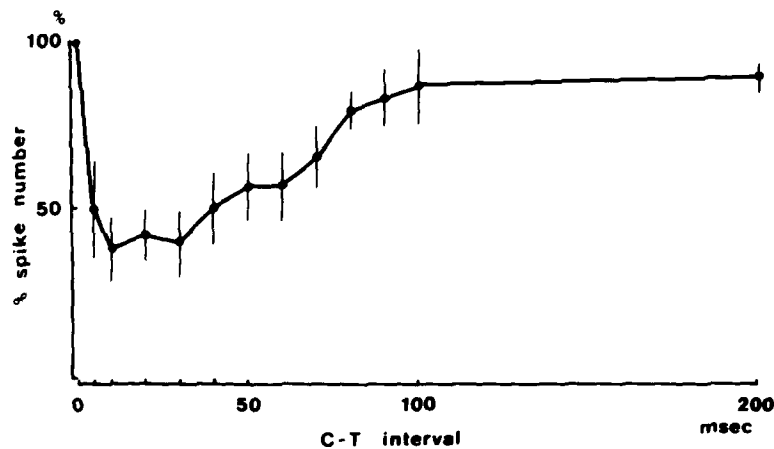


FIGURE 3. Effects of conditioning stimulation of the medial vestibular nucleus on neuron activities of the lateral vestibular nucleus elicited by the test stimulus to the vestibular nerve at various conditioning and testing time intervals (C-T interval). Each point indicates mean percentage changes in spike number of 11 neurons. Vertical bar of each point: standard error.

*Effects of LVN Stimulation on MVN Neurons Activated by
Vestibular Nerve Stimulation*

When the stimulus was applied to the vestibular nerve, the MVN neurons fired spikes monosynaptically with a mean latency of 1.6 ± 0.1 mseconds ($n=16$) ranging from 1.0 to 1.9 mseconds (FIGURE 4A). The spikes could not follow a frequency stimulation of over 50 Hz. These 16 MVN neurons monosynaptically

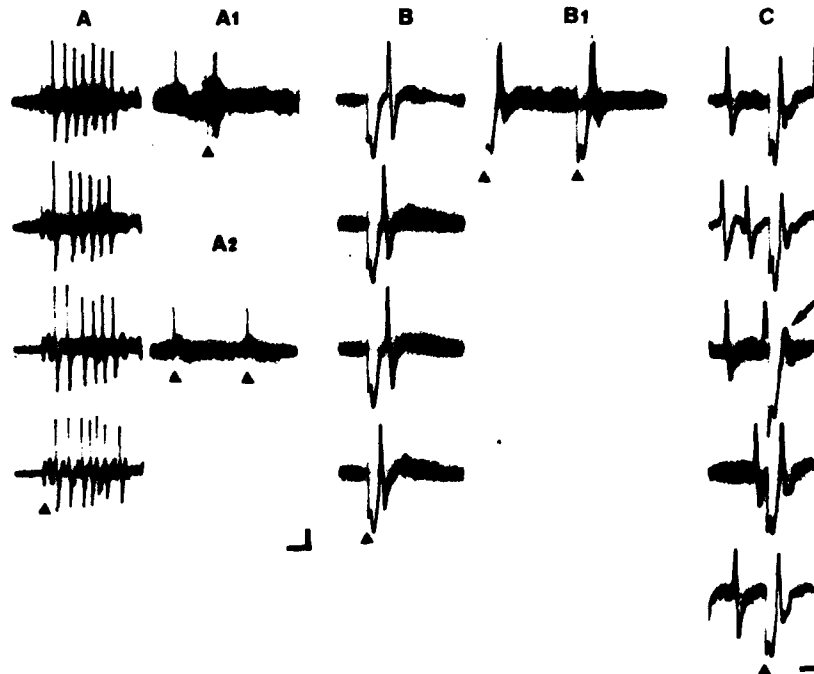


FIGURE 4. Spikes of medial vestibular nucleus neuron elicited by stimulation of the vestibular nerve (A) and lateral vestibular nucleus (B and C). A₁ and A₂: superimposed spikes following high-frequency stimuli of 20 Hz and 50 Hz to the vestibular nerve, respectively. B₁: superimposed spikes following high-frequency stimuli of 100 Hz to the lateral vestibular nucleus. In C, collision block of spikes (arrow) upon lateral vestibular nucleus stimulation occurs with the preceding orthodromic spike by vestibular nerve stimulation. Solid triangles indicate the stimulus artifacts. Calibration: 5 mseconds, 0.2 mV for A; and 2 mseconds, 0.2 mV for B and C.

activated by vestibular nerve stimulation also responded to LVN stimulation with a short and consistent latency (FIGURE 4B). The mean spike latency with LVN stimulation was 1.1 ± 0.1 mseconds, and the spikes followed a high-frequency stimulation up to 200 Hz (FIGURE 4B₁). In addition, collision block of the spike produced by LVN stimulation was observed with the preceding spontaneous firing, or orthodromic spike, by vestibular nerve stimulation, as shown in FIGURE 4C. These results indicate that the spike was antidromically activated by LVN stimulation.

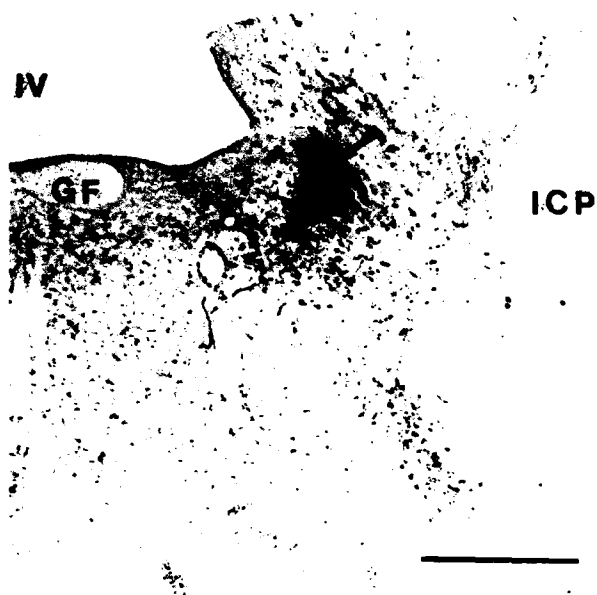


FIGURE 5. Ejection site of horseradish peroxidase in the lateral vestibular nucleus (arrow). Abbreviations: GF, genu of facial nerve; ICP, inferior cerebellar peduncle; IV, fourth ventricle. Calibration mark: 1.0 mm.

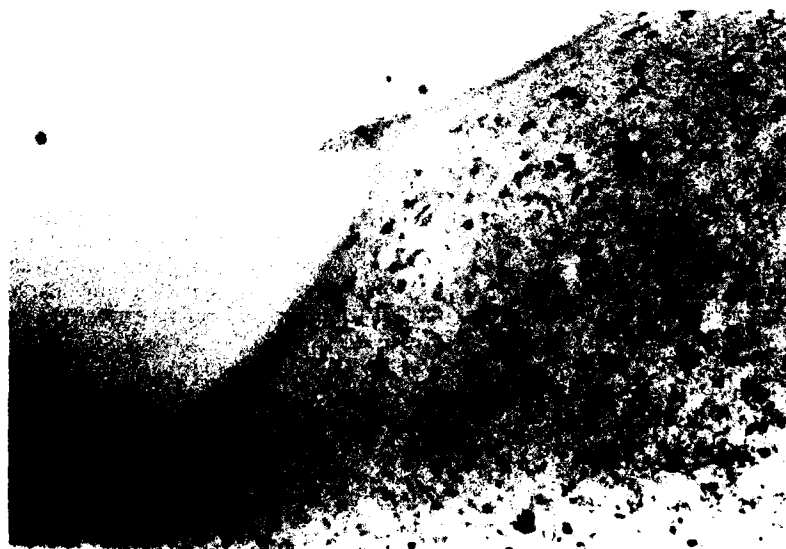


FIGURE 6. Horseradish peroxidase-positive cells in the medial vestibular nucleus. Magnification: 60x.

HRP Studies

When excitatory or inhibitory effects of MVN stimulation were obtained on an LVN neuron monosynaptically activated by vestibular nerve stimulation, HRP was iontophoretically ejected to the immediate vicinity of the neuron recorded. Under these conditions, the dense core of HRP reaction product in the ejection site of the LVN was restricted to within 0.3 mm in diameter and there was no leakage of HRP into the cerebral peduncle, MVN, and neighboring structures. FIGURE 5 is a histological picture showing the ejection site in the LVN. The HRP reaction product was seen in the cells in the immediate vicinity of the ejection site; however, a uniform brown or blue coloration was not observed usually in the fibers surrounding the ejection site.

HRP-positive cells with stippling of HRP reaction product were found in the

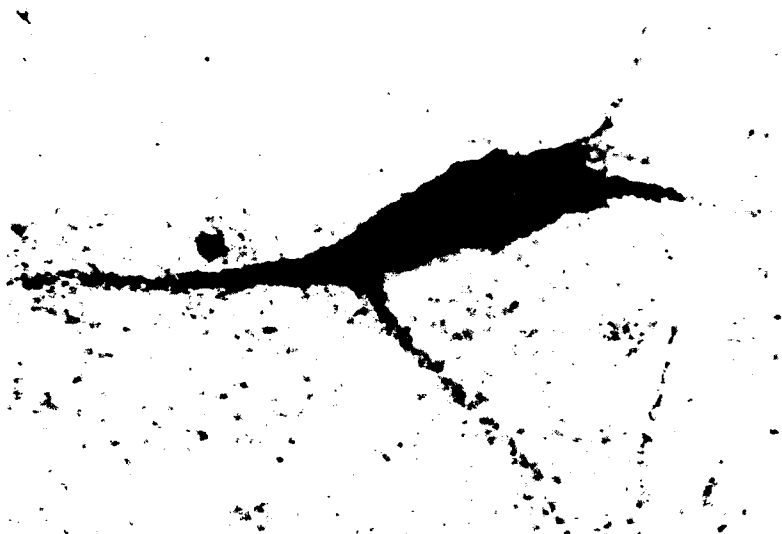


FIGURE 7. High magnification of horseradish peroxidase-positive cell in the medial vestibular nucleus. Magnification: 600 \times .

MVN. The number of HRP-positive cells in the MVN was 3-8 in a single section. A typical HRP-positive cell in the MVN is demonstrated in FIGURES 6 and 7.

DISCUSSION

Stimulation of the MVN produced a spike generation with a short latency in the LVN neurons monosynaptically activated by vestibular nerve stimulation. However, these neurons could not respond to a high-frequency stimulation to the MVN over 50 Hz, indicating that the LVN neurons were monosynaptically excited with MVN stimulation. These results suggest that the LVN neurons might receive a direct and, at least, excitatory input from the MVN.

Other LVN neurons monosynaptically activated by vestibular nerve stimulation were inhibited with a conditioning stimulus to the MVN. The inhibition occurred within 5 mseconds of the C-T interval; however, it remains to be determined whether the inhibition was monosynaptically produced. The possibility that the excitatory and inhibitory effects of MVN stimulation on the LVN neurons may have been due to stimulating nerve fibers passing through the MVN can probably be ruled out for the following reason: the MVN neuron was excited by vestibular nerve stimulation with a short latency, but the spike did not follow a high-frequency stimulation to the nerve over 50 Hz, indicating that the spike was monosynaptically activated by the stimulation. The same MVN neuron was antidromically excited by LVN stimulation, as the spike followed a high-frequency stimulation up to 200 Hz with a short and consistent latency, and a collision block of the spike did occur.

There is a further question that the MVN neurons may be activated by stimulation of nerve fibers merely passing through the LVN. This possibility cannot be excluded completely, but the results of HRP study strongly suggest the existence of direct innervation from the MVN to the LVN. When a small amount of HRP was iontophoretically ejected in the immediate vicinity of an LVN neuron that monosynaptically received input from the vestibular nerve, a localized deposit of HRP was obtained in the LVN and HRP-positive cells were found in the MVN, regardless of the excitatory or inhibitory effects of MVN stimulation on the LVN neurons. Nauta et al. reported that cells labeled by retrograde transport were stippled by the reaction product of HRP and evenly stained cells and axons were not labeled by a physiological uptake and retrograde transport.¹⁴ Since the HRP-positive neurons obtained in the MVN contained stippling, it seems unlikely that HRP was taken up from the nerve fibers passing through the LVN.

In conclusion, our results suggest the existence of excitatory and inhibitory input from the MVN to the LVN neurons monosynaptically activated from the vestibular nerve.

ACKNOWLEDGMENT

We thank M. Ohara for critical reading of the manuscript.

REFERENCES

1. BRODAL, A. 1974. Anatomy of the vestibular nuclei and their connections. In *Handbook of Sensory Physiology*. H. H. Kornhuber, Ed. 6: 239-352. Springer-Verlag, Berlin, Heidelberg & New York.
2. GACEK, R. R. 1971. Anatomical demonstration of the vestibulo-ocular projections in the cat. *Acta Otolaryngol. (Stockh.) Suppl.* 293: 1-63.
3. GOLDBERG, J. M. & C. FERNÁNDEZ. 1975. Vestibular mechanisms. *Ann. Rev. Physiol.* 37: 129-162.
4. MCMASTERS, R. E., A. H. WEISS & M. B. CARPENTER. 1966. Vestibular projections to the nuclei of the extraocular muscles. Degeneration resulting from discrete partial lesions of the vestibular nuclei in the monkey. *Am. J. Anat.* 118: 163-194.
5. PRECHT, W. 1979. Vestibular mechanisms. *Am. Rev. Neurosci.* 2: 265-289.
6. ITO, M. & M. YOSHIDA. 1964. The cerebellar-evoked monosynaptic inhibition of Deiters' neurones. *Experientia* 20: 515-516.
7. PRECHT, W. 1974. The physiology of the vestibular nuclei. In *Handbook of Sensory*

- Physiology. H. H. Kornhuber, Ed. 6: 353-416. Springer-Verlag. Berlin, Heidelberg & New York.
8. WILSON, V. J., M. KATO, R. C. THOMAS & B. W. PETERSON. 1966. Excitation of lateral vestibular neurons by peripheral afferent fibers. *J. Neurophysiol.* **29**: 508-529.
 9. SNIDER, R. S. & W. T. NIEMER. 1961. *A Stereotaxic Atlas of the Cat Brain*. University of Chicago Press. Chicago, Ill.
 10. SHIMAZU, H. & W. PRECHT. 1965. Tonic and kinetic responses of cat's vestibular neurons to horizontal angular acceleration. *J. Neurophysiol.* **28**: 991-1013.
 11. MATSUOKA, I., E. F. DOMINO & M. MORIMOTO. 1975. Effects of cholinergic agonists and antagonists on nucleus vestibularis lateralis unit discharge to vestibular nerve stimulation in the cat. *Acta Otolaryngol. (Stockh.)* **80**: 422-428.
 12. SASA, M., S. FUJIMOTO, S. IGARASHI, K. MUNEKIYO & S. TAKAORI. 1979. Microiontophoretic studies on noradrenergic inhibition from locus coeruleus of spinal trigeminal nucleus neurons. *J. Pharmacol. Exp. Ther.* **210**: 311-315.
 13. CHIKAMORI, Y., M. SASA, S. FUJIMOTO, S. TAKAORI & I. MATSUOKA. 1980. Locus coeruleus-induced inhibition of dorsal cochlear nucleus neurons in comparison with lateral vestibular nucleus neurons. *Brain Res.* **194**: 53-63.
 14. NAUTA, H. J. W., M. B. PRITZ & R. J. LASEK. 1974. Afferents to the rat caudoputamen studied with horseradish peroxidase. An evaluation of a retrograde neuroanatomical research method. *Brain Res.* **67**: 219-238.

THE ASCENDING TRACT OF DEITERS' AND HORIZONTAL GAZE

S. M. Highstein and H. Reisine

*Department of Neuroscience
Rose F. Kennedy Center
Albert Einstein College of Medicine
Bronx, New York 10461*

Rapid advances are being made in unraveling the substrate for the generation and control of eye movement.^{1,18} Specifically, the recording of signals carried by individual neurons that participate in vestibular compensatory eye movements permits relevant neuronal connectivity and signal transformations to be defined. The head velocity information of semicircular canal afferents provides input to several interconnected parallel processing systems that ultimately effect eye movements via the control of the 12 extraocular muscles. The direct pathway of primary vestibular afferent to central vestibular neuron to ocular motoneuron is one such system that plays a prominent role in maintaining gaze during head movement.⁴ Although horizontal gaze and vertical gaze are organized slightly differently, they share common mechanisms of information transfer. A head velocity signal from the vestibular labyrinth is transmitted directly to all six classes of extraocular motoneurons, while neural information encoding rapid eye movement (saccades or quick phases of nystagmus) travels to the motoneurons over different pathways.

Horizontal conjugate gaze involves the cocontraction and/or corelaxation of the medial rectus extraocular muscle of one eye and the lateral rectus of the other acting as a yoked team in opposition to the other pair of medial and lateral recti. This conjugation of the medial and lateral recti of the two eyes is a product of physiologic activity transmitted from the abducens nucleus to the contralateral medial rectus motoneuron pool by abducens internuclear neurons (Ab. Int.).^{3,16,17} Signals afferent to the abducens nucleus arise from several sources.^{1,2,19-22,28,29} The ipsi- and contralateral horizontal semicircular canals transmit head velocity signals via medial vestibular nucleus relay neurons to the abducens nucleus.^{20,28} Both ipsi- and contralateral relay neurons encode gaze-related signals that consist predominantly of eye position sensitivity with only a weak coupling to eye velocity. The dorsomedial gigantocellular tegmental field projects to the contralateral abducens nucleus to encode pause signals related to quick phases of nystagmus,²¹ and pontine reticular neurons mediating quick phases have recently been shown to project directly to the ipsilateral abducens nucleus.²⁸ The medial rectus motoneuron pool, on the other hand, receives only two direct signals from the posterior brain stem.^{2,17} They are transmitted by the internuclear neuron of the abducens nucleus via the medial longitudinal fasciculus (MLF) and by the ventral lateral vestibular neuron via the ascending tract of Deiters' (ATD).^{3,26,27} Abducens internuclear signals resemble those of medial rectus motoneurons, discharging strictly in relation to gaze.⁶ They emit a burst of impulses for saccades and/or quick phases in the on direction, and pause for quick phases or saccades in the off direction. Eye position is also very accurately encoded. Therefore, we can infer that the abducens afferent reticular signals are contained in internu-

clear activity in an already processed form. These signals are apparently necessary for the control of horizontal gaze but reach the medial rectus only indirectly via the internuclear pathway.¹⁶ The signals carried by the second pathway to the medial rectus, the ATD, are the subject of this report.

We have investigated these neurons in anesthetized paralyzed, decerebrate, and alert cats. Our studies indicate that the ascending tract of Deiters' terminates with excitation on medial rectus motoneurons and that the signals carried by these neurons are related both to head velocity and to gaze.^{2,26,27} Muskens, Winkler, Buchanan, and Gacek have described the ascending tract of Deiters'.^{7,12-14,25,29} To further delineate this tract and to determine the cell bodies of origin of the tract, we placed horseradish peroxidase (HRP) in the oculomotor nucleus and lesioned the brachium conjunctivum (BC) and MLF to eliminate labeling of the cells of origin of these known ascending pathways^{5,6} from the posterior brain stem. Lesions were extensive, interrupting the entire left pontine tegmentum from the MLF lateral to the BC. On the right, the MLF and BC were transected, sparing the area between these tracts. FIGURE 1 illustrates the location of neurons projecting to the oculomotor nucleus via pathways other than the MLF and BC. Labeled neurons reside predominantly in the ventral lateral vestibular nucleus, with some overlap to other vestibular nuclei. Sections A1-6 are 500 microns apart; each dot represents a labeled neuron present on the actual section illustrated or in the section 50 microns anterior or posterior. Labeled neurons on the right side were backfilled via axons traveling between the right MLF and BC, the area encompassing the ascending tract of Deiters'. There is an additional possibility of transport by axons between the MLF and BC that do not belong to the ATD system. Retrograde transport via these axons probably accounts for some of the labeled neurons on the left side of sections A1-6. As the right MLF lesion was intentionally more restricted than that on the left, a part of the extreme lateral wing of the MLF may have been spared. Thus, left-sided labeled cells probably comprise a crossed projection to the oculomotor nucleus. Interestingly, the group of "smaller cells" in the medial nucleus (Reference 12, page 13, Figure 5; FIGURE 1, arrowheads A3,4,5) apparently contributes to the ascending tract of Deiters', as suggested by Gacek.^{12,13} FIGURE 1B is a single section through the ventral lateral vestibular nucleus from another experiment.²³ HRP was placed in the ipsilateral cut MLF 4 mm rostral to the abducens nucleus. Labeled neurons are found in locations that overlap the sites of origin of the ATD. This area of the vestibular nuclei also contains the relay neurons for the horizontal canal projection to the abducens nucleus.²² Therefore, it is apparent that the ventral lateral and medial vestibular nuclei contain a mixture of neurons that relay horizontal canal signals to the abducens nucleus via a direct projection, relay horizontal canal signals to the medial rectus subgroup via the ATD, and relay vertical canal signals to the IIIrd nucleus via the crossed MLF.

Results of acute lesions to determine the course of the ATD in the pontine tegmentum indicate a middle course between the MLF and BC. FIGURE 1C illustrates a lesion of the area between the MLF and brachium that abolished the antidromic field evoked by IIIrd nucleus stimulation.

The comparative synaptic efficacy of the ventral lateral vestibular and abducens internuclear projection to the medial rectus motoneuron pool was evaluated by intracellular recording from medial rectus motoneurons during stimulation of both pathways.¹⁷ The abducens nucleus was stimulated to activate the internuclear neurons directly, and the VIIIth nerve to activate the ATD transsynaptically. The abducens-evoked EPSP is usually larger than the ascending Deiters'-evoked PSP (FIGURE 2B arrows, first component of each

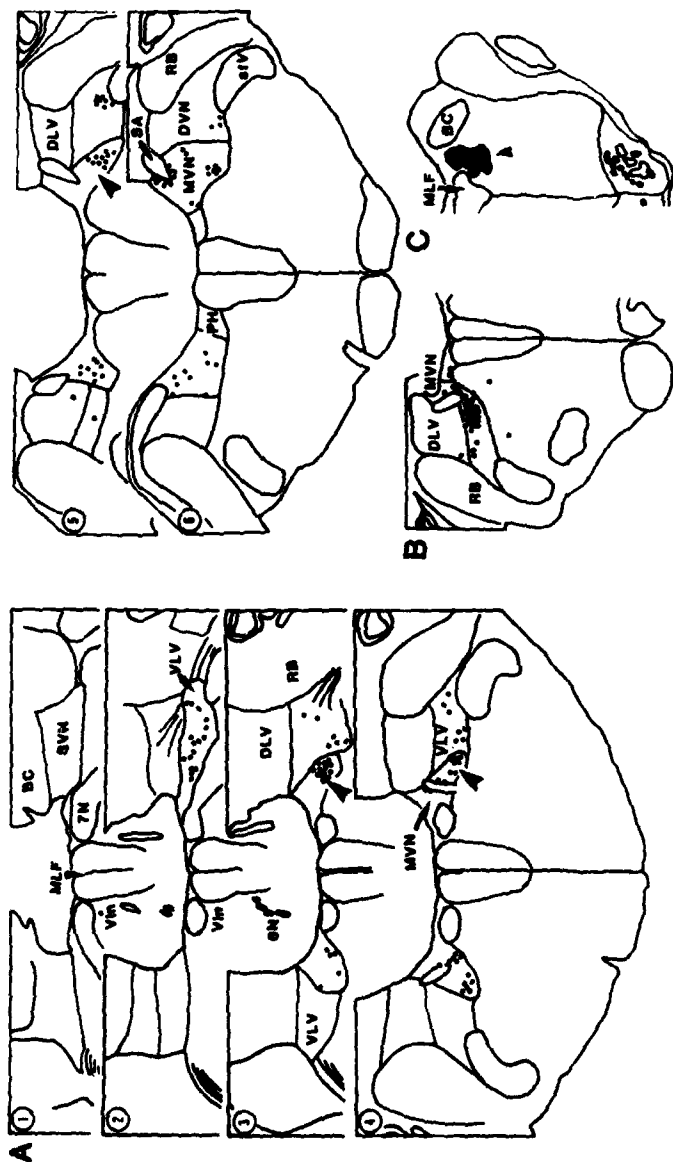


FIGURE 1. A1-6: representative coronal sections through the medulla. Sections are 500 microns apart. Each drawing (1-6) is a composite of three 50-micron sections to illustrate the location of neurons labeled by retrograde transport of horseradish peroxidase from an injection into the oculomotor nucleus. Immediately after the injection, the left pontine tegmentum from the midline lateral to the brachium conjunctivum was lesioned as were the right MLF and brachium conjunctivum. Each dot represents one labeled neuron. B: a single representative coronal section through the medulla to illustrate the location of neurons labeled by retrograde transport of horseradish peroxidase from the MLF. A small cut transected the left MLF exclusively (P-2 level), and a pledget of peroxidase was placed in the cut. C: a coronal section through the pons to illustrate the site of a lesion that abolished the antidromic field recorded in the ventral lateral vestibular nucleus following IIIrd nucleus stimulation. Arrowhead points to the lesion illustrated in black. Abbreviations: BC, brachium conjunctivum; DLV, dorsal lateral vestibular nucleus; DVN, descending vestibular nucleus; MVN, medial vestibular nucleus; RB, restiform body; SVN, superior vestibular nucleus; VIn, abducens nucleus; 6N, abducens nerve rootlets; VLV, ventral lateral vestibular nucleus.

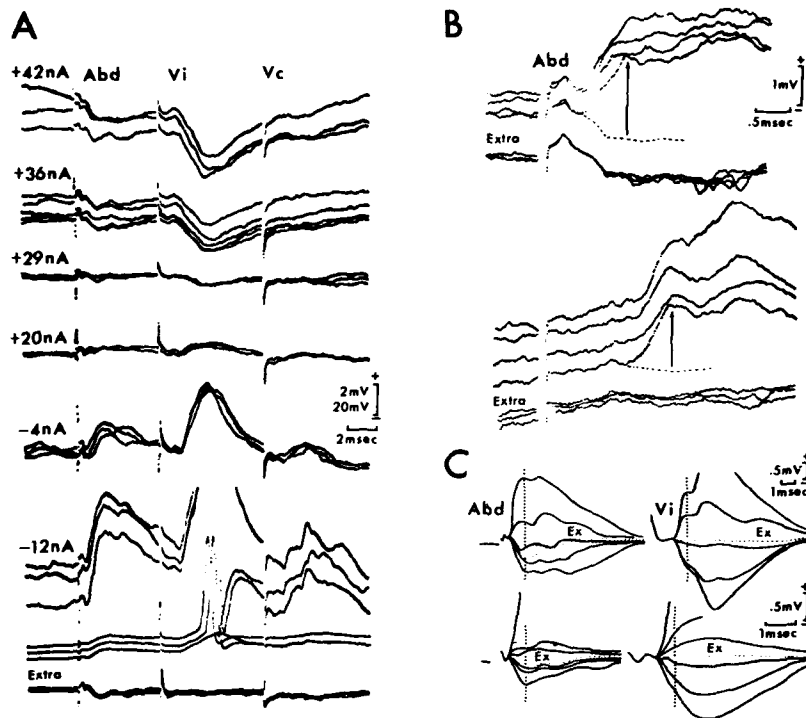


FIGURE 2. Comparison of EPSP reversal profiles for three separate excitatory pathways on medial rectus motoneurons. **A:** application of polarizing current in a left medial rectus motoneuron following stimulation of the right abducens nucleus (Abd), left vestibular nerve (Vi), and right vestibular nerve (Vc) at 2, 2.5, and 3 \times threshold (T), respectively. Currents as indicated, and explanation in text. **B:** comparison of the amplitude and rise time of the abducens excitation and ipsilateral vestibular nerve-evoked excitation in medial rectus motoneurons following 2 \times T stimulation, respectively. **C:** a comparison of the reversal potential profiles in two medial rectus motoneurons at different sweep speeds following abducens and ipsilateral vestibular nerve stimulation to show the waveform characteristics near the equilibrium potential for the EPSPs. Arrows in B and dotted lines in C are drawn through peaks of EPSPs to facilitate comparison of the reversal properties. [Modified from Highstein and Baker, Reference 17.]

PSP).^{*} The complete reversal of these EPSPs with depolarizing currents passed through the microelectrode (FIGURE 2A, Abd and Vi) indicates chemical synaptic transmission between these oculomotor afferent inputs and medial rectus motoneurons. The ascending Deiters'- and abducens-evoked EPSPs reverse with nearly identical current-voltage relationships, which suggests similar spatial distribution of synapses over the somadendritic tree. However, upon careful reconstruction, the ascending Deiters'-evoked EPSP reverses earlier than the abducens-evoked PSP and shows more responsiveness to polarizing current.

^{*}PSP, postsynaptic potential; EPSP, excitatory postsynaptic potential; IPSP, inhibitory postsynaptic potential.

This analysis indicates a roughly comparable synaptic potency of the ATD and internuclear inputs to the medial rectus motoneurons.

To study the input to ATD neurons, ventral lateral vestibular neurons were penetrated with glass microelectrodes in anesthetized paralyzed cats. Stimulation of the ipsilateral VIIIth nerve evoked monosynaptic EPSPs in these neurons (FIGURE 3A,B), while stimulation of the oculomotor nucleus provided antidromic identification. The passage of hyperpolarizing currents through the microelectrode augmented the ipsilateral vestibular-evoked EPSP's amplitude, while depolarizing currents decreased the amplitude and ultimately caused the reversal of the PSP (FIGURE 3C). The complete reversal of the EPSP is presumptive evidence for chemical synaptic transmission between vestibular primary afferents and ventral lateral vestibular neurons. In addition, ATD neurons are strongly modulated by contralateral vestibular stimulation, indicating the presence of powerful commissural inhibition (FIGURE 4). Amino acid studies indicate that there is no reciprocity between the two ventral lateral vestibular

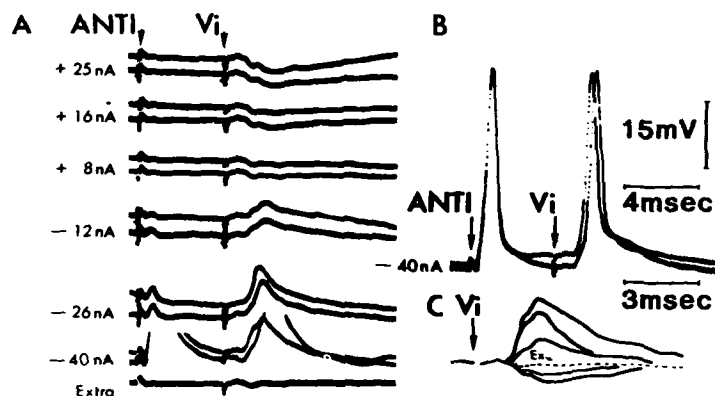


FIGURE 3. Intracellular records obtained from ventral lateral vestibular neurons. ANTI indicates stimulation of the oculomotor nucleus, and Vi stimulation of the ipsilateral labyrinth. Polarizing currents injected through the microelectrode as indicated. C is a drawing of a superimposition of the polarized EPSPs. Ex is extracellular field.

nuclei,²⁴ i.e., the commissural inhibitory neurons do not reside in the contralateral ventral lateral vestibular nucleus.

The morphology of ATD neurons was ascertained utilizing intracellular injection of horseradish peroxidase in physiologically identified neurons. These neurons have elongated somas; they measure approximately 15 by 50 microns and have simple, poorly developed dendritic trees that are oriented roughly perpendicular to the incoming VIIIth nerve fibers. The neurons are more extensive in the sagittal than in the coronal plane.²⁷

The sensitivity of these neurons to head velocity was determined in the decerebrate cat.²⁸ ATD neurons were isolated with an extracellular recording electrode and physiologically identified by their anti- and orthodromic responses. Responses to table rotation are type I (FIGURE 5).^{9,15} Antidromic testing at 1/second was maintained throughout the period during which the table was rotated to ensure the identity of the unit. The maximal amplitude of table rotation

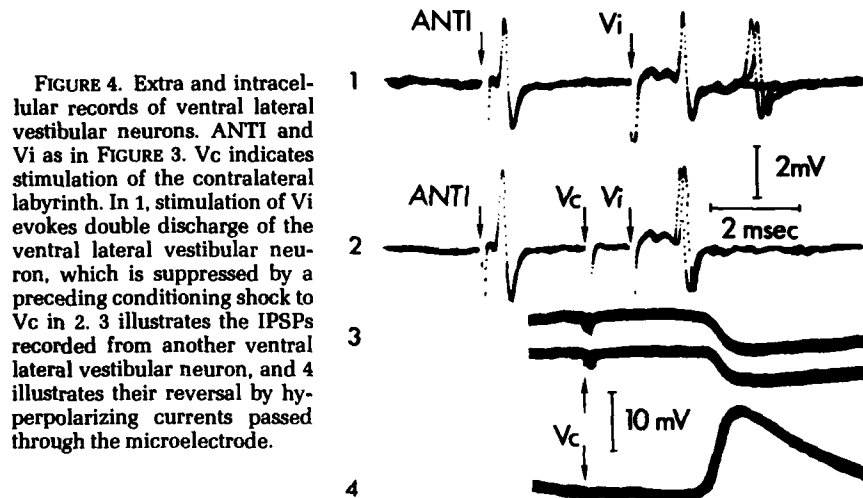


FIGURE 4. Extra and intracellular records of ventral lateral vestibular neurons. ANTI and Vi as in FIGURE 3. Vc indicates stimulation of the contralateral labyrinth. In 1, stimulation of Vi evokes double discharge of the ventral lateral vestibular neuron, which is suppressed by a preceding conditioning shock to Vc in 2. 3 illustrates the IPSPs recorded from another ventral lateral vestibular neuron, and 4 illustrates their reversal by hyperpolarizing currents passed through the microelectrode.

was 30° , the maximum velocity was $\pm 30^\circ/\text{second}$, and the frequency of rotation ranged from 0.4 to 0.65 Hz. All units ($n = 19$) display a type I response to table rotation.^{9,15} Discharge rate increases with table rotation to the ipsilateral side and decreases with table rotation to the contralateral side. The maximal firing rate of the unit illustrated is approximately 55 spikes/second with the testing paradigm employed. The discharge rate however decreased to zero during some part of the contralateral rotation, displaying a clipped response. Hand analysis of this clipped type I response of 5 units (cf., Reference 26) was conducted according to the theory of Melvill Jones and Milsum. All responses had some degree of skewing; for example, the peak of the response in FIGURE 5 record D was skewed

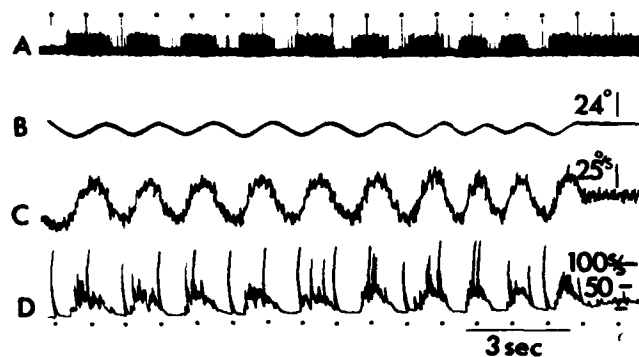


FIGURE 5. Response of an identified ascending tract of Deiters' neuron to head rotation in the plane of the horizontal semicircular canal. A: extracellular record (filtered) of a neuron similar to FIGURE 4. Dots above stimulus artifacts and below lower traces indicate oculomotor nucleus stimulation at 1/second. B: table position. C: table velocity. D: frequency of firing of the neuron in A. Calibration as indicated. (From Reisine and Highstein, Reference 26, with permission of the publisher.)

22.5° from the midpoint of the velocity curve. After correction for the skews of the response curves, the responses, although scattered, were observed to have an average phase lead of 9° (range +46° to -32°) to the angular velocity over all frequencies tested. Response gains were in the range of 0.5 to 1.7 spikes/second per degree/second. These results are similar to data obtained on other vestibular nucleus neurons^{11,15} (cf., Reference 13) and suggest that ascending tract of Deiters' neurons carry a canal signal related to head velocity.

In a third set of experiments in the alert animal, eye movements were measured by electro-oculography, during recording from ascending Deiters' neurons.²⁷ Cats were mounted on a turntable with their heads held 30° below the horizontal to place the lateral semicircular canals in the plane of rotation. Stimulating electrodes were implanted chronically on one abducens nerve at the base of the brain stem, over the bony ampulla of the horizontal semicircular canal, and within the oculomotor complex. A chamber was fitted over the posterior cerebellar vermis for hydraulic microdrive advance of 3-mm diameter glass pipettes to the brain stem. These electrodes were filled with a 10% solution of horseradish peroxidase in 0.5 M KCl, 50 mM tris buffer, pH 7.0. The abducens antidromic field potential was used as a reference to guide the placement of the recording electrode to the ventral lateral vestibular nucleus.

Physiological activity was recorded intra-axonally. When an axon was penetrated, responses to electric pulse stimulation of the labyrinth and IIIrd nucleus were ascertained, and the relation to gaze and rotation in the horizontal plane studied. When adequately characterized, the axon was injected with 3-600 nA-minutes of depolarizing pulses through the microelectrode. Animals survived 36 hours post injection, were then perfused, and the brain tissues processed for HRP. Data presented in eye position and rate plots were analyzed by hand, eye

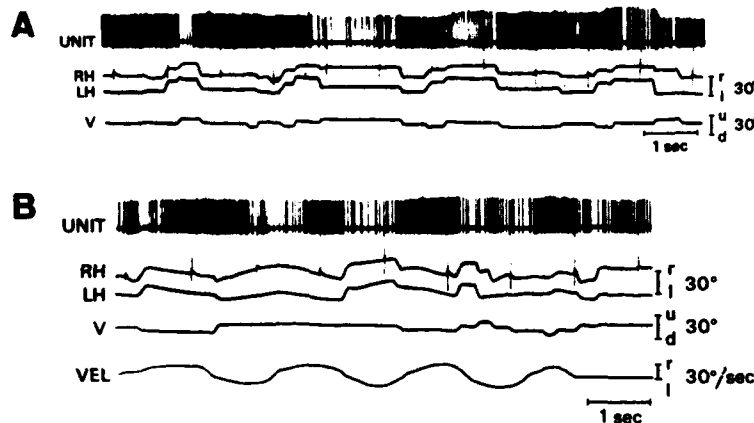
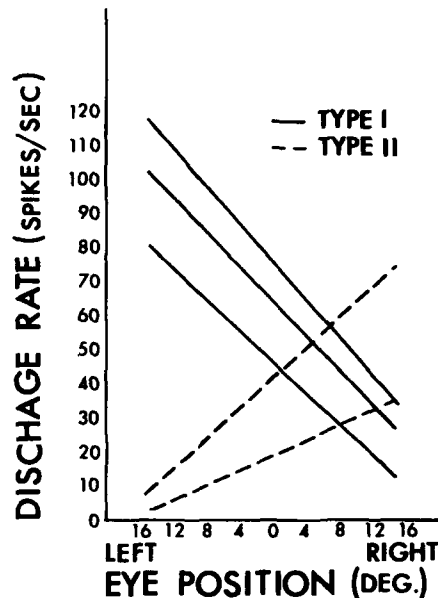


FIGURE 6. Relation of the unitary discharge rate of an ascending tract of Deiters' neuron to eye and head motion. A: UNIT, Intra-axonal record (0.1-10 kHz) recorded in the ventrolateral vestibular nucleus. RH, Electro-oculographic (EOG) record of right horizontal eye movement. Vertical lines are stimulus artifacts resulting from oculomotor nucleus stimulation at 1/second. LH, left horizontal EOG. V, vertical EOG. B: traces as in A except VEL, which is table (head) velocity. Calibrations as labeled. (From Reisine, Strassman, and Highstein, Reference 27, and reproduced with permission of the publisher.)

FIGURE 7. Discharge rate in spikes/second versus eye position. Solid lines are ascending tract of Deiters' neurons, and dotted lines are type II neurons recorded within the ventral lateral vestibular nucleus.



position versus discharge rate was plotted, and the correlation coefficient and regression line were determined.

When the microelectrode penetrated the brain stem 2 mm lateral to the abducens nucleus slightly above or below the level of the abducens, neurons were encountered that could be monosynaptically activated by ipsilateral labyrinth stimulation and antidromically activated by stimulation of the oculomotor nucleus. These neurons were previously identified in decerebrate and anesthetized cats as ATD neurons. Twelve neurons were studied. In FIGURE 6, records of spontaneous eye movement and neuronal discharge illustrate the relation between gaze and firing frequency. During spontaneous eye movement with the head fixed, neuronal activity is well correlated with eye position, increasing with contralateral eye position (left) and decreasing with ipsilateral eye position (right). Although the discharge rate approximates a linear function (correlation coefficient 0.83, slope 2.3 spikes/second per degree for FIGURE 7 lowest solid line), it must be noted that these neurons do not encode eye position with the same precision as an ocular motoneuron or an abducens interneuron. The differential relation to gaze of motoneurons versus ATD neurons is emphasized by the inconsistent response to saccades or quick phases of nystagmus of ATD cells. However, some coupling to rapid eye movements is apparent, as the neuron sometimes bursts for on-direction and pauses for off-direction saccades. These neurons also encode head velocity, type I response.

In summary, ATD neurons lie in the ventral lateral vestibular nucleus and manifest eye position and little rapid eye movement sensitivity. In addition, strong modulation of neuronal activity is manifest in response to head rotation (velocity) in the horizontal plane (type I response).

Although the values of rate-position slope of ATD neurons overlap that of Ab. Int. and ocular motoneurons, gaze-related signals present on ATD cells are

apparently insufficient by themselves to strongly activate the medial rectus extraocular muscle. Yet after MLF lesions, it is possible that the remaining horizontal vestibulo-ocular reflex in the abducting gaze field¹⁰ is due to ascending horizontal canal signals contained in ATD neurons. In the intact brain stem, ATD and abducens internuclear signals apparently interact at the level of medial rectus cells to produce the horizontal vestibulo-ocular reflex and conjugate horizontal gaze.

REFERENCES

1. BAKER, R. & A. BERTHOZ, Eds. 1977. *Control of Gaze by Brain Stem Neurons*. Elsevier/North Holland Biomedical Press. Amsterdam, The Netherlands.
2. BAKER, R. & S. M. HIGHSTEIN. 1978. Vestibular projections to medial rectus subdivision of oculomotor nucleus. *J. Neurophysiol.* **41**: 1629-1646.
3. BAKER, R. & S. M. HIGHSTEIN. 1975. Physiological identification of interneurons and motoneurons in the abducens nucleus. *Brain Res.* **91**: 292-298.
4. BAKER, R., N. MANO & H. SHIMAZU. 1969. Postsynaptic potentials in abducens motoneurons induced by vestibular stimulation. *Brain Res.* **15**: 577-580.
5. BENDER, M. B. & E. A. WEINSTEIN. 1950. The syndrome of the median longitudinal fasciculus. *Res. Publ. Assoc. Nerv. Ment. Dis.* **28**: 414-420.
6. BENDER, M. B. & E. A. WEINSTEIN. 1944. Effects of stimulation and lesion of the median longitudinal fasciculus in the monkey. *Arch. Neurol. Psychiatry* **52**: 106-113.
7. BUCHANAN, A. R. 1937. The course of the secondary vestibular fibers in the cat. *J. Comp. Neurol.* **67**: 183-204.
8. DELGADO-GARCIA, J., R. BAKER & S. M. HIGHSTEIN. 1977. The activity of internuclear neurons identified within the abducens nucleus of the alert cat. In *Control of Gaze by Brain Stem Neurons*. R. Baker & A. Berthoz, Eds.: 291-301. Elsevier/North-Holland Biomedical Press. Amsterdam, The Netherlands.
9. DUENSING, F. & K. P. SCHAEFFER. 1958. Die Aktivität einzelner Neurone im Bereiche der Vestibulariskerne bei Horizontalbeschleunigungen unter besonderer Berücksichtigung des vestibulären Nystagmus. *Arch. Psychiatr. Nervenkr.* **198**: 224-252.
10. EVINGER, C., A. FUCHS & R. BAKER. 1977. Bilateral lesions of the medial longitudinal fasciculus in monkeys; effects on the horizontal and vertical components of voluntary and vestibular induced eye movements. *Exp. Brain Res.* **28**: 1-20.
11. FUCHS, A. F. & J. KIMM. 1975. Unit activity in vestibular nucleus of the alert monkey during horizontal angular acceleration and eye movement. *J. Neurophysiol.* **38**: 1140-1161.
12. GACEK, R. R. 1971. Anatomical demonstration of the vestibulo-ocular projections in the cat. *Acta Oto-Laryngol. (Stockh.)* **293**: 1-63.
13. GACEK, R. R. 1971. Anatomical demonstration of the vestibulo-ocular projections in the cat. *Laryngoscope* **81**: 1559-1595.
14. GACEK, R. R. 1969. The course and central termination of first order neurons supplying vestibular end-organs in the cat. *Acta Otolaryngol.* **254**: 1-66.
15. GERNANDT, B. E. 1949. Response of mammalian vestibular neurons to horizontal rotation and caloric stimulation. *J. Neurophysiol.* **12**: 173-184.
16. HIGHSTEIN, S. M. 1977. Abducens to medial rectus pathway in the MLF: a possible cellular basis for the syndrome of internuclear ophthalmoplegia. In *Eye Movements*. B. A. Brooks & F. J. Bajandas, Eds.: 127-144. Plenum Press. New York, N.Y.
17. HIGHSTEIN, S. M. & R. BAKER. 1978. Excitatory synaptic termination of abducens internuclear neurons on medial rectus motoneurons: relationship to syndrome of internuclear ophthalmoplegia. *J. Neurophysiol.* **41**: 1647-1661.
18. HIGHSTEIN, S. M. & H. REISINE. 1979. Synaptic and functional organization of vestibulo-ocular reflex pathways. *Prog. Brain Res.* **50**: 431-442.
19. HIKOSAKA, O., Y. IGUSA, S. NAKAO & H. SHIMAZU. 1978. Direct inhibitory synaptic

- linkage of pontomedullary reticular burst neurons with abducens motoneurons in the cat. *Exp. Brain Res.* **33**: 337-352.
20. HIKOSAKA, O., M. MAEDA, S. NAKAO, H. SHIMAZU & Y. SHINODA. 1977. Presynaptic impulses in the abducens nucleus and their relation to postsynaptic potentials in motoneurons during vestibular nystagmus. *Exp. Brain Res.* **27**: 355-376.
 21. HIKOSAKA, O. & T. KAWAKAMI. 1977. Inhibitory reticular neurons related to the quick phase of vestibular nystagmus—their location and projection. *Exp. Brain Res.* **27**: 377-396.
 22. MACIEWICZ, R. J., K. EAGEN, C. R. S. KANEKO & S. M. HIGHSTEIN. Vestibular and medullary brain stem afferents to the abducens nucleus in the cat. *Brain Res.* **123**: 229-240.
 23. MACIEWICZ, R. J., et al. (In preparation.)
 24. MACIEWICZ, R. J. & S. M. HIGHSTEIN. (In preparation.)
 25. MUSKINS, L. J. J. 1913-14. An anatomico-physiological study of the posterior longitudinal bundle in its relation to forced movements. *Brain* **36**: 352-426.
 26. REISINE, H. & S. M. HIGHSTEIN. 1979. The ascending tract of Deiters' conveys a head velocity signal to medial rectus motoneurons. *Brain Res.* **170**: 172-176.
 27. REISINE, H., A. STRASSMAN & S. M. HIGHSTEIN. Eye position and head velocity signals are conveyed to medial rectus motoneurons in the alert cat by the ascending tract of Deiters'. *Brain Res.* (In press.)
 28. SASAKI, S. & H. SHIMAZU. 1981. Reticulovestibular organization participating in generation of horizontal fast eye movement. *Ann. N.Y. Acad. Sci.* (This volume.)
 29. WINKLER, C. 1918. The central course of the nervus octavus and its influence on motility. *Opera Omnia* **T4**: 357-535.

NONLINEAR CHARACTERISTICS OF SINGLE NEURONS IN THE VESTIBULAR NUCLEI*

Jai H. Ryu, Brian F. McCabe, and Richard W. Babin

*Department of Otolaryngology
and Maxillofacial Surgery
College of Medicine
University of Iowa
Iowa City, Iowa 52242*

INTRODUCTION

In the early 1930s, Steinhausen proposed the first operational mathematical model of the semicircular canals.^{1,2} The classic model of Steinhausen can be described by the second-order differential equation

$$\theta \ddot{\xi} + \pi \dot{\xi} + \Delta \xi = \theta \alpha,$$

which is known as a highly damped torsion pendulum model. During the past 50 years, many investigators have tried to validate the Steinhausen model, to determine the parameters of the model, and to modify the model by utilizing either theoretical considerations of the physical properties of the semicircular canals or anatomical and physiological experimental data. Although there are variations among the models, most of them are based on the highly damped torsion pendulum model. Some of the models developed recently are based on the relationship between input and output of the semicircular canal system utilizing linear system theory.³⁻⁵ The transfer function describing the system can be expressed with the assumption that the semicircular canal system behaves basically as a linear system.

It is important to investigate the canal system directly; however, various difficulties prevent making direct observations or measurements of the system. Since the single unit in the vestibular nuclei reflects directly the changes in the semicircular canal system, it is possible to study the question of whether or not the semicircular canal system behaves as a linear system by measuring the single-unit responses to canal stimulation. The study reported herein was concerned with the validity of the assumption that the semicircular canal system can be considered within the context of linear system theory.

MATERIALS AND METHODS

A total of 65 adult cats weighing 2.5 to 4.0 kg were used in this study. A total of 110 canal-sensitive neurons in the vestibular nuclei were recorded extracellularly.

Surgical Procedures

Each animal was anesthetized with an intraperitoneal injection of 35 mg/kg pentobarbital sodium followed by 25-mg supplemental doses as needed. A

*This study was supported by the Medical Research Service of the Veterans Administration and by the Department of Otolaryngology and Maxillofacial Surgery.

20-mm parieto-occipital trephine was made, and the posterior half of the bony tentorium was removed. The dura matter over the cerebellum was excised, and sterile mineral oil used to prevent dehydration. The animal was then transferred to a stereotaxic apparatus. The head of the animal was fixed on the stereotaxic device such that the horizontal canals were positioned in the horizontal plane (the head was tilted forward 25°).⁶ Using a stereotaxic atlas as a guide, a tungsten microelectrode (tip diameter = 2.0 micra; impedance = 1.0 to 2.0 megohms) was placed in the vestibular nuclei area through the intact cerebellum.⁷

Recording Procedures

Activity of single neurons in the vestibular nuclei was recorded extracellularly. When a canal-sensitive neuron was found, spikes (action potentials) of neurons were amplified, and the amplified signals were sent to a spike analyzer via the slip rings of the rate table. Spikes were discriminated from noise and were fed into an instrument computer for on-line data analysis. Experimental data were retrieved in both analog and digital form, and were also stored on magnetic tapes. Audio monitoring was routinely employed.

Stimulating Procedures

The horizontal canals were stimulated by angular acceleration utilizing the rate table controlled by the preprogrammable function generator. The two types of angular accelerations used in this study were (A) impulse and (B) step (FIGURE 1).

Impulse acceleration, which consists of 32 equally spaced (period between impulses varied from 1.24 to 4.9 seconds) and uniform magnitude impulses, was generated by the 10°/second angular velocity change in 0.1 second (equivalent to 100°/second² acceleration with 0.1-second duration). Step acceleration consists of 2, 4, 6, or 8°/second² constant acceleration for a given period.

Histological Procedures

At the end of each experiment, the animal was given an overdose of sodium pentobarbital intravenously, and a small electrolytic lesion (0.3-mm lesion was made by applying a constant current of 1.0 mA for 5 seconds) was made at the last spot recorded. The brain stem was removed, and it was serially sectioned and stained (Klüver and Barrera method).⁸ The vestibular nuclei were identified by the criteria of Brodal *et al.*⁹ The locations of recorded neurons were determined by using the recorded coordinates and by utilizing the stereotaxic atlas.

EXPERIMENTAL RESULTS

The resting discharge rate and the response characteristics of 110 canal-sensitive neurons were studied. Utilizing the neuron classification used by Duensing and Schaefer, Shimazu and Precht, and Ryu and McCabe,¹⁰⁻¹² 62 (56%) neurons were classified as type I and 48 (44%) neurons as type II. A total of 11 units exhibited a superimposed cyclic firing pattern (this type of neuron is

probably reflecting the cyclic nature of the ultraslow brain wave) (FIGURE 2) or unstable resting discharge rate (FIGURE 3). These neurons were considered unsuitable for analysis, and they were excluded from the study. The remaining 99 neurons were analyzed.

The resting discharge rate varied from neuron to neuron in the same preparation; firing rates ranged from 1.0 spike per second (sps) to 97 sps, and the average was 21.3 sps with a standard deviation (SD) of 12.6 sps. The average resting discharge rate of type I neurons (mean = 21.9 sps; SD = 13.1 sps) was slightly higher than that of type II neurons (mean = 20.4 sps; SD = 9.7 sps). An

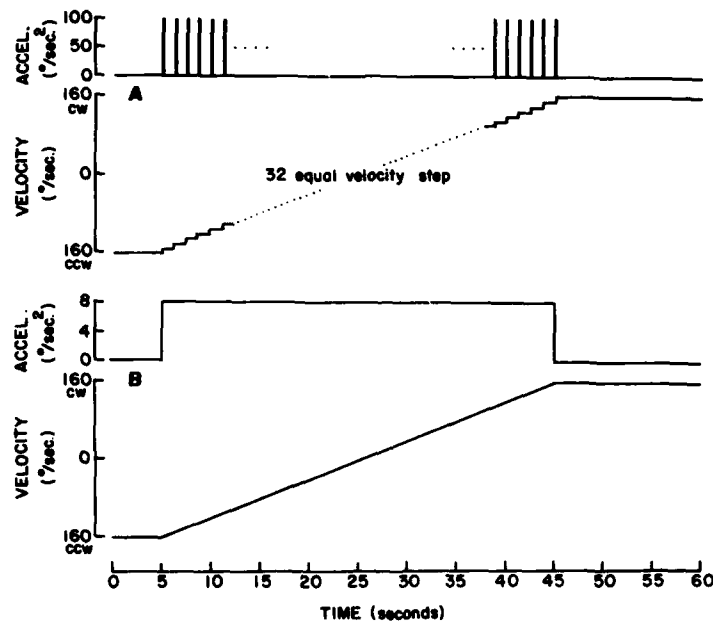


FIGURE 1. Paradigms of stimulus applied in this experiment. (A) illustrates impulse acceleration, and (B) illustrates step acceleration.

independent sample t-test at a confidence level of $p = 0.05$ showed that there was no significant difference in the resting discharge rate between the two types.

The maximum response varied from neuron to neuron. However, the maximum response increased with an increase in the magnitude of acceleration for a given unit. The average maximum response of neurons varied nonlinearly from 14.9 sps for the $2^\circ/\text{second}^2$ to 26.7 sps for the $8^\circ/\text{second}^2$ acceleration (FIGURE 4 and TABLE 1).

The time required to reach maximum response (t_{max}) decreased with the increase in magnitude of acceleration. The average t_{max} also varied nonlinearly from 35.4 seconds for the $2^\circ/\text{second}^2$ to 13.9 seconds for the $8^\circ/\text{second}^2$ acceleration (FIGURE 5 and TABLE 1).

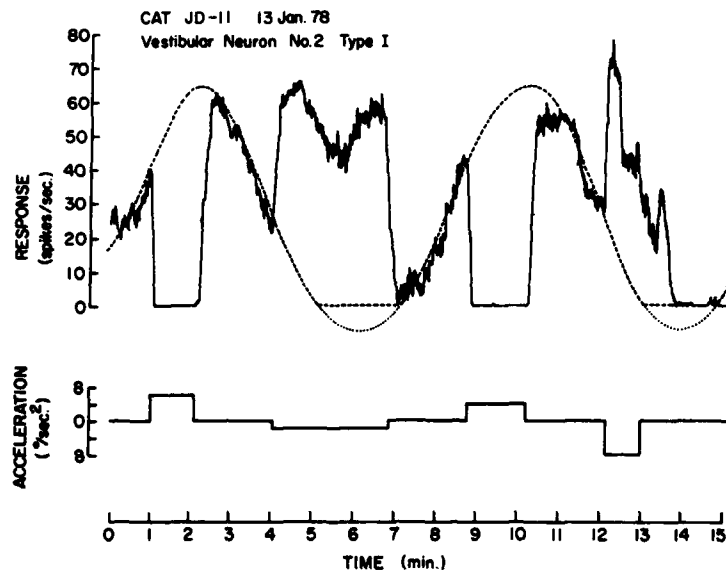


FIGURE 2. Neuron exhibiting cyclic firing. When the neuron was subjected to stimulation, the change of firing rate was superimposed on the inherent cyclic firing pattern. This type of neuron is probably reflecting the ultraslow brain wave.

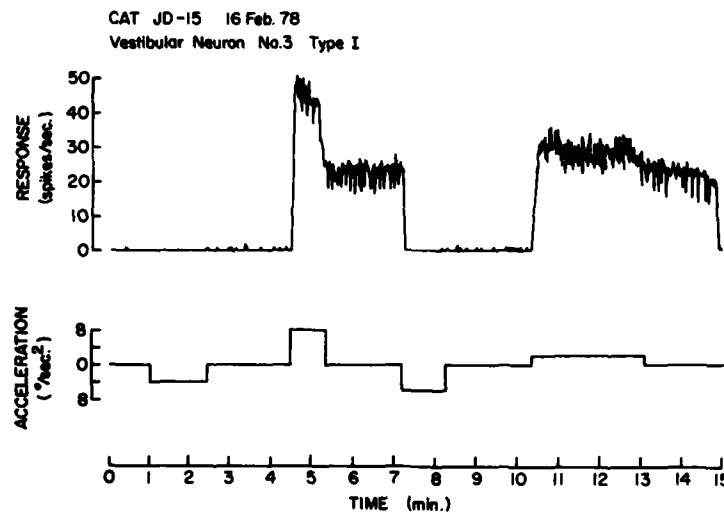


FIGURE 3. Neuron exhibiting unstable resting discharge rate. Initially, the neuron was a kinetic type; however, the neuron became a tonic type after excitatory stimulation (gains resting activity). The established resting activity disappeared after the inhibitory stimulation; the neuron acted as a kinetic neuron.

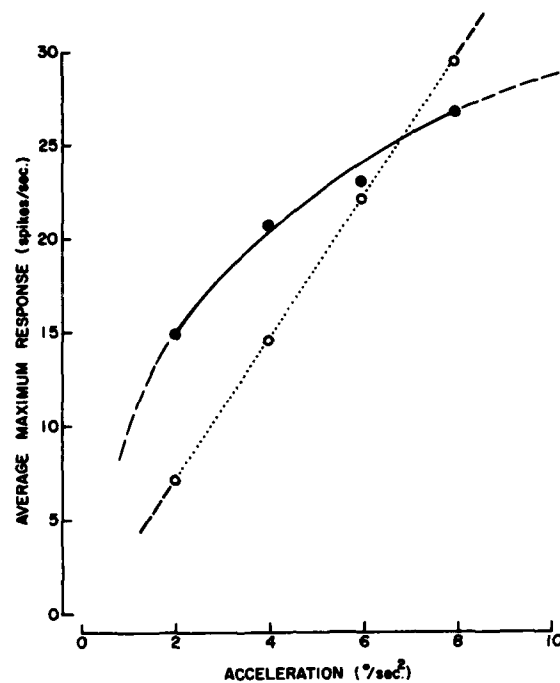


FIGURE 4. Average maximum response (spikes/second) was plotted against the magnitude of step acceleration. The relationship was nonlinear, and the average maximum response increased with an increase in the magnitude of step acceleration. Open circles connected by the dotted line represent the computer simulation results of the Fernández and Goldberg model, showing the linear relationship between the average maximum response and the magnitude of stimulus.

TABLE 1
AVERAGE MAXIMUM RESPONSE AND t_{\max} VS. RATE OF ACCELERATION

Stimulus	Average Maximum Response (spikes per second)	
	Mean	Standard Deviation
2°/sec ²	14.9 sps	11.2 sps
4°/sec ²	20.6 sps	14.2 sps
6°/sec ²	22.9 sps	13.3 sps
8°/sec ²	26.7 sps	13.7 sps
Stimulus	Average t_{\max} (seconds)	
	Mean	Standard Deviation
2°/sec ²	35.4 sec	13.4 sec
4°/sec ²	23.3 sec	4.6 sec
6°/sec ²	19.1 sec	3.8 sec
8°/sec ²	13.9 sec	3.4 sec

Neither the maximum response nor the t_{\max} appeared to be related to the resting discharge rate; the results of an independent sample t-test ($p = 0.05$) showed that there was no correlation between the maximum response and the resting discharge rate, or between the t_{\max} and the resting discharge rate. Furthermore, there was no correlation between the maximum response and t_{\max} utilizing a matched-pair t-test ($p = 0.05$).

In the beginning, the neural responses to successive impulse acceleration were additive. After the magnitude of neural response to impulse acceleration reached a maximum level, the peak-to-peak response to each successive impulse gradually decayed (FIGURES 6 and 7). This phenomenon was also observed when the period between two impulses was varied (FIGURE 8).

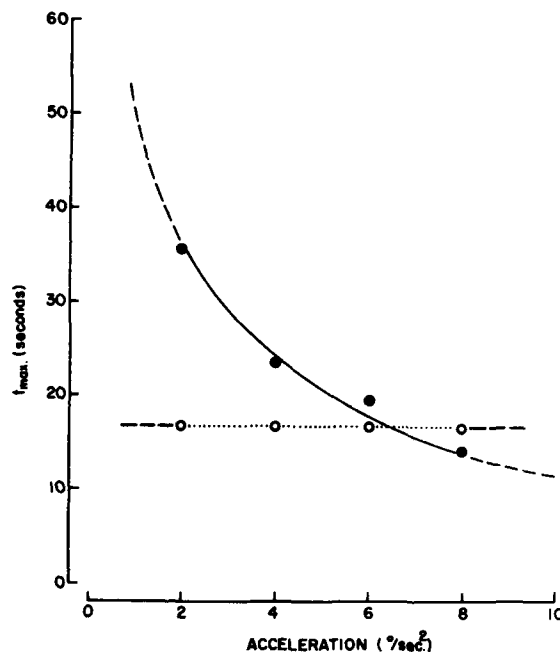


FIGURE 5. The relationship between t_{\max} and the magnitude of acceleration showed that t_{\max} decayed nonlinearly with an increase in the magnitude of acceleration. Open circles connected by dotted lines illustrate the computer simulation results of the Fernández and Goldberg model, showing a linear system property.

The majority of the neurons (both type I and II) showed that the response to inhibitory stimulation was not a mirror image of the response to excitatory stimulation. Usually, the excitatory response was greater than the inhibitory one. Furthermore about 10% of vestibular nuclei neurons were the kinetic type that responded only to excitatory stimulation.

Mathematical models describing the dynamic characteristics of the semicircular canals were reviewed (TABLE 2), and some of the existing models were simulated by utilization of the IBM Continuous System Modeling Program (CSMP/360). The input paradigm used for simulation was the same as the

stimulus paradigm used in the experiment.

... used in the experimental procedures. Some of these simulation results are shown in FIGURES 4 and 5 along with the experimental results. The simulation results indicated that the semicircular canals behave as a linear system. The sample of a simulation plot (Fernández and Goldberg model) is shown in FIGURE 3.

DISCUSSION

Most investigative work on the semicircular canal system has assumed that it behaves like a highly damped torsion pendulum (see TABLE 2). Furthermore, the dynamics of the system have been considered within the context of linear system theory. If the semicircular canal system behaves as a linear system, then the

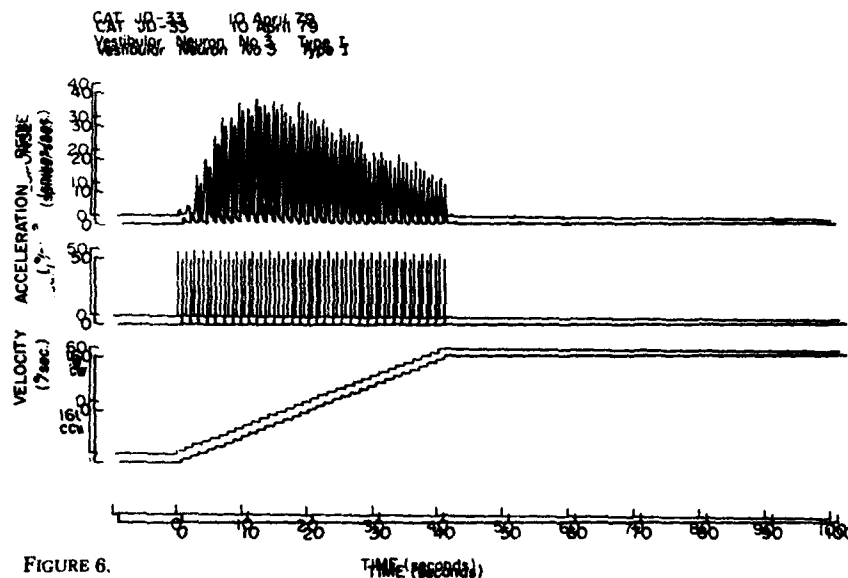


FIGURE 6.
Neural response of a kinetic neuron to impulse acceleration showing that the amplitude varies while the frequency of each impulse stimulus is constant.

system must possess two properties: (1) homogeneity property—a k -fold increase in the input causes a k -fold increase in the output for any value of k ; and (2) superposition property—if there are several inputs acting on the system, then the total output is the sum of all output components computed by considering one input at a time.

The computation results of the existing canal models show that they meet the above conditions. However, the experimental results indicate that the vestibular nuclear complex to semicircular canal stimulation are nonlinearities. The most striking nonlinearity is the nonhomogeneity property, and possess neither homogeneity nor superposition property. The nonlinearity represents variations in k_{canal} which increase

CAT JD-35 25 April 79
Vestibular Neuron No.1 Type I

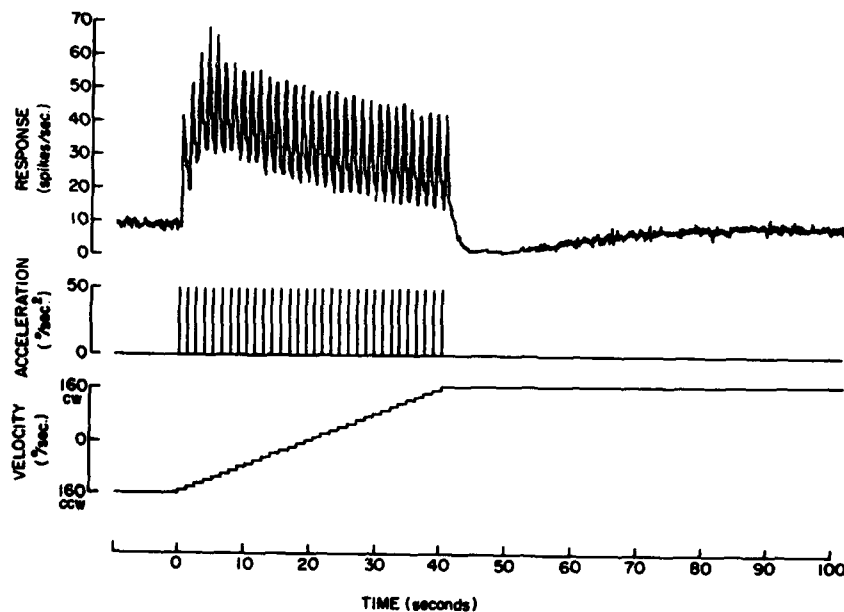


FIGURE 7. Neural response to impulse acceleration. Although each impulse had an equal magnitude of stimulus, the neural response showed that it was additive at the beginning until it reached the maximum level, then it decayed gradually. The averaged response was very similar to the neural response when the canal was stimulated by step acceleration.

Cat JD-28 5 October 78
Vestibular Neuron No.1 Type II

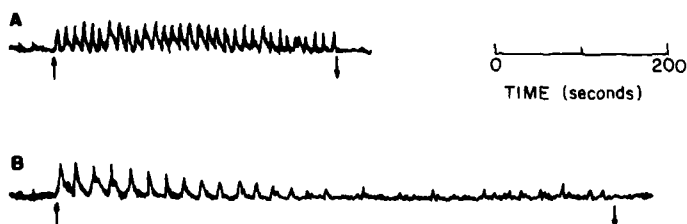


FIGURE 8. Neural response to impulse acceleration. Upward arrow represents the beginning of the 1st impulse stimulus, and downward arrow represents the end of the 32nd impulse stimulus. (A) illustrates the response to impulse acceleration with a 10-second period between two impulses; and (B), with a 20-second period between two impulses.

TABLE 2
REVIEW OF MATHEMATICAL MODELS OF THE SEMICIRCULAR CANALS

Names(s) of investigator(s) and the year	Model(s) and values of parameter(s)	Comments
Anliker and van Buskirk (1970 & 1971)	$\ddot{\xi}_p + (\pi/\theta)\dot{\xi}_p + (\Delta/\theta)K_c\xi_p = \alpha$ $(\pi/\theta) = 11.0$; $(\Delta/\theta) = 0.0058$; $K_c = ?$	1. A theoretical model 2. Based on an erroneous concept -- cupula movement is due to perilymph flow
Aschan et al. (1952)	$\ddot{\xi} + (\pi/\theta)\dot{\xi} + (\Delta/\theta)\xi = \alpha$ $(\pi/\Delta) = 11.0$ (range 6 to 24)	1. Nystagmus responses of 320 human subjects
Barnes and Benson (1979)	$A(s) = \frac{s}{(1 + 90s)(1 + 70s)}$ (Canal + Adaptation) $H(s) = \frac{s}{(1 + 250s)(1 + 44s)}$ (Heating effect)	1. Nystagmus responses of human subjects 2. Bithermo caloric test
Barnes et al. (1978)	$\frac{\theta_v}{\theta_c} = \frac{K \tau_b(1 + \tau_a s)}{(1 + \tau_b s)(1 + \tau_c s)}$ $\tau_a = 0.25$; $\tau_b = 15.0$; $\tau_c = 0.01$; $K = 0.7$	1. Based on study of human visual-vestibular interaction due to vestibular and visual stimulations
Benson (1966)	$\ddot{\xi} + (\pi/\theta)\dot{\xi} + (\Delta/\theta)\xi = \alpha$ $(\pi/\Delta) = 12.0$	1. Nystagmus responses and subjective sensation of human subjects 2. Angular acceleration modified by direction & magnitude of linear acceleration

Name(s) of investigator(s) and the year	Model(s) and values of parameters(s)	Comments
Benson (1967)	$\bar{\xi} + (\pi/\theta)\bar{\xi} + (\Delta/\theta)\xi = \alpha$ (π/θ) nystagmus = 15.0; (π/θ) sensation = 35.0	1. Post-rotational nystagmus responses and subjective sensation of human subjects
Cappel (1966)	$\frac{F_{out}}{F_{in}} = \frac{K \omega_n(s + \alpha)}{s^2 + 2\zeta\omega_n s + \omega_n^2}$ (π/θ) = 0.25; (Δ/θ) = 4×10^{-4} ; at $K = 6.0$, $\omega_n = 0.02$	1. Analog computer curve fitting method 2. Based on data collected by Crampton (single neuron activity in the vestibular nuclei of the cat)
Fernández and Valentiniuzzi (1968)	$\bar{\xi} + (\pi/\theta)\bar{\xi} + (\Delta/\theta)\xi = \alpha$ (π/θ) cat = 657; (π/θ) pigeon = 360	1. Theoretical calculation from anatomical dimensions of end organs of cat and pigeon 2. Pigeon data (Money, 1966)
Fernández and Goldberg (1971) Goldberg and Fernández (1971a & 1971b)	$H(s) = \frac{\tau_2(s)(1 + \tau_1 s)}{(1 + \tau_1 s)(1 + \tau_2 s)(1 + \tau_3 s)}$ $\tau_1 = 0.003$; $\tau_2 = 5.7$; $\tau_3 = 30 \sim 80$; $\tau_4 = 0.013 \sim 0.094$	1. Data from the neural activity of first-order neurons in the squirrel monkey 2. Stimulus: constant angular acceleration and sinusoidal angular rotation
Groen et al. (1952)	$\bar{\xi} + (\pi/\theta)\bar{\xi} + (\Delta/\theta)\xi = \alpha$ (π/θ) = 35.0; (π/Δ) = 35.0; (Δ/θ) = 1.0	1. Responses of the primary fiber of elasmobranch 2. Torsion swing

(continued)

TABLE 2 (continued)

Name(s) of investigator(s) and the year	Model(s) and values of parameter(s)	Comments
Green (1965)	$\ddot{\xi} + (\pi/\theta)\dot{\xi} + (\Delta/\theta)\xi = \alpha$ Infant: $(\pi/\Delta)_1 \text{ day} = 22.0$; $(\pi/\Delta)_{100 \text{ days}} = 10.0$ Dog: $(\pi/\Delta)_1 \text{ day} = 30.0$; $(\pi/\Delta)_{25 \text{ day}} = 15.0$	1. Post-rotatory nystagmus from birth to 100 days 2. Inhibitor of (π/Δ) value is coming from the CNS
Guedry (1968)	$\ddot{\xi} + (\pi/\theta)\dot{\xi} + (\Delta/\theta)\xi = \alpha$ $(\pi/\Delta) = 14.0$	1. Post-rotatory nystagmus of human subjects 2. (π/Δ) value decreases with head tilt 3. Result is identical to Benson's (1974) work
Hallpike and Hood (1953)	$\ddot{\xi} + (\pi/\theta)\dot{\xi} + (\Delta/\theta)\xi = \alpha$ $(\pi/\Delta) = 12.6$; $(\pi/\theta) = 10.99$; $(\Delta/\theta) = 0.86$	1. Nystagmus responses and subjective sensation of human subjects 2. Constant angular acceleration
Lowenstein et al. (1964) Lowenstein (1966)	$\ddot{\xi} + (\pi/\theta)\dot{\xi} + (\Delta/\theta)\xi = \alpha$ $(\pi/\Delta) = 22.0$; $(\pi/\theta) = 36.0$; $(\Delta/\theta) = 1.64$; $\omega_n = 1.3$	1. Measurements from the primary fiber of the ray 2. Sinusoidal rotation
Malcolm (1968 & 1973) Malcolm and Melvill Jones (1970)	$\frac{\theta_e}{\theta_h} = K \left\{ \frac{s}{(\tau_1 s + 1)} - \frac{s}{(\tau_1 s + 1)(\tau_g s + 1)} \right\}$ $\tau_1 = 15.0$; $\tau_g = 73.4$	1. Relationship between slow-phase nystagmus velocity and angular velocity of the head of human subjects

Name(s) of investigator(s) and the year	Model(s) and values of parameter(s)	Comments
Mayne (1950)	$\ddot{\xi} + (\pi/\theta)\dot{\xi} + (\Delta/\theta)\xi = \alpha$ $(\pi/\theta) = 200.0$; $(\Delta/\pi) = 0.12$; $(\Delta/\theta) = 24.0$	1. Theoretical analysis 2. Anatomical and physiological data obtained by Mowrer (1932 & 1935)
Mayne (1965)	$\ddot{\xi} + (\pi/\theta)\dot{\xi} + (\Delta/\theta)\xi = A\omega^2 \sin \omega t$ $(\tau_1)_{\text{mammal}} = 5.5 \sim 7.2$; $(\tau_1)_{\text{fish}} = 10.4 \sim 26.5$	1. Theoretical analysis 2. Anatomical and physiological data obtained by Melvill Jones and Spell (1965)
McDonald et al. (1965)	$\ddot{\xi} + (\pi/\theta)\dot{\xi} + (\Delta/\theta)\xi = \alpha$ $(\pi/\Delta) = 11.0$	1. Post-rotatory nystagmus of human subject 2. Reduction of (π/Δ) value due to bilateral radiation of 500 rads to end organ
Melvill Jones and Milsom (1970 & 1971)	$\frac{d}{dt} \xi(s) = \frac{K \tau_1 \tau_2^5}{(\tau_1 s + 1)(\tau_2 s + 1)}$ $\tau_1 = 3.6$; $\tau_2 = \frac{1}{657}$; $w = 7.89 \times 10^{-3}$ dyne-cm/sec; $\Delta = 2.05 \times 10^{-3}$ dyne-cm; $K = 1264$ spikes per sec/deg of cupular deflection	1. Theoretical analysis utilizing existing data (Fernández and Valentiniuzzi, 1968)
Milsom (1966)	$\ddot{\xi} + (\pi/\theta)\dot{\xi} + (\Delta/\theta)\xi = \alpha$ $(\pi/\Delta) = 10.0$; $(\theta/\pi) = \frac{1}{200}$	1. Theoretical analysis

(continued)

TABLE 2 (continued)

Name(s) of investigator(s) and the year	Model(s) and values of parameter(s)	Comments
Niven and Hixon (1963)	$\ddot{\xi} + (\pi/\theta)\dot{\xi} + (\Delta/\theta)\xi = a \sin \omega t$ $(\pi/\Delta) = 14.8$	1. Nystagmus responses of human subjects
Niven et al. (1965 & 1966)	$\ddot{\xi} + (\pi/\theta)\dot{\xi} + (\Delta/\theta)\xi = a \sin \omega t$ $(\pi/\Delta) = 12.0$	1. Nystagmus responses of human subjects 2. (π/Δ) value varies as a function of stimulus frequency
Peterka et al. (1976)	$H(s) = \frac{2.46(0.48^2 + 0.041s + 1)}{(2.09s + 1)(0.25 + 1)(0.061s + 1)}$	1. Response of first-order neuron of the cat 2. White noise rotational stimulation
Ryu et al. (1973)	$H(s) = \frac{\tau_A s}{(1 + \tau_A s)} \frac{(1 + \tau_L s)}{(1 + \tau_1 s)(1 + \tau_2 s)}$ $\tau_A = 40.0; \tau_L = 0.05; \tau_1 = 6.0; \tau_2 = 0.003$	1. Single neuron activity in vestibular nuclei of the cat 2. Constant angular acceleration
Steer (1967 & 1968)	$\frac{\ddot{\xi}}{a}(s) = \frac{0.22}{s^2 + 220 \left(1 + \frac{4.5 \times 10^{-6}}{\Delta B} \right) s + 0.07c}$ $(\pi/\theta) = 220; (\Delta/\theta) = 0.07c$	1. Theoretical analysis utilizing the Navier-Stokes equations of fluid dynamics 2. Anatomical data (Igarash, 1967)

Name(s) of investigator(s) and the year	Model(s) and values of parameter(s)	Comments
Valentinuzzi (1970a)	$\ddot{\xi} + (\pi/\theta)\dot{\xi} + (\Delta/\theta)\xi = a$ $(\pi/\Delta) = 6.0; (\pi/\theta) = 16.6$ $(\theta/\pi) = 0.06; (\Delta/\theta) = 2.7$ $\xi = 5.0; \omega_n = 1.6$	1. Velocity of slow-component nystagmus of the cat
van Ruskirk (1977)	$\ddot{\xi} + (\pi/\theta)\dot{\xi} + (\Delta/\theta)\xi = a$ $(\pi/\Delta) = 17.0; (\theta/\pi) = 0.0033$	1. Theoretical model
van Egomond et al. (1949)	$\ddot{\xi} + (\pi/\theta)\dot{\xi} + (\Delta/\theta)\xi = a$ $(\pi/\theta) = 10.0; (\Delta/\theta) = 1.0$	1. Nystagmus responses and subjective sensation 2. Impulse acceleration and sinusoidal rotation
van Egomond and Groen (1955)	$\ddot{\xi} + (\pi/\theta)\dot{\xi} + (\Delta/\theta)\xi = a$ $(\pi/\Delta) = 16.0$	1. Cupulometric of human subject
Mall et al. (1978)	$H(s) = \frac{6.26(1.95s + 1)(0.15s + 1)}{(12.05s + 1)(1.72s + 1)(0.25s + 1)}$	1. Vestibulo-ocular responses of human subjects 2. White noise rotational stimulus
Young and Oman (1968 & 1969)	$\frac{\theta_e}{\theta_i}(s) = \frac{10.5 s^2}{(s + 25)(s + 0.0625)(s + 0.008)}$	1. Theoretical analysis of nystagmus responses and subjective sensation

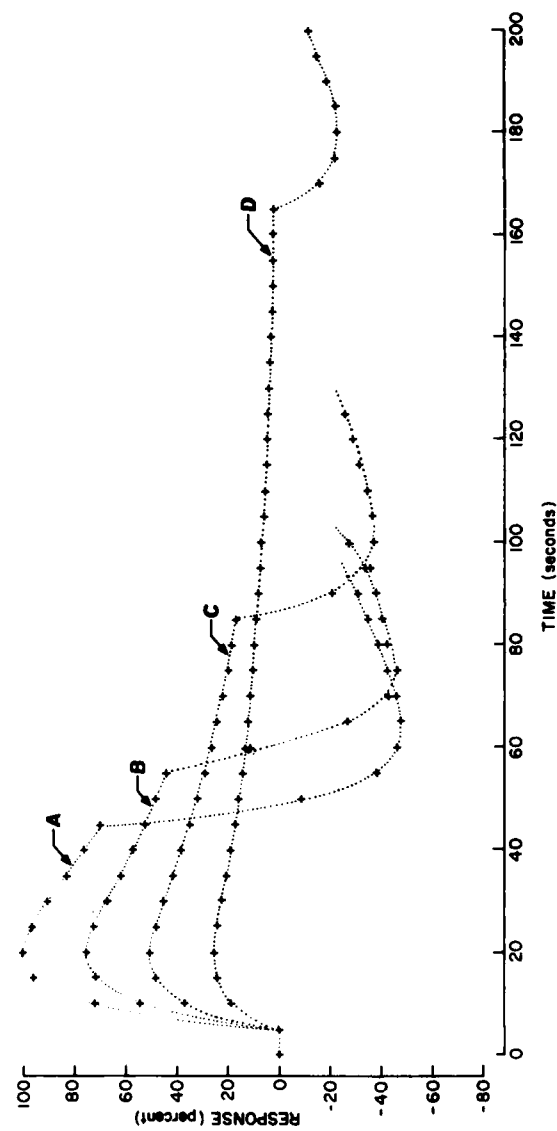


FIGURE 9. The CSMP/360 simulation results of the model developed by Fernández and Goldberg. (A) Percent response to $8^\circ/\text{second}^2$ step acceleration of 40 seconds; (B) $6^\circ/\text{second}^2$, 53 seconds; (C) $4^\circ/\text{second}^2$, 80 seconds; and (D) $2^\circ/\text{second}^2$, 160 seconds. This linear model showed that the maximum response level increases linearly with the magnitude of the stimulus level; t_{max} remains at the same level regardless of the strength of the stimulus (a property of a linear system).

nonlinearly with a decrease in the magnitude of a stimulus (FIGURE 5), and in the magnitude of the maximum response of a neuron, which also increases nonlinearly with an increase in the magnitude of a stimulus (FIGURE 4). Other nonlinearities were observed in the neural response to semicircular canal stimulation: (1) asymmetry between the excitatory and inhibitory responses of a given neuron was very striking; (2) the unidirectional response of a kinetic neuron.

If the canal system is linear, then the responses to repeated impulse stimuli should be equal, but the experimental results showed that the maximum response level to successive impulses was first increased and then gradually decayed (FIGURES 6, 7, and 8). Furthermore, when the interimpulse interval was short, the response to the impulse was additive at the beginning and the averaged

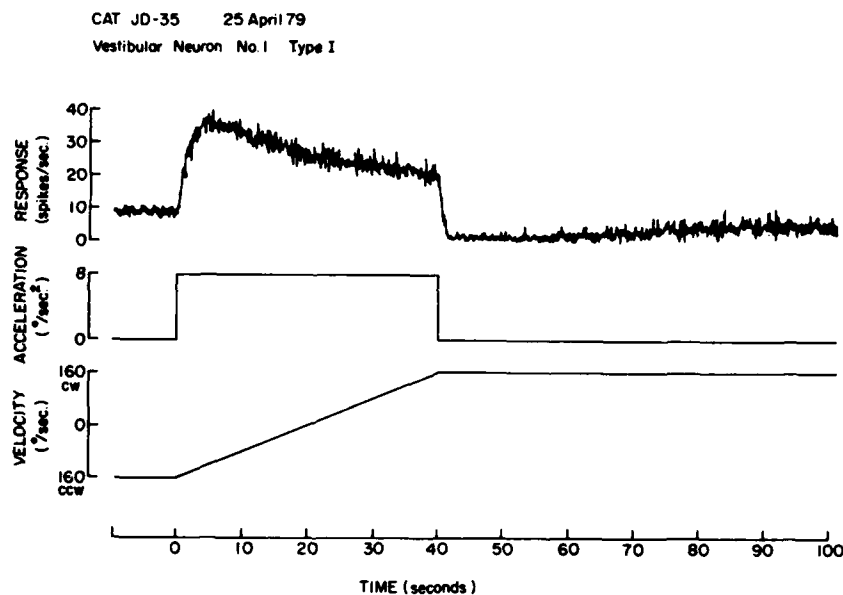


FIGURE 10. Neural response to step acceleration.

responses assumed the configuration of the response to the step acceleration (FIGURES 7 and 10). The decay of response after reaching the maximum level might be reflecting vestibular adaptation occurring either at the end-organ level or neural level. However, the additive response at the beginning and the response decay after the maximum response were nonlinear; these responses could not be accounted for by the linear model.

The nonlinearities observed in the responses of the vestibular nuclei neurons may have a complex origin. It is possible that these nonlinearities are due to (1) nonlinear behavior of the cupula-endolymph system, (2) the influence of the vestibular efferent system, (3) the influence of the other central nervous system

(viz., cerebellum, eye muscle nuclei), or (4) the inherent neural properties of the vestibular nuclei. Much investigative work is needed before a satisfactory explanation, incorporating this nonlinear behavior, can be offered.

The existing linear models for the semicircular canal system (TABLE 2) cannot account for the nonlinear responses observed. Consequently, these models do not explain the physical properties of the system.

SUMMARY

The characteristics of response of 99 vestibular nuclei neurons were investigated in the cat anesthetized with pentobarbital sodium. All neurons responded to stimulation of the horizontal semicircular canals (HSCC) with prolonged 2, 4, 6, or 8°/second² angular acceleration. Neural response was recorded utilizing the single-neuron recording technique. The vestibular neurons responded nonlinearly to stimulation of the HSCC. Specifically (1) the time required to reach the maximum response level decreased nonlinearly with an increase in stimulus magnitude (SM); (2) the maximum response level increased nonlinearly with the increase in SM; (3) the neural response to excitatory stimulus was not the mirror image of that to an inhibitory stimulus. Several existing mathematical models were simulated by utilization of the IBM Continuous System Modeling Program, and comparison was made to the experimental data. None of the models could account for the nonlinear response of the vestibular nuclei neurons. The nonlinearities observed in the responses may be due to (1) nonlinear behavior of the end organ, (2) the influence of the CNS including the vestibular efferent system, or (3) the inherent neural properties of the vestibular nuclei.

REFERENCES

1. STEINHAUSEN, W. 1931. Über den Nachweis der Bewegung der cupula in der intakten Bogengangsampulle des Labyrinthes bei der natürlichen rotatorischen und calorischen Reizung. *Pfluegers Arch. Gesamte Physiol. Menschen Tiere* **228**: 322.
2. STEINHAUSEN, W. 1933. Über die Beobachtung der cupula in den Bogengangsampullen des Labyrinths des lebenden Hechtes. *Pfluegers Arch. Gesamte Physiol. Menschen Tiere* **232**: 500.
3. FERNANDEZ, C. & J. M. GOLDBERG. 1971. Physiology of peripheral neurons innervating semicircular canals of the squirrel monkey. II. Response to sinusoidal stimulation and dynamics of peripheral vestibular system. *J. Neurophysiol.* **34**: 661.
4. SCHNEIDER, L. W. & J. ANDERSON. 1976. Transfer characteristics of first and second order lateral and vestibular neurons in gerbil. *Brain Res.* **112**: 61.
5. PETERKA, R. J., D. P. O'LEARY & D. L. TOMOKO. 1978. Linear system techniques for the evaluation of semicircular canal afferent responses using white-noise rotational stimuli. In *Vestibular Mechanisms in Health and Disease*: 10. Academic Press, London, England.
6. BLANKS, R. H. I., I. S. CURTHOYS & C. H. MARKHAM. 1972. Planar relationships of semicircular canals in the cat. *Am. J. Physiol.* **223**: 55.
7. BERMAN, A. L. 1968. *The Brain Stem of the Cat*. University of Wisconsin Press, Madison, Wis.
8. KLÜVER, H. & E. BARRERA. 1953. A method for the combined staining of cells and fibers in the nervous system. *J. Neuropathol. Exp. Neurol.* **12**: 400.
9. BRODAL, A., O. POMPEIANO & F. WALBURG. 1962. *The Vestibular Nuclei and Their Connections*. Charles C. Thomas, Publishers, Springfield, Ill.

10. DUENSING, F. & K. P. SCHAEFER. 1958. Die Aktivität einzelner Neurone in Bereich der Vestibulariskerne bei Horizontalbeschleunigungen unter besonderer Berücksichtigung des vestibulären Nystagmus. *Arch. Psychiatr. Nervenkr.* **198**: 225.
11. SHIMAZU, H. & W. PRECHT. 1965. Tonic and kinetic responses of the cat's vestibular neurons to horizontal angular acceleration. *J. Neurophysiol.* **28**: 991.
12. RYU, J. H. & B. F. MCCABE. 1973. Neural activity in the vestibular nuclei of the cat. *Ann. Otol. Rhinol. Laryngol.* **82** (Suppl. 9).

RETICULOVESTIBULAR ORGANIZATION PARTICIPATING IN GENERATION OF HORIZONTAL FAST EYE MOVEMENT*

S. Sasaki and H. Shimazu

Department of Neurophysiology
Institute of Brain Research
School of Medicine
University of Tokyo
Tokyo, Japan

INTRODUCTION

Unit activities that are closely related to eye movements have been recorded in both the vestibular nuclei and the reticular formation in the alert animal.¹⁻¹⁰ Among these, four groups of neurons have been identified in the cat as immediate premotor neurons participating in activation or suppression of abducens motor activity during horizontal fast eye movement, i.e., excitatory and inhibitory secondary vestibular neurons and excitatory and inhibitory reticular burst neurons (EBNs and IBNs).¹¹⁻¹⁵

The locations of these neurons in the brain stem and their axonal projections to the abducens nuclei have been verified in these studies. Excitatory and inhibitory secondary vestibular neurons are located predominantly in the ventrolateral part of the medial vestibular nucleus. The former send axons to the contralateral abducens nucleus, and the latter to the ipsilateral (FIGURE 1).¹⁴ EBNs are located in the dorsomedial reticular formation immediately rostral to the abducens nucleus and project to the ipsilateral abducens nucleus.¹⁵ In contrast, IBNs are found mainly in the region caudal to the abducens nucleus and send their axons to the contralateral abducens nucleus (FIGURE 1).¹⁶

The discharge pattern of these neurons related to horizontal nystagmus has also been specified. FIGURE 1 (right) shows their activities in one nystagmic cycle. At the beginning of the quick phase, EBNs and IBNs on the same side as the direction of fast eye movement exhibit high-frequency burst activity, and tonic discharges of secondary vestibular neurons on the same side are abruptly suppressed.^{12,15,16} Synaptic mechanisms of this spike suppression of secondary vestibular neurons were investigated.¹⁴ The results indicated that the spike suppression was caused by an abrupt generation of inhibitory postsynaptic potentials (IPSPs) in these neurons. These IPSPs are suggested to originate from activity of type II vestibular neurons, on the basis of the findings that type II neurons exhibited burst activity during the pause of secondary vestibular neurons and that type II neurons made monosynaptic inhibitory connection with secondary vestibular neurons in the same nucleus as revealed by postspike averaging technique (FIGURE 1).¹³ However, the origin of input causing burst activity of type II neurons is so far unknown.

In view of the neural connection shown in FIGURE 1, synchronous generation of a burst of EBNs, IBNs, and type II vestibular neurons on the same side appears

*Supported by Grants-in-Aid for Scientific Research 248106 and 548095 from the Japan Ministry of Education, Science and Culture.

to be important for well-coordinated activity of bilateral abducens motoneurons during fast, conjugate eye movement. The present paper will describe further study on firing characteristics and axonal projections of EBNs. It will also be shown that EBNs are likely to play an important role in the formation of the synchronism between burst activity of IBNs or type II vestibular neurons and suppression of spikes of secondary vestibular neurons during fast eye movement.

METHODS

Experiments were performed on cats prepared under ether anesthesia and artificial respiration. The animal was mounted on a stereotaxic frame, which was fixed on the turntable. The upper cervical cord was transected. Surgical proce-

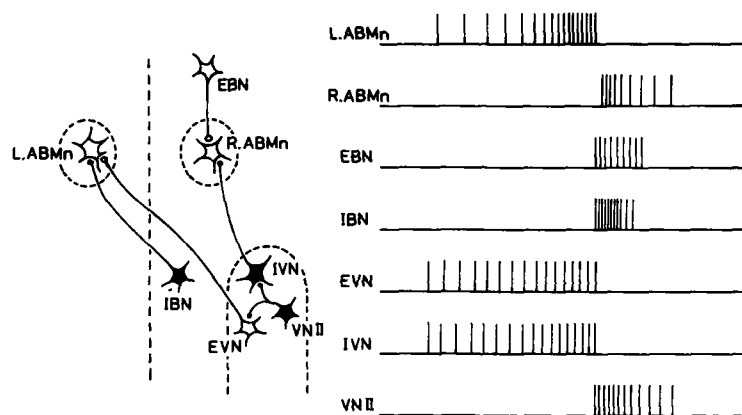


FIGURE 1. Schematic representation of immediate premotor mechanisms for activation or suppression of abducens motoneurons during fast eye movement. Neural connections (left) and discharge patterns of each neuron (right) are drawn on the basis of previous studies.¹¹⁻¹⁷ In the left scheme showing a horizontal view of the brain stem, neurons of open and filled shapes indicate excitatory and inhibitory neurons, respectively. In the right diagram, the quick phase directed to the right side occurs at the time of conversion of spike activity from L. ABMn to R. ABMn. L. and R. ABMn: left and right abducens motoneurons. EBN: excitatory burst neuron. IBN: inhibitory burst neuron. EVN: excitatory type I vestibular neuron. IVN: inhibitory type I vestibular neuron. VNII: type II vestibular neuron.

dures and the conditions for care of the animal were essentially similar to those described in a previous paper.¹² After cessation of ether inhalation, incision and pressure points were carefully infiltrated with 4% Xylocaine. Abducens nerve discharges were used as the neural correlate of nystagmus. A glass microelectrode filled with 2 M NaCl solution saturated by Fast Green, having an electrical resistance of 1.0-1.7 MΩ, was used to record extracellular activity from single neurons. Intracellular recording from abducens motoneurons was made with a glass micropipette filled with 3 M KCl solution. For stimulation, a microelectrode—either glass-coated tungsten wire or a micropipette filled with 2 M NaCl

agar—was inserted into the abducens nucleus and its surrounding structures, the dorsomedial reticular formation, and the vestibular nuclei. A fine steel electrode was inserted into the ventral funiculus of the spinal cord at C2. Rectangular cathodal currents of 0.1 msecond duration were applied. Field potentials in the abducens nucleus were summed with a digital averaging computer (Signal Processor, 7T07, San-ei) over a 10-msecond sweep duration from 5 mseconds before to 5 mseconds after spikes of single burst neurons. Recording sites were marked by electrophoretic ejection of the dye from the recording microelectrode and identified histologically. Stimulation sites were located by an electrolytic mark in histological sections.

RESULTS

The dorsomedial reticular formation was explored 1–4 mm rostral to the center of the abducens nucleus. During nystagmus induced by horizontal rotation of the turntable or electrical stimulation of the vestibular nerve, unit spikes that exhibited burst activity at the quick phases were recorded. In the present paper, 62 burst neurons whose activity occurred only at the quick excitatory phase of the ipsilateral abducens nerve (unidirectional burst neurons) will be dealt with.

Discharge Pattern of EBNs

Unidirectional burst neurons located in the dorsomedial reticular formation immediately rostral to the abducens nucleus may be divided into two classes in terms of their discharge pattern. A class of burst neurons exhibited burst of spikes at the beginning of the quick phases. The maximum intraburst spike frequency was 300/second in the neuron of FIGURE 2A and attained 400/second in other neurons. When the direction of nystagmus was reversed, the neurons were silent or fired sporadically without any relation to nystagmus. The onset of burst activity preceded ipsilateral abducens nerve discharges by 5–10 mseconds and was approximately coincident with or less than 5 mseconds before the onset of the steep negative deflection of the field potential in the ipsilateral abducens nucleus. The onset of the negative field potential is known to be synchronous with the mean onset time of steep depolarization in motoneurons at the quick phase.¹² These characteristics appear to correspond to those of unidirectional *medium-lead* burst neurons found in the pontine reticular formation of the alert monkey.^{1,10} These discharge patterns are essentially similar to those of IBNs located caudally on the same side, except that intraburst frequency of IBNs was 300–750/second and was approximately two times as high as that of EBNs.¹⁶

The other class of burst neurons was differentiated from the above by their characteristic onset time of spike activity related to the quick phases: they exhibited irregular low-frequency activity preceding rapid activation of the ipsilateral abducens nerve by 20–80 mseconds and displayed a burst of spikes (150–400/second) at the beginning of or slightly prior to the steep negative deflection of the field potential in the abducens nucleus (FIGURE 2B). During nystagmus directed to the contralateral side, these neurons were also silent or exhibited sporadic spikes unrelated to nystagmic cycle. This class of neurons resemble unidirectional *long-lead* burst neurons in the monkey pontine reticular formation in terms of their firing characteristics.^{1,10}

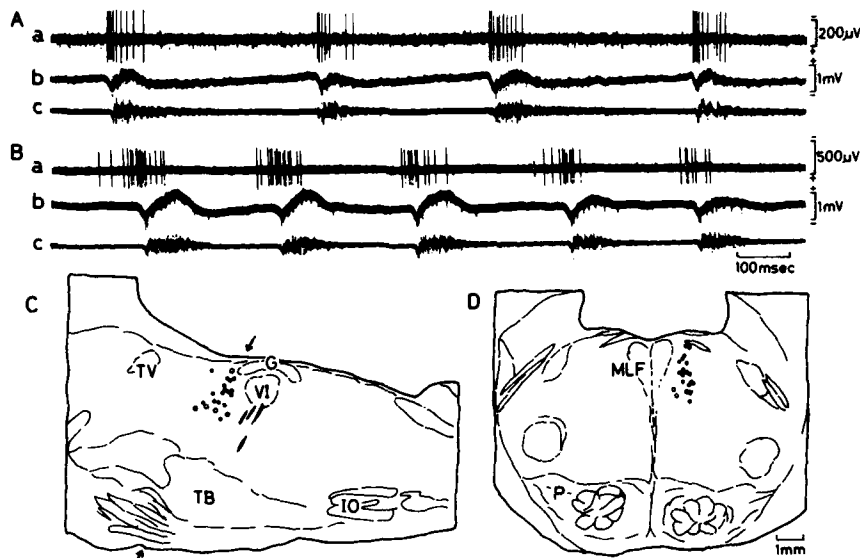


FIGURE 2. Discharge patterns and locations of EBNs. **A:** medium-lead EBN. **B:** long-lead EBN. In **A** and **B:** **a,** unit spikes of EBN; **b,** field potentials in the ipsilateral abducens nucleus; **c,** ipsilateral abducens nerve activity. **C** and **D:** locations of EBNs identified by antidromic activation from the ipsilateral abducens nucleus or by postspike averaging of unitary field potential. Marked spots for recording sites are projected to the parasagittal plane (**C**) and the transverse plane (**D**) indicated by oblique arrows in **C**. Filled and open circles represent medium-lead and long-lead EBNs, respectively. **G:** genu facialis. **IO:** inferior olive. **MLF:** medial longitudinal fasciculus. **P:** pontine nucleus. **TB:** trapezoid body. **TV:** ventral tegmental nucleus. **VI:** abducens nucleus.

Termination of EBN Axons in the Ipsilateral Abducens Nucleus

Most EBNs were antidromically activated by microstimulation within the ipsilateral abducens nucleus. An example is shown in FIGURE 3. The neuron was identified as a medium-lead burst neuron by observing its firing characteristics. Microstimulation of less than 20 μ A intensity was applied each 100 μ m along dorsoventral tracks at intervals of 200 μ m through and near the ipsilateral abducens nucleus (FIGURE 3A). The neuron was antidromically activated from two distinctly separated sites in this transverse plane (dorsal and ventral spots). FIGURE 3B shows antidromic spikes induced from the dorsal effective spot within the abducens nucleus at threshold-straddling intensity. Its antidromic nature was confirmed by a collision block of spontaneous and induced spikes (not illustrated).

The above finding indicates that the neuron sends its axon to or through the ipsilateral abducens nucleus. To confirm the termination of the axon within the nucleus, postspike averaging of the field potential was employed at and near the sites where microstimulation induced antidromic spikes. The field potential was averaged over a 10-millisecond sweep duration before and after the neuron discharges, with a digital computer (FIGURE 3C). FIGURE 3Ca shows the distribu-

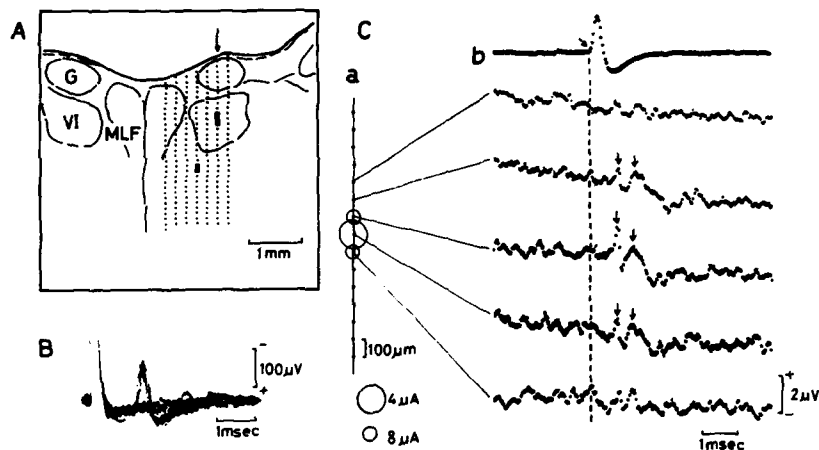


FIGURE 3. Antidromic activation of a medium-lead EBN from the ipsilateral abducens nucleus and postspike average of field potentials in the abducens nucleus induced by activity of the single EBN. **A:** microelectrode tracks (dotted lines) for antidromic stimulation. Thick lines indicate effective sites for antidromic activation at stimulus intensity of less than $10 \mu\text{A}$. **B:** antidromic response of the EBN to threshold-straddling stimulation of the dorsal effective site within the abducens nucleus. **Ca:** thresholds for antidromic activation measured at $100\text{-}\mu\text{m}$ steps along the electrode track shown by arrow in **A**. The diameter of each circle indicates the threshold current as shown below the diagram. Dots without circles indicate ineffective sites with stimulus currents less than $10 \mu\text{A}$. **Cb:** averaged field potentials (10,000 sweeps) triggered by spikes of the EBN shown at top. Vertical broken line indicates the onset time of trigger spike (oblique arrow). Voltage calibration applies to field recording.

tion of thresholds for antidromic activation along the electrode track through the dorsal effective spot in FIGURE 3A (arrow). Within these effective sites, the postspike average of the field potential revealed an early positive-negative spike followed by a late slow negative wave (FIGURE 3Cb, second to fourth traces). No appreciable field was obtained more dorsally or ventrally along this track.

The interval between the trigger spike and the early positive peak of the average field potential (first arrow) was 0.8 msecond . This value corresponded to the latency of antidromic activation of the EBN, 1.0 msecond at stimulus intensity of 1.2 times the threshold, when allowance of 0.2 msecond was made for the latency of spike initiation at the stimulated site. The initial positive-negative spike field in the averaged record was therefore presumed to represent the arrival of impulses coming from the EBN. The interval between the initial positive peak of the presynaptic impulse and the onset of late negativity (first and second arrows in FIGURE 3Cb) was 0.45 msecond , which corresponded to a single synaptic delay time. Therefore the late slow negative field potential was attributed to postsynaptic currents induced by synaptic action of the single EBN. Its negative polarity suggests that the synaptic action of the burst neuron is excitatory in nature as demonstrated in the spinal and trigeminal motor nuclei.^{18,19} This view was consistent with the finding that the burst activity was always in phase with rapid excitation of motoneurons in the abducens nucleus to which the axon of the EBN projected.

Similar results were obtained with long-lead burst neurons located in the

region rostral to the abducens nucleus: they were antidromically activated from the restricted sites in the ipsilateral abducens nucleus (see FIGURE 4C). Postspike averaging of the field potential was employed with a few long-lead burst neurons. It revealed a monosynaptic unitary negative field, suggesting that at least some of the long-lead burst neurons also send axons to the ipsilateral abducens nucleus and make monosynaptic excitatory connection with motoneurons and/or interneurons.

Location of EBNs

Recording sites of medium-lead and long-lead EBNs identified by antidromic activation from the localized area in the ipsilateral abducens nucleus were studied in histological sections. They were immediately rostral to the abducens

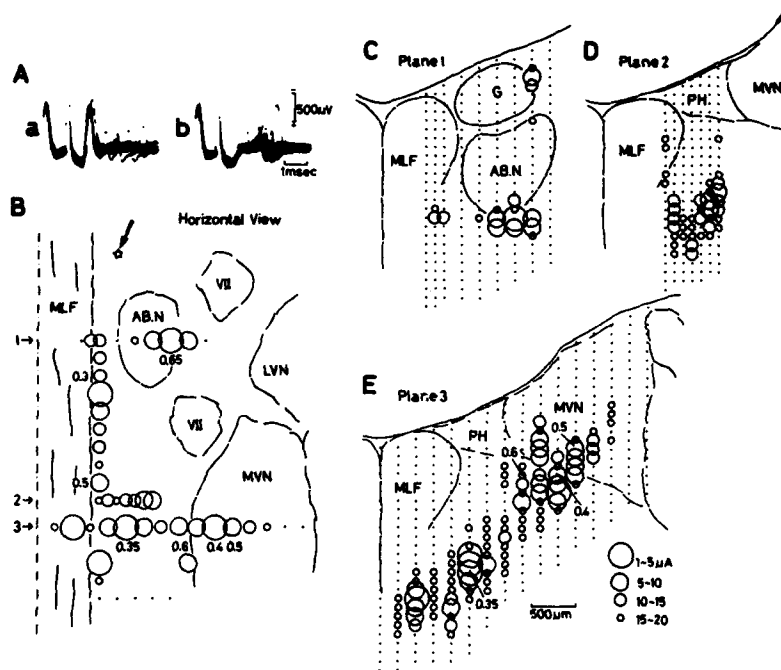


FIGURE 4. Antidromic activation of a long-lead EBN from the ipsilateral abducens nucleus, IBN area, and medial vestibular nucleus. A: an example of collision block test. The sweeps were triggered by rotation-induced spikes that were followed by antidromic stimulation. Stimulation in b failed to evoke spikes in contrast to full activation with slightly delayed stimulation in a. B: horizontal view of the brain stem, showing effective sites for antidromic activation of the EBN whose location is indicated by oblique arrow. C-E: transverse view of three planes indicated by horizontal arrows 1, 2, and 3 in B. The diameter of each circle indicates the threshold current as shown in the bottom-right. Dots without circles indicate threshold currents greater than $20 \mu A$. The diameter of each circle in B represents the lowest threshold value in each track of stimulating microelectrode. Numerals in B and E indicate latencies in mseconds of antidromic response of the EBN from respective spots. AB.N: abducens nucleus. LVN: lateral vestibular nucleus. MVN: medial vestibular nucleus. PH: prepositus hypoglossi nucleus. VII: facial nerve.

nucleus (FIGURE 2C and D). The ventrally located EBNs were found in the dorsocaudal portion of the paramedian pontine reticular formation (PPRF) delineated in the cat by Graybiel;²⁰ but the location of many EBNs, especially medium-lead ones, extended farther dorsally outside the PPRF. Since sampling is small in number, it cannot be stated at the present stage of study whether there is any tendency toward different locations between medium-lead and long-lead EBNs.

Collateral Projection of EBN Axons in the Brain Stem

It was investigated whether the axons of EBNs project only to the ipsilateral abducens nucleus or to other regions in the brain stem or the spinal cord as well. For this purpose, microelectrode tracking was made in a wide area caudal to the level of the abducens nucleus for antidromic activation of single EBNs. FIGURE 4 exemplifies the distribution of effective sites for antidromic activation of a single long-lead EBN with stimulus currents of less than 20 μ A. A collision-block test was employed to exclude the possibility of orthodromic activation or of antidromic activation of a neighboring neuron that was spontaneously silent and had a shape of spikes similar to that of the neuron concerned (FIGURE 4A). The effective spots were found not only in the ipsilateral abducens nucleus (FIGURE 4C) but also farther caudally along the zone ventrolateral to the ipsilateral medial longitudinal fasciculus (FIGURE 4B-E). In the frontal plane 2 and 3 in FIGURE 4B, the effective region in the dorsomedial reticular formation corresponded well to the area of IBNs (FIGURE 4D and E).¹⁶ The effective sites were found farther laterally in the rostral part of the medial vestibular nucleus as well (FIGURE 4E).

It was noted that the low threshold spots were separated by relatively high threshold sites in the region of IBNs as well as in the ventral area of the medial vestibular nucleus. These results suggest that the axon of the single EBN extends caudally and that collaterals emerging from the stem axon give off a number of ramifications in the ipsilateral IBN region and the medial vestibular nucleus. Antidromic latencies were not always shorter at the proximal sites than at the distal sites relative to the location of the EBN cell. There was jumping of latencies at different spots close to each other, as indicated by several samples of latencies in FIGURE 4B and E. Therefore the distribution of effective spots in FIGURE 4 cannot be attributed to the simple course of a single passing axon, but supports the view that a single EBN axon issues collateral branches and may terminate in the IBN region and the medial vestibular nucleus.

Most long-lead EBNs, which were antidromically activated from the ipsilateral abducens nucleus, projected to the ipsilateral IBN area and the medial vestibular nucleus. Some medium-lead EBNs were also antidromically activated from these regions. None of the EBNs, however, could be activated antidromically from the spinal cord at the C2 level.

During exploration of the region immediately rostral or rostroventral to the abducens nucleus for single-unit recording, we often encountered neurons that were antidromically activated from both the ipsilateral abducens nucleus and the C2 spinal cord. The conduction velocities of the descending axons to the spinal cord were estimated to be 60-90 m/second. These values were an approximation, because they were calculated from the antidromic latency and the conduction distance with a single spinal-stimulating electrode, on the assumption that the latency of spike initiation at the stimulated site was 0.15 msecond. These reticulospinal neurons were intermingled with ventrally located EBNs, and their

location appeared to be in the dorsocaudal region of the PPRF. An example is shown in FIGURE 5. FIGURE 5A shows collision block between spontaneous spikes and spikes induced by stimulation of the spinal cord (a) or the abducens nucleus (b), indicating antidromic activation from these two structures. In and near the ipsilateral abducens nucleus, lower threshold spots for antidromic activation were separated by intervening higher-threshold sites (FIGURE 5B), suggesting axonal branching in and near the abducens nucleus. Postspike averaging of field potentials in the abducens nucleus triggered from spikes of this class of neurons

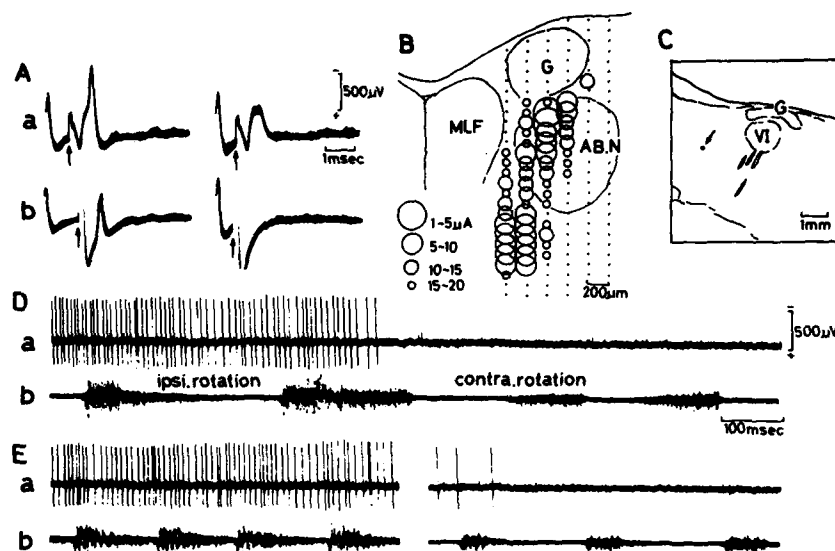


FIGURE 5. Discharge pattern of a reticular neuron projecting to the abducens nucleus and spinal cord. A: collision test. Rotation-induced spikes were followed by antidromic stimulation of the spinal cord at C2 (a) and abducens nucleus (b). Arrows indicate stimulus artifacts. In the right record of a, spinal cord stimulation induced only field potential without unit spikes concerned. B: mapping of thresholds at effective sites in and near the ipsilateral abducens nucleus for antidromic activation of the neuron. C: location of the neuron (arrow). D: response of the neuron to horizontal rotation of the turntable. Spikes were increased in frequency (a) during ipsilateral rotation (left half) without any relation to ipsilaterally directed quick phases of abducens nerve discharges (b). They were silent during contralateral rotation (right half) inducing nystagmus in the reversed direction. E: response of the neuron after repetitive stimulation of the ipsilateral vestibular nerve. The interval between left and right record was 1 second.

revealed a unitary negative field (not illustrated). It is therefore suggested that a number of reticulospinal neurons located in the region rostroventral to the abducens nucleus send their axon collaterals to the ipsilateral abducens nucleus and therein terminate with excitatory synapses. Their axonal branching in the abducens nucleus appeared to be more profuse than that of EBNs (compare FIGURE 5B with FIGURE 3A or 4C).

It should be stressed, however, that these reticulospinal neurons have never exhibited unidirectional burst activity related to the ipsilaterally directed quick

phases of nystagmus. Their firing frequency was smoothly increased with ipsilateral angular acceleration and decreased with contralateral acceleration (type I response), even though ipsilaterally or contralaterally directed quick phases were clearly recorded in the abducens nerve during sinusoidal horizontal rotation (FIGURE 5D). Immediately after electrical stimulation of the ipsilateral vestibular nerve, their firing frequency was tonically increased when the frequency of nystagmus was high (left record in FIGURE 5E). As the neuron became gradually less active, the frequency and amplitude of nystagmic discharges in the abducens nerve also gradually decreased (right record in FIGURE 5E). Thus, these neurons do not seem to be related directly to generation of fast eye movement, but probably provide abducens motoneurons with a background excitatory input that facilitates burst activity of the motoneurons at the time of arrival of EBN input in the abducens nucleus.

Target Neurons of EBN Axons

The area immediately rostral to the abducens nucleus was stimulated with a tungsten microelectrode to find possible target neurons with which EBN axons might make direct connection. The tip of the microelectrode was placed in the area where EBNs were densely located, i.e., 1.2 mm lateral to the midline and 1.5 mm in depth from the surface of the brain stem along the electrode track indicated by arrows in FIGURE 2C. The stimulation sites were later confirmed histologically. The axons of single EBNs terminated in the abducens nucleus, and probably in the IBN region and the medial vestibular nucleus as described above. Therefore, abducens motoneurons, IBNs, and type I and II vestibular nucleus neurons were selected for studying effects of microstimulation of the EBN area.

Intracellular recording was made from abducens motoneurons that were identified by antidromic stimulation of the abducens nerve. When the ipsilateral EBN area was stimulated at the intensity of 20 μ A (0.1 msecond in duration), EPSPs were produced in motoneurons (FIGURE 6C). The latency of EPSPs was 1.0 msecond (0.8–1.2 mseconds in other motoneurons), suggesting a monosynaptic connection with motoneurons on the basis of antidromic latencies of EBNs, ranging from 0.4–1.3 mseconds, from the abducens nucleus. The amplitude of EPSPs induced by single shocks was relatively small (less than 2 mV). With double shock stimulation at short intervals, the monosynaptic EPSP in response to the second shock was markedly increased in amplitude (FIGURE 6C). The time-to-peak of the second EPSP was 1.6 mseconds, which was approximately the same as that of the first EPSP. This suggests that the observed increase in amplitude of the second EPSP was not due to delayed polysynaptic effects but mainly due to facilitation of the monosynaptic EPSP. The time course of the facilitation relative to the interval of double shocks is shown in FIGURE 6B: appreciable amount of facilitation lasted for approximately 20 mseconds after the first shock. The origin of this facilitation is not clear at the present stage. There are at least two possibilities: (1) microstimulation delivered at the EBN area may excite not only cell somata located there but also presynaptic fibers terminating on EBNs. Activation of presynaptic fibers caused by the first conditioning shock would expand the subliminal fringe of EBNs and thereby facilitate the response of abducens motoneurons to the second test shock; (2) the observed facilitation would be caused by frequency potentiation at the terminals synapsing with abducens motoneurons.

Extracellular spikes of IBNs were recorded in the area caudal to the abducens nucleus. They were identified by observing burst activity during the quick phases

directed to the ipsilateral side and antidromic activation in response to microstimulation of the contralateral abducens nucleus¹⁶ (FIGURE 6Fa). The identified IBNs were activated by microstimulation of the ipsilateral EBN area at a stimulus intensity of 20 μ A. In FIGURE 6Fb, single-shock stimulation did not induce spikes, while double shocks clearly evoked spikes of the IBN with fluctuating latencies, indicating a transsynaptic activation. The latencies ranged from 1.3 to 2.2

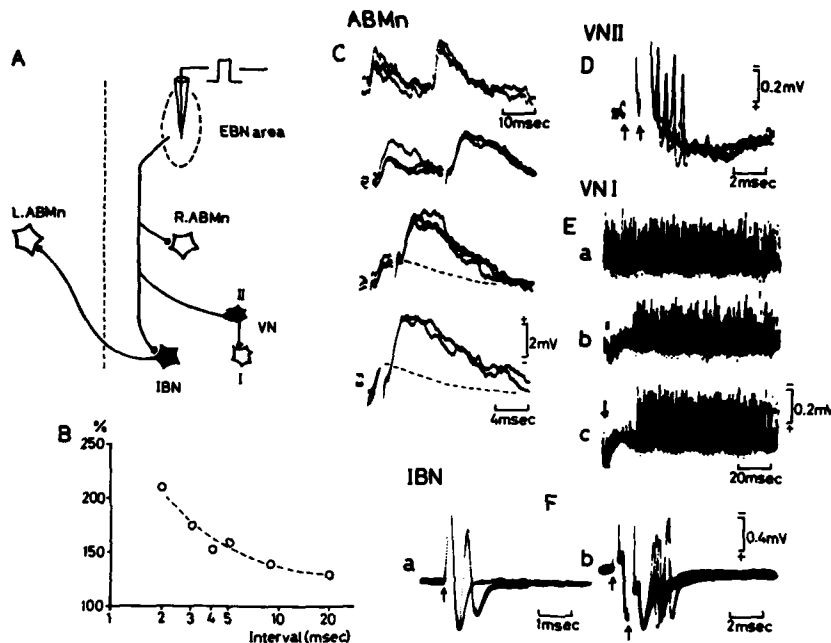


FIGURE 6. Effects of microstimulation of the EBN area on abducens motoneurons, IBNs, and type I and II vestibular nucleus neurons. A: schematic diagram showing relevant neural connections. B: facilitation of second EPSPs in an abducens motoneuron with double shocks to the EBN area at varied intervals. C: specimen records of EPSPs in the same abducens motoneuron. Intervals between two shocks were varied. Time scale of 4 mseconds applies to the second to fourth traces. Dotted lines are drawn on the basis of averaged EPSPs induced by a single shock. D: spikes of a type II vestibular neuron (four superimposed traces) in response to double shocks (arrows) to the EBN area. Single shock stimulation induced no spikes. E: inhibition of spikes of a type I vestibular neuron (50 superimposed traces). a: spontaneous spikes without stimulation. b: response to triple shocks (mark) to the EBN area. c: response to single shock (arrow) to the contralateral vestibular nerve. F: response of an IBN. a: antidromic response to microstimulation (arrow) of the contralateral abducens nucleus. b: spikes induced by double shocks (arrows) to the EBN area. Single-shock stimulation induced no spikes. Intensity of stimulus currents at the EBN area was 20 μ A (0.1-msecond duration) in each case.

mseconds from the effective shock. These latency values for spike evocation suggest the existence of monosynaptic excitatory connection with IBNs from the EBN area, taking into account that the antidromic latencies of EBNs from the IBN area were 0.3–1.0 msecond.

Spikes of type II neurons were extracellularly recorded in the ventral part of

the medial vestibular nucleus. Type II neurons were identified by observing an increase in spike frequency during contralateral horizontal angular acceleration and a decrease in frequency with ipsilateral acceleration.²¹ Type II neurons that were activated by single shocks to the contralateral vestibular nerve with relatively short latencies (2.5–3.5 mseconds)²² were selected for further study. When microstimulation (20 μ A) was delivered at the ipsilateral EBN area, spikes of these type II neurons were induced with varied latencies (1.1–2.5 mseconds) (FIGURE 6D), indicating a transsynaptic activation. The shortest latency of evoked spikes after the effective second shock, 1.1 mseconds, suggests that there is also a monosynaptic excitatory connection from the EBN area to horizontal type II neurons. No antidromic activation was found in type II neurons after stimulation of the EBN area.

Spike activity of horizontal type I vestibular neurons²¹ was suppressed for approximately 20 mseconds after microstimulation of the EBN area (2–3 shocks at intervals of 1–2 mseconds) (FIGURE 6Eb). Suppression of type I spike activity can well be explained by the above-mentioned activation of type II neurons, because the latter exert an inhibitory action on the former.¹³ The duration of suppression of type I spikes was similar to that of commissural inhibition through type II neurons (FIGURE 6Ec).²²

DISCUSSION

Locations of abducens motoneurons, IBNs, and type II vestibular neurons were consistent with the areas to which the axon collaterals of single EBNs projected. Microstimulation confined to the EBN area monosynaptically activated ipsilateral abducens motoneurons, IBNs, and type II vestibular neurons. These results suggest, though they do not directly demonstrate, that EBNs provide a common excitatory input to induce burst activity of these three kinds of neuron.

The ventral part of the EBN area contains nonbursting reticulospinal neurons that send axon collaterals to the abducens nucleus (FIGURE 5). On the basis of their anatomical locations, these neurons may correspond to a class of morphologically identified reticulospinal neurons that send axon collaterals to the abducens nucleus, the dorsomedial reticular formation caudal to the abducens nucleus, and the medial vestibular nucleus, ipsilaterally.²³ Although the functional identity of their target neurons in the dorsomedial reticular formation and the medial vestibular nucleus has been unknown, there is a possibility that monosynaptic excitatory action on IBNs and type II vestibular neurons after electrical stimulation of the EBN area also involves the action of collateral projection of these reticulospinal neurons. However, so far as nystagmus is concerned, the reticulospinal neurons in the EBN area did not exhibit unidirectional burst activity during ipsilaterally directed fast eye movement. These reticulospinal neurons therefore would not be a candidate for a common input causing burst activity of abducens motoneurons, IBNs, and type II vestibular neurons. Further study is needed to find a possible burster providing a common source of ocular and spinal associated activity.

A previous intracellular study on cat abducens motoneurons described characteristics of changes in the membrane potential of motoneurons in association with quick phases of vestibular nystagmus, and revealed component postsynaptic potentials composing the membrane-potential changes.²⁴ At the beginning of the quick phase, a burst of spikes in the agonist was induced by a steep depolariza-

tion of motoneurons, which consisted of sudden production of EPSPs and disinhibition. In the antagonist, the spike activity was rapidly suppressed at the time of steep hyperpolarizing deflection of the membrane potential. The hyperpolarization was found to consist of sudden production of IPSPs and disfacilitation. These postsynaptic potential changes are attributable to activities of at least four classes of identified premotor neurons located in both the reticular formation and the vestibular nuclei. The steep depolarization in agonistic abducens motoneurons to initiate fast eye movement is explained well by excitatory synaptic action originating from ipsilateral EBNs plus disinhibition due to sudden cessation of preexisting activity of ipsilateral inhibitory type I vestibular neurons.^{12,14} The concomitant steep hyperpolarization in antagonistic abducens motoneurons is caused by inhibitory synaptic action originating from contralateral IBNs plus disfacilitation due to sudden cessation of preexisting activity of contralateral excitatory type I vestibular neurons.^{12-14,16,17}

It was further shown that the steep depolarization in agonistic motoneurons and the steep hyperpolarization in antagonistic motoneurons occurred synchronously at the beginning of quick phases of both optokinetic and vestibular nystagmus in the alert cat.²⁵ This synchronism appears to be attributed to the specific connection of collateral axons of single EBNs with their target neurons. Simultaneously with activation of agonistic abducens motoneurons due to burst activity of EBNs, a burst of IBNs induced by EBN activity inhibits contralateral abducens motoneurons as an antagonistic inhibition. At the same time, EBNs activate type II vestibular neurons that inhibit ipsilateral excitatory and inhibitory premotor type I vestibular neurons, thus causing disfacilitation and disinhibition of abducens motoneurons. These mechanisms should be responsible, at least in part, for the synchronism of abrupt changes in activities of premotor reticular and vestibular neurons and thereby assure well-coordinated activity of the lateral rectus muscles of both eyes during horizontal conjugate fast eye movements. The possibility cannot be excluded, however, that other neurons—such as those located in the prepositus hypoglossi nucleus or other areas in the reticular formation—may also act as premotor neurons for the generation of horizontal fast eye movements.

Keller proposed a hypothesis that medium-lead burst neurons receive an inhibitory influence from pause neurons that exhibit tonic discharges except during fast eye movements.¹⁰ It has recently been reported that pause neurons are antidromically activated from the IBN area and that IBNs are monosynaptically inhibited by stimulation of the pause neuron area, supporting the view that burst activity of IBNs may be caused by release of the inhibition from pause neurons.²⁶ This may be related to the finding that intraburst frequency of IBNs was much higher than that of EBNs on average. The excitatory input from EBNs plus the above-described disinhibition may be effective for producing extremely high frequency burst of IBNs.

An input to EBNs should arise originally from the ipsilateral horizontal canal so far as rotation-induced fast eye movements are concerned. The pathway from secondary vestibular neurons to EBNs appears to be polysynaptic on the basis of long-latency activation of EBNs after stimulation of the ipsilateral vestibular nerve. It is not known, however, how slow-phase discharges in secondary vestibular neurons are converted into intermittent burst activity of EBNs. The initiation of burst could be either due to membrane properties of EBNs themselves or caused by local neuronal circuits.

The present study has shown that long-lead EBNs also terminate in the abducens nucleus. This was unexpected, because an intracellular study on

abducens motoneurons had shown that there was no slowly depolarizing potential before abrupt EPSPs were produced at the beginning of the quick phase.²⁴ The summated EPSPs, which were produced by low-frequency activity of EBNs as a prelude to a high-frequency burst, might be obscured by an intense IPSP arising from inhibitory vestibular neurons during the slow phase.¹² Such a mechanism infers an important role of inhibitory vestibular neurons in generation of burst activity of abducens motoneurons, by means of disinhibition due to sudden cessation of their spike activity at the quick phase. Alternatively, a possible frequency potentiation at EBN terminals (see above) might be functionally significant. The low-frequency prelude activity of EBNs would cause only small EPSPs, while the high-frequency burst would produce a large depolarization due to frequency potentiation. These possibilities remain to be studied at the single-neuron level.

ACKNOWLEDGMENTS

The authors express their thanks to Drs. Y. Igusa and N. Isu for their helpful assistance in parts of experiments, to Miss C. Utena for histological preparation, and to Mrs. K. Katagiri for secretarial assistance.

REFERENCES

1. LUSCHEI, E. S. & A. F. FUCHS. 1972. Activity of brain stem neurons during eye movements of alert monkeys. *J. Neurophysiol.* **35**: 445-461.
2. MILES, F. A. 1974. Single unit firing patterns in the vestibular nuclei related to voluntary eye movements and passive body rotation in conscious monkeys. *Brain Res.* **71**: 215-224.
3. FUCHS, A. F. & J. KIMM. 1975. Unit activity in vestibular nucleus of the alert monkey during horizontal angular acceleration and eye movement. *J. Neurophysiol.* **38**: 1140-1161.
4. KELLER, E. L. & P. D. DANIELS. 1975. Oculomotor related interaction of vestibular and visual stimulation in vestibular nucleus cells in alert monkey. *Exp. Neurol.* **46**: 187-198.
5. KELLER, E. L. & B. Y. KAMATH. 1975. Characteristics of head rotation and eye movement-related neurons in alert monkey vestibular nucleus. *Brain Res.* **100**: 182-187.
6. WAESPE, W., V. HENN & T. S. MILES. 1977. Activity in the vestibular nuclei of the alert monkey during spontaneous eye movements and vestibular or optokinetic stimulation. *Dev. Neurosci.* **1**: 269-278.
7. SPARKS, D. L. & R. P. TRAVIS, JR. 1971. Firing patterns of reticular formation neurons during horizontal eye movements. *Brain Res.* **33**: 477-481.
8. COHEN, B. & V. HENN. 1972. The origin of quick phases of nystagmus in the horizontal plane. *Bibl. Ophthalmol.* **82**: 36-55.
9. COHEN, B. & V. HENN. 1972. Unit activity in the pontine reticular formation associated with eye movements. *Brain Res.* **46**: 403-410.
10. KELLER, E. L. 1974. Participation of medial pontine reticular formation in eye movement generation in monkey. *J. Neurophysiol.* **37**: 316-332.
11. MAEDA, M., H. SHIMAZU & Y. SHINODA. 1971. Rhythmic activities of secondary vestibular efferent fibers recorded within the abducens nucleus during vestibular nystagmus. *Brain Res.* **34**: 361-365.
12. HIKOSAKA, O., M. MAEDA, S. NAKAO, H. SHIMAZU & Y. SHINODA. 1977. Presynaptic impulses in the abducens nucleus and their relation to postsynaptic potentials in motoneurons during vestibular nystagmus. *Exp. Brain Res.* **27**: 355-376.

Sasaki & Shinohara & H. SHIMAZU. 1977. Responses of medial vestibular nucleus to horizontal rotation of the head. *Neurosci. Abstr.* 3: 545.

13. SCHOR, R. H., S. NAKAO & H. SHIMAZU. 1980. Postsynaptic inhibition underlying spike neurons during vestibular nystagmus. *J. Neurosci.* **1**: 540-547.
14. HIKOSAKA, O., S. NAKAO & H. SHIMAZU. 1980. Postsynaptic inhibition underlying spike neurons during quick phases of vestibular nystagmus. *Brain Res.* **18**: 21-26.
15. IGUSA, Y., S. SASAKI & T. AWAKAMI. 1977. Inhibitory reticular neurons related to the quick phase of vestibular nystagmus—their location and projection. *Exp. Brain Res.* **27**: 377-386.
16. HIKOSAKA, O., S. NAKAO & H. SHIMAZU. 1978. Direct inhibitory synaptic connections by spike-triggered averaging. I. Spindle muscle receptor connections. *J. Neurophysiol.* **39**: 1375-1392.
17. HIKOSAKA, O., E. K. STAUFFER, A. TAYLOR, R. M. REINKING & D. G. STUART. 1976. Linkage of primary and secondary vestibular nuclei by spike-triggered averaging. II. Vestibular nucleus-related pontomedullary reticular burst neurons. *Neurosci. Lett.* **1**: 21-26.
18. WATT, D. G., J. A. STEPHENS, G. SOMJEN, K. APPENTENG & M. J. O'DONOVAN. 1978. Analysis of primary and secondary vestibular nuclei by spike-triggered averaging for plotting synaptic projections. *Brain Res.* **18**: 21-26.
19. TAYLOR, A. J. 1977. Direct and indirect preculo-motor pathways of the brainstem: a cytoarchitectural study of the pontine reticular formation in the cat. *J. Comp. Neurol.* **158**: 344-378.
20. GRAVANA, R. & K. P. SCHAEFER. 1958. Die Aktivität einzelner Neurone im Bereich der Vestibulären Nuclei bei Horizontalbeschleunigungen unter besonderer Berücksichtigung des Vestibulären Nystagmus. *Arch. Psychiatr. Nervenkr.* **198**: 225-252.
21. DUMMER, F. & W. PRECHT. 1966. Inhibition of central vestibular neurons from the labyrinth and its mediating pathway. *J. Neurophysiol.* **29**: 467-492.
22. SHIMAZU, H., S. BAKER & A. GRANTYN. 1980. Morphological and physiological identification of vestibular nucleus-related pontine reticular neurons projecting to the cat abducens nucleus. *Brain Res.* **198**: 221-228.
23. GRAVANA, R. & H. SHIMAZU. 1972. Nature of synaptic events in cat abducens nucleus during slow and quick phase of vestibular nystagmus. *J. Neurophysiol.* **35**: 273-283.
24. MURRAY, M. L., S. SASAKI & H. SHIMAZU. 1977. Nuclear delay of impulse transmission in abducens motoneurons during fast eye movements of visual and vestibular origin in the cat. *J. Neurophysiol.* **40**: 1415-1423.
25. SHIMAZU, H., S. SASAKI & I. S. CURTHOYS. 1979. Direct projection of pauser cells to the vestibular nucleus-related pontomedullary reticular burst neurons. *Neurosci. Lett.* **1**: 21-26.
26. MURRAY, C. H., S. SASAKI & H. SHIMAZU. 1977. Nuclear delay of impulse transmission in abducens motoneurons during fast eye movements of visual and vestibular origin in the cat. *J. Neurophysiol.* **40**: 1415-1423.

HORIZONTAL EYE MOVEMENT SIGNALS IN SECOND-ORDER VESTIBULAR NUCLEI NEURONS IN THE CAT*

A. Berthoz, K. Yoshida,† and P. P. Vidal

Laboratory of Neurosensory Physiology
National Center for Scientific Research (CNRS)
75270 Paris Cedex 06, France

INTRODUCTION

The functional role of the vestibulo-ocular reflex is to decrease retinal slip induced by head movements. This is performed by compensatory eye movements in the direction opposite to the head. The neuronal organization underlying the vestibulo-ocular reflex (VOR), since its initial description by Lorente de Nó,¹ has been studied extensively in acute preparations. In his initial concept of the organization of the reflex, Lorente de Nó recognized that the reflex was articulated around a three-neuron arc. The first-order neuron was the vestibular primary afferent terminating in the vestibular nucleus, the second-order neuron was a vestibular nucleus neuron with an axon terminating in the nuclei containing the eye muscle motoneurons, and the last neuron was the motoneuron. Lorente de Nó suggested that second-order vestibular neurons were merely relay neurons, transmitting the tonic input from the labyrinth to the motoneurons. In his schema concerning the generation of vestibular nystagmus, he proposed that the fast phase of vestibular nystagmus would be produced by a reticular generator, receiving a collateral from the vestibular nucleus neurons and feeding forward a pulsatile activity to the motoneurons. However, he recognized that some activity was fed back from the reticular centers to the vestibular nucleus neurons, and thought that this loop was essentially contributing to reexcitation. Evidence that the activity of second-order vestibular neurons during vestibular nystagmus was not purely tonic, but was modulated in relation with the eye movements, was provided in the cat by recordings of identified axons of second-order vestibular neurons, presumably terminating in the abducens and trochlear nuclei.²⁻⁵ It was demonstrated that inhibitory vestibular neurons projecting to the ipsilateral side (Vi) or excitatory vestibular neurons terminating in the contralateral motor nuclei (Vc) showed modulation of their firing activity together with the slow and the quick phases of vestibular nystagmus.

In addition, considerable evidence has been accumulated concerning the presence in the vestibular nucleus of eye movement-related activity. Results obtained in the cat were generally obtained from acute preparations.⁶⁻⁸ In the monkey, the combination of head- and eye-movement signals carried by vestibular nucleus neurons was mainly studied in alert animals.⁹⁻¹⁴ However, in these studies only incomplete identification of vestibular nuclei neurons was made, and consequently it was not possible to assert whether the findings obtained from identified second-order vestibular neurons in the acute cat during vestibular nystagmus could be confirmed for all types of eye movements in the alert animals.

*This research was supported by CNRS.

†Supported by grants from INSERM and Fondation de France. Present affiliation: Institute of Basic Medical Sciences, University of Tsukuba, Niihari Gun, Ibaraki Ken 300-31, Japan.

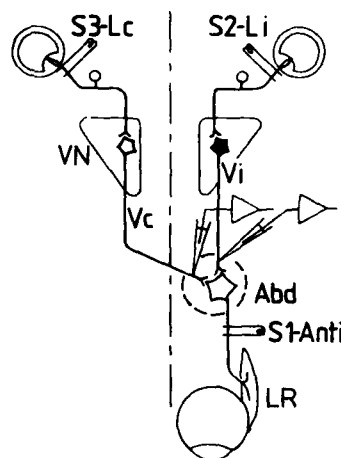
In the present work, we have attempted to record in the alert cat from axons of second-order vestibular neurons identified by electrophysiological and/or morphological methods in order to study the precise discharge characteristics of these neurons during either spontaneous or vestibular-evoked eye movement. We shall report only preliminary results concerning horizontal type I second-order Vi and Vc neurons terminating in the abducens nucleus. Other preliminary results concerning the morphology and physiology of horizontal and vertical neurons have been given elsewhere.¹⁷⁻¹⁹

METHODS

Eye Movement Recording

Eye movements were recorded in the alert cat by the search coil technique.¹⁵ Search coils were implanted chronically around the orbit, and the animal was placed in a magnetic field, pulsating at 10 kHz, which allowed the recording of

FIGURE 1. Intra-axonal recording of second-order vestibular neurons in the alert cat. Schema of the experimental paradigm: stimulation and recording sites. Stimulating electrodes (S2, S3) are implanted in the ipsi- (Li) and contralateral (Lc) labyrinth for identification of second-order vestibular nucleus (VN) neurons by orthodromic stimulation. The intracellular recording site of the axons of ipsi- (Vi) or contralateral (Vc) vestibular neurons is identified in the abducens nucleus with the help of the antidromic stimulation of the abducens nerve (S1-Anti). Only the axonal branch of second-order vestibular neurons terminating in the abducens nucleus is shown here. Other branches (see, for example, FIGURE 5) have been omitted for the sake of clarity. LR, lateral rectus.



vertical and horizontal components of eye movements. The bandwidth of the recording system (Skalar) was 300 Hz, the precision was on the order of 10 minutes of arc. Eye movements were calibrated by moving the magnetic field around the head of the cat.

Procedure for the Identification of Vestibular Nucleus Neurons

Axons from vestibular nuclei neurons were recorded in the vicinity of the abducens nucleus (FIGURE 1). The abducens nucleus was identified by chronically implanted stimulation electrodes, placed on the abducens nerve as it exits from the brain stem. Single-shock stimulation of the antidromic stimulating electrodes evoked field potentials in the abducens nucleus, which allowed the identification of the exact location of the nucleus. In addition, the vestibular

nerves were stimulated with bipolar fine silver ball electrodes, chronically implanted in the labyrinth on both sides. Single shock of vestibular nerves by these electrodes evoked spike discharges in axons of vestibular neurons projecting to the ipsilateral (Vi) or contralateral (Vc) side. The axonal character of the recording was evidenced by (a) the lack of synaptic potentials; and (b) the latency of evoked spike potentials, which fluctuated at threshold intensity and shortened considerably with increasing stimulus intensity, indicating the transsynaptic nature of activation. When tested with stimulus intensities of 1.5 to 2 times the threshold, the latencies ranged from 0.6 to 0.9 msecond. In addition, the spike potentials were superimposed on small negative field potentials, attributable to second-order vestibular fibers in the abducens nucleus. This method of identification has some limitations, because only vestibular neurons activated from the contralateral labyrinth (Vc) can be identified with certainty. The reason for this ambiguity is that, when recording an axon in the abducens nucleus, if this axon is stimulated by the ipsilateral labyrinth, it can be either a true vestibular nucleus neuron projecting to the ipsilateral side (Vi) or a neuron that crosses the midline after its passage in the nucleus and is therefore an axon of Vc type. For this reason, we have complemented the identification by electrophysiological methods with intracellular injection of horseradish peroxidase (HRP) in the axons of the neurons. The details of this method have been presented elsewhere.¹⁶⁻¹⁹ It allows the complete reconstruction of the neuron from the soma to the terminal arborizations and, therefore, the description of both the functional and the morphological properties of these neurons.

Recording of Neuronal Activity

Recordings were obtained with intracellular penetration of the axons of vestibular neurons. The axons were recorded by glass microelectrodes (1- to 2-micron tip) that penetrated the brain stem through the intact cerebellum. To have access to the cerebellum, a small hole 3-5 mm in diameter was made on the lambdoidal ridge, and in between sessions, this hole was covered with a thin film of Silastic and bone wax. Microelectrodes were filled with 3 M KCl solution, and for morphological studies, micropipettes were filled with 10% solution of HRP in tris-buffer (pH 7.2) and 0.5 M KCl. Electrode resistance varied from 15 to 30 megohms.

Vestibular Stimulation

The cats were immobilized in a stereotaxic apparatus, and the head inclined in order to place the semicircular canals in the horizontal plane. This apparatus was mounted on a velocity-controlled turntable that provided horizontal sinusoidal oscillation, stimulating the labyrinth. In the present work, frequencies of 0.1 to 0.3 Hz were used, with peak velocities ranging from 20 to 200°/second. A large shutter facing the head of the cat was mounted on the turntable, allowing the experimenters to test the neuronal activity either in light or in darkness. A typical protocol was the recording of spontaneous eye movements in the dark, followed by vestibular stimulation in the dark at one or more sinusoidal frequencies with different amplitudes. These two measurements were then repeated after the opening of the shutter in order to obtain information concerning the behavior of the neurons in the light.

Data Processing

Eye movement components, neuronal discharge, and table velocity were recorded on analog magnetic tape and processed on a digital computer (HP 5451 B and HP 1000). Eye velocity was calculated by filtering the data with a digital polynomial filter introducing no phase shift. Instantaneous firing rate was calculated, and in some cases, averaged over 50-millisecond bins. For the calculation of the range of firing rate of each neuron in relation to eye position (rate-position curve), a mean eye position was calculated by averaging all the eye movements of the cat over a period of several minutes. This gave an approximate evaluation of the resting eye position in the orbit.

RESULTS

A general observation—based on recordings of more than 50 axons, including type I and type II neurons of Vi and Vc types—was that the behavior of a given neuron with respect to the characteristics of the eye movement signals it carries could vary from one moment to another depending on the state of alertness of the animal. This calls for some caution in the interpretation of quantitative data concerning eye position or eye velocity sensibility of these neurons. Systematic studies on this problem—such as the one made by Buettner *et al.* in the monkey²⁰—will have to provide quantitative measurements. In the present report, we shall not attempt to give statistical values because the number of cells analyzed so far allows us to describe only the main features of the behavior of these neurons. However, because information concerning identified second-order vestibular neurons in the alert cat is not yet available, we feel that it can be useful at this point to describe these preliminary results.

Second-Order Vestibular Neurons Activated from the Contralateral Labyrinth

In order to avoid confusion, the activity of the neurons will be described with reference to their soma. For example, if the activity of an axon was recorded on the left side, and if it was activated monosynaptically by right vestibular nerve stimulation, or if horseradish peroxidase injection revealed that the soma was in the right vestibular nucleus, the modulation of discharge of the neuron was identified as Vc. In addition, it was said to be of type I if it discharged when the head of the animal turned in the horizontal plane to the right.

A first clear finding concerning Vc neurons is that they exhibit eye movement sensitivity that can be related to either the horizontal or vertical components of eye movements.^{18,19} Because our turntable could only provide rotation in the horizontal plane, we could not test the vestibular sensitivity (vertical semicircular canals or otoliths) of the neurons related to vertical eye movements. We shall now restrict our description to the main features of discharge patterns of horizontal type I Vc neurons.

FIGURES 2 and 3 show the behavior of one of these neurons during spontaneous eye movements in darkness and during table rotation either in darkness or in light (optokinetic and vestibular nystagmus). The instantaneous firing rate of this neuron induced by horizontal rotation is related to horizontal eye movements and head velocity. The on direction is when the eye moves to the right. As the

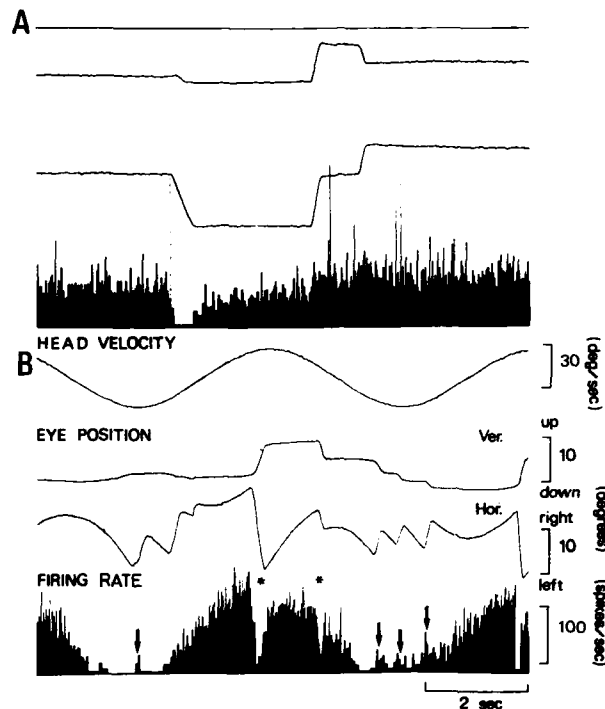


FIGURE 2. Discharge characteristics of a second-order Vc axon recorded in the right abducens nucleus and whose soma is in the left vestibular nucleus. **A.** Discharge characteristics during spontaneous eye movements in darkness. From top to bottom: table velocity, vertical and horizontal eye position, instantaneous firing rate. Calibrations indicated in **B.** **B.** Type I modulation of the discharge of the same neuron during sinusoidal rotation in the illuminated laboratory (combination of optokinetic and vestibular nystagmus). The asterisks and arrows respectively indicate the decrease and the increase of the firing rate associated with off- and on-direction quick phases. Calibrations are valid for A and B.

soma of the cell is in the left vestibular nucleus, the on direction is contralateral to the soma.

FIGURE 2A shows the instantaneous firing rate during a horizontal off-direction saccade (left). After the pause, the firing rate increases to an average value that is lower than during the preceding fixation. Note that it takes about 1 to 1.5 seconds for the firing rate to attain its final mean value. During the on-direction horizontal saccades, an irregular increase of discharge rate occurs. It will be seen with more clarity in FIGURE 3.

FIGURE 2B shows the behavior of the neuron during vestibular nystagmus in the light at 0.2 Hz. A typical type I modulation of firing rate appears nearly in phase with head velocity. Large pauses occur during quick phases in the off direction. The changes in firing rate during the two quick phases at the center of the figure (asterisks) are respectively about 125 spikes/second for a quick phase of 18° and about 70 spikes/second for a quick phase of 4° . Conversely, during

on-direction quick phases, small transient increases in firing rate are seen (arrows).

The behavior of the same neuron is shown in FIGURE 3, in which firing rate has been averaged in 50-millisecond bins. FIGURE 3A shows spontaneous eye movements in darkness. Note the pauses (asterisks) during off-direction saccades and transient increases in activity during on-direction saccades (arrows). The

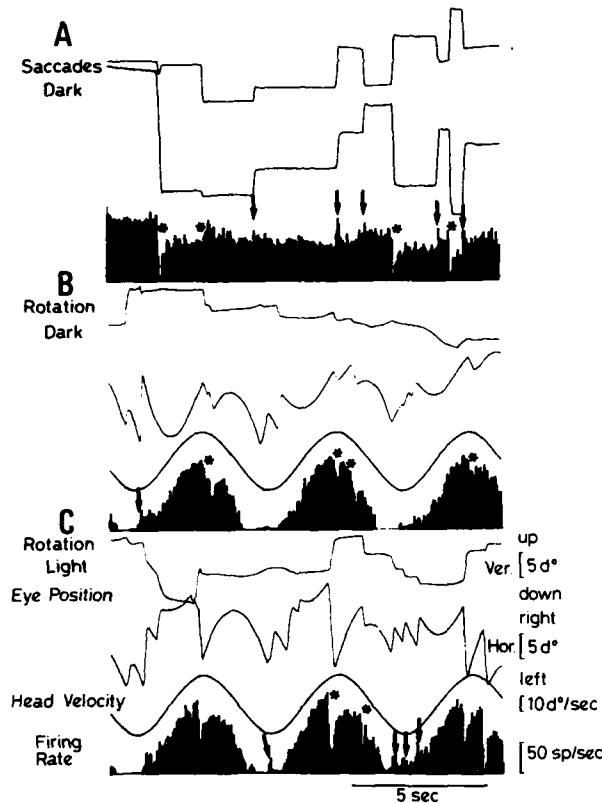


FIGURE 3. Comparison of the discharge characteristics of a second-order Vc axon during spontaneous saccades and nystagmus (same neuron as in FIGURE 2). **A.** From top to bottom: vertical and horizontal eye movements, firing rate averaged over 50-millisecond bins. Calibrations as in C. The figure shows a series of fixations in darkness. Note that the eye position sensitivity and saccadic eye velocity sensitivity (pauses and transient increases shown by asterisks and arrows during off- and on-direction saccades) occur in the absence of visual input. **B.** Discharge characteristics of the same neuron during sinusoidal rotation of the table at 0.2 Hz in darkness. From top to bottom: vertical and horizontal eye position, head velocity, firing rate. Calibration as in C. Note that, superimposed on the clear type I modulation in phase with head velocity, there is a clear eye position and saccadic eye velocity (asterisks and arrows) sensitivity. **C.** Same as in B but during sinusoidal rotation in the illuminated laboratory (summation of vestibular and optokinetic nystagmus). Calibrations shown here are also valid for A and B.

rate-position curves for this neuron indicate an eye position sensitivity of about 1.3 spikes/second per degree (correlation highly significant at $p < 0.01$). It reveals no relation with vertical eye movements.

FIGURE 3B shows the discharge pattern of the same neuron during vestibular nystagmus in darkness. At a frequency of horizontal sinusoidal rotation of 0.2 Hz, the discharge rate is modulated nearly in phase with head velocity. (Peak firing rate slightly leads peak head velocity.) During quick phases toward the on direction, small increases (arrows) of activity can be seen; their amplitude (about 0.3 spikes/second per degree/second) is small with respect to the head velocity-related discharge modulation (rough calculation of head velocity sensitivity gives for this neuron about 2.4 spikes/second per degree/second). Consequently, the excitatory action of the eye velocity-related signals in the on direction produces only a weak change in the head velocity-related discharge.

In contrast, off-direction quick phases are associated with a clear decrease in firing rate (asterisks). Interestingly, the high-amplitude quick phases in the off direction seen in FIGURE 3C occur at peak firing rate of the neuron. For a quick-phase amplitude of about 18° and peak eye velocity of about $100^\circ/\text{second}$, a rough calculation gives an off-direction saccadic eye velocity sensitivity of about 1 spike/second per degree/second.

It is interesting to compare the behavior of the neuron in darkness (FIGURE 3A and B) with that when the animal is rotated in the light (FIGURE 3C). Recording conditions in FIGURE 3B and C are the same, but in FIGURE 3C, the animal was oscillating in the illuminated laboratory. Therefore, optokinetic stimulation was

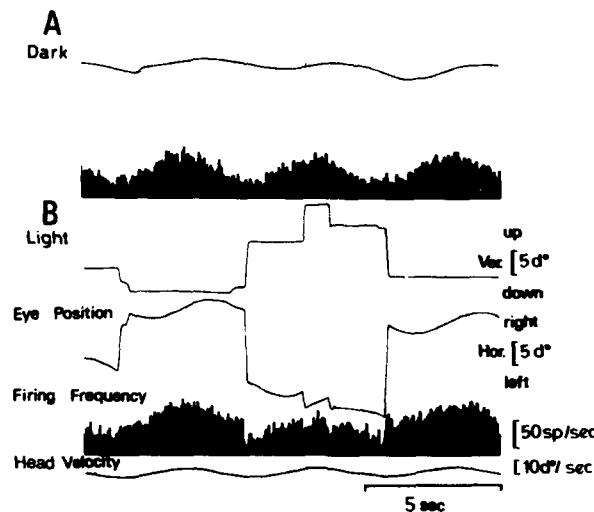


FIGURE 4. Discharge characteristics of the same neuron as in FIGURES 2 and 3 during low-amplitude vestibular stimulation. **A.** Discharge characteristics of the neuron during vestibular nystagmus in the dark. Upper trace: horizontal component of eye position. Lower trace: firing rate of the cell (averaged over 50-msecond bins). Calibrations as indicated in B. **B.** Discharge characteristics of the same neuron as in A during sinusoidal rotation in the illuminated laboratory. (Summation of vestibular and optokinetic nystagmus). From top to bottom: vertical and horizontal components of eye movements, firing rate, and head velocity. The head velocity record is the same for A and B.

TABLE 1
NUMERICAL VALUES OF SACCADIC EYE MOVEMENT SENSITIVITY FOR SEVEN TYPE I
SECOND-ORDER NEURONS OF VC AND VI TYPE (SEE TEXT)

Eye Position							
	Unit	Type	On Direction	Coefficient of Correlation*	Slope (spikes/sec per degree)	Intercept (spikes/sec)	Eye Velocity
Vc	1	I	Contra	0.45 (S)	1.1	43	yes
	2	I	Contra	0.90 (S)	5.8	22	yes
	3	I	Contra	0.72 (S)	1.3	64	yes
	4	I	Contra	NS	0.4	56	weak (no pause)
Vi	5	I	Contra	0.41 (S)	1.7	53	yes
	6	I	Contra	0.87 (S)	8.7	82	yes
	7	I	Contra	0.34 (S)	0.8	33	weak

*S means significant. NS means not significant.

combined with vestibular stimulation. Comparison between the modulation of firing rate in these two conditions reveals how the presence of the moving visual environment affects the discharge pattern of the neuron: (a) the overall gain of the sinusoidal modulation by head rotation is practically unchanged; (b) large pauses (asterisks), transient increases (arrows), and tonic changes in firing rate related to eye movements can be observed. However, they can be predicted from the eye movement sensitivity in the dark (FIGURE 3A) and are not in this case due to a visual component. This finding is consistent with the observations of Lisberger and Miles in the monkey;¹⁴ they demonstrated that at a frequency of 0.2 Hz, no significant effect of the visual environment of the response of type I horizontal "vestibular plus saccade" neurons could be observed.

FIGURE 4 shows the behavior of the same neuron as in FIGURE 2 but in the case of a smaller amplitude of vestibular stimulation. In the dark (FIGURE 4A), spontaneous eye movements are rare and the modulation is clearly sinusoidal. In the light (FIGURE 4B), large spontaneous saccades, which are superimposed with vestibular nystagmus, lead to changes in firing rate that are consistent with the description made above.

TABLE 1 gives additional information concerning four Vc type I second-order neurons. The table indicates in mean values (a) the direction of the eye position sensitivity with respect to the soma of the cell (on direction); (b) the correlation coefficient of the relationship between horizontal eye position and firing rate; (c) the slope of the regression line for this relationship; (d) the intercept between this regression line and the zero eye position (resting discharge); and (e) the presence of eye velocity sensitivity. Note that unit 4 is similar to a "vestibular only" neuron, although it has a small eye-position sensitivity.

Second-Order Neurons Activated from the Ipsilateral Labyrinth

We have recorded a number of axons activated monosynaptically from the ipsilateral labyrinth. For the reasons given in the methods section, the exact identification of these axons is not possible, and although quantitative analysis of these data presently is being done, we shall refer here only to the behavior of the Vi neurons identified by intra-axonic injection of horseradish peroxidase.^{16,18,19}

FIGURE 5 shows an example of such a neuron, whose soma is in the medial vestibular nucleus (FIGURE 5C). Its terminal arborizations, although they did not seem to reach the abducens nucleus, may have contacted the dendrites of abducens motoneurons around and below the sixth nucleus. Axonal terminations of these neurons were also seen in the ipsilateral caudal prepositus nucleus, reticular formation, and nucleus of Roller.

FIGURE 5A shows, at fast sweep speed, the behavior of the neuron (instantaneous firing rate) during spontaneous saccades in the dark. This neuron, whose soma was in the right side of the brain stem, stops firing during saccades to the right and discharges during saccades to the left (contralateral side). This is consistent with the general rule that second-order type I vestibular neurons terminating in or around the abducens nucleus seem to discharge during horizontal eye movements directed toward the contralateral side. FIGURE 5A also shows the time relationship between the onset of ipsilateral rightward and downward saccade and onset of pause, and the onset of contralateral leftward saccade and the onset of firing.

FIGURE 5B shows the behavior of the neuron with respect to eye position and saccadic eye velocity during spontaneous saccades in darkness. In this case, the firing rate has been averaged with 50-millisecond bins. Eye position sensitivity is

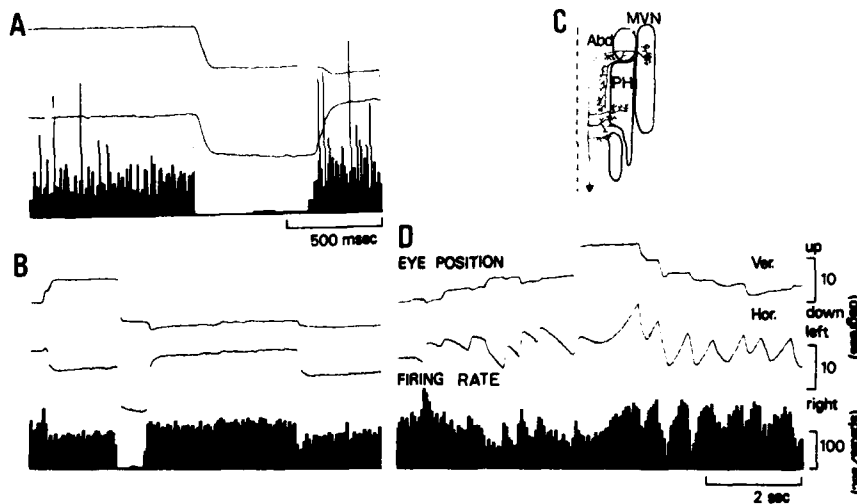


FIGURE 5. Morphological and physiological characteristics of a second-order Vi neuron. A. Detail of the discharge characteristics, at fast sweep speed, of the neuron during spontaneous saccades in the dark. From top to bottom: vertical and horizontal eye movements, instantaneous firing rate. Time calibration in milliseconds, amplitude calibrations as in D. B. Discharge of the same neuron in darkness with a slower sweep speed and an averaged firing rate (50-millisecond bins). Time and amplitude calibrations as indicated in D. C. Morphology of this neuron revealed by the reconstruction after intracellular injection of HRP. The soma lies in the medial vestibular nucleus (MVN); the axon descends ipsilaterally to the spinal cord, giving off collaterals around the abducens nucleus (Abd), caudal prepositus hypoglossi (PH), medullary reticular formation, and nucleus of Roller. D. Modulation of the discharge rate of the same neuron during sinusoidal rotation in the illuminated laboratory. Combination of optokinetic and vestibular nystagmus. Calibrations are valid for B.

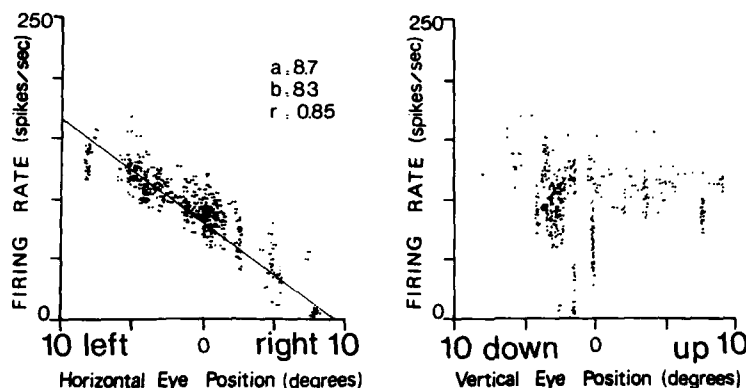


FIGURE 6. Relationship between instantaneous firing rate and eye position for the neuron illustrated in FIGURE 5. Computer-plotted data points. Each data point was calculated by averaging instantaneous firing rate and eye position over periods of 25 mseconds during eye fixation. The left side of the figure shows the linear relationship between the amplitude of the horizontal component of the eye position (on abscissa) and the firing rate (on ordinate) during fixations in darkness. On the abscissa, 0 indicates the center of gaze. The right side of the figure illustrates the lack of correlation between the vertical component of the eye position (on abscissa) and the firing rate (on ordinate). The parameters of the computed regression line for the horizontal component are inserted: a, slope in spikes/second per degree; b, intercept with the y-axis (zero-degree eye position); r, correlation coefficient.

high; it is illustrated in FIGURE 6 in the horizontal rate-position curve with a sensitivity of about 8.6 spikes/second per degree (correlation coefficient 0.87, highly significant at $p < 0.01$). The large pause during a rightward fixation in FIGURE 5B is from the same record as the one that is shown in FIGURE 5A. This neuron has a rather small saccadic eye velocity sensitivity.

In FIGURE 5D, the behavior of this neuron during vestibular nystagmus in darkness is shown at 0.1 Hz sinusoidal oscillation. In our study, three type I horizontal Vi neurons were recorded and injected with HRP. They all show a similar pattern of relationship with eye position and velocity. However, a detailed quantitative analysis remains to be done before general conclusions can be drawn.

TABLE compares examples of the numerical values of saccadic eye movement sensitivity for three Vi type I neurons.

DISCUSSION

The above results, although still preliminary, demonstrate that horizontal type I second-order vestibular neurons carry information concerning eye position and eye velocity in addition to head velocity. They are of the "vestibular plus eye position" type of Fuchs and Kimm in the monkey vestibular nucleus.¹¹ The eye position sensitivity of most of the neurons encountered varies between 1 to about 8 spikes per second per degree. The phases of discharge modulation by the vestibular stimulus were studied by Shinoda and Yoshida and by Keller and Precht.^{21,22} These last authors found a bimodal distribution in the histograms of

the phases of discharge rate with respect to head acceleration, which at 0.2 Hz would suggest the existence of two populations of cells, one with a small lag (about 60 to 70°) and another with a large phase lag (about 100 to 120°) with respect to head acceleration. The present state of our results does not allow us to say which one of these populations is more clearly related with the eye movement, and in fact, it is probable that further investigations will reveal a variety of behaviors. Keller and Precht, recording a number of Vi axons (25 cells), reported that they saw in these neurons, pauses with a discharge rate during ipsilaterally directed quick-phase eye movements.²² It is possible that only some of these axons were actually projecting to the ipsilateral abducens nucleus, for the reasons stated in the methods section. However, their observation is in agreement with the present results, which show that in both Vc and Vi axons, the pauses always occur for rapid eye movements in the contralateral direction. The detailed analysis of instantaneous firing frequency has revealed in our study small, but consistent, saccade- and quick phase-related bursts of activity in those cells with eye velocity sensitivity. The small amplitude of these changes in firing frequency during the saccade (0.2 to 0.3 spikes/second per degree/second) may not be immediately perceptible on visual analysis of raw records and therefore requires quantitative calculation. It is not possible to say yet whether this is a burst tonic type of activity, such as the one present in motoneurons, or whether it is an eye velocity sensitivity, although we would favor the latter interpretation.

The existence of a time constant after the saccade-related burst or pause, which can be as high as 1 to 2 seconds (before the cell reaches a stable mean firing rate during the subsequent fixation), cannot be explained at this point. It may, however, be itself responsible for the slow decay in firing rate seen in many motoneurons.^{4,23,28}

The present results suggest that vestibular nucleus second-order neurons are not mainly relay neurons, carrying tonic information to the oculomotor nuclei as thought by Lorente de Nó,¹ but are highly complex neurons integrating a number of signals in order to control eye movement from a premotor level.

If one considers that in the cat, second-order vestibular neurons receive afferents from the neck, from the flocculus of the cerebellum, and from sources of visual origin,²⁴ it is therefore necessary to reconsider the role of these neurons and return to one of the other concepts proposed by Lorente de Nó: the vestibulo-ocular reflex would be organized by the interactive action of several networks of neurons obeying the so-called law of reciprocity of innervation. This means that many structures along this network would receive influences from the structures it innervates. What we have to understand now is the reason why an eye movement modulation of second-order neurons is useful for the normal operation of the vestibulo-ocular reflex. The pauses during saccades could have an evident functional use: this is to interrupt inhibition (in the case of Vi axons) of the agonist muscles during the saccade and to suppress the excitation of the antagonist (in the case of Vc axons).

Such a powerful suppression of the VOR during a saccade is also necessary during rapid rotation of the head to one side. It has been shown in man and in the cat that at the onset of rapid active or passive head rotation around a vertical axis, after a short-lasting compensatory deviation of the eyes due to the VOR, a large anticompany saccade or quick phase is triggered, whose function is probably to bring the eye in the direction of the head movement.²⁵⁻²⁷ This saccade can take place only if a nearly complete suppression of the VOR is possible. We have indeed seen in the present results that in the light, a nearly complete suppression of the VOR often occurs during saccades. The origin of this suppression is yet

unclear. Inhibitory burst neurons (IBNs) located caudally to the abducens nucleus have been shown to give monosynaptic inhibition to the contralateral abducens motoneurons.³ These neurons are the immediate premotor neurons for all types of rapid eye movements and terminate not only in the abducens nucleus but also in the contralateral medial vestibular nucleus, prepositus nucleus, and reticular formation.^{16,17} However, they cannot be directly at the origin of the pause in type I neurons, but most probably produce a pause in type II neurons.

Given the remarkable variety of morphological characteristics of vestibular neurons revealed by intracellular horseradish peroxidase injection,¹⁷⁻¹⁹ more data are needed before definite conclusions can be drawn. In particular, the fact that a number of horizontal second-order vestibular neurons project not only to the abducens nucleus but also to the spinal cord suggests investigations in which neck-oculomotor coordination is studied.

ACKNOWLEDGMENT

Dr. R. McCrea participated in some of the experiments concerning the identification of the neurons by HRP as reported elsewhere.¹⁶⁻¹⁹

REFERENCES

1. LORENTE DE NÓ, R. 1933. Vestibulo-ocular reflex arc. *Arch. Neurol. Psychiatry* **30**: 245-291.
2. MAEDA, M., H. SHIMAZU & Y. SHINODA. 1972. Nature of synaptic events in cat abducens motoneurons at slow and quick phase of vestibular nystagmus. *J. Neurophysiol.* **35**: 279-296.
3. HIKOSAKA, O. & T. KAWAKAMI. 1977. Inhibitory reticular neurons related to the quick phase of vestibular nystagmus. Their location and projection. *Exp. Brain Res.* **27**: 377-396.
4. BAKER, R. & A. BERTHOZ. 1974. Organisation of vestibular nystagmus in the oblique oculomotor system. *J. Neurophysiol.* **37**: 195-217.
5. BERTHOZ, A., R. BAKER & J. GOLDBERG. 1974. Neuronal activity underlying vestibular nystagmus in the oculomotor system of the cat. *Brain Res.* **71**: 233-238.
6. SPIEGEL, E. 1933. Role of vestibular nuclei in the cortical innervation of the eye muscles. *Arch. Neurol. Psychiatry* **29**: 1084-1097.
7. DUENSING, F. & K. P. SCHAEFFER. 1958. Die Aktivität Einzelner Neurone im Bereich der Vestibulariskerne bei Horizontal-Beschleunigungen unter Besonderer Berücksichtigung des Vestibulären Nystagmus. *Arch. Psychiatr. Nervenkr.* **198**: 225-252.
8. AZZENA, G. B., M. T. AZZENA & R. MARINI. 1974. Optokinetic nystagmus and the vestibular nuclei. *Exp. Neurol.* **42**: 158-168.
9. KELLER, E. L. & P. D. DANIELS. 1975. Oculomotor related interaction of vestibular and visual stimulation in vestibular nucleus cells in alert monkey. *Exp. Neurol.* **46**: 187-198.
10. MILES, F. A. 1974. Single unit firing patterns in the vestibular nuclei related to voluntary eye movements and passive body rotation in conscious monkeys. *Brain Res.* **71**: 215-224.
11. FUCHS, A. F. & J. KIMM. 1975. Unit activity in vestibular nucleus of the alert monkey during horizontal angular acceleration and eye movement. *J. Neurophysiol.* **38**: 1140-1161.
12. KELLER, E. L. & B. Y. KAMATH. 1975. Characteristics of head rotation and eye movement related neurons in alert monkey vestibular nucleus. *Brain Res.* **100**: 182-187.

13. WAESPE, W. & V. HENN. 1977. Neuronal activity in the vestibular nuclei of the alert monkey during vestibular and optokinetic stimulation. *Exp. Brain Res.* **27**: 523-538.
14. LISBERGER, S. G. & F. A. MILES. 1980. Role of primate medial vestibular nucleus in long term adaptive plasticity of vestibulo-ocular reflex. *J. Neurophysiol.* **43**: 1725-1745.
15. ROBINSON, D. A. 1963. A method of measuring eye movement using a scleral search-coil in magnetic field. *IEEE Trans. Bio-Med. Eng.* **10**: 137-145.
16. YOSHIDA, K., R. MCCREA, A. BERTHOZ & P. P. VIDAL. 1979. Morphological and physiological characteristics of burst inhibitory neurons in the alert cat. In Abstracts, Ninth Annual Meeting of the Society for Neuroscience, Houston, Texas (USA) **5**: 391.
17. YOSHIDA, K., R. MCCREA, A. BERTHOZ & P. P. VIDAL. 1981. Properties of immediate premotor inhibitory burst neurons controlling horizontal eye movements in the cat. *Prog. Oculomotor Res.* (In press.)
18. MCCREA, R. A., K. YOSHIDA, A. BERTHOZ & R. BAKER. 1980. Eye movement related activity and morphology of second order vestibular neurons terminating in the cat abducens nucleus. *Exp. Brain Res.* **40**: 468-473.
19. MCCREA, R., K. YOSHIDA, C. EVINGER & A. BERTHOZ. 1981. The location, arborization and termination sites of eye movement related secondary vestibular neurons demonstrated by intra-axonal HRP injection in the alert cat. *Prog. Oculomotor Res.* (In press.)
20. BUETTNER, V. W., V. BUETTNER & V. HENN. 1978. Transfer characteristics of neurons in vestibular nuclei of the alert monkey. *J. Neurophysiol.* **41**: 1614-1628.
21. SHINODA, Y. & K. YOSHIDA. 1974. Dynamic characteristics of responses to horizontal head angular acceleration in the vestibulo-ocular pathway in the cat. *J. Neurophysiol.* **37**: 653-673.
22. KELLER, E. L. & W. PRECHT. 1979. Visual vestibular responses in vestibular nuclear neurons in the intact and cerebellectomized cat. *Neuroscience* **4**: 1599-1613.
23. GOLDBERG, J. 1980. Activity of abducens nucleus units in the alert cat. Ph.D. Thesis. University of California. Berkeley, Calif.
24. BAKER, R., W. PRECHT & R. LLINAS. 1972. Cerebellar modulatory action on the vestibulo-trochlear pathway in the cat. *Exp. Brain Res.* **15**: 364-385.
25. MELVILL JONES, G. 1964. Predominance of anticomensatory oculomotor response during rapid head rotation. *Aerosp. Med.* **35**: 965-968.
26. BARNES, G. R. 1979. Vestibulo-ocular function during co-ordinated head and eye movements to acquire visual targets. *J. Physiol. London* **287**: 127-147.
27. BERTHOZ, A., M. JEANNEROD, F. VITAL-DURAND & J. L. OLIVERAS. 1975. Development of vestibulo-ocular responses in visually deprived kittens. *Exp. Brain Res.* **23**: 425-442.
28. YOSHIDA, K., P. P. VIDAL & A. BERTHOZ. (Unpublished observations.)

A TRANSSYNAPTIC AUTORADIOGRAPHIC STUDY OF
THE PATHWAYS CONTROLLING THE EXTRAOCULAR
EYE MUSCLES, USING [125 I]B-II₆ TETANUS TOXIN
FRAGMENT*

J. A. Büttner-Ennever, P. Grob, and K. Akert

Brain Research Institute
University of Zurich
CH-8029 Zurich, Switzerland

B. Bizzini
Pasteur Institute
92420 Marnes la Coquette, France

INTRODUCTION

Tetanus toxin has been shown to be taken up by peripheral nerve terminals and transported intra-axonally in a retrograde fashion to the corresponding cell bodies.^{16,18,40,44,51} Additional studies demonstrated that this agent is a reliable and highly sensitive retrograde tracer substance, which can be injected into the brain in minute quantities and detected in afferent fibers and their cell bodies at the light microscope level.⁴³ In addition to its retrograde transport into the cell soma, tetanus toxin also has been detected by electron microscopy in the presynaptic terminals,^{41,42,45} and in a recent report it could be demonstrated in presynaptic axons, distal to a crush, with the light microscope.¹⁷ Theoretically, therefore, tetanus toxin could be used as a transsynaptic retrograde tracer substance, although up to now it has not been used for this purpose. Our study was designed to explore this possibility. The experiments were performed on the medial rectus eye muscle of the monkey because, first, the connectivity of its motoneurons and especially the synaptic inputs from the abducens internuclear neurons and the vestibular nuclei are well defined,^{2,11,15,23,26} and second, large volumes of tetanus toxin can be injected into the extraocular eye muscles without fear of directly contaminating intracranial structures. The results show that tetanus toxin can be used as a transsynaptic retrograde tracer and detected by light microscopy in the cell bodies of both primary and secondary neurons, but that problems of interpretation arise through the use of large injections.⁴³

METHODS

Experiments were carried out on five anesthetized (Nembutal, 40 mg/kg) monkeys (*Macaca fascicularis*). The surgical procedure used to expose the medial rectus muscle of the right eye involved cutting the medial margin of the palpebral fissure, and an incision of the conjunctiva. Between 17 and 50 μ l of [125 I] tetanus toxin B-II₆ fragment were injected by a mechanically driven syringe, over a period of one to three hours, into the belly of the muscle. The atoxic fragment had

*This work was supported by the Swiss National Science Foundation Nr. 3.636.75 and 3.611.75, the Dr. Eric Slack-Gyr Foundation, and the EMDO-Stiftung.

been isolated from crude tetanus toxin by a freezing-thawing procedure and labeled with radioactive iodine [^{125}I].^{4,50} TABLE 1 provides experimental details. The animals were perfused through the heart with 300 ml of a 1:1 mixture of Ringer solution and Macrodex®, a plasma expander, followed by 1 l of 1% paraformaldehyde and 2.5% glutaraldehyde in a 0.1 M phosphate buffered solution (PBS) at pH 7.4, and finally 0.1% paraformaldehyde, 4% glutaraldehyde, and 5% sucrose in 0.1 M PBS.³⁶ The brains were removed and stored in a 0.1 M PBS with 30% sucrose for three days at 4°C. Frozen sections (30 μ) were taken in the transverse stereotaxic plane from the rostral mesencephalon to the caudal medulla,⁴⁷ except in experiment 79-206. In this case, serial sections were only taken from the rostral mesencephalon back to the rostral pons; in addition a small separate block from the abducens nucleus, contralateral to the side of injection, was processed for autoradiography. Every fifth section was mounted and dipped in NTB₂ photographic emulsion, at 45°C, diluted 1:1 with distilled water. The sections were exposed for four weeks at 4°C in the dark, then developed with Kodak Dektol at 18°C for 1½ minutes, washed, fixed with 30% sodium thiosulfate, washed for two hours, then counterstained with cresylviolet, and covered. All sections were examined for silver grain deposits under magnifications of at least 100 times. Grain counts were taken from an area of 0.01 mm², at magnifications of 1,000. The average count of various structures from 10 different fields is given in TABLE 2. For each structure, background counts were evaluated by sampling 10 sites around the labeled area.

RESULTS

In three experiments, the injection of [^{125}I] tetanus toxin into the medial rectus led to the deposit of silver grains over many brain-stem structures (TABLE 1). In experiment 78-833, only weak labeling over extraocular motoneurons was found. Two distinctly different patterns of silver grains could be found: diffuse, and clusters lying over cell bodies. In some regions both were superimposed. The location and relative density of labeling in experiment 79-538, regardless of its type of pattern, is shown diagrammatically in FIGURE 1. Similar patterns of silver grain deposits were seen in experiments 79-206 and 79-486. In addition, grain counts were taken from several structures of experiments 79-538 (TABLE 2) in order to make quantitative comparisons between their labeling. In TABLE 2 the background counts around each structure are given in the final column. Areas that were weakly labeled—such as the principal sensory trigeminal nucleus, the pretectal olivary nucleus, and the nucleus reticularis tegmenti pontis (nrtp)—had counts about 10 times greater than background. However, grain counting was not

TABLE 1
EXPERIMENTAL DETAILS

Experiment	Volume (μl)	Concentration ($\mu\text{Ci}/\mu\text{l}$)	Specific Activity ($\mu\text{Ci}/\mu\text{g}$)	Total Activity (μCi)	Survival Time (days)	Transsynaptic Labeling
78.833	17	5.0	10	85	1½	—
79.206	50	2.5	3.4	125	6	++
79.486	50	3.3	3	125	6	+
79.538	45	1.3	10.4	58	6	++

TABLE 2
GRAIN DENSITIES IN SELECTED STRUCTURES*

Structure	Average Grains/0.01 mm ²		
	Right Side	Left Side	Background
Oculomotor nucleus	>800	>800	7 ± 3
Trochlear nucleus	>800	>800	7 ± 2
Abducens nucleus	>800	>800	7 ± 2
Facial nucleus	>800	55 ± 15	7 ± 2
Trochlear nerve	13 ± 4	310 ± 30	9 ± 2
Abducens rootlets	132 ± 24	9 ± 2	9 ± 4
Facial nerve	54 ± 10	9 ± 2	9 ± 4
Rostral interstitial nucleus of the MLF	117 ± 22	133 ± 27	7 ± 2
Interstitial nucleus of Cajal	273 ± 58	182 ± 30	12 ± 3
Anteromedian nucleus	562 ± 40	140 ± 12	4 ± 1
Olivary nucleus (pretectal)	61 ± 9	80 ± 11	10 ± 3
Medial longitudinal fasciculus	76 ± 16	29 ± 6	6 ± 3
Nucleus reticularis tegmenti pontis	67 ± 13	55 ± 5	6 ± 2
Superior colliculus	17 ± 3	17 ± 3	6 ± 3
Spinal trigeminal nucleus	226 ± 105	10 ± 3	9 ± 3
Principal sensory trigeminal nucleus	70 ± 20	9 ± 3	9 ± 3
Superior vestibular nucleus	60 ± 12	100 ± 26	7 ± 1
Medial vestibular nucleus	59 ± 20	73 ± 11	11 ± 4
Lateral vestibular nucleus	194 ± 65	66 ± 14	8 ± 1
Nucleus prepositus hypoglossi	240 ± 50	53 ± 16	9 ± 3
y group	164 ± 13	100 ± 11	9 ± 3

*Each grain count is the mean of counts made within 10 different 0.01-mm² areas. The background counts were taken from the area surrounding the labeled structure.

used to verify the presence or absence of a projection; this was decided on the basis of visual inspection of serial sections. The location, strength, and pattern of labeling will be described below, and the interpretation of whether the labeling is the result of direct retrograde, anterograde, or transsynaptic transport will be considered in the discussion.

The most rostral structure labeled in the material studied was the rostral interstitial nucleus of the medial longitudinal fasciculus (rostral iMLF), see FIGURE 1. The silver grain deposits were equally strong on both sides and often were concentrated over cell bodies. Comparing the three positive cases (TABLE 1), the labeling in 79-206 was strongest. Moving caudally to the interstitial nucleus of Cajal (iC), the pattern of silver grains became more diffuse, although from TABLE 2 it can be seen that the iC labeling was stronger on the side contralateral to the injection. On slides where the caudal end of the rostral iMLF and the rostral tip of the iC appeared in the same section, their silver grain deposits could be distinguished from each other. No labeling was present over nucleus Darkschewitsch or the nuclei of the posterior commissure. The rostral anteromedian nucleus was diffusely covered with silver grains ipsilaterally (FIGURE 1 and TABLE 2); however, this was not clearly separate from halo effects around the adjacent oculomotor neurons, which were heavily labeled.

In every case, the oculomotor rootlets were covered with silver grains, on the side ipsilateral to the injection, and motoneuron pools in the oculomotor nucleus supplying individual eye muscles from that side were also labeled. The classical medial rectus subgroup, indicated as subgroup A in FIGURE 2b and lying in the

EXP 78-536

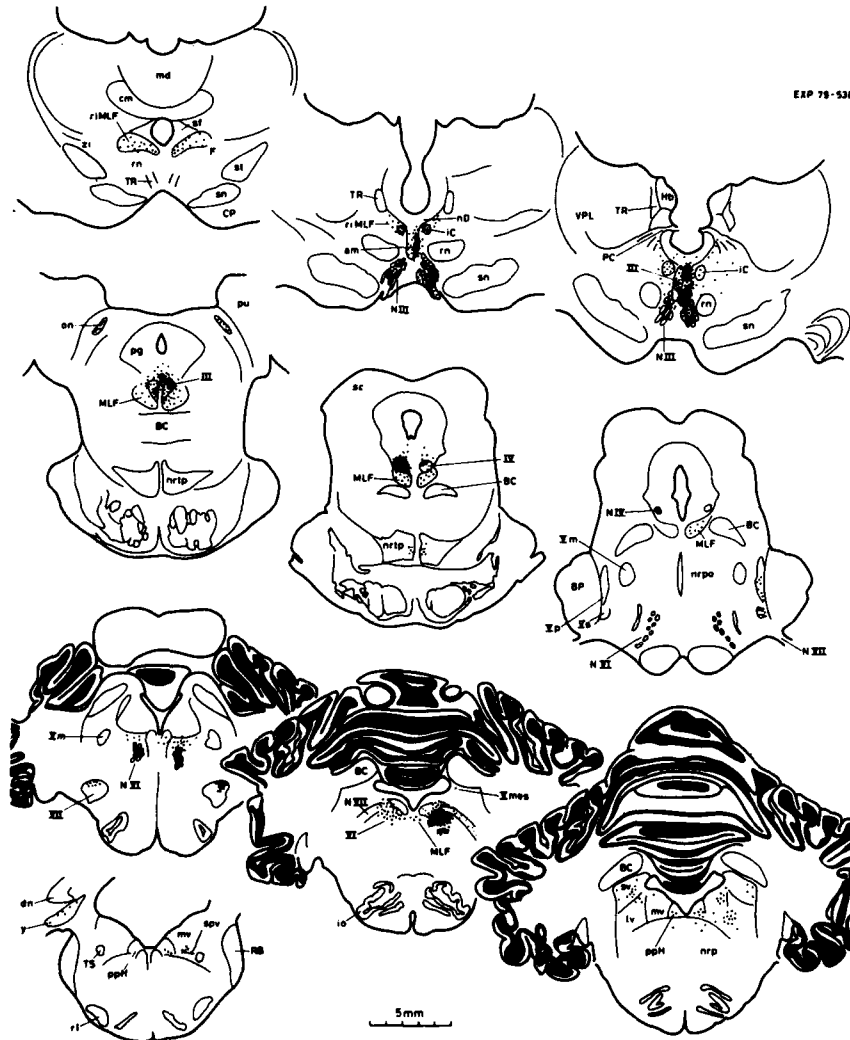


FIGURE 1. Experiment 79-538. Selected transverse sections drawn to show the distribution of silver grains in the brain stem after injection of [125 I]tetanus toxin into the right medial rectus muscle. The distribution of dots indicates the relative intensity of labeling, regardless of type (diffuse or clustered over cell bodies). See Appendix for a list of abbreviations.

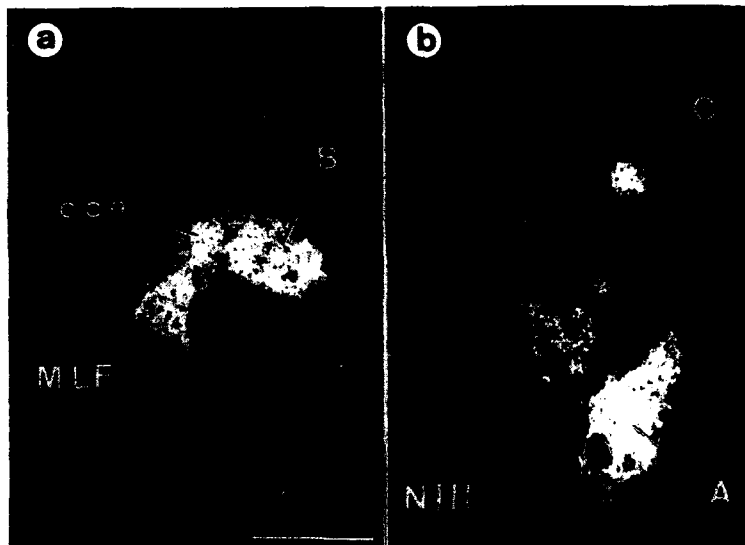


FIGURE 2. Experiment 79-538. Transverse sections through the oculomotor nucleus, photographed under dark-field illumination, to show the silver grain deposits over (a) caudal levels and (b) mid-levels, after injection of tetanus toxin into the medial rectus muscle. The three heavily labeled subgroups of medial rectus motoneurons are marked A, B, and C. The motoneurons of the superior rectus (sr), which lie on the contralateral side, and those of the levator palpebrae in the central caudal nucleus (ccn) are also heavily labeled. Calibration = 1 mm.

Edinger-Westphal nucleus. The halo of silver grains around these motoneurons may obscure some weak labeling in the Edinger-Westphal nucleus. However, since there was no increase in silver grain density associated with the nucleus itself, we must conclude that there was no significant labeling of this structure. The third medial rectus motoneuron subgroup, B, located in the dorsal part of the caudal oculomotor nucleus, was labeled as heavily as the other two subgroups. It is shown in FIGURE 2a adjacent to the central caudal nucleus, which contained strongly labeled motoneurons of levator palpebrae, distributed bilaterally. The motoneurons of the superior rectus lie in the oculomotor nucleus contralateral to the injection site. They were labeled and are clearly visible in FIGURE 2a and b, while the ipsilateral subgroups of inferior rectus and inferior oblique, lying beneath medial rectus subgroup C, were less dramatically labeled. In all experiments, the contralateral trochlear nucleus was heavily covered with silver grains (FIGURE 3a). In experiment 79-206, the intensity of the labeling, in fact, appeared equal to that of the medial rectus. A much weaker and diffuse deposit of silver grains was found over the dorsal part of the ipsilateral trochlear nucleus as well. This is shown in the inset of FIGURE 3a.

Other cell groups to be labeled at these levels, outside the oculomotor complex, were the olivary nucleus in the pretectum and the medial part of the nrtp. The pattern of silver grains was, in both instances, diffuse and equally strong on both sides (FIGURE 1 and TABLE 2).

A clear lateralization could be observed in the number of silver grains over

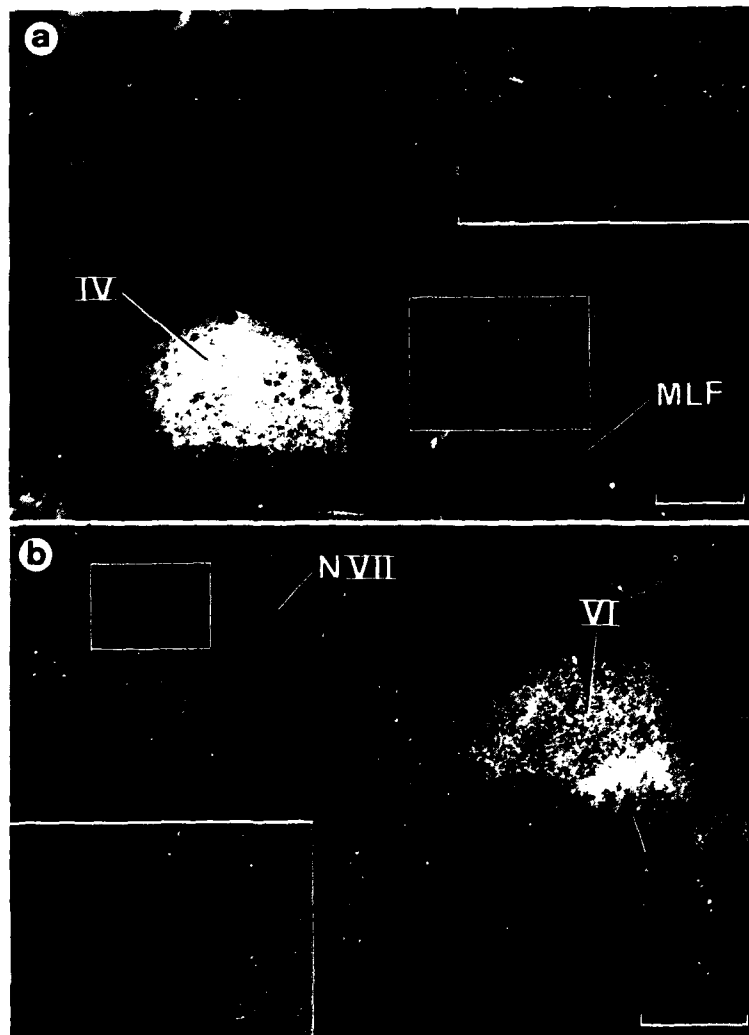


FIGURE 3. Experiment 79-538. Direct and transneuronal retrograde transport of tetanus toxin. (a) Transverse section at the level of the trochlear nucleus, photographed under dark-field illumination, to show the direct strong labeling of the motoneurons of the contralateral superior oblique after leakage from an injection of tetanus toxin into the neighboring medial rectus. The framed area is enlarged in the inset to show the diffuse pattern of silver grains confined to the dorsal portion of the contralateral trochlear nucleus. (b) Heavy direct labeling in the abducens nucleus (VI) on the side of the injection; the more intensely labeled cell group just ventral to the VI is thought to be the motoneurons of the accessory lateral rectus muscle "slip" (arrow). The framed area is enlarged in the inset to demonstrate the weaker, but significant, transneuronal labeling of the contralateral VI. Calibrations = 0.5 mm in (a) and 1.0 mm in (b).

the trochlear nerves, abducens rootlets, facial nerves, and MLF. Under visual inspection (100 \times , dark field), the MLF as well as abducens and facial nerves ipsilateral to the injection, and the contralateral trochlear nerve (proximal to the decussation), were clearly above background (TABLE 2). The cell groups of the trigeminal complex were labeled ipsilaterally. In all cases, silver grain deposits over the principal sensory and spinal trigeminal nuclei were found, but the motor trigeminal nucleus was only labeled in 79-486. The grain counts over the trigeminal nerve in the latter case were about three times greater than background, which implies some transport from the periphery. Only one cell in the mesencephalic trigeminal nucleus was labeled (experiment 79-538). The orbicularis oculi division of the facial nucleus contained radioactive deposits, bilaterally. However, the side ipsilateral to the injection was covered with a dense cluster of silver grains, while the contralateral side was only weakly labeled in comparison. On both sides the pattern of silver grains was of the diffuse type.

The ipsilateral abducens nucleus was strongly labeled, but the motoneurons of the accessory lateral rectus muscle "slip," which lie just ventral to the main abducens nucleus,⁴⁶ were even more heavily marked (FIGURE 3b). On the contralateral side, only the main abducens nucleus was covered with silver grains, the labeling being distinctly weaker than on the other side (FIGURE 3b). But the deposits lay in clusters over cell bodies (FIGURE 4c). This was visible most easily around the periphery of the nucleus, where the labeling was less dense.

The vestibular nuclei, the nucleus prepositus hypoglossi (ppH), and the y group were labeled on both sides of the brain, but there was a striking difference in the patterns and intensities of the deposits. Clusters of silver grains covered individual neurons of the ipsilateral ppH and lateral and medial vestibular nucleus (lv and mv), as well as the contralateral mv and superior vestibular nucleus (sv). The cells were often, but not always, surrounded by diffuse deposits (FIGURE 4a and b). These labeled areas were well demarcated and did not stretch throughout the rostrocaudal extent of these nuclei. The silver grain deposits were confined to the smaller neurons in the ventromedial part of the lv and not found in the large Deiters' neurons (FIGURE 4a and b). Labeled cell bodies could also be seen in the medial vestibular nucleus (mv) dorsal to the deposits in the lv, but otherwise the labeling in the rest of the vestibular nuclei was diffuse, and weaker than in the areas described above. The only part of the medullary reticular formation that was found to have a concentration of silver grains higher than background was just below the ppH (FIGURE 1). The y group labeling was confined to the dorsal division of the nucleus and tended to lie over neuronal perikarya. No silver grain deposits were found at the level of the nucleus intercalatus of Staderini, which represented the most caudal level inspected.

DISCUSSION

A disappointing feature of this study is that although tetanus toxin was injected into the medial rectus muscle, all the motoneuron pools supplying extraocular muscles in the same orbit—in particular, the contralateral trochlear nucleus—are heavily labeled. This situation, however, can be turned to our advantage since the labeled secondary pathways are being multiplied. It is explained by the fact that tetanus toxin is taken up by nerve terminals in a highly efficient manner,^{44,45} and with the massive doses injected in this study, some tetanus toxin was seen to leak out of the medial rectus into the orbit where the agent was taken up by the neighboring muscles—especially the superior oblique

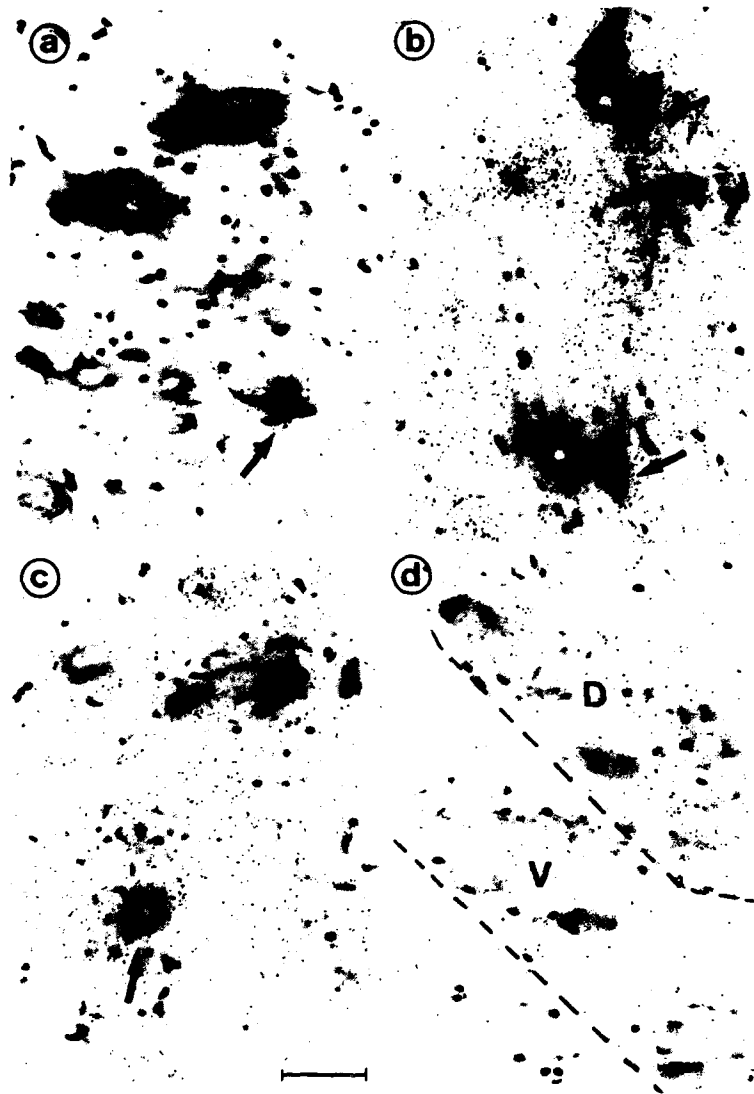


FIGURE 4. Experiment 79-538. Light-field photographs to show the transsynaptic retrograde labeling of cell bodies in (a) the lateral vestibular nucleus, ipsilateral to the injection (arrow); note that the two large Deiters' neurons are not labeled; (b) another region of the same lateral vestibular nucleus where silver grains are associated with perikarya (arrow) and diffusely distributed throughout the neuropil; (c) the abducens nucleus, contralateral to the injection. Arrow indicates a labeled internuclear neuron. Silver grains are also diffusely distributed over the neuropil; (d) the y group contralateral to the injected side; D marks the dorsal division over which there is a significant accumulation of silver grains, not clearly associated with cell bodies. V is the ventral division, which remains unlabeled. Calibration for all photos = 50μ .

(innervated by the contralateral trochlear nucleus), being closest to the medial rectus—thus involving the respective oculomotor nuclei. This would also account for the higher grain densities in the facial nerve of the right side (TABLE 2) and the massive labeling of the orbicularis oculi division of the ipsilateral facial nucleus.⁵² Another possibility would be the cross contamination within the oculomotor nerve itself, but this could not produce labeling of the facial nucleus. Contamination of the motoneurons via the blood supply is also less likely because one would not expect only one specific division of the facial nucleus to be labeled. This orbital contamination leads to difficulties in interpretation of the autoradiograms. However, if one considers only the patches of labeling in which distinctly labeled cell bodies were found, the interpretation becomes relatively simple.

Clusters of silver grains were found over perikarya in the contralateral sv, mv, and abducens nuclei; in the ipsilateral lv, mv, and ppH; and bilaterally in the rostral iMLF. The labeling within the abducens nucleus does not arise from uptake in the periphery, since the rootlets of the sixth nerve on that side have silver grain counts equal to background (TABLE 2). Neither is tetanus toxin likely to be transported across from the contralateral abducens, since no interconnections have ever been found between the two nuclei. However, there is anatomical and physiological evidence for a strong projection to the medial rectus motoneurons from the internuclear cells of the contralateral abducens nucleus.^{11,12,15,19,23,24,26,49} The afferent axons cross the midline at the level of the abducens nucleus, and ascend in the MLF to innervate only the medial rectus subgroups of the oculomotor nucleus. This pathway is well labeled in these experiments. These findings are consistent with the interpretation of retrograde transport of tetanus toxin to the medial rectus motoneurons and subsequent transsynaptic movement into the presynaptic terminals of the abducens internuclear neurons, then retrograde transport within the ipsilateral MLF back to the cell bodies in the contralateral abducens nucleus. An example of such a labeled neuron is shown in FIGURE 4c. There is a reciprocal pathway that arises from internuclear neurons in the medial rectus subgroups of the oculomotor nucleus, projecting back to the contralateral abducens nucleus.^{5,33,53} Since tetanus toxin also is transported in an anterograde fashion,⁴³ this pathway also will be labeled and the pattern of silver grains over the terminals will obscure the labeling of the cell bodies and account for the difficulty in detecting clusters of silver grains over abducens neurons in the center of the nucleus.

The ventral part of the rostral lv nucleus is known to send a strong projection to medial rectus motoneurons via the ascending tract of Deiters'.^{20,27,29} This pathway is part of the vestibulo-ocular (three-neuronal) arc. The medium-sized cells of this area are strongly labeled, leaving the large Deiters' neurons free of silver grains (FIGURE 4a). The rostral iMLF also has clearly labeled perikarya, bilaterally. This region is known to be a premotor structure involved in the generation of fast vertical eye movements;^{5,9,10,22,31,32} it projects directly onto the motoneuron subgroups of the vertical eye muscles and not to the medial rectus.^{6,13} As these vertical motor neuron subgroups are labeled with tetanus toxin, especially the trochlear nucleus, transsynaptic retrograde transport is expected to lead to neuronal labeling in the rostral iMLF. This was indeed the case, and labeling was strongest in experiment 79-206, in which the contralateral trochlear nucleus was most heavily involved.

There is anatomical evidence from this laboratory that the caudal ppH projects exclusively to the ipsilateral medial rectus motoneuron subgroups,⁶ and the present experiments support this result, since distinctly labeled neurons could be found in the caudal ppH region. Dorsolateral to the ppH, in the lateral

part of the mv, is another patch of silver grains covering perikarya. Cells in the mv are known to carry the posterior semicircular canal signal directly to the contralateral trochlear nucleus, while others send monosynaptic inhibitory projections into the ipsilateral abducens nucleus.^{1,25,27,29,30,39} Both these pathways could provide a source of tetanus toxin for the ipsilateral mv, and both are part of the vestibulo-ocular (three-neuronal) arc. The trochlear connection would carry more label, since the trochlear nucleus was more heavily labeled than was the ipsilateral abducens (FIGURE 3). The trochlear nucleus also receives a strong monosynaptic input from the sv of the same side.^{30,39} These cells in the central portion of the sv relay anterior semicircular canal inhibition to the trochlear motoneurons. Neurons in the ventral sv, contralateral to the injection site, are in fact strongly labeled with silver grains (FIGURE 1). Finally, the only other cell group containing labeled cell bodies is a small cluster in the medial part of the mv, contralateral to the injection site. Cells here are known to project to the abducens nucleus on the other side, which in this experiment was strongly labeled (FIGURE 3b).³⁸

The abducens internuclear pathway and the connections of the vestibulo-ocular (three-neuronal) arc are known to be powerful inputs to oculomotor neurons.^{26,38} The synaptic connectivity of the rostral iMLF and ppH to these cells has not been tested, but would be expected to be strong. Therefore, all the cell groups containing clearly labeled cell bodies have, as far as is known, strong projections to either medial rectus or superior oblique motoneurons, the two most heavily labeled primary targets of our experiments. For this reason it appears that tetanus toxin seems suitable as a transsynaptic retrograde tracer.

The diffuse patterns of silver grains are less easy to interpret. If a cell is retrogradely filled with tetanus toxin, then some labeling will be associated with the dendrites.¹⁸ In the autoradiogram, this will appear as a diffuse pattern of silver grains as shown in FIGURE 4b. Breakdown of the [¹²⁵I] tetanus toxin molecule followed by [¹²⁵I] diffusion is an additional possibility that should be considered. Structures that are only weakly labeled by retrograde transport may also appear diffusely covered with silver grains, for example the bilateral labeling of the y group (FIGURES 1 and 4d). The dorsal part of the y group, called the infracerebellar nucleus by Gacek,²¹ is labeled. It is known to carry saccule information to the oculomotor complex,^{23,27,28,49} and Gacek has demonstrated a bilateral y group input to the trochlear nucleus.²¹ The ventral portion, which receives the direct saccule input, is not significantly labeled. Diffuse silver grains may also be the result of anterograde transport, directly from the periphery, or subsequent to retrograde transport into the motoneurons. An example of the latter is possibly provided by the weak, diffuse deposits lying bilaterally close to the midline in the nrtp. A projection from the oculomotor nucleus to this area in the cat was described by Maciewicz and Spencer and Graybiel.^{24,34} The same group of cells receives an input from the superior colliculus and, in turn, projects to the cerebellar vermis. The projection from the oculomotor nucleus is described for the first time here in the monkey, and may serve as a criterion for the presence of, and for quantifying, retrograde-antegrade transport.

Diffuse patterns of silver grains were also found in the trigeminal complex and in the contralateral facial nucleus. The contralateral facial nucleus may be labeled via internuclear neurons of the ipsilateral facial nucleus, the latter being invaded by tetanus toxin spread into the orbicularis oculi muscle (see above). The diffuse labeling of the neurons of the trigeminal complex, Vp and Vs, could have been achieved by anterogradely transported toxin taken up by sensory receptor terminals within the orbit including those situated in the extrinsic eye muscles.³⁵ The diffuse deposits in the vestibular nuclei on both sides can be attributed to

several pathways interconnecting the nuclei with the oculomotor complex.^{29,30} (See also recent reviews of these pathways.)^{7,27,38}

It is surprising that only diffuse, and not individual neuron, labeling could be seen in the iC. Horseradish peroxidase has been shown to strongly label the contralateral iC after injections into the oculomotor nucleus,^{23,49} and the iC is assumed to exert an effective monosynaptic control on trochlear motoneurons.⁴⁶ The diffuse labeling in the dorsal division of the trochlear nucleus supplying the unoperated orbit (FIGURE 2a) is also an unexpected finding. It does not come from the periphery, since the trochlear nerve remained unlabeled (TABLE 2). Therefore, it may represent a central connection (as yet unknown). Finally, the bilateral labeling of the pretectal olivary nucleus is also diffuse. This nucleus is thought to be involved in the control of the pupillary light reflex by receiving a direct retinal input and projecting to the Edinger-Westphal nucleus.^{3,14,37,49} It is not clear at the moment as to which pathway was used by the tracer.

Transsynaptic retrograde labeling of neurons, as indicated by accumulations of silver grains over cell bodies, could be reliably found in areas known to send strong projections to the cell groups labeled by direct retrograde transport from the injection site.

In conclusion, these experiments using the oculomotor system as a model have shown that tetanus toxin is transported in a retrograde fashion not only directly but also transsynaptically in sufficient quantities to be detected at the light microscope level in the cell body of the second neuron.

ACKNOWLEDGMENTS

The authors are most grateful to A. Fähr, M. Stella, C. Dudli, and R. Bürki for their technical assistance, to D. Savini for photography, R. Emch for the drawings, and I. Roth for the preparation of the manuscript.

Prof. W. Horst kindly provided the facilities of the Department of Nuclear Medicine and Radiotherapy, University of Zürich, to label the tetanus toxin with [¹²⁵I].

REFERENCES

1. BAKER, R., N. MANO & H. SHIMAZU. 1969. Postsynaptic potentials in abducens motoneurons induced by vestibular stimulation. *Brain Res.* **15**: 577-580.
2. BAKER, R. & S. M. HIGHSTEIN. 1978. Vestibular projections to medial rectus subdivision of oculomotor nucleus. *J. Neurophysiol.* **41**: 1629-1646.
3. BENEVENTO, L. A., M. REZAK & R. SANTOS-ANDERSON. 1977. An autoradiographic study of the projections of the pretectum in the rhesus monkey (*Macaca mulatta*): evidence for sensorimotor links to the thalamus and oculomotor nuclei. *Brain Res.* **127**: 197-218.
4. BIZZINI, B., K. STOECKEL & M. E. SCHWAB. 1977. An antigenic polypeptide fragment isolated from tetanus toxin: chemical characterization, binding to gangliosides and retrograde axonal transport in various neuron systems. *J. Neurochem.* **28**: 529-542.
5. BÜTTNER-ENNEVER, J. A. 1977. Pathways from the pontine reticular formation to structures controlling horizontal and vertical eye movements in the monkey. *Dev. Neurosci.* **1**: 89-99.
6. BÜTTNER-ENNEVER, J. A. 1979. Organization of reticular projections onto oculomotor neurons. *Prog. Brain Res.* **50**: 619-630.
7. BÜTTNER-ENNEVER, J. A. Vestibular oculomotor organization. In *The Neural Control of Eye Movements*. A. F. Fuchs & W. Becker, Eds. Elsevier. Amsterdam, the Netherlands. (In press.)

8. BÜTTNER-ENNEVER, J. A. Anatomy of medial rectus subgroups in the oculomotor nucleus of the monkey. In *The Neural Control of Eye Movements*. A. F. Fuchs & W. Becker, Eds. Elsevier, Amsterdam, the Netherlands. (In press.)
9. BÜTTNER, U., J. A. BÜTTNER-ENNEVER & V. HENN. 1977. Vertical eye movement related unit activity in the rostral mesencephalic reticular formation of the alert monkey. *Brain Res.* **130**: 239-252.
10. BÜTTNER-ENNEVER, J. A. & U. BÜTTNER. 1978. A cell group associated with vertical eye movements in the rostral mesencephalic reticular formation of the monkey. *Brain Res.* **151**: 31-47.
11. BÜTTNER-ENNEVER, J. A. & K. AKERT. Medial rectus subgroups and their abducens internuclear input in the oculomotor nucleus of the monkey. *J. Comp. Neurol.* (In press.)
12. CARPENTER, M. B., R. E. MCMASTERS & G. R. HANNA. 1963. Disturbances of conjugate horizontal eye movements in the monkey. I. Physiological effects and anatomical degeneration from lesions of the abducens nucleus and nerve. *Arch. Neurol.* (Chicago) **8**: 231-247.
13. CARPENTER, M. B., J. W. HARBISON & P. PETER. 1970. Accessory oculomotor nuclei in the monkey: projections and effects of discrete lesions. *J. Comp. Neurol.* **140**: 131-154.
14. CARPENTER, M. B. & R. J. PIERSON. 1973. Pretectal region and the pupillary light reflex. An anatomical analysis in the monkey. *J. Comp. Neurol.* **149**: 271-300.
15. CARPENTER, M. B. & R. R. BATTON. 1980. Abducens internuclear neurons and their role in conjugate horizontal gaze. *J. Comp. Neurol.* **189**: 191-209.
16. CARROLL, P. T., D. L. PRICE, J. W. GRIFFIN & J. MORRIS. 1978. Tetanus toxin: immunocytochemical evidence for retrograde transport. *Neurosci. Lett.* **8**: 335-339.
17. DUMAS, M., M. E. SCHWAB, R. BAUMANN & H. THOENEN. 1979. Retrograde transport of tetanus toxin through a chain of two neurons. *Brain Res.* **165**: 354-357.
18. ERDMANN, G., H. WIEGAND & H. H. WELLHONER. 1975. Intraaxonal and extraaxonal transport of ¹²⁵I-tetanus toxin in early local tetanus. *Naunyn Schmiedeberg's Arch. Pharmacol.* **290**: 357-373.
19. FUSE, G. 1912. Ueber den Abduzenskern der Säuger. *Arch. Hirnanat. Inst. Univ. Zürich* **6**: 407-447. (Bergmann. Wiesbaden, Federal Republic of Germany.)
20. GACEK, R. R. 1971. Anatomical demonstration of the vestibulo-ocular projections in the cat. *Acta Otolaryngol.* (Stockh.) **293**: 1-63.
21. GACEK, R. R. 1979. Location of trochlear vestibulo-ocular neurons in the cat. *Exp. Neurol.* **66**: 692-706.
22. GRAYBIEL, A. M. 1977. Organization of oculomotor pathways in the cat and rhesus monkey. *Dev. Neurosci.* **1**: 79-88.
23. GRAYBIEL, A. M. & E. A. HARTWIEG. 1974. Some afferent connections of the oculomotor complex in the cat: an experimental study with tracer techniques. *Brain Res.* **81**: 543-551.
24. GRAYBIEL, A. M. 1977. Direct and indirect preoculomotor pathways of the brainstem: an autoradiographic study of the pontine reticular formation in the cat. *J. Comp. Neurol.* **175**: 37-78.
25. HIGHSTEIN, S. M. 1973. The organization of the vestibulo-oculomotor and trochlear reflex pathways in the rabbit. *Exp. Brain Res.* **17**: 285-300.
26. HIGHSTEIN, S. M. & R. BAKER. 1978. Excitatory termination of abducens internuclear neurons on medial rectus motoneurons: relationship to syndrome of internuclear ophthalmoplegia. *J. Neurophysiol.* **41**: 1647-1661.
27. HIGHSTEIN, S. M. & H. REISINE. 1979. Synaptic and functional organization of vestibulo-ocular reflex pathways. *Prog. Brain Res.* **50**: 431-442.
28. HWANG, J. C. & W. F. POON. 1975. An electrophysiological study of the saccule-ocular pathways in cats. *Jpn J. Physiol.* **25**: 241-251.
29. ITO, M., N. NISIMURA & M. YAMAMOTO. 1976. Pathways for the vestibulo-ocular reflex excitation arising from semicircular canals of rabbits. *Exp. Brain Res.* **24**: 257-271.
30. ITO, M., M. NISIMURA & M. YAMA. 1976. Postsynaptic inhibition of oculomotor neurons involved in vestibulo-ocular reflexes arising from semicircular canals of rabbits. *Exp. Brain Res.* **24**: 273-283.
31. KÖMPF, D. 1978. Verticale Augenbewegungen. *Nervenarzt* **49**: 377-384.

32. KING, W. M. & A. F. FUCHS. 1979. Reticular control of vertical saccadic eye movements by mesencephalic burst neurons. *J. Neurophysiol.* **42**: 861-876.
33. MACIEWICZ, R. J., C. R. S. KANEKO, S. M. HIGHSTEIN & R. BAKER. 1975. Morphological identification of interneurons in the oculomotor nucleus that project to the abducens nucleus of the cat. *Brain Res.* **96**: 60-65.
34. MACIEWICZ, R. J. & R. SPENCER. 1977. Oculomotor and abducens internuclear pathways in the cat. *Dev. Neurosci.* **1**: 99-108.
35. MANNI, E. & R. BORTOLAMI. 1979. Peripheral and central organization of the extraocular muscle proprioception in the ungulate. *Prog. Brain Res.* **50**: 291-299.
36. MESULAM, M. M. 1978. Tetramethyl benzidine for horseradish peroxidase neurochemistry: a non-carcinogenic blue reaction product with superior sensitivity for visualizing neural afferents and efferents. *J. Histochem. Cytochem.* **26**: 106-117.
37. PIERSON, R. J. & M. B. CARPENTER. 1974. Anatomical analysis of the pupillary reflex pathways in the rhesus monkey. *J. Comp. Neurol.* **158**: 121-144.
38. PRECHT, W. 1978. *Neuronal Operations in the Vestibular System*. Springer-Verlag, Berlin, Federal Republic of Germany.
39. PRECHT, W. & R. BAKER. 1972. Synaptic organization of the vestibulo-oculomotor pathway. *Exp. Brain Res.* **14**: 158-184.
40. PRICE, D. L., J. W. GRIFFIN, A. YOUNG, K. PECK & A. STOCKS. 1975. Tetanus toxin: direct evidence for retrograde intraaxonal transport. *Science* **188**: 945-947.
41. SCHWAB, M. E. & H. THOENEN. 1976. Electron microscopic evidence for a transsynaptic migration of tetanus toxin in spinal cord motoneurons: an autoradiographic and morphometric study. *Brain Res.* **105**: 213-227.
42. SCHWAB, M. E. & H. THOENEN. 1977. Selective transsynaptic migration of tetanus toxin after retrograde axonal transport in peripheral sympathetic nerves. A comparison with nerve growth factor. *Brain Res.* **122**: 459-474.
43. SCHWAB, M. E., Y. AGID, J. GLOWINSKI & H. THOENEN. 1977. Retrograde axonal transport of ¹²⁵I-tetanus toxin as a tool for tracing fiber connections in the central nervous system: connections of the rostral part of the rat neostriatum. *Brain Res.* **126**: 211-224.
44. SCHWAB, M. E. & H. THOENEN. 1978. Selective binding, uptake and retrograde transport of tetanus toxin by nerve terminals in the rat iris. An electron microscopic study using colloidal gold as a tracer. *J. Cell Biol.* **77**: 1-13.
45. SCHWAB, M. E., K. SUDA & H. THOENEN. 1979. Selective retrograde transsynaptic transfer of a protein tetanus toxin, subsequent to its retrograde axonal transport. *J. Cell Biol.* **82**: 798-810.
46. SCHWINDT, P. C., W. PRECHT & A. RICHTER. 1974. Monosynaptic excitatory and inhibitory pathways from medial midbrain nuclei to trochlear motoneurons. *Exp. Brain Res.* **20**: 223-238.
47. SHANTA, T. R., S. L. MANOCHA & G. H. BOURNE. 1968. *A Stereotaxic Atlas of the Java Monkey Brain*. Karger, Basel, Switzerland.
48. SPENCER, R. & J. D. PORTER. Phylogenetic changes in the innervation and structure of monkey extraocular muscles. *J. Comp. Neurol.* (Submitted for publication.)
49. STEIGER, H. J. & J. A. BÜTTNER-ENNEVER. 1979. Oculomotor nucleus afferents in the monkey demonstrated with horseradish peroxidase. *Brain Res.* **160**: 1-15.
50. STÖCKEL, K., U. PARAVICINI & H. THOENEN. 1974. Specificity of the retrograde axonal transport of nerve growth factor. *Brain Res.* **76**: 413-421.
51. STÖCKEL, K., M. E. SCHWAB & H. THOENEN. 1975. Comparison between the retrograde axonal transport of nerve growth factor and tetanus toxin in motor, sensory and adrenergic neurons. *Brain Res.* **99**: 1-16.
52. SZENTAGOTHAI, J. 1948. The representation of facial and scalp muscles in the facial nucleus. *J. Comp. Neurol.* **88**: 207-220.
53. TSUCHIDA, U. 1906. Ueber die Ursprungskerne der Augenbewegungsnerven und über die mit diesen in Beziehung stehenden Bahnen im Mittel- und Zwischenhirn. *Arch. Hirnanat. Inst. Zürich* **2**: 1-205. (Bergmann, Wiesbaden, Federal Republic of Germany.)

APPENDIX
ABBREVIATIONS

III	oculomotor nucleus
IV	trochlear nucleus
Vm	motor trigeminal nucleus
Vmes	mesencephalic trigeminal nucleus
Vp	principal sensory trigeminal nucleus
Vs	spinal trigeminal nucleus
VI	abducens nucleus
VII	facial nucleus
N III	oculomotor nerve
N IV	trochlear nerve
N VI	abducens nerve
N VII	facial nerve
am	anteromedian nucleus
BC	brachium conjunctivum
BP	brachium pontis
ccn	central caudal nucleus
cm	centromedian nucleus
dn	dentate nucleus
F	H fields of Forel
Hb	habenula complex
iC	interstitial nucleus of Cajal
io	inferior olive
lv	lateral vestibular nucleus (Deiters')
md	nucleus medialis dorsalis thalami
MLF	medial longitudinal fasciculus
mv	medial vestibular nucleus
nD	nucleus of Darkschewitsch
nrp	nucleus reticularis parvocellularis
nrpo	nucleus reticularis pontis oralis
nrtpt	nucleus reticularis tegmenti pontis
on	olivary nucleus of the pretectum
PC	posterior commissure
pg	periaqueductal gray
ppH	nucleus prepositus hypoglossi
pu	pulvinar
RB	restiform body
riMLF	rostral interstitial nucleus of the MLF
rl	nucleus reticularis lateralis
rn	red nucleus
sc	superior colliculus
sn	substantia nigra
so	superior olive
spv	spinal vestibular nucleus
sr	superior rectus division of III
st	subthalamic nucleus
sv	superior vestibular nucleus
TR	tractus retroflexus
TS	tractus solitarius
VPL	nucleus ventralis posterior lateralis
y	y group
zi	zona incerta

SOME THOUGHTS ABOUT THE THREE NEURONS IN THE VESTIBULAR OCULAR REFLEX*

R. Baker, C. Evinger, and R. A. McCrea

*Department of Physiology and Biophysics
New York University Medical Center
New York, New York 10016*

The three-neuron arc envisioned by Lorente de Nó (1933) and popularized by Szentagothai (1943, 1950) has generated considerable scientific interest because of the apparent simplicity with which it produces compensatory eye movement following head rotation.^{46,70,71} The reciprocal organization of inhibitory and excitatory second-order vestibular neurons has offered a structural basis that adequately explains visual stabilization by coordinating the activity of agonist-antagonist extraocular motoneurons. Several years ago, however, Robinson pointed to a number of problems in signal processing intrinsic to translating discharge rate on the three neurons in the vestibular ocular reflex (VOR) into muscle active-state tension.^{61,62} This paper traces the development of conceptual and experimental findings, with emphasis on recent understanding of the neural signals recorded on each of the three neurons in the VOR.

Although few new data are presented, a few significant insights are offered by this exercise. First, many of the recent data on neural signals in respect to information coding via discharge rate during the VOR in cat are presented, and can be compared to that in the primate. In so doing, we find that central VOR organization in the two species is very similar and suggest that neural processing may be essentially the same. Second, it is argued that understanding the three-neuron VOR pathway has important implications for studying the central organization of other oculomotor subsystems (e.g., saccadic and pursuit) but, most relevantly, provides information concerning fixation (e.g., eye position). Third, some of the difficulties in modeling the VOR with neurons reflecting population (i.e., mean) values are discussed. The wide range of unique physiological sensitivities extending from sensory to motor periphery argues for tuned channels responding selectively throughout the oculomotor range to specific frequencies of head movement. Finally, morphological evidence pointing to the location of the integrator is suggested. This review begins by presenting the ideas underlying the type of information to be coded at the final common pathway—the motoneuron.

THE VOR IN OPERATION

The purpose of the VOR is to maintain stable vision by rotating the eye in the head with exactly the same time course, but in the opposite direction, as head movement. Robinson (1975) first described the neural signals needed to create this movement.^{61,62} Since head acceleration (\ddot{H}) is the second derivative of head position (H) and the former stimulates the semicircular canals, then from the

*These thoughts were supported by United States Public Health Service Grants No. NS 13742 from the NINCDS and EY-02007 from the NEI.

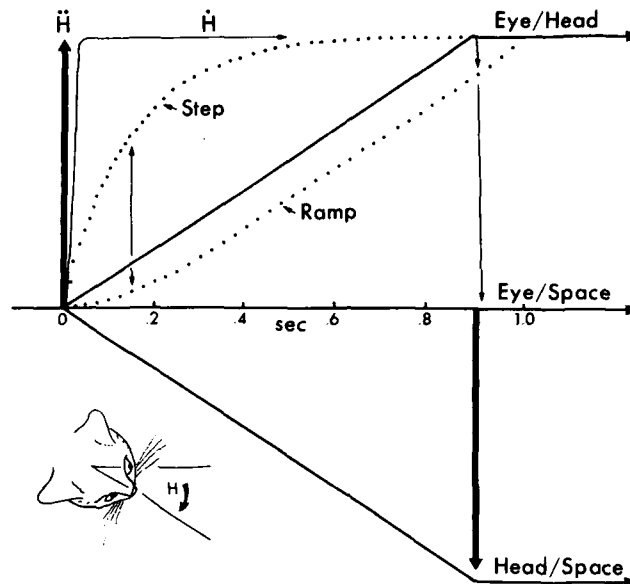


FIGURE 1. Signal processing in the vestibulo-ocular reflex. Step displacement of the head as illustrated in the lower left produces a change in head position (H), with the overall effect of altering its angle in respect to space. This movement produces a pulse of head acceleration (\ddot{H}), which is signaled as a step of head velocity (\dot{H}). The \dot{H} signal (i.e., frequency) on first- and second-order vestibular neurons would also be described by a similar waveform. The step and ramp functions were calculated assuming an orbital time constant of 0.15 seconds.²¹ Combining $0.15 \, d\theta/dt$ with θ produces the compensatory eye motion depicted as eye in respect to head. The net result is stabilization of the eye in respect to space. The downward directed arrow indicates the 0.15-second delay before the ramp signal approaches eye velocity.

standpoint of neural processing, the purpose of the VOR is to recover the latter signal. The compensatory eye movement in response to a pulse of head acceleration is a smooth, constant-velocity motion in the opposite direction, but due to oculomotor plant dynamics, a step change in motoneuron activity would produce an eye movement exponentially approaching a new position (FIGURE 1). Given the orbital time constant to be roughly 0.15 seconds in the cat,²¹ then the movement would last for about 0.5 seconds; but if this signal were transferred as such through the three-neuron VOR, then within 0.15 seconds the eye would begin to be in phase with head velocity (\dot{H}), which clearly would not be compensatory to the change in head position. If the increase in firing rate were in the form of a ramp, then a pursuitlike movement would be produced that exponentially approached a constant velocity but in which the amplitude was less than that of the head movement.⁶¹ Thus, it is clear that to make the eye change rapidly in the VOR, the step must be combined with the ramp and the neural signals must be proportional to both eye position (E) and eye velocity (\dot{E}).⁶² Therefore, it is important to know whether primary and secondary vestibular neurons provide extraocular motoneurons with the combined signal and, if so, how the cat and monkey compare in this respect.

Historically it is important to note that Skavenski and Robinson (1973) pointed out that the above algorithm combining E and \dot{E} works relatively well for

combinations of all eye movements, irrespective of whether \dot{E} is produced by either vestibular (\dot{E}_v), pursuit (\dot{E}_p), or saccadic (\dot{E}_s) pathways.⁶⁸ In the case of the VOR, a command proportional to desired eye velocity could in fact be obtained directly from second-order vestibular connections ($\dot{H} \approx \dot{E}$), and this transformation was never questioned. However, the additional phase lag necessary to produce eye position was postulated to occur via a polynuclear network consisting of reverberating collaterals (Lorente de N6, 1933)⁴⁶ in the pontine reticular formations (see Reference 60, page 521, Figure 2). The separation into parallel pathways had often been argued for because of its analytical convenience,^{42,68} even though evidence began to appear that second-order vestibular neurons were modulated during all phases of nystagmus.^{3,31,47} More recently, the eye-movement-related behavior of the horizontal and vertical VOR neurons in the alert cat and the "presumed" second-order vertical vestibular neurons in the

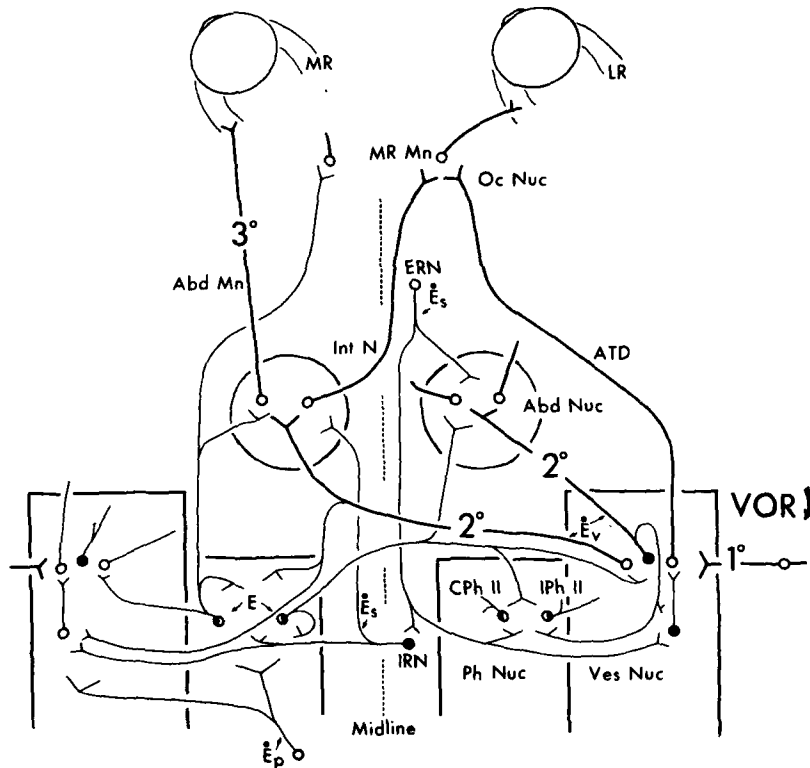


FIGURE 2. Schematic diagram illustrating neurons involved in production of the vestibulo-ocular reflex. The three neurons in the VOR expected to be active during a head movement to the right are shown by heavy lines. Most abbreviations are similar to those utilized in the text. Others are: IPh II and CPh II are ipsi- and contralateral projecting prepositus neurons. ERN and IRN are inhibitory and excitatory reticular neurons. \dot{E}_p , \dot{E}_s , and \dot{E}_v are pursuit, saccadic, and vestibular velocity signals, respectively. In every case, only one set of connections is illustrated. Since many of these pathways are indeed schematic and/or incomplete, original papers mentioned in the text should be consulted before adopting them for other purposes. Filled and open neurons are inhibitory and excitatory, respectively.

primate have been studied well enough so that the reciprocal inhibitory and excitatory second-order vestibular projections to horizontal extraocular motoneurons may be utilized as examples for discussing VOR operation (FIGURE 2).^{5,41,49,50,56,73,75}

MOTONEURONS AND MOTOR UNITS

Logically it is not possible to evaluate the types of information encoded on first- and second-order vestibular neurons without recourse to the hypothesis that motoneuronal discharge is directly translated into muscle active-state tension, which itself creates the eye movement.¹⁰ Based upon records from extraocular motoneurons, Robinson suggested a descriptive equation in which firing rate was correlated to eye position and velocity by a first-order differential equation:⁵⁹

$$R = k(\theta - \theta_i) + r d\theta/dt \quad (1)$$

where R was motoneuron discharge rate, θ was eye position, $d\theta/dt$ was eye velocity, k and r were slopes of the rate position and velocity relationship, respectively, and θ_i was the intercept of the rate-position plot (i.e., threshold; see FIGURE 3).

Subsequent studies indicated that motoneurons could be characterized by unique values of θ_i , k , and r , which is useful for comparing data between the cat and monkey.^{20,21,27,39,40,63,68} These values have important implications because they provide a means to estimate the neural output to the orbital mechanics.^{37,39} The relationship between the net muscle force (i.e., active-state tension) and globe rotation had also been approximated by a similar first-order differential equation, which assumed that the mechanical impedance of the eye and its attachments consisted mainly of elastic and viscous elements that could be approximated by a single elasticity in the form:⁵⁹

$$F = \chi\theta + \rho d\theta/dt \quad (2)$$

Essentially χ and ρ have been substituted by K and R , representing elastic and viscous coefficients whose ratio R over K reflects the time constant of the mechanical load. The latter is envisioned to be constant. The above equation is only useful as an approximation because fourth-order, and even higher, linear differential equations (even nonlinear) are necessary to model the mechanical impedance of the eye.^{37,59,68} This cautionary concession is important because a distinctive feature of extraocular organization is the wide range in mechanical properties of individual muscle fibers with, of course, subsequent inference as to innervation by motoneurons with suitably matching proportionality constants (r/k).

The maximum tetanic tension of different motor units, as well as their fusion frequencies, varies by more than an order of magnitude.^{10,11,23,37,42} In light of variable levels of thresholds for recruitment (θ_i) and the remarkable sensitivity of muscle fibers to frequency potentiation, it is clear that total muscle force is always, in part, a function of both the number of motoneurons firing and their individual rate. Thus, nearly any attempt with present-day approaches to show a highly ordered relationship between muscle force and individual motoneuron discharge rate definitely would be nonlinear. This conclusion is apparent from the observation that about 10% of extraocular motoneurons generate more than 25% of the maximum muscle tension.³⁷ The above ideas are important factors in

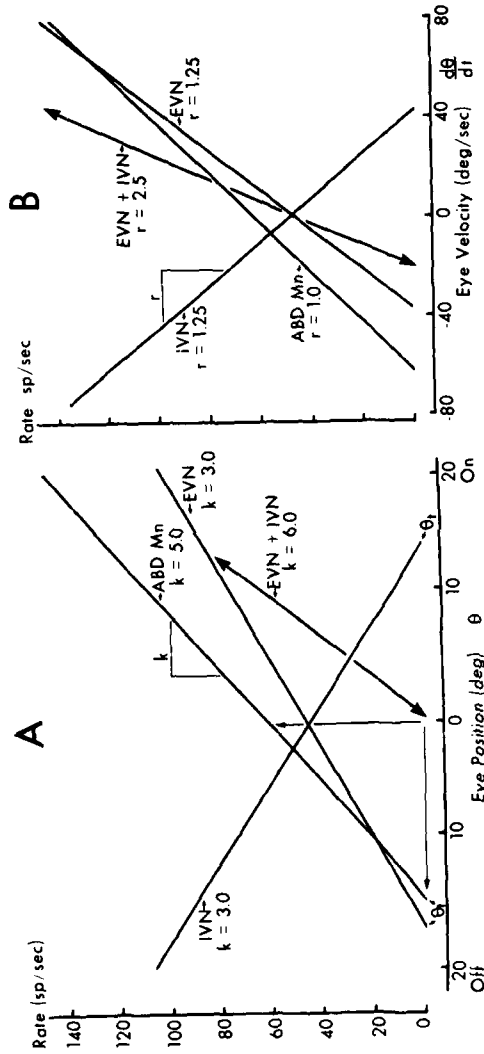


FIGURE 3. Rate position and velocity diagrams for vestibular neurons and motoneurons. A: rate-position plots with k values employed in the text are shown for inhibitory (INN) and excitatory (EVN) vestibular neurons including Abd Mns. The plot for EVN + IVN is indicated to pass through the center of gaze. Remember that it reflects the combined synaptic effect on the target motoneuron. The two arrows pointing to the plot of the Abd Mn [i.e., from threshold (θ_1) to 60 spikes/second] indicate the range over which additional position signals may be required. B: rate-velocity curves for the same neurons shown in A in which the proportionality constants (r) are the same as those discussed in the text. The EVN + IVN plot reflects combined velocity sensitivity on target Abd Mns.

determining the point-to-point causal relationships between first- and second-order vestibular neurons and motoneurons.

Robinson has argued that if motoneuron discharge rate is directly translated into muscle force, then the position and velocity proportionality constants (k and r in Equation 1) should have nearly the same ratio as the comparable parameters for the force equation (K and R in Equation 2) in order to approximate the time constant of the mechanical load.⁵⁹ In the primate, k ranged from 1.1 to 14.5 spikes/second per degree with a mean of 4.0 spikes/second per degree.^{37,59,63,68} The value of r determined with sinusoidally induced eye movement in the VOR ranged from 0.25–5.0 spikes/second per degree/second, with a peak near 0.6 spike/second per degree/second.⁶³ Although r and k ranged over a magnitude, the average ratio was 4/1. Depending on number selection, the mean time constants ranged from 0.15 to 0.25 seconds.^{37,59,63,68} Another way to calculate the time constant is to measure the phase lag between eye position and motoneuron discharge during sinusoidal eye movement. Since eye movement is described by $\theta = \sin \omega t$, the latter may be substituted in Equation 1 so that the phase lag between eye position and discharge rate is equivalent to $\tau = \text{tangent}^{-1}(\omega T)$, where ω is frequency in radians, T is time, and τ is the time constant. Since $\tau = r/k$, a more convenient way to write the equation is:

$$\frac{r}{k} = \frac{\tan \theta}{2\pi F} \quad (3)$$

By employing the calculated value for the velocity proportionality constant (r) in the primate, τ was found to be 0.2 seconds, suggesting both methods for its approximation to be reasonably comparable. In identified cat motoneurons, k was found to range between 1.8–9.9 spikes/second per degree, with a mean of 5.3 spikes/second per degree.²¹ The value of r determined with saccadic eye movement ranged from 0.63–1.23 spikes/second per degree/second, yielding a mean time constant of 0.16 second. The time constant calculated from phase lag during sinusoidal vestibular VOR was 0.142 second.²¹ Thus, the ratio of orbital time constants in the cat vs. the primate as determined (a) by sinusoidal responses is 140 vs. 200 mseconds and (b) by the step responses to electrical stimulation of the nerve is 45 vs. 68 mseconds.^{21,56} The nearly three to one difference in both species indicates that larger, higher-tension motor units need to be weighted more heavily in calculation of the overall (i.e., population) neuronal time constants (see References 21 and 37).

A priori, one might have envisioned that the findings showing that motoneurons and motor units were not quantitatively a homogeneous population coupled with the vast range in their morphological and electrophysiological architecture, added to the disparity in neural vs. mechanical time constants, would argue conclusively for motoneuronal channels as being "highly tuned" conduits of specific types of eye movements.^{4,11,25,28,42,70} In fact, early studies reasonably expected the diversity of eye position and velocity sensitivities to be correlated with discharge pattern wherein the neuronal time constants might be logically correlated to motor unit characteristics.^{63,68} Yet every study in the monkey failed to find such relationships (cf., Reference 27). All neurons in the extraocular motor nuclei appeared to participate in all types of eye-movement-related behavior, extending from "tonic" during fixation to "phasic" during saccades. Thus, the overall thrust of most arguments has been to deny the long-standing hypothesis for separate (i.e., discontinuous) populations of "tonic" and "phasic" motoneurons that might be correlated specifically with slower (i.e., vergence) and faster (i.e., saccadic) eye movements. On the other hand, the above assertion simply

may be *too encompassing*, especially in view of recent work on primary and secondary vestibular neurons, including motoneurons and motor units. The ability to match neuronal time constants with appropriate motor units in the primate may have failed because of the latter's extensive oculomotor range, containing a large number of intermediate- and low-threshold units responding during all types of eye movements *rather than* the absence of such relationships. The cat's limited oculomotor range and broad range for motoneuronal recruitment threshold as well as velocity sensitivity before saturation should offer a better opportunity to resolve this question.²¹ Tonic motoneuronal discharge exists throughout the oculomotor range in both species. Even in the three neurons of the VOR, it would be important to weight recruitment from the multiply to the singly innervated fibers such that both the motoneuronal and vestibular neuron time constants would reflect a continuous function of recruitment and/or frequency potentiation into the ongoing compensatory eye movement. The strength of the above suggestion is that it would not interfere with use of any prior data from either the monkey or the cat as long as they were obtained in a defined state of alertness (see later discussion).

The above points serve to reemphasize the use Robinson really wanted to make of the neural time constant ratio, namely, to suggest that variation in r and k at the motoneuronal level indicated separate prenuclear structures to be involved with each type of eye movement.⁵⁹ For example, the range of variation in r for pursuit vs. vestibular eye movement indicated that cells with the same values for position could have quite different velocity parameters. This suggested that one prenuclear structure might generate the command concerned with fixation (position), and another with velocity (e.g., in the VOR). It also led to subsequent studies of other velocity command sources (i.e., pursuit, vergence, saccades, etc.), which themselves produced unique proportionality values (r and k) for motoneurons. Most important, the work emphasized for the first time that "fixation" was an active process, as much so as movement, and in fact that generation of eye position (i.e., k) might be via a separate neural control system independent of any other.⁶² Locating the central neural circuit(s) underlying eye position is therefore an important undertaking.

The finding that each motoneuron and vestibular neuron may be described by a unique set of response properties (r and k) suggests that each preferentially responds to or in conjunction with certain types of eye movement. To be specific for the VOR, this implies that each cell of the three-neuron arc may be tuned to the speed of head movement, thereby providing a continuum of information from low to high frequency. The evidence to date suggests that this "uniqueness" in respect to head velocity (i.e., r) may not be averaged out by synaptic convergence in the three-neuron VOR. Certainly the fixation signal (i.e., eye position, k) appears to be distributed in a ubiquitous, but ordered, fashion on each of the final two stages of the three-neuron VOR. In spite of our general feeling that use of averaged proportionality constants is not the best way to model the three-neuron VOR, they essentially may not be incorrect and, in fact, may offer some further insight to remaining problems. In that spirit—

PRIMARY AFFERENT VESTIBULAR NEURONS

Two measures of vestibular semicircular canal afferent activity are resting discharge rate and sensitivity to head acceleration. In primates, the average rate was found to be equivalent to 90 spikes/second and the mean sensitivity to head acceleration was 2.24 spikes/second per degree/second² (throughout the

frequency range of 0.03–1 Hz).^{18,22} Dividing the population value for constant acceleration by the effective time constant of the cupula (5.7 seconds) yielded an average sensitivity to head velocity of 0.39 spike/second per degree/second. Thus, primate vestibular afferent discharge (PVR_p) may be described by:

$$PVR_p = 90 \text{ spikes/second} - 0.4 \text{ spike/second per degree/second } \dot{H}$$

where \dot{H} equals head velocity and the minus sign indicates coordinates chosen so that the eyes move in the opposite direction to the head.⁵⁶

In the cat, the average vestibular firing rate was about 60 spikes/second;^{1,7,15,17,67,69} and this value is close to that in the alert cat.⁷ The acceleration sensitivity of canal afferents ranged from 0.11–5.6 spikes/second per degree/second², and the canal cupular time constant between 3.0 and 4.9 seconds.^{1,6,17,51,67,69} A mean acceleration sensitivity of 1.8 spikes/second per degree/second and a mean time constant of 4.0 seconds may be calculated, thereby describing the cat primary afferent discharge rate (PVR_c) as:

$$PVR_c = 60 \text{ spikes/second} - 0.4 \text{ spike/second per degree/second } \dot{H}$$

Thus, all recent work argues that cat primary vestibular neurons are very similar to those in the primate, including such features as high-frequency enhancement and phase lead. Most significantly, the distribution and mean values for sensitivity and phase were nearly the same regardless of the animals' state of alertness. This invariant feature makes the conversion of \dot{H} from first- to second-order vestibular neurons one of the easiest to address. However, of specific relevance to the earlier ideas regarding motoneuronal time constants is the recent finding on cat primary vestibular afferents suggesting them to be tuned to respond maximally to certain head movements.^{69,74} Afferents innervating different portions of the crista have different dynamic properties, as shown by use of wide-band stimuli and subsequent estimation of the system transfer function, where it was concluded that use of an average transfer function was an oversimplification.⁶⁹ Clearly the sensitivity, dominant time constant, and resting discharge rate are three important properties of every canal afferent that determines the cells behavior under a variety of conditions (see Figure 6 in Reference 69). Nearly every study of second-order vestibular neurons suggests that between-cell differences do not appear to be averaged out by convergence of primary vestibular afferents with different characteristics.^{5,8,19,38,52,57,65,67,75}

SECONDARY VESTIBULAR NEURONS

Traditionally, both anesthetized and alert cats and primates have been studied, and population values from nonidentified neurons in the vestibular nucleus have given expected wide-ranging values. Even so, Fuchs and Kimm, in an interesting comparison of the *cat* and *monkey* vestibular nuclei neurons, concluded that there was little difference in respect to *gain* (average values were 0.76 spike/second per degree/second in the frequency range of 0.25–1.5 Hz versus 0.53 spike/second per degree/second in the range of 0.5–0.93 Hz) and *phase* (78.6° and 77.20°).¹⁹ The only notable finding was a lower spontaneous firing rate in the absence of vestibular stimulation, where cat neurons responded around 20 spikes/second yet the primate was always in excess of 70 spikes/second.^{52,65,67} These numbers became more specific for the VOR when Pola and Robinson and King et al. utilized values recorded from axons of presumed

second-order vestibular neurons located in the medial longitudinal fasciculus (MLF) of alert primates.^{41,56} In this case, the average discharge rate was an even higher 130 spikes/second (at central gaze position) and \dot{H} sensitivity during the VOR was found to be nearly 0.98 spike/second per degree/second. Combined with an eye position (E) sensitivity of 2.5 spikes/second per degree, second-order vestibular neuron rate (SVR_p) could be described by:

$$SVR_p = 130 \text{ spikes/second} + 2.5 \text{ spikes/second per degree } E \\ - 0.98 \text{ spike/second per degree/second } \dot{H}$$

In the cat, based upon records from axons of identified second-order vestibular neurons in the MLF, the mean resting discharge rate was found to be 45 spikes/second.^{5,49,75} Eye position values ranged from 1.0–9.0 spikes/second per degree, and the population value equaled 3.0 spikes/second per degree. In the alert cat, \dot{H} was estimated for identified VOR neurons (Equation 3 and measurements), and values ranged from 0.5–4.0 spikes/second per degree/second, with a population mean of 1.25 \dot{H} . Thus, cat second-order vestibular neuron discharge (SVR_c) may be described by:

$$SVR_c = 45 \text{ spikes/second} + 3.0 \text{ spikes/second per degree } E \\ - 1.25 \text{ spikes/second per degree/second } \dot{H}$$

The first notable point is that \dot{H} sensitivity is nearly doubled in both the cat and primate from the first- to second-order vestibular neuron in either the alert or anesthetized animal. In the latter respect, \dot{H} has been often calculated on cat second-order neurons, and the range of 0.3–3.0 spikes/second per degree/second is quite comparable to the alert cat values.^{21,38,52,65,67} Secondly, most prior views have assumed the increase of \dot{H} sensitivity to be due to vestibular commissural inhibition, in spite of the high synaptic efficacy between first- and second-order vestibular neurons.^{35,57,64} The only direct commissural vestibular connection in the cat horizontal VOR appears to be on the excitatory vestibular pathway projecting via the ascending tract of Deiters' (ATD) to medial rectus motoneurons.^{29,34} Undoubtedly, in the alert cat and other preparations (e.g., References 3, 47, 66, and 67), there is an inhibitory interaction between VOR neurons, but whether it really is "vestibular sensitivity" (i.e., \dot{H}) or an action through indirect pathways (e.g., via the Ph integrator) is not known. The more parsimonious assumption is that mean (not range of) \dot{H} is larger on second-order VOR neurons because of the synaptic arrangement between first- and second-order neurons. This argument indirectly supports highly tuned synaptic convergence between primary and second-order VOR neurons.

In the primate, an average smooth pursuit sensitivity (\dot{E}_p) of 0.5 spike/second per degree/second was also found on MLF fibers,^{56,72} thereby clearly indicating (as suggested earlier by Robinson)⁵⁹ that the same prenuclear neurons could carry one velocity signal for pursuit and another for vestibular but that in both cases the proportionality constants for eye position were the same. Qualitatively, \dot{E}_p has been shown on identified cat second-order vestibular neurons, but as yet no reliable values have been calculated to compare it with \dot{E}_p . Since primate MLF neurons paused for saccades in both directions, the saccadic velocity (\dot{E}_s) signal was (–) and 1.0 spike/second per degree/second. However, cat VOR neurons only pause for saccades in the off direction and often exhibit a weak velocity sensitivity in the on direction for both horizontal and vertical VOR.^{5,49,75} Thus, in both species there are clearly separate pathways from the reticular formation for \dot{E}_v to be superimposed on second-order VOR neurons.^{32,76} The various combinations of the above eye velocity signals (\dot{E}_v , \dot{E}_p , and \dot{E}_s) on identified cat vestibular

and abducens motoneurons are well summarized in Berthoz et al. and Goldberg.^{5,21}

Vestibular neuron position sensitivity (E) can and does vary with the state of alertness, yet the \dot{H} signal is relatively invariant. A decrease in k is equivalent to reducing the stiffness of the oculomotor plant, which undoubtedly shifts the eye away from perfect compensation during vestibular stimulation.¹⁰ In fact, it has been noticed in the drowsy cats and monkeys that as sensitivity to eye position decreases, sinusoidal head rotation creates a strong change in the phase (i.e., a lead) of neuronal discharge relative to head acceleration.^{5,8,14,21} This effect is illustrated by comparison of data from the alert cat (References 5, 21, 49, and 75 and unpublished data) with that described in the decerebrate,⁶⁷ in which the neural and mechanical orbital time constants differed by an order of magnitude yet the population values for \dot{H} on first- and second-order and motoneurons in the VOR were nearly the same. In view of the fact that velocity sensitivity (r) appears to be less dependent on the behavioral state, then active muscle-force tension generated in the plant from contributing motoneurons becomes a function of averaging the wide-ranging, but unique, time constants. Given that r and k for cat vestibular and motoneurons range over an order of magnitude $[(10-12)/1]$, it may be argued that the oculomotor system spring constant is an important feature compensated for centrally with neural signals *strategically placed on both classes of neurons* for that precise purpose. In fact, Goldberg has pointed out that the limited oculomotor range in cats and their capacity to generate a larger stiffness in peripheral musculature imply that their oculomotor plant is capable of responding faster to step changes in both innervational input and sinusoidal than that of the monkey, even though cats' eye movements are generally slower.²¹ Others have recently commented on the state dependency of eye movements,^{9,12,13,16,21} with the reasonable extrapolation now being that to understand *normal operations of the VOR*, it must be studied in the alert, intact animal because of the strong dependence of the eye position signal on central processing. The importance of this idea can be visualized in another fashion by considering the contributions of second-order vestibular neurons to the phase of eye movement, which, secondarily, offers the advantage of pointing out some structural features of the "integrator." By contending nothing more than that the vestibular neuron and its associated position signal reflect an output of the integrator, it is possible to construct a Bode plot like that shown in FIGURE 4. The numerical values arise from picking appropriate r , k , and θ values for elements in the cat VOR throughout the frequency range of 0.01 to 10 Hz and inserting them in Equation 3. It is possible to conclude from this figure that nearly all the necessary phase shift, including that of the more than 90° required at low frequencies (0.01-0.1 Hz), could in fact be produced by the straightforward logical progression of signals from the semicircular canal end organ to the motor unit. In view of the above features of the three neurons in the VOR, it now is possible to inquire about other implications for normal VOR operation.

To this point, the proportionality constants for the three VOR neurons have been used to illustrate the point-to-point average neural conversion. As is clear from preceding discussion, this exercise may be misleading unless it eventually falls into agreement with morphological data. Some immediate advantages and limitations may be drawn by comparing the descriptive equations for cat horizontal second-order vestibular neurons and motoneurons:²¹

$$\begin{aligned} \text{SVNR}_c &= 45 \text{ spikes/second} + 3.0 \text{ spikes/second per degree } E \\ &\quad - 1.25 \text{ spikes/second per degree/second } \dot{H} \end{aligned}$$

$$\text{Abd Mn}_c = 60 \text{ spikes/second} + 5.0 \text{ spikes/second per degree } E \\ + 1.0 \text{ spike/second per degree/second } \dot{E}$$

The range of position (E) values on cat vestibular neurons (k , 1-9.9 spikes/second per degree) could be significant both in respect to phase and gain of the signal provided at the motoneuron, depending of course on the spatial-temporal convergence pattern in which the number of synaptic possibilities is likely only limited by adherence to the tuned filter concept. A straightforward literal

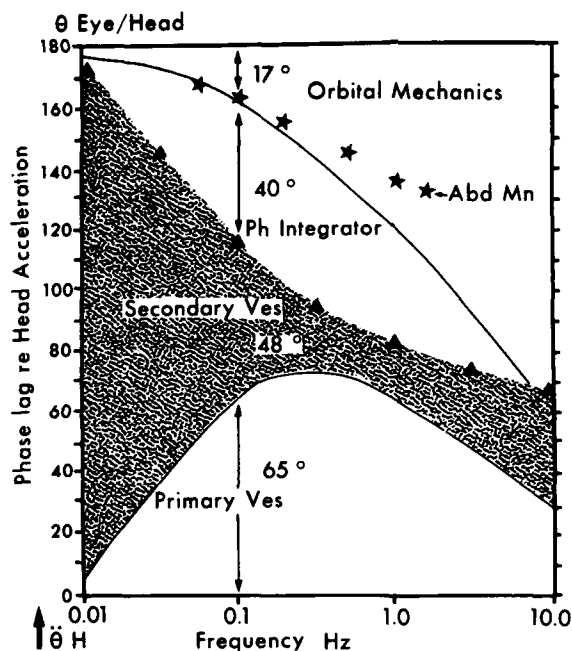


FIGURE 4. Bode diagram summarizing the phase shifts with respect to head position of identifiable elements in the VOR, beginning with primary vestibular and extending to orbital mechanics (dynamics of extraocular muscle, motoneurons, etc.) for frequencies of sinusoidal head rotations from 0.01-10 Hz. The bottom horizontal line $\ddot{\theta}_H$ is head acceleration, which leads the head position by 180° (the top line). Therefore, moving from the bottom to the top of this graph shows a phase lag. The values for primary vestibular afferents and orbital mechanics are direct from Reference 68, but they have been redrawn slightly differently. The shaded area is the phase lag contributed by secondary vestibular neurons. It was calculated from Equation 3, assuming constant r values of 1.0 spike/second per degree/second and k values ranging from 1-8 spikes/second per degree. The filled triangles represent the upper limit (i.e., $k = 8$) for a lag contributed by this vestibular element. The difference between secondary vestibular neurons and orbital mechanics is labeled Ph Integrator. It is the phase that remains to be contributed by an additional integration in central neural processing. The relative phase lags from each of the elements are indicated at 0.1 Hz because the latter is a representative frequency as well as the point where the largest additional position signal is required. The stars represent calculated values of Abd Mns in the cat from Reference 21 and suggest that phase lag contributed from orbital mechanics is less in the cat than in the primate. Note that since the cat VOR (References 21 and 13) exhibits a 3-5° phase lead to head position throughout the above frequency range, the lag in orbital mechanics is further reduced.

translation (i.e., spike for spike) from one level to another without reference to correlative morphological or topographical organization is illogical,⁶⁸ because by itself it would lead to the conclusion that the neural signals (i.e., gain) on vestibular neurons are probably sufficient to drive motoneurons. This synaptic arrangement could become quite generous because reciprocal vestibular pathways (medial rectus excluded) drive motoneurons in a push-pull fashion, so both H and E are effectively doubled, which results in:

$$\begin{aligned} \text{EVN} - (-\text{IVN}) \rightarrow \text{Abd Mn}_c &= 60 \text{ spikes/second} \\ &+ 6.0 \text{ spikes/second per degree } E \\ &- 2.5 \text{ spikes/second per degree/second } \dot{H} \end{aligned}$$

The argument in respect to doubling \dot{H} at individual motoneuronal levels is really applicable throughout the oculomotor range; however, intuitively there are limitations in respect to E . There seemingly is no way to avoid a balance or a null point for vestibular inhibitory-excitatory interaction very close to the center of fixation (see FIGURE 3). Irrespective of the synaptic arrangement, there will always be a fixation point where vestibular inhibition offsets excitation and a zero position signal (i.e., 0.0 E) results. The sharpness and range of θ_i for such effects are unknown, and any null-point argument need not be extended until the distribution of vestibular inputs (with unique r and k proportionality constants) is correlated with equally well identified postsynaptic targets. Yet the above observation is important because it implies that another afferent source imparts E in a continuous and/or graded fashion, but maybe not equally well throughout the entire oculomotor range (?). Secondly, since most rate-position curves for vestibular neurons intersect near central fixation (around 0°), where the vast majority of motoneurons still require a significant E signal, then their role appears to be directed toward production of eccentric fixation angles (i.e., laterality). Fortunately, it is possible to conclude that second-order vestibular neurons in respect to \dot{H} sensitivity are utilized exactly as expected (i.e., in a continuous and increasingly sensitive fashion throughout a wider part of the oculomotor range). To establish any realistic transfer function between first- and second-order vestibular and extraocular motoneurons first requires establishing the synaptic relationship between individual cells with measured r and k values. As yet, there is no compelling argument for abandoning the proposed role of "average" burst tonic neurons and adopting the concept of high- and low-frequency tuned channels, but there is little doubt that second-order vestibular neurons with large head velocity sensitivities preferentially contact higher threshold motoneurons with similar properties and that those with high position sensitivities synapse extensively with lower threshold "tonic" motoneurons. Interestingly, the tonic activity found on second-order vestibular neurons clearly consists of, in part, a head position signal (i.e., spontaneous activity of first-order vestibular neurons)¹⁵ plus an added-on eye position signal. Their termination on lower threshold motoneurons whose distributed mechanical properties range from the smaller amplitude, low- to medium-range head velocities indeed provides the largest fixation angle throughout which the oculomotor system operates. In this scheme, the "population" responses are limited to the central part of the oculomotor range where the uncertainties in synaptic organization and role (e.g., described in FIGURE 3) caution against their unqualified use to further model VOR organization. The continuity of synaptic connectivity extending from the mechanical structure of the canal itself to the level of the motor unit in which higher head velocities are preferentially passed onto mechanical units

with dynamic characteristics appropriate for compensating the VOR to that head velocity needs to be explored in more detailed models.^{42,55}

THE INTEGRATOR

The preceding section has made it clear that in addition to the eye position signal described on second-order vestibular neurons, another source seems to be required at the level of extraocular motor nuclei. Diverse pieces of evidence strongly suggest that the prepositus nucleus (a subdivision of the perihypoglossal complex)² is the source of this extra position input. The argument can be illustrated best in relationship to horizontal eye movement during the VOR. The prepositus nucleus projects directly to both the abducens and medial rectus nuclei.^{2,26,30,48} Physiological evidence has confirmed that the neural signal is related to both the eye position and velocity ($E + \dot{E}$).^{44,45}

The most relevant morphological finding is the extent of synaptic connectivity between second-order VOR neurons with the prepositus nucleus and its reciprocal connections to the vestibular nuclei.^{33,48-50} By the process of exclusion (i.e., absence of other connectivity), one must assume that the role of the above neurocircuitry is to produce eye position. For the VOR, this conclusion is in fact indirectly supported by study of excitatory and inhibitory reticular neurons related to eye velocity and their reciprocal organization with the prepositus including the vestibular nuclei.^{9,24,26,30,32,48,76} Also of obvious important reference is the established role of the flocculus in smooth pursuit and fixation, with its reciprocally organized connections to the prepositus and vestibular nuclei.^{2,43,48,53,54,77} In summary, the most parsimonious conclusion is that at least the structure and/or part of the neurocircuit primarily generating eye position is located in the posterior brain-stem in the medulla. Furthermore, in view of its detailed cytoarchitectonic organization, including intrinsic and extrinsic connections (Reference 49 and McCrea and Baker, 1982, unpublished), it is logical to conclude that the prepositus nucleus is the site for the "integrator."

Finally, one of the interesting features of the diagram illustrated in FIGURE 1 is its conceptual similarity to that of Robinson entitled "a circuit diagram for the pons," in which the sequence of signal flow was depicted for all eye-movement-related activity.⁶² The neural wiring in FIGURE 1 fits nearly perfectly with the above description! Especially relevant is the feature of being able to correlate the morphological and physiological organization of not only the vestibular projection to the extraocular nuclei but that to and from the prepositus, including the reticular nuclei. Although it would be reasonable to suggest on the basis of our present experimental understanding of the prepositus that it is the additional source for the eye position signal required by the extraocular motor nuclei (FIGURE 4, Ph integrator), it clearly would be presumptuous. The major problem is that, to date, most of the detailed physiology and morphology is not yet in agreement. As one example, prepositus neurons are predominantly type II (i.e., respond like Abd Mns), and although there are both ipsi- and contralateral projecting type II axonal patterns, each seems to be restricted to only one side of the brain stem as illustrated in FIGURE 1 (References 30 and 48 and unpublished data). This would imply that the extensive ramifications of an individual prepositus neuron need to be excitatory in some cases (i.e., as in the contralateral vestibular nucleus) but inhibitory at other levels (i.e., the abducens nucleus (?). Furthermore, the prepositus activity recorded to date in the medial rectus subdivision of the oculomotor complex is consistent with an inhibitory action on

target cells.⁴⁵ These connections are confusing because "excitatory" position signals would seem to be more desirable for both motoneurons and internuclear neurons. Given that the range of prepositus proportionality constants (r , k , and θ) overlaps those of Abd Mns,⁴⁴ the probability of a null point around the center of gaze would result from a reciprocal inhibitory and excitatory afferent convergence onto target cells. Thus, we actually wonder how the above problem is solved by a direct integrator output connection to the extraocular motor nuclei. One interesting explanation would be a bilateral, asymmetrically organized excitatory influence directly onto motoneurons (also vestibular and prepositus) but close interaction with a reciprocally organized inhibitory-excitatory connection (i.e., like the VOR). Such connections would imply that inhibition of antagonist motoneurons (and vestibular neurons) is indirectly relayed through the integrator. In fact, the above organization is compatible with pathways to the medial rectus subdivision, including the activity of internuclear neurons in the abducens nucleus. Thus we conclude that the prepositus may provide a separate source of E and \dot{E}_p to motoneurons, as shown in FIGURE 2. In fact, the latter argument appears to be necessary on the basis of "exclusion" (i.e., all other sources of neurons projecting to the abducens nucleus have been identified, and their signals assessed). However, in view of the sparse synaptic density of the vestibular and certainly of the prepositus terminations in the abducens nucleus (R. Spencer, unpublished), it still seems to be more desirable to have an additional source of cells available in the posterior brain stem to provide the above function. None of these problems will be resolved until the individual prepositus neurons are identified as to their eye-movement-related signal and the pattern of their synaptic connectivity is established in the alert cat, as has been done for the identified second-order vestibular neurons.^{5,49,75}

Although the location of the "integrator" presumably has been narrowed to the prepositus nucleus, its intrinsic operation remains a mystery. Central processing in a simple structure ($\dot{E} \rightarrow E$) has been discussed by Robinson and in a more complex integrator (storage of \dot{E}) by Raphan and Cohen.^{58,62} Given the cytoarchitectonic diversity of the prepositus,^{2,49} it is reasonable to conclude that there is a suitable morphological substrate for any of the above functions, and more. The addition of some analytical concepts with the neuronal connections discussed herein hopefully will focus future research in the direction of the prepositus, as it may be the key for understanding not only the VOR but also all other types of eye movements.

REFERENCES

1. ANDERSON, J. G., R. H. I. BLANKS & W. PRECHT. 1978. Response characteristics of semicircular canal and otolith systems in cat. I. Dynamic responses of primary vestibular fibers. *Exp. Brain Res.* **32**: 491-507.
2. BAKER, R. 1977. The nucleus prepositus hypoglossi. In *Eye Movements*. B. Brooks & F. J. Bajandes, Eds.: 145-178. Plenum Publishing Corp. New York, N.Y.
3. BAKER, R. & A. BERTHOZ. 1974. Organization of vestibular nystagmus in oblique oculomotor system. *J. Neurophysiol.* **37**: 195-217.
4. BAKER, R. & R. MCCREA. 1979. The parabducens nucleus. In *Integration in the Nervous System*. V. Wilson & H. Asanuma, Eds.: 97-121. Igakaku Shoin Ltd. Tokyo, Japan.
5. BERTHOZ, A., K. YOSHIDA & P. P. VIDAL. 1981. Horizontal eye movement signals in second-order vestibular nuclei neurons in the cat. *Ann. N.Y. Acad. Sci.* (This volume.)
6. BLANKS, R. H. I., M. S. ESTES & C. H. MARKHAM. 1975. Physiologic characteristics of

- vestibular first-order canal neurons in the cat. II. Response to constant angular acceleration. *J. Neurophysiol.* **38**: 1250-1267.
7. BLANKS, R. H. I. & W. PRECHT. 1978. Response properties of vestibular afferents in alert cats during optokinetic and vestibular stimulation. *Neurosci. Lett.* **10**: 225-229.
 8. BUETTNER, V. W., V. BUETTNER & V. HENN. 1978. Transfer characteristics of neurons in vestibular nuclei of the alert monkey. *J. Neurophysiol.* **41**: 1614-1628.
 9. BUETTNER-ENNEVER, J. A. & V. HENN. 1976. An autoradiographic study of the pathways from the pontine reticular formation involved in horizontal eye movements. *Brain Res.* **108**: 155-164.
 10. COLLINS, C. C. 1971. Orbital mechanics. In *The Control of Eye Movements*. P. Bach-y-Rita & C. C. Collins, Eds.: 283-325. Academic Press, Inc. New York, N.Y.
 11. CRANDALL, W. F., J. S. WILSON & S. J. GOLDBERG. 1977. Branching axons to "functionally independent" muscles in the cat oculomotor system. *Neurosci. Abstr.* **3**: 153.
 12. CROMMELINCK, M. & A. ROUCOUX. 1976. Characteristics of cat's eye saccades in different states of alertness. *Brain Res.* **103**: 574-578.
 13. DONAGHY, M. 1980. The cat's vestibulo-ocular reflex. *J. Physiol.* **300**: 337-351.
 14. ECKMILLER, R. & M. MACKEBEN. 1976. Functional changes in the oculomotor system of the monkey at various stages of barbiturate anesthesia and alertness. *Pfluegers Arch.* **363**: 33-42.
 15. ESTES, M. S., R. H. I. BLANKS & C. H. MARKHAM. 1975. Physiologic characteristics of vestibular first-order canal neurons in the cat. I. Response plane determination and resting discharge characteristics. *J. Neurophysiol.* **38**: 1232-1249.
 16. EVINGER, C. & A. FUCHS. 1978. Saccadic, smooth pursuit and optokinetic eye movements of the trained cat. *J. Physiol. London* **285**: 209-229.
 17. EZURE, K., R. H. SCHOR. & K. YOSHIDA. 1978. The response of horizontal semicircular canal afferents to sinusoidal rotation in the cat. *Exp. Brain Res.* **33**: 27-39.
 18. FERNÁNDEZ, C. & J. M. GOLDBERG. 1971. Physiology of peripheral neurons innervating semi-circular canals of the squirrel monkey. II. Response to sinusoidal stimulation and dynamics of peripheral vestibular system. *J. Neurophysiol.* **34**: 661-675.
 19. FUCHS, A. F. & J. KIMM. 1975. Unit activity in vestibular nucleus of the alert monkey during horizontal angular acceleration and eye movement. *J. Neurophysiol.* **38**: 1140-1161.
 20. FUCHS, A. F. & E. S. LUSCHEI. 1970. Firing patterns of abducens neurons of alert monkeys in relationship to horizontal eye movement. *J. Neurophysiol.* **33**: 382-392.
 21. GOLDBERG, J. 1980. Activity of abducens nucleus units in the alert cat. Ph.D. Dissertation. University of California. Berkeley, Calif.
 22. GOLDBERG, J. M. & C. FERNÁNDEZ. 1977. Conduction times and background discharge of vestibular afferents. *Brain Res.* **122**: 545-550.
 23. GOLDBERG, S. J., G. LENNERSTRAND & C. D. HULL. 1976. Motor unit responses in the lateral rectus muscle of the cat; intracellular current injection of abducens nucleus neurons. *Acta Physiol. Scand.* **96**: 58-63.
 24. GRANTYN, R., R. BAKER & A. GRANTYN. 1980. Morphological and physiological identification of excitatory pontine reticular neurons projecting to the cat abducens nucleus and spinal cord. *Brain Res.* **198**: 221-228.
 25. GRANTYN, R. & A. GRANTYN. 1978. Morphological and electrophysiological properties of cat abducens motoneurons. *Exp. Brain Res.* **31**: 249-274.
 26. GRAYBIEL, A. M. 1977. Direct and indirect pre-oculomotor pathways of the brainstem: an autoradiographic study of the pontine reticular formation in the cat. *J. Comp. Neurol.* **175**: 37-78.
 27. HENN, V. & B. COHEN. 1973. Eye muscle motoneurons with different functional characteristics. *Brain Res.* **45**: 561-565.
 28. HENNEMAN, E., G. SOMJEN & D. O. CARPENTER. 1965. Functional significance of cell size in spinal motoneurons. *J. Neurophysiol.* **28**: 560-580.
 29. HIGHSTEIN, S. M. & H. REISINE. 1981. The ascending tract of Deiters' and horizontal gaze. *Ann. N.Y. Acad. Sci.* (This volume.)
 30. HIKOSAKA, O. & Y. IGUSA. 1980. Axonal projection of the prepositus hypoglossi and reticular neurons in the brainstem of the cat. *Exp. Brain Res.* **39**: 441-452.
 31. HIKOSAKA, O., M. MAEDA, S. NAKAO, H. SHIMAZU & Y. SHINODA. 1977. Presynaptic

- impulses in the abducens nucleus and their relation to postsynaptic potentials in motoneurons during vestibular nystagmus. *Exp. Brain Res.* **27**: 355-376.
32. IGUSA, Y., S. SASAKI & H. SHIMAZU. 1980. Excitatory premotor burst neurons in the cat pontine reticular formation related to the quick phase of vestibular nystagmus. *Brain Res.* **182**: 451-456.
 33. ISHIZUKA, N., H. MANNEN, S. SASAKI & H. SHIMAZU. 1980. Axonal branches and terminations in the cat abducens nucleus of secondary vestibular neurons in the horizontal canal system. *Neurosci. Lett.* **16**: 143-148.
 34. ITO, M., N. NISIMARU & M. YAMAMOTO. 1976. Inhibitory interaction between the vestibulo-ocular reflexes arising from the semi-circular canals of rabbits. *Exp. Brain Res.* **26**: 89-103.
 35. KAWAI, W., M. ITO & M. NOZUE. 1969. Postsynaptic influences in the vestibular non-Deiters nuclei from primary vestibular nerve. *Exp. Brain Res.* **8**: 190-200.
 36. KELLER, E. L. 1974. Participation of medial pontine reticular formation in eye movement generation in monkey. *J. Neurophysiol.* **37**: 316-332.
 37. KELLER, E. L. 1981. Oculomotor neuron behavior. In *Models of Oculomotor Behavior and Control*. B. L. Zuber, Ed. CRC Press, Cleveland, Ohio. (In press.)
 38. KELLER, E. L. & W. PRECHT. 1979. Adaptive modification of central vestibular neurons in response to visual stimulation through reversing prisms. *J. Neurophysiol.* **42**: 896-911.
 39. KELLER, E. & D. ROBINSON. 1972. Abducens unit behavior in the monkey during vergence movements. *Vision Res.* **21**: 369-382.
 40. KING, W. M. 1976. Quantitative analysis of the activity of neurons in the accessory oculomotor nuclei and the mesencephalic reticular formation of alert monkeys in relation to vertical eye movements induced by visual and vestibular stimulation. Ph.D. Dissertation. University of Washington. Seattle, Wash.
 41. KING, W., S. LISBERGER & A. FUCHS. 1976. Response of fibers in medial longitudinal fasciculus (MLF) of alert monkeys during horizontal and vertical conjugate eye movement evoked by vestibular or visual stimuli. *J. Neurophysiol.* **39**: 1135-1149.
 42. LENNERSTRAND, G. 1974. Motor units in eye muscles. In *Basic Mechanisms of Ocular Motility and Their Clinical Implications*. P. Bach-y-Rita & G. Lennerstrand, Eds.: 337-374. Pergamon Press, Oxford, England.
 43. LISBERGER, S. G. & A. F. FUCHS. 1977. Role of the primate flocculus in smooth pursuit eye movements and rapid behavioral modification of the vestibulo-ocular reflex. *Dev. Neurosci.* **1**: 381-390.
 44. LOPEZ-BARNEO, J., C. DARLOT, A. BERTHOZ & R. BAKER. 1981. Neuronal activity in the prepositus nucleus correlated with eye movement in the alert cat. *J. Neurophysiol.* (In press.)
 45. LOPEZ-BARNEO, J., J. RIBAS & J. M. DELGADO-GARCIA. 1981. Identification of prepositus neurons projecting to the oculomotor nucleus in the alert cat. *Brain Res.* (In press.)
 46. LORENTE DE NÓ, R. 1933. Vestibulo-ocular reflex arc. *Arch. Neurol. Psychiatry* **30**: 245-291.
 47. MAEDA, M., H. SHIMAZU & Y. SHINODA. 1971. Rhythmic activities of secondary vestibular efferent fibers recorded within the abducens nucleus during vestibular nystagmus. *Brain Res.* **34**: 361-364.
 48. MCCREA, R., R. BAKER & J. DELGADO-GARCIA. 1979. Afferent and efferent organization of the prepositus hypoglossi nucleus. *Prog. Brain Res.* **50**: 653-665.
 49. MCCREA, R., K. YOSHIDA, A. BERTHOZ & R. BAKER. 1980. Eye movement related activity and morphology of second order vestibular neurons terminating in the cat abducens nucleus. *Exp. Brain Res.* **40**: 468-473.
 50. MCCREA, R. A., K. YOSHIDA, C. EVINGER & A. BERTHOZ. 1981. The location, axonal arborization and termination sites of eye movement related secondary vestibular neurons demonstrated by intra-axonal HRP injection in the alert cat. *Prog. Oculomotor Res.* (In press.)
 51. MELVILL JONES, G. & J. MILSUM. 1970. Characteristics of neural transmission from the semi-circular canal to the vestibular nuclei of cats. *J. Physiol. London* **209**: 295-316.
 52. MELVILL JONES, G. & J. MILSUM. 1971. Frequency response analysis of central vestibulo-

- lar unit activity resulting from rotational stimulation of the semi-circular canals. *J. Physiol. London* **219**: 191-215.
53. MILES, F. A. 1977. The primate flocculus and eye-head coordination. In *Eye Movements*. B. A. Brooks & F. J. Bajandas, Eds.: 75-92. Plenum Publishing Corp. New York, N.Y.
 54. NODA, H., R. ASOH & M. SHIBAGAKI. 1977. Floccular unit activity associated with eye movements and fixation. *Dev. Neurosci.* **1**: 371-380.
 55. O'LEARY, D. P., R. F. DUNN & V. HONRUBIA. 1966. Analysis of afferent responses from isolated semicircular canal of the guitar fish using rotational acceleration white noise inputs. I. Correlation of response dynamics with receptor innervation. *J. Neurophysiol.* **39**: 631-644.
 56. POLA, J. & D. A. ROBINSON. 1978. Oculomotor signals in medial longitudinal fasciculus of the monkey. *J. Neurophysiol.* **41**: 245-259.
 57. PRECHT, W. & H. SHIMAZU. 1965. Functional connections of tonic and kinetic vestibular neurons with primary vestibular afferents. *J. Neurophysiol.* **28**: 1014-1028.
 58. RAPHAN, T. & B. COHEN. 1980. Integration and its relation to ocular compensatory movement. *M. Sinai J. Med. N.Y.* **47**: 410-417.
 59. ROBINSON, D. A. 1970. Oculomotor unit behavior in the monkey. *J. Neurophysiol.* **33**: 393-404.
 60. ROBINSON, D. A. 1971. Models of oculomotor neural organization. In *The Control of Eye Movements*. P. Bach-y-Rita & C. C. Collins, Eds.: 519-538. Academic Press, Inc. New York, N.Y.
 61. ROBINSON, D. A. 1975. Eye movements: a round table discussion. In *The Vestibular System*. R. F. Naunton, Ed.: 400-418. Academic Press, Inc. New York, N.Y.
 62. ROBINSON, D. A. 1975. Oculomotor control signals. In *Basic Mechanisms of Ocular Motility and Their Clinical Implications*. P. Bach-y-Rita & G. Lennerstrand, Eds.: 337-374. Pergamon Press. Oxford, England.
 63. ROBINSON, D. A. & E. KELLER. 1972. The behavior of eye movement motoneurons in the alert monkey. *Bibl. Ophthalmol.* **82**: 7-16.
 64. SHIMAZU, H. 1967. Mutual interaction between the bilateral vestibular nuclei and their significance in motor regulation. In *Neurophysiological Basis of Normal and Abnormal Motor Activities*. Raven Press. New York, N.Y.
 65. SHIMAZU, H. & W. PRECHT. 1965. Tonic and kinetic responses of cat's vestibular neurons to horizontal angular acceleration. *J. Neurophysiol.* **28**: 991-1013.
 66. SHIMAZU, H. & W. PRECHT. 1966. Inhibition of central vestibular neurons from the contralateral labyrinth and its mediating pathway. *J. Neurophysiol.* **29**: 467-492.
 67. SHINODA, Y. & K. YOSHIDA. 1974. Dynamic characteristics of responses to horizontal head angular acceleration in the vestibuloocular pathway in the cat. *J. Neurophysiol.* **37**: 653-673.
 68. SKAVENSKI, A. & D. ROBINSON. 1973. Role of abducens neurons in vestibulo-ocular reflex. *J. Neurophysiol.* **36**: 724-738.
 69. SPENCER, R. F. & P. STERLING. 1977. An electron microscope study of motoneurons and interneurons in the cat abducens nucleus identified by retrograde intra-axonal transport of HRP. *J. Comp. Neurol.* **176**: 65-86.
 70. SZENTAGOTHAÏ, J. 1943. Die zentrale Innervation der Augenbewegungen. *Arch. Psychiatr.* **116**: 721-760.
 71. SZENTAGOTHAÏ, J. 1950. The elementary vestibulo-ocular reflex arc. *J. Neurophysiol.* **13**: 395-407.
 72. TOMLINSON, R. D. & D. A. ROBINSON. 1980. Responses of vestibular nuclei cells during vertical vestibular and pursuit eye movements. *Soc. Neurosci. Abstr.* **6**: 477.
 73. TOMKO, D. L., R. J. PETERKA, R. H. SCHOR & D. P. O'LEARY. 1981. Response dynamics of horizontal canal afferents in barbiturate anesthetized cats. *J. Neurophysiol.* **45**: 376-396.
 74. YAGI, T., N. E. SIMPSON & C. H. MARKHAM. 1977. The relationship of conduction velocity to other physiological properties of the cat's horizontal canal neurons. *Exp. Brain Res.* **30**: 587-600.
 75. YOSHIDA, K., A. BERTHOZ, P. VIDAL & R. A. MCCREA. 1981. Eye movement related

activity of identified second order vestibular neurons in the alert cat. *Prog. Oculomotor Res.* (In press.)

76. YOSHIDA, K., R. MCCREA, A. BERTHOZ & P. P. VIDAL. 1979. Morphological and physiological characteristics of burst inhibitory neurons in the alert cat. *Soc. Neurosci. Abstr.* 5: 391.
77. ZEE, D. S., A. YAMAZAKI & G. GUCER. 1978. Ocular motor abnormalities in trained monkeys with floccular lesions. *Soc. Neurosci. Abstr.* 4: 168.

CAT MEDIAL PONTINE NEURONS IN VESTIBULAR NYSTAGMUS

Charles H. Markham

*Reed Neurological Research Center
University of California School of Medicine
Los Angeles, California 90024*

Shozo Nakao

*Department of Physiology
Tottori University School of Medicine
Yanago City 683, Japan*

Ian S. Curthoys

*Department of Psychology
University of Sydney
Sydney, New South Wales 2006, Australia*

Two main events take place in abducens motoneurons at the quick phase of vestibular nystagmus. One is the high-frequency bursts of agonist abducens motoneurons, which results in a quick ipsilateral deviation of the eye. The other event is the abrupt cessation of firing of the contralateral abducens motoneurons, which results in termination of the slow phase to the opposite side. In the normal human and animal, these events are highly coordinated and synchronous.

The high-frequency discharge in the agonist motoneurons could be caused by several groups of neurons. Several classes of neurons in the medial pontine reticular formation (PRF) that discharge in bursts have been suggested to provide the necessary excitatory drive.¹⁻³ Recently Igusa *et al.* have shown that certain pontine medium-lead burst neurons make monosynaptic connections with neurons in the ipsilateral abducens nucleus.⁴ Monosynaptic Vc axons in the abducens nucleus, whose cell bodies lie in the opposite vestibular nucleus, do have rhythmic discharges with nystagmus; but they usually begin to fire several milliseconds after the abducens motoneurons begin abrupt depolarization, which ushers in the spike burst.⁵ Monosynaptic Vi neurons, inhibitory neurons in the ipsilateral vestibular nucleus, do cease firing at the quick phase and result in disinhibition,^{5,6} but active excitation appears to be a more powerful influence.

Termination of the discharge of abducens motoneurons responsible for the slow phase of vestibular nystagmus is brought about by burst inhibitory neurons (BINs), premotor neurons that are predominantly located caudal to one abducens nucleus and that terminate on contralateral abducens motoneurons and possibly abducens interneurons. These neurons have been demonstrated to be inhibitory.^{7,8} Which neurons regulate the behavior of BINs? Suggestions have been made that pause neurons (PNs), a class of neurons that fire tonically but cease firing just prior to a quick eye movement in any direction, play a role in regulating saccadic discharges of eye motoneurons.^{2,9}

The present paper analyzes the firing patterns of a number of groups of pontine reticular formation neurons in relation to vestibular nystagmus in the cat and analyzes the behavior of neural firing at the quick phase.

METHODS

Adult cats were anesthetized with halothane and were placed in a stereotaxic frame, which was angulated 20° nose down and placed in the center of a turntable. Using an orbital approach, the abducens nerve and medial rectus portion of the third nerve were dissected free and mounted on Ag-AgCl electrodes for recording compound action potentials. The floor of the fourth ventricle was exposed by aspirating the midline cerebellum. In some animals, a bipolar stimulating electrode made of 80- μ m wire was inserted stereotaxically into the flocculus. Stainless-steel screw electrodes were placed in the skull over the anterior cerebral cortex for monitoring electroencephalographs (EEG). A bilateral pneumothorax was performed to reduce brain pulsations. Arterial blood pressure and heart rate were continuously monitored via a femoral arterial catheter. All wound edges and pressure points were infiltrated with 1% procaine, and the animal was immobilized by intravenous gallamine triethiodide (Flaxedil). The halothane was discontinued at least two hours before recording started.

Local anesthesia was maintained by repeated administration of procaine throughout the experiment. Maintenance of a pain-free condition was judged by observing changes in heart rate, blood pressure, pupillary size, and EEG at rest.^{6,10-14} The animals were considered to be comfortable when the heart rate was regular and in a range from 140-180/minute, the blood pressure stable in the 100-160 mm of mercury range, the pupil of the remaining eye either slitlike or in mid-dilation, and the EEG showing 5-7/second activity with infrequent 3-4/second spindles. These precautions, plus the considerable personal experience of one of us (CHM) during human neurosurgical procedures performed under only local anesthesia, plus consultations with neurosurgeons and ophthalmologists on operations done under local anesthesia, give us further evidence that the present experiments were conducted in a humane and pain-free state.

Horizontal vestibular nystagmus in both directions was induced by manual oscillation of the turntable. In some animals, regular nystagmus in one direction was elicited by destruction of one labyrinth. In most experiments, the vision of the remaining eye was blocked by holding the eyelid closed with a moist bit of cotton.

Stimulation of the brain stem was carried out with shielded glass micropipettes filled with 2 M NaCl and Fast Green FCF dye and having 0.5-1.0 megohm impedance, and occasionally with fine-wire bipolar electrodes. All electrical stimuli consist of 0.1-millisecond rectangular pulses. When the glass microelectrodes were used for stimulation, cathodal currents of less than 40 and usually around 20 μ A were used.

Recording of extracellular spikes was carried out with glass micropipettes filled with 2 M NaCl solution saturated with Fast Green FCF dye (with 1-2 megohm resistance). Intracellular recording was performed with glass electrodes containing 3 M KCl or 2 M K-citrate and had resistance of 10-20 megohms. Extracellular unitary spikes and the compound action potentials of abducens and medial rectus nerves were recorded with single-ended a.c. amplifiers (1-millisecond time constant). Intracellular potentials were recorded using d.c. amplifiers (1-millisecond time constant). These potentials were led to oscilloscopes and either were photographed on Polaroid film or were recorded on motion-picture film.

Recording and stimulation sites in the brain stem were marked by electrophoretic injection of Fast Green FCF dye. Electrolytic lesions were made in the

flocculus. Histological examination was carried out on Nissl-stained serial sections 50 μm thick.

RESULTS

The identification and classification of brain stem neurons related to eye movement depend on (1) the presence of brisk normal nystagmus for eye movements in which the end of the slow phase and the beginning of the quick phase are abrupt. This depends on the cat being alert and pain free. (2) It is important to have an accurate indicator of eye movement. We have chosen to use the compound action potentials of the eye motor nerves. Precision of timing is particularly important for analyzing eye-movement-related neurons intracellularly. (3) Neural events can be related to the moment of abrupt termination of abducens or medial rectus nerve activity at the end of the slow phase, these indicating the onset of postsynaptic potentials (PSPs) in abducens motoneurons.⁶ (4) Extracellular spikes of single neurons were distinguished from axonal responses because the spikes had a negative polarity with an inflection on the rising phase and a decline in height during repetitive discharge,^{15,16} and because the neuron could be recorded from while the micromanipulator was manipulated over a 100–200 μm range.

Neurons were examined in an area from immediately caudal to the abducens nucleus to rostral to the trochlear nucleus and from the midline to about 2 mm lateral. The main area explored was from midline to 0.75 mm lateral, since this is where most of the nystagmus-related units were found. Over 300 nystagmus-related units were examined. These could be classified as medium-lead burst neurons, long-lead burst neurons, burst-tonic neurons, pause neurons, and tonic neurons (just one of the last was found) using the terminology of Luschei and Fuchs and Keller.^{2,3} Burst inhibitory neurons (BINs)⁷ also were examined.

Before discussing the behavior of the neurons, it is instructive to see their locations. As may be seen in FIGURE 1, long-lead burst and two types of medium-lead burst neurons are closely intermingled and lie in the nucleus of the raphé in the central division of the tegmental reticular nucleus, which corresponds to the nucleus reticularis tegmenti pontis, and in the most medial part of the gigantocellular tegmental field (FTG). Burst-tonic units typically were found in a localized area of the dorsal median reticular formation close to and sometimes within the medial longitudinal fasciculus (MLF), and clearly dorsal to the burst units. Pause units all were encountered within a narrow strip between the midline and 0.5 mm lateral, most being concentrated at the rostral pole of the abducens nucleus in a small region of the nucleus raphé pontis.

Medium-Lead Burst Units

Ninety-one of 269 units were medium-lead burst units related to horizontal vestibular nystagmus. Thirty of these units fired high-frequency bursts of spikes specifically at the quick phase of nystagmus directed to the ipsilateral side. These were therefore called medium-lead unidirectional burst units. FIGURE 2A-1 shows a typical unit. When the quick phase was directed to the ipsilateral side (first two and last two beats), this neuron fired bursts of spikes at the time of the quick inhibitory phase of the contralateral abducens nerve (FIGURE 2A-2) and at

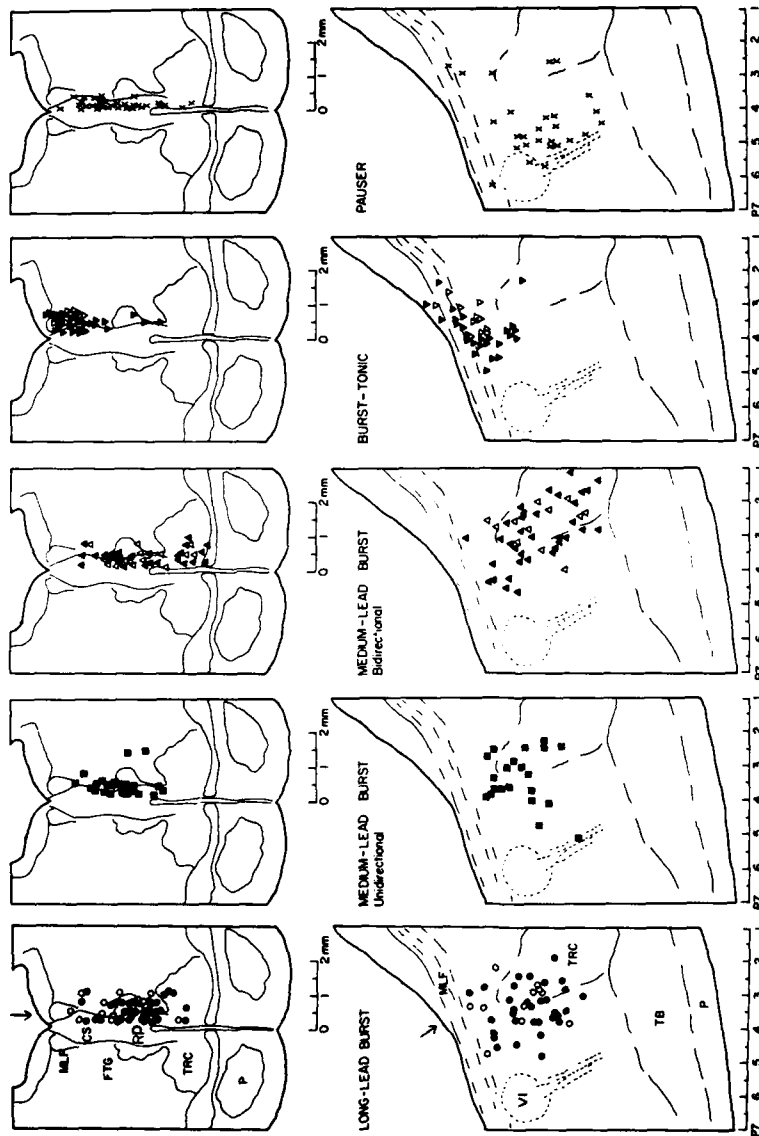


FIGURE 1. Location of PRF units projected on transverse (top) and sagittal sections (bottom). Vertical arrow in left upper drawing indicates plane of the sagittal sections, and a black arrow in the first lower drawing indicates the level and direction of the transverse sections. Long-lead burst units were divided into two groups: with (open circles) and without (filled circles) a discharge prelude before bursts. Medium-lead bidirectional burst neurons consist of those without a preferred direction (filled triangles) and with a preferred direction (open triangles) to the ipsilateral side. Burst-tonic units were divided into augmenting (filled reversed triangles) and nonaugmenting (open reversed triangles) types. The abscissae of the sagittal sections indicate stereotaxic coordinates. Definitions: MLF, medial longitudinal fasciculus; CS, superior central nucleus of the raphe; FTG, gigantocellular tegmental field; RP, nucleus raphe pontis; TRC, central division of nucleus reticularis tegmenti pontis; P, pyramidal tract; TB, trapezoid body; VI, abducens nucleus and nerve, projected into the plane of this section.

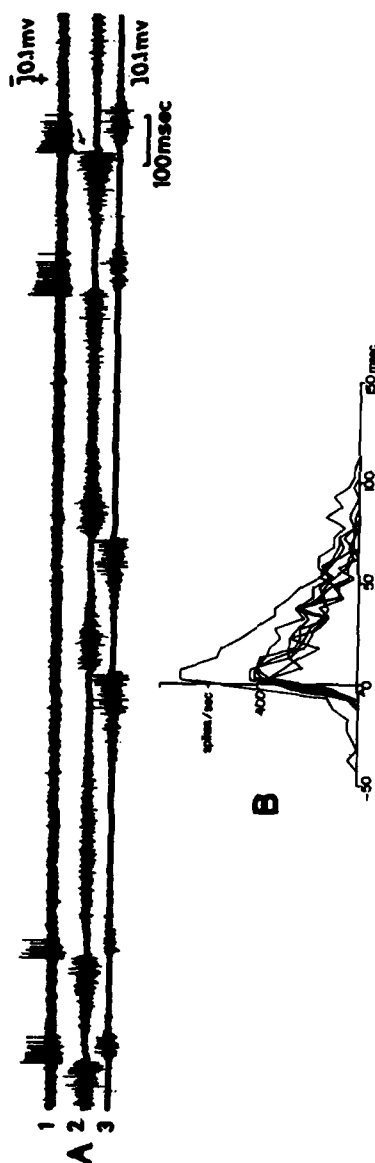


FIGURE 2. Firing pattern of medium-lead unidirectional burst units during vestibular nystagmus. A1 shows extracellular spikes of the burst units, A2 the compound action potential of contralateral abducens nerve, and A3 the compound action potential of contralateral medial rectus nerves. The burst unit discharges only with nystagmus beats with the quick phase to the ipsilateral side. B shows successive spike frequencies of seven units with each trace showing the firing pattern of the neuron over 10 beats of nystagmus. Arrowhead indicates the mean onset of firing. In this and following figures, 0 time indicates the abrupt end of abducens or medial rectus slow-phase discharge.

the quick excitatory phase of the contralateral medial rectus nerve (FIGURE 2A-3). It was completely silent during nystagmus in the opposite direction (middle two beats). The onset of bursts preceded the abrupt cessation of slow-phase abducens nerve discharge by $3.4 \text{ mseconds} \pm 5.2$, $n = 7$. The burst onset clearly preceded the medial rectus discharge at the quick phase by about 8 mseconds on the average. In order to actually compare this with the start of the quick movement of the eyeball,^{2,3} one can add about 5 mseconds, giving a total of 13 mseconds. This is approximately the lead found in medium-lead burst neurons in the monkey PRF (7-12 mseconds).² FIGURE 2B shows the firing pattern of 7 units in this category. The duration of bursts was 60-100 mseconds. Most units fired with a maximum firing frequency of around 400/second.

Sixty-one units were medium-lead bidirectional burst units, so named because they fired a burst at quick phase of nystagmus in both directions and were silent or fired sporadically during the slow phase of nystagmus. They were silent when there was no nystagmus present. In other respects, their bursting characteristics were similar to the unilateral type.

Long-Lead Burst Units

Seventy-one of 269 units fell in this category. All these units exhibited a burst of firing related only to the quick phase directed to the ipsilateral side. Fifty of these units responded with a clear-cut burst and usually were silent during the period before and after the burst. FIGURE 3A-1 shows the firing pattern of a unit of this type during nystagmus in both directions, which is indicated by the rhythmic alteration of activity of the contralateral abducens (FIGURE 3A-2) and the medial rectus nerves (FIGURE 3A-3). The firing pattern of 15 of these neurons related to the ipsilateral quick phase is shown graphically in FIGURE 3C. The bursts started $17.8 \text{ mseconds} \pm 6.9$ (standard deviation) before the end of the slow-phase nerve discharge. The mean latency is shown by the small arrowhead on the x-axis, and time zero corresponds to the end of the slow phase. The duration of the burst usually was 40-80 mseconds, and the maximum firing rate typically was 200-400 spikes/second.

The remaining 21 units in the long-lead burst category showed a prelude of firing before the burst itself (FIGURE 3B-1), as has been reported in the monkey.^{2,3} The prelude in the 8 neurons shown in FIGURE 3D started $45.3 \text{ mseconds} \pm 25.2$ before the end of the slow-phase nerve discharge. The burst itself resembled very closely the bursts in the long-lead neurons without preludes.

Burst-Tonic Units

Sixty-six of 68 units in this category exhibited tonic firing during the slow phase to the contralateral side and a burst of spikes during the quick phase in the same direction. When the nystagmus was absent, they fired tonically and had discharge rates related to eye nerve discharge activity. During horizontal rotation of the turntable, these units respond in a type I fashion (increase in firing rate during ipsilateral angular acceleration and decrease during contralateral acceleration). Only 2 burst-tonic units discharged during ipsilaterally directed eye movements. They showed a type II response to turntable rotation.

Most burst-tonic units were close to or even within the MLF. Thus, on the basis of firing pattern alone, they could be mistaken for axons of internuclear

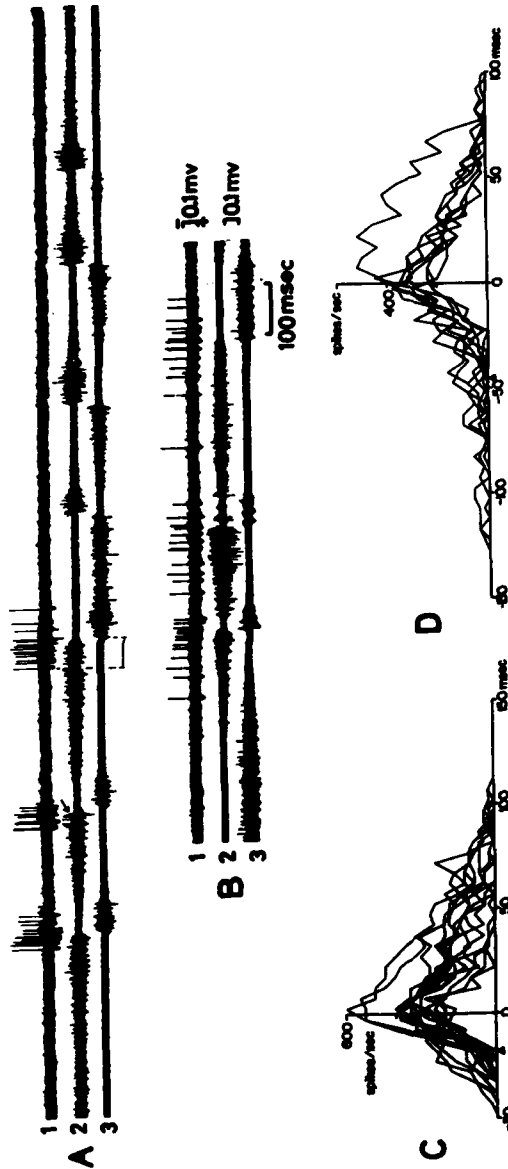


FIGURE 3. Firing pattern of long-lead burst units during vestibular nystagmus. A-D, same arrangements as in FIGURE 2. A1 shows a neuron without discharge prelude before burst activity. The horizontal bar below A3 indicates the latency from the onset of burst to quick-phase activity of medial rectus nerve. B shows another unit with a prelude. C shows successive spike frequencies of 15 units without a prelude, and D has 8 units with a prelude.

neurons of the abducens nucleus in their ascending path to the oculomotor nucleus. The burst-tonic neurons discussed here fulfilled the criteria of cell body responses as noted in an earlier section of this paper.

Pause Units

Thirty-nine of 269 units were in this category. They exhibited a steady discharge during the slow phase in both directions and ceased firing slightly prior to and during the quick phases in both directions. FIGURE 4A-1 shows the discharge pattern of one of these units. During the slow phase in either direction, pause units typically maintained a fairly steady firing rate of 150–200 spikes/second (FIGURE 4B and C). The tonic firing in the slow phase abruptly ceased $12.9 \text{ mseconds} \pm 4.5$, $n = 9$, prior to the end of the slow phase in the contralateral direction and 13.6 ± 7.6 , $n = 9$, prior to the end of the slow phase in the ipsilateral direction. At rest in the absence of nystagmus and during rotation that induced only spindlelike eye nerve discharges, most of the pause units displayed a quite regular firing independent of the amplitude of the nerve discharge.

Miscellaneous Units

A number of nystagmus-unrelated units were found, most of which showed a type I response to rotation. Only one unit had its firing rate clearly related to eye position and could be classified as a *tonic unit*. Its firing rate was proportional to the amplitude of the contralateral abducens nerve discharge directed to the contralateral side but was not related to any quick-phase discharge.

Comparison of Firing Patterns of PRF Units and Identified Premotor Neurons

The firing pattern of each category of PRF units described above was compared to the firing pattern of abducens motoneurons ($n = 4$), internuclear neurons of the abducens nucleus ($n = 3$), and BINs ($n = 5$). Abducens motoneurons were identified by being antidromically activated from the abducens nerve, abducens internuclear neurons by being antidromically activated by a bipolar fine-wire electrode placed in the contralateral MLF, and BINs by their location and characteristic firing pattern.⁷

FIGURE 5 shows the mean firing rate of PRF units in each category. The averages were obtained from 5–15 units. The compound action potentials of ipsilateral abducens and medial rectus nerves associated with nystagmus are shown schematically at the top of the figure. Vertical lines indicate the end of slow-phase discharge of the abducens or medial rectus nerves. Careful perusal of the figure allows speculation on which of these neuronal groups might influence another and has led to some of the experiments discussed below.

Projection of PRF Neurons to the Abducens Nucleus

A number of physiologically identified PRF units were studied during electrical stimulation of the ipsilateral abducens nucleus. These consisted of 22 long-lead burst, 12 medium-lead unidirectional burst, 18 medium-lead bidirec-

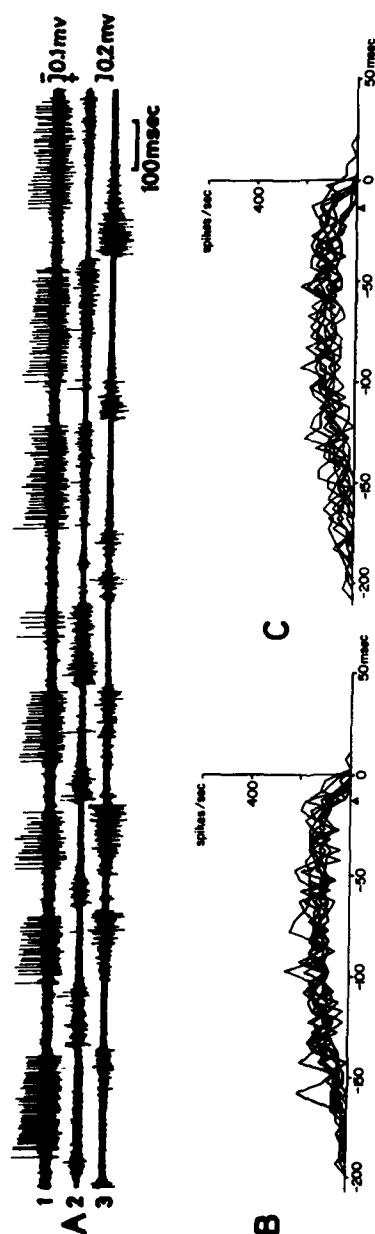


FIGURE 4. Firing pattern of pause units during vestibular nystagmus. A, same arrangement as in FIGURE 2A. B and C, successive spike frequencies of pause units during the quick phase directed to the ipsilateral (B) and contralateral (C) side. Arrowheads on abscissae indicate the mean time of discharge cessation.

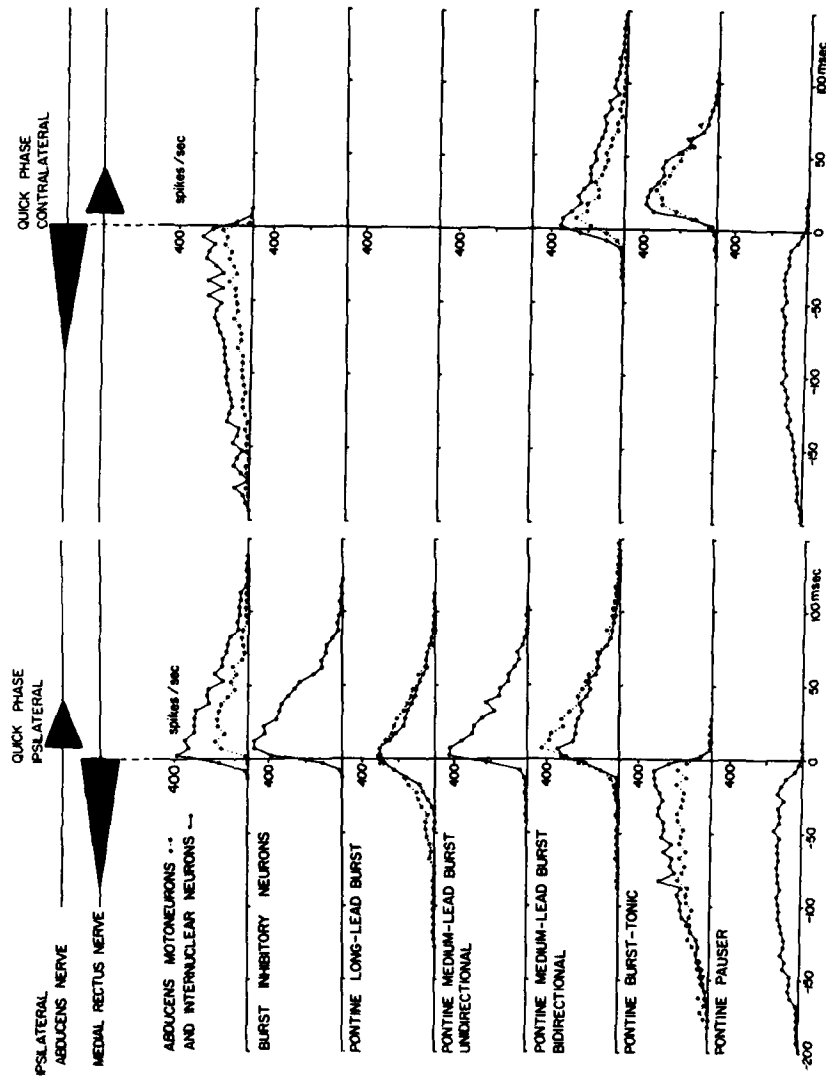


FIGURE 5. Comparison of average firing patterns of PRF units during vestibular nystagmus. Solid-line and dotted-line diagrams show the mean spike frequency of each category and subcategory. The diagrams of PRF units were made by averaging 7-15 units, while 5 units were used for the BIN, 4 for the abducens, and 3 for the internuclear neuron diagrams respectively.

tional burst, 16 burst-tonic, 29 pause, and 28 PRF units that responded to angular acceleration but whose firing patterns were not related to nystagmus. Stimulation was applied through fine-wire bipolar electrodes or monopolarly with a glass microelectrode placed in the abducens nucleus. In both cases, the electrode tip was positioned by monitoring the antidromic field potential in response to stimulation of the abducens nerve. The site of the stimulating electrode was verified later by histological examination. Of all the PRF units with firing patterns related to nystagmus, only two long-lead burst neurons were antidromically evoked from the abducens nucleus. FIGURE 6 shows the response to single shock stimulation in the ipsilateral abducens nucleus, the site being indicated by a dot surrounded by a circle in FIGURE 6C. The spikes had a fixed latency of 0.5 msecond and fired in an all-or-none fashion at threshold intensity. They

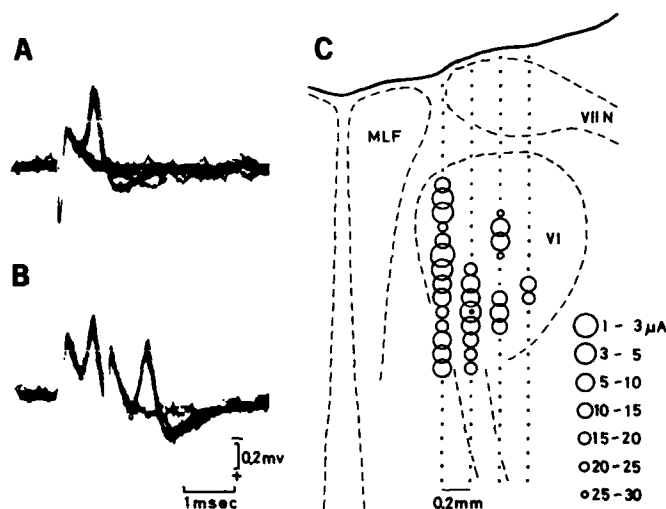


FIGURE 6. The response of a long-lead burst unit to microstimulation of the *ipsilateral* abducens nucleus. A and B, responses to single shock stimulation at threshold-straddling intensity (A) and double shocks at suprathreshold intensity (B) of the abducens nucleus, stimulation site being shown by a large dot surrounded by a circle in C. C, current thresholds obtained on systematic tracking in and around the abducens nucleus. VI, abducens nucleus; VII N, facial nerve; MLF, medial longitudinal fasciculus.

followed double shocks at short intervals of 0.9 msecond (FIGURE 6B). These results indicate that the response was induced antidromically. Activation of the unit was studied further by systematic tracking with the stimulating electrode in and around the abducens nucleus (FIGURE 6C). The electrode was advanced in a dorsal-ventral direction in 100-μm steps. The threshold current at each step was measured and is represented by circles of graded size. Low-threshold foci were separated by noneffective sites or intermingled with higher-threshold foci, suggesting that the axon branched in this region. The cell body of this long-lead burst unit was within the distribution of similar units as shown in FIGURE 1.

No medium-lead burst units could be shown to project to the abducens nucleus. It should be noted that all the units specifically tested lay within 0.75

mm of midline. However, Igusa, Sasaki, and Shimazu clearly demonstrated that some medium-lead unidirectional burst neurons made monosynaptic connection with neurons in the ipsilateral abducens nucleus.¹⁷ The neurons in that study were located about 1.5 mm from the midline, outside of the area we explored intensively.

Many PRF neurons that did not fire in relation to nystagmus could be antidromically activated by microstimulation of the ipsilateral abducens nucleus. Several were examined with systematic tracking of the stimulating microelectrode within the abducens nucleus and showed current thresholds consistent with axonal branching. These neurons were in a fairly well localized area at the rostral pole of the nucleus reticularis pontis caudalis and the tail of the nucleus reticularis oralis. Most of these neurons had a weak type I response to rotation.

Projection to the Flocculus

In endeavoring to find structures that might be influenced by the numerous eye-movement-related PRF neurons, we examined the flocculus.¹⁸ This was not unreasonable, since the flocculus has an important role in the vestibulo-ocular reflex and single-unit studies of flocculus Purkinje cells, interneuron fibers, and mossy fibers during saccades and vestibular nystagmus have shown various firing patterns in relation to rapid eye movement.¹⁹⁻²² Further, there is some anatomic evidence for projection from the PRF to the flocculus.²³⁻²⁵

FIGURE 7 shows the discharge pattern of a bidirectional medium-lead burst neuron. FIGURE 7A-1 shows the discharge pattern of the neuron during nystagmus in both directions. On stimulation of the ipsilateral flocculus, spikes were evoked at a fixed latency of 0.7 msecond in an all-or-none fashion at threshold intensity (FIGURE 7B). The spikes followed double shocks with an interval of 1.3 mseconds (FIGURE 7C). Collision testing (not shown) confirmed the antidromic activation of this neuron from the ipsilateral flocculus. FIGURE 7D, E, and F show the results of collision testing on another medium-lead burst neuron. Spikes of this neuron were evoked from ipsilateral flocculus stimulation with a latency of 1.6 mseconds (FIGURE 7D). The oscilloscope was triggered by spontaneous spikes, and stimulation of the ipsilateral flocculus was delivered at various intervals after the spontaneous spikes. The shortest interval between the spontaneous spikes and evoked spikes was 4.2 mseconds (FIGURE 7F). This value was much longer than the refractory period of the neuron determined by double shocks to the flocculus—1.1 mseconds (FIGURE 7E). These results exclude the possibility of orthodromic activation of the neuron by flocculus stimulation and strongly suggest that the activation was antidromic. The sum of the orthodromic (1.6 mseconds) plus antidromic (1.6 mseconds) conduction times, plus refractory period of the neuron (1.1 mseconds), was 4.3 mseconds, approximately the value of the shortest collision-test interval. No PRF neuron was activated synaptically by flocculus stimulation, suggesting that stimulation was localized within the flocculus. The sites of stimulation were marked by electrolytic lesion and later confirmed histologically.

Antidromic activation from the ipsilateral flocculus was demonstrated for 9 medium-lead burst neurons of both ipsilateral and bilateral discharging types; for 5 long-lead burst neurons; for 8 burst-tonic neurons; and for 15 other PRF neurons that were unrelated to horizontal vestibular nystagmus but some of which showed a type I response to horizontal turntable rotation. A few neurons of the above types also were activated by stimulating the contralateral flocculus.

It is noteworthy that no pause neurons were activated by stimulating either the ipsilateral or contralateral flocculus.

Projection of Inhibitory Pause Neurons to Burst Inhibitory Neurons

Extracellular spike activities of PNs and BINs during vestibular nystagmus were directly compared. See FIGURE 8 and the appropriate parts of FIGURE 5. When there was horizontal vestibular nystagmus with quick phase in the ipsilateral direction, a given pause neuron exhibited a tonic discharge during the

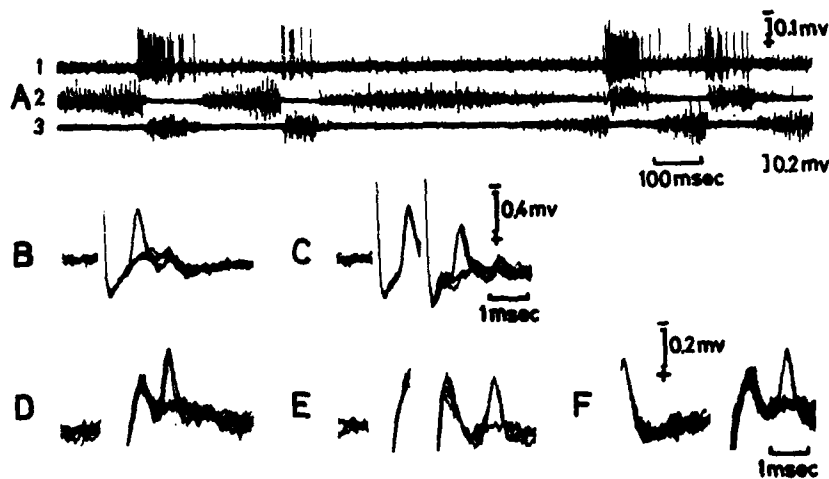


FIGURE 7. Discharge pattern during vestibular nystagmus and activation by ipsilateral flocculus stimulation of medium-lead burst neurons. A, simultaneous recording of extracellular spike potentials of a medium-lead bidirectional burst neuron (1) and discharges of the contralateral abducens (2) and medial rectus (3) nerves during nystagmus. B and C were recorded from the same neuron as in A, while D to F show responses of another neuron to ipsilateral flocculus stimulation. B and D, responses to single shock stimulation at threshold-straddling intensity. C and E, responses to double shocks at suprathreshold intensity. F, collision test between spontaneous spikes and evoked spikes at the shortest possible interval. Stimulation was at the same intensity as used in E. (Reproduced from Reference 18 with permission of Elsevier/North Holland Biomedical Press.)

slow phase of the contralateral abducens nerve (FIGURE 8A). The tonic discharge of the PN abruptly stopped 10–20 mseconds before the end of the slow phase. In contrast, the BIN emitted a high-frequency burst of spikes specifically at the quick phase coinciding with complete suppression of abducens nerve activity. When the direction of nystagmus was reversed (not shown), the PN maintained a tonic discharge during the slow phase and again ceased to fire 10–20 mseconds before the end of the slow phase. All PNs studied ceased firing prior to the quick phase of horizontal nystagmus in either direction. In FIGURE 8A, the BIN was recorded using a d.c. amplifier. It may be seen that each burst of spikes occurred on the crest of a negative field potential. In FIGURE 8B, it may be seen that the

onset of the negative field potential was approximately synchronous with the abrupt cessation of the tonic discharge of the PN. This temporal relation is also seen in FIGURE 8C, in which each spike of the PN discharge during the latter part of the slow phase for 10 beats of nystagmus is represented by a dot and a vertical line shows the onset of the negative field potential. FIGURE 8D shows the average spike frequency of this PN and for others using the same alignment procedure.

PNs were studied during microstimulation of the ipsilateral and contralateral BIN areas. The location of the stimulating electrode in the BIN area was determined by prior recording of the activity of BINs through the same electrode. FIGURE 9A shows responses of a PN to single shock stimulation to the ipsilateral BIN area at threshold-straddling intensity ($12 \mu\text{A}$). The evoked spikes had a fixed latency of 0.7 msecond occurring in an all-or-none fashion. The spikes could follow double shocks with a minimum interval of 1.5 mseconds at a supra-

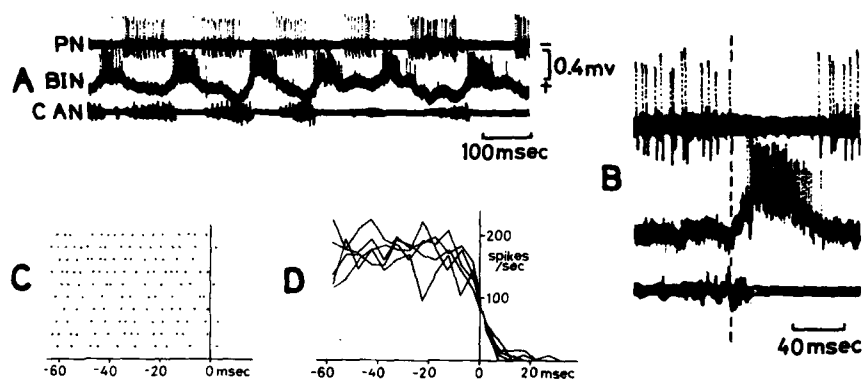


FIGURE 8. Temporal relations between activity of PNs, BINs, and extracellular field potential in the BIN area. **A**, simultaneous recording of a PN, a BIN recorded using a d.c. amplifier, and compound action potential of the contralateral abducens nerve (CAN). **B**, same as in **A** but with expanded time scale. Vertical broken line indicates the onset of the negative field potential. **C**, dot display of spikes of another PN toward the end of the slow phase for 10 beats of nystagmus. **D**, spike-frequency changes of 5 PNs at the end of the slow phase. The time 0 on the abscissae in **C** and **D** indicates the onset of the negative field potential in the BIN area.

threshold intensity, and the second spikes also had a fixed latency (FIGURE 9B). A collision test was performed, with the oscilloscope sweep being triggered by spontaneous PN spikes and stimulation of the ipsilateral BIN area delivered at decreasing intervals after the spontaneous PN spikes. The shortest interval between the spontaneous and evoked spikes was 2.7 mseconds (FIGURE 9C). These results indicate that the activation of the PN was antidromic.

Antidromic activation of PNs was studied further by systematic tracking with stimulating microelectrodes in and around the ipsilateral BIN area (FIGURE 9E and F). The stimulating electrode was advanced from the surface of the brain stem, and threshold currents for antidromic activation of single PNs were measured at $100\text{-}\mu\text{m}$ intervals. FIGURE 9E shows the threshold distribution for one PN when the brain stem was explored in a sagittal plane, while FIGURE 9F shows the threshold distributions for another neuron explored in transverse section P

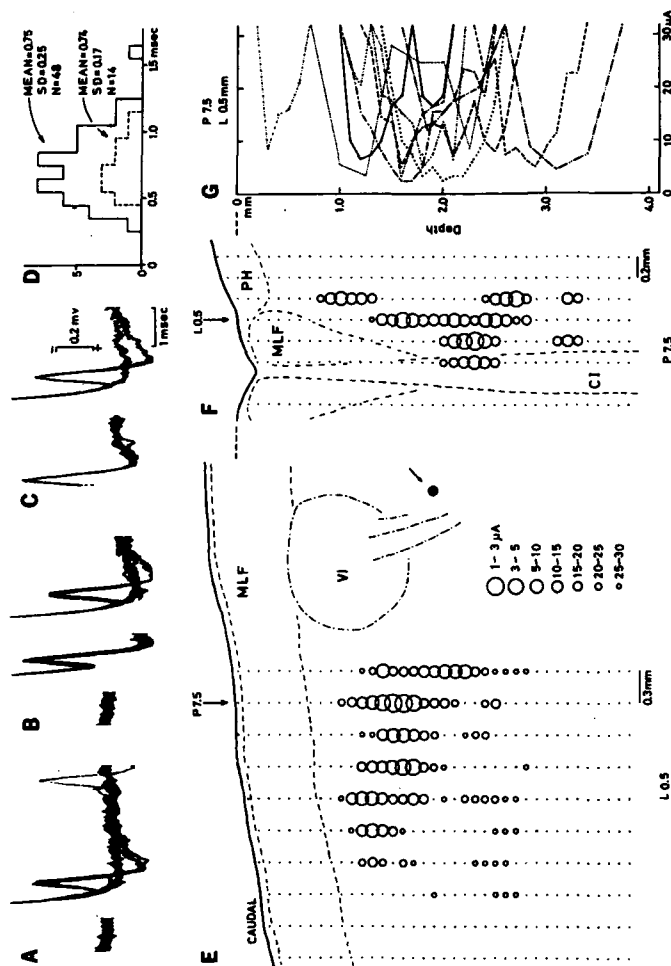


FIGURE 9. Antidromic spike responses of PN to microstimulation of BIN area and location of effective stimulation sites. A-C: spike responses of a PN to single shocks at threshold-straddling intensity (A) and double shocks at suprathreshold intensity (B) for first spikes applied to the ipsilateral BIN area, and responses of neuron to collision testing (C). D, latency histograms of antidromic spikes in response to stimulation of the ipsilateral (solid lines) and contralateral (broken lines) BIN areas. E and F, distribution of effective sites for antidromic activation of PNs in the sagittal (E) and transverse (F) planes in the ipsilateral BIN area. In each track, threshold currents for antidromic activation (less than $30 \mu A$) were measured at every $100 \mu m$ and are represented by open circles of various sizes. Effective stimulation sites in E were obtained from the same neuron shown in A through C, and those in F were obtained from another neuron. The filled circle with arrow in E indicates the recording site of the tested neuron projected into this plane. The vertical arrow in E indicates the rostral-caudal level of the transverse plane in F, and the arrow in F indicates the section of the sagittal plane of E. MLF, medial longitudinal fasciculus; PH, prepositus hypoglossi nucleus; CL, inferior central nucleus of the raphe; VI, abducens nucleus (projected). Depth-threshold traces for antidromic activation of 9 PNs on stimulation of the ipsilateral BIN area.

7.5. FIGURE 9G shows depth-threshold curves of nine PNs tested by antidromic stimulation in the ipsilateral BIN area. The distribution of effective antidromic stimulation sites for the PNs in both sagittal and transverse planes corresponds to the location of most BINs.⁷ The tracking experiments demonstrate that there were low-threshold foci interposed by high-threshold foci and indicate that PNs have axon branches in the BIN area.

The contralateral BIN area was studied less intensively than the ipsilateral area but clearly showed effective sites intermingled with noneffective sites, suggesting that axons of some PNs also terminate in this area. No PNs were antidromically activated from the neighboring MLF or abducens nucleus on either side. One neuron was activated antidromically from the ipsilateral prepositus hypoglossi nucleus.

The effect of microstimulation of the PN area on spontaneous discharges of single BINs was studied. When single shocks at two per second and at an intensity of 30 μ A were applied to the ipsilateral PN area, spontaneous spikes were suppressed for 15 to 20 mseconds after stimulation. When weak repetitive stimulation was delivered to the PN area, not only was the rhythmic activity of the single BIN being recorded suppressed, but the triangular-shaped d^+ charges of the abducens nerve indicating the presence of regular nystagmus were replaced by irregular tonic activity. The baseline on which the individual BIN spikes appeared was shifted in a positive direction throughout the repetitive stimulation. This effect was limited to the PN area as shown in FIGURE 1. For some BINs, the similar inhibitory effects were produced on stimulation of the contralateral PN area.

Intracellular recording from a BIN is shown in FIGURE 10. In FIGURE 10A, the nystagmus is with quick phase to the ipsilateral side, the BIN firing near the end of the contralateral abducens nerve discharge (CAN). The membrane potential revealed rhythmic changes consisting of a relatively steep depolarization generating a burst of spikes at the quick phase and a tonic hyperpolarization during the slow phase. In FIGURE 10C, the onset of steep membrane depolarization (vertical broken line) is better seen. The rhythmic changes of the membrane potential also are shown in another neuron (FIGURE 10D and E) in which the spike-generating mechanism has deteriorated.

Microstimulation of the ipsilateral PN area (20 μ A) induced a hyperpolarizing potential with a latency of 0.9 msecond in the BIN shown in FIGURE 10F. When the recording electrode was withdrawn from the cell, a small positive field potential was produced at about the same latency (FIGURE 10G). In 25 BINs, the mean latency of hyperpolarization was 1.04 mseconds (FIGURE 10H). The mean latency for antidromic stimulation of PNs from the ipsilateral BIN area was 0.75 mseconds (see FIGURE 9D). The difference between the mean synaptic and antidromic latencies, namely, 0.29 msecond, is explained as a single synaptic delay. Similar results were seen in a few BINs on stimulating the contralateral PN area.

Electrophoretic injection of chloride ions Cl^- into BINs during intracellular recording inverted the hyperpolarization as shown in FIGURE 10F to a depolarizing potential (not shown). Under the condition of Cl^- injection, membrane-potential changes were studied during vestibular nystagmus. In nystagmus with quick phase to the ipsilateral side, the previously observed hyperpolarizations during the slow phase were inverted to depolarization. Further, when the direction of nystagmus was reversed, the membrane potential during the slow phase could now be seen to be at a more depolarized level than at the quick phase. These results suggest that BINs are directly inhibited by inhibitory

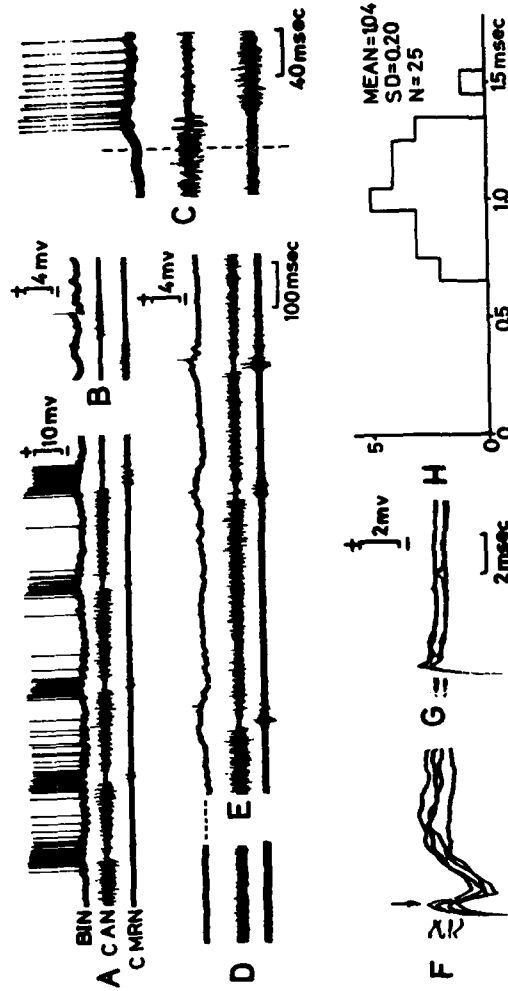


FIGURE 10. Intracellular recording from BINs during vestibular nystagmus and stimulation of ipsilateral PN area. A-C, membrane-potential changes and generation of burst of spikes of a BIN during nystagmus with the quick phase directed to the ipsilateral (A, C) and contralateral (B) side. The contralateral abducens nerve (CAN) and the contralateral medial rectus nerve (C MRN) also are shown. In C, the vertical broken line indicates the onset of steep membrane depolarization. D and E, intracellular recording from another BIN during nystagmus with the quick phase to the ipsilateral side (E) and in the absence of nystagmus (D). The recording was made after the spike-generating mechanism had deteriorated. F and G, membrane hyperpolarization of one BIN (F) and a small positive field potential (G), recorded just outside the BIN following 20- μ A intensity stimulation of the ipsilateral PN area. The arrow of F indicates the onset of hyperpolarization. H, latency histogram of the hyperpolarizing responses of 25 BINs.

postsynaptic potentials (IPSPs) from the PN area during the slow phase of nystagmus in both directions.

DISCUSSION

A number of studies, largely in the monkey, have shown that the medial pontine reticular formation (PRF) is important in rapid horizontal eye movements.¹ A small lesion in the PRF profoundly affects saccades and quick phases of vestibular and optokinetic nystagmus in the horizontal plane and produces paralysis of conjugate gaze to the ipsilateral side.^{26,27} Electrical stimulation produces horizontal eye movements with a short latency directed to the ipsilateral side, except for a limited midline region rostral of the abducens nucleus, which, when stimulated, inhibits all eye movements.^{2,28,29} PRF neurons exhibit various patterns of firing related to visual or vestibular-induced rapid eye movements,^{1-3,30} and these have been classified into several main types: burst units, burst-tonic units, pause units, and tonic units.

These several types of neurons are clearly related to eye movements, particularly saccades and quick phase of vestibular nystagmus. But what do they do? In recent years, a considerable speculative literature has developed on what these neurons should do or might do. As specific synaptic relations become known with the same clarity that exists in the vestibular-eye motoneuron relations, the basic control mechanisms in eye movements can be better understood. Three recent major steps have been made in identifying immediate premotor neurons in the PRF. These are BINs, most of which are clustered caudal to the abducens nucleus and directly inhibit contralateral abducens motoneurons;^{5,7} a small group of medium-lead excitatory burst neurons that terminate on ipsilateral abducens motoneurons;¹⁷ and internuclear neurons of the abducens nucleus terminating on contralateral medial rectus motoneurons.³¹⁻³³ The role of other PRF neurons to eye movement has to be approached with caution, in part because the present study shows that there are neurons in the PRF that are not nystagmus related but that terminate in the abducens nucleus.

The present series of studies was directed to analysis of synaptic events in horizontal nystagmus-related PRF nerves in the cat (see FIGURE 5). It may be surmised that there are several ways these PRF neurons may modulate nystagmus: (1) as immediate premotor neurons; (2) providing signals equivalent to the activity of eye motoneurons to the PRF and other structures involved in eye movements and thus serving a "corollary discharge" function; (3) projecting to other centers concerned with the precision of eye movement, such as the cerebellum; and (4) directly controlling the action of immediate premotor neurons.

In the group of long-lead burst neurons, we found a few that did terminate in the abducens nucleus and may, therefore, excite motoneurons and/or internuclear neurons. However, proof of this awaits further experimentation. We were surprised to find that none of the medium-lead burst neurons in the area we explored carefully within about 0.7 mm of the midline showed terminal branching patterns in the abducens nucleus. This does not alter the clear observation of Igusa and his colleagues that medium-lead unidirectional neurons lying in a cluster about 1.5 mm from the midline made monosynaptic connections with neurons in the ipsilateral abducens nucleus.¹⁷

Our failure to find tonic neurons may be related to our search techniques, which depended on firing patterns closely linked to nystagmus, or may be related

to the lack of proprioceptive input from eye muscles in our Flaxedil-paralyzed preparations.

When we examined eye-movement-related neurons in the brain stem projecting to the flocculus, we fairly easily demonstrated a number of such neurons. It is possible that the relative ease of finding such neurons may have some bearing on their number. Be that as it may, we did find, using antidromic identification, that burst-tonic neurons and long-lead and medium-lead burst neurons projected to the flocculus. These neurons fell in the general distribution of the neurons illustrated in FIGURE 1. These neurons appear to be the cells of origin of the afferents to Purkinje cells recorded by Noda and Suzuki.³⁴ It should be noted that we found no pause neurons that projected to the flocculus.

The burst-tonic units in the PRF exhibited discharge patterns quite similar to type IIB neurons in the prepositus hypoglossi nucleus.⁶ It is unlikely that PRF burst-tonic units are premotor neurons. They may receive excitatory input from the abducens nucleus, probably from internuclear neurons, and serve as a source of corollary discharge to other brain stem structures involved in eye movements. The same assumption is possible for prepositus hypoglossi neurons, since there is evidence that abducens interneurons are antidromically activated from the prepositus hypoglossi nucleus.³⁵

We can conclude on the following grounds that pause neurons make direct inhibitory connections with BINs and produce IPSPs in BINs during the slow phase of vestibular nystagmus:

1. There were positive field potentials in the BIN area during slow phase.
2. PNs were antidromically activated from the BIN areas bilaterally.
3. Systematic microstimulation of the BIN area leading to antidromic activation revealed a pattern consistent with terminal axonal branching in the BIN area.
4. Repetitive microstimulation of the PN area induced a positive shift in the field potential in the BIN area and suppressed bursts of BINs and nystagmic activity of the contralateral abducens nerve.
5. Microstimulation of the PN area during intracellular recording of BINs induced monosynaptic latency hyperpolarizing potentials that could be reversed by Cl^- injection.
6. During intracellular recording from BINs during vestibular nystagmus in either direction, the membrane potential during the slow phases had a tonic hyperpolarization that was shown to be due to IPSPs by means of Cl^- injection.

REFERENCES

1. COHEN, B. & V. HENN. 1972. The origin of quick phase of nystagmus in the horizontal plane. *Bibl. Ophthalmol.* **82**: 36-55.
2. KELLER, E. L. 1974. Participation of medial pontine reticular formation in eye movement generation in monkey. *J. Neurophysiol.* **37**: 316-332.
3. LUSCHEI, E. S. & A. F. FUCHS. 1972. Activity of brain stem neurons during eye movements of alert monkeys. *J. Neurophysiol.* **35**: 445-461.
4. IGUSA, Y., S. SASAKI & H. SHIMAZU. 1980. Excitatory premotor burst neurons in the cat pontine reticular formation related to the quick phase of vestibular nystagmus. *Brain Res.* **182**: 451-456.
5. HIKOSAKA, O., M. MAEDA, S. NAKAO, H. SHIMAZU & Y. SHINODA. 1977. Presynaptic impulses in the abducens nucleus and their relation to post synaptic potentials in motoneurons during vestibular nystagmus. *Exp. Brain Res.* **27**: 355-376.

6. MAEDA, M., H. SHIMAZU & Y. SHINODA. 1972. Nature of synaptic events in cat abducens motoneurons at slow and quick phase of vestibular nystagmus. *J. Neurophysiol.* **35**: 279-296.
7. HIKOSAKA, O. & T. KAWAKAMI. 1977. Inhibitory reticular neurons related to the quick phase of vestibular nystagmus—their location and projection. *Exp. Brain Res.* **27**: 377-396.
8. HIKOSAKA, O., Y. IGUSA & H. IMAI. 1978. Firing pattern of prepositus hypoglossi and adjacent reticular neurons related to vestibular nystagmus in the cat. *Brain Res.* **144**: 395-403.
9. ROBINSON, D. A. 1975. Oculomotor control signals. In *Basic Mechanisms of Ocular Motility and Their Clinical Implications*. G. Lennerstrand & P. Bach-y-Rita, Eds.: 337-374. Pergamon Press, New York, N.Y.
10. LENOX, J. R. 1970. Effect of hypnotic analgesia on verbal report and cardiovascular responses to ischemic pain. *J. Abnorm. Psychol.* **75**: 199-206.
11. HILGARD, E. R., H. MAC DONALD, G. D. MARSHALL & A. H. MORGAN. 1974. Anticipation of pain and of pain control under hypnosis: heart rate and blood pressure responses in the cold pressor test. *J. Abnorm. Psychol.* **38**: 561-568.
12. WOLF, S. & J. D. HARDY. 1941. Studies in pain. Observations on pain due to local cooling and on factors involved in the "cold pressor" effect. *J. Clin. Invest.* **20**: 521-533.
13. KRYZHANOVSKY, G. N. 1976. Experimental central pain and itch syndromes: modeling and general theory. *Adv. Pain Res. Ther.* **1**: 225-230.
14. RÖMER, D. 1968. A sensitive method of measuring analgesic effects in the monkey. In *Pain*. A. Soulaïrac, J. Cahn & J. Carpentier, Eds.: 165-170. Academic Press, Inc. New York, N.Y.
15. FUORTES, M. G., K. FRANK & M. C. BECKER. 1957. Steps in the production of motoneuron spikes. *J. Gen. Physiol.* **40**: 735-752.
16. KANDEL, E. R. & W. A. SPENCER. 1961. Electrophysiology of hippocampal neurons. II. After potential and repetitive firing. *J. Neurophysiol.* **24**: 243-259.
17. IGUSA, Y., S. SASAKI & H. SHIMAZU. 1980. Excitatory premotor burst neurons in the cat pontine reticular formation related to the quick phase of vestibular nystagmus. *Brain Res.* **182**: 451-456.
18. NAKAO, S., I. S. CURTHOYS & C. H. MARKHAM. 1980. Eye movement related neurons in the cat pontine reticular formation: projection to the flocculus. *Brain Res.* **183**: 291-299.
19. ITO, M. 1972. Neural design of the cerebellar motor control system. *Brain Res.* **40**: 81-84.
20. LISBERGER, S. G. & A. F. FUCHS. 1978. Role of primate flocculus during rapid behavioral modification of vestibulo-ocular reflex. II. Mossy fiber firing patterns during horizontal head rotation and eye movement. *J. Neurophysiol.* **41**: 764-777.
21. LLINAS, R., J. I. SIMPSON & W. PRECHT. 1976. Nystagmus modulation of neuronal activity in rabbit cerebellar flocculus. *Pfluegers Arch. Gesamte Physiol. Menschen Tiere* **367**: 7-13.
22. NODA, H., R. ASOH & M. SHIBAGAKI. 1977. Floccular unit activity associated with eye movements and fixation. *Dev. Neurosci.* **1**: 371-380.
23. ALLEY, K. 1977. Anatomical basis for interaction between cerebellar flocculus and brainstem. *Dev. Neurosci.* **1**: 109-117.
24. BRODAL, A., E. TABER & F. WALBERG. 1960. The raphe nuclei of the brain stem in the cat. II. Efferent connections. *J. Comp. Neurol.* **114**: 239-259.
25. HODDEVIK, G. H. 1978. The projection from nucleus reticularis tegmenti pontis onto the cerebellum in the cat. *Anat. Embryol.* **153**: 227-242.
26. COHEN, B., A. KOMATSUZAKI & M. B. BENDER. 1978. Electrooculographic syndrome in monkeys after pontine reticular formation lesions. *Arch. Neurol.* **18**: 78-92.
27. GOEBEL, H. H., A. KOMATSUZAKI, M. B. BENDER & B. COHEN. 1971. Lesions of the pontine tegmentum and conjugate gaze paralysis. *Arch. Neurol.* **24**: 431-440.
28. COHEN, B. & A. KOMATSUZAKI. 1972. Eye movements induced by stimulation of the pontine reticular formation. Evidence for integration in oculomotor pathways. *Exp. Neurol.* **35**: 101-117.

29. NAKAO, S., I. S. CURTHOYS & C. H. MARKHAM. 1980. Direct inhibitory projection of pause neurons to nystagmus-related pontomedullary reticular burst neurons in the cat. *Exp. Brain Res.* **40**: 283-293.
30. SPARKS, D. L. & R. P. TRAVIS. 1971. Firing patterns of reticular formation neurons during horizontal eye movements. *Brain Res.* **33**: 477-481.
31. HIGHSTEIN, S. M. & R. BAKER. 1978. Excitatory termination of abducens internuclear neurons on medial rectus motoneurons: relationship to syndrome of internuclear ophthalmoplegia. *J. Neurophysiol.* **41**: 1647-1661.
32. NAKAO, S. & S. SASAKI. 1978. Firing pattern of interneurons in the abducens nucleus related to vestibular nystagmus in the cat. *Brain Res.* **144**: 389-394.
33. NAKAO, S. & S. SASAKI. 1980. Excitatory input from interneurons in abducens nucleus to medial rectus motoneurons mediating conjugate horizontal nystagmus in the cat. *Exp. Brain Res.* **29**: 22-32.
34. NODA, H. & D. A. SUZUKI. 1979. Processing of eye movement signals in the flocculus of the monkey. *J. Physiol.* **294**: 349-364.
35. MCCREA, R. A. & R. BAKER. 1978. Neurons in the oculomotor, trochlear and abducens nuclei project caudally in the MLF to the prepositus nucleus. *Neurosci. Abstr.* **4**: 166.

IS TRANSMISSION BETWEEN THE VESTIBULAR
TYPE I HAIR CELL AND ITS PRIMARY
AFFERENT CHEMICAL?

D. A. Schessel and S. M. Highstein*

Department of Neuroscience
Rose F. Kennedy Center
Albert Einstein College of Medicine
Bronx, New York 10461

Understanding of the mode of synaptic transmission between the vestibular type I hair cell and its primary afferent is complicated by the unusual anatomical configuration of the contact between the hair cell and afferent ending.^{1,4,5,10,16} Each type I cell is surrounded almost completely by a characteristic expansion of the primary afferent that has been termed a calyx or nerve chalice. Ultrastructural descriptions of presynaptic bars or ribbons surrounded by synaptic vesicles opposite postsynaptic membrane thickenings suggest chemical synaptic transmission, but these structures are relatively rare in type I cells.^{3,6,11} Calculations based upon published electron micrographs indicate a ratio of about one synaptic body per type I cell.¹¹ Further, in mammals, cytoplasmic protrusions of the calyx are reported to invaginate the type I hair cells.^{6,11,12,14} The hair cell and calyx are separated by a regular extracellular space of 30–35 nm with the exception of the sites of cytoplasmic protrusions from the calyx into the hair cell, where the space decreases to 6–7 nm. This "close" apposition of membranes in the invaginations is significantly greater than the narrow 2-nm intercellular space found at gap junctions between electrically coupled cells, and freeze-fracture studies have not demonstrated the presence of typical gap-junctional particle arrays at the calyceal invaginations or elsewhere along the hair cell-calyx apposition. Furthermore, ultrastructural studies are by necessity performed on nonliving tissue, and results often cannot be extrapolated to a physiological situation. If, for example, the type I hair cell-afferent synapse were structurally labile, the ultrastructural correlates of chemical transmission might not be observable after routine fixation procedures. Siegal and Brownell have demonstrated that synaptic bars and vesicles, usually absent from cochlear outer hair cells, are present in profuse numbers when the tissue is fixed in the presence of a high concentration of magnesium.² However, because at least one synaptic bar per hair cell can usually be documented, there are grounds for the reasonable supposition of chemical synaptic transmission. Nevertheless, the function of the calyx and its reason for existence still remain unclear. With this background in mind, we undertook a morphophysiological study with intracellular electrodes loaded with horseradish peroxidase to record from the vestibular primary afferents that are contacted by type I hair cells.

The lizard *Calotes versicolor*, known to have type I and type II hair cells,¹⁷ was selected as the experimental animal. Lizards were spinalized, artificially respired, and kept warm. The base of the ampulla of the horizontal semicircular canal was exposed by a lateral approach, and the nerve visualized. Glass microelectrodes were filled with a 10% solution of horseradish peroxidase (HRP)

*To whom all correspondence should be addressed.

in 500 mM KCl, 50 mM tris buffer pH 7, and had d.c. resistances of 100-150 M Ω . Microelectrodes were inserted into the horizontal canal nerve, and axons penetrated at the level of the basement membrane. Spontaneous action potentials and subsynaptic activity were recorded; no mechanical stimulation has been employed to date. Upon successful penetration and recording, depolarizing pulses (60-150 nA minutes total) were passed directly through the microelectrodes to fill the recorded process with HRP. Animals survived for several hours; labyrinths were perfused with a buffered mixed aldehyde fixative and reacted with a standard diaminobenzidine, cobalt-chloride protocol to develop the horseradish reaction product. Labyrinths were embedded in epon, and 2- μ sections cut with glass knives for light microscopy.

Both regular and irregular units were recorded, indicating a similarity in the spectrum of responses for this labyrinth to that of others. This report will be limited to the morphophysiology of irregular fibers. When the microelectrode

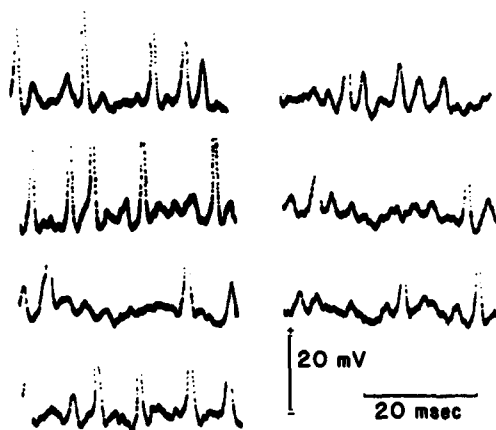


FIGURE 1. Spontaneous activity recorded from the primary afferent illustrated in FIGURE 2. Selected, nonsequential segments of action potentials and subthreshold activity. Calibrations as indicated.

penetrates a fiber in the center of the horizontal canal nerve, a resting potential of 50 to 65 mV negative appears, with superimposed action potentials irregularly spaced. As FIGURE 1 illustrates, subthreshold depolarizing activity is also observed. During the experiment, the impression of a barrage of synaptic activity similar to that observed at the neuromuscular junction or at other synapses known to be chemical can be observed. Subthreshold activity can often be seen to underlie the spontaneous action potentials (FIGURE 1). With increased recording time, the action potentials decrease in number and finally fail, leaving an unchanged resting potential of 50-65 mV with substantially unchanged subthreshold activity. Hyperpolarization of the membrane via a bridge circuit often leads to an increase in the amplitude of the subthreshold depolarizations. Records illustrated in FIGURE 1 were obtained from the neuron shown in FIGURE 2. Serial sections through the injected neuron demonstrate that it is a multiple calyx enveloping five type I hair cells. The recording site (horizontal arrow) was within a few microns of the calyx. No type II cells innervated this fiber. In every

case so far studied, nerve fibers with irregular activity terminate with calyceal endings in the cristae and are innervated by type I hair cells. In two cases, in addition to a calyx there were small processes originating from the calyx itself, which traveled through the sensory epithelium of the cristae to be innervated by type II cells.

Although the frequency and pattern of the subthreshold activity are sugges-



FIGURE 2. Photomicrograph through the crista of the horizontal semicircular canal. A calyx and primary afferent extending toward the horizontal canal nerve have been filled with horseradish peroxidase. The arrowhead points to one of five type I hair cells innervating the recorded primary afferent. The arrow points to the recording site.

tive of chemical synaptic transmission, the shape of the depolarizations (post-synaptic potentials, PSPs) is not typical of chemical excitatory postsynaptic potentials (EPSPs) in that the rising and falling phases are rather symmetrical. This can be interpreted as indicating a short time constant of the calyceal membrane resulting in a very rapid decay or falling phase of the PSP. Similar EPSPs with symmetrical rising and falling phases can be seen occasionally in

central-nervous-system neurons. Such symmetrical PSPs also are observed when recording goldfish saccular afferent activity in response to a moderately high-frequency sound.⁹

Further evidence suggestive of chemical transmission can be gleaned from an experiment in which records were taken from an irregular fiber subsequently found to have a calyceal terminal innervated by a single type I hair cell. The records were virtually identical to those illustrated in FIGURE 1, i.e., EPSPs of varying sizes occurring at irregular frequencies were recorded.

Several conclusions can be drawn from these experiments. First, every irregular fiber studied to date terminates in a calyx that is innervated by type I hair cells, although some may have branches that innervate type II cells. The records from a single calyceal terminal expansion innervated by a single type I hair cell are particularly revealing, as we can attribute the origin of all of the recorded postsynaptic activity to a single presynaptic element. In that case, the amplitude of the PSPs varied between 4 and 15 mV. If type I hair cells could generate action potentials and these were transmitted electrotonically to the calyx, presumably all postsynaptic activity would be of uniform amplitude and not, as observed, varying over a twofold range. Therefore we feel confident that electronically transmitted hair cell action potentials (if present) do not account for the recorded postsynaptic activity. The most convincing records of vestibular hair cell receptor potentials have been obtained from saccular hair cells of the bullfrog.¹³ These neurons generate biphasic receptor potentials of 10-15 mV when maximally mechanically stimulated. If these or other^{7,8} hair cell potentials were electrotonically transmitted to the calyx, some electrotonic decrement in amplitude should be expected. Yet our spontaneous monophasic depolarizing PSPs are often 15 mV or larger. Thus it seems unlikely that electrotonic transmission from hair cells to primary afferents can account for these results.

Further the absence of specialized junctions between the neck of the nerve calyx and the type I cell, which might limit current flow into the extracellular space, and the possible presence of half calyces also mitigate against ephaptic transmission. On the basis of EPSP shape, the type I synaptic structure has a very short time constant. This might serve to curtail the falling phase of synaptic input, insuring independent transmission of each unitary potential between a hair cell and the nerve calyx, and thus may minimize summation of individual postsynaptic events.¹⁵

In summary, we have recorded from irregular primary afferents of the cristae of the horizontal semicircular canal of the lizard and have filled the afferents with HRP. Morphophysiological studies indicate that irregular fibers terminate in a calyx that is innervated by from one to five type I hair cells. Interpretation of records suggests chemical synaptic transmission between type I hair cells and vestibular primary afferents.

REFERENCES

1. ADES, H. W. & H. ENGSTRÖM. 1965. Form and innervation of the vestibular epithelia. In *The Role of the Vestibular Organs in the Exploration of Space*: 23-40. NASA Report No. SP-77. U.S. Naval School of Aviation Medicine. Pensacola, Fla.
2. BROWNELL, W. E. & J. H. SIEGEL. 1980. Synaptic bars in outer hair cells of the chinchilla cochlea. Abstract, Third Midwinter Research Meeting, Associated Researchers of Otolaryngology, January 21-23.
3. FAVRE, D. & A. SANS. 1977. Synaptogenesis of the efferent vestibular nerve endings of the cat: ultrastructural study. *Arch. Oto-Rhino-Laryngol.* **215**: 183-186.

4. FAVRE, D. & A. SANS. 1978. The development of vestibular efferent nerve endings during cat maturation: ultrastructural study. *Brain Res.* **142**: 333-337.
5. FAVRE, D. & A. SANS. 1979. Embryonic and postnatal development of afferent innervation in cat vestibular receptors. *Acta Otolaryngol.* **87**: 97-107.
6. FAVRE, D. & A. SANS. 1979. Morphological changes in afferent vestibular hair cell synapses during the postnatal development of the cat. *J Neurocytol.* **8**: 765-775.
7. FETTIPLACE, R. & A. C. CRAWFORD. 1978. The coding of sound pressure and frequency in cochlear hair cells of the terrapin. *Proc. R. Soc. London Ser. B* **203**: 209-218.
8. FETTIPLACE, R. & A. C. CRAWFORD. 1978. Ringing responses in cochlear hair cells of the turtle. *J. Physiol.* **284**: 120P-122P.
9. FURAKAWA, T., Y. ISHII & S. MATSUURA. 1972. Synaptic delay and time course of post-synaptic potentials at the junction between hair cells and eighth nerve fibers in the goldfish. *Jpn J. Physiol.* **22**: 617-635.
10. GRAYBIEL, A. 1967. Paper presented at the Third Symposium on the Role of the Vestibular Organs in Space Exploration, January 24-26. Naval Aerospace Medical Institute Naval Aerospace Medical Center. Pensacola, Fla.
11. GULLEY, R. L. & D. BAGGER-SJOBACK. 1979. Freeze-fracture studies on the synapse between the type I hair cell and the calyceal terminal in the guinea-pig vestibular system. *J. Neurocytol.* **8**: 591-603.
12. HAMILTON, D. W. 1968. The calyceal synapse of type 1 vestibular hair cells. *J. Ultrastruct. Res.* **23**: 98-114.
13. HUDSPETH, A. J. & D. P. COREY. 1977. Sensitivity, polarity, and conductance change in the response of vertebrate hair cells to controlled mechanical stimuli. *Proc. Nat. Acad. Sci. USA* **74**: 2407-2411.
14. LINDEMAN, H. H. 1969. *Studies on the Morphology of the Sensory Regions of the Vestibular Apparatus.* Springer-Verlag. Berlin, Heidelberg & New York.
15. ROSSI, M. L., P. VALLI & C. CASELLA. 1977. Fibers of the posterior semicircular canal in the frog. *Brain Res.* **135**: 67-75.
16. SMITH, C. A. & G. RASMUSSEN. 1967. Nerve endings in the maculae and cristae of the chinchilla vestibule, with a special reference to the efferents. *In Third Symposium on the Role of the Vestibular Organs in Space Exploration*: 183-200. NASA Report No. SP-152. U.S. Government Printing Office. Washington, D.C.
17. WERSALL, J. & D. BAGGER-SJOBACK. 1974. Morphology of the vestibular sense organ. *In Handbook of Sensory Physiology.* H. H. Kornhuber, Ed. **6**: 123, 171. Springer-Verlag. Berlin, Heidelberg & New York.

ORGANIZATION OF THE AVIAN ACCESSORY OPTIC SYSTEM*

Nicholas C. Brecha† and H. J. Karten†‡

†Department of Neurobiology and Behavior
‡Department of Psychiatry and Behavioral Sciences
State University of New York
Stony Brook, New York 11794

The retina of all vertebrates projects in a comparable fashion upon several separate targets within the brain. These targets include the optic tectum, the pretectal complex, the dorsal and ventral thalamus, the suprachiasmatic nucleus of the hypothalamus, and the nuclei of the accessory optic system (AOS).^{1,2} The specific functional role of each of these retinal targets in visual behavior remains unknown. Conversely, identification of the specific structure responsible for particular visual functions often has proven difficult to establish with certainty. With the possible exception of the pupillary reflex, there are few instances in visual system function where we can draw the complete circuit diagram of input-output that might specifically account for a defined operation of the visual system. A parallel problem to that of the specific function of each central target of the retina pertains to the retina itself. Do particular types of ganglion cells project upon specific central targets?

Our research of the last several years has provided some clarification of these questions, with particular relevance to the subjects of this conference. This research has led us to concentrate our efforts upon one of the less well studied central retinal targets, the nuclei of the AOS. Our research has indicated that the AOS plays an important and specific role in retino-oculomotor control mechanisms.

The accessory optic nuclei, which are components of the accessory optic system (AOS), were first recognized in 1881³ and have been identified in all vertebrate classes (see References 4 and 5 for reviews). The AOS includes the accessory optic nuclei, which are located along the mesodiencephalic border, and a distinct fascicle or fascicles of retinal axons that terminate upon these nuclei. The most prominent and consistently described components of the AOS are (1) a fascicle of retinal axons, generally known as the basal optic root or the tractus peduncularis transversus in nonmammalian and mammalian vertebrates respectively, and (2) a main accessory optic nucleus. This main accessory optic nucleus is known as the nucleus ectomammillaris or the nucleus of the basal optic root (nBOR) in nonmammalian vertebrates. In mammals, this nucleus also is called the nucleus tractus peduncularis transversus, the medial terminal nucleus, or the medial accessory nucleus.^{6,7}

The second-order connections as well as the functions of the AOS have remained obscure until recently. A variety of speculations as to the functions of this system have been proposed previously, including a role in rapid orienting responses to a peripheral stimulus, participation in the discrimination of luminous flux, and/or mediation of the photic modulation of the pineal gland.⁸⁻¹³ Recently, several studies have suggested that this system plays an important role

*Supported by National Institutes of Health Grants No. NS12078 and EY02146 to H.J.K.

in oculomotor function. Anatomical studies have demonstrated that the main accessory optic nucleus gives rise to axonal projections upon several central nervous system structures, such as the oculomotor complex and vestibulocerebellum, which play a prominent role in oculomotor behavior.^{5,14} Physiological studies have demonstrated that neurons within the accessory optic nuclei have large receptive fields and respond best to large, slow-velocity, vertically moving stimuli.¹⁵⁻¹⁷ In addition, behavioral studies have demonstrated an impairment of optokinetic nystagmus following lesions of the AOS and an enhancement of the metabolic activity of the AOS in response to vertical moving stimuli.¹⁸⁻²⁰ In this review, much of the evidence suggesting a role of the AOS in oculomotor function will be presented.

Retinal Projections upon the Accessory Optic System

In birds, a unique class of retinal ganglion cells known as the displaced ganglion cells of Dogiel are the predominant, if not sole, source of a retinal projection via the basal optic root (BOR) upon the nucleus of the basal optic root (nBOR).²¹⁻²⁶ In pigeons, the BOR forms into a separate and distinct tract just caudal to the optic chiasm and is present along the ventral aspect of the brain

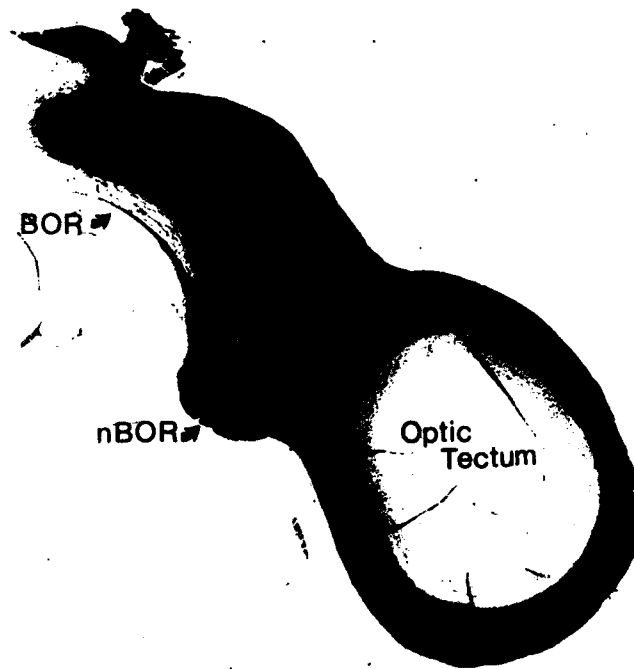


FIGURE 1. Photomicrograph of a horizontal section through the pigeon brain stem illustrating the distribution of label in the BOR and nBOR after an intraocular injection of 1 mCi of ³H-proline. Bright-field photograph. BOR, basal optic root; nBOR, nucleus of the basal optic root; TrO, tractus opticus.

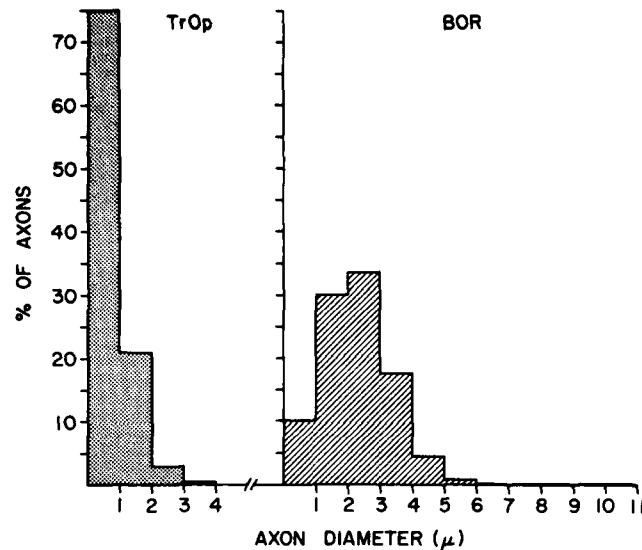


FIGURE 2. A comparison of the axon diameters of the BOR and adjacent TrOp. TrOp, tractus opticus.

stem just lateral to the hypothalamus and medial to the optic tract (FIGURE 1). This tract is characterized by large myelinated fibers that measure from 1-11 μm in diameter. In comparison, the majority of axons within the adjacent optic tract, many of which are unmyelinated, measure 1 μm in diameter or less (FIGURE 2). The BOR axons represent about 0.2% of the total number of retinal axons; quantitative analyses of the BOR and optic nerve have estimated about 4,800 axons in the BOR and 2.4 million axons in the optic nerve.²⁷

Injections of horseradish peroxidase (HRP) confined primarily to the nBOR complex result in the labeling of displaced ganglion cells of the contralateral retina, which appear to be morphologically identical to these cell types as described from Golgi impregnation material.²²⁻²⁶ Displaced ganglion cells are characterized as having a particularly large somata located at the border at the inner nuclear layer and the inner plexiform layer, and dendritic processes that arborize over a wide horizontal field in lamina 1 of the inner plexiform layer (FIGURE 3). In pigeon, the displaced ganglion cells that give rise to a projection upon the nBOR complex are widely spaced, distributed predominantly within peripheral retinal regions, and found in the greatest densities in superior nasal and inferior temporal retinal fields^{24,28} (FIGURE 4). About 5,000 displaced ganglion cells project upon the contralateral nBOR complex.²⁶ This estimate closely matches the estimated number of axons within the BOR and strongly suggests that this tract is derived exclusively from the axons of displaced ganglion cells. In contrast, HRP injections into the optic tectum do not result in labeling of displaced ganglion cells. These injections do, however, result in the labeling of cells within a restricted portion of the ganglion cell layer corresponding to that retinal area known to project upon the optic tectum.^{24-26,28} Therefore, the morphology, distribution, and spacing of displaced ganglion cells suggest that they

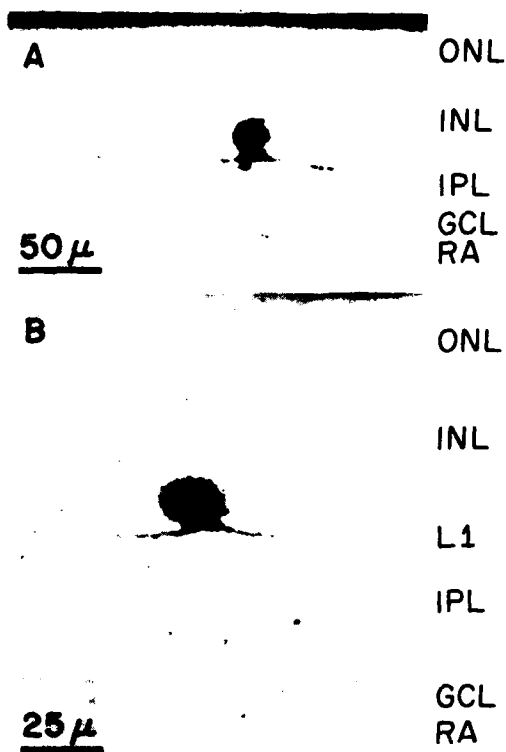


FIGURE 3. Photomicrographs of labeled displaced ganglion cells after an injection of HRP into the contralateral nBOR complex. Note labeled axon entering the retinal axon layer in A. ONL, outer nuclear layer; INL, inner nuclear layer; IPL, inner plexiform layer; GCL, ganglion cell layer; RA, retinal axon layer. (From Fite et al.,²⁶ with permission of the publisher.)

may be involved in the detection of movements in peripheral visual fields, rather than playing a role in visual acuity processes.^{24,26}

Organization of the nBOR Complex

The nBOR complex includes three distinct subdivisions: the nucleus of the basal optic root (nBOR), the nucleus of the basal optic root pars dorsalis (nBORd), and the nucleus of the basal optic root pars lateralis (nBORl).⁵ On the basis of Golgi impregnations, Nissl stains, and retrograde HRP filling of cells, the nBOR complex has been found to contain several different populations of cells including large basophilic stellate cells, medium ovoid cells, and small spindle cells.^{5,29-32} All of these cell types appear to receive a direct retinal projection and give rise to projections upon the targets of the nBOR complex^{5,31,32} (TABLE 1).

The efferent projections of the nBOR complex have been demonstrated

following unilateral injection of ^3H -leucine/ ^3H -proline mixtures into the nBOR complex.^{5,14} The nBOR complex gives rise to prominent bilateral projections upon (1) the vestibulocerebellum, (2) the inferior olivary complex, (3) the oculomotor nuclear complex, (4) the nucleus interstitialis; contralateral projections upon (5) the nBOR complex; and ipsilateral projections upon (6) the nucleus lentiformis mesencephali pars magnocellularis. These efferent systems have been confirmed following HRP injections into each of the targets of the nBOR complex (TABLE 1). Detailed descriptions of the projections and terminal patterns of the nBOR complex have been published elsewhere.⁵ In this review, the projections of the nBOR complex upon the vestibulocerebellum, the inferior olivary complex, and the oculomotor complex will be discussed. The existence of these projection systems strongly supports the contention that the accessory optic system plays a role in oculomotor function.

nBOR Complex Projections upon the Vestibulocerebellum

Axons originating from the nBOR complex that are destined for the cerebellum join the descending axons of the nucleus spiriformis medialis to form the brachium conjunctivum cerebellopetale.³³ This tract projects caudally as a compact fascicle and enters the cerebellum via the ipsilateral brachium conjunctivum. Axons originating from the nBOR complex pass through and between the medial and lateral deep cerebellar nuclei and distribute bilaterally, predominantly within the granule cell layer of the vestibulocerebellum, which includes

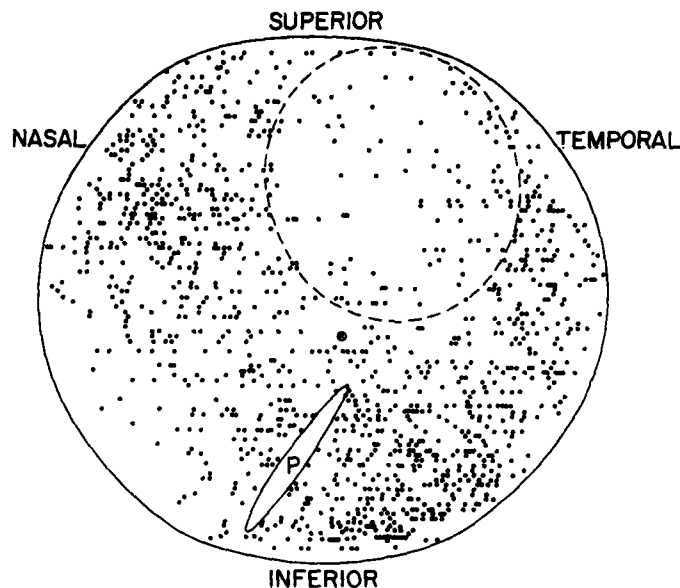


FIGURE 4. Reconstruction of the distribution of labeled displaced ganglion cells in the contralateral retina after an injection of HRP into the contralateral nBOR complex. P, pecten; F, approximate location of the fovea. (From Fite et al.,²⁸ with permission of the publisher.)

folia IXc,d and the parafoolculus (FIGURE 5). The nBOR axons end as mossy fiber terminals within the external one-third to one-half of the granule cell layer immediately adjacent to the Purkinje cell layer. The mossy fiber terminals spread horizontally within the vestibulocerebellum, frequently merging to form a continuous band of terminals that varied in density in an apparently random manner.

The bilateral nBOR complex projection upon the cerebellum was also suggested following injections of HRP into folia IXc,d of the vestibulocerebellum.^{5,14,30} Unilateral injections of HRP confined to the parafoolculus or folia IXc,d resulted in bilateral retrograde labeling of both medium and large cells within the nBOR complex (TABLE 1). Unilateral HRP injections into folia IXc,d also

TABLE 1
SUMMARY OF THE NUMBER OF LABELED CELLS WITHIN THE nBOR COMPLEX FOLLOWING
UNILATERAL HRP INJECTIONS INTO THE nBOR COMPLEX TARGETS*

	Ipsilateral			Contralateral		
	nBOR	nBORd	nBORl	nBOR	nBORd	nBORl
Vestibulocerebellum-folia IXc,d						
193t	72	11	1	52	11	2
199s	23	3	1	15	0	0
206t	159	10	11	132	12	6
207t	95	12	4	105	13	3
208t	30	0	2	31	0	1
Inferior olivary complex						
169t	15	17	0	4	8	0
170t	10	10	0	2	3	0
Oculomotor nuclear complex						
62t	0	5	0	8	0	0
74t	0	10	0	9	0	0
92t	0	2	0	3	0	0
Contralateral nBOR complex						
153t	—	—	—	22	11	6
154t	—	—	—	20	9	1
Lentiformis mesencephali						
129s	66	26	8	—	—	—
109lt	15	12	2	—	—	—
109rt	14	2	0	—	—	—

*From Brecha *et al.*,⁵ with permission of the publisher.

resulted in labeling of cells within vestibular, reticular, and spinal regions as well as in the contralateral dorsal division of the medial accessory olive.⁵ The projection of these systems upon the vestibulocerebellum is consistent with current proposals that visual, vestibular, and spinal inputs are integrated within this region.³⁴

nBOR Complex Projections upon the Inferior Olivary Complex

The inferior olivary complex in birds has been well described and is directly comparable to the inferior olivary complex of mammals.³⁵ Axons of the nBOR complex project bilaterally upon the medial regions of the inferior olive. This

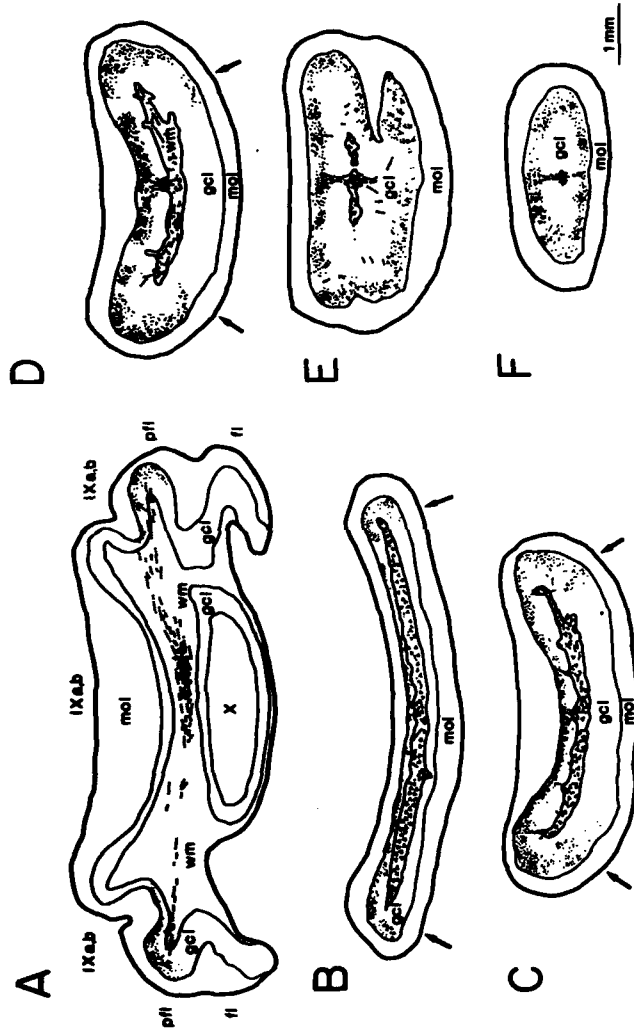


FIGURE 5. Distribution of label within folia IXc,d and paraflocculus following a unilateral injection of ^3H -leucine into the nBOR complex. Label is distributed within the white matter and the superficial regions of the granule cell layer. Chartings are of transverse sections arranged in a rostral (A) to caudal (F) sequence. B-E show only folia IXc,d. Note paucity of projection upon folium IXd. Arrows indicate the border between folia IXc and IXd. mol, molecular layer; fl, flocculus; pfl, paraflocculus; wm, white matter; gcl, granule cell layer; IXa,b, cerebellar folia IXa,b; IXc,d, cerebellar folia IXc,d; X, cerebellar folia X. (From Brecha *et al.*,⁵ with permission of the publisher.)

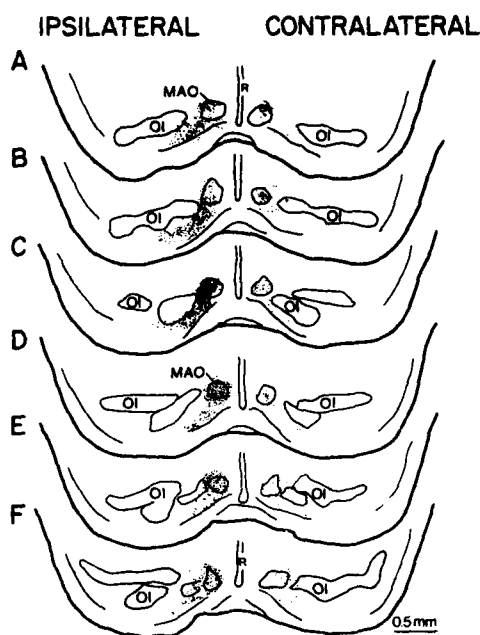


FIGURE 6. Bilateral distribution of label within the inferior olivary complex following a unilateral injection of ^3H -proline/ ^3H -leucine mixture into the nBOR complex. Label is distributed predominantly within the medial regions of the ipsilateral inferior olivary complex. Chartings are of horizontal sections arranged in a dorsal (A) to ventral (F) sequence. OI, nucleus olivaris inferior; MAO, medial accessory olive; R, nucleus raphes. (From Brecha *et al.*,⁵ with permission of the publisher.)

zone reportedly corresponds to the dorsal division of the medial accessory olive of mammals.⁵ The nBOR complex projection upon the ipsilateral medial accessory olive is greater than that upon the contralateral medial accessory olive, as evident in both the number of axons within the ventral tegmental tracts and the density of label within the inferior olivary nucleus (FIGURE 6).

Unilateral HRP injections placed in the region of the inferior olivary nucleus resulted in bilateral retrograde labeling of small spindle cells in both the nBOR and nBORd (TABLE 1). The greatest number of labeled cells were found within the ipsilateral nBOR complex, confirming the suggestion, based upon anterograde studies, that the nBOR complex projection upon the ipsilateral inferior olive is greater than that upon the contralateral inferior olive.

Inferior Olivary Projections upon the Vestibulocerebellum

As mentioned above, HRP injections into folia IXc,d of the vestibulocerebellum resulted in retrograde cell labeling within the same region of the contralateral medial accessory olive that receives a bilateral visual input from the nBOR.³⁶ Autoradiographic studies have demonstrated that this region of the inferior olivary complex gives rise to a projection upon the internal portion of the molecular layer of the vestibulocerebellum in a pattern characteristic of climbing fibers in the bird.³⁷ These anatomical studies thus provide evidence for a visual climbing fiber system that terminates upon the same region of the cerebellum that receives the nBOR mossy fiber input.³⁶ The function of the visual climbing fiber system in birds, which has yet to be investigated with electrophysiological techniques, is likely to be similar to that described for mammals.^{36,39}

nBOR Complex Projections upon the Oculomotor Complex

On the basis of normal cytoarchitectonic appearance, the avian oculomotor nuclear complex contains four prominent divisions: the Edinger-Westphal nucleus and the dorsolateral, the dorsomedial, and the ventral (medial and lateral divisions) oculomotor nuclei. The latter four nuclei contain the oculomotor neurons that project upon the inferior rectus, medial rectus, superior rectus, and inferior oblique extraocular muscles.

Axons of the nBOR complex give rise to substantial projections upon the ipsilateral ventromedial and contralateral dorsolateral divisions of the oculomotor nuclear complex⁵ (FIGURE 7). Axons of the nBOR complex run in a dorsomedial direction lateral to the oculomotor nerve to enter the ipsilateral ventral nuclei. Some axons also cross the midline just ventral to the oculomotor nuclear complex and run within the fasciculus longitudinalis medialis to terminate within the contralateral dorsolateral nucleus. A very sparse projection of the

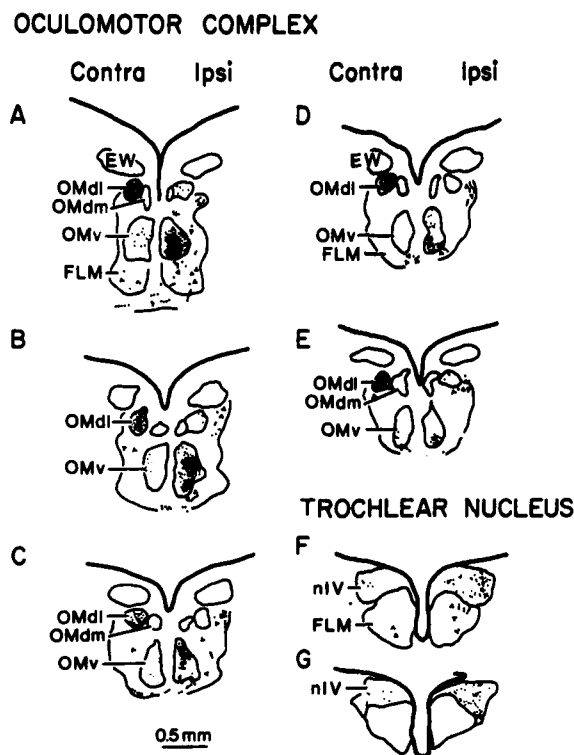


FIGURE 7. Distribution of label within the oculomotor nuclear complex and the trochlear nucleus following a unilateral injection of ³H-leucine into the nBOR complex. Chartings are of transverse sections arranged in a rostral (A) to caudal (G) sequence. EW, nucleus of Edinger-Westphal; OMDl, nucleus nervi oculomotorii, pars dorsolateralis; OMDm, nucleus nervi oculomotorii, pars dorsomedialis; OMv, nucleus nervi oculomotorii, pars ventralis; FLM, fasciculus longitudinalis medialis; nIV, nucleus nervi trochlearis. (From Brecha et al.,⁵ with permission of the publisher.)

nBOR upon the contralateral ventromedial and ipsilateral dorsolateral divisions of the oculomotor complex also has been observed. In addition, sparse bilateral projections have been observed over the trochlear nuclei, with the ipsilateral trochlear nucleus being somewhat more heavily labeled than the contralateral trochlear nucleus. No labeling was ever observed over either the ipsilateral or contralateral dorsomedial division of the oculomotor complex, the Edinger-Westphal nucleus, or the abducens nucleus. In the oculomotor nuclear complex and trochlear nucleus, the autoradiographic grains were clustered immediately adjacent to the somata and proximal dendrites of oculomotor neurons (FIGURE 8).

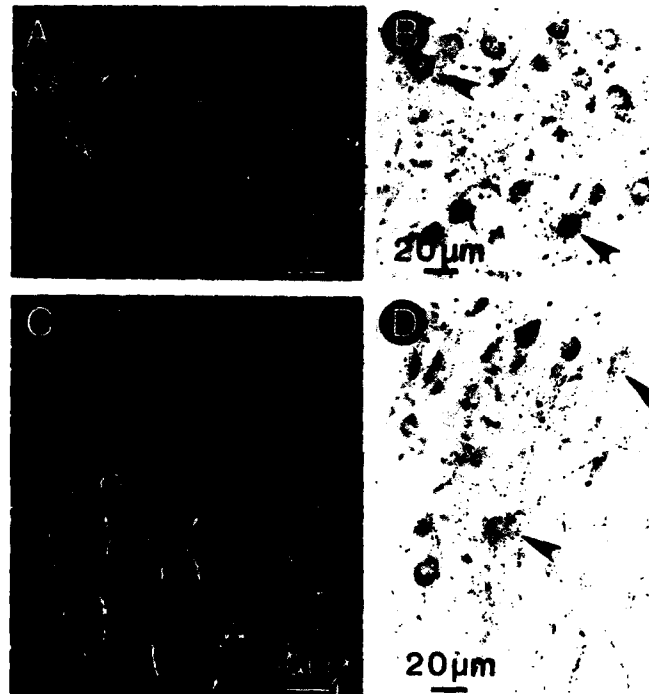


FIGURE 8. Photomicrographs of the distribution of label within the oculomotor nuclear complex. Note the clustering of label around cell bodies (arrows) and the suggestion of labeled axons by the continuous alignment of label. A and B: parasagittal sections through the contralateral dorsolateral division of the oculomotor nuclear complex. C and D: parasagittal sections through the ipsilateral ventral division of the oculomotor nuclear complex. (From Brecha *et al.*,⁵ with permission of the publisher.)

This distribution of label, which probably represents axonal terminals, implies that nBOR neurons form synaptic contacts with the somata and proximal dendrites of oculomotor neurons. This suggests that the nBOR complex has a very strong influence upon the physiological properties of oculomotor neurons.

Discrete, unilateral injections of HRP into the oculomotor nuclear complex and the trochlear nucleus have confirmed the anterograde transport studies and result in the retrograde labeling of medium and large cells (TABLE 1) within the contralateral nBOR and somewhat smaller cells located throughout the full extent of the ipsilateral nBORd.

Oculomotor Complex Projections upon the Extraocular Muscles

HRP injections into individual extraocular muscles result in the labeling of motor neurons within the oculomotor nuclear complex, trochlear nucleus, and abducens nucleus. The labeling patterns within these nuclei are similar to those described in other vertebrates. Of particular note are the projections of the dorsolateral and ventromedial nuclei of the oculomotor nuclear complex upon the ipsilateral inferior rectus and contralateral superior rectus, respectively. The dense projection of the nBOR complex upon these divisions of the oculomotor nuclear complex suggests that the accessory optic system plays a prominent role in the control of vertical eye movements.

Functional Organization of the Accessory Optic System

Anatomical studies suggest that in bird the retinal input to the main accessory optic nucleus is derived from displaced ganglion cells.²⁴⁻²⁶ In other vertebrates, including the turtle, rabbit, and chinchilla, the retinal input to the main accessory optic nucleus also appears to be derived from a limited population or populations of retinal ganglion cells.⁴⁰⁻⁴² For instance in rabbit retina, about 2,000 ganglion cells terminate upon the medial terminal nucleus.⁴¹ These retinal ganglion cells appear to have a large uniform size, occur with the highest density in and near the visual streak, and have similar physiological properties.^{16,41} In turtle and chinchilla retina, a widely spaced population of large ganglion and displaced ganglion cells also have been reported to project upon the nBOR or medial terminal nucleus.^{40,42} All of these studies thus suggest that the accessory optic system in several, and perhaps all, vertebrates receives a retinal projection from a unique and distinct population or populations of retinal ganglion cells.

Studies of the secondary projections of the AOS have strongly supported the contention that this system plays a significant role in oculomotor function.^{5,14,30,43-45} The avian nBOR complex projects upon several nuclei, all of which appear to be involved directly or indirectly in the control of eye and neck movements.^{5,14} These projections include those upon the vestibulocerebellum, the olivary nuclear complex, and the oculomotor nuclear complex as well as the interstitial nucleus of Cajal.⁵ Both retrograde and anterograde tracing studies have demonstrated that the accessory optic nuclei of several vertebrates, including the catfish, turtle, and chinchilla, give rise to a direct projection upon the vestibulocerebellum that presumably terminates as a mossy fiber system.^{5,14,42-45} In addition, in both birds and mammals, a bisynaptic retinal projection upon the inferior olivary complex has been described.^{5,36} This region of the inferior olivary complex in turn gives rise to a climbing fiber system upon the vestibulocerebellum. The existence of both mossy and climbing fiber systems that convey visual input to the cerebellum via the AOS suggests that this system plays an important role in the visual modification of cerebellar oculomotor control systems and perhaps plays a role in the vestibulo-ocular reflex.

Perhaps the most compelling argument for a role of the AOS in oculomotor functions is the existence of bisynaptic retinal inputs to the oculomotor complex.^{5,14,44,46} In birds, the nBOR complex gives rise to a direct and prominent projection upon the contralateral dorsolateral and the ipsilateral ventromedial nuclei of the oculomotor complex (FIGURE 9). These nuclei in turn give rise to projections upon the inferior rectus and superior rectus extraocular muscles of the same eye.⁵ This projection system could be the mechanism by which rapid adjustments of the oculomotor muscles are made to a peripheral visual stimulus.

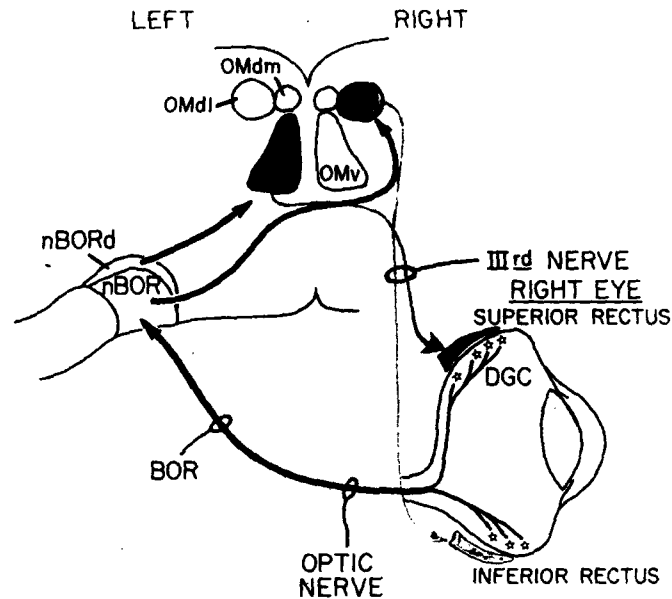


FIGURE 9. Schematic representation of (1) the nBOR complex projection upon the oculomotor nuclear complex and (2) the oculomotor nuclear complex upon the extraocular muscles.

In addition, this projection system strongly argues that the nBOR system plays a role in vertical eye movements.

Electrophysiological studies have demonstrated that neurons within the avian nBOR complex and rabbit medial terminal nucleus have large receptive fields that respond almost exclusively to large, slow-velocity, vertically moving stimuli.¹⁵⁻¹⁷ In addition, these neurons respond poorly or not at all to horizontally moving stimuli or small, slow-velocity, vertically moving stimuli. In the chicken, whose accessory optic system is organized in a manner similar to that of the pigeon, a functional organization of the nBOR complex has been described recently; neurons within the dorsal portion of the nBOR complex respond best to upward movements, while those in the ventral portion respond best to downward movements.¹⁷ These observations demonstrate a matching of the physiological and anatomical organization of the nBOR complex. That is, nBOR neurons that are responsive to upward movements are located in the dorsal region of the nBOR complex, and this region projects bisynaptically upon the superior rectus extraocular muscle. Conversely, nBOR neurons that are responsible to downward movements are located in the ventral region of the nBOR complex, and this region projects bisynaptically upon the inferior rectus extraocular muscle. Thus a downward- or upward-moving stimulus may elicit, via a bisynaptic pathway, a corresponding downward or upward movement of the eye.

Finally, behavioral studies have suggested that the accessory optic system plays a role in oculomotor behavior. In amphibians, large lesions of the AOS reportedly eliminate optokinetic nystagmus resulting from stimuli moving in the contralateral visual field.¹⁸ In turtles and pigeons, bilateral lesions of the AOS

result in a reduction in head nystagmus resulting from a horizontally moving optokinetic stimulus at high stimulus velocities.¹⁹ However, to date, no studies have evaluated the effects of AOS lesions on vertical optokinetic nystagmus. Recently, vertical optokinetic stimulation has been shown to activate the AOS selectively. In chickens, the nBOR complex can be activated by slowly moving vertical or torsional stripes but not by slowly moving horizontal stripes.²⁰ This enhancement of the metabolic activity of the nBOR complex by vertically moving stimuli implies that this system plays a role in vertical oculomotor systems.

In summary, recent anatomical studies have demonstrated that a seemingly distinct class of retinal ganglion cells give rise to a projection upon the main accessory optic nucleus (FIGURE 10). This nucleus in turn gives rise to projections upon several regions that are critical for oculomotor function, including the oculomotor nuclear complex, the inferior olivary complex, and the vestibulocerebellum. These anatomical observations, in combination with electrophysiological and behavioral studies, have thus suggested that the AOS plays an important role in oculomotor function; this role may include the initiation of an orienting movement of the eyes and neck, as suggested by Herrick,⁸ and/or the stabilization of eye and neck movements.

The apparently restricted functions of this system thus stand in marked contrast to the extremely diverse functions attributed to areas such as the optic tectum and striate cortex. The fundamental pattern of organization of the AOS is similar in all classes of vertebrates studied, and presumably reflects the essential nature of the behavior mediated by this circuit.

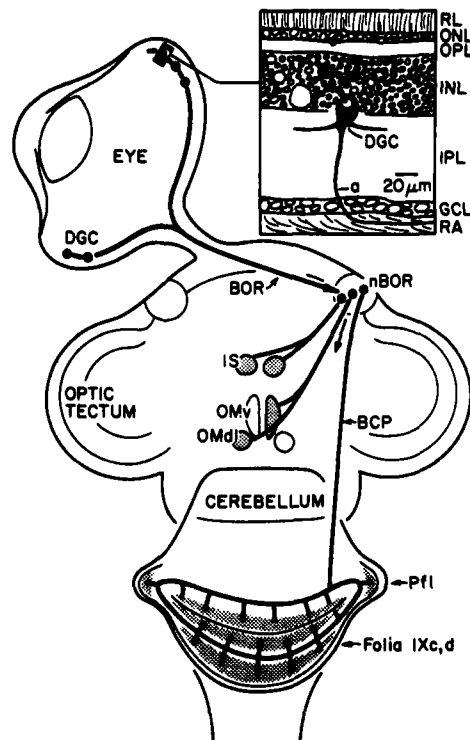


FIGURE 10. Summary schematic of the displaced ganglion cell projection upon the nBOR complex and the nBOR complex projections upon the nucleus interstitialis (IS), oculomotor nuclear complex (OMv, OMdl), and the vestibulocerebellum. (From Brecha *et al.*,⁵ with permission of the publisher.)

ACKNOWLEDGMENTS

We would like to thank Drs. C. Gall and A. Reiner for their critical reading and helpful comments in the preparation of this manuscript.

REFERENCES

1. EBBESSON, S. O. E. 1970. On the organization of central visual pathways in vertebrates. *Brain Behav. Evol.* **3**: 178-194.
2. KARTEN, H. J. 1979. Visual lemniscal pathways in birds. In *Neural Mechanisms of Behavior in the Pigeon*. A. M. Granda & J. H. Maxwell, Eds.: 409-430. Plenum Publishing Corp. New York, N.Y.
3. GUDDEN, B. 1881. Über den Tractus Peduncularis Transversus. *Arch. Psychiatr.* **11**: 415-423.
4. MAI, J. K. 1978. The accessory optic system and the retinohypothalamic system. A review. *J. Hirn. Forsch.* **19**: 213-288.
5. BRECHA, N., H. J. KARTEN & S. P. HUNT. 1980. Projections of the nucleus of the basal optic root in the pigeon. An autoradiographic and horseradish peroxidase study. *J. Comp. Neurol.* **189**: 615-670.
6. MARBURG, O. 1903. Basale Opticus Wurzel und Tractus Peduncularis Transversus. *Arb. Neurol. Inst. Univ. Zentbl. Physiol.* **17**: 30-31.
7. HAYHOW, W. R. 1959. An experimental study of the accessory optic fiber system in the cat. *J. Comp. Neurol.* **113**: 281-314.
8. HERRICK, C. J. 1948. *The Brain of the Tiger Salamander*. University of Chicago Press. Chicago, Ill.
9. PASIK, T. & P. PASIK. 1971. The visual world of monkeys deprived of striate cortex: effective stimulus parameters and the importance of the accessory optic system. *Vision Res. Suppl.* **3**: 419-435.
10. PASIK, T. & P. PASIK. 1973. Extrageniculostriate vision in the monkey. IV. Critical structures for light vs no light discrimination. *Brain Res.* **56**: 165-182.
11. PASIK, P. & T. PASIK. 1973. Extrageniculostriate vision in the monkey. V. Role of accessory optic system. *J. Neurophysiol.* **36**: 450-457.
12. MOORE, R. Y., A. HELLER, R. J. WURTMAN & J. AXELROD. 1967. Visual pathway mediating pineal response to environmental light. *Science* **155**: 220-223.
13. MOORE, R. Y. 1969. Pineal response to light: mediation by the accessory optic system in the monkey. *Nature* **222**: 781-782.
14. BRECHA, N. & H. J. KARTEN. 1979. Accessory optic projections upon oculomotor nuclei and the vestibulocerebellum. *Science* **203**: 913-916.
15. WALLEY, R. E. 1967. Receptive fields in the accessory optic system of the rabbit. *Exp. Neurol.* **17**: 27-43.
16. SIMPSON, J. I., R. E. SOODAK & R. HESS. 1979. The accessory optic system and its relation to the vestibulocerebellum. *Prog. Brain Res.* **50**: 715-724.
17. BURNS, S. & J. WALLMAN. 1981. Relation of single unit properties to the oculomotor function of the nucleus of the basal optic root (accessory optic system) in chickens. (Personal communication.)
18. LAZAR, G. 1973. Role of the accessory optic system in the optokinetic nystagmus of the frog. *Brain Behav. Evol.* **5**: 443-460.
19. FITE, K. V., A. REINER & S. P. HUNT. 1979. The accessory optic system and optokinetic nystagmus. *Brain Behav. Evol.* **16**: 192-202.
20. MCKENNA, O. & J. WALLMAN. 1980. Metabolic mapping of avian brain areas responsive to retinal slip. *Soc. Neurosci. Abstr.* **6**: 840.
21. DOGIEL, A. S. 1891. Ueber die nervösen Elemente in der Retine des Menschen. *Arch. Mikrosk. Anat.* **30**: 317-344.
22. DOGIEL, A. S. 1895. Die Retina der Vogel. *Arch. Mikrosk. Anat.* **44**: 622-648.
23. CAJAL, S. R. 1893. La retine des vertebres. *La Cellule* **9**: 17-257.

24. KARTEN, H. J., K. V. FITE & N. BRECHA 1977. Specific projection of displaced retinal ganglion cells upon the accessory optic system in the pigeon (*Columba livia*). *Proc. Nat. Acad. Sci. USA* **74**: 1753-1756.
25. REINER, A., N. BRECHA & H. J. KARTEN. 1979. A specific projection of retinal displaced ganglion cells to the nucleus of the basal optic root in the chicken. *Neuroscience* **4**: 1679-1688.
26. FITE, K. V., N. BRECHA, H. J. KARTEN & S. P. HUNT. 1981. Displaced ganglion cells and the accessory optic system of pigeon. I. *Comp. Neurol.* **195**: 279-288.
27. BINGGELI, R. L. & W. J. PAULE. 1969. The pigeon retina: quantitative aspects of the optic nerve and ganglion cell layer. *J. Comp. Neurol.* **137**: 1-18.
28. HAMDI, F. A. & D. WHITTERIDGE. 1954. The representation of the retina on the optic tectum of the pigeon. *Q. J. Exp. Physiol.* **39**: 111-119.
29. REPERANT, J. 1973. Nouvelles donnees sur les projections visuelles chez le pigeon (*Columba livia*). *J. Hirn. Forsch.* **14**: 151-187.
30. BRAUTH, S. E. & H. J. KARTEN. 1977. Direct accessory optic projections to the vestibulo-cerebellum: a possible channel for oculomotor control systems. *Exp. Brain Res.* **28**: 73-84.
31. RIO, J.-P. 1979. The nucleus of the basal optic in the pigeon: an electron microscope study. *Arch. Anat. Microsc. Morphol. Exp.* **68**: 17-27.
32. KORTE, G. E., H. J. KARTEN & N. BRECHA. 1981. Anatomical organization of the pigeon accessory optic nucleus—the nucleus of the basal optic root. (In preparation.)
33. KARTEN, H. J. & T. E. FINGER. 1976. A direct thalamocerebellar pathway in pigeon and catfish. *Brain Res.* **102**: 335-338.
34. ITO, M. 1978. Cerebellar control mechanisms of movements investigated in connection with vestibular functions. *Neuroscience* **3**: 117-118.
35. KOOY, F. H. 1917. The inferior olive in vertebrates. *Folia Neurobiol.* **10**: 205-369.
36. BRECHA, N. & H. J. KARTEN. 1978. A visual climbing fiber input to the vestibulocerebellum: an accessory optic-inferior olivary-vestibulocerebellar projection system. *Soc. Neurosci. Abstr.* **4**: 621.
37. FREEDMAN, S. L., J. VOOGD & G. J. VIELVOYE. 1977. Experimental evidence for climbing fibers in the avian cerebellum. *J. Comp. Neurol.* **175**: 243-252.
38. MAEKAWA, K. & J. I. SIMPSON. 1972. Climbing fiber activation of Purkinje cells in the flocculus by impulses transferred through the visual pathway. *Brain Res.* **39**: 245-251.
39. MAEKAWA, K. & J. I. SIMPSON. 1973. Climbing fiber responses evoked in vestibulocerebellum of rabbit from visual system. *J. Neurophysiol.* **36**: 649-666.
40. REINER, A. 1981. A projection of displaced ganglion cells and giant ganglion cells to the accessory optic nuclei in turtle. *Brain Res.* **204**: 403-409.
41. OYSTER, C. W., J. I. SIMPSON, E. S. TAKAHASHI & R. E. SOODAK. 1981. Retinal ganglion cells projecting to the rabbit accessory optic system. *J. Comp. Neurol.* **190**: 49-61.
42. KIMM, J., J. A. WINFIELD & A. E. HENDRICKSON. 1979. Visual-vestibular interactions and the role of the flocculus in the vestibulo-ocular reflex. *Prog. Brain Res.* **50**: 703-713.
43. WINFIELD, J. A., A. E. HENDRICKSON & J. KIMM. 1979. Anatomical evidence that the medial terminal nucleus of the accessory optic tract in mammals provides a visual mossy fiber input to the flocculus. *Brain Res.* **151**: 175-182.
44. FINGER, T. E. & H. J. KARTEN. 1978. The accessory optic system in teleosts. *Brain Res.* **153**: 144-149.
45. REINER, A. & H. J. KARTEN. 1978. A bisynaptic retinocerebellar pathway in the turtle. *Brain Res.* **150**: 163-169.
46. MONTGOMERY, N., K. V. FITE & L. BENGSTON. 1979. The anuran accessory optic system: neuroanatomical analysis. *Soc. Neurosci. Abstr.* **5**: 798.

VISUAL-VESTIBULAR INTERACTION IN
VESTIBULAR NEURONS:
FUNCTIONAL PATHWAY ORGANIZATION*

Wolfgang Precht
Brain Research Institute
University of Zurich
CH-8029 Zurich, Switzerland

Visual information signaling motion of large parts of the visual surround may reach the brain via crossed or both crossed and uncrossed retinofugal fibers and generates through central circuits eye and/or head movements that try to compensate for surround motion, thereby stabilizing a given visual image on the retina. The input-output relationship of this velocity control system has been studied particularly well for the horizontal optokinetic eye nystagmus (OKN) in rabbit, cat, and monkey;¹⁻⁵ but relatively little is known about the pathway organization from the retina to ocular motoneurons. Thus, it has been shown that in foveate animals, OKN is still present after complete removal of the bilateral visual cortex.^{6,7} More specifically, it is only the OKN evoked by temporonasal surround motion that is little affected by cortical ablation, whereas nasotemporally directed stimuli produce a very poor OKN response in the absence of the visual cortex. Foveate animals without visual cortex, therefore, show an OKN pattern similar to that found in intact afoveate animals such as the rabbit and rat.^{1,8} Recent work employing the split optic chiasma paradigm or unilateral section of the optic tract has revealed that the system most independent of the visual cortex is the crossed retinofugal system responding to temporonasal surround motion.⁷ All other systems (uncrossed temporonasal and nasotemporal and crossed nasotemporal) either are not able to generate OKN without the cortex or mediate only very poor responses. Therefore, the OKN mediated by the crossed retinofugal system is the most basic one, requires only the integrity of the brain stem, and is present in all vertebrates so far studied.

In investigating OKN pathways, it is therefore reasonable to start out with this phylogenetically old system. We have chosen the rat as an experimental animal, since in this afoveate species, only the crossed temporonasal system generates significant OKN responses with monocular stimulation.^{7,8} For a comparison, we studied the OKN pathways in the cat, which has an area centralis and may be considered a representative of the foveate species.

Based on studies of the exact time course of the OKN generated by velocity steps of surround motion, the existence of direct and indirect pathways has been postulated.⁵ The *direct* path very rapidly brings the OKN slow-phase velocity to a fraction of the final steady-state velocity, and the *indirect* path provides the additional slower rise of OKN velocity to the steady-state value observed during prolonged stimulation. In anatomical terms, the direct path may consist of a three-neuron arc composed of the axons of the optic nerve and central relay neurons whose axons directly contact ocular motoneurons. Anatomical evidence for such connections exists in birds and amphibia.^{9,10} The indirect path is polysynaptic in nature and involves the vestibular nuclei on its way to motoneurons. It is this pathway that is of particular relevance in the context of the present paper.

*Supported by Grants No. 3.505.79 and 3.616.80 of the Swiss National Foundation for Scientific Research and the Dr. Eric Slack-Gys Foundation.

There is overwhelming evidence that vestibular nuclear neurons (Vn) of various species respond not only to vestibular but also to pure optokinetic stimuli and the responses evoked by the two systems interact synergistically.^{8,11-15} Since many of the Vn project directly or indirectly to ocular motoneurons, the transvestibular optokinetic path has a powerful access to the final motor output stage. The importance of the vestibular system for OKN is also demonstrated by the fact that both OKN and optokinetic after-nystagmus, the latter of which is an expression of a velocity storage mechanism, are severely affected by a bilateral labyrinthectomy.^{16,17} The experiments to be described here were designed to elaborate the pathways mediating optokinetic responses of Vn in the rat and cat.

MATERIAL AND METHODS

Details have been described in previous publications.^{8,18-20} In brief, all single unit recordings were performed in alert (paralyzed or unparalyzed) rats (DAHAN) or cats prepared under anesthesia for chronic recording. Electrolytic lesions of various brain structures were performed from a few hours up to three days prior to recording. Recording sites were marked by Pontamine Blue electrophoretically ejected from the recording pipettes. All experimental brains were sectioned and stained with the Nissl technique to delineate the extent of the lesions or the position of dye marks.

In many animals, the horizontal electro-oculogram (EOG) was recorded prior to and after the lesion, and the eye movements evoked by horizontal rotation in the dark (vestibulo-ocular reflex, VOR) and by moving a large patterned surround (OKN) were measured (for details, see Reference 20).

Pure vestibular stimulation was achieved by applying trapezoidal or sinusoidal rotations with a Toennies turntable in the dark; they served to identify the units as type I or type II neurons of the horizontal canal system. Pure optokinetic stimuli were produced by a Toennies shadow projector producing a stripe pattern on a cylinder surrounding the animal; stimulus velocities could be varied from 0.2-60°/second.

To ascertain alertness, particularly in the paralyzed state, amphetamine (0.5 mg/kg) was injected prior to the recording session and renewed once during longer sessions.

The signal from the microelectrode was amplified by conventional electronics, displayed on an oscilloscope, and played over an audiomonitor. The same signal after amplitude discrimination with a window detector was converted to the instantaneous discharge rate and also smoothed with a first-order filter and displayed on a brush recorder together with table position or drum velocity.

In 14 rats, stimulating electrodes consisting of stainless-steel wires, insulated except for the tip, were inserted into various brain structures (see below) for monopolar stimulation.

RESULTS AND DISCUSSION

Optokinetic Responses of Vestibular Neurons in Control Animals

In both rat and cat, nearly all type I and type II Vn neurons responded to optokinetic stimulation in a direction-specific manner. As shown in FIGURE 1 and TABLE 1, type I Vn increased their discharge rate on surround motion directed

contralaterally to the recording side, and a decrease in firing occurred on opposite stimulus direction. Responses of type II Vn were mirror images of those of type I. Thus, the optokinetic responses of both types of Vn were synergistic with their vestibular responses, which increased or decreased their firing rates on rotation in the dark always in directions opposite to those of the optokinetic stimuli.

FIGURE 1 illustrates some important features of the time course of the optokinetic responses. There was often a delay of one to three seconds following the onset of the stimuli before a change in firing occurred. After this delay, the firing changed gradually to reach a plateau, which could be maintained or slightly reduced during the remainder of the stimulation. As shown in FIGURE 2, the mean peak increases and decreases in the rat occurred at retinal-slip

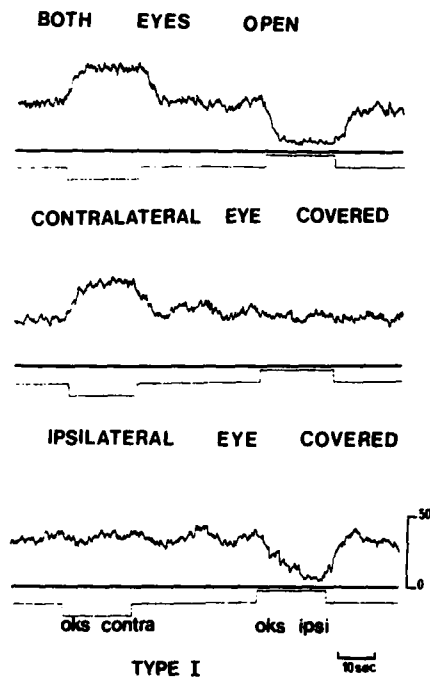


FIGURE 1. Response behavior of rat type I vestibular neuron to optokinetic stimulation (OKS) in binocular and monocular conditions. Upper trace in each set of records shows smoothed instantaneous frequency of a single unit, middle trace indicates zero level of discharge, and lower trace gives the stimulus profile, i.e., velocity of OKS ($1^\circ/\text{second}$). Note that recordings were obtained in paralyzed state.

velocities of $1^\circ/\text{second}$, whereas in the cat the peak occurred at higher velocities of ca. $10^\circ/\text{second}$.

Another important difference between Vn responses in rat and cat was noted when monocular stimuli were applied. In the rat (FIGURE 1, TABLE 1), monocular stimulation changed the bidirectionally selective responses seen in binocular condition to unidirectionally selective response patterns. In the cat, however, response bidirectionality was maintained in monocular condition,¹⁵ i.e., both temporonasal and nasotemporal stimulus directions gave responses. It is noteworthy to mention that the actual $\pm \Delta f$ (frequency of spike firing) values in monocular condition were very similar (TABLE 1). Further details are described elsewhere and are of minor interest in the present context.⁸

TABLE 1
RESPONSE PATTERNS OF TYPE I AND TYPE II VESTIBULAR NEURONS TO BINOCULAR AND MONOCULAR
OPTOKINETIC STIMULATIONS (1°/SECOND) IN PARALYZED ANIMALS*

	Both Eyes Opened		Ipsilateral Eye Covered		Contralateral Eye Covered	
	Type I (n = 51)	Type II (n = 34)	Type I (n = 16)	Type II (n = 29)	Type I (n = 19)	Type II (n = 15)
OKS	Excitation	Inhibition	No	No	Excitation	Inhibition
Contralateral	+ $\Delta f = 18.22 \pm 10.39$	- $\Delta f = 11.96 \pm 4.89$	Excitation	Inhibition†	+ $\Delta f = 19.93 \pm 9.15$	- $\Delta f = 10.08 \pm 4.56$
OKS	Inhibition	Excitation	Inhibition	Excitation	No	No
Ipsilateral	- $\Delta f = 11.84 \pm 6.43$	+ $\Delta f = 17.71 \pm 9.91$	- $\Delta f = 10.32 \pm 5.61$	+ $\Delta f = 15.72 \pm 8.11$	Inhibition	Excitation†

* Δf = mean frequency increase (+ Δf) or decrease (- Δf) of Vn discharge in impulses/second.
†9% of the units showed a small change in firing ($\Delta f = 3$ impulses/second).

Effects of Lesions on Vn Responses

In our attempt to study optokinetic pathways to Vn, we first placed lesions in various nuclei and fiber tracts. We then measured in these lesioned animals the Vn responses to optokinetic stimuli and compared them to the control values described above. Both qualitative (i.e., directionality of responses) and quantitative measures ($\pm \Delta f$ values) were taken with the same stimulations as in the control studies.

Lesions of the Pretectum

There is strong experimental evidence suggesting that the pretectum is a crucial, first link in the afferent path of the horizontal optokinetic reflex arc in the rabbit.²¹ Among the various pretectal nuclei, the nucleus of the optic tract (NOT)

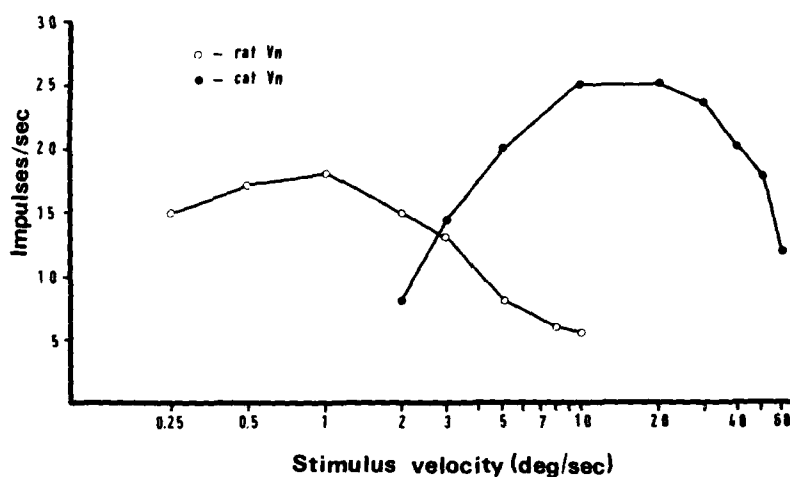


FIGURE 2. Mean values of frequency increase (mean steady state minus mean resting rate) of Vn of cat (●) and rat (○) measured in paralyzed state.

is probably the most crucial one since its neurons in the rabbit and cat have response characteristics compatible with OKN and very similar to those recorded in Vn and they receive direct projections from the retina.^{22,23} Furthermore, electrical stimulation of the NOT generated nystagmus, while lesions abolished OKN.^{21,22}

To test the importance of the pretectum for optokinetic responses in Vn and OKN, we placed unilateral and bilateral lesions in this area and recorded Vn activity and OKN thereafter. FIGURE 3 shows a projection drawing of the extent of a lesion in the left pretectum of the rat and the effects of this lesion on the optokinetic responses of type I and type II Vn recorded in the right vestibular nucleus. With unilateral lesions, the responses became unidirectional with binocular viewing and were thus similar to those obtained in control animals with monocular viewing. In addition, as seen in TABLE 2, monocular viewing with

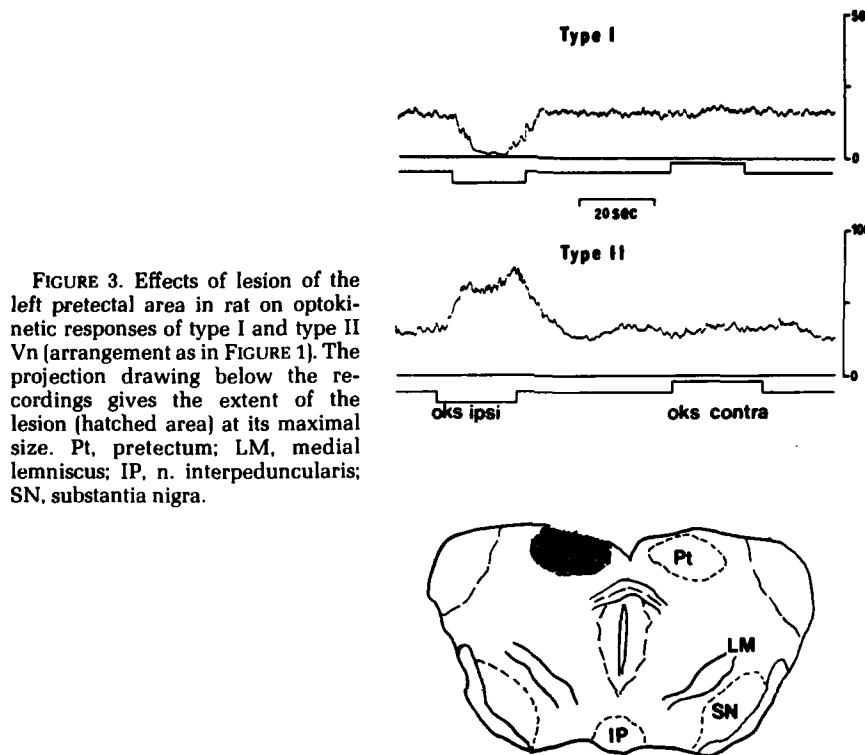


FIGURE 3. Effects of lesion of the left pretectal area in rat on optokinetic responses of type I and type II Vn (arrangement as in FIGURE 1). The projection drawing below the recordings gives the extent of the lesion (hatched area) at its maximal size. Pt, pretectum; LM, medial lemniscus; IP, n. interpeduncularis; SN, substantia nigra.

the ipsilateral eye gave no responses in lesioned animals. This finding shows that in the rat, uncrossed retinotectal fibers cannot drive Vn. It should be noted (TABLE 2) that the Δf values of Vn in lesioned animals were not significantly different from control values, indicating that the contralateral pretectum does not contribute much to the response sensitivity. Needless to say, bilateral lesions abolished all responses in Vn.

TABLE 2
EFFECTS OF UNILATERAL PRETECTAL LESIONS ON OPTOKINETIC RESPONSES OF TYPE I AND TYPE II Vn (STIMULUS VELOCITY = 1°/SECOND) IN PARALYZED RATS WITH BOTH EYES OPEN*

	Lesioned Side		Intact Side	
	Type I (n = 12)	Type II (n = 15)	Type I (n = 5)	Type II (n = 11)
OXS Contralateral	Excitation $+\Delta f = 16 \pm 6.78$	Inhibition $-\Delta f = 9.93 \pm 4.24$	No Excitation	No Inhibition
OXS Ipsilateral	No Inhibition	No Excitation	Inhibition $-\Delta f = 11 \pm 4.05$	Excitation $+\Delta f = 15.05 \pm 7.33$

* Δf = mean frequency increase (+ Δf) or decrease (- Δf) of Vn discharge in impulses/second.

In the cat, bilateral pretectal lesions including the NOT almost abolished optokinetic responses in Vn, and unilateral lesions caused a strong reduction of normal responses on either side of the lesion (TABLE 3). Since in the cat monocular optokinetic stimulation gives bidirectional responses (see above) and uncrossed fibers are capable of carrying the optokinetic signal, the remaining ca. 30% of qualitatively normal responses found in unilaterally lesioned animals are readily explained. It should be noted, however, that the sensitivity of these apparently normal Vn responses was strongly reduced (see Δf in TABLE 3). Our results, therefore, strongly support the notion that both in rat and cat, the pretectum is a crucial link in the central optokinetic path to the vestibular nuclei.

Lesion of the Nucleus Reticularis Tegmenti Pontis (NRTP)

In the preceding section, it was demonstrated that the integrity of the pretectum is essential for obtaining optokinetic responses from Vn. Since apparently there are no direct pretectal projections to Vn,^{24,25} we searched for possible

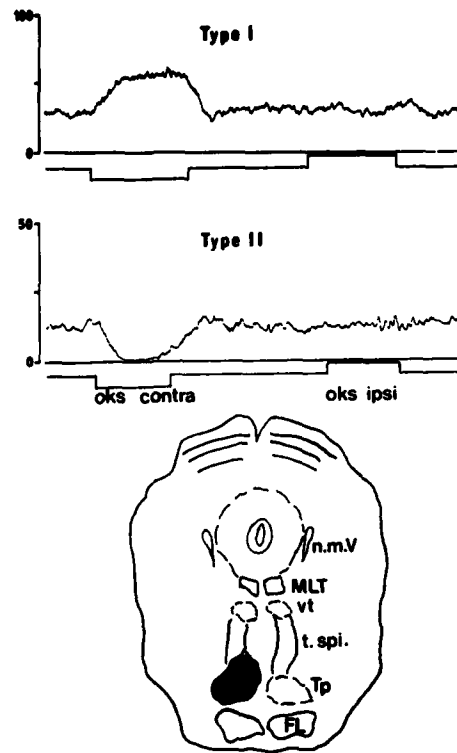
TABLE 3
SUMMARY OF THE RESPONSES OF TYPE I AND TYPE II NEURONS IN THE VESTIBULAR
NUCLEI TO OPTOKINETIC STIMULI: EFFECTS OF VARIOUS LESIONS IN THE CAT

Type of Lesion	Units Tested	Normal Response	No Response	Uni-directional	Inverted	+ Δf (imp/sec)
Bilateral Pretectum	78	4 (5.2%)	54 (69.2%)	7 (9%)	13 (16.7%)	11.0
Unilateral Pretectum	77	25 (32.5%)	21 (27.3%)	22 (28.6%)	9 (11.7%)	17.0
Bilateral Ret. Tgm. Pontis	152	37 (24.3%)	87 (57.2%)	26 (17.1%)	2 (1.3%)	12.7
Bilateral Ventrolateral Midbrain	33	18 (54.5%)	5 (15.1%)	8 (24.2%)	2 (6.1%)	13.6
Central Tgm. Tract	44	37 (84.4%)	2 (4.5%)	3 (11.4%)	0	26.2
Intact Animals	62	58 (93.5%)	3 (4.8%)	1 (1.6%)	0	26.0

relay nuclei and found that lesions of the NRTP in the rat (TABLE 4) and in the cat (TABLE 3) abolished optokinetic responses in Vn.

FIGURE 4 gives an example of an experiment in which the left NRTP of a rat has been lesioned; the response deficits are very similar to those described above for pretectal lesions. Lesions placed in the same anterior-posterior level but more dorsally and involving the tectospinal tracts, ventral tegmental nuclei, or medial longitudinal fascicle had no appreciable effects on Vn responses. When the lesions were placed between pretectum and NRTP deep in the midbrain, effects were similar to those after pretectal or NRTP lesions. This finding suggests that pretectofugal fibers after leaving the pretectum run ventrally in the midbrain to the region of NRTP. Whether these fibers actually terminate there cannot be told from lesion studies. Single unit recordings from NRTP neurons during optokinetic stimulation are required to answer this question. They will be described later.

FIGURE 4. Effects of lesion of the NRTP in rat on optokinetic responses of type I and type II Vn (arrangement as in FIGURE 1). Extent of lesion is shown in the projection drawing. FL, fasciculus longitudinalis; MLT, medial longitudinal tract; n.m.V., nucleus mesencephalicus V.; TP, n. reticularis tegmenti pontis; t. spi., tractus tectospinalis; VT, n. ventralis tegmenti.



Lesion of the Vestibular Commissure

In control rats, it has been demonstrated that with binocular viewing, type I and type II Vn responded with a decrease or increase respectively to ipsilaterally directed stimuli and showed an increase or decrease on reverse stimulation (TABLE 1). Response bidirectionality was abolished with monocular viewing (TABLE 1): type I and type II Vn located ipsilaterally to the covered eye decreased

TABLE 4
EFFECTS OF UNILATERAL LESION OF NRTP ON VN IN RAT*

	Lesioned Side		Intact Side	
	Type I (n = 13)	Type II (n = 18)	Type I (n = 6)	Type II (n = 2)
OKS Contralateral	Excitation $+ \Delta f = 11.04 \pm 3.13$	Inhibition $- \Delta f = 11 \pm 5.42$	No Excitation	No Inhibition
OKS Ipsilateral	No Inhibition	No Excitation	Inhibition $- \Delta f = 10.83 \pm 6.55$	Excitation $+ \Delta f = 9 \pm 1.41$

*Arrangement as in TABLE 2.

or increased, respectively, their firing on ipsilateral surround motion and showed no responses on contralateral stimuli; on the contralateral side, Vn showed the reverse responses.

When the vestibular commissure was interrupted,²⁶ the response pattern changed: with binocular viewing, Vn responded as they did during monocular stimulation in intact animals (TABLE 5). The same pattern was noted in commissurotomized animals when the eye ipsilateral to the recording side was covered; however, no responses occurred when the contralateral eye was covered (TABLE 5, FIGURE 5). This finding clearly indicates that no effective transfer of optokinetic signals occurs rostral to the vestibular nuclei, e.g., between the pretecta. It also implies that in the rat, the bidirectionality of the Vn responses to optokinetic stimuli is achieved by the vestibular commissure. Thus, temporonasal surround motion presented to either eye is transmitted via the commissure to Vn on both sides, and due to the reversal in signs in the inhibitory commissure,²⁶ the bilateral Vn responses always are mirror images.

Other Lesions

Lesions of well-defined descending tracts, such as the tectospinal tract, the medial longitudinal fascicle, and the central tegmental tracts, had no appreciable effect on optokinetic Vn responses of cat and rat.^{18,20}

Removal of the visual cortex or the superior colliculi in the rat likewise did not abolish Vn responses. In the cat, however, bilateral removal of the visual cortex rendered Vn responses unidirectional in monocular viewing, i.e., they were similar to those seen in intact rats. The OKN recorded simultaneously in these animals was likewise asymmetrical, i.e., the response to nasotemporal stimuli was weak or absent. This finding is in keeping with the view that the visual cortex is required for optokinetic responses mediated by the uncrossed retinofugal fibers as well as those carried by the crossed nasotemporal system.⁷

In cats with only the optic chiasma split, Vn responses were qualitatively normal, indicating that with the visual cortex intact the uncrossed system alone can generate the typical optokinetic responses in Vn. Splitting the optic chiasma in rats abolished both OKN and Vn responses.

After the discovery of a visual-evoked response in the cerebellar flocculus,²⁷ an optokinetic route from the pretectum via the flocculus to the Vn has been widely discussed. The latter was shown to receive optokinetic and vestibular inputs via both mossy and climbing fiber afferents and to project via Purkinje cell axons to Vn (for references, see 28). Of relevance for this hypothesis is the finding that the pretectum projects to the inferior olive,^{24,25} which in turn projects via climbing fibers to the flocculus. Also, optokinetically driven cells in the NOT were antidromically fired by stimulation of the olive.²⁹ As for the optokinetic responses mediated to the flocculus by the mossy fibers, it is of interest to note that there is some evidence that the NRTP is of importance.³⁰ The latter also projects directly to the flocculus.³¹

It has been shown recently, however, that either complete cerebellar ablation or selective floccular ablations in cat and rat had no effect on optokinetic Vn responses at the qualitative level.^{15,16} Vn responses were, however, less sensitive, particularly at higher stimulus velocities (FIGURE 6). These findings suggest that the transcerebellar route has a modulatory role but is not an essential link in the optokinetic path to Vn and the motor system.

TABLE 5
EFFECTS OF SECTIONING THE VESTIBULAR COMMISSURE IN RATS ON THE RESPONSES OF VN TO OPTOKINETIC STIMULI
(OKS VELOCITY = 1°/SECOND) IN ONE- OR TWO-EYES OPENED CONDITION*

	Both Eyes Opened		Ipsilateral Eye Covered		Contralateral Eye Covered	
	Type I (n = 21)	Type II (n = 17)	Type I (n = 13)	Type II (n = 6)	Type I (n = 13)	Type II (n = 6)
OKS Contralateral	No Excitation	No Inhibition	No Excitation	No Inhibition	No Excitation	No Inhibition
OKS Ipsilateral	Inhibition $\Delta f = 10.59 \pm 6.56$	Excitation $\Delta f = 13.32 \pm 9.91$	Inhibition $\Delta f = 12 \pm 5.59$	Excitation $\Delta f = 9 \pm 5.40$	No Inhibition	No Excitation

*Numbers give mean $\pm \Delta f$ values obtained in 38 units in six rats. Of these, only 3 units showed weak responses to OKS contralateral, presumably due to incomplete sectioning of the commissure.

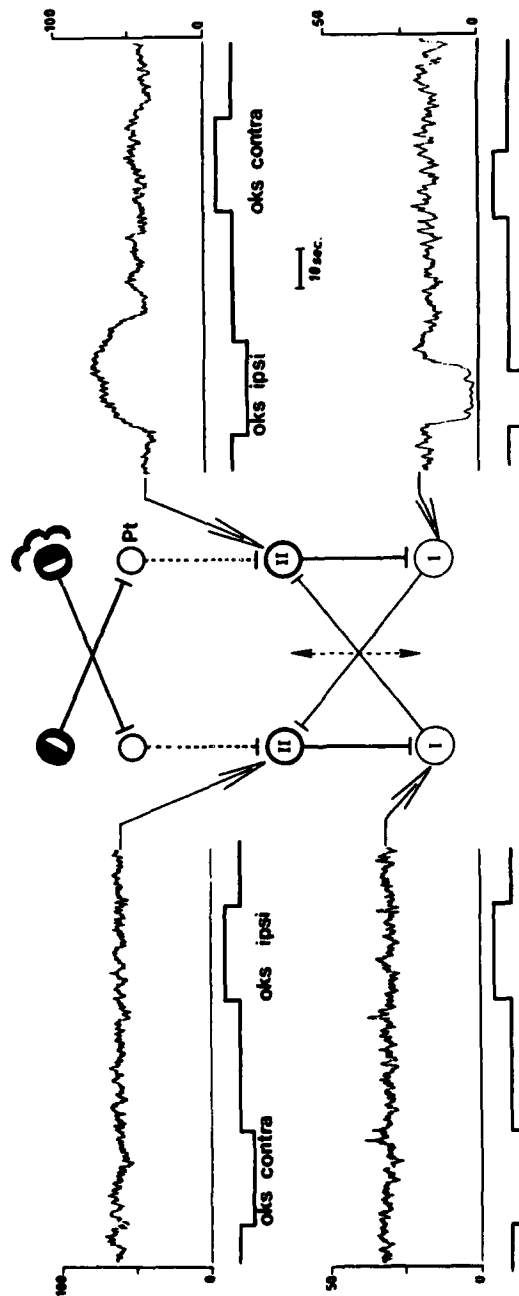


FIGURE 5. Effects of midline section of the vestibular commissure on monocular optokinetic responses of type I and II vestibular neurons. Note the lack of response to OKS (1°/second) on the side contralateral to the covered eye. On the ipsilateral side, responses are unidirectional and only elicited by OKS ipsilateral to the recording side. The schematic between the recordings gives the basic wiring of the commissural connections. Note that type II neurons are inhibitory and type I excitatory in nature in this simplified diagram (for details, see text and FIGURE 11).

Effects of Lesions on OKN and Visual-Vestibular Interactions

Since the OKN is one of the final motor acts in the optokinetic system, it would be of interest to know whether lesions abolishing optokinetic responses in Vn (i.e., in presumed premotor neurons) would also affect OKN. We therefore recorded OKN in animals with pretectal, NRTP, and cortical lesions, all of which affected optokinetic Vn responses (see above).

Cats who had undergone a bilateral removal of the visual cortex showed a highly asymmetrical OKN when viewing monocularly a moving visual surround; the asymmetry was caused by a poor response to nasotemporal surround motion.⁷ The gain of the temporonasal stimuli was affected only slightly. When the same operation was performed in rats, no major change in OKN occurred, i.e., the responses to temporonasal stimuli were present and the nasotemporal ones were absent as in control animals. Thus, the OKN data obtained after cortical ablations paralleled those reported for Vn.

In both cat and rat (FIGURE 7), unilateral lesions of the pretectum or NRTP strongly reduced or abolished the OKN induced by surround motion toward the side of the lesion.^{18,20} Bilateral lesions abolished OKN in both directions. This finding indicates that when the brain-stem relay of the crossed retinofugal fibers is destroyed, the uncrossed system apparently is not capable of producing an OKN with a gain comparable to that noted in cats with optic chiasma lesions.

When an animal turns its head in the light, vestibular and optokinetic systems work together to generate a perfectly compensatory VOR over a wide range of stimulus velocities. Alternatively, fixation mechanisms may be used to suppress vestibular nystagmus. When the optokinetic system was impaired by the lesions just described, these so-called visual-vestibular interactions were likewise deficient.^{7,20} For example, in cats with bilateral cortex ablations, postrotatory nystagmus no longer could be suppressed when the vestibular slow phase was directed nasally. Similarly, when animals were rotated at low frequencies and velocities, the phase and gain changes occurring when comparing the VOR elicited in dark and light were missing or poor.

Responses of Units in the Pretectum and NRTP to Optokinetic and Vestibular Stimuli

To support the tentative conclusion derived from our lesion experiments that the pretectum and NRTP are crucial links in the horizontal optokinetic system, we recorded from neurons in these nuclei in the rat during optokinetic stimulations. For unit recording, rats were always paralyzed (see Methods) so that optokinetic-stimulus velocities equaled retinal-slip velocities. To test for possible visual-vestibular interaction, most units were also tested with horizontal table rotation in the dark.

TABLE 6 summarizes the different unit responses obtained in the pretectum and NRTP. It is important to note that in both the pretectum and the NRTP, the majority of neurons had their firing increase when the stimuli were presented in the temporonasal direction to the eye contralateral to the recording side; other stimuli were unable to change the resting rates of these units. The implication of these data will be discussed in the next section. It should also be noted, however, that in addition to the most typical responses, other response types have been found, indicating that pretectal and NRTP neurons may subservise several functional systems.

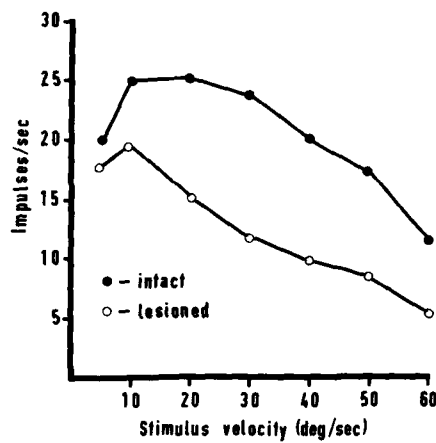


FIGURE 6. Effects of removal of the entire cerebellum in cat on mean responses of Vn to optokinetic stimulation.

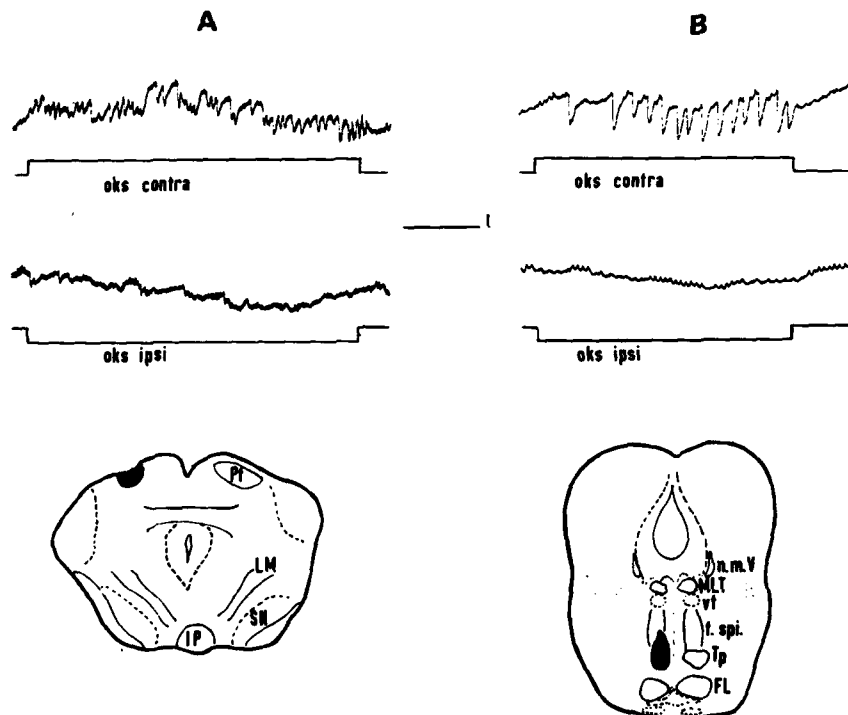


FIGURE 7. Effects of pretectal and NRTP lesions on OKN. In **A** (pretectal) and **B** (NRTP), EOG recordings and projection drawing of the lesions are shown. OKN was evoked by surround motion with a velocity of 5° /second. Both eyes were open. Note absence of OKN when the pattern moved in the direction of lesion. Calibrations: time, 5 seconds; amplitude of eye movement, 1° .

TABLE 6
OPTOKINETIC RESPONSE PATTERNS OF SINGLE UNITS IN PRETECTUM, NRTP, AND VN TO
MONOCULAR (IPSI- AND CONTRALATERAL EYE) OPTOKINETIC STIMULATION
(VELOCITY STEPS OF 0.25-15°/SECOND)*

	Pattern of Optokinetic Responses	Ipsilateral Eye		Contralateral Eye		Number of Units	Vestibular Type
		T-N	N-T	T-N	N-T		
Pretectum	Unidirectional	—	—	↑	—	30 (48%)	—
	Bidirectional	↓	—	↑	—	10 (16%)	—
	Selective	—	—	↑	↓	4 (6%)	—
	Nonselective	↑	—	↑	—	2 (3%)	—
		↑	↑	—	↑	10 (16%)	—
NRTP	Bidirectional	—	—	↓	↓	6 (9.5%)	—
	Nonselective	—	—	↑	—	1 (1.5%)	—
		↑	—	—	—	16 (43%)	II
		↑	—	—	—	3 (8%)	I
Vn	Bidirectional	—	—	↑	—	6 (16%)	II
	Nonselective	—	—	↑	—	12 (33%)	I
		↑	—	—	—	34 (40%)	II
Vn	Selective	↑	—	↑	—	51 (60%)	I
		↑	—	↑	—	51 (60%)	I

*T-N, temporonasal; N-T, nasotemporal stimulus direction. Column on the far right-hand side gives response to pure vestibular stimuli. Symbols indicate: —, no response; ↑, increase and ↓, decrease of resting rate.

Comparing the typical optokinetic response patterns of pretectal (FIGURE 8) and NRTP (FIGURE 9) neurons, it is apparent that the discharge of the former shows a much faster time to peak levels than that of the latter and likewise the decay times are different.

Other very important differences between the two populations of neurons were observed when pure vestibular stimuli were applied. Whereas pretectal neurons showed no response to this stimulation, the typical NRTP units all showed a type II response pattern (TABLE 6).

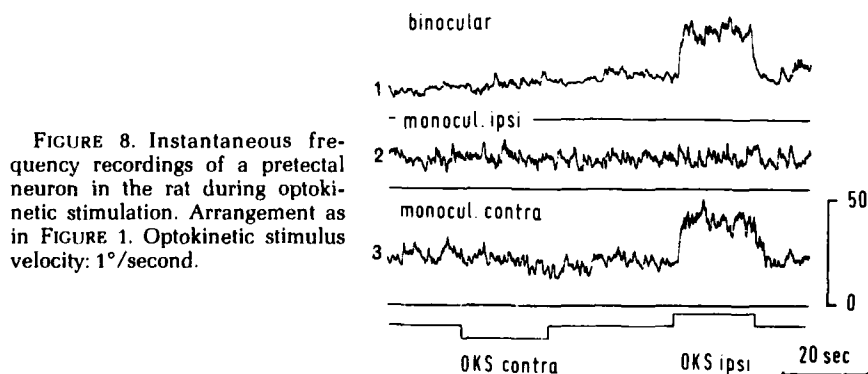


FIGURE 8. Instantaneous frequency recordings of a pretectal neuron in the rat during optokinetic stimulation. Arrangement as in FIGURE 1. Optokinetic stimulus velocity: 1°/second.

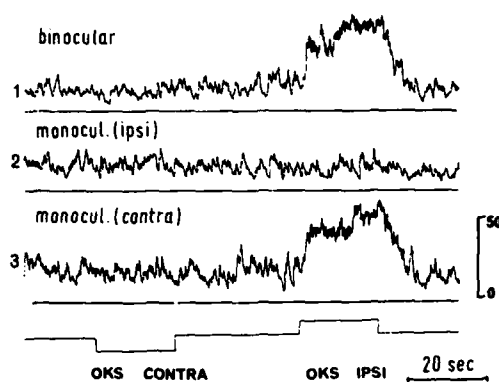


FIGURE 9. Instantaneous frequency recordings of a neuron located in the NRTP. Arrangement as in FIGURE 1.

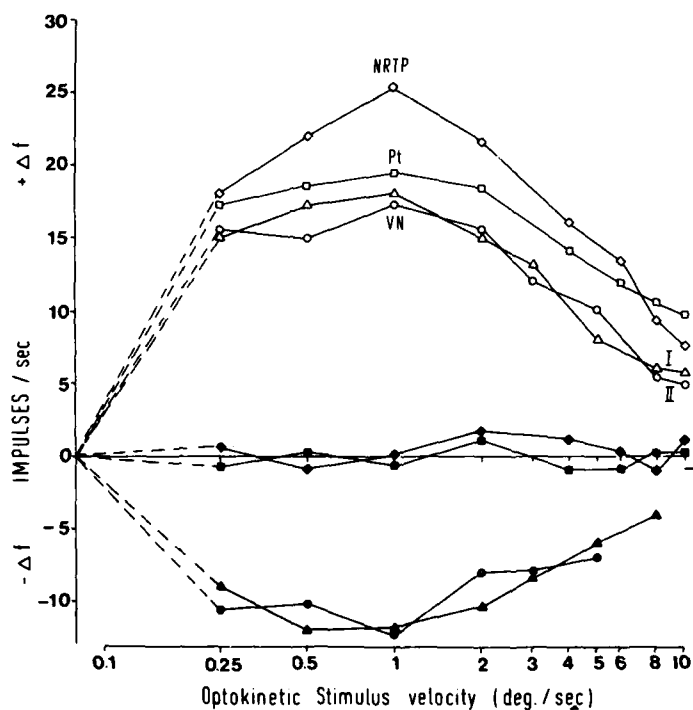


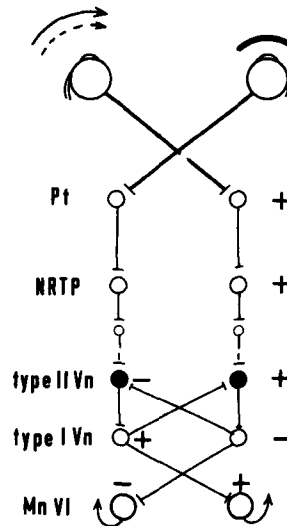
FIGURE 10. Responses of vestibular, pretectal, and NRTP neurons to optokinetic velocity steps. Mean values of frequency increase ($+\Delta f$) and decrease ($-\Delta f$) elicited in type I (Δ , \blacktriangle) and in type II (\circ , \bullet) vestibular neurons (VN); binocular OKS contralateral and OKS ipsilateral evoked increase (Δ) and decrease (\blacktriangle) in type I units, respectively, and decrease (\bullet) and increase (\circ) in type II neurons. Responses of pretectal (Pt; \square , \blacksquare) and NRTP (\circ , \bullet) neurons to OKS ipsilateral (open symbols) and contralateral (filled symbols).

Comparison between Optokinetic Responses of Pretectal, NRTP, and Vestibular Neurons

The results described above have shown that the majority of prepectal and NRTP neurons increase their firing when the contralateral eye is viewing a temporonasally moving pattern and show no change in resting discharge on reverse stimulus directions or on the stimulation of the ipsilateral eye (TABLE 6, FIGURE 10). Such a response pattern is also noted in type II Vn (FIGURE 10). Concurrently, type I Vn recorded on the same side show a decrease in discharge. Type I Vn on the side ipsilateral to the stimulated eye increase and type II decrease their firing (TABLE 1) providing the vestibular commissure stays intact.

At the quantitative level, the response properties of these three types of neurons are likewise strikingly similar. FIGURE 10 compares the mean frequency increases ($+\Delta f$) of prepectal, NRTP, contralateral type II, and ipsilateral type I

FIGURE 11. Tentative schematic diagram of the horizontal, indirect optokinetic path to Vn and abducens motoneurons. On the right-hand side, the response signs—i.e., increase (+) and decrease (–) in firing—are indicated for an optokinetic stimulus being temporonasal for the left eye (right eye covered). This stimulus causes an OKN with the slow phase to the right, i.e., firing noted in abducens motoneurons is appropriate. On the left-hand side, neuronal groups are identified: Pt, prepectum; NRTP, n. reticularis tegmenti pontis; Vn, vestibular neuron; Mn VI, abducens motoneuron. Note that broken line indicates polysynaptic path and neurons shown in filled symbols are inhibitory in nature.



Vn as well as the frequency decreases ($-\Delta f$) of contralateral type I and ipsilateral type II Vn obtained with different magnitudes of optokinetic stimulation. It can be seen that all responses have their mean maxima at a stimulus velocity of ca. $1^\circ/\text{second}$ (here equal to retinal-slip velocity) and that the absolute maxima are also similar. These qualitative and quantitative data strongly indicate that the three neuronal populations are parts of a common system.

Circuitry of the Optokinetic Path to Vn

From the above, it seems fair to state that the prepectum is the first central relay in the horizontal optokinetic reflex path through Vn (FIGURE 11). A particular class of units (see FIGURE 8, TABLE 6) has the proper response polarity,

tuning curves, and response time course to relay the optokinetic signal to lower centers. Lesion data described here also are compatible with this concept.

How does the pretectal signal reach the Vn? It is quite certain that it does not get there directly, since no such connections have been found.^{24,25} Furthermore, Vn spike latencies after electrical stimulation of the pretectum are beyond the monosynaptic range,¹⁸ and clear differences in the time course of the responses of the two populations exist. Therefore, there should be at least one more link between pretectal neurons and Vn, and this might be the NRTP (FIGURE 11). Neurons in this nucleus have all the response properties that pretectal units have in common with Vn, plus the proper response time course and vestibular convergence. Also, there exists in the rat a pretectal projection to NRTP.²⁵ Indirect pretectal-NRTP projections may play some role too.

Assuming the NRTP is a link in the pathway to Vn, one must now ask, How does the signal reach Vn from the NRTP? Our electrical stimulation experiments do not support a direct projection. The recordings were done extracellularly from identified type I and type II Vn, with the former being inhibited and the latter excited by ipsilateral NRTP stimulation. The mean latencies for type II excitation and type I inhibition were ca. 3 mseconds, and the shortest latency for type II excitation was 1.1 mseconds (1 unit). These latencies, for the most part, exclude direct projections, a notion that is also in agreement with negative anatomical data.³² We conclude then that the NRTP projects via oligosynaptic chains to Vn. At present it is not known where these additional neurons are located.

Based on a model proposed by Robinson,³³ it seems reasonable to suggest that the NRTP represents the site where retinal-slip signals and an eye-velocity signal get together. This combined signal is then transmitted to the neural network subserving the velocity storage mechanism,⁵ which in turn projects to Vn. Future work is needed to (1) identify the location of the velocity storage network and (2) demonstrate its connection to Vn.

Previous studies have shown that central afferents to Vn may inhibit type I neurons via excitation of the inhibitory type II neurons.^{34,35} In the system described here this may likewise be the case, since the thresholds for type II activation from pretectum and NRTP were lower and the latencies shorter than those for type I inhibition. Furthermore, the mirror image responses recorded concurrently in the contralateral Vn are likely to be mediated by the vestibular commissure (see above), which would lead to type II decrease by disfacilitation and increased type I firing by disinhibition. It is of interest to point out that the optokinetic responses obtained from Vn after systemic injection of picrotoxin are compatible with this hypothesis since in this condition only type II excitation following temporonasal stimulation of the contralateral eye is preserved.¹⁸

REFERENCES

1. COLLEWIJN, H. 1969. Optokinetic eye movements in the rabbit: input-output relations. *Vision Res.* **9**: 117-132.
2. HONRUBIA, V., B. J. SCOTT & P. H. WARD. 1967. Experimental studies on optokinetic nystagmus. I. Normal cats. *Acta Oto-Laryngol.* **64**: 388-402.
3. EVINGER, C. & A. R. FUCHS. 1979. Saccadic, smooth pursuit, and optokinetic eye movements of the trained cat. *J. Physiol.* **285**: 209-229.
4. MONTAROLO, P. G., W. PRECHT & P. STRATA. 1981. Functional organisation of the horizontal optokinetic nystagmus in the cat. *Neuroscience*. (In press.)
5. COHEN, B., V. MATSUO & T. RAPHAN. 1977. Quantitative analysis of the velocity

- characteristics of optokinetic nystagmus and optokinetic after-nystagmus. *J. Physiol. London* **270**: 321-344.
6. WOOD, C. C., P. D. SPEAR & J. J. BRAUN. 1973. Direction-specific deficits in horizontal optokinetic nystagmus following removal of visual cortex in the cat. *Brain Res.* **60**: 231-237.
 7. PRECHT, W. 1980. Functional organisation of the pathways mediating horizontal optokinetic eye nystagmus. *Proc. Int. Union Physiol. Sci.* **14**: 0506.
 8. CAZIN, L., W. PRECHT & J. LANNOU. 1980. Optokinetic responses of vestibular nucleus neurons in the rat. *Pfluegers Arch.* **384**: 31-38.
 9. BRECHA, N. & H. J. KARTEN. 1979. Accessory optic projections upon oculomotor nuclei and vestibulocerebellum. *Science* **203**: 913-916.
 10. MONTGOMERY, N., K. FITE & L. BENGSTON. 1979. The anuran accessory optic system: neuroanatomical analysis. *Soc. Neurosci. Abstr.* **5**: 798.
 11. DICHGANS, J. & TH. BRANDT. 1972. Visual-vestibular interaction and motion perception. *Bibl. Ophthalmol.* **82**: 327-338.
 12. DICHGANS, J., C. L. SCHMIDT & W. GRAF. 1973. Visual input improves the speedometer function of the vestibular nuclei in the goldfish. *Exp. Brain Res.* **18**: 319-322.
 13. ALLUM, J. H. J., W. GRAF, J. DICHGANS & C. L. SCHMIDT. 1976. Visual-vestibular interactions in the vestibular nuclei of the goldfish. *Exp. Brain Res.* **26**: 463-485.
 14. WAESPE, W. & V. HENN. 1977. Neuronal activity in the vestibular nuclei of the alert monkey during vestibular and optokinetic stimulation. *Exp. Brain Res.* **27**: 523-538.
 15. KELLER, E. L. & W. PRECHT. 1979. Visual-vestibular responses in vestibular nuclear neurons in the intact and cerebellectomized, alert cat. *Neuroscience* **4**: 1699-1613.
 16. COHEN, B., T. UEMURA & S. TAKEMORI. 1973. Effects of labyrinthectomy on optokinetic nystagmus (OKN) and optokinetic after-nystagmus (OKAN). *Equilibrium Res.* **3**: 88-93.
 17. COLLEWIJN, H. 1976. Impairment of optokinetic (after-) nystagmus by labyrinthectomy in the rabbit. *Exp. Neurol.* **52**: 146-156.
 18. CAZIN, L., W. PRECHT & J. LANNOU. 1980. Pathways mediating optokinetic responses of vestibular nucleus neurons in the rat. *Pfluegers Arch.* **384**: 19-29.
 19. CAZIN, L., W. PRECHT & J. LANNOU. 1980. Firing characteristics of neurons mediating optokinetic responses to rat's vestibular neurons. *Pfluegers Arch.* **386**: 221-230.
 20. PRECHT, W. & P. STRATA. 1980. On the pathway mediating optokinetic responses in vestibular nuclear neurons. *Neuroscience* **5**: 777-787.
 21. COLLEWIJN, H. 1975. Oculomotor areas in the rabbit's midbrain and pretectum. *J. Neurobiol.* **6**: 3-22.
 22. COLLEWIJN, H. 1975. Direction-selective units in the rabbit's nucleus of the optic tract. *Brain Res.* **100**: 489-508.
 23. HOFFMANN, K.-P. & A. SCHOPPMANN. 1975. Retinal input to direction selective cells in the nucleus tractus opticus of the cat. *Brain Res.* **99**: 359-366.
 24. BERMAN, N. 1977. Connections of the pretectum in the cat. *J. Comp. Neurol.* **174**: 227-254.
 25. TERESAWA, K., K. OTANI & J. YAMADA. 1979. Descending pathways of the nucleus of the optic tract in the rat. *Brain Res.* **173**: 405-417.
 26. SHIMAZU, H. & W. PRECHT. 1966. Inhibition of central vestibular neurons from the contralateral labyrinth and its mediating pathway. *J. Neurophysiol.* **29**: 467-492.
 27. MAEKAWA, K. & J. I. SIMPSON. 1973. Climbing fiber responses evoked in vestibulocerebellum of rabbit from visual system. *J. Neurophysiol.* **36**: 649-666.
 28. PRECHT, W. 1978. Neuronal operations in the vestibular system. In *Studies of Brain Function*. V. Braitenberg, Ed. **2**: 226. Springer-Verlag, Berlin, Heidelberg & New York.
 29. HOFFMANN, K.-P., K. BEHREND & A. SCHOPPMANN. 1976. A direct afferent visual pathway from the nucleus of the optic tract to the inferior olive in the cat. *Brain Res.* **115**: 150-153.
 30. MIYASHITA, Y., M. ITO, P. J. JASTREBOFF, K. MAEKAWA & S. NAGANO. 1980. Differential roles of mossy and climbing fiber visual inputs to the cerebellar flocculus in controlling eye movements of rabbits. *Proc. Int. Union Physiol. Sci.* **14**: 2477.

31. BLANKS, R. H. & J. C. BLANKS. 1980. Afferents to the cerebellar flocculus in cat conveying visual input. In *Proceedings of a meeting of the Association of Research in Vision and Ophthalmology*, Sarasota, Fla.
32. POMPEIANO, O., T. MERGNER & N. CORVAJA. 1978. Commissural, perihypoclossal and reticular afferent projections to the vestibular nuclei in the cat. An experimental anatomical study with the method of the retrograde transport of horseradish peroxidase. *Arch. Ital. Biol.* **116**: 130-172.
33. ROBINSON, D. A. 1977. Vestibular and optokinetic symposia: an example of explaining by modelling. *Dev. Neurosci.* **1**: 49-58.
34. MARKHAM, C. H., W. PRECHT & H. SHIMAZU. 1966. Effect of stimulation of interstitial nucleus of Cajal on vestibular unit activity in the cat. *J. Neurophysiol.* **29**: 493-507.
35. SHIMAZU, H. & C. M. SMITH. 1971. Cerebellar and labyrinthine influences of single vestibular neurons identified by natural stimuli. *J. Neurophysiol.* **34**: 493-508.

NEURAL ACTIVITY IN THE NUCLEUS RETICULARIS TEGMENTI PONTIS IN THE MONKEY RELATED TO EYE MOVEMENTS AND VISUAL STIMULATION*

E. L. Keller and W. F. Crandall

Smith-Kettlewell Institute of Visual Sciences
San Francisco, California 94115

INTRODUCTION

Significant progress has been made recently in understanding the operation of and delimiting the neural pathways involved in the optokinetic system and its close ties to the vestibular system. Careful measurement of the reflex eye movements induced by a variety of full-field visual or vestibular stimuli given alone or in combination has produced a deeper understanding of the qualitative behavior of these reflex systems for visual stabilization.^{1,2} Mathematical models based on similar measurements have generated theoretical conceptions of the neurological organization of these systems.¹⁻³ The most interesting new feature derived from these behavioral and modeling studies is the delimitation of a central positive feedback loop or velocity storage mechanism. This theoretical mechanism is presumed to be a neural network that is shared by both the visual and vestibular inputs and provides much of the steady-state behavior of both systems.

In terms of understanding the neurophysiological operation of the optokinetic system, the discovery that vestibular nucleus neurons (Vn) respond in a direction-selective manner to whole-visual-field motion as well as to vestibular stimulation has been a major advance.^{4,5} The exact nature of this visually induced signal in Vn is still being investigated. Although it is clear that it can be uncoupled from the optokinetic drive to the eye muscles under certain conditions,⁶ we will continue in the present paper to refer to this modulation in Vn as an optokinetic response.

Interest now has been directed toward uncovering the pathways mediating this complex optokinetic response in Vn. Attention first was focused on a possible pathway through the cerebellum, but the response has been shown to persist following total cerebellar ablations.⁷ More recently a new pathway has been proposed in rat and cat, which includes as early relay stations the pretectal region followed by the nucleus reticularis tegmenti pontis (NRTP).^{8,9} In addition, the response properties of NRTP neurons indicated that this structure might be involved in the velocity storage mechanism discussed above.¹⁰

The present paper explores the relationship of this latter nucleus (NRTP) to optokinetic and vestibular responses in the primate. Although a small percentage of NRTP cells in the monkey respond to whole-visual-field motion, their velocity-tuning properties are completely different from those observed in Vn in this animal for similar stimuli. In contrast, NRTP in primates seems to play a more important role in relaying visual information about discrete visual targets, their motion, and accompanying saccadic and pursuit eye movements to the cerebellum.

*The research was supported by NIH Grants R01 EY-03280-01 and 5P 30 EY-01186, and by the Smith-Kettlewell Eye Research Foundation.

METHODS

Microelectrode recordings in the region of the NRTP were conducted in three previously trained juvenile monkeys (*Macaca fascicularis*). The methods used in the chronic preparation and training of these animals have been described previously.¹¹ Briefly, under pentobarbital sodium anesthesia and aseptic conditions, a stainless-steel chamber was implanted stereotaxically on the skull in a frontal plane at a 25° angle from the vertical above the NRTP. During subsequent daily recording sessions, tungsten microelectrodes were driven through the chamber with an eccentric, hydraulic drive system. The dura was left intact, and electrodes were passed through it within a sterile cannula. A light aluminum crown was bolted to the skull to provide a platform for restraining the monkey's head during recording sessions. A Teflon[®]-insulated stainless-steel coil was also implanted on one eye during this same surgical period. During subsequent recording sessions, eye movements were measured using the search coil in a magnetic field method.¹² During experiments, the monkey sat upright in its primate chair with its head fixed. As the microelectrode was driven into the region of the NRTP, an optokinetic drum was oscillated about a vertical axis at a low frequency (about 0.1 Hz) around the animal as a searching stimulus. The drum was four feet in diameter, included the entire upper visual field with a striped ceiling and down 30° into the lower visual field, contained alternating black and white vertical stripes of random width (1–8° of visual angle each), and was uniformly illuminated at a mean luminance of 9.1 cd/m² (contrast = 0.82). The drum was rotated by a servocontrol system and could be retracted quickly into the ceiling above the animal when desired. The monkey attended to a dimly lighted light-emitting diode (LED) located at the primary position (which subtended about 0.25°) when it was on and suppressed its optokinetic nystagmus (OKN). This will be called the fixation condition. When the LED was extinguished during drum rotation, normal OKN resulted.

Vestibular stimulation was provided by a mechanical oscillator previously described.¹³ This oscillator provided sinusoidal motion of the whole animal about a vertical axis passing through the center of its head. The angular position of the animal's head was measured by a high-resolution potentiometer. Vestibular tests were carried out in total darkness.

Smooth-pursuit and saccadic eye movements were induced with an oscilloscope projection system. The OK drum was raised, and images from the face of the oscilloscope were back projected onto a translucent tangent screen located 40 cm from the monkey. The image on the screen was a dim spot that subtended about one degree of visual angle. When the fixed LED at the primary position was lighted, the animal attended to it and did not follow the projected spot, which could be used as a stimulus to explore visual fields of NRTP units. When the LED was extinguished, the animal followed the projected spot with its eyes. Saccades were triggered by target steps, while sinusoidal spot motion resulted in smooth-pursuit movements.

Unit activity and analog signals for horizontal and vertical eye position, OK drum velocity, head position, and discrete-target-spot position were recorded on an instrument-grade magnetic tape recorder for subsequent analysis. Detailed analysis of unit activity and its relationship to the various visual, optokinetic, vestibular, or eye-movement parameters was carried out with a special program on a PDP-11 computer.

An electrolytic lesion was made through the tip of the recording electrode at the site of a supposed NRTP unit in one monkey. The lesion was verified to be in the NRTP on histological brain-stem sections (25- μ sections stained with cresyl

violet). Recording sites on other electrode tracks were reconstructed from this marked location. In the other two animals, we first located the oculomotor nucleus on the basis of its characteristic neural activity related to eye movements. Subsequent electrode penetrations were offset stereotaxically to enter the region of the nearby, but ventrally displaced, NRTP. Since the neural activity in this nucleus was also unique (and this was confirmed by the histology in the first animal), we considered this method to be sufficient for localization.

RESULTS

Electrode penetrations in this study were concentrated in the medial portion of the NRTP (out to about 2.0 mm from the midline) but throughout its whole rostral to caudal extent. We have not yet explored the lateral portion (the *processus tegmentosus lateralis*). Within this medial region, the activity of 100 neurons in or in the close vicinity of the NRTP were recorded in the three monkeys. Of this population, only 12% (12 cells) responded to the stimulation provided by motion of the visual surround. In contrast, 72 cells showed a relationship to saccadic eye movements, generally with a burst or pause of activity associated with certain saccades. The discharge of 16 neurons was exclusively related to the motion of the small discrete visual target and the accompanying smooth-pursuit eye movement but not to large visual-field motion. In this paper we will concentrate on providing a description of the first set of neurons because they are related to OK stimulation, but will briefly describe the two latter classes since they constitute the vast majority of the units in the NRTP in the primate.

Optokinetic-Related Cells

All 12 neurons of this group were spontaneously active at very low, irregular rates in a stationary visual surround and were not related to spontaneous eye movements. Each unit responded in a direction-selective manner to horizontal motion of the OK drum (FIGURE 1). The magnitude of the response was similar whether the eyes moved in response to drum motion or fixated the suppression target. The units were excited by one direction of horizontal drum rotation (7 for the right and 5 for the left direction) and were totally inhibited by the opposite direction of visual motion. Vertical or oblique directions of motion were not tested.

When the motion of the drum was a velocity trapezoid (FIGURE 2), the units all showed a latency of about 400 mseconds from the onset of drum motion before any change in activity and then began a rapid buildup in response to a maximum level within another 0.5 to 1 second. This level was maintained with irregularly spaced fluctuations for the entire period (1 minute was the maximum tested duration) of drum rotation. The time course of this profile of activation was not affected by the magnitude of the constant-acceleration phase (for accelerations from 10 to 100°/second²).

None of these units responded to discrete visual stimuli either fixed or moving (FIGURE 3A) or during smooth-pursuit eye movements (FIGURE 3B). Finally, this type of unit did not respond to vestibular stimulation (FIGURE 3C).

The anatomic location of these 12 units is shown in FIGURE 4. They were found at scattered locations within the dorsomedial portion and just dorsal to the NRTP. There was no obvious grouping of units responding to left or right drum

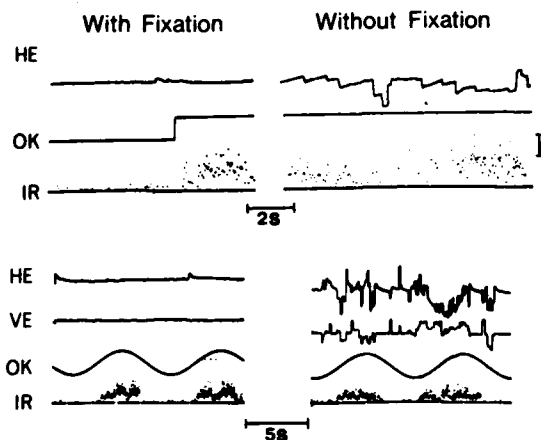


FIGURE 1. The response of a typical OK-type NRTP neuron. The upper panels show responses during constant-velocity ($10^\circ/\text{second}$) drum rotation, while the lower panels illustrate sinusoidal drum motion at 0.1 Hz (peak velocity = $5^\circ/\text{second}$). The panels on the left show the fixation condition, while those on the right the condition without a stationary fixation point. In each panel the traces are horizontal eye position (HE), vertical eye position (VE), drum velocity (OK), and instantaneous firing rate of the neuron (IR). The vertical calibration applies to all traces, and represents in the upper panels 25° for HE, $10^\circ/\text{second}$ for OK, and 40 spikes/second for IR. In the lower panels, it represents 5° for HE and VE, $10^\circ/\text{second}$ for OK, and 40 spikes/second for IR.

rotation. In order to quantify the behavior of this type of unit for comparison to the optokinetic response of Vn in the monkey, the activity in response to about eight consecutive sinusoidal (0.1-Hz) drum rotations during the fixation condition was averaged for several different values of peak drum velocity from 0.5 to $50^\circ/\text{second}$. An example of the cycle histogram for one unit is shown in FIGURE 5

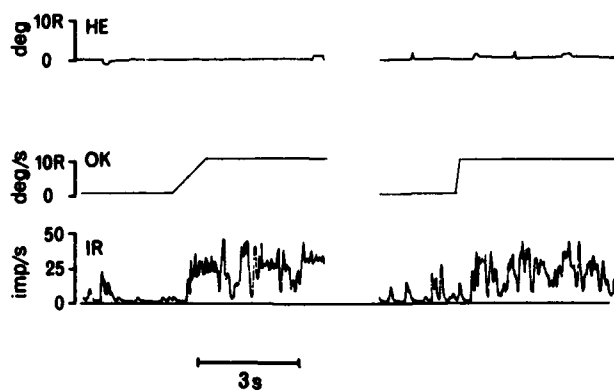


FIGURE 2. The onset of NRTP unit responses to OK velocity trapezoid stimulation. Symbols and traces the same as FIGURE 1. In the left panel the period of the acceleration phase was 1 second, and in the right panel it was 0.1 second. Final OK velocity was the same. Fixation condition during both tests.

for peak velocities of 1, 5, and 10°/second. Four units showed a maximum response amplitude by 1°/second, while the rest (like the example in FIGURE 5) had a soft saturation that was evident at 5 to 10°/second (FIGURE 6). All units continued to respond at nearly maximum level at the highest tested value of drum velocity (50°/second). The phases of the averaged responses were all in phase or just slightly leading drum velocity at this test frequency (0.1 Hz).

Several units were tested over a similar range of constant-velocity drum rotations, with identical response magnitudes to the peak values obtained by the sinusoidal tests. Therefore, the peak values of the cycle histograms obtained for each peak velocity of the sinusoidal type of stimulation were averaged over the group of units, and the results at each velocity are shown as the open circles in FIGURE 7. These averaged values were normalized to the value obtained at 5°/second so that they could be compared to similarly normalized average values

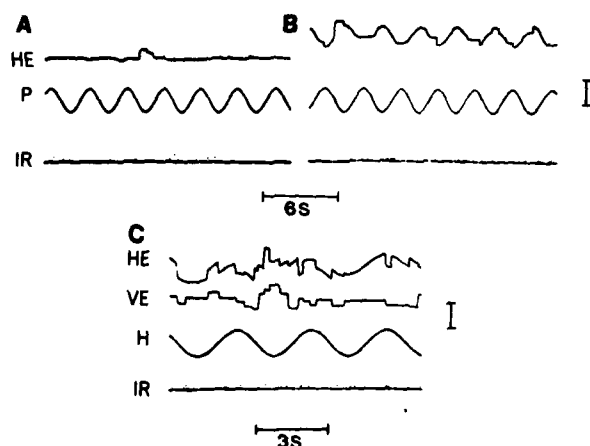


FIGURE 3. The total lack of response of optokinetic-type NRTP neurons to discrete visual targets moving across the fovea (A), to smooth-pursuit eye movements (B), or to vestibular stimulation in dark (C). The trace labeling is the same as in FIGURE 1 except for the position of the discrete visual target (P) and the position of the head (H). Vertical calibration in B applies to the upper panels and represents 10° for HE and P and 40 spikes/second for IR. Vertical calibration in C represents 20° for HE, VE, and H and 40 spikes/second for IR.

obtained from data in Buettner and Büttner in monkey Vn during suppression of OK eye movements (filled circles, FIGURE 7).⁶ The opposite trends are apparent. The NRTP unit response to OK stimulation saturates at low drum velocities (certainly by 5°/second) and then decreases somewhat at higher values of velocity. The response of Vn is barely evident at 5°/second, but increases almost linearly over the range 5 to 60°/second.

Saccade-Related Neurons

Sixty-six cells were recorded in the NRTP that burst in association with certain saccades, while six additional cells showed a saccade-related pause in spontaneous activity. Only the former, large class will be described here. The

most important property of the majority of these saccadic burst neurons was that they showed a movement-field organization similar to that observed in deeper layer superior colliculus cells in the monkey.¹⁴⁻¹⁶ Most units were totally silent or had a small, irregular spontaneous discharge with the monkey fixating the discrete visual target in the primary position. The step movement of the target to the center of the unit's movement field induced in some cases an early visual response (latency from 65-100 mseconds) followed by an intense burst of

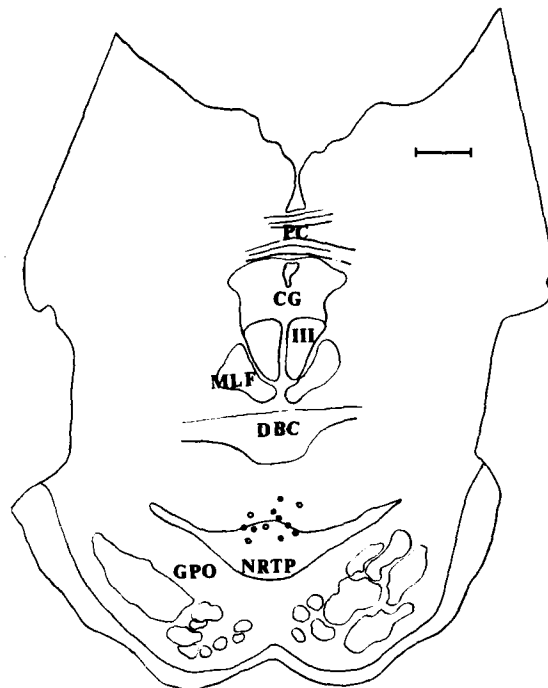


FIGURE 4. Anatomic location of optokinetic-type NRTP units projected onto one representative frontal section at a stereotaxic coordinate of A6.0. Monkey's right side shown on the right. Open circles are units that are excited by leftward OK drum rotation, filled circles are units excited by rightward rotation. Calibration mark is 2 mm. PC, posterior commissure; CG, central gray; III, oculomotor nucleus; MLF, medial longitudinal fasciculus; DBC, decussation of the brachium pontis; NRTP, nucleus reticularis tegmenti pontis; GPO, pontine nuclei.

discharge preceding the saccade by about 20 mseconds to the center of the cell's movement field (FIGURE 8A). When the target step was smaller in amplitude (FIGURE 8B) or larger (FIGURE 8C) or of the same amplitude but in a different direction (FIGURE 8D), no visual response (or a greatly attenuated response) was obtained and the saccade-related response was likewise attenuated. The movement-related response was still present for spontaneous saccades to the region of the movement field in total darkness (FIGURE 8E). The visual and saccadic-

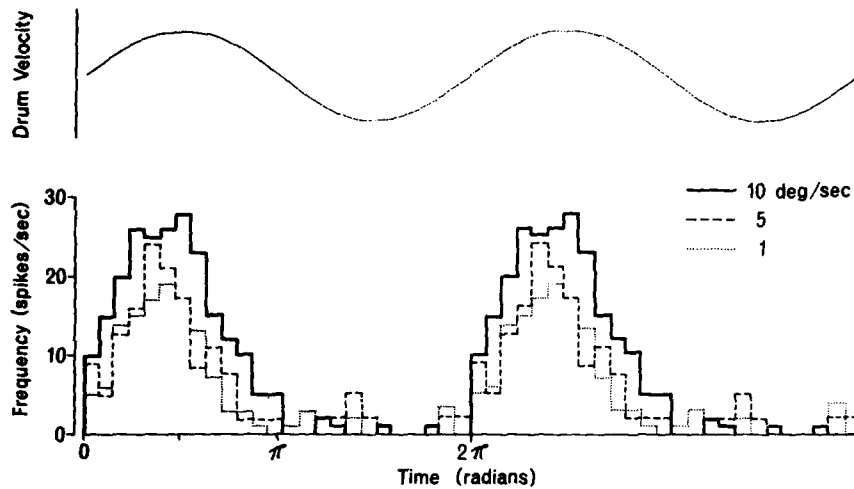


FIGURE 5. Cycle-averaged responses of a typical NRTP neuron to sinusoidal OK drum motion (0.1 Hz) of 1, 5, and 10°/second peak velocity. Unit response separated into 25 bins per cycle and averaged for eight cycles. Two identical cycle averages are shown for clarity. All data obtained during suppression of OKN.

related responses were retinotopically organized and thus were not dependent on initial eye position before the saccade, at least over a range of $\pm 20^\circ$ of initial position. The parameters quantifying the burst portion of the units' discharge (burst duration, average burst frequency, and number of spikes in the burst) were not related to the saccadic metrics. Thus the burst for a saccade made to the

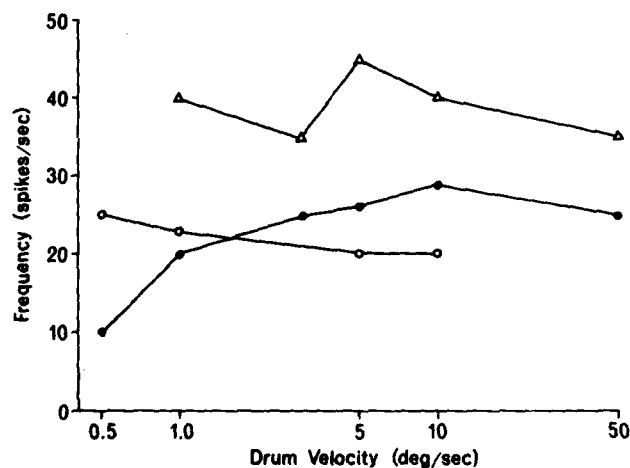


FIGURE 6. Velocity-tuning characteristics for three typical NRTP units (different symbols for each unit). Peak unit response obtained from cycle histograms (FIGURE 5) are plotted as a function of peak sinusoidal drum velocity (all at 0.1 Hz).

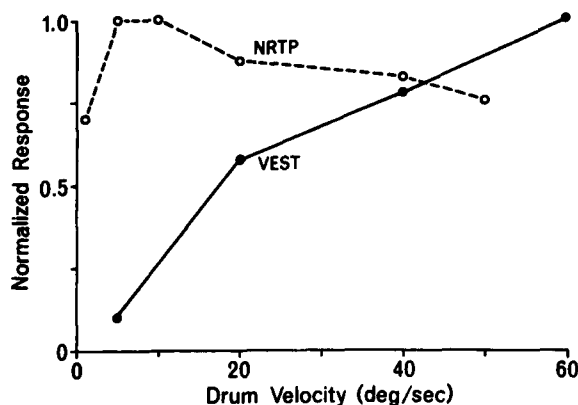


FIGURE 7. Comparison of the velocity-tuning properties of monkey NRTP units (open circles and dashed lines) and Vn units (filled circles and solid lines) to OK stimuli. The data on Vn units are normalized and replotted from those given in Buettner and Büttner.⁶ Both sets of data were obtained during suppression of OKN.

middle of the movement field for a unit with its field at 5° of eccentricity was very similar to that in another unit for a saccade to the middle of its movement field at 20° of eccentricity.

One example of a typical unit's movement field is shown in FIGURE 9. The number of spikes in the burst for a large number of saccades to different regions of visual space is shown. Some activity occurred for saccades over a considerable region of space, but a clear peak occurs for saccades that move the eyes about 7° right. The proximal side of the mound representing discharge intensity was generally much more sharply tuned. For units with movement-field centers at 20° of eccentricity, or larger, it was difficult to show any decrease in response for very large saccades in the preferred direction. Some movement fields included a full quarter or more of the visual field.

Units Responding to Discrete-Visual-Target Motion

Only a preliminary study has been completed on this type of NRTP unit. Since these units never responded to the OK stimulation provided by the drum rotation (our searching stimulus), their relative number in the NRTP may be significantly higher than that indicated here. When the drum was retracted and the target spot was moved sinusoidally on the tangent screen, a clearly modulated response (FIGURE 10) was seen in this type of unit. For the unit illustrated in FIGURE 10, the response was similar whether the eyes remained fixated at the primary position and the visual stimulus was moved across the fovea (FIGURE 10B) or when the eyes tracked the same stimulus (FIGURE 10A). In some other units of this type, the response was more closely related to the pursuit eye movement and the response was greatly diminished in the fixation condition. For most units of this type, the peak discharge frequency was nearly in phase with target velocity (and eye velocity when tracking was permitted). However, in a

few units like the one shown in FIGURE 10, the peak discharge frequency lagged stimulus velocity by almost 90° . For these units, discharge was approximately in phase with target position (or acceleration).

DISCUSSION

The major conclusion that can be drawn from this study is that the primate NRTP is organized quite differently from that of the rat. The majority of units in the rat NRTP respond to OK stimuli, and furthermore, the unit response is quantitatively very similar to the OK response observed in Vn in the same animal.^{10,17} Thus in the rat, it has been hypothesized that the NRTP is a direct link

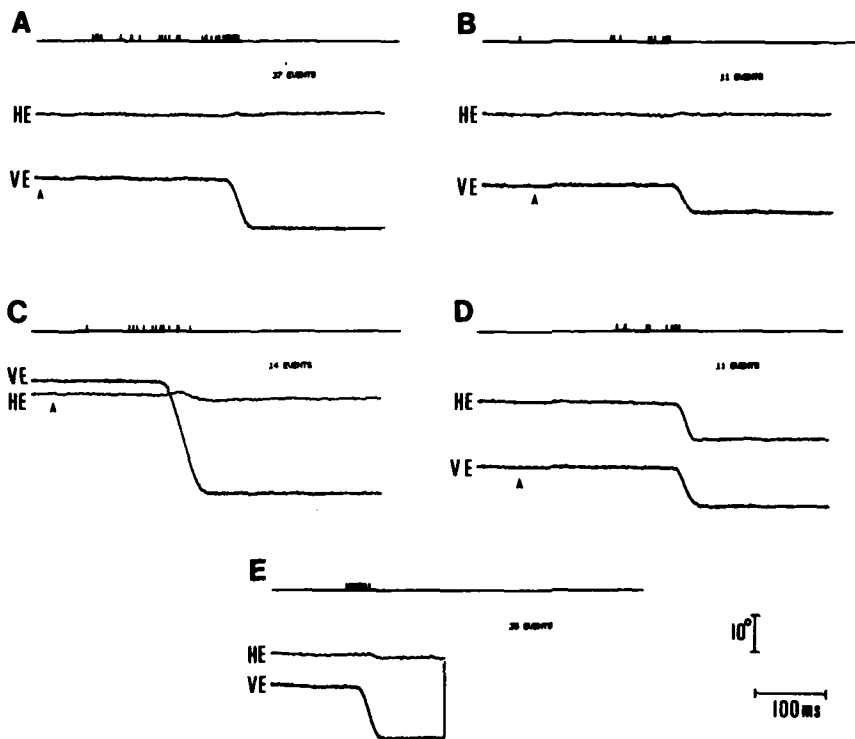


FIGURE 8. The activity pattern of an NRTP saccadic burst unit. In all panels, the upper trace shows the computer-generated marks (events) for each neural discharge, the next trace shows horizontal eye position (HE), and the bottom trace shows vertical eye position (VE). The arrowheads mark the points in time when the visual target shifted position evoking the following saccades: (A) Eye movement to the center of this unit's movement field (down 14°). (B) Smaller pure down movement with less vigorous unit burst. (C) Larger pure down movement also with smaller burst. (D) An oblique eye movement with a vertical component equal to that in A with little discharge. (E) Spontaneous saccade in darkness to the center of the movement field showing a burst similar to A but without the early visual response.

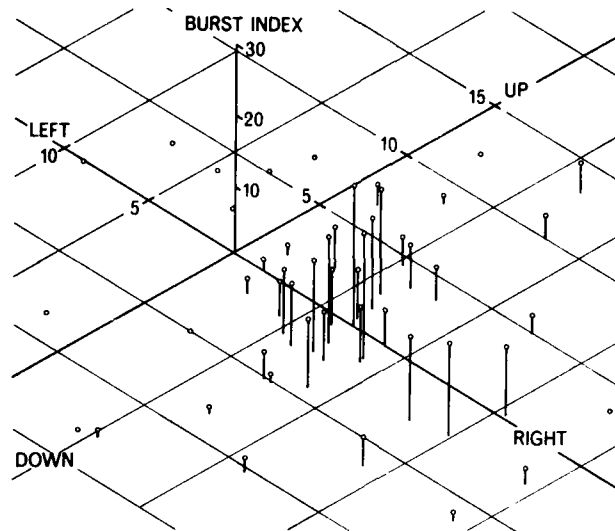


FIGURE 9. Movement field of a typical NRTP burst neuron shown in a three-dimensional representation. Each symbol represents one saccade with the horizontal and vertical coordinates indicated in the plane in degrees. The height of each symbol represents the number of spikes (burst index) in the high-frequency portion of the unit's discharge for that saccade. The center of this unit's movement field was about 7° pure right.

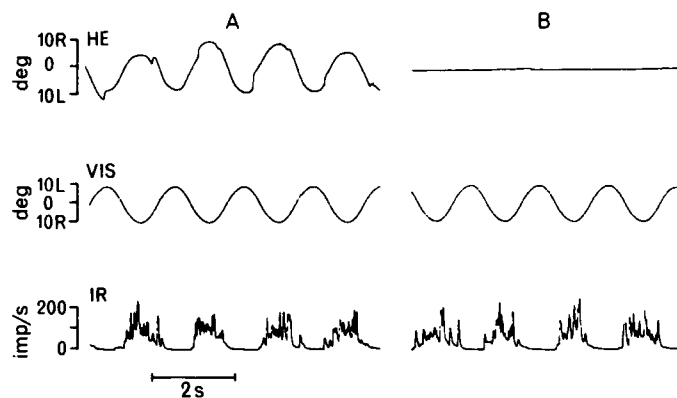


FIGURE 10. Activity pattern of an NRTP neuron responding to discrete visual targets. In both plates, the upper trace is horizontal eye position (HE), the middle trace is horizontal target position (VIS), and the lower trace is the unit's instantaneous discharge rate (IR). (A) The monkey is tracking the target as it moves sinusoidally at 0.6 Hz. (B) Target motion is the same, but the monkey is now fixating the stationary LED.

in the neural pathway carrying visual responses to the vestibular nucleus and that this pathway is also instrumental in generating optokinetic nystagmus. Based on the unit activity observed in the primate NRTP, this nucleus in the monkey seems more related to the saccadic and smooth-pursuit systems. Not only are units that can be modulated by OK stimuli extremely rare in the monkey NRTP, but their pattern of discharge clearly is not similar to that observed in Vn. Instead they saturate at very low velocities of surround motion. In this feature they resemble the response recorded in a majority of motion-sensitive neurons in the nucleus of the optic tract in rabbit and cat.^{18,19} However, they appear to have somewhat more broadly tuned velocity responses, particularly at velocities above 10°/second, than do units observed in this pretectal region.

This type of NRTP unit still could be involved in generating the slow phase of OKN. Koerner and Schiller reported that open-loop OK-eye-movement response peaks for a stimulus of about 5°/second in the monkey,²⁰ which is similar to the unit response we observed. The similarity in response of this type of unit when the monkey was fixating or tracking the drum motion can probably be explained by the low-velocity soft-saturation effect. Close inspection of FIGURE 1 shows that the response was consistently a little larger when the eyes were fixed (and retinal slip created by drum was equal to surround velocity) than when the eyes were following the drum and retinal image slip was very low.

Monkey NRTP optokinetic units differ in two other significant ways from units recorded in this nucleus in the rat. First, the buildup of activity following a step or ramp initiation of drum motion is almost immediate in monkey NRTP units in contrast to the several-second time course observed in rat NRTP neurons. This slow buildup of activity led Cazin *et al.* to hypothesize that NRTP units might form part of the velocity storage mechanism for the OK system.¹⁰ Such a role does not seem possible for monkey NRTP units, in view of their rapid response. Secondly, all rat NRTP cells that respond to OK stimuli also respond to pure vestibular stimulation. No units responding to vestibular stimuli have been found in the monkey NRTP.

The saccade-related response observed in most NRTP burst units resembles most closely that observed in neurons found in the deeper layers of the colliculus.¹⁴⁻¹⁶ Anatomic work supports the idea of an extensive projection from the superior colliculus to the NRTP in the monkey.²¹ Furthermore, some NRTP units resemble that particular class of collicular neurons having both a visual field and a movement field. Collicular cells with this characteristic typically are located in the intermediate gray layer just below the optic layer.^{22,23} Mohler and Wurtz have suggested that neurons of this type form one output of the colliculus,²² and our findings in NRTP support this hypothesis.

The most interesting point concerning this class of NRTP neurons stems from the fact that almost the total efferent projection of the NRTP goes to the cerebellum.²⁴ This indicates that the combined visual/movement field type of information is probably projected onto the cerebellum. Thus the cerebellum receives both visual information about intended target position and information about the saccade to this target. Furthermore, both pieces of information are spatially coded. On the basis of current reports concerning cerebellar discharge related to saccadic eye movements, it appears that Purkinje cell (cerebellar cortex output) activity is temporally coding saccadic metrics.²⁵⁻²⁷ Therefore, a spatial-to-temporal transformation may be hypothesized to occur in this part of the brain.

The discovery that many units in the primate NRTP respond in a direction-selective fashion to the motion of discrete visual targets came as a surprise to us and emphasizes again the differences in the neural organization of the foveate and nonfoveate OK pathways. It seems unlikely that these units play a role in generating OK eye movements or the OK response in Vn, since they did not respond at all to the motion of the drum. However, Koerner and Schiller found that discrete spots of the same size (1° of angle) used in the present study could induce "optokinetic" following movements in their monkeys under open-loop conditions.²⁰ It might be argued that such movements are smooth-pursuit eye movements, but in any case, the more complex nature of OK eye movements and its neural organization, including the NRTP in the primate as compared to the rabbit or rat, is thus further underscored.

ACKNOWLEDGMENTS

We thank Helen Sullivan for photography, Jim Brodale for illustrations, and Jona Countie for secretarial assistance.

REFERENCES

1. COHEN, B., V. MATSUO & TH. RAPHAN. 1977. Quantitative analysis of the velocity characteristics of optokinetic nystagmus and optokinetic after-nystagmus. *J. Physiol. London* **270**: 321-344.
2. RAPHAN, TH., V. MATSUO & B. COHEN. 1979. Velocity storage in the vestibulo-ocular reflex arc (VOR). *Exp. Brain Res.* **35**: 229-249.
3. ROBINSON, D. A. 1977. Vestibular and optokinetic symbiosis: an example of explaining by modelling. *Dev. Neurosci.* **1**: 49-58.
4. ALLUM, J. H. J., W. GRAF, J. DICHGANS & C. L. SCHMIDT. 1976. Visual-vestibular interactions in the vestibular nuclei of the goldfish. *Exp. Brain Res.* **26**: 463-485.
5. WAESPE, W. & V. HENN. 1977. Neuronal activity in the vestibular nuclei of the alert monkey during vestibular and optokinetic stimulation. *Exp. Brain Res.* **27**: 523-538.
6. BUETTNER, U. M. & U. BÜTTNER. Vestibular nuclei activity in the alert monkey during suppression of vestibular and optokinetic nystagmus. *Exp. Brain Res.* **37**: 581-593.
7. KELLER, E. L. & W. PRECHT. 1979. Visual-vestibular responses in vestibular nuclear neurons in intact and cerebellectomized, alert cat. *Neuroscience* **4**: 1599-1613.
8. PRECHT, W. & P. STRATA. 1980. On the pathway mediating optokinetic responses in vestibular nuclear neurons. *Neuroscience* **5**: 777-787.
9. CAZIN, L., W. PRECHT & J. LANNOU. 1980. Pathways mediating optokinetic responses of vestibular nucleus neurons in the rat. *Pfluegers Arch.* **384**: 19-29.
10. CAZIN, L., W. PRECHT & J. LANNOU. Firing characteristics of neurons mediating optokinetic responses to rat's vestibular neurons. *Pfluegers Arch.* (In press.)
11. KELLER, E. L. 1974. Participation of medial pontine reticular formation in eye movement generation in monkey. *J. Neurophysiol.* **37**: 316-332.
12. FUCHS, A. F. & D. A. ROBINSON. 1966. A method for measuring horizontal and vertical eye movements chronically in the monkey. *J. Appl. Physiol.* **21**: 1068-1070.
13. KELLER, E. L. & P. D. DANIELS. 1975. Oculomotor related interaction of vestibular and visual stimulation in vestibular nucleus cells in alert monkey. *Exp. Neurol.* **46**: 187-198.
14. SCHILLER, P. H. & F. KOERNER. 1971. Discharge characteristics of single units in superior colliculus of the alert rhesus monkey. *J. Neurophysiol.* **34**: 920-924.
15. WURTZ, R. H. & M. E. GOLDBERG. 1972. Activity of superior colliculus in behaving monkey. III. Cells discharging before eye movement. *J. Neurophysiol.* **35**: 575-586.

16. SPARKS, D. L., R. HOLLAND & B. L. GUTHRIE. 1976. Size and distribution of movement fields in the monkey superior colliculus. *Brain Res.* **113**: 21-34.
17. CAZIN, L., W. PRECHT & J. LANNOU. 1980. Optokinetic responses of vestibular nucleus neurons in the rat. *Pfluegers Arch.* **384**: 31-38.
18. COLLEWIJN, H. 1975. Direction-selective units in the rabbit's nucleus of the optic tract. *Brain Res.* **100**: 489-508.
19. HOFFMANN, K.-P. & A. SCHOPPMANN. 1975. Retinal input to direction selective cells in the nucleus tractus opticus of the cat. *Brain Res.* **99**: 359-366.
20. KOERNER, F. & P. SCHILLER. 1972. The optokinetic response under open and closed loop conditions in the monkey. *Exp. Brain Res.* **14**: 318-330.
21. HARTING, J. K. 1977. Descending pathways from the superior colliculus: an autoradiographic analysis in the rhesus monkey (*Macaca mulatta*). *J. Comp. Neurol.* **173**: 583-612.
22. MOHLER, C. W. & R. H. WURTZ. 1976. Organization of monkey superior colliculus: intermediate layer cells discharging before eye movements. *J. Neurophysiol.* **39**: 722-744.
23. MAYS, L. E. & D. L. SPARKS. 1980. Dissociation of visual and saccade-related responses in superior colliculus neurons. *J. Neurophysiol.* **43**: 207-232.
24. BRODAL, A. & J. JANSEN. 1946. The ponto-cerebellar projection in the rabbit and cat. *J. Comp. Neurol.* **84**: 31-118.
25. LLINAS, R. & J. W. WOLFE. 1977. Functional linkage between the electrical activity in the vermal cerebellar cortex and saccadic eye movements. *Exp. Brain Res.* **29**: 1-14.
26. KASE, M., D. C. MILLER & H. NODA. 1980. Discharges of Purkinje cells and mossy fibres in the cerebellar vermis of the monkey during saccadic eye movements and fixation. *J. Physiol. London* **300**: 539-555.
27. WATERHOUSE, B. D. & J. G. MCELLIGOTT. 1980. Simple spike activity of Purkinje cells in the posterior vermis of awake cats during spontaneous saccadic eye movements. *Brain Res. Bull.* **5**: 159-168.

VISUAL-VESTIBULAR INTERACTIONS IN VISUAL CORTICAL CELLS IN THE CAT*

Robert H. Lahue, Jr. and Stanislav Reinis

*Renison College and Department of Psychology
University of Waterloo
Waterloo, Ontario, Canada N2L 3G1*

Jack P. Landolt and Kenneth E. Money

*Defence and Civil Institute of Environmental Medicine
Downsview, Ontario, Canada M3M 3B9*

INTRODUCTION

The number of other papers in this volume that detail various interactions between the visual and vestibular systems attest to the fertility of this area of investigation, although it is not yet clear how such interactions subserve the well-known phenomena of the constancy of visual perceptions. In fact, relatively little is known about the impact that vestibular input has upon the processing of information in the primary visual system.

The functional architecture of this system, especially at the level of the visual cortex, is quite elaborate and, after early visual experience, quite rigidly fixed.¹⁻⁴ The functional characteristics of individual cells in the system can be described rigorously in terms of the parameters of stimuli presented in the visual field to which they respond. In the few studies that have examined the effects of vestibular stimuli upon the processing of visual information, the order and predictability that might have been expected from the nature of this system have not been found.⁵⁻¹⁷

The present work investigated the effects of alterations in vestibular inputs upon the receptive field properties of cells in the visual cortex of the cat, using the basic techniques described by Hubel and Wiesel.¹⁻⁴ Data are presented on 24 cells in which vestibular input was varied by tilting the animal's head. Data are also presented on 8 other cells in which vestibular input was varied by intravenous injection of deuterium oxide (heavy water).¹⁸ Both types of vestibular manipulation produced pronounced changes in the receptive field characteristics of cortical cells that have not been reported in previous studies.

METHODS

Animal Preparation and Data Collection

Under general anesthesia, a clamping block was mounted stereotaxically on the skull of each mature, normal cat. When an animal was to be used in an

*This work was supported by Defence and Civil Institute of Environmental Medicine Research Contracts 3277037/8SU78-00126 and 3279017/8SU79-00225. DCIEM Research Paper 80P39.

electrophysiological experiment, always at least one week after mounting the clamping block, this block allowed the animal to be positioned in a standard stereotaxic device without being subjected to pressure points or known sources of painful stimulation. Under halothane-O₂ anesthesia, the animal was positioned in the stereotaxic device, holes were drilled through the skull over the visual cortex to admit tungsten microelectrodes, and the exposed skin edges were infiltrated periodically with xylocaine. Intravenous and endotracheal cannulae were introduced, and contact lenses were inserted to protect the corneas. The nictitating membranes were retracted with phenylephrine, and atropine was used to dilate the pupils. At least 90 minutes prior to recording, the halothane-O₂ anesthesia was discontinued, the animal was immobilized by the intravenous injection of pancuronium bromide (Pavulon), and artificial ventilation was initiated. Electroencephalograph (EEG), electrocardiograph (ECG), core temperature, and expired CO₂ were monitored periodically.

Visual stimuli, as bars of light, were projected with a hand-held ophthalmoscope on a Plexiglas screen covered with Albanene tracing paper, which was positioned 81 cm in front of the animal. The projections of the optic disks were plotted on the screen, and their positions were rechecked periodically to verify that the eyes had not moved. Muscular paralysis prevented any such movement in all animals. The receptive fields of individual visual cortical neurons were plotted on the tracing paper, which provided a permanent record. The audio output of a standard microelectrode amplifier (GRASS P511) provided the primary means of distinguishing the responsivity of the cell being examined, although a digitized output also was available.

After plotting the receptive field with the animal's head in a horizontal position (orientation), the head was tilted 30° to the animal's right (right-tilt orientation) and the receptive field was plotted again. When possible, the field was plotted again with the head tilted 30° to the left of horizontal (left-tilt orientation). Receptive field plotting was commenced within 1 or 2 minutes after the head was moved. The characteristics of the receptive fields remained stable for the periods of more than one hour during which the head was usually left in a particular orientation. Whenever possible, the receptive field for the horizontal orientation was replotted after returning the animal's head to the horizontal orientation. In all such cases, the characteristics of the replotted receptive field were identical to those initially observed in the horizontal orientation. The actual movement of the head to one side or the other often resulted in the loss of the unit being investigated, which prevented the completion of a full set of receptive field plots for some cells. In some animals, following the receptive field plot in the horizontal orientation, heavy water (deuterium oxide) was introduced intravenously (4 ml/kg) and the receptive field was replotted at 15-minute intervals.

Calculation of Receptive Field Characteristics

When the animal's head was in the horizontal orientation, the positions of the optic axes of the eyes were plotted on the stimulus screen and joined by a line. The position of the axis about which the animal's head was rotated also was plotted on the screen. A line passing through this axis of rotation and perpendicular to the line joining the optic axes was equidistant from each eye and, thus, equally divided the visual field. It was also vertical, i.e., in line with the gravitational force vector. When the animal's head was tilted 30° from the horizontal, this line also tilted by an equal amount and maintained its relation-

ship to the positions of the optic axes. Of course, with the head tilted, the line no longer was parallel to gravity. Since the position of this line was defined with reference to the visual field, or animal, and not to the gravitational vertical, it was termed the subjective vertical meridian. This subjective vertical meridian and the position of the axis of rotation were used as reference points for calculation of receptive field characteristics.

For data analysis, the geometric center of each receptive field plotted was determined and the perpendicular distance between this point and the subjective vertical meridian was measured. The dimensions of the receptive field were also measured. A line was constructed that passed through the center of the receptive field and was parallel to the long, or major, axis of the receptive field. The intersection of this line with the subjective vertical meridian was used to determine the angle of the major axis.

Details of receptive field characteristics were obtained from 24 cells with the animal's head in both the horizontal orientation and at least one tilt orientation. For 17 cells, data were obtained for both right- and left-tilt orientations. Thus, 41 distinct receptive field plots were made, with each plot deriving from a particular cell with the head in a particular tilt orientation. The receptive field characteristics of each of these 41 cell-tilt combinations were compared with those obtained for the same cell with the head in the horizontal orientation. Thus, the horizontal orientation data obtained for each cell served as the baseline, or control, comparison for the data obtained from the same cell after the head was tilted. The receptive field characteristics for each cell-tilt combination were expressed as changes (i.e., changes in distance from the subjective vertical meridian, changes in area, and changes in major axis angle) from the control comparison.

RESULTS

Receptive Field Plots

If alterations in vestibular information had no impact upon visual cortical cells, then all characteristics of the receptive field plot obtained in the horizontal orientation should remain unchanged following head tilt except for a rotation in the same direction and by the same amount as the rotation of the head. Since the receptive field characteristics were calculated relative to the subjective vertical meridian, the values obtained from a particular cell in the tilted orientation in this case would be identical to those obtained in the horizontal orientation for the same cell. This would be true as long as tilting did not affect the positions of the eyes in their orbits, which in these experiments was the case. Thus, stimulation of the same retinal coordinates would drive the cortical cell regardless of head orientation.

FIGURE 1 includes the experimentally determined receptive field plots for a cell with the head in the horizontal, right-tilt, and left-tilt orientations. The plots with the dashed borders are identical to the horizontal plot except that they have been rotated geometrically 30° to the left and the right and, therefore, demonstrate "no change" relative to the subjective vertical meridian. These "no-change" plots indicate how the receptive field plots of this cell would appear after head tilting if, in fact, head tilt had no effect upon the cell. Subsequent calculations for each cell can be conceptualized as comparisons of the various characteristics of experimentally determined fields with such no-change plots.

The experimentally determined receptive field plots for six cells are reproduced in FIGURE 2. The plots in FIGURE 2A are the same as those shown in FIGURE 1. For the sake of compactness, plots obtained in both the right- and left-tilt orientations have been rotated geometrically 30° back toward the horizontal. No-change plots, such as those in FIGURE 1, would be exactly superimposable upon and indistinguishable from the horizontal plot in all cases following such geometrical rotations. FIGURE 2 demonstrates the extent to which this does not occur with actual experimental plots. As a general rule, the horizontal receptive field characteristics are not reproduced exactly after tilting.

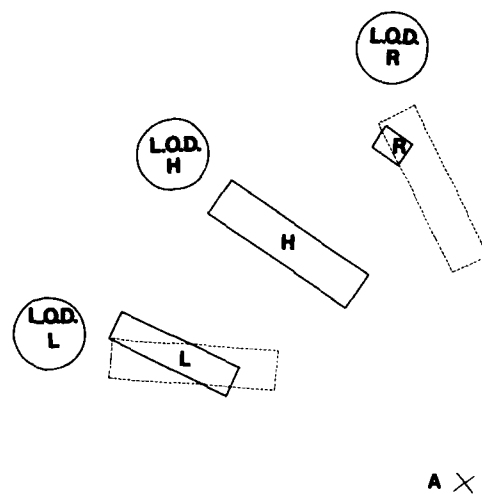


FIGURE 1. The rectangles with the solid borders represent receptive fields of a visual cortical cell plotted with the animal in the horizontal (H), right-tilt (R), and left-tilt (L) orientations. The cell was monocularly driven through the left eye and is identified as A in FIGURE 2 and TABLE 1. The right- and left-tilt rectangles with the dashed borders represent the no-change plots that are produced by simple 30° geometrical rotations of the experimentally determined horizontal receptive field. These no-change plots would be identical to the right- and left-tilt receptive fields if changes in head position did not affect the cell. In the case of this cell, tilting resulted in changes in receptive field positions, areas, and major axis angles. Legend: left optic disk (L.O.D.) locations in the horizontal (H), right-tilt (R), and left-tilt (L) orientations; the \times symbol indicates the position of the axis of rotation.

Changes in Receptive Field Characteristics following Tilting

Changes in the perpendicular distance from the subjective vertical meridian of the receptive field center for each of the 41 cell-tilt combinations relative to its horizontal orientation comparison are summarized in FIGURE 3. In 39% of these cell-tilt combinations, the distance between the receptive field center and the subjective vertical meridian was reduced by more than 10% compared to the distance in the horizontal orientation. In 29% of the cell-tilt combinations, the distance increased by more than 10%. Increases or decreases of 10% or less characterized the remaining cell-tilt combinations. As indicated in TABLE 1, only

3 of the 11 cell-tilt combinations in the examples from FIGURE 2 fell into this latter, "unchanged," classification.

In FIGURE 2, cell A is the only one in which the effect on distance was in the same direction (i.e., increased) for both left and right tilts. However, data on both tilts were available for 17 of the 24 cells, and of these, 8 demonstrated tilt-induced distance shifts in the same direction (i.e., either increases or decreases following both left and right tilts).

Changes in the receptive field area for each of the 41 cell-tilt combinations relative to its horizontal orientation comparison are summarized in FIGURE 4. In 54% of the cell-tilt combinations, the receptive field area decreased by more than 10% compared to the area in the horizontal orientation. In 34% of the cell-tilt

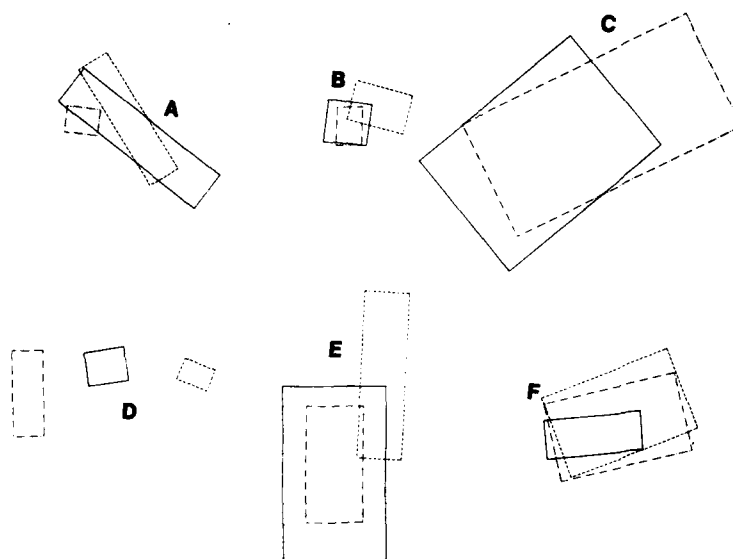


FIGURE 2. Examples of tilting effects on six cells. The right-tilt (R) and left-tilt (L) receptive fields have been rotated 30° back toward the horizontal (H) receptive field for the sake of comparison and compactness. If tilting had no effect on receptive field characteristics, then the R and L fields would be superimposed exactly upon the H field.

combinations, the area increased by more than 10%. The remaining cell-tilt combinations exhibited either increases or decreases of 10% or less. None of the 11 cell-tilt combinations reproduced in FIGURE 2 were classified as unchanged in area. The increases and decreases in area for these examples are detailed in TABLE 1.

In 3 of the cells in FIGURE 2, both left and right tilts influenced area changes in the same direction (i.e., either increases or decreases in area following both tilts). Of the total of 17 cells available for such comparison, 10 exhibited tilt-induced area changes in the same direction. At least for area changes, knowledge of the response of a cell to tilting in one direction allows some predictability about the response of the cell following a tilt in the other direction.

The correspondence between simultaneous changes in both distance and

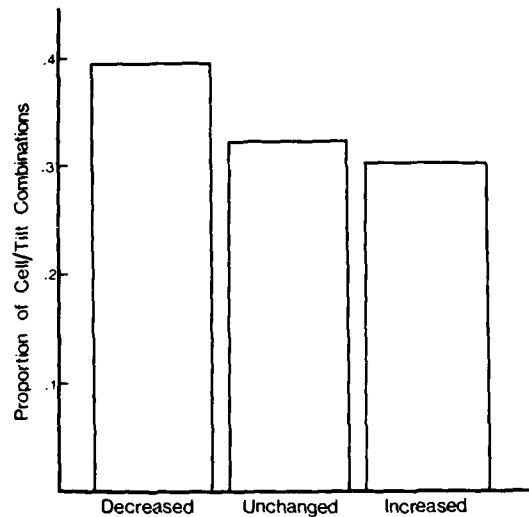


FIGURE 3. Changes in distance following tilt. The perpendicular distance from the subjective vertical meridian to the center of the receptive field for each cell-tilt combination ($n = 41$) was compared with that observed for the same cell when the animal was in the horizontal orientation. Receptive fields were classified according to whether the distance from the subjective vertical meridian increased (by more than 10%), decreased (by more than 10%), or remained unchanged (increases or decreases of 10% or less) following tilting.

area following a single tilt is very small. In only 15 of the 41 cell-tilt combinations were the effects of tilt the same on both variables (i.e., increases or decreases or no changes in both variables). As noted in TABLE 1, the examples in FIGURE 2 include 5 of these 15 cell-tilt combinations.

Changes in the angle of the major axis of the receptive field for each cell-tilt combination relative to its horizontal orientation comparison are summarized in FIGURE 5. If the angle of the major axis of a receptive field remained unchanged

TABLE 1
CLASSIFICATION OF CHARACTERISTICS OF RECEPTIVE FIELDS SHOWN IN FIGURE 2

Cell	Tilt	Distance	Area	Angle
A	right	increased	decreased	full compensation
	left	unchanged	decreased	partial compensation
B	right	unchanged	decreased	large overshoot
	left	decreased	increased	partial compensation
C	right	decreased	increased	moderate overshoot
	left	increased	increased	large overshoot
D	right	decreased	decreased	full compensation
	left	unchanged	decreased	no compensation
E	right	decreased	decreased	no compensation
	left	increased	increased	no compensation
F	right	increased	increased	moderate overshoot
	left	increased	increased	moderate overshoot

($\pm 7^\circ$) with respect to the subjective vertical meridian, the cell-tilt combination was classified as "none," i.e., showing no compensation for the tilt. Approximately 32% of the cell-tilt combinations fell into this category. In the greatest number of cell-tilt combinations, the angle of the major axis shifted in the direction of the tilt. Shifts of more than 7° but not more than 25° were classified as "moderate overshoot" and accounted for nearly 20% of the cell-tilt combinations. Shifts in excess of 25° , "large overshoot," occurred in 27% of the cell-tilt combinations. Major axes that shifted by more than 25° in a direction opposite to that of the head tilt were said to exhibit "full" compensation. Full compensation was seen in 10% of the cell-tilt combinations, while 12% exhibited "partial" compensation, which was defined as shifts of more than 7° but not more than 25° in a direction opposite to that of the head tilt.

It should be noted that the method used to determine the angle of the major axis was independent of the distance and size variables. For example, in FIGURE 2, although the areas and distances for cell E shift somewhat after tilting, the major axes in both cell-tilt combinations demonstrated no compensation. Examples of all five categories of major axis angle change are included in FIGURE 2, and TABLE 1 provides a key to the categorization.

There does not appear to be any relationship between the angle of the major

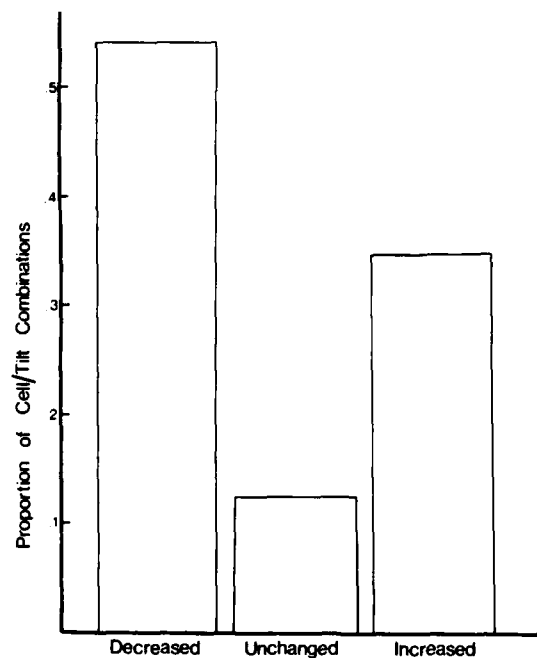


FIGURE 4. Changes in area following tilt. The area of the receptive field for each cell-tilt combination ($n = 41$) was determined and compared with that observed when the animal was in the horizontal orientation. Receptive fields were classified according to whether their area increased (by more than 10%), decreased (by more than 10%), or remained unchanged (increases or decreases of 10% or less) following tilting.

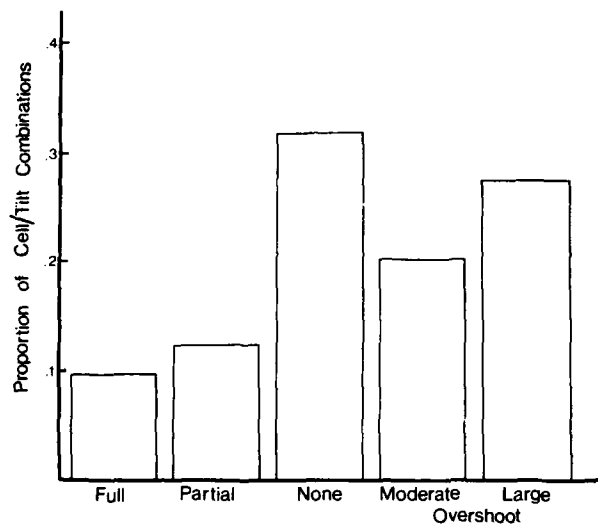


FIGURE 5. Tilt compensation of major axis. The effects of tilting upon the angle of the major axis of the receptive field relative to the subjective vertical meridian are categorized. Major axes that remained stable ($\pm 7^\circ$) with respect to the subjective vertical meridian following tilting exhibited no compensation (i.e., "none"). Axes that shifted in the direction of the tilt exhibited either "moderate overshoot" (shifts of more than 7° but not more than 25°) or "large overshoot" (shifts in excess of 25°). Axes that shifted in a direction opposite to that of the tilt exhibited either "partial" compensation (shifts of more than 7° but not more than 25°) or "full" compensation (shifts in excess of 25°). For each cell-tilt combination ($n = 41$), shifts were determined by comparison with the angle of the major axis when the animal was in the horizontal orientation.

axis following tilting in one direction and the angle following tilting in the opposite direction. Furthermore, it has not been possible to establish any relationship between the effects of tilting on the angle of the major axis and either the distance or area variables.

Changes in Receptive Field Characteristics following Heavy Water

Receptive field characteristics were plotted for eight cells immediately before and for several hours after an intravenous injection of heavy water (4 ml/kg). All plots were made with the animal in the horizontal orientation. For each cell, the plot made immediately before the administration of heavy water was used as the baseline, or control, comparison for subsequent plots. These subsequent plots were made at 15-minute intervals for more than 5 hours after the administration of heavy water.

Postinjection changes in receptive field area were calculated for each receptive field plot for each cell relative to its preinjection control comparison. FIGURE 6 summarizes these results by presenting averages for the eight cells at 15-minute intervals following the heavy-water injection. The general trend was a rapid and

large increase in receptive field area following the administration of heavy water. The increased area remained more or less constant for a period of time, after which the receptive field gradually returned to its original size and remained stable. The most rapid return to original size required only 1.25 hours, while the slowest return required 4.75 hours. The average time required was 3.25 hours. Following the return to original size, these receptive fields remained stable for as long as they were observed, which was, in some cases, for several additional hours.

FIGURE 6 unfortunately obscures the fact that in three of these eight cells, the increase in receptive field area was preceded by a more transient decrease in relative area. In two of these cells this transient phase lasted for over 1 hour, while in the third it lasted only 10 minutes. FIGURE 7 provides a composite of the receptive field plots for this third cell, which includes the plots made 5 and 10 minutes after the administration of heavy water.

In general, there was little change in the perpendicular distance of the receptive field centers following the administration of heavy water. Only one of the eight cells showed a fluctuation of the angle of the major axis of the receptive field greater than $\pm 2^\circ$.

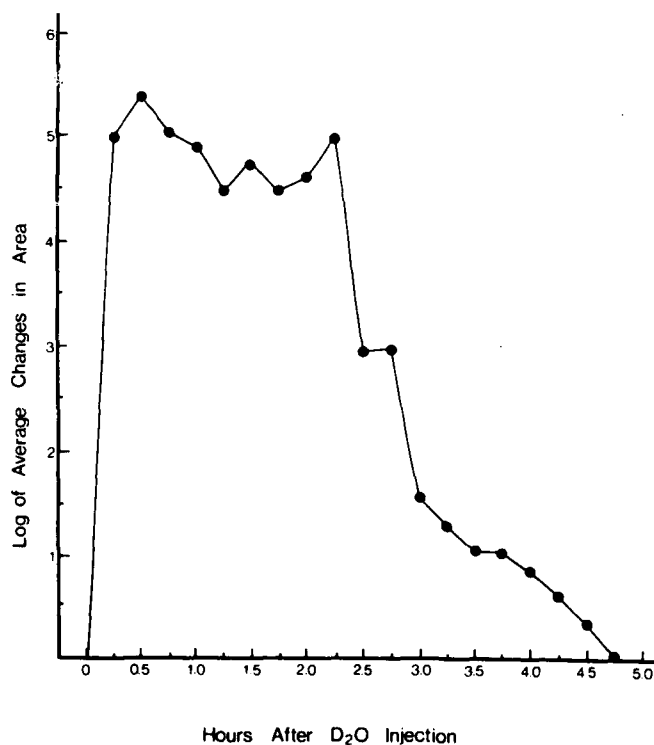


FIGURE 6. Log of the average changes in receptive field area as a function of time following the intravenous administration of heavy water (D₂O) is presented for eight cells examined in the horizontal orientation.

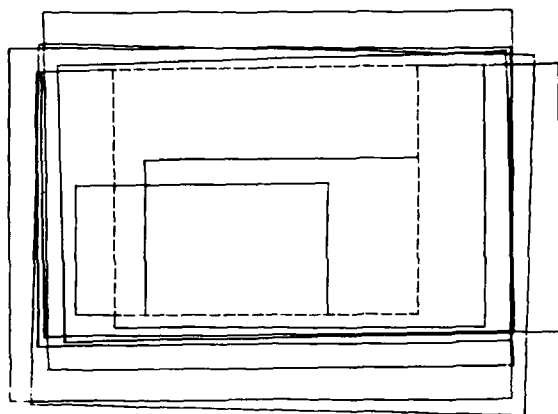


FIGURE 7. Composite of the receptive field plots for a single cell both before (dashed rectangle) and after the administration of heavy water. The two smaller fields were plotted 5 and 10 minutes after the administration of heavy water. The next plot was made 5 minutes later, and subsequent plots were made at 15-minute intervals until the receptive field returned to its original size.

DISCUSSION

Once the receptive field of a given cortical cell was determined with the animal's head in the horizontal orientation, it was easy to determine the expected position of the receptive field following head tilting if, in fact, the visual system does not respond to changes in head orientation. Given the fact that no eye movement accompanied tilting, the only receptive fields that would correspond to stimulation of the same portions of the retina would be no-change plots such as those depicted in FIGURE 1. None of the receptive fields in the 41 cell-tilt combinations reported here corresponded with such no-change plots for all three of the variables.

Thus, the receptive field of a given visual cortical cell and, correlatively, the retinal area that activates that cell are not rigidly fixed but, rather, vary according to the information received from other sensory systems concerning head position. There have been other reports that suggest that the response properties of visual cortical cells are not immutable.¹⁹⁻²⁴ Fluctuations in preferred stimulus orientation and direction of movement have been reported to occur as a function of time with no other known correlates.^{7,25} Such time-dependent fluctuations are not widely supported in the literature,^{26,27} and were not observed with the variables measured here.

The only study in the literature that is nearly comparable with the present one examined the effects of head tilt on only one variable, namely, orientation specificity.⁵ Of the 33 cell-tilt combinations reported there, 36% exhibited no compensation, which compares favorably with the 32% indicated in FIGURE 5. Only 33% of the cell-tilt combinations exhibited overshoot, in contrast to the 44% shown in FIGURE 5. More recently, a similar study reported that 44% of the cell-tilt combinations exhibited no compensation with 30% exhibiting overshoot and 26% demonstrating some compensation.⁹ Other investigators, after tilting the whole body, reported that the majority of cells exhibited either no compensation

or overshoot.⁶⁻⁸ A small number of cells exhibited alterations in receptive field size or shape.

Confirmation of the role of the vestibular system in producing the tilt-induced receptive field alterations derives from the heavy-water experiment. The ingestion of heavy water produces a profound vestibular effect that closely resembles positional alcohol nystagmus.¹⁸ This effect is apparently due to the creation of a heavy area in the endolymph ring of the semicircular canals when heavy water is acquired from the circulation. No other interactions of heavy water with either the sensory or nervous systems have been reported. Since heavy water produced a large effect on the area variable, a very much smaller effect on the distance variable, and no effect on the angle of the major axis, the area variable would appear to be the one most clearly established as being affected by vestibular input. However, while some other source of information about orientation, such as the proprioceptors, may influence the other variables, the heavy-water effect does not rule out the possibility of a vestibular interaction.

Preliminary analysis of some, as yet incomplete, data indicates that both head tilt and heavy-water administration increase the background, or spontaneous (i.e., the nonvisually driven), firing rate of visual cortical neurons but not of nonvisual cortical neurons. Similar reports of vestibular influence on spontaneous activity in the visual system have previously appeared,^{14-16,28} but it is impossible to speculate upon the relationship between such variations in spontaneous activity and the receptive field lability shown here. Reported effects of visual stimulation on the vestibular system only serve to emphasize the likely complexity of visual-vestibular interactions.^{29,30} Recent work with humans demonstrating that visual perceptions are sensitive to both proprioceptive and auditory inputs while vestibular input is varied, dramatically emphasizes the need for further information on any such interactions.³¹

REFERENCES

1. HUBEL, D. H. & T. N. WIESEL. 1959. Receptive fields of single neurons in the cat's striate cortex. *J. Physiol.* **148**: 574-591.
2. HUBEL, D. H. & T. N. WIESEL. 1962. Receptive fields, binocular interaction and functional architecture in the cat's visual cortex. *J. Physiol.* **160**: 106-154.
3. HUBEL, D. H. & T. N. WIESEL. 1965. Receptive fields and functional architecture in two non-striate visual areas (18 and 19) of the cat. *J. Neurophysiol.* **28**: 229-289.
4. HUBEL, D. H. & T. N. WIESEL. 1979. Brain mechanisms of vision. *Sci. Am.* **241**(3): 150-162.
5. DENNEY, D. & C. ADORJANI. 1972. Orientation specificity of visual neurons after head tilt. *Exp. Brain Res.* **14**: 312-317.
6. HORN, G. 1965. The effect of somaesthetic and photic stimuli on the activity of units in the striate cortex of unanesthetized, unrestrained cats. *J. Physiol.* **179**: 263-277.
7. HORN, G. & R. M. HILL. 1969. Modifications of receptive fields of cells in the visual cortex occurring spontaneously and associated with body tilt. *Nature* **221**: 186-188.
8. HORN, G., G. STRECKLER & R. M. HILL. 1972. Receptive fields of units in the visual cortex of the cat in the presence and absence of bodily tilt. *Exp. Brain Res.* **15**: 113-132.
9. TOMKO, D. L., N. M. BARBARO & F. M. ALI. 1978. Effect of head tilt on receptive field orientation of simple cells in area 17 of unanesthetized cats, *Soc. Neurosci. Abstr.* **4**: 615.
10. METZLER, J. & D. N. SPINELLI. 1979. Tilt-constant receptive fields in the kitten visual cortex. *Brain Res.* **183**: 344-348.

11. BLAKEMORE, C. & J. PAPAIOANNOU. 1974. Does the vestibular apparatus play a role in the development of the visual system. *J. Physiol.* **236**: 373-385.
12. BISTI, S., L. MAFFEI & M. PICCOLINO. 1972. Variations of the visual responses of the superior colliculus in relation to body roll. *Science* **175**: 456-457.
13. RIEGER, P. & M. STRASCHILL. 1973. The effect of body tilt upon the transfer and output function of neurons of the cat's superior colliculus. *Pfluegers Arch.* **344**: 187-193.
14. PAPAIOANNOU, J. 1969. Vestibular influences on the spontaneous activity of neurons in the lateral geniculate nucleus of the cat. *J. Physiol.* **202**: 87P.
15. PAPAIOANNOU, J. N. 1973. Changes in the light-evoked discharges from lateral geniculate nucleus neurons in the cat, induced by caloric labyrinthine stimulation. *Exp. Brain Res.* **17**: 10-17.
16. MAGNIN, M., M. JEANNEROD & P. PUTKONEN. 1974. Vestibular and saccadic influences on dorsal and ventral nuclei of the lateral geniculate body. *Exp. Brain Res.* **21**: 1-18.
17. KENNEDY, H., M. MAGNIN & M. JEANNEROD. 1976. Receptive field responses of LGB neurons during vestibular stimulation in awake cats. *Vision Res.* **76**: 119-120.
18. MONEY, K. E. & W. S. MYLES. 1974. Heavy water nystagmus and effects of alcohol. *Nature* **247**: 404-405.
19. PETTIGREW, J. D., T. NIKARA & P. O. BISHOP. 1968. Responses to moving slits by single units in cat striate cortex. *Exp. Brain Res.* **6**: 373-390.
20. BISHOP, P. O., J. S. COOMBS & G. H. HENRY. 1971. Responses to visual contours: spatio-temporal aspects of excitation in the receptive fields of simple striate neurons. *J. Physiol.* **219**: 625-657.
21. FRIES, W., K. ALBUS & O. D. CREUTZFELDT. 1977. Effects of interacting visual patterns on single cell responses in cat's striate cortex. *Vision Res.* **17**: 1001-1008.
22. FRIES, W. & K. ALBUS. 1976. Static and dynamic properties of receptive fields of some simple cells in cat's striate cortex. *Vision Res.* **16**: 563-566.
23. BISHOP, P. O., J. S. COOMBS & G. H. HENRY. 1973. Receptive fields of simple cells in the cat striate cortex. *J. Physiol.* **231**: 31-60.
24. GOODWIN, A. W. & G. H. HENRY. 1978. The influence of stimulus velocity on the responses of single neurones in the striate cortex. *J. Physiol.* **277**: 467-482.
25. DONALDSON, I. M. L. & J. G. R. NASH. 1975. Variability of the relative preference for stimulus orientation and direction of movement in some units of the cat visual cortex (areas 17 and 18). *J. Physiol.* **245**: 305-324.
26. HAMMOND, P., D. P. ANDREWS & C. R. JAMES. 1975. Invariance of orientational and directional tuning in visual cortical cells of the adult cat. *Brain Res.* **96**: 56-59.
27. HAMMOND, P. & D. P. ANDREWS. 1978. Orientation tuning of cells in areas 17 and 18 of the cat's visual cortex. *Exp. Brain Res.* **31**: 341-351.
28. GRUSSER, O. J. & U. GRUSSER-CORNHILS. 1972. Interaction of vestibular and visual inputs in the visual system. *Prog. Brain Res.* **37**: 573-583.
29. WAESPE, W. & V. HENN. 1978. Conflicting visual-vestibular stimulation and vestibular nucleus activity in alert monkeys. *Exp. Brain Res.* **33**: 203-211.
30. ALLUM, J. H. J., W. GRAF, J. DICHGANS & C. L. SCHMIDT. 1976. Visual-vestibular interactions in the vestibular nuclei of the goldfish. *Exp. Brain Res.* **26**: 463-485.
31. LACKNER, J. R. & A. GRAYBIEL. 1979. Parabolic flight: loss of sense of orientation. *Science* **206**: 1105-1108.

CIRCULARVECTION: PSYCHOPHYSICS AND SINGLE-UNIT RECORDINGS IN THE MONKEY*

U. Büttner and V. Henn

*Department of Neurology
University Hospital
University of Zurich
CH-8091 Zurich, Switzerland*

In humans the sensation of self-rotation can be induced by moving a large visual field around the stationary subject. This sensation was first investigated by Mach and later called circularvection (CV).¹⁷ This visually induced sensation of self-rotation implies a high degree of visual-vestibular convergence in central nervous structures.

In neurophysiological studies such interaction already has been demonstrated at the level of the vestibular nuclei, only one synapse away from the vestibular nerve.^{1,11,15,19} Additional visual-vestibular interaction along the vestibulocortical pathway has been demonstrated at both the thalamic and the cortical level.^{8,7,9}

In functional terms, the vestibular end organ can only detect accelerations whereas the visual system can also detect constant-velocity rotation. Convergence of these two inputs therefore should make it possible to derive an output encoding actual velocity over a wide range, from constant velocity to high accelerations. Analysis of single-unit recordings in the vestibular nuclei supports this notion.²⁰

Experiments were designed to explore the upper frequency limit of sinusoidal rotation of the visual surround, which can lead either to CV in humans or to modulation of vestibular-unit activity in the monkey. In the experiments, two paradigms were used:

1. Human subjects were exposed to sinusoidal rotation of an optokinetic cylinder totally enclosing the subject. Stimulus frequency of cylinder rotation was increased until subjects no longer experienced CV and only perceived motion of the surround. All subjects experienced at least partial CV, even at stimulus frequencies above 1 Hz.

2. Monkeys also were exposed to sinusoidal cylinder rotation of different frequencies, and single-unit responses were measured in the vestibular cortex (area 2v).^{8,13} Comparison of these responses to those of the vestibular nuclei shows that cortical neurons respond over a wider range of visual frequencies and therefore must receive additional visual input.

METHODS

Psychophysics

Six healthy subjects (25-40 years old) with normal peripheral vision and no history of vestibular disorders participated. Subjects sat on a chair that was completely surrounded by a cylinder (diameter, 140 cm) covered with vertical

*Supported by Swiss National Foundation for Scientific Research 3.343-78.

black and white stripes, each 7.5° wide (FIGURE 1). The cylinder was driven by a torque motor and rotated sinusoidally around the stationary subject. The applied frequencies, accelerations, velocities, and position changes are shown in TABLE 1. Trials were given in random order, with an intermission to keep subjects alert and to avoid motion sickness. Each stimulus sequence, which lasted about 1 hour, was repeated three times.

Subjects were instructed to indicate verbally the maximal amount of CV (i.e., sensation of self-rotation) that they experienced during each sinusoidal cycle. It ranged from full CV (100%; only self-rotation, no cylinder rotation, perceived) to no CV (0%; only cylinder rotation). Intermediate values were given in percent of self-rotation in five steps (20, 40, 50, 60, and 80%). Fifty percent would indicate the perception that total relative motion is half cylinder and half self-rotation.

Neurophysiology

Monkeys were prepared chronically for single-unit recordings.⁵ Eye position was recorded with implanted d.c. Ag-AgCl electrodes.

Monkeys sat upright in a primate chair with the head fixed and tilted 25° forward in order to bring the horizontal semicircular canals in the plane of rotation. For pure vestibular stimulation, animals were sinusoidally rotated about a vertical axis at frequencies between 0.005 and 1 Hz in the dark. For visual stimulation, a striped cylinder similar to the one shown in FIGURE 1 was rotated sinusoidally around the stationary monkey. Parameters for visual stimulation are given in TABLE 2.

All relevant data (neuronal activity, horizontal and vertical eye position, cylinder and turntable velocity) were stored on FM magnetic tape. For analysis, data were written out on a six-channel oscillograph. Unit activity was analyzed using instantaneous and average frequency, i.e., running average over 250 mseconds with display update every 100 mseconds. Phase relations of vestibular neurons were determined using a Fourier analysis program on a PDP 11/40 computer.⁶

RESULTS

Psychophysics

The amounts of CV during different frequencies of stimulation and accelerations for one subject are shown in FIGURE 2. This subject experienced CV at all frequencies when maximal acceleration was $5^\circ/\text{second}^2$. The highest frequency was limited to 2 Hz at this acceleration. At 5 Hz, total cylinder displacement would be only 0.01° , which cannot be detected reliably if no stationary points of reference are visible. Therefore, the upper frequency limit was chosen to be that frequency at which all subjects still perceived object motion. The amount of CV decreases with higher accelerations and higher sinusoidal-stimulus frequencies.

At low frequencies, periods of full CV alternate with periods of pure object motion during one cycle.³ Also, the relative amount of CV changes during the course of one sinusoidal cycle. Therefore, subjects were instructed to indicate only the maximal CV for each trial.

All subjects experienced full CV at low-frequency stimulation and low acceleration (FIGURE 3). With increasing frequencies and accelerations, all expe-



FIGURE 1. Optokinetic cylinder with sliding doors to completely enclose the subject.

TABLE 1
PARAMETERS OF SINUSOIDAL CYLINDER ROTATION USED FOR PSYCHOPHYSICAL
EXPERIMENTS IN HUMANS

Frequency (Hz)	Maximum Acceleration* (deg/sec ²)	Maximum Velocity† (deg/sec)	Total Position Change (degrees)
0.01	5; 10	80; 159	2546; 5062
0.02	5-20	40-159	636-2532
0.05	5-40	16-127	102-808
0.07	5-40	11-91	50-414
0.1	5-40	8-64	25-204
0.2	5-160	4-127	6.4-202
0.5	5-160	1.6-51	1.0-32
1.0	5-160	0.8-25	0.26-8.1
2.0	5-160	0.4-12.7	0.06-2.0
5.0	20-160	0.6-5.1	0.04-0.32

*Maximum accelerations were chosen in steps as 5, 10, 20, 40, 80, or 160°/second².

†Maximal velocities were limited to 159°/second.

perienced a combined sensation of CV and object motion. During combined sensation, object motion and CV are sensed in opposite directions.³ Partial CV was definitely present at 1 and 2 Hz (FIGURES 2 and 3). At these frequencies, all subjects had some CV for all accelerations, at least in one trial. At 5 Hz, CV was greatly reduced but was not zero. All subjects still experienced some CV, at least in one trial. The curves of FIGURES 2 and 3 indicate that 5 Hz is probably the upper frequency limit for perceiving CV.

Neurophysiology

Neurons were recorded in the region of the vestibular cortical projection (area 2v).^{6,9,13,16} It is located in the transition zone of areas 2, 5, and 7.⁴ Vestibular cortex neurons can be classified as type I or II according to the nomenclature of Duensing and Schaefer.¹² Type I neurons are activated with angular acceleration to the ipsilateral side; type II neurons, to the contralateral side.

Average activity was low (about 8 impulses/second) and irregular. Neurons showed no additional modulation with eye movements.⁶

TABLE 2
PARAMETERS OF SINUSOIDAL CYLINDER ROTATION USED FOR SINGLE-UNIT RECORDINGS IN
THE VESTIBULAR CORTEX (AREA 2v) OF THE ALERT MONKEY

Frequency (Hz)	Maximum Acceleration (deg/sec ²)	Maximum Velocity (deg/sec)	Total Position Change (degrees)
0.01	5.6/6.9	90/110	2466/3503
0.05	22/28	70/90	445/573
0.1	28/44	45/70	143/223
0.2	38/57	30/45	48/72
0.5	50/69	16/22	10/14
1.0	75	12	3.8

Unit activity was related to turntable velocity using a Fourier analysis program. During sinusoidal rotation at 0.1 Hz in the dark, neurons showed a phase advance of 0-20° relative to turntable velocity (FIGURE 4). There was no difference in the response of type I and II neurons. These values are similar to those found in the vestibular nuclei and in the thalamus of the alert monkey.^{5,8,14}

Vestibular cortex neurons also responded to large moving visual fields, which induce optokinetic nystagmus. They did not respond to small moving objects or to light-on or -off. In most instances, turntable and cylinder had to move in opposite directions to elicit an activation. Under these conditions, vestibular and optokinetic nystagmus beat into the same direction.

When tested with sinusoidal cylinder rotation, vestibular cortex neurons consistently responded over a wide frequency range. Responses were then in phase with cylinder velocity (FIGURE 5). For most neurons, the sensitivity (impulses/second per degree/second) increased with stimulus frequencies above 0.1 Hz (FIGURES 5 and 6). These response characteristics are different from those found in the vestibular nuclei (monkey, personal observation; cat, Reference 16), where most neurons display a decreasing gain with increasing stimulus frequencies of the optokinetic cylinder.

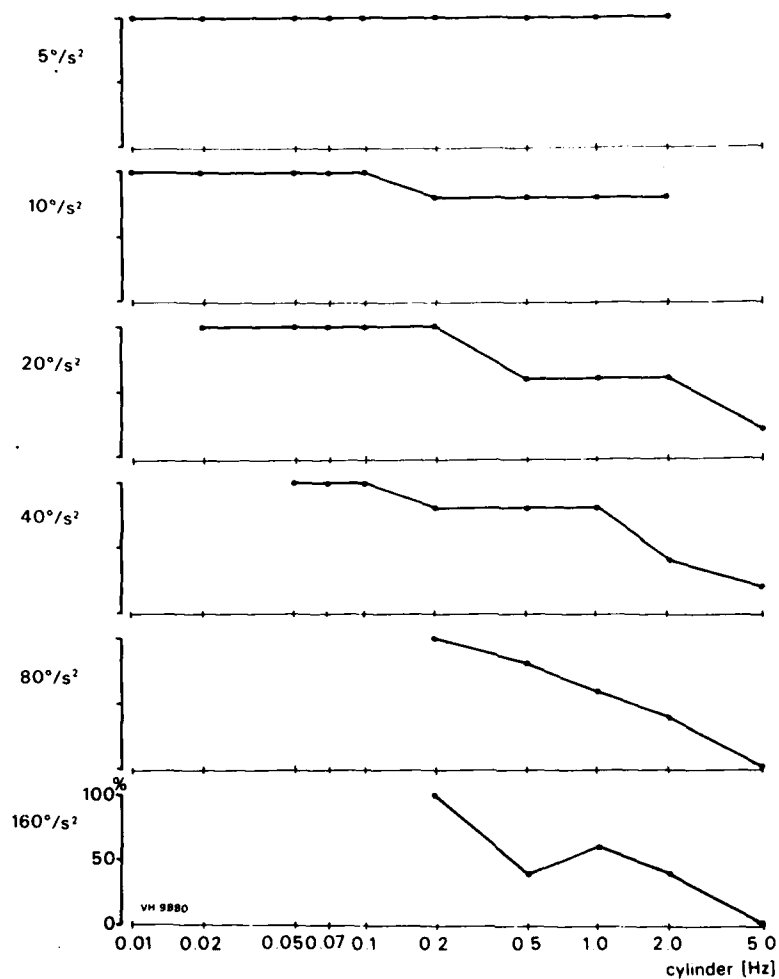


FIGURE 2. Circularvection (CV) of one subject during different frequencies (abscissa) and accelerations ($5\text{--}160^{\circ}/\text{second}^2$) of sinusoidal cylinder rotation. Ordinate indicates the relative amount of CV ranging from 0% (only cylinder rotation perceived, no CV) to 100% (pure CV, no cylinder rotation). Values in between indicate a combined perception of cylinder rotation and CV. The subject was asked to indicate the maximal perceived CV. The relative amount of CV decreases with higher frequencies and accelerations.

DISCUSSION

Psychophysics

Experiments were performed to measure the range of frequencies and accelerations under which CV can be experienced. CV could be elicited reliably up to 2 Hz. An upper frequency limit seems to occur around 5 Hz (FIGURE 3). In

similar experiments, linearvection (LV, self-motion perception induced by linear visual motion) was still present at 1 Hz, the highest frequency tested.^{2,10}

The development of CV is highly dependent on additional parameters like acceleration and velocity, and probably also on the size of position changes. Brandt *et al.* showed that CV increases linearly up to 120°/second constant stimulus velocity.³ With few exceptions, we kept maximal velocities below 120°/second (TABLE 1). Results show that CV decreases if accelerations exceed

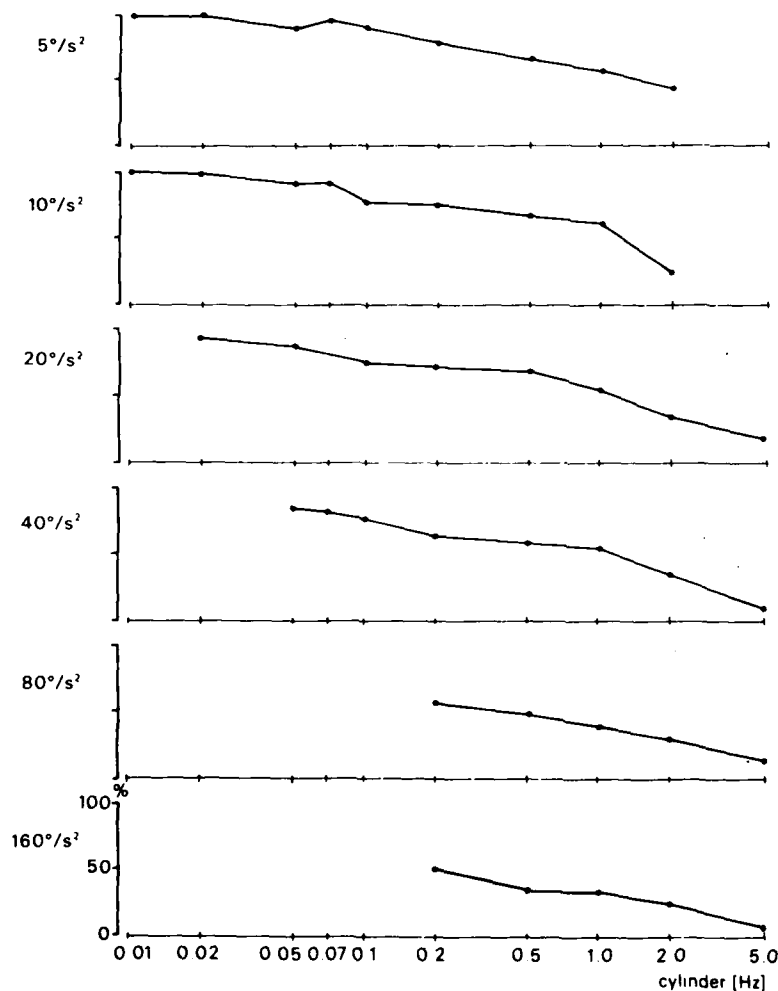


FIGURE 3. Averaged CV of six subjects (each subject, three trials) during different frequencies and accelerations of sinusoidal cylinder rotation. Same format as FIGURE 2. The relative amount of CV decreases little up to 0.1 Hz, but strongly at higher frequencies. At 5 Hz, only a minimal amount of CV remains. CV also decreases at a given frequency with increasing accelerations, particularly above 20°/second².

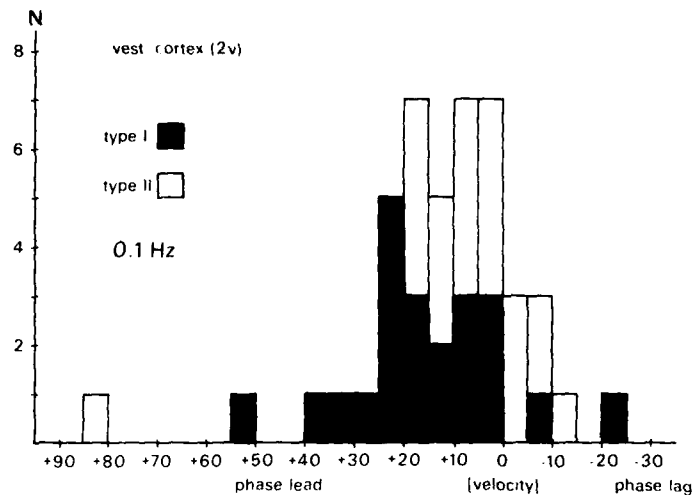


FIGURE 4. Phase relation of 44 (22 type I, 22 type II) vestibular cortex neurons during sinusoidal rotation of the monkey at 0.1 Hz in the dark. Ordinate, number of neurons; abscissa, phase relation between neuronal activity and turntable velocity. Most neurons show a phase advance between 0-20°.

10-20°/second². The perception of CV, depending on so many limiting factors, is highly nonlinear.

For the perception of self-motion, the central vestibular system seems to depend primarily on two sensory channels: the visual input for stimuli in the low-frequency range up to about 0.1 Hz, and the vestibular input for higher frequencies. These input ranges are well tuned to the optimal working parameters of the receptor systems, with low accelerations and constant velocities for the visual input and high accelerations for the peripheral vestibular organ. A model of how these two inputs combine has been proposed.²¹ Basically, the two inputs

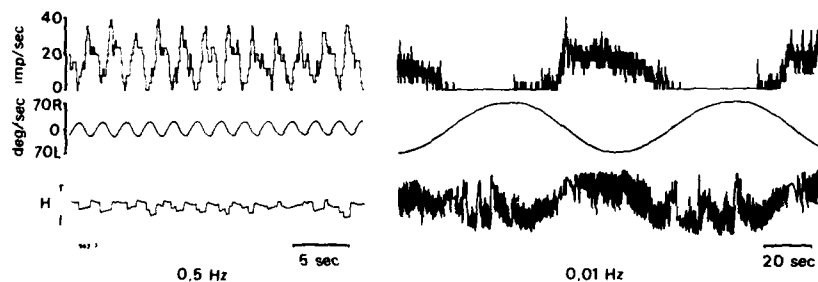


FIGURE 5. Vestibular cortex neuron (type I, recorded on the right side) during sinusoidal cylinder rotation at 0.5 and 0.01 Hz. The monkey is stationary. From above: neuronal activity (running average), cylinder velocity, and horizontal eye position. Neuronal activity is in phase with cylinder velocity. The sensitivity of the neuron in relation to cylinder velocity is much higher at 0.5 than at 0.01 Hz.

are compared with an internal parameter representation and weighted accordingly.

In our experiments, the peripheral vestibular input was zero at all times. Still, a reliable response was present at visual frequencies of 1–2 Hz, a range that is usually considered to lie within the working range of the vestibular system, with the gain of the vestibulo-ocular reflex near unity. Our results show that with adequate visual stimuli, i.e., the whole visible surround physically moving, there is a wide overlap of frequency ranges of visual and vestibular inputs for the perception of self-motion.

A related problem is how the vestibulo-ocular reflex can operate at a gain of unity in the high-frequency range, if not constantly recalibrated by visual input. Recently, Melvill Jones (this volume) showed that subjects wearing spectacles that produce a right-left inversion of visual input, perfectly adapt and reverse

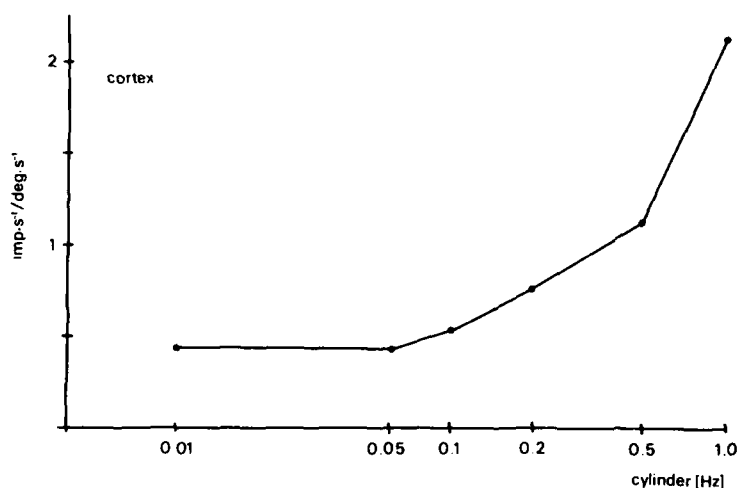


FIGURE 6. Average sensitivity (impulses/second per degree/second) of 14 vestibular cortex neurons (8 type I, 6 type II) during different frequencies of sinusoidal cylinder rotation. Sensitivity increases at stimulus frequencies above 0.1 Hz.

their vestibulo-ocular reflex even at high frequencies (3 Hz). This is another example of how powerful the visual input can be at high frequencies. It shows that although the gain of the optokinetic nystagmus might be very low at stimulus frequencies above 0.5 Hz, the visual input still can modify other responses.

Neurophysiology

The quantitative analysis of the vestibular responses of cortical neurons in area 2v shows that neurons carry a head-velocity signal at a medium-frequency range (0.1 Hz), similar to that in the vestibular nuclei.^{5,14} This indicates a transfer of vestibular information over only a few synapses, which agrees well with electrophysiological studies,¹⁶ although the anatomical pathway has not been worked out yet.⁹

The prominent visual response of vestibular cortex neurons at high frequencies of sinusoidal cylinder rotation is different from that seen in the vestibular nuclei. This indicates an additional visual input, the origin of which is not known. It should be noted that there has been no clinical report of a patient who has lost the sense of motion after focal cortical lesions. This implies that there is probably no single primary vestibular projection area responsible for motion sensation (see also Reference 9). A direct comparison of the single-unit data and the psychophysical measurements reveals the discrepancy of the gain decrease for CV at high frequencies and the gain increase for the unit data. This might imply that these neurons do not encode a signal about self-motion. However, the neurophysiological data clearly demonstrate that the cortex receives converging information about motion from the vestibular and visual systems. These neurons could function as an input to association areas, where a signal about self-motion then could be reconstructed.

SUMMARY

In psychophysical experiments, human subjects indicated the amount of circularvection (CV) that they experienced during sinusoidal rotation (0.01–5 Hz) of the visual surround. Accelerations varied between 5 and 160°/second²; maximal velocities did not exceed 160°/second. Below 0.1 Hz and 20°/second², most subjects experienced full CV; above, CV was only partial. Subjects then perceived a combination of CV and object motion. All subjects still had some CV at 2 Hz. The upper frequency limit seemed to occur around 5 Hz.

In related neurophysiological studies, single units were investigated in the vestibular cortex (area 2v) of the alert monkey. Neurons responded to animal rotation in the dark as well as to sinusoidal rotation of the visual surround (0.01–1 Hz). Units responded to the visual stimulus in the high-frequency range with a gain increase.

These experiments demonstrate the prominent influence of the visual system on vestibular neurons even at high frequencies.

ACKNOWLEDGMENTS

We thank Ms. V. Isoviita for assistance during the experiments, Mr. E. Solcá for taking care of the electronic equipment, and Mr. J. Müller for photographic work.

REFERENCES

1. ALLUM, J. H. J., W. GRAF, J. DICHGANS & C. L. SCHMIDT. 1976. Visual-vestibular interactions in the vestibular nuclei of the goldfish. *Exp. Brain Res.* **26**: 463–485.
2. BERTHOZ, A., B. PAVARD & L. R. YOUNG. 1975. Perception of linear horizontal self-motion induced by peripheral vision (linearvection). Basic characteristics and visual-vestibular interactions. *Exp. Brain Res.* **23**: 471–489.
3. BRANDT, TH., J. DICHGANS & E. KOENIG. 1973. Differential effects of central versus peripheral vision on egocentric and exocentric motion perception. *Exp. Brain Res.* **16**: 476–491.
4. BRODMAN, K. 1905. Beiträge zur histologischen Lokalisation der Grosshirnrinde. Dritte Mitteilung: Die Rindenfelder der niederen Affen. *J. Psychol. Neurol.* **4**: 177–226.

5. BUETTNER, U. W., U. BÜTTNER & V. HENN. 1978. Transfer characteristics of neurons in the vestibular nuclei of the alert monkey. *J. Neurophysiol.* **41**: 1614-1628.
6. BÜTTNER, U. & U. W. BUETTNER. 1978. Parietal cortex (2v) neuronal activity in the alert monkey during natural vestibular and optokinetic stimulation. *Brain Res.* **153**: 392-397.
7. BÜTTNER, U. & V. HENN. 1976. Thalamic unit activity in the alert monkey during natural vestibular stimulation. *Brain Res.* **103**: 127-132.
8. BÜTTNER, U., V. HENN & H. P. OSWALD. 1977. Vestibular-related neuronal activity in the thalamus of the alert monkey during sinusoidal rotation in the dark. *Exp. Brain Res.* **30**: 435-444.
9. BÜTTNER, U. & W. LANG. 1979. The vestibulocortical pathway: neurophysiological and anatomical studies in the monkey. *Prog. Brain Res.* **50**: 581-588.
10. CHU, W. H. N. 1976. Dynamic response of human linearvection. Masters Thesis. Department of Aeronautics and Astronautics. Massachusetts Institute of Technology. Cambridge, Mass.
11. DICHCANS, J., C. L. SCHMIDT & W. GRAF. 1973. Visual input improves the speedometer function of the vestibular nuclei in the goldfish. *Exp. Brain Res.* **18**: 319-322.
12. DUENSING, F. & K. P. SCHAEFER. 1958. Die Aktivität einzelner Neurone im Bereich der Vestibulariskerne bei Horizontalbeschleunigungen unter besonderer Berücksichtigung des vestibulären Nystagmus. *Arch. Psychiatr. Nervenkr.* **198**: 225-252.
13. FREDRICKSON, J. M., U. FIGGE, P. SCHEID & H. H. KORNUBER. 1966. Vestibular nerve projection to the cerebral cortex of the rhesus monkey. *Exp. Brain Res.* **2**: 328-337.
14. FUCHS, A. F. & J. KIMM. 1975. Unit activity in vestibular nucleus of the alert monkey during horizontal angular acceleration and eye movement. *J. Neurophysiol.* **38**: 1140-1161.
15. HENN, V., L. R. YOUNG & C. FINLEY. 1974. Vestibular nucleus units in alert monkeys are also influenced by moving visual fields. *Brain Res.* **71**: 144-149.
16. KELLER, E. L. & W. PRECHT. 1979. Visual-vestibular responses in vestibular nuclear neurons in the intact and cerebellectomized, alert cat. *Neuroscience* **4**: 1599-1613.
17. MACH, E. 1875. *Grundlinie der Lehre von den Bewegungsempfindungen*. Engelmann. Leipzig, Germany. (Also 1967. Bonset. Amsterdam, the Netherlands.)
18. SCHWARZ, D. W. F. & J. M. FREDRICKSON. 1971. Rhesus monkey vestibular cortex: a bimodal primary projection field. *Science* **172**: 280-281.
19. WAESPE, W. & V. HENN. 1977. Neuronal activity in the vestibular nuclei of the alert monkey during vestibular and optokinetic stimulation. *Exp. Brain Res.* **27**: 523-538.
20. WAESPE, W. & V. HENN. 1979. The velocity response of vestibular nucleus neurons during vestibular, visual, and combined angular acceleration. *Exp. Brain Res.* **37**: 337-347.
21. ZACHARIAS, G. L. & L. R. YOUNG. 1981. Influence of combined visual and vestibular cues on human perception and control of horizontal rotation. *Exp. Brain Res.* **41**: 159-171.

SIGMA-MOVEMENT AND SIGMA-NYSTAGMUS: A
NEW TOOL TO INVESTIGATE THE GAZE-PURSUIT
SYSTEM AND VISUAL-MOVEMENT PERCEPTION
IN MAN AND MONKEY*

Birgit Adler, H. Collewijn,† G. Curio, O.-J. Grüsser,‡ M. Pause,
Ursula Schreiter, and L. Weiss

Department of Physiology
Free University of Berlin
1 Berlin 33, Federal Republic of Germany

VISUAL MOVEMENT PERCEIVED WITH STABILIZED RETINAL STIMULI

The simple observation that started our experiments has an age-old tradition in the history of science. Aristotle (384-322 B.C.) was presumably the first to describe that after looking into the sun or another bright light, a long-lasting afterimage persists and is seen thereafter in the respective line of sight.¹ Such an afterimage is, of course, a perfectly stabilized retinal image; however, it can be seen to change its position in the extrapersonal space whenever the eyes move voluntarily. A small afterimage placed within 2° to 3° around the fovea centralis can be used to elicit smooth-pursuit eye movements in darkness when one tries to fixate it intentionally. During the pursuit movements, the afterimage is seen moving in the direction of the eye movements.^{2,3,4} This von Helmholtz afterimage movement illusion was explained by 19th century physiologists as being caused by a central interaction of premotor commands controlling gaze movement and the afferent visual-signal flow.^{2,5,6}

Visual movement perceived with a stimulus pattern that is stationary on the retina but with moving eyes is called *efferent movement perception*, while the visual movement elicited by a change in position of the retinal stimuli is called *afferent movement perception*.^{7,8} To our knowledge, the first block diagram of the interaction between afferent sensory signals and the corollary discharges of efferent motor signals was published in the general scheme "Merkwelt-Wirkwelt-Koppelung" by J. von Uexküll.⁹ This model (FIGURE 1a) contains the essential properties that later became known as the *efference copy hypothesis*:^{10,11,12,13} an efference copy of the motor commands interacts with the afferent sensory-signal flow; the result of this interaction constitutes the percept and simultaneously the signals driving the pursuit mechanisms.

Despite its long existence, the efference copy interaction model rarely has been analyzed quantitatively and no systematic experiments have been performed with nonhuman primates. The afterimage paradigm is difficult to apply in animal experiments. We have therefore, during the last eight years, used another paradigm (FIGURE 1b).^{14,15} A row of equally spaced stationary black and white stripes or black dots of the spatial period P_s is illuminated stroboscopically at the flash frequency f_s (flash duration half-time, 56 μ seconds). When the center

*Supported by grants from the Deutsche Forschungsgemeinschaft (Gr 161) and a Twinning Grant of the European Science Foundation-ETP Strassburg.

†Department of Physiology, Erasmus University, Rotterdam, the Netherlands.

‡To whom correspondence should be addressed.

$$\bar{V}_g = k \cdot P_s \cdot f_s [\text{degrees/second}] \quad (1)$$

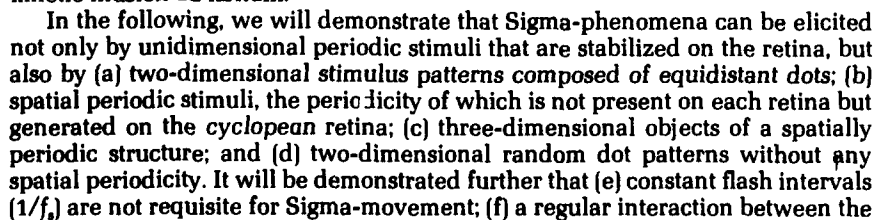
a

The diagram illustrates a closed-loop control system. It consists of the following components and connections:

- M** (Motor): Labeled "control of motor act" and "Handlungsorgan".
- P** (Perceptor): Labeled "central perceptory system" and "Merkorgan".
- R** (Receptor): Represented by a circle.
- E** (Effector): Represented by a shaded rectangle.

The flow of the system is as follows:

- A solid arrow points from **M** to **E**.
- A solid arrow points from **E** to **P**.
- A solid arrow points from **P** to **M**.
- A dashed arrow points from **R** to **P**.
- A feedback loop is shown as a solid arrow starting from the output of **E**, passing through a junction point (a circle with a cross), and then entering **P**. This junction point is labeled "reference copy".



vestibulo-ocular reflex and Sigma-movement was found; and (g) Sigma-phenomena are elicitable in awake monkeys; thus, the phenomenon is accessible to further neurophysiological exploration.

The experiments were performed in man (12 subjects) and 8 Java monkeys (*Macaca fascicularis*). The horizontal and vertical electro-oculogram (EOG) was recorded in monkeys by chronically implanted Ag-AgCl electrodes, in man by skin Ag-AgCl electrodes. In addition, the electromagnetic search coil technique (EMOG) was applied.^{18,19} For details of the experimental techniques, the reader is referred to other reports.^{17,20,21}

SIGMA-MOVEMENT DEPENDS ON THE SPATIAL PERIOD P_s AND THE FLASH FREQUENCY f_s

Experiments in Man

The law expressed by Equation 1 was fulfilled within a wide range. The perceived speed of the apparent Sigma-movement increased with the period P_s of the stationary stimulus pattern and the flash frequency f_s , as did the angular

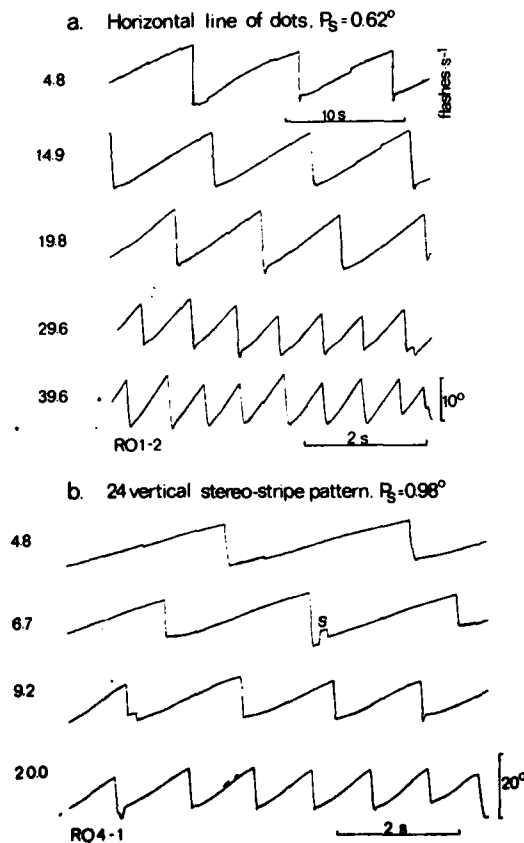


FIGURE 2. (a) Sigma-OKN in man. Recording with the electromagnetic search coil technique (EMOG).^{18,19} A horizontal line of dots 0.62° apart was illuminated stroboscopically with different flash frequencies as indicated. (b) Sigma-OKN elicited by a vertical stereo-stripe pattern. The stereo-strips generated on the cyclopean retina were 0.98° apart. Different flash frequencies as indicated.

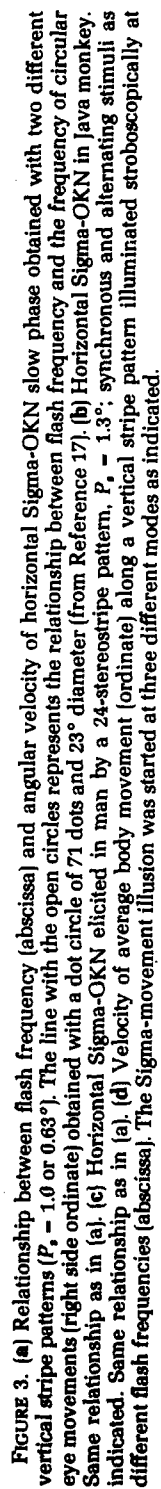


FIGURE 3. (a) Relationship between flash frequency (abscissa) and angular velocity of horizontal Sigma-OKN slow phase obtained with two different vertical stripe patterns ($P_s = 1.0$ or 0.63°). The line with the open circles represents the relationship between flash frequency and the frequency of circular eye movements (right side ordinate) obtained with a dot circle of 71 dots and 23° diameter (from Reference 17). (b) Horizontal Sigma-OKN in Java monkey. Same relationship as in (a). (c) Horizontal Sigma-OKN elicited in man by a 24-stereostripe pattern, $P_s = 1.3^\circ$; synchronous and alternating stimuli as indicated. Same relationship as in (a). (d) Velocity of average body movement (ordinate) along a vertical stripe pattern illuminated stroboscopically at different flash frequencies (abscissa). The Sigma-movement illusion was started at three different modes as indicated.

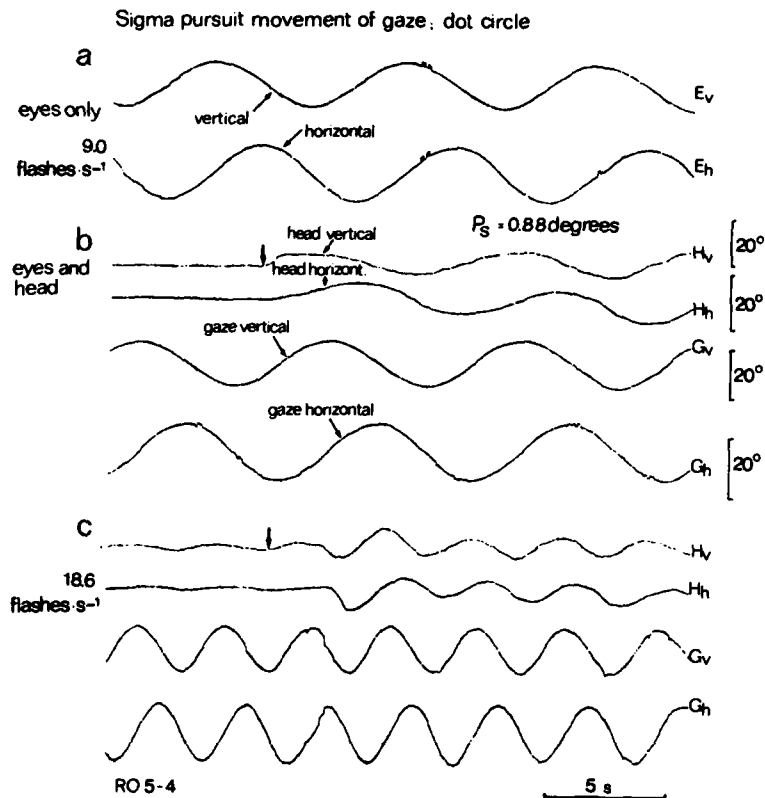


FIGURE 4. Sigma-pursuit movements elicited by stroboscopic illumination of a stationary dot circle, 23° diameter, 71 dots. (a) Head fixed, circular movements of eyes; 9 flashes/second. (b) Eye and head movements; 9.0 flashes/second. (c) Eye and head movements; 18.6 flashes/second. Recording of gaze position and head position by EMOG, one coil on the sclera, the other on the forehead.

velocity of the center of gaze V_g during Sigma-OKN. With fixed head, V_g was identical to the angular velocity of the eyes, V_e (FIGURE 2a). The Sigma-movement perceived was smooth and continuous, and its speed was correlated to the angular velocity of the Sigma-OKN slow phase V_o . The latter increased with P_s and f_s according to Equation 1 (FIGURES 2a and 3a).

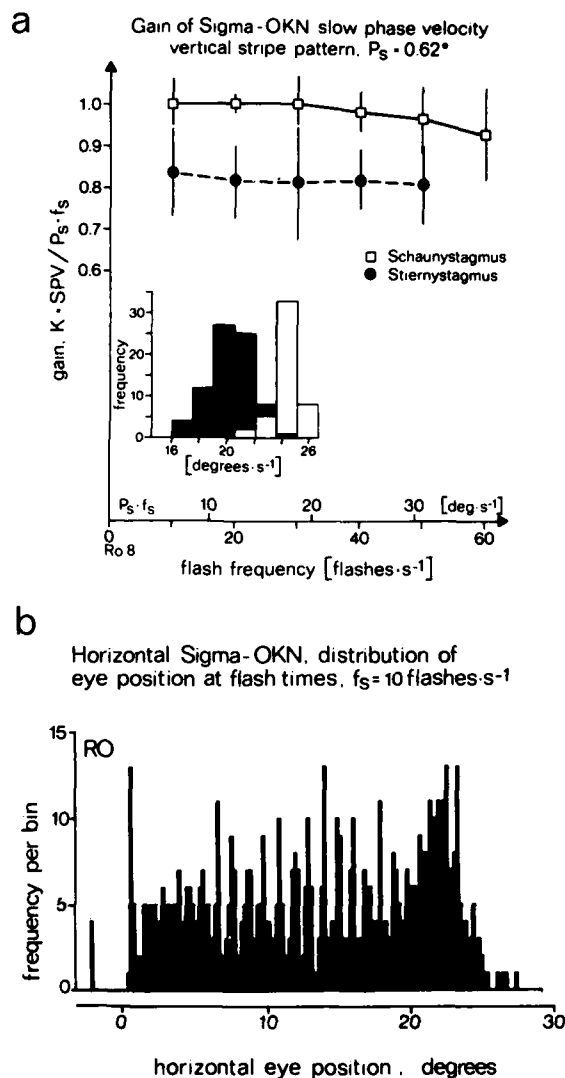
Identical retinal stimulus patterns were no longer elicited from flash to flash in the case of a circle, ellipse, or any other closed figure composed of equidistant dots. Then, only the fovea received identical stimuli from flash to flash. With such a stimulus pattern, continuous Sigma-PM were easily maintained for long periods and the subject perceived a large part of the dot figure as rotating in the direction of the gaze-pursuit movements. With fixed head, the circular Sigma-PM along a dot circle (composed of n dots) led to a sine-wave horizontal and vertical EOG shifted by a phase angle of 90° (FIGURE 4). The angular speed of the eye-pursuit movements during such Sigma-PM again was described well by

Equation 1. Consequently, the period P_s of the circular eye movements in an attentive subject corresponded exactly to

$$P_s = \frac{n}{f_s} [\text{seconds}] \quad (2)$$

i.e., the gain of the Sigma-PM was 1. The upper frequency limit of $1/P_s$ was 0.8–1.2 Hz and corresponded to the limiting frequency of circular eye movements elicited by a spot of light rotating in a circle of comparable diameter.

FIGURE 5. (a) Gain of horizontal Sigma-OKN slow-phase angular velocity. Vertical stripe pattern illuminated at different flash frequencies. Two states of attentiveness: "Schaunystagmus" and "Stiernystagmus." Inset: distribution of individual velocities of Sigma-OKN slow phases at 40 flashes/second for Schaunystagmus and Stiernystagmus. (b) The distribution of the individual eye positions at the time of each flash is represented in a frequency histogram. The eye position was sampled by triggering with the flash signals. Peaks in the frequency histogram appear at integer values of P_s (1.1°); $f_s = 10$ flashes/second. Midline of gaze field at about 12°.



In normal OKN, it has been well known since the work of ter Braak that the angular speed of the OKN slow phase depends not only on the stimulus velocity but also on the type of subject attentiveness ("Schaunystagmus" versus "Stiernystagmus").²² This difference also was found with Sigma-OKN. The constant k of Equation 1 was on the average about 1 when the subject was attentive and applied "foveal" pursuit, but k decreased significantly below 1 when the subject was in a state of lowered attentiveness and had a Sigma-Stiernystagmus (FIGURE 5a). This reduction in gain was also observed when the fovea moved across an empty field and the stripe pattern was restricted to the peripheral part of the retina.¹⁷ When the gain fell below 1, the perceived speed of Sigma-movement did not change. It therefore is probable that the retinal displacement signals (retinal Phi-movement) are added to the efference copy signals before the "perceptual level" is reached.

Even when the average gain of the Sigma-OKN slow-phase velocity was 1, some fluctuation in the individual slow-phase velocities still was present. Despite this variability, the distribution of the center of gaze position measured at the moment of every flash was not at random but with a higher probability at the "correct target" rather than in between the targets (FIGURE 5b).

The laws and the perception of Sigma-movement (Equations 1 and 2) were independent of whether the head was fixed and the oculomotor system alone determined the movement of gaze or the center of gaze was moved by head and eye movement (FIGURE 4). Thus Sigma-phenomena are related to gaze movement and not to eye movements per se.

Experiments in Monkeys

To elicit Sigma-OKN, Java monkeys were placed with the head fixed in a monkey chair surrounded by a stationary drum of 120-cm diameter covered on its inside wall by a precise pattern of vertical black and white stripes (silk-screen prints) of 1.15° or 2.3° period. After the monkey was lured into a Sigma-state (for details see Reference 21), his Sigma-OKN frequently continued for several minutes. Increasing the flash frequency f_s led, as in man, to an immediate increase in the angular velocity of the Sigma-OKN slow phase. Equation 1 was found to be valid (FIGURES 6 and 3b). Now and then, the monkey's oculomotor system "jumped" into the mode 2 with $k = 2$ in Equation 1, but most of the experiments were performed with mode 1. Any stationary object presented to the monkey within his visual field led to an immediate interruption of the Sigma-OKN by fixation of the object.

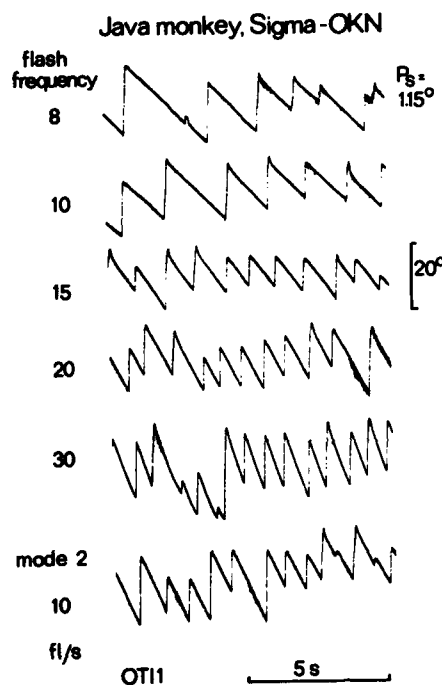
SIGMA-MOVEMENT ELICITED BY STROBOSCOPICALLY ILLUMINATED STATIONARY STEREOPATTERNS

Sigma-phenomena were also elicitable with periodic stimulus patterns that were not visible with monocular vision but were generated on the *cyclopean retina*. We used a 16- or 24-vertical-stripe Julesz stereogram.²³ All subjects with normal stereovision saw stationary stereostripes when the left eye and right eye patterns were synchronously illuminated at a flash frequency of ≥ 2 flashes/second. The subjects induced smooth-pursuit eye movements across the stationary stereopattern by fixating a small spot of light moving at a constant angular speed across the pattern. As the angular speed of the eyes (head fixed) reached a

value near that given by Equation 1, the whole stereopattern was seen moving in the direction of the eye movements. During this movement illusion, the surface structure of the pattern changed because the different stereostripes of the stereogram had variable distributions of their respective black and white random dots. After some training, all subjects could elicit Sigma-PM and Sigma-OKN across the stationary stereostripe pattern, and the angular velocity of the Sigma-OKN slow phase again depended on f_s and P_s as expressed by Equation 1 (FIGURES 2b and 3c).

Sigma-movement and Sigma-OKN were also elicitable when, instead of synchronous dichoptic flashes, a time delay Δt between the left- and right-eye

FIGURE 6. Horizontal Sigma-OKN in Java monkey. Vertical stripe pattern of 1.15° period. Flash frequencies as indicated. In the lowest line, a recording at 10 flashes/second is demonstrated, whereby the oculomotor system was in mode 2, i.e., the constant k of Equation 1 was 2. Compare this Sigma-OKN with that in mode 1 at 20 flashes/second.



stimuli was introduced. The apparent depth of the stereopattern decreased when Δt increased. With alternating dichoptic stimuli ($\Delta t = \frac{1}{2} f_s$), the stereocomponents of the stripe pattern had disappeared, but paradoxically the stripes were still seen moving in the direction of the eye-pursuit movements but in the plane of the random dot background. A variation in Δt did not change the relationship expressed by Equation 1.²⁴

SIGMA-MOVEMENT OF THREE-DIMENSIONAL OBJECTS

From the data presented in the preceding section, we could expect that Sigma-movement and corresponding gaze-pursuit movements were also elicitable by three-dimensional, spatially periodic objects. Two different stimulus

patterns were used: a round plastic plate of 65-cm diameter on which a circle of 40 equally spaced rods was mounted; and a set of 100 equally spaced white balls fixed at equal distances on a steel wire forming a complex three-dimensional figure (FIGURE 7a and b). When such three-dimensional, spatially periodic objects were illuminated stroboscopically and gaze-pursuit movements were initiated at an adequate speed, Sigma-movement was perceived in three-dimensional space. The eyes then performed smooth-pursuit movements at a speed determined by the condition that the center of gaze moved from flash to flash from one of the periodically repeated objects (rods or balls) to the next, independent of the changes in angle, distance, shape, and relative orientation with respect to the subject's eyes. In the case of the rod circle, the circle was seen moving in space at a constant speed while the speed of the eyes in the orbita (head fixed), of course, depended on the perspective projection relative to the eyes. In the case of the complex three-dimensional figure, a correspondingly more complex Sigma-PM was performed (FIGURE 7b). The average speed of this Sigma-PM increased with f_s and the time P_g the center of gaze needed to move once around the whole figure was

$$P_g = \frac{n}{f_s} \text{ [seconds]} \quad (3)$$

whereby n is the number of periodic objects in the whole figure.

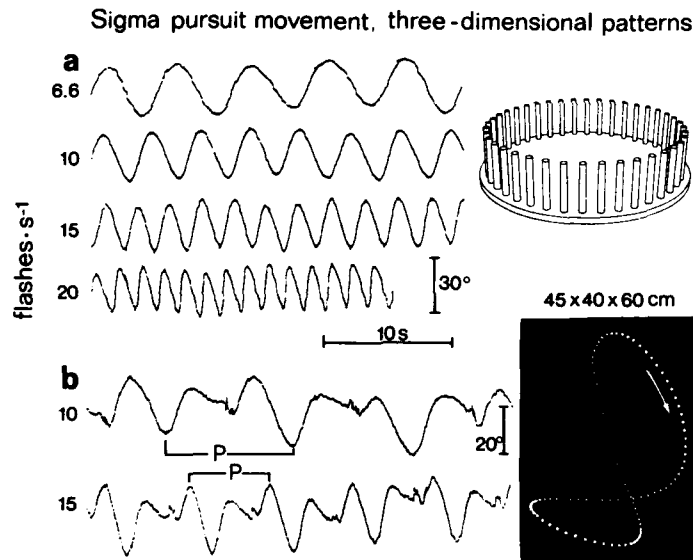


FIGURE 7. (a) Sigma-PM recorded in man (horizontal EOG) when Sigma-movement was elicited by a stroboscopically illuminated rod circle of 65-cm diameter. Flash frequencies as indicated; inspection angle, 52°; distance between eyes and center of rod circle, 136 cm. (b) Complex Sigma-pursuit movements elicited by a three-dimensional object with 100 periodic balls. Flash frequencies as indicated. Horizontal EOG recordings. P_g - period of pursuit movements. Observation distance about 110 cm.

SIGMA-MOVEMENT DURING ACTIVE BODY MOVEMENTS

Total body movements also were suitable to maintain Sigma-movement. The inner wall of a cylinder of 280-cm diameter and 240-cm height was covered with vertical black and white stripes of 3.7-cm period. A white mark was placed at eye height on two of the black stripes, 100 periods apart. The subject initiated Sigma-movement perception and Sigma-OKN by pursuing a finger moving at an adequate speed. Thereafter, he started to walk around the wall of the cylinder at the speed at which the body velocity corresponded to the speed of the Sigma-movement. The subject was asked to press a stopwatch as soon as the center of gaze moved across the first and the second white mark. The time between the two signals was read off, and the subject continued to repeat the same measurements with the same or a different flash frequency. FIGURE 3d demonstrates that the average speed of body movement \bar{V}_b depended on f_s as predicted by Equation 1 and on the mode at which Sigma-movement was induced.

EXPERIMENTS DESIGNED TO REFUTE THE SIGMA PARADIGM: RANDOM COMPONENTS OF THE FLASH SEQUENCE

Experiments in Man

As mentioned above, the individual Sigma-OKN slow phase did not necessarily have to correspond exactly to the speed predicted by Equation 1. This observation (FIGURE 5a and inset) indicated that Sigma-movement was generated by signals representing an approximative mean of gaze velocity and retinal change in position signals averaged over several hundred milliseconds. It therefore was predictable that the first condition of the original Sigma-paradigm (FIGURE 1b), namely, an exactly periodic flash sequence, is not a necessary requisite to elicit the Sigma-phenomena. Testing this conclusion, we applied random-interval flash sequences of a constant average rate and a Gaussian interval distribution.^{16,17} At a flash rate of 20 flashes/second and a coefficient of variation (c.v. = standard deviation/mean interval) smaller than 0.12, Sigma-movement of a periodic black-and-white stripe pattern was not affected. At a coefficient of variation $0.12 \leq \text{c.v.} \leq 0.3$, however, the subjects saw the Sigma-movement interrupted by irregular jerks, but their Sigma-OKN persisted with little disturbance of the slow phase. Only when the coefficient of variation was larger than 0.36 was the Sigma-movement frequently totally interrupted and no continuous Sigma-OKN present. The Sigma-movement illusion and the Sigma-PM were more sensitive to temporal irregularities of the flash sequences when the dot circle was applied instead of a periodic stripe pattern. Smooth Sigma-PM were still elicitable at a coefficient of variation of 0.1. At higher flash irregularities, the Sigma-movement of the dot circle was still perceived, but it was interrupted by irregular jerks that frequently led to saccades interrupting the smooth-pursuit movement.^{16,17}

Experiments in Monkeys

Essentially the same data were obtained in monkey Sigma-OKN. FIGURE 8 indicates that the systems involved in Sigma-movement and Sigma-OKN in

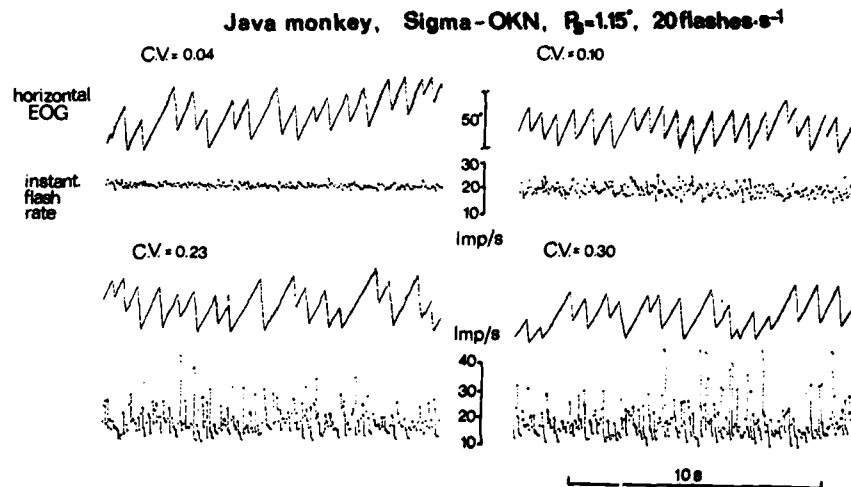


FIGURE 8. Sigma-OKN in Java monkey. Vertical stripe pattern of 1.15° period. Average flash rate, 20 flashes/second. The different amounts of temporal noise in the flash sequences are characterized by the coefficients of variation (c.v.) of the Gaussian flash interval distributions (as indicated).

monkeys also tolerate a considerable contingency of the temporal signal sequence. Thus the condition that from flash to flash identical retinal stimulus patterns are necessary, can be refuted.

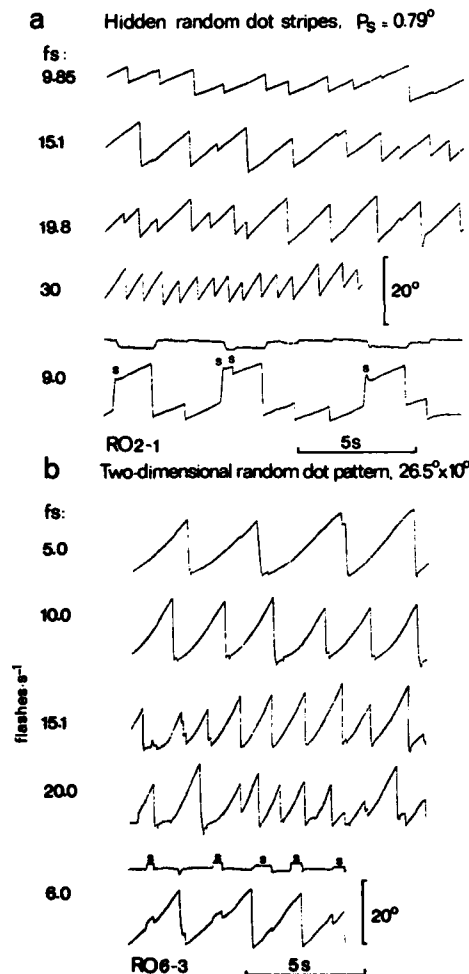
A FURTHER MODIFICATION OF THE SIGMA-PARADIGM: SIGMA-MOVEMENT OF RANDOM DOT PATTERNS

Spatial periodicity is the second condition of the original Sigma-paradigm (FIGURE 1b). In two experimental series, we tested how far the condition "spatial periodicity" has to be fulfilled. Firstly, instead of periodic stripes or dots, a stripe pattern composed of identical random dot stripes interspersed with uncorrelated random dot stripes was investigated. Such a pattern of correlated and uncorrelated spatial noise stripes did not give the appearance of striation. When smooth-pursuit eye movements were initiated by a target moving at an appropriate speed across the stroboscopically illuminated pattern ($f_s \geq 9$ flashes/second), the subjects suddenly could see a vertical grid pattern composed of identical stripes moving in the direction of the eye pursuit movements and in front of a "snowstorm" background. This Sigma-movement led to a corresponding Sigma-OKN, which perpetuated the movement illusion and the perception of the stripe pattern. Equation 1 was found to be valid.^{16,17} During Sigma-movements, the subject could gaze about the stripe pattern, whereby the apparent movement usually was not interrupted (FIGURE 9a). If interruption of Sigma-movement occurred, however, the stripes disappeared immediately into the masking background.

A second step in the analysis was the application of a two-dimensional,

random dot pattern.²⁰ When such a pattern was illuminated stroboscopically and pursuit movements were performed across it, the random dot structure was seen moving in the direction of the eye-pursuit movements, and this Sigma-movement could be used to elicit a Sigma-OKN (FIGURE 9b). A careful analysis of the Sigma-OKN slow phases indicated, however, that the velocity during a given slow phase changed much more than with periodic stripe patterns and that the variability between successive Sigma-OKN slow phases was rather high. In addition, the relationship between flash frequency and angular velocity of the Sigma-OKN slow phase was not described by Equation 1 and, except for a slight tendency of V_s to increase with f_s , the high variability of V_s was a dominant feature in these experiments (FIGURE 11c). The important result of these experiments, however, was the fact that Sigma-movement was seen in a direction opposite to that expected from the retinal displacement signals.

FIGURE 9. (a) Sigma-OKN performed during stroboscopic illumination of a vertical random dot stripe pattern; $P_s = 0.79^\circ$. Different flash frequencies as indicated. In the lower part, recording of horizontal and vertical EMOG. The subject performed voluntary inspection saccades (s) across the apparently moving pattern in vertical or oblique direction. These saccades did not interrupt the apparent Sigma-movement perception. (b) Horizontal Sigma-OKN performed across a stroboscopically illuminated two-dimensional random dot pattern, individual dot size about 0.05° . Flash frequencies as indicated. In the lower part, the vertical and the horizontal EOGs are shown. Oblique or vertical voluntary inspection saccades (s) did not interrupt the apparent movement perception and the Sigma-OKN.



AFTEREFFECTS OF SIGMA-MOVEMENTS

Experiments in Man

Our subjects, who sat in front of a tangent screen or within a stationary vertical stripe cylinder, did not perceive any circularvection during the kinetic illusion of Sigma-movement when P_s of the stripe pattern was 1.15° . Experiments with larger stripe patterns are in progress. When the stroboscopic illumination was turned off after a Sigma-OKN period longer than 20 seconds, a strong circularvection was perceived. The subject had the impression of being turned smoothly in the direction of the preceding Sigma-movement or Sigma-OKN slow phases. The strength of the vection decreased approximately exponentially with time and depended on the duration of the preceding Sigma-OKN. As a rule, we could not record an optokinetic after-nystagmus (Sigma-OKAN) during these periods of vection, but in some subjects slow eye deviations were observed.

Experiments in Monkeys

The aftereffects of Sigma-OKN were rather different in the monkey. A strong optokinetic after-nystagmus (Sigma-OKAN I and II) was observed (FIGURE 10). This difference corresponded to the difference in normal OKAN between man and monkey.²⁵

INTERACTION OF THE VESTIBULO-OCULAR REFLEX AND SIGMA-OKN

Experiments in Man

Two results of our studies about the interaction of Sigma-OKN and the responses to vestibular stimulation will be described.²⁶

A. The subject sat on a turntable surrounded by a vertical cylinder of 120-cm diameter and was rotated sinusoidally around the vertical axis, while the subject's head was fixed to the rotating chair and the stripe pattern on the inner wall of the cylinder remained earth fixed. The subject was asked to fixate one particular stripe. In doing so, the center of gaze remained stable in space when $f_s > 4$ flashes/second and the gain of the vestibulo-ocular reflex (VOR) thus was 1. When, in addition, the subject initiated a horizontal Sigma-OKN, a linear superposition of the Sigma-OKN slow-phase velocity and the angular eye velocity caused by the VOR was found:

$$V_e = P_s \cdot f_s + A \omega \cos \omega t \text{ [degrees/second]} \quad (4)$$

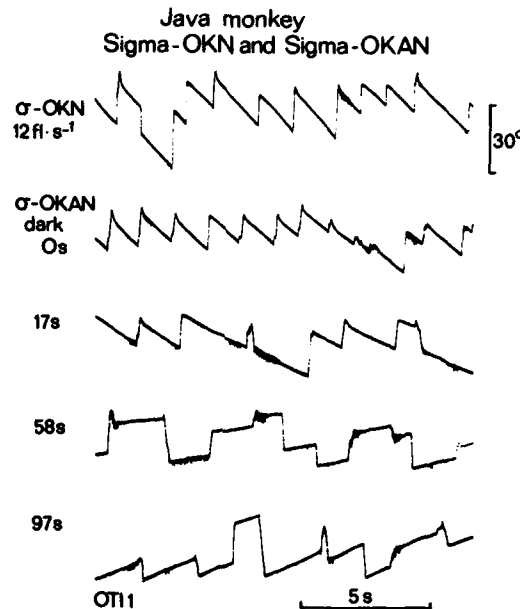
whereby A is the amplitude and ω the angular frequency of the chair rotation (FIGURE 11a). Equation 4 simply states that the speed of the center of gaze V_e with respect to earth-fixed coordinates remained constant during the slow Sigma-OKN phases.

During the interaction of VOR and Sigma-OKN, the subject perceived the stripe cylinder as rotating at a constant speed in the extrapersonal space. He perceived himself, however, as moving back and forth in the direction of the Sigma-movement and opposite to it, whereby in the first case, his speed could be faster or slower than the Sigma-movement. When the subject's speed was faster

than the speed of the apparent Sigma-movement, his eyes moved with respect to the head coordinates in the opposite direction to the Sigma-movement. From these findings it is evident that the perceived Sigma-movement was not correlated to the eye movements with respect to head coordinates but to the movement of gaze with respect to the coordinates of the earth-fixed extrapersonal space.

B. In another set of experiments, the vertical stripe cylinder was mechanically coupled to the rotating chair. Before the Sigma-movement was initiated, the subject's VOR was measured in darkness and the gain was found to be about 0.7. Thereafter, the stripe pattern was illuminated stroboscopically and the sinusoidally rotating subject fixating one particular stripe of the cylinder could suppress the VOR completely when $f_s > 8-10$ flashes/second. When, in addition, the

FIGURE 10. Sigma-OKN and Sigma-OKAN in Java monkey. Vertical stripe pattern 1.15° period. Sigma-OKN at 12 flashes/second. The Sigma-OKAN was recorded in darkness at different times after completion of a 60-second Sigma-OKN. Sigma-OKAN I changed into Sigma-OKAN II after 35 seconds.



subject initiated a horizontal Sigma-OKN, V_e approximated the values predicted by Equation 1 for $f_s > 10$ flashes/second. Thus in these experiments, the VOR also was suppressed during Sigma-OKN. Despite the constant V_e values, the subjects reported seeing a variable Sigma-movement speed changing with the back-and-forth rotation of the chair, i.e., Sigma-movement again was related to the speed of gaze with respect to earth-fixed coordinates and not to the speed of the eyes with respect to head coordinates.

Experiments in Monkeys

The experiments A and B were repeated in Java monkeys, and essentially the same results were obtained, as indicated by FIGURES 11b and 12. In contrast to an

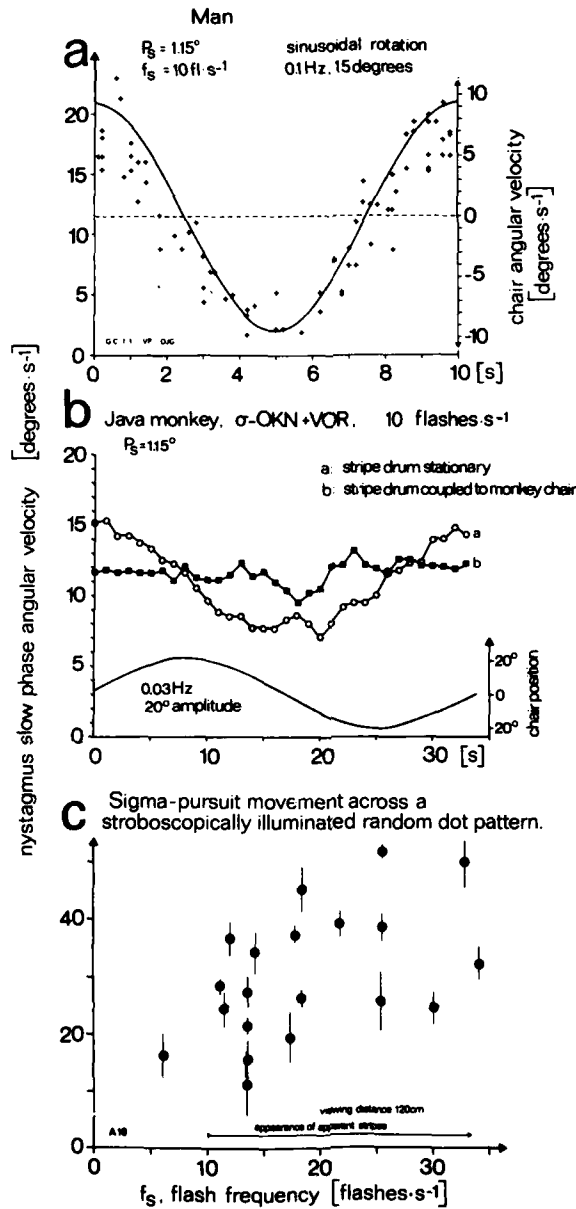


FIGURE 11. (a) Angular velocity of Sigma-OKN measured in man at different times of horizontal sinusoidal movement. The vertical stripe pattern of 1.15° period was earth fixed. (b) Angular velocity of Java monkey Sigma-OKN measured at different times of horizontal sinusoidal movement. The vertical stripe pattern was either stationary or coupled to the sinusoidally rotating chair. (c) Sigma-OKN and Sigma-PM across a two-dimensional random dot pattern. Coordinates as in FIGURE 3a. Means of 10 successive measurements and standard deviations.

attentive human subject, however, the monkeys quite frequently lost the Sigma-state during VOR. Thus, fairly time-consuming experiments were necessary to collect enough data about the interaction of Sigma-OKN and VOR in monkeys.

DISCUSSION

A model explaining the kinetic illusion of Sigma-movement has to take into consideration that Sigma-movement velocity was only correlated to the actual eye velocity in the experiments with the head fixed. In the experiments in which the head was actively moved or the subject was rotated by the turntable, the direction of the perceived movement corresponded to that of the gaze movement

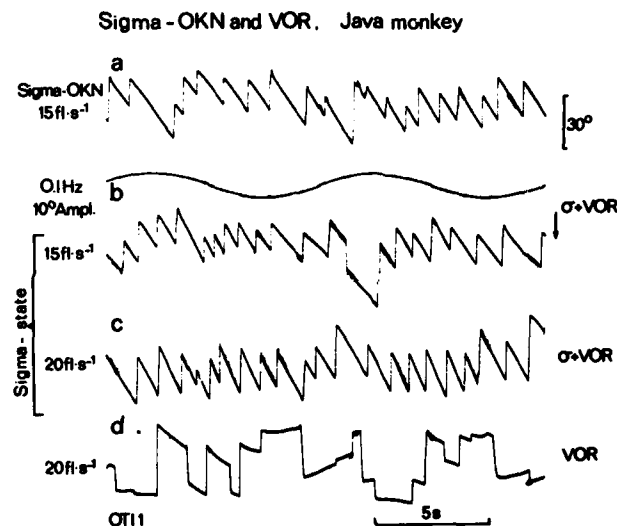


FIGURE 12. Horizontal EOG of Java monkey. Superposition of Sigma-OKN and vestibulo-ocular reflex (VOR). Stationary vertical stripe pattern; $P_s = 1.15^\circ$. The monkey was horizontally and sinusoidally rotated. (a) Sigma-OKN without rotation, $f_s = 15$ flashes/second. (b) Additional sinusoidal rotation: 0.1 Hz, 10° amplitude. (c) Flash frequency increased from 15 to 20 flashes/second. (d) VOR at 20 flashes/second; no Sigma-nystagmus.

relative to the earth-fixed coordinates of the extrapersonal space. The Sigma-movement speed was then correlated to the angular velocity of gaze and not to that of the eyes. In the experiments in which the subject was turned sinusoidally back and forth together with the vertical stripe cylinder, the Sigma-OKN slow-phase angular velocity was almost constant with respect to head coordinates but gaze velocity in space exhibited a cosine-shaped variation and corresponded to the perceived Sigma-movement.

Sigma-movement is a typical example of efferent visual-movement perception and may be explainable by the assumption that somewhere in the central visual system, an efference copy signal interacts with the afferent visual-signal

flow. The simplest way to explain our data is the assumption that this efference copy signal originates from gaze-movement commands (related to the coordinates of the extrapersonal space) and not from oculomotor signals (FIGURE 13). Under these conditions, the VOR signals stabilizing gaze are not directly included in the efference copy signals, because they enter the oculomotor system below the branching-off point of the gaze-command efference copy (circled arrow in FIGURE 13). Vestibular signals with respect to the subject's own movement in space, however, are directly included in the movement perception. Suppression of the VOR during Sigma-OKN is attained by automatic regulation of the central-gaze-velocity command via retinal error signals. This corrected

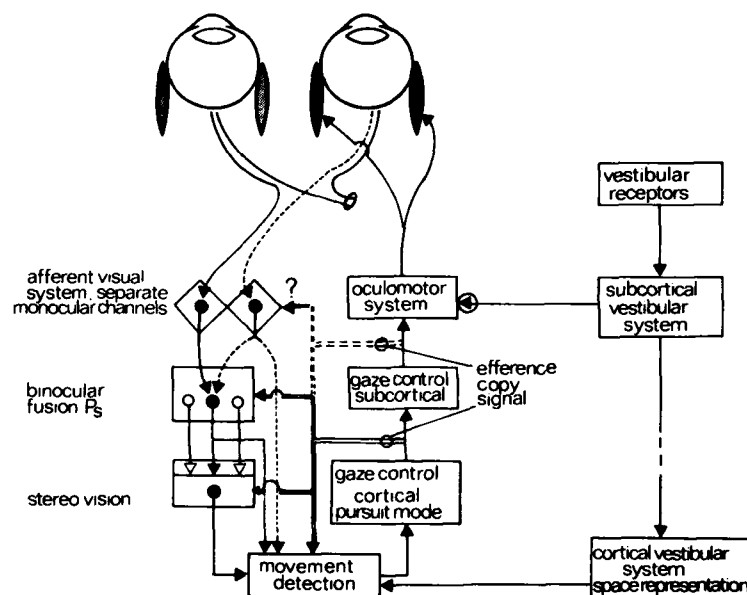


FIGURE 13. Block diagram of the interaction of binocular afferent visual signals, efference copy signals of gaze movement, and central vestibular signals. For details, see text.

gaze-velocity command counteracts the vestibular reflex signals and leads to constant eye velocity when the stripe drum is coupled to the rotating chair.

The experiments with dichoptic stimuli provide further clues to the location of the interaction between efference copy and afferent movement signals. The efference copy signals that lead to the illusion of Sigma-movement seem to be included in visual-signal processing at or beyond the level of binocular fusion and stereopsis. This process of interaction evidently does not take individual retinal signals into consideration, but rather retinal position signals averaged over several hundred milliseconds. Otherwise the experiments with flash sequences of a Gaussian interval distribution are hardly explainable. The interaction between afferent visual-movement signals and efference copy signals is probably not a simple algebraic summation, as postulated in earlier models.¹⁰ Sigma-movement seen with random dot patterns (FIGURE 9b) indicates that under

certain conditions the efference copy signal is stronger than the counteracting retinal displacement signals.

Our present results do not exclude an interaction of oculomotor efference copy signals and afferent visual signals at a subcortical level. However, we have no positive evidence so far that such a mechanism is important for the generation of Sigma-movement. Man and monkey exhibit practically the same properties for Sigma-OKN, and one therefore can assume that monkeys also perceive *Sigma-movement*. One difference between man and monkey Sigma-phenomena is fortunate for the monkey experiments. It is the strong Sigma-OKAN, which is present in monkeys but nonexistent or very rudimentary in man. The Sigma-OKAN is the reason why a short closure of the eyelids does not interrupt Sigma-OKN in monkey. Therefore, once monkeys are lured into Sigma-nystagmus, they remain in the Sigma-state over a rather long period without being specially rewarded. Experiments are in progress in which we are exploring the neurophysiological basis of Sigma-phenomena by means of microelectrode recordings from the monkey brain.

ACKNOWLEDGMENTS

We thank Mrs. J. Dames for careful technical assistance, Mr. H. Dannenberg, Mr. J. Lerch, Ing. J. Petsch, and Ing. P. Rickmeyer for their help in building part of the mechanical and electronic equipment.

REFERENCES

1. ARISTOTLE. On the soul. Parva naturalia. On breath. With an English translation by W. S. Hett. 1964. Cambridge University Press. Cambridge, Mass.
2. VON HELMHOLTZ, H. 1866. Handbuch der physiologischen Optik. Voss. Leipzig, Germany.
3. KOMMERELL, G. & U. KLEIN. 1971. Vision Res. **11**: 905-920.
4. KOMMERELL, G. & R. TÄUMER. 1972. Investigations of the eye tracking system through stabilized retinal images. In Cerebral Control of Eye Movements and Motion Perception. J. Dichgans & E. Bizzi, Eds.: 288-297. S. Karger. Basel, Switzerland.
5. MACH, E. 1886. Die Analyse der Empfindungen. G. Fischer. Leipzig, Germany.
6. HERING, E. 1879. Der Raumsinn und die Bewegungen des Auges. In Handbuch der Physiologie. L. Hermann, Ed. **3**: 343-601. Vogel. Leipzig, Germany.
7. GRÜSSER, O.-J. & U. GRÜSSER-CORNEHLS. 1966. Ergeb. Physiol. **61**: 178-265.
8. JUNG, R. 1973. Visual perception and neurophysiology. In Handbook of Sensory Physiology. R. Jung, Ed. **7/3A**: 1-152. Springer Verlag. Berlin, Heidelberg & New York.
9. VON UEXKÜLL, J. 1920. Theoretische Biologie. Springer Verlag. Berlin, Germany.
10. VON HOLST, E. & H. MITTELSTAEDT. 1950. Naturwissenschaften **20**: 464-465.
11. SPERRY, R. W. 1950. J. Comp. Physiol. Psychol. **43**: 482-489.
12. TEUBER, H. L. 1960. Perception. In Handbook of Physiology. I. Field, Ed. **3**: 1595-1668. Williams and Wilkins. Baltimore, Md.
13. HENN, V., B. COHEN & L. R. YOUNG. 1980. Visual-vestibular interaction in motion perception and the generation of nystagmus. Neurosci. Res. Program Bull. **18**: 458-651.
14. STOPER, A. E. 1967. Vision during pursuit movement: the role of oculomotor information. Ph.D. Thesis. Brandeis University. Waltham, Mass.
15. LAMONTAGNE, C. 1973. Perception **2**: 167-180.
16. BEHRENS, F. & O.-J. GRÜSSER. 1978. Bewegungswahrnehmung und Augenbewegungen bei Flickerbeleuchtung unbewegter visueller Muster. In Augenbewegungsstörungen.

en. G. Kommerell, Ed.: 273-284. J. F. Bergmann. München, Federal Republic of Germany.

17. BEHRENS, F. & O.-J. GRÜSSER. 1979. *Exp. Brain Res.* **37**: 317-336.
18. COLLEWIJN, H. 1977. *J. Physiol. London* **266**: 471-498.
19. STEINMAN, R. M. & H. COLLEWIJN. 1980. *Vision Res.* **20**: 415-429.
20. ADLER, B. & O.-J. GRÜSSER. 1979. *Exp. Brain Res.* **37**: 537-550.
21. GRÜSSER, O.-J., M. PAUSE & U. SCHREITER. 1979. *Exp. Brain Res.* **35**: 519-526.
22. TER BRAAK, J. G. W. 1936. *Arch. neerl. Physiol.* **21**: 309-376.
23. JULESZ, B. & R. A. PAYNE. 1968. *Vision Res.* **8**: 433-444.
24. ADLER, B. & O.-J. GRÜSSER. (Submitted.)
25. COHEN, B., V. MATSUO & T. RAPHAN. 1977. *J. Physiol. London* **270**: 321-344.
26. COLLEWIJN, H., G. CURIO & O.-J. GRÜSSER. 1980. Interaction of vestibulo-ocular reflex and Sigma-optokinetic nystagmus in man. *Prog. Oculomotor Res.* (In press.)

MOTION SICKNESS DUE TO VISION REVERSAL: ITS ABSENCE IN STROBOSCOPIC LIGHT

G. Melvill Jones and G. Mandl
Aviation Medical Research Unit
Department of Physiology
McGill University
Montreal, Quebec, Canada H3G 1Y6

INTRODUCTION

Motion sickness apparently cannot be generated in the absence of an intact, functioning vestibular system, either in man or animals.¹⁻⁵ However, while abnormal vestibular stimulation effectively provokes the condition, it is not a necessary prerequisite for the development of symptoms.⁶ Such symptoms can be induced equally well by moving visual stimuli when these conflict with normal vestibular stimulation,^{7,8} i.e., in a static flight simulator equipped with a moving visual scene,⁹ or when wearing distorting optics during normal patterns of body and head movement.¹⁰ Significantly, in these latter circumstances the time course of symptomatic amelioration closely parallels marked and long-lasting adaptive changes in the vestibulo-ocular reflex (VOR).¹¹ It was therefore particularly interesting to find that when performing comparable adaptive experiments with vision reversal in stroboscopic light, none of the subjects ever experienced nausea or associated symptoms, even though there was overt visual-vestibular conflict as well as adaptive changes in the VOR.¹² An additional observation in these strobe experiments suggested the possibility that the patterns of adaptive VOR change were highly selective, which in turn might account for the peculiar lack of motion sickness noted in the strobe-light condition.

To appreciate the significance of this argument, it is necessary to recall relevant details of previous adaptive experiments in normal light. Thus after vision reversal in normal light, voluntary head oscillation at 2-3 Hz (with prisms temporarily removed) invariably leads to oscillatory destabilization of the visual scene, even as early as 10-15 minutes after commencing the vision-reversed experience. Evidently, significant adaptive changes occur in the high-frequency range of VOR at an early stage in the adaptive response. In marked contrast to this, there never was any sign of such high-frequency image destabilization during similar head-shake tests in subjects adapted to vision reversal in strobe light (and tested as before in normal light). It seemed that although adaptive changes in VOR are evident when tested at low frequency as described below, such changes might not be manifest over the upper frequency range in subjects adapted in strobe light. The following experiments aimed to investigate this possibility in an attempt to elucidate the peculiar absence of motion sickness in such subjects. Some aspects of the results have been briefly reported previously.¹²

METHODS

As detailed elsewhere, subjects were fitted with goggles containing dove prisms arranged to produce horizontal (but not vertical) image reversal while

permitting direct forward vision, albeit with a restricted visual field of view (around 50° solid angle).¹¹ The goggles were fitted first in normal light, with the head fixed by means of a dental bite-board to prevent head movement and thus avoid activation of conflicting visual-vestibular stimulation in normal light. The head was released only after replacing the normal light with stroboscopic illumination of 4-Hz flash frequency and 3- μ second flash duration. The flash frequency was chosen to be in the range of other experiments performed in strobe light and to avoid epileptogenic stimuli.¹³ The short flash duration ensured elimination of significant smooth slippage of the retinal image during the flash. Particular care was taken to screen completely any continuous light emerging from laboratory equipment.

Seven subjects were exposed to these conditions, each for a period of six hours. During this period they made more or less continuous attempts to "navigate" themselves around the laboratory, avoiding equipment, chairs, benches, etc., placed as suitable obstructions. For safety they were always accompanied by an attendant. No systematic "forcing" was undertaken on the turntable, but when resting on a chair subjects were encouraged to continue making active head movements while looking at the stroboscopically illuminated surroundings. At least one week later, control experiments were performed on four of the subjects in strobe light with the reversing prisms removed from the goggles.

Ocular gain, defined as slow-phase eye angular velocity per head velocity, was estimated in two different ways according to whether testing was performed at low or high frequencies. For low-frequency testing, the subject was rotated sinusoidally about a vertical axis on a servo-driven turntable, with head fixed to the turntable and the stereotaxic skull-horizontal tilted 20° nose down. These oscillations were conducted at 0.17 Hz and peak-to-peak amplitude 120° (peak head angular velocity $60^\circ/\text{second}$), with eyes open in complete darkness and the subject performing mental arithmetic to maintain arousal. Horizontal eye movements were recorded by conventional d.c. electro-oculography (3 dB at 250 Hz). A previously described computer-assisted method was used to estimate ocular gain in these circumstances,^{14,22} after constructing curves of cumulative eye position (CEP curves, Reference 15). Two control runs, each including 10 cycles of oscillation, were performed before commencing the six-hour period in strobe light, and two similar test runs were made at the end of this period. Thus the magnitude of adaptive influence was estimated by comparison of mean control and test values, each obtained from a total of 20 cycles of low-frequency stimulation.

A different method was used for high-frequency testing,^{16,18} since the available equipment was not capable of producing whole-body oscillation in the required frequency range. Instead, subjects performed voluntary head oscillations about a vertical axis in response to a sinusoidally modulated sound (centered at 1 kHz). Head angular position was measured by means of mechanical coupling, which employed a miniature "parallel-arm" device clamped to a dental bite at one end and to a precision (earth-fixed) rotary potentiometer at the other. The parallel-arm system was similar to, but much smaller than, that familiarly employed on the draftsman's drawing board. With this arrangement, the potentiometer registers only horizontal rotation of the head while rejecting any linear components of dental-bite movement. The system was accurate to at least 0.25° head rotation, with no significant response to the amplitudes of linear components of dental-bite movements encountered during the experiments. As before, conventional d.c. electro-oculography recorded eye movement relative to

the skull. The gain of ocular response, expressed as peak eye velocity per peak head velocity, was estimated from at least 20 cycles of head and eye movement. Records were obtained at 1.75-Hz and 3-Hz head oscillation and approximately 5° and 3° amplitude respectively. These frequencies cover the range over which visual tracking per se fails and hence the VOR becomes particularly important for the production of image stabilization.^{17,27,28} The chosen amplitudes ensured that peak head velocity was on the same order of magnitude (60°/second) as in the low-frequency tests.

In order to suppress the confusing influence of reflex anticomensatory eye movements likely to occur in these circumstances without vision,²⁹ the present high-frequency tests were always conducted with eyes open in normal light. Moreover it is clear from results described below in connection with FIGURE 1 that changes of ocular gain obtained with this form of voluntary high-frequency head oscillation closely paralleled corresponding changes of VOR gain obtained with low-frequency oscillation in the dark.

In order to follow up the "head-shake" observations that led to these experiments (see Introduction), two subjects underwent an additional perceptual "blur-test" regime. For this they looked at a white disc with black radial lines marked at 5° intervals, while voluntarily oscillating the head in a horizontal plane at around 3 Hz and 3° amplitude.¹⁷ In these circumstances, discrepancies in gain and/or phase between head and eye movements are manifested as well-defined perceptual distortions of the disc's image. Specifically, lines closely parallel to the plane of image slip stand out progressively more against orthogonal lines as the degree of slip increases. It proves a simple matter to ascribe values of 0, 1, 2, and 3 to four magnitudes of such distortion, while an experienced subject can choose values lying between these numbers, as seen in the diamond-shaped points in FIGURE 1.

RESULTS

Vision Reversal in Normal Light: Low-Frequency Tests

Previously reported experiments conducted on human subjects with vision reversal in normal light demonstrated consistent attenuation of VOR as tested with whole-body oscillation at low frequency (0.17 Hz; 60° amplitude) with eyes open in the dark [see Methods].^{11,12} Thus an average of approximately 40% attenuation of VOR gain (smooth-pursuit eye angular velocity/head angular velocity) was observed in three subjects after the first day of vision-reversed exposure during ordinary locomotor activity (i.e., no forcing on the turntable).¹¹

Vision Reversal in Normal Light: High-Frequency Tests

With voluntary head oscillations at higher frequencies, conducted as described in Methods above, attenuation of the ocular response also was observed previously, although the magnitude of attenuation was somewhat less than that recorded at 0.17 Hz. Specifically in the same three subjects, the average gain was attenuated by approximately 30% at 1.75 Hz and 25% at 3.0 Hz after the first day of exposure.¹⁸

As an example of such high-frequency attenuation, FIGURE 1 (continuous line,

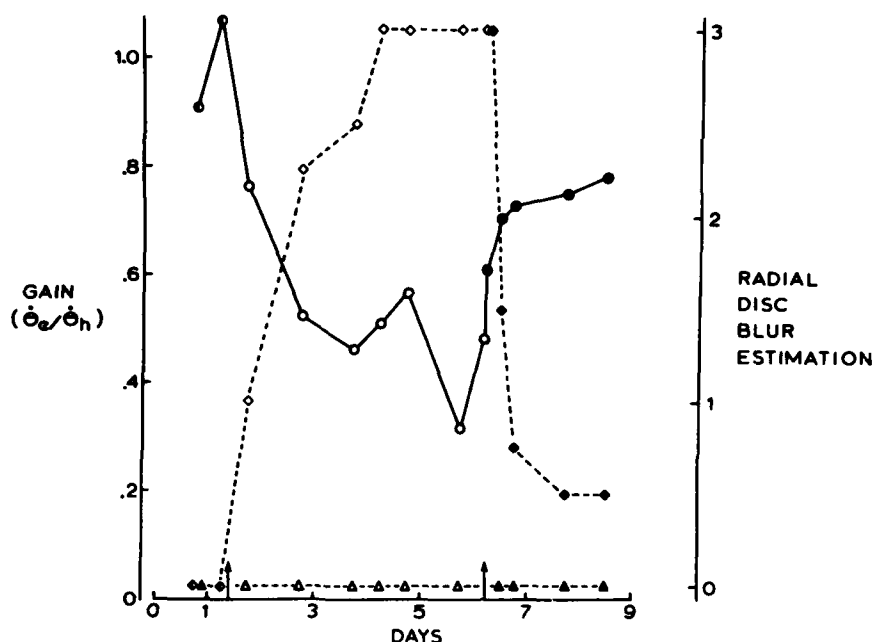


FIGURE 1. Changes in VOR gain (solid line, left ordinate) and blur estimation (interrupted lines, right ordinate) during voluntary head shake, at a frequency of 1.75 Hz, without prisms. Units on right ordinate indicate subjective estimates for a radial disc blur, with 3 denoting the largest blur. The duration of the experiment is plotted along the abscissa (days), with vertical arrows bracketing five days of vision reversal. Each point representing gain is a mean of 10 consecutive head-shake cycles before (\bullet), during (\circ), and after (\bullet) vision reversal. Each diamond denotes the subject's single estimate of blur, made at the end of each test run, before (\diamond), during (\diamond), and after (\diamond) vision reversal. The subject's blur estimation during head oscillations (at 1.75 Hz) in the vertical (sagittal) plane is similarly presented by triangular symbols. Note that there was no optical reversal of vision in the sagittal plane. (From Reference 19.)

left-hand ordinate) shows the time course of gain change measured in one subject at 1.75-Hz head shake during and after a five-day period of continuous vision reversal in normal light.¹⁸ After two control tests (half-filled circles) performed on two consecutive days, reversing prism goggles were donned at the time indicated by the first vertical arrow on the abscissa. Whereas the mean control gain was close to 1, the first test run conducted approximately five hours after commencing vision reversal produced a corresponding value of 0.76. Thereafter there was a progressive decline of gain (open circles), followed after prism removal (second arrow) by a gradual return to normal (closed circles). These changes are generally very similar to (although of lower magnitude than) those found in the same subject with low-frequency testing of the VOR in the dark (compare FIGURE 1 with Figure 6A of Reference 11). The two data sets exemplify the consistent relationship between low-frequency and high-frequency responses that was found in all subjects examined with these methods.

The dashed curve with diamond-shaped points illustrates the corresponding blur-test results (right ordinate), using the radial line disc as described in Methods. The gain attenuation seen on the first day was associated with significant (magnitude-1) image distortion during head shake, the degree of distortion becoming progressively more marked as gain decreased further. Quite different were the blur-test results obtained with similar head shake in the sagittal plane (vertical plane, dashed line with triangle-shaped points). In this plane there was never any sign of disc distortion. Bearing in mind that the dove prisms produced reversal in the horizontal, but not in the vertical (sagittal), plane, this complete lack of adaptive change in sagittal response indicates a high degree of geometric specificity in the adaptive mechanism.²⁰ The difference between the two dashed-line data sets reflects well the meaningful character of information content in the blur-test results, the significance of which in the present context will become apparent below.

In summary, the results obtained with vision reversal in normal light demonstrate a generally broad frequency spectrum of adaptive change in the oculomotor system, which is in accord with corresponding animal studies.²¹⁻²³

Vision Reversal in Stroboscopic Light: Low- and High-Frequency Tests

The present stroboscopic-light experiments were conducted over a period of one day only (six hours of vision reversal during locomotor and free-head-movement activity). Nevertheless, as reported earlier,¹² all of seven subjects tested at low frequency demonstrated significant VOR attenuation, although in these circumstances the rate of change of VOR gain was only about half that in normal light. However, not previously reported is the fact that *no measurable change of high-frequency gain was seen in the four subjects tested at 1.75 Hz and 3.0 Hz after the same duration of exposure to vision reversal in the stroboscopic light*. These results are seen in FIGURE 2. At 1.75 Hz, the mean gains were 1.01 and 1.02 before and after the vision-reversed exposure, respectively; at 3.0 Hz, the corresponding values were 1.04 and 1.03. Evidently, no measurable adaptive change was manifest at these frequencies of head oscillation. Supporting this

1.75Hz ◀ HEAD OSCILLATION ▶ 3.0Hz				
	Before	After	Before	After
1	1.07	0.96	1.17	1.02
2	0.99	1.02	0.97	0.99
3	0.99	1.11	0.99	1.07
4	1.00	0.98	1.03	1.03
MEAN	1.01	1.02	1.04	1.03

FIGURE 2. Ocular gain during active head oscillation in four subjects, before and after six hours vision reversal in 4-Hz strobe light. Note the absence of any adaptation-related gain changes.

conclusion is the fact that after the six-hour adaptive period in strobe light no subject ever noted any degree of image distortion in the blur test (conducted in normal light, in the horizontal plane, at the end of experiment).

FIGURE 3 shows an interesting feature that parallels an earlier observation,¹² namely, that control subjects exposed to strobe light *without* vision reversal tended to demonstrate increased VOR gain as tested at low frequency in the dark. At both high frequencies of head shake, there was a consistent tendency for the ocular gain to be enhanced after six hours of free movement in the stroboscopic light with nonreversed vision.

Motion Sickness

As reported elsewhere,¹⁰ all subjects exposed to vision reversal in *normal* light tended to experience marked symptoms of motion sickness, especially during the first day. Indeed symptoms were sufficiently severe to necessitate

1.75Hz <HEAD OSCILLATION> 3.0Hz				
	Before	After	Before	After
1	1.06	1.14	1.11	1.20
2	1.06	1.09	1.07	1.19
3	1.03	1.17	1.00	1.00
4	0.95	1.05	0.95	1.01
MEAN	1.03	1.11	1.03	1.10

FIGURE 3. Ocular gain during active head oscillation before and after six hours normal vision in 4-Hz strobe light. Note the increase in gain after exposure to nonreversed strobe vision. Same four subjects as in FIGURE 2.

considerable periods of recumbancy with head still. And yet none of the subjects with vision reversal in *strobe* light ever experienced such symptoms throughout the experiment. This was true even in the one subject common to both sets of experiments, who was strongly disposed to expect an unpleasant day of sickness.

DISCUSSION

This study set out to examine, over an extended frequency range, the modification of oculomotor control incurred by a period of vision reversal in stroboscopic light. The objective was to detect physiological correlates that might account for the absence of motion sickness in these conditions. As an outcome it transpires that whereas adaptive changes were found over a broad frequency spectrum after vision reversal in normal light, these changes were restricted to a low-frequency range in the stroboscopic illumination. Even at 0.17 Hz, the

adaptive attenuation, although distinctly present, was less marked than with normal light. It seems clear, therefore, that the physiological drive to bring about adaptive change was itself considerably attenuated by the stroboscopically illuminated environment, with specific elimination of the adaptive response in the tested high-frequency range 1.75-3.0 Hz. The findings thus would seem to imply a functional association between the incidence of motion sickness and the prevailing "strength" and/or frequency range of the adaptive drive.

Origin of the Adaptive Drive

It seems likely, if not certain, that the vector of the retinal image slip during head movement provides an essential element in the source signal responsible for activating adaptive modifications in the neural organization of oculomotor control.^{11,12,24} Consequently one might have expected that—with strobe illumination of flash duration too short for significant image slip to occur during the flash—this source element would have been eliminated, and hence also the adaptive response. Evidently it was not, at least as tested at 0.17 Hz.

As discussed elsewhere,¹² this finding probably stems from the fact that at least in cat, some retinal image movement detectors in the central nervous system respond in a meaningful way even when an image is moved discontinuously across the retina.²⁵ However, it seems obvious that for such a signal to be meaningful there must be some spatiotemporal limitations to the pattern of discontinuous image displacements on the retina. For example, as the frequency of relative image oscillation approaches that of the sequential image placements on the retina, the problem of deducing discrepancies between head and compensatory eye velocities from retinal image information would become progressively more complicated. Thus, at the 0.17-Hz test frequency (six seconds/cycle) and 4-Hz strobe flash frequency, 24 image impressions would occur per cycle of head oscillation; but at the 3-Hz head frequency, there only would be close to 1 impression per cycle. Hence, if during the period of exposure to strobe light the frequency content of head movement extended over the range of frequencies tested in normal light, then the above argument would imply that an effective adaptive drive should have been manifest only at the low-frequency end of the spectrum. In view of this, the present findings lead to the interesting suggestion that in these experiments any gain change incurred by the low-frequency range of exposure to head movement was not carried over into the high-frequency range. If so, this would be particularly interesting on account of the apparent lack of frequency specificity after adaptation to vision reversal in normal light conditions, as described above.^{19,21-23}

In this connection it is intriguing to compare the results shown in FIGURES 2 and 3. Why should there have been no high-frequency change after the vision-reversed state, and yet an upward increment of high-frequency gain after no reversal? Recall that with low-frequency testing, strobe-exposed subjects *did* show effects with and without prisms, i.e., gain attenuation after prism adaptation and gain augmentation after strobe exposure with no prisms. As suggested earlier,¹² the latter result could derive from an initially low and inadequately boosted VOR gain associated with low-frequency head movement in the strobe environment. The resulting (discontinuous) retinal image slip would then be in a direction calling for augmentation of the VOR.²⁶

At high frequency in strobe light, the VOR gain presumably would be augmented initially toward unity due to the inherent frequency response of the

normal reflex.^{27,30} Hence, in the absence of prisms, the amplitude of image slip would be correspondingly small, and its significance (i.e., magnitude and direction) therefore easily detectable. This then could account for the observed high-frequency gain augmentation in subjects exposed to strobe light *without* vision reversal (see FIGURE 3). With prisms in place, however, strobe exposure at high frequency would be accompanied by very much larger retinal image displacements, resulting in spatiotemporal pattern dispersions devoid of any meaningful velocity information, with a corresponding absence of any high-frequency change in VOR gain (see FIGURE 2).

Reviewing the findings as a whole, it is clear that imposing vision reversal in *normal* light disturbs the normally harmonious relation between visual and vestibular inputs. The resulting sensory conflict provokes both motion sickness and an adaptive drive calling for resolution of this conflict. With such resolution, there is a progressive diminution of both the adaptive drive and the severity of motion sickness.

During adaptation in *strobe* light, no motion sickness was ever noted. This, together with the previously demonstrated reduction in the rate of strobe-induced adaptation at low frequencies,¹² favors a functional relation between the rate and range of the adaptive process, and the severity of induced motion sickness.³¹ In turn, the findings suggest the possibility of producing functionally useful adaptation without the penalty of disabling motion sickness, by controlling the rate of the adaptive process by means of an appropriate stroboscopically illuminated environment.

REFERENCES

1. SJOBERG, A. A. 1929. Experimental studies of the eliciting mechanism of sea sickness. *Acta Oto-Laryngol.* **13**: 343-347.
2. KENNEDY, R. S. & A. GRAYBIEL. 1965. The Dial Test: A Standardized Procedure for the Experimental Production of Canal Sickness Symptomatology in a Rotating Environment. Report NSAM-930, NASA Order No. R-93. Naval School of Aviation Medicine. Pensacola, Fla.
3. GRAYBIEL, A. 1965. Functional disturbances of vestibular origin of significance in space flight. In *Second International Symposium on Basic Environmental Problems of Man in Space*: 1-30. U.S. Naval Aviation Medical Center. Pensacola, Fla.
4. MONEY, K. E. & J. FRIEDBERG. 1964. The role of the semicircular canals in causation of motion sickness and nystagmus in the dog. *Can. J. Physiol. Pharmacol.* **42**: 793-801.
5. WANG, S. C. & H. I. CHINN. 1956. Experimental motion sickness in dogs: importance of labyrinth and vestibular cerebellum. *Am. J. Physiol.* **105**: 617-623.
6. WITKIN, H. A. 1949. Perception of body position and of the position of the visual field. *Psychol. Mon.* **63**: 1-46.
7. MONEY, K. E. 1970. Motion sickness. *Physiol. Rev.* **50**: 1-39.
8. REASON, J. T. & J. J. BRAND. 1975. *Motion Sickness*. Academic Press, Inc. London & New York.
9. MILLER, J. W. & J. E. GOODSON. 1960. Motion sickness in a helicopter simulator. *Aerosp. Med.* **31**: 204-212.
10. GONSHOR, A. & G. MELVILL JONES. 1960. Postural adaptation to prolonged optical reversal of vision in man. *Brain Res.* **102**: 239-248.
11. GONSHOR, A. & G. MELVILL JONES. 1976. Extreme vestibulo-ocular adaptation induced by prolonged optical reversal of vision. *J. Physiol.* **256**: 381-414.
12. MELVILL JONES, G. & G. MANDL. 1979. Effects of strobe light on adaptation of vestibulo-ocular reflex (VOR) to vision reversal. *Brain Res.* **164**: 300-303.

13. CYNADER, M. & G. CHERNENKO. 1976. Abolition of direction selectivity in the visual cortex of the cat. *Science* **193**: 504-505.
14. MELVILL JONES, G. & P. DAVIES. 1976. Adaptation of cat vestibulo-ocular reflex to 200 days of optically reversed vision. *Brain Res.* **103**: 551-554.
15. MEIRY, J. L. 1966. The Vestibular System and Human Dynamic Space Orientation. Report No. NASA CR-628. National Aeronautics and Space Administration. Washington, D.C.
16. MELVILL JONES, G., P. DAVIES & A. GONSHOR. 1977. Long-term effects of maintained vision reversal: Is vestibulo-ocular adaptation either necessary or sufficient? *Dev. Neurosci.* **1**: 59-68.
17. MELVILL JONES, G. & D. H. DRAZIN. 1962. Oscillatory motion in flight. In *Human Problems of Supersonic and Hypersonic Flight*. A. B. Barbour & H. E. Whittingham, Eds.: 134-151. Pergamon Press. London, England.
18. MELVILL JONES, G. & A. GONSHOR. Oculomotor response to rapid head oscillation (0.5-5.0 Hz) after prolonged adaptation to vision-reversal: "simple" and "complex" effects. *Exp. Brain Res.* (Submitted.)
19. GONSHOR, A. 1974. An investigation of plasticity in the human vestibuloocular reflex arc. Ph.D. Thesis. Department of Physiology. McGill University. Montreal, Canada.
20. BERTHOZ, A., G. MELVILL JONES & A. BEGUE. 1980. Long term effects of dove prism vision on torsional VOR and head-eye coordination. In *Proceedings of Symposium on Neuronal Plasticity in Sensory Motor Systems*, Bremen, July 10-12. (In press.)
21. ROBINSON, D. A. 1976. Adaptive gain control of the vestibulo-ocular reflex by the cerebellum. *J. Neurophysiol.* **39**: 954-969.
22. DAVIES, P. R. 1978. Neural adaptation in humans and cats subjected to long term optical reversal of vision: an experimental and analytical study of plasticity. Ph.D. Thesis. Department of Electrical Engineering. McGill University. Montreal, Canada.
23. MILES, F. A. & B. B. EICHMY, 1980. Long-term adaptive changes in primate vestibulo-ocular reflex. I. Behavioural observations. *J. Neurophysiol.* **43**: 1406-1425.
24. MILES, F. A. & S. G. LISBERGER. 1981. Plasticity in the vestibulo-ocular reflex: a new hypothesis. *Ann. Rev. Neurosci.* **4**: 273-299.
25. OUTERBRIDGE, J., G. MANDL & M. GORAYEB. 1977. How do visual cells synthesise responses to moving light stimuli? *Neurosci. Abstr.* **3**: 572.
26. COLLEWIJN, H. & A. F. GROOTENDORST. 1979. Adaptation of optokinetic and vestibulo-ocular reflexes to modified visual input in the rabbit. *Prog. Brain Res.* **50**: 772-781.
27. BENSON, A. J. & G. R. BARNES. 1978. Vision during angular oscillation: the dynamic interaction of visual and vestibular mechanisms. *Aviat. Space Environ. Med.* **49**(2): 340-345.
28. FUCHS, A. F. 1967. Periodic eye tracking in the monkey. *J. Physiol.* **193**: 161-171.
29. MELVILL JONES, G. 1964. Predominance of anticomensatory oculomotor response during rapid head rotation. *Aerosp. Med.* **35**: 965-988.
30. BARNES, G. R. & L. N. FORBAT. 1979. Cervical and vestibular afferent control of oculomotor response in man. *Acta Oto-Laryngol.* **88**: 79-87.
31. GRAYBIEL, A. 1968. Prevention of motion sickness in the slow rotating room by incremental increases in strength of stimulus. In *Fourth Symposium on the Role of the Vestibular Organs in Space Exploration*: 109-116. Report No. NASA SP-187. National Aeronautics and Space Administration. Washington, D.C.

NATURAL RETINAL IMAGE MOTION: ORIGIN AND CHANGE*

H. Collewyn

*Department of Physiology I
Erasmus University
3000DR, Rotterdam, the Netherlands*

A. J. Martins and R. M. Steinman†

*Department of Psychology
University of Maryland
College Park, Maryland 20742*

It is generally accepted that "the function of the vestibulo-ocular reflex (VOR) is to maintain a stable retinal image during head rotations by generating appropriate compensatory eye movements."¹ There have been numerous expressions of enthusiasm for the effectiveness with which this reflex achieves retinal image stability, for example, "the remarkable fact emerges that the reflex produces virtually perfect compensation."²

We share this enthusiasm, but we believe that the true function of the VOR is more subtle than has been suspected. We believe that the VOR serves not simply to stabilize the retinal image of a fixated object during movement but, rather, to produce and maintain retinal image motion within each eye and between the eyes that is optimal for binocular vision.

It became possible for us to entertain this idea only recently because supporting evidence requires accurate measurement of binocular retinal image motion in freely moving human beings. When it became possible to make such measurements, we found that natural eye movement compensation was not virtually perfect and, furthermore, that compensation was different within each of the eyes.³ Subjectively, vision remained clear, fused, and stable under all but the most violent, active head rotations we studied despite such "imperfections" of oculomotor compensation.

The present experiments continue this line of research. First, we extended our results on natural binocular retinal image motion to a larger sample of subjects, making these observations with passive, as well as active, rotations. Second, we measured binocular retinal image motion with sinusoidal stimulation of fixed frequencies and amplitude, allowing estimates of retinal image speed at each of several frequencies. Third, we determined the degree and speed with which the VOR (in the dark and when supplemented by vision) could be modified by changing the correlation between the amount of retinal image motion and a given degree of eye rotation. These adaptation experiments were undertaken to determine whether the observed departures from virtually perfect compensation arose from limitations inherent in the compensatory subsystems or from the desire of the compensatory subsystems to maintain retinal image motion at some nonzero value that might be optimal for vision.

We will show that (1) compensation is rarely virtually perfect; (2) even when

*Supported by National Science Foundation Grants No. BNS 77-16474, 80-25344, and 80-13508.

†To whom correspondence should be addressed.

compensation is virtually perfect in one eye, it is not in the other eye, which leads to noncorrespondence of fixation positions between the eyes and high vergence velocities; (3) the degree of compensation in the light is the same with active and passive rotations; (4) the VOR in the light adapts completely within minutes (adaptation is complete in the sense that it reestablishes retinal image velocities observed prior to the introduction of novel optical arrangements); and (5) the VOR in the dark also adapts within minutes to as much as 90% of the required change.

METHODS

Recording

A revolving magnetic-field-sensor coil eye-movement monitor was used to record binocular eye and head rotations. Our instrument is based on the idea, suggested by Hartmann and Klinke, that Collewijn developed and used to measure eye movements on the horizontal meridian in the freely moving rabbit.^{4,5} Steinman and Collewijn subsequently used Collewijn's revolving field monitor with freely moving human subjects.³ Detailed descriptions of Collewijn's instrument are given in the prior papers. Here we will review only briefly its basic principle and then describe the Maryland instrument used in the present experiments.

Two horizontal a.c. magnetic fields of equal magnitude, in spatial and phase quadrature, generate a magnetic vector of constant magnitude rotating with uniform angular velocity through 360° during every period of the field frequency. The phase of the voltage induced in a sensor coil placed in the field varies linearly with the angular orientation of the sensor coil, and thus by phase detection the angular orientation of any object fitted with a sensor coil can be measured. It is crucial that the magnetic field be homogeneous in direction and magnitude and truly orthogonal in space and phase. The simple arrangement used by Collewijn and copied at Maryland for creating a uniform magnetic field was described by Rubens.⁶

The rotating field frequency of the Maryland instrument was 976 Hz. The orthogonality of the sinusoidal currents at this frequency and the strength of the magnetic field were maintained by a feedback loop receiving input from a (10-cm diameter) field-sensing coil located near the center of the magnetic chamber, which was 2.43 m on a side. The control accuracy of this magnetic-field servo loop was such as to compensate for departures from orthogonality (phase shift from 90°) smaller than 1°. The measured homogeneity of the magnetic field was within 1 part in 1,000 for translations of ± 24 cm, as expected from Rubens' analysis. The Maryland instrument is digital, and both magnetic field control and phase-detecting circuits were controlled by reference to a 200-MHz crystal clock. The bandwidth for phase measurement was 178 Hz (-3 dB). The noise level with the weak magnetic field used (0.278 gauss) and type of sensor coils attached to the eyes and head was $< 40^\circ$. Phase indications were linear to better than 1% in 360°. The instrument was stable, i.e., the angular orientation of a fixed sensor coil drifted $< 6^\circ$ during periods ranging from 1 second to 24 hours.

Eye movements were measured with the silicone-annulus sensor coils described by Collewijn, Van der Mark, and Jansen.⁷ These silicone annuli are shaped so as to suck onto the eye when they are inserted with the tool described by the inventors.⁷ The fidelity with which these annuli follow the eye was

determined originally by asking subjects to make a rapid series of twenty 20° saccades.⁷ No detectable differences in fixation position were observed following these saccades. We repeated this kind of experiment for two reasons. First, because the prior measurements had been made with an instrument less accurate than ours. Second, because we planned to elicit larger eye movements in our experiments and felt that the stability of the annulus should be verified under the conditions to be employed. Therefore, two of us (HC and AM) fixated a red diffraction-limited point target, located 12.2 m away, for 12.8 seconds with our heads supported on a bite-board. We then got off the bite-board and recorded while making large head and eye movements for an equal period of time. We then returned to the bite-board and recorded another fixation trial. HC recorded 30 pairs of such trials, and AM recorded 22 pairs. The annuli did not change position on the eye under these extreme conditions. The standard deviations of the mean fixation position were small (HC, standard deviation = 3.8' and AM, SD = 3.5'); both values are within the range of standard deviations of eye positions observed during fixation trials. These results—where the scatter around the mean fixation position is similar to the average scatter of the line of sight during periods of maintained fixation of the same target—show that a properly inserted annulus does not change its position with respect to the eye. Very occasionally, an annulus will lose its grip. Such occurrences are easily detected because the annulus no longer follows the eye and saccades, therefore, are no longer seen in the records. More often than not, a loose annulus falls out of the orbit. A properly inserted and seated annulus must be grasped with forceps and peeled off the eye at the end of each recording session. Ours typically lasted 20 to 45 minutes. Head movements were recorded from a sensor coil mounted on a contoured polycarbonate strip that was strapped and taped to the forehead.

Stimulation

The fixation stimulus was a colorful object (a yellow-orange polyurethane duck's-head hand puppet with red eyes) subtending 56' vertically and 42' horizontally. This target, located 12.2 m from the subject, was seen at the center of a 4.7° diameter circular field composed of a black and white random square array, each square subtending 2.8'. Subjects were required to fixate the duck's head while they sat either actively rotating their heads or while their heads were supported by a dental bite-board and their chair was rotated. The frequencies of the active rotations, which were paced by a metronome, were 0.33, 0.66, or 1.33 Hz. The passive rotations were provided by a motor-driven chair equipped with a cam and lever that produced approximately sinusoidal movements at 0.0, 0.33, or 0.66 Hz. The peak-to-peak amplitude of the passive rotations was set at 34°—the amplitude of head rotation that subjects felt was comfortable and natural, i.e., did not lead to neck strain when they attempted paced sinusoidlike active rotations.

Data Acquisition and Analysis

Digital eye position and head samples were acquired at 976 Hz. Four samples from each of three channels (right eye, left eye, and head) were averaged, converted to minutes of arc, and stored on tape at the end of each 12.8-second trial. The stored data, after averaging and scaling, describe eye and head position for successive 5-millisecond periods, which means that our effective bandwidth was

100 Hz. The stored samples represent the positions of the eyes and head with respect to an earth-fixed framework. For a subject not wearing spectacles, these eye-position samples, which we will call "gaze," are equivalent to the position of the fixation target image on the retina. However, eye position measured with reference to an earth-fixed framework for a subject wearing spectacles must be corrected for the magnification factor of the spectacles before gaze (or retinal image position) is determined because, for example, a myope wearing a spectacle with a negative correction will have more retinal image motion for a given-amplitude eye rotation than will an emmetrope not wearing spectacles. Similarly, an individual wearing spectacles with a positive correction will have a smaller retinal image displacement for a given amplitude of eye rotation than will the person not wearing spectacles. Magnification factors for those of our subjects (HC, WC, and AM) who required and wore spectacles during the experiments were determined by a behavioral technique that will be described later. It should be noted, however, that whenever we speak of gaze or retinal image motion, the values reported or plotted incorporate appropriate corrections for the spectacle wearers.

Eye- and head-position samples served as the basis for the calculations of velocities and gains. These measures were calculated as follows.

A sliding-window technique was used to calculate velocity. The window—35 mseconds wide—contained seven position samples, and the slope of the line—fitted by least squares—through the seven positions provided a single estimate of "instantaneous" velocity. The window was then moved 5 mseconds later in time (one position sample), and the next velocity estimate was calculated. Velocity samples were then used to detect and remove saccades. Saccades were detected by an acceleration criterion, viz., each velocity sample was compared to the previous velocity sample and if it differed by more than $15\% + 300^\circ/\text{second}^2$, the velocity sample meeting this criterion was flagged as saccade onset. This criterion was checked against a large sample of eye-position records and listings of the velocities associated with these records. The criterion detected all saccades—the microsaccades occurring during maintained fixation and the large saccades occurring during high-velocity smooth compensatory eye movements. When a saccade was detected, 40 mseconds of data were removed, providing the saccade ended within this period. Most did. The determination of whether the saccade had ended was made by comparing eye speed at the end of the 40-msecond period during which samples were removed to eye speed preceding detection of the saccade. A saccade was judged to be over when eye speed was below the saccade-detection criterion. If the saccade had not ended, additional samples were removed until the criterion was met or 100 mseconds had elapsed.

Gain (35-msecond eye-in-head velocity/35-msecond head velocity) was calculated from the velocities determined with the sliding-window technique (described above) after saccades were removed and after the velocity of the eye in the head was determined by subtracting eye-in-space velocity from head-in-space velocity. Negative gains (periods during which the eye went in the same direction as the head) were not included in the summaries of gain (gain was negative in $< 2\%$ of the calculations). Negative gains were observed only near changes in direction of head rotation.

Subjects

We examined natural retinal image motion in seven subjects (four myopes and three emmetropes). Five of the seven subjects served in a extensive series of experiments, and only their data will be described in detail (the other two

subjects did not differ in any significant way). All three of the authors served as subjects, but only HC and RS had served in oculomotor experiments before. AM was completely inexperienced as an oculomotor subject. The other two subjects (EK and WC), whose performance will be described in detail, had served in prior oculomotor research, but neither had participated with free heads or the silicone annulus technique. Their experience was confined to contact lens optical lever and double Purkinje image tracker experiments. Subjects ranged in age from 21 to 64 years old. All had 20:20 Snellen acuity naturally or with their normal spectacle corrections.

RESULTS

Binocular retinal image motion was determined by recording positions of the eyes and head in space relative to an earth-fixed framework while the subjects maintained fixation of a distant target for 12.8 seconds. Recording sessions began

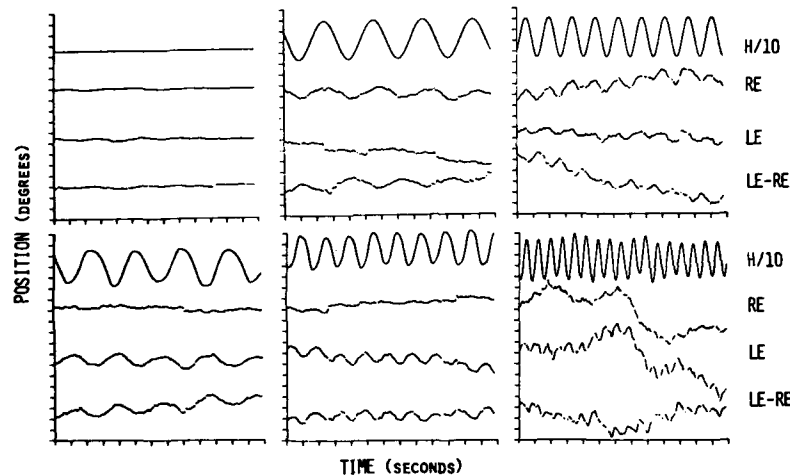


FIGURE 1. Six illustrative records of horizontal smooth compensatory eye and head movements of subject RS fixating a distant target while his head was passively or actively rotated. The top three records were made with the head supported by a bite-board while the body was rotated at three frequencies: 0.00 Hz (left), 0.33 Hz (center), and 0.66 Hz (right). The bottom three graphs were made during active head rotation paced by a metronome at three frequencies: 0.33 Hz (left), 0.66 Hz (center), and 1.33 Hz (right). The time-scale marks signify one-second intervals. The position-scale marks signify 1° distances. The head-position traces (H/10) show the position of the head scaled to 1/10 of its actual value. The gaze (retinal image position) of the right eye (RE) is shown just below the head trace, the gaze of the left eye (LE) is shown just below the right eye trace, and the vergence of the eyes (LE-RE) is shown at the bottom of each record. Upward changes in the head and eye traces signify leftward movements. Upward changes in the vergence traces signify divergence. Saccades have been removed from all eye traces. Saccades were detected by an acceleration criterion (see text), and the gaze traces were corrected for the changes in position introduced by saccades by assuming that smooth compensatory eye movements continued during the saccade at the velocity present just prior to saccade onset. Small gaps in the traces signify when saccades occurred and were removed.

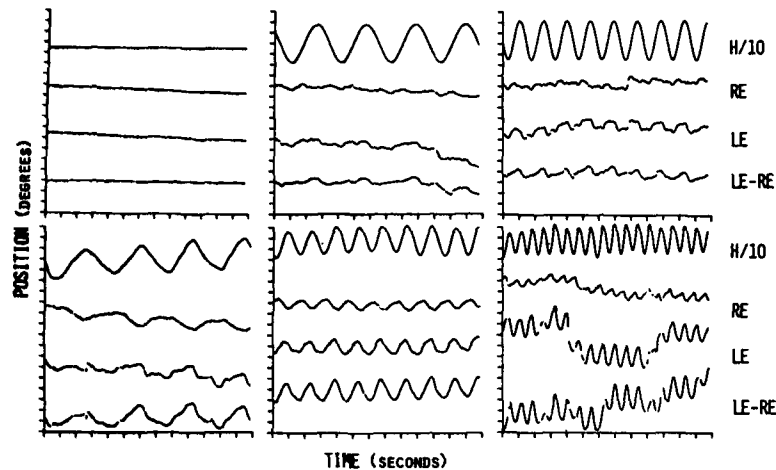


FIGURE 2. Six illustrative records of horizontal smooth compensatory eye and head movements of subject HC, a myope wearing his normal corrective spectacles, fixating a distant target while his head was passively or actively rotated. Gaze traces have been corrected for his spectacles. See FIGURE 1 for other details.

with the subject's head supported by a dental bite-board. This unnatural condition (0.00 Hz) permits examination of slow compensatory eye movements (VOR supplemented by vision) when head movement is minimal. Next, recordings were made while the subject's head remained supported by the bite-board as his chair was oscillated sinusoidally at 0.33 or 0.66 Hz with peak-to-peak amplitude set to 34° (peak velocities = 35° or 70°/second). The subject then removed his head from the bite-board, and a series of recordings were made during active head rotations whose frequencies were paced by a metronome (0.33, 0.66, or 1.33 Hz where peak velocity = 140°/second). Subjects tried to make sinusoidal movements and keep amplitude similar to the amplitude of the passive rotations. The results of these experiments are illustrated in FIGURES 1-5 and summarized in TABLES 1 and 2.

The retinal image of the fixation target moved very little only when the head was supported artificially. All five subjects, whose results are described in detail, performed similarly in this condition (the upper-left recording reproduced in each plate). Note, however, that the head movements, which did occur when the head was stabilized, were only modestly compensated by eye movements (see TABLES 1 and 2). The mean speed of these head movements on the bite-board was 31°/second (SD = 0.37). The mean oculomotor compensation for these small, relatively slow head movements was modest, i.e., only 30% (SD = 23). Now consider the illustrative eye- and head-movement records made during active and passive rotation. If compensation were virtually perfect, gaze and vergence traces would approximate horizontal straight lines—they do when the head is almost stabilized by the bite-board and vestibular compensation is not required to maintain gaze stability. There are very few instances, off the bite-board, during which it seems appropriate to speak of virtually perfect compensation, and even in these cases virtual perfection is achieved by only one eye. This causes considerable imperfection in the control of vergence. See, for example, subject

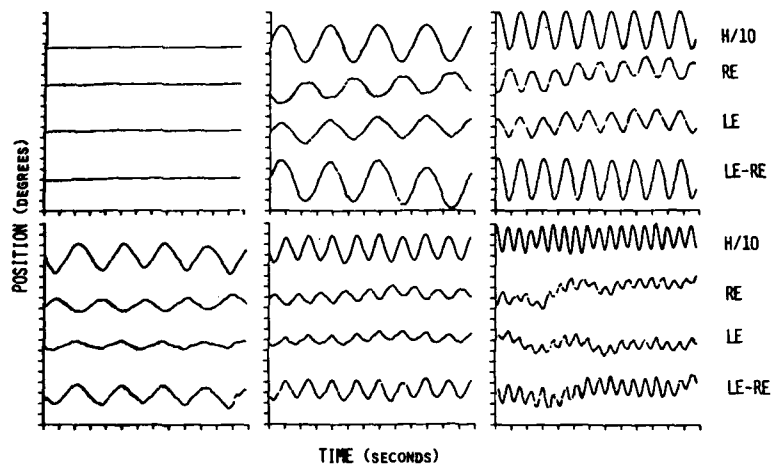


FIGURE 3. Six illustrative records of horizontal smooth compensatory eye and head movements of subject AM, a myope wearing his normal corrective spectacles, fixating a distant target while his head was passively or actively rotated. Gaze traces have been corrected for his spectacles. See FIGURE 1 for other details.

RS's gaze and vergence during passive rotation at 0.33 Hz (top center in FIGURE 1) and at 0.33 and 0.66 Hz during his active rotations (bottom left and center). Subject HC's right-eye gaze during passive rotation at 0.33 Hz (top center in FIGURE 2) and to a lesser degree at 0.66 Hz (top right) is almost as good as when his head is held. In all other instances (subjects and/or eyes), the differences

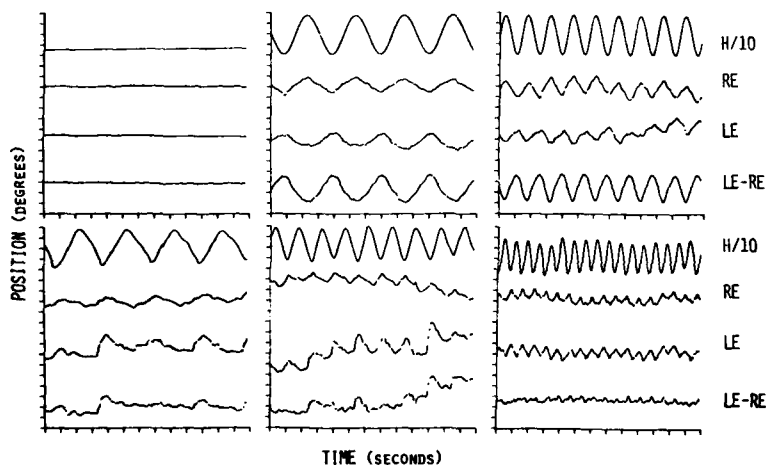


FIGURE 4. Six illustrative records of horizontal smooth compensatory eye and head movements of subject WC, a myope wearing his normal corrective spectacles, fixating a distant target while his head was passively or actively rotated. Gaze traces have been corrected for his spectacles. See FIGURE 1 for other details.

between compensation during head movement and during artificial head stabilization are striking. These "failures" in compensation arise from both overcompensation and from undercompensation. When the eye movement undercompensates, the gaze trace in these records moves in the same direction as the head. When the eye movement overcompensates, the gaze trace moves in the direction opposite to the head. See, for example, FIGURE 3. This subject, AM, undercompensates with his left-eye movements and overcompensates with his right-eye movements under all conditions. The other subjects show similar "failures," but they tend to vary with conditions of stimulation, e.g., WC in FIGURE 4 overcompensates with both eyes during active rotation, but his right eye undercompensates while his left eye continues to overcompensate during passive rotations. WC's performance in these records was idiosyncratic but consistent. He always

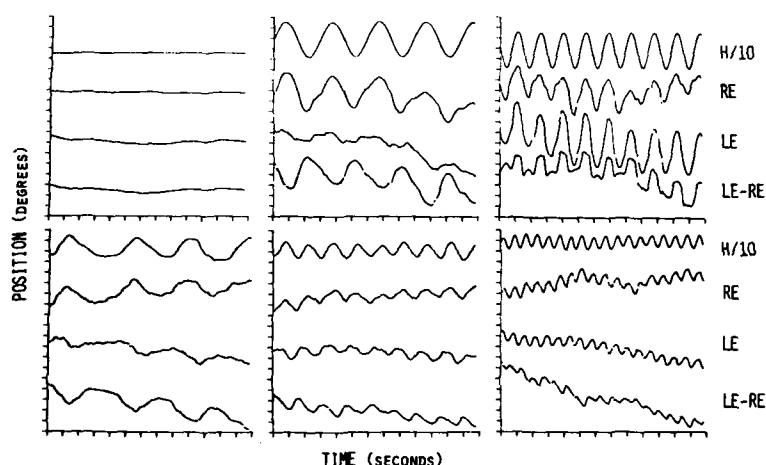


FIGURE 5. Six illustrative records of horizontal smooth compensatory eye and head movements for subject EK, a myope wearing her corrective corneal contact lenses, fixating a distant target while her head was passively or actively rotated. Gaze traces did not require correction. See FIGURE 1 for details.

shows these patterns, as do the other subjects, each of whom has his own binocular compensatory signature.

Despite these differences in gaze characteristics within and between individuals, there is considerable consistency in the overall pattern of data summarized in TABLE 2. The grand mean head-movement speed compensated under natural conditions (i.e., excluding measures on the bite-board) was 95% (SD = 2.1). Compensation was the same during active (mean = 95%, SD = 2.4) and during passive rotation (mean = 95%, SD = 1.9). Vergence speed increased very markedly once the head was allowed to move. The grand mean increase in vergence speed was 329% (SD = 249). The increase was greater under passive rotation for four subjects (mean = 429%, SD = 249) than under active rotation (mean = 178%, SD = 102). The opposite result was obtained with the other subject (HC), where active mean increase was 290% (SD = 164) and passive mean increase was 114% (SD = 59). These comparisons could be made only for

TABLE 1
MEAN BINOCULAR RETINAL IMAGE AND HEAD SPEED (MIN ARC/SEC) DURING ACTIVE AND PASSIVE HEAD ROTATION AT SEVERAL FREQUENCIES*

Condition		Head	LE	RE	LE-RE
Subject RS (n = 8000)					
Passive	0.00 Hz	25 (20)	24 (19)	21 (17)	30 (23)
	0.33 Hz	1,408 (650)	32 (37)	49 (36)	67 (44)
	0.66 Hz	2,999 (1,445)	79 (62)	103 (70)	124 (89)
Active	0.33 Hz	1,072 (760)	42 (34)	34 (35)	50 (49)
	0.66 Hz	2,281 (1,472)	62 (54)	43 (41)	68 (68)
	1.33 Hz	5,006 (2,742)	129 (119)	86 (80)	113 (97)
Subject HC (n = 4000)					
Passive	0.00 Hz	39 (29)	23 (21)	24 (21)	29 (23)
	0.33 Hz	1,361 (677)	55 (60)	44 (56)	50 (42)
	0.66 Hz	2,927 (1,472)	93 (76)	70 (55)	74 (63)
Active	0.33 Hz	908 (448)	58 (53)	43 (32)	76 (58)
	0.66 Hz	1,971 (1,010)	104 (76)	65 (44)	149 (87)
	1.33 Hz	3,862 (1,870)	257 (190)	113 (112)	313 (200)
Subject AM (n = 9000)					
Passive	0.00 Hz	43 (33)	20 (17)	25 (20)	31 (23)
	0.33 Hz	1,412 (656)	80 (40)	79 (53)	150 (80)
	0.66 Hz	2,947 (1,490)	168 (84)	154 (106)	307 (164)
Active	0.33 Hz	1,081 (483)	45 (32)	50 (18)	85 (49)
	0.66 Hz	2,042 (922)	83 (50)	83 (53)	157 (77)
	1.33 Hz	3,410 (1,796)	146 (62)	136 (93)	256 (137)
Subject WC (n = 4000)					
Passive	0.00 Hz	45 (34)	19 (16)	23 (19)	27 (20)
	0.33 Hz	1,424 (685)	58 (40)	57 (38)	98 (103)
	0.66 Hz	3,166 (1,531)	105 (74)	126 (66)	208 (101)
Active	0.33 Hz	1,207 (489)	76 (100)	47 (37)	65 (80)
	0.66 Hz	2,461 (960)	105 (100)	77 (52)	86 (80)
	1.33 Hz	4,584 (2,156)	149 (84)	131 (91)	107 (76)
Subject EK (n = 5000)					
Passive	0.00 Hz	22 (17)	23 (18)	21 (17)	30 (23)
	0.33 Hz	1,321 (652)	70 (56)	99 (77)	113 (83)
	0.66 Hz	2,807 (1,357)	340 (215)	213 (140)	184 (181)
Active	0.33 Hz	632 (359)	44 (35)	58 (43)	67 (47)
	0.66 Hz	1,106 (487)	73 (56)	82 (52)	79 (52)
	1.33 Hz	1,907 (919)	133 (97)	167 (93)	116 (73)

*Standard deviations are given in parentheses. Speeds are based on 35-msec velocity samples after removal of saccades. The approximate number (n) of speeds contributing to the mean speeds is shown for each subject. The column labeled LE-RE represents the speed of vergence eye movements.

TABLE 2
PERCENT OF HEAD MOVEMENT SPEED COMPENSATED IN EACH EYE AND THE
PERCENT INCREASE IN VERGENCE SPEED DURING ACTIVE AND
PASSIVE ROTATIONS AT SEVERAL FREQUENCIES*

Condition		LE	RE	LE-RE
Subject RS (n = 8000)				
Passive	0.00 Hz	4	16	
	0.33 Hz	98	97	123
	0.66 Hz	97	97	313
Active	0.33 Hz	96	97	67
	0.66 Hz	97	98	127
	1.33 Hz	97	98	277
Subject HC (n = 4000)				
Passive	0.00 Hz	41	38	
	0.33 Hz	96	97	72
	0.66 Hz	97	98	155
Active	0.33 Hz	94	95	162
	0.66 Hz	95	97	414
	1.33 Hz	93	97	979
Subject AM (n = 9000)				
Passive	0.00 Hz	53	42	
	0.33 Hz	94	94	384
	0.66 Hz	94	95	890
Active	0.33 Hz	96	95	174
	0.66 Hz	96	96	406
	1.33 Hz	96	96	726
Subject WC (n = 4000)				
Passive	0.00 Hz	58	49	
	0.33 Hz	96	96	263
	0.66 Hz	97	96	670
Active	0.33 Hz	94	96	141
	0.66 Hz	96	97	219
	1.33 Hz	97	97	296
Subject EK (n = 5000)				
Passive	0.00 Hz	-4	5	
	0.33 Hz	95	93	277
	0.66 Hz	88	92	513
Active	0.33 Hz	93	91	123
	0.66 Hz	93	93	163
	1.33 Hz	93	91	286

*The percent compensation is based on the ratio of eye speed to head speed. The percent increase in vergence speed is based on the ratio of vergence speed during rotation to vergence speed at 0.00 Hz (head on bite-board).

0.33 and 0.66 Hz. It should be emphasized at this point that all subjects always saw the fixation field as fused, clear, and stable during the course of these experiments.

We conclude that virtually perfect compensation of head rotation by the VOR, supplemented by vision, is rarely observed when head rotations are within "the natural dynamic range of semicircular canal stimulation."⁸ The proportion of head speed that is compensated during natural head rotation is greater than when the head is artificially stabilized on a bite-board, which permits only very small, slow head rotations. The fact that compensation is particularly poor for very small rotations has been reported before by Skavenski, Hansen, Winterson, and Steinman.⁹ These authors proposed that incomplete compensation may aid vision by guaranteeing sufficient retinal image motion when bodily movement is very modest. Similar results were obtained subsequently in rabbit.¹⁰

Adaptation experiments were undertaken to determine whether the rather high retinal image speeds observed in all of our subjects during relatively large bodily movements arose from limitations of their oculomotor compensatory subsystems or from the teleologically attractive alternative suggested by Skavenski et al.⁹ Adaptation experiments can make it plausible to assert that the compensatory subsystems adjust their degree of compensation so as to guarantee some nonzero value of retinal image speed that subsequently might be shown in psychophysical experiments to be useful and perhaps essential to visual processing. This possibility becomes plausible if it can be shown that the amount of compensation preferred by a given subject remains the same when the VOR is forced to change its gain when a new correlation between the degree of head movement and the resulting displacement of the retinal image is introduced.

We knew from prior work that adaptation of the human VOR was possible but likely to be both slow and incomplete. Gauthier and Robinson reported that Gauthier partially adapted to a 2 \times telescope, which he wore continually for 5 days.¹² Gonshor and Melvill Jones produced adaptation by using mirrors or dove prisms to reverse the direction of eye movement to head movement.^{8,13} Sixteen minutes of adaptation with the mirror on 3 consecutive days led to a modest cumulative reduction in VOR gain (VOR gain in the dark started at about 0.75 and went down to about 0.5). Adaptation of 14 days with continuously worn dove prisms led to complete elimination, and possibly to the beginning of reversal, of the VOR. Complete adaptation would be evidenced by negative gains of 0.75. Research with the rhesus monkey gave similar expectations of slow and incomplete adaptation.^{1,14} Monkeys fitted with 2 \times telescopes required 3 days to reach 60% of the required increase in VOR gain and stayed at this level during 5 subsequent days. Monkeys fitted with -0.5 \times telescopes required 24 hours to achieve their stable level at 54% of the required reduction in VOR gain.

We began our experiments in this context and proceeded accordingly, viz., we measured VOR baselines in the dark and in the light, fitted magnifying or minifying spectacles, measured VOR performance with these spectacles, and then wore them continually for 24 hours, after which we once again measured the VOR both in the light and in the dark. When, after about a month of such experiments, it became possible to determine what had been happening, we found a great deal of adaptation of the VOR within minutes of fitting our magnifying or minifying spectacles. It did not change during the next 24 hours. This unexpected observation led to specific experiments on short-term adaptation, which will now be described. (The data obtained over longer periods of adaptation will be described elsewhere.)

Three of the subjects (the authors) served in these experiments. Two (HC and

AM) are myopic and had worn their normal negative corrective spectacles during the earlier experiments in which their natural retinal image motion was measured. The technique we use to make the correction for spectacle wearers when we describe or plot their gaze will be described here because the rationale underlying these corrections is the same as that used when altering the normal relation between rotations of the head and movements of the fixation target on the retina. There are two ways to determine the magnification factor required to convert eye in space to gaze for an individual wearing spectacles. First, the power of the spectacle and distance to the center of the eye's optics can be measured. This distance is difficult to determine accurately. The second method, the one employed, is behavioral. It permits an accurate determination because measurements are limited only by the stability of the fixating eye, which in all of our subjects was better than 5'.

Our behavioral measurement proceeded as follows. The subject's head was supported on a bite-board attached to his chair. The chair could be rotated through a known angle. The subject's task was to maintain monocular fixation of a distant target while wearing his normal spectacles. Fixation was recorded while the head faced the target and the subject looked through the center of his spectacle. The spectacles were secured to the head by tape during these measurements and during all subsequent experiments. The head was then rotated, to the right or to the left, 17°, and recordings were made while the subject once again fixated the same target monocularly. Now his eye was looking at the target, but the line of sight passed through an off-center portion of the spectacle lens. The amount of rotation of the eye required to place the line of sight on the fixation target depends on the power of the spectacle and its distance from the eye. If no spectacle is worn, the required rotation of the eye in the head will be equal in size, but opposite in direction, to the rotation of the head, i.e., the magnification factor equals one. If a negative spectacle is worn, the rotation of the eye in the head will be less than the rotation of the head and the magnification factor will be less than one. Positive spectacles will give magnification factors greater than one. This behavioral technique was reliable, i.e., the magnification factors for a given subject's left and right eye and particular pair of spectacles were highly reproducible. The validity of the technique was determined by making similar measurements for an emmetrope (RS) whose magnification factor for each of his eyes, when no spectacles were worn, was within 1% of unity and also for EK, a myope wearing corneal contact lenses concurrent with sensor-coil annuli who also had, as she should, a magnification factor of one.

The same behavioral technique was used to calibrate the spectacles that were used to encourage adaptive changes in the VOR. Subjects HC and AM, whose normal spectacles incorporate about -5 D corrections, were fitted with +5 D spectacles and then calibrated behaviorally in the manner described above. We determined that both subjects, wearing the +5 D spectacles, would have to increase rotations of their eye in space by 33% if they wished to maintain the same stability of gaze they prefer when they wear their normal negative spectacles. Requiring a myope to wear a positive spectacle, however, introduces considerable visual blur. It was for this reason that we used a relatively large colorful fixation target. This target, even when grossly defocused, provided a discriminable chromatic region that was clearly visible within what was now seen as a fuzzy grey background.

Following the calibration of the novel noncorrective spectacles, the short-term adaptation experiment was done as follows. A sensor coil was fitted to the right eye, and the positive spectacles were fitted. The subject was placed in

darkness and required to move his head sinusoidally in pace with a metronome set at 0.66 Hz. Very shortly after he began to move, a 12.8-second recording was made. The subject was instructed to imagine that he was looking at the distant fixation target while he moved his head in darkness. This record provided an estimate of VOR gain before adaptation. The blinds then were opened, and the subject continued moving at 0.66 Hz while he viewed the distant defocused fixation target. A 12.8-second trial in the light was recorded at this time. The subject continued adapting by fixating the defocused target while moving his head for 40 minutes thereafter. At 5-minute intervals, he was placed in total darkness and a recording was made followed immediately by a recording of his eye-movement pattern while fixating the visible target. HC continued wearing the positive spectacles for 24 hours, and recordings were then made both in the light and in the dark.

RS, a presbyopic emmetrope, served in an analogous experiment. He, however, was fitted with a -5 D pair of spectacles that required him to reduce his compensatory responses by 9% (measured behaviorally). We chose this experiment for this subject because, although RS does not require spectacle correction for normal distance vision, he has in recent years found it necessary to use a variety of magnifiers to read and to perform other close work. We wished to avoid any contamination of his adaptation results by such prior exposures to positive adaptations and therefore required him to reduce, rather than increase, his compensatory responses. RS's data were obtained last in a brief experiment in which we only examined the adaptation of his VOR in darkness because we already knew from our measurements of HC and AM that adaptation with a visual stimulus was almost instantaneous. We also expected that a 9% change would be completed very quickly.

The results of these experiments are summarized in FIGURE 6. The preadaptation gain of the VOR of HC and AM, the myopic subjects who will be fitted with

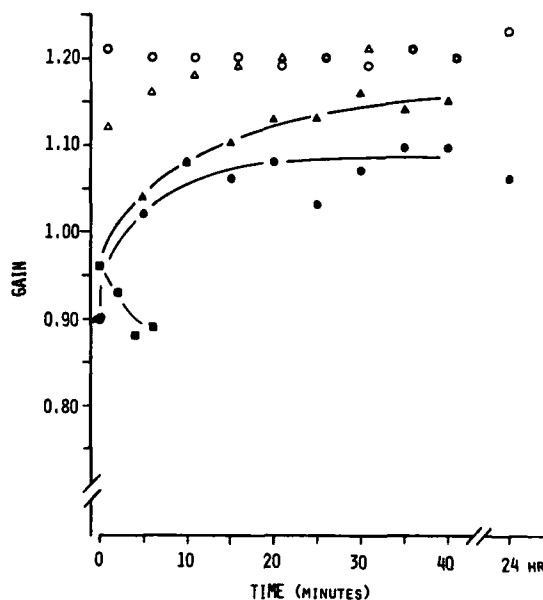


FIGURE 6. VOR gain (35-msec eye-in-head velocity/35-msec head velocity) in the light (open symbols) and in the dark (closed symbols) as a function of adaptation time. Subject HC's performance is shown by circles, AM's by triangles, and RS's by squares.

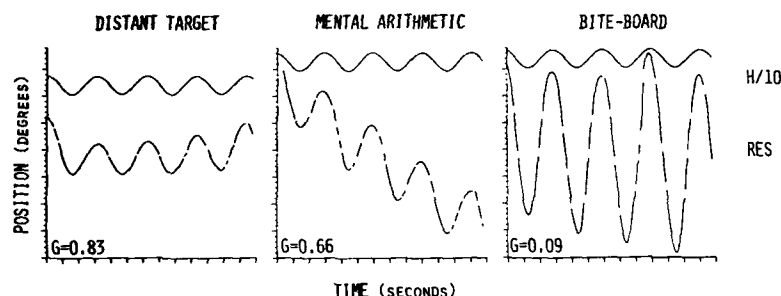


FIGURE 7. Three representative records of subject AM imagining a distant target (left), doing mental arithmetic (center), or imagining a target attached to his bite-board holder (right). Recordings were made in total darkness while AM's head was supported by a bite-board and his chair was rotated at 0.33 Hz. The time-scale marks signify one-second intervals. The position-scale marks signify 1° distances. The trace labeled H/10 shows the position of the head scaled to 1/10 of its actual value. The trace labeled RES shows the position of the right eye in space. Gaps in the eye traces show when saccades have been removed. Mean gains (G) are also given.

positive spectacles, is shown at time zero. Both fail to compensate completely with their right eyes in the light as well as in the dark—both gains = 0.90. Exact compensation for the introduction of the positive spectacles would require their gain to increase to 1.21. Both HC and AM accomplished this adjustment very rapidly in the light; HC attained this level within 1 minute of starting the experiment. AM required only 11 minutes to reach asymptote. Adaptation of the VOR working alone in the dark was slower and less complete. Both subjects, however, achieved a great deal in only 40 minutes. AM's VOR accomplished about 90% of the required change in this time, and HC's about 70%. The circles at the right show HC's gains in the light and in the dark after 24 hours during which he continued to wear the positive spectacles. These values fall within the range observed during the later portion of the initial period of adaptation. RS's adaptation to the negative spectacles, requiring a 9% reduction in gain, is also reproduced in this figure (filled squares). His baseline gain shown at time zero was 0.96, the highest natural VOR gain observed in the dark in any of our subjects under these conditions. RS accomplished about 85% of the required reduction within 6 minutes.

Some comment about the gain of the VOR in the dark is both necessary and possible at this time. It has been claimed on the basis of behavioral, but never absolute, calibrations made with insensitive eye movement monitors (EOG) that the average gain of the VOR in the dark can be as high as 1.00. Unity gain was observed very rarely in our experiments except when gain was forced up by artificial optical arrangements. The average gain of the natural VOR in the dark was less than 1.00. Similar observations were made previously in a smaller series of experiments in Rotterdam and also in Boston.^{3,9} It also has been claimed that the gain of the VOR in the dark can be altered markedly and systematically by giving specific instructions to the subject.¹¹

We undertook to examine this second claim, also based on behavioral calibrations of EOG, now that we knew that the first was fallacious. AM participated in this experiment. He was chosen because of his relative inexperience as an oculomotor subject and researcher. The results are summarized in FIGURE 7 where his VOR in the dark is shown under three instructions: imagining

the distant fixation target mounted on the wall, during the course of mental arithmetic, and while imagining a target attached to the front of his bite-board holder.

We recorded five trials under each condition. Their mean gains are included in the illustrative analog records. Instructions clearly make a systematic difference. Distraction in the form of mental arithmetic will reduce gain noticeably, and almost complete cancellation of the VOR can be obtained by asking a subject to imagine a target moving with his head. Note, however, that imagining a distant target attached to the wall gave a mean gain of 0.83 not 1.00. The highest right-eye average gain observed for this subject imagining a distant stationary target was 0.90. His left-eye average was slightly higher, 0.92.

We have shown quantitatively in FIGURE 6 that the gain of the VOR can exceed one, but this unnatural state required adaptation with appropriate stimulation. By appropriate stimulation we mean novel optical arrangements that forced the compensatory subsystems to increase their response in the effort to reduce the retinal image slip of the fixation target. FIGURES 8 and 9 illustrate the changes in the oculomotor pattern of the myopic subjects (HC and AM) during the course of adaptation with +5 D spectacles that required them to increase gain well beyond unity.

All of these records show head position in space and the position of the right eye in space (RES). The top records, which illustrate performance in the light, also show the gaze of the right eye (RE) after correction for spectacles. The first pair of records in each plate illustrate preadaptation performance in the light (top) and in the dark (bottom). These baselines are typical of the right eyes of

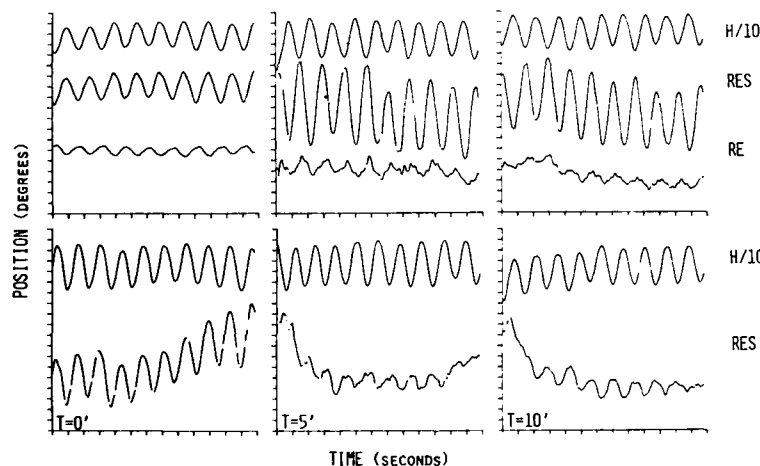


FIGURE 8. Six records of a myopic subject's (HC) short-term adaptation to +5 D spectacles. The upper three records were recorded in the light and the lower three records in total darkness while the subject actively rotated his head at 0.66 Hz. The time (T) these records were obtained relative to the start of adaptation (T=0) is indicated. The time-scale marks within each record signify one-second intervals. The position-scale marks signify 1° distances. The trace labeled H/10 shows the position of the head scaled to 1/10 of its actual value. The trace labeled RES shows the position of the right eye in space. The trace labeled RE shows the gaze (retinal image position) of the right eye after correction for the magnifying spectacles. Gaps in the eye traces show when saccades were removed.

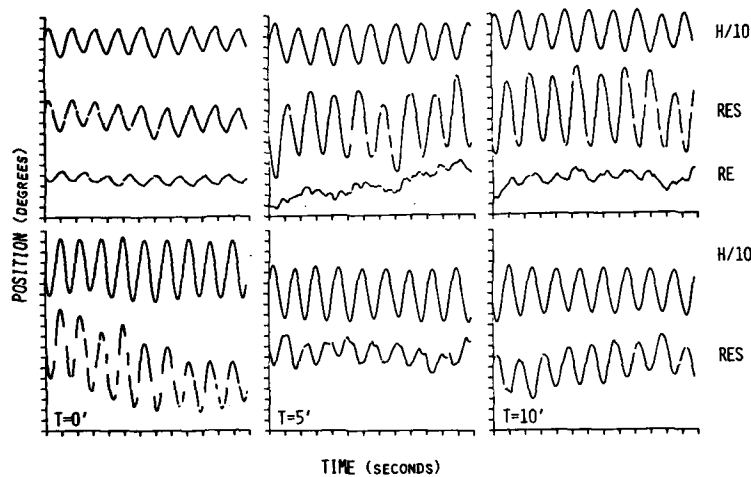


FIGURE 9. Six records of a myopic subject's (AM) short-term adaptation to +5 D spectacles. See FIGURE 8 for other details.

these subjects, namely, both overcompensate head movement [i.e., the eye in space trace (RES) moves opposite to the direction of the head] and both show considerable retinal image motion. (The mean head speed compensated by HC was 97% and by AM was 96%.) The middle records in these plates show performance after about 5 minutes of adaptation. Gain at this time had already exceeded 1.00; the eyes in space both in the light (top) and in the dark (bottom) are now moving *opposite* in direction to movements of the head (see RES traces before and after adaptation). Adaptation was almost over in the records shown on the right, which were made about 10 minutes into the adaptation period.

The gaze traces (RE) are of particular interest because they show the retinal image motion that the compensatory subsystems chose as optimal before and after adaptation. Note that marked changes in gain produced by novel optical arrangements reestablished the pattern of retinal image motion preferred before adaptation. The mean head speed compensated in the light after adaptation, when gain had increased 33%, was 95% for HC and 97% for AM—values very similar to the compensation shown by these subjects when they wore their normal corrective spectacles before adaptation. It is important to realize that when we pushed the compensatory subsystems from their natural low gain to an unnatural high gain, gain moved through values that would have allowed virtually perfect stabilization of the retinal image. Had virtually perfect stability been the goal of the compensatory subsystems, they should have stopped adapting at this time. They did not. This result permits us to conclude that the compensatory subsystems seek some appreciable nonzero retinal image speed rather than virtually perfect image stability.

DISCUSSION

We report two kinds of observations. Some extend our prior work on natural binocular image motion and others begin to examine its origin and change.

We confirmed, in additional subjects, our observations initially made in the Netherlands that natural binocular retinal image motion is appreciable,³ and extended the observations to show that this is equally true with active and passive rotations. We also confirmed that the gain of the VOR in the dark can be changed by instructions.¹¹ We did not find that instructions can produce natural average unity gain of the VOR in the dark. This last observation does not seem to require discussion beyond calling attention to the fact that we, unlike all others, used a sensitive instrument for measuring eye movement that is calibrated absolutely rather than behaviorally.

Our other observations were completely unexpected. Our demonstration that the slow compensatory subsystems adjust their gain very rapidly and almost completely in the dark to novel visual demands conflicts with prior reports both for man and infrahuman primates.^{1,8,12-14} If, for the sake of discussion, we take these prior EOG measurements at face value, we can discuss two more-or-less plausible explanations.

Perhaps we obtained such rapid and almost complete adaptation because we challenged the vestibular system only modestly. Prior authors generally required much larger changes in oculomotor compensation: $2\times$ in Gauthier and Robinson and complete reversal in Gonshor and Melvill Jones.^{8,12,13} It is only in the infrahuman primate literature that we have data on adaptation to a relatively modest change—in line with the demands we made. Miles and Eighmy required their monkeys to reduce VOR gain by 50%.¹ We required 33% increases in gain. Miles and Eighmy observed that adaptation proceeded faster when they required a 50% change than when they required a 100% change. However, their monkey's adaptation in the dark to 50% minification was only 54% complete after 24 hours and showed no signs of going further over 8 days. We obtained 70% changes for one subject and 90% changes for the other subject when we required a 33% increase. Our changes, which were accomplished within 40 minutes, were stable for periods as long as 24 hours. This difference in results may arise simply from the species difference. If this proves to be the explanation, rhesus would seem to be a poorer animal model for the human than most physiologists would like to believe.

There is another difference between our experiments and prior human and animal work. Namely, we used simple spectacles to change magnification factors both upwards and downwards. This optical arrangement is cost effective, but it has severe adverse effects on the clarity of vision. It is possible, although it seems unlikely to us, that our failure to provide a sharply focused visual world allowed the vestibular system to be more plastic than it would be when the clarity of vision is preserved. This explanation, as well as the possibility of slower vestibular adaptation to larger challenges than we have tried thus far, must be tested empirically.‡ Despite the desirability of examining these possibilities, the fact remains that a small, blurred foveal stimulus is sufficient to promote rapid and marked adaptation of the VOR.

We proposed at the beginning of this paper that the goal of compensatory eye movements might be to establish nonzero gaze velocities (retinal image motions) that are optimal for vision. We have added plausibility to this idea by demonstrating that the compensatory subsystems rapidly adapt to some nonzero value of gaze velocity. We now must study individual visual capacities with known gaze

‡Note added in proof: We found in subsequent research that rapid adaptation occurs when clear vision is preserved.

velocities and show that the gaze velocities preferred by an individual are optimal for that individual's visual requirements.

ACKNOWLEDGMENTS

We thank W. Cushman, B. Geisert, E. Kowler, and J. Z. Levinson for serving as subjects, making valuable suggestions, and providing technical assistance. We also thank G. Davis, M. Fritz, J. Giganti, and I. Nicholson for technical assistance.

REFERENCES

1. MILES, F. A. & B. B. EICHMAY. 1980. Long-term adaptive changes in primate vestibulo-ocular reflex. I. Behavioral observations. *J. Neurophysiol.* **43**: 1406-1425.
2. WILSON, V. J. & G. MELVILL JONES. 1979. *Mammalian Vestibular Physiology*: 287. Plenum Press, New York, N.Y.
3. STEINMAN, R. M. & H. COLLEWIJN. 1980. Binocular retinal image motion during active head rotation. *Vision Res.* **20**: 415-429.
4. HARTMANN, R. & R. KLINKE. 1976. A method for measuring the angle of rotation (movements of body, head, eye in human subjects and experimental animals). *Pfluegers Arch. Gesamte Physiol. Menschen Tiere* **362**: R 52.
5. COLLEWIJN, H. 1977. Eye and head movements in freely moving rabbits. *J. Physiol.* **266**: 471-498.
6. RUBENS, S. R. 1945. Cube-surface coil for producing a uniform magnetic field. *Rev. Sci. Instrum.* **16**: 243-245.
7. COLLEWIJN, H., F. VAN DER MARK & T. C. JANSEN. 1975. Precise recording of human eye movements. *Vision Res.* **15**: 447-450.
8. GONSHOR, A. & G. MELVILL JONES. 1976. Short-term adaptive changes in the human vestibulo-ocular reflex arc. *J. Physiol. London* **256**: 361-379.
9. SKAVENSKI, A. A., R. HANSEN, R. M. STEINMAN & B. J. WINTERSON. 1979. Quality of retinal image stabilization during small natural and artificial body rotations in man. *Vision Res.* **19**: 675-683.
10. WINTERSON, B. J., H. COLLEWIJN & R. M. STEINMAN. 1979. Compensatory eye movements to miniature rotations in the rabbit: implications for retinal image stability. *Vision Res.* **19**: 1155-1159.
11. BARR, C. C., L. W. SCHULTHEIS & D. A. ROBINSON. 1976. Voluntary, non-visual control of the human vestibuloocular reflex. *Acta Oto-Laryngol.* **81**: 365-375.
12. GAUTHIER, G. M. & D. A. ROBINSON. 1975. Adaptation of the human vestibulo-ocular reflex to magnifying lenses. *Brain Res.* **82**: 331-335.
13. GONSHOR, A. & G. MELVILL JONES. 1976. Extreme vestibulo-ocular adaptation induced by prolonged optical reversal of vision. *J. Physiol. London* **256**: 381-414.
14. MILES, F. A. & J. H. FULLER. 1974. Adaptive plasticity in the vestibulo-ocular responses of the rhesus monkey. *Brain Res.* **80**: 512-516.

VESTIBULAR HABITUATION IN MAN AND MONKEY DURING SINUSOIDAL ROTATION*

J. Jäger and V. Henn†

Department of Neurology
University Hospital
University of Zurich
CH-8091 Zurich, Switzerland

INTRODUCTION

Sailors or airplane pilots, who through their professions are regularly exposed to vestibular stimuli or unusual combinations of visual-vestibular stimulation, have nystagmus on the Bárány rotatory chair in the dark that is of shorter than average duration. In these professionals, initial side effects also soon subside when exposed to unexpected combinations of visual-vestibular interaction that otherwise commonly lead to motion sickness.¹ Until about 1920, a "good" vestibular response was considered to be nystagmus of long duration. Therefore, many of the most experienced airplane pilots of the United States Air Force were barred from further flying after vestibular testing on rotatory chairs had been introduced. This led to a prolonged controversy, more studies were performed, and the pilots were finally reinstituted in their jobs. The fact that a short nystagmus duration after repeated exposure to vestibular stimulation is based on habituation is therefore not only acknowledged scientifically but also accepted legally.^{7,15}

In all studies, habituation has been achieved by repeated exposures to stimuli that induce vestibular nystagmus, which include pulses of acceleration and caloric irrigation of the external ear. Habituation seems to be direction specific,¹² and transfer from one mode of stimulation to any other is limited (for review, see Reference 6). Pulses of angular acceleration in the dark, i.e., velocity steps, regularly lead to a shortening of nystagmus. Mathematically, a velocity step can be thought of as the sum of sine waves of different frequencies. Gonshor and Melvill Jones have shown for humans, and Kleinschmidt and Collewyn for rabbits, that continued sinusoidal rotation at a frequency of 0.16 Hz does not lead to habituation.^{9,13} Therefore the question remained whether only combinations of frequencies like velocity steps are effective, or whether single frequencies also are effective when applied separately.

We will address ourselves to the following questions. What stimuli lead to habituation? How can it be measured? How does it relate to unit activity in the neurons along the vestibulo-ocular reflex arc (VOR)? How can animal experiments be related to human physiology and the subjective sensation of motion?

METHODS

Monkeys (*Macaca mulatta*) were prepared chronically with implantation of eye electrodes, a microdrive receptacle for single-unit recordings, and bolts for

*Supported by a grant from the Swiss National Foundation for Scientific Research 3.343-0.78.

†To whom correspondence should be addressed.

head fixation. Animals were seated on a servo-controlled turntable. They received amphetamine (0.5 mg/kg intramuscularly) to maintain a constant level of alertness. All relevant data were stored on FM tape and written out on an oscillograph, from which measurements were made.

In human subjects, eye movements were recorded with d.c. oculography. Subjective motion sensation was indicated by turning a handle fixed to the shaft of a potentiometer. One subjective 360° turn was indicated by one full turn of the handle. Data processing was the same as for monkeys.

Time constants of nystagmus, motion sensation, or single-unit data were measured from velocity steps or the response to sinusoidal rotation at different frequencies. The decline time constant after pulses of angular acceleration was determined as the time elapsed between maximum response at the end of acceleration and the time the response had declined to $1/e$ (37%) of the initial value. Time constants also were determined from frequency response curves: the two frequencies that lay below or above the point of 45° phase advance were determined, and the curve was extrapolated to the value at 45°. The frequency at this value was then taken to calculate the time constant.⁸

RESULTS

Habituation in the Monkey

After it had been shown that pulses of angular acceleration lead to habituation (review in Reference 6), the question remained as to whether rotation with a sinusoidal velocity profile is equally effective. In a systematic study, monkeys were rotated with different sinusoidal frequencies.¹¹ Habituation always occurred if the stimulus frequency was below 0.1 Hz. An example is shown in FIGURE 1. Above, two selected frequencies of rotation in the naive animal. Below, the same two frequencies tested again after the monkey was habituated. There is an increase in phase angle between stimulus and nystagmus slow-phase velocity, and a concomitant decrease in gain. This monkey was rotated at different frequencies between 0.002 and 0.5 Hz in 17 sessions, each lasting about 60 minutes. This led to a shift of the frequency response curve, as shown in FIGURE 2. Initially, the point of 45° phase advance occurred at a frequency of about 0.0045 Hz, corresponding to a time constant of 36 seconds. After the habituation, the point of 45° phase advance shifted to a frequency of 0.015 Hz. This corresponds to a time constant of less than 11 seconds or a reduction to less than one-third of the initial value.

The curves in FIGURE 2 show the greatest divergence in a medium-frequency range between 0.005 and 0.05 Hz. At frequencies above or below, the curves converge. Specifically, neither phase angles nor gain changes at rotational frequencies above 0.1 Hz. This confirms earlier studies by Gonshor and Melvill Jones and Kleinschmidt and Collewyn,^{9,13} and can be generalized: habituation only occurred with a stimulus frequency at which the naive animal already had exhibited some phase advance. This phase angle then increased during habituation. Extended rotation with only a single medium frequency nevertheless led to a shift of the whole frequency response curve, similar to that shown in FIGURE 2. Even if a frequency was chosen at which the naive animal already had exhibited a phase advance of 90°, habituation occurred, with a shift of the frequency response curve, although no great change could be observed at the stimulus frequency that was already in phase with acceleration. An example is shown in

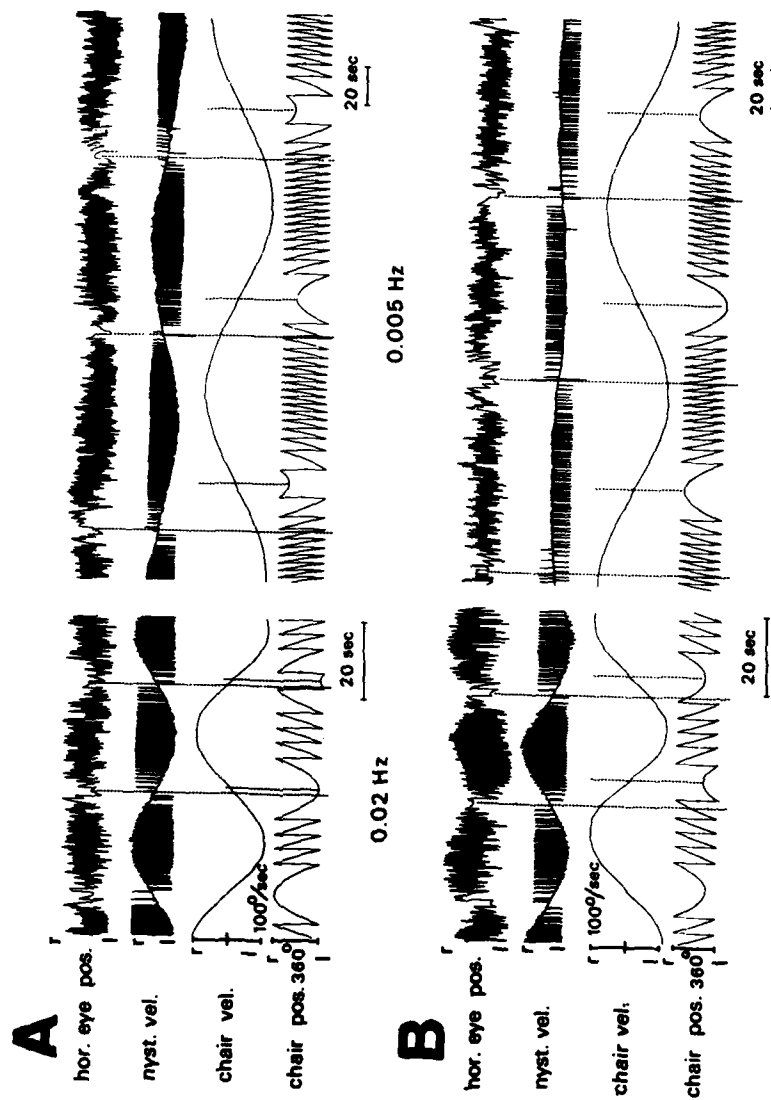


FIGURE 1. Increase in phase angle and decrease in gain during sinusoidal rotation of a monkey in the dark. From above: horizontal eye position, horizontal eye velocity, turntable velocity, turntable position. A, measurements from the naive monkey. B, the same stimulus frequencies in the same, habituated monkey. The phase advance at 0.02 Hz in the habituated animal is about 40° , a value that in the naive animal occurred at a frequency of 0.005 Hz (A).

FIGURE 3. This animal was rotated at a frequency of 0.002 Hz for 1 hour eight times over a period of 35 days. Before the first trial and after the last one, a pulse of acceleration was given. Time constants could then be measured as response decline. Time constants measured in this way, or calculated from frequency response curves, correspond well with each other. The insert in FIGURE 3 shows the reduction of the time constant over several sessions. The recovery from one session to the next is very little, and differentiates habituation from fatigue.

These results show that prolonged rotation with a sinusoidal velocity profile leads to habituation. Acquisition is fast and can occur over half an hour. Retention, once the time constant has been reduced to values of less than 15 seconds, is long—in the range of months. The time constant has been found to be a good and sufficient characterization of the state of habituation, since different modes of measurement (sinusoidal rotation or step responses) can be compared.

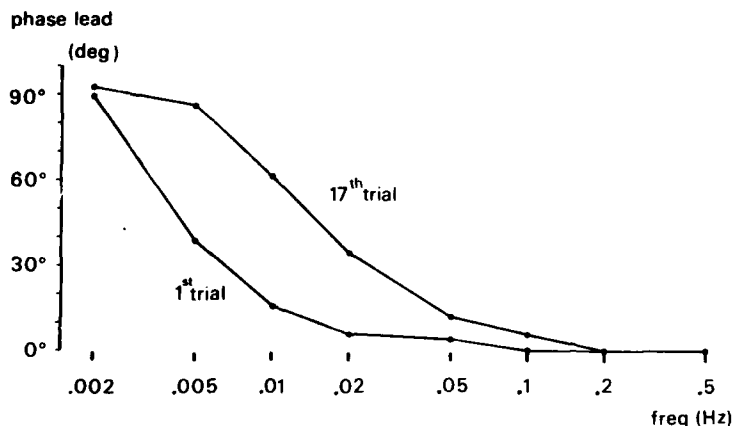


FIGURE 2. Frequency response curve from one animal before and after 17 sessions of sinusoidal rotation at the frequencies indicated on the abscissa. The greatest change in phase angle occurs at frequencies between 0.005 and 0.02 Hz. The gain shows a corresponding decrease. At frequencies above 0.1 Hz, no change is evident.

Habituation as Reflected in Neuronal Activity along the VOR Pathway

Fernández and Goldberg recorded from single fibers of the vestibular nerve in anesthetized squirrel monkeys.⁸ Time constants of neuronal activity were 6 seconds on average, with little variation. Büttner and Waespe recorded from vestibular nerve fibers in alert rhesus monkeys, specifically comparing time constants of neuronal activity with the simultaneously measured nystagmus, after pulses of acceleration.⁵ Fibers always had a time constant of about 6 seconds, while nystagmus time constants were always longer, varying between 8 and 24 seconds in their sample.

Activity of neurons in the vestibular nuclei always shows a close correspondence to nystagmus velocity during angular acceleration in the dark. Experimentally naive monkeys have long time constants both for nystagmus and for neuronal activity in the vestibular nuclei.³ In habituated animals, the time

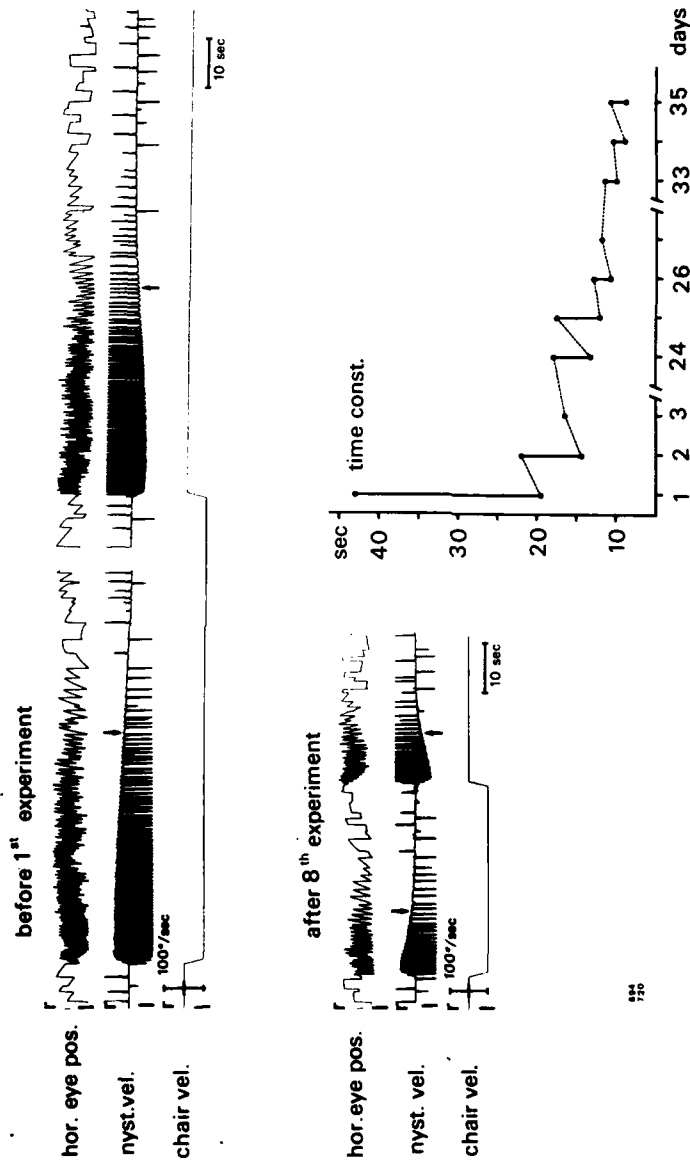


FIGURE 3. Reduction of time constant in a monkey after eight 90-minute periods of rotation at a frequency of 0.002 Hz. The time constant (arrow) is reduced from a value of 43 seconds to about 10 seconds. The insert gives the course of the change. Once the time constant has been reduced, there is little recovery even over periods of three weeks (between second and third sessions on days 2 and 24).

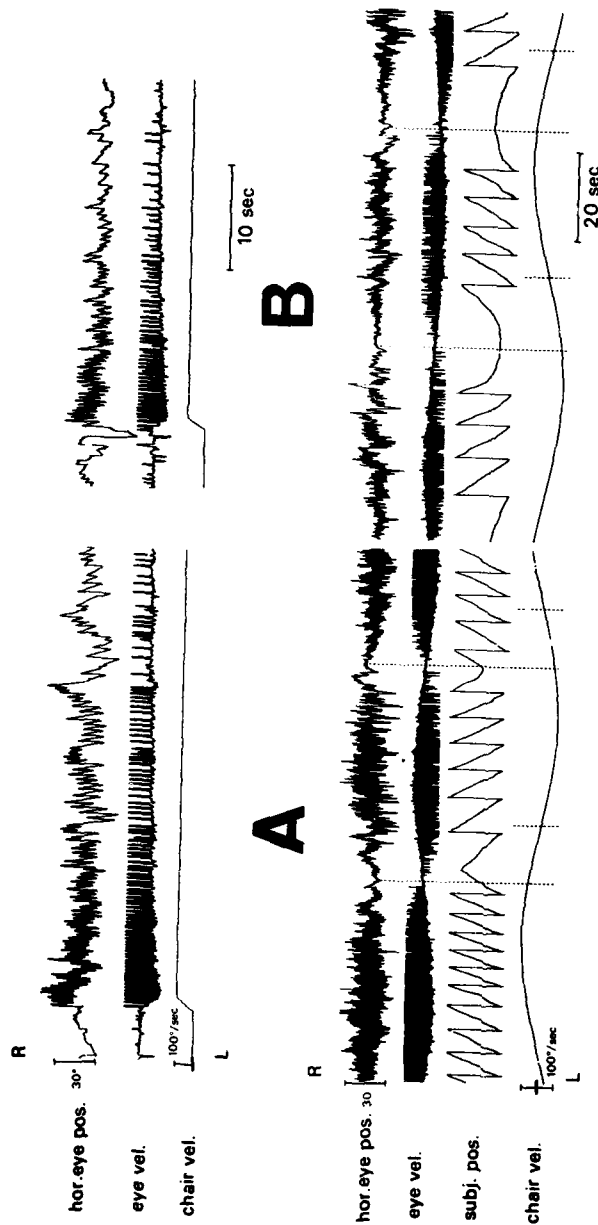


FIGURE 4. Habituation of vestibular nystagmus and motion sensation in a human subject. Above: a velocity step in the dark before (A) and after (B) 77 minutes of continued rotation at a frequency of 0.01 Hz. Below: the second and the last cycle of the sinusoidal rotation. The shortening of the time constant is seen as an increase in phase angle for both nystagmus and motion sensation, as well as a decrease in gain.

constants for both nystagmus and unit activity are similar and short. This places the process of habituation beyond the first-order neuron. How it is achieved and what anatomical structures are involved are not known. However, the effect of habituation can be measured in all second-order neurons of the vestibular nuclei.

Habituation in Humans

Stipulated by the results from animal experiments, a similar series was performed in humans. FIGURE 4 shows the response from one subject before (A) and after (B) 77 minutes of continued rotation with a sinusoidal velocity profile.

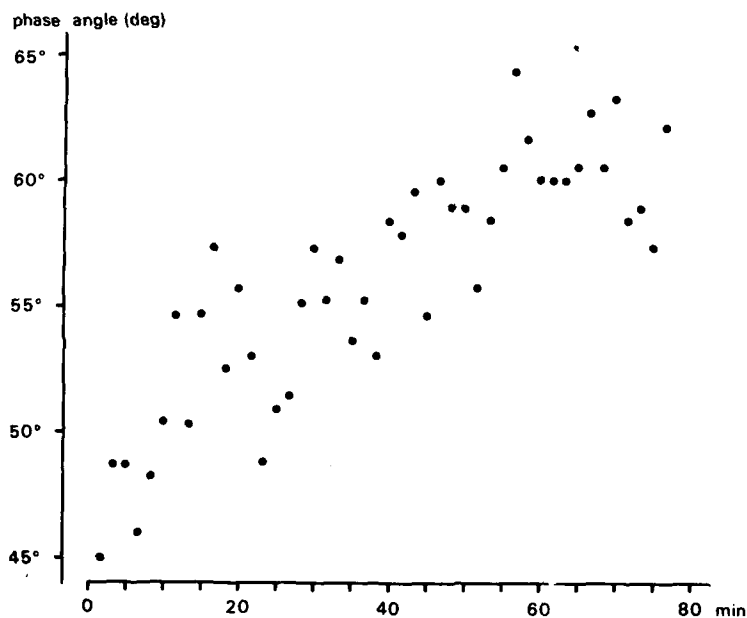


FIGURE 5. Increase in phase angle of nystagmus velocity for one human subject during continued rotation at a frequency of 0.01 Hz. During the first cycle, the phase angle is 45°. It steadily increases until it reaches a plateau at about 60° after one hour rotation.

In the upper part of this figure is the response to a velocity step. The initial decay time constant of nystagmus was 23 seconds. After 77 minutes rotation, it had declined to a value of 13 seconds. In the lower part, the 2nd cycle is shown along with the 46th cycle, which completes this session of continued rotation at a frequency of 0.01 Hz. There is an increase in phase angle together with a decrease in gain. Subjective velocity, continuously indicated as subjective position, shows a similar change. Acquisition of habituation was as fast as in the monkey. FIGURE 5 shows the phase angles for consecutive individual cycles of rotation at the subject's first session. Phase angles continuously increase and then

tend to level off at a plateau. The gain exhibits a corresponding decrease over the same time. Retention is also similar to that seen in monkeys. Once the time constant had been reduced to a value below 15 seconds, it tended to stay at that value over periods of at least several weeks.

In an initial series, 10 human subjects were continuously rotated at a frequency of 0.01 Hz only. This was carried out using different protocols. Single rotation periods were systematically varied between 30 and 80 minutes repeated daily over periods of five days. Results were essentially the same, independent of protocol details. In most cases, the initial time constant, which ranged between 15 and 30 seconds, was reduced to values between 8 and 15 seconds.

This shows that in humans, as in monkeys, rotation with a single frequency can lead to habituation if that frequency is smaller than 0.1 Hz. In each case, the entire frequency curve is shifted as the result of habituation.

Subjective velocity estimation changes in parallel to the nystagmus. Velocity estimation tends to have a slightly higher threshold and an even shorter time constant. Signs of motion sickness were not observed. On the contrary, subjects usually and spontaneously reported that they enjoyed the rotation with a sinusoidal velocity profile. Some of the subjects in other tests of visual-vestibular interaction initially complained about motion sickness, which often forced such experiments to be terminated. All subjects, after the habituation process, had a clearly raised threshold for motion sickness.

CONCLUSIONS

Experiments on vestibular habituation performed in monkeys as well as in humans led to essentially similar results. Prolonged rotation with a sinusoidal velocity profile is a powerful stimulus that leads to habituation if a stimulus frequency smaller than 0.1 Hz is chosen. Similar results were obtained by Blair and Gavin.² The full transfer function of nystagmus for naive and habituated monkeys has been described by Buettner *et al.*⁴ Even if only a single frequency was applied, the whole frequency response curve shifted toward values of greater phase angles. The state of habituation can be characterized by a single number, the value of the dominant time constant. It can be reduced to values smaller than 10 seconds, but probably not below the time constant of activity in the vestibular nerve, which is 6 seconds in the monkey.

In humans, nystagmus and subjective motion sensation were measured. Both parameters had similar values, with motion sensation usually having a slightly higher threshold and a shorter time constant.

In monkeys, nystagmus and single units in the vestibular nuclei were recorded. Time constants for both were similar and always varied together. This places the process of habituation into central neural structures. The earlier studies that link nystagmus duration to peripheral parameters like cupula stiffness need therefore to be reinterpreted.¹⁰ On more theoretical grounds, Mach has already stipulated that nystagmus duration cannot be equated with actual cupula motion.¹⁴

Most forms of vestibular stimulation in the dark lead to a shortening of time constants. No stimulus condition has been worked out yet that would lead to a lengthening of the vestibular time constant. This has to be taken into account when patients are repeatedly tested. One then has to differentiate between the physiological effects of habituation and an altered response based on pathology. Our experimental results imply that there is no single normal value for the

nystagmus time constant. Instead, there is a wide range between at least 10-30 seconds, all of which can be found in normal, healthy subjects depending on their current state of habituation. If average values were taken from a large population, a single value with a rather small standard deviation might emerge. However, this would be an artifact, caused by our rather similar sedentary life-styles.

Might there be an advantage for humans to have a short vestibular time constant? Preliminary experiments have shown that humans might be less prone to the symptoms of motion sickness. Habituation with sinusoidal velocity profiles were uniformly reported as a pleasant experience. This stands in contrast to the experience with the usual programs that are aimed at reducing motion sickness. It remains to be investigated whether habituation with sinusoidal stimulation would lead to a measurable relief from motion sickness, or even from pathological dizziness in patients.

SUMMARY

Habituation of the vestibular system by repeated steps of angular velocity leads to a shortening of nystagmus. These steps can be broken down into different frequency sinusoids. High-frequency sinusoidal rotation (above 0.1 Hz) generally was found to be ineffective, while low-frequency stimulation (0.0015-0.05 Hz) led to a dramatic shortening of time constants after only a few cycles of stimulation. In the alert monkey, time constants of vestibular nystagmus and single units, recorded from the vestibular nuclei, are always similar and covary together. Experiments in humans, with measurement of nystagmus and subjective velocity sensation, suggest similar processes for habituation.

REFERENCES

1. ABELS, H. 1906. Ueber Nachempfindungen im Gebiete des kinästhetischen und statischen Sinnes. *Z. Psychol.* **43**: 268-422.
2. BLAIR, S. & M. GAVIN. 1979. Response of the vestibulo-ocular reflex to differing programs of acceleration. *Invest. Ophthalmol.* **18**: 1086-1090.
3. BUETTNER, U. W., U. BÜTTNER & V. HENN. 1978. Transfer characteristics of neurons in vestibular nuclei of the alert monkey. *J. Neurophysiol.* **41**: 1614-1628.
4. BUETTNER, U. W., V. HENN & L. R. YOUNG. 1981. Frequency response of the vestibulo-ocular reflex (VOR) in the monkey. *Aviat. Space Environ. Med.* **52**: 73-77.
5. BÜTTNER, U. & W. WAESPE. 1981. Vestibular nerve activity in the alert monkey during vestibular and optokinetic nystagmus. *Exp. Brain Res.* **41**: 310-315.
6. COLLINS, W. E. 1974. Habituation of vestibular responses with and without visual stimulation. In *Handbook of Sensory Physiology*. H. H. Kornhuber, Ed. **612**: 369-388. Springer Verlag, Berlin, Heidelberg & New York.
7. DUNLAP, K. 1919. The nystagmus test and practice. *J. Am. Med. Assoc.* **73**: 54-55.
8. FERNÁNDEZ, C. & J. M. GOLDBERG. 1971. Physiology of peripheral neurons innervating semicircular canals of the squirrel monkey. II. Response to sinusoidal stimulation and dynamics of peripheral vestibular system. *J. Neurophysiol.* **34**: 661-675.
9. GONSHOR, A. & G. MELVILL JONES. 1969. Investigation of habituation to rotational stimulation within the range of natural movement. In *Proceedings, Aerospace Medicine Association Meeting*, San Francisco, Calif.: 94-95.
10. GROEN, J. J. 1957. Cupulometry. *Laryngoscope* **67**: 894-905.
11. JÄGER, J. & V. HENN. 1981. Habituation of the vestibulo-ocular reflex (VOR) in the monkey during sinusoidal rotation in the dark. *Exp. Brain Res.* **41**: 108-114.

12. JEANNEROD, M., G. CLEMENT, J. H. COURJON & R. SCHMID. 1981. Unilateral habituation of vestibulo-ocular responses in the cat. *Ann. N.Y. Acad. Sci.* (This volume.)
13. KLEINSCHMIDT, H. J. & H. COLLEWIJN. 1975. A search for habituation of vestibulo-ocular reactions to rotatory and linear sinusoidal acceleration in the rabbit. *Exp. Neurol.* 47: 257-267.
14. MACH, E. 1875. *Grundlinien der Lehre von den Bewegungsempfindungen*. W. Engelmann. Leipzig, Germany. (Also 1967. Bonset, Amsterdam, the Netherlands.)
15. MOWRER, O. H. 1934. The modification of vestibular nystagmus by means of repeated elicitation. *Comp. Psychol. Monogr.* 9: 1-48.

UNILATERAL HABITUATION OF VESTIBULO-OCULAR RESPONSES IN THE CAT

M. Jeannerod, G. Clement, and J. H. Courjon
Laboratory of Experimental Neuropsychology
INSERM U94
69500 Bron, France

R. Schmid
Institute of Computer and Systems Science
University of Pavia
I-27100 Pavia, Italy

INTRODUCTION

Vestibular habituation is known to be direction specific. When the animal is submitted to repeated unidirectional accelerations or unilateral calorization (vestibular training), the vestibulo-ocular reflex (VOR) decreases in one direction only.¹⁻⁴

Unidirectional VOR decline also can be obtained by repeatedly presenting a stationary subject with large visual scenes moving in one direction (optokinetic training). In that case, the progressive VOR decrease occurs for responses to subject's rotations in the direction opposite to that of the previous pure visual stimulation.⁵⁻⁸

Based on these results, Young and Henn concluded that the necessary condition for vestibular habituation to take place is the generation of a repeated and consistent motion sensation,⁷ which actually can be produced by either vestibular or optokinetic stimulation.⁹ However, whether VOR decline during vestibular habituation induced by repeated vestibular and visual stimulations relies upon a single mechanism (and eventually upon a single neural structure) has not yet been established. A comparative description of the two phenomena is needed to answer this question. In the present study, unilateral VOR changes have been reinvestigated in cats exposed to vestibular and/or optokinetic training. The transfer of vestibular habituation acquired with one type of stimulation to oculomotor responses induced by the other type also has been examined.

METHODS

Adult cats were implanted under Nembutal anesthesia (35 mg/kg, intraperitoneally) with AgCl electrodes for recording eye movements in the horizontal plane. A head-fixation device also was sealed to the skull.

Experiments were not begun until the fourth postoperative day. Each animal underwent an experimental protocol that involved preexposure testing, exposure to vestibular or optokinetic training, and postexposure testing.

During testing sessions as well as during training sessions, animals were placed in a hammock, with their head secured at the center of rotation of a horizontal servo-controlled turntable. The turntable was surrounded by a cylindrical drum, 1 m in diameter, the inner wall of which was covered with

alternating black and white vertical stripes (10° of visual angle each). The drum could be maintained in light or in darkness, and could be rotated independently from the turntable or mechanically coupled to it.

Eye position was monitored on a polygraph and stored on magnetic tape.

Preexposure Testing

Both vestibular nystagmus (VN) and optokinetic nystagmus (OKN) were tested.

VN was tested by using different profiles of turntable velocity. Namely, a "ramp-step" profile first was applied in each direction, clockwise (CW) and counterclockwise (CCW). Such a velocity profile consisted of a constant subthreshold ramp acceleration ($0.18\text{--}0.22^\circ/\text{second}^2$) up to a velocity of $80^\circ/\text{second}$, followed by a step change reducing velocity from $80^\circ/\text{second}$ down to $0^\circ/\text{second}$ in about 200 mseconds. A subthreshold value of acceleration was determined previously for each cat, by the lack of vestibular nystagmus during the ramp.

Sinusoidal oscillations with a peak velocity of $80^\circ/\text{second}$ then were applied at frequencies of 0.03, 0.05, 0.07, and 0.1 Hz. Corresponding peak-to-peak amplitudes were 849, 509, 364, and 255° respectively.

OKN was tested by rotating the drum around the stationary animal at constant velocities of 15, 30, and $45^\circ/\text{second}$ in each direction.

Cats with a clear asymmetry in either VN or OKN during preexposure testing were discarded. Seven cats were retained for the following experiments.

Unidirectional Vestibular Training

During each session, cats were submitted to a series of eight ramp steps in the same direction. Each ramp started one minute after the occurrence of the previous step. Sessions were repeated twice a day (morning and afternoon) for five consecutive days unless VN had almost disappeared earlier. Between sessions, cats were kept in a normal environment.

The direction of vestibular training (CW or CCW) will be defined as the direction opposite to that of table rotation before the stop. By this definition, each stop of a CW training produces an excitation of the right labyrinth, and gives rise to a vestibular nystagmus with the slow phase to the left. In these experiments, two cats were submitted to a CW training and two others to a CCW training.

Unidirectional Optokinetic Training

During each session, cats were submitted to a constant-velocity ($30^\circ/\text{second}$) optokinetic stimulation in one direction. Each session lasted 30 minutes. Sessions were repeated twice a day for four days. Between sessions, animals were kept in the dark.

The direction of optokinetic training will be defined as the direction of drum rotation during the training sessions. By this definition, during a CW training the slow phase of OKN is directed to the right. In these experiments, one cat was submitted to a CW training and two cats to a CCW training.

Postexposure Testing

For six cats, postexposure testing started immediately after the end of the last training session and consisted of the same sequence of stimulation as that used during preexposure testing. In one of these animals, previously submitted to vestibular training, testing was repeated over time up to 10 days after the end of training in order to follow recovery from habituation.

The seventh cat was submitted to optokinetic training and tested at the end of each session by the use of only sinusoidal vestibular stimulations.

Data Processing

VN was analyzed by constructing manually the slow cumulative eye position (SCEP).¹⁰ In the case of step responses, the parameters C_m (peak value of SCEP) and t_o (time to SCEP peak) were computed (see Reference 11 for a more detailed definition of these parameters). In the case of responses to sinusoidal oscillations, the average peak-to-peak values of SCEP during CW and CCW rotations, $C_m(R)$ and $C_m(L)$, were computed. The ratio $C_m(R)/C_m(L)$ gives a measure of VOR symmetry. Since no calibration of eye movements was available, C_m , $C_m(R)$, and $C_m(L)$ were expressed in arbitrary units.

The phase shift between the peaks of SCEP and the corresponding peaks of table position in response to sinusoidal oscillations were measured and averaged.

Finally, SCEP also was constructed for optokinetic responses, and its slope representing the average value of nystagmus [slow-phase velocity (SPV)] was measured. The ratio between average SPV (in arbitrary units) and the optokinetic stimulus velocity was assumed to represent the gain of the optokinetic reflex.

RESULTS AND COMMENTS

Vestibular Training

When unidirectional steps were repeated, a marked variation of VOR was observed. A typical example of a habituated response recorded at the end of a CW vestibular training is shown in FIGURE 1. The CW response is reduced to only a few beats occurring during the primary phase of nystagmus, which lasts less than 10 seconds. Secondary nystagmus is almost absent. No spontaneous nystagmus could be observed at any stage of habituation.

This process can be followed in a quantitative way by plotting the value of C_m (in percent with respect to the value obtained in the first response) and of t_o , for the first and the last response of each training session, for successive sessions. Both C_m and t_o decreased within each session (acquisition) and across sessions (retention) (FIGURE 2). For the four cats examined, C_m decreased down to a value ranging between 50% and 10% of the initial value; t_o decreased down to 46%–27% of its initial value, which ranged between 20 and 30 seconds. The asymmetry of the oculomotor responses at the end of unidirectional vestibular training could be appreciated clearly during postexposure testing. A head-velocity step in the direction opposite to that of training would produce a response (record D in FIGURE 1) quite comparable to that recorded in the

preexposure testing (record B in FIGURE 1) for the same direction. Quantitatively, C_m and t_0 had not varied by more than about $\pm 10\%$ (FIGURE 2).

Unilaterality of habituation also was apparent in responses to sinusoidal stimulation (i.e., not used during training). FIGURE 3 gives the results of sinusoidal tests performed on a cat before and after a CCW vestibular training. The values of $C_m(R)$ and $C_m(L)$ in preexposure responses are given in arbitrary units by assuming the value of $C_m(L)$ at 0.03 Hz to be equal to 1. Note that there is a decrease of $C_m(R)$ and $C_m(L)$ with the frequency, due to the fact that the same peak stimulus velocity (and not the same peak amplitude) was maintained throughout all frequencies. In order to appreciate the amount of $C_m(R)$ and $C_m(L)$ changes due to habituation and their possible frequency dependence, the values of $C_m(R)$ and $C_m(L)$ in postexposure tests are given in percent of the corresponding preexposure values at the same frequency. It can be noted easily that $C_m(R)$ (CW rotation) did not change from preexposure to postexposure tests. On the contrary, $C_m(L)$ was reduced to about 60% at all frequencies.

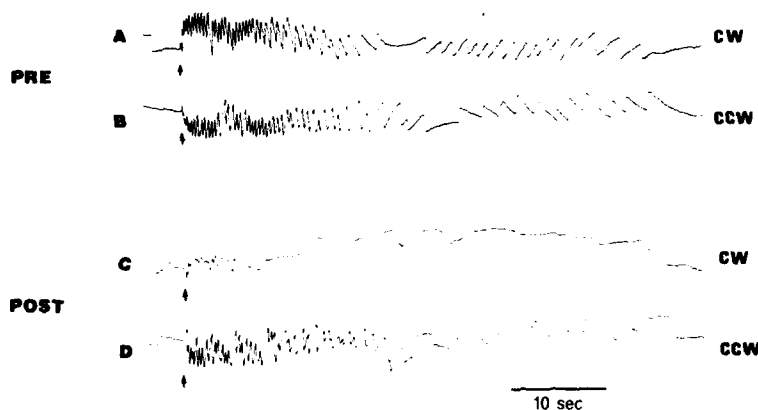


FIGURE 1. Clockwise (CW) and counterclockwise (CCW) responses to velocity steps before and after a CW vestibular training. After training, the CW response is virtually abolished, whereas the CCW response is unchanged.

A strong asymmetry also occurred in the phase shifts of postexposure responses. An increase of the phase lead during rotations toward the "trained" labyrinth and a decrease during rotations in the opposite direction were observed in one cat (FIGURE 3). The remaining three cats presented a large phase-lead increase during rotations toward the "trained" labyrinth, but no significant variations of phase lead during rotations in the opposite direction.

Recovery from habituation was tested in one animal with one velocity step applied in both directions every 2 days up to the 10th day following the end of vestibular training. C_m was found to increase slowly from 40% up to 65% of its initial value. Hence a significant retention still was present after 10 days.

The possibility of obtaining unilateral habituation by a unidirectional vestibular training,^{1,3} as confirmed by the present results, excludes a role of unspecific factors, such as changes in the state of vigilance, in producing the observed

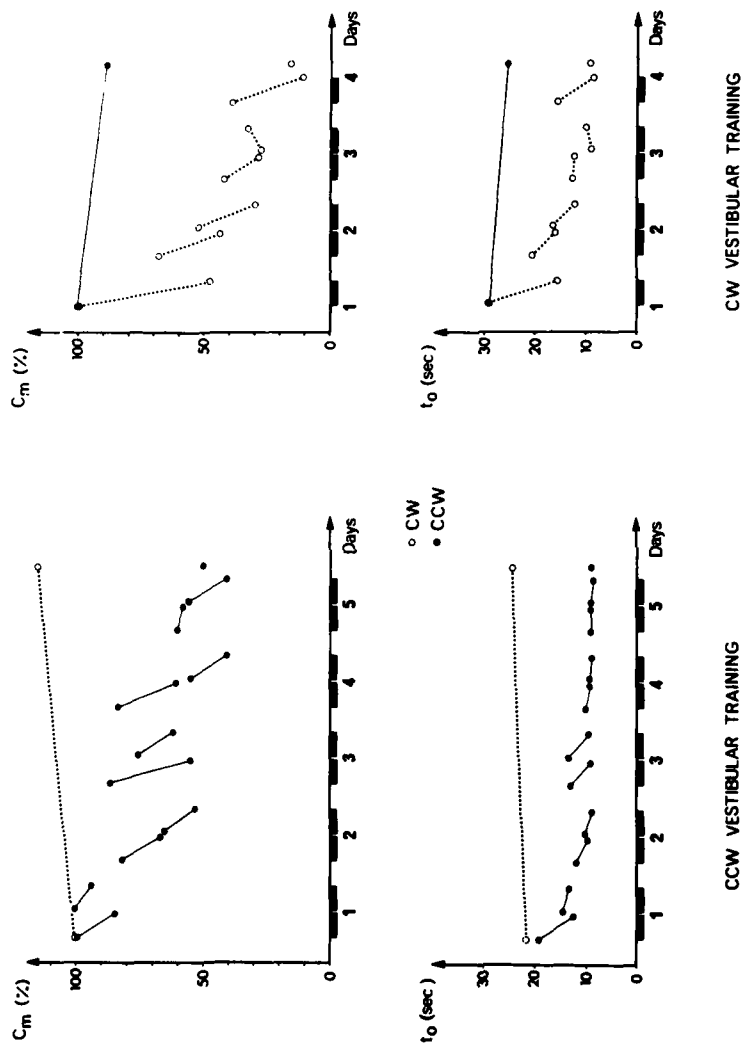


FIGURE 2. Time course of the parameters C_m (peak amplitude of the slow cumulative eye position) and t_0 (time to peak) in responses to velocity steps during a CCW (diagrams on the left) and during a CW (diagrams on the right) vestibular training. C_m is given in percent with respect to its initial value, t_0 in seconds. For the "trained" side, values of C_m and t_0 are given for the first and the last response of each session, and for the step response in the postexposure testing (last value on the abscissae). For the "untrained" side, values of C_m and t_0 are given for the step responses in the preexposure and in the postexposure tests.

modifications of VOR. Rather, we had suggested in a previous paper dealing with bilateral habituation that habituation is due to a selective mechanism that modifies not only the gain but also the dynamic characteristics of the vestibulo-ocular reflex.¹¹

The results of the present experiments tend to confirm our previous suggestion. The unilateral increase in phase lead observed in the responses to postexposure sinusoidal oscillations and the unilateral decrease of t_0 in responses to

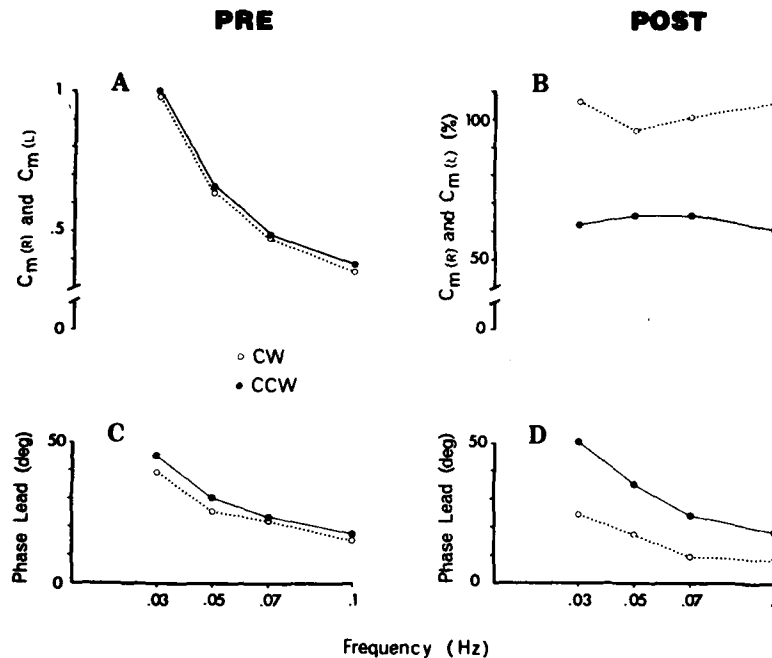


FIGURE 3. CCW vestibular training. A: amplitude relationships in the responses to sinusoidal oscillations before a CCW vestibular training. $C_m(R)$ and $C_m(L)$ are given in arbitrary units by assuming the peak-to-peak value equal to 1 during CCW rotation at 0.03 Hz. The small differences between $C_m(R)$ and $C_m(L)$ indicate the high degree of symmetry of the responses. B: amplitude relationships in the responses to sinusoidal oscillations after a CCW vestibular training. The values of $C_m(R)$ and $C_m(L)$ are given in percent of the corresponding pretraining values at the same frequency. The amplitude of CCW responses is reduced to 60% independently of the frequency. C and D: phase relationships in pre- and postexposure tests, showing an increase of phase lead during rotations toward the "trained" labyrinth.

velocity steps both indicate a progressive quickening of the VOR dynamics, restricted to rotations toward the "trained" labyrinth.

The absence of spontaneous nystagmus at any stage of unilateral habituation by vestibular training, in spite of the large asymmetry in the amplitude of the vestibulo-ocular responses, shows that habituation can produce unilateral gain changes without introducing an additional imbalance between the two vestibular

pathways in the resting condition. This effect could be obtained by changing the gain of secondary vestibular neurons with no spontaneous resting discharge, such as kinetic neurons or tonic neurons with zero resting discharge.¹² A change of their gain therefore should not modify the balance of the system in the resting condition. On the other hand, when kinetic and tonic units work in parallel to produce a given response in dynamic conditions, that response will be more or less rapid depending on the relative contribution of these two types. Kinetic units, which discharge proportionately to the derivative of the input signal, tend to make the response faster and to increase its phase lag. Since VOR dynamics became progressively faster, it should be inferred that it is the relative contribution of tonic neurons with zero resting discharge that is progressively decreased.

The absence of any appreciable effect of a previous vestibular training on OKN could suggest that the parametric variations occurring during habituation take place at the peripheral level of the vestibular system. This would be in contradiction to the general belief that habituation is a central process. More likely, the open-loop gain of the optokinetic reflex is modified by the parametric variations of habituation. This modification is masked, however, by the fact that the closed-loop gain and therefore the slow-phase velocity of OKN do not vary appreciably. The closed-loop nature of the optokinetic reflex thus allows the mechanism controlling vestibular habituation to focus its action on the vestibulo-ocular reflex in keeping intact the function of the optokinetic reflex in spite of the interaction of the two systems at the level of the vestibular nuclei.¹³

Optokinetic Training

In a preliminary experiment, OKN slow-phase velocity (SPV) was measured at different times during the same session of a unidirectional optokinetic training. It was found to increase almost linearly. After 30 minutes of exposure, SPV was increased by about 30% with respect to the preexposure values for both directions of drum rotation. This effect was of short duration, since when OKN was retested after a few minutes of rest in darkness, SPV almost had returned to its preexposure value for both CW and CCW responses (FIGURE 4). This finding explains the results obtained when optokinetic training sessions were repeated (avoiding exposure to reversed optokinetic stimulation). During each session, an increase of SPV by 25% on the average was observed, although there was no significant retention of this SPV increase from one session to the next (FIGURE 5).

At the end of each session, when the light in the optokinetic drum was switched off, a marked spontaneous nystagmus in the direction opposite to the previous OKN and to the optokinetic after-nystagmus (OKAN) was recorded, which could last from several minutes to more than one hour. In fact, a similar (albeit weaker) spontaneous nystagmus also could be observed even after the short optokinetic tests (30 to 60 seconds) performed in the preexposure session. In contrast, a short reversal of the optokinetic stimulus after 30 minutes of unidirectional optokinetic training, as tested in one animal, prevented spontaneous nystagmus from appearing when the light was switched off.

During postexposure testing, OKN appeared to be symmetrical for both directions of stimulation, and the values of SPV did not differ from preexposure values. This confirms the very short-lasting nature of the SPV increase during each training session.

Postexposure testing of the vestibulo-ocular reflex was made by using both velocity steps and sinusoidal oscillations. The value of C_m in the step response

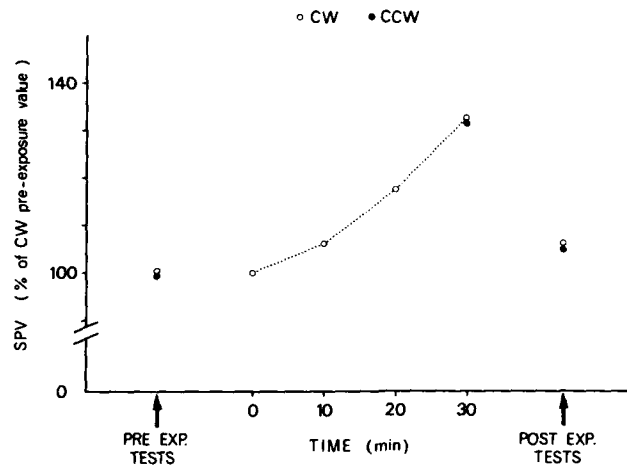


FIGURE 4. CW optokinetic stimulation. Time course of OKN slow-phase velocity (SPV) during a prolonged CW optokinetic stimulation. SPV is given in percent of the preexposure value. The increase of SPV is bilateral and of short duration, as shown by the postexposure SPV values.

induced by excitation of the labyrinth contralateral to the direction of the optokinetic training was decreased by 55% with respect to the preexposure value. In the response to the step in the opposite direction, Cm decreased by 30% only (FIGURE 6). Remarkable changes also were observed in gain and phase shift of responses to sinusoidal oscillations during rotation in the direction opposite to that of optokinetic training (FIGURE 7). The amount of these changes was frequency dependent. The gain decreased by about 50% at 0.03 Hz down to 25% at 0.1 Hz, whereas the phase lead increased by about 25° at 0.03 Hz down to 10° at 0.1 Hz. No significant gain variation and a small decrease in phase lead were observed during the periods of sinusoidal oscillation in the opposite direction. These results confirm that a unilateral vestibular habituation can be produced by

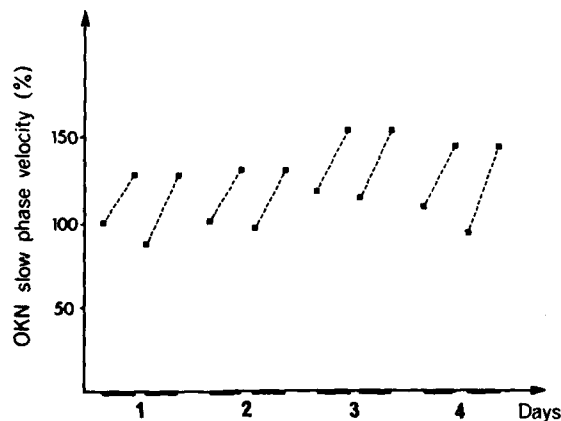


FIGURE 5. Slow-phase velocity (SPV) values at the beginning and at the end of a CCW optokinetic training. SPV is given in percent of the initial value. Note acquisition without any significant retention.

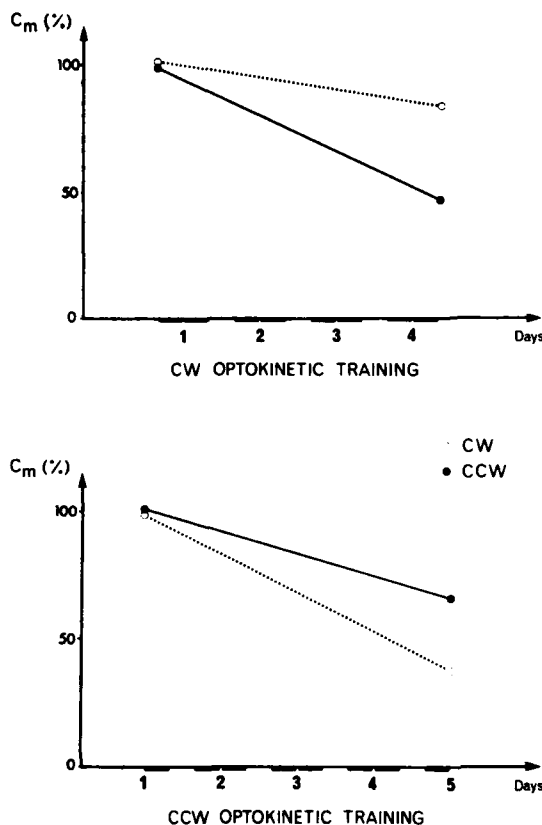


FIGURE 6. Values of C_m in responses to velocity steps before and after a CW (upper diagram) and a CCW (lower diagram) optokinetic training. There is a significant unidirectional vestibular effect with a greater depression of the side contralateral to the direction of optokinetic training.

unidirectional optokinetic training, the habituated side being that contralateral to the direction of optokinetic training.

In order to investigate the time course of acquisition and retention of vestibular habituation induced by optokinetic training, one cat was submitted to sinusoidal oscillations in the dark before and after each session of a five-day CCW optokinetic training. The results are shown in FIGURE 8, where the ratio $C_m(R)/C_m(L)$ is reported for the different frequencies examined. Already at the end of the first session, the CW gain was significantly decreased with respect to the CCW gain, and a strong directional preponderance to the left was present. This effect was observed at all frequencies, with the same frequency dependence as previously mentioned. This pattern repeated itself in each session, without indication of a significant retention from one session to the next.

Prolonged moving visual stimulation produces two distinct effects. First, it improves the optokinetic responses, an improvement that amounted to about 25% in our cats. This effect also has been observed in man.¹⁴ In terms of open-loop gain, this variation of SPV represents a tremendous change. Actually, by assuming an initial value of 0.75 of the closed-loop gain (in order to explain a 25% SPV increase), the open-loop gain should be changed from 3 to about 16.

If such a gain variation were taking place in the pathways used also by the vestibulo-ocular reflex, which is an open-loop system, an enormous increase of

the contralateral VOR should be expected. This does not actually occur, since the contralateral VOR is in fact significantly depressed after optokinetic training. Thus this result tends to exclude a gain increase within the optokinetic pathways going through the vestibular nuclei, at least through the part of these pathways shared with the vestibulo-ocular reflex. The observed improvement of OKN therefore should be due to a gain enhancement within visuomotor pathways reaching oculomotor nuclei without interacting with the vestibulo-ocular reflex.

Prolonged moving visual stimulation also produces static and dynamic VOR changes. The spontaneous nystagmus in the direction opposite to that of the previous OKN and OKAN already has been mentioned in man and monkey (Young and Henn, Brandt et al., Büttner et al., and Waespe et al.).^{6,7,15-17} These authors show that although the spontaneous nystagmus increases with the duration of the optokinetic stimulation, it also can be observed after very short exposures, as we also noticed. This spontaneous nystagmus has been considered by Waespe et al. as a central activity of counterregulation rather than as a simple reversal of OKAN related to the dynamics of the return of the optokinetic system

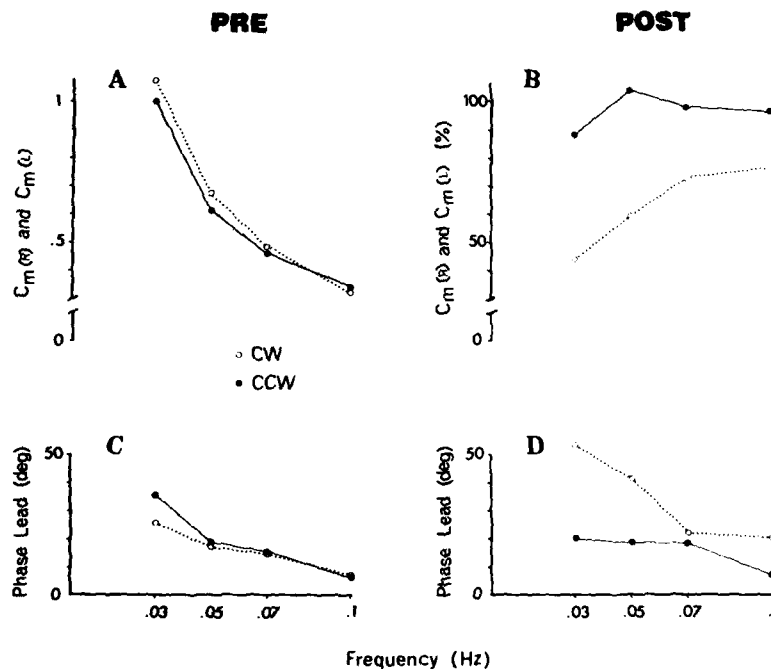


FIGURE 7. CCW optokinetic training. A: amplitude relationships in the responses to sinusoidal oscillations before a CCW optokinetic training. The values of $C_m(R)$ and $C_m(L)$ are given in arbitrary units by assuming the peak-to-peak value during CCW rotation at 0.03 Hz as equal to 1. B: amplitude relationships in the responses to sinusoidal oscillations after a CCW optokinetic training. The values of $C_m(R)$ and $C_m(L)$ are given in percent of the corresponding pretraining values at the same frequency. The amplitude of the response to CW rotation of the animal is significantly decreased. The ratio $C_m(R)/C_m(L)$ gives a measure of the asymmetry of the vestibular response due to optokinetic training. C and D: phase relationships in pre- and postexposure tests. At all frequencies there is a remarkable increase of the phase lead during rotation in the direction opposite to that of the optokinetic training.

to the resting condition.¹⁷ In other words, the appearance of a spontaneous nystagmus would not be a direct effect of the parameter modifications introduced to improve OKN, but rather a different phenomenon.

Our suggestion would be that information about subject rotation in space (as provided by both the visual and the vestibular systems) always is interpreted in a natural way as a rotation of the subject in a stationary visual surround. During a prolonged unidirectional optokinetic stimulation, due to the absence of any dynamic response from the vestibular system, the same pattern of signals as in the case of an imbalance between the resting activity of the two vestibular pathways is received centrally. As a central regulation is generated to counteract this apparent imbalance, a real imbalance actually is produced. Hence a sponta-

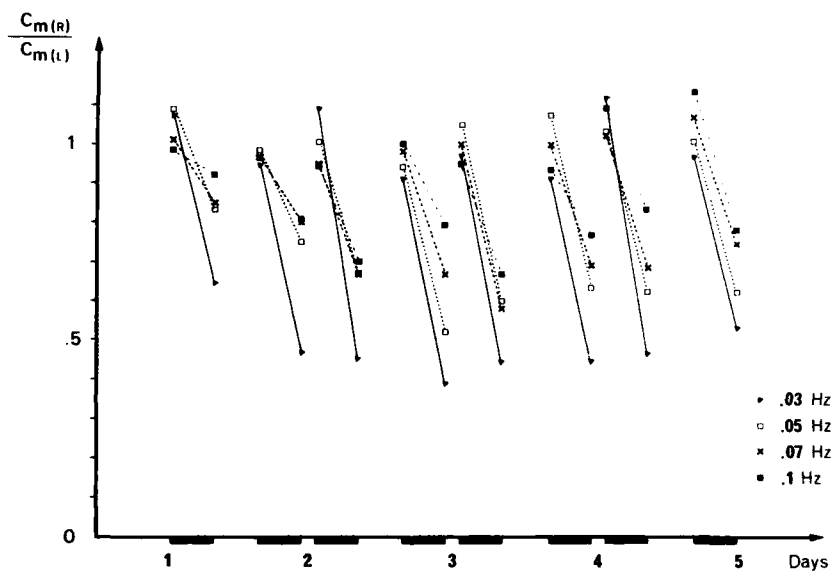


FIGURE 8. Time course of acquisition and retention of vestibular habituation induced by optokinetic training in one cat submitted to sinusoidal oscillations in the dark before and after each session of a five-day CCW optokinetic training.

neous nystagmus takes place, in the direction opposite to that of the previous optokinetic stimulation. The production by optokinetic training of a VOR directional imbalance similar to that observed after vestibular training thus could be interpreted as the dynamic aspect of the same counterregulation that, in the resting condition, gives rise to the spontaneous nystagmus.

The presence of a static VOR imbalance following optokinetic training, and not vestibular training, could account for the main difference between the effects produced by the two conditions, i.e., the different degree of retention of habituation. Following optokinetic training, it is likely that an active compensation process begins after cessation of the stimulation, in order to re-equilibrate the system and to suppress the spontaneous nystagmus. In achieving a symmetrical VOR, this process simultaneously would oppose retention.

REFERENCES

1. CRAMPTON, G. H. 1962. Directional imbalance of vestibular nystagmus in cat following repeated unidirectional angular acceleration. *Acta Oto-Laryngol. Stockh.* **55**: 41-48.
2. COLLINS, W. E. & B. P. UPDEGRAFF. 1965. A comparison of nystagmus habituation in the cat and in the dog. *Acta Oto-Laryngol. Stockh.* **62**: 19-26.
3. MERTENS, R. A. & W. E. COLLINS. 1967. Unilateral caloric habituation of nystagmus in the cat. Effects on rotational and bilateral caloric responses. *Acta Oto-Laryngol. Stockh.* **64**: 281-297.
4. COLLINS, W. E. 1974. Habituation of vestibular responses with and without visual stimulation. In *Vestibular System. Part 2. Psychophysics, Applied Aspects and General Interpretations*. H. H. Kornhuber, Ed.: 369-388. Springer-Verlag. Berlin, Federal Republic of Germany.
5. PFALTZ, C. R. & I. KATO. 1974. Vestibular habituation. Interaction of visual and vestibular stimuli. *Arch Oto-Laryngol Stockh.* **100**: 444-448.
6. YOUNG, L. R. & V. HENN. 1974. Selective habituation of vestibular nystagmus by visual stimulation. *Acta Oto-Laryngol. Stockh.* **77**: 159-166.
7. YOUNG, L. R. & V. HENN. 1976. Selective habituation of vestibular nystagmus by visual stimulation in the monkey. *Acta Oto-Laryngol. Stockh.* **82**: 165-171.
8. PFALTZ, C. R. & B. NOVAK. 1978. The effect of optokinetic training on vestibular responses. In *Vestibular Mechanisms in Health and Disease*. J. D. Hood, Ed.: 288-293. Academic Press. London, England.
9. BRANDT, TH., J. DICHGANS & E. KOENIG. 1973. Differential effects of central versus peripheral vision on egocentric and exocentric motion perception. *Exp. Brain Res.* **18**: 476-491.
10. MEIRY, J. L. 1965. The vestibular system and human dynamic space orientation. Sc. D. Thesis. Massachusetts Institute of Technology. Cambridge, Mass.
11. JEANNEROD, M., M. MAGNIN, R. SCHMID & M. STEFANELLI. 1976. Vestibular habituation to angular velocity steps in the cat. *Biol. Cybern.* **22**: 39-48.
12. SHIMAZU, H. & W. PRECHT. 1965. Tonic and kinetic responses of cat's vestibular neurons to horizontal angular acceleration. *J. Neurophysiol.* **28**: 991-1013.
13. WAESPE, W. & V. HENN. 1979. The velocity response of vestibular nucleus neurons during vestibular, visual, and combined angular acceleration. *Exp. Brain Res.* **37**: 337-347.
14. MIYOSHI, T., C. R. PFALTZ & P. PIFFKO. 1973. Effect of repetitive optokinetic stimulation upon optokinetic and vestibular responses. *Acta Oto-Laryngol. Stockh.* **75**: 259-265.
15. BRANDT, TH., J. DICHGANS & W. BÜCHELE. 1974. Motion habituation: inverted self-motion perception and optokinetic after-nystagmus. *Exp. Brain Res.* **21**: 337-352.
16. BÜTTNER, U., W. WAESPE & V. HENN. 1976. Duration and direction of optokinetic after-nystagmus as a function of stimulus exposure time in the monkey. *Arch. Psychiatr. Nervenkr.* **222**: 281-291.
17. WAESPE, W., TH. HUBER & V. HENN. 1978. Dynamic changes of optokinetic after-nystagmus caused by brief visual fixation periods in monkey and man. *Arch. Psychiatr. Nervenkr.* **226**: 1-10.

VISUALLY INDUCED SELF-MOTION SENSATION ADAPTS RAPIDLY TO LEFT-RIGHT REVERSAL OF VISION*

Charles M. Oman and Otmar L. Bock†

Man Vehicle Laboratory
Massachusetts Institute of Technology
Cambridge, Massachusetts 02139

INTRODUCTION

Both visual and vestibular motion cues are known to contribute to self-motion perception in a complementary fashion.¹ In everyday life, head rotation results in an equal and oppositely directed angular motion of the visual scene relative to the head. This association between normal active head rotation and relative scene motion is believed to account for the phenomenon of "circularvection" (CV): a pattern of stripes rotating around a stationary observer soon elicits a compelling sensation of self-rotation in the opposite direction.^{2,3}

When human subjects wear optics that either left-right ("mirror") reverse or invert (rotate by 180°) vision, the normal relationship between left-right head rotation and relative visual scene motion is reversed. For example, head rotation to the right then is accompanied by relative scene motion to the right with respect to the head, with the result that the seen world is no longer perceived as stationary.^{4,5} Spatial orientation is severely impaired. However, after an extended period of vision reversal (days to weeks), the seen world appears more stable and subjective visual "normalcy" and coordinated movement are gradually restored.⁴⁻¹⁰ Active movement by the subject is thought to play a vital role in the adaptation process.¹¹ The slow-phase component of the horizontal vestibulo-ocular reflex (VOR), which contributes to perceptual stabilization under normal vision, has been shown to reverse after a week of vision reversal.¹² The neural pathways believed to mediate adaptive changes in the VOR recently have been explored in animals.^{13,14} One might also expect that the neural interpretation of visual self-rotation cues would reverse, and be manifest perceptually in a reversal of the CV phenomenon. We have demonstrated such a reversal, accompanied by only a modest reduction in vestibulo-ocular reflex gain, in 10 of 15 subjects within a brief (one- to three-hour) period of exposure. Reversed CV was demonstrated only when the moving stripe display size was limited to the field of view conditioned by exposure. A preliminary report has appeared.¹⁵

METHODS

Three experiments, which differed somewhat in protocol details, were conducted using 15 adult volunteers with no overt oculomotor or vestibular disorders. As symptoms of motion sickness often occur under vision reversal,

*This work was supported by National Aeronautics and Space Administration Grant NSG-2032 and NASA Contract NAS9-15343.

†Dr. Bock was supported by a NATO Science Fellowship.

drugs (scopolamine, 0.5 mg; or scopolamine, 0.4 mg/dexedrine, 5.0 mg) were administered orally prior to Experiments 1 and 2. In all experiments, left-right vision reversal was achieved using the prism goggles shown in FIGURE 1, which permitted a binocular field of vision subtending approximately 45° horizontally and 28° vertically.† Two Dove prisms, mounted base to base, were held in front of each eye (with bases in a sagittal plane) by a Plexiglas frame fixed to the head by an adjustable band. A black shield closely fitted to the face and the prisms excluded all nonreversed visual information.



FIGURE 1. Subject wearing prism goggles and EOG electrodes.

In all experiments, CV was tested before and immediately after a period of exposure to reversed vision ("preliminary" and "final" tests). For all subjects in Experiment 2, and for one subject in Experiment 3, CV also was tested at intervals during the exposure period. Subjects were seated in the closed, motionless cabin of a flight simulator (Link GAT-1). Equal width (6.4°) vertical

†Prism axes were adjusted to eliminate diplopia at a distance of three meters. The monocular field of view through each eye was 28° by 28° .

light and dark stripes, moving left or right at $8^\circ/\text{second}$, were back projected onto the translucent front window, about 70 cm from the subject. During testing without the goggles before and after exposure, the shape of the moving display could be varied using appropriate masks applied to the window, whereas in tests made during exposure, the shape corresponded to the field of view of the goggles. Subjects were asked to report verbally the onset and disappearance of any CV. Because of the transposition of the visual location of the hands with goggles on, subjects were asked to report their perceived direction of self-motion with respect to the direction of seen stripe motion, or with respect to their left and right eyes, or both. Motion reports made using these two different methods were always consistent.

The gain and phase of the horizontal VOR were tested in the dark before and after exposure using sinusoidal simulator angular velocity (0.2 Hz, $30^\circ/\text{second}$ peak velocity, 6–8 cycles). Eye movement was measured in the dark using conventional d.c. electro-oculography (EOG). Subjects performed mental arithmetic to maintain alertness. (In the case of certain subjects, we also performed one or more additional brief tests during the preliminary and final test sessions. These included acceleration threshold measurements, an evaluation of gaze stabilization during active head movement, an oculogyral illusion test, and a pseudorandom cabin motion nulling test. Results of these additional tests will be reported elsewhere.) The present paper will focus on circularvection and VOR test results.

When not participating in the brief perexposure tests, our subjects explored their reversed visual environment by walking through the laboratory buildings in the company of an observer. Head and body movements in the horizontal plane were encouraged. When they occurred, motion sickness symptoms were maintained at an acceptable level by intervals of eye closure and/or head immobilization.

RESULTS

Experiment 1

In this experiment (five subjects), we first confirmed that preexposure CV direction was opposite to seen stripe motion ("normal CV") using the 63° (horizontal) by 28° rectangular stripe display shown in FIGURE 2A. Latency of CV onset ranged from 8 to 47 seconds. Then, after the prism goggles were fitted, the subjects exposed themselves to vision reversal for 180 to 230 minutes.

After the exposure period, the prism goggles were removed and CV was tested using a 30° (horizontal) by 19° display, shown in FIGURE 2B, that stimulated only the field of view previously exposed to the goggles. After a latency of between 10 and 42 seconds, all five subjects reported an unequivocal sensation of motion in the *same direction* as the seen stripe motion. Subjects usually likened the sensation to being "pulled along with the stripes." We refer to this perception as "reversed circularvection" (RCV). Four of the five subjects in Experiment 1 experienced compelling sustained RCV until we suddenly, some 30 to 60 seconds later, increased the display size to 63° (horizontal) by 28° . Subjects then reported that RCV immediately ceased and, after several seconds, that normal (unreversed) CV appeared. Changing back to the narrow field abolished normal CV, and RCV was reestablished after several seconds. This sequence could be demonstrated repeatedly over several minutes. Active head movements (eyes



FIGURE 2A. 63° by 28° moving stripe display used in Experiment 1. Schematic of display as seen from a position inside the GAT-1 simulator cabin, above and behind the head of the seated subject.

open in light) appeared to abolish RCV. Our fifth subject experienced an initial 17-second period of compelling RCV, followed by periods of normal CV and RCV, even though the display area remained narrow.

Experiment 2

To define more systematically the time course of CV adaptation, seven additional subjects participated in a second experiment in which CV was tested every 30 to 40 minutes during a 190-minute exposure period. To demonstrate more clearly the dependency of CV direction on the region of the visual field stimulated, CV was measured both before and after exposure using a rectangular "central-visual-field" display (CVF, 29° horizontal by 17°) shown in FIGURE 3A, and also by using a "peripheral-visual-field" display (PVF, 180° horizontal by 23°, with a dark mask of the CVF display area, FIGURE 3B). Before exposure, the CVF test was preceded by a PVF test. After exposure, two CVF tests (both directions of stripe movement) were followed by a PVF test, and the head was immobilized in an effort to avoid readaptation. Subjects were asked to report verbally the first appearance of CV, its direction, and their sensation of self-rotation in 45° increments. For purposes of comparison between subjects, we

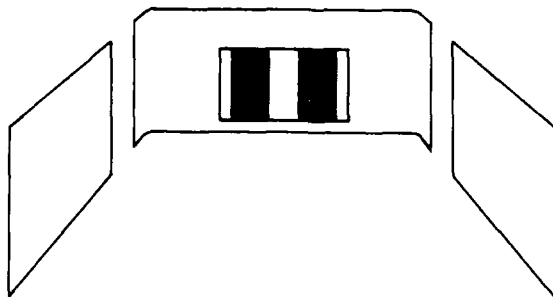


FIGURE 2B. 30° by 19° moving stripe display used in Experiment 1.

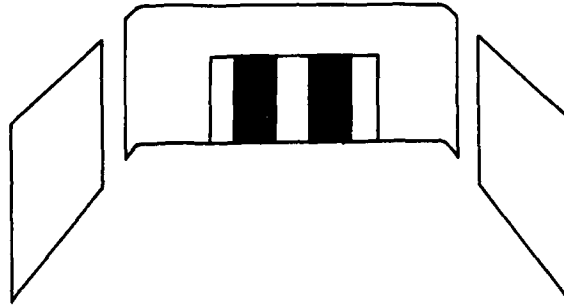


FIGURE 3A. Central-visual-field (CVF) moving stripe display used in Experiment 2 (29° by 17°).

converted these reports to a four-bin velocity scale, described in TABLE 1. When vection could not be demonstrated using the display alone, we attempted to trigger it with a brief rotation of the simulator cab, thus providing a transient semicircular canal motion cue (present during normal head rotation, but absent using conventional CV test procedures). As shown in TABLE 1, four subjects demonstrated RCV. The first RCV episode occurred after 95 to 190 minutes of exposure.

Experiment 3

Three additional subjects underwent an exposure period (which ranged from 150 to 220 minutes), but used no anti-motion-sickness drugs. Symptoms were controlled only by eye closure and head-movement limitation. Two of the subjects were tested as in Experiment 1, but using only the 63° by 28° front window display. RCV was not found after the exposure, perhaps because we failed to test with the narrow 30° by 19° display. The third subject underwent a protocol similar to Experiment 2, and demonstrated RCV after 80 minutes of exposure with goggles on, and with the CVF display in final testing with goggles removed.

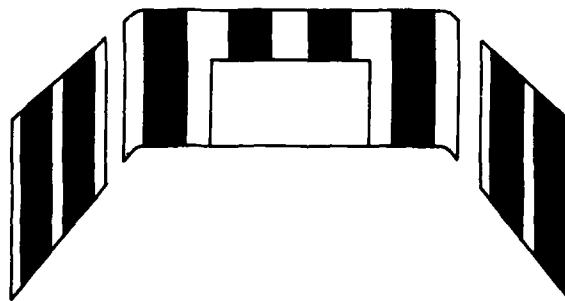


FIGURE 3B. Peripheral-visual-field (PVF) moving stripe display used in Experiment 2 (180° by 23°).

TABLE 1
EXPERIMENT 2 CIRCULARVECTION TEST RESULTS*

Subject	Preliminary Testing		Goggles-On Testing during Exposure Period					Final Testing	
	PVF	CVF	1	2	3	4	5	CVF	PVF
B1	4(+++)	— (/)	4(+++)	7(+++)	7.5(+++)	3(+)	5.5(+++)	1.5(+++)	2(+++)
B2	7(+++)	5.5(+++)	5(+++)	11(+++)	19.5(+++)	4(+++)	5(+++)	1.5(+++)	19(+++)
B3	11.5(+++)	8(+++)	5(+++)	21(+++)	— (+)	14(+++)	16.5(+++)	21(+++)	9(+++)
B4	9(+++)	— (/)	— (/)	— (/)	18(+++)	121(+++)	5(+++)	15(+++)	3(+++)
B5	— (+)	— (+)	23(+++)	18(+++)	12.5(+++)	63(+++)	8(+++)	9(+++)	3.5(+++)
B6	10(+++)	— (+)	12(+++)	— (+)	12(+++)	10(+++)	60(+++)	— (+)	20.5(+++)
B7	— (+)	— (/)	— (/)	— (+)	— (/)	— (/)	— (/)	— (/)	35(+++)

*Boxed-off numbers designate occurrence of reversed circularvection. For each test, latency is given in seconds, followed by magnitude on a four-bin scale: (+++) is strong vection greater than 25% of stripe velocity; (++) is vection present; (+) indicates sustained vection present after triggering simulator rotation stopped; (/) denotes no vection, even with triggering rotation. Dashes (—) indicate CV latency not measured.

Vestibulo-Ocular Reflex Tests

VOR slow-phase velocity gain and phase re trainer velocity were measured in all experiments before the first preexposure CV test, and after the exposure just before the goggles were removed. Data from 2 subjects in Experiment 1 could not be analyzed due to technical problems. In the remaining 10 subjects in Experiments 1 and 2, VOR gain decreased from 0.72 (standard error = 0.35) to 0.55 (SE = 0.29) after exposure. This change was significant (paired-sample t-test, $p < 0.001$). Among those 7 subjects in Experiments 1 and 2 who experienced RCV, gain decreased from 0.80 (SE = 0.39) to 0.64 (SE = 0.31), also a significant change ($p < 0.005$). Slow-phase eye velocity of the 10 subjects lagged trainer velocity by 180° (SE = 7°) prior to exposure and lagged by 176° (SE = 11°) after exposure. The slow-phase VOR gain of the 3 Experiment 3 subjects who did not use drugs decreased from 0.74 (SE = 0.30) to 0.47 (SE = 0.17). We were unable to demonstrate significant differences between the drug and nondrug groups in terms of VOR gain decrease. As confirmed by direct inspection of the eye-movement records, none of our subjects showed any evidence of reversal of the VOR slow-phase component. (Apparently systematic changes in the occurrence of the fast component of nystagmus were, however, observed.)

DISCUSSION

Our subjects showed approximately a 20% reduction in VOR slow-phase gain over their brief exposure period. This short-term gain reduction could be due to uncontrolled changes in alertness caused by motion sickness or fatigue. Scopolamine is known to depress oculomotor responses,¹⁸ but the gain reduction in our drug and nondrug groups appeared similar. Alternatively, the gain reduction we observed may represent the early stages of the adaptive VOR change described by Gonshor and Melvill Jones.¹² Their subjects, who did not use drugs, showed similar gain changes during the first day of exposure.

Our results imply that vision reversal soon produces a corresponding reversal of the interpretation of visual self-rotation cues from that portion of the field of view (referred to the head) that has been conditioned by the exposure. This change is adaptive in that it appears directed towards the goal of veridical self-motion perception. The reversal of circularvection presumably is mediated by a central mechanism that establishes a new association between the direction of motion of the visual input relative to the head and self-rotation direction information provided by nonvisual (e.g., vestibular) sensory modalities during body movement. Nonvisual self-rotation information is not available at the retinal level. It therefore can be argued that the adaptive process is central in origin, and not a retinal phenomenon.

RCV could be demonstrated only when the field of view was limited to or less than the field of view of the goggles. With a wide field stimulus (as in Experiment 1), RCV appeared to be overwhelmed by normal vection. In Experiment 2, normal CV response to PVF stripe motion was, if anything, enhanced by exposure of the central field to vision reversal. Our findings suggest that visual information from the exposed central field of view is transmitted centrally along pathways that are separate from those carrying information from the peripheral visual field, and that each of these pathways may be modified separately as a

result of sensory experience. The occasional presence of alternating normal CV and RCV during early perexposure tests indicates that RCV may not develop gradually. Instead, it is as if a second, competitive mechanism develops.

It is important to point out that RCV cannot be explained simply as a "negative aftereffect,"¹⁷ since RCV was demonstrated without preceding unreversed CV. Similarly, RCV is distinctly different from the brief episodes of "inverted self-motion perception" reported to occur during prolonged (4- to 12-minute) optokinetic stimulation.¹⁶ RCV could be demonstrated after distinctly shorter latencies (order of seconds) with no preceding normal vection, was sustained for periods greater than 5 seconds (usually 20 seconds to more than a minute), and could be manipulated quickly and consistently by altering the display size.

It is not surprising that the RCV velocity magnitudes reported were modest, given the narrow field of view of the goggles, as normal CV can be elicited more effectively if peripheral retinal areas are exposed to the moving display.¹⁹ In this regard, we note that demonstration of RCV or lack of it within the allowed exposure period appeared to be correlated with CV strength produced with a narrow field stimulus. In Experiment 2, subjects B1-B4 showed strong, normal CV at least once, either in CVF preexposure tests or during the first four perexposure sessions, and they were the only subjects in this experiment to show RCV. Test-scheduling constraints limited exposure to 190 minutes in Experiment 2. Had the exposure for subjects B5-B7 been extended, it is conceivable that they, too, would have shown RCV. The exposure duration in Experiment 1 was not so constrained. All five subjects in Experiment 1 experienced RCV.

In animals, convergence of visual and vestibular head rotation information is known to occur in vestibular nucleus neurons,^{20,21} which are thought to determine the slow-phase velocity of vestibular and optokinetic nystagmus under many conditions. The extent to which vestibular nucleus neurons contribute to rotation perception is unknown, although there appears to be a close relationship between the time course of normal CV in man and the response pattern of some vestibular nucleus neurons in animals.²⁰⁻²⁴ It would be interesting to know if a reversal in visual sensitivity of vestibular nucleus neurons can be demonstrated in animals after several hours of active exposure to vision reversal.

CONCLUSIONS

1. Reversed circularvection (RCV) was demonstrated in 10 of 15 subjects after one to four hours of active head movement while wearing left-right vision-reversing goggles.
2. Exposure to left-right visual reversal apparently reversed the perceptual interpretation of visual information only from the conditioned portion of the subject's field of view.
3. Development of RCV appears adaptive, i.e., directed toward the goal of veridical self-motion perception, and is probably of central, rather than retinal, origin.
4. RCV is abolished quickly when active head movements are made eyes open in the light with goggles off.
5. RCV cannot be explained as a negative aftereffect artifact or as an inverted self-motion perception resulting from prolonged stimulation. RCV was demonstrated in one subject without the use of anti-motion-sickness drugs.

6. Horizontal VOR slow-phase gain decreased similarly in both the drug and nondrug groups. No evidence of VOR slow-phase reversal was found.

SUMMARY

After one to three hours of active movement while wearing vision-reversing goggles, 10 of 15 (stationary) human subjects viewing a moving stripe display experienced a self-rotation illusion in the same direction as seen stripe motion, rather than in the opposite (normal) direction, demonstrating that the central neural pathways that process visual self-rotation cues can undergo rapid adaptive modification.

ACKNOWLEDGMENTS

We thank J.-K. Huang, our subjects, and also Professors R. Sivan, L. Young, and R. Held and Dr. O. Garriott, M. Pankratov, and E. Boughan.

REFERENCES

1. DICHGANS, J. & TH. BRANDT. 1978. In *Handbook of Sensory Physiology. Perception*. R. Held, H. Leibowitz & H. L. Teuber, Eds. 7: Chapter 25. Springer-Verlag. Berlin, Federal Republic of Germany.
2. FISHER, M. & A. KORNMULLER. 1930. *J. Psychol. Neurol. Leipzig* 41: 273-308.
3. MACH, E. 1875. *Grundlinien der Lehre von den Bewegungsempfindungen*. Engleermann. Leipzig, Germany.
4. STRATTON, G. 1896. *Psychol. Rev.* 4: 341-360.
5. STRATTON, G. 1896. *Psychol. Rev.* 5: 611-617.
6. EWERT, P. 1930. *Genet. Psychol. Monogr.* 7: 177-363.
7. ERISMAN, T. 1947. *Proc. Congr. German Psychol. Assoc. Bonn*: 54.
8. KOTTENHOFF, H. 1957. *Acta Psychol.* 13: 79-97, 151-161.
9. KOHLER, I. 1964. *Psychol. Issues* 3: 1-72.
10. HARRIS, C. 1965. *Psychol. Rev.* 72: 419-444.
11. HELD, R. 1962. *J. Nerv. Ment. Dis.* 132: 26-32.
12. GONSHOR, A. & G. MELVILL JONES. 1976. *J. Physiol.* 256: 381-414.
13. KELLER, E. & W. PRECHT. 1979. *J. Neurophysiol.* 42: 896-911.
14. HADDAD, G., J. DEMER & D. ROBINSON. 1980. *Brain Res.* 185: 265-275.
15. OMAN, C., O. BOCK & J.-K. HUANG. 1980. *Science* 209: 706-708.
16. BENSON, A. & J. BRAND. 1968. *Q. J. Exp. Physiol.* 53: 296-311.
17. THALMANN, W. 1921. *Am. J. Psychol.* 32: 429-441.
18. BRANDT, TH., J. DICHGANS & W. BUCHELE. 1974. *Exp. Brain Res.* 21: 337-352.
19. BRANDT, TH., J. DICHGANS & E. KOENIG. 1973. *Exp. Brain Res.* 16: 476-491.
20. DICHGANS, J., C. SCHMIDT & W. GRAF. 1973. *Exp. Brain Res.* 18: 319-322.
21. HENN, V., L. YOUNG & C. FINLEY. 1974. *Brain Res.* 71: 144-149.
22. YOUNG, L. 1979. In *Posture and Movement*. R. Talbot & D. Humphrey, Eds.: 177-187. Raven Press. New York, N.Y.
23. ALLUM, J., W. GRAF, J. DICHGANS & C. SCHMIDT. 1976. *Exp. Brain Res.* 26: 463-485.
24. WAESPE, W., B. WAESPE & V. HENN. 1978. *Pfluegers Arch. Gesamte Physiol. Menschen Tiere* 373 (Suppl. R87).

PATTERNS OF VESTIBULAR AND NECK RESPONSES
AND THEIR INTERACTION: A COMPARISON
BETWEEN CAT CORTICAL NEURONS
AND HUMAN PSYCHOPHYSICS*

T. Mergner, L. Deecke, and W. Becker

Department of Neurology and
Section of Neurophysiology
University of Ulm
D-7900 Ulm, Federal Republic of Germany

INTRODUCTION

So far, human psychophysical data have been compared with results obtained for first-order vestibular neurons in animals, as well as with the theoretical deflection of the cupula and with nystagmus in man.^{7,12} However, it would be more appropriate to relate the psychophysical data to the neuronal responses obtained from the cortex as the site of conscious experience. The ideal approach would be the comparison in the same animal experiment. At present, however, we can only report on neuronal responses recorded from the anterior suprasylvian (ASS) cortex in cats subjected to labyrinthine, neck, and combined stimulation in the horizontal plane, and on preliminary results from human psychophysics. In particular, we were interested to know what naive humans report when subjected to the same stimuli as the animals. We shall consider mainly basic features rather than quantitative details when comparing the results of the two experimental series.

METHODS AND RESULTS

Horizontal Canal Stimulation

Neuronal Responses in the ASS Cortex of the Cat

Extracellular spike activity of neurons in the left ASS cortex was recorded in chronically prepared awake cats, which were paralyzed during the recording sessions. Sinusoidal stimuli at 0.05, 0.2, and 1 Hz with peak angular velocities ranging from 5 to 80°/second as well as position trapezoids ($\dot{\theta} = 35^\circ/\text{second}$, 1.8 seconds duration) were applied in the dark. Impulse density histograms were constructed by a laboratory computer, which averaged over 4-16 double cycles of the stimulus. For quantitative analysis, the phase (fundamental from Fourier analysis) and the amplitude of excitatory responses to sinusoidal stimulation were compared with chair velocity.

In continuation of our previous experiments,^{2,4,13} we recorded 104 additional neurons from the ASS cortex. Thirty-three of them revealed a type I response, and 62 a type II response, to sinusoidal stimulation. Overall resting rate was low (11 spikes/second). The modulation in discharge rate around resting level tended

*Supported by Deutsche Forschungsgemeinschaft, SFB 70.

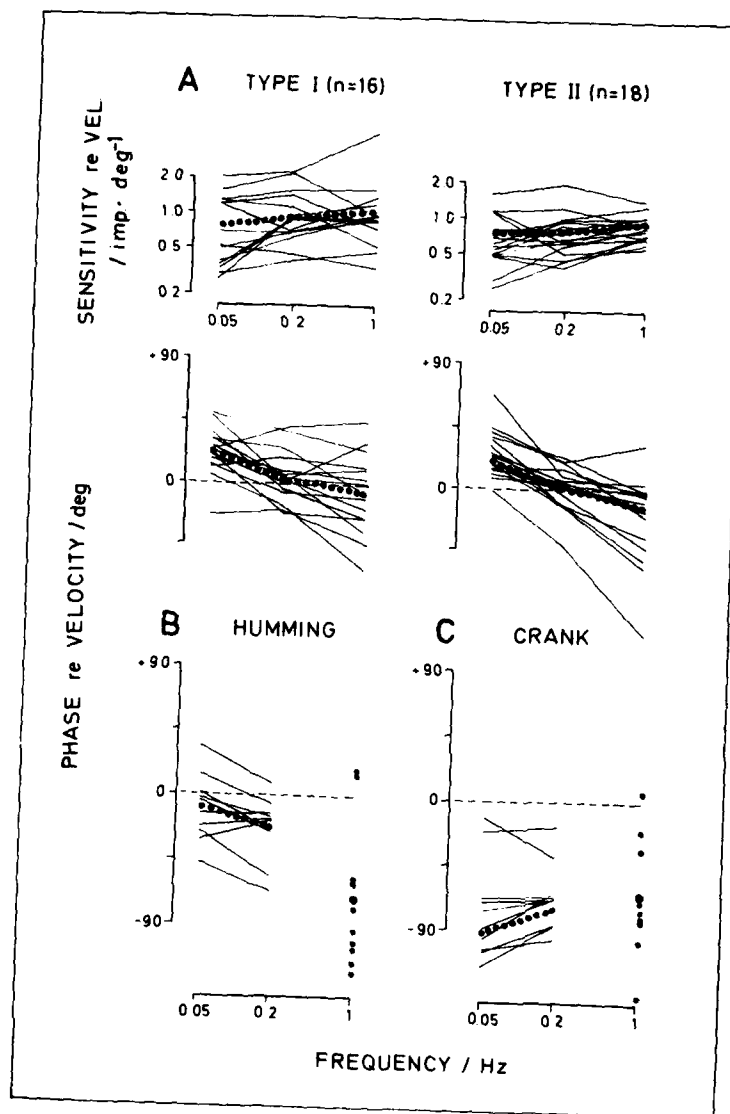


FIGURE 1. Responses to sinusoidal whole-body rotation in the horizontal plane (labyrinthine stimulus). A: Neuronal responses of cat ASS cortex. Bode diagrams giving sensitivity and phase (referred to angular velocity; $\dot{\psi} = 20^\circ/\text{second}$) of type I and type II neurons as a function of stimulus frequency. Thin lines refer to individual neurons; dotted lines give the mean values. B and C: Human turning sensation. Concurrent indication by humming (B) and crank turning (C) of 10 subjects. Bode diagrams giving the phase of the middle of humming periods or of crank turning periods (referred to peak angular velocity; $\dot{\psi} = 10^\circ/\text{second}$) as a function of stimulus frequency. Thin lines represent mean response curves of individual S; dotted lines show average of the individual curves. Since results at 1 Hz showed a large variability, their means are not linked to the average curves. (2 S are not included in the average in C.)

to be asymmetric with increasing stimulus intensity; there was an abrupt saturation of the "inhibitory" responses above $5^\circ/\text{second}$, and a more gradual saturation of the excitatory responses was evident above $20^\circ/\text{second}$. Mean sensitivity with our standard stimulus (0.2 Hz , $\phi = 20^\circ/\text{second}$) was ca. $0.8 \text{ spike/second per degree/second}$, for both types of neurons. Both were also similar in their mean phases, which were closely related to stimulus velocity ($+4.0^\circ$ and -2.0° , respectively). Mean phases showed a slight phase advance at 0.05 Hz (FIGURE 1A). The phase characteristics of the individual neurons showed large variations. When using position trapezoids, the following response patterns could be distin-

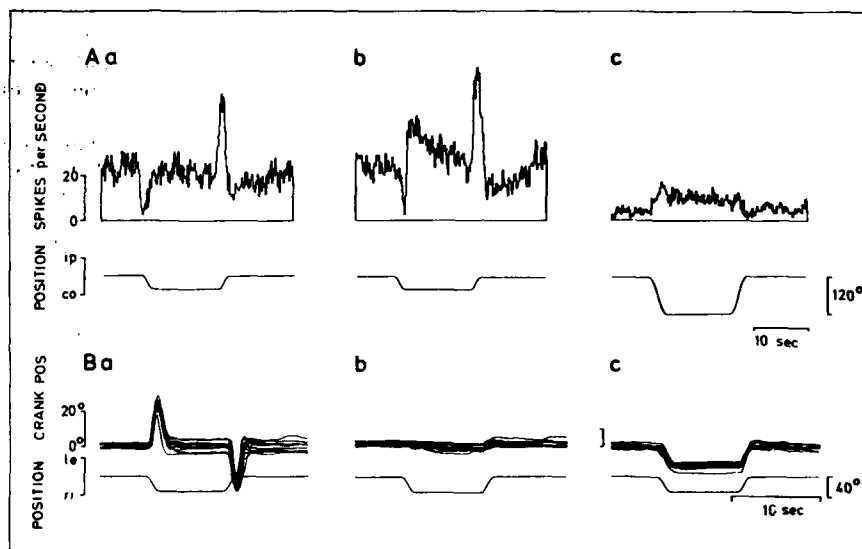


FIGURE 2. Responses to trapezoidal whole-body rotations. Lower traces give chair position. A: Neuronal responses. Spike density histograms from three different neurons. a: Phasic response. b: Phasic response followed by a slowly decaying ("quasi-tonic") overshoot in opposite direction. c: Essentially tonic response with slow decay. B: Human subject concurrent sensation indications by crank turning. Superposition of 10 consecutive trials. Three different instructions were given: a: Indicate speeding up and slowing down of chair rotation; b: Indicate any turning sensation that follows after the rapid chair rotation; c: Keep the crank pointing to the north during chair rotation.

guished: (1) almost purely phasic responses essentially related to stimulus velocity (FIGURE 2A-a); (2) phasic responses followed, after the end of the stimulus, by a long-lasting "quasi-tonic" overshoot in a direction opposite to the initial phasic response (FIGURE 2A-b); (3) predominantly tonic responses with slow decline (FIGURE 2A-c)—they appeared to be related to angular displacement when testing with angles up to ca. 200° ; and (4) phasic responses with or without overshoot, which had a delayed rising and/or falling slope. These different trapezoid responses often could not be predicted from the response characteristics obtained with sinusoidal stimuli.

Concurrent Indication of Turning Sensation by Human Subjects

Ten naive subjects (*S*; student physical therapists) were rotated in the horizontal plane, their heads being fixed in a 30° nose-down position to a frame by means of a bite-bar, which was molded from each *S*'s dental impression. The *S* were blindfolded; auditory cues were excluded by plugging the external ear openings and by applying noise via earphones. The only instruction given was to indicate the sensation of being turned to one direction of the *S*'s own choice. The same experimental setup and the same stimulus parameters ($\dot{\theta} = 10^\circ/\text{second}$, otherwise as above) as with the animal experiments were used. Two modes of sensation indication were used consecutively: (1) humming, which was recorded by a throat microphone and displayed as a phonogram on a strip chart recorder together with chair position, and (2) horizontal turning of a crank that was coupled to a potentiometer. The phase relation between the sensation indication and the stimulus was analyzed by relating the middle of the indication period to peak angular velocity.

Indication by humming. With sinusoidal stimuli, 7 *S* chose rightward and 3 *S* leftward rotation for sensation indication. The mean values ($n = 10$) for the humming indication of the individual *S* and the overall means are shown in FIGURE 1B, in which the absolute on direction, however, is disregarded. At 0.05 Hz, humming tended to be almost in phase with chair angular velocity ($\bar{\phi} \pm \text{standard deviation} = -9.2 \pm 23.4^\circ$), while it clearly lagged velocity at 0.2 Hz ($\bar{\phi} = -22.6 \pm 22.8^\circ$). Phase values at 1 Hz showed large variations (+19.7 to -124.6°). The *S* reported that it was impossible for them to keep up with the stimulus at this frequency. When tested with position trapezoids, they started humming slightly after stimulus onset and finished shortly after stimulus end (not shown).

Indication by crank turning. With sinusoidal stimuli, 9 *S* started crank turning during rightward rotation (2 had changed on direction as compared to humming) and 1 during leftward rotation. Two *S* made crank excursions that were almost in phase with chair velocity (upper two curves in FIGURE 1C), although slightly lagging those obtained with humming at 0.05 Hz ($\Delta\phi = -9.6^\circ$ and -35.0°) and at 0.2 Hz ($\Delta\phi = -24.3^\circ$ and -12.1°). The remaining *S* started crank excursion almost at the same instant, but reset it clearly later. In these cases, excursion periods tended to lag chair velocity by almost 90° at 0.05 Hz ($\bar{\phi} = -90.6 \pm 17.9^\circ$) and at 0.2 Hz ($\bar{\phi} = -75.1 \pm 12.3^\circ$). The slope of the mean phase characteristic was different from that obtained with humming in that there was a relative phase lag instead of phase lead at 0.05 Hz compared to 0.2 Hz. Similar with humming, no reliable values were obtained at 1 Hz. Taken together, crank excursion was roughly in phase with chair position. The subjects seemed not to be aware of this fact when asked after the experiments.

When tested with position trapezoids, the subjects started crank excursion during chair rotation, but tended to maintain the crank's new position after the end of the stimulus. In order to overcome this tendency, special instructions were given to 5 other *S*. They were asked to indicate turning sensations during rotation in either direction, and to pay attention to the instances of speeding up and slowing down of chair rotation. During the experiments they turned the crank in the same direction as chair rotation, the profile of the crank excursion resembling that of chair velocity, although it was slightly delayed and broadened (FIGURE 2B-a). The *S* reported that they experienced, after the end of this stimulus, a slight and long-lasting rotation in the opposite direction. In a further set of trials, they

were asked to indicate any weak turning sensation they might experience after the end of the rapid rotation. With this instruction, they generally executed a small and long-lasting excursion after the end of the stimulus. The signal was opposite in sign with respect to the one that they had produced with the previous instruction (cf., FIGURE 2B-b). In a final set of trials, the spontaneous indication of angular displacement (position), which the first 10 S had produced, was further explored. The 5 new S were told that in the initial chair position, the direction straight forward was north. They had to turn the crank so that it always would point to the north while they were turned. Crank excursion was, of course, now opposite to that in the first experiment. The signals were related rather well to the trapezoidal chair displacements (FIGURE 2B-c) apart from two aspects: first, chair displacement tended to be underestimated; second, there was a slight backward drift. On request, the subjects related this drift to the weak sensation of counterrotation they had indicated in the previous experiments.

In summary, crank excursion turned out quite suitable for the indication of angular displacement, but appeared to be less suited for indication of the turning sensation. In the following sections dealing with turning sensations during isolated trunk rotation and isolated head rotation, results obtained with this method will not be considered.

Stimulation of Neck Afferents

Neck stimulation was achieved by rotation of the trunk while the head was kept stationary. The scheme on top of FIGURE 4A gives our definition of its on direction relative to the other stimuli used: the reference is the labyrinthine stimulus (L) during whole-body rotation (in the example, counterclockwise), which excites primary horizontal canal afferents on the side to which the animal is rotated. The neck stimulus is called (plus) N, when the chair is rotated to the same side as in condition L; in this situation stretch of the neck, which we consider to be the excitatory stimulus, occurs on the same side as the canal afferent excitation. If the two stimuli are combined during rotation of the head with stationary trunk, the neck is stretched contralateral to the canal excited. Thus we refer to this stimulus as L minus N. The same stimuli as shown for the cat were also applied to the human subjects.

Neuronal Responses

About 80% of the vestibular ASS neurons also responded to neck stimulation. Mean neck sensitivity (1.04 spikes/second per degree/second) was slightly higher than mean labyrinthine sensitivity. Neck type I responses were about as frequent as neck type II responses (definition as with labyrinthine responses; Reference 5). With our standard stimulus, the mean phase of the neck responses lagged that of labyrinthine responses by about 10° . The frequency characteristics of the individual neurons showed large variations. In most of the neurons, they could be related to the following two response patterns obtained with position trapezoids: (1) neurons behaving like a leaky integrator of acceleration during sinusoidal stimulation (in phase with velocity at 0.2 and 1 Hz, reduced gain and a phase lead at 0.05 Hz) gave almost purely phasic responses with position trapezoids

(30%; $n = 56$); (2) neurons behaving like a position-plus-velocity signaling system (in phase with velocity at 0.2 and 1 Hz, increased gain and a phase lag at 0.05 Hz) gave phasic-tonic responses (both components in the same direction) (41%). The remaining neurons (29%) had more complex frequency characteristics and response patterns (e.g., a phasic response in one direction followed by a tonic response in the opposite direction; cf., FIGURE 3A). In the latter neurons, trapezoid responses often could not be predicted from the sinusoid responses.

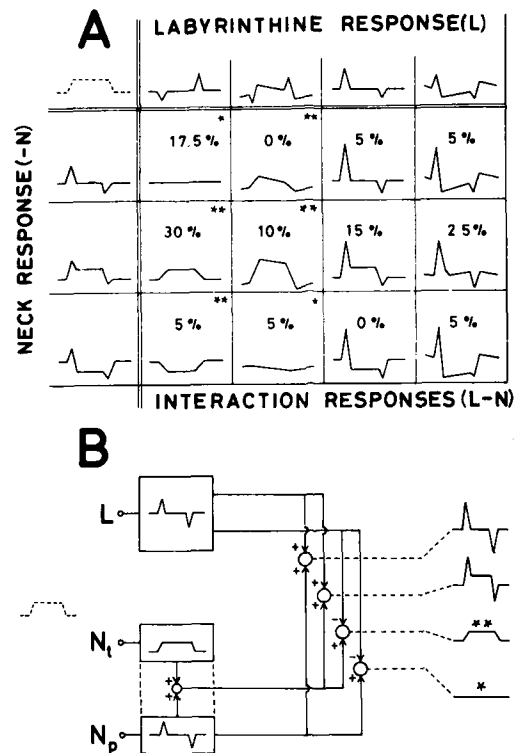


FIGURE 3. Schematic summary of the most common patterns of labyrinthine-neck convergence and interaction obtained with trapezoidal stimuli (dashed curves). **A:** ASS cortex. Horizontal row on top of matrix shows major patterns of labyrinthine responses (L); left vertical column gives neck responses ($-N$, on-direction reversed). The elements of the matrix show the interaction responses ($L - N$) resulting from the combined labyrinthine-neck stimulation during isolated head rotation. Note that basically four different patterns of interaction responses result: subtraction of phasic response components yields (1) little or no response (one asterisk) or (2) tonic responses (two asterisks); addition of phasic response components yields enhanced phasic responses (3) with or (4) without additional tonic components. **B:** Vestibular nuclei. Signal diagram summarizing the basic patterns of labyrinthine-neck convergence and interaction observed.¹ Two sensors are hypothesized in the neck, one (N_t) having static and the other (N_p) having dynamic properties. Four different patterns of interaction responses result, which resemble those found in the ASS cortex.

Turning Sensations of the Subjects

In the first 10 S mentioned, whole-body rotations were intermittently replaced by rotations of the trunk alone, by keeping the frame with the head stationary while the chair rotated. All S indicated a turning sensation (humming). Five of them indicated the same on direction as with whole-body rotation ($\bar{\phi} = -18.7^\circ$ at 0.05 Hz, $\bar{\phi} = -41.8^\circ$ at 0.2 Hz), while the other 5 reversed the on direction ($\bar{\phi} = -187.7^\circ$ at 0.05 Hz, $\bar{\phi} = -208.3^\circ$ at 0.2 Hz). Thus in both groups, the humming periods were almost in phase with the angular velocities in the respective on direction (cf., FIGURE 4B). After the experiments, all subjects reported that they had been able to distinguish between whole-body rotation and trunk rotation. Those in the first group had focused their attention on the trunk and had indicated its rotation. However, they experienced at the same time a head rotation in the opposite direction, which they had disregarded. This apparent head rotation had been indicated by the second group of S, who reported that they had focused their attention on head rotation. Taken together, trunk rotation induced two different sensations: a prominent turning sensation in the direction of actual trunk rotation, and a sensation of apparent head rotation in the opposite direction.

Combined Labyrinthine and Neck Stimulation

The stimulus condition already has been described under Stimulation of Neck Afferents. It should be pointed out once more that according to our definition, the two receptor systems are reciprocally activated during head rotation, so at first glance a confusing variety of possible convergences resulted. Thus we give the neck input during interaction a negative sign. For sinusoidal rotation, this corresponds to a shift in phase of the stimulus and of the response by 180° ; for trapezoidal rotation, this corresponds to a reversal of the on and off directions.

Neuronal Responses

The four different response patterns obtained with labyrinthine stimulation (see section on Horizontal Canal Stimulation) could combine with those obtained with neck stimulation (see section on Stimulation of Neck Afferents) during head rotation, so at first glance a confusing variety of possible convergences resulted. However, the majority of neurons (40/56) tested with position trapezoids in all of the stimulus conditions could be arranged in the scheme of FIGURE 3A. This scheme shows the convergences of the most common labyrinthine responses (pure phasic responses or phasic response with "quasi-tonic" overshoot) and neck responses (purely phasic responses or phasic responses with an additional tonic component either in the same or in the opposite direction). The phasic components of the labyrinthine and neck responses had either opposite on directions during head rotation (antagonistic convergence, left half of FIGURE 3A) or the same on direction (synergistic convergence, right half of FIGURE 3A). For the sake of simplicity, the absolute directionality of the neurons (type I or type II) was disregarded. Antagonistic convergence was found in 67.5% of the neurons, while 32.5% of the neurons showed a synergistic convergence. The relative

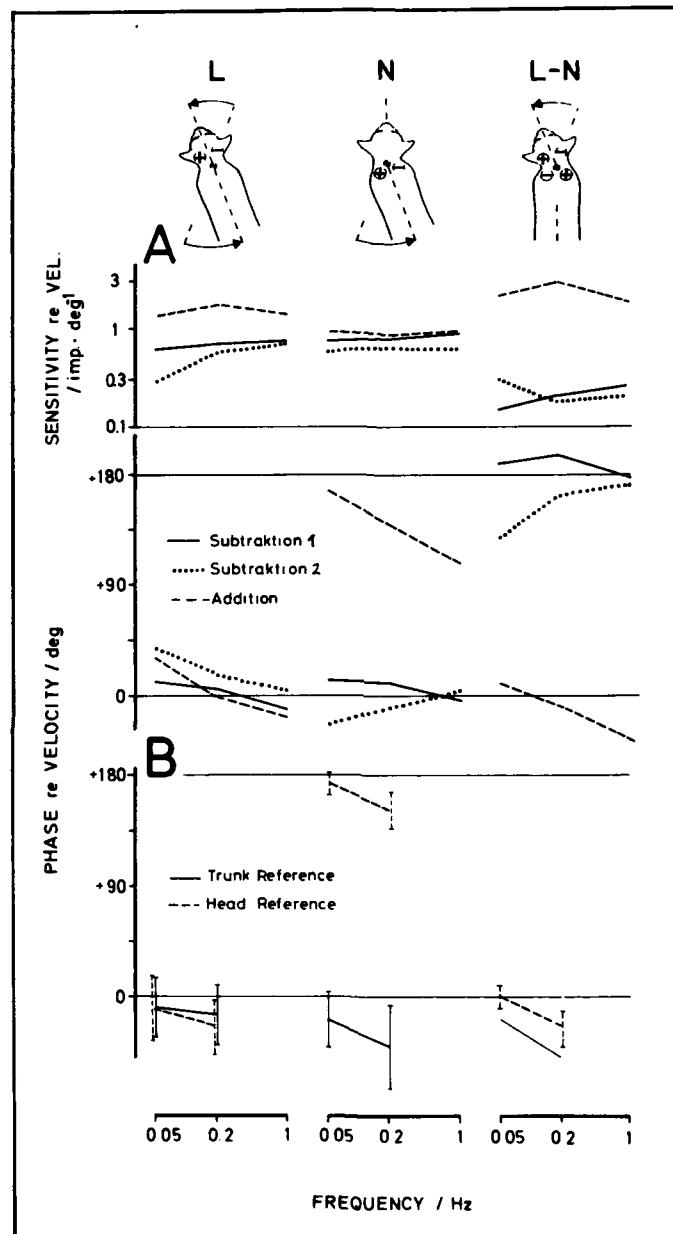


FIGURE 4. Responses during labyrinthine-neck interaction obtained with sinusoidal stimulation. Bode diagrams, same presentation as in FIGURE 1. On top of A, the three stimulus conditions used are shown schematically for an instant of counterclockwise rotation of either chair or head. L, labyrinthine stimulus (whole-body rotation); N, neck stimulus (trunk rotation); L - N, combined stimulation (head rotation). The plus and minus

frequency of the individual combinations is given by the percentage numbers in FIGURE 3A.

In considering the outcome of interaction, essentially four basic patterns of interaction responses could be distinguished: (1) little or no response during head rotation, due to subtraction of phasic and/or tonic response components (one asterisk in FIGURE 3A); (2) tonic responses mainly of neck origin, remaining after subtraction of phasic response components (two asterisks in FIGURE 3A); (3) enhanced phasic responses without tonic component, due to addition of phasic labyrinthine and neck responses either without tonic components or with tonic components canceling each other; and (4) enhanced phasic responses with additional tonic components, which were usually of neck origin but in a few cases stemmed from or had contributions from the labyrinthine response.

In the neurons with additive interaction, the enhancement of the excitatory response during head rotation could be explained rather well by assuming linear summation of the two inputs. However, in the neurons with antagonistic interaction, a strong excitatory response to one stimulus was often canceled by a weak "inhibitory" response to the other stimulus. The most likely explanation would be that the excitatory response has an almost equal "inhibitory" counterpart at subcortical level, which is reduced on the way to the cortex together with the decrease in resting rate. Thus the interaction observed at cortical level is probably performed, at least in part, in subcortical structures. In fact, neurons in the vestibular nuclei (VN) of the cat showed linear subtraction or linear addition of labyrinthine and neck response with the same stimuli.¹ A schematic description of the basic convergences and interactions found in the VN is given in FIGURE 3B. The basic features of the interaction responses obtained in the VN resemble those obtained in the ASS cortex, although the latter resulted from a much larger variety of convergences.

In our earlier studies, we mainly had used sinusoidal stimuli.^{2,4,13} These stimuli also were applied to some neurons in the present study. The results confirmed our earlier data, and they were also consistent with the four major response patterns described above. Examples are given in FIGURE 4A. In the first neuron (subtraction 1, solid line), labyrinthine and neck responses are similar with respect to their sensitivity and phase at the three frequencies tested. In the L - N condition, the sensitivity of the neuron is greatly reduced at all stimulus frequencies. The second neuron (subtraction 2, dotted lines) represents a similar case of subtraction; but at 0.05 Hz, the neck response shows a phase lag, and the response remaining during interaction is shifted in phase towards position (the neuron belonged to the group of interaction responses in which phasic

signs refer to excitation respective to "inhibition" of horizontal canal and neck receptors. A: Three examples of ASS neurons. In the first neuron (subtraction 1, solid lines), responses to the L- and the N- stimuli are similar; they subtract during L - N at all frequencies tested. In the second example (subtraction 2, dotted lines), subtractive interaction tends to be incomplete in the lower frequency range. In the third neuron (addition, dashed lines), L- and N- response are 180° out of phase; their interaction is additive. B: Concurrent indication of turning sensation by humming. Same S as in FIGURE 1B. Five of the S had chosen the trunk as reference (solid lines); their turning sensations were similar during L and N stimulation, and were either absent (2 S) or weak (3 S, thin line) with the L - N stimulation. The other 5 S had chosen the head as reference; their turning sensations during the N stimulation were about 180° out of phase, and during L - N stimulation almost in phase, with those obtained during L stimulation.

response components were canceled by subtraction while the tonic neck component remained). In the third neuron (addition, dashed lines), the neck response is about 180° out of phase with respect to the labyrinthine response. During head rotation, the interaction response is enhanced.

Turning Sensations of the Subjects

In the 10 subjects described above, whole-body or trunk rotation was intermittently replaced by rotation of the head while the trunk was kept stationary. In the first group of S, who had chosen the trunk as reference, 3 out of 5 produced only a weak humming (in the direction of head rotation) and the remaining 2 produced no humming at all (cf., FIGURE 4B). On request they reported that they had little or no turning sensation. The other 5 S, who had chosen the head as reference, indicated a prominent turning sensation in the same direction as during whole-body rotation (at 0.05 Hz, $\phi = +0.1^\circ$; at 0.2 Hz, $\phi = -24.4^\circ$) (cf., FIGURE 4B). On request they reported that the sensation was as strong or even stronger than during whole-body rotation. Taken together, it appears that during head rotation there are two possible turning sensations: one refers to the trunk and results from antagonistic interaction of labyrinthine and neck input, while the other refers to the head and results from a synergistic interaction of the two inputs.

DISCUSSION

In human subjects, the turning sensation during sinusoidal horizontal rotation is closely related to the theoretical deflection of the cupula, which during most naturally occurring head movements signals angular velocity.^{6,7} Furthermore, the ability to estimate angular displacement in the horizontal plane as well as after-sensations of apparent counterrotation is well documented in the psychophysical literature.^{3,6,7,8} Our own preliminary psychophysical experiments confirmed these findings. We tried to use as few instructions and as simple methods of indication as possible. Our aim was to gain a close access to the actual sensations of the subjects and not to stress their ability to perform elaborate tasks related to these sensations. Concurrent sensation indication with humming slightly lagged angular velocity in phase. This phase lag might be due to the fact that sensation onset was approached from subthreshold level whereas the end of the sensation was approached from suprathreshold level (the threshold in the former case being higher than in the latter case). On the other hand, we cannot exclude that the subjects had introduced additionally a relative phase advance by prediction to compensate for their reaction time. With the crank turning as indication, most subjects tended to indicate angular position. The phase characteristics with crank turning resemble that of a second-order system (with the acceleration as input) with a lead element at the higher frequencies. However, the frequency range tested was too small and responses in the upper frequency range too inaccurate to allow a final conclusion. Therefore, in the further experiments, we restricted ourselves to the indication by humming, which we consider to be closer to the actual turning sensation.

The ASS cortex in the cat was found to contain neurons that basically perform operations similar to those necessary to explain the psychophysical findings. These operations include coding of angular velocity, measurement of angular displacement, and an aftereffect equivalent to an apparent counterrotation

following position trapezoids. The operation required to obtain the angular displacement information is an integration of the velocity signal over time. The tonic neurons in the ASS cortex conceivably represent a first step toward displacement information. As to the "quasi-tonic" overshoots observed in a considerable number of the cortical neurons, they possibly may be related to the long-lasting after-sensations of counterrotation after the end of the trapezoid stimuli. Both the neuronal and psychophysical aftereffects appear to involve adaptational processes already starting in the cupula and the primary afferents (cf., Reference 16); similar overshoots were observed also in neurons of the vestibular nuclei, but with clearly smaller amplitudes.¹ Thus the overshoots appear to be enhanced relative to the phasic response component on the way to the cortex. This suggests that central processes also contribute to the human after-sensation.

In the majority of neurons, convergence of labyrinthine and neck input was found to be antagonistic. In some of these neurons, there was little or no response during head rotation. This was due to an almost complete subtraction of the individual labyrinthine and neck responses. In contrast, these neurons showed prominent responses when the trunk was rotated either in isolation (neck response) or together with the head (whole-body rotation, labyrinthine response). Thus these neurons appear to code rotation of the trunk. In other neurons with antagonistic convergence, subtractive interaction affected only the phasic response components while a tonic neck signal remained. In neurons with synergistic convergence, the phasic response components especially were enhanced by additive interaction. The interaction of labyrinthine and neck afferents appeared to be based on a linear summation of the two inputs (for parallels in earlier behavioral observations, cf. References 11 and 15).

In our psychophysical study on labyrinthine-neck interaction, we found that neck stimulation resulting from trunk rotation induces a strong sensation of trunk turning and an additional sensation of (apparent) head rotation in the opposite direction. During isolated head rotation, one would expect that the labyrinthine turning sensation and the sensation of trunk turning tend to cancel each other because they are of opposite sign in this stimulus condition. In fact, our subjects who used the trunk as reference indicated no or only weak turning sensations during head rotation. In contrast, the illusion of head rotation during neck stimulation should be synergistic with the labyrinthine turning sensation, if these two stimuli are combined during head rotation. Although not quantified, this appeared to hold true in the five subjects who used the head as reference; some of them reported that their turning sensation in this situation was stronger than during whole-body rotation.

It is interesting to compare these findings to those obtained for postural reflexes of labyrinthine and neck origin. It generally is assumed that during head movements the two reflexes act antagonistically on the limbs.^{9,10,15} This may be so because head movements have little or no effect on trunk stability. In contrast, the two reflexes appear to act additively on the neck musculature during passive head rotation, as judged from a recent study by Peterson and collaborators (Reference 14 and this volume); they consider this interaction to be essential for head versus trunk stabilization. A possible function of additive interaction for turning sensation might be to optimize the measurement of head displacement in space, if one considers that the labyrinthine stimulus alone is underestimated. Another role of neck input may be to compensate for after-sensations of labyrinthine origin. However, these hypotheses need further support from experimental work.

SUMMARY

The present study provides evidence that during whole-body rotation and during isolated rotation of either the head or the trunk, essentially the same processing of labyrinthine and neck afferent inputs takes place in neurons of the cat's ASS cortex and in humans who try to distinguish these stimulus conditions. This processing includes, among others, (1) measurement of angular velocity and displacement during labyrinthine stimulation (whole-body rotation); (2) indication of trunk rotation as well as of an apparent head rotation in the opposite direction during neck stimulation (isolated trunk rotation); and (3) subtraction as well as addition of labyrinthine and neck afferent inputs during combined stimulation (isolated head rotation). Subtraction provides a basis for the discrimination between whole-body rotation and isolated head rotation; addition may optimize the indication of movement and position of the head in space.

REFERENCES

1. ANASTASOPOULOS, D. & T. MERGNER. 1981. Horizontal vestibular-neck interaction in neurons of the vestibular nuclei. *Pfluegers Arch.* **389** (Suppl.) R31.
2. BECKER, W., L. DEECKE & T. MERGNER. 1979. Neuronal responses to natural vestibular and neck stimulation in the anterior suprasylvian gyrus of the cat. *Brain Res.* **165**: 139-143.
3. BÉKÉSY, G. VON. 1955. Subjective cupulometry. *Arch. Otolaryngol.* **61**: 16-28.
4. DEECKE, L., W. BECKER, R. JÜRGENS & T. MERGNER. 1979. Interaction of vestibular and somatosensory afferents for perception and postural control. *Agressologie* **20**: 179-184.
5. DUENSING, F. & K. P. SCHAEFER. 1958. Die Aktivität einzelner Neurone im Bereich der Vestibulariskerne bei Horizontalbeschleunigungen unter besonderer Berücksichtigung des vestibulären Nystagmus. *Arch. Psychiatr. Nervenkr.* **198**: 225-252.
6. EGMOND, A. A. J. VAN, J. J. GROEN & L. B. W. JONGKEES. 1949. The mechanics of the semicircular canals. *J. Physiol. London* **110**: 1-17.
7. GUEDRY, F. E. 1974. Psychophysics of vestibular sensation. In *Handbook of Sensory Physiology*. H. H. Kornhuber, Ed. **6/2**: 3-154. Springer-Verlag, Heidelberg, Federal Republic of Germany.
8. GUEDRY, F. E., C. W. STOCKWELL, J. W. NORMAN & G. G. OWENS. 1971. Use of triangular waveforms of angular velocity in the study of vestibular function. *Acta Oto-Laryngol.* **71**: 439-448.
9. HOLST, E. VON & H. MITTELSTAEDT. 1950. Das Reafferenzprinzip (Wechselwirkungen zwischen Zentralnervensystem und Peripherie). *Naturwissenschaften* **37**: 464-475.
10. KORNUBER, H. H. 1966. Physiologie und Klinik des zentralvestibulären Systems (Blick- und Stützmotorik). In *Hals- Nasen- Ohrenheilkunde*. J. Berendes, R. Link & F. Zöllner, Eds. **3/3**: 2150-2351. Thieme, Stuttgart, Federal Republic of Germany.
11. MAGNUS, R. 1924. *Körperstellungen*. Springer Verlag, Berlin, Federal Republic of Germany.
12. MAYNE, R. 1974. A systems concept of the vestibular organs. In *Handbook of Sensory Physiology*. H. H. Kornhuber, Ed. **6/2**: 493-580. Springer Verlag, Heidelberg, Federal Republic of Germany.
13. MERGNER, T. 1979. Vestibular influences on the cat's cerebral cortex. *Prog. Brain Res.* **50**: 567-579.
14. PETERSON, B. W., G. BILOTTO, J. H. FULLER, J. GOLDBERG & B. LEEMAN. Interaction of vestibular and neck reflexes in the control of gaze. *Prog. Oculomotor Res.* (In press.)
15. ROBERTS, T. D. M. 1978. *Neurophysiology of Postural Mechanisms*. 2nd edit. Butterworths, London, England.
16. WILSON, V. J. & G. MELVILL JONES. 1979. *Mammalian Vestibular Physiology*. Plenum Publishing Corp. New York, N.Y.

RESPONSES OF VESTIBULOSPINAL NEURONS
TO NECK AND MACULAR VESTIBULAR INPUTS
IN THE PRESENCE OR ABSENCE
OF THE PALEOCEREBELLUM*

R. Boyle and O. Pompeiano†
*Institute of Human Physiology
University of Pisa
56100 Pisa, Italy*

INTRODUCTION

In the normal, active animal, signals arising from macular vestibular or neck receptors are elicited during deviations of the head relative to space or to body. The resulting information is processed in the brain stem and thus allows the motor system to maintain a stable position of the body against external disturbances. Although the importance of macular vestibular and neck receptors in maintenance of posture is well known,^{7,22,23} the interaction of corresponding afferent signals on central nervous structures is poorly understood. Von Holst and Mittelstaedt postulated an antagonistic interaction of tonic vestibular and neck reflexes on postural mechanisms involving the limb musculature¹³ (cf., References 25 and 32). Inclination experiments in decerebrate cats have shown that the responses of ipsilateral forelimb extensors to independent stimulation of macular and neck receptors are opposite in sign,^{7,19,22-24} and are appropriate to explain why directional changes in head position—when both tonic labyrinth and neck reflexes act together—leave the position of the limbs unchanged (cf., References 13, 25, and 32).

To account for these findings, one might postulate that the stability of postural activity during head rotation is the result of an integration of opposite influences arising from macular and neck receptors, converging through independent channels on either spinal motoneurons or neurons of supraspinal descending pathways subserving postural regulation. Tonic neck reflexes have been observed after upper cervical transection²² (cf., however, Reference 41) and may thus control the activity of fore- and hindlimb motoneurons by utilizing propriospinal mechanisms (cf., References 15 and 17). On the other hand, the tonic labyrinth reflexes utilize mainly the vestibulospinal reflex arc passing through the lateral vestibular nucleus (LVN) of Deiters²¹ (cf., References 28 and 43). These two apparently independent anatomical pathways, however, are functionally linked at the level of the LVN itself: LVN neurons may process afferent signals originating not only from macular receptors (see 3 and 27 for references) but also from neck receptors.^{4,5,11,12,26,33-35,40}

*This investigation was supported by Public Health Service Research Grant NS 07685-12 from the National Institute of Neurological and Communicative Disorders and Stroke, National Institutes of Health, by a grant from the Consiglio Nazionale delle Ricerche, and by a grant in Biologia e Medicina Spaziale from the CNR, Italy. Financial assistance was also given to R.B. by a grant from the CNR.

†To whom correspondence should be addressed.

The present report summarizes a series of experiments designed to determine how the conflict between asymmetric responses arising from macular and neck receptors is resolved at the level of the LVN. The relative contribution of the cerebellum in determining the response characteristics of LVN units to the two afferent signals also was investigated.

METHODS

The experiments were performed on 34 adult cats decerebrated at the precollicular level under ether anesthesia. In 18 experiments, the cerebellar vermal cortex and fastigial nuclei were aspirated until visualization of the floor of the fourth ventricle. The dorsal neck muscles—biventer cervicis, complexus, and splenius—were disconnected bilaterally from the occipital bone; the ventral rami of C₁–C₃ were crushed, and the skin of the neck was disconnected from the underlying musculature and fully denervated.

In 20 experiments, the animals were immobilized with pancuronium bromide (Pavulon, N.V. Organon Oss) and artificially ventilated. Systematic arterial pressure, rectal temperature, and end-tidal P_{CO₂} were monitored and maintained within physiological limits.

The animal's head was placed in a stereotaxic frame and fixed in horizontal position, pitched 10° nose down. The axis vertebra was held at the level of the exposed spinous process of C₂ by a clamp secured on a tilting table; the lower trunk was clamped to a spinal cord frame, and pins were inserted through the great trochanter of both femoral bones to prevent body sway. Fore- and hindlimbs were extended and clamped. Sinusoidal oscillations of the neck, whole animal (tilt), or head alone about the animal's longitudinal axis were accomplished by independent hydraulic systems (cf., Reference 8). In particular, rotation of the neck clamp and table simultaneously beneath a stationary head produced stimulation of neck receptors (*neck input*). Rotation of the entire stereotaxic equipment and table together produced stimulation of labyrinth receptors (*macular input*). And finally, rotation of the head while the C₂ clamp and table remained stationary elicited costimulation of both receptors (*neck + macular inputs*). Since detectable responses to the individual neck and macular inputs were ensured using sinusoidal stimulation at 0.026 Hz, 5 to 10° peak amplitude of displacement, these parameters will be referred to as the standard parameters of angular rotation.

To activate vestibulospinal neurons, three stimulating electrodes with an interelectrode distance of 1.5 mm, and made of insulated 200- μ m stainless-steel wire were implanted into the ventral quadrant of the right cervical cord (between C₃ and C₄). Stimuli for identification of vestibulospinal neurons consisted of single 0.2-millisecond rectangular pulses applied in a bipolar manner between two of the three electrodes. Standard criteria for antidromic activation were followed (cf., Reference 30). For extracellular recording of single units, glass microelectrodes (5–10 M Ω impedance) filled with 2% Pontamine Sky Blue dye in 0.5 M sodium acetate were used.

The unit activity was filtered, amplified, and converted to standard pulses and averaged (sequential pulse density histograms, SPDH). The analog output of the signal averager (Correlatron 1024, Laben) was plotted on an x-y plotter (HP 7035P), and the digital data were stored on punch tape and processed off-line with a computer system (HP 2100/A) equipped with a fast Fourier analyzer (HP 5451/B).

Results are based on the cross-spectral analysis of the averaged unit activity with respect to the first harmonic of response (output) during the rotational stimuli (input).

The sensitivity of the fundamental component of response was defined as the percentage increase (half of peak-to-peak) of mean firing rate per degree of peak displacement, while the corresponding gain was expressed in impulses/second per degree. According to the terminology used by Lindsay *et al.*,¹⁹ the direction of stimulus orientation was designated side-down when the head or spinous process of C₂ was rotated towards the side of the recorded unit, and side-up for rotations in the opposite sense. The phase angle of response was expressed in arc degrees with respect to the peak of side-down position of the head or neck, indicated by 0°. A coherence coefficient was computed to provide a measure of reliability between the input and output. We consider to be positive only those units displaying a stable resting discharge, and a response to successive cycles of stimulation with a coherence coefficient higher than 0.8, a sensitivity usually greater than 0.4, and a harmonic distortion less than 25%.

At the end of each penetration, the location of recorded units was marked and later identified on serial sections stained with the Neutral Red method. The vestibular nuclei were identified following the anatomical criteria described by Pompeiano and Brodal.²⁰ The criteria for the subdivision of the LVN into rostroventral and dorsocaudal parts can be found in previous papers.^{3,4}

RESULTS

General Considerations

The activity of 231 neurons identified histologically in the LVN has been recorded. These neurons have been separated into two main groups. In the first group, 100 units were obtained from preparations with the cerebellum intact. The LVN was subdivided anatomically into its rostroventral (cLVN; $n = 33$ units) and dorsocaudal (ILVN; $n = 67$ units) aspects, which are known to project to cervical and lumbosacral segments of the spinal cord, respectively. Thirty-five units were activated antidromically from the spinal cord and have been assigned to their division of the LVN. In the second group, 131 units were recorded in preparations following partial cerebellectomy, i.e., complete destruction of the vermal cortex of anterior lobe and the fastigial nuclei, and included 53 cLVN and 78 ILVN units. Ninety units were classified as vestibulospinal neurons. Neurons located in other vestibular nuclei have been excluded from this report.

Response Characteristics of LVN Neurons to Macular Vestibular Stimulation

Among the population of 231 units studied during sinusoidal tilt of the animal (0.026 Hz, 5 or 10°), the majority displayed a reliable periodic modulation of their firing rate to the stimulus both in preparations with intact cerebellum ($n = 75$, i.e., 75.0%) or with partial cerebellectomy ($n = 94$, i.e., 71.8%); the remaining units in either type of preparation were unaffected by this stimulus.

Three main points emerge upon inspection of the data of TABLE 1. First, the proportion of cLVN units responding to angular tilt was higher than that of ILVN units in both preparations. Second, the average response sensitivity of cLVN units was significantly greater than that of ILVN in both preparations

TABLE 1
RESPONSES OF LVN NEURONS TO SINUSOIDAL TILT OF THE ANIMAL (MACULAR VESTIBULAR INPUT) OR ROTATION OF THE NECK (NECK INPUT)
AT STANDARD PARAMETERS IN INTACT CEREBELLUM AND PARTIALLY CEREBELLECTOMIZED PREPARATIONS*

	Intact Cerebellum										Cerebellar Ablation									
	Macular Input					Neck Input					Macular Input					Neck Input				
	Anti-dromic LVN	cLVN	ILVN	ILVN	Total LVN	Anti-dromic LVN	cLVN	ILVN	ILVN	Total LVN	Anti-dromic LVN	cLVN	ILVN	ILVN	Total LVN	Anti-dromic LVN	cLVN	ILVN	ILVN	Total LVN
Number of units	35	33	67	100	35	33	67	100	35	33	67	100	90	90	131	90	90	131	90	131
Responsive (R) units	29	30	45	75	24	25	31	56	24	25	31	56	63	63	94	48	48	78	48	94
	(82.9%)	(90.9%)	(67.2%)	(75.0%)	(68.6%)	(75.8%)	(46.3%)	(56.0%)	(70.0%)	(77.4%)	(77.4%)	(77.4%)	(70.0%)	(70.0%)	(71.8%)	(53.3%)	(53.3%)	(51.3%)	(51.3%)	(48.9%)
Nonresponsive units	6	3	22	25	11	8	36	44	11	8	36	44	27	27	37	42	42	29	38	67
	(17.1%)	(9.1%)	(32.8%)	(25.0%)	(31.4%)	(24.2%)	(53.7%)	(44.0%)	(30.0%)	(22.6%)	(22.6%)	(22.6%)	(30.0%)	(30.0%)	(28.2%)	(46.7%)	(46.7%)	(48.7%)	(48.7%)	(51.1%)
Firing rate of R-units in impulses/sec.	38.6	46.9	39.0	42.2	35.6	45.1	40.6	42.6	37.4	37.4	27.4	39.6	34.3	36.2	29.2	36.2	29.2	38.5	35.0	35.0
	± 43.3	± 61.4	± 43.0	± 50.4	± 28.2	± 38.3	± 36.1	± 37.0	± 25.1	± 21.2	± 21.2	± 29.0	± 25.6	± 24.7	± 20.0	± 24.6	± 20.0	± 24.6	± 22.9	± 22.9
and (mean \pm SD)																				
Sensitivity of R-units (mean \pm SD)	2.66	3.72	1.82	2.58	2.64	3.89	2.36	3.04	1.84	3.45	1.54	2.37	1.49	1.88	1.38	1.57	1.70	1.70	1.70	1.57
	± 2.93	± 3.41	± 1.86	± 2.73	± 2.35	± 4.96	± 2.22	± 3.75	± 2.60	± 3.36	± 1.65	± 2.40	± 2.67	± 2.67	± 1.70	± 2.06	± 2.06	± 2.06	± 2.06	± 2.06
Gain of R-units (mean \pm SD)	0.42	0.54	0.29	0.39	0.40	0.56	0.41	0.48	0.30	0.40	0.25	0.31	0.23	0.23	0.21	0.22	0.23	0.21	0.22	0.22
	± 0.22	± 0.53	± 0.30	± 0.41	± 0.63	± 0.84	± 0.39	± 0.59	± 0.32	± 0.45	± 0.28	± 0.33	± 0.22	± 0.22	± 0.24	± 0.26	± 0.24	± 0.24	± 0.24	± 0.26
From +45° lead to -45° lag	15	13	19	32	10	10	8	18	20	20	18	38	12	12	5	10	10	10	10	15
	(51.7%)	(43.3%)	(42.2%)	(42.7%)	(41.7%)	(40.0%)	(25.8%)	(32.1%)	(31.7%)	(48.8%)	(34.0%)	(40.4%)	(25.0%)	(25.0%)	(20.8%)	(25.0%)	(25.0%)	(25.0%)	(25.0%)	(23.4%)
From +135° lead to -135° lag	2	7	6	13	11	7	18	23	35	13	32	45	23	23	13	20	20	20	20	33
	(6.9%)	(23.3%)	(13.3%)	(17.3%)	(45.8%)	(28.0%)	(51.6%)	(41.1%)	(55.6%)	(31.7%)	(60.4%)	(47.9%)	(47.9%)	(47.9%)	(50.0%)	(50.0%)	(50.0%)	(50.0%)	(50.0%)	(51.6%)
From +45° to +135° and from -45° to -135°	12	10	20	30	3	8	7	15	8	8	3	11	13	13	6	10	10	10	10	16
	(41.4%)	(33.3%)	(44.5%)	(40.0%)	(12.5%)	(32.0%)	(22.6%)	(26.8%)	(12.7%)	(19.5%)	(5.6%)	(11.7%)	(27.1%)	(27.1%)	(25.0%)	(25.0%)	(25.0%)	(25.0%)	(25.0%)	(25.0%)

*Abbreviations used: LVN, lateral vestibular nucleus; cLVN and ILVN, rostral and dorsocaudal parts of LVN, respectively; gain, change of mean firing rate per degree of peak displacement; sensitivity, percentage change of mean firing rate per degree. Phase angle of the first harmonic of responses is relative to ipsilateral side-down displacement.

($p < 0.01$, t-test for difference of means); no significant difference in response sensitivity was observed between the two preparations for each respective subdivision of the LVN as well as the whole population of LVN neurons (FIGURE 1A), or in mean firing rates within and across the two populations of units. And third, the majority of responding units were maximally excited by the direction of

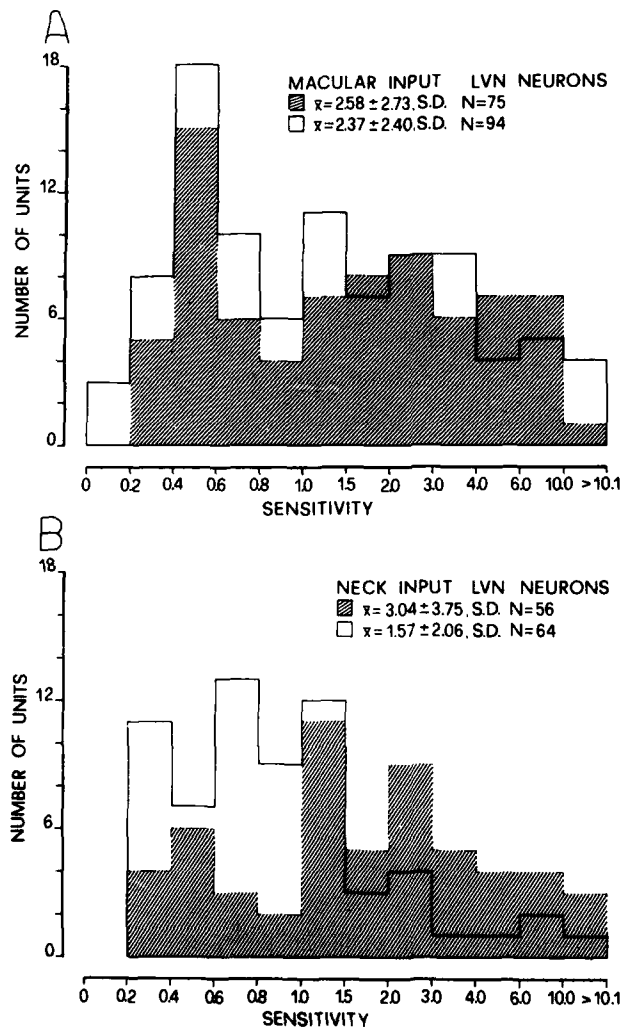


FIGURE 1. Response sensitivity of LVN units to individual macular vestibular (A) and neck (B) stimulation. Histograms plot the sensitivity of unit responses to selective stimulation of macular vestibular or neck receptors at standard parameters (10° peak displacement at 0.026 Hz) in preparations with intact cerebellum (hatched columns) or following partial cerebellectomy (white columns). Values in this and subsequent figures refer to the first harmonic of responses.

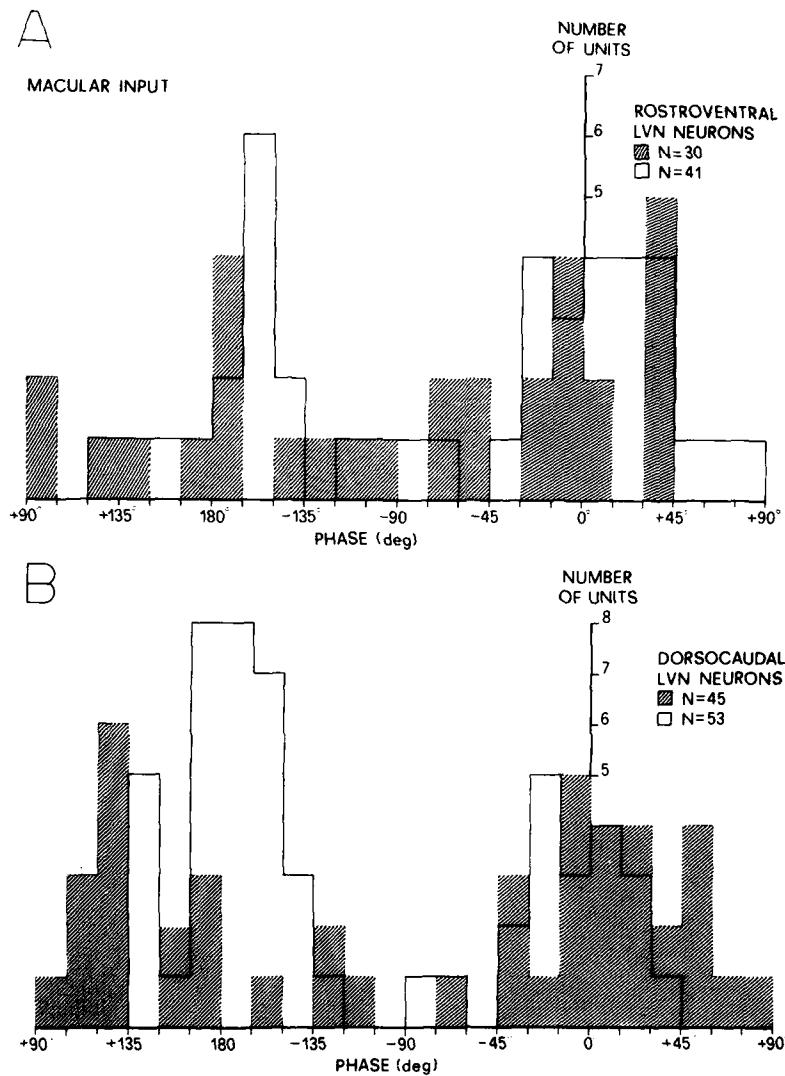


FIGURE 2. Distribution of the phase angle of unit responses in the cLVN (A) and lLVN (B) to sinusoidal macular stimulation. The units were tested during lateral tilting of the animal at standard parameters. Positive numbers in abscissae indicate in degrees the phase lead, whereas negative numbers indicate the phase lag of responses with respect to extreme side-down position of the animal, as indicated by 0° . The units were recorded either in preparations with intact cerebellum (hatched columns) or after partial cerebellectomy (white columns). Values ranging from $+90^\circ$ to 180° , representing phase lags from the peak of side-up position of the animal, have been plotted at the left-hand side of each histogram to better illustrate unit responses for this direction of stimulus orientation.

stimulus orientation both in intact cerebellum ($n = 45$, i.e., 60.0%) or partial cerebellectomized ($n = 83$, i.e., 88.3%) preparations.

This last point, i.e., the phase relation of unit response during angular tilt, deserves a more detailed description. FIGURE 2 demonstrates that following partial cerebellectomy, the proportion of unit responses related to the direction of animal orientation was higher than in preparations with intact cerebellum, particularly at the level of ILVN (94.4% and 55.5%, respectively). Furthermore, within the cLVN, units responding with an increased firing rate during side-down and a reduction during side-up tilt (alpha response) predominated over those displaying the opposite pattern of response (beta response) in both types of preparations (FIGURE 2A). On the other hand, within the ILVN, there was a predominance of the alpha over the beta responses in preparations with intact cerebellum, whereas after partial cerebellectomy, the majority of unit responses were of the beta type and only three (5.6%) neurons showed a response that was not closely related to either direction of stimulus orientation (FIGURE 2B).

In summary, both the sensitivity and the proportion of units responding to angular tilt were greater within the cLVN than the ILVN in preparations with intact cerebellum; the corresponding parameters were not modified greatly after partial cerebellectomy. The preferred direction of stimulus orientation to elicit unit responses was side-down tilt for both divisions of LVN in intact cerebellum preparations. After partial cerebellectomy, cLVN units maintained this phase relationship. However, concerning the ILVN units, most of the responses at phase angles intermediate between the two extreme positions of tilt in preparations with the cerebellum intact became related to the side-up direction of tilt following partial cerebellectomy.

Response Characteristics of LVN Units to Neck Stimulation

Among the population of units studied at standard parameters ($n = 231$), approximately one-half responded to neck rotation in both preparations (TABLE 1). The major findings are the following. In intact cerebellum preparations, the proportion of cLVN units (75.8%) responding to neck rotation was higher than that of ILVN units (46.3%); no significant difference was observed in their response sensitivities. Following partial cerebellectomy, a significant reduction of response sensitivity within both divisions of the LVN was observed (FIGURE 1B; $p < 0.05$, t-test for difference of means). Similar to the macular responses, the majority of units responded preferentially to the direction of neck orientation both in intact cerebellum (73.2%) and partial cerebellectomized (75.0%) preparations.

Concerning the phase relation of responses (FIGURE 3), the majority of units by two fold responded preferentially to side-up orientation of the neck, the only exception being within the cLVN in preparations with intact cerebellum. This latter group of neurons underwent the most detectable changes after partial cerebellectomy: a reduced proportion of responding units (45.3% compared to 75.8%), a decreased response sensitivity (1.88 ± 2.67 standard deviation compared to 3.89 ± 4.98 SD), and a reversal of the preferred direction of neck orientation were observed. This latter effect is illustrated in FIGURE 3A.

In summary, in the absence of the paleocerebellum, there was a reduction in sensitivity of unit responses during neck rotation. Concomitant changes in phase

relation of unit responses were also observed within the cLVN. This contrasts with the results obtained during macular stimulation in which no change in response sensitivity was found in both divisions of the LVN following partial cerebellectomy. On the other hand, changes in the phase relation of unit responses were observed only in the lLVN.

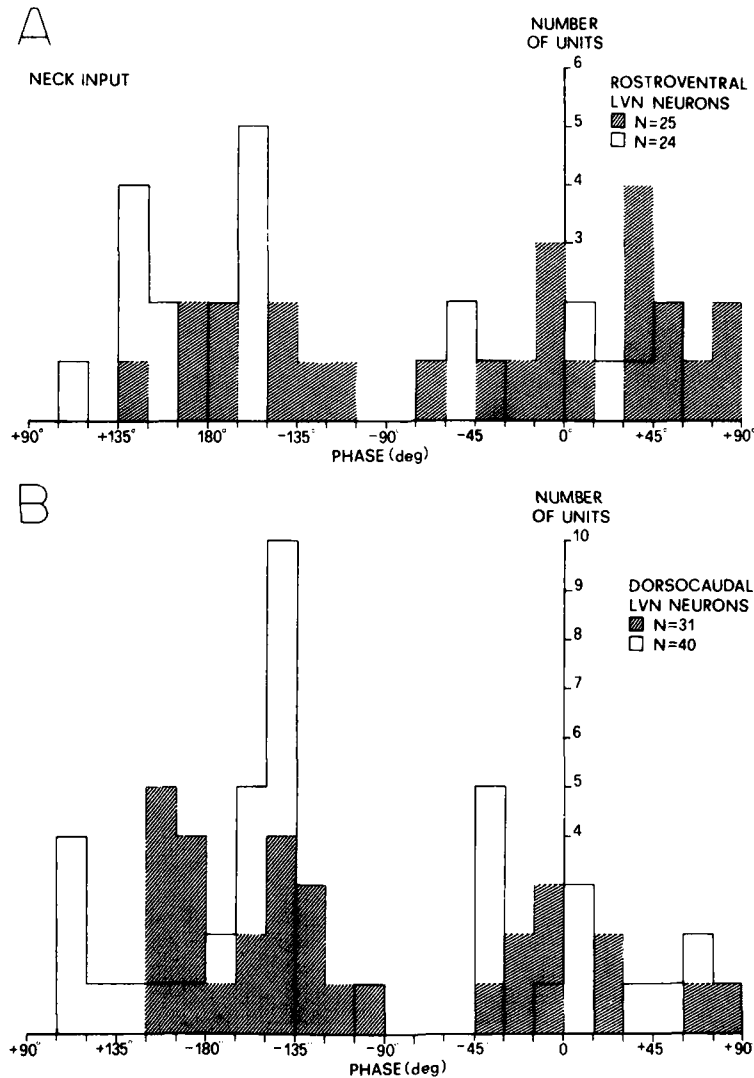


FIGURE 3. Distribution of the phase angle of unit responses in the cLVN (A) and lLVN (B) to sinusoidal neck rotation. The units were tested during neck rotation at standard parameters. Description as in FIGURE 2.

TABLE 2
CONVERGENCE OF BOTH MACULAR AND NECK INPUTS AT STANDARD PARAMETERS ON LVN NEURONS
IN INTACT CEREBELLUM AND PARTIALLY CEREBELLECTOMIZED PREPARATIONS*

	Intact Cerebellum				Cerebellar Ablation			
	Antidromic LVN	cLVN	ILVN	Total LVN	Antidromic LVN	cLVN	ILVN	Total LVN
Number of units	35	33	67	100	90	53	78	131
Units responsive to both inputs	22 (62.9%)	24 (72.7%)	28 (41.8%)	52 (52.0%)	44 (48.9%)	24 (45.3%)	35 (44.9%)	59 (45.1%)
Units responsive to macular input only	7 (20%)	6 (18.2%)	17 (25.4%)	23 (23.0%)	19 (21.1%)	17 (32.1%)	18 (23.1%)	35 (26.7%)
Units responsive to neck input only	2 (5.7%)	1 (3.0%)	3 (4.5%)	4 (4.0%)	4 (4.4%)	0 (0.0%)	5 (6.4%)	5 (3.8%)
Units not responsive to both inputs	4 (11.4%)	2 (6.1%)	19 (28.3%)	21 (21.0%)	23 (25.6%)	12 (22.6%)	20 (25.6%)	32 (24.4%)
S_N/S_M (mean \pm SD)	1.85 \pm 1.67	0.95 \pm 0.79	2.52 \pm 1.86	1.79 \pm 1.37	1.41 \pm 1.73	0.90 \pm 0.85	1.82 \pm 1.95	1.45 \pm 1.50
$\Delta\phi > 90^\circ$ (mean \pm SD)	148.4 \pm 21.3° n = 12	146.2 \pm 21.3° n = 14	142.4 \pm 23.6° n = 19	144.0 \pm 22.6° n = 33	135.3 \pm 29.8° n = 22	139.9 \pm 29.7° n = 12	132.9 \pm 29.4° n = 19	135.6 \pm 29.5° n = 31
$\Delta\phi < 90^\circ$ (mean \pm SD)	42.6 \pm 17.9° n = 10	46.5 \pm 26.5° n = 10	46.5 \pm 22.5° n = 9	46.5 \pm 24.6° n = 19	38.2 \pm 23.5° n = 22	23.9 \pm 17.1° n = 12	42.0 \pm 23.9° n = 16	34.2 \pm 21.0° n = 28
Ipsi-macular Contra-neck	4 (11.2%)	5 (20.8%)	7 (25.0%)	12 (23.1%)	5 (11.4%)	7 (29.2%)	3 (8.6%)	10 (16.95%)
Contra-macular Ipsi-neck	1 (4.5%)	1 (4.2%)	1 (3.6%)	2 (3.8%)	9 (20.5%)	2 (8.3%)	8 (22.9%)	10 (16.95%)
Ipsi-macular Ipsi-neck	7 (31.8%)	4 (16.7%)	5 (17.8%)	9 (17.3%)	2 (4.5%)	1 (4.2%)	1 (2.8%)	2 (3.4%)
Contra-macular Contra-neck	0 (0.0%)	0 (0.0%)	1 (3.6%)	1 (1.9%)	13 (29.5%)	5 (20.8%)	12 (34.3%)	17 (26.8%)
Not positional	10 (45.5%)	14 (58.3%)	14 (50.0%)	28 (53.9%)	15 (34.1%)	9 (37.5%)	11 (31.4%)	20 (33.9%)

*Abbreviations used: S_N/S_M , ratio between sensitivity of neck responses (S_N) and sensitivity of macular responses (S_M); $\Delta\phi$, difference in phase angles between macular and neck responses ($\Delta\phi > 90^\circ$, reciprocal responses; $\Delta\phi < 90^\circ$, parallel responses); Ipsi-macular and Ipsi-neck, units excited during side-down (from $+45^\circ$ lead to -45° lag) tilt of the whole animal or rotation of the neck; Contra-macular and Contra-neck, units excited during side-up (from $+135^\circ$ lead to -135° lag) animal tilt or neck rotation; not positional, units whose response to one or both inputs showed phase angles intermediate between the values reported above.

Convergence of Both Macular and Neck Inputs on LVN Neurons

Approximately one-half of the units in both preparations responded to independent stimulation of both receptors (TABLE 2). In preparations with intact cerebellum, the percentage of units receiving a convergent input was greater within the cLVN (72.7%) than the lLVN (41.8%). This relationship vanished after partial cerebellectomy. Fewer cLVN units (45.3%) responded to both inputs in the latter preparations, thus reaching the proportion found for the lLVN units (44.9%). Nevertheless, the average ratio of sensitivity of the neck responses over macular responses (S_N/S_M) was greater by two fold within the lLVN than the cLVN in both preparations ($p < 0.01$, t-test for difference of means). This latter finding indicates that regardless of the anatomical integrity of the cerebellum, there is a greater influence of the macular signal on the neck and forelimb region of the LVN (cLVN), whereas the neck input is more effective on the hindlimb region of the LVN (lLVN).

From the polar diagram and histogram in FIGURE 4A (see also TABLE 2), it appears that the majority of units (33/52, i.e., 63.5%) in intact cerebellum preparations displayed responses that were roughly out of phase with one another with an average difference in phase angle ($\Delta\phi$) of $144.0 \pm 22.6^\circ$ SD; the preferred unit response in both divisions of the LVN in these preparations was characterized by excitation during side-down tilt of animal and side-up neck rotation. On the other hand, the remaining units (19/52, i.e., 36.5%) showed parallel responses to the two inputs with an average $\Delta\phi$ of responses of $46.5 \pm 24.6^\circ$ SD. Following partial cerebellectomy, the units tested to the two inputs were distributed equally between the two groups showing reciprocal ($\Delta\phi > 90^\circ$) or parallel ($\Delta\phi < 90^\circ$) responses. The major observation following this lesion was the dramatic increase in number of units responding preferentially to both side-up tilt of animal and side-up neck rotation (28.8%), as opposed to that observed in intact cerebellum preparations (1.9%; see FIGURE 4B and TABLE 2).

Interaction of Macular and Neck Responses during Head Rotation

Among the 111 LVN units receiving a convergent input from macular and neck receptors in both preparations, 52 also were examined in detail during combined receptor activation elicited by head rotation at standard parameters. Of this sample, 36 units (23 of which were recorded after partial cerebellectomy) were identified antidromically as vestibulospinal neurons.

The 52 unit responses to head rotation were usually in good agreement with those predicted as a result of vectorial summation of responses to the individual macular and neck inputs. This finding was observed in the two divisions of the LVN in both preparations, regardless of the fact that the two inputs produced reciprocal ($n = 27$) or parallel ($n = 25$) responses. FIGURE 5 plots the predicted (vectorial) values of both the sensitivity (A) and phase angle (B) of responses against the corresponding values obtained experimentally during head rotation; the degree of correspondence was striking for both functions ($\chi^2 < 0.01$). In fact, the difference between the actual and predicted response sensitivities corresponded on the average to $20.3 \pm 14.6\%$ SD, and the difference between the actual and predicted phase angles of responses averaged $8.8 \pm 11.8^\circ$ SD.

FIGURE 6 presents the data of the 52 units in a three-dimensional diagram. It can be seen from the figure that when the responses of a unit to the macular and neck inputs are about 180° out of phase, the more prominent the response

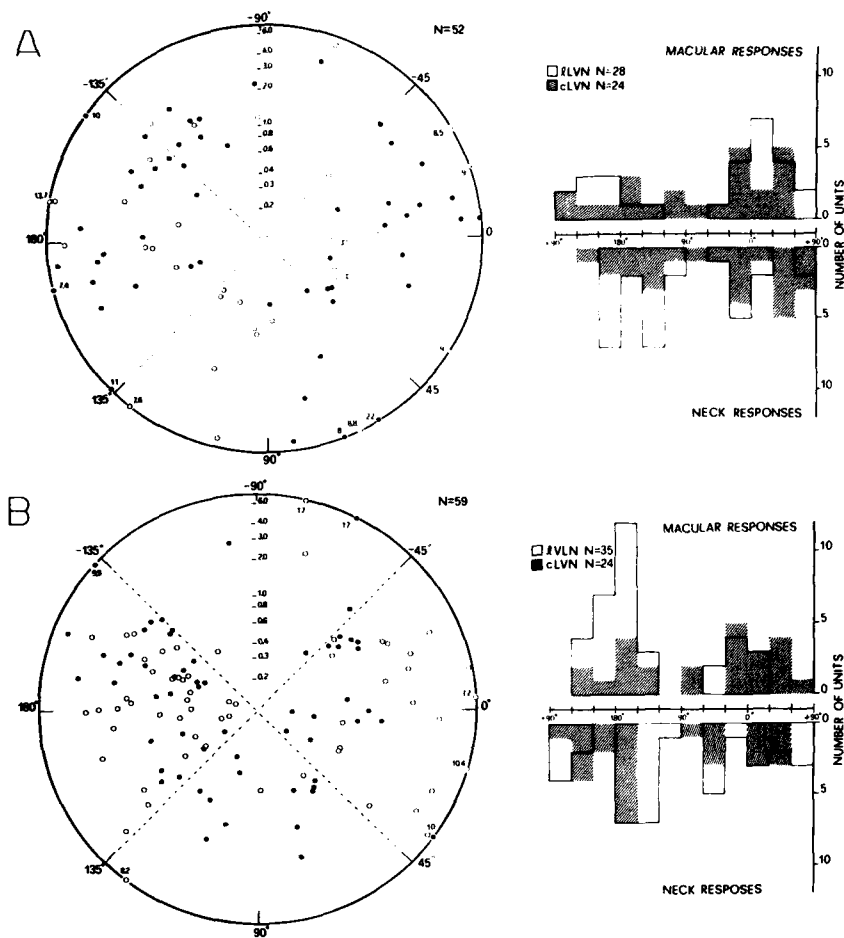


FIGURE 4. Responses of LVN neurons receiving convergent inputs from macular and neck receptors, both in preparations with intact cerebellum (A) and with partial cerebellectomy (B). Each unit responded to both neck input (dots) and macular input (circles). The sensitivity of responses of each unit to individual inputs is indicated by the distance of the corresponding symbol from the center of the diagram (see the scale along vertical meridian). The relative position of each symbol from 0° meridian indicates in degrees the phase lead (positive values) or phase lag (negative values) of the peak of response with respect to peak of side-down displacement either of the animal or of the neck only. The histograms on the right-hand side of each polar diagram provide the phase angle distribution of unit responses to each input in both preparations.

sensitivity to one input over the other, the smaller was the difference in phase angle of response to head rotation with respect to that elicited by the prominent input. This finding is illustrated by the population of 11 units located in the lower left-hand corner along the x-axis. On the other hand, when the response sensitivities to macular and neck inputs were comparable, the phase angle of

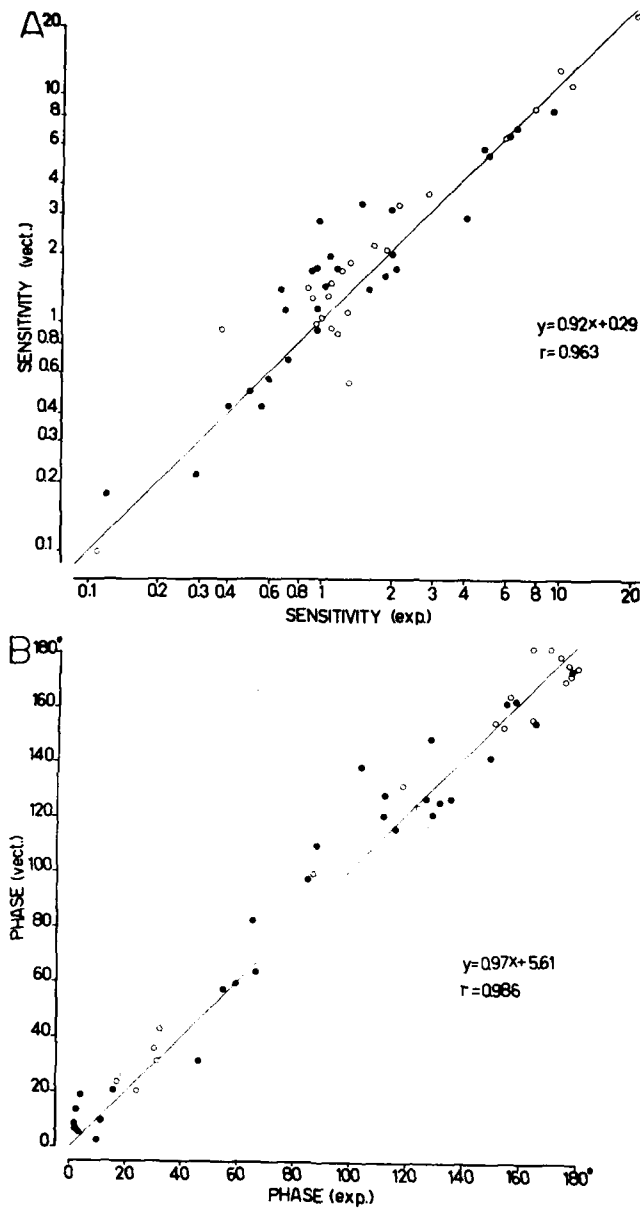


FIGURE 5. Comparison between the experimental parameters of responses of LVN neurons to combined stimulation of neck-macular receptors and the corresponding predicted values. Among the 52 LVN units receiving a convergent input from both neck and macular receptors, 29 (dots) were recorded in preparations with intact cerebellum and 23 (circles) after partial cerebellectomy. Both sensitivity (A) and phase angle (B) of responses to combined neck-macular inputs (exp.) have been plotted against the corre-

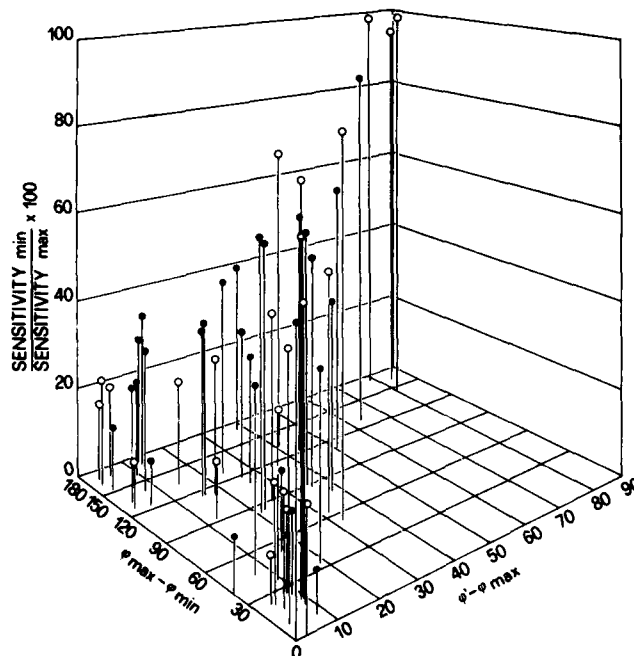


FIGURE 6. Three-dimensional diagram relating response characteristics of LVN neurons to neck, macular, and combined inputs. Of 52 unit responses to individual stimulation of macular and neck receptors (0.026 Hz, 5 or 10°), 28 (dots) displayed a higher response sensitivity to neck input than to macular input, while 24 (circles) showed a predominance of the macular over neck response. The same units shown in FIGURE 5 are plotted here irrespective of the preparation from which they were collected. $\text{Sensitivity}_{\min} / \text{Sensitivity}_{\max} \times 100$: percent ratio of response sensitivities to the least and most effective (macular or neck) input, respectively. $\phi_{\max} - \phi_{\min}$: difference in degrees between phase angles of responses of same units to the most and least effective input, respectively. $\phi - \phi_{\max}$: difference in degrees between phase angle of response elicited by combined receptor stimulation (head rotation) and phase angle of response of same unit to the most effective (macular or neck) input alone, respectively. Additional explanation in text.

response to head rotation approached an intermediate value (about 90°) in those instances in which the responses were almost in opposition of phase; however, this value progressively decreased below 90° when the phase angles of the two separate responses became more and more in phase. This is actually what one would expect on the basis of a vectorial summation of responses.

FIGURE 7 illustrates the cancelation of a unit response during combined receptor activation (head rotation). In this instance, the responses of the same unit to individual macular and neck inputs were of approximately equal magni-

sponding components of the vector (vect.) calculated by summation of the two separate responses. Linear regression and correlation coefficient functions for all the recorded units are indicated. The lines of slope 1 would apply if experimental and predicted sensitivities and phase angles of responses were equal.

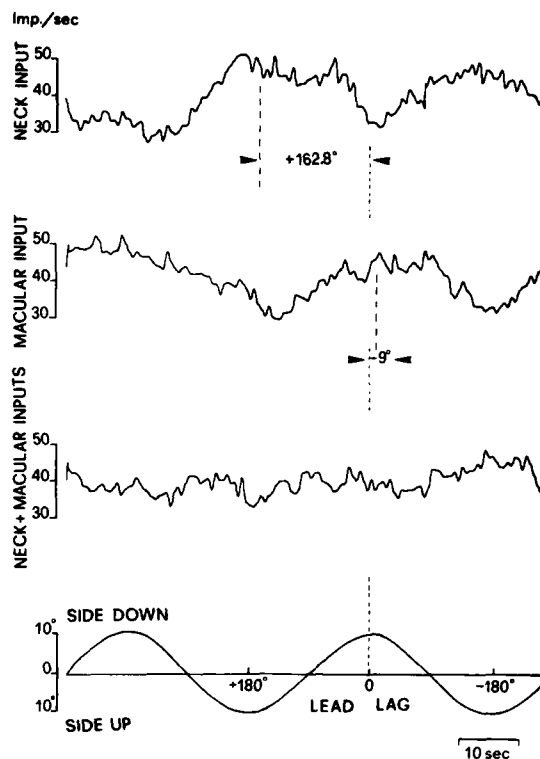


FIGURE 7. Cancellation of the reciprocal neck and macular responses of a vestibulospinal neuron during head rotation. SPDH averaged over five sweeps (128 bins, 0.6-second bin width) showing the responses of an LVN unit to sinusoidal stimulation of neck, macular, and combined receptors at standard parameters. Lower trace indicates animal position. The mean firing rate of unit was 40.8 impulses/second. The neuron received a convergent input from both types of receptors and displayed a response of approximately equal magnitude to both the neck input (sensitivity, 1.44) and macular input (sensitivity, 1.40), but the responses were reciprocally arranged ($\Delta\phi \sim 171.8^\circ$). Phase angle of unit response to each input is indicated by dashed lines. The responses to individual neck and macular inputs were highly coherent (>0.9) and were suppressed when both inputs were elicited during head rotation.

tude but 180° out of phase, and as a consequence, the unit displayed no modulation of firing rate during head rotation. This was not a common observation because one input normally dominated over the other and the phase angles of responses usually were not in perfect opposition of phase (see FIGURE 6).

In addition to the units reported above, 65 units were studied during head rotation. In these instances, the units were unresponsive to one or both stimuli. For example, when one input alone was effective, the unit response during head rotation closely mimicked that obtained for the individual (effective) input. Two examples of this type of response are illustrated in FIGURE 8. Further, it was observed that when the unit responses to both individual inputs were negligible, a reliable response could be elicited during head rotation, suggesting that both

inputs—subliminal on these units when taken individually—now became effective.

The responses of vestibulospinal neurons to macular, neck, and combined inputs finally were examined against changes in frequency of stimulation. FIGURE 9 illustrates the results obtained from two of these units in preparations with intact cerebellum (A) or with partial cerebellectomy (B). Maximum angular acceleration ranged from 0.02 to 8.9°/second² for the former and from 0.9 to 8.9°/second² for the latter unit. The phase relation and sensitivity of unit response to combined stimulation of both macular and neck receptors (●) approximated that predicted vectorially (×) over the range of frequencies

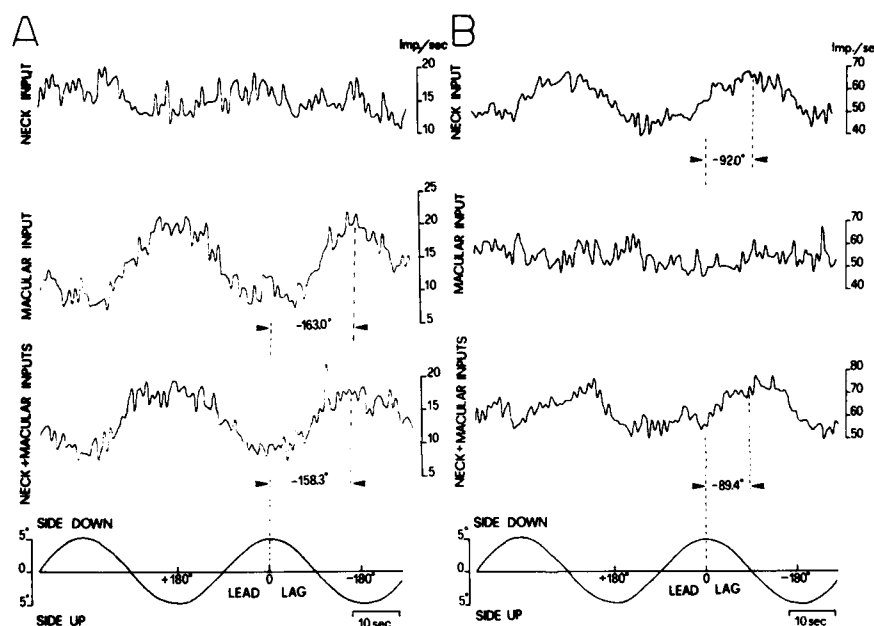


FIGURE 8. Unit responses during head rotation of vestibulospinal neurons receiving only one separate input. SPDH showing the changes in discharge rate of two vestibulospinal neurons located in the rostroventral (A) and dorsocaudal (B) part of the LVN during sinusoidal rotation at 0.026 Hz, 5° of body alone (neck input), of both head and body (macular input), and of head alone (neck + macular inputs). Five sweeps were accumulated for each record (128 bins, 0.6-second bin width). The lowest traces signal the direction and amplitude of displacement of the neck and/or head during the different experimental conditions. A: the unit response to neck input (upper record) was negligible (coherence coefficient, 0.60). The response to macular input (middle record) had a sensitivity of 8.0 and a phase lag of -163.0° , and that to combined neck and macular inputs had a sensitivity of 6.7 and a phase lag of -158.3° . These responses to successive cycles were highly coherent (0.992 and 0.999, respectively). B: the unit response to macular input (middle record) was negligible (coherence coefficient, 0.42). The response to neck input (upper record) had a sensitivity of 2.2 and a phase lag of -92.0° and was comparable to the response to both neck and macular inputs, which had a sensitivity of 1.43 and a phase lag of -89.4° . These responses to successive cycles were highly coherent (0.970 and 0.960, respectively). The mean discharge rate of unit A was 14.8 impulses/second, and that of unit B was 56.3 impulses/second, and both remained constant throughout the experiment.

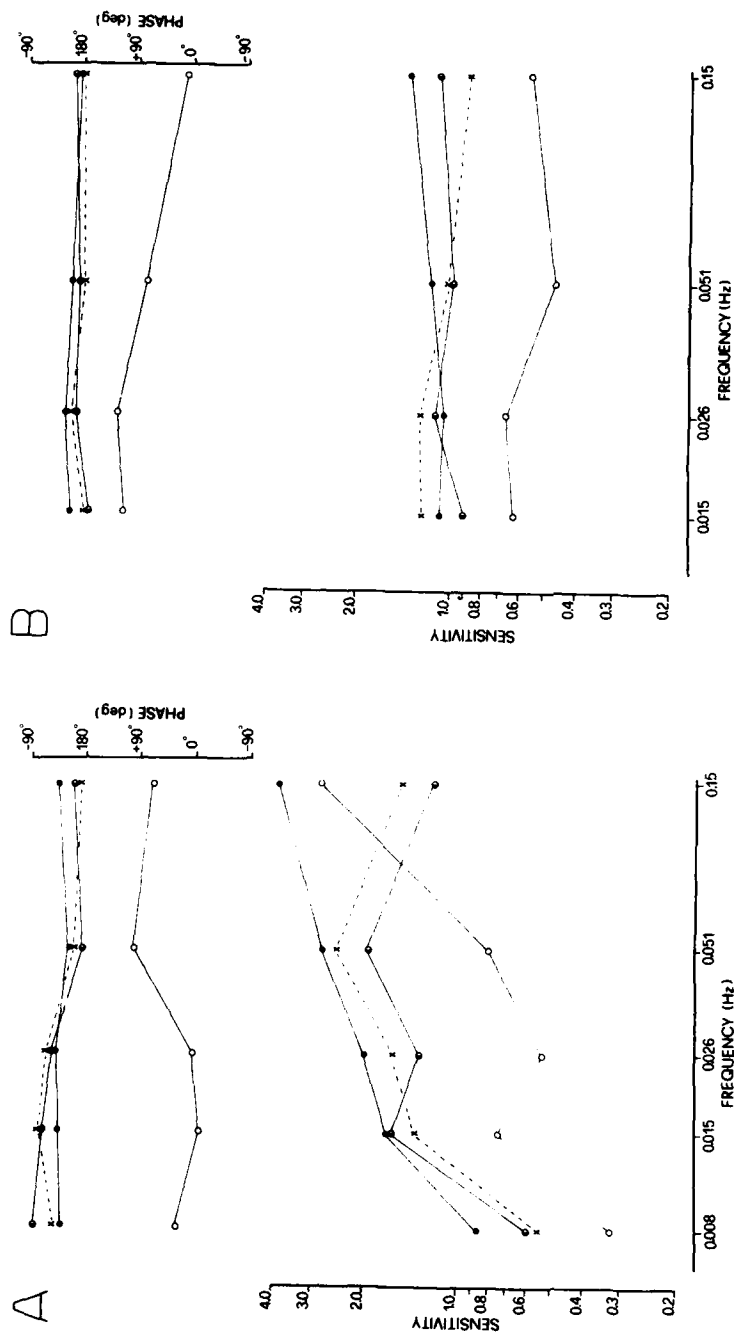


FIGURE 9. Interaction of neck-vestibular inputs in LVN neurons at changing frequencies of stimulation in preparations with intact cerebellum (A) and following partial cerebellectomy (B). The sensitivity (lower diagrams) and phase relation (upper diagrams) of response of individual vestibulospinal neurons located in the cLVN (A) and ILVN (B) have been evaluated during sinusoidal rotation at peak amplitude of 10° for increasing frequencies of displacement of the body alone (neck responses, dots), of both head and body (vestibular responses, circles), and of head alone (neck + vestibular responses, \circ). The predicted vectorial responses of the same unit to combined neck and vestibular stimulation for increasing frequency of head rotation are indicated by crosses. The sensitivity of responses is expressed in percentage change of mean firing rate per degree of rotation; phase angle of responses is expressed in degrees of phase lead (positive values) or lag (negative values) with respect to peak of side-down position, indicated by 0° .

employed for both populations of units, again indicating that the unit response is the result of a predictable integration of the two inputs regardless of the particular dynamics of each frequency response.

DISCUSSION

At maximum angular accelerations of animal tilt employed here, i.e., less than or equal to $0.26^\circ/\text{second}^2$, the responses of LVN neurons can be attributed in large part to stimulation of macular vestibular receptors³⁰ (cf., Reference 30). The unit responses elicited during neck rotation can be considered the result of stimulation of deep neck receptors, i.e., joint and/or muscle spindle receptors related to atlanto-occipital and atlantoaxial membranes innervated from dorsal root ganglia C₁-C₂,^{24,31} in the absence of inputs from the labyrinth or skin of neck (cf., Reference 4). Our experimental paradigm to elicit the neck input should not be confused with that employed by others who used entire neck rotation, thereby permitting larger amplitudes of displacement.¹¹

A main result of the present study is the demonstration that a large proportion of LVN neurons in the presence or absence of the paleocerebellum responded with a periodic modulation of their firing rates to both types of tests, whereas fewer units responded to the macular or neck input alone. Therefore, selective elaboration either of the macular input or, to a lesser extent, neck input is rather uncommon in the investigated area. Further, unit responses to combined stimulation of both types of receptors elicited during head rotation closely corresponded to those obtained by vectorial summation of the individual neck and macular responses. This additive mode of interaction of inputs was observed in both divisions of the LVN in the two different preparations.[‡] However, the possibility that a multiplicative process may occur under parameters of neck-vestibular stimulation different from those employed here cannot be excluded by our experiments.²⁸

Sensitivity of LVN Unit Responses to Macular and Neck Stimulation

A major finding emerges when the response sensitivity of LVN neurons to individual macular and neck stimulation is compared across the two preparations used in the present experiments. Not surprising, the sensitivity of LVN neurons to the macular input was unmodified following partial cerebellectomy, since primary vestibular afferents innervating the macular receptors impinge monosynaptically but also disynaptically on LVN neurons (cf., Reference 43). On the other hand, the sensitivity of LVN units to neck stimulation was reduced significantly by one-half following partial cerebellectomy. This finding can be attributed to the fact that the neck input is not transmitted directly to the LVN, as described for the macular signal, but by way of both reticular (cf., Reference 5) and cerebellar (cf., Reference 6) structures.

Regional differences of unit responses to both stimuli were found within the rostroventral (cLVN) and dorsocaudal (lLVN) aspects of Deiters' nucleus, which are known to project to cervical and lumbosacral segments of the spinal cord, respectively.²⁹ A comparison of unit responses in these divisions may help us to understand the role of LVN in the tonic labyrinth and neck reflexes acting on

[‡]A similar vectorial addition of separate responses of vestibular nuclear neurons to ampullar and visual inputs recently has been reported.¹⁸

neck and limb extensors in decerebrate cats.^{7,18,19,22-24,32,41,42} As expected, the proportion of units responsive to the macular input and their sensitivity were greater in the cLVN than in the lLVN in both preparations (see TABLE 1, cf., References 3 and 27), since the former division represents the primary site of termination of first-order afferents from macular receptors (cf., Reference 43). A similar observation concerning the proportion of responding units also was found for the neck input in preparations with intact cerebellum. These findings may explain why tonic labyrinth and neck reflexes are more effective on neck and forelimb extensor muscles than on hindlimb extensors.

Although the two inputs were particularly effective on the cLVN, their relative distribution, as evaluated from the ratio S_N/S_M , was not comparable for cLVN and lLVN neurons receiving a convergent input from both sources. Our findings indicate that the macular input has a relatively greater influence on the cLVN, whereas the neck input, due to a dramatic reduction of the macular signal, has a predominant influence on the lLVN.

Phase Relation of LVN Unit Responses to Macular and Neck Stimulation

The majority of LVN units were excited preferentially by the direction of animal or neck orientation in both preparations. In preparations with intact cerebellum, the majority of unit responses were characterized by excitation during side-down tilt of animal and side-up neck rotation. These unit responses, which were approximately out of phase ($\Delta\phi > 90^\circ$), are appropriate for the observed asymmetric changes in postural activity of fore- and hindlimb muscles during the tonic labyrinth and neck reflexes. Since the LVN exerts an excitatory influence on ipsilateral extensor motoneurons²¹ (cf., References 28 and 43), unit responses in this nucleus may explain why side-down tilt produces contraction of ipsilateral and relaxation of contralateral limb extensors¹⁹ (cf., however, Reference 37) whereas side-down neck rotation produces the opposite posture.^{7,18,22-24} The persistence of a residual response of LVN units during combined macular and neck stimulation appears in contrast with the observation that in decerebrate animals changes in head position leave the status of the limbs unmodified³² (cf., also, References 1 and 10). From our experiments, the cancelation of a unit response during head rotation in the LVN could occur only if both afferent signals were of equal magnitude and 180° out of phase. Although this was observed in isolated instances, the majority of unit responses to the two inputs were neither of equal magnitude nor perfectly out of phase. Therefore, a final integration of both inputs leading to resolution of the conflicting influences probably occurs at segmental levels in the spinal cord.

The functional significance of LVN units showing parallel responses to macular and neck stimulation ($\Delta\phi < 90^\circ$) would be better understood if a more detailed knowledge of the muscle field(s) under the control of individual LVN units were available. It is tempting to suggest that these units intervene in synergistic influences of both macular and neck receptors on some limited groups of motoneurons controlling neck, axial, and/or limb muscles. Unfortunately, the exact projection of these neurons to the spinal cord is not known, nor are the muscle fields under their control.

Major changes in phase angle distribution were observed following partial cerebellectomy. These differences were confined mainly to the dorsocaudal (lLVN) aspect of Deiters' nucleus (see TABLE 1) concerning macular responses, but were most evident in units located in the rostroventral (cLVN) aspects of

Deiters' nucleus concerning neck responses. Both these findings may explain why the reciprocal arrangement of macular and neck responses is reduced in this preparation. Opposite patterns of responses to individual macular and neck inputs were recorded from Purkinje (P) cells of the cerebellar vermis projecting to the LVN as well as from the fastigial nucleus,^{8,9,38,39} i.e., from that corticonuclear region destroyed in the present experiments, indicating that cerebellar processing may participate in the production of reciprocal changes in firing rate of LVN neurons for the same direction of animal or neck rotation. Vectorial addition also was observed during combined receptor activation in these P-cells and fastigial neurons. Indeed, the anatomical integrity of the cerebellum is important to produce reciprocal responses of LVN neurons and forelimb muscles during vestibular stimulation.^{2,14,20}

In conclusion, the present findings indicate that interaction of both macular and neck inputs fulfills the requirements of linear summation and the recorded units are capable of monitoring the absolute position of head and body in space and relative to each other. The anatomical integrity of the cerebellum is not essential for this additive mode of interaction of inputs, but has an important influence on the phase relation and/or sensitivity of LVN unit responses during macular or neck stimulation and may have a regulating action on the limb musculature during the tonic labyrinth and neck reflexes. In this context, the design of additional experiments to study the gain and phase adjustments exerted by cerebellar structures on postural mechanisms offers new possibilities of extending our observations.

SUMMARY

1. The role of the paleocerebellum in determining the responses of lateral vestibular nucleus (LVN) neurons either to independent or combined stimulation of macular vestibular and neck receptors has been investigated in decerebrate cats. Sinusoidal rotation around the longitudinal axis at 0.026 Hz, 5-10°, represented the constant input parameters. Among the tested neurons, 100 and 131 units were recorded in animals with intact cerebellum and following partial cerebellectomy, respectively. The units were classified according to their anatomical location in either the rostroventral (cLVN) or dorsocaudal (lLVN) part of the LVN; units also were activated antidromically from the spinal cord.

2. The majority of units responded to stimulation of macular receptors both in preparations with intact cerebellum (75.0%) or with partial cerebellectomy (71.8%), the response being primarily in phase with the direction of animal orientation. The proportion of responding units and their response sensitivity were greater in the cLVN than lLVN in each preparation; no significant differences in mean firing rate and response sensitivity were observed between the two preparations for each subdivision of the LVN. In animals with cerebellum intact, the majority of cLVN and lLVN units were excited during side-down tilt; following partial cerebellectomy, this predominant response pattern still was present in cLVN but was reversed in lLVN.

3. About one-half of the units responded to sinusoidal stimulation of neck receptors in both preparations, the response being mainly in phase with the direction of neck orientation. In the intact cerebellum preparations, the proportion of cLVN units responding to neck rotation was greater than that of lLVN units, but no difference in response sensitivity was observed between these units.

Following partial cerebellectomy, the proportion of cLVN units responsive to the neck input was reduced but that of lLVN units was not; however, the average response sensitivity was halved for both cLVN and lLVN units. In preparations with cerebellum intact, most of the cLVN units were excited during side-down neck rotation, whereas lLVN units were excited mainly by rotation in the opposite sense; following partial cerebellectomy, the majority of units were excited during side-up neck rotation, not only in lLVN but also in cLVN.

4. Units receiving a convergent input from both receptors were more numerous in cLVN (72.7%) than lLVN (41.8%) in preparations with intact cerebellum; following partial cerebellectomy, this disproportion of responsive units in the two divisions (45.3% and 44.9%, respectively) disappeared, due to a reduced number of cLVN units responding to the neck input. In both preparations, the macular input had a relatively greater influence on the cLVN whereas the neck input was more effective on the lLVN.

5. The unit responses to head rotation leading to combined stimulation of macular and neck receptors agreed with those predicted on the basis of vectorial summation of the individual neck and macular responses. This was observed in cLVN and lLVN units in both preparations. This additive mode of interaction also was observed over the frequency domain, despite the particular dynamics of each frequency response.

6. The results are reviewed in terms of the role that the LVN exerts in postural regulation. The influence of the cerebellum in the gain regulation and/or phase adjustment of LVN unit responses to macular and neck inputs is also discussed.

REFERENCES

1. AJALA, G. F. & R. E. POPPELE. 1967. Some problems in the central actions of vestibular inputs. In *Neurophysiological Basis of Normal and Abnormal Motor Activities*. M. D. Yahr & D. P. Purpura, Eds.: 141-154. Raven Press. New York, N.Y.
2. ANDERSON, J. H., J. F. SOECHTING & C. A. TERZUOLO. 1977. Dynamic relations between natural vestibular inputs and activity of forelimb extensor muscles in the decerebrate cat. I. Motor output during sinusoidal linear accelerations. *Brain Res.* **120**: 1-15.
3. BOYLE, R. & O. POMPEIANO. 1980. Reciprocal responses to sinusoidal tilt of neurons in Deiters' nucleus and their dynamic characteristics. *Arch. Ital. Biol.* **118**: 1-32.
4. BOYLE, R. & O. POMPEIANO. 1980. Responses of vestibulospinal neurons to sinusoidal rotation of neck. *J. Neurophysiol.* **44**: 633-649.
5. BRINK, E. E., N. HIRAI & V. J. WILSON. 1980. Influence of neck afferents on vestibulospinal neurons. *Exp. Brain Res.* **38**: 285-292.
6. BRODAL, A., O. POMPEIANO & F. WALBERG. 1962. The Vestibular Nuclei and Their Connections, Anatomy and Functional Correlations. William Ramsay Henderson Trust Lecture: viii-193. Oliver and Boyd. Edinburgh & London.
7. DE KLEIJN, A. 1920. Tonische Labyrinth- und Halsreflexe auf die Augen. *Pfluegers Arch.* **186**: 82-97.
8. DENOTH, F., P. C. MAGHERINI, O. POMPEIANO & M. STANOJEVIĆ. 1979. Responses of Purkinje cells of the cerebellar vermis to neck and macular vestibular inputs. *Pfluegers Arch.* **381**: 87-98.
9. DENOTH, F., P. C. MAGHERINI, O. POMPEIANO & M. STANOJEVIĆ. 1980. Responses of Purkinje cells of the cerebellar vermis to sinusoidal rotation of the neck. *J. Neurophysiol.* **43**: 46-59.
10. EHRHARDT, K. J. & A. WAGNER. 1970. Labyrinthine and neck reflexes recorded from spinal single motoneurons in the cat. *Brain Res.* **19**: 87-104.

11. FREDRICKSON, J. M., D. SCHWARZ & H. H. KORNHUBER. 1966. Convergence and interaction of vestibular and deep somatic afferents upon neurons in the vestibular nuclei of the cat. *Acta Oto-Laryngol. Stockh.* **61**: 168-188.
12. HIKOSAKA, O. & M. MAEDA. 1973. Cervical effects on abducens motoneurons and their interaction with vestibulo-ocular reflex. *Exp. Brain Res.* **18**: 512-530.
13. HOLST, E. V. & H. MITTELSTAEDT. 1950. Das Reafferenzprinzip. Wechselwirkungen zwischen Zentralnervensystem und Peripherie. *Naturwissenschaften* **37**: 464-476.
14. HOSHINO, K. & O. POMPEIANO. 1977. Responses of lateral vestibular neurons to stimulation of contralateral macular labyrinthine receptors. *Arch. Ital. Biol.* **115**: 237-261.
15. ILLERT, M., A. LUNDBERG, Y. PADEL & R. TANAKA. 1978. Integration in descending motor pathways controlling the forelimb in the cat. 5. Properties of and monosynaptic excitatory convergence on C₃-C₄ propriospinal neurones. *Exp. Brain Res.* **33**: 101-130.
16. KELLER, E. E. & W. PRECHT. 1979. Visual-vestibular responses in vestibular nuclear neurons in the intact and cerebellectomized, alert cat. *Neuroscience* **4**: 1599-1613.
17. KENINS, K., H. KIKILLUS & E. D. SCHOMBURG. 1978. Short and long-latency reflex pathways from neck afferents to hindlimb motoneurons in the cat. *Brain Res.* **149**: 235-238.
18. KIM, J. H. & L. D. PARTRIDGE. 1969. Observations on types of response to combination of neck, vestibular and muscle stretch signals. *J. Neurophysiol.* **32**: 239-250.
19. LINDSAY, K. W., T. D. M. ROBERTS & J. R. ROSENBERG. 1976. Asymmetric tonic labyrinth reflexes and their interaction with neck reflexes in the decerebrate cat. *J. Physiol. London* **261**: 583-601.
20. LINDSAY, K. W. & J. R. ROSENBERG. 1977. The effect of cerebellectomy on tonic labyrinth reflexes in the forelimb of the decerebrate cat. *J. Physiol. London* **273**: 76-77P.
21. LUND, S. & O. POMPEIANO. 1968. Monosynaptic excitation of alpha-motoneurons from supraspinal structures in the cat. *Acta Physiol. Scand.* **73**: 1-21.
22. MAGNUS, R. 1924. *Körperstellung: xiii-740.* Julius Springer. Berlin, Germany.
23. MAGNUS, R. & A. DE KLEIJN. 1912. Die Abhängigkeit des Tonus der Extremitätenmuskeln von der Kopfstellung. *Pfluegers Arch.* **145**: 455-548.
24. MCCOUCH, G. P., I. D. DEERING & T. H. LING. 1951. Location of receptors for tonic neck reflexes. *J. Neurophysiol.* **14**: 191-195.
25. MITTELSTAEDT, H. 1964. Basic control patterns of orientational homeostasis. *Symp. Soc. Exp. Biol.* **18**: 365-385.
26. MORI, S. & A. MIKAMI. Excitation of Deiters' neurons by stimulation of the nerves to neck extensor muscles. *Brain Res.* **56**: 331-334.
27. PETERSON, B. W. 1970. Distribution of neural responses to tilting within vestibular nuclei of the cat. *J. Neurophysiol.* **33**: 750-767.
28. POMPEIANO, O. 1975. Vestibulo-spinal relationships. In *The Vestibular System*. R. F. Naunton, Ed.: 147-180. Academic Press. New York, San Francisco & London.
29. POMPEIANO, O. & A. BRODAL. 1957. The origin of vestibulospinal fibres in the cat. An experimental-anatomical study, with comments on the descending medial longitudinal fasciculus. *Arch. Ital. Biol.* **95**: 166-195.
30. PRECHT, W. 1974. The physiology of the vestibular nuclei. In *Handbook of Sensory Physiology. Vestibular System. Basic Mechanisms*. H. H. Kornhuber, Ed. **6/1**: 353-416. Springer Verlag. Berlin, Heidelberg & New York.
31. RICHMOND, F. J. R. & V. C. ABRAHAMS. 1979. What are the proprioceptors of the neck? *Prog. Brain Res.* **50**: 245-254.
32. ROBERTS, T. D. M. 1978. *Neurophysiology of Postural Mechanisms*. 2nd edit.: xv-415. Butterworths. London, England.
33. RUBIN, A. M., S. R. C. LIEGREN, A. C. MILNE, J. A. YOUNG & J. M. FREDRICKSON. 1977. Vestibular and somatosensory interaction in the cat vestibular nuclei. *Pfluegers Arch.* **371**: 155-160.
34. RUBIN, A. M., J. H. YOUNG, A. C. MILNE, D. W. F. SCHWARZ & J. M. FREDRICKSON. 1975. Vestibular-neck integration in the vestibular nuclei. *Brain Res.* **96**: 99-102.

35. SCHWARZ, D. W. F., A. M. RUBIN, R. D. TOMLINSON, A. C. MILNE & J. M. FREDRICKSON. 1975. Studies on the integrative activity of the vestibular nuclei complex. *Can. J. Otolaryngol.* **4**: 378-382.
36. SHIMAZU, H. & W. PRECHT. 1965. Tonic and kinetic responses of cat's vestibular neurons to horizontal angular acceleration. *J. Neurophysiol.* **28**: 989-1013.
37. SOECHTING, J. F., J. H. ANDERSON & A. BERTHOZ. 1977. Dynamic relations between natural vestibular inputs and activity of forelimb extensor muscles in the decerebrate cat. III. Motor output during rotations in the vertical plane. *Brain Res.* **120**: 35-47.
38. STANOJEVIĆ, M. 1980. Responses of cerebellar fastigial neurons to neck and macular vestibular inputs. *Pfluegers Arch.* (In press.)
39. STANOJEVIĆ, M., L. ERWAY, B. GHELARDUCCI, O. POMPEIANO & W. D. WILLIS, JR. 1980. A comparison of the response characteristics of cerebellar fastigial and vermal cortex neurons to sinusoidal stimulation of macular vestibular receptors. *Pfluegers Arch.* **385**: 95-104.
40. THODEN, U., R. GOLSONG & J. WIRBITZKY. 1975. Cervical influence on single units of vestibular and reticular nuclei in cats. *Pfluegers Arch.* **355**: R 101, n. 201.
41. WENZEL, D. & U. THODEN. 1977. Modulation of hindlimb reflexes by tonic neck positions in cats. *Pfluegers Arch.* **370**: 277-282.
42. WENZEL, D., U. THODEN & A. FRANK. 1978. Forelimb reflexes modulated by tonic neck positions in cats. *Pfluegers Arch.* **374**: 107-113.
43. WILSON, V. J. & G. MELVILL JONES. 1979. *Mammalian Vestibular Physiology*: xi-365. Plenum Press. New York and London.

DYNAMICS OF VESTIBULO-OCULAR, VESTIBULO-COLLIC, AND CERVICOCOLLIC REFLEXES*

Barry W. Peterson, Gerardo Bilotto, Jefim Goldberg,
and Victor J. Wilson

*The Rockefeller University
New York, New York 10021*

Activation of semicircular canal receptors leads to reflex movements of the eye, head, and body. The functional role of the vestibulo-ocular reflex (VOR)—stabilization of the position of the eyes in space—is well established, and the dynamics of the reflex have been studied extensively.^{1,2} Extraocular motoneuron discharge, relative to eye position, behaves as a first-order lead signal, i.e., it is in phase with head angular velocity at higher frequencies. Such motoneuron behavior compensates for the predominantly viscous load of the eye. As a result, the vestibulo-ocular reflex produces compensatory eye movements over a wide frequency range even though it appears to operate essentially open loop, without feedback. Much less is known about the vestibulocollic reflex (VCR), whose dynamics have been studied only in the open-loop mode (i.e., whole-body rotations with the head immobilized) and over a restricted frequency range. Outerbridge and Melvill Jones have suggested that, functioning in its normal closed-loop mode (head free to counterrotate in response to whole-body rotations), the VCR acts to stabilize the position of the head in space during rotation of the body.³ Another reflex that also is involved in head stabilization, although not of vestibular origin, is the cervicocollic reflex, or CCR. This reflex is evoked by activity of receptors in neck muscles or joints, which occurs when the head is rotated with respect to the body.

The goal of this paper is to describe in some detail the dynamics of the horizontal VCR and CCR and the interaction of the two reflexes, and to discuss their functional role.

VESTIBULOCOLLIC REFLEX

The horizontal VCR has been studied previously in decerebrate cats where it was evoked by sinusoidal horizontal rotation limited to frequencies below 1 Hz.⁴ (This limitation is a serious drawback since head movements of normal cats have frequency components of significant amplitude to frequencies of 6.5–7 Hz.)^{5,6} Results of experiments, conducted in the open-loop mode, showed that reflex motor output lags input acceleration by 150° in the midfrequency range near 0.1 Hz, and that above this frequency a phase lead develops.^{4,7} Frequencies above 1 Hz have been studied recently in experiments in which the stimulus consisted of sinusoidal polarization of canal afferents.⁸ Results showed that the central pathways of the horizontal VCR introduced a first-order lag at low frequencies and a first-order lead at high frequencies. The time constant of the latter was

*Research supported in part by Grants EY 02249, EY 00100, and NS 02619 of the National Institutes of Health.

estimated to be 0.1 second. We now have studied the properties of the VCR with natural stimulation over an extended frequency range and compared them with properties of the VOR.

Experiments were performed on precollicular decerebrate cats prepared for recording of the bitemporal electro-oculogram (EOG), for bipolar recording of electromyographic (EMG) signals from various neck muscles, and for extracellular recording from identified abducens motoneurons. The animal's body was secured firmly to a rotating turntable with squeeze plates and a clamp attached to the first thoracic vertebra. Its head was attached to the turntable by a head holder that permitted rotation of the head about a vertical axis passing through the C_1 - C_2 joint. Servomotors under computer control were used to produce rotation of the

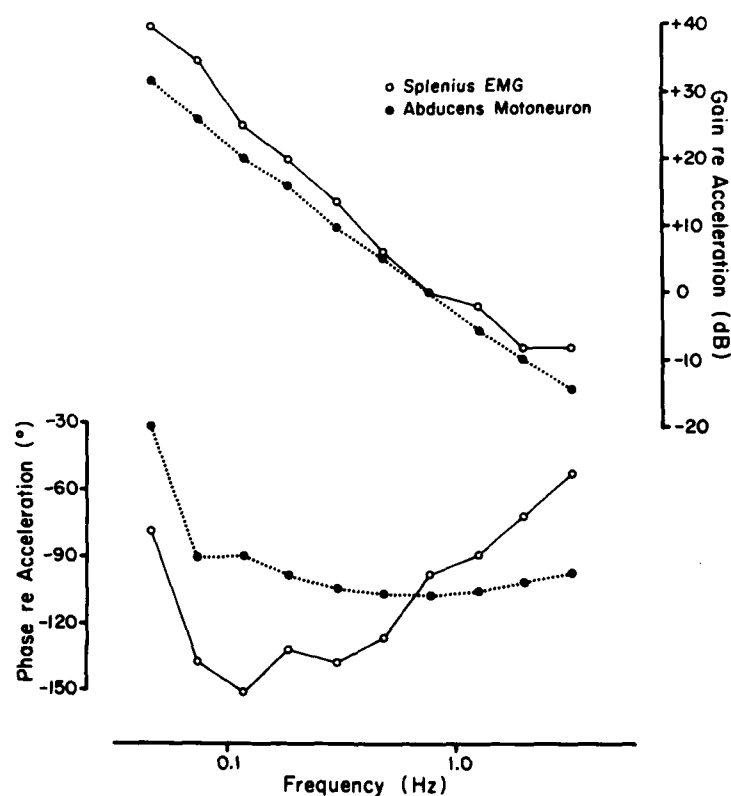


FIGURE 1. Frequency response of splenius muscle (open circles) and abducens motoneuron (filled circles) activity recorded simultaneously during horizontal angular rotation of the whole animal. The peak angular acceleration of the body produced by the composite stimulus waveform (a sum of 10 sinusoids with frequencies ranging from 0.046 to 3.2 Hz) was approximately $720^\circ/\text{second}^2$. In this and subsequent figures, the muscle gain represents the percent modulation of EMG activity per degree/second² and the phase is calculated in reference to the peak counterclockwise angular acceleration of the body. Gains were normalized (0 dB) relative to the gain of each response at 0.77 Hz. Motoneuron gain was computed as spikes/second per degree/second².

body or head about this axis. Rotational angle was modulated either as a single sinusoid at frequencies between 0.01 and 5 Hz or as a sum of 8-10 sinusoids spanning the same frequency range. The computer that generated the rotational stimuli also recorded rectified EMG activity of several dorsal neck muscles, abducens motoneuron discharge, horizontal EOG, horizontal head torque, and angular position of the turntable and head. Analysis procedures described in Wilson et al. and Peterson et al. were used to compute the amplitude and phase of modulation of the above signals at each of the component frequencies in the stimulus waveform as well as estimates of harmonic distortion and signal-to-noise ratio.^{8,9} In the recordings of CCR and VCR responses described below, harmonic distortion typically was less than 30%, signal-to-noise ratio greater than 2:1. Phase and gain (response amplitude/stimulus amplitude) of the responses did not vary with stimulus intensity, indicating that the reflex systems behaved linearly.

One of the Bode plots in FIGURE 1 (open circles) shows the response of the splenius muscle to a stimulus consisting of 10 superimposed sine waves with a maximum frequency of 3.2 Hz. As in the results of Ezure and Sasaki,⁴ there is a phase lag with respect to angular acceleration, of about 150° at 0.1 Hz. Below this frequency, the phase lag decreases because of the relatively short time constant of central integration in this experimental animal. Above this frequency, the phase lag decreases to about 50° at 3.2 Hz. Gain drops at the rate of 8-10 dB/octave in the low-frequency range and considerably less steeply above 1 Hz. These properties approach the behavior of a second-order lag-lead system. At 0.1 Hz, the input acceleration has been integrated nearly twice (i.e., a phase lag of 180°) to provide a motor output approximately in phase with position. At 3.2 Hz, the output leads angular velocity by about 40° (or, as shown in FIGURE 1, lags angular acceleration by about 50°) and appears to be approaching a phase of 0° with respect to angular acceleration.

The filled symbols show the behavior of a typical abducens motoneuron recorded simultaneously with the neck muscle EMG activity. The 90° phase lag of abducens discharge at 0.1 Hz is comparable to the data of Shinoda and Yoshida.² As with the VCR, the integration of the signal with respect to head angular acceleration is poor at low frequencies. Above 0.1 Hz, abducens discharge lags acceleration by approximately 90°, i.e., it remains approximately in phase with angular velocity. At high frequencies, abducens discharge lags considerably behind the neck EMG, behaving as a first-order lead signal with respect to horizontal eye position.¹ Corresponding to this first-order phase characteristic, the gain has a slope of about 7 dB/octave over the whole frequency range.

Role of the Medial Longitudinal Fasciculus in the Vestibulocollic Reflex

The horizontal canal signal responsible for the VCR is relayed by second-order neurons in the vestibular nuclei, and some of these project directly to neck motoneurons.¹⁰ The physiological function of these second-order fibers, which are known to exert an excitatory and inhibitory influence on motoneurons responsible for contraction of neck muscles,¹¹ remains to be determined. Transection of the medial longitudinal fasciculus (MLF) does not change the dynamic properties of the reflex evoked by natural stimulation at frequencies up to 0.4 Hz or the properties of the central pathways activated by sinusoidal polarization at frequencies up to 6 Hz.^{8,12} In the present experiments we have studied the effect

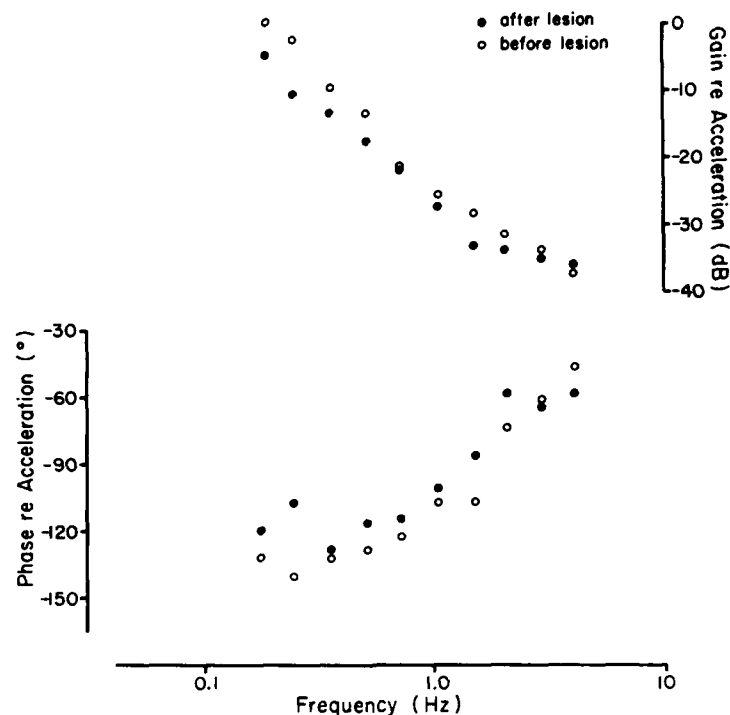


FIGURE 2. Phase and gain response of the splenius muscle during the horizontal vestibulocollic reflex before (open circles) and after (filled circles) transection of the MLF. The peak angular acceleration of the body produced by the composite stimulus waveform (a sum of 10 sinusoids with frequencies ranging from 0.185 to 4.1 Hz) was approximately $810^\circ/\text{second}^2$.

of MLF transection on behavior of the reflex evoked by sinusoidal rotation at frequencies ranging from 0.5 to 4 Hz.

FIGURE 2 illustrates the results of one experiment. In this case, neither phase nor gain at any frequency is affected by the lesion. This lack of change in phase is typical of the data from five cats. In three animals, the lesion produced a uniform drop in gain at all frequencies, which could be due to the trauma of the lesion or to a specific effect of MLF interruption. In two experiments, the gain of the VCR dropped while that of the VOR remained unchanged, while the opposite result has not been obtained. This selective effect suggests that the drop in gain that is seen is not entirely due to trauma and that the descending pathways in or near the MLF, including the second-order pathway, contribute to the horizontal VCR.

CERVICOCOLLIC REFLEX

The presence of a CCR was demonstrated in a behavioral context by Bizzi *et al.*,¹⁹ but the dynamic properties of this reflex have not been investigated. We

now have studied the dynamic properties of the CCR and compared them to those of the VCR. The dots in FIGURE 3 show the response of the complexus muscle to a stimulus consisting of rotation of the body in the horizontal plane about the C_1 - C_2 joint with the head held fixed in space. Superimposed sine waves ranging in frequency from about 0.1 to 5 Hz were used. The response is very similar to the VCR response illustrated in FIGURE 1, and suggests that the CCR also can be considered to be a second-order lag-lead system. The solid lines in the figure indicate that the data in fact can be approximated closely by the response of the second-order lag-lead system whose equation is given in the figure.

To compare the gains of horizontal CCR and VCR in the same animal, we compared the percent modulation of EMG activity in several different neck muscles when the cat was subjected to identical sinusoidal rotation (a) of the whole body (VCR) or (b) of the body with the head fixed in space (CCR). In this way, 13 pairs of matched VCR and CCR gains were obtained from five cats (one-four neck muscles sampled per cat). The ratio of CCR gain to VCR gain in these 13 cases ranged from 0.4 to 3.1 with a median of 1.2. In over half the cases, the range was from 0.8 to 1.8. Therefore the gains of these two reflexes do not differ greatly in these preparations.

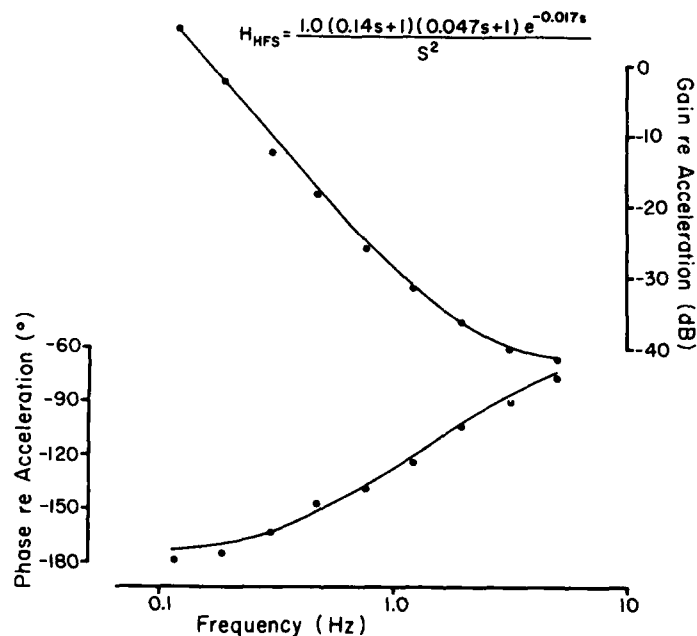


FIGURE 3. Frequency response to complexus muscle during the horizontal cervicocollic reflex. Dots refer to the actual data points, while solid lines illustrate the phase and gain response of the above second-order transfer function. The peak angular acceleration of the body (head fixed in space) rotating about the C_1 - C_2 joint produced by the composite stimulus waveform (a sum of nine sinusoids with frequencies ranging from 0.115 to 5 Hz) was approximately $1,043^\circ/\text{second}^2$.

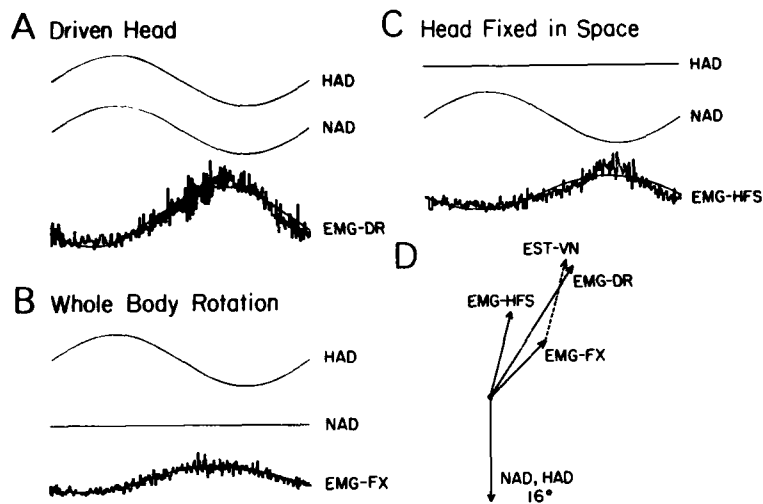


FIGURE 4. Interaction of the horizontal vestibulocollic and cervicocollic reflexes produced by 0.2 Hz sinusoidal rotation with an amplitude of 16° . Part A shows the reflex response during combined activation of vestibular and neck afferents produced by forced rotation of the head while the body remained stationary in space. The head (HAD) and the neck (NAD) angular deviations are identical in this case. The response of the right splenius muscle is shown by its rectified EMG activity together with the best-fitting sinusoid at the fundamental frequency (EMG-DR). Part B indicates the response (EMG-FX) obtained during whole-body rotation (i.e., activation of vestibular receptors), and part C the response (EMG-HFS) obtained during rotation of the body about the C_1 - C_2 joint while the head remained fixed in space (HFS, activation of neck afferents). In part D, the EMG response of the splenius muscle, during three different paradigms (DR, FX, HFS), and the stimulus are plotted as vectors in polar coordinates (solid lines). Each vector length represents the amplitude of EMG modulation, and the polar angle denotes the phase of this modulation measured with respect to the peak rightward deviation of the turntable. The dotted line vector (EST-VN) represents the sum of the EMG-FX and EMG-HFS vectors, which closely approximates the EMG-DR vector obtained during the experiment in part A. (From Reference 14 with permission of Elsevier/North Holland Biomedical Press.)

INTERACTION OF VESTIBULOCOLLIC REFLEX AND CERVICOCOLLIC REFLEX

Because normal head movements must activate both the VCR and CCR, it is of considerable interest to determine how these two reflexes interact. Part A of FIGURE 4 shows the EMG response to forced rotation of the head on a stationary body, a stimulus that elicits the two reflexes in combination. The reflexes are studied individually in parts B (whole-body rotation, VCR) and C (rotation of body with head fixed in space, CCR). The diagram in part D shows that vectorial addition of the VCR (EMG-FX) and CCR (EMG-HFS) components yields an estimated combined response (EST-VN) that closely approximates the response to forced head rotation (EMG-DR). From this we conclude that the two reflexes add linearly to reinforce each other during such a movement. It must be kept in mind that in the closed-loop situation, i.e., during body rotation with the head free to move, the two reflexes would oppose each other: compensatory head rotation evoked by the VCR will evoke a CCR acting in the opposite direction. In

measurements in the same decerebrate cat preparation, we showed that as a result of this effect the total compensatory head movement never exceeded one-third of the applied body rotation.¹⁴

COMMENT

An important finding in our recent work is that, while they originate in different receptors, the two major reflexes elicited by angular rotation of the head (the CCR and VCR) have similar dynamics over a broad frequency range. The most striking aspect of this similarity is the second-order phase advance and gain increase that are seen at higher frequencies. This high-frequency behavior is qualitatively different from that of the VOR, which behaves as a first-order system.^{1,2,15} Just as the first-order behavior of the VOR is appropriate to overcome the viscoelastic load imposed by extraocular mechanics,¹ the second-order signal observed on neck motoneurons during the CCR and VCR would be appropriate to control the predominantly inertial load imposed by the mechanics of the head-neck system. In other words, it appears that the central output of both the VCR and CCR is adapted to the load that these reflexes normally encounter.

At what stage in the vestibulomotor pathways are the differences we have observed between vestibulocollic and vestibulo-ocular signals likely to develop? The similarity of responses of all second-order vestibular neurons in decerebrate cats to sinusoidally modulated semicircular canal input (including second-order neurons that do and do not project to the spinal cord)⁶ suggests that the difference must arise at the level of higher order premotor neurons in the brain stem or spinal cord. The existence of reticulospinal neurons carrying both the low-frequency phase-lagging and high-frequency phase-leading portions of the VCR signal⁹ indicates that the signal transformations required in the VCR pathway may occur in premotor centers within the brain stem. It also is conceivable that the signal carried to the spinal cord by the extensive second-order projections¹⁰ is transformed at the level of spinal interneurons to provide appropriate input to motoneurons. In any case our observation that the dynamic behavior of the VCR is not altered by MLF lesions that interrupt the axons of all second-order neurons of the horizontal VCR system indicates that direct pathways, while they may contribute to the VCR, are not required.

A final question to be raised concerns the functional roles of the CCR and VCR. The action of these reflexes will be considered under three situations: (1) where external forces tend to change the intended position of the head; (2) where the body undergoes angular rotation, thus requiring counterrotation of head and eyes to maintain gaze stability; and (3) where the animal must maintain head stability on a stationary body.

Bizzi *et al.* studied the CCR in isolation in labyrinthectomized monkeys and concluded that this reflex is too weak to provide effective compensation for external loads applied during active head movements.¹³ Our data do not bear directly on the gain of the CCR in a behavioral context, but they do indicate that the CCR and VCR have equivalent gains over a broad frequency range in the decerebrate cat. If the gains also are equal in alert animals, this would suggest that neither the CCR nor the VCR is able to provide effective compensation for external forces applied to the head.

As mentioned above, because the VCR opposes rotation of the head in space while the CCR opposes rotation of the head with respect to the body, the two reflexes tend to oppose one another in the closed-loop situation in which the

body is subjected to rotation resulting in a counterrotation of the head. Thus unless the CCR is suppressed during such rotation, the VCR, impeded by the CCR, would not be effective in compensating for angular movement of the body. The possibility that the gain of the VCR may exceed greatly that of the CCR under appropriate conditions is suggested by Outerbridge and Melvill Jones' observation that some human subjects can produce rotations of the head that effectively compensate for low-frequency sinusoidal oscillation of the body.³

In situations where their gains are equivalent, the two reflexes would function most effectively to counter or to damp out rotations of the head on the stationary body. Under such conditions, the second-order dynamics of the two reflexes should give them the capability of effectively damping potential oscillations due to the inertial component of the load imposed by the head-neck system.

Further quantitative studies of the gains and dynamics of the CCR and VCR are required to clarify their functional role in the three situations discussed above.

REFERENCES

1. SKAVENSKI, A. A. & D. A. ROBINSON. 1973. Role of abducens neurons in vestibuloocular reflex. *J. Neurophysiol.* **36**: 724-738.
2. SHINODA, Y. & K. YOSHIDA. 1974. Dynamic characteristics of responses to horizontal head angular acceleration in vestibuloocular pathway in the cat. *J. Neurophysiol.* **37**: 653-673.
3. OUTERBRIDGE, J. A. & G. MELVILL JONES. 1971. Reflex vestibular control of head movements in man. *Aerosp. Med.* **42**: 935-940.
4. EZURE, K. & S. SASAKI. 1978. Frequency-response analysis of vestibular induced neck reflex in cat. I. Characteristics of neural transmission from horizontal semicircular canal to neck motoneurons. *J. Neurophysiol.* **41**: 445-458.
5. WATT, D. G. D. & M. C. WETZEL. 1977. Linear head movements of walking and trotting cats. *Neurosci. Abstr.* **3**: 280.
6. DONAGHY, M. 1980. The cat's vestibulo-ocular reflex. *J. Physiol.* **300**: 337-351.
7. BERTHOZ, A. & J. H. ANDERSON. 1971. Frequency analysis of vestibular influence on extensor motoneurons. I. Response to tilt in forelimb extensors. *Brain Res.* **34**: 370-375.
8. WILSON, V. J., B. W. PETERSON, K. FUKUSHIMA, N. HIRAI & Y. UCHINO. 1979. Analysis of vestibulocollic reflexes by sinusoidal polarization of vestibular afferent fibers. *J. Neurophysiol.* **42**(2): 331-346.
9. PETERSON, B. W., K. FUKUSHIMA, N. HIRAI, R. H. SCHOR & V. J. WILSON. 1980. Responses of vestibulospinal and reticulospinal neurons to sinusoidal vestibular stimulation. *J. Neurophysiol.* **43**: 1236-1250.
10. WILSON, V. J. & G. MELVILL JONES. 1979. *Mammalian Vestibular Physiology*. Plenum Press, New York, N.Y.
11. WILSON, V. J. & M. MAEDA. 1974. Connections between semicircular canals and neck motoneurons in the cat. *J. Neurophysiol.* **37**: 346-357.
12. EZURE, K., S. SASAKI, Y. UCHINO & V. J. WILSON. 1978. Frequency-response analysis of vestibular induced neck reflex in cat. II. Functional significance of cervical afferents and polysynaptic descending pathways. *J. Neurophysiol.* **41**: 459-471.
13. BIZZI, E., P. DEV, P. MORASSO & A. POLIT. 1978. Effect of load disturbances during centrally initiated movements. *J. Neurophysiol.* **41**(3): 542-556.
14. PETERSON, B. W., G. BILOTTO, J. H. FULLER, J. GOLDBERG & B. LEEMAN. Interaction of vestibular and neck reflexes in the control of gaze. *Prog. Oculomotor Res.* [In press.]
15. HONRUBIA, V., D. B. REINGOLD, C. G. Y. LAU & P. H. WARD. 1979. Neural correlates of nystagmus in abducens nerve. *J. Neurophysiol.* **42**: 1282-1290.

EARLY DIRECTIONAL INFLUENCE OF VISUAL MOTION CUES ON POSTURAL CONTROL IN THE FALLING MONKEY*

M. Lacour, P. P. Vidal,† and C. Xerri

*Laboratory of Psychophysiology
University of Aix-Marseille I
13397 Marseille Cedex 13, France*

INTRODUCTION

The sudden change in acceleration that occurs at the onset of a free-fall produces muscular responses in many muscles throughout the body. Early electromyographic (EMG) responses develop in the feet extensor muscles, with latencies of about 75–80 mseconds in man, 55 mseconds in the cat, and 30 mseconds in the monkey.^{7,8,13,20} Many authors reported that the early muscle responses were not modified by blindfolding or when subjects fell in total darkness. They took these results as an argument against the role of vision in the genesis of these postural reactions. Because these reactions were found in extensor as well as flexor muscles and disappeared in man when the subject triggered the fall himself, they were interpreted as a startle reaction of vestibular origin. A different explanation was proposed by Melvill Jones and Watt, Watt, and our group.^{8,9,13,20} On the basis that totally labyrinthectomized animals or only "plugged" semicircular canal preparations did not exhibit such reactions to fall, it was assumed that the reactions represent an otolith-originating reflex assisting landing.

However, we have demonstrated that stabilization of the visual surround with respect to the monkey's head produces a strong motor depression.¹⁷ This experimental condition suppresses all visual motion cues. By contrast, only a slight motor reduction was recorded in total darkness.¹⁷ These results confirmed previous findings in man and supported the initial suggestion of Nashner and Berthoz that vision intervenes at an early stage in postural control.^{15,18} The dramatically enhanced effect of visual stabilization in labyrinthectomized monkeys agrees also with this view.¹⁰

In this paper we report the main findings of recent experiments that consisted of a study of the dynamics of visual and vestibular control of rapid postural reactions in the intact falling monkey.¹¹ These experiments were performed by modifying the amplitude of the acceleration of fall and by changing the speed and the direction of the visual surround relative to the monkey's head.

METHODS

Preparation

Experiments were performed on six baboons (4–8 kg). Chronic EMG recording electrodes were implanted bilaterally in head extensor and lateral flexor

*This work was supported by ERA 272 CNRS and CRL 806007 6 INSERM.

†Laboratoire de Physiologie du Travail du CNRS, Département de Physiologie Neurosensorielle, Centre Universitaire des Cordeliers, Paris, France.

muscles (splenius capitis) and in distal extensor (soleus) and flexor (tibialis anterior) muscles. The techniques are described fully in Lacour *et al.*⁸⁻¹¹

Free-Fall Device

The monkey was seated in a chair (see FIGURE 1A) maintained in the initial position by two electromagnets and suddenly dropped 0.9 m. The end of the fall was slowed by an elastic system. The chair was guided by two vertical rails so that the vertical axis was parallel to the head-trunk axis of the monkey. For recordings, the monkey's hindlimbs were fixed in a standard position and his

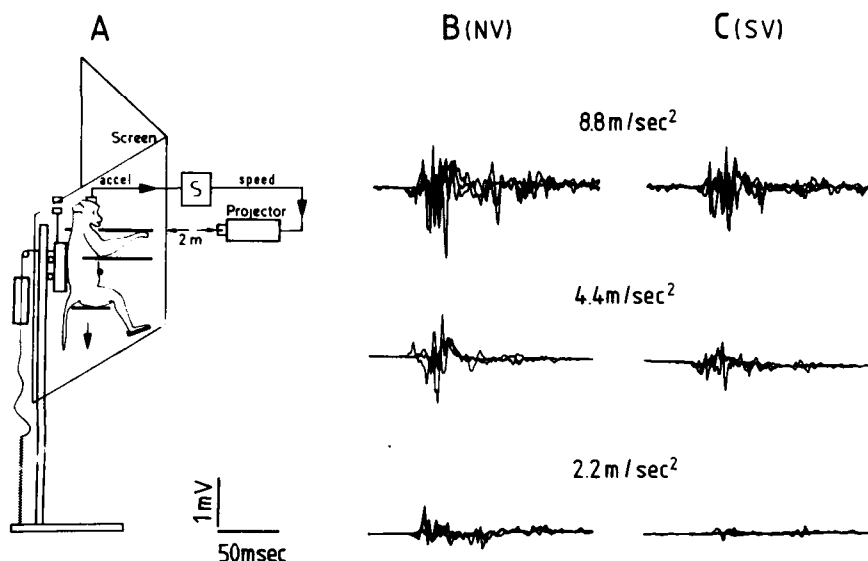


FIGURE 1. A-C: Experimental setup and typical muscle responses to fall. A: Experimental setup (see text). Five conditions of visual surround are used: (a) the images remain stationary on the screen (NV); (b) the visual scene moves upward with a velocity 0.6, 0.75, 1, 1.5, or 3 times the velocity of the falling monkey (EV); (c) the visual scene moves downward with a velocity 0.6 or 0.75 times the one of the falling monkey (RV); (d) the visual scene moves downward with the same velocity as that of the falling monkey (SV); and (e) total darkness. B: Three superimposed raw EMG recordings from the splenius capitis during falls with normal vision (NV) at 8.8 m/second², 4.4 m/second², and 2.2 m/second². C: Three superimposed raw EMG recordings from the same muscle, in the same monkey, during falls with visual stabilization (SV) at the same rates of acceleration. Note the reduction in energy as the acceleration decreases, and the motor depression in the SV condition.

head was restrained, allowing only a few degrees of head movement in each direction.

Five maximum peak accelerations were used (8.8 m/second², 6.6 m/second², 4.4 m/second², 3.3 m/second², and 2.2 m/second²), corresponding for the highest and the lowest to a duration of fall of 452 mseconds and 904 mseconds,

respectively. The vertical acceleration was recorded by an accelerometer placed on the chair.

Visual Environment during Falls

A V-shaped stationary retroprojection screen, folded in a 90° angle, was placed in front of the monkey in order to occlude all his visual field (cf., FIGURE 1A and Reference 10). A film, consisting of a random black and white pattern, was projected onto the screen. The film motion in the projector was commanded by a servo-controlled system, which received the integrated output of the accelerometer. This velocity signal could be multiplied, divided, and/or inverted. A photoelectric cell measured the speed of the pattern on the screen. Using this device, the baboon was submitted to five types of visual surroundings, all occurring in a random order:

1. Normal vision (NV). The images remain stationary on the screen. Velocity of the falling monkey is at any moment equal and opposite to the relative velocity of the visual scene.

2. Enhanced vision (EV). The film motion is directed upward with a speed at any moment equal to 0.6, 0.75, 1, 1.5, or 3 times the velocity of the falling monkey.

3. Reduced vision (RV). The film motion is directed downward with a speed equal to 0.6 or 0.75 times the velocity of the falling monkey.

4. Stabilized vision (SV). The film motion again is directed downward but with the same speed as that of the monkey. In this case, the visual motion cues are suppressed totally. This condition represents the limit case of the RV condition. We also used speeds of the film that were 1.5 and 3 times greater than the velocity of the monkey. In these situations, as the monkey falls down, the visual scene motion is similar to the one that would be produced by upward motion of the chair.

5. Total darkness (D). The monkey's head is covered by a box, and the experiments are done in total darkness.

Data Processing

The latency and energy (surface of the integrated EMG) of the muscular responses developed in the 20- to 120-millisecond interval after release of fall were stored by a T 1600 computer. The energy recorded in the EV, RV, SV, and D conditions was expressed in a Z score relative to the mean value recorded in the NV condition, i.e., to a value normalized to zero. This statistical evaluation was done for each pair of muscles and for each acceleration of fall. The confidence intervals were calculated with $p < 0.01$. In FIGURE 3, we have calculated the relative velocity of the visual surround by adding (EV condition) or by subtracting (RV or SV conditions) the absolute velocity of the visual scene on the screen from the normal relative velocity of the visual scene during normal vision. The relative velocities resulting from the visual manipulations were expressed in proportion to the relative velocity in the NV condition.

TABLE 1
LATENCY OF THE SPLENIUS MUSCLE RESPONSES DURING FALLS*

Visual Condition†	Acceleration of Fall	8.8 m/sec ²	4.4 m/sec ²	2.2 m/sec ²
NV		22.5 ± 1.2	26 ± 2.5	29 ± 2.3
D		28 ± 1.4	32 ± 1.7	34 ± 3.3
SV		32 ± 1.9	32 ± 2.1	49 ± 3.8

*In milliseconds ± standard deviation.

†NV, normal vision; D, total darkness; SV, stabilized vision.

RESULTS

The present results show that the early motor reactions to fall are modified either by reducing the amplitude of acceleration (the visual surround remaining normal) or by changing the relative velocity of the visual surround (for a given acceleration).

Muscle Responses in Normal Vision: Effects of Reducing the Acceleration of Fall

Bilateral and symmetrical modifications occur in all tested muscles when the acceleration is reduced. The most important effects are observed in the neck muscles and in the distal extensor muscles. These modifications consist first of a progressive increase in the latency of the EMG response as the acceleration decreases. TABLE 1 presents these results concerning the splenius muscle.

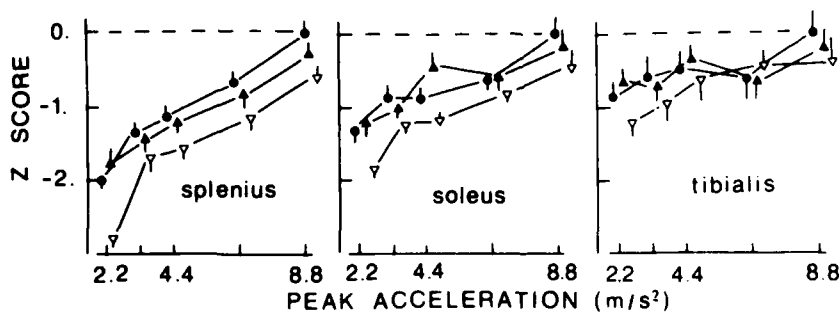


FIGURE 2. Influence of the amplitude of the acceleration and of the visual conditions on the energy of the early EMG responses. Mean values (three normal baboons) recorded from splenius, soleus, and tibialis anterior muscles. On the abscissa: value of the acceleration in m/second². On the ordinates: energy of the muscular response expressed as the Z score relative to the energy recorded at 8.8 m/second² in normal vision (values normalized to zero). EMG activities are recorded during falls in normal vision (dots), in total darkness (filled triangles), and with visual stabilization (open triangles). Each point is represented with its 1% confidence interval.

Second, the duration of the motor reactions is not altered significantly, but the energy decreases progressively as acceleration is reduced, as already shown in man.⁶ Three superimposed raw EMG recordings from the splenius for three consecutive falls in one monkey are illustrated for the three main peaks of acceleration (8.8 m/second^2 , 4.4 m/second^2 , 2.2 m/second^2) in FIGURE 1B. The statistical evaluation is presented in FIGURE 2. One can observe that the decrease in the muscular energy follows an almost linear function from 8.8 m/second^2 to 2.2 m/second^2 , and that the slope of the curves is more accentuated in the splenius and soleus muscles than in the tibialis anterior muscles.

Muscle Responses during Visual Manipulations

Results in Total Darkness (D)

We confirm our previous findings concerning falls at 8.8 m/second^2 ,¹⁷ and we extend these conclusions to falls at lower accelerations. In total darkness, the motor reactions show two modifications when compared to those recorded in normal vision. The latency is slightly enhanced whatever the acceleration of fall (cf., TABLE 1), and the energy is slightly, but significantly, reduced. In all tested muscles, the reduction of the muscular energy as the acceleration decreases is closely parallel to that recorded in normal vision (cf., FIGURE 2). This suggests that the reduction observed in total darkness is not dependent on the amplitude of acceleration or on the amount of energy recorded in the NV condition.

Results with Visual Stabilization (SV)

In this situation, all visual motion cues are suppressed but the static visual input relative to position remains. The effects of visual stabilization, however, are strongly accentuated when compared to the slight modification recorded in total darkness. The latency is considerably longer, and especially so during falls at low acceleration (cf., TABLE 1). The energy is depressed strongly in the splenius and soleus muscles, with the most important effects occurring again during falls at low acceleration (cf., FIGURE 1C). With acceleration at 2.2 m/second^2 , a total motor suppression sometimes is observed. The reduction of the EMG energy (cf., FIGURE 2) is parallel to that recorded in the NV and D conditions from 8.8 m/second^2 to 3.3 m/second^2 peak accelerations. There is a sudden drop for the lowest acceleration (2.2 m/second^2), indicating that the visual motion cues intervene predominantly during slow falls.

Results with Enhanced (EV) or Reduced (RV) Visual Input

We found a visually induced modulation of the early muscular responses. This effect is predominant for falls at low accelerations and for the splenius and soleus muscles. FIGURE 3 presents results from the splenius and soleus muscles for the highest (8.8 m/second^2) and lowest (2.2 m/second^2) peak accelerations. For high accelerations, the muscular energy recorded in the RV condition progressively decreases as the relative speed of the visual scene is reduced, with a maximal reduction in the SV condition. The EMG responses recorded in the EV

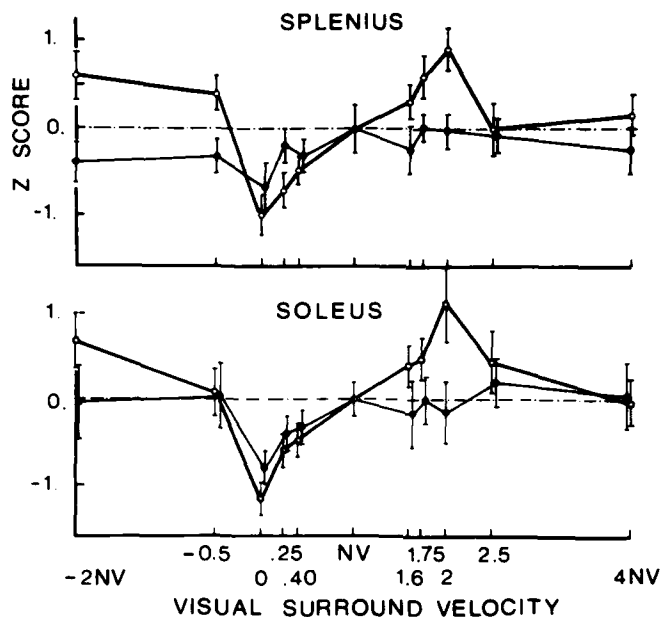


FIGURE 3. Directional influence of visual motion cues on the energy of the early EMG responses. Mean values (three normal baboons) recorded from splenius and soleus muscles during falls at 8.8 m/sec^2 (thin line, dots) or 2.2 m/sec^2 (thick line, circles). On the abscissae: relative velocity of the visual surround (see techniques). Values between 0 (SV condition) and 1 (NV condition) represent the RV condition (reduced visual input). Values above 1 correspond to the EV condition (enhanced visual input). On the ordinates: energy of the EMG response expressed as the Z score relative to the energy recorded in normal vision (values normalized to zero). Note the progressive increase in the energy as the relative velocity of the visual scene increases, in the range 0-2 NV.

condition are not modified when compared to the control (energy in the NV condition). For falls at low acceleration, the motor reduction observed in the RV condition is significantly greater and is again maximal when all visual motion cues are suppressed (SV). By contrast with higher accelerations, the EV condition produces a strong increase of the muscular energy. This effect saturates at about a relative velocity of the visual scene twice the normal relative velocity. In conclusion, in the range 0-2 NV, the modulation is proportional to the relative speed of the visual surround. Above the value 2 NV, the EMG energy is comparable to the control. Under the value 0 NV, the EMG energy is either paradoxically increased (low acceleration) or close to the control (high acceleration).

DISCUSSION

The present report indicates that the early motor reactions to fall are heavily dependent on the amplitude of acceleration and, therefore, probably on the

vestibular input. These early muscle responses can be modulated visually. The visual modulations are direction specific, a function of the relative speed of the visual scene, and dependent on the amplitude of acceleration. Taking into consideration that the responses do not habituate with the repetition of falls, and that changing the acceleration or manipulating the visual surround modifies the muscle responses, it is concluded that these early motor reactions cannot be compared to a startle reaction. Instead we propose that the rapid postural reactions to fall constitute a reflexively triggered landing preparation that would be efficient functionally when the height of fall is short. Visual and vestibular cues interact in the elaboration of these postural reactions. The vestibular input would dominate the response at high accelerations, the visual one at low accelerations.

A first paradox arises when one considers the different effects produced by the total suppression of both static and dynamic visual cues (total darkness) and by the simple suppression of the visual motion cues (visual stabilization). The more drastic modifications are found when the visual scene is stabilized with respect to the monkey's head. The fact that the early role of vision in postural control was underestimated is due for us to the fact that darkness or blindfolding really does not test the role of vision, but only the successful capacity of the animal to compensate for an expected lack of visual cues. A modification of the gain of the reflex pathways or a change in the state of alertness of the monkey may constitute such a supplying mechanism. The visual stabilization method escapes this criticism. Indeed, we recorded similar motor reactions when stabilizing the visual scene, by using either the box covering the monkey's head, the film motion technique, or the stroboscopic light.^{11,17} These paradigms exclude a presetting of the gain of the reflex pathways and the expectation of the deprivation of visual cues. Therefore it is concluded that visual motion cues are crucial information for rapid postural control. The motor reductions observed with the visual stabilization method would result from an intersensory conflict: the otoliths detecting a downward vertical acceleration while the peripheral retina does not signal any movement. This conflict theory is proposed to explain the well-known vection phenomena, such as linear vection.^{1,12}

A second paradox arises when one considers the dynamic characteristics of the otolith system. The otoliths have a very low threshold (<0.005 g) and provide good directional information, as shown by Fernández and Goldberg in primary vestibular afferents and by Daunton and Melvill Jones in vestibular second-order neural units.^{3,5} But a certain ambiguity exists between measurements of gravity and linear acceleration. It thus may be hypothesized that visual motion cues contribute to distinguishing between a translational movement relative to the inertial space and a position relative to the gravitational vertical. It might be the reason why Melvill Jones and Young found that human subjects remained confused about the direction of movement during low vertical accelerations in the absence of vision.¹⁴

Various structures within the central nervous system receive visual, vestibular, and somatic inputs. Among them, the vestibular nuclei have been extensively studied. Daunton and Thomsen demonstrated visual-vestibular interactions in otolith-dependent units at the vestibular nuclei level.⁴ Seventy six percent of the units that responded to a linear acceleration also were activated by a large visual stimulus moving linearly in the opposite direction. Waespe and Henn have recorded canal-dependent units in the vestibular nuclei in the alert monkey during conflicting visual-vestibular stimulation.¹⁹ Their experimental paradigm

in fact is equivalent to our visual stabilization condition. They found a reduction of the neuronal discharge that could be the neural correlate of the reduction in the EMG energy that occurs in the falling monkey during visual stabilization. Recent observations by Thoden *et al.* pointed to a direction-specific modulation of spinal reflexes in cat that is opposite for optokinetic and vestibular stimuli.¹⁸ These different experimental results suggest that visual-vestibular interactions underlying our results may take place in the vestibular nuclei. Our data in hemilabyrinthectomized monkeys also support this view.¹⁰ However, it is well known that the visual effects in the vestibular nucleus are observed mainly for low-frequency stimulation and have a long time constant. This apparently is not the case in the parietal cortex (area 2v) of the monkey, which receives visual and vestibular inputs.² Visual-vestibular interactions in the superior colliculus and the pontine reticular formation also may be of functional importance for postural control in the falling baboon.

ACKNOWLEDGMENT

The authors thank Dr. A. Berthoz for his advice and encouragement during the course of the experiments.

REFERENCES

1. BERTHOZ, A., B. PAVARD & L. R. YOUNG. 1975. Perception of linear horizontal self motion induced by peripheral vision (linear vection). Basic characteristics and visual-vestibular interactions. *Exp. Brain Res.* **23**: 471-489.
2. BUTTNER, U. & V. W. BUETTNER. 1978. Parietal cortex (2v) neuronal activity in the alert monkey during natural vestibular and optokinetic stimulation. *Brain Res.* **153**: 392-397.
3. DAUNTON, N. & G. MELVILL JONES. 1973. Directional representation of horizontal and vertical acceleration in the neural activity of cat vestibular nuclei. Abstr., Proceedings of the Annual Science Meeting of the Aerospace Medicine Association, Las Vegas, Nev.
4. DAUNTON, N. & D. THOMSEN. 1979. Visual modulation of otolith dependant units in cat vestibular nuclei. *Exp. Brain Res.* **37**: 173-176.
5. FERNÁNDEZ, C. & J. M. GOLDBERG. 1976. Physiology of peripheral neurons innervating otolith organs of squirrel monkey. III. Response dynamics. *J. Neurophysiol.* **39**: 996-1008.
6. GREENWOOD, R. J. & A. P. HOPKINS. 1974. Muscle activity in falling man. *J. Physiol. London* **241**: 26-27.
7. GREENWOOD, R. J. & A. P. HOPKINS. 1976. Muscle responses during sudden falls in man. *J. Physiol. London* **254**: 507-518.
8. LACOUR, M., C. XERRI & M. HUGON. 1978. Muscle responses and monosynaptic reflexes in falling monkey: role of the vestibular system. *J. Physiol. Paris* **74**: 427-438.
9. LACOUR, M., C. XERRI & M. HUGON. 1979. Compensation of postural reactions to fall in the vestibular neurectomized monkey: role of the remaining labyrinthine afferences. *Exp. Brain Res.* **37**: 563-580.
10. LACOUR, M. & C. XERRI. 1980. Compensation of postural reactions to fall in vestibular neurectomized monkey: role of the visual motion cues. *Exp. Brain Res.* **40**: 103-110.
11. LACOUR, M., P. P. VIDAL & C. XERRI. 1981. Visual influences on vestibulospinal reflexes during vertical linear motion in normal and hemilabyrinthectomized monkeys. *Exp. Brain Res.* (In press.)

12. LESTIENNE, F., J. F. SOECHTING & A. BERTHOZ. 1977. Postural readjustments induced by linear motion of visual scenes. *Exp. Brain Res.* **28**: 363-384.
13. MELVILL JONES, G. & D. G. D. WATT. 1971. Muscular control of landing from unexpected falls in man. *J. Physiol. London* **219**: 729-737.
14. MELVILL JONES, G. & L. R. YOUNG. 1978. Subjective detection of vertical acceleration: a velocity dependent response. *Acta Otolaryngol.* **85**: 45-53.
15. NASHNER, L. & A. BERTHOZ. 1978. Visual contribution to rapid motor responses during postural control. *Exp. Brain Res.* **150**: 403-407.
16. THODEN, U., J. DICHCANS & TH. SAVIDIS. 1977. Direction-specific optokinetic modulation of monosynaptic hindlimb reflexes in cats. *Exp. Brain Res.* **30**: 155-160.
17. VIDAL, P. P., M. LACOUR & A. BERTHOZ. 1979. Contribution of vision to muscle responses in monkey during free-fall: visual stabilization decreases vestibular dependent responses. *Exp. Brain Res.* **37**: 241-252.
18. VIDAL, P. P., A. BERTHOZ & M. MILLANVOYE. 1981. Difference between eye closure and visual stabilization in the control of the posture in man. (In press.)
19. WAESPE, W. & V. HENN. 1978. Conflicting visual vestibular stimulation and vestibular nucleus activity in alert monkeys. *Exp. Brain Res.* **33**: 203-211.
20. WATT, D. G. D. 1976. Responses of cat to sudden falls: an otolith originating reflex assisting landing. *J. Neurophysiol.* **39**: 257-265.

INFLUENCE OF LABYRINTHINE HYPOACTIVITY ON GROSS MOTOR DEVELOPMENT OF INFANTS

Kimitaka Kaga, Jun-Ichi Suzuki, Roger R. Marsh,*
and Yoshisato Tanaka

*Department of Otolaryngology
Teikyo University School of Medicine
Tokyo 173, Japan*

INTRODUCTION

In adults, bilateral dysfunction of the vestibular labyrinths may be manifested by unsteadiness, but loss of postural control is rare so long as visual cues are available. In infants and children with hypoactive labyrinths, however, loss of postural control is much more common and development of gross motor function is delayed.^{1,2} These children do catch up with normals because proprioceptive, visual, and motor systems compensate for the deficit, but the length of the delay in acquiring normal gross motor skills is a controversial issue.

Many authors have pointed out that vestibular impairment most likely is to be found in children with severe or profound hearing loss since the vestibular end organ and cochlea are closely related in their anatomy and ontogeny and may be affected by the same developmental or noxious factors.^{1,3-7} Those deaf infants and children who do have an accompanying vestibular dysfunction are reported to be delayed in acquisition of head control, sitting, and walking.^{1,2} These reports, however, have lacked data about the vestibular responses of normal control groups of the same age range. Although the vestibular end organ apparently is fully mature at birth, myelination within the central nervous system continues for some time, so that the vestibular reflexes of infants may not be comparable to those of adults.^{8,9} For this reason, it is particularly important in the evaluation of young deaf patients that their vestibular function is judged with reference to that of their age-mates.

Several kinds of rotation tests, such as Barany's method, the subthreshold rotation test, and the torsion swing test, have been used to elicit vestibular responses in infants and children, perrotatory and postrotatory nystagmus being measured as an index of maturation of the vestibular system.¹⁰⁻¹⁴ The primary result of these studies has been that the duration of nystagmus and the number of beats increase with increasing age. These rotation tests stimulate both labyrinths, but Eviatar employed caloric stimulation of each labyrinth separately and found that vestibular responses matured over time, with patterns that correlate with gestational age and weight at birth.¹³

The present investigation had as its primary objective the longitudinal study of patients with congenital hearing impairment and delayed acquisition of gross motor function. To accomplish this, we first obtained quantitative data on the development of these skills in normal infants and children, along with measures of the maturation of their vestibular responses to the damped-rotation test. We then compared these data with those of congenitally deaf children, relating degree of vestibular impairment to delay in reaching milestones of gross motor development.

*Present affiliation: Children's Hospital of Philadelphia, Philadelphia, Pa. 19104.

METHODS

Subjects

In the control group were 30 infants in the first year of life, 30 children one to six years of age, and 10 adults. All the children were examined by pediatricians, with special attention to neurological status, and were considered to have no abnormalities. Their hearing was determined to be normal on the basis of auditory brain-stem responses or behavioral-observation, conditioned-orienting-reflex, or pure-tone audiometry.¹⁵

The hearing-impaired group included 14 infants less than one year old, 21 children one year old, and 33 children two to five years of age, all of whom were being followed in our clinic, which is devoted to speech and hearing disorders in children. These patients had been evaluated by brain-stem responses or conditioned-orienting-reflex audiometry, and only those whose thresholds were above 85 dB were selected for this study. All have received extensive diagnostic and rehabilitation evaluations, and any children identified as having central nervous system impairment—mental retardation or cerebral palsy, for instance—were excluded from this study.

Procedure

Vestibular responses were assessed by means of the damped-rotation test. Electrodes were applied just lateral to the eyes to record horizontal eye movements, and the subject was seated in a rotating chair or, in the case of infants, held on the mother's lap. The chair then was accelerated to a maximum rotational velocity of 200°/second, maximum acceleration being 300°/second².

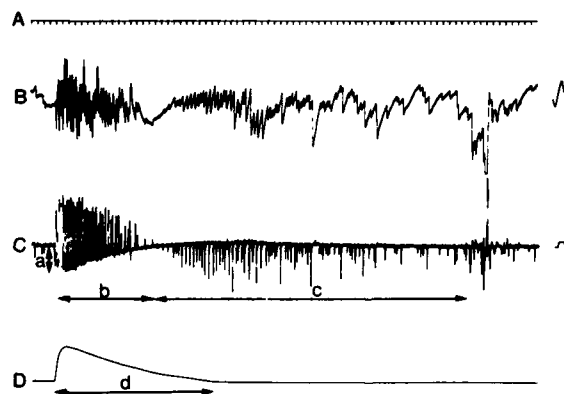


FIGURE 1. Typical recording of perrotatory and postrotatory nystagmus of normal adult, in response to clockwise damped rotation. A: Time scale (one division per second). B: Angular displacement of eyes (time constant, 0.3 second; calibration signal, 10°). C: Rotational velocity of eyes (time constant, 0.003 second, calibration signal, 20°/second); a, maximum slow-phase velocity during rotation; b, duration of perrotatory nystagmus; c, duration of postrotatory nystagmus. D: Angular velocity of rotating chair; d, duration of rotation.

Velocity then decayed to 0° over a period of 20 seconds, approximately six revolutions. The test was performed twice for clockwise and twice for counter-clockwise rotation. The velocity-time function of the chair is shown in FIGURE 1D, along with the response of a normal adult (FIGURE 1B and C). Responses were recorded according to duration and number of beats of perrotatory nystagmus. These measures are more reliable than velocity of slow phase, since young infants and deaf children cannot cooperate in the calibration procedure that is required for accurate velocity measurements.

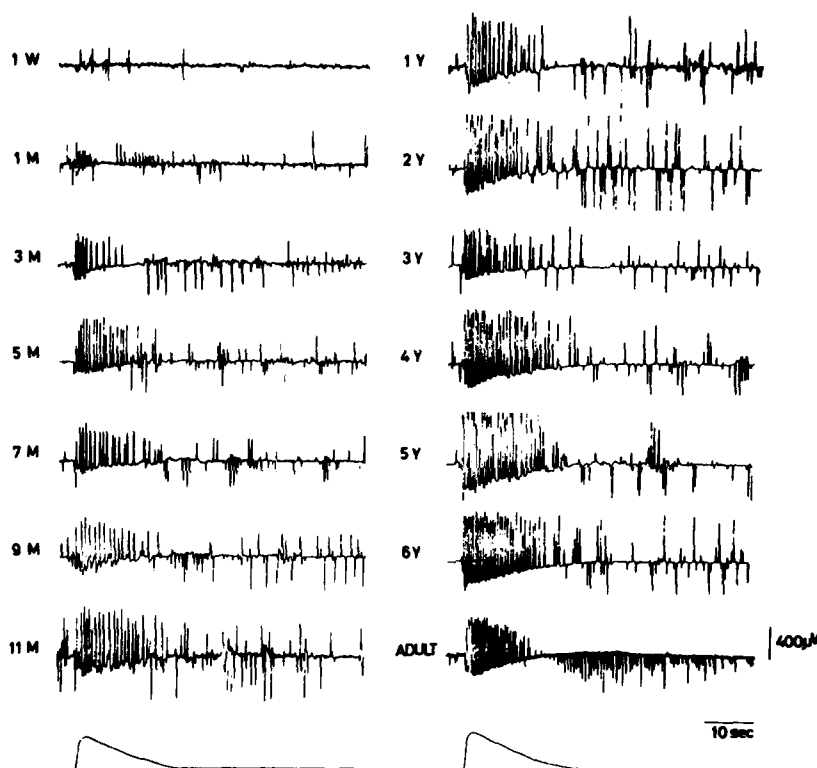


FIGURE 2. Examples of perrotatory and postrotatory nystagmus with damped-rotation test, recorded from normal subjects ranging from neonate to adult.

RESULTS

FIGURE 2 shows examples of perrotatory and postrotatory nystagmus elicited by the damped-rotation test from subjects ranging from a neonate to an adult. In the first year of life, the number of beats and the duration of perrotatory nystagmus clearly increase with age. Postrotatory nystagmus is more variable in this period because body movements interfere with the weak responses of

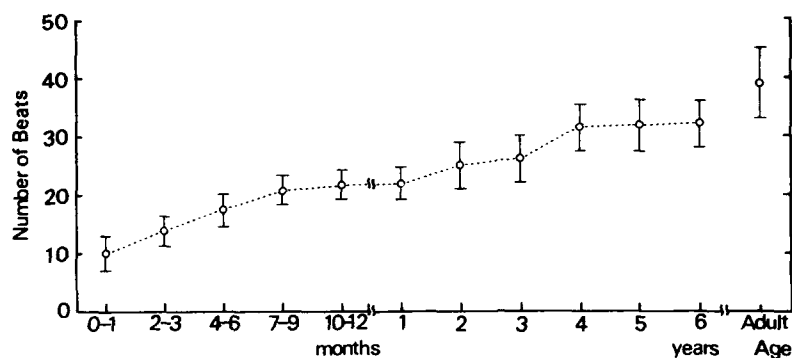


FIGURE 3. Mean number of beats of perrotatory nystagmus as a function of age. Error bars indicate ± 1 SD for each age group.

infancy. The head is inclined forward at 30° during the test, and infants resist being held in this position for more than a few seconds.

These responses suggest that number of beats or the duration of perrotatory nystagmus, rather than of postrotatory nystagmus, may be an appropriate parameter for evaluation of vestibular ocular reflexes in infants.

Control Group

FIGURE 3 shows the relationship between mean number of beats of perrotatory nystagmus and age; error bars indicate \pm one standard deviation (SD). With increase in age, the number of beats increases, the mean at one year being approximately twice that of neonates and half that of adults.

The relationship between the duration of perrotatory nystagmus and age appears in FIGURE 4. The duration increases with age, up to six years. The increase is especially marked during the first year of life. One-year-olds have

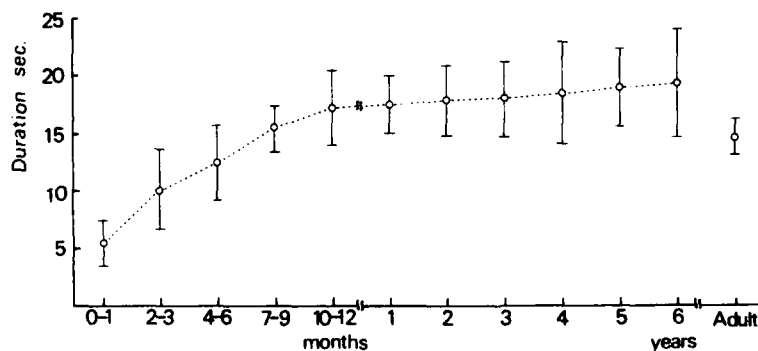


FIGURE 4. Relation between mean duration of perrotatory nystagmus and age. Error bars indicate ± 1 SD.

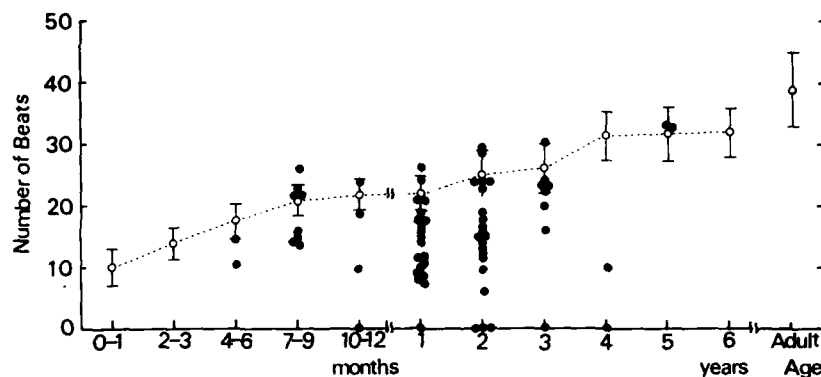


FIGURE 5. Number of beats of perrotatory nystagmus in congenitally hearing-impaired infants and children, superimposed on the data of normal subjects shown in FIGURE 3. Each black circle indicates one case at the indicated age.

scores approximately thrice those of the neonates, but the difference between one-year-olds and six-year-olds is very small. The adults' data show a somewhat shorter duration and a narrow standard deviation.

Congenitally Hearing-Impaired Group

In FIGURE 5, the number of beats for each case of congenital hearing impairment is indicated by a black circle plotted on the data of FIGURE 3. Among the hearing-impaired group, 22 cases (33%) had normal responses, 38 cases (57%) showed hypoaffective responses (more than 1 SD below the mean), and in 7 cases (10%) responses were absent.

In FIGURE 6, the duration of perrotatory nystagmus of each case, indicated by

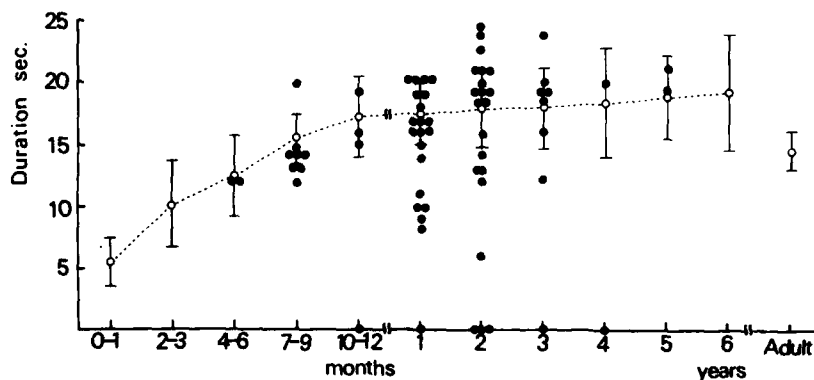


FIGURE 6. Duration of perrotatory nystagmus of congenitally hearing-impaired infants and children. Each black circle, superimposed on the normal duration-age function, indicates one case of that age.

a black circle, is plotted on the normal duration-age function. Forty-six cases (69%) fall within one SD. This is twice as many as were within the normal range on the measure of the number of beats. Therefore, the number of beats was used as the basis for classifying the cases for the analysis of gross motor milestones.

TABLE 1 shows the ages at development of head control and at initial walk for the hearing-impaired cases, classified according to vestibular function, along with the ages of the control group. Vestibular function was defined as normal, hypoactive, or absent on the basis of the number of beats of perrotatory nystagmus. Hypoactivity or absence of vestibular function was associated with marked delay; in the present series, every child with absent function was late in reaching the gross motor milestones, as were most but not all of the children with reduced function.

There was one child, excluded from TABLE 1, who still does not walk at four years of age. Head control in this case began at four months, and no neurological

TABLE 1
AGE AT REACHING GROSS MOTOR MILESTONES

Diagnosis		Head Control (month)				First Walk (month)			
Auditory	Vestibular	n	\bar{X}	SD	Range	n	\bar{X}	SD	Range
Normal	Normal	30	3.4	0.6	3-3.8	30	12.4	0.5	11-12
Impaired	Normal	22	3.7	1.5	3-7	18	13.7	2.8	11-20
Impaired	Hypoactive	38	5.3	2.2	3-9	29	21.4	6.5	21-40
Impaired	Absent	6	7.3	3.1	6-12	5	25.6	8.1	18-41

signs had been found, except for disequilibrium and hypotonus of the legs. The brain computerized-tomography (CT) scans (FIGURE 7) show marked dilation of the lateral and third ventricles. In this case, vestibular dysfunction and intracranial pathophysiology both may contribute to this remarkable delay in walking.

DISCUSSION

Our data provide further evidence for the thesis that vestibular dysfunction may delay the achievement of head control and independent walking in infants. There was found to be a 55% incidence of hypoactivity of the vestibulo-ocular reflex among children with congenital hearing impairment, and the reflex was absent in another 10%. It is clear that impairment or absence of this reflex was associated with delay of gross motor landmarks in these children but that the children were able to acquire these skills eventually, provided that other functions were not impaired as they were in the case with abnormal CT-scan findings.

Normally, the vestibulo-ocular reflex regulates eye-head coordination of gaze, while the vestibulospinal reflex helps to maintain postural control.^{16,17} Therefore, these two reflexes are important for the development of balance and locomotion. It follows that impairment of these reflexes in infancy may lead to delayed achievement of gross motor milestones. However, the delay seems to be compensated for easily by plasticity of the central nervous system and by development of proprioceptive, visual, and motor systems. Compensation in later

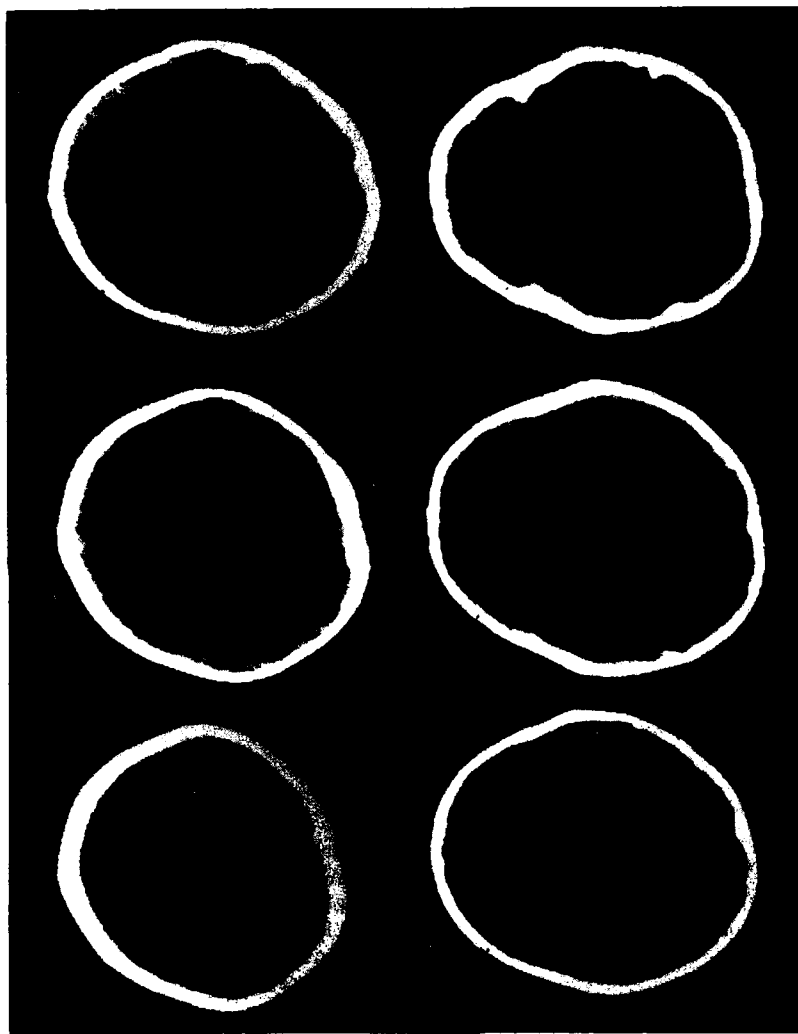


FIGURE 7. Brain CT scan of congenitally deaf child who still cannot walk at the age of four years. No abnormal neurological signs have been noted, except disequilibrium and hypotonus of legs. Remarkable dilation of the lateral and third ventricles is apparent.

childhood is quite good, so that special tests may be required to elicit any abnormality of gait due to vestibular dysfunction.¹

If the prognosis is so good in cases of vestibular impairment, one may wonder why detection of the problem is of concern. One answer is that delay of gross motor landmarks is suggestive of a variety of disabilities having less favorable outcomes, notably cerebral palsy, mental retardation, and minimal brain dysfunction.^{1,2,18} Failure to identify correctly a peripheral vestibular lesion may lead to increased anxiety on the part of the parents, or even to a misdiagnosis of neurological impairment.^{1,2} In order to avoid this error in the case of hearing-impaired children who have "floppy" heads or who are late walkers, Rapin has emphasized that all deaf children should undergo vestibular testing as a part of their total evaluation.

For this purpose, caloric and rotational tests of various kinds have been used.¹⁰⁻¹⁴ The caloric test permits testing of each labyrinth separately, but unilateral lesions are not a great handicap as far as gross motor development is concerned because one labyrinth provides sufficient information for the vestibular reflexes. In any event, it is difficult to obtain children's cooperation for this test and to observe their responses, since the procedure often elicits startle responses or crying. The rotational tests do not permit independent stimulation of the left and right labyrinths, but they are more practical for the clinical examination of infants and children.

Several kinds of rotation tests have been applied to the evaluation of infants and children, and the reports of these tests have devoted much discussion to the various measures of perrotatory and postrotatory nystagmus that have been considered as indices of vestibular dysfunction.¹⁰⁻¹⁴ The speed of the slow component is regarded as the best measure of the degree of vestibular stimulation, a high speed being considered an expression of high peripheral activity.¹⁰ In infants and children, this measure is more precise than number of beats or duration according to Tibbling, who reports that the latter measures correlate with speed and amplitude less well in infants than in adults.¹¹ Tibbling also found the amplitude and duration measures to diverge in infancy; the responses tend to be of shorter duration but higher amplitude. In clinical practice, however, the present results suggest that the number of beats of the perrotatory nystagmus can be used readily as an indicator of vestibular function in infancy. This measure appeared to discriminate cases of hypofunction from those of hearing impairment with normal vestibular function, and has a practical advantage in that amplitude calibration, a difficult or impossible task with infants, need not be performed.

The systematic increase in number of beats and duration as a function of age suggests also that rotation tests may have some value in developmental evaluations of children who have normal peripheral function but who are at risk for central nervous system involvement. The present data do not elucidate the basis for the maturational changes in the vestibulo-ocular reflex, but we may speculate that myelination within the central nervous system, which continues after birth, may play an important role by enhancing conduction velocity.

In recent years we have seen increased recognition of the need for early and aggressive habilitation of hearing-impaired children. Comprehensive evaluations—including but not limited to auditory, neurological, and intellectual status—are essential to the implementation of an individualized treatment plan. In view of the prevalence of vestibular hypofunction among these children and its impact in their early development, we concur that vestibular assessment should be an essential part of this evaluation.

REFERENCES

1. RAPIN, I. 1974. Hypoactive labyrinths and motor development. *Clin. Pediatr.* **13**: 922-937.
2. EVIATAR, L. & A. EVIATAR. 1978. Neurovestibular examination of infants and children. *Adv. Oto-Rhino-Laryngol.* **23**: 169-191.
3. GUILDER, R. P. & L. A. HOPKINS. 1936. Auditory function studies in an unselected group of pupils at the Clarke School for the Deaf. III. Relation between hearing acuity and vestibular function. *Laryngoscope* **46**: 190-197.
4. ARNVIG, J. 1955. Vestibular function in deafness and severe hardness of hearing. *Acta Otolaryngol.* **45**: 283-288.
5. ROSENBLÜT, B., R. GOLDSTEIN & W. M. LANDAU. 1960. Vestibular responses of some deaf and aphasic children. *Ann. Otol. Rhinol. Laryngol.* **69**: 747-755.
6. SWISHER, L. P. & R. P. GANNON. 1968. A comparison of auditory and vestibular responses in hearing-impaired children. *Acta Otolaryngol.* **66**: 89-96.
7. SANDBERG, L. E. & K. TERKILDSEN. 1965. Caloric tests in deaf children. *Arch. Otolaryngol.* **81**: 350-354.
8. ANSON, B. J. 1973. Developmental anatomy of the ear. In *Otolaryngology*. M. M. Paparella & D. A. Shumrick, Eds. 1: 3-74. W. B. Saunders Company, Philadelphia, Pa.
9. YAKOVLEV, P. I. & A-R. LECOURS. 1967. The myelogenetic cycles of regional maturation of the brain. In *Regional Development of the Brain in Early Life*. A. Minkowski, Ed.: 3-70. Blackwell Scientific Publications, Oxford, England.
10. MICHISHITA, K. 1967. Studies of normal vestibular reaction in children. *J. Otolaryngol. Soc. Jpn.* **70**: 37-60. (In Japanese.)
11. TIBBLING, L. 1969. The rotatory nystagmus response in children. *Acta Otolaryngol.* **68**: 459-467.
12. VAN DER LAAN, F. L. & W. J. OOSTERVELD. 1974. Age and vestibular function. *Aerosp. Med.* **45**: 540-547.
13. EVIATAR, L., S. MIRANDA, A. EVIATAR, K. FREEMAN & M. BORKOWSKI. 1979. Development of nystagmus in response to vestibular stimulation in infants. *Ann. Neurol.* **5**: 508-514.
14. ORNITZ, E. M., C. W. ATWELL, D. O. WALTER, E. E. HARTMANN & A. E. KAPLAN. 1979. The maturation of vestibular nystagmus in infancy and childhood. *Acta Otolaryngol.* **88**: 244-256.
15. KAGA, K. & Y. TANAKA. 1980. Auditory brainstem response and behavioral audiometry. *Arch. Otolaryngol.* **106**: 564-566.
16. BIZZI, E., R. E. KALIL & V. TAGLIASCO. 1971. Eye-head coordination in monkeys: evidence for centrally patterned organization. *Science* **173**: 452-454.
17. MOLINA-NEGRO, P., R. A. BERTRAND, E. MARTIN & A. GIOANI. 1980. The role of the vestibular system in relation to muscle tone and postural reflexes in man. *Acta Otolaryngol.* **89**: 524-533.
18. TOROK, N. & M. A. PERLSTEIN. 1962. Vestibular findings in cerebral palsy. *Ann. Otol. Rhinol. Laryngol.* **71**: 51-67.
19. HENRIKSSON, N. G. 1955. The correlation between the speed of the eye in the slow phase of nystagmus and vestibular stimulus. *Acta Otolaryngol.* **45**: 120-136.

VELOCITY STORAGE, NYSTAGMUS, AND VISUAL-VESTIBULAR INTERACTIONS IN HUMANS*

Bernard Cohen, Volker Henn,† Theodore Raphan,
and Debra Dennett

*Department of Neurology
Mount Sinai School of Medicine
City University of New York
New York, New York 10029*

INTRODUCTION

A mechanism that stores activity related to slow-phase eye velocity plays an important role in producing vestibular nystagmus, optokinetic nystagmus (OKN) and visual-vestibular interactions.^{1,2} This mechanism is present in a wide range of species (see Reference 3 for review) and has been studied extensively in monkeys. Stored activity promotes ocular following during OKN and is responsible for optokinetic after-nystagmus (OKAN).¹ During vestibular nystagmus, stored activity lengthens the time over which compensatory eye movements are maintained.^{2,4} Modeling of the vestibulo-ocular reflex (VOR) has shown that a single storage element is capable of mediating these responses and can reproduce many phenomena of visual-vestibular interactions.²

Manifestations of stored activity also are found in neurons in the vestibular nuclei of the monkey. Canal afferents in the vestibular nerve have a decay time constant of about 5-6 seconds after pulses of acceleration.⁵ The decay time constant of neurons in the vestibular nuclei always is longer than that of canal afferents, usually varying between 10 and 30 seconds depending on the state of habituation.^{6,7} These same central neurons also are activated during OKN and OKAN. This demonstrates stored activity in firing rates of vestibular nuclei neurons and supports the theory of a common storage element.

While this storage mechanism has been studied in animals, it is not known whether it plays a role in generating or modulating nystagmus in humans. Because the dominant time constant of the cupula-endolymph system and of activity in semicircular canal afferents cannot be determined directly in man, other ways have to be found to demonstrate the presence of stored activity in the oculomotor response. One way is by the presence of OKAN. OKAN represents the steady discharge of activity related to slow-phase velocity stored during exposure to a moving surround.^{1,8-12} Storage of activity also is manifest in visual-vestibular interactions. Mowrer and Ter Braak were the first to show that postrotatory nystagmus is weaker after rotation in light than in darkness. They inferred that OKAN had summated with the vestibular after-nystagmus to reduce or abolish it. In similar experiments on humans, after-nystagmus was reduced

*Supported by National Institutes of Health Research Grant NS 00294, National Eye Institute Academic Investigator Award EY 00157 (T.R.), and a grant from the Roche Research Foundation for Scientific Exchange and Biomedical Collaboration.

†Faculty of Medicine, University of Zurich, CH-8091 Zurich, Switzerland.

after rotation in light.¹⁶ The purpose of this study was to determine whether stored activity related to slow-phase eye velocity is present in humans and whether it contributes to visual-vestibular interactions.

METHODS

Experiments were done on five individuals ranging in age from 13 to 48. Eye movements were recorded with electro-oculography (EOG) using d.c. coupling. The recording system had an upper bandpass of 150 Hz. Eye movements were calibrated before and after each trial. Horizontal and vertical eye movements were recorded on paper and on FM magnetic tape along with slow-phase velocity and signals representing illumination, table position, OKN drum velocity and perceived rotation. Subjects estimated rotation by moving a handle fixed to the shaft of a potentiometer that was part of a bridge circuit. Each complete revolution of the handle represented 360° of subjective rotation. This is designated in the figures as "rotation sensation."

During experiments, subjects sat in a chair on a rotating platform. The platform was situated inside a rotating optokinetic drum that had alternating 7.5° black and white stripes. The drum and platform could be rotated together or separately by servo-controlled motors. The maximum acceleration of the platform was 100°/second². The platform and drum could be coupled mechanically to provide a fixed visual field during rotation. Steps of platform velocity in darkness were used to study vestibular nystagmus, steps of surround velocity in light were given to study OKN and OKAN, and subjects were rotated in an earth-stationary lighted surround to study the effects of visual-vestibular interactions on per- and postrotatory nystagmus. After each of these stimuli, the after-nystagmus was recorded in darkness. To test for effects of fixation suppression of nystagmus, subjects were shown a stationary surround for variable periods of time during postrotatory nystagmus or OKAN, and the recovery velocity of nystagmus was determined after they were put back into darkness.

RESULTS

Vestibular nystagmus, OKN, and OKAN for one subject are shown in FIGURE 1. During vestibular nystagmus induced by a step in velocity in darkness, eye velocity rose to a maximum value, then declined slowly over a period of 45 to 75 seconds (FIGURE 1A). There usually was a plateau in eye velocity at the onset of the per- or postrotatory nystagmus in humans as in the monkey.² During acceleration in darkness, subjects signaled that they were rotating. During constant-velocity rotation, the sensation of rotation gradually dissipated and subjects felt that they were stationary, although they often still had nystagmus (FIGURE 1A). During deceleration, an oppositely directed postrotatory response was elicited; its characteristics were similar to those of the perrotatory nystagmus. The gain of vestibular nystagmus (peak slow-phase eye velocity/stimulus velocity) varied from 0.3-0.7 in the five individuals. The gain of the subject whose responses are shown in FIGURE 1 is plotted in FIGURE 2A. VOR gains in humans were less than in the monkey, which usually has a gain close to unity.^{2,17-19}

OKN elicited by surround rotation is shown in FIGURE 1B. At the onset of stimulation, there was a rapid rise in eye velocity to a steady-state level.

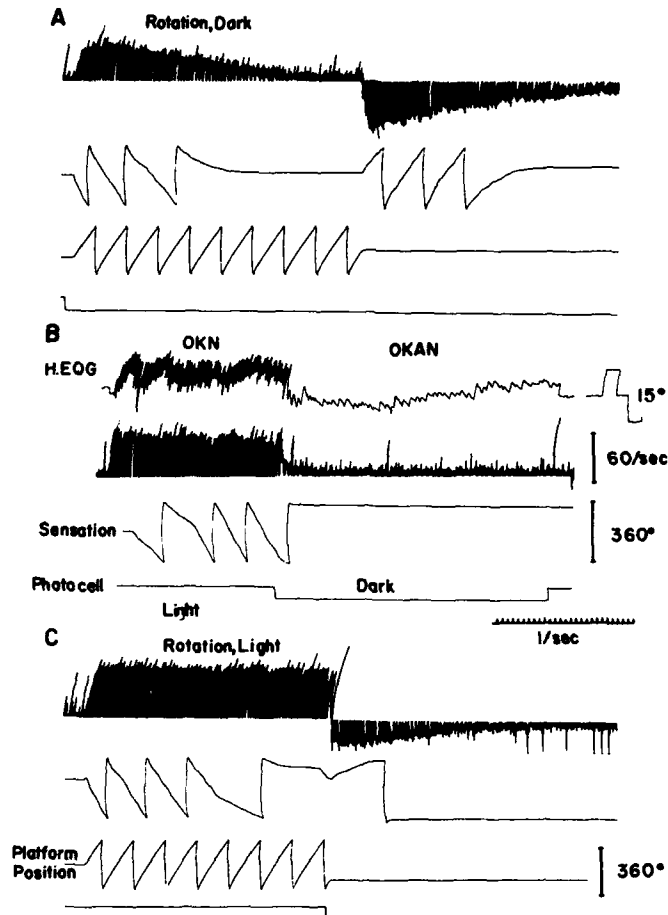


FIGURE 1. Vestibular nystagmus, OKN, and OKAN of a human subject in response to platform rotation (A, C) or surround rotation (B) at $60^\circ/\text{second}$. In A, the entire test was in darkness. In B and C, the surround or subject, respectively, was rotated in light and the OKAN or postrotatory nystagmus was recorded in darkness. From above: horizontal eye position, slow-phase eye velocity, rotation sensation, and photocell showing the presence or absence of light. Rotation sensation was determined subjectively by turning a potentiometer; one full turn equals 360° . Note the weak OKAN after OKN at $60^\circ/\text{second}$ (B). Note also the decrease in slow-phase velocity and sensation of rotation after rotation in light (C), compared with that after rotation in dark (A).

Maximum velocities were reached in the first beat. This is different from OKN in the monkey, which is characterized by both a rapid and a slow rise to a steady-state level. The slow rise is associated with charging of the storage mechanism responsible for OKAN.¹ The gain of OKN in humans was close to unity up to $60\text{--}90^\circ/\text{second}$ (FIGURE 2B).^{20,21} Within 5–6 seconds after the onset of full-field motion, a sensation of self-rotation, circularvection, was elicited.^{10,11,21} It

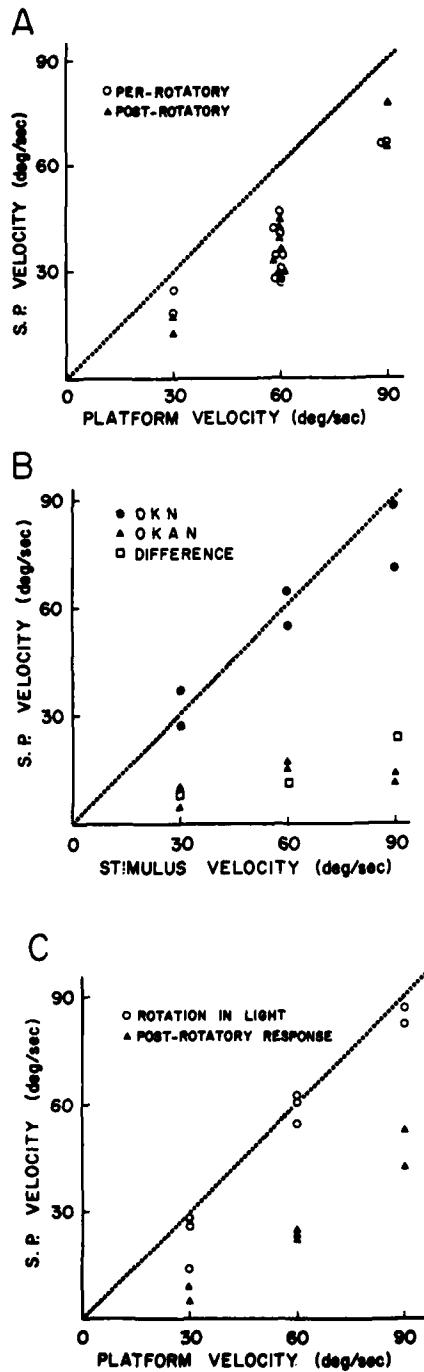


FIGURE 2. Vestibular nystagmus, OKN, OKAN, and the visual-vestibular interaction in one subject. **A:** slow-phase velocities of per- and postrotatory nystagmus induced by steps of platform velocity of 30, 60, and 90°/second in darkness. The dotted line indicates unity gain in this and subsequent parts of this figure. **B:** OKN, OKAN, and the difference between postrotatory nystagmus after rotation in light and in dark. Note that the gain of OKN was close to unity. Note also that the difference in peak velocities of postrotatory nystagmus (squares) was approximately equal to the value of OKAN (triangles). **C:** slow-phase velocities during rotation in an earth-stationary lighted surround and during the after-nystagmus recorded in darkness. The squares of FIGURE 2B were derived by subtracting values represented by the triangles in FIGURE 2C from those in FIGURE 2A.

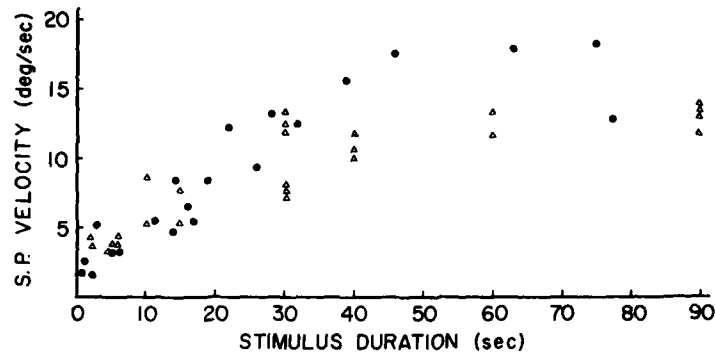


FIGURE 3. Effects of varying the period of exposure of moving full-field stimulus on the development of OKAN. The stimulus velocity was $60^\circ/\text{second}$. Responses are shown for two subjects. In each of these individuals, the OKAN was evoked maximally by about 30-40 seconds of exposure to the stimulus.

persisted for the duration of stimulation (FIGURE 1B). At the end of rotation, there was weak OKAN, which lasted for 45-50 seconds.^{10,11,21-24} It was unaccompanied by a sensation of rotation in our subjects. The gain of OKN or OKAN did not depend on the presence of circularvection. In the five subjects tested, the velocity of OKAN was maximally $15-20^\circ/\text{second}$ (FIGURE 2B). In monkeys, OKAN velocities reach values of $90-120^\circ/\text{second}$.¹

While there was no apparent slow rise in nystagmus velocity during OKN, stored activity responsible for OKAN built up slowly. To investigate this, two subjects were exposed to varying periods of surround rotation of from 2-90 seconds.^{1,24} OKAN elicited by the period of stimulation was recorded in darkness. The time constant of the rise in OKAN was about 20 seconds (FIGURE 3). The fall of OKAN velocity in darkness was somewhat longer. It had a time constant of about 25 seconds. This is different from the monkey, which has a charging time constant of OKAN of 3-5 seconds and a falling time constant of 10-30 seconds. This demonstrates that in humans the storage mechanism responsible for OKAN accumulates activity more slowly and does not reach values that are as high as in the monkey.

Rotation in a lighted stationary surround elicits both vestibular nystagmus and OKN. At the onset of rotation, eye velocity rose to a steady-state level that was maintained for the duration of stimulation (FIGURE 1C). When subjects were decelerated and lights turned off, there was oppositely directed after-nystagmus. It always was weaker than the nystagmus that followed rotation in darkness (compare FIGURE 1A and C). The sensation of rotation during the after-response also was attenuated markedly following rotation in light. Up to about $30^\circ/\text{second}$, there was no after-sensation. The percept was simply that one had stopped suddenly. At higher velocities, there was more after-sensation, but it was always less than that following rotation in darkness at a similar velocity.

The response to testing at various velocities in one subject is shown in FIGURE 2C. The circles show the maximum perrotatory slow-phase velocities in light, and the triangles the velocities of the after-nystagmus recorded in darkness. This can be compared to the velocity of the postrotatory responses that followed rotation in

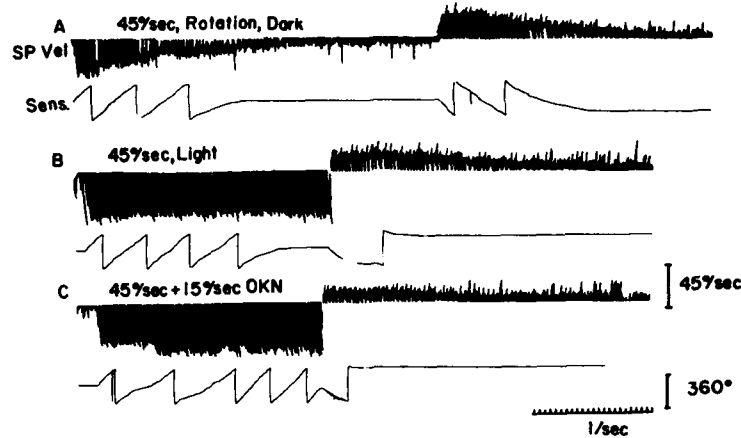


FIGURE 4. Effects of adding OKN during rotation (C) on the postrotatory response recorded in darkness. In each instance the vestibular stimulus was a step in velocity at 45°/second in dark (A) and in light (B). Both the postrotatory nystagmus and the sensation of movement were weaker after OKN had been added during rotation.

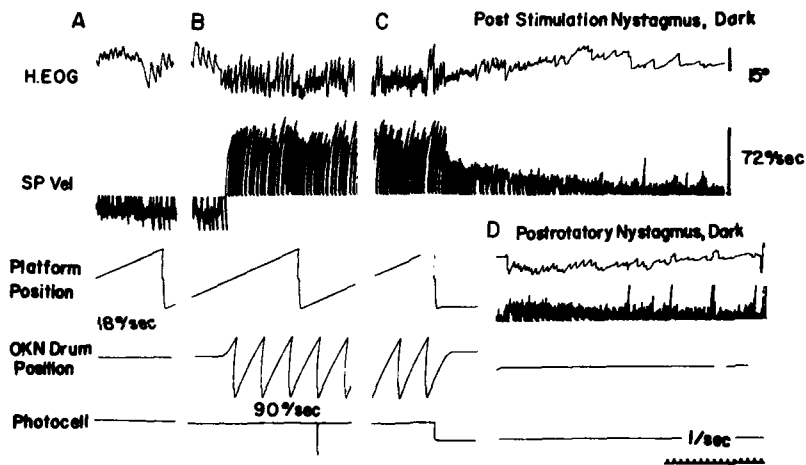


FIGURE 5. Enhancement of postrotatory nystagmus by OKAN. In A, the subject was rotated at 18°/second in an earth-stationary lighted surround. In B, the OKN drum was rotated in the same direction but at a velocity of 90°/second. This created a reversal in the relative direction of surround movement of 72°/second; eye velocity was close to that level. In C, the platform was halted and poststimulus nystagmus was recorded in darkness. The maximal velocity of the postrotatory nystagmus was about 30°/second. This was about 18°/second more than the postrotatory nystagmus recorded after a step of velocity in darkness, shown in D.

dark in this same individual (triangles, FIGURE 2A). At each stimulus velocity, the maximum response after rotation in light was 15 to 20°/second less than after rotation in dark. This difference is plotted in FIGURE 2B by the squares. It is similar to the OKAN induced by stimulation at each of these velocities (triangles, FIGURE 2B). This suggests that activity stored during optokinetic stimulation was responsible for the difference in after-nystagmus that followed rotation in light and in dark (see also Reference 25).

Postrotatory nystagmus also could be enhanced or reduced by varying the relative velocity between the subject and the surround. During platform rotation,

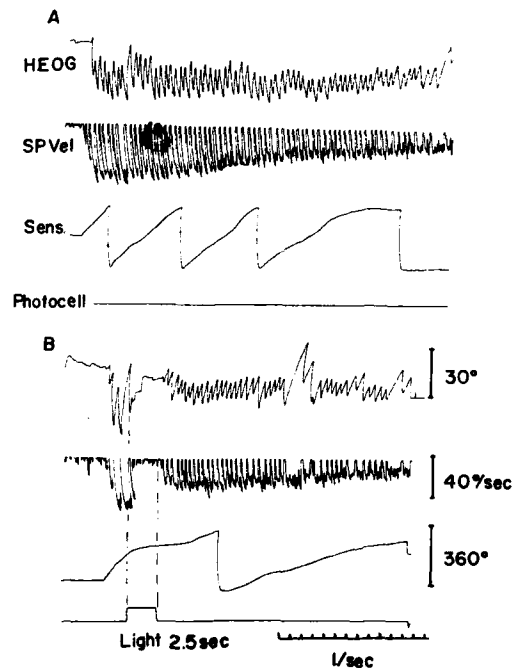


FIGURE 6. A: postrotatory nystagmus induced by rotation at 60°/second. In B, the subject had a 2.5-second period of exposure to a stationary lighted surround. This reduced both the sensation of rotation and the recovery velocity of nystagmus. The reduction in slow-phase velocity was about 15°/second.

the optokinetic cylinder was rotated separately to increase or decrease relative motion between subject and surround. If during platform rotation at 45°/second the drum was rotated at 15°/second in the opposite direction, the visual surround moved with a relative velocity of 60°/second. This caused the OKN velocity to go to 60°/second (FIGURE 4C). After deceleration, the postrotatory nystagmus was reduced beyond that after rotation in light (FIGURE 4B) or in darkness (FIGURE 4A). The effective range over which nystagmus velocity could be manipulated was about 15–20°/second. This is the maximum velocity of OKAN in this individual.

Rotating the surround in the same direction as the subject but at a faster speed causes relative motion of the visual world in the direction of rotation. This

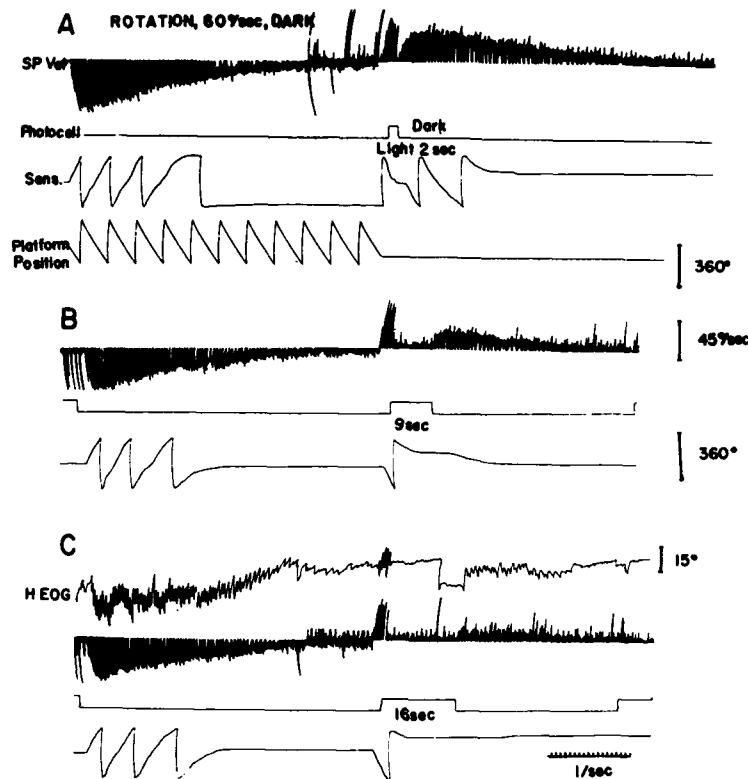


FIGURE 7. Effects of varying the period of exposure to an earth-stationary visual surround on postrotatory nystagmus. There was a progressive decline in slow-phase velocity and sensation of motion as the period of exposure was increased (A-C). Note the slow rise in slow-phase velocity during the recovery nystagmus. This suggests recharge of the velocity storage mechanism, presumably due to continued deflection of the cupula. See text for details.

produces OKN that is opposite to the direction of nystagmus induced in a stationary surround. A result of this is that when the subject is stopped, OKAN now is in the same direction as the postrotatory nystagmus, and the two should summate. With the platform rotating at $45^\circ/\text{second}$ and the drum at $60^\circ/\text{second}$, there was a relative difference of $15^\circ/\text{second}$. This did not cause significant enhancement of the postrotatory nystagmus, although the postrotatory sensation was more intense.

At lower velocities of platform rotation, however, larger relative retinal slips were induced and postrotatory nystagmus velocities were increased. Such an experiment is shown in FIGURE 5. The subject was rotated at $18^\circ/\text{second}$ in light (A). Then the drum was rotated in the same direction at $90^\circ/\text{second}$. This created an OKN stimulus velocity of $72^\circ/\text{second}$, and eye velocity was close to that value (B). When the platform was stopped and the lights were turned off, the postrotatory nystagmus was about $30^\circ/\text{second}$ (C). This was about $18^\circ/\text{second}$ more than

after a similar step of rotation in darkness (D). Thus the stored activity induced by optokinetic stimulation added to or subtracted from velocities induced by vestibular stimulation. The limit was the saturation value for OKAN. This is consistent with the concept of a common storage mechanism for vestibular nystagmus, OKN, and OKAN.

Besides being canceled by OKAN, postrotatory nystagmus in monkeys can be reduced by exposure to a stationary visual surround.² Similarly, in humans, exposure to a stationary visual field during nystagmus caused a loss of stored activity and an attenuation of the response. When lights were turned off after such an exposure, nystagmus velocity was reduced beyond the velocity that would be expected if there had been no period of fixation. FIGURE 6A shows a control postrotatory response to a step of velocity in darkness. In FIGURE 6B, the subject was exposed to a stationary lighted surround for 2.5 seconds during postrotatory nystagmus. When the stationary surround became visible, there was a sudden drop in eye velocity and the eyes were held stable. When lights were turned off again, nystagmus returned. Eye velocity rose slowly to a peak value that was about 15–20°/second less than if there had been no period of fixation. Associated with this, there was a reduction in the sensation of rotation.

There were two differences between the responses of humans and monkeys to periods of fixation suppression during postrotatory nystagmus. In humans, eye velocity was close to zero during fixation suppression. In the monkey, there almost always is some nystagmus during this period. Secondly, in the monkey, 6–10 seconds of exposure to a stationary surround usually is adequate to discharge activity responsible for vestibular nystagmus.² In humans, even 16 seconds of exposure to a stationary field were not sufficient to abolish nystagmus (FIGURE 7). Similar results were found by Koenig and Dichgans.²⁵ The mechanism that discharged, or "dumped," activity from the velocity storage integrator also was not as effective during OKAN in humans as in monkeys. In a typical human

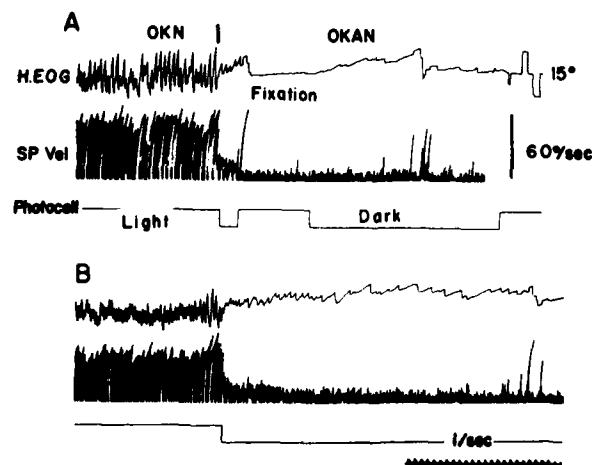


FIGURE 8. Effect of eight-second period of visual fixation on OKAN. The presence of nystagmus after the period of visual fixation indicates that the velocity storage mechanism had not discharged its activity completely during the period of exposure to the stationary surround.

subject, 8 seconds of exposure to a stationary visual surround were inadequate to discharge the activity responsible for OKAN (FIGURE 8). In the monkey, such long values rarely are encountered, and after some practice, OKAN is lost completely after 2-3 seconds of fixation.¹

DISCUSSION

These data demonstrate a number of manifestations of stored activity related to slow-phase eye velocity in humans: (1) OKAN was present after optokinetic stimulation; (2) postrotatory nystagmus velocity measured in darkness was reduced after rotation in light; (3) the velocity storage mechanism became partially charged by exposure to full-field motion for short periods of time; (4) it was discharged by exposure to a fixed visual field; and (5) various rates of field motion relative to the subject increased or decreased postrotatory nystagmus in a predictable fashion.

Lacking information about the dynamics of the cupula, the finding that the visual system is capable of discharging activity associated with postrotatory nystagmus probably is the most direct demonstration that stored activity contributes to the vestibular response in man. (This assumes that the visual system is not capable of affecting VIIIth nerve activity in man as in monkey.) The maximal amount of stored activity for OKN was between 15 and 20°/second. This is similar to that found by Koenig and Dichgans,²⁵ and is considerably less than in the monkey. It would dictate a considerable amount of postrotatory nystagmus in darkness after rotation at higher velocities in light. This was observed consistently.

Previously, by modeling OKN, OKAN, and the visual-vestibular interaction, a number of organizational aspects of the VOR and of visual-oculomotor pathways became apparent.^{1,2} An insight from this work was the recognition that there are direct and indirect pathways from the visual and vestibular systems to the oculomotor system. The direct visual pathway is responsible for the rapid rise in OKN at the onset of stimulation. The indirect pathway utilizes the velocity storage mechanism and provides a common element for coupling both the visual and the vestibular input to the oculomotor output.

Interpreting data presented in this report in the framework of this scheme, it would appear that the direct visual pathways are predominant in humans during OKN, and that visual coupling to the oculomotor system through the indirect pathways is weaker in man than in monkey. Weak coupling is suggested by the long time constant of charge and the low saturation value of OKAN slow-phase velocity relative to OKN velocity. Also, fixation of a stationary environment did not discharge the integrator and reduce nystagmus velocity as rapidly or as completely as in the monkey. A high gain of the direct pathway is suggested by the finding that at the onset of OKN, eye velocity jumps immediately to the stimulus velocity with a gain close to unity, and there is no slow rise as in the monkey. If lights are turned off after optokinetic stimulation, there is a rapid drop in eye velocity to a maximum of 15-20°/second. We interpret this as inactivation of the direct pathways. The gain of direct pathways in man probably is close to unity, whereas in the monkey it is about 0.6.¹ Thus, humans depend much more on activity in direct pathways to sustain optokinetic nystagmus, and the velocity storage mechanism probably contributes much less to OKN. This would lead to the postulate that activation of neurons in the vestibular nuclei during full-field stimulation would be less in man than in monkey. This would explain why

labyrinthectomy has a much more limited effect on OKN in humans than in monkeys.²⁶

Although the velocity storage mechanism makes only a limited contribution to production of OKN, this contribution has two important effects in mediating visual-vestibular interactions. The after-nystagmus following prolonged head rotations is considerably weaker if vision is permitted during rotation, and the after-sensation is strongly reduced. Generally, the sensation of rotation appears to covary with activity in the velocity storage mechanism, but the sensation of motion can be dissociated from nystagmus under certain circumstances. There may be no sensation of rotation at a time when there is nystagmus induced by the velocity storage mechanism, such as during OKAN (FIGURE 1A). Also, the sensation of rotation can be present without the occurrence or intensification of nystagmus. This occurs, for example, during acceleration in a visual field that is stationary with reference to the subject.²⁷

Another question is what role velocity storage might play in producing vestibular nystagmus. Without knowledge of the dynamics of the cupula, the relative contribution of peripheral and central activity to the nystagmus response cannot be measured directly. The return of nystagmus after a period of fixation could occur either if the storage integrator were being reexcited or if the stored activity had not been discharged. The slow rise in eye velocity after 9 seconds of fixation (FIGURE 7B) suggests that the velocity storage integrator was being charged in the period that followed fixation.^{2,28} Presumably, the cupula still was deflected 9-10 seconds after the end of rotation, causing activity in the vestibular nerve to reexcite the storage mechanism, although other sources could contribute to this activity. This suggests that the dominant time constant of human semicircular canal afferents is longer than in the monkey, probably in the range of 7-8 seconds.

Two other lines of evidence are consistent with this suggestion. Humans are larger than the laboratory primates usually used in vestibular research. Therefore, their canals would be larger.²⁹ This causes a shift in canal dynamics,²⁹ giving them a somewhat longer time constant. In addition, in the monkey, the postrotatory response after off-vertical axis rotation is in the range of 3-5 seconds, whereas in humans it is in the range of 7-8 seconds.^{30,31} We have postulated that the shortening of postrotatory nystagmus after off-vertical rotation is due to discharge of activity in the velocity storage integrator.³² If correct, the time constant of nystagmus in this condition closely reflects the time constant of activity in the vestibular nerve. The longer time constant of vestibular nystagmus in humans than in monkeys after off-vertical axis rotation, therefore, could be due to a longer time constant of activity in their canal afferents.

Thus in summary, a velocity storage mechanism is present in man. It appears to play less of a role in producing optokinetic and vestibular responses in the human than in the monkey. However, this mechanism is important for mediating visual-vestibular interactions. Moreover, pathological disturbances of this mechanism could have important effects in producing vertigo in various disease states.

ACKNOWLEDGMENTS

We thank Walter Waespe, Bruno Waespe, and Nathaniel Cohen for serving as subjects.

REFERENCES

1. COHEN, B., V. MATSUO & T. RAPHAN. 1977. Quantitative analysis of the velocity characteristics of optokinetic nystagmus and optokinetic after nystagmus. *J. Physiol.* **270**: 321-344.
2. RAPHAN, T., V. MATSUO & B. COHEN. 1979. Velocity storage in the vestibulo-ocular reflex arc (VOR). *Exp. Brain Res.* **35**: 229-248.
3. HENN, V., B. COHEN & L. R. YOUNG. 1980. Visual vestibular interaction in motion perception and the generation of nystagmus. *Neurosci. Res. Program Bull.* **18**: 459-651.
4. ROBINSON, D. A. 1975. Oculomotor control signals. In *Basic Mechanisms of Ocular Motility and Their Clinical Implications*. G. Lennerstrand & P. Bach-y-Rita, Eds: 337-374. Pergamon Press, Oxford, England.
5. GOLDBERG, J. M. & C. FERNÁNDEZ. 1971. Physiology of peripheral neurons innervating semicircular canals of the squirrel monkey. I. Resting discharge and response to constant angular accelerations. *J. Neurophysiol.* **34**: 635-660.
6. WAESPE, W. & V. HENN. 1977. Neuronal activity in the vestibular nuclei of the alert monkey during vestibular and optokinetic stimulation. *Exp. Brain Res.* **27**: 523-538.
7. JÄGER, J. & V. HENN. 1981. Vestibular habituation in man and monkey during sinusoidal rotation. *Ann. N.Y. Acad. Sci.* (This volume.)
8. OHM, J. 1921. Ueber optischen Drehnystagmus. *Klin. Monatsbl. Augenheilkd.* **68**: 234-235.
9. KRIEGER, H. P. & M. B. BENDER. 1956. Optokinetic after nystagmus in the monkey. *Electroencephalogr. Clin. Neurophysiol.* **8**: 97-106.
10. BRANDT, T. & J. DICHGANS. 1972. Circularvection, optische Pseudocoriolis-Effekte und optokinetischer Nachnystagmus. *Albrecht von Graefes Arch. Klin. Exp. Ophthalmol.* **184**: 42-57.
11. BRANDT, T., J. DICHGANS & W. BUECHELE. 1974. Inverted self motion perception and optokinetic after-nystagmus. *Exp. Brain Res.* **21**: 337-352.
12. WAESPE, W. & V. HENN. 1977. Vestibular nuclei activity during optokinetic after-nystagmus (OKAN) in the alert monkey. *Exp. Brain Res.* **30**: 323-330.
13. MOWRER, O. H. 1934. The modification of vestibular nystagmus by means of repeated elicitation. *Comp. Psychol. Monogr.* **9**: 1-48.
14. MOWRER, O. H. 1937. The influence of vision during bodily rotation upon the duration of post-rotational vestibular nystagmus. *Acta Otolaryngol. Stockh.* **25**: 351-364.
15. TER BRAAK, J. W. G. 1936. Untersuchungen über optokinetischen Nystagmus. *Arch. Neerl. Physiol.* **21**: 309-376.
16. JUNG, R. 1948. Die Registrierung des postrotatorischen und optokinetischen Nystagmus und die optisch-vestibuläre Integration beim Menschen. *Acta Otolaryngol. Stockh.* **36**: 199-202.
17. SKAVENSKI, A. A. & D. A. ROBINSON. 1973. Role of abducens motoneurons in the vestibulo-ocular reflex. *J. Neurophysiol.* **36**: 724-738.
18. KELLER, E. 1978. Gain of the vestibulo-ocular reflex in monkey. *Vision Res.* **18**: 311-315.
19. MILES, F. A. & B. B. EIGHMY. 1980. Long term adaptive changes in primate vestibulo-ocular reflex. I. Behavioral observations. *J. Neurophysiol.* **93**: 1406-1425.
20. GRUETTNER, R. 1979. Experimentelle Untersuchungen über der optokinetischen Nystagmus. *Z. Sinnesphysiol.* **68**: 1-48.
21. DICHGANS, J. & T. BRANDT. 1978. Visual-vestibular interactions. Effects on self-motion perception and postural control. In *Handbook of Sensory Physiology*. R. Held, H. Liebowitz & H. L. Teuber, Eds. 7: 755-804. Springer Verlag, New York, N.Y.
22. MACKENSEN, G., G. KOMMERELL & D. SILBERSEN. 1961. Untersuchungen zur Physiologie des optokinetischen Nachnystagmus. *Albrecht von Graefes Arch. Ophthalmol.* **163**: 170-187.
23. MACKENSEN, G. 1958. Zur Theorie des optokinetischen Nystagmus. *Klin. Monatsbl. Augenheilkd.* **132**: 769-780.
24. KOMMERELL, G. & H. THIELE. 1970. Der optokinetische Kurzreiznystagmus. *Albrecht von Graefes Arch. Klin. Exp. Ophthalmol.* **179**: 230-234.

25. KOENIG, E. & J. DICHGANS. 1981. Aftereffects of vestibular and optokinetic stimulation and their interaction. *Ann. N.Y. Acad. Sci.* (This volume.)
26. ZEE, D. S., R. D. YEE & D. A. ROBINSON. 1976. Optokinetic responses in labyrinthine-defective human beings. *Brain Res.* **113**: 423-428.
27. WAESPE, B., W. WAESPE & V. HENN. 1980. Subjective velocity estimation during conflicting visual-vestibular stimulation. *Arch. Psychiatr. Nervenkr.* **228**: 109-116.
28. COHEN, B. & T. RAPHAN. 1981. Stored neural activity in the vestibulo-ocular reflex and the response to vestibular testing. In Conference Volume on Ototoxicity of Aminoglycosides. Little Brown & Co. Boston, Mass. (In press.)
29. MELVILL JONES, G. 1974. The functional significance of size in the semicircular canals. In *Handbook of Sensory Physiology*. H. H. Kornhuber, Ed. **6/2**: 171-184. Springer Verlag. New York, N.Y.
30. GUEDRY, F. E. 1965. Orientation of the rotation axis relative to gravity: its influence on nystagmus and the sensation of rotation. *Acta Otolaryngol. Stockh.* **60**: 30-48.
31. BENSON, A. J. & H. A. BODIN. 1966. Interaction of linear and angular accelerations on vestibular receptors in man. *Aerosp. Med.* **37**: 144-154.
32. RAPHAN, T., B. COHEN & V. HENN. 1981. Effects of gravity on rotatory nystagmus in monkeys. *Ann. N.Y. Acad. Sci.* (This volume.)

AFTEREFFECTS OF VESTIBULAR AND OPTOKINETIC STIMULATION AND THEIR INTERACTION

E. Koenig and J. Dichgans

Neurological Clinic
University of Tübingen
D-7400 Tübingen, Federal Republic of Germany

INTRODUCTION

In recent years, the interaction of optokinetic and vestibular stimuli on the slow-phase velocity (SPV) of nystagmus and on the perception of body motion has gained increasing interest. The resulting research work has improved our understanding of how man compensates for a sensory deficit: there is no receptor signaling constant angular or linear body velocity. The adequate inputs to the semicircular canals are angular accelerations; and to the otoliths, linear accelerations.

With vestibular stimuli of high frequency (sinusoidal stimulation above 0.1 Hz), this deficit is compensated for by the inertia of the cupula, which integrates the acceleration to a velocity signal of the head in space.¹ With lower frequencies of vestibular stimulation, the output of the peripheral vestibular system undergoes a phase shift. It is less and less proportional to head velocity, but eventually—at frequencies below 0.005 Hz²—corresponds to head acceleration. The mechanical integration of the cupula is reflected in the time constant (3–5 seconds) of the peripheral vestibular nerve.¹ An additional central integrator³—presumably located in the vestibular nuclei storing the neuronal activity from the peripheral nerve—extends to lower frequencies the range of frequencies eliciting a vestibulo-ocular reflex (VOR) in phase with head velocity.² This central integration prolongs the peripheral time constant (3–5 seconds) to the time constant (15–28 seconds) of the first phase of vestibular after-nystagmus (VAN I).^{4,5}

In spite of its integrative properties, the vestibular system is not able to provide an adequate velocity signal during motion with constant angular velocity. In the presence of visual cues, this can be compensated for by the visual system. When the whole visual surround moves with uniform velocity, a sensation of self-motion is induced (circularvection).^{6,7} The neurophysiological basis for this perception is a convergence of visual inputs on the premotor structures of the vestibular system.^{8–11} Features common to vestibular (VAN I) and optokinetic after-nystagmus (OKAN I), as well as recordings from vestibular neurons during OKAN, indicate that the convergence of the two inputs has to be located at or prior to the level of the central integrator in the vestibular nuclei mentioned above.^{4,5,12} Thus OKAN I and the prolongation of the peripheral time constant (3–5 seconds) to that of VAN I could be accomplished by the same integrator (VAN I-integrator).

A second integrator, however, is required to explain secondary vestibular (VAN II) and secondary optokinetic after-nystagmus (OKAN II), as OKAN II at least is independent of OKAN I.^{13,14} The interaction of the two integrators was studied in our experiments. The experimental setup was designed such that it resembled a natural combination of vestibular and optokinetic stimuli, with the

vestibular stimulus at the beginning. In a second set of experiments, the simplest paradigm of vestibular and optokinetic interaction, i.e., fixation of a pattern at zero velocity, was employed to determine the effect of different durations of visual stimulation on after-nystagmus.

METHODS

Subjects

Four subjects (two male, two female; aged between 22 and 26 years) with normal vestibular function volunteered for our experiments. They were familiar with the apparatus from previous experiments.

Apparatus

For testing, subjects were seated on a chair that rotated about the axis of a surrounding cylindrical drum (Tönnies, Freiburg, 1.4 m in diameter), which served as the visual surround. The inner wall of the drum was covered with 48 alternating black and white stripes, each subtending 7.5° of visual angle. The pattern filled the entire visual field including the retinal periphery. A small band at eye level, extending 10° vertically, was displayed in addition. It was covered with colored comic-strip figures and served as foveal fixation. Both the chair and the drum could be rotated (independently or coupled) at servo-controlled velocities up to $180^\circ/\text{second}$. Horizontal (and vertical) eye movements were recorded using Beckman Ag-AgCl electrodes. After d.c. amplification, eye movements and acceleration signals from drum and chair were recorded on paper charts using a Siemens Mingograph four-channel high-pressure-jet galvanometer system. Calibrations of eye movements were taken from voluntary saccades (four targets at 15° and 30° left and right). These were repeated between trials.

Experimental Procedure

Each subject was seated with the head restrained in a headrest and was asked to pursue attentively the moving pattern or to fixate the stationary pattern when the drum was coupled rigidly to the chair. Acoustic cues from the motors driving the chair and the drum were masked by music from a cassette-recorder, presented via earphones. The stimuli used and the responses obtained are depicted schematically in FIGURE 1. For comparison, pure vestibular stimulation (chair accelerations and decelerations of 3, 6, 9, 12, and $18^\circ/\text{second}^2$ for 10 seconds in the dark, FIGURE 1a) and pure optokinetic stimulation (pattern motions of 30, 60, 90, 120, and $180^\circ/\text{second}$ for 1 minute, FIGURE 1b) also were applied. To test fixation suppression of the VOR (FIGURE 1c), the chair was accelerated with 3, 6, 9, 12, and $18^\circ/\text{second}^2$ for 10 seconds in the dark with the drum rigidly coupled to it. Within the first second after the end of the acceleration, the light was switched on to present the pattern, which was stationary relative to the subject turning at constant speed.

In a second set of experiments, the effect of different time intervals of fixation on the SPV of vestibular nystagmus was studied quantitatively. For vestibular

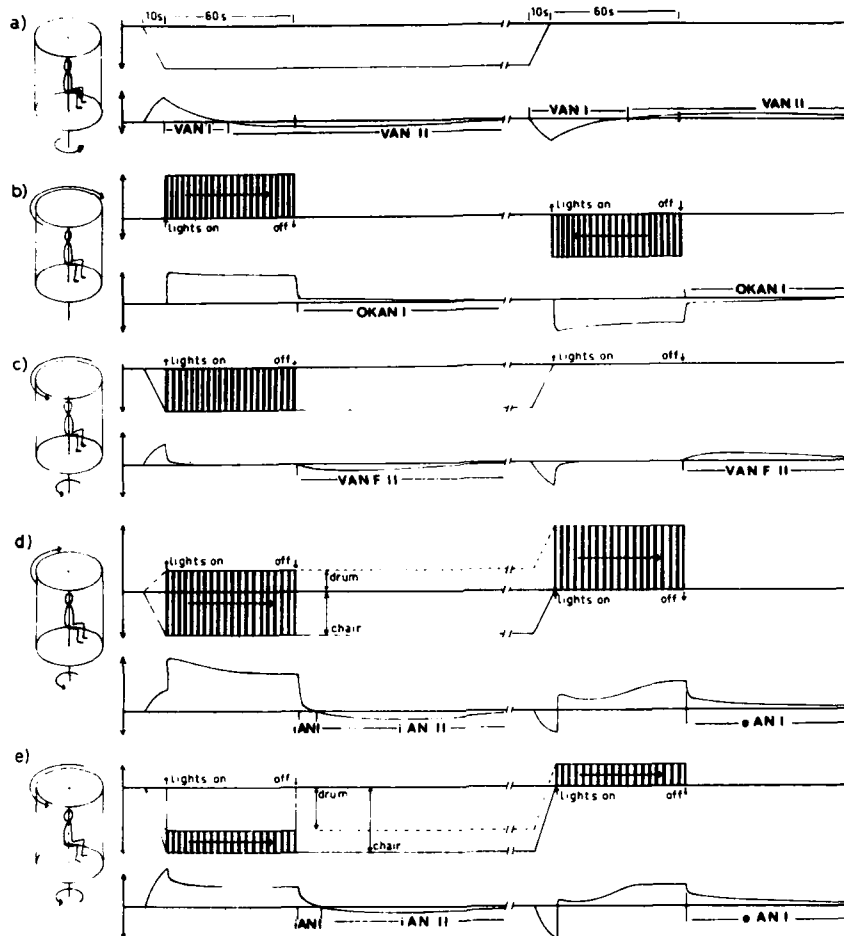


FIGURE 1. The vestibular and optokinetic stimuli used and their combinations, as well as a schematic illustration of the resulting slow-phase velocity of nystagmus (see legend of FIGURE 4 for the meaning of the abbreviations). (a) Pure vestibular stimulation, by chair acceleration to the left, and deceleration of the chair. (b) Pure optokinetic stimulation by a drum rotation for 1 minute to the right and a subsequent drum rotation to the left for the same time. (c) Fixation suppression of vestibular nystagmus for 1 minute by the presentation of a visual surround, stationary in respect to the observer, after the termination of the vestibular stimulus. (d) Combination of a weak acceleration with a high optokinetic pattern velocity, eliciting nystagmus into the same direction after the acceleration and into opposite directions after the deceleration. (e) Combination of a strong acceleration with a low optokinetic pattern speed, resulting in a decrease of SPV after the beginning of optokinetic stimulus.

stimulation, the rotating chair and drum, rigidly coupled to each other, were accelerated with $18^\circ/\text{second}^2$ for 10 seconds in the dark. Within the first second after termination of the acceleration, the light was switched on, presenting the stationary pattern to the subject for the following time intervals: 2, 5, 10, 20, and

30 seconds, and 1, 2, and 3 minutes. Then the light was switched off, and after-nystagmus was recorded until it definitely had ceased.

So as to test interaction (FIGURE 1d and e), the chair was accelerated (or decelerated after an extended period of constant velocity) in the dark for 10 seconds (3, 6, 9, 12, and $18^\circ/\text{second}^2$). Then within 1 second after the end of the acceleration, the light was switched on so as to illuminate the drum. The speed of the drum was adjusted to generate a velocity difference between drum and chair of 30, 60, 90, 120, or $180^\circ/\text{second}$. The subject thereby was exposed to an optokinetic stimulus eliciting nystagmus either toward the same direction as the previous vestibular nystagmus or toward the opposite direction. After 1 minute, the light was switched off and after-nystagmus was recorded until it ceased. The combination of five accelerations and five pattern velocities resulted in 25 trials. For technical reasons (limited maximal speed of the drum), in the first part of each trial, vestibular and optokinetic nystagmus had the same direction; whereas in the second part (deceleration), they were opposite. The 40 trials (including pure vestibular, pure optokinetic, and fixation suppression experiments) were split up into four separate sessions on different days. So as to balance sequential effects, the order of the trials was reversed for two subjects.

RESULTS

Aftereffects of Pure Vestibular Stimulation

After reaching a peak at the end of the acceleration phase lasting 10 seconds, SPV of VAN I declines approximately exponentially. After an acceleration of $18^\circ/\text{second}^2$ (FIGURE 2), the average time constant of this decline was 12.5 seconds and the average duration of VAN I was 36.5 seconds. Thereafter, the second phase (VAN II), with the slow phase toward the opposite direction, started. It ceased on average 175 seconds after the termination of acceleration. The average cumulative amplitude of VAN II was 635° after an acceleration of $18^\circ/\text{second}^2$. For comparison with the aftereffects of the interaction trials (tested after accelerations of 3, 6, 9, 12, and $18^\circ/\text{second}^2$ and a subsequent 1-minute optokinetic stimulation), VAN II cumulative amplitude and duration after pure vestibular stimulation also were measured for the corresponding time interval. This interval started 1 minute after termination of the acceleration. Prior to this time interval, VAN I had decayed and VAN II had started. Cumulative amplitude of VAN II is plotted in FIGURE 4. VAN II following the acceleration is plotted below the abscissa. VAN II following the deceleration is plotted above. Cumulative amplitude (and duration) of VAN II increases with increasing acceleration. In our experiments, cumulative VAN II was considerably weaker (only 62%) after deceleration.

Vestibular Aftereffects despite Prior Fixation Suppression

Starting immediately after termination of the acceleration ($18^\circ/\text{second}^2$), a stationary visual surround was presented for different time intervals (2, 5, 10, 20, and 30 seconds, 1, 2, and 3, minutes). The attempt to fixate the stationary pattern invariably resulted in a sharp drop of SPV. This drop was roughly exponential, leading to a gain of 0.16 (as compared to the SPV prior to fixation) within the first 2-second interval. A complete suppression of nystagmus was reached after 12

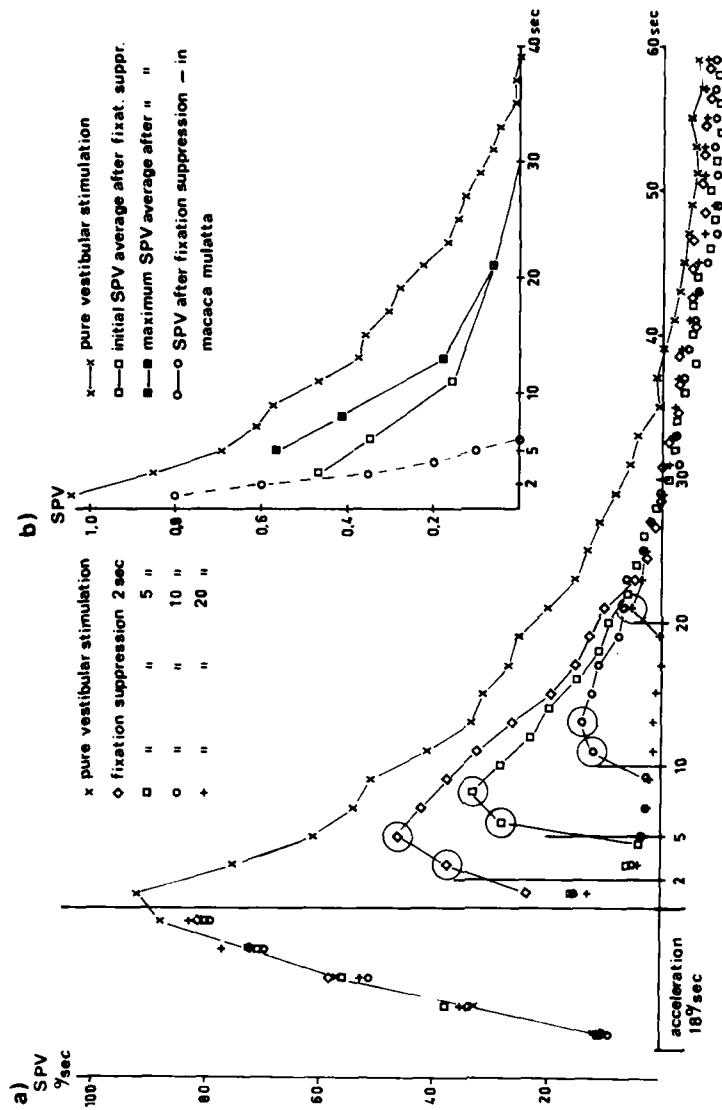


FIGURE 2: (a) Average SPV of four subjects for pure vestibular stimulation and fixation suppression intervals of 2, 5, 10, and 20 seconds. (b) Normalized average SPV of four subjects for pure vestibular stimulation, the initial 2-second average of SPV (encircled in FIGURE 2a) after fixation suppression intervals of 2, 5, 10, and 20 seconds (open squares), and the maximum SPV (also encircled in FIGURE 2a) two seconds later after the same fixation intervals (dark squares). For comparison, SPV after fixation found in *Macaca mulatta* (open circles) also is plotted.^{4,5}

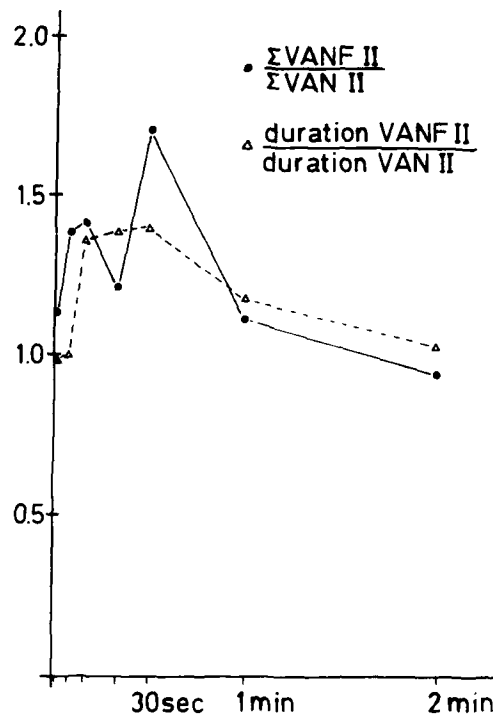


FIGURE 3. Comparison of VANF II and VAN II by the ratio of cumulative amplitude of VANF II and VAN II (dark circles) and the ratio of the duration of VANF II and VAN II (open triangles). For a fixation interval of 3 minutes, the ratios were not calculated, as VANF II was observed only in one of our four subjects.

seconds on average. With fixation intervals lasting up to 2 minutes, nystagmus invariably recovered after the lights were switched off. With the shorter fixation intervals (up to 20 seconds), VAN I reappeared (FIGURE 2). This occurred also when nystagmus had ceased completely during fixation. VAN I, however, did not reach the same velocity as without prior fixation at corresponding times. After the termination of fixation, an increase of SPV over several seconds (2-4 seconds) invariably was found. This increase was rapid at first and then progressively slower. Thereafter, SPV slowly declined and ceased only slightly earlier (28.8 seconds) than VAN I without fixation suppression (36.5 seconds). To compare VANF I* in humans to the data obtained with a similar method in *Macaca mulatta*,^{4,5} VANF I was normalized by calculating the ratio between SPV after fixation and SPV immediately prior to fixation. The average values from our four subjects are plotted in FIGURE 2b. The open squares represent the initial 2-second average of SPV after fixation termination (encircled in FIGURE 2a); and the dark squares, the maximal SPV two seconds later (see also FIGURE 2a). For comparison, the normalized values of VAN I in humans (without prior fixation) and Raphan's data obtained in *Macaca mulatta* also are plotted in FIGURE 2b. The

*Vestibular after-nystagmus I after fixation.

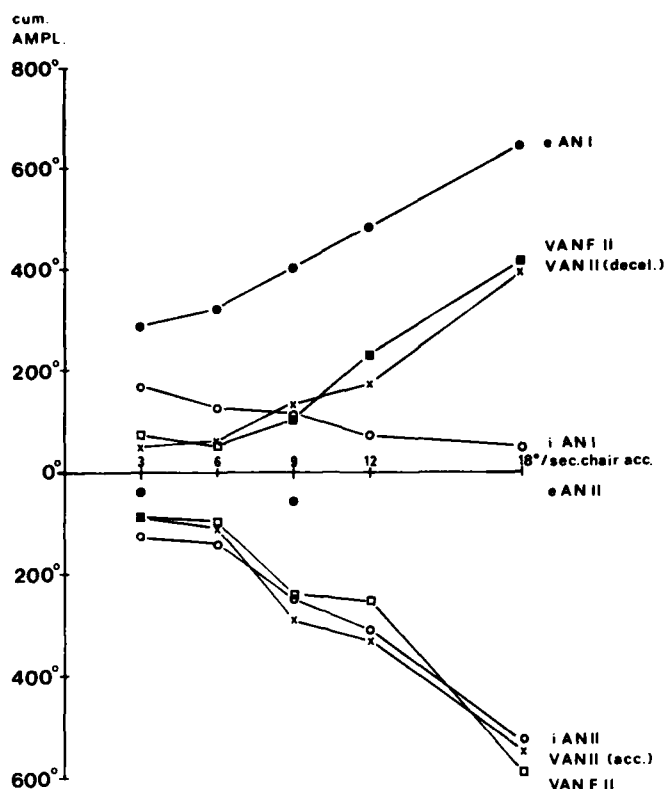


FIGURE 4. The influence of the five accelerations tested on the cumulative amplitude of vestibular after-nystagmus II (VAN II), vestibular after-nystagmus II after fixation suppression (VANF II), after-nystagmus I and II during inhibiting interaction of the aftereffects (iAN I, iAN II), and after-nystagmus I and II during enhancing interaction (eAN I, eAN II).

figure shows a much faster decline of the recovered SPV after fixation in the monkey as compared to humans. The effect of different fixation suppression intervals on the second phase of vestibular after-nystagmus (VANF II) also was studied. Fixation during VAN I did not shorten, but rather tended to prolong, the duration of VANF II (FIGURE 3) and increased its cumulative amplitude. VANF II was observed in all four subjects after 2 minutes of fixation and even after 3 minutes in one subject. FIGURE 3 plots the duration of VANF II after different fixation intervals in relation to VAN II (175 seconds) without fixation (duration of VANF II/duration of VAN II). The cumulative amplitudes of VANF II in relation to VAN II also are plotted (Σ VANF II/ Σ VAN II). With fixation intervals exceeding 30 seconds, VANF II was curtailed. Cumulative VAN II therefore was compared to corresponding parts of VAN II. FIGURE 3 shows that both duration and cumulative amplitude of VANF II tended to be increased by a prior fixation. This effect was maximal for a fixation interval of 30 seconds. The effect of a prior fixation suppression on VANF II also was tested using different accelerations (3, 6, 9, 12, and $18^\circ/\text{second}^2$) but a constant fixation interval of 1 minute. VANF II

invariably was observed. As with VAN II, its cumulative amplitude and duration (not plotted) increased with increasing accelerations (FIGURE 4). VANF II again was weaker after the deceleration phase (70%, as compared to the one after the acceleration phase). Cumulative amplitudes and durations of VANF II were very similar to VAN II without fixation (FIGURE 4), although vestibular nystagmus was canceled almost completely during fixation. VAN II therefore cannot be the response to vestibular nystagmus, but must be elicited by the vestibular stimulus proper.

Optokinetic After-Nystagmus

After 1 minute of optokinetic stimulation, optokinetic after-nystagmus (OKAN) was observed only toward the direction of previous optokinetic nystagmus (OKN). Its duration averaged 45 seconds and was independent of speed. There was no second phase (OKAN II). Average cumulative amplitudes for the five velocities tested were 187, 249, 259, 272, and 238° to the right and 203, 220, 300, 379, and 212° to the left. Since in contrast to the effects of vestibular stimulation, the order of presentation was not critical, measurements of OKAN were averaged for both directions. FIGURE 5 shows that within the range tested, OKAN is largely independent of pattern speed. It increased only slightly with increasing stimulus velocities up to 120°/second and was weaker after a 180°/second pattern motion.

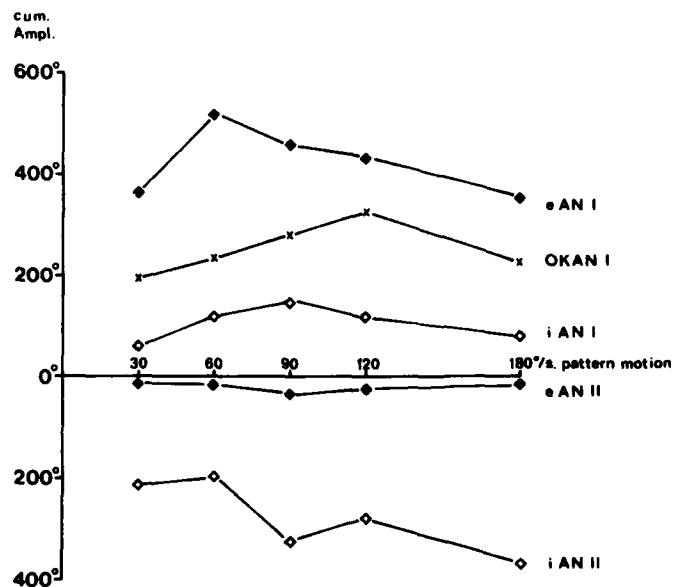


FIGURE 5. The influence of the five velocities of optokinetic stimulus on the cumulative amplitudes of optokinetic after-nystagmus I (OKAN I), iAN I, iAN II, eAN I, and eAN II (see legend of FIGURE 4 for an explanation of the abbreviations).

Aftereffects of Visual-Vestibular Interaction

We demonstrated OKAN I after 1 minute of optokinetic stimulation and also demonstrated that VANF II is independent of the occurrence of nystagmus (VAN I). So both mechanisms driving after-nystagmus should be active 1 minute after termination of the acceleration, and the aftereffects of optokinetic and vestibular stimulation should combine to a single SPV output. When vestibular nystagmus and OKAN during stimulation are of the same direction, their aftereffects should inhibit each other because VAN II and OKAN I are opposite. When vestibular nystagmus is opposite in direction to the optokinetic nystagmus, VAN II and OKAN I have the same direction, presumably enhancing each other. To test this, cumulative amplitudes and durations of after-nystagmus during inhibitory (iAN) and enhancing interaction (eAN) were measured. To determine the effects of vestibular accelerations and optokinetic pattern speed, we averaged cumulative amplitudes, either across pattern speeds or across accelerations, and thus were able to plot first the average effect of a prior optokinetic stimulus in relation to the five accelerations employed (FIGURE 4) and second the average effect of a prior acceleration in relation to the five pattern speeds used (FIGURE 5). With the inhibiting interaction of the aftereffects, OKN is followed by a short after-nystagmus toward the same direction (iAN I), then a secondary nystagmus of long duration and slow velocity follows (iAN II). The comparatively shorter OKAN drive soon was overpowered by the VAN II tendency. FIGURE 4 shows that iAN I is strongest with low accelerations and decreases with higher accelerations, indicating the strong inhibitory effect of the VAN II drive. The effect of pattern speed—a slight increase with increasing velocity up to $90^\circ/\text{second}$ (FIGURE 5)—is comparatively minor. A comparison of the traces labeled OKAN and iAN I in FIGURE 5 shows that the inhibitory interaction of VAN II on OKAN largely is independent of pattern velocity.

The effects of the mutually enhancing combination are similar in principle. With enhancing interaction of the aftereffects, OKAN is followed by a strong after-nystagmus of long duration (eAN I). FIGURE 4 again shows that similarly to VAN II, eAN I increases with increasing accelerations. Pattern velocity is less influential (FIGURE 5). eAN II was observed only occasionally in two subjects with accelerations of 3 and $9^\circ/\text{second}^2$ (FIGURES 4 and 5). We assume that eAN II is a vestibular aftereffect corresponding to VAN III, occasionally observed after vestibular stimulation. An analysis of the duration of the different forms of after-nystagmus showed the same characteristics; therefore, these data are not shown.

DISCUSSION

The characteristics of VAN I in the dark conform well with earlier findings.^{15,16} VAN I is elicited by both integrators mentioned earlier: the inertia of the cupula and the central VAN I-integrator. It is not possible, however, to assess from our data how much each integrator contributes to the response. A rough estimate for the peripheral time constant may be obtained from the peripheral time constant (3–5 seconds) of the squirrel monkey.¹ In man, because of his larger body mass, this time constant probably is slightly longer. If we assume a time constant of 7 seconds for the decay of the cupula deflection, there still should be a small vestibular input after 20 seconds. This could very well be the reason for the partial recovery of VANF I observed after the termination of fixation suppres-

sion, as suggested by B. Cohen at this symposium. The rise of SPV within the subsequent 2–4 seconds after termination of fixation then may be explained by a recharge of the central VAN I-integrator by the continuing neuronal input from the periphery. The fact that VANF I after fixation does not reach the velocity of VAN I at the corresponding time has to be attributed to a discharge of the central VAN I-integrator during fixation.^{4,5}

This hypothesis, however, hardly explains the data from *Macaca mulatta* (FIGURE 2b), with an abolishment of VANF I after a fixation interval of 6 seconds.^{4,5} With a cupula time constant of 3–5 seconds,¹ there still should be a considerable peripheral input 6 seconds after the termination of the vestibular stimulus, which should give rise to VANF I when the stationary visual surround is removed. The missing recovery of VANF I suggests an additional process.

Assuming that the presence of the visual surround in the fixation-suppression paradigm is equivalent to an optokinetic input (drum velocity in space) opposite to the slow phase of vestibular nystagmus, its aftereffect would correspond to OKAN I and its direction would be opposite to VAN I, thus explaining the missing recovery of VANF I in the monkey. It seems probable that the difference between man and monkey results from the stronger input of the optokinetic system into the vestibular nuclei of the monkey. This results in a higher optokinetic gain with high stimulus velocities, in a much stronger OKAN, and after fixation suppression, in an effective suppression of the continuing vestibular stimulation by the only gradually decaying cupula deflection. The necessary basic assumption is that in the fixation-suppression paradigm, a large moving visual stimulus—although stationary with respect to the moving head—is equivalent to retinal image motion.

Besides the VAN I-integrator with its rapid rise time, high gain, and short decay time constant, vestibular stimulation charges a second integrator generating VAN II, with a low gain and a long decay time constant. That the VAN II-integrator (as also observed with OKAN II)^{13,14} is charged by the adequate stimulus (vestibular, optokinetic respectively) and not by the preceding nystagmus is demonstrated by the missing reduction of VANF II after fixation compared to VAN II (FIGURES 3 and 4). The boost of VANF II (FIGURE 3) by fixation may be explained again by the addition of a presumed OKAN I, as the aftereffect of an optokinetic signal counter-coupled to VAN I. A similar boost of OKAN II was observed with fixation suppression of OKAN I.¹⁴ These parallels between VAN II and OKAN II suggest that one integrator elicits both aftereffects. However, the short-term adaptation of VAN II (VAN II and VANF II were considerably weaker after the deceleration than after the acceleration) was not found in OKAN II.^{17,18}

Our findings considering the influence of optokinetic pattern velocity on OKAN I are in good agreement with an earlier study.¹⁹ After an optokinetic stimulation of 1 minute, OKAN II was observed frequently.¹³ The absence of OKAN II in our study probably has to be attributed to the large interindividual variation of OKAN, as our subjects showed OKAN II after 2 minutes of optokinetic stimulation.

During the inhibiting interaction of the aftereffects, a VAN II tendency subtracts from the optokinetic aftereffects. Therefore, the cumulative amplitude of iAN I always is considerably smaller than that of OKAN I (FIGURE 5). As VAN II increases with acceleration, the inhibition of OKAN I becomes more effective, resulting in a decrease of iAN I with increasing accelerations.

Surprisingly, cumulative amplitude of iAN II is approximately the same as that of VAN II, although OKAN I should have subtracted from VAN II early after

the termination of optokinetic stimulation. Since after an optokinetic stimulation for 1 minute, OKAN II frequently is observed,¹³ a possible explanation would be an OKAN II tendency that might add to VAN II and thereby compensate for the inhibition by OKAN I. With enhancing interaction of the aftereffects (eAN I), the addition of VAN II and OKAN I leads to a considerably larger cumulative amplitude than either VAN II (FIGURE 4) or OKAN I (FIGURE 5) alone. Calculations showed that at least for enhancing interaction, the cumulative amplitude of eAN I is close to the algebraic sum of VAN II and OKAN I when elicited separately. So linear addition—earlier proposed for the interaction of optokinetic and vestibular inputs during stimulation^{20,21,16}—also seems to take place during after-nystagmus.

SUMMARY

In humans the influence of prior vestibular stimulation (3, 6, 9, 12, and 18°/second² for 10 seconds) and subsequent whole-field optokinetic stimulation (30, 60, 90, 120, and 180°/second for 1 minute) or the presentation of a stationary pattern on after-nystagmus (AN) was studied. For comparison, pure vestibular and pure optokinetic stimuli also were employed. The presentation of a stationary pattern resulted in suppression of vestibular nystagmus, which recovered after the termination of fixation. Fixation during the period of AN I did not inhibit an AN II. During the combinations of vestibular and optokinetic stimuli when the elicited vestibular (VN) and optokinetic nystagmus (OKN) had the same direction, there was a weak AN I toward the direction of the preceding VN and OKN, and a strong AN II toward the opposite side. When VN had been opposite to the subsequent OKN, there was a strong AN I toward the direction of OKN; AN II toward the opposite direction was small or mostly absent. Thus, AN was always stronger into the direction opposite to the previously elicited VN, indicating that the vestibular afference is the predominant input to the VAN II-integrator.

REFERENCES

1. FERNÁNDEZ, C. & J. M. GOLDBERG. 1971. Physiology of peripheral neurons innervating semicircular canals of the squirrel monkey. II. Response to sinusoidal stimulation and the dynamics of the peripheral vestibular system. *J. Neurophysiol.* **34**: 661-675.
2. BUETTNER, U. W., U. BÜTTNER & V. HENN. 1978. Transfer characteristics of neurons in vestibular nuclei of the alert monkey. *J. Neurophysiol.* **41**: 1614-1628.
3. ROBINSON, D. A. 1977. Vestibular and optokinetic symbiosis: an example of explaining by modelling. *Dev. Neurosci.* **1**: 49-58.
4. RAPHAN, T., B. COHEN & V. MATSUO. 1977. A velocity-storage mechanism responsible for optokinetic nystagmus, optokinetic after-nystagmus and vestibular nystagmus. *Dev. Neurosci.* **1**: 37-47.
5. RAPHAN, T., V. MATSUO & B. COHEN. 1979. Velocity storage in the vestibulo-ocular reflex arc. *Exp. Brain Res.* **35**: 229-248.
6. FISCHER, M. H. & A. E. KORNMÜLLER. 1930. Optokinetisch ausgelöste Bewegungswahrnehmungen und optokinetischer Nystagmus. *J. Psychol. Neurol. Leipzig* **41**: 273-308.
7. BRANDT, TH., J. DICHGANS & E. KOENIG. 1973. Differential effects of central versus peripheral vision on egocentric and exocentric motion perception. *Exp. Brain Res.* **18**: 476-491.
8. KLINKE, R. & C. L. SCHMIDT. 1970. Efferent influence of the vestibular organ during active movements of the body. *Pfluegers Arch.* **318**: 325-332.

9. DICHGANS, J., C. L. SCHMIDT & W. GRAF. 1973. Visual input improves the speedometer functions of the vestibular nuclei in goldfish. *Exp. Brain Res.* **18**: 319-322.
10. HENN, V., L. R. YOUNG & C. FINLEY. 1974. Vestibular nucleus units in alert monkeys are also influenced by moving visual fields. *Brain Res.* **71**: 144-149.
11. WAESPE, W. & V. HENN. 1977. Neuronal activity in the vestibular nuclei of the alert monkey during vestibular and optokinetic stimulation. *Exp. Brain Res.* **27**: 523-538.
12. WAESPE, W. & V. HENN. 1977. Vestibular nuclei activity during optokinetic afternystagmus in the alert monkey. *Exp. Brain Res.* **30**: 323-330.
13. BRANDT, TH., J. DICHGANS & W. BÜCHELE. 1974. Motion habituation: inverted self-motion perception and optokinetic after-nystagmus. *Exp. Brain Res.* **21**: 337-352.
14. WAESPE, W., TH. HUBER & V. HENN. 1978. Dynamic changes of optokinetic afternystagmus (OKAN) caused by brief visual fixation periods in monkey and in man. *Arch. Psychiatr. Nervenkr.* **226**: 1-10.
15. BROWN, J. H. & G. H. CRAMPTON. 1964. Quantification of the human nystagmic response to angular acceleration. Prediction formulae and nomograph. *Acta Oto-Laryngol.* **58**: 555-564.
16. KOENIG, E., J. H. H. ALLUM & J. DICHGANS. 1978. Visual-vestibular interaction upon nystagmus slow phase velocity in man. *Acta Oto-Laryngol.* **85**: 397-410.
17. COLLINS, W. E. 1974. Habituation of vestibular responses with and without visual stimulation. In *Handbook of Sensory Physiology. Vestibular System*. H. H. Kornhuber, Ed. **6/2**: 369-388. Springer-Verlag, Berlin, Heidelberg & New York.
18. WAESPE, W. & V. HENN. 1978. Reciprocal changes in primary and secondary optokinetic after-nystagmus produced by repetitive optokinetic stimulation in the monkey. *Arch. Psychiatr. Nervenkr.* **225**: 23-30.
19. MACKENSEN, G. & O. WIEGMANN. 1959. Untersuchungen zur Physiologie des optokinetischen Nachnystagmus. I. Die Abhängigkeit des optokinetischen Nachnystagmus von der Drehrichtung und der Winkelgeschwindigkeit des Reizmusters. *Albrecht von Graefes Arch. Ophthalmol.* **160**: 497-509.
20. ROBINSON, D. A. 1977. Linear addition of optokinetic and vestibular signals in the vestibular nucleus. *Exp. Brain Res.* **30**: 447-450.
21. LAU, C. C. Y., V. HONRUBIA, H. A. JENKINS, R. W. BALOH & R. D. YEE. 1978. Linear model for visual-vestibular interaction. *Aviat. Space Environ. Med.* **49**: 880-885.

THE ROLE OF THE DENTATE NUCLEUS AND Y-GROUP IN THE GENERATION OF VERTICAL SMOOTH EYE MOVEMENTS*

M. Carroll Chubb and Albert F. Fuchs

*Department of Physiology and Biophysics
and Regional Primate Research Center
University of Washington
Seattle, Washington 98195*

The dentate nucleus and the nearby y-group of the vestibular nuclear complex have been implicated in the generation of vertical eye movements by several lines of evidence. Cells in the y-group of the monkey and in the homologous region in cats (referred to as either the infracerebellar nucleus or the y-group) project onto the oculomotor nuclei.¹⁻⁴ In cats, neurons in the y-group, especially the dorsal part, are activated antidromically by electrical stimulation of the oculomotor nuclei.⁵ In rabbits, field potentials evoked by electrical stimulation in the y-group are most prominent in cell groups innervating vertical extraocular muscles.⁶ Many studies also have reported direct projections from the dentate nucleus to the oculomotor nucleus, again particularly to those cell groups innervating the vertical extraocular muscles⁶⁻⁸ (see, however, References 2 and 3). In alert monkeys, electrical stimulation in the dentate nucleus elicits upward eye movements.^{9,10} Thus projections from the y-group and probably the dentate nucleus to the oculomotor nucleus, as well as the effects of electrical stimulation in the dentate nucleus, suggest that these two structures are involved in the generation of vertical eye movements.

We investigated the role of the dentate nucleus and the y-group in the generation of vertical smooth eye movements by examining the relation of their neuronal activity to vertical eye movements and adequate vestibular stimulation and by electrically stimulating this region at sites of neurons whose activity was related to eye movements. Only our preliminary results are presented here.

METHODS

Three adolescent rhesus macaques (*Macaca mulatta*) were trained to track a small visual target while undergoing vertical sinusoidal angular acceleration. The tracking task allowed us to obtain various combinations of passive head rotation and eye movements. Recordings of neuron activity were made in all three monkeys, but electrical stimulation was applied to only one monkey.

Eye movements were measured with the electromagnetic search coil technique,¹¹ which permitted eye movements as small as 15 minutes of arc to be detected (d.c. to 300 Hz, -3 dB). The monkey's experimental situation is shown in FIGURE 1. The monkey sat in a chair in a vestibular stimulator with its head fixed firmly to the chair.¹² The chair, and with it the monkey's head, was rotated sinusoidally with a peak-to-peak amplitude of 20° in the sagittal plane at 0.5 Hz (harmonic distortion less than 3%).

*This study was supported by National Institutes of Health Grants RR00166, EY00745, and GM00260.

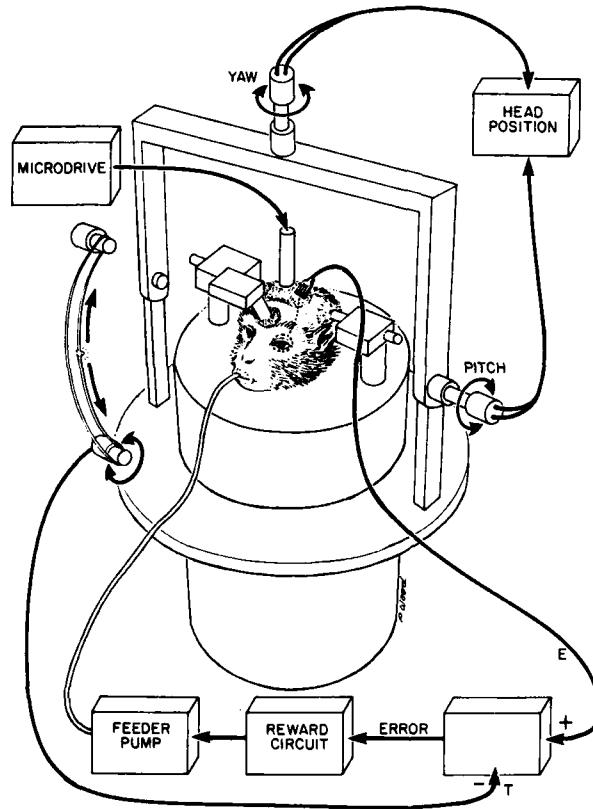


FIGURE 1. Schematic diagram of monkey's experimental situation.

The monkeys tracked a visual target for an applesauce reward. The target was a movable, red-light-emitting diode, 0.5 to 2° in diameter, driven by a servo-controlled motor. The three most frequently studied behavioral conditions were (1) sinusoidal smooth pursuit; (2) suppression of the vestibulo-ocular reflex (VOR), which was obtained during sinusoidal head rotation by holding the target fixed with respect to the monkey, so that its eyes remained stationary in its head; and (3) target stable in the world during sinusoidal head rotation, which was obtained with the target fixed in space to produce compensatory eye movements approximately equal and opposite to head movements.

Extracellular single-unit activity was recorded using methods previously described.¹² In brief, to permit electrodes to be introduced into the brain, stainless-steel chambers were implanted surgically over holes trephined in the skull. The electrode was guided into the brain through a cannula and advanced with a hydraulic microdrive. The signal from the electrode was amplified using conventional methods and recorded on analog tape for later analysis. Based on previous work using the same recording conditions,¹³ units having extracellular action potentials with triphasic positive-negative-positive and diphasic positive-negative waveforms were classified as fibers, while those having diphasic

negative-positive waveforms whose time from onset to peak positivity was 200 μ seconds or more were classified as somata.

As the electrode was advanced, the monkey continually was rotated sinusoidally through $\pm 10^\circ$ in the sagittal plane while tracking the target in one of four conditions: (1) target stable in the world, (2) suppression of the VOR, (3) target motion in phase with chair, and (4) target motion 180° out of phase with chair and about $\pm 25^\circ$ in amplitude.

Data were collected only on units with activity related to the stimuli.

In one monkey, some electrodes were used for both recording and electrical stimulation. Stimulation current was controlled by a Nuclear Chicago (model 7150) constant current stimulator and delivered through a stimulus isolation unit (Tektronix 2620). The return current path passed through a surgically implanted ground wire. Trains of bipolar pulses, each pulse 250 μ seconds in duration, were used. The current intensities were either 10 or 20 μ A.

Unit activity during sinusoidal stimulation either was analyzed using a computer with modified versions of programs used by Lisberger and Fuchs or was written on high-speed photosensitive paper and analyzed by hand.^{14,15} A more complete description of the analysis programs will be given in a paper on the quantitative description of the unit activity (in preparation).

The responses to electrical stimulation were analyzed by hand using high-speed ultraviolet recordings of data previously stored on the analog tape recorder.

So that unit locations and stimulation sites could be reconstructed, lesions were made at or near some of the units with activity related to the stimuli. At the end of each experiment, the monkey was deeply anesthetized and sacrificed by intracardiac perfusion with saline followed by 10% formalin. The brains were frozen and cut in 40- μ m frontal sections and stained with cresyl violet. Unit and stimulation sites were reconstructed from their positions relative to the lesions.

RESULTS

Upward Head and Eye Velocity Units

In the y-group and dentate nucleus region, most units exhibited increases in firing rate related to upward eye velocity during smooth pursuit (FIGURE 2, eye movement only) and upward head velocity during suppression of the VOR (FIGURE 2, head movement only). When the rotating monkey fixated a target stable in the world, so that its head and eyes moved in opposite directions, the modulation in unit activity was much reduced and in some cases no significant modulation remained (FIGURE 2, eye and head movement). A total of 51 units with activity related to upward head and eye velocity (UHEV units) were recorded. The activity of 31 of these units showed little or no relation to eye position, while 15 showed substantial sensitivity to eye position as well as to upward head and eye velocity. The 5 remaining UHEV units yielded insufficient data for us to determine whether activity also was related to eye position. The activity of most UHEV units was related to saccades; usually the units fired a burst of action potentials during saccades in all directions.

The UHEV units were recorded in the rostral half of the dentate nucleus, in the y-group, and in the "white matter" dorsal, lateral, and rostral to the dentate nucleus. This white matter does include cell bodies (unpublished observation).

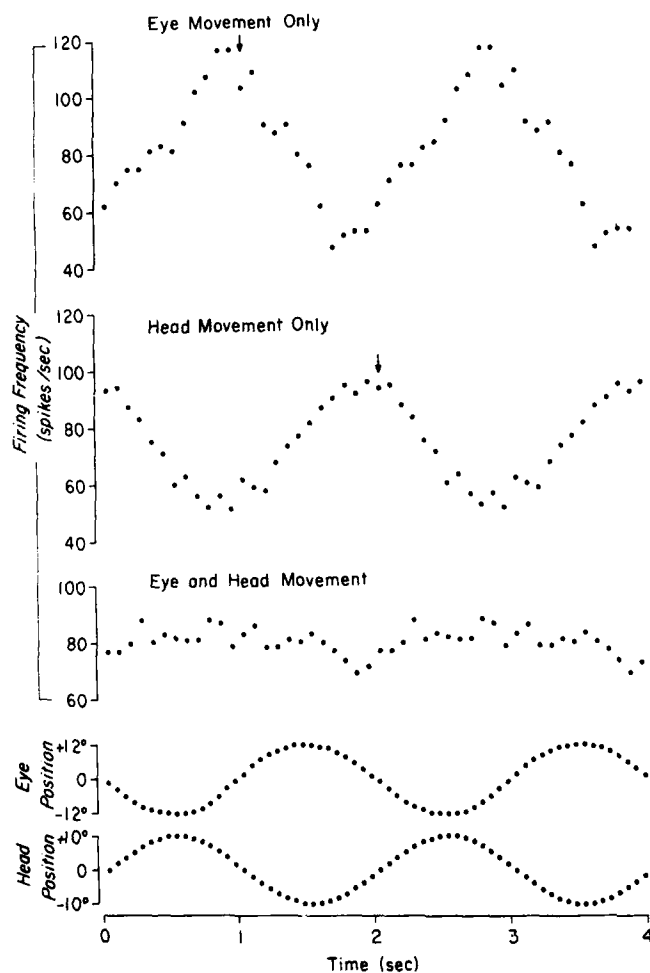


FIGURE 2. Discharge characteristics of UHEV unit averaged over 10 cycles. During smooth pursuit (eye movement only), the peak firing rate occurs near the time of maximum upward eye velocity (arrow). During suppression of the VOR (head movement only), the peak firing rate occurs at about the time of peak upward eye velocity (arrow). During compensatory eye movements (eye and head movement), there is little or no modulation in activity. Here and in FIGURE 4, the same cycle has been repeated to facilitate visualization of periodic events.

Two of the lesions made at the sites of UHEV units are shown in FIGURE 3. Based on the waveform of the action potentials, the great majority of the recordings were from somata. Thus the y-group, the dentate nucleus, and the cells in the adjacent cerebellar white matter form a functional region in which the activity of many of the neurons is related approximately to upward gaze velocity.



FIGURE 3. Lesion at sites of UHEV units in the y-group (A, arrow) and dentate nucleus (B).

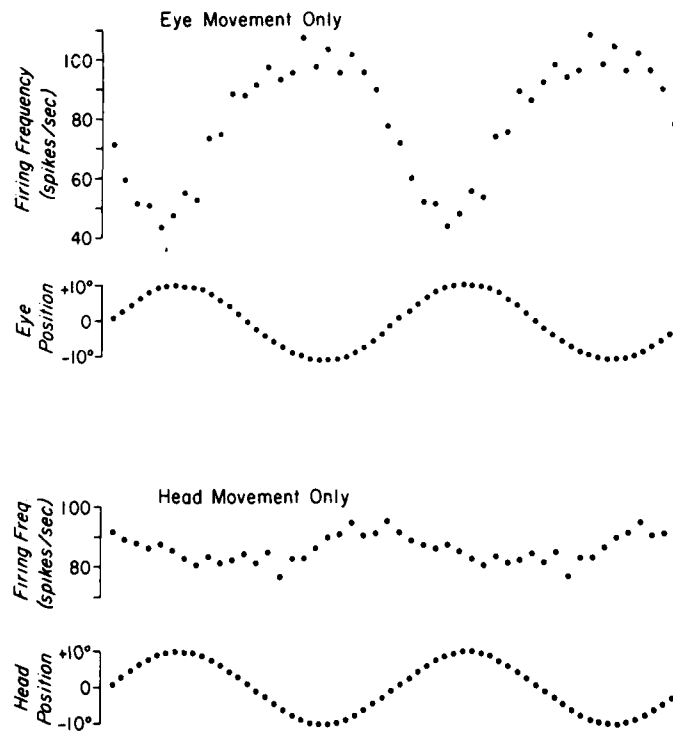


FIGURE 4. Discharge characteristics of down eye position unit averaged over 10 cycles. During smooth pursuit (eye movement only), the peak activity occurred when the monkey looked in a downward (negative) direction. During suppression of the VOR (head movement only), there was little or no modulation in activity.

Non-UHEV Units

In addition to the UHEV units, other units in the vicinity fired in relation to vertical smooth eye movements or vestibular stimulation. Units with activity related to downward eye position but with little or no modulation during suppression of the VOR for rotation in the sagittal plane (FIGURE 4) were found intermingled with UHEV units. The action potential waveforms indicated that almost all of these unit recordings were from cell bodies. Twelve units with activity related to downward eye position were recorded in or near the dentate nucleus, while two were recorded in the y-group. Only two units were tested for firing rate modulation during suppression of the VOR with rotation in other vertical planes, and the pattern of response indicated that the activity of both was strongly related to rotation in the coronal plane.

The other units with activity related to eye movements or vestibular stimulation usually were located at the edge of the area containing UHEV units. These included eight units with activity related to downward head velocity or position, four with activity related to upward eye velocity, and four with activity related to

upward eye movement. Of four units with activity related to both eye and head movements, one had activity modulated with downward head and eye velocity. This unit was recorded slightly more caudally than any UHEV unit. Unfortunately, because of poor recording conditions, we were not able to determine the relation of unit activity in the caudal part of the dentate nucleus to eye movements and vestibular stimulation.

Electrical Stimulation

If the UHEV units are premotor neurons involved in the generation of vertical smooth eye movements, then electrical stimulation with low current intensity at the sites of UHEV units should elicit vertical smooth eye movements.

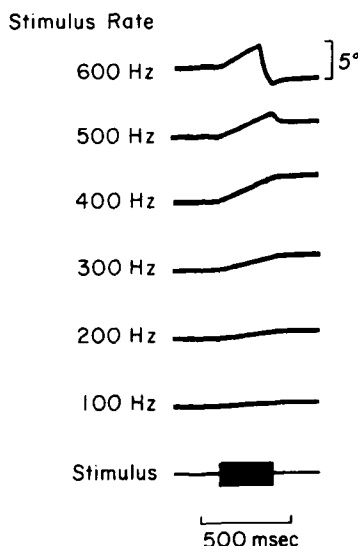


FIGURE 5. Upward eye movements elicited by microstimulation in the center of the y-group. Higher stimulus frequencies produced faster smooth eye movements. Stimulus train duration was 300 mseconds, and current strength was 20 μ A.

Application of trains of 10 or 20 μ A to three sites at which UHEV units had been recorded caused the eyes to rotate smoothly upward; little or no horizontal eye movement response was seen.

If the firing frequency of the UHEV units determines eye velocity, then increasing the pulse frequency of electrical stimulation should increase eye velocity. When stimulus duration was held constant at either 300 or 500 mseconds and the pulse frequency was varied (FIGURE 5), the maximum eye velocity was found to increase with the stimulus pulse frequency at all three UHEV-unit sites. These results support the hypothesis that UHEV units drive upward smooth eye movements.

CONCLUSIONS

In the y-group, the dentate nucleus, and the white matter rostral, dorsal, and lateral to the dentate nucleus, neurons were recorded with activity related to upward eye velocity and upward head velocity. Therefore, based on the correlation of unit activity with smooth eye movements and passive sinusoidal rotation of the monkey, this region forms a functional unit. Electrical stimulation in this area with low current intensities evokes upward smooth eye movements, with the velocity of the response increasing as a function of the frequency of the stimulus. These results implicate the UHEV units in the generation of vertical smooth pursuit and visual modification of the vertical VOR.

Since many cells in the monkey's y-group have been shown to project onto the oculomotor nuclei,^{1,2} and since the UHEV units were the only frequently encountered unit type with activity related to eye movements recorded in the y-group, it is likely that UHEV units send their axons to the oculomotor nucleus. The monkey flocculus contains Purkinje cells with activity related to ipsilateral eye velocity and head velocity and a group with activity related to downward eye velocity, which were not tested during head rotation in the sagittal phase.^{14,16} The flocculus projects heavily onto the y-group in the monkey (Langer, personal communication), suggesting that the UHEV units of the y-group are modulated by inhibition from Purkinje cells with activity related to downward head and eye velocity and that they relay this vertical gaze velocity signal to the vertical oculomotor neurons.

REFERENCES

1. GRAYBIEL, A. M. 1977. Organization of oculomotor pathways in the cat and rhesus monkey. *Dev. Neurosci.* **1**: 79-88.
2. STEIGER, J.-J. & J. A. BÜTTNER-ENNEVER. 1979. Oculomotor nucleus afferents in the monkey demonstrated with horseradish peroxidase. *Brain Res.* **160**: 1-15.
3. GACEK, R. R. 1977. Location of brain stem neurons projecting to the oculomotor nucleus in the cat. *Exp. Neurol.* **57**: 725-749.
4. GRAYBIEL, A. M. & E. A. HARTWIEG. 1974. Some afferent connections of the oculomotor complex in the cat: an experimental study with tracer techniques. *Brain Res.* **81**: 543-551.
5. HWANG, J. C. & W. F. POON. 1975. An electrophysiological study of the sacculo-ocular pathways in cats. *Jpn. J. Physiol.* **25**: 241-251.
6. HIGHSTEIN, S. M. 1973. The organization of the vestibulo-oculomotor and trochlear reflex pathways in the rabbit. *Exp. Brain Res.* **17**: 285-300.
7. CARPENTER, M. B. & N. L. STROMINGER. 1964. Cerebello-oculomotor fibers in the rhesus monkey. *J. Comp. Neurol.* **123**: 211-230.
8. CHAN-PALAY, V. 1977. *Cerebellar Dentate Nucleus*. Springer-Verlag, Berlin, Federal Republic of Germany.
9. COHEN, B., K. GOTO, S. SHANZER & A. H. WEISS. 1965. Eye movements induced by electrical stimulation of the cerebellum in the alert cat. *Exp. Neurol.* **13**: 145-162.
10. RON, S. & D. A. ROBINSON. 1973. Eye movements evoked by cerebellar stimulation in the alert monkey. *J. Neurophysiol.* **36**: 1004-1022.
11. FUCHS, A. F. & D. A. ROBINSON. 1966. A method for measuring horizontal and vertical eye movement chronically in the monkey. *J. Appl. Physiol.* **21**: 1068-1070.
12. FUCHS, A. F. & E. S. LUSCHEI. 1970. Firing patterns of abducens neurons of alert monkeys in relationship to horizontal eye movements. *J. Neurophysiol.* **33**: 382-392.
13. KING, W. M., S. G. LISBERGER & A. F. FUCHS. 1976. Response of fibers in medial longitudinal fasciculus (MLF) of alert monkeys during horizontal and vertical

- conjugate eye movements evoked by vestibular or visual stimuli. *J. Neurophysiol.* **39**: 1135-1149.
14. LISBERGER, S. G. & A. F. FUCHS. 1978. Role of primate flocculus during rapid behavioral modification of vestibuloocular reflex. I. Purkinje cell activity during visually guided horizontal smooth-pursuit eye movements and passive head rotation. *J. Neurophysiol.* **41**: 733-763.
 15. FUCHS, A. F. & J. KIMM. 1975. Unit activity in vestibular nucleus of the alert monkey during horizontal angular acceleration and eye movement. *J. Neurophysiol.* **38**: 1140-1161.
 16. MILES, F. A., J. H. FULLER, D. J. BRAITMAN & B. M. DOW. 1980. Long-term adaptive changes in primate vestibuloocular reflex. III. Electrophysiological observations in flocculus of normal monkeys. *J. Neurophysiol.* **43**: 1437-1476.

THE BRAIN-STEM PROJECTION TO THE CEREBELLAR FLOCCULUS RELEVANT TO OPTOKINETIC RESPONSES IN CATS

Tadashi Kawasaki,* Isao Kato,† Yu Sato,* and
Kanemasa Mizukoshi‡

*Faculty of Medicine
Toyama Medical and Pharmaceutical University
Toyama 930-01, Japan*

INTRODUCTION

The cerebellar flocculus has relevance to immediate modification of the vestibulo-ocular reflex by vision.¹⁻³ The Purkinje cells in the flocculus are activated from the retina through not only the climbing fibers but also the mossy fibers.^{4,5} The dorsal cap of the inferior olive is identified as the origin of the visually driven climbing fibers terminating in the flocculus, while the origin of the visually driven mossy fibers terminating in the flocculus is still open to scrutiny.^{4,6,7}

Recently, the nucleus reticularis tegmenti pontis (Bechterew) (NRTP) has been proposed as a candidate for the origin of the visually driven mossy fibers terminating in the flocculus in rabbits.^{8,9} On the other hand, it has been reported that the NRTP may be a relay nucleus of an optokinetic pretectofugal pathway that does not reach the cerebellum but the vestibular nuclei.¹⁰ In view of these findings, a further study is necessary on the precerebellar nuclei in the brain stem that terminate as the mossy fibers in the flocculus.

The present experiments were aimed at identifying the origin of the mossy fibers terminating in the flocculus. For this purpose, histochemical tracer experiments were carried out in cats by means of the retrograde axonal transport of horseradish peroxidase (HRP), while physiological experiments were undertaken to affirm the observations of the tracer experiments. Besides these, optokinetic nystagmus (OKN) was investigated to clarify a role of the NRTP as a candidate for mediating optokinetic effects on OKN.

METHODS

HRP (Toyobo grade-1-C) injections were tried in 24 cats (weighing 1-1.5 kg) anesthetized with pentobarbital sodium (40 mg/kg intraperitoneally). The cats were mounted in a stereotaxic apparatus, and the bone just posterior to the tentorium was removed to expose the unilateral cerebellar hemisphere. Glass micropipettes (tip diameters, 30-50 μ m) filled with 10% HRP (Tris HCl buffer

*Department of Physiology.

†Department of Otolaryngology, School of Medicine, Yamagata University, Yamagata City 990-23, Japan.

‡Department of Otolaryngology.

solution, pH 8.6) were inserted stereotaxically into the flocculus while passing a negative d.c. current (10 μ A). HRP was iontophoresed into the flocculus by passing a positive current (2–6 μ A) at a frequency of 1 Hz for 20 minutes. The conditions for later histochemical procedures were the same as described previously.¹¹

Electrophysiological experiments were performed in 15 cats (weighing 2–3 kg) anesthetized with an intraperitoneal injection of a mixture of α -chloralose (50 mg/kg) and urethane (0.6 g/kg). Stimulating electrodes were inserted stereotaxically into the brain stem through the cerebellum. Orthodromic evoked potentials were recorded from the flocculus with steel electrodes inserted stereotaxically. The position of each electrode was marked with an electrolytic lesion by the passing of a positive d.c. current (1 mA, for 10 seconds) at the termination of each experiment, and the location of electrode tip position was determined histologically.

Optokinetic responses were recorded in 12 cats (weighing 2–3 kg) prepared chronically. The method of preparation is described elsewhere.¹² OKN and visual suppression (VS) of caloric nystagmus were tested before and after destruction of the NRTP in 7 of 12 cats and before and after destruction of the pontine nucleus (PN) in 3 of 12 cats. In the remaining 2 cats, the unilateral cerebellar hemisphere was aspirated. The lesion was made by passing a positive d.c. current (1 mA) for 1–2 minutes through a steel electrode inserted stereotaxically into the brain stem. The methods of optokinetic stimulation, caloric stimulation, and recording of eye movement were the same as described previously.^{12–14} Slow-phase OKN velocity was used as the parameter for evaluating the optokinetic response. It was assumed that OKN slow-phase velocity is equal to OKN stimulus velocity at low speeds.¹⁵ Slow-phase velocity was calibrated from the eye speed in response to a 20°/second stimulus.

RESULTS

Projection from the Brain Stem to the Flocculus

HRP reaction product was found only within the flocculus in 11 of the 24 cats, after incubation of the sections of the cerebellum in 3-3'-diaminobenzidine- H_2O_2 solution (FIGURE 1A). The extent of HRP reaction product varied in each cat, but could cover approximately the rostral three-fourths of the flocculus in these 11 animals.

Neurons labeled with HRP were recognized in the lateral reticular nucleus (of the side ipsilateral to the injection site), the dorsal cap of the inferior olive (contralateral), the inferior central nucleus of the raphe (bilateral), the perihypoglossal complex (bilateral), the vestibular nuclei (bilateral), the superior central nucleus of the raphe (bilateral), the caudal part of the dorsal nucleus of the raphe (bilateral) (DNR), and the NRTP (bilateral), in agreement with the results of previous reports^{6,7,11,16–20} (FIGURES 1B and 2).

The present experiments were focused on the labeled neurons in the NRTP and the caudal part of the DNR. When HRP was injected accurately within the flocculus, labeled neurons were found only in the medial part of the NRTP (FIGURE 1B), in agreement with the results of previous reports.^{11,16} Only when diffusion of the tracer involved the paraflocculus were labeled neurons recog-

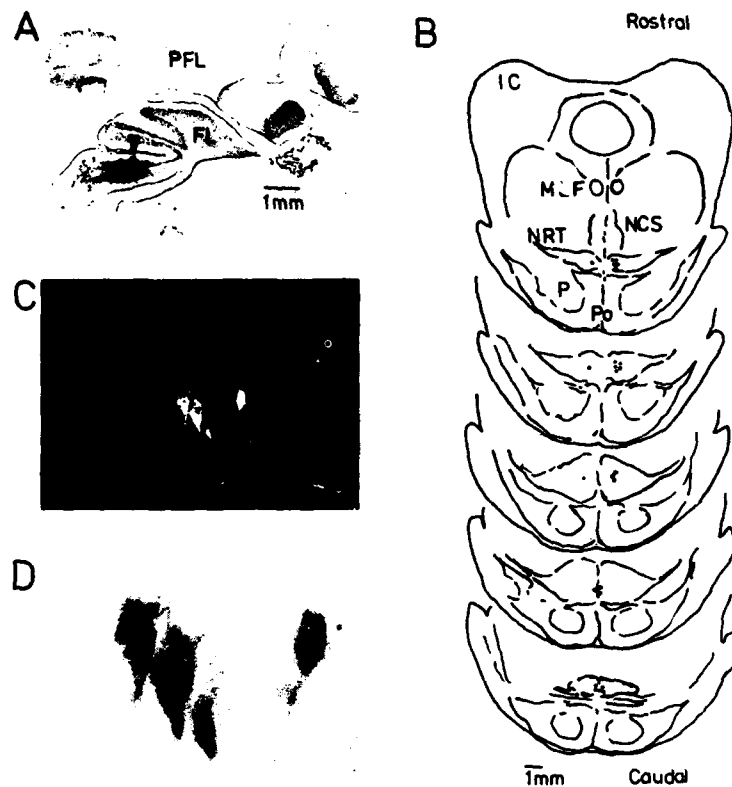


FIGURE 1. **A:** photograph of injection site in the flocculus. **B:** line drawings of selected transverse sections of the brain stem. The distance from each section to the other is 0.48 mm. For each section, a dot represents an HRP-labeled neuron. Abbreviations: FL, flocculus; IC, inferior colliculus; MLF, medial longitudinal fasciculus; NCS, superior central nucleus of the raphe; NRT, nucleus reticularis tegmenti pontis; P, pyramidal tract; PFL, parafofoculus; Po, pontine nucleus. **C** and **D:** dark field ($\times 130$) and bright field ($\times 260$) photomicrograph of HRP-labeled neurons in the NRTP.

nized in the processus tegmentosus lateralis and PN. Even when a fairly large amount of HRP was injected only within the flocculus, only few labeled neurons could be found in the NRTP (FIGURE 1B). These findings suggest that the NRTP may project weakly to the flocculus.

The neurons in the DNR are medium sized and multipolar.²¹ Medium-sized and multipolar neurons were labeled with HRP in the small area along the midline of the brain stem (FIGURE 2B). This area corresponded to the most caudal part of the DNR. A fairly large number of labeled neurons could be counted. Even when a large amount of HRP was injected only into the flocculus or when the diffusion of tracer involved the parafofoculus, no labeled neurons could be recognized in the rostral part of the DNR.

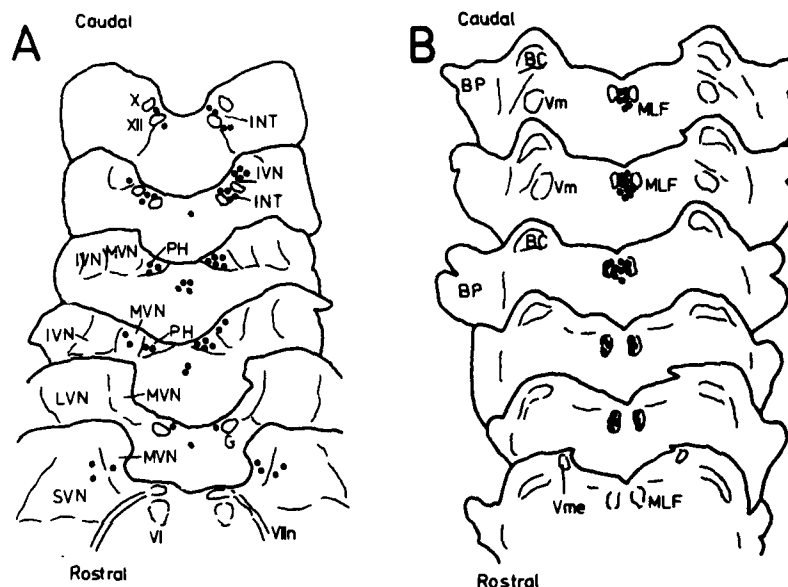


FIGURE 2. Line drawings of selected transverse sections of the brain stem. For each section, a dot represents two HRP-labeled neurons. The distance of each section to the other is 1.2 mm in A and 0.36 mm in B, respectively. Abbreviations: BC, brachium conjunctivum; BP, brachium pontis; G, genu of facial nerve; INT, nucleus intercalatus; IVN, inferior vestibular nucleus; LVN, lateral vestibular nucleus; MLF, medial longitudinal fasciculus; MVN, medial vestibular nucleus; NRT, nucleus reticularis tegmenti pontis; PH, nucleus prepositus hypoglossi; SVN, superior vestibular nucleus; Vm, motor trigeminal nucleus; Vme, mesencephalic trigeminal nucleus; VI, abducens nucleus; VII, facial nerve; X, vagal nucleus; XII, hypoglossal nucleus.

Field Potentials in the Flocculus following NRTP and DNR Stimulation

The projections from the NRTP and the most caudal part of the DNR to the flocculus mentioned in the preceding paragraph were affirmed by electrophysiological experiments. Electrical stimulation (pulse width, 0.05 msecond) of the NRTP elicited orthodromic evoked potentials in the flocculus contralateral to the stimulating site, which were characterized by negative potentials with two components occurring at a peak latency of 0.8 msecond and of 1.5 mseconds (FIGURE 3A). This response followed the stimulus to frequencies as high as 50 Hz. As shown in FIGURE 3B, the positions of the stimulating electrode, with threshold current of lower than 150 μ A, were limited to one area of the NRTP. The lowest threshold was 50 μ A. Furthermore, electrical stimulation of the NRTP could not elicit evoked potentials in the flocculus ipsilateral to the stimulating site.

On the other hand, electrical stimulation (pulse width, 0.05 msecond) of the most caudal part of the DNR also elicited evoked potentials in the flocculus, which were characterized by negative potentials occurring at a peak latency of 2-2.6 mseconds (FIGURE 4A) and following stimulation frequencies of as high as 50 Hz. The positions of the stimulating electrode, with threshold current of lower than 150 μ A, were limited to the most caudal part of the DNR (FIGURE 4B and C).

The lowest threshold current was 60 μ A. It should be noted that extracellular unitary spikes activated antidromically by electrical stimulation of the flocculus were recorded in the region corresponding to the area where the threshold current for the evoked potentials was lower than 150 μ A (not illustrated).

Effect of NRTP Lesion on Optokinetic Responses

In order to clarify a role of the NRTP in optokinetic responses, OKN and VS of caloric nystagmus were tested in seven cats with NRTP lesion, three cats with PN lesion, and two unilaterally hemicerebellectomized cats, respectively.

After destruction of the NRTP, slow-phase OKN velocity toward the direction ipsilateral to the lesion site did not increase as the OKN stimulus velocity increased (FIGURE 5A), while slow-phase OKN velocity fell in the normal range in the cats with PN lesion (FIGURE 5C). These findings suggest that the NRTP may have relevance to optokinetic responses in cats. It should be noted, however, that the impaired pattern of slow-phase OKN velocity in the cats with NRTP lesion was different from that in the unilaterally hemicerebellectomized cats: the slow-phase OKN velocity was approximately in the normal range at the OKN stimulus velocities of less than 30°/second in the hemicerebellectomized cats (FIGURE 5D); in the cats with NRTP lesion, it fell in a lower range than normal even at an OKN velocity of 10°/second (FIGURE 5C).

The impairment of OKN in the cats with NRTP lesion persisted for more than three weeks after the lesion had been made, while loss of VS of caloric

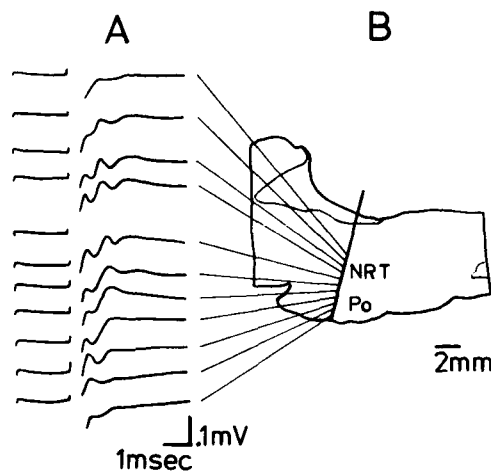


FIGURE 3. Field potentials in the flocculus evoked by electrical stimulation of the NRTP. **A:** field potentials in the flocculus evoked by electrical stimulation (150 μ A) of the medial part of the NRTP contralateral to the recording site. Potentials were averaged during 10 successive sweeps at a rate of 1 Hz. **B:** line drawing of a sagittal section of the brain stem showing a stimulating electrode track, which is indicated by a line drawn in the dorsoventral direction. Diagonal lines between A and B indicate that a response in A was recorded at a region where a diagonal line crosses the electrode track in B. Abbreviations: NRT, nucleus reticularis tegmenti pontis; Po, pontine nucleus.

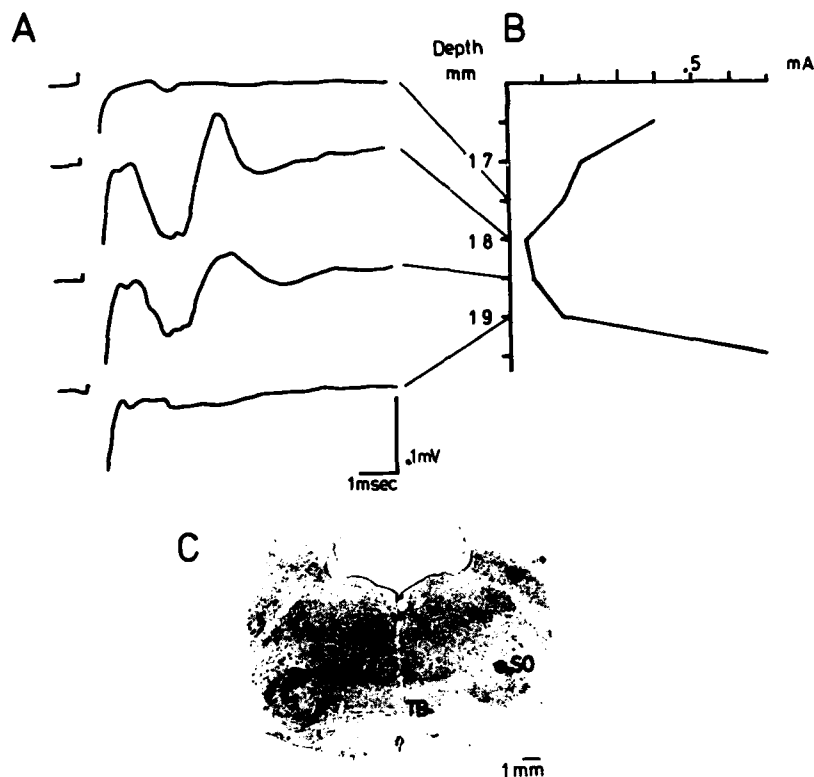


FIGURE 4. Field potentials in the flocculus evoked by electrical stimulation of the most caudal part of the DNR. A: field potentials evoked by electrical stimulation ($150 \mu\text{A}$) of the most caudal part of the DNR. Potentials were averaged during 10 successive sweeps at a rate of 1 Hz. B: relation between the depth of the stimulating electrode and the threshold current. The number at the left of the ordinate indicates the depth from the surface of the cerebellum. C: histological verification of the stimulated site of the lowest threshold in B. This section corresponds well with motor trigeminal nuclear levels of FIGURE 2B. Abbreviations: SO, superior olive; TB, trapezoid body; Vm, motor trigeminal nucleus.

nystagmus was transient in all cats with NRTP lesion (not illustrated)—it was observed only for a few days after the lesion was made.

DISCUSSION

Projection from the NRTP to the Flocculus

The projection from the NRTP to the flocculus was bilateral with a contralateral preponderance (FIGURE 1B). Only few neurons labeled with HRP were found in the medial part of the NRTP, in agreement with the results of previous reports.^{11,16} In rabbits, however, large numbers of neurons labeled with HRP were recognized in the NRTP, including the processus tegmentosus lateralis.^{8,20}

This discrepancy may be due either to a difference in animal species or to whether or not the tracer diffused to the parafoveolus.^{11,16,20}

A projection from the medial part of the NRTP to the contralateral flocculus may be supported by the electrical experiments: electrical stimulation of the

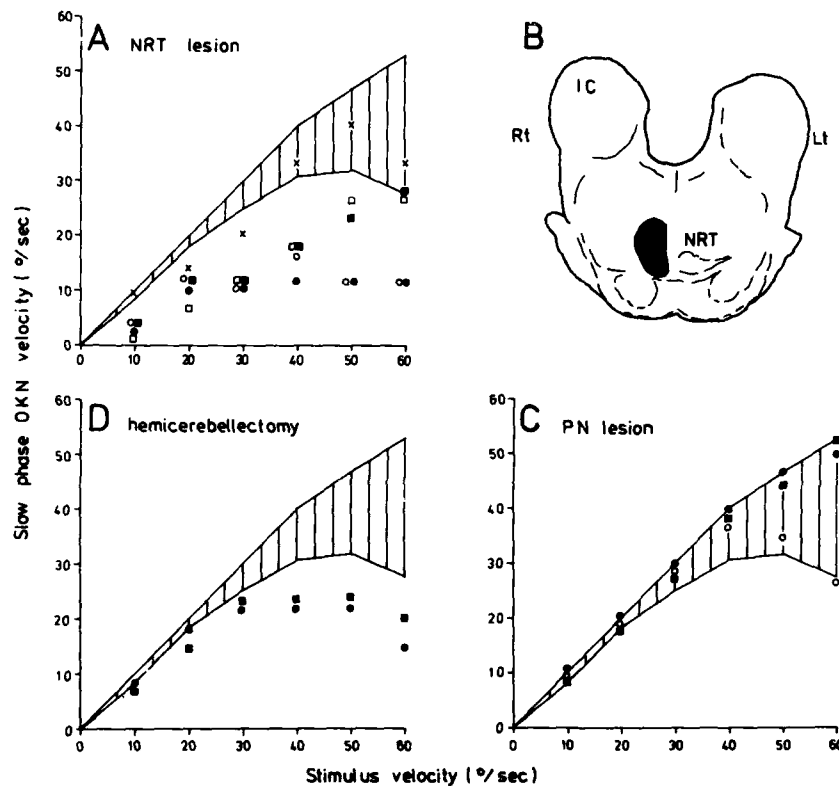


FIGURE 5. The gain of OKN in normal, NRTP-lesioned, PN-lesioned, and hemiserebellectomized cat. The hatched area indicates the normal range of the slow-phase OKN velocity obtained from 12 cats before the lesion was made. A: the relation between slow-phase OKN velocity and OKN stimulus velocity (OKN stimulus toward the right and slow-phase eye movement toward the right) in 5 cats with the right-side NRTP lesion. Note that the slow-phase OKN velocity toward the lesion site is clearly in a lower range than normal, even at OKN stimulus velocities of less than 20°/second in cats with the NRTP lesion, except one cat. In this cat, only the caudal part of the NRTP was found to be affected by the lesion. B: schematic representation of the lesion site in the brain stem. The lesion site was found in the rostral half of the NRTP. Abbreviations: IC, inferior colliculus; NRT, nucleus tegmenti pontis; Lt, left; Rt, right. C: the relation between slow-phase OKN velocity and OKN stimulus velocity in 3 cats with PN lesion. Slow-phase OKN velocity fell in the normal range in these cats. D: the relation between slow-phase OKN velocity and OKN stimulus velocity (OKN stimulus toward the right and slow-phase eye movement toward the left) in 2 cats with hemiserebellectomy on the right-hand side. Note that slow-phase OKN velocity is approximately in the normal range at the lower OKN stimulus velocities of less than 30°/second, while it is in a lower range than normal at the higher OKN stimulus velocities of more than 40°/second.

medial part of the NRTP elicited evoked potentials in the flocculus contralateral to the stimulating site, while stimulation of the lateral part of the NRTP did not. Furthermore, the threshold current evoking field potentials in the flocculus was lower than $150\ \mu\text{A}$ (FIGURE 3A) and the positions of stimulating electrode, with threshold current of lower than $150\ \mu\text{A}$, were limited to the medial part of the NRTP.

Regarding the possibility for transmission of visual information to the flocculus via the NRTP, it seems that most of these transmissions may be mediated through the pretectum, which sends fibers to the medial part of the NRTP, while some may be mediated through the superior colliculus, which sends fibers to the mediodorsal part of the NRTP.²²⁻²⁵ These areas project in turn to the flocculus.^{11,16} This pathway may be a part of the route responsible for visually induced mossy fiber potentials in the flocculus.⁵

Projection from the Caudal Part of the DNR to the Flocculus

A projection of the DNR to the cerebellum has not been described anatomically, except for our preliminary report.¹¹ A projection of the most caudal part of the DNR to the flocculus may be supported by several findings obtained from the stimulation experiments. First, the threshold current necessary to evoke field potentials in the flocculus was low, with $60\ \mu\text{A}$ being the lowest threshold current (FIGURE 4A and B). Second, the positions of the stimulating electrode, with threshold current of lower than $150\ \mu\text{A}$, were limited to a small area corresponding to the most caudal part of the DNR (FIGURE 4C). Third, antidromic extracellular unit activities induced by electrical stimulation of the flocculus were recorded in the most caudal part of the DNR.

Regarding a function of the projection of the most caudal part of the DNR to the flocculus, it seems that the most caudal part of the DNR may be involved in eye movement control, since this region appears to correspond to the recording site of the pause unit reported by Raybourn and Keller and Evinger *et al.*, which ceased its firing during saccade eye movements.^{26,27} Furthermore, units activated by both sinusoidal rotation stimulation and antidromic electrical stimulation of the flocculus also were recorded in the vicinity of the caudal part of the DNR.²⁸ On the other hand, retinal ganglion cells having y-cell type characteristics send their axons to the DNR.²⁹ These cells have been known to be sensitive to rapidly moving stimuli.³⁰ There exists another possibility—that the visual information relevant to rapidly moving stimuli may be mediated via the DNR to the flocculus.

Role of the NRTP in OKN

In the present experiments, NRTP and PN lesions were made by the same method: the lesion was made by the passing of a positive d.c. current through a steel electrode inserted stereotaxically into the brain stem through the cerebellum. The lesion site in the PN was about 3 mm below the NRTP. In spite of this fact, PN lesion did not produce any effect on optokinetic responses, while NRTP lesion impaired slow-phase OKN velocity (FIGURE 5A and C). These findings suggest that the NRTP may have an important role in induction of optokinetic responses. It should be emphasized that the impaired pattern of slow-phase OKN velocity in the cats with NRTP lesion was different from that in the hemicerebel-

lectomized cats (FIGURE 5A and D). This finding was consistent with those in previous reports.^{10,15} Furthermore, in patients with a cerebellar tumor, slow-phase OKN velocity was impaired at higher OKN stimulus velocities, while it was normal at lower OKN stimulus velocities.³¹ These facts lead us to suppose that the cerebellum may not be essential for elicitation of OKN at lower OKN stimulus velocities and that the NRTP may be a relay nucleus mediating visual information relevant to OKN not to the flocculus but to the vestibular nuclei. This view may be supported by the results reported by Precht and Strata.¹⁰

Candidate for the Precerebellar Nucleus Relevant to Optokinetic Responses

In the present experiments, the precerebellar nucleus that processes optokinetic responses could not be determined. However, it seems that the DNR may be a candidate for one of the precerebellar nuclei mediating visual information relevant to optokinetic responses to the flocculus, since ganglion cells having y-cell type characteristics send fibers to the DNR and y-cells in the retina are sensitive to rapidly moving stimuli.^{29,30} It seems very probable that a pathway mediating this kind of visual information to the flocculus has an important role in optokinetic responses to rapidly moving stimuli and that an interruption of this pathway may cause impairment of slow-phase OKN velocity at higher OKN stimulus velocities.

REFERENCES

1. ITO, M. 1976. Cerebellar learning control of vestibulo-ocular mechanisms. In *Mechanisms in Transmission of Signals for Conscious Behaviour*. T. Desiraju, Ed.: 1-22. Elsevier/North Holland Biomedical Press. Amsterdam, the Netherlands.
2. TAKEMORI, S. & B. COHEN. 1974. Loss of visual suppression of vestibular nystagmus after flocculus lesions. *Brain Res.* 72: 213-224.
3. LISBERGER, S. G. & A. F. FUCHS. 1978. Role of primate flocculus during rapid behavioral modification of vestibuloocular reflex. I. Purkinje cell activity during visually guided horizontal smooth-pursuit eye movements and passive head rotation. *J. Neurophysiol.* 41: 733-763.
4. MAEKAWA, K. & J. I. SIMPSON. 1973. Climbing fiber responses evoked in vestibulocerebellum of rabbit from visual system. *J. Neurophysiol.* 36: 649-666.
5. MAEKAWA, K. & T. TAKEDA. 1975. Mossy fiber responses evoked in the cerebellar flocculus of rabbits by stimulation of the optic pathway. *Brain Res.* 98: 590-595.
6. ALLEY, K. A., R. BAKER & J. I. SIMPSON. 1975. Afferents to the vestibulocerebellum and the origin of the visual climbing fibers in the rabbits. *Brain Res.* 98: 582-589.
7. ALLEY, K. A. 1977. Anatomical basis for interaction between cerebellar flocculus and brainstem. *Dev. Neurosci.* 1: 109-117.
8. MAEKAWA, K. & T. TAKEDA. 1978. Origin of the mossy fiber projection to the cerebellar flocculus from the optic nerves in rabbits. In *Integrative Control Function of the Brain*. M. Ito et al., Eds.: 110-112. Kodansha Scientific. Tokyo, Japan.
9. MAEKAWA, K., T. TAKEDA & M. KIMURA. 1979. Activities of nucleus reticularis tegmenti pontis (Bechterew) which transfer optic signals through mossy fiber afferents to the cerebellar flocculus of rabbits. *J. Physiol. Soc. Jpn.* 41: 320.
10. PRECHT, W. & P. STRATA. 1980. On the pathway mediating optokinetic responses in vestibular nuclear neurons. *Neuroscience* 5: 777-787.
11. KAWASAKI, T. & Y. SATO. 1980. Afferent projection from the dorsal nucleus of the raphe to the flocculus in cats. *Brain Res.* 197: 496-502.
12. KATO, I., M. AOYAGI, T. KAWASAKI & Y. SATO. 1979. Visual suppression of caloric nystagmus in cats. *Acta Otolaryngol.* 87: 108-112.

13. KATO, I., T. KAWASAKI, M. AOYAGI, Y. SATO & K. MIZUKOSHI. 1979. Loss of visual suppression of caloric nystagmus in cats. *Acta Otolaryngol.* **87**: 499-505.
14. KATO, I., T. KAWASAKI, Y. SATO, M. AOYAGI & Y. KOIKE. 1980. Visual suppression of caloric nystagmus and optokinetic responses in cats. *Acta Otolaryngol.* **89**: 497-503.
15. KELLER, E. L. & W. PRECHT. 1979. Visual-vestibular responses in vestibular nuclear neurons in the intact and cerebellectomized, alert cat. *Neuroscience* **4**: 1599-1613.
16. HODDEVIK, G. H. 1978. The projection from nucleus reticularis tegmenti pontis onto the cerebellum in the cat. *Anat. Embryol.* **153**: 227-242.
17. KOTCHABHAKDI, N., G. H. HODDEVIK & F. WALBERG. 1978. Cerebellar afferent projections from the perihypoglossal nuclei: an experimental study with the method of retrograde axonal transport of horseradish peroxidase. *Exp. Brain Res.* **31**: 13-29.
18. KOTCHABHAKDI, N., G. H. HODDEVIK & F. WALBERG. 1978. Cerebellar afferent projections from the vestibular nuclei in the cat: an experimental study with the method of retrograde axonal transport of horseradish peroxidase. *Exp. Brain Res.* **31**: 591-604.
19. WALBERG, F., N. KOTCHABHAKDI & G. H. HODDEVIK. 1979. The olivocerebellar projections to the flocculus and paraflocculus in the cat, compared to those in the rabbit. A study using horseradish peroxidase as a tracer. *Brain Res.* **161**: 389-398.
20. YAMAMOTO, M. 1979. Topographical representation in rabbit cerebellar flocculus for various afferent inputs from the brain stem investigated by means of retrograde axonal transport of horseradish peroxidase. *Neurosci. Lett.* **12**: 29-34.
21. TABER, E., A. BRODAL & F. WALBERG. 1960. The raphe nuclei of the brain stem in the cat. I. Normal topography and cytoarchitecture and general discussion. *J. Comp. Neurol.* **144**: 161-187.
22. BERMAN, N. 1977. Connections of the pretectum in the cat. *J. Comp. Neurol.* **174**: 227-254.
23. GRAYBIEL, A. M. 1974. Some efferents of the pretectal region in the cat. *Anat. Rec.* **178**: 365.
24. ALTMAN, J. & M. B. CARPENTER. 1961. Fiber projections of the superior colliculus in the cat. *J. Comp. Neurol.* **116**: 157-178.
25. KAWAMURA, K., A. BRODAL & G. H. HODDEVIK. 1974. The projection of the superior colliculus onto the reticular formation of the brain stem. An experimental anatomical study in the cat. *Exp. Brain Res.* **19**: 1-19.
26. RAYBOURN, M. S. & E. L. KELLER. 1977. Colliculoreticular organization in primate oculomotor system. *J. Neurophysiol.* **40**: 861-878.
27. EVINGER, C., C. R. S. KANEKO, G. W. JOHANSON & A. F. FUCHS. 1977. Omnipuser cells in the cat. *Dev. Neurosci.* **1**: 337-340.
28. NAKAO, S., I. S. CURTHOYS & C. H. MARKHAM. 1980. Eye movement related neurons in the cat pontine reticular formation: projection to the flocculus. *Brain Res.* **183**: 291-299.
29. FOOTE, W. E., E. TABER-PIERCE & L. EDWARDS. 1978. Evidence for a retinal projection to the midbrain raphe of the cat. *Brain Res.* **156**: 135-140.
30. FUKUDA, Y. & J. STONE. 1975. Direct identification of the cell bodies of y-, x- and w-cells in the cat's retina. *Vision Res.* **15**: 1034-1036.
31. SATO, Y., T. KAWASAKI, I. KATO & K. MIZUKOSHI. 1981. Role of the cerebellum on optokinetic nystagmus. *Acta Med. Biol.* **28**: 161-167.

VISUAL MOSSY FIBER INPUTS TO THE FLOCCULUS OF THE MONKEY*

Hiroharu Noda

Brain Research Institute
Departments of Physiology and Anatomy
University of California
Los Angeles, California 90024

INTRODUCTION

Recent single-unit studies in monkeys, trained to track a slowly moving visual target, implicate the cerebellar flocculus in the control of smooth-pursuit eye movements.¹⁻⁴ A smooth-pursuit eye movement is the result of an attempt to match the angular velocity of eye movement to the velocity of a moving object, and consequently the object's image is held relatively stationary on the moving retina. It has been observed that discharge rates of some Purkinje cells in the flocculus are modulated typically in relation to the velocity of eye movements during smooth pursuit in the absence of head rotation.^{2,3} In this situation, since the image of the object moves with the retina, the modulation in Purkinje cell activity reflects primarily eye velocity signals arising in the oculomotor system. On the other hand, when eye velocity is smaller than object velocity, the eye movement lags behind the moving object and there occurs slippage of its retinal image. The velocity of the moving object then corresponds to the algebraic sum of eye velocity and retinal image velocity. Neural activity reflecting the sum of such velocity signals should, therefore, be observed in some brain structures thought to be constituents of the smooth-pursuit system. In order to qualify as a part of the smooth-pursuit control system, the flocculus may have to receive information about retinal image motion from the visual system. The existence of visual inputs to the flocculus of the monkey has been reported.^{1,4,5} However, partially because the fibers carrying visual information comprise only a small percentage of the afferent fibers, the properties of visual input signals to the monkey flocculus mostly are unknown. The aim of the present investigation was to study the characteristics of visual signals that are brought to the flocculus of the monkey.

METHODS

The present study was based on 19 visually responsive mossy fiber units, which were selected from a total of 1,858 units recorded from the flocculus of seven monkeys (*Macaca nemestrina*). Among the 1,858 units, 116 units were identified as mossy fibers on the basis of the criteria used in a preceding study.⁷ A detailed account of the surgical procedures for implanting electro-oculogram (EOG) electrodes, experimental condition, procedures for training monkeys, and methods of recording neuronal activity together with the EOGs and anatomical locations of recording sites are described elsewhere.^{3,8} In brief, the monkeys were trained to fixate a small spot of red light, which was generated from a neon laser.

*Supported by National Institutes of Health Grant R01 EY01051.

The dispensing of a juice reward was contingent upon the release of a lever during a brief presentation of a green spot following the red-spot period.

During an experiment, a monkey was seated in a primate chair designed to offer a clear view of the central 30° from the midgaze point. By inserting two pairs of bars into two transverse tubes on the skull, the head of the monkey was affixed to a frame that provided support for the chair. This system resulted in complete immobilization of the head without application of painful pressure and prevented dynamic input signals from the labyrinths. The animal was placed in a small room facing a window that had been furnished with a rear-projection screen. When the animal was placed 57 cm from it, the screen subtended 110° of the visual angle horizontally and 90° vertically. A background random-dot pattern (interspot luminance: 0.035 ft-L) was projected on and filled the tangent screen. When the visual pattern was not projected, the small room was completely dark. In order to test responses of units to visual stimulation, the random-dot background was moved sinusoidally during fixation of a stationary target presented at the midgaze position of the screen. The velocity of background movement typically was within the range of monkey's smooth-pursuit eye movement. The most commonly used background movements were sinusoidal oscillations in the horizontal plane between 10° right and 10° left at frequencies from 0.1 Hz to 0.7 Hz.

RESULTS

Mossy fibers showing responses to movements of the random-dot background were encountered in the white matter of the flocculus. Out of 116 mossy fiber units, 19 responded to movements of visual patterns. The others discharged in bursts associated with saccadic eye movements. The bursts with saccades persisted even in complete darkness, indicating that they represented signals related to oculomotor activity and did not reflect quick retinal image motion that accompanied the rapid motion of the eyes during saccades. Details of the discharge patterns of mossy fibers in relation to saccadic eye movements already have been described.⁷ Visually responsive mossy fiber units studied in the present experiment were intermingled with these saccade-related mossy fibers.

A common feature of the responses of visual mossy fiber units was directional selectivity. Each unit had a preference for the direction of stimulus movement and showed a vigorous response only when the stimulus moved in the preferred direction. Stimulus movements in the other direction usually were not associated with discharges. The second and perhaps more important feature of the responses was their sensitivity to the velocity of stimulus movements in the velocity range of smooth-pursuit eye movements. Based on whether or not the unit activity was related to changes in the velocity of sinusoidal stimulus movement less than 50°/second, the visual mossy fiber units were classified into two groups. The first group showed only directional selectivity, and the second group showed both directional preference and velocity sensitivity.

Direction-Only Visual Mossy Fibers

Of the 19 mossy fiber units, visual responses of 7 units were observed to convey direction, but not velocity, information. These responses were characterized by discharges when the background was moved in a specific, preferred

direction. Regardless of whether the background movement was sinusoidal or triangle waveform, the units showed an early peak in discharge rates with a latency between 100 and 200 mseconds from the changes in direction of background movements (turnabout). The early peak was prominent in some units (4 units) and was not in others (3 units) but always was followed by a plateau or a gradual downhill activity. There was no elevation at the midway where sinusoidal movements reached the peak velocity. Movements in the nonpreferred direction always were associated with almost complete silence. When tested with constant-velocity triangle-waveform movements, the responses almost were identical with those to sinusoidal movements, indicating that these units did not respond to the sinusoidal change in velocity. The units also showed analogous responses even when the frequency of sinusoidal movement was changed without changing the magnitude of the oscillation (or changing the magnitude at the same frequency, hence changing the peak velocity of the sinusoidal movement).

FIGURE 1 shows an example of direction-only visual mossy fiber units. FIGURE 1A shows the original film record of instantaneous discharge rate (IR), spikes, horizontal (H) and vertical (V) EOGs, and background motion signal (Bg). FIGURE 1B shows rasters, displaying response-to-response variation and the time course of the responses. FIGURE 1C shows phase histograms, illustrating activity changes

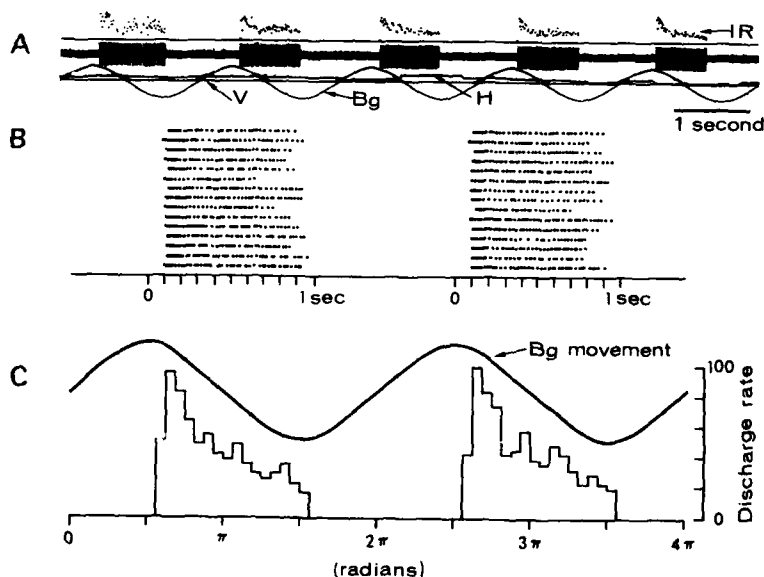


FIGURE 1. Responses of a mossy fiber unit to sinusoidal background movements. A: original film record, showing instantaneous discharge rates (IR), spike train, horizontal (H) and vertical (V) EOGs, and background position (Bg) signals. Upward shifts of the horizontal and vertical EOGs and the background position signals in this and the following figures indicate movements to the right, up, and right, respectively. B: raster, showing temporal relationship between the discharges and stimulus movements. Responses are aligned with respect to the right-to-left turnabout. C: phase histograms, showing the change in discharge rate with background position. To facilitate visualization, responses to consecutive two cycles were sampled and displayed.

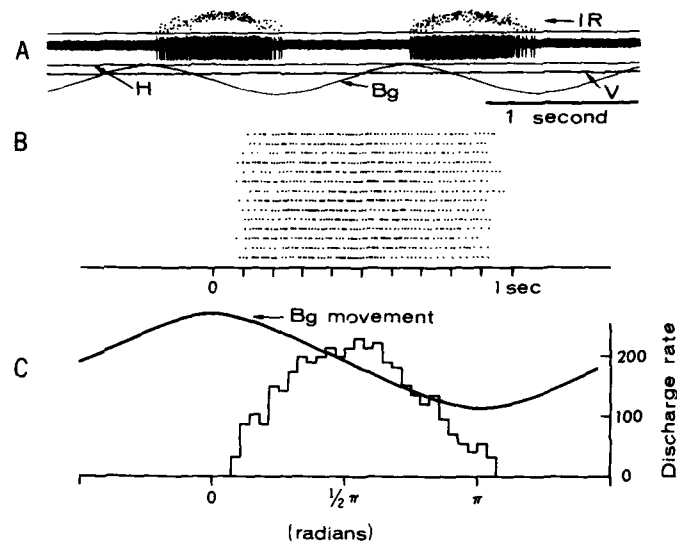


FIGURE 2. Responses of a mossy fiber unit to sinusoidal background movements. A: original film record, showing instantaneous discharge rate (IR), spike train, horizontal (H) and vertical (V) EOGs, and background position (Bg) signals. Note that the peak activity appeared approximately in phase with the peak velocity of the background movements to the left. B: a raster, showing temporal relationship between the discharges and stimulus movements. Responses are aligned with respect to the right-to-left turnabout. C: phase histogram, showing the change in discharge rate in relation to the change in background position.

with respect to the cycle of sinusoidal background movements. The response started with a burst, which decayed gradually and occasionally finished even before the turnabouts, as seen in the last response of the film record. The latency of the peak activity with respect to the turnabouts varied from cycle to cycle, as evidenced in the rasters. The latency of the first spike of the bursts measured from the turnabouts ranged from 78 to 107 mseconds, with a mean of 96.5 mseconds. For the seven direction-only mossy fiber units, sinusoidal background movements at 0.5 Hz were associated with an average latency of 102 mseconds (range: 85 to 157 mseconds).

Direction- and Velocity-Related Visual Mossy Fibers

In 12 out of the 19 visual mossy fibers, responses were related also to the sinusoidal changes in the velocity of the stimulus movements. When tested with sinusoidal background movements, discharges of these units started with short latencies after the turnabouts and increased along with the sinusoidal increment of the velocity up to the point of maximum velocity, and then—again with short latencies—the firing rate started to slow down and returned to zero after the background started moving in the opposite direction. Within the velocity range of

monkey's smooth-pursuit eye movements (from 0 to about 50°/second), the discharge rates of this group of mossy fibers were related to the velocity. As the frequency of sinusoidal movements was increased, without changing the magnitude of the oscillation, the peak discharge rates increased monotonically with higher frequencies.

A typical example of a visual mossy fiber unit, showing velocity-related activity, is shown in FIGURE 2. In response to sinusoidal movements of background, the unit discharged when it was moved to the left (A). The raster (B) shows the temporal relationship of the responses with respect to background movements. The delays of the first spikes from the right-to-left turnabout ranged from 75 to 145 msec, with a mean of 112 msec. The phase histogram (C), evaluated from 30 cycles of sinusoidal movements, showed that the peak discharge rate appeared with a phase lag slightly more than $\pi/2$ radians from the turnabout. The modulation in activity reflected the sinusoidal changes in the velocity of background movements in a range from 0 to about 35°/second at 0.5 Hz. The sensitivity to the stimulus velocity was about 5.2 spikes/second per degree/second. The response of the unit exhibited a frequency dependency, with peak discharge rates of 70, 108, 145, 180, and 210 spikes/second being observed at 0.2, 0.3, 0.4, 0.5, and 0.6 Hz (magnitude of oscillation: 20°), respectively.

FIGURE 3 shows another example of a velocity-sensitive visual mossy fiber,

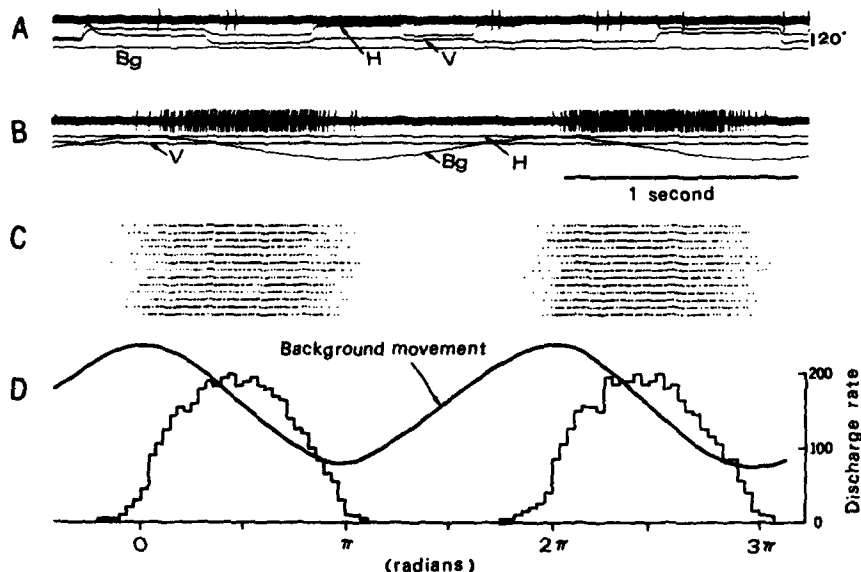


FIGURE 3. Responses of a mossy fiber unit to sinusoidal movements of the background. A: discharges during spontaneous eye movements in total darkness. Note that spontaneous discharge rate was about 3 spikes/second. B: discharges during fixation of a stationary target while the background was oscillated sinusoidally at approximately 0.5 Hz. C: raster, showing responses during 13 repetitions of two cycles of background movements. D: phase histograms. Note that the firing started before the nonpreferred to preferred turnabout of stimulus movements.

exhibiting activity changes in relation to sinusoidal movements of the random-dot background. During spontaneous saccades and fixation in complete darkness, the unit discharged randomly at 2-3 spikes/second (A). There was no discharge associated with saccadic eye movements. When background was moved sinusoidally at 0.5 Hz during steady fixation of a stationary target, the unit discharged with the background movement to the left (B). The rasters (B) and the phase histograms (C) show that discharge rates reflected the sinusoidal changes in the velocity of background movements. Although the unit discharged predominantly with the movement to the left, the responses started even before the change in direction of background movements. In contrast with the relatively simple velocity-sensitive mossy fibers as exemplified in FIGURE 2, this unit responded more exactly to the changes in the velocity of sinusoidal motion. The responses of the unit shown in FIGURE 2 had certain latencies in both the start and the end as well as in the peak with respect to the turnabouts and the maximum stimulus velocity, respectively. Such latencies were not observed in this unit. Similar responses were found also in four other units. Fourier analyses revealed that the fundamental components of such half-sinusoidal visual responses had 44° phase lag relative to the background-movement curve. The other four units also showed similar phase lags, ranging from 42.7° to 46.3° , with a mean value of 44.3° . Therefore, their activity curves almost were in phase with the velocity curve of the sinusoidal stimulus movements. With available data, there is no convincing explanation at present as to how the latencies of visual inputs were compensated to match the velocity of the stimulus movements. As to the firings before the turnabout, it may well be that inhibitory visual signals also converge on the same mossy fiber unit during stimulus movements in the nonpreferred direction. The spontaneous discharge rate was about 2.5 spikes/second in this unit (A). During movements in the nonpreferred direction, discharge rate fell down to zero, suggesting the possibility of suppression by the inhibitory inputs.

When velocity-sensitive visual mossy fibers were tested with sinusoidal movements of the background, their responses were characterized by smooth elevation of discharge rates, which reached a peak approximately at the maximum velocity. The response curves in these cases had a phase lag of about 45° (or $\pi/2$ radians) relative to the stimulus curve (background motion). When the same units were tested with triangle-waveform movements (constant velocity), their responses were associated with an early peak, which was followed by a plateau. Examples of such responses are seen in FIGURE 4, where discharges of a mossy fiber unit during sinusoidal (A) and triangle-wave (B) movements of the random-dot background are illustrated. It is clear that the response curve of the unit during constant-velocity stimulation almost was identical with those of direction-only mossy fiber units (FIGURE 1). When latencies of the responses were measured from the turnabout of ramp background movements, they varied from 86.2 mseconds to 121.4 mseconds, with a group mean of 108.3 mseconds (for all visual mossy fibers).

Based on the difference of whether or not the unit was sensitive to sinusoidal changes in velocity in a range up to $50^\circ/\text{second}$ (e.g., 0.8 Hz; magnitude, 20°), visual mossy fibers were classified into direction-only or direction-and-velocity sensitive units. In individual units, however, the responses were not always clear-cut. A continuous variation occurred in the responses that filled the gap between the two classes of units. Reading raw data frequently did not provide an indication of whether a unit was sensitive to velocity or not in many units. Velocity-related activity could be seen in such units only after processing the

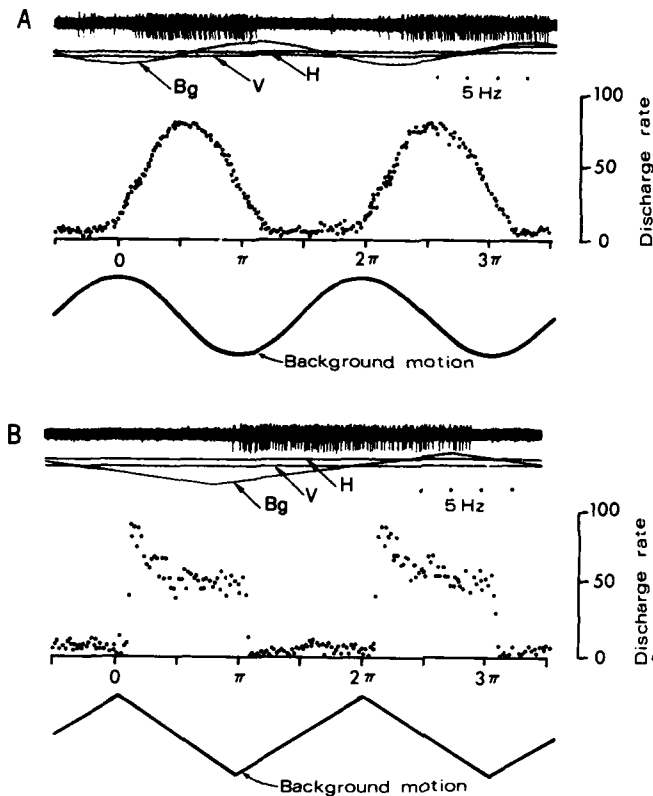


FIGURE 4. Responses of a visual mossy fiber to sinusoidal (A) and ramp (B) movements of the background. Discharge rates in the phase histograms were evaluated from 30 repetitions of two cycles of stimulus movements.

responses to repeated trials. FIGURE 5 shows an example. In response to ramp movements at a constant velocity of $30^\circ/\text{second}$, the unit showed an early peak followed by a relatively flat level (A-C). The discharge rate of the flat portion was 57 spikes/second. The latency ranged from 80 to 134 mseconds, with a mean of 110 mseconds. When tested with the ramp movements at $15^\circ/\text{second}$, the average level of activity decreased to 28.7 spikes/second (D-F). The latency ranged from 102 to 234 mseconds, with a mean of 130 mseconds. The discharge pattern of this unit did not show clear velocity-dependent changes in response to individual cycles of the sinusoidal movements (G and J). The responses started inconsistently at low velocity, resulting in a considerable variation in the latencies from response to response (H-K). The latencies ranged from 86 to 260 mseconds with a mean of 185 mseconds during sinusoidal movements at 0.5 Hz. The mean latency increased to 300 mseconds at 0.25 Hz (K). Because of such variability in the latencies, the phase histogram (L) showed a response curve that, as a result, resembled very closely the change in velocity of sinusoidal movements. The peak discharge rate appeared with a phase lag slightly more than $\pi/2$ radians from the

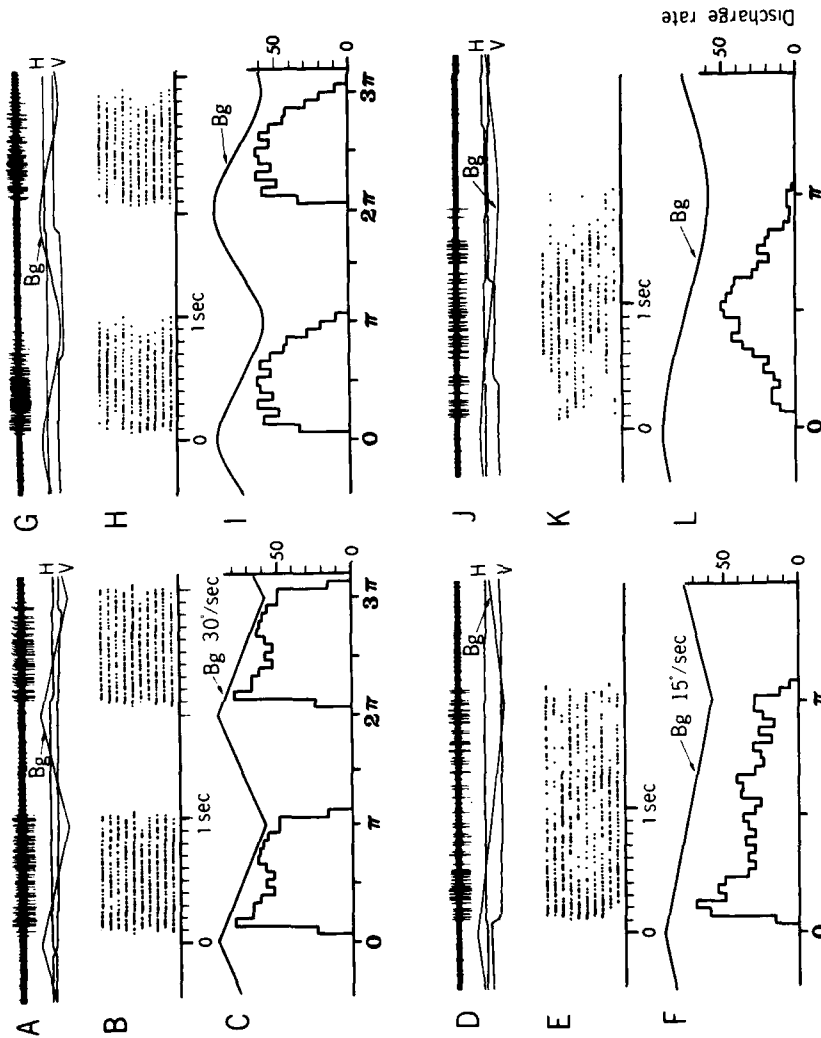


FIGURE 5. Responses of a mossy fiber unit to ramp and sinusoidal movements of the background. A, D, G, & J: original film records. B, E, H, & K: rasters. C, F, I, & L: phase histograms. A-C: during constant-velocity ramp movements at $15^\circ/\text{second}$. G-I: during sinusoidal movements at 0.5 Hz. J-L: during sinusoidal movements of 0.25 Hz.

turnabout, indicating that the point where there is the highest probability of finding spikes occurs slightly after the appearance of peak velocity.

The observation made in this unit provided us with a hint showing how the velocity signals were refined in the process of transmission of visual signals. During sinusoidal movements of the visual pattern, the delay of the responses varied from cycle to cycle of the stimulus movements (H and K). In a sinusoidal movement, the velocity gradually increases from zero to the peak. The period of near-zero velocity continues for some time, and a cell discharges only when the background movement reaches a certain velocity. The velocity threshold of the cell may be determined by the sensitivity of the cell. The velocity sensitivity may vary from time to time due to changes in the excitability of the cell. It also is possible that the velocity of retinal image, which is the difference between the stimulus and eye velocities, may vary associated with small saccades or momentary drifts of eye positions during the stimulus movements. All these factors may cause the variability in the latency of responses to sinusoidal movements. As a result, the probability of seeing discharges may increase with a higher velocity and the highest activity may appear when the stimulus movement reaches the peak velocity, as seen in FIGURE 5L. On the other hand, when the unit was tested with ramp stimulus movements, the latency was relatively regular, as the constant stimulus movement began immediately after the turnabout. Due to such regular latencies, the phase histograms (C and F) were a simple summation of individual responses that were nicely aligned with respect to the turnabouts (B and E).

In reality, such temporal summation as seen in the histograms (I and L) may occur as a spatial summation of impulses arriving from different presynaptic cells. Supposing that a brain-stem cell that is the origin of a mossy fiber receives visual signals from a group of cells with different velocity sensitivities to low-velocity stimulus movements, it is possible that the number of presynaptic cells that are activated at a certain time may increase as the stimulus velocity is increased. The latency of responses may vary from one synaptic cell to another, depending upon the velocity sensitivity of the cell. Thus, the total number of impulses coming to the cell of the mossy fiber may increase as the stimulus velocity is increased sinusoidally from zero to the peak velocity.

It is known that most neurons in the visual system are activated by moving stimuli, but the neuronal mechanisms for the detection and signaling of the velocity of motion are unknown. Some relation to stimulus velocity may be found in visual neurons in the sense that above and below a certain preferred velocity, the response falls off sharply. However, only few neurons in the mammalian visual system have shown a strictly positive functional correlation between discharge rate and stimulus velocity (see Reference 8 for a review). This suggests that velocity detection may require the successive activation of a population of neurons with similar directional selectivity but different sensitivity to the velocity, by passing of the image across the retina.

DISCUSSION

The present investigation has demonstrated clearly that the visual system is an important source of sensory input to the flocculus in the monkey. It is known in the rabbit that floccular Purkinje cells are activated from the optic nerves not

only through the climbing fiber but also through the mossy fiber pathway.^{9,10} However, the significance of the visual input to the flocculus has been controversial in the monkey (see Reference 11 for a review). When the monkey tracks ramp movements of the target, there exists a transient phase where the target already has changed the direction but the eyes still are moving in the same direction. The eyes change direction with latency of 50–150 mseconds and catch up to the target with a saccade. Lisberger and Fuchs analyzed Purkinje cell activity during such a transient period and found that 12 out of 20 cells displayed transient overshoots (or undershoots) in firing rate.² Although the possibility that the transient overshoots might have reflected eye acceleration signals could not be ruled out, the study suggested possible neuronal correlates of retinal image motion in the flocculus of the monkey. The latter possibility has been supported by Miles *et al.*, based on almost identical experiments.⁴ The significance of the visual input with which the flocculus may serve to improve the stability of retinal images of the visual field during free head movements has been suggested in the monkey. Takemori and Cohen demonstrated that the horizontal vestibulo-ocular reflex provoked by caloric stimulation, alcohol administration, or labyrinthectomy was depressed by visual input, and this effect was lost when the flocculus had been removed.^{12,13} This observation would indicate that the flocculus is a medium through which the visual system can alter or modify vestibular reflexes. In spite of the implications concerning the visual control of eye movements, single-unit recordings of visual input signals in the monkey flocculus so far have been unsuccessful (see Reference 11 for a review). The present data have shown that mossy fiber activity recorded in the white matter of the flocculus was related to the direction and velocity of visual stimulus movements. It is now indisputable that the visual modulation of simple spike activity of floccular Purkinje cells is due to mossy fiber inputs. The existence of velocity-related mossy fiber activity indicates that the flocculus receives signals related to the velocity of retinal image movements. It is demonstrated that the flocculus qualifies as one of the constituents of the smooth-pursuit control system.

The average latency of visual mossy fibers of the flocculus was about 108 mseconds in response to the change in the direction of ramp stimulus movements. On the other hand, the latency of the flash-evoked field potentials recorded from the flocculus of the rabbit was 30–40 mseconds.⁹ The field potentials responded fairly well to that of single-unit responses. The latency of climbing fiber responses of Purkinje cells to the onset of light in their receptive fields was 35–40 mseconds.¹⁴ As compared with these values in the rabbit flocculus, the latency observed in the present study—based on the mossy fiber responses of the monkey flocculus—was very long. It is possible that visual signals brought to the flocculus by mossy fibers may take entirely different pathways from those for climbing fibers. It also is possible that the cells of mossy fibers receive visual signals through various routes, such as the brain-stem visual pathways and by way of the higher visual cortices.^{15,16} This possibility is supported by the observation that response latencies of rostral pontine neurons to flashes of light exhibited a considerably wide distribution. Baker *et al.* observed that the majority of visual cells in these structures of the cat responded to flashes with latencies from 15 to 70 mseconds.¹⁶ In 14 out of 95 cells, the latency was greater than 100 mseconds. Supposing that the flocculus of the monkey receives mossy fibers also from these nuclei, the present units, which responded primarily to retinal image motion of the velocity range of smooth-pursuit eye movements, may originate from the cells of the long-latency group.¹⁶

ACKNOWLEDGMENTS

The author is grateful to Dr. T. Warabi, Dr. R. Asoh, Mr. D. A. Suzuki, and Mr. M. Shibagaki for their assistance.

REFERENCES

1. MILES, F. A. & J. H. FULLER. 1975. Visual tracking and the primate flocculus. *Science* **189**: 1000-1002.
2. LISBERGER, S. D. & A. F. FUCHS. 1978. Role of primate flocculus during rapid behavioral modification of vestibulo-ocular reflex. I. Purkinje cell activity during visually guided horizontal smooth pursuit eye movements and passive head rotation. *J. Neurophysiol.* **41**: 733-763.
3. NODA, H. & D. A. SUZUKI. 1979. The role of the flocculus of the monkey in fixation and smooth pursuit eye movements. *J. Physiol. London* **294**: 335-348.
4. MILES, F. A., J. H. FULLER, D. J. BRAITMAN & B. M. DOW. 1980. Long-term adaptive changes in primate vestibuloocular reflex. III. Electrophysiological observations in flocculus of adapted monkeys. *J. Neurophysiol.* **43**: 1437-1476.
5. NODA, H. & R. ASOH. 1976. Discharges of monkey flocculus units in eye movements. *Neurosci. Abstr.* **2**: 115.
6. NODA, H. & D. A. SUZUKI. 1979. The role of the flocculus of the monkey in saccadic eye movements. *J. Physiol. London* **194**: 317-334.
7. NODA, H. & D. A. SUZUKI. 1979. Processing of eye movement signals in the flocculus of the monkey. *J. Physiol. London* **194**: 349-364.
8. BROOKS, B. A. & R. JUNG. 1973. Neuronal physiology of the visual cortex (areas 17, 18 and 19). In *Handbook of Sensory Physiology*. R. Jung, Ed. 7/3: 324-440. Springer-Verlag, Berlin, Federal Republic of Germany.
9. MAEKAWA, K. & J. I. SIMPSON. 1973. Climbing fiber responses evoked in vestibulo-cerebellum of rabbit from visual system. *J. Neurophysiol.* **36**: 649-666.
10. MAEKAWA, K. & T. TAKEDA. 1975. Mossy fiber responses evoked in the cerebellar flocculus of rabbits by stimulation of the optic pathways. *Brain Res.* **98**: 590-595.
11. PRECHT, W. 1977. Influence of supranuclear structures on brain stem neurons. A. Vestibulo-cerebellar regulation of eye and head movements. *Dev. Neurosci.* **1**: 417-424.
12. TAKEMORI, S. & B. COHEN. 1974. Visual suppression of vestibular nystagmus in rhesus monkey. *Brain Res.* **72**: 203-212.
13. TAKEMORI, S. & B. COHEN. 1974. Loss of visual suppression of vestibular nystagmus after flocculus lesion. *Brain Res.* **72**: 213-224.
14. MAEKAWA, K. & T. NATSUI. 1973. Climbing fiber activation of Purkinje cells in rabbit's flocculus during light stimulation of the retina. *Brain Res.* **59**: 417-420.
15. GLICKSTEIN, M., J. STEIN & R. A. KING. 1972. Visual input to the pontine nuclei. *Science* **178**: 1110-1111.
16. BAKER, J., A. GIBSON, M. GLICKSTEIN & J. STEIN. 1976. Visual cells in the pontine nuclei of the cat. *J. Physiol. London* **255**: 415-433.

MOSSY FIBER ACTIVATION OF THE CEREBELLAR FLOCCULUS FROM THE VISUAL SYSTEM*

Kyoji Maekawa, Minoru Kimura, and Toshiaki Takeda

Department of Physiology
Fichi Medical School
Tochigi-ken, Japan 329-04

INTRODUCTION

Previous studies on rabbits have demonstrated that the cerebellar flocculus receives visual signals bilaterally through climbing fiber as well as mossy fiber afferent pathways.¹⁻⁵ The climbing fiber pathways are mediated by the dorsal cap of the contralateral inferior olive.⁶⁻¹⁰ They have been traced with both electrophysiological and morphological techniques. Optic signals from the eye ipsilateral to the flocculus cross at the optic chiasm and, after being relayed by the dorsal terminal nucleus of the accessory optic tract as well as the nucleus of the optic tract (NOT), descend through the brain stem to the dorsal cap.^{1,2,8,9,11,12} Optic signals from the contralateral eye enter the ipsilateral accessory optic tract, crossing through the posterior commissure to the contralateral side.³ After being relayed by a cell group located in the ventromedial tegmentum, they descend to the rostral part of the dorsal cap.^{8,9,13}

On the other hand, the visual mossy fiber pathways long have been obscure. In this report, we attempt to summarize studies in our laboratory to trace visual mossy fiber pathways in rabbits by means of electrophysiological and morphological (horseradish peroxidase) methods. Parts of this report have been published previously.^{14-17,40}

CHARACTERISTIC FEATURES OF MOSSY FIBER ACTIVATION OF PURKINJE CELLS

Characteristic features of mossy fiber activation of a Purkinje cell in the flocculus evoked by optic chiasm (CH) stimulation are illustrated in FIGURE 1. Electrical double shocks (1.3-millisecond interval) to the CH evoked a positive field potential (P_2 wave of mossy fiber potential)¹⁸ with a latency of 4.7 mseconds, which was followed by typical complex spike discharges of a Purkinje cell due to climbing fiber activation, with a latency of 10.2 mseconds (Figure 1A-1).

As the stimulus intensity to the CH (once per second) was decreased from A-1 to A-3, the latency of the P_2 wave of mossy fiber potentials became longer, from 5.0 mseconds in A-2 to 6.9 mseconds in A-3. On the other hand, the latency of complex spike discharges was fairly constant through A-1 to A-3. This indicates that the visual mossy fiber pathways to the flocculus may be more complicated polysynaptically than those of the climbing fiber pathways.

It is well known that one of the major differences between mossy fiber and climbing fiber activation of Purkinje cells is the ability to follow high-frequency repetitive stimulation.^{18,19} As seen in FIGURE 1B, the P_2 wave of mossy fiber activation was resistant to repetitive CH stimulation at 30 Hz, while climbing

*This work was supported by Grant 311401 to K.M., Grant 577080 to M.K., and Grant 377060 to T.T. from the Ministry of Education of Japan.

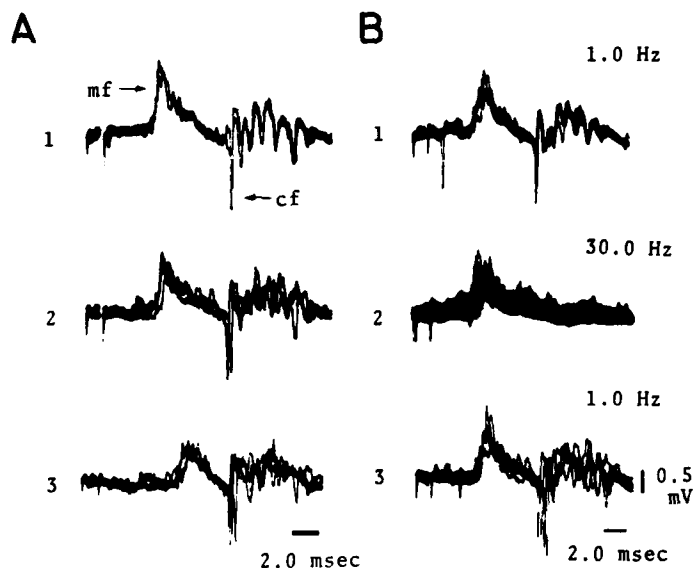


FIGURE 1. Mossy fiber (mf) and climbing fiber (cf) responses evoked in the cerebellar flocculus by optic chiasm stimulation. **A:** chiasm stimulation was given once per second. In A-1, P₂ wave of mossy fiber potential (mf) with a latency of 4.7 mseconds was followed by a complex spike discharge (cf) of a Purkinje cell due to climbing fiber activation with a latency of 10.2 mseconds. As stimulus intensities were decreased from A-1 to A-3, latencies of mossy fiber potentials became longer—5.0 mseconds in A-2 and 6.9 mseconds in A-3. On the other hand, latency of complex spikes was fairly constant regardless of stimulus intensities. **B:** effects of repetitive stimuli. With high-frequency repetitive stimuli (B-2, 30 Hz) to the chiasm, complex spikes disappeared while mossy fiber potentials were attenuated only slightly. In B-3, as stimulus frequency was decreased to 1 Hz, complex spikes reappeared with slight fluctuation in latencies. (Maekawa & Takeda, 1978, unpublished.)

fiber activation was eliminated completely during repetitive stimulation (B-2). This susceptibility of climbing fiber responses to repetitive stimulation is due to potent inhibitory synaptic action occurring at inferior olivary neurons.¹⁹

ORIGIN OF VISUAL MOSSY FIBER AFFERENTS TO THE FLOCCULUS

Horseradish Peroxidase Injection into the Flocculus

To find the origin of mossy fiber afferents to the flocculus, a small amount of horseradish peroxidase (HRP) was injected iontophoretically into the flocculus, and labeled neurons were examined in the brain stem.

Before HRP injection, the right flocculus was mapped by a glass microelectrode to find the portion in the flocculus with a prominent mossy fiber field potential evoked from both the contra- (L-OT) and ipsilateral (R-OT) optic tract (FIGURE 2A).⁵ Then the recording microelectrode was replaced by a glass pipette filled with 10% HRP solution, and the pipette was either advanced or withdrawn

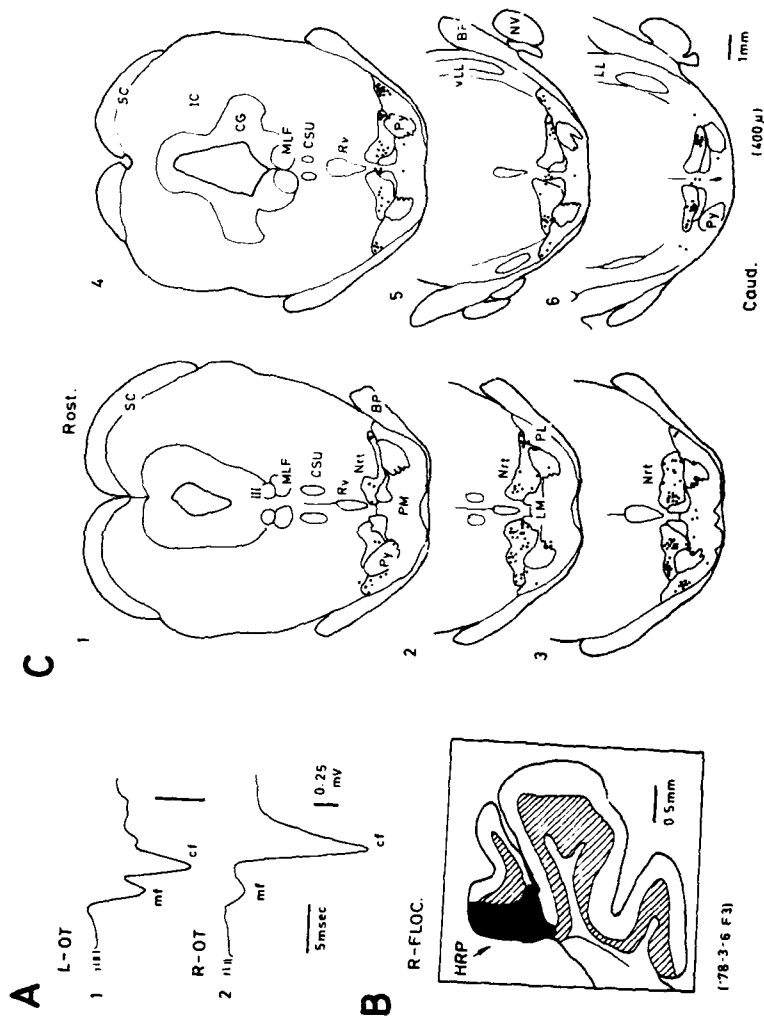


FIGURE 2. HRP injection into the right flocculus. **A:** HRP injection site was selected in the flocculus so that mossy fiber responses were produced by the left (A-1) and right (A-2) optic tract stimuli. mf and cf, mossy (N_1 wave) and climbing fiber response in the molecular layer. **B:** a frontal section of the right flocculus shows HRP injection area (shaded). **C:** chart drawings of six transverse sections (0.4 mm apart from each other) on which labeled cells were superimposed and plotted (dots). Rost., rostral; Caud., caudal. Abbreviations in this and in the following figures: BC, brachium conjunctivum; BP, brachium pontis; CSU, central superior nucleus; FL, flocculus; HP, habenulopeduncular tract; LC, locus ceruleus; LL and LM, lateral and medial lemniscus; MG, medial geniculate nucleus; NOT, nucleus of the optic tract; Nrt, nucleus reticularis tegmenti pontis; NVm and NVs, motor and sensory nerve of the Vth nucleus; PA and PP, anterior and posterior pretectal nucleus; PL and PM, lateral and medial pontine nucleus; PN, pontine nucleus; Py, pyramidal tract; RN, red nucleus; Rv, ventral raphe nucleus; SC, superior colliculus; SN, substantia nigra; VM and Vs, motor and sensory nuclei of the Vth nerve; III and IV, third and fourth nuclei. (Maekawa & Takeda, 1978, unpublished.)

until its tip was located in the granular layer indicated by an N_2 - P_2 wave of mossy fiber potentials,¹⁸ where HRP was injected iontophoretically by positive d.c. current.

The injection area was confined to the rostromedial part of the dorsal folium of the flocculus (FIGURE 2B).⁵ Labeled cells found in eight of the 50- μ m sections (400 μ m) were superimposed and plotted on six line drawings of frontal sections (FIGURE 2C). In the pontine region, labeled neurons were found bilaterally in the nucleus reticularis tegmenti pontis (NRTP), and some were found in the lateral pontine nucleus (FIGURE 2C-3 and 4).^{10,14,20,21}

Mossy Fiber Potentials Evoked by NRTP Stimulation

To examine electrophysiologically that the NRTP transfers optic signals to the flocculus, interaction between mossy fiber potentials evoked from the left optic tract (L-OT) (FIGURE 3A-1 and B-1) and those evoked by NRTP stimulation (FIGURE 3A-2 and B-2) was examined in the right flocculus by varying intervals. Latencies of mossy fiber potentials from the L-OT and from the NRTP were 5.5 mseconds and 3.0 mseconds, respectively. FIGURE 3C shows an interaction curve when NRTP test stimuli were preceded by L-OT conditioning stimuli by 0-60 mseconds. Peak amplitudes of the mossy fiber test potentials (T) relative to those

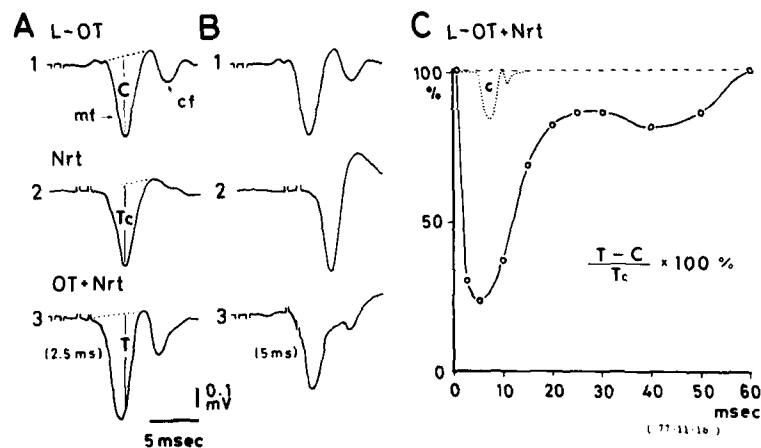


FIGURE 3. Interaction between mossy fiber potentials in the right flocculus evoked from the left optic tract (L-OT) and from the NRTP. A-1 and B-1: conditioning stimuli to the L-OT evoked a mossy fiber potential (N_2 wave, mf) with a latency of 5.5 mseconds, which was followed by a climbing fiber potential (cf) with a latency of 10 mseconds. A-2 and B-2: test stimuli to the right NRTP evoked a mossy fiber potential with a latency of about 3.0 mseconds. A-3 and B-3: both conditioning (L-OT) and test (Nrt) stimuli were delivered with a time interval of 2.5 mseconds (A) and 5 mseconds (B). C: amplitudes of test mossy fiber potentials ($T - C$) relative to control value (T_c) (ordinate, percentages) are plotted as a function of conditioning-test intervals (abscissa, in mseconds). The time course of a conditioning response is shown schematically as a dotted line (c). All potentials in A and B were constructed by summing 30 successive responses evoked at 1 Hz. Upward = positive. C, conditioning response; T_c , test control response; T, test response with a preceding conditioning shock. (Maekawa & Takeda, 1977, unpublished.)

of control potentials (Tc) (ordinate) were plotted as a function of conditioning-test stimulus interval (abscissa, in mseconds). It is shown clearly that mossy fiber responses evoked from the L-OT and from the NRTP occluded each other during a period of mossy fiber conditioning potential (dotted line, C) that was followed by a long-lasting inhibition for about 50 mseconds.

When a stimulating electrode was inserted stereotaxically into the pontine region, the area of the lowest threshold current required to elicit mossy fiber potentials in the flocculus always was in the NRTP and the threshold current increased abruptly as the tip of a stimulating electrode entered the pontine nucleus; thus the pontine nucleus was excluded from the origin of mossy fiber activation of the flocculus. These findings suggested electrophysiologically that optic signals that produce mossy fiber responses in the flocculus pass through the NRTP.

Neuronal Activity of NRTP Neurons

To study how NRTP neurons do transfer optic signals to the flocculus, neuronal activities were recorded extra- and intracellularly in the NRTP.¹⁵

Albino rabbits ($n = 25$) were anesthetized with α -chloralose-urethane, immobilized by gallamine triethiodide, and artificially respired with N_2O-O_2 mixture plus halothane. The middle portion of the cerebellum was aspirated to expose the fourth ventricle floor, through which a recording glass microelectrode (2 M NaCl) was inserted perpendicularly into the NRTP. Optic tracts and flocculi on both sides were stimulated electrically. Before insertion of stimulating electrodes, the flocculus was mapped with a recording microelectrode to find areas with prominent mossy fiber responses produced from both optic tracts. The recording microelectrode was replaced with a bipolar stimulating electrode and positioned at sites where N_2 waves of visual mossy fiber responses reversed polarity to positive to stimulate mossy fiber afferent terminals effectively.

Orthodromic and Antidromic Activation

FIGURE 4 shows examples of intracellular recordings of neurons in the left NRTP. Both the ipsilateral (FIGURE 4A, OT-L) and the contralateral (4B, OT-R) optic tract stimuli evoked excitatory postsynaptic potentials (EPSPs) associated with action potentials. Latencies of EPSPs were 3.2 mseconds (A-1) and 3.7 mseconds (B-1). When the neuron was hyperpolarized slightly by current injection through a recording microelectrode, action potentials were blocked, revealing underlying EPSPs (FIGURE 4A-2 and B-2).

Ipsilateral flocculus stimulation evoked an action potential with a constant latency (1.0 mseconds) (A-1 and B-1, FL-L). The FL-response could follow high-frequency repetitive stimulation (100 Hz) (FIGURE 4C). A fairly constant response latency and the ability to follow high-frequency repetitive stimulation indicated that this response was due to antidromic invasion of an impulse from the flocculus. As a floccular stimulation was delivered immediately (14 mseconds) after orthodromic activation from the optic tract (A-1 and B-1, FL-L), most antidromic impulses from the flocculus failed to invade the soma, leaving a small depolarization (3 mV) of a constant latency, which is presumably the M potential of the antidromic activation.²² The failure of antidromic invasion in A-1

and B-1 may be due to a slight hyperpolarization. Presumably there are inhibitory postsynaptic potentials (IPSPs) following orthodromic activation from the optic tract. The location of the neuron of FIGURE 4A-C is indicated in D (a dot with an arrow).

Figure 4E-G was recorded in another NRTP neuron, which was activated

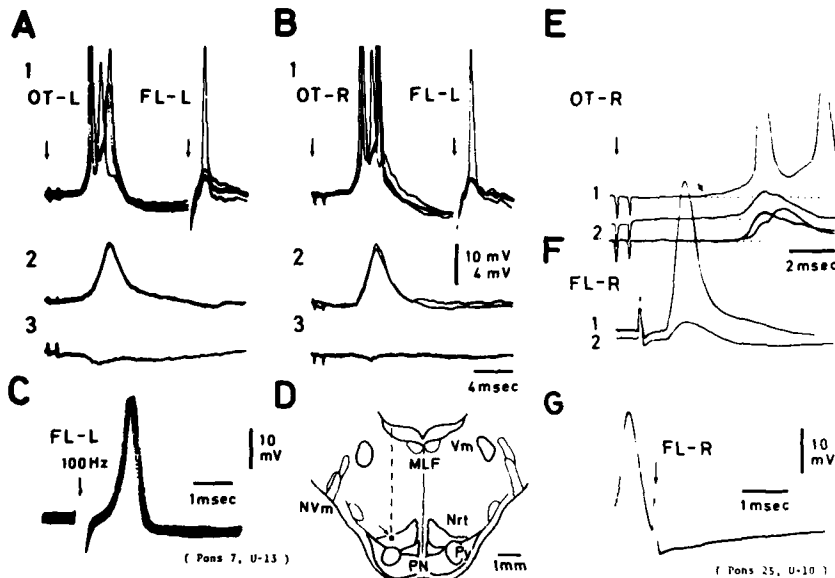


FIGURE 4. Intracellular recording of NRTP neurons. A-C were recorded from one NRTP neuron, and E-G from another NRTP neuron. A-1 and B-1: ipsilateral (OT-L) and contralateral (OT-R) optic tract stimulation evoked EPSPs associated with spikes. Latencies of EPSPs were 3.2 and 3.7 mseconds, respectively, and were followed by slight hyperpolarization. Ipsilateral floccular stimulation (FL-L) evoked an antidromic spike with 1.0-msecond latency. M components were revealed when antidromic impulses failed to invade the soma. A-2 and B-2: membrane hyperpolarization induced by current injection through the recording microelectrode blocked spike generation and revealed underlying EPSPs. A-3 and B-3: field potentials evoked from optic tracts just outside of the cell. Voltage calibration bar of 10 mV applies to A-1 and B-1 and 4 mV to A-2, A-3, B-2, and B-3. C: antidromic activation following high-frequency stimulation (100 Hz) of the ipsilateral flocculus. D: a line drawing of a frontal section showing an electrode track (dashed line) and the recording site in the NRTP (a dot with an oblique arrow). E-G: taken from another NRTP neuron. E-1: contralateral optic tract (OT-R) stimulation evoked a slow-rising EPSP (3.7-msecond latency) with associated spikes. Horizontal dotted lines indicate membrane potential level, and an oblique arrow points to the beginning of the EPSP. E-2: slight hyperpolarization by current injection revealed underlying EPSPs. F-1: antidromic activation from the contralateral flocculus (FL-R). When the antidromic spike failed to invade the soma due to membrane hyperpolarization, the M component was revealed (F-2). G: collision between a spontaneously firing spike and antidromic activation. An oscilloscope sweep was triggered by a spontaneous spike. Note that even the M component could not be seen after FL-R stimulation. The location of this neuron is shown in FIGURE 6-4 (a downward arrow). [From Reference 15 with permission of Elsevier/North-Holland Biomedical Press.]

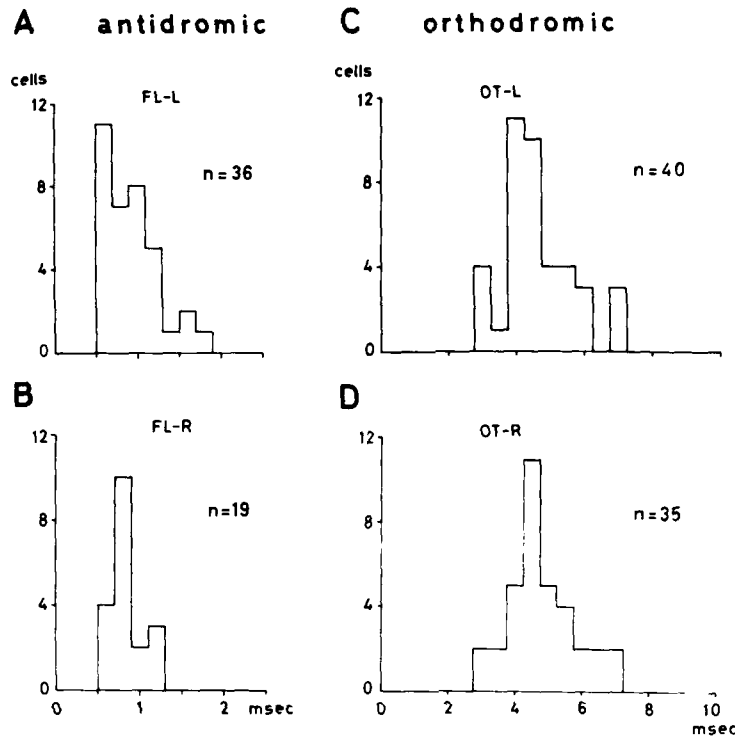


FIGURE 5. Latency distributions of NRTP neurons ($n = 55$). **A** and **B**: antidromic latency distribution for NRTP neurons from the ipsilateral (**A**, FL-L) and contralateral (**B**, FL-R) flocculus. **C** and **D**: orthodromic latency distribution for either the EPSP or the first spike activated from the ipsilateral (**C**, OT-L) and contralateral (**D**, OT-R) optic tract. Abscissa, latency in msec; ordinate, number of neurons. Sample sizes (n) are indicated in each part. Mean plus SD (msec) is 0.98 ± 0.33 (**A**), 0.88 ± 0.29 (**B**), 4.63 ± 1.06 (**C**), and 4.80 ± 0.98 (**D**). NRTP neurons were invaded antidromically either from the ipsi- (**A**, FL-L) or contralateral (**B**, FL-R) flocculus but never from both flocculi. Thirty-six percent of samples (20 out of 55) were activated orthodromically from both ipsi- and contralateral optic tracts. (From Reference 15 with permission of Elsevier/North-Holland Biomedical Press.)

orthodromically from the contralateral optic tract (**E**, OT-R) but not from the ipsilateral optic tract (not shown). The orthodromically evoked EPSPs had a 3.7-msec latency (an oblique arrow) but rose very slowly, leading to associated spikes after a long latency (**E-1**). A slight hyperpolarization blocked action potentials and revealed slowly rising, multicomponent EPSPs (**E-2**). The contralateral flocculus stimulation (**F**, FL-R) antidromically activated the neuron, with a latency of 0.65 msec (**F-1**). A slight hyperpolarization blocked antidromic invasion, leaving a small (4-mV) depolarizing wave, presumably the M component of the antidromic activation.

The antidromic nature of the activation from the contralateral flocculus stimulation was confirmed by a collision block of the floccular activation by a spontaneously firing spike (**FIGURE 4G**). The time interval between a spontaneous

spike and the onset of the stimulus (FL-R, a vertical arrow) was 1.0 msecond. The refractory time was not measured in this neuron. However, the short latency (0.65 msecond) from the flocculus (F-1) strongly suggested the collision of a spontaneous spike with an impulse generated antidromically from the flocculus. The failure of appearance of an M component in FIGURE 4G also may indicate that the collision occurred at a site far from the soma, probably at or near the stimulating site in the flocculus. The location of the neuron of E-G is indicated by a downward arrow in FIGURE 6-4.

Latency Distribution

In total, 55 neurons were sampled intra- and extracellularly in the left NRTP. FIGURE 5 shows latency distributions of activations antidromically from the flocculus (A and B) and orthodromically from the optic tract (C and D). Thirty-six out of 55 neurons were activated antidromically from the ipsilateral flocculus (FIGURE 5A, FL-L), and the other 19 neurons from the contralateral flocculus (B, FL-R). None were invaded antidromically from both flocculi. Antidromic spike latencies (mean and standard deviation) are 0.98 ± 0.33 msecond ($n = 36$) from the ipsilateral flocculus (FIGURE 5A) and 0.88 ± 0.29 msecond ($n = 19$) from the contralateral flocculus (5B). They are not significantly different.

Twenty neurons out of 55 were activated orthodromically from the ipsilateral and 15 neurons from the contralateral optic tract. The other 20 neurons were activated from both the ipsi- and contralateral optic tract.

Orthodromic latencies were measured either for the first spike of extracellular repetitive firings or in a few cells for the evoked EPSP. Latencies (mean and SD) are 4.63 ± 1.06 mseconds ($n = 40$) from the ipsilateral optic tract (FIGURE 5C,

Recording Sites ($n=47$)

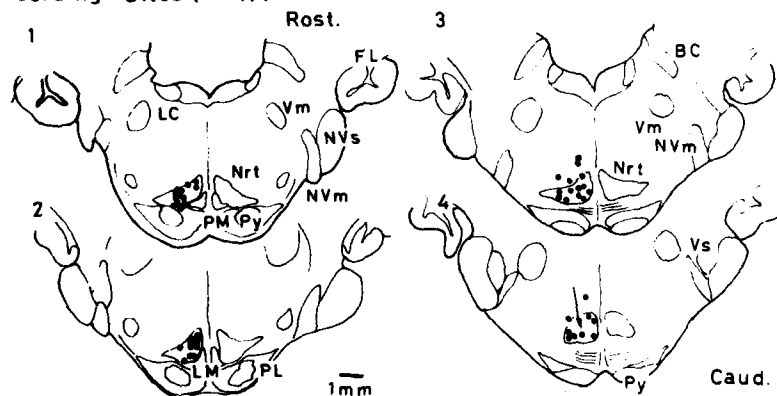


FIGURE 6. Histological distribution of NRTP neurons sampled. 1-4: chart drawings of frontal sections of the pons. Distance between 1 and 2 is 0.4 mm, and between 2 and 3 and between 3 and 4 is 0.3 mm. Each dot represents one cell. Forty-seven neurons out of 55 were superimposed and plotted on four frontal sections. Since another four neurons were identified in the NRTP at a level 0.5 mm caudal to 4, they are not included. The remaining four neurons were not identified histologically. An arrow in 4 points at a neuron of FIGURE 4 E-G. Rost., rostral; Caud., caudal. (Modified from Reference 15.)

OT-L) and 4.80 ± 0.98 mseconds ($n = 35$) from the contralateral optic tract (5D, OT-R). They are not significantly different.

Histological Examination of Recording Sites

Recording sites of neurons were identified by reference to extracellularly ejected dye spots (fast green FCF) and/or to depth readings of a micromanipulator along electrode tracks from the fourth ventricle floor on histological sections.

Out of 55 neurons, locations of 51 were identified histologically. In FIGURE 6, histologically identified locations of 47 neurons are superimposed and plotted on four frontal sections. Another 4 neurons, located at a level 0.5 mm caudal to FIGURE 6-4, were not included. Recording sites were confined to the NRTP, except for a few cells that were located dorsally (FIGURE 6-3 and 4).

PRETECTAL RELAY NEURONS

To trace further rostrally the relay neurons that convey optic signals to the NRTP and that are involved in the mossy fiber pathways to the flocculus, the following experiments were performed: (1) HRP injection into the NRTP;¹⁶ (2) stimulation threshold mapping in the pretectal region to produce mossy fiber responses in the flocculus; and (3) recording of neuronal activities in the pretectal region.⁴⁰

HRP Injection into the NRTP

A small amount of HRP was injected iontophoretically into the NRTP. In these experiments, the midline cerebellum was aspirated and the fourth ventricle floor was exposed, through which the glass pipette containing 10% HRP solution was inserted into the NRTP. Results of an experiment are shown in FIGURE 7. In B, HRP injection sites are indicated in two frontal sections that are 500 μ m apart. Dotted areas indicate the most densely stained areas, which were well confined in the left NRTP. In FIGURE 7A, three frontal sections of the border of the mesodiencephalon, 300 μ m apart from each other from the rostral (A-1) to the caudal (A-3) level. Labeled cells found in six of the 50- μ m serial sections were superimposed and plotted as dots. Labeled cells were found almost exclusively ipsilaterally in the nucleus of the optic tract (NOT), in the anterior pretectal nucleus (PA), and in the mesencephalic reticular formation.

Stimulation Threshold Mapping in the Pretectal Region

Stimulating currents required to evoke mossy fiber potentials in the ipsilateral flocculus were mapped in the lateral pretectal region. In these experiments, the posterior part of the cerebral cortex was aspirated and the caudolateral part of the diencephalon and rostromedial part of the superior colliculus were exposed. An array of three fine-platinum-wire stimulating electrodes were inserted lateromedially into the lateral pretectal area. The area of the lowest threshold current always was found in and around the NOT.¹⁶

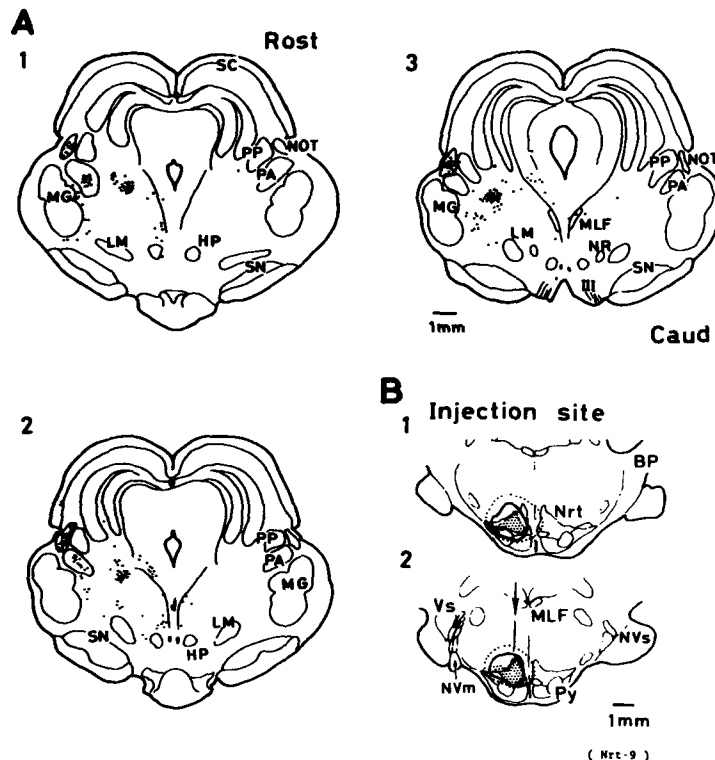


FIGURE 7. HRP-labeled cells in the mesodiencephalon after HRP injection into the NRT. A: line drawings of frontal sections of the mesodiencephalon, 300 μ m apart from each other from rostral (A-1) to caudal (A-3). A dot represents an HRP-labeled cell body. In each drawing, labeled cells are plotted by superimposing six successive 50- μ m sections. B: line drawings of frontal sections showing the injection site, 500 μ m apart from each other from rostral (B-1) to caudal (B-2). The dotted areas indicate the most densely stained region. Thick lines encircle the less densely stained area, and the whole extent of faint brownish colored areas is indicated by dotted lines. A vertical arrow in B-2 indicates an HRP electrode track. Abbreviations, see FIGURE 2. (Maekawa & Kimura, 1980, see Reference 16.)

Neuronal Activity of the Pretectal Region

Using a glass microelectrode, neuronal activities were recorded extracellularly in the lateral pretectal region after exposing the surface by aspiration of the overlying cortex. The optic chiasm (CH) was stimulated by a stereotactically inserted bipolar electrode. One bipolar platinum-wire stimulating electrode was inserted caudorostrally into the ipsilateral NRT, and the other electrode into the ipsilateral inferior olive.

Neuronal spikes orthodromically activated from the CH and antidromically invaded from the NRT and/or the inferior olive were recorded.^{8,11,23} FIGURE 8 shows examples of neuronal responses recorded in the NOT. The neuron was activated orthodromically from the CH with a latency of 1.75 mseconds (FIGURE 8A) and invaded antidromically from the NRT with a latency of 0.75 msecond

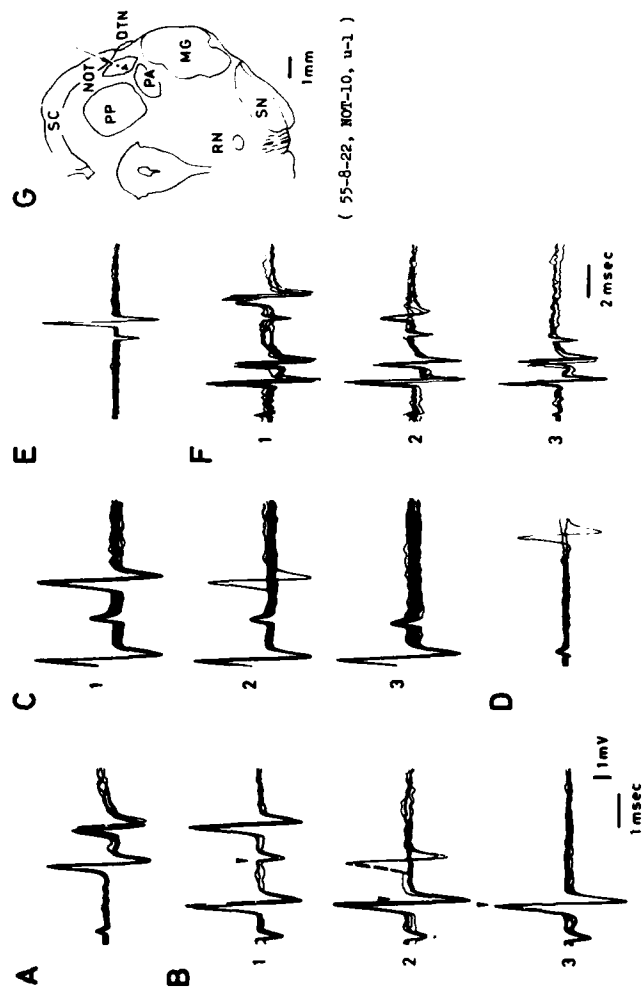


FIGURE 8. Extracellular recordings of an NOT neuron. A: orthodromic spike responses from the optic chiasm with a latency of 1.75 msec. B: antidromic responses from the NRTTP with a latency of 0.75 msec. Double shocks were delivered at varying intervals. A downward arrowhead indicates the onset of the second shock. Intervals are 2.3 msec (B-1), 1.2 msec (B-2), and 1.1 msec (B-3), thus showing a refractory period of 1.2 msec (B-2). C: oscilloscope traces were triggered by a spontaneously firing spike, and NRTTP stimuli were delivered at varying intervals—1.5 msec (C-1), 1.4 msec (C-2), and 1.3 msec (C-3). Collisions began to occur at C-2. D: stimulation to the ipsilateral inferior olive did not produce any response. A spontaneously firing spike is seen on the right. E-F: collision test. E: the control spikes from the NRTTP. F: time intervals between the second spike orthodromically evoked from the optic chiasm and the NRTTP stimulus were decreased from 2.8 msec (F-1), to 1.8 msec (F-2) to 1.4–1.5 msec (F-3). Collision occurred every time in F-3. Voltage scale of 1 mV in B-3 applies to all records. Time scale of 1 msec in B-3 applies to A-D, and time scale of 2 msec in F-3 applies to E-F. G: a line drawing of a transverse section at the mesencephalon, showing the histologically identified locations of neurons. A downward arrow depicts the direction of a microelectrode insertion and points at the recording site (a dot). In this transverse section, four neurons (dots) were recorded in the NOT, which were identified physiologically as relay neurons. (Maekawa & Kimura, 1980, unpublished, see Reference 16.)

(B). The refractory time for NRTP responses was 1.2 mseconds when double shocks were given to the NRTP (B-2). Stimulation to the inferior olive did not activate the neuron (D). The antidromic nature of NRTP responses was evidenced by a collision test (FIGURE 8C and F). In C, oscilloscope sweeps were triggered by spontaneous spikes and NRTP stimuli were delivered at varying intervals: 1.5 mseconds (C-1), 1.4 mseconds (C-2), and 1.3 mseconds (C-3). Most trials of NRTP stimuli in C-2 failed to activate the neuron, showing a collision of a spontaneous spike with an antidromically initiated impulse from the NRTP. Collisions of an orthodromically evoked spike with an impulse from the NRTP are shown in F. Control responses evoked from the NRTP are shown in E. NRTP stimuli given at 2.8 mseconds after the second spike evoked from the CH elicited a spike every time (F-1); however, latencies of NRTP responses were slightly but significantly longer (0.9 msecond) than those of control responses (0.7 msecond in E).²⁴ A strong deflection on the rising phase of a spike indicated a delay for invasion of impulse from the initial segment (IS) to the soma-dendritic (SD) segment of the cell.²² As the time interval was decreased to 1.8 mseconds (F-2), NRTP stimuli either failed to activate the cell or produced only an early component of the spike, presumably the IS component.²² Further decrease of the time intervals between a preceding spike and the NRTP stimulus to 1.4–1.5 mseconds led to a failure of the NRTP stimuli to elicit spikes (F-3), even at intervals longer than the refractory period of this cell. These findings are clear evidence that NRTP responses were antidromic.

An oblique arrow in FIGURE 8G, showing the direction of a microelectrode insertion, points at the location (a dot) of this neuron. In this preparation, four neurons (dots) were sampled in a transverse plane, all of which were identified histologically in the NOT.

Thus, 43 neurons in total were sampled in the caudolateral part of the pretectal area that were activated orthodromically from the CH and invaded antidromically from the NRTP. Out of 43 neurons, 31 (72%) were identified histologically in the laterocaudal portion of the NOT, 4 (9%) were identified in the dorsal portion of the anterior pretectal nucleus (PA), and 7 (16%) were presumably in the ventral part of the NOT—however, since we were not quite sure whether they were in the NOT or just outside of it, these neurons were classified tentatively as border cells. The remaining neuron was not identified.

TABLE 1 shows mean latencies with standard deviations (mseconds) for 43 neurons in and around the NOT, orthodromic latency from the CH, and

TABLE 1
LATENCY OF SPIKE RESPONSES

Cells	Stimulating Sites			
	CH (msec)	NRTP (msec)	CH + NRTP* (msec)	OT (msec)
PT†	1.86 ± 0.35	0.97 ± 0.22	2.83 ± 0.39	—
NRTP‡	—	—	—	4.63 ± 1.06

*CH + NRTP: sum of the orthodromic (CH) and antidromic (NRTP) latencies.

†Latency of orthodromic spike responses from the optic chiasm (CH) and antidromic spike responses from the NRTP in 43 pretectal (PT) neurons.

‡Orthodromic latencies from the ipsilateral optic tract (OT) in 40 NRTP neurons. (Data taken from Figure 5C.)¹⁸ Figures are mean ± standard deviation.

antidromic latency from the NRTP. For comparison with the orthodromic latency for 40 NRTP neurons from the ipsilateral optic tract (4.63 ± 1.06 mseconds, FIGURE 5C),¹⁵ the mean and standard deviation of the sum of CH and NRTP latencies for each pretectal neuron also are listed under CH + NRTP. The mean latency difference between these two values—1.8 mseconds—may indicate that a few neurons would be intercalated in the NRTP region before optic signals activate NRTP neurons that send mossy fiber afferents to the flocculus.

Three out of 43 neurons were activated antidromically from both the NRTP and the inferior olive. The mean latency of antidromic activation from the inferior olive ($n = 3$) was 1.3 mseconds.

COMMENTS

These series of experiments clearly demonstrated that optic signals, after being transferred by NOT neurons, descend in the brain stem to activate the ipsi- and/or contralateral NRTP neurons. The signals eventually reach the flocculus and cause the mossy fiber activation of floccular Purkinje cells, which are known to project to the vestibular nuclei and to modify eye movements.

Pretectal projections to the ipsilateral NRTP have been demonstrated anatomically in cats, rabbits, and rats, but the exact origin of these neurons in the pretectal region has not been identified.^{12,25-27} Recent autoradiographic studies in tree shrews and rabbits showed NOT projections to the dorsal pontine nucleus but not to the NRTP.^{28,29}

A close relation between optokinetic nystagmus and the NOT has been demonstrated in rabbits by Collewyn.^{30,31} Neurons in the NOT responded to movements of a large, textured pattern to the contralateral eye from temporal to nasal, which is the most effective stimulus in eliciting optokinetic nystagmus.³⁰ Further, small lesions in the lateral pretectum abolished optokinetic nystagmus, and electrical stimulation of the NOT region elicited horizontal nystagmus.³¹ Similar properties of responses of neurons in the NOT were reported in cats.³² The involvement of the NOT in the pathways evoking optokinetic neuronal responses in the vestibular neurons also has been suggested.^{33,34}

Recently, Miyashita *et al.* demonstrated in rabbits that the gain of the optokinetic responses was reduced significantly in the eye contralateral to a lesion made in the NRTP, while the horizontal vestibulo-ocular reflex did not show any change due to NRTP lesions.³⁵ When the lesioned rabbits were rotated continuously with a slit light presented to the eye contralateral to the NRTP lesions, the gain of the vestibulo-ocular reflex increased adaptively as in control rabbits.³⁶⁻³⁹

Thus the visual mossy fiber pathway presented in this study through the NOT-NRTP to the flocculus contributes to optokinetic eye movements but not to visually guided adaptive change of the vestibulo-ocular responses.

REFERENCES

1. MAEKAWA, K. & J. I. SIMPSON. 1972. Climbing fiber activation of Purkinje cells in the flocculus by impulses transferred through the visual pathway. *Brain Res.* **39**: 245-251.
2. MAEKAWA, K. & J. I. SIMPSON. 1973. Climbing fiber responses evoked in vestibulo-cerebellum of rabbit from visual system. *J. Neurophysiol.* **36**: 649-666.
3. MAEKAWA, K. & T. TAKEDA. 1976. Electrophysiological identification of the climbing

- and mossy fiber pathways from the rabbit's retina to the contralateral cerebellar flocculus. *Brain Res.* **109**: 169-174.
4. SIMPSON, J. I., W. PRECHT & R. LLINÁS. 1974. Sensory separation in climbing and mossy fiber inputs to cat vestibulocerebellum. *Pfluegers Arch.* **351**: 183-193.
 5. MAEKAWA, K. & T. TAKEDA. 1975. Mossy fiber responses evoked in the cerebellar flocculus of rabbits by stimulation of the optic pathway. *Brain Res.* **98**: 590-595.
 6. ALLEY, K., R. BAKER & J. I. SIMPSON. 1975. Afferents to the vestibulo-cerebellum and the origin of the visual climbing fibers in the rabbit. *Brain Res.* **98**: 582-589.
 7. HODDEVIK, G. H. & A. BRODAL. 1977. The olivocerebellar projection studied with the method of retrograde axonal transport of horseradish peroxidase. V. The projections to the flocculonodular lobe and the paraflocculus in the rabbit. *J. Comp. Neurol.* **176**: 269-280.
 8. MAEKAWA, K. & T. TAKEDA. 1977. Afferent pathways from the visual system to the cerebellar flocculus of the rabbit. *Dev. Neurosci.* **1**: 187-195.
 9. TAKEDA, T. & K. MAEKAWA. 1980. Bilateral visual inputs to the dorsal cap of inferior olive: differential localization and inhibitory interactions. *Exp. Brain Res.* **39**: 461-471.
 10. YAMAMOTO, M. 1979. Topographical representation in rabbit cerebellar flocculus for various afferent inputs from the brain stem investigated by means of retrograde axonal transport of horseradish peroxidase. *Neurosci. Lett.* **12**: 29-34.
 11. TAKEDA, T. & K. MAEKAWA. 1976. The origin of the pretectoolivary tract. A study using the horseradish peroxidase method. *Brain Res.* **117**: 319-325.
 12. MIZUNO, N., K. MOCHIZUKI, C. AKIMOTO & R. MATSUSHIMA. 1973. Pretectal projections to the inferior olive in the rabbit. *Exp. Neurol.* **39**: 498-506.
 13. MAEKAWA, K. & T. TAKEDA. 1979. Origin of descending afferents to the rostral part of dorsal cap of inferior olive which transfers contralateral optic activities to the flocculus. A horseradish peroxidase study. *Brain Res.* **172**: 393-405.
 14. MAEKAWA, K. & T. TAKEDA. 1978. Origin of the mossy fiber projection to the cerebellar flocculus from the optic nerves in rabbits. In *Integrative Control Functions of the Brain*. M. Ito, N. Tsukahara, K. Kubota & K. Yagi, Eds. **1**: 93-95. Kodansha Scientific. Tokyo, Japan. Elsevier. Amsterdam, the Netherlands.
 15. MAEKAWA, K., T. TAKEDA & M. KIMURA. 1981. Neural activity of nucleus reticularis tegmenti pontis—the origin of visual mossy fiber afferents to the cerebellar flocculus of rabbits. *Brain Res.* **210**: 17-30.
 16. MAEKAWA, K. & M. KIMURA. 1980. Midbrain neurons relaying optic signals which induce mossy fiber response in the cerebellar flocculus. *J. Physiol. Soc. Jpn* **42**: 260.
 17. MAEKAWA, K., T. TAKEDA & M. KIMURA. 1981. Visual mossy fiber pathway to the cerebellar flocculus of rabbits. *Prog. Oculomotor Res.* (In press.)
 18. ECCLES, J. C., M. ITO & J. SZENTAGOTHAÏ. 1967. *The Cerebellum as a Neuronal Machine*. Springer-Verlag. Berlin, Heidelberg & New York.
 19. ECCLES, J. C., L. PROVINI, P. STRATA & H. TABOŘÍKOVÁ. 1968. Analysis of electrical potentials evoked in the cerebellar anterior lobe by stimulation of hindlimb and forelimb nerves. *Exp. Brain Res.* **6**: 171-194.
 20. BRODAL, A. & P. BRODAL. 1971. The organization of the nucleus reticularis tegmenti pontis in the cat in the light of experimental anatomical studies of its cerebral cortical afferents. *Exp. Brain Res.* **13**: 90-110.
 21. HODDEVIK, G. H. 1978. The projection from nucleus reticularis tegmenti pontis onto the cerebellum in the cat. A study using the methods of anterograde degeneration and retrograde axonal transport of horseradish peroxidase. *Anat. Embryol.* **153**: 227-242.
 22. ECCLES, J. C. 1957. *The Physiology of Nerve Cells*: 47-50. Johns Hopkins Press. Baltimore, Md.
 23. HOFFMAN, K-P., K. BEHREND & A. SCHOPPMANN. 1976. A direct afferent visual pathway from the nucleus of the optic tract to the inferior olive in the cat. *Brain Res.* **115**: 150-153.
 24. FULLER, J. H. & J. D. SCHLAG. 1976. Determination of antidromic excitation by the collision test: problems of interpretation. *Brain Res.* **112**: 283-298.
 25. BERMAN, N. 1977. Connections of the pretectum in the cat. *J. Comp. Neurol.* **174**: 227-254.

26. GRAYBIEL, A. M. 1974. Some efferents of the pretectal region in the cat. *Anat. Rec.* **178**: 365.
27. TERASAWA, K., K. OTANI & J. YAMADA. 1979. Descending pathways of the nucleus of the optic tract in the rat. *Brain Res.* **173**: 405-417.
28. WEBER, J. T. & J. K. HARTING. 1980. The efferent projections of the pretectal complex: an autoradiographic and horseradish peroxidase analysis. *Brain Res.* **194**: 1-28.
29. HOLSTAGE, G. & H. COLLEWIJN. 1980. The efferent connections of the nucleus of the optic tract of the rabbit. *Neurosci. Lett.* [Suppl. 5]: S183.
30. COLLEWIJN, H. 1975. Direction-selective units in the rabbit's nucleus of the optic tract. *Brain Res.* **100**: 489-508.
31. COLLEWIJN, H. 1975. Oculomotor areas in the rabbit's midbrain and pretectum. *J. Neurobiol.* **6**: 3-22.
32. HOFFMANN, K-P. & A. SCHOPPMANN. 1975. Retinal input to direction selective cells in the nucleus tractus opticus of the cat. *Brain Res.* **99**: 359-366.
33. KELLER, E. L. & W. PRECHT. 1979. Visual-vestibular responses in vestibular nuclear neurons in intact and cerebellectomized, alert cat. *Neuroscience* **4**: 1599-1613.
34. PRECHT, W. & P. STRATA. 1980. On the pathway mediating optokinetic responses in vestibular nuclear neurons. *Neuroscience* **5**: 777-787.
35. MIYASHITA, Y., M. ITO, P. J. JASTREBOFF, K. MAEKAWA & S. NAGAO. 1980. Effect upon eye movements of rabbits induced by severance of mossy fiber visual pathway to the cerebellar flocculus. *Brain Res.* **198**: 210-215.
36. ITO, M., T. SHIIDA, N. YAGI & M. YAMAMOTO. 1974. Visual influence on rabbit horizontal vestibulo-ocular reflex presumably effected via the cerebellar flocculus. *Brain Res.* **65**: 170-174.
37. ITO, M. & Y. MIYASHITA. 1975. The effects of chronic destruction of the inferior olive upon visual modification of the horizontal vestibulo-ocular reflex of rabbits. *Proc. Jpn. Acad.* **51**: 716-720.
38. ITO, M. 1977. Neuronal events in the cerebellar flocculus associated with an adaptive modification of the vestibulo-ocular reflex of the rabbit. *Dev. Neurosci.* **1**: 391-398.
39. ROBINSON, D. A. 1976. Adaptive gain control of vestibuloocular reflex by the cerebellum. *J. Neurophysiol.* **39**: 954-969.
40. MAEKAWA, K. & M. KIMURA. 1981. Electrophysiological study of the nucleus of the optic tract that transfers optic signals to the nucleus reticularis tegmenti pontis—the visual mossy fiber pathway to the cerebellar flocculus. *Brain Res.* **220**. (In press.)

INPUT-OUTPUT ACTIVITY OF THE PRIMATE FLOCCULUS DURING VISUAL-VESTIBULAR INTERACTION*

W. Waespe, U. Büttner, and V. Henn

Neurological Clinic
University of Zurich
CH-8091 Zurich, Switzerland

INTRODUCTION

Cerebellar lesions in patients lead to deficits in pursuit eye movements, reduced optokinetic nystagmus, and the inability to suppress vestibular nystagmus by visual fixation.¹⁻³ Lesions of the flocculus in primates lead to the same clinical syndrome.^{4,5} We will show that floccular Purkinje cells modulate their activity to either enhance optokinetic nystagmus or suppress vestibular nystagmus during various paradigms of visual-vestibular interaction. Our hypothesis is that the flocculus and the vestibular nuclei process visual-vestibular information in a complementary way: floccular Purkinje cells are modulated when vestibular nuclei activity is insufficient to move the eyes with adequate velocity, or when vestibular nuclei neurons still are modulated but nystagmus is suppressed.^{6,7}

METHODS

Monkeys (*Macaca mulatta*) were prepared chronically for single-unit recordings (for details, see Reference 8). A ring for fixing the micropositioner above a trephine hole in the skull, Ag-AgCl electrodes to monitor eye position, and skull bolts to clamp the animal's head during experiments were implanted. Animals were placed on a servo-controlled turntable with their heads bent forward 25° and fixed in that position to bring the lateral semicircular canals into the horizontal plane. The turntable was enclosed totally by an optokinetic cylinder, which could be accelerated independently. For vestibular stimulation, monkeys were rotated about a vertical axis in complete darkness; for optokinetic stimulation, the cylinder was illuminated from within (photopic range) and rotated around the stationary monkey. During conflicting visual-vestibular stimulation, the cylinder was fixed mechanically to the turntable and both were rotated together. One monkey was trained to fixate a small spot of light using the paradigm of Wurtz.⁹ One fixation light was attached to the turntable and rotated with the monkey to suppress vestibular nystagmus (VOR suppression). When stationary, the monkey could suppress optokinetic nystagmus during rotation of the visual surround (OKN suppression). Another light was attached to the cylinder for tracking eye movements while the cylinder was moving in darkness (smooth pursuit).

Unit activity in the flocculus was recorded extracellularly mainly from the anterior part (folia 4 to 10). Neuronal activity was classified according to criteria

*Supported by a grant from the Swiss National Foundation for Scientific Research 3.343-2.78

suggested by other authors:¹⁰⁻¹² discharge pattern, spike configuration, recording sites with respect to layers, method of isolation. Neurons were classified into Purkinje cells (P-cells) and non-Purkinje cells (non-P-cells). P-cells were characterized by an irregular simple spike (SS) activity and the occurrence of complex spikes (CS). Non-P-cells were characterized by a more regular resting discharge. Some units exhibited typical patterns of fiber recordings (mossy fibers, MF), while others had recording characteristics more typical of cell bodies (granule cells).

All relevant data—neuronal activity, horizontal and vertical eye position, turntable and optokinetic stimulus velocity, a photocell signal, and a digital time code—were stored on an FM tape machine. For analysis, the instantaneous and averaged neuronal activity (running average over 250 or 500 mseconds) and other relevant data were written out on a rectilinear oscillograph from which further measurements were taken. Horizontal eye position was differentiated to obtain eye velocity. Nystagmus direction always refers to the direction of the fast phase. In all figures, an upward deflection of the stimulus profile or of eye velocity corresponds to movements to the ipsilateral side (recording side).

RESULTS

The flocculus, like other parts of the cerebellar cortex, receives information via two inputs—a mossy fiber (MF) and a climbing fiber (CF) input. The only output originates from the Purkinje cells (P-cells) and is characterized by simple (SS) and complex spike (CS) activity. We will confine our description to input activity (mossy fibers and granule cells) and output activity (P-cells).

Input Activity

Neuronal activity that reflects MF-input (mossy fibers and granule cells) can be separated into two groups. In one group, activity is related exclusively to parameters of fast eye movements and/or eye position. This input has been described extensively.^{12,13} In the other group, activity can be related to parameters of visual-vestibular stimulation. Most of these units show characteristics similar to neurons in the vestibular nuclei.^{8,14-17} A smaller percentage is modulated only when visual image slip is present.

Input reflecting vestibular nuclei activity comprises more than 90% of the recordings of the second group. During *vestibular stimulation* (rotation of the monkey about a vertical axis in darkness), units were modulated in either a type I (48%) or a type II (52%) fashion. The decay time constant of neuronal activity after the end of acceleration varied between 10 and 50 seconds and always was similar to the time constant of vestibular nystagmus (VN, see FIGURE 1B). All units also were modulated during *optokinetic stimulation* (rotation of the visual surround around the stationary monkey). Modulation always was bidirectional. Units were activated during vestibular and optokinetic stimulation when nystagmus had the same direction. Neurons were modulated at low optokinetic stimulus velocities and were saturated on average at 60°/second, whereas optokinetic nystagmus (OKN) could reach higher values (FIGURE 2). During sudden presentation of the optokinetic stimulus, neuronal activity built up slowly with a time constant of 4-6 seconds. Eye velocity, however, jumped to a velocity of around 30°/second and then rose more slowly. When lights were turned off

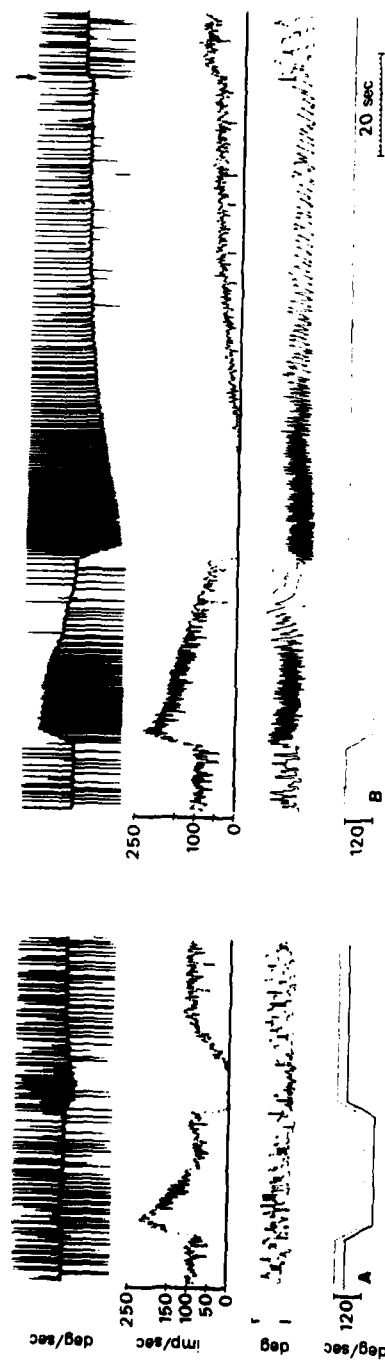


FIGURE 1. Type II input unit during conflicting (A) and vestibular (B) stimulation. From above: horizontal eye velocity (fast phases clipped at an arbitrary level); neuronal activity (running average, 250 mseconds); horizontal eye position; and stimulus profile (acceleration and deceleration, $40^{\circ}/\text{second}^2$). During conflicting stimulation, the nystagmus response is attenuated but peak neuronal activity is the same as during vestibular stimulation.

during high-velocity optokinetic stimulation, neuronal activity slowly declined. Eye velocity, however, immediately dropped to a velocity of around $50^\circ/\text{second}$ and only then slowly declined, similar to unit activity. *Conflicting visual-vestibular stimulation* (rotation of the turntable and visual surround mechanically fixed together) led to an attenuation of neuronal activity at low ($10^\circ/\text{second}^2$) but not at high accelerations ($40^\circ/\text{second}^2$), when compared to the values at the same accelerations in the dark. Nystagmus was attenuated or was suppressed completely. The decay time constant of both nystagmus and neuronal activity was shortened to less than 6-8 seconds (FIGURE 1A).

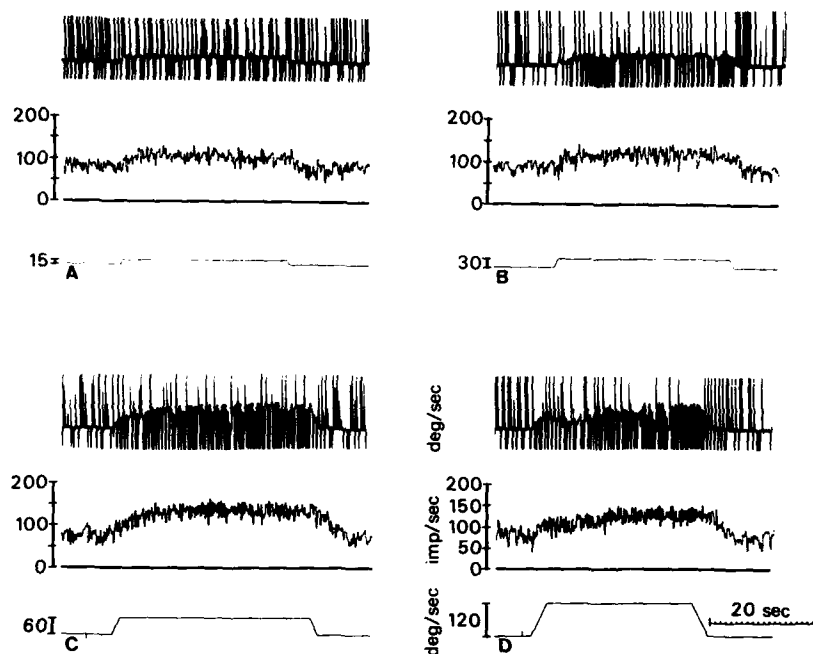


FIGURE 2. Same neuron as in FIGURE 1 during optokinetic stimulation at different velocities between 15 and $120^\circ/\text{second}$. Same display as in FIGURE 1, without the horizontal eye position signal. Neuronal activity increases with stimulus velocities to the side opposite to that which gives rise to activation during vestibular stimulation. In both cases, this leads to nystagmus (VN and OKN) in the same direction (contralateral to the side of unit recording).

Characteristics of floccular input most closely resembled type I vestibular-plus-eye movement neurons in the vestibular nuclei. Few neurons were recorded that could be modulated by vestibular but not by optokinetic stimulation. These neurons also had a short decay time constant of five-six seconds. Their modulation with rapid eye movements excluded a peripheral vestibular origin.

Input activity reflecting visual image slip constitutes only 5% of all recordings. The term image slip is used instead of retinal slip. The amount of image or

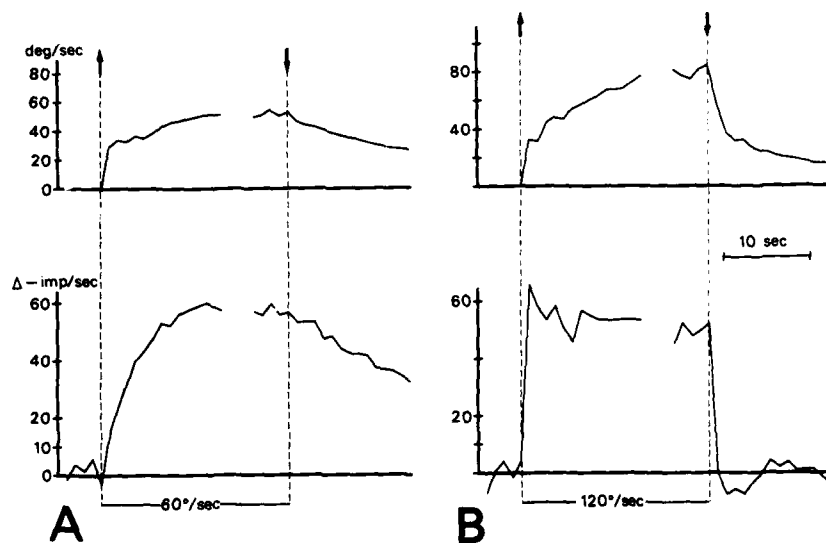


FIGURE 3. Comparison of input unit (A) and P-cell (B) activity during optokinetic nystagmus and after-nystagmus. On top, nystagmus slow-phase velocity; on bottom, average frequency increase of five input units in A (three type I, two type II) and of seven type I P-cells in B. Values were taken every second for a period of 4 seconds before until 14 seconds after the start of stimulation (lights on and off). Lights were switched on (upward arrow) during rotation of the optokinetic drum at a velocity of 60°/second (A) or 120°/second (B). After 20-30 seconds, the lights were switched off (downward arrow).

retinal slip is the same; the direction is inverted by the optics of the eyes. During all conditions of whole-field visual stimulation, the velocity and direction of image slip were coded by these units. With one exception, modulation was bidirectional. Units were not modulated during vestibular stimulation or during optokinetic after-nystagmus (OKAN). One unit was recorded in the trained monkey. Although whole-field image slip clearly modulated this unit, it was not

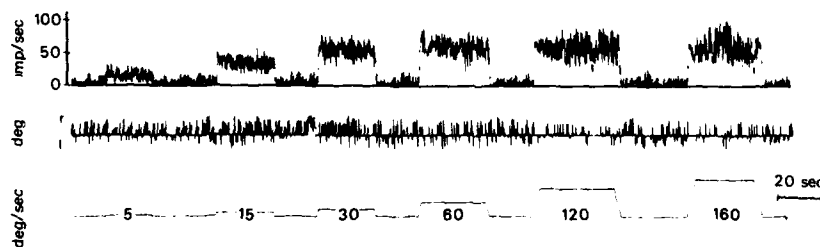


FIGURE 4. Visual input unit during optokinetic stimulation at different velocities between 15 and 160°/second. During stimulation, any nystagmus is suppressed by fixation of a stationary light. First trace, unit activity (running average, 250 mseconds); second trace, horizontal eye position; third trace, stimulus velocity.

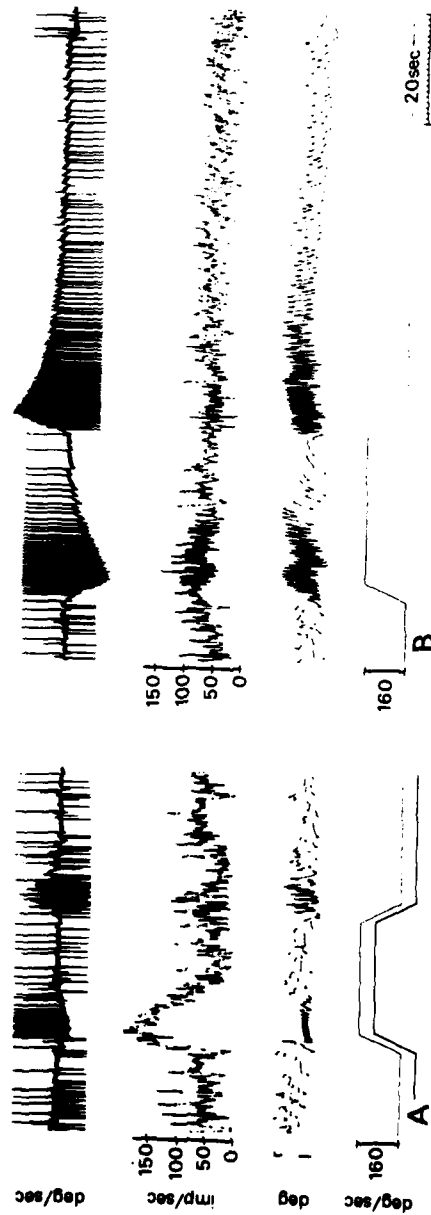


FIGURE 5. Simple spike (SS) activity (with its typical irregular resting discharge) of a type I P-cell during vestibular (B) and conflicting (A) stimulation. Same display as in FIGURE 1. Acceleration and deceleration, 40°/second²; end velocity, 160°/second. Note irregular burst activity with saccades to the left (to the side of recording).

influenced during smooth pursuit. During OKN-suppression, the same unit showed a monotonic increase in activity up to $30^\circ/\text{second}$ and then saturated when optokinetic stimulus velocity was increased further to $160^\circ/\text{second}$ (FIGURE 4).

Output Activity

Purkinje cells (P-cells) constitute the only output elements of the cerebellar cortex. They were tested during conflicting visual-vestibular and optokinetic stimulation. About 10-20% showed a modulation of their simple spike (SS) activity during conflicting stimulation and half of them also during constant-velocity optokinetic stimulation.

During conflicting stimulation, P-cells were modulated only at high accelerations ($40^\circ/\text{second}^2$). Acceleration at $10^\circ/\text{second}^2$ had little or no effect.

The same P-cells showed a small or no response during vestibular stimulation even with high accelerations (FIGURES 5 and 6A). About 90% of the P-cells were activated during acceleration to the ipsilateral side, similar to vestibular type I cells. Less than half of them showed a bidirectional response with inhibition during acceleration to the contralateral side (FIGURE 6B).

Optokinetic stimulation activated P-cells only at velocities of $60^\circ/\text{second}$ or above (FIGURES 7 and 9). Stimulus direction for activation is the same as for conflicting stimulation, but elicits nystagmus to the opposite direction. This is a decisive difference between type I vestibular nuclei and floccular input units. Although nystagmus directions are opposite for conflicting and optokinetic stimulation, visual image slip goes in the same direction toward the ipsilateral side. In the fully alert animal, SS activity can be related to image slip velocity over a wide range. During periods of inattention, when nystagmus velocity is reduced, SS activity does not increase. This shows that the signal that drives activity in P-cells is derived from image slip velocity but cannot be directly equated to velocity of motion across the retina (FIGURE 7D). Presenting the optokinetic stimulus suddenly by turning lights on during drum rotation led to a sudden increase in SS activity similar as for eye velocity. When lights were turned off, P-cell activity immediately returned to the level of resting discharge although nystagmus only slowly decayed as OKAN (FIGURE 3B). Complex spike (CS) activity was modulated in a reciprocal manner to SS activity under all stimulus conditions and was equivalent to image slip velocity and direction. However, the responses were not mirrorlike. CS activity was bidirectional and responded to a constant-velocity optokinetic stimulation of $30^\circ/\text{second}$ (FIGURE 8).

DISCUSSION

Clinical studies and lesion experiments in animals suggest a major role in visual-vestibular information processing for the flocculus. Therefore, the flocculus should receive visual and vestibular information independently via separate input channels.¹⁹ Our results, however, show that the most frequently recorded MF-input carries a signal that already combines different sensory inputs together with motor information. This input most probably arises from type I vestibular-plus-eye-movement units from both sides of the vestibular nuclei. These neurons

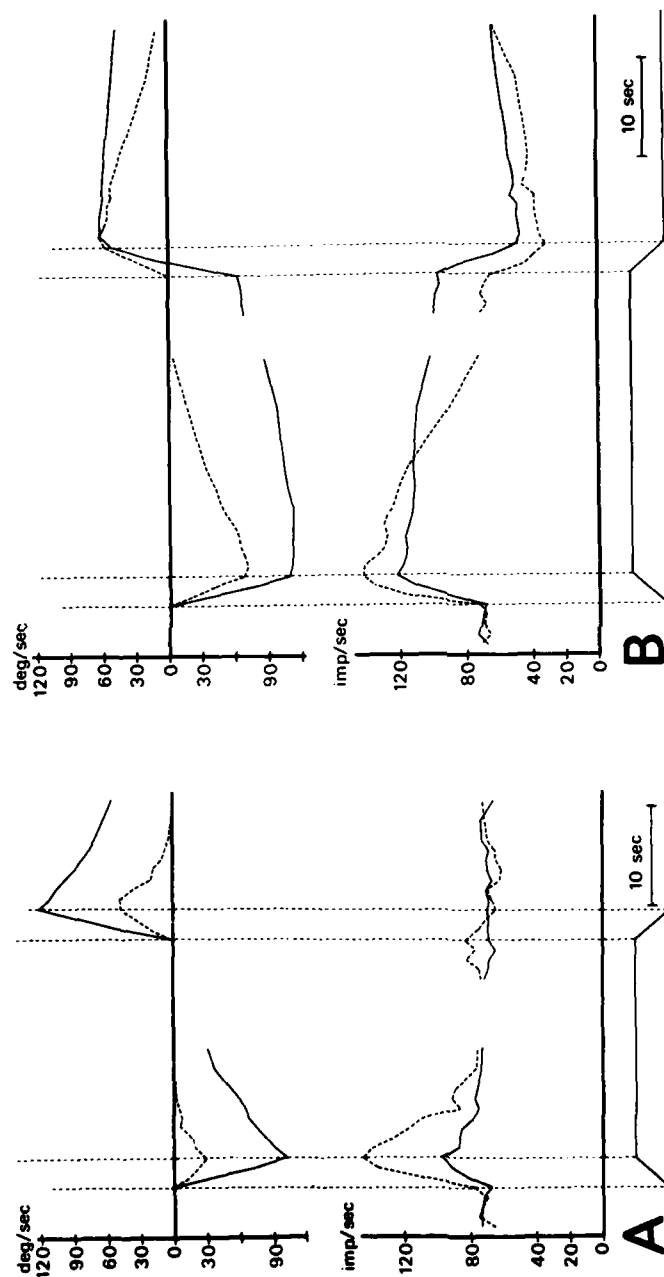


FIGURE 6. Averaged SS activity of type I P-cells and eye velocity during conflicting (dashed line) and vestibular (solid line) stimulation. In A, activity of seven neurons from two monkeys with a short time constant of vestibular nystagmus. In B, six neurons from monkey 51, which had a time constant of VN greater than 50 seconds. Values were taken every second for a period of 4 seconds before to 14 or 25 seconds after start of acceleration and deceleration ($40^\circ/\text{second}^2$). In A during vestibular stimulation, P-cells were modulated only weakly. During conflicting stimulation, modulation was unidirectional. In B, P-cells were modulated also during vestibular stimulation in a bidirectional way.

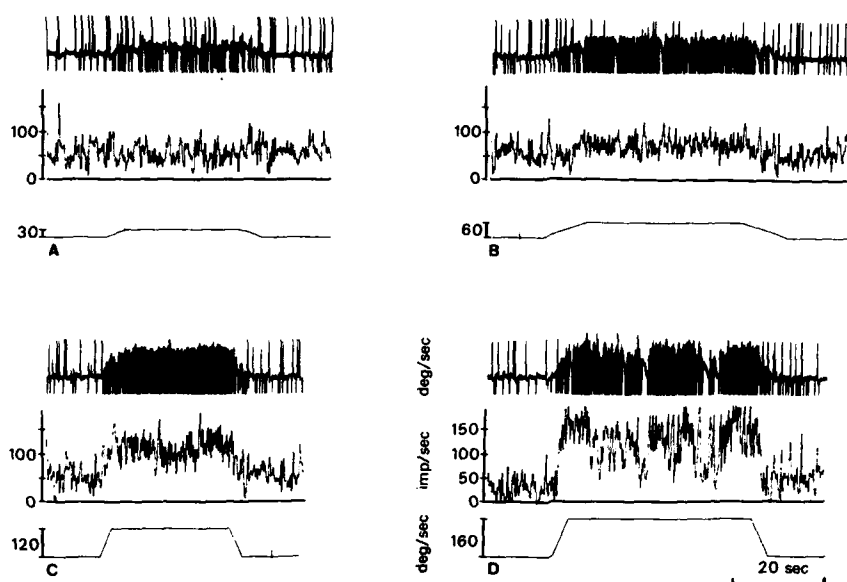


FIGURE 7. Same P-cell as in FIGURE 5 during optokinetic stimulation toward the recording side at different velocities between 30 and 160°/second. At 160°/second, SS activity decreases whenever nystagmus slow-phase velocity decreases.

reacted to vestibular and visual (optokinetic) stimulation, and the majority also were modulated with fast eye movements and/or eye positions.^{8,14-17} Another, less often encountered input exclusively carries information about velocity of visual image slip. We could not record neuronal activity similar to that of the vestibular nerve, although vestibular nerve fibers are known to project to the flocculus.^{19,20}

Our results suggest a two-stage processing of visual-vestibular information in the vestibular nuclei and the flocculus. It therefore is necessary to compare activity in these two structures during the different stimulus combinations. Our hypothesis is that P-cells are modulated when activity in the vestibular nuclei is not adequate to move the eyes with the required velocity.^{6,7} During suppression of vestibular nystagmus, eye velocity can be zero although vestibular nuclei cells are activated. During high-velocity optokinetic stimulation, nystagmus velocity saturates at a level higher than vestibular nuclei activity. Another example is conflicting stimulation at high accelerations (40°/second²), when activity in the vestibular nuclei is similar to the input from the labyrinths but observed nystagmus velocity is much slower. This could be achieved by the opposing influence from the flocculus. Using low acceleration values (less than 10°/second²) neuronal activity in the vestibular nuclei is much reduced, as is nystagmus velocity, when compared to the response during vestibular stimulation in darkness. These examples show that the flocculus can provide an extra input to the oculomotor system to either enhance or slow down nystagmus velocity. It is not clear how and where the two outputs from the vestibular nuclei and the flocculus converge. To provide this extra signal to the oculomotor system, the flocculus must utilize a second input, which carries information about

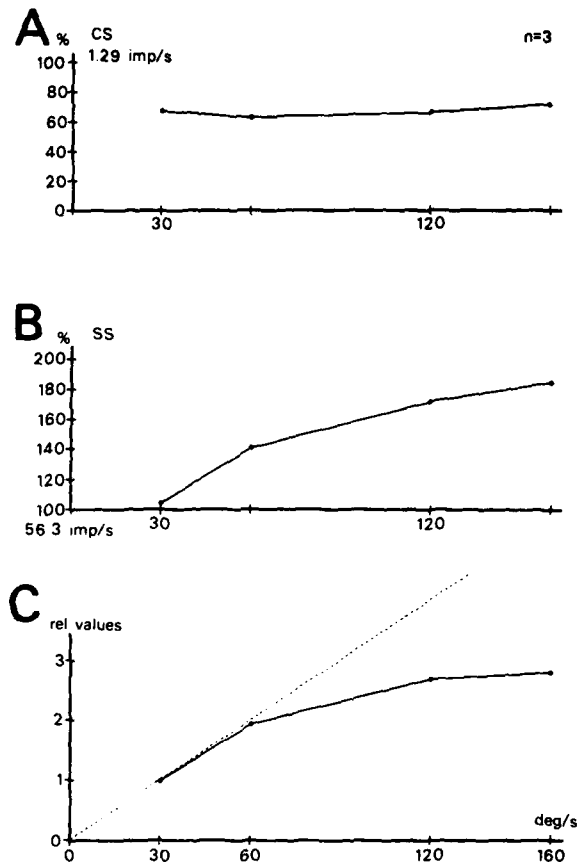


FIGURE 8. Averaged CS (A) and SS (B) activity together with OKN slow-phase velocity (C) for three type I P-cells. Optokinetic stimulation at different velocities to the ipsilateral side. Activity increase in A and B is expressed in percent of the resting discharge. Resting discharge was 1.3 impulses/second for CS and 56.5 impulses/second for SS activity. Note opposite modulation for CS and SS activity. SS activity increases with higher velocities, while CS activity is depressed by a constant amount.

large-field visual image slip. This input can indicate whether nystagmus response is compensatory or not. The origin of this input is not clear. During optokinetic stimulation, activity in the input units from the vestibular nuclei increases up to velocities of 60°/second (FIGURE 9, left) and during OKAN, decreases in parallel with the slow-phase eye velocity. Floccular P-cells become modulated only at velocities of 40–60°/second or above (FIGURE 9, right). They show no modulation during OKAN. If lights are turned off during high-velocity OKN, the sudden loss of activity in floccular cells might be responsible for the initial drop in nystagmus velocity. Our findings are corroborated by lesion studies. After flocculectomy, monkeys can generate OKN only up to velocities of

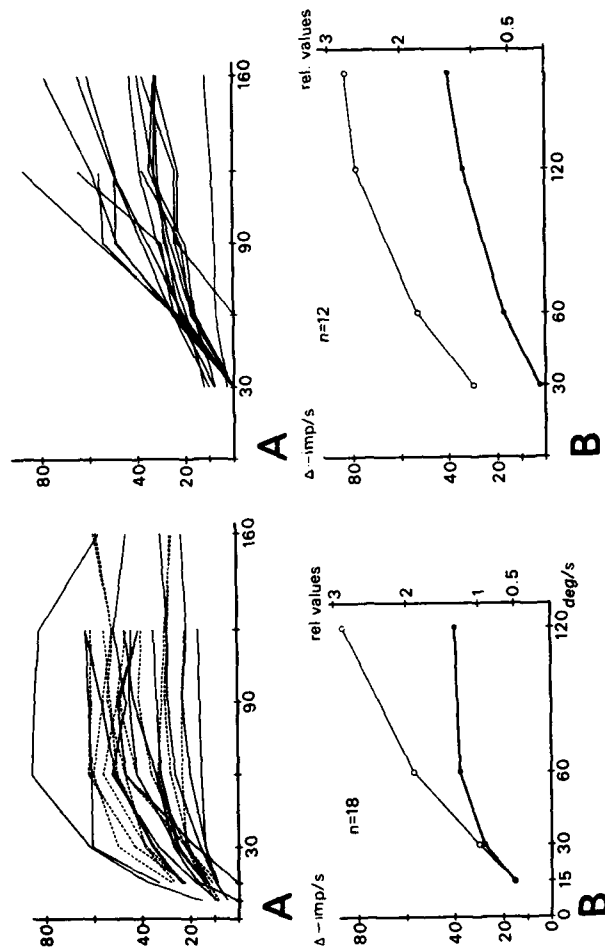


FIGURE 9. Frequency increase (ordinate) during constant-velocity optokinetic stimulation at different velocities (abscissa) for vestibular input units (left) and P-cells (right). A: values for individual units; solid lines indicate type I units; dotted lines, type II units. B: averaged values for several units (thick line) with concomitant slow-phase optokinetic nystagmus velocity (thin line, values normalized to a velocity of 30°/second).

40 to 60°/second; visual suppression of VN is lost;⁴ OKAN is not altered.⁵ OKN velocity also is reduced in cats.²¹

These findings can be interpreted within the frame of the modified model of Raphan and Cohen.²² This model has an "indirect" visual pathway going through a "velocity-storage" integrator via the vestibular nuclei. Within this pathway OKAN is generated. A second, "direct" visual pathway bypasses the integrator and the vestibular nuclei. This pathway does not contribute to OKAN, but is responsible for the fast increase of OKN and the sudden velocity drop in OKAN velocity after high-velocity optokinetic stimulation.²³ Both pathways combine at a stage beyond the vestibular nuclei. Some of the functions ascribed to the direct pathway can be found in activity of floccular P-cells.

SUMMARY

In the primate flocculus, unit activity was recorded during vestibular (rotation of the monkey about the vertical axis in complete darkness), optokinetic (rotation of the visual surround around the stationary monkey), and conflicting (rotation of the visual surround and the turntable fixed together) stimulation. Activity indicating two different mossy fiber inputs was recorded. One carried a signal that was similar to that in the vestibular nuclei: during optokinetic stimulation, neurons saturated at a velocity of 60°/second; and during conflicting stimulation, neuronal activity was attenuated only at low accelerations. This input combines vestibular, visual, and oculomotor information. Another mossy fiber input carried information about visual image slip only. This input indicates instances when nystagmus is not compensatory. Purkinje cells were modulated in their simple spike activity during optokinetic stimulation only at high stimulus velocities of 40–60°/second and above, and during conflicting stimulation at high accelerations. This suggests a complementary information processing of the flocculus and the vestibular nuclei during visual-vestibular stimulation. The findings are corroborated by lesion studies in primates.

ACKNOWLEDGMENTS

We thank V. Isoviita for her assistance during the experiments, E. Solcà for taking care of the electronic equipment, and J. Müller for photographic work.

REFERENCES

1. DICHGANS, J. & R. JUNG. 1975. Oculomotor abnormalities due to cerebellar lesions. In *Basic Mechanisms of Ocular Motility and Their Clinical Implications*. G. Lennerstrand & P. Bach-y-Rita, Eds.: 281–298. Pergamon Press, Oxford & New York.
2. VON REUTERN, G. M. & J. DICHGANS. 1977. Augenbewegungsstörungen als cerebelläre Symptome bei Kleinhirnbrückenwinkeltumoren. *Arch. Psychiatr. Nervenkr.* **223**: 117–130.
3. ZEE, D. S., R. D. YEE, D. G. COGAN & D. A. ROBINSON. 1976. Ocular motor abnormalities in hereditary cerebellar ataxia. *Brain* **99**: 207–234.
4. TAKEMORI, S. & B. COHEN. 1974. Loss of visual suppression of vestibular nystagmus after floccular lesions. *Brain Res.* **72**: 213–224.
5. ZEE, D. S., A. YAMAZAKI & G. GUCER. 1978. Ocular motor abnormalities in trained monkeys with floccular lesions. Abstr. 575, Eighth Neuroscience Meeting, St. Louis, Mo., November 5–9.

6. WAESPE, W., U. BÜTTNER & V. HENN. 1981. Visual-vestibular interaction in the flocculus of the alert monkey. I. Input-activity. *Exp. Brain Res.* (In press.)
7. WAESPE, W. & V. HENN. 1981. Visual-vestibular interaction in the flocculus of the alert monkey. II. Purkinje cell activity. *Exp. Brain Res.* (In press.)
8. WAESPE, W. & V. HENN. 1977. Neuronal activity in the vestibular nuclei of the alert monkey during vestibular and optokinetic stimulation. *Exp. Brain Res.* **27**: 523-538.
9. WURTZ, R. H. 1969. Visual receptive fields of striate cortex neurons in awake monkeys. *J. Neurophysiol.* **32**: 727-742.
10. LISBERGER, S. G. & A. F. FUCHS. 1978. Role of primate flocculus during rapid behavioral modification of vestibuloocular reflex. I. Purkinje cell activity during visually guided horizontal smooth-pursuit eye movements and passive head rotation. *J. Neurophysiol.* **41**: 733-763.
11. MILES, F. A., J. H. FULLER, D. J. BRAITMAN & B. M. DOW. 1980. Long-term adaptive changes in primate vestibuloocular reflex. III. Electrophysiological observations in flocculus of normal monkeys. *J. Neurophysiol.* **43**: 1437-1476.
12. NODA, H. & D. A. SUZUKI. 1979. Processing of eye movement signals in the flocculus of the monkey. *J. Physiol. London* **294**: 349-364.
13. LISBERGER, S. G. & A. F. FUCHS. 1978. Role of primate flocculus during rapid behavioral modification of vestibuloocular reflex. II. Mossy fiber firing patterns during horizontal head rotation and eye movement. *J. Neurophysiol.* **41**: 764-777.
14. WAESPE, W. & V. HENN. 1977. Vestibular nuclei activity during optokinetic after-nystagmus (OKAN) in the alert monkey. *Exp. Brain Res.* **30**: 323-330.
15. WAESPE, W. & V. HENN. 1978. Conflicting visual-vestibular stimulation and vestibular nucleus activity in alert monkeys. *Exp. Brain Res.* **33**: 203-211.
16. WAESPE, W. & V. HENN. 1979. The velocity response of vestibular nucleus neurons during vestibular, visual, and combined angular acceleration. *Exp. Brain Res.* **37**: 337-347.
17. WAESPE, W. & V. HENN. 1979. Motion information in the vestibular nuclei of alert monkeys: Visual and vestibular input vs. optomotor output. *Prog. Brain Res.* **50**: 683-693.
18. ITO, M. 1972. Neural design of the cerebellar motor control system. *Brain Res.* **40**: 81-84.
19. BÜTTNER, U. & W. WAESPE. 1981. Vestibular nerve activity in the alert monkey during vestibular and optokinetic nystagmus. *Exp. Brain Res.* **41**: 310-315.
20. CARPENTER, M. C., B. M. STEIN & P. PETER. 1972. Primary vestibulocerebellar fibers in the monkey: distribution of fibers arising from distinctive cell groups in the vestibular ganglia. *Am. J. Anat.* **135**: 221-250.
21. KELLER, E. L. & W. PRECHT. 1979. Visual-vestibular responses in vestibular nuclear neurons in intact and cerebellectomized, alert cats. *Neuroscience* **4**: 1599-1613.
22. RAPHAN, TH. & B. COHEN. 1981. The role of integration in oculomotor control. In *Models of Oculomotor Behavior and Control*. B. L. Zuber, Ed. CRC Press. (In press.)
23. COHEN, B., V. MATSUO & TH. RAPHAN. 1977. Quantitative analysis of the velocity characteristics of optokinetic nystagmus and optokinetic afternystagmus. *J. Physiol. London* **270**: 321-344.

DIRECTIONAL PLASTICITY OF THE VESTIBULO-OCULAR REFLEX IN THE CAT*

Lex W. Schultheis and David A. Robinson

*The Wilmer Institute
The Johns Hopkins Medical School
Baltimore, Maryland 21205*

INTRODUCTION

As an individual moves, the eyeballs must rotate at the same speed, but in the opposite direction, as head rotation for images to be stabilized on each retina. Such movements are made automatically by the vestibulo-ocular reflex (VOR). Its effectiveness may be measured by the gain of the reflex: eye velocity divided by head velocity. Normally the gain is close to 1.0, so that images do not slip on the retina when the head moves. The VOR must have some type of maintenance system that monitors its gain (by vision) and corrects it when it falls out of calibration. In a young animal this system is responsible for maintaining calibration as the organism grows. Growth of the skull—which alters the angular relations between the orbits¹ and the semicircular canals—and changes in the mechanical parameters of the eyeball and eye muscles must be compensated if the system is to continue working. In the mature animal the task becomes one of preserving the gain of the vestibulo-ocular system in spite of the continual disturbing effects of cell death during aging. The enormous anatomical variations between members of a species suggest that genetic programming alone cannot maintain the VOR.² The mechanism responsible for optimizing the VOR has been described as a motor-learning system capable of making parametric changes by modifying synaptic strengths.^{3,4}

The ability of this repair mechanism to change the VOR has been demonstrated by adapting animals and humans to optical devices that change the relationship between the apparent motion of visual objects and head rotation. Melvill Jones and his colleagues have studied the effect of chronic vision through Dove prisms.⁵⁻⁷ These prisms reverse the seen world from left to right and make it appear to move in the same direction as the head when the latter moves. After an adaptation period, the gain was found to be reduced. Miles and his colleagues found that a telescope lens system that magnifies the visual world can be used to raise the VOR gain.^{8,9} In each of these and similar situations, the gain always rose or fell in such a way as to lessen or eliminate retinal image slip during head movements. This form of adaptive motor plasticity now has been well established in a variety of species.

Not only must the speed of a compensatory eye movement be correct, its direction must be just opposite to that of the head to keep the line of sight stationary in the visual environment. We can think of vestibular eye compensatory movements as occurring in a plane parallel to the plane of head rotation. The wrong orientation of the plane of the eye movement would cause images to slip on the retina. If the planes of action of pairs of extraocular muscles were exactly parallel to those of synergistic pairs of semicircular canals, the arrangement

*This research was supported by Training Grant No. EY07047 (L.W.S.) and by Research Grant No. EY00598 (D.A.R.) from the National Eye Institute, National Institutes of Health.

would be simple. Stimulation of one pair of canals would create a movement by only one pair of muscles for each eye. Should the system become inaccurate over time, it could be recalibrated simply by changing the gains of the direct pathways between single canal pairs and their target muscles. No changes between a given canal pair and other muscles would be necessary. The eye muscle planes, however, are not parallel to the planes of the semicircular canals, so the pattern of connectivity is more complicated. This fact means that a head rotation in the plane of one canal pair must cause a response in all pairs of eye muscles. It has been shown, in fact, that stimulation of any single ampullary nerve results in an eye movement driven by tension changes in every eye muscle; stimulation of the left anterior canal nerve in alert cats increased tension in the left medial and the right lateral rectus as well as in the vertical muscles.^{10,11} Normally, in this example, symmetrical connections from the right anterior canal to the left-ducting horizontal muscles prevent a vertical head rotation from causing horizontal eye movements. This report will show that visual experience can unbalance these connections so that vertical head rotations can be made to cause reflexive horizontal eye movements.

More generally, the wiring of the semicircular canals to the extraocular muscles may be described mathematically as a coordinate transformation as shown in FIGURE 1. A head rotation may be described as a vector, \vec{H} , directed along the axis about which the head is spinning (and perpendicular to the plane of rotation) with components in an earth-fixed Cartesian coordinate system. This head rotation stimulates the three canal pairs, the activity of which represents the same vector, but described now as \vec{C} with components in the coordinate system of the canals (column vector on the right in FIGURE 1). The vector \vec{C} then is transformed by a brain-stem connections matrix $[B]$, shown as the 3×3 array in FIGURE 1. The numbers in the array describe the strengths of all the projections from the canals to the muscles of the left eye. The original vector \vec{H} now is

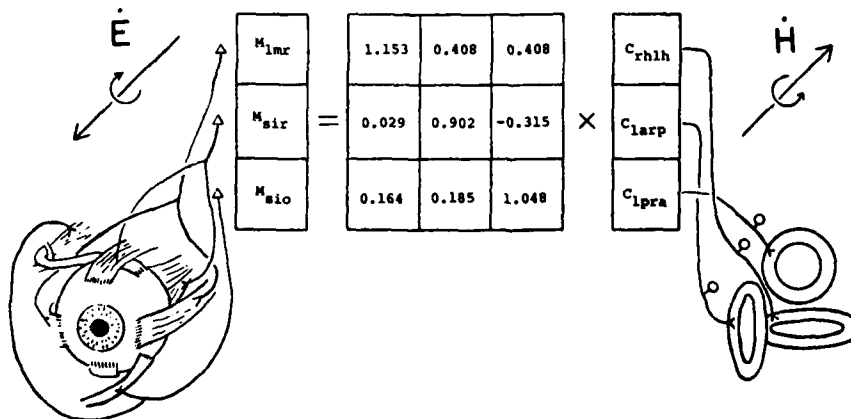


FIGURE 1. The neural connections between synergistic semicircular canal pairs and antagonist extraocular muscle pairs for each eyeball are represented by a matrix of weighting elements. See text for description. rhlh, right and left horizontal canal pair; larp, left anterior right posterior canal pair; lpra, left posterior right anterior canal pair; lmr, lateral medial recti; sir, superior inferior recti; sio, superior inferior obliques.

represented as a vector \vec{M} in the coordinate system of the muscles (the column vector on the left in FIGURE 1). This motor vector then creates an eye rotation, \vec{E} , expressed in the same earth-fixed Cartesian coordinate system as \vec{H} .

Normally, the vector \vec{E} must equal $-\vec{H}$ for compensatory eye movements. In that case, since the transformation from \vec{H} to \vec{C} can be calculated by geometry, as can the transformation from \vec{M} to \vec{E} , the middle transformation matrix [B], shown in FIGURE 1, can be calculated. For the numerical values shown, we considered the lateral canals to be tilted backwards by 30° from a plane horizontal with respect to the head and the vertical canals to lie in vertical planes oriented at $\pm 45^\circ$ from a parasagittal plane. This allowed calculation of the rotation matrix between \vec{H} and \vec{C} . The relationship between the vectors \vec{M} and \vec{E} was determined from Table I of the calculations of Robinson for the primary position.¹² These assumptions then led to the calculation of the values in the matrix [B] in FIGURE 1. The values of these elements are only approximate since they are based on some anatomical assumptions, but they should, nonetheless, indicate roughly the relative overall strengths of connections between the three coplanar canal pairs and the three antagonist pairs of extraocular muscles on a given eyeball. Since each canal of a pair excites one muscle and inhibits its antagonist, each element in the matrix represents 4 neural pathways so that 36 pathways actually are involved. For eye movements to compensate for head rotation so that image slip on the retina is a minimum, each part of this matrix must be correct. If the strength of any of those pathways changes due, for example, to cell death from disease or aging, eye movements will fail to be compensatory in speed and direction. To reestablish calibration, the remaining synapses must carry more than their original share of the signal. This requires selective plastic changes to restore individual components of the matrix to their original values.

We felt that it should be possible to simulate this type of plastic adjustment by altering the direction of retinal slip relative to the direction of head movement. Such visual-vestibular experience might induce plastic changes in the individual contributions to eye movements from different semicircular canal pairs. These artificially induced changes in the off-diagonal elements of the transformation matrix should change the direction in which the eye moves as well as its speed. Vestibular nystagmus then would contain a component outside the plane of head rotation.

The first experiments to study modification of the plane of the vestibulo-ocular reflex were done by John Hay and others.¹³⁻¹⁶ Human subjects in a dark room tracked a dim luminous dot that moved horizontally in synchrony with vertical head nodding. For example, as a subject's head rotated down, the dot was tracked to the left; up rotation moved the target dot to the right. After a training period, the subject reported an illusory horizontal movement of a stationary dot during vertical head movement. This illusory movement was in the direction opposite to that of the dot during training. Since the dot was not moving, it was presumed that some type of motor learning must have occurred to drive the subject's eyes in the same direction as during training. This suggests that the vestibulo-ocular reflex was plastically modified outside of the plane of head rotation. No eye movements were measured in these experiments. Also, active head movements were used, so the development of some sort of predictive tracking based on an intended head movement cannot be ruled out. We wanted to confirm these results objectively and chose the cat for our experimental subject because previous studies had shown that plasticity of the gain of the VOR was abolished by vestibulocerebellectomy.¹⁷ If one thinks of a vestibular eye

movement as a vector with both magnitude and direction, it would seem reasonable to suppose that vestibulocerebellectomy also would abolish plasticity of the direction of the VOR, and we wanted to test this idea.

METHODS

Eight, healthy, female cats weighing between seven and nine pounds were prepared chronically with a skull implant, to prevent voluntary head movements, and a subconjunctival search coil by which eye movements could be monitored.¹⁸ The magnetic-field method of measuring eye movements has been described elsewhere.¹⁹ Cats were restrained in a plastic box that was able to rotate in pitch $\pm 25^\circ$ about an interaural axis within the magnetic field. A wooden frame supporting the magnetic-field coils and the cat box could rotate in yaw. Horizontal head position was sensed by a potentiometer coupled to the wooden frame. A second search coil attached to the cat box provided a measurement of vertical angular head position. Since the cat's head moved within the magnetic field during vertical head rotation, vertical eye position in the orbit was derived by electronic subtraction of vertical head displacement from vertical eye displacement with respect to the field. The entire system had a sensitivity of 0.25° over a bandwidth of 0-1,000 Hz.

An optokinetic drum, which surrounded the animal, could be driven by a feedback control system so that horizontal drum position was proportional to vertical head position (see FIGURE 2). The distance that the drum rotated horizontally for a given vertical head rotation was adjustable. Typically, drum motion was 50% greater than head motion. Eye movements were monitored continuously to be certain that the animal was alert.

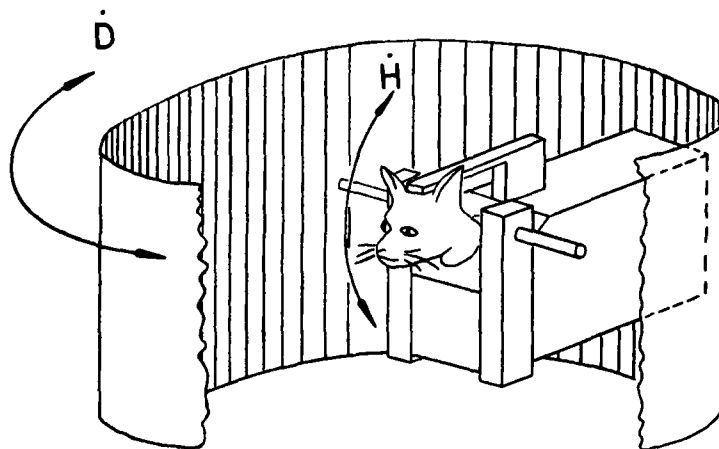


FIGURE 2. The experimental method. Vertical head velocity (\dot{H}) was created by forced oscillations about an interaural axis. This motion was made to cause proportional horizontal movement of an optokinetic drum (\dot{D}). This entire system was attached to a wooden frame that could be rotated horizontally.

After an initial demonstration of plasticity in two cats, their vestibulocerebellum (nodulus and flocculi) was removed by aspiration under visual control through trephine holes over the posterior fossa. The cats subsequently were sacrificed, and their cerebellums examined grossly to verify that the appropriate lobes were removed. Histology was not available at the time this report was written.

RESULTS

After a training period in which the optokinetic drum moved horizontally in synchrony with vertical head oscillations, the VOR was measured in the dark and compared to control values obtained before training. In normal animals before training, vestibular nystagmus generated by quasi-sinusoidal vertical head rotation, shown in FIGURE 3A, was entirely vertical with no horizontal component, as shown in FIGURE 3B. This is an example of pure vertical head movements producing horizontal eye movements in the dark. This demonstrated what we called cross-axis plasticity. The ratio of eye velocity of the horizontal component of nystagmus to vertical head velocity, we called the cross-axis ratio. In an untrained animal this was zero. All eight animals exhibited a cross-axis horizon-

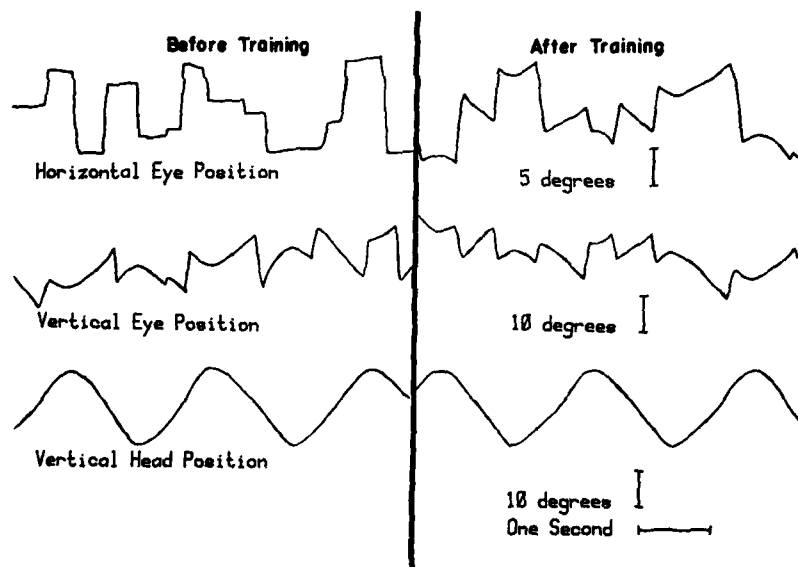


FIGURE 3. Horizontal cross-axis nystagmus during vertical head oscillation. (A) Before training, there was no horizontal nystagmus in the dark when the cat was rotated in pitch. (B) After training, horizontal eye movements were generated in the dark when the cat was oscillated vertically. These horizontal eye movements moved in the same direction as the drum did during training. There was no change in the gain of the vertical VOR. Upward and rightward movements are on the recordings. Note different scales for horizontal and vertical movements.

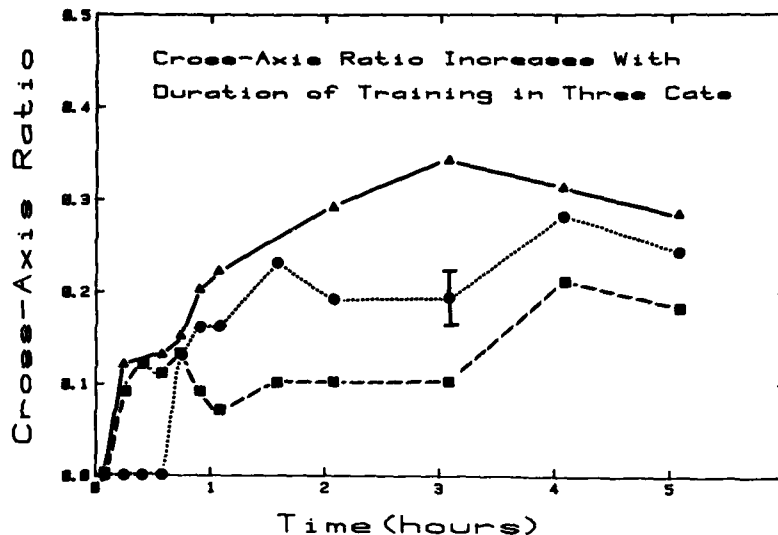


FIGURE 4. The cross-axis ratio (peak horizontal eye velocity/peak vertical head velocity) increased with the duration of training. After about three to five hours, the cross-axis ratio ranged from 0.33 to 0.18 with a typical value of 0.25 and a typical standard deviation of ± 0.03 , as shown for one cat at three hours. The three different traces apply to three different cats.

tal nystagmus after training. The cross-axis ratio increased with the amount of time that the animal was exposed to a situation in which horizontal retinal slip was correlated with vertical head rotation. FIGURE 4 shows that after five hours of sinusoidal rotation in this visual-vestibular conflict situation in which drum velocity was 50% greater than vertical head velocity, the slow phases of horizontal nystagmus had a peak velocity that was 20 to 30% of peak vertical head velocity.

If the cat then remained in the restraint box overnight without moving its head, the horizontal nystagmus generated by vertical head movements persisted, indicating that a plastic change had occurred, a change that was stable over time in the absence of any new visual-vestibular experience. On the other hand, if an animal that had been adapted for several hours then was rotated vertically in the light with the optokinetic drum removed, the cross-axis nystagmus disappeared within about half an hour. The cross-axis nystagmus is unlearned more quickly than it is learned.

In one adapted cat with a cross-axis ratio of 0.29, no change in either the vertical or horizontal components of the VOR themselves was observed in the dark. During a vertical head movement, the vertical component of eye speed was normal; and during a horizontal head movement, the eye moved at the normal speed horizontally. Thus, off-diagonal terms of the transformation matrix in FIGURE 1 could be changed plastically without affecting the main diagonal elements. Furthermore, in an adapted cat, the established cross-axis ratio was not decreased by rotating the cat horizontally in a stationary visual environment. Therefore, visual-vestibular experience in one plane did not modify visual-

vestibular learning in another plane. This implies that the neural maintenance mechanism can effect repairs in the parts of the reflex that are malfunctioning without changing those pathways that are driving the eyes appropriately.

We suspected that an altered correlation between retinal image slip signals and canal afference was responsible for modification of the direction of the vestibulo-ocular reflex. To test this, we adapted each of three cats with different ratios of horizontal drum velocity to vertical head velocity. The difference between drum velocity and horizontal eye velocity is horizontal retinal slip velocity. By rotating the animals through a small amplitude (7°) at a high frequency (0.5 Hz), peak horizontal eye velocity was relatively constant regardless of peak drum speed, because the optokinetic system is unable to keep up with such drum speeds and frequencies. Consequently, we could vary retinal slip independently of the efferent command to the eye muscles. In three cats the cross-axis ratio that developed after two hours of training increased as a function of peak horizontal retinal slip velocity during training. The ratio increased from a typical value of 0.12 when peak retinal slip was small ($10^\circ/\text{second}$) to a value of 0.2 when slip was large ($30^\circ/\text{second}$).

We wondered if this change of the direction of the VOR occurred only at the training frequency or if the system's modifications extended over all stimulus frequencies. Three cats were adapted at 0.25 Hz for two hours and then rotated in the dark at higher frequencies (0.5 and 1.0 Hz) and a lower frequency (0.125 Hz). The peak velocity of the stimulating waveform was kept constant at all frequencies. Some horizontal nystagmus was observed at all frequencies, but in the dark at the training frequency, the cats exhibited a larger cross-axis ratio than they did at the high frequencies by a factor of 60%. The cross-axis ratio at half the training frequency was equal to or slightly higher than the cross-axis ratio at the training frequency. Thus, adaptation was seen at all frequencies, but was greater over a range of low frequencies near the training frequency.

When the cat box was rotated with a step change of vertical angular displacement, a horizontal slow phase appeared that took off at the same time as the vertical slow phase. Since both the normal vertical VOR and the learned horizontal nystagmus appeared to have the same latency, it seems reasonable that the cross-axis movements probably resulted from a modification of the vestibulo-ocular reflex and were not some learned pursuit movement that could be made in the dark.

To see if cerebellar lesions could affect plastic changes in VOR direction as well as VOR speed, we surgically removed the nodulus and both flocculi by aspiration in two cats. It was necessary to remove the lateral aspects of the paraflocculus and lobule IX and part of VIII in the vermis to reach the vestibular structures. Preoperatively, both cats had been rotated passively to demonstrate the development of a cross-axis VOR. One cat had a cross-axis ratio of 0.26, and the other a ratio of 0.36, after three hours of training. The cats were able to walk and feed themselves within two days after surgery. One week later each cat was rotated passively while wearing Dove prisms to determine if gain plasticity remained. Both cats exhibited a horizontal VOR gain of close to 1.0 in the dark before rotation. No significant change was observed after three hours of oscillation with reversed vision. This result indicated that gain plasticity had been abolished as shown previously¹⁷ and helped to confirm, in the living animal, that the vestibulocerebellum had been removed successfully.

Next, plasticity of the VOR direction was examined. Neither cat produced a horizontal nystagmus after three hours of training to develop a cross-axis VOR.

Six weeks after surgery further attempts to change the direction of slow-phase eye movements during passive rotation in pitch produced negative results. These lesions appear to have abolished the ability to make plastic changes in the directional plane of the vestibulo-ocular reflex.

DISCUSSION

Cross-axis nystagmus was found in every cat we trained. We conclude that it is a general phenomenon normally present in all members of the species. Since the cross-axis eye movements had the same latency as the VOR, cross-axis plasticity probably represents a modification of the normal vestibulo-ocular wiring, as shown in FIGURE 1, as a consequence of the system's ability for self-repair, rather than some learned following movement that can occur in the dark. Vestibulo-ocular plasticity across axes—like plasticity of the gain of the reflex within the plane, which appears to have the purpose of eliminating retinal slip during head motion—seemed to depend on the magnitude and direction of image slip on the retina during training. The stimulus appeared to be an altered correlation between head movement and retinal slip rather than a comparison between head movement and the resultant eye movement during this learning. The sensitivity of each pathway from every canal to every eye muscle probably can be changed independently as needed, so that the whole reflex can be optimized. These data, taken together, suggest that gain plasticity within the plane of head rotation is a special case of a more general vestibulo-ocular plasticity where the direction in which the eye moves is controlled as well as its speed.

Although the anatomical locus of these plastic changes remains unknown, the pathways must have certain special characteristics. They must have a large number of parallel components with similar connections to preserve the overall functional integrity in spite of, say, cell death. They also must have the ability to modify selectively individual pathways from every canal to every muscle. This could be accomplished by the convergence of signals from more than one canal onto cells whose dendritic synapses can be altered selectively by retinal slip. The site of vestibulo-ocular plasticity must have the memory storage capacity to retain changes in the VOR when they are needed and to erase those that are no longer appropriate. The cerebellar cortex certainly satisfies the requirements of redundant connections and canal convergence;^{20,21} however, it is less certain that it contains the mechanism for memory.^{22,23} It may be that VOR plasticity is not confined to a single locus, but rather is distributed along a set of serial circuits so that a number of small synaptic changes in cascade can effect a large overall change in the reflex. We suggest, nevertheless, that the cerebellum is an important component of the learning machine that enables modification of the direction as well as the gain of the reflex, although its exact mode of action remains unknown.

ACKNOWLEDGMENTS

We thank Corena Bridges for vital assistance with the animal surgery, Adrian Lasker for technical help, and Andrea McCracken for secretarial assistance.

REFERENCES

1. MESCHAN, I. 1959. *An Atlas of Normal Radiographic Anatomy*: 253. W. B. Saunders Company. Philadelphia, Pa.
2. BLANKS, R. H. I., I. S. CURTHOYS & C. H. MARKHAM. 1972. Planar relations of semicircular canals in the cat. *Am. J. Physiol.* **223**: 55-62.
3. ROBINSON, D. A. 1975. Oculomotor control signals. In *Basic Mechanisms of Ocular Motility and Their Clinical Implications*. G. Lennerstrand & P. Bach-y-Rita, Eds.: 337-374. Pergamon Press. New York, N.Y.
4. DAVIES, P. & G. MELVILL JONES. 1976. An adaptive neural model compatible with plastic changes induced in the human vestibulo-ocular reflex by prolonged optical reversal of vision. *Brain Res.* **103**: 546-550.
5. MELVILL JONES, G. & P. DAVIES. 1976. Adaptation of cat vestibulo-ocular reflex to 200 days of optically reversed vision. *Brain Res.* **103**: 551-554.
6. GONSHOR, A. & G. MELVILL JONES. 1976. Short-term adaptive changes in the human vestibulo-ocular reflex arc. *J. Physiol. London* **256**: 361-379.
7. GONSHOR, A. & G. MELVILL JONES. 1976. Extreme vestibulo-ocular adaptation induced by prolonged optical reversal of vision. *J. Physiol. London* **256**: 381-414.
8. MILES, F. A. & J. H. FULLER. 1974. Adaptive plasticity in the vestibulo-ocular responses of the rhesus monkey. *Brain Res.* **80**: 512-516.
9. MILES, F. A. & B. B. EIGHMY. 1980. Long-term adaptive changes in primate vestibulo-ocular reflex. I. Behavioral observations. *J. Neurophysiol.* **43**: 1406-1436.
10. COHEN, B., J. I. SUZUKI & M. B. BENDER. 1964. Eye movements from semicircular canal nerve stimulation in the cat. *Ann. Otol. Rhinol. Laryngol.* **73**: 153-169.
11. SUZUKI, J. I. & B. COHEN. 1964. Head, eye, body and limb movements from canal nerves. *Exp. Neurol.* **10**: 393-405.
12. ROBINSON, D. A. 1975. A quantitative analysis of extraocular muscle cooperation and squint. *Invest. Ophthalmol.* **14**: 801-825.
13. HAY, J. C. 1968. Visual adaptation to an altered correlation between eye movement and head movement. *Science* **160**: 429-430.
14. HAY, J. C. 1971. Does head-movement feedback calibrate the perceived direction of optical motions? *Percept. Psychophys.* **10**: 286-288.
15. WALLACH, H., K. J. FREY & G. ROMNEY. 1969. Adaptation to field displacement during head movement unrelated to the constancy of visual direction. *Percept. Psychophys.* **5**: 253-256.
16. WALLACH, H. & K. J. FREY. 1972. Differences in the dissipation of the effect of adaptation to two kinds of field displacement during head movements. *Percept. Psychophys.* **11**: 31-34.
17. ROBINSON, D. A. 1976. Adaptive gain control of the vestibuloocular reflex by the cerebellum. *J. Neurophysiol.* **39**: 954-969.
18. JUDGE, S. T., B. J. RICHMOND & F. C. CHU. 1980. Implantation of magnetic search coils for measurement of eye position: an improved method. *Vision Res.* **20**: 535-538.
19. ROBINSON, D. A. 1963. A method of measuring eye movement using a scleral search coil in a magnetic field. *IEEE Trans. Bio-Med. Electron.* **10**: 137-145.
20. BLANKS, R. H. I., W. PRECHT & M. L. GIRETTI. 1977. Response characteristics and vestibular receptor convergence of frog cerebellar Purkinje cells. A natural stimulation study. *Exp. Brain Res.* **27**: 181-201.
21. PRECHT, W., R. VOLKIND & R. H. I. BLANKS. 1977. Functional organization of the vestibular input to the anterior and posterior vermis of the cat. *Exp. Brain Res.* **27**: 143-160.
22. KELLER, E. L. & W. PRECHT. 1979. Adaptive modification of central vestibular neurons in response to visual stimulation through reversing prisms. *J. Neurophysiol.* **42**: 896-911.
23. LISBERGER, S. G. & F. A. MILES. 1980. Role of primate medial vestibular nucleus in long-term adaptive plasticity of vestibuloocular reflex. *J. Neurophysiol.* **43**: 1725-1745.

THE "ERROR" SIGNALS SUBSERVING ADAPTIVE GAIN CONTROL IN THE PRIMATE VESTIBULO-OCULAR REFLEX

F. A. Miles and S. G. Lisberger

*Laboratory of Neurophysiology
National Institute of Mental Health
Bethesda, Maryland 20205*

The vestibulo-ocular reflex (VOR) functions to maintain ocular stability during head turns by generating compensatory eye movements that offset the head rotation. The ultimate purpose of these compensatory eye movements is to prevent head movements from seriously disturbing the retinal image, and in the monkey they do so very well: the VOR has a gain (measured as magnitude of compensatory eye movement divided by magnitude of head rotation in the dark) close to unity.¹ A number of studies in a variety of species have demonstrated that the VOR is very sensitive to prolonged optical disturbances of the visual input associated with head turns.¹⁻¹⁶ Magnifying telescopic spectacles, for example, elicit a gradual increase in the gain of the reflex, while diminishing spectacles bring about a decrease. Since these visually mediated changes operate always to improve the stability of the retinal image during head rotations, the reflex is said to possess *adaptive gain control*, the purpose of which is to establish and maintain appropriate calibration of the system. In order to do this, the system must be able to detect gain errors and utilize them to effect an appropriate gain adjustment. However, gain is a derived physical measure of the VOR's performance that is not directly available to the nervous system, and the purpose of this paper is to discuss the mechanism(s) by which the system computes VOR gain errors.

Any shortcomings in the gain of the VOR will result in persistent retinal slip during head turns, and the associated visual inputs will signal the need for gain adjustment. Of course, the system cannot diagnose gain errors from retinal slip alone and must relate it in some way to the ongoing head movement. The directional relationship between the slip and the head movement reliably indicates the direction in which the VOR gain needs to be changed to achieve better image stabilization, and most models of the adaptive mechanism invoke some directionally selective visual influence on transmission in vestibular pathways.^{4,7,17} The ultimate dependency on visual and vestibular inputs is clearly obligate since they alone provide the central nervous system with the relevant information about the physical world. However, this need not mean that the system necessarily uses visual and vestibular signals per se to guide calibration—any reliable central correlates of the same might serve equally well.

Substitutes for Vestibular (Head-Velocity) Signals?

Animals like the rabbit that never track moving targets use smooth eye movements solely to compensate for head rotations, always with the object of stabilizing their eyes with respect to the stationary surroundings. In such animals,

the mechanism regulating VOR gain might utilize eye-velocity signals rather than head-velocity (vestibular) signals to decipher errors: if smooth eye movements are accompanied consistently by retinal slip in the same direction as the eye movements, it would indicate that the compensatory eye velocities in general are not large enough, a situation that could be remedied by increasing the gain of the VOR; conversely, if slip and eye velocity are in opposing directions, it would indicate the need for a decrease in the gain of the VOR. There is evidence that this, indeed, is the mode of operation in the rabbit, i.e., the system computes VOR gain errors using eye-velocity signals rather than head-velocity signals.¹¹ With optical devices such as magnifying or reducing telescopic spectacles that call merely for an increase or decrease in the gain of the VOR, such a mechanism would be expected to operate appropriately and be indistinguishable from one deriving error information from retinal slip and head-velocity signals. However, there are other optical arrangements that can be used to distinguish between the two mechanisms. Collewijn and Grootendorst observed that when the rabbit was oscillated passively in optical situations producing left-right, or mirror, reversal of the visual input, the gain of the VOR decreased for the first hour or so but thereafter showed a gradual and consistent increase. On examining the original eye-movement records, they observed that for the first hour or so, the animal's compensatory eye movements in the light were attenuated and normally directed but thereafter showed reversal.¹¹ Thus, while the directional relationship between retinal image slip and head movement remained unchanged throughout, the directional relationship between retinal image slip and eye movement underwent a reversal at the time that the VOR gain stopped falling and began to increase. When retinal image slip and eye movements were in opposing directions, VOR gain decreased, and when the two movements were in the same direction, VOR gain increased. Further evidence that the velocity of the eyes rather than of the head is the relevant parameter is the demonstration that the gain of the rabbit's VOR can be increased merely by exposing the animal to sinusoidal optokinetic stimulation with its head fixed in position.¹¹ In this situation the animal experiences retinal image slip that is always in the same direction as its smooth eye movements; the fact that those eye movements are elicited by tracking rather than the VOR seems to be unimportant. Thus, in the rabbit, VOR gain changes can be elicited in the total absence of head movements. Similar mechanisms probably operate in the goldfish since prolonged sinusoidal optokinetic stimulation also is known to increase the gain of the VOR in this species.¹⁶

We have carried out similar experiments on the monkey and conclude that in this species, eye movements per se are irrelevant so far as adaptive gain control of the VOR is concerned. When the normal monkey was subjected to passive sinusoidal oscillations while wearing Dove prism spectacles that produced left-right reversal of visual inputs, the gain of the animal's VOR consistently showed a gradual decrease. However, the animal's compensatory eye movements were very variable during exposure to the reversed vision, showing reversal during some cycles but not others. Thus, from the viewpoint of the directional association between retinal slip and the movements of the eyes and head, the situation was ambiguous. A clear distinction between mechanisms using signals encoding eye velocity as against head velocity is possible only when both vision and the associated "compensatory" eye movements are reversed consistently. Then, if head velocity were the relevant parameter, VOR gain would decrease while if eye velocity were involved, VOR gain would increase. In order to insure consistently reversed eye movements during oscillation with

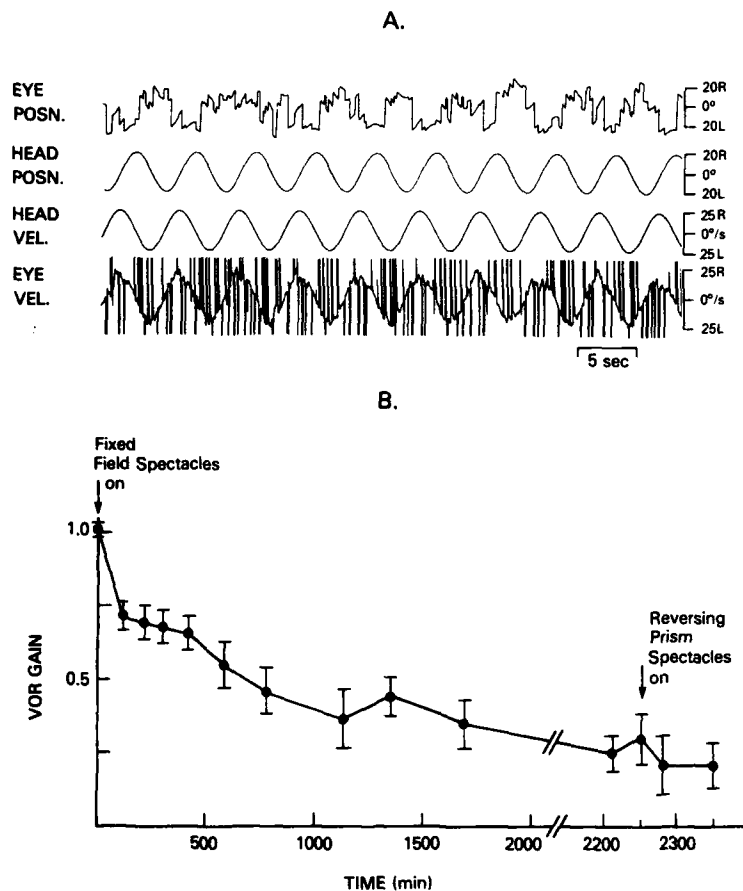


FIGURE 1. Effect of reversed vision and reversed "compensatory" eye movements on the monkey's horizontal VOR gain. **A:** Sample records showing the reversed "compensatory" eye movements of a monkey with low VOR gain during passive oscillation in the light while wearing left-right reversing Dove prism spectacles (0.2 Hz, $\pm 20^\circ$). **B:** Time course of the changes in a monkey's VOR gain resulting from passive oscillation (0.2 Hz, $\pm 20^\circ$) while wearing fixed-field goggles, later replaced by left-right reversing Dove prism spectacles. Time refers to time actually spent looking through the spectacles and was estimated from continuous polygraph records of the animal's eye movements. Error bars indicate standard deviations.

the Dove prism spectacles, we first reduced the VOR gain to very low levels by fitting the monkey with goggles that provided a visual field that always was fixed with respect to the head.¹ When these goggles subsequently were replaced with reversing-prism spectacles, the animal's compensatory eye movements during passive oscillation in the light showed consistent reversal (FIGURE 1A). Though the gain of the VOR (as usual, measured in the dark) already was very low, it actually showed a further slight decrease after the animal was oscillated with reversed vision (FIGURE 1B). Thus, the adaptive mechanism in the monkey always responds to the reversed-vision situation in the same way that it responds to

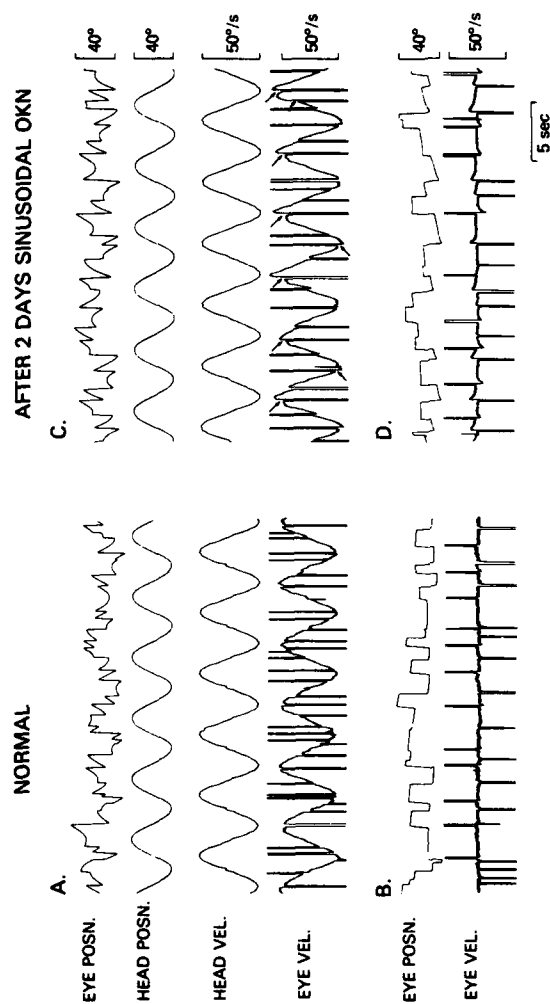


FIGURE 2. Effect of prolonged sinusoidal optokinetic stimulation (horizontal) on the monkey's horizontal eye movements in the dark. A and B: Sample records of the normal animal's eye movements when passively oscillated about the vertical (the usual VOR test situation: 0.2 Hz , $\pm 20^\circ$) and when stationary, respectively. C and D: Sample records of the animal's eye movements after two days inside an oscillating optokinetic drum (0.2 Hz , $\pm 25^\circ$ sinusoids) when passively oscillated about the vertical (0.2 Hz , $\pm 20^\circ$) and when stationary, respectively. Note the transient postsaccadic ocular drifts when the animal is stationary and the postsaccadic surges in eye velocity during oscillation (see arrows).

reducing spectacles; that both optical situations share the same kind of relationship insofar as the directions of the slip and head movement are concerned, while differing in regard to the directions of the slip and eye movement, indicates that eye movements per se are irrelevant. The computation of VOR gain errors in the monkey, therefore, appears to utilize some direct, internal measure of head velocity, with the vestibular signal itself, of course, presumably a prime candidate.

In view of the above findings, it was expected that prolonged sinusoidal optokinetic stimulation would have no significant effect on VOR gain in the monkey, and this is borne out by experiment. However, such stimulation does result in gradual changes in the monkey's saccadic control signals, and in some test situations these might be mistaken for VOR gain changes. Prolonged sinusoidal optokinetic stimulation of the monkey induces postsaccadic ocular drift, which takes the form of an exponential backward movement of the eyes after each saccade, with a time constant of a few hundred milliseconds (FIGURE 2D). During the sinusoidal oscillations used to determine the gain of the VOR, the postsaccadic ocular drifts associated with the resetting saccades have the effect of boosting the peak eye velocity (see arrows in FIGURE 2C), hence increasing the magnitude of the compensatory eye movements and the apparent gain of the VOR. However, if suitable allowance is made for these postsaccadic ocular drifts, then no significant change in VOR gain is evident. In our view, these changes are not due to adaptation in the vestibular system and show a strong resemblance to recently reported adaptive changes in the saccadic system.¹⁸

The neural commands underlying saccadic eye movements each consist of a dynamic component, or pulse, which quickly moves the eyes to a new position, and a static component, or step, which then holds the eyes there. If these two components are not matched appropriately, the eyes drift away from the new fixation point. Optican and Miles recently demonstrated that the step components are matched to the pulse components by an adaptive mechanism that, at least in part, senses postsaccadic retinal image slip.¹⁸ Using a special optical arrangement to drift the visual scene after each saccadic eye movement, these workers showed that monkeys exposed to postsaccadic retinal slip for a prolonged period exhibit exponential postsaccadic ocular drifts, which operate to minimize the artificially imposed image slip. It seems likely that the postsaccadic ocular drifts following prolonged sinusoidal optokinetic stimulation have a similar etiology. Optokinetic nystagmus consists of smooth tracking eye movements in the direction of the stimulus movement, interrupted at intervals by resetting saccades in the contrary direction. Since the velocity of the eyes consistently falls short of the velocity of the optokinetic stimulus, the animal experiences considerable retinal slip and, more particularly, postsaccadic retinal slip. Further, there is a consistent relationship between the direction of the saccadic eye movements and the direction of the retinal slip—exactly the same stimulus configuration as the one that was used to induce adaptation in the pulse-step innervation ratio for saccadic eye movements.¹⁸

Substitutes for Retinal Slip Signals?

When suddenly confronted with, say, magnifying telescopic spectacles, the normal monkey at first must endure some retinal slip during head turns, and the resulting visual signals could be used as an index of errors in the VOR. In

addition, these visual signals will activate the pursuit system, which will operate to supplement the now inadequate VOR in an attempt to stabilize the shifting images seen through the spectacles. So long as VOR gain is inadequate, pursuit will be invoked to improve retinal image stability. As the VOR gain adapts to the new conditions, the dependence on pursuit decreases. Clearly, the extent to which pursuit is consistently deployed during head turns is itself an index of the "error" in the VOR, and some central correlate of this pursuit involvement conceivably might substitute for frank visual signals in the adaptive process. This idea first occurred to us as a result of recent work on the flocculus, a structure known to be very important in the regulation of VOR gain.

In all of the species so far studied (cat, rabbit, fish, and monkey), lesions of the flocculus have resulted in severe deficits in adaptive control of VOR gain.^{7,12,19,20} It has been usual to regard the flocculus as a side loop of the VOR pathway that contains the modifiable synapses presumed to subserve adaptive gain control^{7,12} and to attribute these lesion deficits directly to loss of the variable gain element. However, the primate flocculus has been shown to have an important role in pursuit tracking. Thus, floccular lesions also result in major deficits in the monkey's performance on various ocular pursuit tasks, and single-unit recordings in the primate flocculus have shown that the activity of the most common type of output Purkinje cell (P-cell) modulates during pursuit tracking and effectively encodes gaze velocity (eye velocity relative to the stationary surroundings).²¹⁻²³ These data raise two further possible explanations for the deficits in VOR adaptation following floccular lesions in the monkey. One is that the adaptation deficits are secondary to an oculomotor insufficiency: the pursuit deficits (presumably due to loss of the gaze-velocity-signal support) effectively disrupt the adaptive mechanism as a side effect of seriously undermining the animal's ability to stabilize the retinal images seen through the telescopic spectacles. Another—and in our view, more likely—explanation is that the gaze-velocity output signals from the flocculus that are so important for pursuit also are directly involved in the induction of the modifications underlying adaptive gain control in the VOR pathways: as a "central correlate of pursuit," the discharge modulation of gaze-velocity P-cells could provide all or part of the error signal guiding recalibration of the reflex. In the remainder of this paper we examine the evidence that leads us to propose this new role for the flocculus in the adaptive regulation of VOR gain.

The Primate Flocculus: An Important Part of the Pursuit System

Our current view of the functional role of the flocculus in the generation of pursuit eye movements—based upon unit recordings, ablation, and electrical stimulation data²¹⁻²⁴—is most easily appreciated with the aid of a block diagram. In FIGURE 5, we have incorporated the gaze velocity P-cells in the flocculus into a simple model of the open-loop VOR and the negative-feedback pursuit system. The gaze-velocity-signal configuration (\dot{e}_w') is achieved by summing together two independent signals separately encoding the velocity of the eyes with respect to the head (\dot{e}_h') and the velocity of the head with respect to the surroundings (\dot{h}_w'). The head-velocity component is assumed to be vestibular in origin and is configured in the model as part of an inhibitory side loop of the vestibulo-ocular pathway. The eye-velocity component is assumed to be derived from the motor command to move the eyes (though it might equally well originate from proprioceptive input) and is configured in the model as part of a positive-feedback loop.

The existence of the latter has long been predicted by theoreticians modeling ocular pursuit,²⁵⁻²⁸ and is assumed to boost the gain of the negative-feedback pursuit system. Lesion studies²¹ suggest that the flocculus may boost the closed-loop gain of the pursuit system by as much as 40%, a very considerable improvement. However, monkeys often accomplish pursuit tasks with combined eye-head movements, substituting part of the eye movement with a head movement. It is in this situation—where the ocular component of pursuit is diminished (and hence the eye-velocity, positive-feedback boost through the flocculus also is diminished)—that the vestibular (head-velocity) component of P-cell discharge plays a crucial role in the process: it exactly compensates for the drop in the eye-velocity component. This ensures that the output from the flocculus provides the same (gaze-velocity) signal in support of tracking whatever combination of eye and head movements the animal chooses to employ.

The Primate Flocculus: A Source of "Error" Information for Adaptive Gain Control?

Since the monkey's VOR gain normally is close to unity, its gaze velocity during head turns (when not tracking) is close to zero and the gaze velocity P-cells in the flocculus show little or no modulation of their activity.^{22,23} Thus, these P-cells normally make little or no contribution to the VOR. However, when the normal monkey first wears the magnifying telescopic spectacles used to elicit VOR adaptation, he is confronted with a tracking task every time he turns his head, and uses his pursuit system to supplement the compensatory eye movements generated by the VOR. These tracking efforts will mean that gaze velocities no longer will be zero during head turns and the activity of the floccular P-cells will modulate accordingly in support of the pursuit. In fact, the discharges of the gaze-velocity P-cells will modulate during head turns whenever the monkey uses pursuit to supplement a VOR whose gain is inappropriate for the visual conditions. Such discharge behavior is exactly that expected of neurons supposedly signaling VOR gain errors.

When the animal has adapted to the magnifying spectacles, the increased magnitude of the compensatory eye movements coupled to head turns (now generated by the VOR and not pursuit) means that the eye-velocity input to the P-cell associated with a given head turn will be proportionately higher than normal; however, unit recordings in the adapted animal²⁹ reveal that this increased eye-velocity input is counterbalanced almost exactly by a proportional change (increase) in the strength of the head-velocity input signal—presumably reflecting a change in synaptic efficacy in the vestibular pathway at gain elements A and/or C in FIGURE 5. The net result of this is that P-cell discharges cease modulation during head turns when adaptation is complete (and dependence on pursuit again is minimal). Once more, this is exactly the behavior expected of neurons signaling VOR gain error. Significantly, it is not the behavior expected of neurons operating as the modifiable gain element, a point that has been argued more completely elsewhere.²⁹

VOR Gain Changes Resulting from Foveal Pursuit Tracking

If the adaptive mechanism deciphers VOR gain errors from the modulation of gaze-velocity P-cell discharge during head movements, it should be possible to

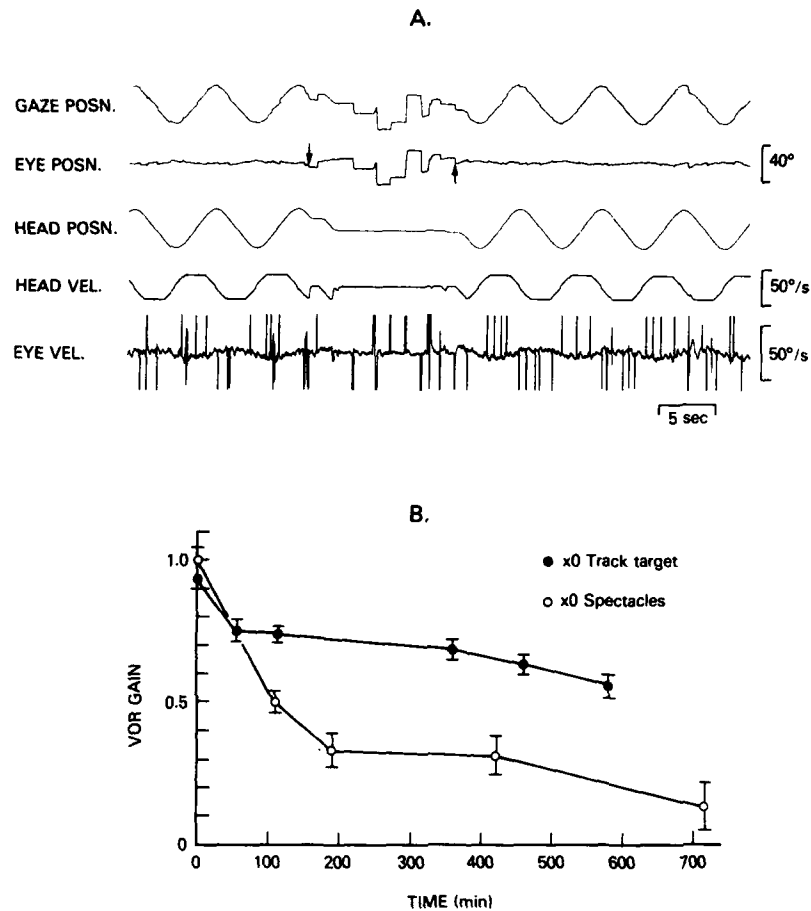


FIGURE 3. Effect on the monkey's horizontal VOR gain of prolonged horizontal oscillation during fixation of a small target that moves with the head (dark background). A: Sample records of a monkey's eye and head movements while performing the tracking task. So long as the monkey kept its eyes continuously positioned within $\pm 3^\circ$ of the target, it received a water reinforcement every 2 seconds. During these fixation periods, both the monkey and the target were oscillated together so as to induce gaze-velocity events similar to those that would be associated with $\times 0$ telescopic spectacles (achieved with fixed-field goggles). If the animal's eyes moved out of the $\pm 3^\circ$ window (e.g., downward arrow), the target spot was extinguished for 100 msec while the chair/head and the target were brought to a halt. When the animal reacquired the target (e.g., upward arrow), movement of the chair/head/target was resumed, but accelerations were very gradual so that the monkey was able to keep on target throughout. Note that gaze represents eye position with respect to the surroundings and is the sum of eye position and head position. B: Time course of the changes in a monkey's VOR gain when passively oscillated while wearing fixed-field goggles (equivalent to $\times 0$ telescopic spectacles) or while tracking a small target spot moving with the head/chair (as in A). Time refers to time actually spent looking through the spectacles or tracking and was estimated from continuous polygraph records of the animal's movements. Error bars indicate standard deviations.

design an experimental situation that elicits VOR gain changes when the only available visual inputs are foveal pursuit targets. We now report experimental evidence that demonstrates that this is indeed the case. Monkeys were seated in a special chair that could be oscillated about the vertical by a torque motor under computer control. The animals' eye movements were monitored by the electromagnetic search-coil technique, and their heads secured to the chair in the stereotaxic plane so that the axis of rotation passed through the interaural line. Fluid-deprived animals were reinforced with water for continuously fixating a small, dim target spot back-projected on to a white screen (via a servo-controlled mirror galvanometer) in otherwise totally dark surroundings. Matters were arranged so that during the periods of fixation, the monkey and the target were moved either in phase (FIGURE 3A) or 180° out of phase (FIGURE 4A) to mimic the gaze-velocity events—and presumably also the P-cell discharge modulation—normally associated with wearing reducing or magnifying telescopic spectacles, respectively. This resulted in "adaptive" changes in the gain of the VOR equal to as much as 50% of the changes produced by an equivalent amount of experience with telescopic spectacles (see FIGURES 3B and 4B). These findings are consistent with the hypothesis that the error signal guiding recalibration of the VOR is in part the modulation of gaze-velocity P-cell discharge. Of course, it is possible that the crucial ingredient in these pursuit experiments is foveal retinal slip rather than gaze velocity.

While it certainly is clear from these experiments that appreciable gain changes can be observed in the absence of peripheral retinal slip, some influence of peripheral visual inputs seems to be indicated since VOR adaptation with the foveal pursuit targets alone was much less than with the equivalent spectacles. In fact, it is possible that the flocculus P-cells provide both gaze-velocity and peripheral retinal-slip signals, especially since there is evidence that some of these cells discharge in relation to motion of the visual surround.^{30,31}

Adaptive Gain Control in the Primate VOR: A New Hypothesis

As a result of the evidence outlined above, we suggest that the modifiable elements mediating adaptive gain control in the primate VOR are located in the brain-stem pathway and are regulated by error signals generated at least in part by the flocculus P-cells. We now shall attempt to link these two ideas into a single hypothesis.

In our scheme (FIGURE 5), the gaze-velocity P-cells have been assigned two quite separate functions with but one purpose—to improve the stability of the retinal image. As a part of the pursuit system, their discharge modulation has an immediate influence upon their target neurons through conventional (inhibitory) synaptic mechanisms. As a part of the system regulating VOR gain, their persistent discharge modulation during head turns indicates errors in the VOR and has a long-term influence on the efficacy of synaptic transmission in the vestibulo-ocular pathway.

An important feature of our hypothesis is that the P-cells exert their two different influences at two different points in the vestibular pathway. Recent evidence (not reviewed here) strongly suggests that the gain of the pursuit system is insensitive to VOR gain changes.³² By contrast, the gain of the pursuit system is very sensitive to lesions of the flocculus,²¹ suggesting that the P-cells' short-term synaptic action in support of pursuit is exerted downstream of their long-term

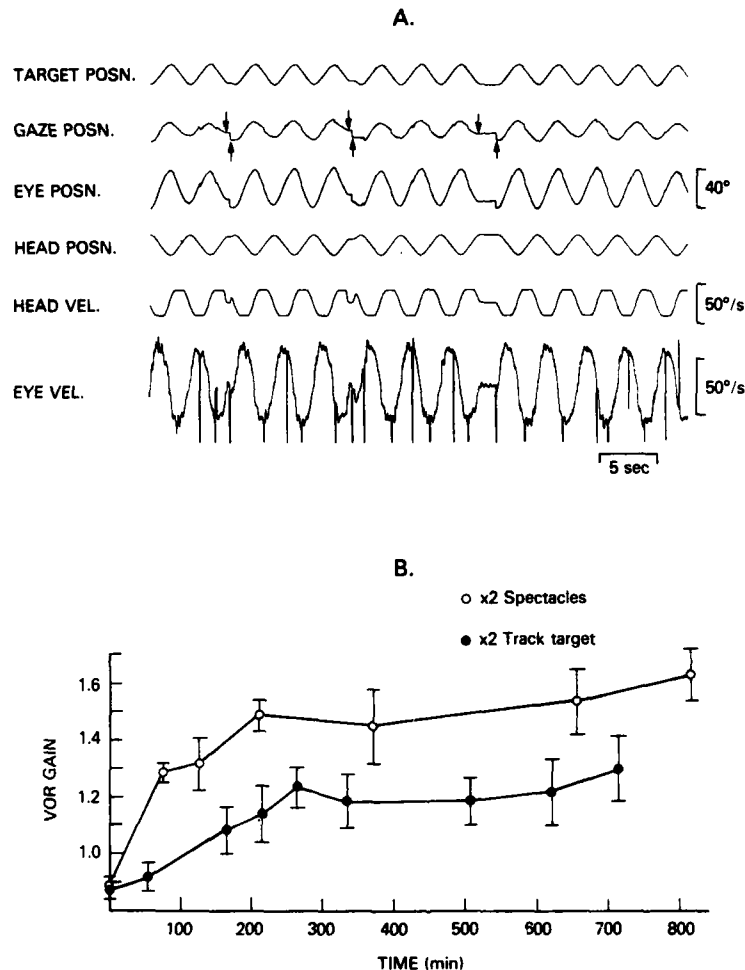


FIGURE 4. Effect on the monkey's horizontal VOR gain of prolonged horizontal oscillation during fixation of a small target that moves 180° out of phase with the head (dark background). **A:** Sample records of a monkey's eye and head movements while performing the tracking task. So long as the monkey kept its gaze (eye position with respect to the surroundings, i.e., the sum of eye position and head position) continuously positioned within $\pm 3^\circ$ of the target, it received a water reinforcement every 2 seconds. During these fixation periods, both the monkey and the target were oscillated 180° out of phase so as to induce gaze-velocity events similar to those that would be associated with $\times 2$ telescopic spectacles. If the animal's gaze moved out of the $\pm 3^\circ$ window (downward arrows), the target spot was extinguished for 100 mseconds while the chair/head and the target were brought to a halt. When the animal reacquired the target (upward arrows), movement of the chair/head/target was resumed, but accelerations were very gradual so that the monkey was able to keep on target throughout. **B:** Time course of the changes in a monkey's VOR gain when passively oscillated while wearing $\times 2$ telescopic spectacles or while tracking a small target spot moving 180° out of phase with the head/chair (as in A). Time refers to time actually spent looking through the spectacles or tracking and was estimated from continuous polygraph records of the animal's eye movements. Error bars indicate standard deviations.

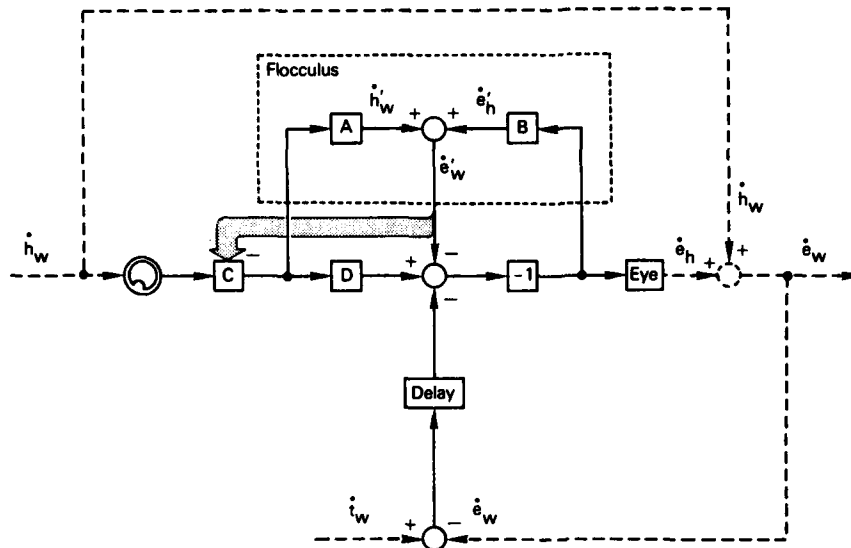


FIGURE 5. Block diagram of the VOR and pursuit system, incorporating the gaze-velocity P-cells in the flocculus. Continuous lines denote signal flow channels within the nervous system; discontinuous lines represent external, physical links denoting head velocity with respect to the world (\dot{h}_w), eye velocity with respect to the head (\dot{e}_h), eye velocity with respect to the world (\dot{e}_w , gaze velocity), and target velocity with respect to the world (\dot{t}_w). A, B, C, and D represent gain elements; \dot{h}_w' and \dot{e}_h' denote the head-velocity and eye-velocity inputs, respectively, to the P-cells in the flocculus whose discharge modulations effectively encode gaze velocity (\dot{e}_w'). Broad arrow indicates the hypothesized long-term regulatory influence of the P-cells on the postulated modifiable gain element in the vestibular pathway (element C).

modulatory action. Another feature of our scheme is that the P-cells' long-term influence must be exerted above the point from which the P-cells derive their own vestibular input. This is assumed to be at gain element C in FIGURE 5 (though parallel changes at gain elements A and D—which would be operationally equivalent, albeit more complex—cannot be ruled out). It is vital for the functioning of our model that there be reciprocal connections between the P-cells and the vestibular relay cells in the brain stem, organized in essence as an internal negative-feedback loop that is concerned with long-term regulation rather than short-term compensation. Thus, we envisage a local feedback loop operating (very slowly) to achieve zero modulation of P-cell discharge during head turns: persistent modulations of P-cell discharge ("errors") induce changes in the gain of the vestibular input that in turn operate to reduce those modulations. Single-unit data²⁹ indicate that the P-cell output is indeed regulated in this manner, producing minimal discharge modulation during head turns in the fully adapted state.

The problem now is to explain how a control loop that is entirely internal and functions to minimize P-cell discharge modulation can at the same time achieve an appropriate VOR gain calibration. The crucial factor is the eye-velocity input to the P-cell: this signal is assumed to retain a reliable, constant relationship to

eye velocity (something that could be achieved by an internal negative-feedback network within the cerebellar cortex) and to provide the internal standard against which everything else must be calibrated.

In order to appreciate how this scheme would work, consider the chain of events set in motion when the normal monkey first wears magnifying telescopic spectacles. Initially, there is considerable retinal slip during head turns and the pursuit system takes on the immediate responsibility of augmenting the compensatory eye movements generated by the now inadequate VOR. In the flocculus, this results in an elevated eye-velocity-signal input to the P-cell, whose discharge as a consequence now modulates during head turns. In effect, this eye-velocity signal is the P-cells' external reference and, together with any visual inputs that they may also receive (not indicated in FIGURE 5), provides the P-cells' only link—albeit indirect, via the pursuit system—with the external visual world. If the monkey continues to wear the spectacles, the persistent modulation of P-cell discharge due to the elevated eye-velocity-signal input is assumed to induce a gradual increase in the gain of element C. This would result in (1) an increase in the gain of the VOR, which would gradually transfer the burden of generating larger compensatory eye movements from the pursuit system to the VOR, and (2) an increase in the head-velocity-signal input to the flocculus P-cells, which would operate to offset the augmented eye-velocity signal and, hence, gradually reduce the P-cells' discharge modulation during head turns. We assume that this process would continue until eventually the P-cells are receiving head-velocity inputs that once more balance their eye-velocity inputs during head turns in the light. (Note that at all times during the adaptation, P-cell discharge modulation will be minimal during head turns in the dark.) When VOR gain becomes appropriate for the visual conditions, head turns in the light will be associated with the same compensatory eye velocities as head turns in the dark and modulation of P-cell discharge will be minimal. At this point, we have come full circle: the responsibility for generating the now larger compensatory eye movements has shifted from the pursuit system back to the vestibular, and the error signal (P-cell discharge modulation) has returned to zero.

REFERENCES

1. MILES, F. A. & B. B. EICHMY. 1980. Long-term adaptive changes in primate vestibulo-ocular reflex. I. Behavioral observations. *J. Neurophysiol.* **43**: 1406-1425.
2. GONSHOR, A. & G. MELVILL JONES. 1971. Plasticity in the adult human vestibulo-ocular reflex arc. *Proc. Can. Fed. Biol. Sci.* **14**: 11.
3. GONSHOR, A. & G. MELVILL JONES. 1976. Short-term adaptive changes in the human vestibulo-ocular reflex arc. *J. Physiol. London* **256**: 361-379.
4. GONSHOR, A. & G. MELVILL JONES. 1976. Extreme vestibulo-ocular adaptation induced by prolonged optical reversal of vision. *J. Physiol. London* **256**: 381-414.
5. GAUTHIER, G. M. & D. A. ROBINSON. 1975. Adaptation of the human vestibulo-ocular reflex to magnifying lenses. *Brain Res.* **92**: 331-335.
6. MILES, F. A. & J. H. FULLER. 1974. Adaptive plasticity in the vestibulo-ocular responses of the rhesus monkey. *Brain Res.* **88**: 512-516.
7. ROBINSON, D. A. 1976. Adaptive gain control of vestibuloocular reflex by the cerebellum. *J. Neurophysiol.* **39**: 954-969.
8. MELVILL JONES, G. & P. DAVIES. 1976. Adaptation of cat vestibulo-ocular reflex to 200 days of optically reversed vision. *Brain Res.* **103**: 551-554.
9. KELLER, E. L. & W. PRECHT. 1979. Adaptive modification of central vestibular neurons in response to visual stimulation through reversing prisms. *J. Neurophysiol.* **42**: 896-911.
10. COLLEWIJN, H. & A. F. GROOTENDORST. 1978. Adaptation of the rabbit's vestibulo-ocular

- reflex to modified visual input: importance of stimulus conditions. *Arch. Ital. Biol.* **116**: 273-280.
11. COLLEWIJN, H. & A. F. GROOTENDORST. 1979. Adaptation of optokinetic and vestibulo-ocular reflexes to modified visual input in the rabbit. *Prog. Brain Res.* **50**: 772-781.
 12. ITO, M., T. SHIIDA, N. YAGI & M. YAMAMOTO. 1974. The cerebellar modification of rabbit's horizontal vestibulo-ocular reflex induced by sustained head rotation combined with visual stimulation. *Proc. Jpn. Acad.* **50**: 85-89.
 13. ITO, M., P. J. JASTREBOFF & Y. MIYASHITA. 1979. Adaptive modification of the rabbit's horizontal vestibulo-ocular reflex during sustained vestibular and optokinetic stimulation. *Exp. Brain Res.* **37**: 17-30.
 14. GREEN, A. E. & J. WALLMAN. 1978. Rapid change in gain of vestibulo-ocular reflex in chickens. *Neurosci. Abstr.* **4**: 163.
 15. SCHAIRER, J. O. & M. V. L. BENNETT. 1977. Adaptive gain control in vestibulo-ocular reflex of goldfish. *Neurosci. Abstr.* **3**: 157.
 16. SCHAIRER, J. O. & M. V. L. BENNETT. 1978. VOR gain changes produced by target rotation without head movement in goldfish. *Neurosci. Abstr.* **4**: 167.
 17. ITO, M. 1972. Neural design of the cerebellar motor control system. *Brain Res.* **40**: 81-84.
 18. OPTICAN, L. M. & F. A. MILES. 1979. Visually induced adaptive changes in oculomotor control signals. *Neurosci. Abstr.* **5**: 380.
 19. SCHAIRER, J. O. & M. V. L. BENNETT. 1980. Cerebellectomy in goldfish prevents adaptive gain control of the VOR without affecting the optokinetic system. In *Neuroscience Satellite Symposium on Vestibular Function and Morphology*. T. Gualtierotti, Ed. Springer-Verlag, New York, N.Y. (In press.)
 20. OPTICAN, L. M., D. S. ZEE, F. A. MILES & S. G. LISBERGER. 1980. Oculomotor deficits in monkeys with floccular lesions. *Neurosci. Abstr.* **6**: 474.
 21. ZEE, D. S., A. YAMAZAKI & G. GUCER. 1978. Ocular motor abnormalities in trained monkeys with floccular lesions. *Neurosci. Abstr.* **4**: 168.
 22. LISBERGER, S. G. & A. F. FUCHS. 1978. Role of primate flocculus during rapid behavioral modification of vestibuloocular reflex. I. Purkinje cell activity during visually guided horizontal smooth-pursuit eye movements and passive head rotation. *J. Neurophysiol.* **41**: 733-763.
 23. MILES, F. A., J. H. FULLER, D. H. BRAITMAN & B. M. DOW. 1980. Long-term adaptive changes in primate vestibuloocular reflex. III. Electrophysiological observations in flocculus of normal monkeys. *J. Neurophysiol.* **43**: 1437-1476.
 24. RON, S. & D. A. ROBINSON. 1973. Eye movements evoked by cerebellar stimulation in the alert monkey. *J. Neurophysiol.* **36**: 1004-1022.
 25. FENDER, D. H. 1962. The eye-movement control system: evolution of a model. In *Neural Theory and Modeling*. R. F. Reiss, Ed.: 306-324. Stanford University Press, Stanford, Calif.
 26. FENDER, D. H. & P. W. NYE. 1961. An investigation of the mechanisms of eye movement control. *Kybernetik* **1**: 81-88.
 27. YOUNG, L. R., J. D. FORSTER & N. VAN HOUTTE. 1968. A revised stochastic sampled data model for eye tracking movements. In *Proceedings, Fourth Annual NASA-University Conference on Manual Control*. NASA SP-192: 489-509. National Aeronautics and Space Administration, Washington, D.C.
 28. ROBINSON, D. A. 1971. Models of oculomotor neural organization. In *The Control of Eye Movements*. P. Bach-y-Rita & C. C. Collins, Eds.: 519-538. Academic Press, Inc., New York, N.Y.
 29. MILES, F. A., D. J. BRAITMAN & B. M. DOW. 1980. Long-term adaptive changes in primate vestibuloocular reflex. IV. Electrophysiological observations in flocculus of adapted monkeys. *J. Neurophysiol.* **43**: 1477-1493.
 30. NODA, H. & D. A. SUZUKI. 1978. Purkinje cell activity in the monkey flocculus during smooth pursuit eye movement. *Neurosci. Abstr.* **4**: 167.
 31. WARABI, T., H. NODA & N. ISHII. 1979. Effect of retinal image motion upon flocculus Purkinje cell activity during smooth pursuit eye movements. *Neurosci. Abstr.* **5**: 108.
 32. LISBERGER, S. G., F. A. MILES, L. M. OPTICAN & B. B. EICHMY. 1981. Optokinetic response in monkey: underlying mechanisms and their sensitivity to long-term adaptive changes in vestibuloocular reflex. *J. Neurophysiol.* **45**: 869-890.

A NEW NEUROTOLOGICAL TEST FOR DETECTING CEREBELLAR DYSFUNCTION

Toshiaki Yagi, Motohiro Shimizu, Suji Sekine,
and Tomokazu Kamio

*Department of Otolaryngology
Nippon Medical School
Tokyo, Japan 113*

Jun-Ichi Suzuki

*Department of Otolaryngology
Teikyo University School of Medicine
Tokyo, Japan 173*

The vestibulo-ocular reflex (VOR) helps maintain a stable retinal image by generating compensatory eye movements to offset the effects of head rotation. This reflex is plastic and adaptable, as demonstrated by observations of human and animal subjects wearing vision-reversal prisms.¹⁻⁴ Recent experiments demonstrated that the visual and vestibular inputs for the VOR are integrated in the vestibulocerebellum,⁵⁻⁹ and Robinson has demonstrated in the cat that the plasticity of the VOR is abolished after removal of the vestibulocerebellum.¹⁰

On the basis of these studies, it can be expected that the observation of the adaptation of the VOR to reversing prisms may lead to detection of cerebellar dysfunction. The present study was undertaken to examine clinical applications of the response of the VOR to right-left image-reversing prisms. Both normal subjects and patients with cerebellar lesions were tested.

METHODS

Twenty-six adults (12 males and 14 females), ranging in age from 19 to 34 years, who were free from vestibular and oculomotor disorders were employed. Subjects sat on a chair that was rotated sinusoidally in a horizontal plane at 0.25 Hz and 30° angular amplitude. Eye movement (E), eye velocity (\dot{E}), and head movement (H) were recorded, using electronystagmography.

FIGURE 1 shows the test sequence of this experiment. First, the subjects were asked to watch a small, dim light fixed approximately two meters in front of the chair in the darkened room (baseline). Next, the subjects' eyes were covered by blackout goggles (initial level). After that, the subjects wore right-left image-reversal prisms. During the image-reversal condition, the subjects were asked to watch the dim light. Every 15 minutes, the subjects wore the blackout goggles over the reversing prisms and E , \dot{E} , and H were recorded in addition to the baseline and initial-level recordings. Each recording consisted of 10 to 20 sinusoidal rotations. Subjects did mental arithmetic to maintain arousal during recordings. The experiment was carried out in darkness, except for the small, dim target light used during forced adaptation.

Gain and phase of the VOR were calculated for each subject as follows. The relative VOR gain (G) was estimated as the ratio of eye velocity in the baseline condition (\dot{E}_b) to the eye velocity in the eyes-covered condition (\dot{E}_x): $G = \dot{E}_b / \dot{E}_x$. In

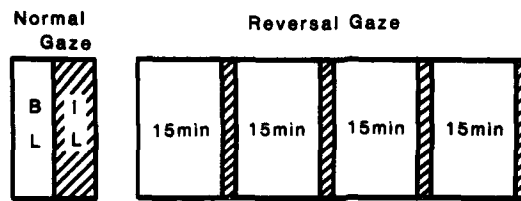


FIGURE 1. Schematic diagram of experimental sequence. VOR measurements were made in the blackout conditions (shaded areas) and expressed as gain relative to measurements in the baseline condition. BL and IL indicate baseline and initial level, respectively.

order to observe net adaptation, the adaptation index also was calculated. The adaptation index can be expressed as the ratio of initial level to gain after 15, 30, 45, and 60 minutes of wearing prisms. Phase was determined at the zero crossing. Phase was calculated as the value in each condition (θ_x) relative to the phase in the baseline condition (θ_{bl}); $\text{VOR phase} = \theta_x - \theta_{bl}$. Gain and phase measurements were based on the means of at least eight cycles.

RESULTS

Means and standard deviations of VOR gain in darkness before (initial level) and after wearing prisms (15, 30, 45, and 60 minutes) were 0.65 ± 0.12 , 0.45 ± 0.16 , 0.38 ± 0.14 , 0.37 ± 0.11 , and 0.33 ± 0.10 , respectively. After forced adaptation by right-left reversal, VOR gain gradually decreased (filled circles in FIGURE 2). VOR gains during the gaze reversal condition in the intervals between the

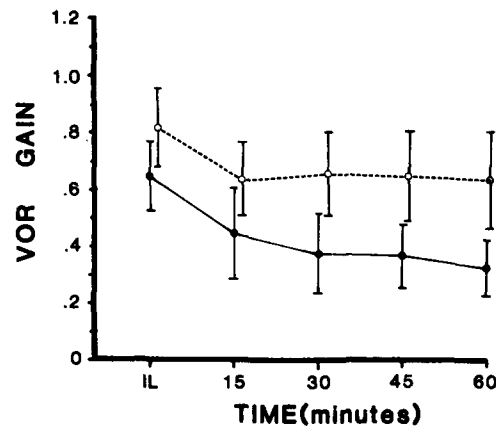


FIGURE 2. Means (filled and open circles) and standard deviations (vertical bars) of the sequential VOR gain changes during 60 minutes of forced vision reversal. Filled circles and open circles indicate mean VOR gains from 26 normal subjects and 26 patients with cerebellar lesions, respectively. IL indicates the initial level (VOR in darkness before gaze reversal).

blackout test period were the same as in the normal gaze condition, but 180° out of phase. The adaptation indexes (VOR gain after gaze reversal/initial level) of each subject also were calculated. Means and standard deviations of adaptation indexes after 15, 30, 45, and 60 minutes were 0.69 ± 0.18 , 0.58 ± 0.17 , 0.58 ± 0.12 , and 0.52 ± 0.12 , respectively.

Means and standard deviations of the VOR phase in darkness before and after wearing prisms (15, 30, 45, and 60 minutes) were 9.1 ± 19.9 , 5.9 ± 14.1 , 7.4 ± 20.7 , 9.4 ± 13.4 , and 10.5 ± 16.4 , respectively. Statistically, no significant difference was found between any two pairs (t-test).

CLINICAL APPLICATION

Twenty-six subjects with cerebellar lesions, which had been confirmed by neurotological examinations and x-ray studies, mainly CT-scan, were tested. The test method was the same as for normal subjects. The diagnoses of these cases were cerebellar atrophy (11), epidermoid tumor (4), acoustic tumor (2), vascular origin (bleeding, 2; arterio-venous (AV) malformation, 2; thrombosis, 1), astrocytoma (1), glomus jugulare tumor (1), and metastatic tumor (1).

The VOR gains from the 26 cases are illustrated in FIGURE 2 (open circles). The mean initial level of gain was 0.83. This value was higher than that of normal subjects (0.65). However, 11 cases among the 26 showed normal values in this situation. Means and standard deviations of VOR gains from these cases 15, 30, 45, and 60 minutes after wearing prisms were 0.64 ± 0.14 , 0.66 ± 0.15 , 0.65 ± 0.16 , and 0.64 ± 0.17 , respectively. These values were clearly higher than those of normal subjects. Also, except for 1 case, no abnormal subject had a normal-range value after 1 hour of vision reversal. As this may be due to the higher initial level, an adaptation index was calculated, as described in the methods section. Means and standard deviations of the adaptation index after wearing prisms for 15, 30, 45, and 60 minutes were 0.79 ± 0.16 , 0.81 ± 0.16 , 0.79 ± 0.16 , and 0.77 ± 0.16 , respectively. This indicates that the net adaptation was reduced in the cases with cerebellar lesions. However, 5 cases among the 26 showed normal values after 60 minutes of forced adaptation.

FIGURE 3 shows the relationship between the initial level and the adaptation index after one hour. From this figure, three different pathological conditions can be noted.

Fifteen cases among the 26 showed abnormally high gain in the initial level. Five of the 15 exhibited normal adaptation after the one-hour forced adaptation task. The other 11 cases out of the 26 showed normal values of VOR gain in the initial level, but abnormal reductions of adaptation were observed. These different conditions are summarized as type A, higher initial level and abnormal adaptation (10 cases); type B, higher initial level and normal adaptation (5 cases); and type C, normal initial level and abnormal adaptation (11 cases).

Among the 10 patients who had type-A responses, there were 6 cases that had initial levels above 0.85 and one-hour adaptation indexes above 0.80. The diagnoses of these cases were atrophy (2), metastatic tumor in the vermis (1), cerebellar bleeding (1), astrocytoma (1), and AV malformation (1). According to the results of neurotological tests and CT-scan, these cases had severe widespread or midline lesions of the cerebellum, and most of the cases showed brain-stem lesions as well.

Two cases among the five patients who showed type-B responses exhibited scores above 0.85 in the initial level and less than 0.80 on the adaptation index.

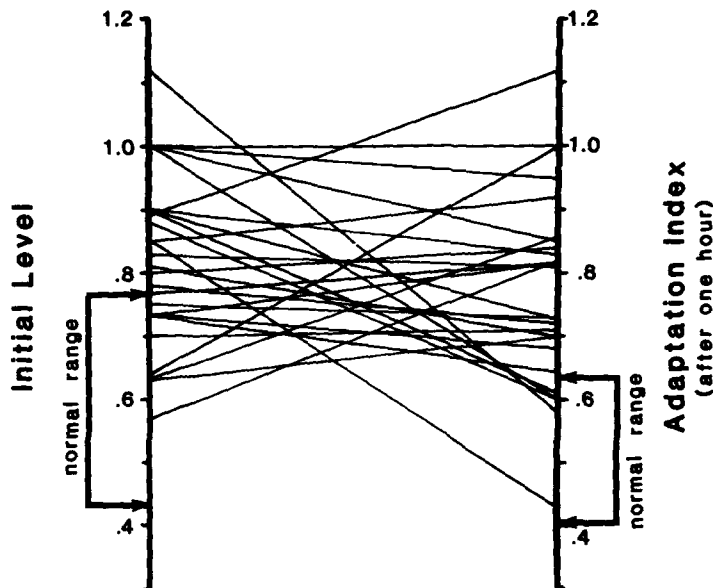


FIGURE 3. Relationship between the initial level of the VOR gain and the adaptation index after the one-hour forced-adaptation task for 26 patients with cerebellar lesions. Normal ranges (two standard deviations) of both initial level and adaptation index are indicated by arrows.

The diagnoses of these two cases were cerebellar atrophy. The results of neurotological examinations and CT-scan revealed that the cerebellar lesions were much milder than those of type-A cases, and there were no findings that indicated brain-stem lesions.

Three cases among the 11 patients who showed type-C responses had scores less than 0.65 in the initial level and above 0.80 on the adaptation index. The diagnoses of these cases were cerebellar tumors. Neurotological examinations and CT-scan revealed that the lesions were located in one side of the cerebellum and that there was little or no brain-stem dysfunction.

Phase changes of the VOR were calculated from 26 patients, but no statistical difference was found between values from abnormal subjects and values from normal subjects.

DISCUSSION

The vestibulo-ocular reflex helps maintain a stable retinal image during head movements. When subjects wearing horizontal reversing prisms are asked to watch a stationary target during sinusoidal rotation, the visual and vestibular inputs will be opposite in direction and there should be slippage of the retinal image. However, the subjects can see the image without blurring because of the adaptive function of the vestibulocerebellum.

Plastic changes of cerebellar function in the VOR, induced by vision-reversal prisms, recently have been studied extensively in human subjects and in animals.^{1-4,10} Gonshor and Melvill Jones reported that in human subjects, the VOR gain was reduced substantially during the first 2 days of vision reversal; reduction of gain continued, reaching a minimum by the end of 1 week at about 25% of normal value.² Melvill Jones and Davies studied VOR adaptation in cats that were exposed to long-term (200 days) horizontal reversal of vision.³ They found rapid attenuation of VOR gain after the initiation of vision reversal. After about 2 weeks, the phase changed sharply in the lagging direction.

Robinson reported the mechanisms of the adaptive control of VOR gain from lesion-making experiments in cats that chronically wore right-left vision-reversal prisms.¹⁰ He observed gain increase and abolition of the plastic changes after removal of the vestibulocerebellum. From these results, he concluded that the adaptation process is distributed widely in the vestibulocerebellum.

In the present study, normal subjects showed rapid adaptation of gain while wearing reversing prisms. The reduction was to about 50% the normal value at the end of one hour of sinusoidal stimulation. This is more rapid than the values that were reported by Gonshor and Melvill Jones,² perhaps because in our experiment the subjects were asked to watch a target light during rotation, while in Gonshor and Melvill Jones' study, the subjects did not receive a forced adaptation task.

Regarding phase changes, the present study showed none within one hour. Since the phase changes are reported by Gonshor and Melvill Jones to start slowly,² this finding seems reasonable.

In the present study, 15 cases among the 26 with cerebellar lesions showed high gain in the eyes-covered condition in the dark (initial level). This abnormally high gain already has been observed by Zee *et al.* and Baloh *et al.*^{11,12} They speculated that the cause of this phenomenon is the absence or reduction of cerebellar inhibition of the VOR. Five cases among these 15 showed normal adaptation (type B) after wearing prisms. This fact suggests that the mechanisms of VOR gain control in darkness and the process of adaptation to vision reversal have different anatomical locations. This speculation is supported further by the findings of the present study. Ten cases exhibited normal reduction of adaptation (type C). Eleven other cases showed both abnormalities: high gain and reduction of adaptation (type A). The cases that showed the clearest type-A responses tended to have severe widespread or midline lesions of the cerebellum. The cases that showed characteristic type-B responses had mild cerebellar atrophy, and the cases that showed typical, clearly defined type-C responses tended to have lesions limited to one side of the cerebellum. From these results, the following speculations can be stated. In order to evoke adequate VOR gain in darkness, it is sufficient to have half of the cerebellum intact. However, in order to produce normal VOR adaptation to image reversal, it is necessary to have the cerebellum intact or, at worst, only mild lesions.

There are several useful neurotological test methods—such as the visual suppression test and the VOR examination test¹¹⁻¹³—for detecting cerebellar dysfunctions. However, although these tests are able to detect dysfunctions of the VOR arc, they cannot identify more precisely the anatomical or functional site of the cerebellar lesions. On the basis of the present study, it may be possible, by observation of the adaptation of the VOR to vision-reversal prisms, to detect cerebellar lesions that are, by their nature or subtlety, impossible to find with established tests.

SUMMARY

The adaptation of the vestibulo-ocular reflex (VOR) was studied in 26 normal subjects and 26 patients with cerebellar lesions, using horizontal vision-reversal prisms. In normal subjects, the adaptation of gain after wearing prisms for one hour was approximately 50% of the VOR value in the dark. In contrast to this, patients with cerebellar lesions showed less adaptation—approximately 20% after a one-hour forced adaptation task. These were type A, higher gain in the initial level and abnormal adaptation (10 cases); type B, higher gain in the initial level and normal adaptation (5 cases); and type C, normal initial level and abnormal adaptation (11 cases). The cases showing the typical type-A responses tended to have severe widespread or midline lesions of the cerebellum. Typical type-B cases had mild cerebellar lesions, and typical type-C cases tended to have lesions restricted to one side of the cerebellum. From these results, it can be speculated that reduction of VOR adaptation occurs when one side of the cerebellum has severe lesions, but it is sufficient to produce a normal vestibulo-ocular reflex if at least half of the cerebellum is intact.

REFERENCES

1. GONSHOR, A. & G. MELVILL JONES. 1976. Short-term adaptive changes in the human vestibulo-ocular reflex arc. *J. Physiol.* **356**: 361-379.
2. GONSHOR, A. & G. MELVILL JONES. 1976. Extreme vestibulo-ocular adaptation induced by prolonged optical reversal vision. *J. Physiol.* **256**: 381-414.
3. MELVILL JONES, G. & P. DAVIES. 1976. Adaptation of cat vestibulo-ocular reflex to 200 days of optically reversed vision. *Brain Res.* **103**: 551-554.
4. MILES, F. A. & J. H. FULLER. 1974. Adaptive plasticity in the vestibulo-ocular responses of the rhesus monkey. *Brain Res.* **72**: 512-516.
5. ITO, M. 1972. Neural design of the cerebellar motor control system. *Brain Res.* **40**: 81-84.
6. ITO, M., N. NISHIMURA & M. YAMAMOTO. 1977. Special patterns of neuronal connections in the control of the rabbit's vestibulo-ocular reflexes by the cerebellar flocculus. *J. Physiol.* **265**: 833-854.
7. MAEKAWA, K. & J. I. SIMPSON. 1973. Climbing fiber responses evoked in vestibulocerebellum of rabbit from visual system. *J. Neurophysiol.* **36**: 649-666.
8. MAEKAWA, K. & T. TAKEDA. 1975. Mossy fiber responses evoked in the cerebellar flocculus of rabbits by stimulation of the optic pathway. *Brain Res.* **98**: 590-595.
9. MAEKAWA, K. & T. TAKEDA. 1976. Electrophysiological identification of the climbing and mossy fiber pathways from the rabbit's retina to the contralateral cerebellary flocculus. *Brain Res.* **109**: 169-174.
10. ROBINSON, D. A. 1976. Adaptation gain control of vestibulo-ocular reflex by the cerebellum. *J. Neurophysiol.* **39**: 954-969.
11. ZEE, D. S., R. D. YEE, D. G. COGAN, D. A. ROBINSON & W. K. ENGEL. 1976. Ocular motor abnormalities in hereditary cerebellar ataxia. *Brain* **99**: 207-243.
12. BALOH, R. W., H. A. JENKINS, V. HONRUBIA, R. D. YEE & C. G. Y. LAU. 1979. Visual-vestibular interaction and cerebellar atrophy. *Neurology* **29**: 116-119.
13. TAKEMORI, S. 1977. Visual suppression test. *Ann. Otol. Rhinol. Laryngol.* **86**: 80-85.

FURTHER OBSERVATIONS ON THE PHENOMENON OF REBOUND NYSTAGMUS

J. D. Hood

*Medical Research Council
Hearing and Balance Unit
Institute of Neurology
National Hospital
London, WC1N 3BG, England*

In 1973 Hood, Kyan, and Leech described a form of spontaneous nystagmus termed rebound, which had certain remarkable distinguishing characteristics.¹ In general the nystagmus, which is vestibular in character, makes its appearance as a first-degree nystagmus on gaze deviation, either to the right or to the left. If, however, the gaze is maintained for some 20 seconds or more, the nystagmus fatigues. Thereafter it may disappear altogether and occasionally may even reverse its direction. If at this point the eyes are returned briskly to the primary position, a transient second-degree nystagmus is induced, beating in the opposite direction to that of the preexisting deviation. In this way a second-degree nystagmus to left or to right which is not normally present can be elicited repeatedly, provided only that the initiating gaze deviation is maintained for a sufficiently long period of time. A typical tracing of rebound nystagmus is shown in FIGURE 1.

In our experience, patients presenting with rebound nystagmus consistently reveal deranged tracking movements and optokinetic nystagmus together with absent or reduced vestibulo-ocular reflex (VOR) suppression, which routinely manifests itself as a marked enhancement of the caloric responses when the tests are carried out in the presence of optic fixation. In addition, there is now a substantial body of evidence that supports our view that this form of nystagmus is associated uniquely with cerebellar disease and in consequence is a diagnostic sign of some significance.²⁻⁵

Since our original report, we have had the opportunity of examining a number of patients with rebound nystagmus who have in addition presented with certain interesting features that seem to be related to the rebound and that throw new light upon its underlying nervous mechanism.

Consider first the form of the nystagmus itself. Originally we made the assumption that, as with other types of vestibular nystagmus, it was brought about by some form of tonic imbalance that provoked the slow component and took the eyes away from the target, so that the fast component could be considered as a corrective movement that returned the eyes thereto. In the normal course of events, electronystagmography is not helpful in establishing with any accuracy the actual position of the eyes relative to the target. However, in some, admittedly rare patients, in whom the nystagmus on sustained gaze deviation actually undergoes a reversal of direction, certain important inferences would seem to be justified.

Consider the trace shown in FIGURE 2. With attempted gaze fixation upon a target deviated 30° to the right, a nystagmus to the right is initiated, which ceases after 15 seconds. Following a short period of steady gaze, it then reappears beating in the opposite direction. It follows that since these are d.c. recordings,

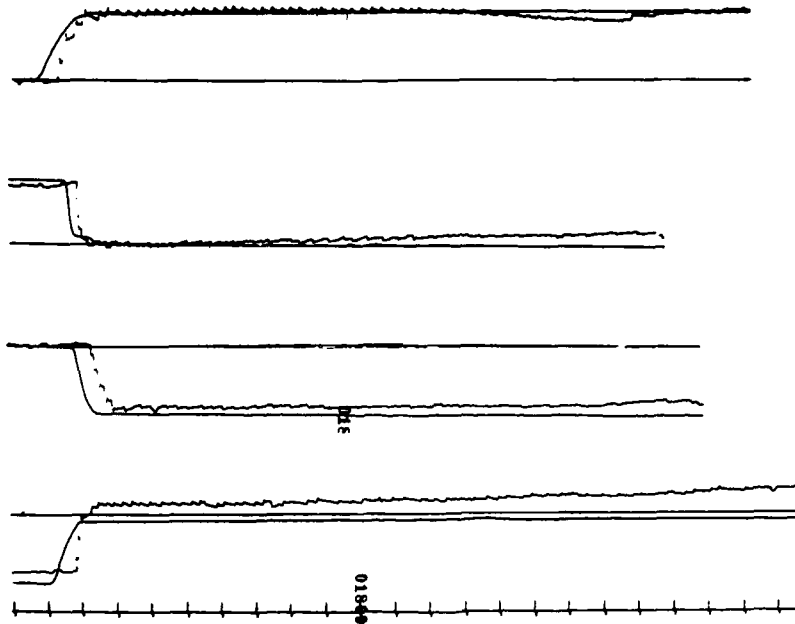


FIGURE 1. Rebound nystagmus. The tracing is continuous throughout and begins with the eyes deviated 30° to the right followed by straight-ahead gaze, deviation 30° to the left, and finally a return to straight-ahead gaze. Note the fatigability of the nystagmus in all directions of gaze and the reversal of the direction of the nystagmus in the two tracings of straight-ahead gaze.

the steady, center part of the tracing can be taken to indicate the patient's line of sight upon the target. Projecting this line to right and to left, it will be seen that it coincides in each case with the termination of the slow phases of the nystagmus. In other words, the surprising conclusion, contrary to our original assumption, is that it is the fast phase of the nystagmus that takes the eyes away from the target and the slow phase that returns it thereto.

These same events now have been observed in a number of patients and seem to mark an important distinction between the underlying mechanism of rebound nystagmus and that of any other form of vestibular nystagmus.

More recently, additional new evidence has come to light derived from six patients, all with well marked rebound nystagmus, upon whom we were able to carry out a variety of other test procedures. The neurological diagnosis was cerebellar atrophy in three patients, multiple sclerosis in two, and cerebellar cyst in one. Similar results were obtained from all of them, and can best be exemplified with one illustrative case.

Let us consider first the spontaneous nystagmus itself. In order to establish the effect of the maintenance of gaze deviation upon the magnitude of the rebound, patients were required to fix their gaze on targets deviated 30° to left or right for varying periods of time from 5 seconds to 30 seconds.

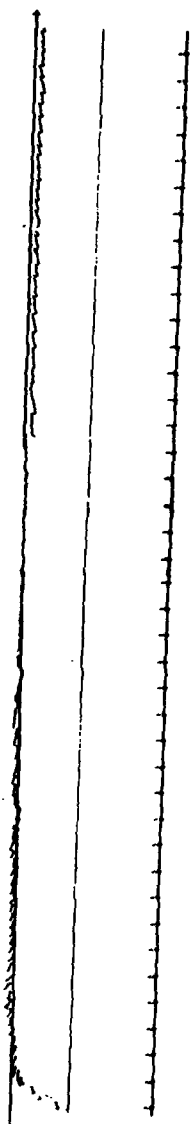


FIGURE 2. Rebound nystagmus showing reversal in direction of nystagmus consequent upon sustained gaze deviation 30° to the right. Lower tracings are enlarged sections of tracings shown above. Time, seconds.

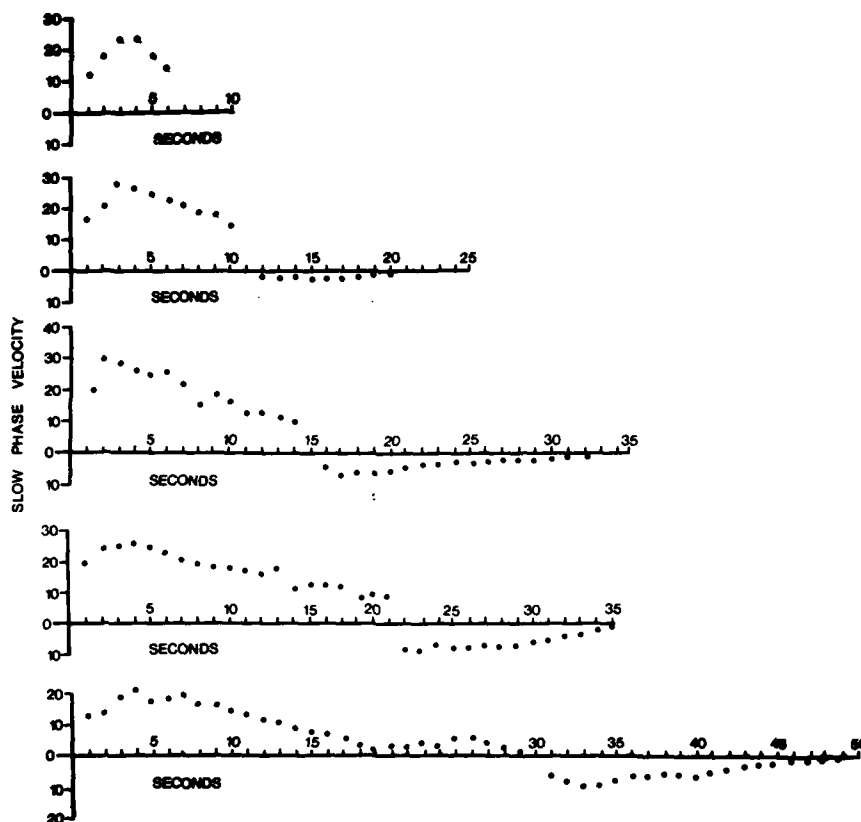


FIGURE 3. Slow-component velocities of rebound nystagmus induced by sustained gaze deviations of 5 to 30 seconds.

The results, expressed for convenience in terms of the slow-component velocity of the nystagmus, are shown in FIGURE 3.

As will be seen, the longer the deviation is sustained, the greater is the magnitude of the rebound, both in respect to its slow-component velocity and to its duration. In fact, the rebound seems to be a reflection of the initial nystagmic response in respect to both these parameters.

These same events are equally apparent in the responses to rotational stimuli shown in FIGURE 4. The stimulus was an impulsive rotation of the chair to $20^\circ/\text{second}$ or $40^\circ/\text{second}$. Thereafter a constant velocity was maintained for a prolonged period of time before the chair was abruptly brought to rest.

The data again are presented in terms of the slow-component velocities of the resultant nystagmic responses, recorded in total darkness with eyes open. Following the initial responses to the start and stop stimuli, it will be seen that the nystagmus undergoes multiple reversal, the duration of each reversal varying randomly from about 50 to 100 seconds. In fact as many as five reversals occur in response to the $40^\circ/\text{second}$ stimulus and three to the $20^\circ/\text{second}$ stimulus.

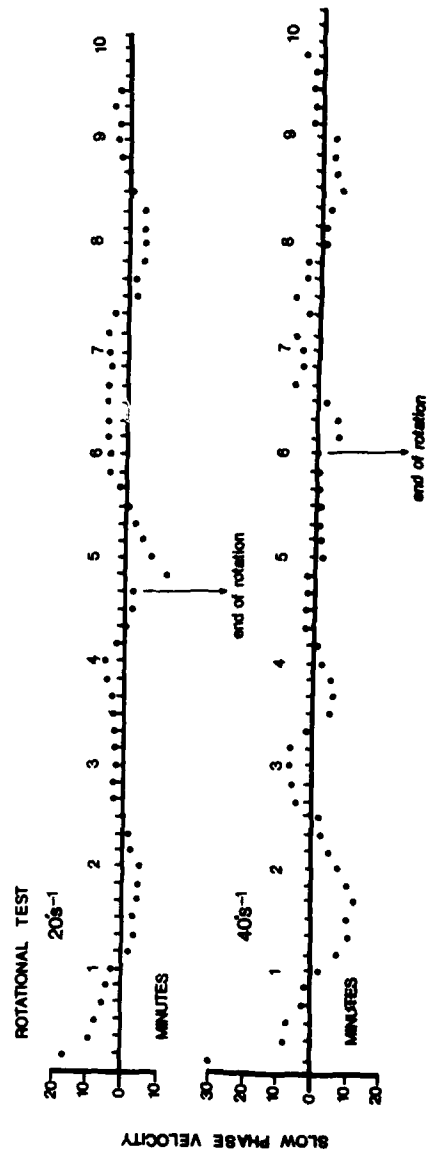


FIGURE 4. Slow-component velocities of nystagmic response to impulsive rotational stimuli of 20°/second and 40°/second. Note multiple rebound to both start and stop stimuli.

In FIGURE 5 are shown the computed responses to a caloric stimulus, again recorded in darkness.

At the termination of the initial response, the nystagmus again undergoes multiple reversal of direction, but on this occasion each reversal is long lasting, reflecting as with the rotational stimulus the duration of the primary response.

It would seem, therefore, that irrespective of the nature of the initiating stimulus, the response rebounds and its magnitude and duration both are functions of the primary response. We had the opportunity of examining one patient strapped to a stretcher, which could be rotated spit-like about the horizontal axis. Rotation at constant velocity in this manner induces a persistent nystagmic response, the mechanism of which remains obscure; nevertheless, even this unusual form of nystagmus underwent multiple reversal. In addition, it is not without interest that Kato *et al.* reported the occurrence of what they termed polyphasic positional nystagmus in four patients, all of whom presented with rebound nystagmus.³ In these patients the initial positional nystagmic response underwent as many as four distinct reversals of direction.

DISCUSSION

On the face of it, these are remarkable phenomena; nevertheless, they bear certain striking resemblances, albeit in an exaggerated form, to similar responses that can be elicited in the normal subject.

Take the rebound nystagmus itself. If gaze is maintained in extreme deviation for a sufficiently long period of time, it is not unusual to induce in a normal subject a fine nystagmus beating in the direction of the gaze. On return to the primary position, a few beats in the opposite direction invariably occur.

In respect to rotational tests, it is unusual nowadays to use impulsive stimuli in excess of 60°/second, and in consequence the finding of a secondary nystagmic response is fairly rare. However, the German vestibular savants of old, who were accustomed to using the Barany chair with stopping velocities of 180°/second, frequently reported multiple reversals, the number of which they specified by the number of nachs they chose to prefix the word nystagmus, as in nach nach nystagmus. Likewise de Kleyn reports that a reversed secondary nystagmic response can be observed in the normal subject following caloric irrigation, provided only that the irrigation is maintained for 15 minutes or more.⁶

By way of explanation, de Kleyn invokes Sherrington's law of successive induction, maintaining that "the reflex arc of one of the vestibular systems during its own activity induces a phase of greater excitability and capacity for discharge in the antagonistic arc."⁶

To this it seems only necessary to add the following conclusions derived from our own findings:

1. The phenomena we have observed in patients with rebound nystagmus would appear to be a manifestation of the same mechanism envisaged by de Kleyn, but one that has been released from inhibitory control so that it operates unchecked.
2. The mechanism probably has its origin in the cerebellum or is mediated by cerebellar influences upon centers in the brain stem.
3. Whatever the storage mechanism that brings about the phase of greater excitability in the antagonistic arc, it has the remarkable capacity for storing not only magnitude but also duration of response.

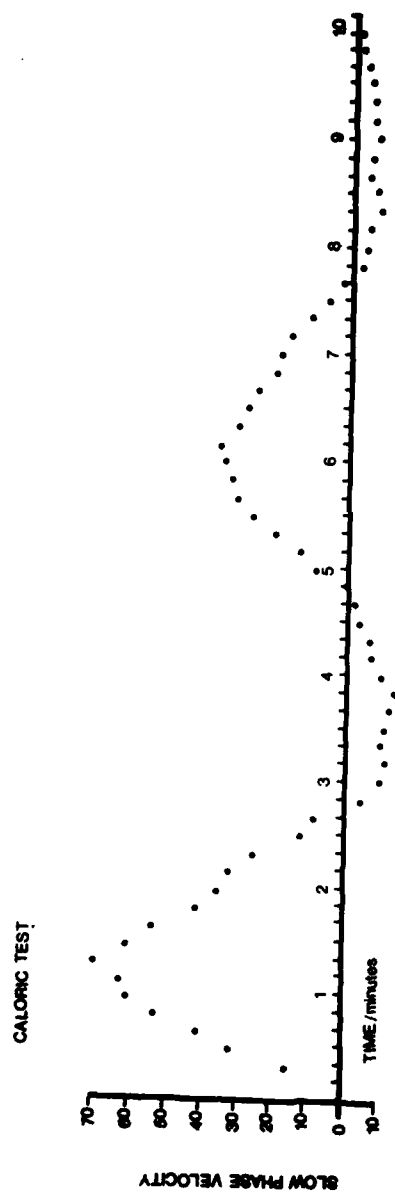


FIGURE 5. Slow-component velocities of nystagmic responses to a caloric test of 44°C. Note multiple rebound, which reflects the duration of the primary response.

4. At least in the presence of optic fixation, its primary mode of action appears to operate upon the fast rather than the slow component of the nystagmus.

Beyond this, little more can be said at the moment other than to draw attention to the interesting parallels in the nystagmic response elicited by electrical or chemical stimulation of the hippocampus, recently described in the rabbit.⁷ These responses, which show similar rebound phenomena and persist for prolonged periods of time, have been attributed to a decrease in excitability of cholinergic components and an increase in excitability of adrenergic components. It may be that similar neurochemical mechanisms are operative in the case of rebound nystagmus.

REFERENCES

1. HOOD, J. D., A. KYAN & J. LEECH. 1973. Rebound nystagmus. *Brain* **96**: 507-526.
2. BALOH, R. W., H. R. KONRAD & V. HONRUBIA. 1975. Vestibulo-ocular function in patients with cerebellar atrophy. *Neurology* **25**: 160-168.
3. KATO, I., M. AOYAGI, K. MIZUKOSHI & K. ISHIKAWA. 1975. Rebound nystagmus, a report of 29 cases. In *Proceedings, Fifth Extraordinary Meeting of the Barany Society*. Masarori Morimoto, Ed.: 237-240. Barany Society and Japan Society for Equilibrium Research. (Int. J. Equilibrium Res. Suppl.)
4. AOYAGI, M., K. MIZUKOSHI, I. KATO, K. ISHIKAWA & Y. WATANABE. 1975. Rebound nystagmus. A report of 18 cases. *Otolaryngology Tokyo* **47**: 175-180.
5. MORALES-GARCIA, C., J. L. CARDENAS, C. ARRIAGADA & J. OTTE. 1978. Clinical significance of rebound nystagmus in neuro otological diagnosis. *Ann. Otol. Rhinol. Laryngol.* **87**: 238-242.
6. DE KLEYN, A. 1939. Some remarks on vestibular nystagmus. *Confin. Neurol.* **2**: 257-292.
7. HINOKI, M., K. NAKANISHI & S. ITO. 1979. Nystagmic responses of hippocampal origin with reference to excitability of cholinergic and adrenergic components involved in hippocampus of rabbits. *Rev. Agressologie* **20**: 11-18.

ACTIVE HEAD ROTATIONS AND EYE-HEAD COORDINATION*

Wolfgang H. Zangemeister† and Lawrence Stark

*Departments of Physiological Optics,
Neurology, and Bioengineering
University of California
Berkeley, California 94720*

INTRODUCTION

Head movements play an important role in gaze; the interaction between eye and head movements involves both their shared role in directing gaze and the compensatory vestibular ocular reflex. This shared role and interaction with respect to body posture and locomotion have attracted the interest of neurologists since the time of Barany, Magnus, and Dodge.

Coordinated gaze movement normally has an initial eye-in-orbit saccade onto the target followed by a synkinetic and much slower head movement. At the level of electromyographic (EMG) signal latencies, these are synchronous; but because the viscoinertial dynamics of head and neck muscles are different from the viscoelastic dynamics of eye and extraocular muscles, the saccade is over before head position has changed. The vestibular ocular reflex (VOR) generated by head acceleration drives the compensatory eye movement (CEM), eye-in-orbit, in the opposite direction so that gaze, eye-in-space, remains on target. The CEM and its VOR component are influenced by visual input and other factors that modify gain;^{11,14,18,22,25,26} resultant overshoots or undershoots are corrected by later saccades. These features have been defined in monkeys and man, and some clinical studies have begun exploration of pathological changes.^{1,3-7,9-13,15,16,18-20,22,24,26}

Beside this classical coordinated gaze movement (type I) (FIGURE 1), other gaze patterns exist, generally determined by asynchronicity of the neural controller signals as reflected in the experimentally recorded EMGs. Sometimes head movement occurs very late (type II), at times with an anticipatory, non-VOR, compensatory eye movement (ACEM) appearing during the interval before the head movement. When the head movement occurs early (type III), eye saccades often are slowed or truncated by the interaction with the ongoing VOR. A very late eye saccade, occurring after the head movement and the VOR are completed (type IV), is a consequence of the early head movement influenced by a variety of experimental protocol conditions. These gaze patterns reflect the increased flexibility of head movements as compared with the rather stereotyped generation of eye saccades.

The methods used for head- and eye-movement recordings are well known and described elsewhere.^{2,20,21,24-26}

*The authors are pleased to acknowledge support from the NCC 2-86 Cooperative Agreement, NASA-Ames Research Center.

†On leave from the University of Hamburg. Address correspondence to the Neurological University Clinic (UKE), University of Hamburg, Martinistr. 52, D-2000 Hamburg 20, Federal Republic of Germany. Supported by Deutsche Forschungsgemeinschaft, Bonn, F.R.G.

RESULTS AND DISCUSSION

Main Sequence

The dynamics of head trajectories can be parameterized to obtain the peak velocity, peak accelerations, the times of these extrema, and the duration of the movement. This parameterization is useful to show lawful relationships in the trajectory dynamics over the wide range of experimental head movements studied, and such a diagram is presented in FIGURE 2. The middle diagram shows the significant increase of peak velocity as a function of amplitude. The range is,

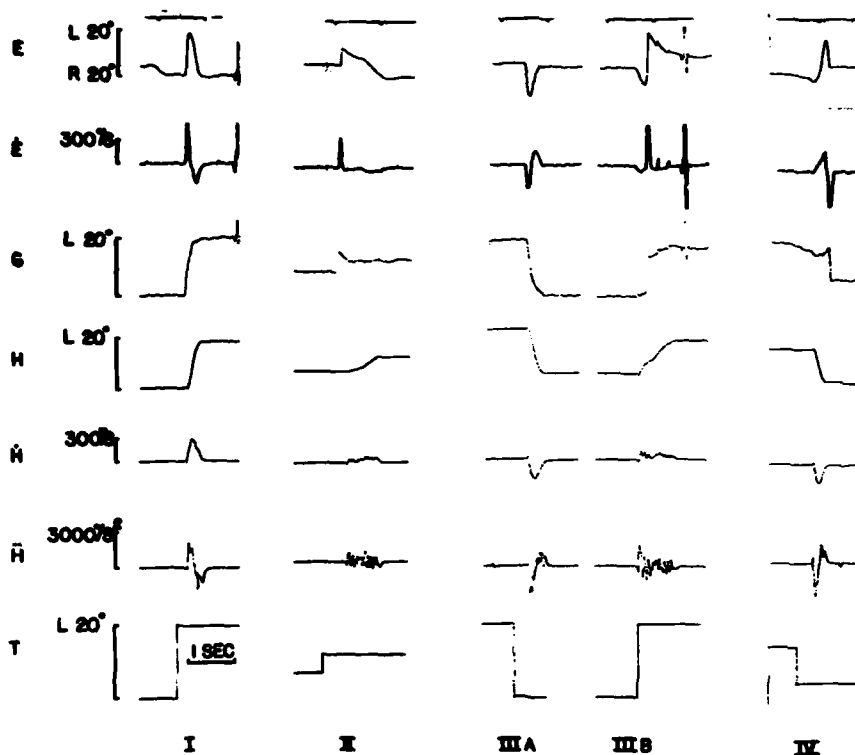


FIGURE 1. Coordinated gaze types. Eye position (E), eye velocity (E), gaze position (G), head position (H), velocity (H), and acceleration (\dot{H}), and target position (T). 40° movements between left (L) and right (R).

of course, quite compressed in this log-log plot. The upper bound of the scatter of experimental results is represented by the main sequence lines; this bound is composed of the fastest movements at any given magnitude. Although velocity and acceleration increase with amplitude, the increase is not proportional, thus indicating a saturation and relative slowing of the movement. The dashed straight line in the middle diagram represents the behavior of a model for head movement simulated on a digital computer.^{17,24}

A comparison between head, eye, and arm main sequence data (FIGURE 2,

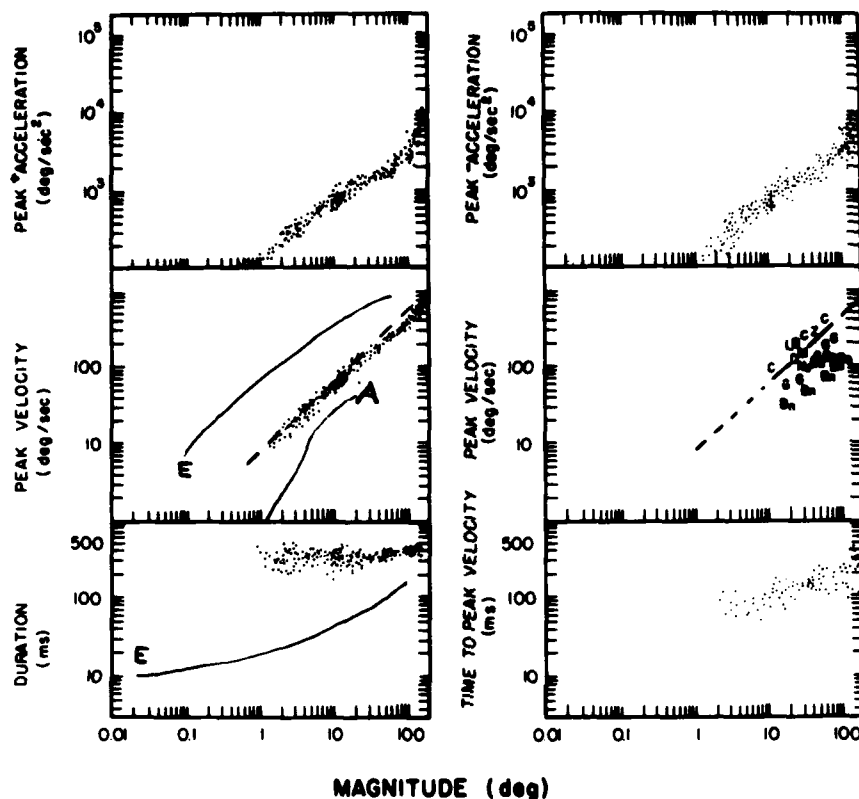


FIGURE 2. Main sequence for head movements. Over 100 fast head movements of a normal subject. Dashed line is a head-movement-model line.^{24,26} Middle right shows comparative data from the literature.² Eye (E) and arm (A) movement main sequence data on the left show similar slopes but viscoinertially caused differing intercepts. Note the comparatively small increase of duration with large head movements.

TABLE 1) shows similar slopes but different intercepts, probably due to the different load. Also, duration increases less significantly in head than in eye movements.

Neck Muscle EMG

Neck Muscle EMG and Details of the Head-Movement Trajectory

The electromyogram is an accessible measure of the neural controller signal that governs head rotation. It thus provides useful information for interpreting and modeling dynamical details of the head-movement trajectory. Head movements are synkinetic with eye movements in gaze. Although similar to eye movements in overall properties, head movements show a contribution of stretch

TABLE 1
COMPARISON OF MAIN SEQUENCE DATA FOR EYE [E], HEAD [H], AND HEAD MODEL (HM)

	E	H	HM	E	H	HM	E	H	HM	E	H	HM	E	H	HM	E	H	HM
Magnitude (degrees)	2.5	2.5	2.5	5.0	5.0	5.0	10.0	10.0	10.0	40.0	40.0	40.0	60.0	60.0	60.0	—	140.0	140.0
Duration (msec)	24.5	260	270	28.5	270	275	37	300	295	78	320	335	110	380	385	—	412	430
v_{max} (deg/sec)	166	22.5	24	320	48	43	519	80	85	791	270	285	850	352	374	—	606	633
t_{max} (msec)	—	90	105	—	95	110	—	105	115	—	125	120	—	125	130	—	150	155
α_{max} (deg/sec ²)	16000	330	310	28000	551	609	41000	994	910	73000	2100	2200	82000	3300	3250	—	6300	5900
α_{min} (deg/sec ²)	—	322	290	—	392	409	—	714	850	—	1850	1900	—	2700	2850	—	3900	4700

reflexes. There are also differences in detailed dynamic features. Electromyograms, representing samples of neurological controller signals, can be used to predict head rotations, which can be either time optimal or non-time optimal depending upon a subject's intent. A major property of neurological control signals is reciprocal innervation, and both pairs of head rotating muscles—splenius and sternocleidomastoideus muscles—demonstrate this (FIGURE 3). The (mostly biphasic and sometimes triphasic) EMG activity appears to fit the concept of optional time-optimal control in head movements, and explains the existence of dynamic overshoot in both large and small head rotations with multiple pulse control of the trajectory, seen as rapid switchings between maximum and minimum. Also demonstrated are quantitative relationships between envelopes of rectified EMG and different velocities and accelerations in head movements of the same amplitude (FIGURE 4). These relationships are lawful and quantitative on a statistical basis with averaged data. Because of the main sequence relationship (FIGURE 2), they also relate the pulse size of EMG envelopes to different head-movement amplitudes.

Kinematic factors, such as operating levels in terms of horizontal rotations, have an important influence on the tonic and phasic aspects of the EMG signal (FIGURE 4). Reciprocally innervated pairs of horizontally rotating muscles become cocontractors for vertical rotation. Correlation of detailed shapes of envelopes of rectified EMGs with detailed acceleration functions are demonstrated in several experimental paradigms. (FIGURE 4). Cocontraction, the stretch reflex, fatigue, and supraspinal influences responding to complex stimuli contribute to variance in both EMG signals and head accelerations. In addition, a number of instrumentation and biological-sampling difficulties may allow the EMG signal to be discordant with the neurological control signal for a particular movement.

Latency studies demonstrate the causal chain from target input to agonistic electromyogram (200 mseconds), to head acceleration (20 mseconds) and initial change in head position (45 mseconds), to final head position (240 mseconds) for

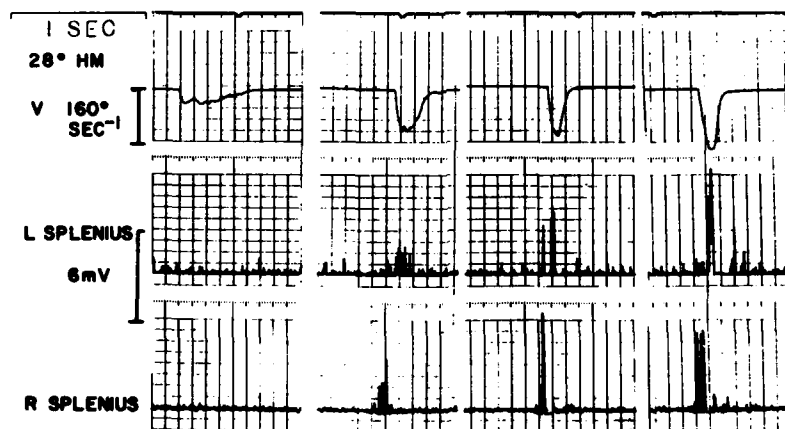


FIGURE 3. Neck-muscle EMG pulse height and pulse width as functions of head velocity (V).

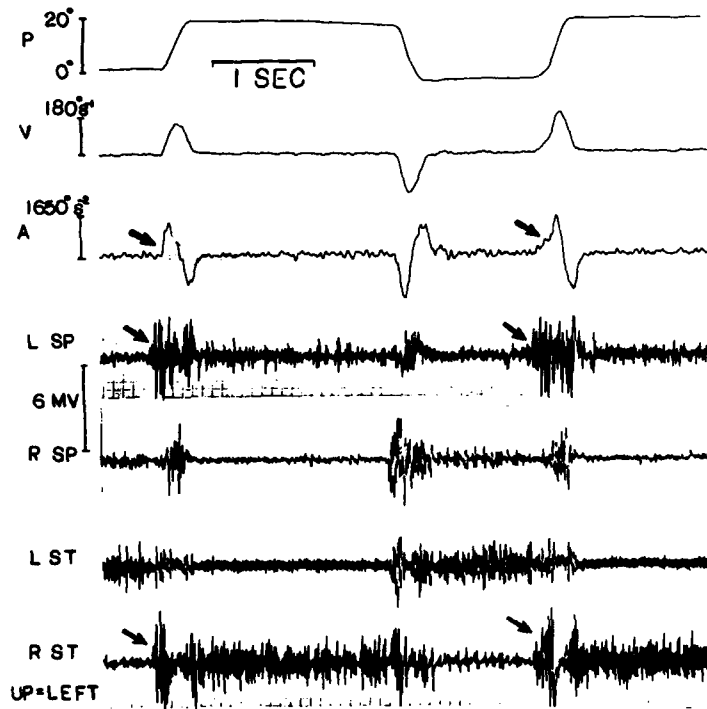


FIGURE 4. Correlation between unrectified EMG of left and right splenius (SP) and sternocleidomastoid (ST) muscles and head acceleration (A), velocity (V), and position (P) traces. Note abrupt onset (left arrows), contrasting with gradual onset (right arrows) of EMG and acceleration.

20° head rotations. Antagonistic EMG, obeying reciprocal innervation, begins about 70 mseconds after agonistic EMG begins. In comparison to eye movements, pulse width is less important than pulse height for the rectified EMG; this also is shown for direct or indirect modeling of head movements.^{17,24,26}

Types of Head Model Accelerations

Experimentally, many different types of head-movement trajectories can be noted (FIGURE 1). One of the uses to which we put our head-movement model was to study the changes in the model that simulate different acceleration types (FIGURE 5). The four horizontal rows represent four different types arranged in decreasing order of maximum acceleration. As can be noted by looking at the right-hand column, the model fits the experimental position trajectory very well for all four types. The model also shows excellent fits to other behavioral features, such as duration, maximum velocity, maximum positive acceleration, and maximum negative acceleration. The timing behavioral parameters,

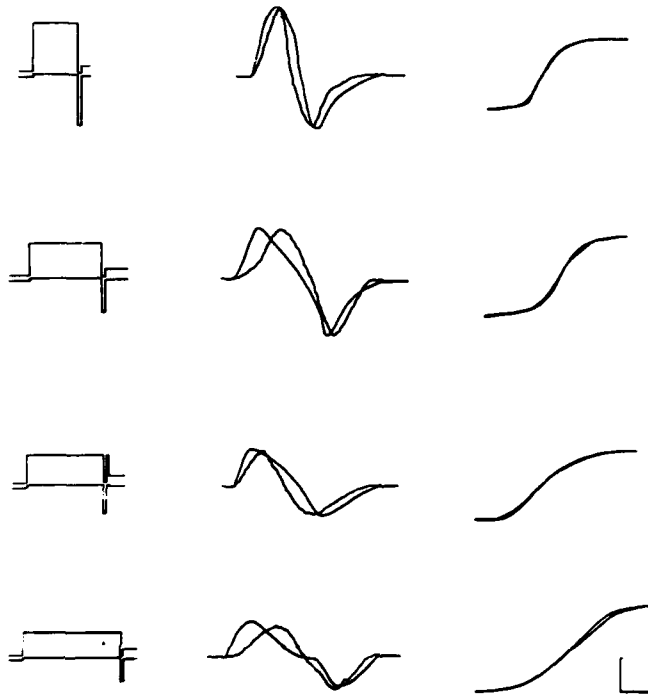


FIGURE 5. Head-movement-model fit for four acceleration types. Left: controller signal envelopes. Middle: acceleration traces (smooth lines equal model traces). Right: position. Calibration mark: abscissa, 100 mseconds; ordinate (for left, middle, and right respectively), 1,000-g force, 1,000°/second per second, 10°.

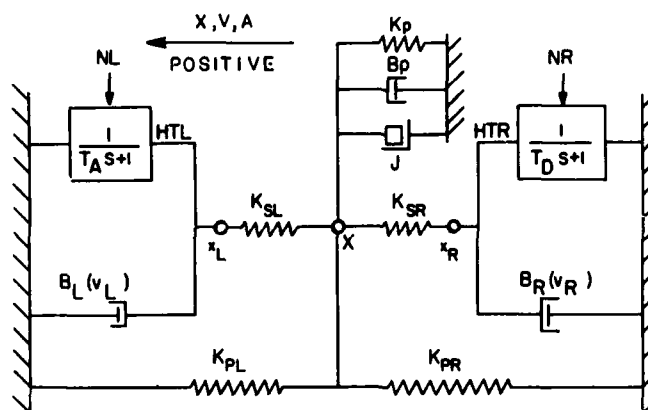


FIGURE 6. Structure of head-movement model. NL, NR: neural control signal left and right; HTL, HTR: hypothetical tensions, left and right. X, V, A: position, velocity, and acceleration. For other parameters, see TABLE 2.

however, were less well fitted, as can be noted in the middle column showing model and experimental acceleration trajectories.

The structure of our head-movement model is shown in FIGURE 6, and the model is compared and contrasted with the eye-movement model¹⁷ in TABLE 2.

Latency of Eye and Head Movement in Coordinated Gaze

The classical coordinated gaze movement may be described as a saccadic eye movement followed by a head movement. Synchronously with the head movement, the compensatory eye movement returns the eye to its primary position in the orbit as an exchange of head movement for eye movement. In this way coordinated gaze obtains a first advantage from the fast eye saccade to rapidly

TABLE 2
COMPARISON OF HEAD AND EYE MODEL PARAMETERS

Definition	Parameter	Units	Eye	Head	Scaling Factor
Inertia	I	$\text{g-sec}^2/\text{deg}$	4.3×10^{-5}	1.8×10^{-1}	10^4
Viscosity	B	g-sec/deg	1.5×10^{-2}	2.0	10^2
Parallel Elasticity	K_p	g/deg	1.5	2.0	1
Series Elasticity	K_{el}	g/deg	1.8	40.0	10^1
Maximum Muscle Force	F_{max}	g	100.0 (10°)	600.0 (10°) 2000.0 (40°)	10^1
Minimum Muscle Force	F_{min}	g	2.0	2.0	1
Activation Time Constant	T_a	sec	4.0×10^{-3}	5.0×10^{-2}	10^1
Deactivation Time Constant	T_d	sec	8.0×10^{-3}	5.0×10^{-2}	(10^1)

place gaze onto a target in space. It obtains a second advantage from having the eye in primary position at the end of the movement for equal ease of next moving in either direction. Although this classical description of a coordinated gaze movement has head movement occurring with a longer latency than eye movement, it must be realized that the head, being a larger mechanical object than the eyeball, requires an increased dynamical lag period in order to move. Thus we might expect that the neck EMG might begin synchronously with eye-movement EMG.

Indeed, neck EMG occurred synchronously with eye movement (FIGURE 7, left arrow), since the eye movement is almost synchronous with its own EMG (about 8 to 12 mseconds).^{6,10,13} This synchronicity suggests the clarification obtained by measuring latency with respect to a controller signal and not with respect to the behavioral movement, which has its own dynamical lags. The first movement of FIGURE 7 shows a large-amplitude head movement, with the agonistic neck-muscle EMG trace (left arrow) turning on approximately 45

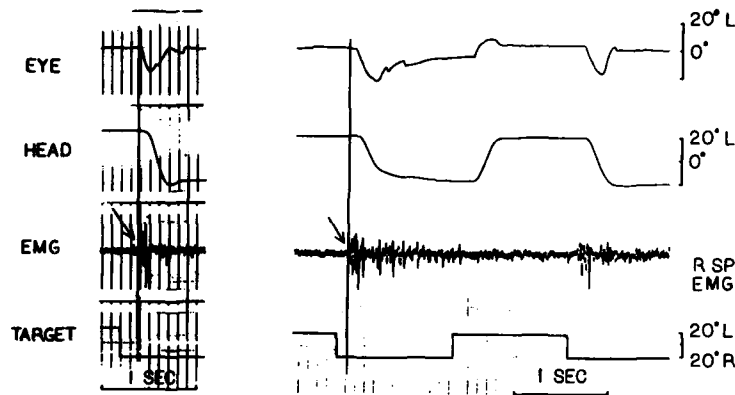


FIGURE 7. Response to a 40° target shift from right (R) to left (L) and back. Left side: unpredictable target shift. Eye movement precedes head (45 mseconds), whereas right splenius EMG (R SP) starts about 10 mseconds before initial eye-position changes. Right side: predictable target shifts. Head predicts comparatively better than does eye.

mseconds before the head movement occurs. The right experimental example shows latencies that are reduced because of prediction by about 100 mseconds. Neck EMG latency is about 50 mseconds less than latency to eye-position change; consequently, neck EMG leads eye EMG by about 40 mseconds in this predictive situation.

The dynamic lag of head movement (position, acceleration, derivative of acceleration) on a magnifying time scale with agonistic and antagonistic EMG is shown in FIGURE 8.

Gaze Latency as Function of (1) Initial Condition, (2) Amplitude, (3) Prediction, and (4) Neurological Disease Process

1. Forced or intended time-optimal coordinated gaze movements have eye-movement latencies that are shorter than head-movement latencies. The gaze-latency diagrams (FIGURE 9) demonstrate this as an offset or difference between two 45° lines. One 45° line, passing through the origin, is the line of synchronicity, that is, if all eye movements and head movements were synchronous with exactly the same latencies, then all data points would lie on this line. For 15° rapid head and eye movements, with instructions to the subject to "force" their head movements as rapidly as possible,²⁴ the elliptical spread of the experimental data points could be fitted by the regression line of head latency on eye latency, for which the correlation coefficient was 0.80. When standard deviations were calculated, they were approximately equal, indicating no special dependence of eye latency on head latency or of head latency on eye latency. This fitted 45° line, with a 40-msecond offset from the origin, represents a model of gaze latencies wherein head latency is 40 mseconds longer than eye latency. This of course is the dynamic head-movement lag. The fit supposes that all of the variation that is

normally seen in gaze-movement latency is a coherent covariability where head latency and eye latency vary together. This is consistent with a neural pathway between stimulus and response, part of which is shared by head and eye movement. When variability occurs in the shared part of the pathway, it is a covariability. Thus with exact covariability, all data should lie along this line; this further assumes that at some point, where there are separate paths to control eye and head movements, variation would give rise to noncoherent covariability.

When the subjects did not force their head movements in tracking the target, but rather made "natural" movements with, as might be expected, longer delays, only head-movement latency increased in this more natural situation ($r = 0.81$; FIGURE 9, upper left). Eye-movement delay seems to be stereotyped, less accessible to intent of the subject, and thus not as influenced by instructions with respect to the goal.

2. The increase of head-latency offset for a natural intent of the tracking task continued when the target amplitudes were increased from 15 to 60° (FIGURE 9, lower left). Again, latency of eye movement did not change whereas latency of head movement increased by approximately 80 mseconds ($r = 0.78$). Also it

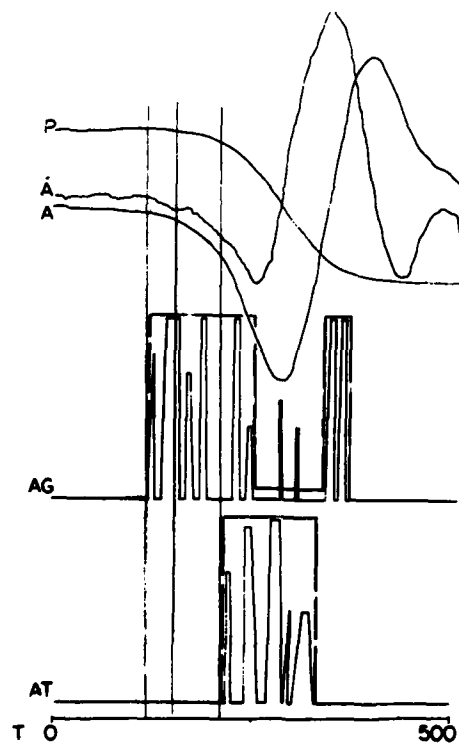


FIGURE 8. Dynamic lag in head movement. Position (P), acceleration (A), and derivative of acceleration (\dot{A}) show the 45-millisecond position delay due to viscoinertial load following start of agonist EMG (AG). Dashed lines represent EMG pulse envelopes.

appears that amplitude for the natural task influenced latencies, that is, the larger the amplitude the longer the head latency. This somewhat smaller effect also was noted clearly by comparing the 15° forced condition with the 60° forced condition (FIGURE 9, upper left). Similarly, head latency rather than eye latency is increased in comparing these conditions.

3. Subjects greatly reduced their latency with prediction, approximately 300 mseconds (FIGURE 9, upper right). This reduction was somewhat more pronounced for head than for eye latency, but occurred to a large extent in a covarying way along the 45° line ($r = 0.95$). The slight shift towards synchrony was attributed to a somewhat more pronounced decrease for latency in head movement. When subjects, still following a predictable target, became fatigued, their predictive latencies were reduced along the covarying 45° line ($r = 0.92$).

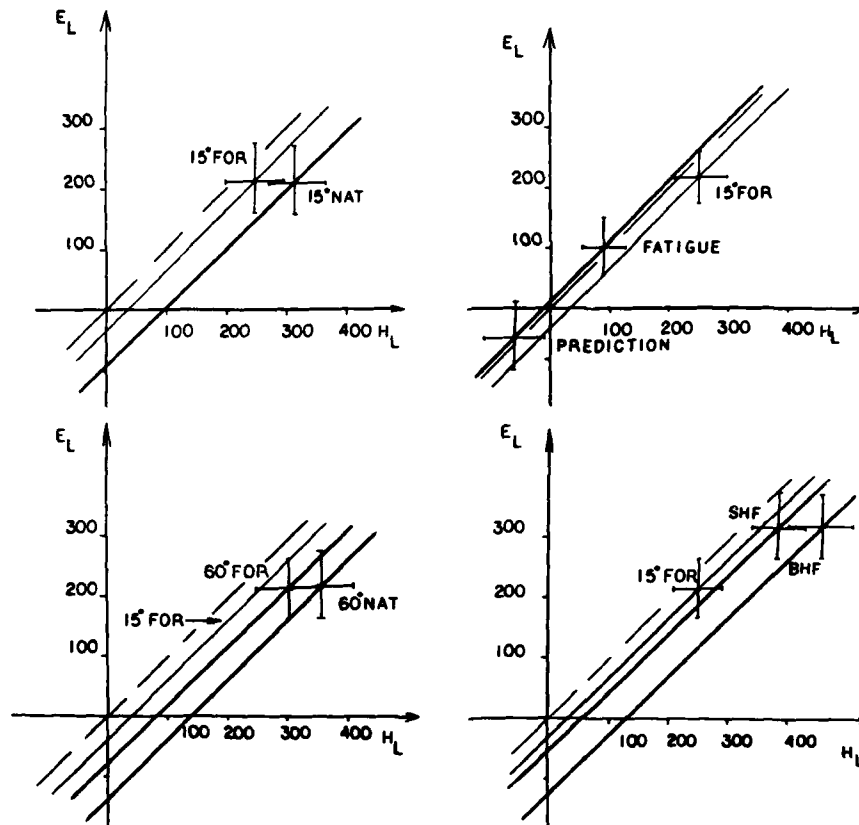


FIGURE 9. Eye- and head-latency correlations with different initial conditions in normal subjects and patients with homonymous hemianopia. 15° forced (FOR) and natural (NAT) head movements to random targets. Predictable targets (prediction) with high and low (fatigue) vigilance; patients with seeing (SHF) and blind (BHF) hemifield. Dashed line is the synchronicity line.

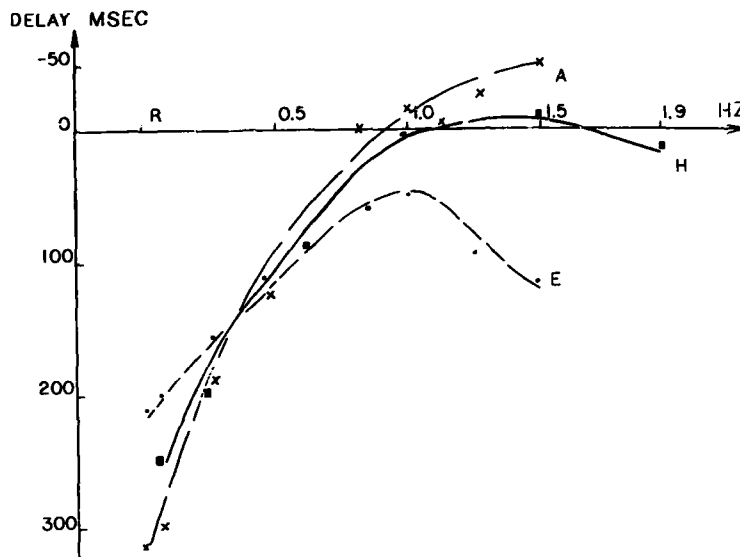


FIGURE 10. Comparison of mean head, arm, and eye delays (H, A, and E). Prediction by head and arm is superior to eye. Note the 1.5-Hz regular target oscillation, while random delay (R) is less for the eye.²¹

4. The gaze-latency diagram also was applied to a neurological disease;¹⁸ patients with homonymous hemianopia were instructed to move their heads as fast and accurately as possible to targets of 10 and 20° amplitude. Great increase occurred in both eye-movement and head-movement latency when the subject gazed into the blind hemifield (BHF) (FIGURE 9, lower right). Quantitatively, this was in part an approximately 110-millisecond increase in delay that was a covarying, or joint, delay for eye-movement latency and head-movement latency, and in part an extra delay that was noncoherent, attributed to head-movement latency only, and equal to about 120 milliseconds ($r = 0.85$). When patients moved their gaze to the seeing hemifield (SHF), they showed only the covarying, approximately 110-millisecond increase in latency for both eye and head movement. The center of this second latency distribution (gaze towards SHF) almost is superimposed on the normal, 15° forced line; it only has moved upwards on this 45° line (FIGURE 9, lower right).

A comparison of the differing mean delay times for head, eye, and arm movements²¹ with random and predictable targets is shown in FIGURE 10.

Coordinated Gaze Types

The experimental time functions of coordinated eye and head gaze movements that have been described give an idea of the variability (FIGURE 1) and suggest a classification for clarification. To understand more deeply these gaze types and their relation to active head trajectories, it is most helpful to discuss

them in terms of a model. This model, the "gaze plane," has the advantage that eye and head movements are displayed as functions of one another with time as only an implicit function of eye and head position (FIGURE 11, right column). In the gaze-plane plot, we see the fast eye saccade occurring first (FIGURE 11, vertical arrow starting from the origin). The line pointing diagonally downwards exemplifies the CEM and the head movement occurring at the same time. Eye position is exchanged for head position, and gaze, that is, eye-in-space, remains on target throughout for the type I gaze movement. This is achieved only when the CEM gain equals unity; higher or lower gains would move gaze slightly off the target during the head trajectory. Normally this would not be a severe disturbance of the target acquisition, since the "postsaccadic snapshot"²¹ already had occurred. Therefore, the target did not need to remain exactly on the fovea; after an intersaccadic interval occurred, corrective saccades could return target onto the fovea. Errors, or differences between gaze angle and target angle, are important to study because both eye and head movements are visual feedback-error-actuated movement patterns. This error function monitored continually by the subject is the important variable to be minimized as the off-foveal eccentricity of the target. Error is minimized in the type I gaze movement, where it persists only for the short eye latency and during the very rapid eye saccade, which is time optimal.^{8,17} However, in the type IV gaze response, there is a much longer period before the fovea acquires the target, since the head movement finishes its trajectory following the head-movement latency (FIGURE 11, right column) before the eye even begins its saccadic trajectory. Thus the error function has a large value for the long time period of approximately 600 mseconds, which includes the 250-msecond latency of the head movement, a long head trajectory of 300 mseconds, and a subsequent fast eye saccadic trajectory of approximately 50 mseconds. This additional "excess error" present in type IV compares with the minimal error present in type I (FIGURE 11). It is represented in the gaze plane by the cross-hatched area encompassing the error during the entire period of head-eye trajectory. The time functions as well as the gaze plane demonstrate the time optimality of type I gaze pattern, considering the minimization of gaze error as the variable to be controlled. The effect of prediction is not taken into account in the gaze plane since time is only an implicit function there. Thus if the head movement of type IV were to begin so early that the late eye saccade of this type actually occurred before the early saccade of type I, then no excess error would occur, but rather a negative error with respect to type I.

The experimental examples (FIGURE 1) demonstrate the gaze patterns and their variability for each of the four gaze types. When we apply the gaze-plane model to the gaze types, we can abstract their basic neurological motor coordination features (FIGURE 11). The "classical" type I gaze shows, as explained, the minimal error, depending only on eye latency. An excess error does not occur. Since head acceleration can vary greatly in this type, additional errors due to nonunity CEM gain and quick-phase-like saccades occasionally take place. Type II gaze shows the delayed head-movement condition with an early gaze acquisition of the target. Typically, an anticipatory compensatory eye movement (ACEM) occurs, which does not depend on the VOR. The ACEM moves gaze off target until the head movement again brings it back onto target. The excess error shows up after the first target acquisition has occurred. Although ACEM velocity often merges indistinguishably with the subsequent CEM, its beginning (vertical line, FIGURE 11) demonstrates its important distinction from the VOR. Low-gain CEMs frequently occur that relate closely to particularly slow head velocities.^{18,28}

Corrective saccades, which would delay additionally the final accurate target acquisition, are not necessary in this case.

The early head movement in type III is not due to delay in the occurrence of the eye saccade but rather to the early appearance of the head movement with its greater flexibility in predicting the target. Thus the excess error with respect to type I frequently is not nearly as great as it might be with random targets; with enough prediction, it even may be a negative quantity. Head movement often

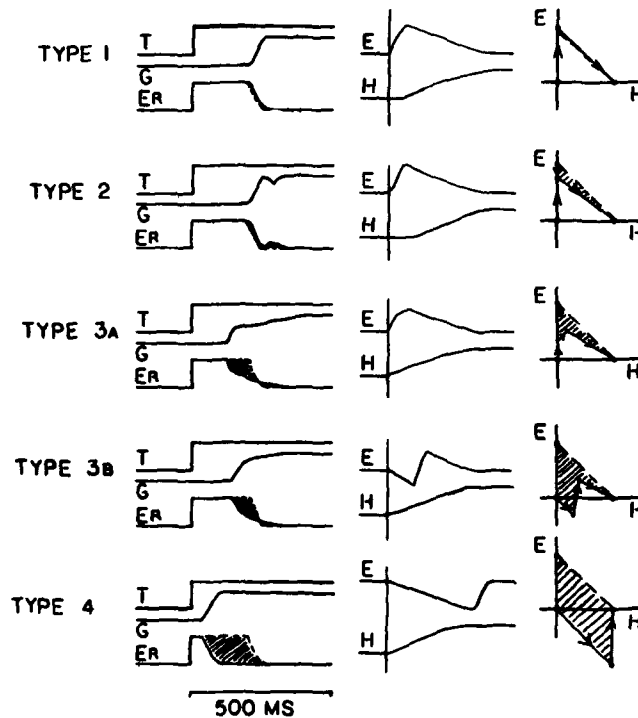


FIGURE 11. Eye and head coordinated gaze types. Left: error displays; dashed lines are excess error (ER) with respect to gaze (G) and target (T) position. Middle: eye (E) and head (H) position; vertical line indicates the relative eye and head latency. Right: gaze plane display with time as an implicit function showing excess error and eye-head interaction for the gaze types in normal subjects.

occurs early with respect to the occurrence of the eye movement, and the dynamical interactions therefore are a significant and major consideration. Two varieties are shown in the abstracted diagrams (FIGURE 11). Type IIIA shows a saccade occurring early during the head trajectory, but late enough to interact with the VOR, which slows down the saccade. When the eye saccade occurs later in the trajectory, as in type IIIB, it may be truncated due to its synchrony with a maximally active VOR occurring at peak positive head acceleration. Often this truncation is compensated for by a lowered CEM gain, which in fact may be the

result of the influence of a saccade on the ongoing VOR. Thus truncation of the saccade could be due to neuromuscular and peripheral biomechanical interactions that are dependent upon the different initial conditions of an oppositely going VOR and that influence the forces of the muscles attempting to generate the saccade.¹⁷ Another explanation for this interaction type could be an interaction of the control signals on a higher central-nervous-system level.¹⁸ We noted also that the fast phases in type IIIB look very much like the quick phases of nystagmus, which relates type III to nystagmus generation in particular. The extreme lateness of the eye saccade in type IV provides for a great deal of excess error, especially when the very early head movement did not anticipate target movement. This excess error shows up both in the time functions and in the gaze plane. Because of the very late normal-velocity eye saccade, no peripheral interaction occurs and the eye saccade finally brings fovea and gaze onto target. However, the importance of the prediction operator is demonstrated in FIGURE 11 (lower left) showing negative excess error. This means that with high prediction, the very late eye saccade actually occurs earlier than the early eye saccade of type I with its minimal standard latency error.

Clinical Examples of Gaze-Plane Analysis

Clinical examples (FIGURE 12) demonstrate the variety of interactions of eye and head in gaze movements in patients with homonymous hemianopia. The upper left shows a gaze movement toward the seeing hemifield (SHH), placed in the upper-right direction in this figure (directions are plotted positively in graphs; θ_E , ordinate; θ_H , abscissa), with eye movement undershooting the target so that the right hemianopic field (represented by diagonal slashes) does not obscure the view of the target either after the first eye saccade or during head movement and CEM, or with the second eye saccade compensating or correcting for initial undershoot (small upward vertical arrow). The upper left also shows a gaze movement toward the blind homonymous hemifield (BHH), which overshoots the target on initial eye movement saccade (vertical arrow downward from the origin) so that the right hemianopic field does not obscure the view of the target. This upper-left corner of FIGURE 12 shows saccadic eye movements adaptive for safe acquisition of target. Contrariwise, maladaptive saccadic eye movements (middle left) overshoot a target in the SHH or undershoot a target in the BHH, so that view of the target is obscured by the hemianopic field.

Similarly, a change in CEM gain can be adaptive (upper middle) or maladaptive (lower middle). Unity gain has a minus 45° slope in contrast to CEM gains, greater with greater slope or lower with less slope. Corrective saccades (small vertical arrow) are required to compensate for nonunity CEM gains. The effect of the ACEM, occurring before actual head movement, is shown on the upper and middle right (FIGURE 12). On gaze to target in the SHH with accurate eye saccade, the occurrence of an adaptive ACEM places the hemianopic field away from the target and permits safe viewing of the target during head movement and CEM. A corrective saccade is necessary (small vertical upward arrow) at the end of gaze movement. A maladaptive ACEM (lower right) moves gaze off the target so that

†KENYON, R. V., et al. 1980. Unequal saccades during vergence. *Am. J. Optom. Physiol. Optics* 57: 586-594.

the BHH obscures view of the target. More frequently occurring clinical examples (FIGURE 12) are interpreted easily in the light of these less often occurring examples. Compensating discrepancies (left) permit safe viewing. With gaze to the SHH, an undershooting saccade (upward vertical arrow) prevents low CEM gain (downward oblique arrow) from obscuring view of the target in many instances (about 60%). Similarly, an overshooting saccade (downward vertical

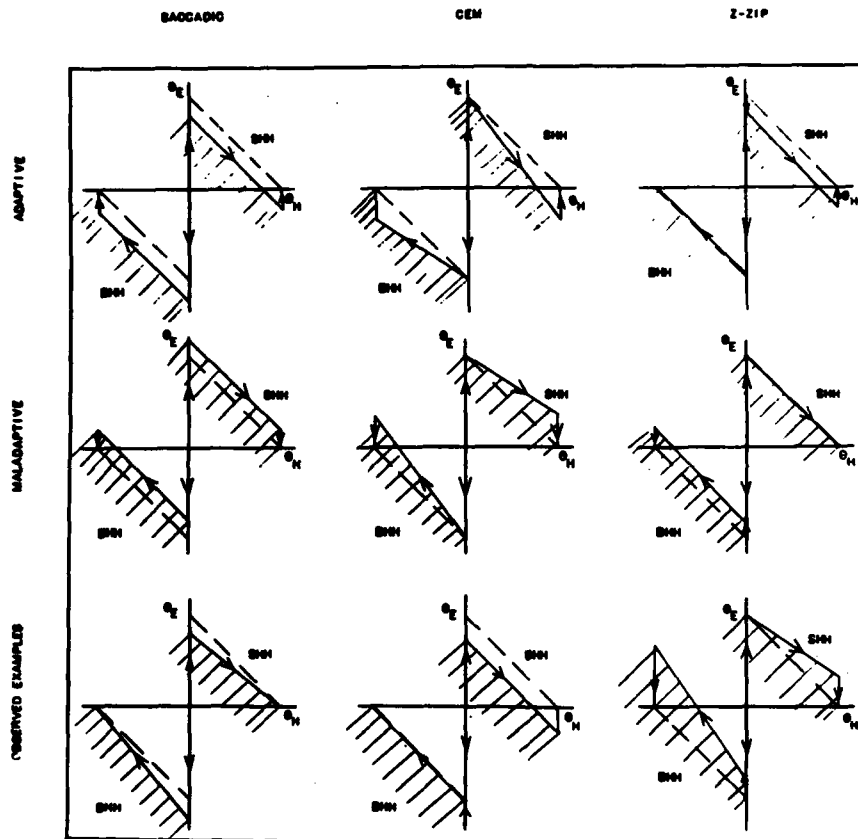


FIGURE 12. Gaze plane display for patients with homonymous hemianopia. Columns show saccadic, CEM, and ACEM (Z-ZIP) mechanisms compensating for the field defect while acquiring targets. Rows show adaptive, maladaptive, and clinically more frequent examples.

arrow) with gaze to the BHH prevents high CEM gain (upward oblique arrow) from obscuring the target in many instances (about 60%).

An especially interesting compensatory discrepancy sometimes occurs (about 25%; FIGURE 12, lowermost row, middle) when saccadic overshoot (large downward vertical arrow) with gaze to the BHH is corrected by an ACEM (small upward vertical arrow) so that the fovea is on target but without a safety margin.

A pure saccadic undershoot discrepancy also sometimes occurs (about 25%; upward vertical arrow), which permits safe target acquisition.

Maladaptive discrepancies may occur (right) with low CEM gain (downward oblique arrow) on gaze to the SHH, or with ACEM (small upward vertical arrow) and high CEM gain (upward oblique arrow). Both place target into the hemianopic field during CEM and require corrective saccades into the BHH.

Instantaneous Change of CEM Gain

A highly interesting difference in interactional modes of head and eye movements was recorded in a patient with congenital homonymous hemianopia (FIGURE 13). In our example, the target moves 20° to the right and returns after 2

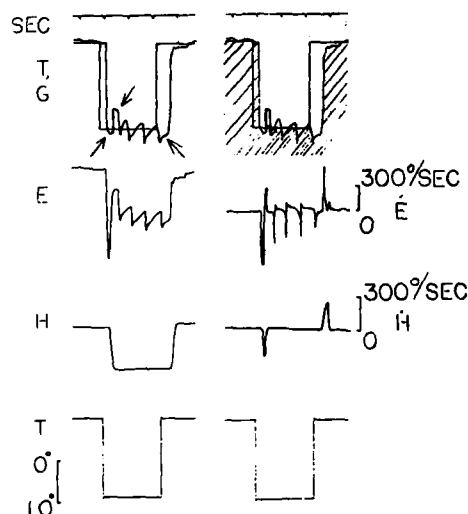


FIGURE 13. Instantaneous change of CEM gain in a patient with congenital hemianopia. Trace descriptions as in FIGURE 1. Hatched field indicates blind hemifield. Note the particularly high-gain CEM (left arrow) with gaze to right blind hemifield (down), the intersaccadic interval before correction saccades occur (middle arrow) together with continual drift, and the almost zero gaze velocity (right arrow) before a saccade and head movement with no CEM occur.

seconds—evidently not predicted in time, as indicated by latencies of 290 and 500 mseconds (eye) and 360 and 450 mseconds (head) to right and left. Normal values for this amplitude are 210 and 250 mseconds.^{20,23,25,26} The initial 22° eye movement, obviously predicted in amplitude, shows small overshoot, which is typical of predictive gaze to the BHH. The fast head movement and the particularly high-gain CEM, together with a continual eye drift interrupted by corrective saccades, characteristic in this patient, bring gaze back to the target. With gaze toward the SHH, eye (10°) and head (13°) movement components place the fovea accurately onto the target. A CEM does not occur.

Here we have two completely different mechanisms or strategies of gaze movement: the first with $\theta_E - \theta_T - \theta_{CEM} - \theta_H$ permitting gaze movement to have

advantages from the speed of the first eye movement, then a continued accurate foveation, when head movement and CEM together trade θ_H for θ_E leaving gaze on target throughout, and finally eye in primary position with respect to orbit; two seconds later, a different target acquisition mode is used where θ_{eye} plus θ_{head} equals θ_{target} , with θ_{CEM} equal to zero. CEM gain clearly is suppressed or canceled; also summation with an equal and opposite smooth pursuit is not a real possibility since smooth pursuit generally would not operate at velocities of the CEM, $150^\circ/\text{second}$, and since smooth pursuit would require about 200 mseconds delay.

Variability

The CEM gain can be changed and also preset^{3,5,14,15,26}—even from unity to zero within two gaze movements in this patient. Another interesting aspect is that the patient's drift is interrupted by multiple small saccades intruding on the slow movement, producing a nystagmus-type movement. A number of small saccades are seen in almost all the types, interrupted by small saccades that intrude upon the VOR reflex and appear as fragments of the fast phases of vestibular nystagmus here also. Conversely, we see in FIGURE 1 that an interrupted acceleration of the head movement appears to be a double movement and to be related to the double saccades seen in fatigued eye movements.² Here the interrupted fast head movement does not interfere with the vestibular ocular reflex that is generated.

What are the primary factors building the gaze types? The most important factor (TABLE 3) is the amount of prediction that the head movement undergoes so that its latency varies with respect to an EMG latency equal to the eye movement, from a late head movement (type II) to a very early head movement (type IV). We have shown that the predictability that the nervous system can use with head movements almost is equivalent to that for arm movements and is more powerful than in the eye-movement control system.^{21,26} The gaze types correlate with acceleration types of head movements. The latter have been studied previously as dynamic responses and confirmed by simulations.^{17,24} The type II late head movement is associated with small amplitudes and rather slow head-movement trajectories, shown by the often "fragmented" acceleration time functions. When the head movement occurs earlier than the eye saccade, we see gaze types III and IV. Both types occur quite frequently with larger amplitudes and therefore often with fast head accelerations.

Head peak positive accelerations mostly are higher than head negative accelerations and also are less "fragmented." Apparently when the head movement is large and also predicted, a highly efficient and time-optimal neural controller signal can be generated, also described in EMG studies.^{6,25} With the "classical" type I gaze, both fast and slow head accelerations can be seen. The possible variability of the head trajectory is noted particularly in this type. It contrasts with the rather stereotyped eye-movement trajectory.

In concluding our observations and analyses, we see how the more intentionally governed head movement influences the eye and gaze patterns on different levels of the central nervous system. Head movement changes on a higher level with various experimental conditions (e.g. prediction), and it acts on a lower level through its variant dynamic trajectories on the VOR and therefore on the eye movement. In addition to responses in healthy subjects to various experimental conditions, patients with homonymous hemianopia demonstrate highly abnormal gaze responses.

TABLE 3
INFLUENCES ON FREQUENCY OF GAZE TYPES*

Condition	Type	I Synchronous Eye-Neck EMG (34%) [†]	II Late Head Movement (4%) [†]	III Early Head Movement (43%) [†]	IV Late Eye Saccade (19%) [†]
Amplitude (60°/15°)		0.90	0.09	3.05	2.10
Intent (forced/natural)		0.73	3.80	2.20	3.50
Predictability (high/low)		0.71	0.85	1.60	2.90
Vigilance (high/low)		0.65	5.90	1.33	0.97
Apparent Target					
Brightness (high/low)		1.88	1.31	0.72	0.60
Helmet Pointer (with/without)		1.04	0.55	1.27	1.11

*The table shows the four experimentally coordinated gaze types (columns) and a variety of experimental protocol conditions (rows). For each condition, a ratio is formed to indicate the influence of that condition on the probability of different gaze types.

[†]Mean percentage of frequency of occurrence.

REFERENCES

1. ATKIN, A. & M. B. BENDER. 1968. Arch. Neurol. Chicago **19**: 559-566.
2. BAHILL, T., M. CLARK & L. STARK. 1975. Exp. Neurol. **48**: 107-122.
3. BARNES, G. 1979. J. Physiol. **287**: 127-147.
4. BARTZ, J. 1965. Science **114**: 1644-1645.
5. BENSON, A. & G. BARNES. 1979. Aviat. Space Environ. Med. **49**: 340-342.
6. BIZZI, E., R. KALIL & V. TAGLIASCO. 1971. Science **173**: 452-454.
7. DICHGANS, J., E. BIZZI, P. MORASSO & V. TAGLIASCO. 1974. Brain Res. **71**: 225-232.
8. FELDBAUM, A. 1965. Optimal Control Systems. Academic Press, Inc. New York, N.Y.
9. FLEMING, D., G. VOSSIUS, G. BOWMAN & E. JOHNSON. 1969. Ann. N.Y. Acad. Sci. **156**: 825-850.
10. FUCHS, A. & E. LUSCHEI. 1970. J. Neurophysiol. **33**: 382-392.
11. FUNK, C. & M. ANDERSON. 1977. Percept. Mot. Skills **44**: 599-610.
12. GREY, M. 1974. Vision Res. **14**: 395-403.
13. HENN, V. & B. COHEN. 1973. J. Neurophysiol. **36**: 115-124.
14. ITO, M., T. SHIIDA, N. YAGI & M. YAMAMOTO. 1974. Brain Res. **65**: 170-174.
15. KASAI, T. & D. ZEE. 1978. Brain Res. **144**: 123-141.
16. KELLER, E. & Y. KAMATH. 1975. Brain Res. **100**: 182-187.
17. LEHMAN, S. & L. STARK. 1979. J. Cybern. Inf. Sci. **2**: 21-43.
18. MEIENBERG, O., W. H. ZANGEMEISTER, M. ROSENBERG, W. F. HOYT & L. STARK. 1980. Ann. Neurol. (In press.)
19. MORASSO, P., E. BIZZI & J. DICHGANS. 1973. Exp. Brain Res. **16**: 492-500.
20. STARK, L., G. VOSSIUS & L. YOUNG. 1962. IEEE Trans. Hum. Factors Electron. **HFE3**: 52-57.
21. STARK, L. 1968. Neurological Control Systems. Plenum Press. New York, N.Y.
22. SUGIE, N. & M. WAKAKUWA. 1970. IEEE Trans. Syst. Sci. Cybern. **SSC6**: 103-109.
23. VAN NOORDEN, G. 1961. Arch. Ophthalmol. **66**: 694-703.
24. ZANGEMEISTER, W. H., A. JONES & L. STARK. 1981. Exp. Neurol. **71**: 76-91.
25. ZANGEMEISTER, W. H., L. STARK, O. MEIENBERG & T. WAITE. 1980. (Submitted.)
26. ZANGEMEISTER, W. H. & L. STARK. 1980. In Proceedings, OMS 80 Conference on Eye Movement Control. California Institute of Technology. Pasadena, Calif.

VESTIBULAR INFLUENCE UPON HEAD-EYE COORDINATION

G. R. Barnes and A. J. Prosser

*Royal Air Force Institute of Aviation Medicine
Farnborough, Hants, GU14 6SZ United Kingdom*

INTRODUCTION

Voluntary rotational movements of the head normally are carried out at a velocity level that provides a very potent stimulus to the angular movement receptors of the vestibular apparatus, the semicircular canals. Such a transient stimulus, whether it is induced by a volitional or a passive head rotation, evokes a reflex eye movement that, even in the absence of visual fixation, consists of two components: an initial saccade in the direction of head movement, and a slower component that returns the eye toward orbital center^{1,2} (FIGURE 1). There is little doubt that the slower component, which compensates for the head movement and stabilizes gaze position at the end of the saccade, corresponds to the slow phase of vestibular nystagmus observed during a passive rotational stimulus. Experiments on visual target acquisition have shown that an exactly similar pattern of eye movement is evoked when the subject makes coordinated head and eye movements to view discrete target sources in the peripheral visual field²⁻⁵ (FIGURE 1).

The question that arises is whether the saccadic eye movement of visual search corresponds to the fast-phase component of vestibular nystagmus or, alternatively, whether the visual and vestibular afferents share a common input to the mechanism of saccadic generation. If either is true, it would be expected that the saccadic component of eye movement during visual search would be modified in the presence of a coexistent stimulus to the vestibular apparatus.

Previous experiments on patients with spontaneous nystagmus of vestibular origin have indicated that such an interaction of the nystagmus fast phase and the saccadic eye movement could be observed during voluntary head movements in the dark.⁶ In the present experiment an attempt has been made to quantify these interactions by instructing the subject to make voluntary head movements during the period of a postrotational vestibular stimulus.

METHODS

Apparatus

The subjects were seated on a small turntable, which was positioned at the center of a semicircular periphery of radius 1.2 m. Embedded into the periphery were small red-light-emitting diodes, each subtending approximately 0.2° at the eye and having a luminance of 2.5 cd/m². The lights were placed at approximately equal (15°) intervals around the periphery to left and right of a center light. The sequence of presentation of the target lights was made under computer control.

A lightweight helmet was worn by the subject (see Reference 2 for details). The crown of the helmet was attached by a flexible coupling to a rotary

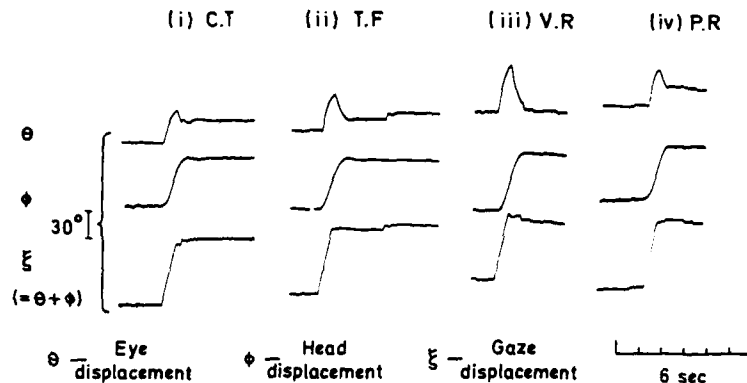


FIGURE 1. The oculomotor response to voluntary head movements in four experimental conditions: (i) CT—continuous target presentation; (ii) TF—target light flashed on for 100 mseconds; (iii) VR—voluntary head movements in the dark; and (iv) PR—passively induced head movements in darkness. (All figures © Ministry of Defense, London, England.)

potentiometer mounted above the subject's head on a support member attached to the turntable. This enabled the angular position of the head to be measured for rotational movements about the vertical axis. An angular accelerometer also was attached to the helmet to measure the acceleration of the head about the axis of rotation.

Eye movements were recorded using the electro-oculographic (EOG) technique with Ag-AgCl electrodes placed beside the external canthi. The subjects wore a red filter visor during the initial setting-up period and throughout the experiments in order to stabilize the corneoretinal potential and hence the gain of the EOG recording. The experiment was carried out in a darkened laboratory in which no visual positional cues were available to the subject other than the target lights.

Eight subjects (three male, five female) took part in the experiment. None had any known visual or vestibular defect, and all had normal mobility of the head and neck.

Experimental Procedure

Subjects were rotated on the turntable for a period of 60 seconds at a velocity of approximately 100°/second. At the end of this period, rotation was stopped abruptly with the subject coming to rest facing in the direction of the center target light. During the ensuing period, in which a potent nystagmus was present, the subjects were exposed to one of the following two experimental conditions.

Target Flash Presentation (TF Condition)

The subject made head and eye movements toward target lights, which appeared for 100 mseconds in random order at offset angles of $\pm 30^\circ$ and $\pm 60^\circ$.

Twenty sequences of target presentation were given; each sequence began with a brief presentation of the center target, which was followed, after a 2-second delay, by the illumination of the offset target. Two seconds elapsed before the start of the next sequence. The advantage of this procedure was that it allowed an indication of target position to be given without continuous fixation so that there was very little, if any, suppression of the postrotational nystagmus. Previous experiments had established that such briefly presented targets would, in normal circumstances, lead to an accurate determination of the required saccadic amplitude.^{2,5,7}

Voluntary Head Rotation in the Dark (VR Condition)

In this experimental condition, the subject voluntarily rotated the head about the yaw axis in the dark, with the eyes open. The discrete movements were made in a set sequence starting from the central position, moving to a random offset position, and then returning to center. There was no instruction to make voluntary eye movements. Each subject made 40 or more individual head movements in approximately the same period (80 seconds) as those in the TF condition.

Each of the two experimental conditions was conducted twice, once following rotation to the left and once after rotation to the right. These four sessions were presented to the subjects in a balanced randomized design.

RESULTS

Qualitative Features

The responses from all subjects showed that the presence of a concurrent vestibular response had a profound effect upon the oculomotor response during visual search (FIGURE 2). When the head displacement was in the opposite direction to the fast phase of the postrotational nystagmus, the onset of the saccade associated with that head movement was delayed and the amplitude of the saccade was reduced; this is illustrated by the first, fourth, sixth, seventh, and ninth head movements in FIGURE 2. Conversely, when the head movements were made in the same direction as the nystagmus fast phase, the saccades were of larger amplitude. There was also less delay between the start of head acceleration and the onset of the saccade when the head was moved in the direction of the fast phase, although it was sometimes difficult to define which saccade actually was related to the head movement.

The interaction of the postrotational nystagmus with head-movement-induced saccades appeared to be similar both in the target flash condition, where there was an indication of retinal target location, and during the voluntary head movements executed in the dark.

Quantitative Features

Data Reduction

The results were analyzed on a computer (HP 9845) with interactive graphics capability. The recordings of head and eye movement were sampled at 5-

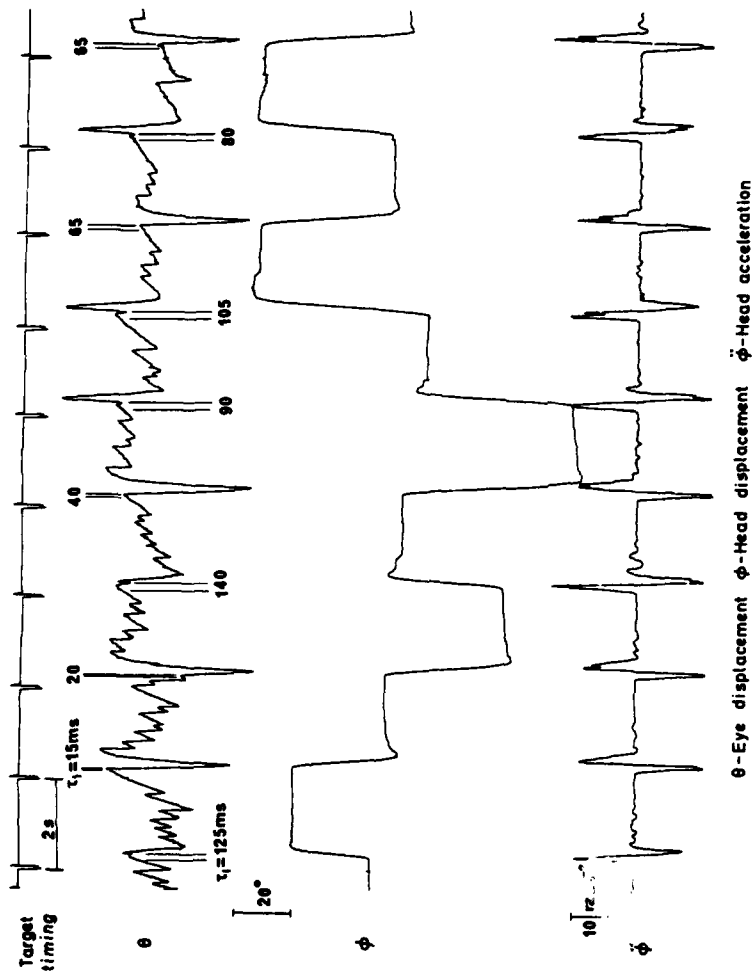


FIGURE 2. The effects of a concurrent postrotational vestibular response on the temporal characteristics of head-eye coordination during acquisition of briefly presented visual targets. t_1 is the delay between onset of head acceleration ($\ddot{\phi}$) and the initiation of the associated saccadic eye movement.

msecond intervals and displayed on the video screen. This enabled each individual response to be analyzed separately with high resolution. The following variables have been analyzed:

1. The latency, τ_1 , between the start of head acceleration and the onset of the saccadic eye movement (FIGURE 2).
2. The duration of the saccadic eye movement (τ_2).
3. The angular velocity of the head at the onset of the saccade (H_v), obtained by integration of the head-acceleration profile.

It had been intended that certain amplitude relationships between head, eye, and gaze position also would be examined. However, this proved extremely difficult because of the inherent drift in the d.c.-recorded EOG, and the problem of defining the intended eye position in the TF condition.

During the period following the cessation of rotation, the slow-phase eye velocity of the nystagmus, induced by the abrupt deceleration, decayed in an exponential manner. The average initial slow-phase velocity was $93^\circ/\text{second}$ for the TF condition and $114^\circ/\text{second}$ for the VR condition. The response decayed to zero within 30–40 seconds and was followed, in all subjects, by a sustained secondary nystagmus with a peak average slow-phase velocity of $-7^\circ/\text{second}$. In the presentation of results that follows, the variables have been considered first with respect to time and second with respect to slow-phase eye velocity.

The Latency (τ_1) of Eye Movement with Respect to Head Acceleration

The relationship between the start of head movement, as monitored by the angular accelerometer attached to the head, and the onset of the saccadic eye movement is plotted in FIGURE 3 as a function of time (t) after the cessation of rotation. The upper traces indicate separately the values obtained when the head movement was made in the opposite direction (τ_1^-) and in the same direction (τ_1^+) as the fast phase of the postrotational nystagmus. In both stimulus conditions, τ_1^- decayed from an initial peak value of 120–130 mseconds in an approximately exponential manner that was similar to the decay of the nystagmus slow-phase eye velocity. Conversely, the value of τ_1^+ increased as slow-phase velocity decayed to the extent that during the period of the secondary nystagmus ($t > 40$ seconds), the mean level of τ_1^+ exceeded that of τ_1^- .

In both experimental conditions, the latencies for head movements made in the same direction as the fast phase were always less than for head movements in the opposite direction. The differences in latency, $d\tau_1 (-\tau_1^- - \tau_1^+)$, were highly significant ($p < 0.001$) for the first 12 seconds of the response and less significant for other periods, as detailed in the lower traces of FIGURE 3.

Correlation of the variables τ_1^- and τ_1^+ with slow-phase eye velocity for individual subjects showed that a linear relationship between these variables could be assumed with a high level of probability ($p < 0.01$).

The majority of the subjects responded with saccadic eye movements that were initiated after the start of head movement, with latencies slightly greater than those observed in a previous experiment.² One subject, however, repeatedly initiated eye movement before or simultaneously with head acceleration during the low-velocity phase of the postrotational response in the target flash condition, though not during voluntary head movements in the dark. It is, however, of interest that in this subject the values of τ_1^- were positive during the initial period of the decaying slow-phase eye velocity and decayed progressively with time, as they did for the other subjects. Thus, it would appear that the vestibular response

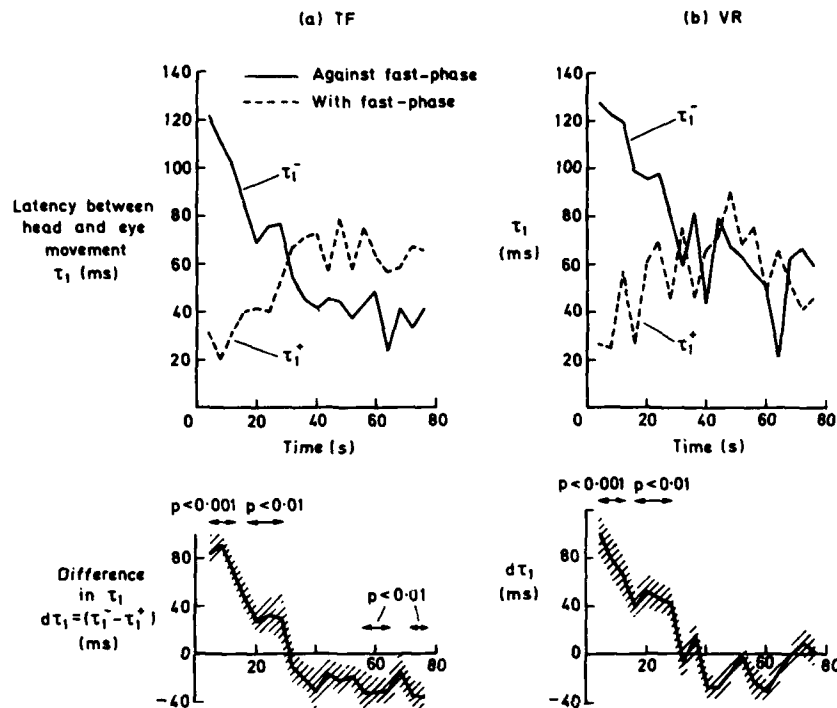


FIGURE 3. The effect of a postrotational vestibular response on the latency between head and eye movement during head movements with (τ_1^+) and against (τ_1^-) the direction of the nystagmus fast-phase component. (a) Target flash (TF) condition. (b) Voluntary head movements (VR) in the dark. Mean of 8 subjects ± 1 standard error of the mean (SEM) in lower traces.

is able to modify the timing of the saccade even when, under normal circumstances, it is initiated before the head movement and is, patently, not of vestibular origin.

The Duration (τ_2) of the Saccadic Eye Movement

In order to obtain some indication of the influence of the postrotational response on the amplitude of the eye movements, the duration of the saccade has been examined. During normal saccadic eye movements of amplitude greater than approximately 10° , the velocity is constant ($\approx 300\text{--}400^\circ/\text{second}$) and the amplitude is proportional to the duration of the saccade.⁸ The results in FIGURE 4 show how the duration (τ_2) of the saccadic eye movement associated with the voluntary head movement was modified by the presence of the postrotational nystagmus. In both experimental conditions, the duration increased as a function of time for head movements against the nystagmus fast phase and decreased for movements in the same direction as the fast phase. The difference in saccadic duration, $d\tau_2 = (\tau_2^- - \tau_2^+)$, was highly significant ($p < 0.001$) for the first 24 seconds of the postrotational response and reversed in polarity during the period

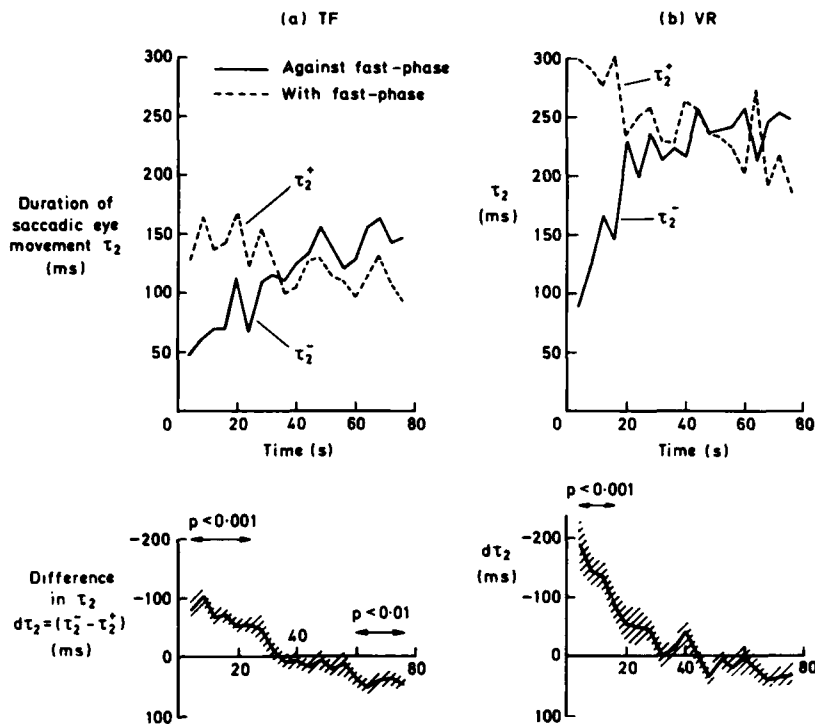


FIGURE 4. The effect of a postrotational vestibular response on the duration of the saccadic eye movement of visual search during head movements with (τ_2^+) and against (τ_2^-) the direction of the nystagmus fast-phase component. (a) Target flash (TF) condition. (b) Voluntary head movements (VR) in the dark. Mean of 8 subjects ± 1 SEM in lower traces.

of the secondary nystagmus. Correlation of saccadic duration with eye velocity revealed a linear relationship between the two variables, which was significant at the 5% level.

Measurement of the saccade duration in these circumstances gives only an approximate indication of the changes to be expected. In the results from the TF condition, considerable variability is present because the responses to both 30° and 60° targets have been analyzed together. Similarly, during the voluntary responses in the dark, the lack of control over the actual amplitude of head movement contributes to the overall variance. Nevertheless, the results do show that the postrotational response has a significant effect on the duration of the saccadic eye movement.

The Velocity of Head Movement (H_v) at the Onset of the Saccade

As the latency between the start of a head movement and the onset of a saccade increases, the actual head velocity achieved before saccadic initiation

also should increase, because there is a longer initial acceleration period. The results shown in FIGURE 5 indicate that, as expected, the head velocity decreased exponentially with time for movements against the fast phase and, conversely, increased for those in the same direction as the fast phase. The difference in head velocity (dH_v) of consecutive pairs of movements also decreased in a manner that closely followed the time course of the slow-phase velocity of nystagmus. In both experimental conditions, it was found that the values of dH_v were significantly greater than zero ($p < 0.001$) for the initial 12 seconds of the response. Correlation of head velocity and slow-phase eye velocity exhibited a highly significant relationship ($p < 0.001$) for all subjects.

It is worthy of note that the mean head velocity at the start of the saccade that corresponded to the normal condition of zero initial slow-phase eye velocity was approximately $35\text{--}40^\circ/\text{second}$. It is clear that such a velocity level is more than sufficient to elicit a response from the semicircular canals, although it should be noted that this measure exhibited wide intersubject variation, with values that ranged from $0^\circ/\text{second}$ in one subject to $74^\circ/\text{second}$ in another.

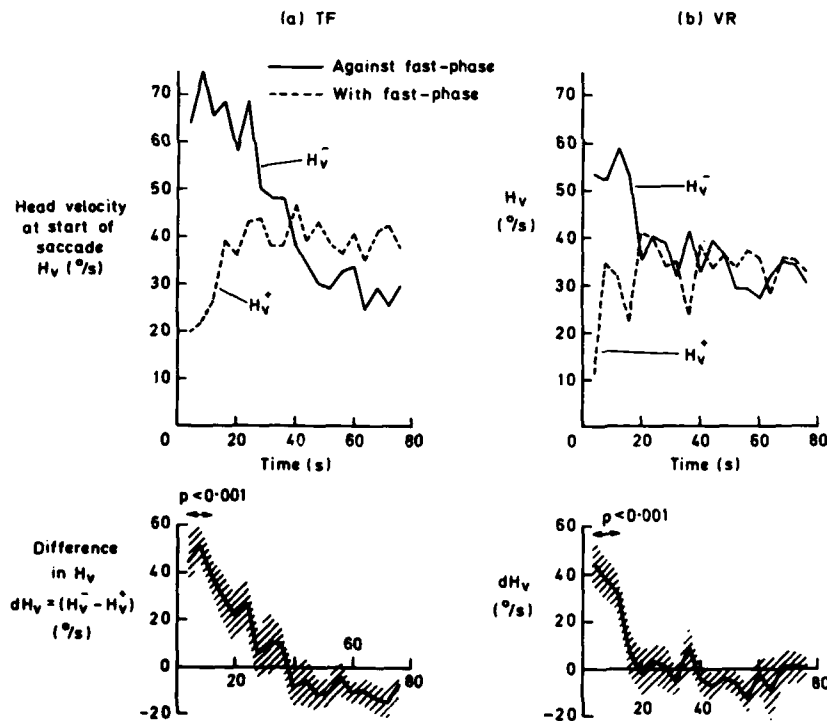


FIGURE 5. The effect of a postrotational vestibular response on the head velocity at the initiation of the saccadic eye movement during head movements with (H_v^+) and against (H_v^-) the direction of the nystagmus fast-phase component. (a) Target flash (TF) condition. (b) Voluntary head movements (VR) in the dark. Mean of 8 subjects ± 1 SEM in lower traces.

DISCUSSION

The results of this experiment demonstrate that the presence of a concurrent stimulus to the vestibular system can significantly modify the temporal characteristics of head-eye coordination during voluntary head movements. This modification of performance was unlikely to have been due simply to the unfamiliar or disorientating nature of the stimulus. Such an effect might well have been expected to lead to an overall modification of the values of the latency τ_1 , but not one that would be dependent on the direction of head movement. There is thus a direct interaction between the output of the vestibular system and the mechanism responsible for generating the saccadic component during visual search. It is probable that this interaction takes place at or before the input to the mechanism of saccadic generation, since any mixing of responses beyond this level would give rise to changes in the amplitude characteristics of the eye movement but not in the temporal relationships.

It is possible that the interaction takes place within the vestibular apparatus itself, since the modification of response is that which would be predicted from the combined effects of the postrotational stimulus and the head-turning movements on the cupulae of the semicircular canals. In earlier experiments it has been shown that a saccadic eye movement, similar to that seen during visual search, can be elicited from stimulation of the lateral canals by head rotation in the dark.^{1,2} In an attempt to model the occurrence of such saccades (and of the fast phase of vestibular nystagmus), it has been suggested that saccades occur whenever the output of the canals, which represents the driving signal proportional to eye velocity, exceeds a certain threshold level.³ During the period of the postrotational nystagmus, the slow-phase eye velocity does not change appreciably during the short course of a voluntary head movement and may be regarded as effectively constant. The head movement itself stimulates the semicircular canals to respond by producing a compensatory driving signal to the eyes, the velocity of which mirrors that of the head. Consequently, when the head movement is in the direction of the nystagmus fast phase, the slow-phase component due to head movement will be added to that of the nystagmus and the resultant eye-velocity driving signal will exceed the threshold after a shorter latency (τ_1^+) and at a lower head velocity (H_v^+) than normal. Conversely, when the head is moved in the opposite direction, the latency (τ_1^-) and the head velocity (H_v^-) would be increased. These predictions are in accord with the experimental results (FIGURES 3 and 5). In the latter condition, it would also be predicted that a reversal of slow-phase eye velocity would occur just prior to the saccade, a feature that was observed frequently in the oculographic recordings (FIGURE 2).

Another prediction of the model was that the duration of the saccade (τ_2) should be related to slow-phase eye velocity,⁴ which in normal circumstances would represent head velocity. It therefore is not surprising to find that the duration was increased when the slow-phase components due to the head movement and the postrotational stimulus were additive (τ_2^+) and decreased when they were subtractive (τ_2^-). This result is in accord with the findings of an earlier experiment, in which the amplitude of the gaze saccade was found to be highly correlated with the velocity of head movement during visual search.²

Thus, the results are not incompatible with the hypothesis that the saccade of visual search is of vestibular origin. However, it is not possible to rule out some other, more complex interactive mechanism between the visual and vestibular

inputs to the saccadic mechanism. There is some evidence for this in the present experiment from the results of the one subject who consistently initiated eye movements before head movement in the target flash condition, a response that clearly rules out any vestibular involvement in saccadic initiation. Nevertheless, even in these responses there was the same modification of the latency (τ_1) and the duration of the saccadic eye movement (τ_2). These findings are consistent with those of a previous experiment, in which it was found that for larger amplitude head movements, the saccade might be initiated by visual or other central means but that the amplitude, and thus also the duration of the saccade, was more closely correlated with the expected output of the vestibular system than with the actual retinal error signal.²

On the basis of previous experiments, it has been argued that there are probably two modes of head-eye coordination.^{2,10} In the primary and dominant mode, which may be termed target acquisition, the saccade is calculated accurately on the basis of a reliable retinal error signal and may be initiated before head movement. In a secondary and subordinate mode, which represents one of visual search rather than target acquisition, the subject makes head movements in the direction of the target location and the saccadic eye movement is generated as a reflex response to the head-turning movement. It is this latter mode that is seen during voluntary head movements in the dark, and probably also when making coordinated movements to locate targets that are positioned more eccentrically in the peripheral visual field. Although in the target flash condition, there was an indication of retinal error, it is probable that the subjects reacted with a visual-search-mode response because the disorientating sensations associated with the postrotational stimulus often gave rise to some uncertainty about the target location.

It therefore is difficult at present to say with any certainty how a saccade that is known to be of visual origin might interact with such a vestibular response. In a future experiment, it is planned to investigate the interaction of the visual and vestibular mechanisms in experimental conditions in which the saccadic eye movement is known to be initiated by the visual system. Preliminary results from this experiment indicate that there is a significant interaction, which can, under some circumstances, lead to the complete elimination of the visual saccade when there is a coexistent nystagmus of vestibular origin.

REFERENCES

1. BARNES, G. R. 1975. The role of the vestibular system in head-eye co-ordination. *J. Physiol. London* **246**: 99-100P.
2. BARNES, G. R. 1979. Vestibulo-ocular function during co-ordinated head and eye movements to acquire visual targets. *J. Physiol. London* **287**: 127-147.
3. BARTZ, P. E. 1966. Eye and head movements in peripheral vision: nature of compensatory eye movements. *Science* **152**: 1644-1645.
4. BIZZI, E., R. E. KALIL, P. MORASSO & V. TAGLIASCO. 1972. Central programming and peripheral feedback during eye-head co-ordination in monkeys. *Bibl. Ophthalmol.* **82**: 220-232.
5. GREY, M. A. 1974. Co-ordination of head and eye movements to fixate continuous and intermittent targets. *Vision Res.* **14**: 395-403.
6. BARNES, G. R. 1979. Head-eye co-ordination in normals and in patients with vestibular disorders. *Adv. Oto-Rhino-Laryngol.* **25**: 197-201.
7. BARNES, G. R. & M. A. GREY. 1973. Characteristics of eye movements to targets of short duration. *Aerosp. Med.* **44**: 1236-1240.

8. ZUBER, B. L., L. STARK & M. COOK. 1965. Microsaccades and the velocity-amplitude relationship for saccadic eye movement. *Science* **150**: 1459-1460.
9. BARNES, G. R. 1977. The Role of the Saccadic Mechanism in Head-Eye Co-ordination; The Development of a Theoretical Model. IAM Report No. 570. RAF Institute of Aviation Medicine. Farnborough, Hants, United Kingdom.
10. BARNES, G. R. 1980. Visual-vestibular interaction in the coordination of voluntary eye and head movements. In *Progress in Oculomotor Research*. A. Fuchs & W. Becker, Eds. Elsevier. New York, N.Y. (In press).

DISTURBANCES OF EYE-HEAD COORDINATION DURING LATERAL GAZE IN LABYRINTHINE DISEASE

Takuya Uemura, Yasuko Arai, and Chiga Shimazaki

*Department of Otolaryngology
Tokyo Women's Medical College
Tokyo 162, Japan*

INTRODUCTION

Patients with acute labyrinthine disorders frequently complain of the visual sensation of movement of the surroundings on head rotation.¹ This optic illusion in unilateral labyrinthine lesion cases occurs when the head moves in a particular direction, and the direction of the illusory motion usually is opposite to that of the head movement.² Although little information is available on retinal image stability in such cases, it is reasonable to suppose that these phenomena may be related to defective eye-head coordination found in bilaterally labyrinthectomized monkeys and labyrinthine-defective human beings.^{3,4}

We have devised an apparatus that enables us to record head rotation without mechanical restraint and have reported on the characteristics of eye-head coordination in normal subjects.⁵⁻⁷ Using this apparatus, we herein analyze the eye-head coordination during lateral gaze in patients with unilateral and bilateral labyrinthine lesions.

METHODS

Horizontal eye movements were recorded by d.c. electro-oculography through bitemporal leads. Horizontal head rotation was recorded using a device containing two terrestrial magnetic sensors. Terrestrial magnetism was reinforced by two pieces of Permalloy placed at both sides of a Hall element, which functioned as a terrestrial magnetic sensor. Two sensors were placed perpendicular to one another and mounted on the subject's head by means of a light plastic helmet. The total weight of the apparatus including the helmet was 450 g. Only a thin wire was necessary to make electrical connection to the apparatus. Thus the subject could move his head without feeling any mechanical restraint or psychological load on head rotation. The output voltage of the sensors was proportional to the angular rotation within a range of $\pm 50^\circ$ with an error of less than 1%.

To examine the accuracy of the present recording techniques for head and eye movements, we measured gaze displacements, i.e., summation of head and eye displacements, of 10° to 50° at the final resting position of lateral gaze in 10 normal subjects. The means of gaze displacement agreed very well with the target angles, and the standard deviations corresponded to approximately 5% of each target angle.⁷ Since normal subjects must fix the target on the fovea at the end of gaze, this proves that the recording methods used in this study are able to record head and eye movements within a gaze displacement of 50° with satisfactory accuracy. Eye position in space, i.e., gaze, was displayed by electrically adding the eye and head movements.

In this report, 11 patients with unilateral and 5 patients with bilateral loss of labyrinthine function (unilateral and bilateral lesions), who showed complete

canal paresis of the involved ear or ears by caloric testing, were examined. Of the unilateral lesion cases, 5 were patients with vestibular neuritis, 3 with Ramsay Hunt syndrome, and 3 with idiopathic aural vertigo. Of the bilateral lesion cases, 2 were patients with ototoxicity due to glycoside antibiotics and the other 3 were of unknown etiology. The periods between the onset of disease and the initial testing were 1 to 13 days in the unilateral lesions and 1 to 9 months in the bilateral lesions.

After at least 15 minutes of dark adaptation, the lateral gaze test and the alternate side-to-side gaze test were performed. The visual targets were red-light-emitting diodes subtending a 0.14° visual angle, which were mounted in a 2-m radius semicircular panorama at 20° and 40° right and left of the central diode. In the lateral gaze test, the subjects sitting at the center of the panorama were instructed to move both their head and eyes to fixate the target as it jumped from the center to one of the four lamps and back to the center 4 seconds later. The order of target presentation was randomized. Each lamp was presented five times and a subject underwent a total of 20 trials. In addition to the continuous mode of target presentation, the subjects were tested in two ways; first by using a target lamp that was turned off after the eye speed had reached $40^\circ/\text{second}$ and relighted 1 second later (eye-triggered mode); and second by using another lamp, which was extinguished during the period of time when the head was moving at a speed of more than $5^\circ/\text{second}$ (head-triggered mode). In the alternate side-to-side gaze test, the subjects were asked to look at one of the two target lamps 40° apart—which were turned on 20 times alternately at intervals of approximately 1 second—with the head fixed and then with the head free. The entire testing procedure took about half an hour. Eye movements were calibrated after the subjects had adapted to the dark and whenever the test conditions were changed.

RESULTS

Unilateral Lesions

When a subject is asked to look at a target, first the eyes move and then the head starts to move. After the sum of eye and head movements, i.e., gaze, has reached the target angle, the eyes stop and thereafter perform a counter-movement (compensatory eye movement) to continue their target fixation during the head movement (FIGURE 1A).

In addition to this normal type of gaze change, patients with unilateral lesions often showed two other types of eye-head coordination. One is the "overshoot" type of FIGURE 1B, in which the eyes and head move to the target similarly to the normal type. However, the compensatory eye movement is not enough to cancel the head movement. Thus the gaze drifts in the direction of head movement and causes an overshoot. The gaze overshoot is corrected by a saccade, as shown by the arrow in FIGURE 1B. In this case, the amplitude of gaze overshoot was 10° and the interval between the onset of the compensatory eye movement and that of the corrective saccade was 580 mseconds. Another pattern is the "rounding" type of FIGURE 1C, in which the eyes stop before the gaze reaches the target. However, since the compensatory eye movement is smaller than the head movement, the gaze continues to move slowly and reaches the target. The ratio of the peak velocity of the compensatory eye movement to the peak head velocity, i.e., VOR

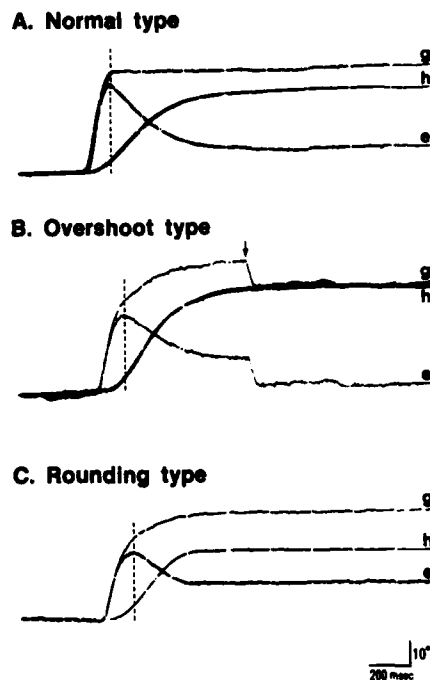


FIGURE 1. Three types of eye-head coordination often seen in patients with labyrinthine disorders. The vertical dotted lines show the end of the eye saccade that corresponds to the onset of compensatory eye movement. The arrow in the overshoot type (B) indicates a saccadic change for correcting gaze overshoot. e, h, and g: records of eye, head, and gaze displacements.

gain, is less than 1.0 in both the overshoot and the rounding types. On the other hand, the pattern of eye-head coordination in which VOR gain is greater than 1.0 is rare.

The appearance rates of abnormal responses with VOR gain less than 1.0 in the lateral gaze tests initially performed in 11 cases are shown in the order of the period of time between the onset of disease and the testing (FIGURE 2, unilateral lesions). Except for one case (Case 9) that was tested 12 days after onset, all cases showed abnormal responses of the overshoot and/or the rounding types. The appearance rates of the abnormal responses are especially high on ipsilateral gaze, and gaze overshoots were found only on the same side.

The lateral gaze tests were repeated in the eye-triggered mode (E-T), in which the target light is extinguished for one second after the start of eye movement, and in the head-triggered mode (H-T), in which the light is off during the period of head movement. As shown by the darker numbers in TABLE 1, the appearance rates of abnormal responses with VOR gain less than 1.0 increased in the majority of cases and reached 100% in a few cases. Even in Case 9, showing no abnormal response in the continuous mode, the rates became 56% and 64% in the eye- and the head-triggered modes respectively. The overshoot-type

VOR < 1 RESPONSES IN PATIENTS WITH LABYRINTHINE LESIONS

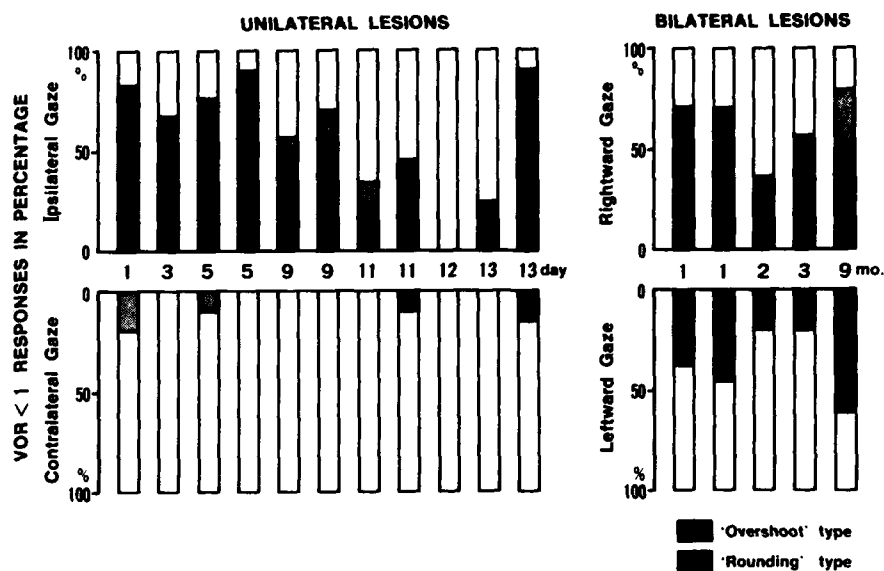


FIGURE 2. The appearance rates of responses with VOR gain less than 1.0 at the initial testing in patients with unilateral and bilateral lesions. On the abscissa is the period of time from the onset of the disease. On the ordinate is the percentage of the normal and abnormal responses of each type.

TABLE 1
PERCENTAGES OF RESPONSES WITH VOR GAIN LESS THAN 1.0 UNDER VARIOUS TEST CONDITIONS IN PATIENTS WITH UNILATERAL LESIONS*

Case	Ipsilateral Gaze				Contralateral Gaze			
	CT.	E-T	H-T	Alter.	CT.	E-T	H-T	Alter.
1	82 (82)	75 (67)	77 (55)	100 (100)	18 (0)	42 (17)	38 (13)	50 (0)
2	67 (42)	67 (17)	78 (61)	100 (37)	0 (0)	11 (0)	0 (0)	6 (6)
3	76 (33)	100 (100)	100 (40)	91 (36)	10 (0)	10 (0)	10 (0)	0 (0)
4	90 (90)	95 (95)	100 (100)	100 (100)	0 (0)	5 (5)	0 (0)	0 (0)
5	55 (15)	26 (5)	66 (33)	62 (0)	0 (0)	0 (0)	0 (0)	0 (0)
6	69 (16)	75 (25)	60 (0)	100 (56)	0 (0)	5 (0)	0 (0)	0 (0)
7	33 (14)	70 (55)	47 (42)	78 (45)	0 (0)	10 (0)	0 (0)	0 (0)
8	45 (15)	50 (50)	85 (85)	75 (75)	10 (0)	0 (0)	9 (0)	11 (11)
9	0 (0)	58 (31)	64 (40)	100 (55)	0 (0)	16 (0)	0 (0)	8 (0)
10	25 (20)	20 (10)	45 (35)	92 (84)	0 (0)	0 (0)	0 (0)	8 (0)
11	90 (50)	80 (30)	95 (74)	88 (25)	15 (0)	25 (0)	10 (0)	19 (13)

*The percentages of overshoot-type responses are given in parenthesis. When the percentage is increased by one or more of the three additional tests—i.e., the lateral gaze test: in the eye-triggered (E-T) and head-triggered (H-T) modes and the alternate side-to-side gaze test (Alter.)—over that of the lateral gaze test in the continuous mode (CT.), in each case, the number is set in bold type.

responses also appeared on contralateral gaze in a few cases, though these were far fewer than on ipsilateral gaze.

The alternate side-to-side gaze tests also revealed much higher positive rates of responses with VOR gain less than 1.0 than did the lateral gaze tests in the continuous mode (TABLE 1). As shown in FIGURE 3, middle, the overshoot- and rounding-type responses tend to occur exclusively on ipsilateral gaze.

The appearance rates of the overshoot-type responses in Case 3, tested frequently during the course of disease, are shown in FIGURE 4. When the lateral

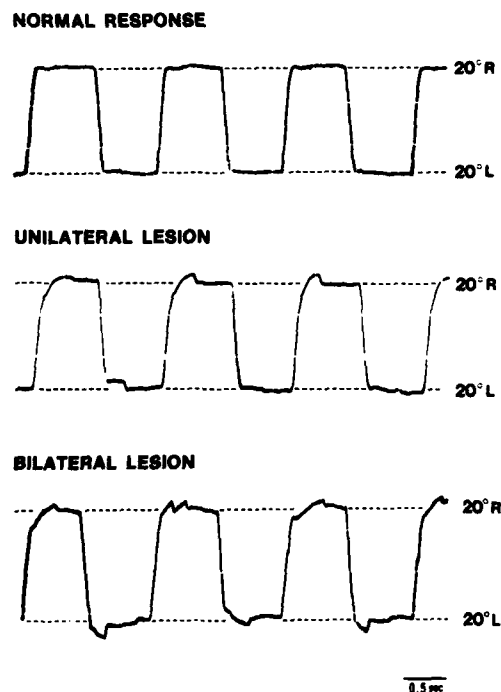


FIGURE 3. Normal and abnormal responses obtained by the alternate side-to-side gaze tests in patients with unilateral and bilateral lesions. Gaze overshoots are seen on gazing toward the involved side (20° right) in unilateral lesion (middle) and on gazing toward both sides in bilateral lesion (bottom).

gaze tests were performed in the continuous mode, the overshoot-type responses disappeared within one month. However, under different test conditions, the gaze overshoots were observed for over one month and disappeared within six months.

Bilateral Lesions

Although patients with bilateral lesions underwent the lateral gaze tests in the continuous mode of target presentation one to nine months after the onset of disease, all five cases showed the overshoot- and the rounding-type responses on

gazing to both sides (FIGURE 2, bilateral lesions). As seen in patients with unilateral lesions, the appearance rates of responses with VOR gain less than 1.0 were markedly increased in almost all cases by means of one or more of the three additional tests, i.e., the lateral gaze tests in the eye- and head-triggered modes and the alternate side-to-side gaze test (TABLE 2).

COMMENTS AND CONCLUSIONS

Under the condition of maintaining natural head motility, we studied eye-head coordination during lateral gaze in patients with unilateral and bilateral labyrinthine lesions.

All patients with unilateral lesions, when tested initially within 11 days after the onset of disease, showed the overshoot- and/or rounding-type responses, in which the ratio of the velocity of eye movement and the head velocity (VOR gain) was less than 1.0. These responses appeared far more frequently on gazing toward the involved side, and the occurrence of gaze overshoot was limited to the same side. This asymmetrical appearance seems to reflect the nonlinear sensitivity of the labyrinth whereby the excitation tends to be greater than the inhibition.^{8,9}

Five patients with bilateral lesions tested 1 to 9 months after the onset of disease showed responses with VOR gain less than 1.0 on gazing toward both the left and the right sides. The durations of abnormal responses were longer than those in patients with unilateral lesions, where they disappeared within approximately one month. This indicates the difficulty of compensation in bilateral lesions.

When the lateral gaze tests were repeated using the target presentation of the

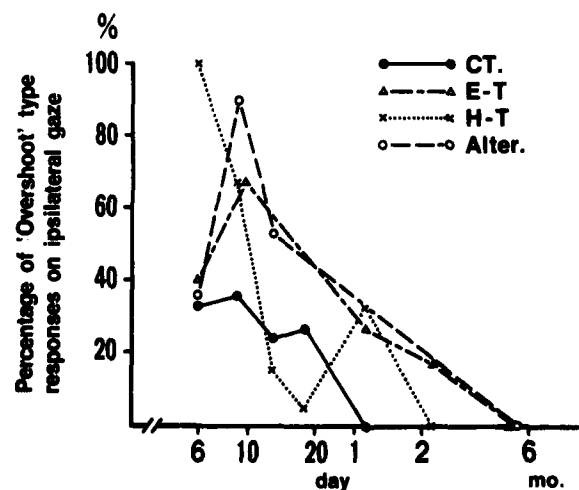


FIGURE 4. Incidences of overshoot-type response on ipsilateral gaze in a patient with vestibular neuritis (Case 3) during the course of disease. CT., E-T, and H-T: the lateral gaze tests in the continuous, eye-triggered, and head-triggered modes of target presentation. Alter.: the alternate side-to-side gaze test.

TABLE 2
PERCENTAGES OF RESPONSES WITH VOR GAIN LESS THAN 1.0 UNDER VARIOUS TEST
CONDITIONS IN PATIENTS WITH BILATERAL LESIONS*

Case	Rightward Gaze				Leftward Gaze			
	CT.	E-T	H-T	Alter.	CT.	E-T	H-T	Alter.
1	70 (30)	90 (30)	41 (0)	100 (100)	37 (21)	48 (32)	38 (19)	60 (40)
2	70 (25)	100 (65)	83 (71)	100 (79)	45 (25)	48 (37)	47 (35)	85 (85)
3	35 (5)	50 (0)	40 (10)	30 (10)	20 (10)	42 (11)	50 (15)	11 (0)
4	55 (10)	90 (67)	73 (47)	100 (40)	20 (5)	72 (33)	51 (8)	70 (40)
5	79 (42)	65 (25)	78 (33)	92 (92)	61 (42)	77 (59)	95 (56)	91 (82)

*The percentages of overshoot-type responses are given in parenthesis. Other features are the same as in TABLE 1.

eye- and the head-triggered modes, the appearance rates of abnormal responses were markedly increased on ipsilateral gaze and gaze overshoots were found even on contralateral gaze, though still infrequently. This tendency also was detected in the alternate side-to-side gaze tests. These results are different from those of Kasai and Zee in labyrinthine-defective subjects.⁴ They reported that various types of gaze changes occurred at approximately the same frequency either in the continuously illuminated target mode or in the target flash mode, and gaze stability was improved markedly when the subjects could anticipate the next position of a jumping target. The difference may be explained by the incompleteness of adaptive strategies to stabilize gaze after labyrinthine lesions in our cases, in which gaze stability depends to a considerable extent on the presence of visual stimuli and is disturbed easily by the repetition of gaze change in the alternate side-to-side gaze tests.

The tests for eye-head coordination mentioned here have two advantages: the subjects are examined during the simple, natural behavior of looking at the target with the head free, and the results correspond well to their subjective symptoms by indicating the presence of visual illusion on head rotation.

REFERENCES

1. J. C. 1952. Living without a balancing mechanism. *N. Engl. J. Med.* **246**: 458-460.
2. BENDER, M. B. & M. FELDMAN. 1967. Visual illusions during head movement in lesions of the brain stem. *Arch. Neurol.* **17**: 354-364.
3. DICHGANS, J., E. BIZZI, P. MORASSO & V. TAGLIASCO. 1973. Mechanisms underlying recovery of eye-head coordination following bilateral labyrinthectomy in monkeys. *Exp. Brain Res.* **18**: 548-562.
4. KASAI, T. & D. S. ZEE. 1978. Eye-head coordination in labyrinthine-defective human beings. *Brain Res.* **144**: 123-141.
5. UEMURA, T., Y. ARAI, N. KIKUCHI, R. ISHIKAWA, C. SHIMAZAKI & H. ITO. 1976. Analysis of eye-head coordination in humans—a preliminary report. *Pract. Otol. Kyoto* **69**: 1819-1823.
6. TAKAHASHI, M., T. UEMURA & T. FUJISHIRO. 1980. Studies of the vestibulo-ocular reflex and visual-vestibular interaction during active head movements. *Acta Otolaryngol.* **90**: 115-124.
7. UEMURA, T., Y. ARAI & C. SHIMAZAKI. 1980. Eye-head coordination during lateral gaze in normal subjects. *Acta Otolaryngol.* **90**: 191-198.

8. TRINKER, D. 1959. Electrophysiological studies of the labyrinth of the guinea pig. II. The changes of the DC potentials inside the ampullae of the semicircular canals during experimental cupula deviations. *Ann. Otol. Rhinol. Laryngol.* **68**: 148-152.
9. GOLDBERG, J. M. & C. FERNÁNDEZ. 1971. Physiology of peripheral neurons innervating semicircular canals of the squirrel monkey. I. Resting discharge and response to constant angular accelerations. *J. Neurophysiol.* **34**: 635-660.

THE INTERACTION BETWEEN ACCURACY OF GAZE WITH AND WITHOUT HEAD MOVEMENTS IN PATIENTS WITH CEREBELLAR ATAXIA*

Natsue Shimizu,† Masahiro Mizuno,‡ Makoto Naito,§ and
Mitsuo Yoshida†

*Jichi Medical School
Tochigi-ken, Japan 329-04*

INTRODUCTION

The unexpected appearance of a visual stimulus initiates a well-defined sequence of motor events to foveate the stimulus in human and monkey, that is, a saccadic eye movement followed by a head movement and a compensatory eye movement for head turning.¹⁻⁴ Investigation of this eye-head coordination in monkeys revealed that the initial saccade and the head movement are completely adequate even when a visual stimulus is turned off just prior to the saccade, and that they are centrally preprogrammed.^{3,5} It also was shown that the saccadic characteristics during head turning are adjusted by a negative vestibulo-ocular feedback.⁶ When the head is free to move, the amplitude, duration, and peak velocity of gaze exactly match those of saccade with the head immobilized.⁶ Here, gaze is defined as the sum of the eye position in orbit and the head position in space.

In patients with cerebellar disorders, gaze dysmetria with and without head movements, and an abnormal vestibulo-ocular reflex (VOR) have been observed.⁷⁻¹⁵ The purpose of this communication is to show how the gaze accuracy at the end of the initial saccade is changed when the head is free to move in comparison with the head-immobilized condition in patients with degenerative cerebellar diseases. We will show that the head-free condition for gaze shift decreases the frequency of occurrence of dysmetric gaze but does not change the amplitude of dysmetria. We also will show that the gain of the VOR does not correlate with dysmetric gaze either in frequency of occurrence or amplitude.

METHODS

Subjects

Sixteen patients, including 11 males and 5 females from 21 to 63 years (mean, 42.8 years), who have had cerebellar ataxia for a duration of from 1 year and 3 months to 27 years (mean, 10.2 years), were examined. The clinical diagnosis was olivopontocerebellar atrophy (OPCA) in 7 patients, Marie's ataxia in 2 patients, dentatorubropallidoluysian atrophy (DRPLA) in 2 patients, other forms of spino-

*This study was supported by a Grant for Research in Spinocerebellar Degeneration from the Ministry of Health and Welfare of Japan.

†Department of Neurology.

‡Department of Otolaryngology.

§Department of Ophthalmology.

TABLE 1
SUMMARY OF CLINICAL FEATURES*

Case	Age & Sex	Clinical Diagnosis	Hereditary	Duration of Symptoms (years)	Gait Disturbance	Dysmetria of Movements	Decomposition of Movements	Intention Tremor	Pyramidal Tract Sign	Extra-pyramidal Tract Sign	ANS Involvement	PNS Involvement
1	51 M	OPCA	-	2.3	+	+	++	-	-	+	+	-
2	63 M	OPCA	+	10	++	+	+	-	±	-	-	-
3	50 M	SCD1	-	40	+	+	+	+	±	+	-	-
4	53 F	OPCA	+	15	++	+	++	-	+	-	-	-
5	45 F	OPCA	-	1.3	++	+	+++	-	-	±	+	-
6	30 M	SCD1	-	1.3	+	±	+	-	-	-	-	-
7	44 M	Marie	+	3	+	±	-	-	+	+	+	-
8	49 M	OPCA	-	4	+++	+	+	-	+	+	+	-
9	61 F	OPCA	-	2.4	++	+	±	-	±	-	++	-
10	35 M	Marie	+	2	+	++	+	-	+	-	-	-
11	58 M	OPCA	-	4.5	++	+	+	-	+	-	+	-
12	29 F	SCD2	-	27	++	±	±	-	+	-	-	++
13	35 M	FSP	+	17	+++	±	+	-	+	-	-	++
14	21 F	DRPLA	+	11	+++	±	+	++	-	++	-	++
15	24 M	DRPLA	+	20	+++	+	+	++	-	++	-	++
16	38 M	Alcohol	-	2.1	+	+	-	+	-	-	-	-

*M: male; F: female. OPCA: olivopontocerebellar atrophy; SCD1: spinocerebellar degeneration, cerebellospinal form. SCD2: spinocerebellar degeneration, predominantly cerebellar form. Marie: Marie's ataxia. FSP: familial spastic paraplegia. DRPLA: dentatorubropallidolysian atrophy. Alcohol: parenchymatous cerebellar degeneration associated with chronic alcoholism. ANS: autonomic nervous system. PNS: peripheral nervous system. Severity of symptoms: - absent; ± minimum; + mild; ++ moderate; +++ severe.

cerebellar degeneration in 4 patients, and parenchymatous cerebellar degeneration associated with chronic alcoholism in 1 patient. The brief clinical features of the patients are summarized in TABLE 1.

Apparatus

Electrodes (Saneisokki Co.) were placed on each outer canthus, above and below the right eye. Horizontal eye movement was recorded by electro-oculogram (EOG) with d.c. coupling, while vertical eye movement was recorded by EOG with a.c. coupling to monitor blinks. Head movement was registered by an x-y tracker, using a high-speed TV-camera system (Hamamatsu TV Co.).¹⁸ A small lamp was placed on the forehead of the subject. The light on the forehead was detected by the TV camera and was followed in both horizontal and vertical directions by the x-y tracker with a sampling rate of 15.75 kHz. The vertical axis of head position was adjusted to a plumb line.

Both the EOG and the x-y tracker have a linearity between the angular displacements of the eyes and head and the corresponding output analog signals over a range of $\pm 35^\circ$, with a sensitivity of about 1° . Gaze was computed electrically by summing horizontal eye-position signals and head-position signals. Head position and EOG were calibrated frequently during the examination.

Experimental Procedures

Each subject had two sessions of examination: one for a test of 30° gaze shifts with and without head movements, the other for various neuro-otological examinations including determination of the gain of the VOR.

For the former, the subject stayed at a low level of illumination for at least 20 minutes to get a reasonably stable EOG and dark adaptation. The subject sat in a chair 1.8 meters from a tangential screen. For head restraint, the head was fixed to a chin-and-forehead holder and was sometimes held by an examiner's hands.

A round, red, luminous target of 0.64° in visual angle was projected continuously on the screen and moved alternately 15° right and left from the center at irregular intervals by a mirror galvanometer. The subject was instructed to follow the target when it shifted. In this procedure, a "triggered mode of eye-head coordination" usually was induced.¹⁷

The neuro-otological examination included examinations of gaze nystagmus, positional and positioning nystagmus, visual suppression of the vestibular nystagmus induced by irrigation of 2 ml of cold water (20°C) to the external auditory meatus for 20 seconds,¹⁸ pursuit eye movements, and optokinetic nystagmus pattern (OKP).¹⁹ The gain of the VOR (maximum amplitude of eye movement/maximum amplitude of chair rotation) was determined by sinusoidally rotating a chair to which the head was fixed, by 60° at 0.25 Hz in complete darkness. Findings of the neuro-otological examinations are summarized in TABLE 2.

Data Analysis

Horizontal gaze to both directions usually was analyzed. When a subject had an asymmetry of gaze dysmetria in frequency and/or amplitude, the gaze to the right or left—whichever was more pathological—was analyzed. Thus, 21 to 107

samples (mean, 49.9) of gaze in the head-free and head-fixed conditions were analyzed in each subject.

RESULTS

Gaze with and without Head Movements

FIGURES 1 and 2 illustrate gaze with and without head movements in two patients (Cases 1 and 10 in TABLES 1 and 2). In FIGURE 1 (Case 1), the patient frequently made hypermetric gaze at the end of the initial saccade irrespective of head movement. In FIGURE 2 (Case 10), the patient made both hypermetric and hypometric gaze when the head was fixed; with head movement, gaze accuracy appeared to be increased.

TABLE 2
SUMMARY OF NEURO-OTOLOGICAL FINDINGS*

Case	Gaze Nystagmus	Saccadic Dysmetria	Abnormality of Pursuit	Abnormality of OKP	Abnormality of VS	Gain of VOR
1	+	++	+	++	+	0.62
2	++	++	+	++	++	0.14
3	++	++	++	++	+	0.63
4	+++	++	+++	+++	†	0.46
5	—	++	+	+	+	0.38
6	++	++	+	++	++	0.61
7	++	++	+	++	†	0.36
8	++	++	+	+++	+	0.48
9	+	++	+	++	++	0.42
10	++	++	+	++	++	0.44
11	+	++	+	+++	++	0.81
12	+	++	++	+++	+	1.0
13	++	++	++	+++	++	1.21
14	+	++	+++	+++	++	1.0
15	++	++	+++	+++	++	1.55
16	+	++	+	+	++	0.76

*OKP: optokinetic pattern. VS: visual suppression of caloric nystagmus. VOR: vestibulo-ocular reflex. Degree of abnormality: — absent; + mild; ++ moderate; +++ severe.

†Caloric nystagmus was not induced.

The frequency histogram of the amplitude of dysmetria, defined as the amplitude of overshoot and undershoot measured from the level of accurate gaze, of those two patients (Cases 1 and 10) is shown in FIGURE 3. In Case 1, the frequency of occurrence of hypermetric gaze was 95.7% with head movements and 96.6% when the head was fixed. The mean amplitude of hypermetria was $8.2^\circ \pm 3.1^\circ$ with the head-free and $8.3^\circ \pm 3.6^\circ$ with the head-fixed condition. The frequency of occurrence and the mean amplitude of hypermetria were not statistically different between the head-free and the head-fixed condition. In Case 10, the frequencies of occurrence of dysmetric, hypermetric, and hypometric gaze were 51.2%, 29.2%, and 22.0% respectively with head movements, and 70.1%, 13.1%, and 57.0% respectively without head movements. The mean

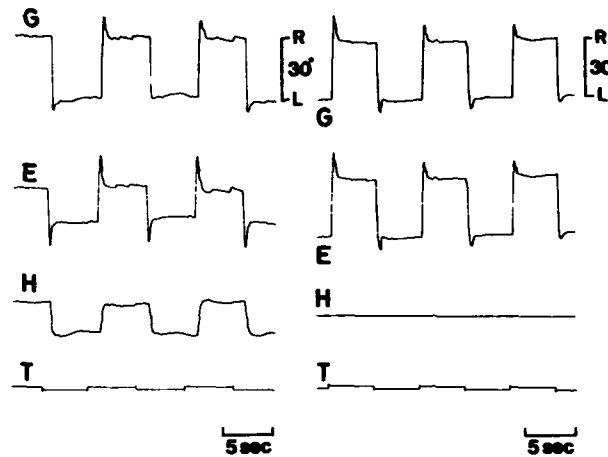


FIGURE 1. Gaze with and without head movements of a patient (Case 1). In this and the following figure: E, eye movement; H, head movement; G (gaze) represents the sum of E and H; and T, target displacement. Hypermetric gaze occurred frequently irrespective of head movements.

amplitudes of hypermetria and hypometria were $4.5^\circ \pm 1.5^\circ$ and $12.1^\circ \pm 9.3^\circ$ respectively with head movements, and $5.2^\circ \pm 1.7^\circ$ and $7.5^\circ \pm 5.3^\circ$ respectively without head movements. The frequencies of occurrence of dysmetric gaze and hypometric gaze were statistically decreased with head movements. The mean amplitude of hypermetria did not differ between these two conditions. On the other hand, the frequency of occurrence of hypermetria and the mean amplitude of hypometria were statistically increased with head movements.

In each patient, the frequency of occurrence and the mean amplitude of dysmetria were compared between the head-free and -fixed condition (FIGURE 4). The results of the statistical analysis of this comparison are given in TABLE 3.

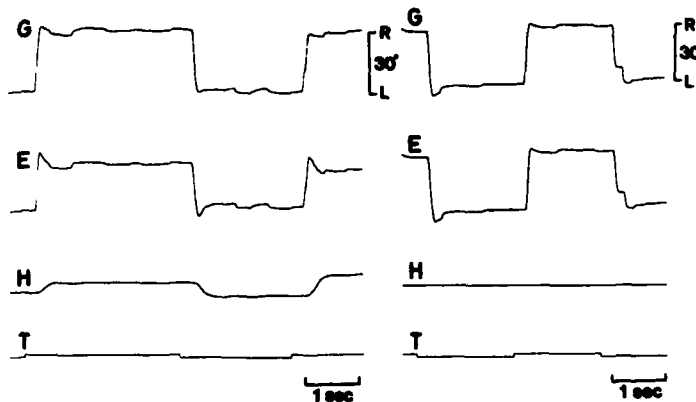


FIGURE 2. Gaze with and without head movements of a patient (Case 10). Both hypermetric and hypometric gaze occurred when the head was fixed.

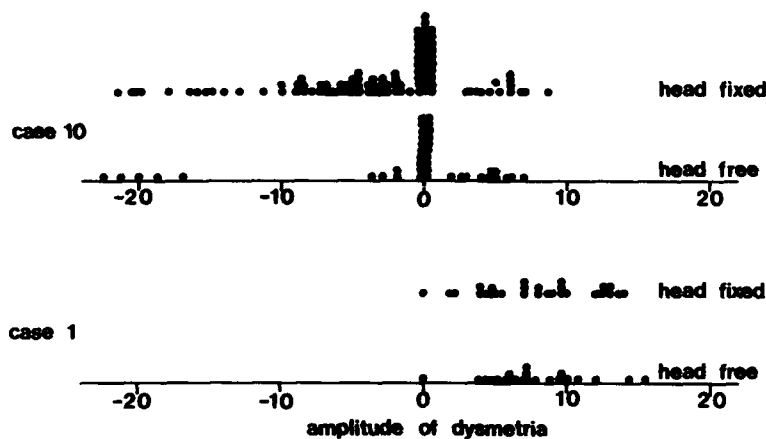


FIGURE 3. The frequency histogram of the amplitude of dysmetria. The abscissa represents the amplitude of dysmetria: zero represents no dysmetria, positive values are hypermetria, and negative values are hypometria. In Case 1, the frequency of occurrence and the amplitude of hypermetria did not differ between the head-free and the head-fixed condition. In Case 10, the frequencies of occurrence of dysmetria and hypometria were decreased with head movements. The mean amplitude of hypermetria did not differ between these two conditions.

With head turning, the frequency of occurrence of dysmetria was decreased in 8 of 16 patients in comparison with that in the head-fixed condition. The frequencies of occurrence of hypermetria and hypometria also were decreased in 7 of 16 patients with head movements (FIGURE 4A, TABLE 3). The mean amplitude of hypermetria did not differ in all of the patients between the head-free and the head-fixed condition. The mean amplitude of hypometria also did not differ in 7 of 15 patients between these two conditions (FIGURE 4B, TABLE 3).

TABLE 3
GAZE ACCURACY UNDER THE HEAD-FREE CONDITION IN COMPARISON WITH THAT UNDER THE HEAD-FIXED CONDITION*

	Decreased†	Unchanged†	Increased†
Frequency of Occurrence			
Dysmetria	8/16	6/16	2/16
Hypermetria	7/16	4/16	5/16
Hypometria	7/16	4/16	5/16
Amplitude of Dysmetria			
Hypermetria	0/11	11/11	0/11
Hypometria	4/15	7/15	4/15

*Gaze accuracy was evaluated at the end of the initial saccade. The amplitude of dysmetria was the amplitude of overshoot and undershoot measured from the level of the accurate gaze at the end of the initial saccade.

†Decreased, unchanged, and increased indicate that the frequency of occurrence or the amplitude of dysmetria was statistically decreased, unchanged, or increased under the head-free condition in comparison with that under the head-fixed condition.

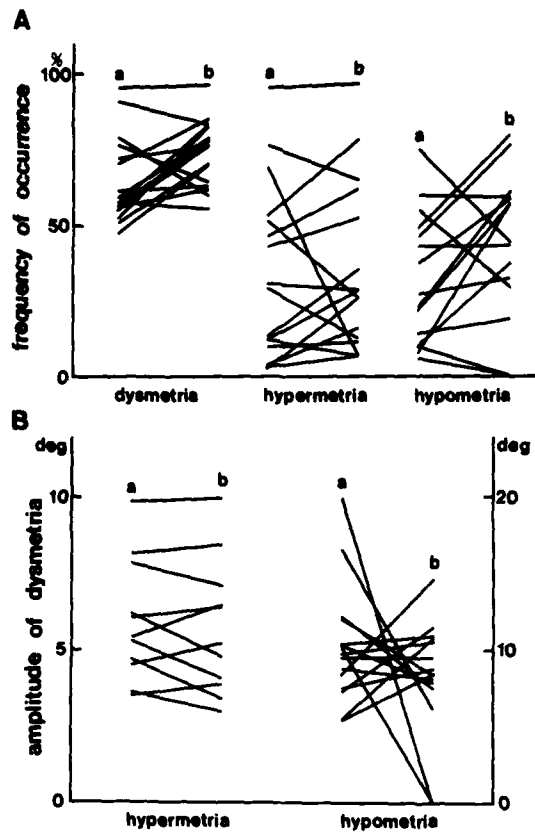


FIGURE 4. The frequency of occurrence (A) and the mean amplitude (B) of dysmetria. The "a" side represents the head-free condition, and the "b" side represents the head-fixed condition. In nearly half of the patients, the frequencies of occurrence of dysmetric, hypermetric, and hypometric gaze were less under the head-free condition than under the head-fixed condition. The mean amplitude of dysmetria did not differ between these two conditions.

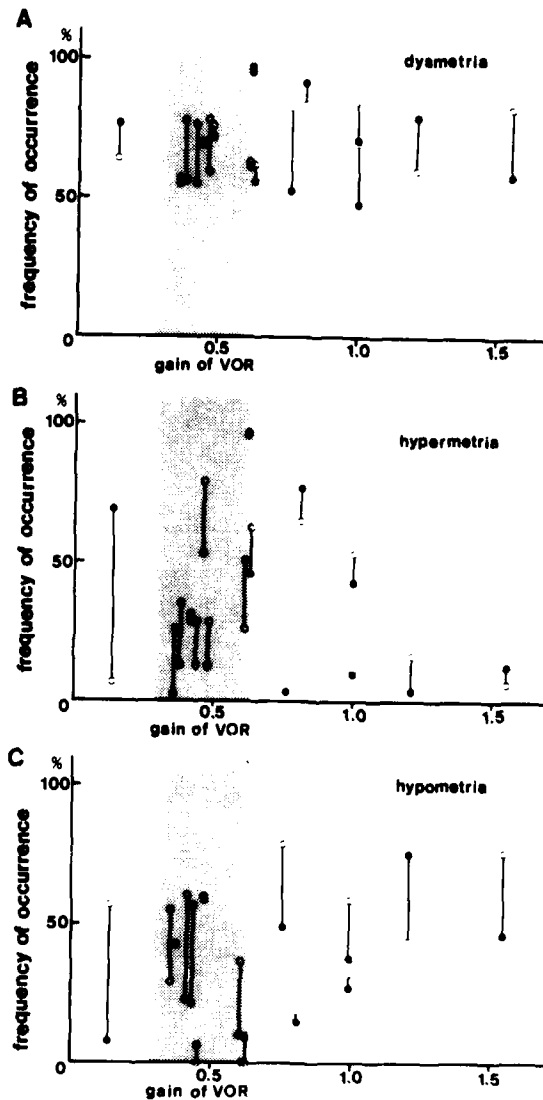


FIGURE 5. The frequencies of occurrence of dysmetria (A), hypermetria (B), and hypometria (C) vs. the gain of the VOR. In this and the following figure, the shadow represents the mean ± 1 SD (0.45 ± 0.17) of normals in our laboratory, the solid circles represent the head-free condition, the open circles represent the head-fixed condition. One circle represents one patient. The gain of the VOR did not correlate to the frequencies of occurrence of dysmetric, hypermetric, or hypometric gaze with or without head movements. The gain of the VOR also did not correlate to the difference of the frequencies of occurrence between the head-free and head-fixed conditions.

In summary, in nearly half of the patients with chronic cerebellar lesions, head movements decreased the frequencies of occurrence of dysmetric, hypermetric, and hypometric gaze, but head movements did not change the mean amplitude of dysmetria, especially that of hypermetria.

The Frequency of Occurrence of Dysmetric Gaze vs. the Gain of the VOR

Since the VOR often is changed in patients with cerebellar diseases and the head movements modify the saccadic characteristics in eye-head coordination, the gain of the VOR was measured in each patient. The frequencies of occurrence of dysmetric gaze, hypermetric gaze, and hypometric gaze were evaluated by the gain of the VOR (FIGURE 5). Some of the patients showed an increased gain of the VOR. However, the gain of the VOR did not correlate to the frequencies of occurrence of dysmetric, hypermetric, and hypometric gaze with or without head movements or to the change of these frequencies of occurrence by head movements.

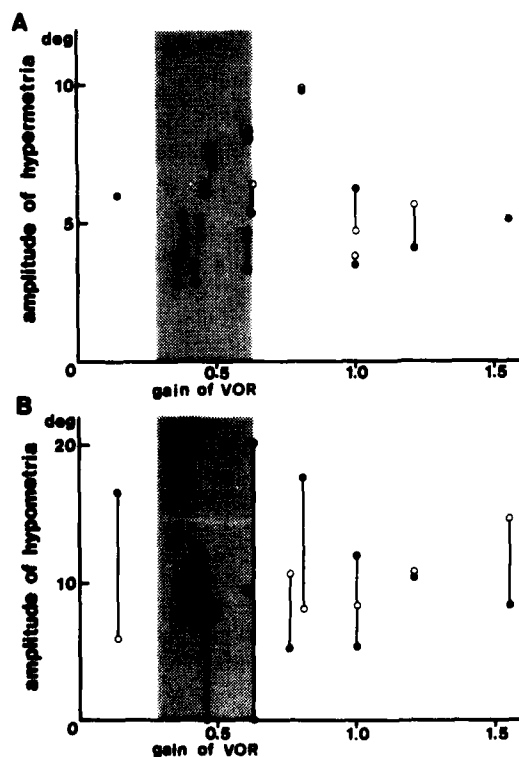


FIGURE 6. The mean amplitudes of hypermetria (A) and hypometria (B) vs. the gain of the VOR. The gain of the VOR did not correlate to the mean amplitude of dysmetria with or without head movements or to the change of the mean amplitude of dysmetria by head turning in comparison to that without head movements.

The Amplitudes of Hypermetria and Hypometria vs. the Gain of the VOR

The amplitudes of hypermetria and hypometria were evaluated by the gain of the VOR (FIGURE 6). The gain of the VOR did not correlate to the mean amplitudes of hypermetria and hypometria with or without head movements or to the change of mean amplitudes of hypermetria and hypometria by head turning.

In summary, the gain of the VOR did not affect the gaze dysmetria either in frequency of occurrence or amplitude.

DISCUSSION

It was shown in eye-head coordination in monkey that saccadic characteristics were changed by head movements.⁹ It also was shown that this change was not the result of the change of the central saccade program but was the result of modification of the programmed saccade by head turning. This modification of saccade was thought to occur through the negative vestibulo-ocular feedback.⁹

When the head was immobilized, saccadic dysmetria frequently was observed in patients with cerebellar lesions.⁹⁻¹² Vermal and paravermal lesions of the posterior lobe of the cerebellum caused saccadic dysmetria in experimental animals.^{20,21} Saccadic eye movement is thought to be under predictive control, because there is no direct feedback connection from retinal error signals or eye-position signals to the oculomotor efferents and the saccade is a very fast motor phenomenon. Thus, saccadic dysmetria with the head-fixed condition is thought to be due to a disturbance of the predictive control of saccades.

On the other hand, change of the VOR has been observed in patients with cerebellar lesions.^{11,13-15} It has been demonstrated in experimental animals that the cerebellum contributes to adaptive gain control of the VOR.²²⁻²⁴ Further, gaze dysmetria was observed during eye and head movements in patients with cerebellar lesions and in monkeys with vermal and paravermal lesions of the cerebellum.^{7,8,15,21} The question is whether an abnormal gain of the VOR causes disturbance of the corrective action of saccades by head turning.

We have shown that head movements improved the frequency of occurrence of gaze dysmetria in nearly half of the patients but not the mean amplitude of dysmetria, and that the gain of the VOR did not correlate to gaze dysmetria in either frequency or amplitude. The saccade associated with head movements is thought to be more reflexive in nature and phylogenetically older than the voluntary saccade without head movements.²⁵ Our results suggest that it is easier to program gaze utilizing the more reflexive system than to program gaze without head movements, and that the abnormal VOR does not change the modification of saccade.

It is concluded that the gain of the VOR does not affect gaze accuracy at the end of the initial saccade, and that the head-free condition improves the gaze but not through the vestibulo-ocular feedback. Dysmetric gaze in patients with cerebellar lesions is thought to be due not to the disturbance of modification of saccade by the VOR, but mainly to the disturbance of the central programming of gaze.

ACKNOWLEDGMENTS

The authors wish to express their thanks to Prof. K. Maekawa and Dr. T. Tango for their advice.

REFERENCES

1. BARTZ, A. E. 1966. Eye and head movements in peripheral vision: nature of compensatory eye movements. *Science* **152**: 1644-1645.
2. FLEMING, D. G., G. W. VOSSIUS, G. BOWMAN & E. L. JOHNSON. 1969. Adaptive properties of the eye-tracking system as revealed by moving-head and open-loop studies. *Ann. N.Y. Acad. Sci.* **156**: 825-850.
3. BIZZI, E., R. E. KALIL & V. TAGLIASCO. 1971. Eye-head coordination in monkeys: evidence for centrally patterned organization. *Science* **173**: 452-454.
4. BARNES, G. R. 1979. Vestibulo-ocular function during co-ordinated head and eye movements to acquire visual targets. *J. Physiol.* **287**: 127-147.
5. DICHGANS, J., E. BIZZI, P. MORASSO & V. TAGLIASCO. 1973. Mechanisms underlying recovery of eye-head coordination following bilateral labyrinthectomy in monkeys. *Exp. Brain Res.* **18**: 548-562.
6. MORASSO, P., E. BIZZI & J. DICHGANS. 1973. Adjustment of saccade characteristics during head movements. *Exp. Brain Res.* **16**: 492-500.
7. ZEE, D. S. 1976. Disorders of eye-head coordination. In *Eye Movements*. B. A. Brooks & F. J. Bajandas, Eds.: 9-39. Plenum Press, New York, N.Y.
8. SHIMIZU, N., M. NAITO & M. YOSHIDA. Eye-head coordination in patients with parkinsonism and cerebellar ataxia. (In press.)
9. KOMATSUZAKI, A. & J. MIZUTANI. 1975. Nystagmus and abnormal eye movement in the cerebellar disease. *Adv. Neurol. Sci.* **19**: 649-661.
10. SELHORST, J. B., L. STARK, A. L. OCHS & W. F. HOYT. 1976. Disorders in cerebellar ocular motor control. I. Saccadic overshoot dysmetria. An oculographic, control system and clinico-anatomical analysis. *Brain* **99**: 497-508.
11. ZEE, D. S., R. D. YEE, D. G. COGAN, D. A. ROBINSON & W. K. ENGEL. 1976. Ocular motor abnormalities in hereditary cerebellar ataxia. *Brain* **99**: 207-234.
12. BALOH, R. W., V. HONRUBIA & A. SILLS. 1977. Eye-tracking and optokinetic nystagmus. Results of quantitative testing in patients with well-defined nervous system lesions. *Ann. Otol. Rhinol. Laryngol.* **86**: 108-114.
13. BALOH, R. W., H. R. KONRAD & V. HONRUBIA. 1975. Vestibulo-ocular function in patients with cerebellar atrophy. *Neurology* **25**: 160-168.
14. BALOH, R. W., H. A. JENKINS, V. HONRUBIA, R. D. YEE & C. G. Y. LAU. 1979. Visual-vestibular interaction and cerebellar atrophy. *Neurology* **29**: 116-119.
15. YOSHIDA, M., N. SHIMIZU, K. NIJIMA & M. MIZUNO. 1980. Pathophysiology of ataxia and ocular disturbance in SCD with quantitative evaluation of TRH treatment. In *Spinocerebellar Degenerations*. I. Sobue, Ed.: 251-256. University of Tokyo Press, Tokyo, Japan.
16. ISHIKAWA, S. & A. YAMAZAKI. 1973. A new instrument for recording of the eye movement. *Jpn. J. Ophthalmol.* **17**: 244-248.
17. BIZZI, E., R. E. KALIL & P. MORASSO. 1972. Two modes of active eye-head coordination in monkeys. *Brain Res.* **40**: 45-48.
18. TAKEMORI, S. 1977. Visual suppression test. *Ann. Otol. Rhinol. Laryngol.* **86**: 80-85.
19. SUZUKI, J. & A. KOMATSUZAKI. 1961. Clinical application of optokinetic nystagmus. Optokinetic pattern test. *Acta Otolaryngol.* **54**: 49-55.
20. ASCHOFF, J. C. & B. COHEN. 1971. Changes in saccadic eye movements produced by cerebellar cortical lesions. *Exp. Neurol.* **32**: 123-133.
21. RITCHIE, L. 1976. Effects of cerebellar lesions on saccadic eye movements. *J. Neurophysiol.* **39**: 1246-1256.
22. ITO, M., T. SHIIDA, N. YAGI & M. YAMAMOTO. 1974. The cerebellar modification of rabbit's horizontal vestibulo-ocular reflex induced by sustained head rotation combined with visual stimulation. *Proc. Jpn. Acad.* **50**: 85-89.
23. MILES, F. A. & J. H. FULLER. 1974. Adaptive plasticity in the vestibulo-ocular responses of the rhesus monkey. *Brain Res.* **80**: 512-516.
24. ROBINSON, D. A. 1976. Adaptive gain control of vestibulo-ocular reflex by the cerebellum. *J. Neurophysiol.* **39**: 954-969.
25. ZEE, D. S., R. D. YEE & H. S. SINGER. 1977. Congenital ocular motor apraxia. *Brain* **100**: 581-599.

NYSTAGMUS, GAZE SHIFT, AND SELF-MOTION PERCEPTION DURING SINUSOIDAL HEAD AND NECK ROTATION

J. M. B. V. de Jong, W. Bles,* and G. Bovenkerk

*Laboratory of Experimental Neurology
University of Amsterdam
1054 EG Amsterdam, the Netherlands*

INTRODUCTION

In man, Bárány's question whether disordered neck reflexes may elicit vertigo and nystagmus is still open.¹ Clinically, an answer is urgently needed, since tenacious dizziness is a frequent symptom following disorders of the neck and a major source of disability in laborers whose jobs involve much work above shoulder level. Our current lack of diagnostic criteria leads to the assessment of cervical vertigo with a degree of license that disturbs all concerned. Since diseases of the spine mostly affect both the cervical proprioceptors and the vertebral neurovascular bundles—comprising the vertebral artery, vein, and sympathetic plexus—clinical studies have provided little help in the attempt to distinguish neck afferent illness from vascular brain-stem disease.

This study of eye movements and perceived horizontal head rotation in healthy medical students will let us compare the responses to sinusoidal visual, vestibular, and cervical stimuli. We will demonstrate that our healthy adult subjects have strong sensations of horizontal head rotation and weak ocular movements upon neck afferent stimulation. This finding corresponds with a similar apparent discrepancy between marked dizziness and minimal ocular signs in many sufferers from neck disease that puzzles the clinician. We will confirm Frenzel's finding that a much greater horizontal gaze shift—Schlagfeldverlagerung—distinguishes the normal cervical from the normal labyrinthine response.^{2,3} Since Guettich's report of 1939, several investigators have paid little or no attention to gaze shift.⁴⁻⁷ Finally, we will show that in man as in various other species, the cervico-ocular signal is added to the vestibulo-ocular response.

METHODS

Using a rotating chair and drum combination (Toennies, Freiburg im Br., Federal Republic of Germany), we examined 26 healthy medical students of either sex, aged 22 to 25. Chair and drum could be rotated separately or together in either direction; we recorded their velocities continuously. A photocell stripe-detection system mounted on the chair measured the relative chair-to-drum velocity. The inside of the optokinetic drum, ϕ 1.5 m, was painted with vertical black and white stripes, each subtending a visual angle of 7.5° . We used sinusoidal movements with a frequency of 0.05 Hz and an amplitude of 90° peak

*Vestibular Laboratory, ENT Department, Free University Hospital, 1007 MB Amsterdam, the Netherlands.

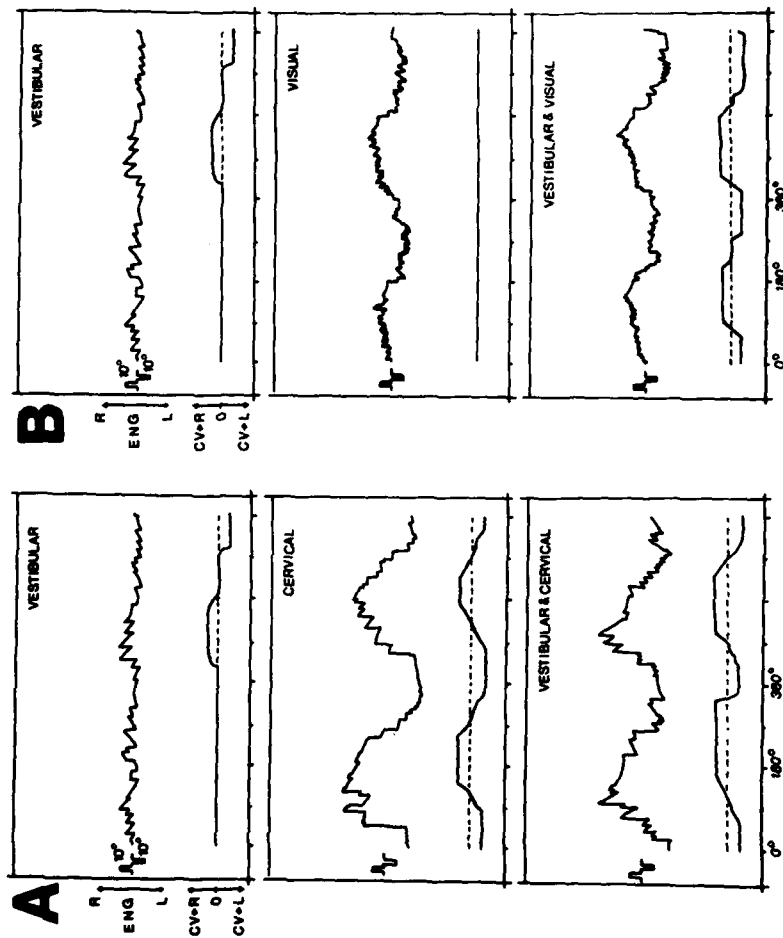


FIGURE 1. Electro-oculographic recordings. Abscissa, cycles of stimulation; ordinate, eye movements and occurrence of circularvection (CV). From top to bottom in this and subsequent figures: A, responses to vestibular, cervical, and vestibular-plus-cervical stimulation; B, responses to vestibular, visual, and vestibular-plus-visual stimulation. R, right; L, left; ENG, electro-oculogram. For better display of interaction, the middle figures of A and B have been shifted over 180° (see Methods).

to peak (p-p), which means an angular velocity of $14.1^\circ/\text{second}$. At frequencies over 0.05 Hz, the mass of the drum distorted the sinusoidal shape of the stimuli.

With the aid of skin electrodes, we recorded horizontal and vertical eye movements by electro-oculography (EOG), using d.c. amplification. In each subject we tested seven stimulus conditions:

1. *Vestibular*. Subject seated with his head supported by a rest mounted on the back of the chair. Rotation in darkness.
2. *Cervical*. Subject seated with his head fixed by a clamp attached to the ceiling of the optokinetic drum. Rotation in darkness of the body relative to the fixed head. Sturdy mechanical constraints prevented the relative head-to-body angle to exceed 45° .
3. *Vestibular plus cervical*. Subject situated as during the cervical condition. Rotation of the clamp relative to the fixed chair in darkness.

Vestibular, cervical, and vestibular-plus-cervical responses are shown in part A of FIGURES 1, 2, 3, and 5.

4. *Visual*. Subject seated in stationary chair. Full-field optokinetic stimulation by drum rotation.
5. *Vestibular plus visual*. Rotation of the chair inside the stationary, internally lighted drum.

Vestibular, visual, and vestibular-plus-visual responses are shown in part B of FIGURES 1, 2, 3, and 5.

6. *Cervical with visual fixation*. Subject tested with his head fixed by a clamp. Internal drum light on. Rotation of the chair while the subject fixated a light spot on the mantle of the drum. Spot ϕ 5 mm.
7. *Vestibular plus cervical with visual fixation*. Subject seated in the chair with his head fixed by the clamp. Internal drum light on. Rotation of the drum—to which the clamp was attached—while the subject fixated the light spot on the mantle of the drum.

Since conditions 6 and 7 never induced systematic EOG deviations from a straight line of more than 1° p-p, we have excluded the possibility of artifacts induced by the head clamp. We instructed our subjects to signal perceived head movement by switching a joystick mounted on an armrest of the chair. Since deviation of the stick to the right (R) meant perceived head motion to the right, stick to the left (L) meant motion to the left, and stick vertical meant no head motion perceived, we obtained discrete data that were given the values of +1, -1, and 0 respectively.

For analysis we fed EOG, velocity, and head-movement signals into a strip-chart recorder (Siemens EM 81.80) and stored them on magnetic tape (Philips Analog 7 recorder). In each experiment, we took the responses to the first two usable sinusoids for independent manual and computer analysis. Manually, we determined the mean (\bar{x}) maximal gaze shift and nystagmus slow-phase velocity of all stimulation modes. We will give these values plus or minus one standard deviation (SD). For analysis on a PDP-8 I computer system, we sampled the data at 10 Hz and calculated the cumulative eye position, skipping across fast nystagmus beats and artifacts on the experimenter's command, by extrapolating over the last 15 samples (1.5 seconds). We subjected the differentiated cumulative

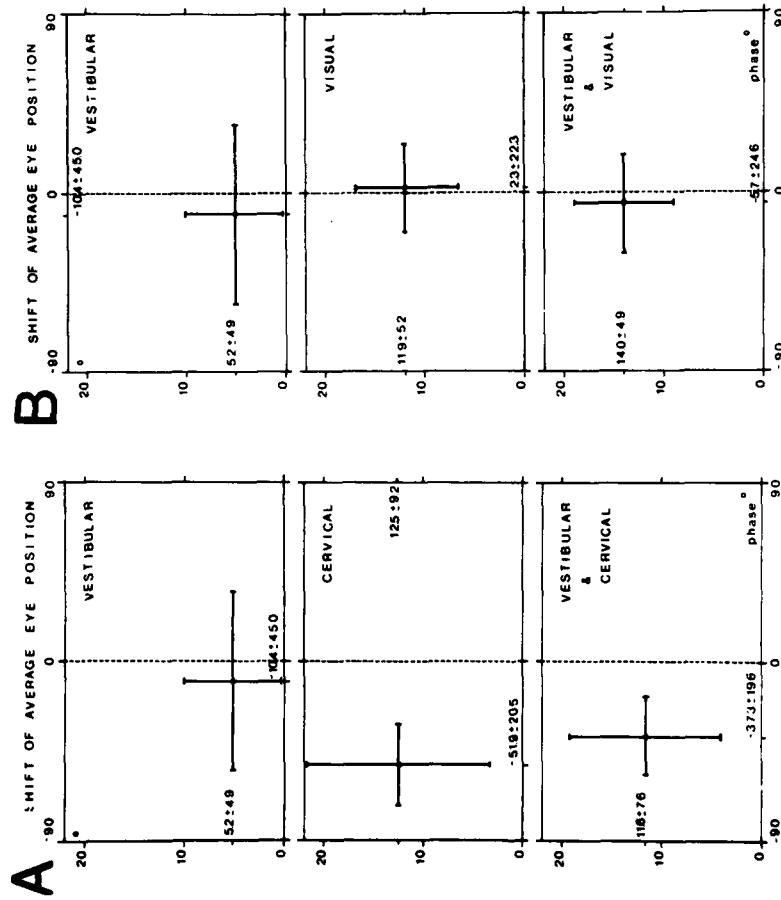


FIGURE 2. Gaze shift, "Schlagfeldverlagerung." Vertical and horizontal bars indicate $\bar{x} \pm SD$ respectively of maximal gaze movement and phase shift. Middle figures of A and B have been shifted over 180° (see Methods).

eye position to Fourier analysis at 0.05 Hz and obtained the mean amplitude and phase of the nystagmus slow-phase velocities. Fourier analysis of the raw data at 0.05 Hz yielded the mean amplitude and phase of the gaze shifts.

By plotting our perceived head rotation values against one stimulus cycle (FIGURE 5), we displayed cumulative circularvection (CV). In this figure, we deleted the negative sign originally allotted to left CV. From the individual CV values, we calculated the \bar{x} and SD of the phase lag (FIGURE 5).

During cervical, vestibular, and vestibular-plus-visual stimulation, we expressed the average stimulus-to-response phase difference with respect to chair velocity. We calculated the phase difference for the visual and the vestibular-plus-cervical conditions with respect to drum velocity. This means that the interacting vestibular and cervical stimuli have a phase difference of 180° during the vestibular-plus-cervical condition. Similarly, the vestibular and visual stimuli have a phase difference of 180° during the vestibular-plus-visual condition. For the reader's convenience, these phase lags have been artificially aligned in FIGURE 3, shifting the vestibular, vestibular-plus-cervical, and vestibular-plus-visual responses over 180° . In FIGURES 1, 2, and 5, we have shifted the cervical and visual responses over 180° .

RESULTS

Gaze Shift (*Schlagfeldverlagerung*)

Neck afferent stimuli gave a pronounced horizontal gaze shift, the resultant of several large anticompany saccades (FIGURE 1). Manually, we found an average maximal cervical gaze shift of $25.0 \pm 18.3^\circ$, and a vestibular one of $10.5 \pm 9.9^\circ$. The computer results expressed relative to orbital midposition were exactly half the size of the manual values, measured p-p. The average visual and cervical gaze shifts were equal and did not differ statistically from the vestibular-plus-visual and vestibular-plus-cervical gaze shifts (FIGURE 2).

The phase shifts of the vestibular-plus-visual and vestibular-plus-cervical responses were about intermediate to the amounts of shift induced by visual, vestibular, and cervical stimuli separately (FIGURE 2).

Nystagmus

Besides anticompany saccades, neck afferent stimuli provoked slow nystagmus beats with a widely variable phase lag (FIGURE 3). Between 90° and 180° , saccades and nystagmus slow phases of the cervical response in FIGURE 1 beat in the same anticompany direction.

We found that cervical and vestibular responses add up, since the peak cervical slow-phase velocity was 5.0 ± 3.6 , the vestibular was 9.4 ± 2.8 , and the vestibular-plus-cervical was $12.8 \pm 3.3^\circ/\text{second}$. The computed cervical and vestibular maximum slow-phase velocities added up as well (FIGURE 3A).

The manually determined maximal slow-phase velocities of our responses were visual, 15.1 ± 2.9 ; vestibular, 9.4 ± 2.8 ; vestibular-plus-visual, 16.1 ± 3.0 ; and vestibular-plus-cervical, $12.8 \pm 3.3^\circ/\text{second}$. Division of these maximal response velocities by the uniform peak stimulus velocity of $14.1^\circ/\text{second}$ yielded the

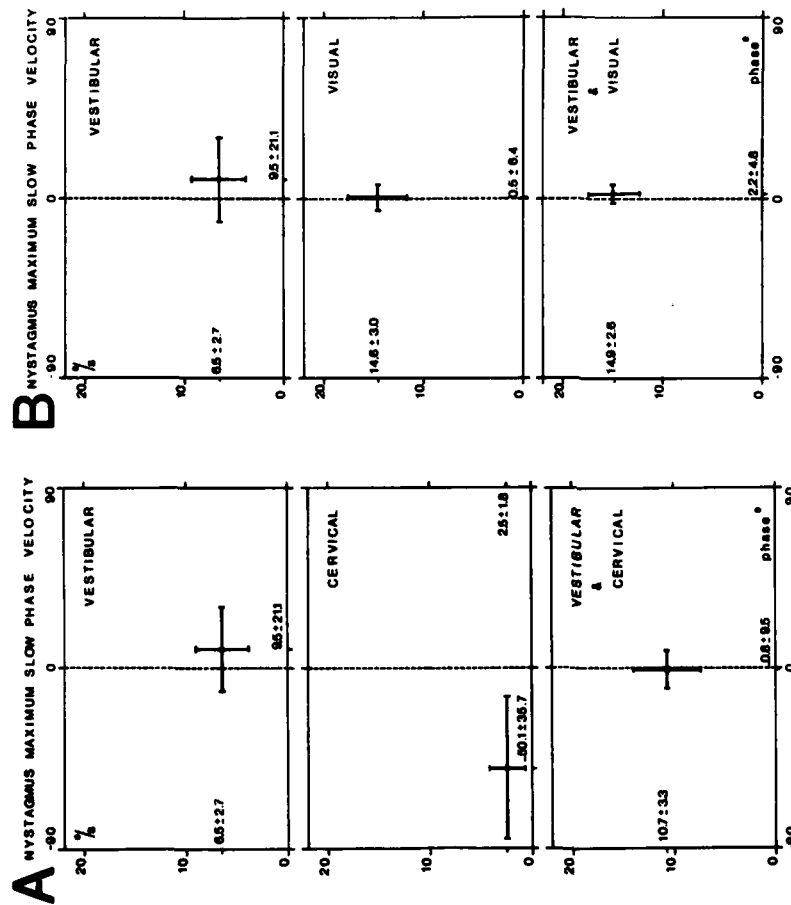


FIGURE 3. Nystagmus maximum slow-phase velocity. Vertical and horizontal bars indicate $\bar{x} \pm SD$ respectively of eye velocity and phase shift. Top and bottom figures of A and B have been shifted over 180° (see Methods).

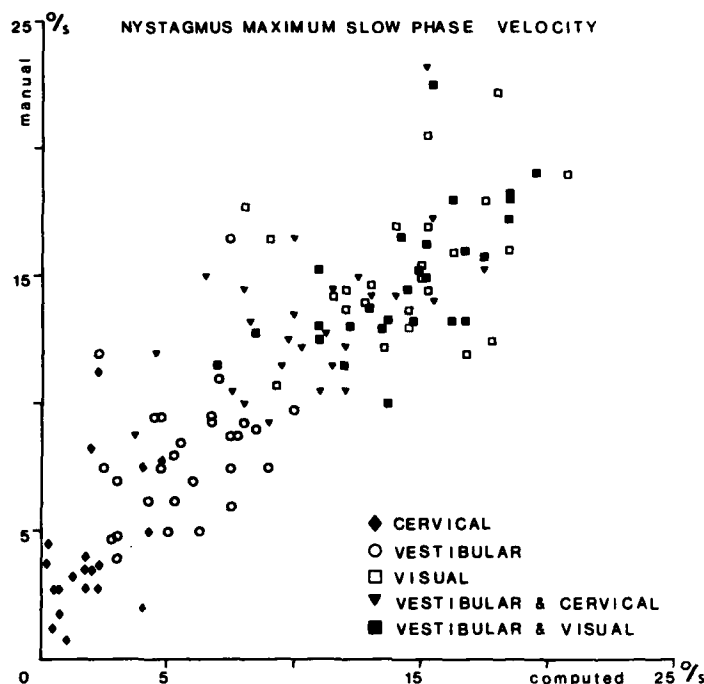


FIGURE 4. Correlogram of manually versus machine determined nystagmus slow-phase velocities. Note the somewhat higher values found manually.

following values for gain: visual, 1.1 ± 0.2 ; vestibular, 0.5 ± 0.2 ; cervical, 0.3 ± 0.2 ; vestibular-plus-visual, 1.1 ± 0.2 ; and vestibular-plus-cervical, 0.9 ± 0.2 . Since we manually measured peak values, whereas the computer fitted a sinus-shaped curve to the response, the manual values were somewhat higher. Otherwise the manual and computer-processed results agreed well (FIGURE 4).

Horizontal Circularvection

Unexpectedly, we found that neck afferent stimuli induced circularvection more frequently than did full-field optokinetic movement. Out of 52 (100%) stimulus cycles (2 per subject) studied for each condition, 49 (95%) vestibular-plus-cervical, 47 (90%) vestibular-plus-visual, 47 (90%) vestibular, 36 (70%) cervical, and only 25 (49%) optokinetic cycles caused horizontal circularvection. During the condition of cervical stimulation with visual fixation, CV was reported in 13.5 (26%) of the cycles. The phase of the vestibular-plus-cervicalvection had moved to about halfway between the phase shifts of the vestibular and the cervical vections separately (FIGURE 5A). The vestibular, visual, and vestibular-plus-visual cumulative responses had the same phase lag (FIGURE 5B).

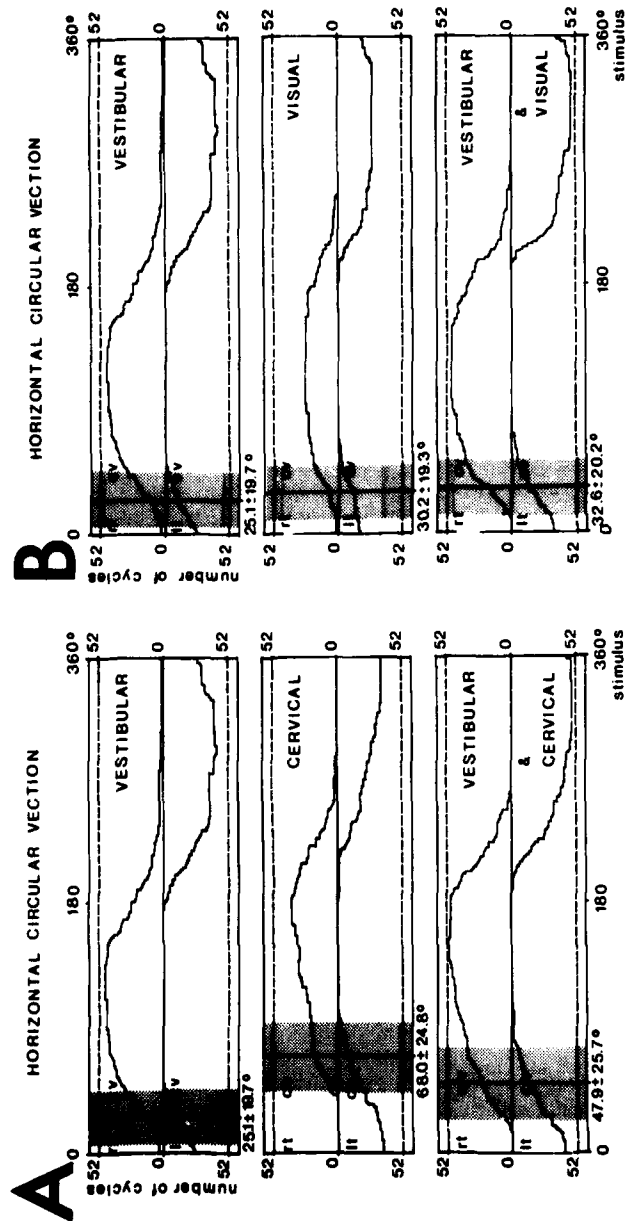


FIGURE 5. Cumulative horizontal circularvection. Vertical lines in center of shaded areas and areas themselves indicate $\bar{x} \pm \text{SD}$ of phase lag. Middle figures of A and B have been shifted over 180° (see Methods).

DISCUSSION

The main new finding of this study is that circularvection occurs more often during cervical than during full-field optokinetic stimulation, whereas the gain of the cervico-ocular loop is much smaller than the optokinetic gain. Even during cervical stimulation with visual fixation, our subjects reported CV in a quarter of the cycles. This unexpected discrepancy between strong circularvection and weak eye movements in healthy students corresponds with a similar contrast between marked dizziness and minimal ocular signs in patients with neck symptoms.

Secondly, our data confirm Frenzel's discovery that a greater gaze shift distinguishes the normal cervical from the normal labyrinthine response and concur with his explanation that the anticomensatory cervical gaze shift facilitates visual orientation during active head movements.^{2,3} Since Melvill Jones has found that the vestibulo-ocular reflexes drive the eyes out of orbital midposition by large anticomensatory saccades only at high head velocities,⁸ the cervico-ocular loop could well do the same during slower head motions. Technical limitations of our equipment, however, prevented us from testing this idea.

As first noted by Guettich, who observed freely moving sharks in the marine aquarium at Heligoland, eye movements are anticomensatory during active and compensatory during passive head movements.⁴ He added that compensatory movements from the neck should have great functional significance in birds and fish, whose bodies frequently are jolted by sudden currents of air or water. This idea is illustrated by Claude Bernard's observation that a finch could not fly after transection of its neck muscles and had to move about by walking or hopping.⁹

In 10 patients, nearly or entirely devoid of labyrinthine function, Frenzel found compensatory slow phases and anticomensatory saccades upon neck rotation, as Magnus, Guettich, and Peterson *et al.* have noted in several other species.^{3,4,10,11} In our subjects, as in those of Takemori and Suzuki,⁶ however, the phase of the slow eye movements varied considerably with respect to the stimulus. Our students were normal and healthy, but we cannot decide whether they also were normal in the sense of meeting a standard of good function. Thus we may conclude no more than that our results provide clinically useful control values.

Thirdly, we have found that in man, as in various other species,^{10,11} cervical slow phases are added to the vestibulo-ocular signal.

Clinically, our study implies that ocular signs may well be a poor measure of dizziness in cervical syndromes.

SUMMARY

Report on eye movements and perceived horizontal head rotation in 26 healthy students during sinusoidal vestibular, visual, cervical, congruent vestibular-plus-visual, or vestibular-plus-cervical stimulation. Circularvection occurred more often during neck afferent than during full-field optokinetic stimuli. In contrast, the cervico-ocular response had a low average velocity. As first noted by Frenzel (1928), a greater gaze shift distinguished the normal cervical from the normal labyrinthine response. The cervico-ocular and vestibulo-ocular responses were found to add up.

Clinically, the results imply that ocular movements may be a poor measure of dizziness in cervical syndromes.

ACKNOWLEDGMENTS

In belated gratitude, de Jong dedicates his share of this work to the teachers of St. Bernardinus College, Heerlen (L), on the occasion of the school's fiftieth anniversary.

We thank Mr. Jorgen Rasmussens for his expert technical assistance and the New York Academy of Sciences for travel support.

REFERENCES

1. BÁRÁNY, R. 1924. Gibt es Schwindel-resp. Nystagmusanfalle als Halsreflex? *Acta Oto-Laryngol.* 7: 1-2.
2. FRENZEL, H. 1928. Rucknystagmus als Halsreflex und Schlagfeldverlagerung des labyrinthären Drehnystagmus durch Halsreflexe. *Z. Hals Nasen Ohrenheilkd.* 21: 177-187.
3. FRENZEL, H. 1931. Halsreflektorisches Augenrucken von vestibulärer Schlagform bei vollstäendig oder nahezu vollstäendig Labyrinthlosen (*Drehunerregbaren*). *Passow-Schaefer Beiträege praktischen theoretischen Hals Nasen Ohrenheilkd.* 28: 305-310.
4. GUETTICH, A. 1939. Ueber den Antagonismus der Hals- und Bogengangsreflexe bei der Bewegung des menschlichen Auges. *Arch. Ohren Nasen Kehlkopfheilkd.* 147: 1-4.
5. MEIRY, J. L. 1971. Vestibular and proprioceptive stabilization of eye movements. In *The Control of Eye Movements*. P. Bach-y-Rita, C. C. Collins & J. E. Hyde, Eds.: 483-496. Academic Press, Inc. New York, N.Y.
6. TAKEMORI, S. & J.-I. SUZUKI. 1971. Eye deviations from neck torsion in humans. *Ann. Otol. Rhinol. Laryngol.* 80: 439-444.
7. BARNES, G. R. & L. N. FORBAT. 1979. Cervical and vestibular control of oculomotor response in man. *Acta Oto-Laryngol.* 88: 79-87.
8. MELVILL JONES, G. 1964. Predominance of anticomensatory oculomotor response during rapid head rotation. *Aerosp. Med.* 35: 965-988.
9. BERNARD, C. 1858. Vingt-sixième leçon. In *Leçons sur la Physiologie et la Pathologie du Système Nerveux*. 1: 495-496. Baillière. Paris, France.
10. MAGNUS, R. 1924. *Körperstellung*. Springer. Berlin, Germany.
11. PETERSON, B. W., G. BILOTTO, J. H. FULLER, J. GOLDBERG & B. LEEHAN. 1980. Interaction of vestibular and neck reflexes in the control of gaze. (In preparation.)

EYE MOVEMENTS IN PATIENTS WITH WALLENBERG'S SYNDROME*

Robert W. Baloh,† Robert D. Yee,‡ and Vicente Honrubia§

University of California School of Medicine
Los Angeles, California 90024

INTRODUCTION

Lesions in the lateral medulla produce a unique disorder of posture known as lateropulsion.^{1,2} Patients with this disorder describe a sensation of being pulled toward the side of their lesion as if an external force were acting upon their body. The eyes also may be pulled to the same side.³⁻⁵ Latropulsion most commonly is caused by infarction of the lateral medulla (Wallenberg's syndrome) but also can result from tumors and demyelination in the same area.⁵ It invariably is accompanied by other signs localized to the lateral medulla.⁶ These include (1) ipsilateral loss of pain and temperature sensation of the face, due to involvement of the descending nucleus and tract of the Vth nerve; (2) contralateral loss of pain and temperature sensation in the trunk and limbs from involvement of the spinothalamic tract; (3) ipsilateral Horner's syndrome from interruption of descending sympathetic fibers; (4) dysarthria and dysphagia from weakness of the palate, pharynx, and larynx secondary to involvement of the nucleus ambiguus; (5) ataxia of the ipsilateral limbs due to involvement of the inferior cerebellar peduncle and cerebellar hemisphere; and (6) vertigo and nystagmus from involvement of the descending and medial vestibular nuclei and their afferent and efferent pathways.

Hagstrom *et al.* were the first investigators to study the tonic conjugate deviation of the eyes toward the side of a lateral medullary infarction.³ When fixation was blocked with eyelid closure or dark opaque contact lenses, the eyes deviated tonically toward the side of the lesion. The patient was unaware of this deviation and had to be instructed to look far to the opposite side in order to bring the eyes back to the mid-position. This conjugate deviation of the eyes was unchanged two years after the infarction. Kommerell and Hoyt recorded eye movements in a similar patient with Wallenberg's syndrome and observed a consistent asymmetry in the amplitude of voluntary and involuntary saccades.⁴ Horizontal saccades were hypermetric toward the side of the lesion and hypometric to the opposite side. Vertical saccades were deflected toward the side of the lesion by an aberrant horizontal component. The authors postulated that a "lateral pulse" in the direction of the infarct was added to each fast eye movement. Since their patient also was unaware of the tonic deviation of the eyes toward the side of the lesion, they proposed that a bias was added to the oculomotor output just before the "prenuclear gaze mechanism."

To evaluate further the nature of lateropulsion and to study its effect on each oculomotor subsystem, we recorded eye movements in six patients with Wallen-

*This study was supported by National Institutes of Health Grant NS 09823.

†Department of Neurology, Reed Neurological Research Center.

‡Department of Ophthalmology, Jules Stein Eye Institute.

§Department of Surgery, Division of Head and Neck Surgery (Otolaryngology).

berg's syndrome. Our data indicate two distinct types of oculomotor bias in these patients—a velocity bias and a position bias. The former resulted in spontaneous nystagmus and asymmetric slow eye movements (vestibular, pursuit, and optokinetic), while the latter caused a marked asymmetry in fast eye movements (saccades). Both resulted in deviation of the eyes toward the side of the infarct. Several differences between these two types of bias suggested that they resulted from different pathophysiologic mechanisms.

CASE MATERIAL

Six patients with a clinical diagnosis of infarction of the lateral medulla (Wallenberg's syndrome) were selected for quantitative eye-movement analysis. Their clinical symptoms and signs are summarized in TABLE 1. The history was similar in each case (for detailed histories on patients 1–3, see Reference 7). All patients complained of the acute onset of vertigo, nausea, and vomiting and reported a sensation of being pulled toward the side of their lesion (lateropulsion). They also reported that their eyes were being pulled in the same direction. Oscillopsia, diplopia, and dysphagia were reported less consistently. On neurologic examination, all six patients exhibited spontaneous nystagmus, loss of pain and temperature sensation on the ipsilateral face, and ataxia of the ipsilateral extremities. An ipsilateral Horner's syndrome was present in five of the six, and three of the six had a skew deviation of the eyes and loss of pain and temperature sensation in the contralateral extremities.

Past medical history revealed prior evidence of vascular disease in only two patients. Patient 2 previously had undergone bypass surgery for coronary artery disease, and patient 6 had long-standing diabetes mellitus and hypertension and required a below-knee amputation for a diabetic foot ulcer. Patient 3 had been taking birth control pills for one year prior to the onset of her acute neurologic symptoms. The other three young patients had no identifiable predisposing factors.

As expected, laboratory studies were of little help in establishing a diagnosis. All patients had normal computed tomography (CT) scans. Lateral medullary infarcts are too small to show up on CT scans, but cerebellar infarction often can be identified. We therefore concluded that either the infarction did not involve the cerebellum or the involvement was minimal. Spinal fluid was remarkable in only one patient. Patient 1 had nine lymphocytes/mm³ and a protein concentration of 54 mg/dl (normal < 45 mg/dl). These findings raised the possibility of a diagnosis of focal encephalitis or an initial bout of demyelinating disease, but there were no other symptoms and signs of infection or multiple sclerosis and the cerebrospinal fluid gamma globulin concentration was normal.

All patients gradually improved after the acute onset of symptoms. However, the rate of improvement varied greatly. In all patients, the spontaneous nystagmus and their complaint of lateropulsion were most pronounced when they were first examined and progressively decreased with each subsequent examination. In five of six patients, the spontaneous nystagmus with fixation had disappeared by the time of discharge from the hospital. Patients 1 and 2 returned to normal activity by one month after the onset of their acute neurologic deficit. The remaining four had a more protracted course requiring prolonged convalescence.

TABLE 1
SYMPTOMS AND SIGNS IN PATIENTS WITH LATERAL MEDULLARY INFARCTION

Patient	Age/ Sex	Symptoms					Signs				
		Vertigo	Nausea & Latero- Vomiting	pulsion	Oscillopsia	Diplopia	Dysphagia	Spontaneous Nystagmus	Ipsilateral Facial Numbness	Ipsilateral Ataxia	Contralateral Extremity Numbness
1	29/F	+	+	+	+	+	+	+	+	+	-
2	58/M	+	+	+	+	+	-	+	+	+	-
3	32/F	+	+	+	-	-	-	+	+	+	+
4	42/M	+	+	+	+	+	-	+	+	+	+
5	32/M	+	+	+	-	-	+	+	+	+	+
6	69/F	+	+	+	+	-	+	+	+	+	-

METHODS

The patients were tested at between 2 and 10 days after the onset of symptoms, based primarily on when their clinical condition was stable enough for them to cooperate with the testing procedure. Eye movements were recorded with d.c. electro-oculography (EOG) and on $\frac{1}{4}$ -inch videotape. Skin electrodes were placed medially and laterally to each eye and above and below the left eye to record bilateral horizontal and unilateral vertical monocular eye movements respectively. Details of the recording system are reported elsewhere.⁶

Fixation stability was evaluated by having the patient fixate on a target in the center of the visual field, 30° to the right and left and 30° up and down. While the patient fixated each target, the lights were turned on and off several times to assess the effects of loss of fixation on spontaneous nystagmus and eye position. Horizontal saccades and smooth pursuit were induced by having the patient track a laser dot projected onto a screen directly in front of the patient. For saccades, the target moved in a stepwise fashion of random amplitude and random interval between jumps. For smooth pursuit, the target moved in a sinusoidal pattern (frequency 0.2 Hz, peak velocity 22.5°/second). Vertical saccades were induced by having the patient refixate between two targets 15° above and below the mid-position. Vertical smooth pursuit was not tested.

Horizontal optokinetic nystagmus (OKN) was induced with the patient seated inside a cloth drum whose interior consisted of alternating white and black vertical stripes (15° apart). This drum produced stimulation of the entire visual field. The drum was rotated at a constant velocity of 30°/second and in a sinusoidal pattern (0.05 Hz, 60°/second peak velocity). After one minute of constant-velocity stimulation, the lights were turned off and optokinetic after-nystagmus (OKAN) was recorded. Patients were instructed to stare at the white stripes as they passed directly in front of them. Sinusoidal rotatory testing (0.05 Hz, 60°/second peak velocity) was performed (1) in the dark (vestibulo-ocular reflex, or VOR), (2) in the light with a fixed surround (visual vestibulo-ocular reflex, or VVOR), and (3) in the dark with a small fixation point attached to the rotatory chair directly in front of the patient (VOR with fixation suppression, or VOR-FIX). In the VOR test, the vestibular system is tested without visual influence, while in the VVOR test, the vestibular and optokinetic systems are stimulated in a synergistic fashion and in the VOR-FIX test, the fixation pursuit system is used to suppress the VOR.

Complete details of the on-line digital computer analysis techniques are reported elsewhere.⁶ In brief, the eye-position signal (digitized at a rate of 200 samples/second) was differentiated to yield an instantaneous velocity record. Saccadic eye movements were identified based on their characteristic velocity profile. For smooth-pursuit and nystagmus data, the gain (peak eye velocity/peak target, drum, or head velocity) was calculated after saccades were identified and removed from the traces.

RESULTS

Eye Deviation with and without Fixation

When patients were sitting quietly without specific instructions, each patient's eyes deviated toward the side of the lesion. However, when asked to fixate on a

target in the mid-position, all were able to maintain gaze at the mid-position for brief periods. Furthermore, each patient had a full range of voluntary movement in all directions by each eye. A skew deviation (ipsilateral eye hypo) was maintained in all gaze positions in three patients.

The eye deviation toward the side of the lesion had two distinct features, and both are illustrated in FIGURE 1. A slow ramp movement toward the side of the lesion was interrupted regularly by corrective saccades back toward the attempted fixation point (i.e., spontaneous nystagmus). These corrective saccades often were too small, and the average eye position deviated progressively in the direction of the slow phase, particularly if the patient was inattentive. In addition, with each eye blink, a horizontal saccade toward the side of the lesion was induced in four of six patients.

The mid-position spontaneous nystagmus was rotatory with a larger horizontal component (i.e., direction of fast phase) toward the intact side in all patients and with a lesser vertical component upward in five patients and downward in the sixth. In three patients, horizontal gaze deviation (30°) toward the side of the lesion changed the direction of the nystagmus so that the eyes now beat toward that side. In the other three patients, the spontaneous nystagmus beat away from the side of the lesion in all gaze positions.

When fixation suddenly was inhibited by turning off the lights, the eye deviation toward the side of the infarct was enhanced in all six patients (FIGURE 2). In four of six, the eyes also deviated downward. The deviation was achieved by a slow or fast eye movement or a combination of the two. The average eye position in the dark varied between 10 and 25° toward the side of the lesion and 0 and 15° downward. The patients were unaware of this deviation, and it

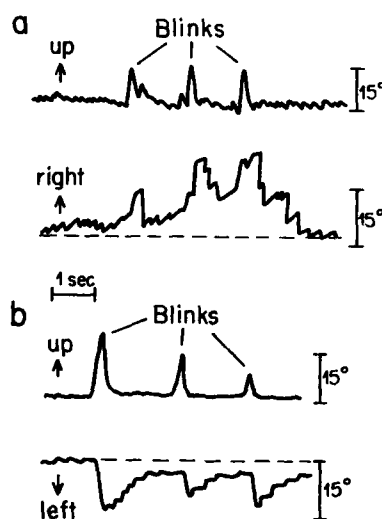


FIGURE 1. Spontaneous eye deviation toward the side of the lesion in patient 3 (a) and patient 4 (b). The patients were instructed to fixate on a target in the mid-position. Upper trace, vertical; lower trace, horizontal.

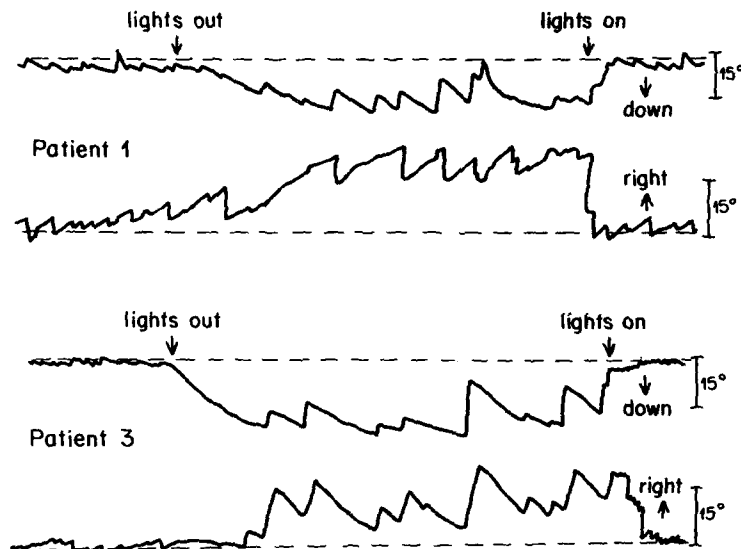


FIGURE 2. Eye deviation toward the side of the lesion with loss of fixation in patients 1 and 3.

remained even when they were urged to look straight ahead. In three of the six patients, the deviation toward the side of the lesion was maintained despite the fact that the horizontal component of their spontaneous nystagmus changed direction in the dark (e.g., patient 3, FIGURE 2). In these three patients, the slow phase now took the eyes away from the side of the lesion. Of note, these were the same three patients whose spontaneous nystagmus changed direction with voluntary gaze toward the side of their lesion.

Voluntary Saccadic Eye Movements

The amplitude of horizontal saccades consistently was asymmetric in all six patients (FIGURE 3). Saccades directed away from the side of the lesion undershot the target, while those directed toward the side of the lesion either overshot or reached the target in a single jump. In the former instance, multiple small-amplitude saccades were needed to reach the target, often taking more than a second for a 30° refixation. The interval between these repetitive saccades frequently was less than 100 mseconds. Attempts at purely vertical refixations resulted in diagonal saccades as though the eyes were deflected toward the side of the lesion (FIGURE 4). This horizontal deflection was most prominent with upward saccades and in two patients occurred only with upward saccades. After the deflection, the eyes returned to the midline with a series of small saccades with an intersaccade interval of approximately 100 mseconds. Despite the amplitude asymmetries, the peak velocities of saccades in all directions consistently were normal for their amplitudes (compared to previously reported normal values).⁹

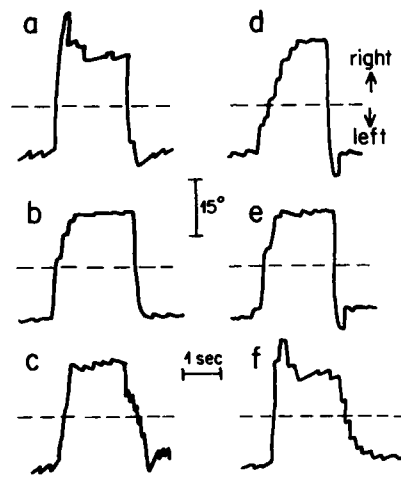


FIGURE 3. Horizontal saccadic eye movements in patients 1-6 (a-f, respectively).

Smooth Pursuit and Optokinetic Nystagmus

Smooth pursuit was asymmetric in all patients—pursuit toward the side of the lesion was better than pursuit toward the intact side (FIGURE 5, TABLE 2). The mean gain (peak eye velocity/peak target velocity) of pursuit toward the side of the lesion was 0.65 ± 0.14 , while that in the opposite direction was 0.20 ± 0.17 (compared to a normal value of 0.96 ± 0.05).¹⁰ Although higher than the gain of pursuit toward the intact side, the gain of pursuit toward the side of the lesion was decreased significantly in all patients compared to that in normal subjects (TABLE 2).

OKN slow-phase velocity showed the same asymmetry as did smooth pursuit. Slow phases toward the side of the lesion (i.e., in the direction of the slow phase of their spontaneous nystagmus) had higher velocity than did slow phases toward

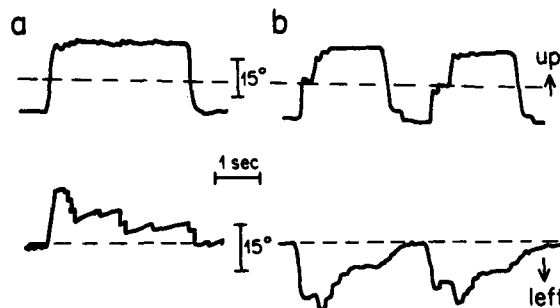


FIGURE 4. Upward vertical saccades induce horizontal saccades toward side of lesion in patients 3 (a) and patient 4 (b). Upper trace, vertical; lower trace, horizontal.

TABLE 2
GAIN OF SLOW EYE MOVEMENTS TOWARD AND AWAY FROM THE SIDE OF THE LATERAL MEDULLARY LESION*

Patient	Side of Lesion	Pursuit		OKN		VOR		VVOR		VOR-FIX	
		Toward	Away	Toward	Away	Toward	Away	Toward	Away	Toward	Away
1	R	0.80	0.11	0.30	0.03	0.80	0.50	1.05	0.90	0.87	0.12
2†	L	0.56	0.46	0.43	0.25	0.23	0.46	0.86	0.70	0.50	0.26
3†	R	0.54	0.36	0.50	0.40	0.26	0.58	0.75	0.87	0.50	0.25
4	L	0.58	0.05	0.41	0.17	0.55	0.42	0.95	0.90	0.33	0.15
5†	L	0.85	0.10	0.56	0.14	0.23	0.57	0.97	0.95	0.49	0.10
6	R	0.56	0.12	0.40	0.05	0.67	0.33	0.83	0.87	0.80	0.24
Patient Mean \pm 1 SD		0.65 \pm 0.14	0.20 \pm 0.17	0.43 \pm 0.09	0.17 \pm 0.14	0.46 \pm 0.25	0.46 \pm 0.09	0.90 \pm 0.11	0.80 \pm 0.13	0.52 \pm 0.12	0.19 \pm 0.07
Normal Mean ¹⁶ \pm 1 SD		0.96 \pm 0.05		0.83 \pm 0.13		0.50 \pm 0.15		0.99 \pm 0.05		0.01 \pm 0.02	

*Gain is peak pursuit or slow-phase velocity/peak stimulus velocity.

†Spontaneous nystagmus changed direction with loss of fixation.

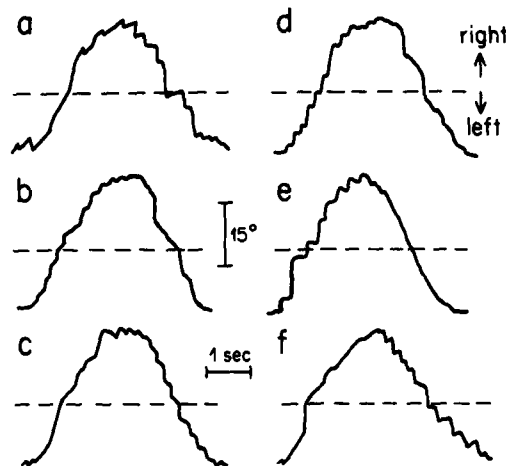


FIGURE 5. Horizontal smooth pursuit in patients 1-6 (a-f, respectively).

the intact side (TABLE 2). For the sinusoidal OKN stimulus (0.05 Hz, 60°/second peak velocity), the average gain toward the side of the lesion was 0.43 ± 0.09 while the average gain away from the side of the lesion was 0.17 ± 0.14 . Average gain values for the constant-velocity stimulus (30°/second) were 0.69 ± 0.08 and 0.23 ± 0.21 toward and away from the side of the lesion respectively. Our normal values for the same sinusoidal and constant-velocity stimuli are 0.83 ± 0.13 and 0.89 ± 0.10 respectively.¹⁰ Thus, in addition to being asymmetric, the OKN gain was decreased significantly in both directions compared to normal subjects.

As with voluntary saccades, OKN fast components toward the side of the lesion consistently were larger than those in the opposite direction (FIGURE 6). This combination of slow-phase and fast-phase asymmetry resulted in a marked asymmetry of OKN frequency. The frequency of OKN induced by drum rotation toward the side of the lesion was on average twice the frequency of OKN induced by drum rotation toward the intact side (FIGURE 6).

Optokinetic after-nystagmus (OKAN) also was asymmetric in all patients. OKAN in the direction of the patients' spontaneous nystagmus (in the dark) had greater slow-phase velocity than did that in the opposite direction. In three of six patients, OKAN occurred only in the direction of the spontaneous nystagmus.



FIGURE 6. Horizontal optokinetic nystagmus in patient 2 induced by the drum moving at a constant velocity of 30°/second. CW, clockwise; CCW, counterclockwise.

Vestibulo-Ocular Reflex

The average gain (peak slow-phase velocity/peak head velocity) of the VOR toward and away from the side of the lesion was not significantly different from that of normal subjects (TABLE 2). However, the VOR gain was asymmetric in all patients, being highest when it was in the direction of the slow phase of their spontaneous nystagmus in the dark. Since the spontaneous nystagmus changed directions from light to dark in three patients, their OKN and VOR slow-phase asymmetries were in opposite directions (e.g., patient 5, FIGURE 7). As with OKN, however, fast components of vestibular-induced nystagmus in all patients were

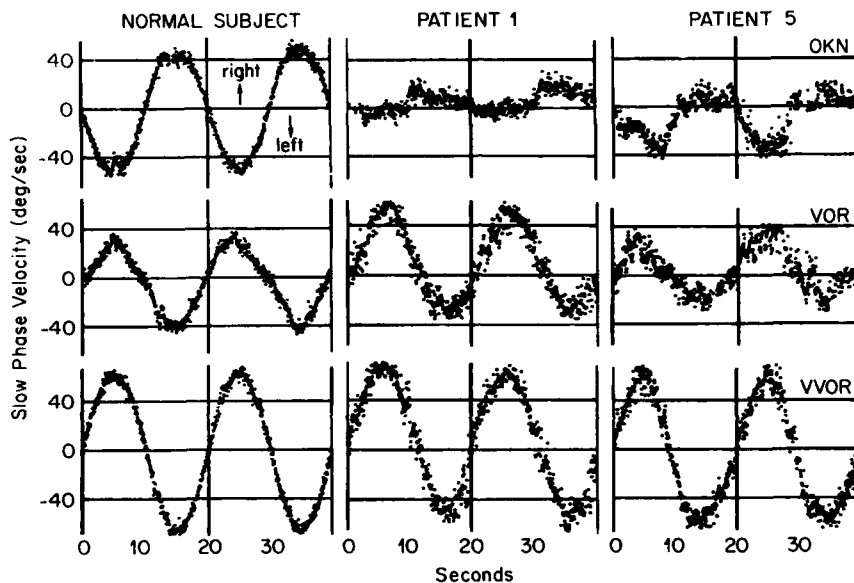


FIGURE 7. Plots of slow-phase velocity vs. time for sinusoidal (0.05 Hz, 60°/second peak velocity) OKN, VOR, and VVOR stimulation. OKN, drum rotating only; VOR, chair rotating in the dark; VVOR, chair rotating in the light with a fixed surround.

larger when directed toward the side of the lesion than when directed toward the intact side.

Visual-Vestibular Interaction

The VVOR responses (a synergistic interaction of OKN and VOR) were surprisingly well preserved (FIGURE 7, TABLE 2). Asymmetry when present was less pronounced than with OKN and VOR testing alone, and the gain (peak slow-phase velocity/peak head velocity) was normal or only slightly below normal. In many cases, the VVOR responses could not be predicted based on a

simple algebraic addition of the OKN and VOR responses. For example, in patient 1 (FIGURE 7), the VOR and OKN gains to the left were 0.50 and 0.03 respectively while the VVOR gain to the left was 0.90. A similar discrepancy was present with the gain measurements of slow phases to the right in patient 5 (FIGURE 7).

All patients had impaired fixation suppression of vestibular nystagmus (i.e., increased VOR-FIX gain) when they were rotated with a fixation point attached to the rotatory chair (TABLE 2). The VOR-FIX slow phases had higher gain when they were in the direction of the slow phase of the patients' spontaneous nystagmus (i.e., toward the side of the lesion) compared to when they were in the opposite direction. In addition to this asymmetry, the gain measurements of the VOR-FIX responses were increased significantly in both directions compared to normal subjects.

DISCUSSION

Our six patients with Wallenberg's syndrome each exhibited a conjugate deviation of the eyes toward the site of their lesion. This deviation occurred with fixation but was more pronounced when fixation was inhibited. Analysis of videotape and EOG recordings of eye movements demonstrated two distinct mechanisms of the eye deviation. When attempting to fixate on a target in the mid-position, each patient had a slow ramp eye movement toward the side of the lesion. This was interrupted regularly by corrective saccades in the opposite direction, generating spontaneous nystagmus toward the intact side. However, the corrective fast components often were inadequate to compensate for the slow components, and the average eye position drifted toward the side of the lesion. This drift was particularly pronounced when the patient was inattentive or fatigued. The second type of eye deviation, a rapid eye movement or saccade, occurred only when fixation was inhibited. In four of six patients, a saccade toward the side of the lesion was induced with each blink. After turning off the lights, each patient's eyes deviated to between 10 to 25° toward the side of the lesion by a combination of slow and fast eye movements.

Voluntary and involuntary horizontal saccades consistently were larger in the direction of the eye deviation than away from it. Vertical saccades, particularly upward saccades, were deflected toward the side of the lesion, resulting in a diagonal trajectory. Slow eye movements also were asymmetric. Smooth pursuit, OKN slow phases, and VOR slow phases had greater velocity in the direction of the slow phase of their spontaneous nystagmus than in the direction of the fast phase. In addition, the gain of smooth pursuit and OKN was decreased significantly in both directions compared to normal subjects. Apparently the lateral medullary lesions interrupted critical pathways needed for generating smooth pursuit and OKN.

We studied two different types of visual-vestibular interaction in these patients—an antagonistic interaction of smooth pursuit and VOR (the VOR-FIX test) and a synergistic interaction of OKN and VOR (the VVOR test). All patients had impaired fixation suppression of vestibular nystagmus (i.e., increased VOR-FIX gain) in both directions compared to normal subjects. In addition, the responses exhibited the same asymmetry observed with other slow eye movements, i.e., slow phases in direction of the slow phase of their spontaneous nystagmus had greater velocity than did those in the opposite direction. These

VOR-FIX responses were consistent with the degree of impairment of smooth pursuit seen in these patients. The VVOR responses, on the other hand, were relatively preserved even though the OKN responses were uniformly abnormal. For example, patients 1, 4, and 5 had normal VVOR gain in both directions despite having markedly decreased and asymmetric OKN gain. Models that assume a linear interaction of OKN and VOR signals would have predicted much lower VVOR responses in these cases.¹¹

Two different types of bias in oculomotor control were observed in our patients—a velocity bias and a position bias. The velocity bias caused the spontaneous nystagmus away from the side of the lesion and the asymmetry of all slow eye movements. The position bias caused the static deviation of the eyes toward the side of the lesion when fixation was inhibited and the amplitude asymmetry of voluntary and involuntary saccades. Two observations suggest that these different types of bias resulted from entirely separate mechanisms. First, the position bias was toward the side of the lesion in all six patients, while the velocity bias was away from the side of the lesion when fixation was inhibited in three patients. In these three patients, voluntary gaze toward the side of the lesion also changed the direction of their spontaneous nystagmus. Second, the velocity bias (i.e., the spontaneous nystagmus) was most prominent in the first few days after the onset of neurologic symptoms and then improved progressively in all patients, while the position bias remained relatively unchanged during the period of observation.

We can only speculate on the pathophysiologic basis of these two types of oculomotor bias since, although the lesions in our patients clinically were localized to the lateral medulla, we did not have anatomical correlation. Even in prior reports where pathologic material was available, clinical symptoms and signs were not well correlated with the location of the lesion.^{6,12} The zone of infarction in Wallenberg's syndrome is variable, and it includes several different pathways known to be important for oculomotor control (e.g., the medial and descending vestibular nuclei, medullary reticular nuclei, the restiform body, and the spinocerebellar tract).⁶ Furthermore, some acute symptoms and signs may be due to edema surrounding the infarct and not to the infarct itself.

We suspect that the velocity bias seen in these patients with lateral medullary lesions was due to asymmetric involvement of central vestibular pathways. Uemura and Cohen observed that unilateral lesions of the caudal lateral vestibular nuclei in the monkey resulted in rotatory nystagmus with horizontal and vertical components similar to those seen in our patients (i.e., slow phase toward the side of lesion and down).¹³ More rostral lesions in the vestibular nuclei resulted in spontaneous nystagmus in the opposite direction. These monkeys did not have eye deviation at rest, and the effect of voluntary gaze deviation on the spontaneous nystagmus was not reported. The spontaneous nystagmus with fixation lasted for 8 to 10 days after the lesion, approximating the duration of spontaneous nystagmus with fixation observed in our patients. Lesions of the labyrinth or VIIIth nerve in humans and monkeys also result in spontaneous rotatory nystagmus with slow phase toward the side of the lesion, but this nystagmus is inhibited more rapidly by fixation (usually within a few days of the lesion).^{13,14}

We agree with Kommerell and Hoyt that the position bias observed in patients with lateral medullary infarction probably results from a false internal reference as to gaze direction.⁴ This internal reference, the so-called corollary discharge or efferent copy, is felt to be important for programming accurate saccades. The bias must be added after the level where the corollary discharge is

evaluated since the patients are unaware of the eye deviation in the absence of fixation.

The paramedian pontine reticular formation (PPRF) is felt to be the immediate pre-nuclear horizontal gaze center.^{15,16} Neurons in the PPRF fire in a burst pattern just before the onset of horizontal saccades to the same side. Unilateral lesions of the PPRF result in eye deviation to the contralateral side and complete inability to move the eyes ipsilaterally beyond the midline. This picture is in direct contrast to the full range of eye movement and deviation toward the side of the lesion seen in our patients. Although the PPRF receives signals from many different areas of the brain, those from the paravermian region of the cerebellum appear to be particularly important for accurate programming of saccades.¹⁷ Lesions of the paravermian region in monkeys result in asymmetric voluntary saccades.¹⁸ The monkeys move their eyes to the contralateral side in a single saccade and return them to the ipsilateral side with a series of smaller saccades (i.e., a pattern similar to but in the reverse direction of that seen in our patients). We have studied eye movements in two patients with isolated unilateral cerebellar lesions and found an asymmetry of voluntary and involuntary saccades the same as that seen in patients with infarction of the lateral medulla, i.e., ipsilaterally directed saccades were larger than contralaterally directed saccades (unpublished data). We therefore suspect that the position bias observed in patients with lesions of the lateral medulla results from interruption of pathways between the paravermian region of the cerebellum and the PPRF pre-nuclear gaze centers.

SUMMARY

We studied electro-oculographic and videotape recordings of eye movements in six patients with Wallenberg's syndrome. With fixation, all patients had a spontaneous rotatory nystagmus with the fast phase directed toward the intact side. With loss of fixation, the patients' eyes deviated tonically toward the side of the lesion. Voluntary and involuntary saccades had larger amplitude when directed toward the side of the lesion than away from it. The spontaneous nystagmus predictably interacted with all slow eye movements, producing asymmetric smooth-pursuit, optokinetic, and vestibular responses. In addition, smooth-pursuit and optokinetic responses were decreased significantly in both directions compared to normal subjects. Fixation suppression of vestibular nystagmus also was impaired in both directions. We concluded that two different types of oculomotor bias were present in these patients—a velocity bias and a position bias. The former resulted from damage to the caudal lateral vestibular nuclei, and the latter from interruption of cerebellopontine pathways.

REFERENCES

1. BARRÉ, M. J. A. 1927. Le nystagmus et le syndrome vestibulaire dans plusieurs cas personnels de syndrome de Babinski-Negeotte et de Wallenberg. *Rev. Oto-neuro-ophthalmol.* 5: 945-959.
2. BJERVER, K. & B. P. SILFVERSKIÖLD. 1968. Lateropulsion and imbalance in Wallenberg's syndrome. *Acta Neurol. Scand.* 44: 91-100.
3. HAGSTRÖM, L., G. HÖRNSTEN & B. P. SILFVERSKIÖLD. 1969. Oculostatic and visual phenomena occurring in association with Wallenberg's syndrome. *Acta Neurol. Scand.* 45: 568-582.

4. KOMMERELL, G. & W. F. HOYT. 1973. Lateropulsion of saccadic eye movements. *Arch. Neurol.* **28**: 313-318.
5. FRISEN, L. 1978. Lateropulsion of the eyes—a localizing brainstem sign. *J. Neurol.* **218**: 171-177.
6. FISHER, C. M., W. E. KARNES & C. S. KUBIK. 1961. Lateral medullary infarction—the pattern of vascular occlusion. *J. Neuropathol.* **10**: 323-379.
7. MEYER, K. T., R. W. BALOH, G. B. KROHEL & R. S. HEPLER. 1980. Ocular lateropulsion. A sign of lateral medullary disease. *Arch. Ophthalmol.* **98**: 1614-1616.
8. BALOH, R. W., L. LANGHOFER, V. HONRUBIA & R. D. YEE. 1980. On-line analysis of eye movements using a digital computer. *Aviat. Space Environ. Med.* **51**: 563-567.
9. BALOH, R. W., W. KUMLEY, A. SILLS & V. HONRUBIA. 1975. Quantitative measurement of saccade amplitude, duration and velocity. *Neurology* **25**: 1065-1070.
10. BALOH, R. W., R. D. YEE, J. KIMM & V. HONRUBIA. 1981. The vestibulo-ocular reflex in patients with lesions of the vestibulocerebellum. *Exp. Neurol.* (In press.)
11. LAU, C. G. Y., V. HONRUBIA, H. A. JENKINS, R. W. BALOH & R. D. YEE. 1978. A linear model for visual-vestibular interaction. *Aviat. Space Environ. Med.* **49**: 880-885.
12. MOBERG, A., L. PREBER, B. P. SILFVERSKIÖLD & S. VALLBO. 1962. Imbalance, nystagmus and diplopia in Wallenberg's syndrome. *Acta Otolaryngol.* **55**: 269-282.
13. UEMURA, T. & B. COHEN. 1973. Effects of vestibular nuclei lesions on vestibulo-ocular reflexes and posture in monkeys. *Acta Otolaryngol. Suppl.* **315**: 1-71.
14. BALOH, R. W. & V. HONRUBIA. 1979. *Clinical Neurophysiology of the Vestibular System*. F. A. Davis Company. Philadelphia, Pa.
15. KELLER, E. L. 1974. Participation of medial pontine reticular formation in eye movement generation in monkey. *J. Neurophysiol.* **37**: 316.
16. HENN, J. & B. COHEN. 1975. Activity in eye motoneurons and brain stem units during eye movements. In *Basic Mechanisms of Ocular Motility and Their Clinical Implications*. G. Lennerstrand & P. Bach-Y-Rita, Eds. **24**: 303-324. Pergamon Press. Stockholm, Sweden.
17. COHEN, B., K. GOTO, S. SHANZER & A. WEISS. 1965. Eye movements induced by electrical stimulation of the cerebellum in the alert cat. *Exp. Neurol.* **13**: 145-162.
18. ASCHOFF, J. C. & B. COHEN. 1971. Changes in saccadic eye movements produced by cerebellar cortical lesions. *Exp. Neurol.* **32**: 123-133.

HEAD NODDING ASSOCIATED WITH IDIOPATHIC CHILDHOOD NYSTAGMUS

Michael Gresty

*Medical Research Council Hearing and Balance Unit
Institute of Neurology
National Hospital
London, WC1N 3BG, England*

G. Michael Halmagyi

*Department of Clinical Neurophysiology
Royal Prince Alfred Hospital
Camperdown 2050, New South Wales, Australia*

INTRODUCTION

There were frequent reports in the earlier literature of children presenting at an early age with a combination of nystagmus and head shaking (e.g., Hancock, 1908).¹ These days the condition apparently is rare and may have declined in incidence because of improvements in diagnosis and community health. Nevertheless, despite its lack of importance as a disease entity, the concurrence of head shaking and nystagmus is of physiological and clinical interest because of implications as to the nature of underlying pathophysiological mechanisms.

Prima facie considerations would suggest two reasons for the association of head shaking and nystagmus: one being that the head movement is in some way compensatory for the nystagmus and helps to stabilize the visual axes; the other is that the shaking is itself an involuntary movement akin to tremor or perhaps chorea. Before investigating these possibilities in actual cases, it is necessary to understand the role of the vestibulo-ocular reflex (VOR) in normal head-eye coordination.

The direction in which the eyes are looking is called "gaze," which is the sum of head position and eye position (eye position in the orbit, i.e., with respect to the head). For good vision, gaze has to be stable; a nystagmus, for example, makes the visual axes oscillate to and fro with the result that gaze never is stable on the target and vision is poor. Under normal conditions, any movement of the head is accompanied by an eye movement that is equal in velocity and opposite in direction to that of the head. The net result is that the direction of gaze remains undisturbed because the head and eye movements cancel each other. These "compensatory" eye movements are generated by the vestibulo-ocular, or "doll's head," reflex. The vestibulo-ocular reflex operates continually even during saccadic eye movements that are made to transfer the direction of fixation. It normally cannot be turned off. These considerations lead us to an important conclusion for the relationship between head shaking and nystagmus.

A person with a nystagmus and a normal VOR who tries to shake his head to compensate for the way his eyes are oscillating will do so in vain, for his head movement will be countereffected by the vestibulo-ocular reflex, leaving the nystagmus to determine the direction of the visual axes. In other words we may formulate the equation, adding head and eye movements together:

Nystagmus + Head Movement + Eye Movement (which is equal to
minus head movement) = Nystagmus = Gaze

In conclusion, a patient with a nystagmus who has a normal VOR cannot shake his head to improve vision; hence, if the head movements are compensatory and help him to see better, then during the shaking he must suppress his VOR in some way. A corollary of this conclusion is that when head shaking does not improve vision, the VOR must be normal and the shaking has no beneficial effect and probably is an involuntary movement of pathological origin.

In fact we have found three patterns of head and eye movements in patients who have had associated nystagmus and head shaking from early life. In the first pattern, the head shaking does not improve vision and probably is an involuntary movement; in the second, the head shaking compensates for the nystagmus, during which the VOR must be suppressed; and in the third type, the nystagmus seems to go away whenever the head is moved, leaving normal vestibulo-ocular reflexes to stabilize gaze.

Head Shaking as an Involuntary Movement (Tremor)

Many more patients fall into this category than into the others. The characteristics are as follows. The nystagmus and associated head shaking probably begin together shortly after birth and persist through life. The nystagmus is of the typical motor-defect type. The head shaking is of low amplitude, perhaps only two or three degrees of displacement, is very regular, and resembles a tremor. The period of the head movement is usually about 250 mseconds and is the same as that of the nystagmus that is present when the head shakes. These periods correspond to a frequency of 4 Hz, which would suggest tremor of cerebellodentothalamic origin.^{2,3} The head movements generally are suppressed and tend to appear only when the patient is tired or engrossed. When old enough to be questioned, these patients are aware of their head shaking and can suppress it when asked. They do not believe that it helps them to see better. Our conclusion is that the head movements in these patients are involuntary, should be classified as tremor, and result from pathology that perhaps is similar to that responsible for the nystagmus.

Since head shaking does not alter visual acuity in these patients, one must presume that they have vestibulo-ocular reflexes that function normally. Because of the low amplitude of head movement in comparison with the nystagmus, it is difficult to detect the vestibulo-ocular reflex component of eye movement during periods of head tremor; however, if the patient shakes his head vigorously, then one can detect readily a modulation of the nystagmus that reflects the head movement.

Other tests of vestibular function, such as rotational stopping stimuli and caloric irrigation, may not be successful because the resulting vestibular nystagmus is confounded with the congenital nystagmus and in some such patients apparently is easily suppressed, presumably because they have a lifetime's experience in dealing with problematic nystagmus.

Head Shaking that Compensates for Nystagmus

We have found two patients with nystagmus who shake their heads with a movement having the same shape as the nystagmus but an opposite direction. The head shaking and the nystagmus, being more or less equal and opposite, tend to cancel each other, thus providing stable gaze. Both of these patients were male

children under 10 years of age. We have been able to follow one of them for two years.

The pattern of head shaking in these children was irregular, consisting of combinations of oscillatory and ramp-shaped movements. The overall amplitude, which corresponded to the size of the nystagmus, was as much as 10° or more. The children both could tell us that the head movements helped them to see; and if one deliberately held their heads still while they concentrated on a visual task, their vision deteriorated markedly.

According to the reasoning detailed above, one must conclude that during head shaking, the VOR was suppressed in these patients. The VOR certainly was not totally absent in these children, for passive oscillation of the head produced eye movements modulated by the head movement.

In the child who was observed longitudinally, there occurred a transition period lasting for several weeks, during which his behavior altered. We were alerted to this by the fact that his parents thought that his head shaking had diminished and that his nystagmus sometimes stopped.

On examination during this time, the child showed several patterns of head and eye movements. At times he produced the usual pattern of compensatory shaking that we already had established and just have described. Within moments of this pattern being recorded, he would switch, as it were, into another mode of control in which the nystagmus disappeared when he shook his head, leaving normal vestibulo-ocular reflexes. This pattern of course is the third type in our classification. At yet other times, the nystagmus would go away completely, its absence lasting from a few seconds to one or two minutes.

All evidence would suggest that people with nystagmus and having compensatory patterns of head shaking eventually lose their nystagmus altogether. The one child we have followed apparently is well on the way to recovery, and we have never come across a report of an adult with this behavior.

From the patient we were able to study, it would seem that such patients can develop strategies for suppressing involuntary eye movements. First the boy "learned" how to switch off his VOR so that he could swing his head in compensation for the nystagmus, and then he learned how to suppress the nystagmus itself, both apparently through the behavioral maneuver of head movement.

*Head Movements that Switch off Nystagmus, "Spasmus Nutans"*⁴

This third category probably forms some kind of continuum, at least in terms of similarity of mechanism, with the second pattern of "compensatory head movements." Excluding the child with compensatory head movements who developed into a Spasmus nutans type, we have observed two other patients, both children in the first five years of life, whose nystagmus went away when they shook their heads. The older child, who was five years of age, was well on the way to recovery according to his parents' report of his development; and we similarly believe that patients with this third pattern of behavior tend to lose their nystagmus as they develop.

Similar to those with compensatory head shaking, these patients report that they see better when they move their head, and vision does deteriorate when their heads are held still. Close examination reveals that during head shaking, they have fairly normal looking dolls-head movements that are unlike the nystagmus present when the head is still.

One may speculate on criteria that distinguish between patients with head tremor and those with compensatory head movements. The waveforms of the nystagmus possessed by patients with head tremor had "null periods" that permitted adequate vision,⁵ whereas patients with compensatory head shaking had nystagmus that was often fast oscillations that did not provide any periods of stable gaze during which they could see. Hence it may be that the children with inadequate vision were driven to develop compensatory strategies, if they could do so.

There are interesting features about children who shake their heads to switch off their nystagmus and those who suppress the VOR during head shaking. In each case, involuntary eye movement is suppressed by a behavioral act. The natural history of the disorder in these children suggests that there is a developmental continuum leading to remission. Although the initial adaptation to the nystagmus is achieved through an overt behavioral maneuver, the final adaptation is internalized totally and the nystagmus is suppressed without head shaking. It is possible that the transition from suppression through overt behavior to internalized suppression follows the type of developmental scheme proposed by Piaget (1962).⁶ At the earliest "sensorimotor" stage, the child is trying to solve problems by overt behavioral acts of experimentation, i.e., in this context he finds that certain maneuvers help his visual problems; from this stage onward, he internalizes the operations as he grows toward the stage of formal reasoning. This ability to construct an internal model of control processes perhaps enables the child with nystagmus eventually to suppress his involuntary eye movements without resorting to overt maneuvers.

Our findings have implications for the physiology and pathology of vestibulo-oculomotor function. First they show that the current twofold classification of congenital nystagmi into sensory and motor-defect types must be incomplete. All our patients would be classified as motor-defect types because they had no evidence of pathology of the visual pathways. However, there probably are differences between the pathologies underlying the nystagmi that are successfully suppressed and those that persist through life. Here the question is open. It may be that the waveforms of the nystagmi that are suppressed do not provide quiescent periods during which gaze is stable, so that the child is forced to explore other strategies for improving his vision. This would be a difference in degree of pathology rather than in kind. Our few observations so far do not allow us to go as far as saying this. What is evident is that the waveforms of some nystagmi that are suppressed, unlike those of the nystagmi that persist, frequently are aperiodic and do not conform readily to an overall pattern. The lack of periodicity may contribute to loss of visual acuity. In addition the nystagmi of the Spasmus nutans type, which also are suppressed, consist of high-frequency oscillations that certainly degrade visual acuity severely and provide no null periods.

The implications of our findings for vestibulo-ocular physiology concern the problem of suppression of the vestibulo-ocular reflex and, generally speaking, of any unwanted, drifting eye movements. There are two hypotheses to account for the suppression of the vestibulo-ocular reflex. One is that vestibular reflexes are canceled by pursuit mechanisms, the other is that there is a specific mechanism that suppresses the reflex. There certainly is a strong relationship between the performance of the pursuit system and that of vestibulo-ocular reflex suppression, for it has been shown that in normal subjects, they break down at similar frequencies and velocities;⁷ so whether the vestibular reflexes are canceled or suppressed, both mechanisms probably share neural structures in common with

the mechanism of smooth pursuit. On the whole, the evidence from patients with congenital nystagmus supports a mechanism of suppression rather than of cancelation, for the children who do switch off their vestibular reflexes or nystagmus during head shaking can hardly do so through the mediation of smooth-pursuit mechanisms. The hypothesis of suppression rather than cancelation also is supported by other clinical data. We frequently have observed that patients who cannot suppress their vestibulo-ocular reflexes may have pursuit that is deranged only moderately, so that there is a mismatch between the performance of suppression and that of pursuit. Similarly—in using the performance of pursuit and suppression to monitor levels of drug toxicity—we have found clear and consistent differences between the decrement in performance of pursuit and of suppression, such that there always is more suppression than one would expect from the capabilities of the pursuit system.

In conclusion, it would seem that although pursuit and suppression are closely related such that when one breaks down the other also is affected, the relationship is not so close that pursuit is wholly responsible for the cancelation of vestibulo-ocular reflexes.

REFERENCES

1. HANCOCK, I. 1908. Head nodding and nystagmus. *The Royal London Ophthalmic Hospital Reports* 17: 104-114.
2. HOLMES, G. 1904. On certain tremors in organic cerebral lesions. *Brain* 27: 360-375.
3. GREY, M. A. & G. M. HALMAGYI. 1979. Abnormal head movements. *J. Neurol. Neurosurg. Psychiatry* 42: 934-939.
4. GREY, M., J. LEECH, M. SANDERS, & H. EGGARS. 1976. A study of head and eye movements in Spasmus nutans. *Br. J. Ophthalmol.* 60: 652-654.
5. DELL'OSSO, L. F. & M. D. DAROFF. 1975. Congenital nystagmus waveforms and foveation strategy. *Doc. Ophthalmol.* 39: 155-182.
6. PIAGET, J. 1962. The stages of the intellectual development of the child. *Bull. Menninger Clin.* 26: 120-128.
7. BENSON, A. J. & G. R. BARNES. 1978. Vision during angular oscillation: the dynamic interaction of visual and vestibular mechanisms. *Aviat. Space Environ. Med.* 49: 340-345.
8. VON BITTENCOURT, P., M. A. GREY & A. RICHENS. 1980. Quantitative assessment of smooth pursuit eye movements in healthy and epileptic subjects. *J. Neurol. Neurosurg. Psychiatry* 43: 1119-1124.

A HYPOTHETICAL EXPLANATION FOR PERIODIC ALTERNATING NYSTAGMUS: INSTABILITY IN THE OPTOKINETIC-VESTIBULAR SYSTEM*

R. John Leigh, David A. Robinson, and David S. Zee

*Departments of Ophthalmology and Neurology
The Johns Hopkins University
School of Medicine
Baltimore, Maryland 21205*

INTRODUCTION

Spontaneous nystagmus that periodically reverses direction has been reported in a variety of circumstances: as a variant of congenital nystagmus; in association with acquired neurological lesions, especially in the region of the craniocervical junction; and as a transient manifestation of anticonvulsant intoxication.¹⁻⁶ Periods of oscillation ranging from a few seconds to minutes have been reported.^{3,7} Sometimes this nystagmus is present only in darkness.² It has been reported in blind patients with no other evidence of neurological disease.⁴ Within the subjects of these reports exists a group of patients who show an indefatigable nystagmus, in light or darkness, which regularly reverses direction with a period often of 3-4 minutes, and in whom acquired disease of the nervous system seems most likely to be the cause.⁸ It is this form of periodic alternating nystagmus (PAN) that we address here, using clinical studies and control-systems analysis to develop a hypothetical explanation, or model, of the phenomenon. We propose that PAN arises from (1) an instability in the brain-stem neural networks that generate slow phases of vestibular and optokinetic nystagmus, (2) the action of an adaptive network that normally acts to null prolonged, inappropriate nystagmus, and (3) an inability to use retinal-error-velocity information.

METHODS

Eye movements were recorded using bitemporal direct-current electro-oculography (EOG). Data were recorded onto magnetic tape and displayed by a pen recorder for analysis by hand. Our entire system had a bandwidth of 0-100 Hz, and eye movements could be measured with a sensitivity of 1° and an accuracy of about 10% over a range of $\pm 40^\circ$.

Patients attempted fixation of an array of small red-light-emitting diodes. Horizontal vestibular responses were induced by use of a servo-driven chair. Pursuit eye movements were tested by asking the patient to track a small spot of light rear-projected onto a semitranslucent screen. This spot was driven in a triangular waveform with velocities of 5-20°/second and amplitudes of 10-20°. A large, patterned, cylindrical drum that surrounded the patient served as an optokinetic stimulus.

*This research was supported by National Institutes of Health Research Grants EY05264 and AG00061 (Dr. Leigh), EY00596 (Dr. Robinson), EY01849 and NS11071 (Dr. Zee), and by a Core Center Grant (EY01765) to the Wilmer Institute.

Patients were dark adapted at the beginning of each session, and frequent calibrations were made throughout to ensure stability of the EOG signal. To ensure optimal alertness and attention, one of the investigators sat with each patient throughout each session, providing constant encouragement. In addition, frequent rest periods were allowed.

CLINICAL MATERIAL

Patient 1

During the summer of 1970, a 39-year-old woman noted an increase in the frequency of her long-standing headaches and increasing fatigability. In December 1970 she developed episodic vertigo, a sensation of fullness in her left ear, intermittent diplopia, and disequilibrium. By January 1971 she had become dysarthric and lethargic, and noted blurred vision. On January 21, 1971, she was admitted to a local hospital where a neurological examination reportedly revealed lethargy, slow speech, nystagmus, dysmetria, and ataxia. A lumbar puncture at that time showed a spinal fluid protein of 110 mg%, glucose of 15 mg%, and 281 white cells/cc, 50% being lymphocytes. The opening pressure was normal. Cerebral arteriography showed hydrocephalus, and a ventriculogram showed a possible IVth-ventricular mass. On February 1, 1971, at the local hospital, she underwent a suboccipital craniotomy. The cerebellar vermis was split, and granulomatous tissue near to the area postrema was biopsied. This showed cryptococcus.

She subsequently was transferred to the National Institutes of Health, where she improved considerably with antifungal chemotherapy and, on discharge, was troubled only by mild oscillopsia and gait ataxia. In 1974 she was noted for the first time to have PAN. She had a mild gait ataxia at that time but no other neurological abnormalities.

When examined clinically in November 1978 (the time of first recording), she had PAN with a period of four minutes, impaired smooth pursuit in all directions (when tested during her null period), and saccades that appeared to be of normal velocity and accuracy. Her neurological examination otherwise was normal. At that time she was unable to work as a schoolteacher because of the impairment of visual acuity due to the nystagmus.

In July 1979 she started taking baclofen, which abolished her PAN and consequently improved her visual acuity so that she could return to work. We recorded her eye movements again at this time.

Patient 2

A 59-year-old woman, with a history of several myocardial infarctions and episodes of congestive heart failure, suddenly developed diplopia, vertigo, numbness, and influenzalike symptoms. Over the course of several weeks, her neurological deficits largely resolved but she complained of intermittent visual impairment. Six months later, in July 1976, she was admitted to Johns Hopkins Hospital when she showed signs of mild congestive heart failure, with a normal blood pressure. Neurological examination showed mild right ptosis, left facial

weakness, and residual right hemiparesis. Oculomotor examination showed alternating nystagmus with a period of 204 seconds. Far eccentric horizontal gaze produced nystagmus with centripetal slow phases regardless of the phase of the cycle of alternating nystagmus. Saccades appeared to be of normal velocity and accuracy. No smooth-pursuit movements were apparent when tested during brief null periods. No vertical nystagmus was noted at that time.

Tomography of the cranial vertebral junction, computed axial tomography of the head, and examination of the spinal fluid all were normal. Carotid arteriography showed about 30% stenosis of the left internal carotid at its origin, and a minimal irregularity of the right common carotid at its origin. However, posterior fossa arteriography showed no vascular abnormality or any tonsillar displacement. Intracranial vessels appeared normal. Blood sugar estimations showed consistently elevated values. Serum tests for syphilis were negative. It was thought most likely that her neurological deficit was due either to a small medullary infarction or to an episode of demyelination.

When she was examined again in September 1979 (time of study), the only change of note was an increase in the length of the period of alternating nystagmus to 220 seconds with no null period. In addition some down-beat nystagmus was noted on far lateral gaze. A trial of baclofen was instituted by her family physician, but although the patient noted some improvement in vision at a dose of 10 mg three times a day, she discontinued the drug because of chest pain and ankle edema.

Patient 3

A 35-year-old shoemaker was referred to the Johns Hopkins Hospital in January 1980, complaining of progressive blurred vision, slurred speech, and unsteady gait. He had been well until age 19, when he suffered head trauma in an automobile accident that resulted in several hours' loss of consciousness. Subsequently his friends remarked that he "looked drunk" and had "dancing eyes" and slurred speech. At age 28, he was admitted to a local hospital. An isotope brain scan and an electroencephalogram were normal; no cause could be found for his complaints. Thereafter he became progressively disabled by his symptoms, which seemed to be made worse by sneezing.

His admission examination was notable for spontaneous nystagmus with periodic head turning, but with a persistent head tilt to the right. With the head erect and fixed, PAN with a period of four minutes was documented. There was prominent gaze-evoked nystagmus with centripetally directed slow phases; and during the few seconds when his horizontal nystagmus was changing direction, down-beating nystagmus was apparent in primary position. He also showed gaze-evoked nystagmus in the vertical plane with centripetally directed slow phases. The patient used head turning to put his eyes in a far lateral position in the orbit and so temporarily nulled his PAN with oppositely directed gaze-evoked nystagmus. He also showed saccadic hypermetria.

Other neurological findings were left-sided facial weakness, a hypoactive gag reflex, limb dysmetria that was more pronounced in the lower extremities, and gait ataxia. Although his skull x-rays were normal, both myelography and computed tomography with metrizamide showed an Arnold-Chiari malformation. On January 25, 1980, a posterior fossa decompression was performed. Subsequently, the PAN persisted, although occasionally the half cycle with slow

phases to the left was replaced by down-beating nystagmus in the primary position. Two months postoperatively, baclofen was started. This abolished PAN, but a persistent down-beating nystagmus remained in all positions of gaze.

RESULTS

Characteristics of PAN

The periods of oscillation were similar in each of our three patients (235, 225, and 220 seconds respectively) in both the light and the dark. An excerpt of the record from patient 1 is shown in FIGURE 1. When slow-phase eye velocity was plotted against time, it was apparent that in none of our patients were the oscillations truly sinusoidal; the velocity built up faster than it declined in each half cycle. For patients 2 and 3, the oscillations were the same while in darkness and during fixation of a light-emitting diode. The peak slow-phase velocity was 37 and 20°/second respectively. For patient 1, however, the peak slow-phase velocity was greater in darkness (20°/second versus 14.5°/second in the light). During attempted fixation of a stationary spot, there were episodes of 7 to 10 seconds—at the time when nystagmus reversed direction—when the eyes were stationary, so-called null periods (FIGURE 2).

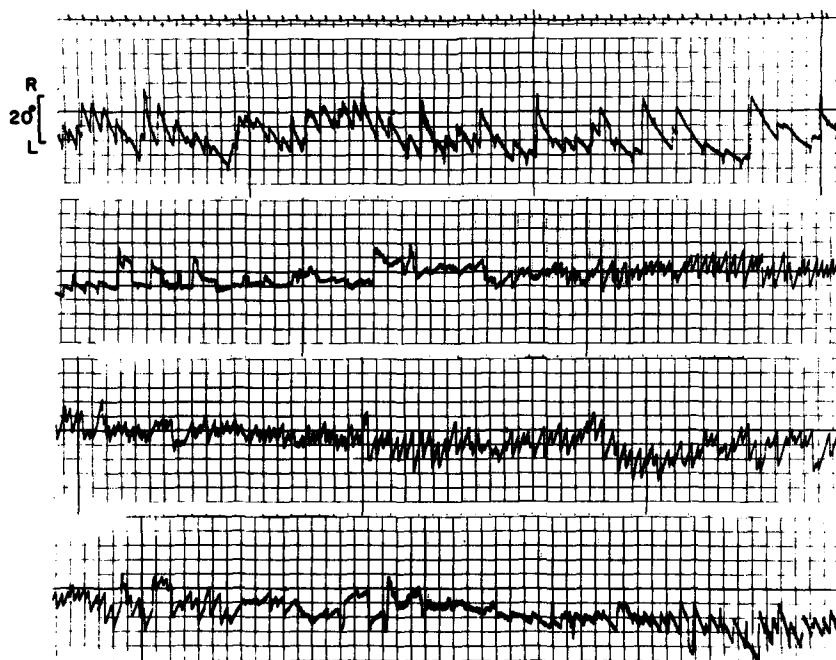


FIGURE 1. Horizontal electro-oculograph record of PAN in patient 1, while in darkness. The time scale at the top is in seconds. The four records shown are continuous.

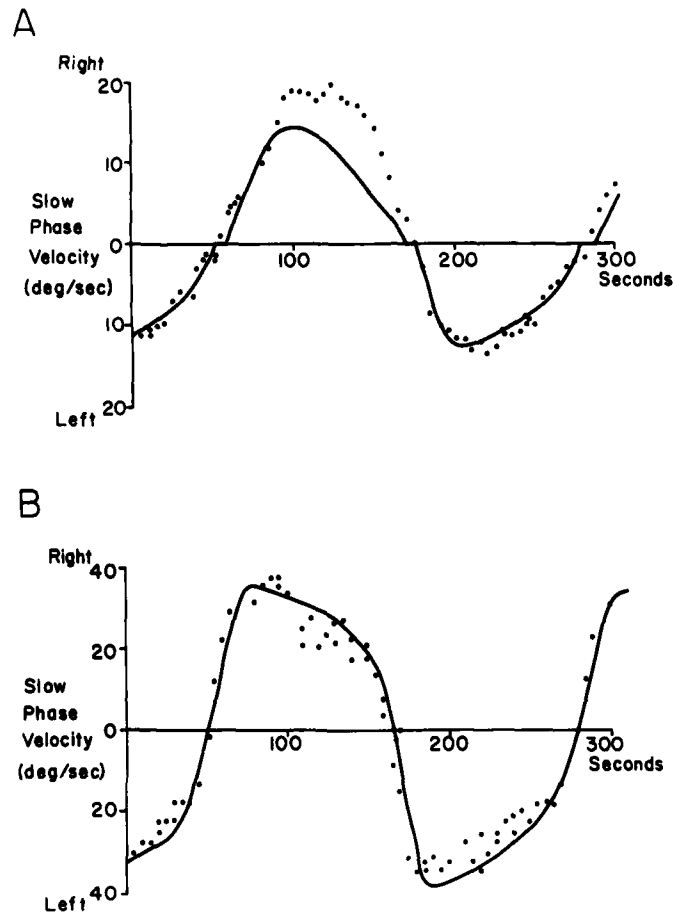


FIGURE 2. Temporal profile of slow-phase velocity of PAN in patients 1 (A) and 2 (B); note the difference in velocity scales. Solid lines indicate PAN during attempted fixation of a light-emitting diode; data points (●) are for PAN while in darkness. Patient 1 showed slower peak slow-phase velocity during attempted fixation in light than in darkness; in light, a "null period" occurred. Patient 2 showed no significant difference of PAN characteristics whether in light or darkness.

Vestibulo-Ocular Responses

Rotational stimuli (velocity steps of $60^\circ/\text{second}$) were applied in darkness at times when the nystagmus was changing direction. In two patients this resulted in compensatory eye velocities with gains (initial eye velocity/initial head velocity) greater than 1 (1.2, 0.9, and 1.1 for patients 1, 2, and 3 respectively). However, the response decayed more rapidly than normal, suggesting a decreased time constant during constant-velocity rotation; a typical value was three seconds. Such rotations "reset" the oscillation, causing a transient change

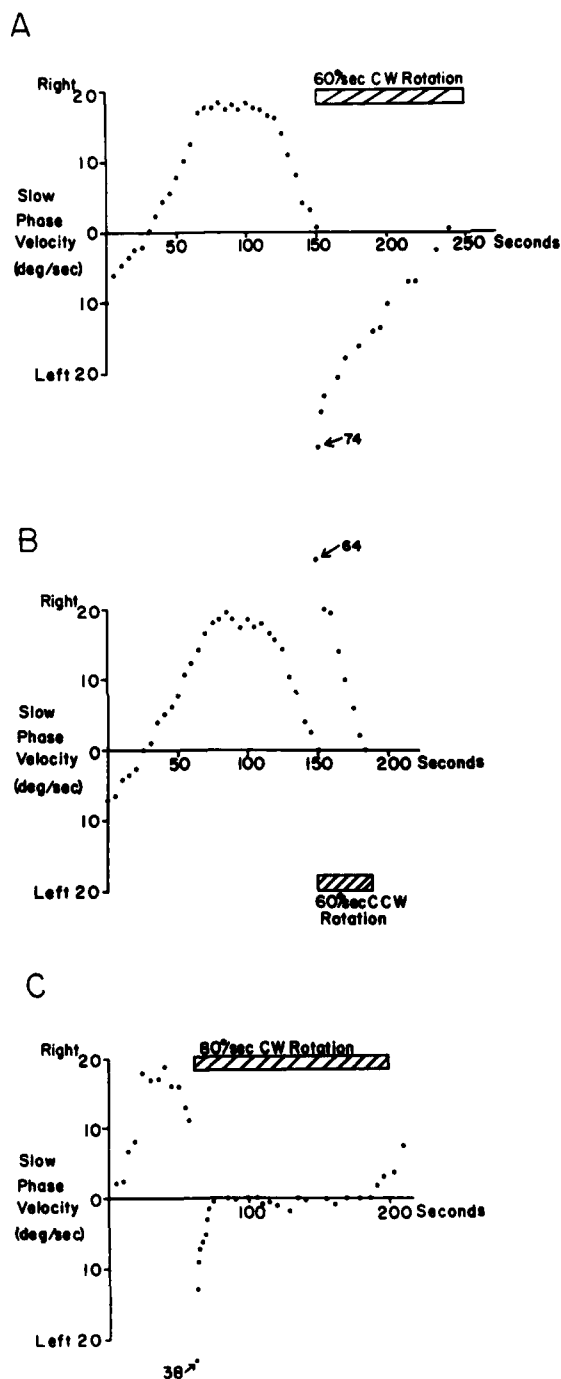


FIGURE 3. The effects of rotational stimuli in darkness (velocity steps) on the PAN of patient 1. Stimuli (striped bars), started at times of reversal of PAN, caused a phase advance in the oscillations in A and phase lag in B. The values of data points off scale are as indicated by arrows. The stimulus in C was chosen to temporarily stop the PAN. These waveforms will be compared to those obtained from a computer simulation (FIGURE 5).

in the amplitude and permanent shift of the phase of the oscillations (FIGURE 3). The significance of this will be discussed later.

Smooth Ocular Pursuit

Neither patient 2 nor 3 showed any preservation of smooth-pursuit tracking. However, patient 1 did show some ability to generate smooth eye movements at low velocities. Pursuit was measured during the brief "null periods." The pursuit gains (eye velocity/target velocity) for target velocities of 5, 10, and 20°/second were 0.65, 0.55, and 0.65 respectively. Once the spontaneous nystagmus began its next half cycle, however, the patient's ability to track smoothly appeared to deteriorate rapidly.

Optokinetic Responses

Because the response of humans to a moving optokinetic drum mainly reflects pursuit function,⁹ we tried to evaluate the performance of the optokinetic system by measuring the after-nystagmus (OKAN) in darkness, following a 50-second period of optokinetic stimulation at 60°/second. OKAN in humans is not striking, and OKAN would be obscured by the ongoing PAN. Consequently, we had to see if the normal course of the PAN, which is quite regular and predictable, was perturbed by the optokinetic stimulus. Judged this way, no patient showed any evidence of optokinetic function: there was no change in predicted slow-phase velocity or any resetting of the PAN.

Effects of Drug Treatment

Patient 1 was able to take the drug baclofen at a dose of 30 mg/day. This abolished the PAN in both light and darkness. However, her smooth-pursuit performance remained impaired but now in an asymmetric manner. Thus at a target velocity of 5°/second, the gain was 0.7 to the right but 0.4 to the left; at 10°/second, 0.6 to the right and 0.2 to the left; and at 20°/second, 0.6 to the right and 0.25 to the left. There was no apparent recovery of optokinetic function, as judged by absence of OKAN. Rotational stimuli applied in darkness produced vestibulo-ocular responses whose gain was 1.1. With sustained rotation of 60°/second, compensatory eye velocity declined in a nonexponential manner; there was an initial rapid fall, lasting about 8 seconds, followed by cessation of eye movements within 40 seconds. A reversal phase of postrotary nystagmus sometimes was evident.

Because of possible cardiac side effects, patient 2 was unable to take baclofen for more than a few days, though she noted some improvement in her vision during this period. Unfortunately we were unable to examine her while she was taking the medication.

On baclofen (30 mg/day), patient 3 showed resolution of PAN. However, marked gaze-evoked nystagmus and a persistent down-beat nystagmus still were evident.

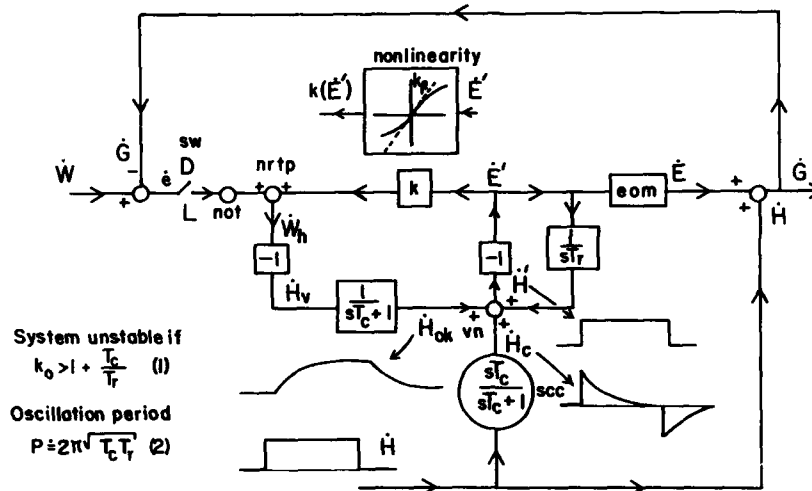


FIGURE 4. A model of the optokinetic system and vestibulo-ocular reflex, which we have used to simulate PAN. Head velocity, H , is transduced by the semicircular canals (scc) into the neural output signal H_c . T_c is the cupula time constant, and s is the Laplace transform complex frequency. H_c passes to the vestibular nucleus, vn , and after a sign change it becomes an eye velocity command E' , which drives the eyes through the extraocular muscles (EOM) at velocity E . This pathway is a simplified version of the vestibulo-ocular reflex. E sums with H to give slow-phase gaze velocity in space, \bar{G} . The optokinetic system is stimulated by retinal-image velocity, e —the difference between the velocity of the visual world, W , and \bar{G} —when the lights are on (indicated by switch, sw , being turned to L ; it is open in darkness, D). The error signal e passes via the nucleus of the optic tract, not , to the nucleus reticularis tegmenti pontis, $nrtp$, where an efference copy of eye velocity E' is added to e to give W_h , the velocity of the environment with respect to the head. Since the seen world never moves, $-W_h$ is the visual system's estimate of head velocity in space, H_v . The high-frequency components of H_v are filtered out, and the resulting optokinetic signal, H_{ok} , is added to H_c in the vn . The sum, H' , is the brain's best estimate of rotational head velocity. A central adaptation operator, $1/(sT_c)$, monitors the slow-phase eye-velocity command E' and acts to eliminate persistent nystagmus by sending a signal back to the vn to cancel the source of vestibular imbalance. Normally the value of gain, k , is slightly smaller than 1.0, but we postulate that for PAN to occur, k 's value increases and if the retinal-error signal e is denied access to the $nrtp$, the system becomes unstable. To constrain the oscillations, we have introduced the nonlinearity shown in the inset, whose output is $k(E')$. For the system to oscillate, the slope of this function at the origin, k_0 , must meet the specifications shown by Equation 1 in the bottom left. The period of these oscillations, P , is approximated by Equation 2.

DEVELOPMENT OF A HYPOTHESIS FOR PAN

On the basis of clinical observations over several years, of a patient who eventually developed PAN, Kornhuber suggested that this phenomenon was an exaggeration of a vestibular response shown by normal subjects: the reversal phase of postrotary nystagmus.⁴ This reversal phase, also called secondary nystagmus or post-postrotary nystagmus, occurs during or on stopping a sustained rotational stimulus (velocity step). After the primary vestibular reaction has died away, a weaker secondary response develops, with slow phases in the opposite

direction (i.e., toward the side of head rotation). This reversal phase has been attributed to a vestibular adaptation or repair process that acts to null persistent unidirectional nystagmus.^{10,11} We also have noted this phenomenon and simulated PAN by using a model of the vestibulo-optokinetic system to which has been added a vestibular adaptation, or repair, circuit that can produce such reversal phases of nystagmus.

Our model makes use of the behavioral and neurophysiological observations that support a symbiotic relationship between the vestibulo-ocular and optokinetic systems. Though the vestibulo-ocular reflex enables compensatory eye movements and hence clear vision for transient head turns, its performance declines during sustained rotations. In this latter circumstance, optokinetic drives maintain compensatory eye movements.^{12,13} Neurophysiological data from primates suggest a linear combination of vestibular and optokinetic signals within the vestibular nucleus.^{14,15} We started with a simple description of the vestibulo-ocular reflex (FIGURE 4). Head velocity, \dot{H} , is transduced by the semicircular canals (with a cupula time constant T_c), and the ensuing neural signal, H_c (after a sign change), becomes an eye-velocity command, \dot{E} . The visual signal that stimulates the optokinetic system is retinal-error velocity (\dot{e}), which is the difference between the velocity of the visual world, W , and slow-phase eye velocity in space or gaze velocity, \dot{G} . (The velocity of the visual world is zero, except under the artificial circumstances of sitting within a rotating optokinetic drum.) In rat, rabbit, and cat, the \dot{e} signal is relayed to the nucleus of the optic tract in the pretectum.¹⁶⁻¹⁸ The main thesis of the optokinetic model is that the visual system deduces head velocity independently of the semicircular canals since, as shown by the inset waveform, the canal signal, H_c , reflects only the transient or high-frequency component of head velocity. To do this, \dot{e} is added to \dot{E} —an internal corollary discharge or efference copy of eye velocity^{19,20}—to obtain W_h , the velocity of the environment with respect to the head (the gain, k , of this pathway is close to 1.0). Since the visual world never moves in nature, $-W_h$ must equal the head velocity in space according to the visual system, \dot{H}_v . To avoid duplicating the transient signal already supplied by H_c , the high-frequency components must be filtered out of \dot{H}_v , so that the filter output, \dot{H}_{ok} , supplies only the sustained signal. Consequently, this filter has the same time constant, T_c , as that of the cupula. The sum of \dot{H}_{ok} and H_c then becomes a good re-creation of actual head velocity, \dot{H} , in the vestibular nucleus (VN).

It now appears that in the rat, a major relay station for optokinetic signals between the nucleus of the optic tract and the VN is the nucleus reticularis tegmenti pontis (NRTP).¹⁶ Moreover, the VN projects back to the NRTP to form a positive feedback loop, as shown in FIGURE 4.²¹ By incorporating this positive feedback loop as shown in the model, we account for several observed features of the optokinetic and vestibular responses.²² In particular, the discrepancy between the time constant of the vestibulo-ocular reflex and cupula time constant is explained. Moreover, the model will account for most optokinetic behavior (open and closed loop) including OKAN. The elements described so far, however, do not account for the reversal phase of postrotary nystagmus (nor do they account for the rather weak reversal phase of optokinetic after-nystagmus—OKAAN). To do this, we have added a central adaptation operator ($1/sT$, in FIGURE 4) similar to that proposed by other workers.^{10,11} This would act to repair or balance the activity in the left and right vestibular nuclei (here represented by positive and negative values). Courjon et al. have shown in the cat that the recovery of nystagmus from peripheral vestibular lesions requires a rebalancing of central vestibular structure that is dependent on both visual and

nonvisual "motor" factors.²³ They showed that motor factors alone could compensate for most of the nystagmus. Since PAN occurs in both light and darkness, we have assumed that the motor factors are important here and have represented their action as a perfect integrator in negative feedback. This integrator monitors slow-phase eye velocity, and if this persists unidirectionally for any length of time (e.g., 10–20 seconds), it begins to send a bias signal back to the VN to eliminate the source of the nystagmus. There can be little doubt that such a mechanism exists, but the neural circuits that effect it are not agreed upon. With this addition, the model simulates both postrotary nystagmus and its reversal phase; it also causes OKAAN, the reversal phase of OKAN.⁹

Using the Model to Simulate PAN

Our first assumption, based on the finding of impaired pursuit and optokinetic function in our patients and the fact that neither of these systems could stop PAN, was that the retinal-error-velocity signal could not be used. Deprived of this input, we postulated that our patients were unable to make the parametric adjustment necessary for normal functioning of the vestibular and optokinetic systems. For example, visual inputs have been shown to be necessary in maintaining the gain of the vestibulo-ocular reflex at an optimal value.²⁴ Loss of this input could account for the abnormally high gain of this reflex in our patients. We postulated that the value of k is adjusted similarly and that when the retinal-error signal is not accessible, parametric adjustment no longer is possible and, for unknown reasons, k increases to a value greater than unity. As k increases in our model, the reversal phase of postrotary nystagmus becomes larger until the system becomes unstable and starts to oscillate. In a linear system, the amplitude of such oscillations would grow unrestrained; but in any biological system, they always are constrained by some limit. Consequently, we have included a nonlinearity, $k(\dot{E})$, in the optokinetic feedback path shown by the inset in FIGURE 4. The slope of this function at the origin, k_0 , must increase beyond $1 + (T_c/T_r)$ before the system begins to oscillate.

Intuitively, if k_0 is too large, the positive feedback loop in FIGURE 4 is unstable because any signal in the loop runs around the loop and adds to itself, causing the signal to increase toward saturation. The repair circuit then is stimulated to generate a bias that will cancel the signal in the optokinetic loop. But when eye velocity becomes zero, the signal in the optokinetic loop simply runs away in the opposite direction. This process continues, eye velocity alternately running away and being "repaired," thereby creating the oscillation of PAN. It may be shown, using small-signal analysis of the system, that the period of oscillation is determined approximately by the optokinetic and adaptive time constants (T_c and T_r , see equations in FIGURE 4). If the former is 5 seconds, then the adaptive time constant, T_r , is required to be about 170 seconds for the system to oscillate with a period similar to that of our patients' PAN. The latter value should not be confused with the time constant of adaptation measured by Malcolm and Melvill Jones,¹¹ which probably partly reflects peripheral vestibular adaptation.

It is not difficult to propose a hypothetical circuit that will oscillate, so we sought some way to test this particular model, that is, to ask the model to predict the behavior of a patient when subjected to some sort of experimental manipulation. There are only two natural stimuli that might affect the system: visual and vestibular. And since these patients' responses to visual stimuli were poor, this left vestibular inputs as a possible stimulus. Our first question was whether the

oscillations could be disturbed by vestibular stimulation. It already had been shown that caloric stimuli could affect PAN,⁴ but we needed a more quantitative demonstration. Thus we submitted our patients to sustained (velocity-step) rotations of different magnitudes and found transient changes in amplitude and permanent changes in phase of PAN. Some of these, shown in FIGURE 3, will be used to support our model, whose predictions are shown in FIGURE 5.

To understand how our nonlinear model predicts the effects of vestibular stimuli on PAN, we found it useful to utilize a phase-plane analysis. This employs a graphic representation for the behavior of the system, with cumulative slow-phase eye position (E) plotted on the abscissa and its first derivative, eye velocity (\dot{E}), plotted on the ordinate. Viewed this way, the oscillations of the system appear roughly as an ellipse called a limit cycle (FIGURE 5A). If k_0 satisfies the criterion for instability shown in FIGURE 4, the system's state (the point defined by instantaneous E and \dot{E}) spirals away from the origin and approaches the limit cycle whose amplitude and shape are determined by the nonlinearity $k(\dot{E})$. Note that when eye velocity crosses through zero, cumulative eye position is maximal and the direction of the nystagmus changes. Efforts to modulate or stop the oscillations by applying external signals will only be temporary and the system eventually will reenter its limit cycle. It is predicting the manner in which vestibular perturbations affect the oscillations and their subsequent return to the limit cycle that comprises our main method of testing the hypothesis.

A simple test stimulus for the model is an impulse of \dot{H}_c . This causes an abrupt change in eye velocity but only a slight immediate change in cumulative eye position. Consequently, an impulse moves the point representing the system's state straight up or down on the phase plane by an amount proportional to the intensity of the stimulus. If one thereby drives the system's state to a point inside or outside the limit cycle, it spirals back out or into the limit cycle. Using phase-plane analysis, it is possible to visualize the nature of the disturbance caused by various impulse stimuli delivered at certain points in the cycle (FIGURE 5). An impulse of the canal signal may be approximated by a step change in head velocity, which causes a signal \dot{H}_c that is a decreasing exponential with a time constant T_c , because the canal time constant is much shorter (T_c is approximately 5 seconds) than the period of PAN (230 seconds); consequently, we compared the behavior of the model and the patients to step changes in head velocity. FIGURE 5 shows the model's behavior when such stimuli are applied at three points in the cycle of oscillation. The phase plane representation may be compared with the corresponding calculated time course of eye velocity, also shown there. Vestibular stimuli applied during the time of reversal of the nystagmus will either phase advance (FIGURE 5C and D) or phase lag (FIGURE 5E and F) the oscillations and cause a transient increase in the amplitude. One impulse response (FIGURE 5G and H) is especially interesting. It is timed so as to drive the eye velocity and cumulative position to zero simultaneously; the oscillations will start to grow again until the limit cycle is reached. This is seen in the phase plane as movement away from the origin along an unstable spiral. These simulation results may be compared with the results obtained from our first patient (FIGURE 3).

We did not attempt an exact duplication of the experimental results; we did not model the fact that in patient 1, peak slow-phase eye velocity in darkness was 20°/second to the right but 14°/second to the left. This probably could be done, for example, by making $k(\dot{E})$ an asymmetric function. The model did, however, produce a waveform similar to our patients' PAN, with eye velocity rising in each half cycle faster than it fell. Peak eye velocity could be adjusted exactly by

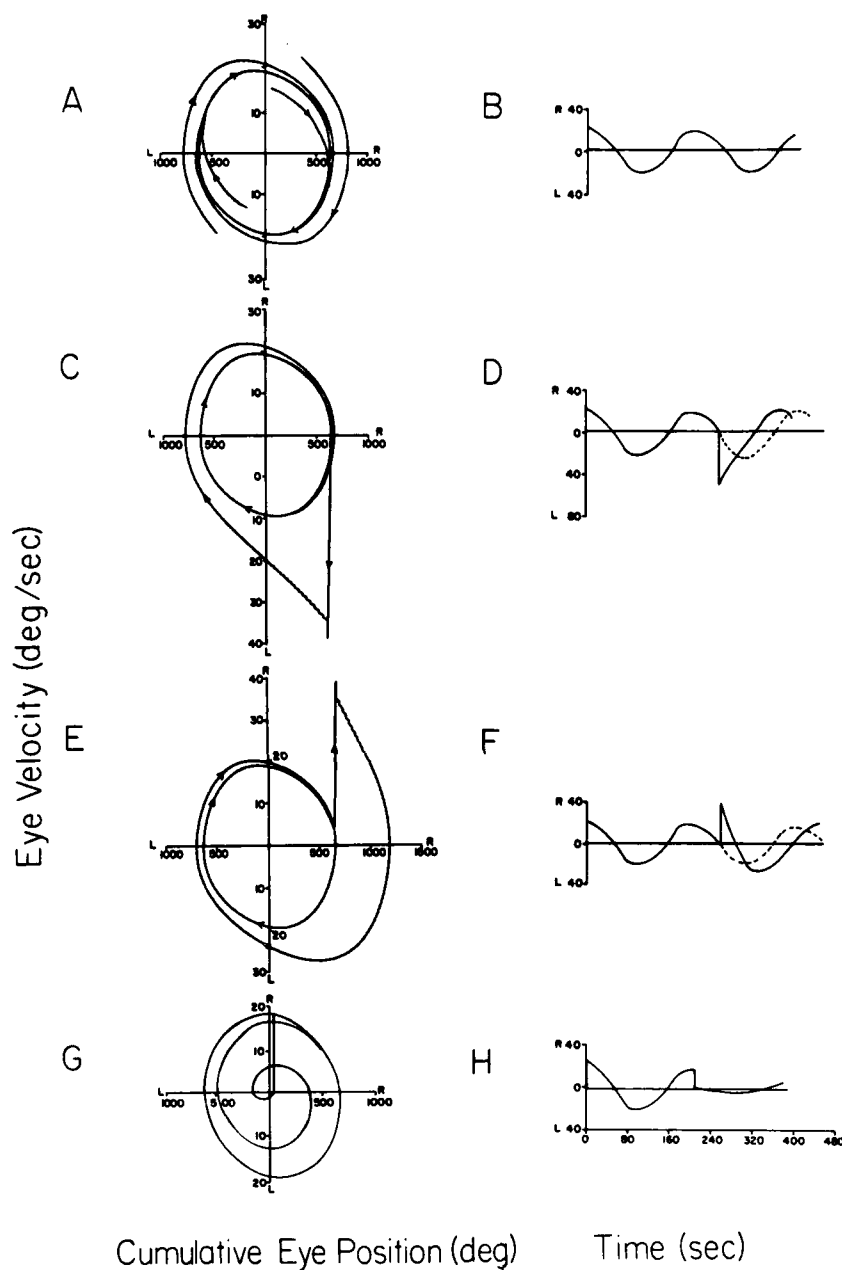


FIGURE 5. Computer simulation of PAN and the effects of rotational stimuli (velocity steps), utilizing the model shown in FIGURE 4. Results are shown as phase planes (A, C, E, and G) and corresponding temporal waveforms (B, D, F, and H); the latter may be compared with the results from patient 1 shown in FIGURES 2 and 3. PAN oscillations are

varying $k(\dot{E})$. The period of oscillation could be changed by varying T_r . We could not simulate exactly the magnitude of the responses produced by steps of head velocity because the intensity of the vestibular impulse is the area under the cupula waveform \dot{H}_c (FIGURE 4), which is $\Delta \dot{H} T_c$, where $\Delta \dot{H}$ is the change in head velocity. All three patients had abnormally small effective values of T_c (about 3 seconds). We could have simulated the step responses quantitatively if we had made T_c small in the model, but this parameter is determined by cupula mechanics and we had no evidence that they had changed. More likely, T_c is made to look small in our patients by some central vestibular mechanism. Apart from this exception, the model did correctly reflect the phase shifts and transient amplitude changes observed when steps of head velocity of various amplitudes and directions were applied at any point in the cycle. Indeed, it allowed us to calculate the vestibular stimulus shown in FIGURE 5G accurately enough to stop the PAN in patient 1 for more than 20 minutes on one occasion (after continuous oscillation for over 5 years). When k_0 is significantly larger than 1.0 (e.g., 1.5), the system is driven close to the limits imposed by the saturation of $k(\dot{E})$. These are called hard oscillations. When velocity steps are applied, the system is disturbed only momentarily and the state quickly comes back to the limit cycle; hence these hard oscillations are difficult to stop, using vestibular stimuli. This was the case for patients 2 and 3.

DISCUSSION

As described elsewhere, our model accounts for a number of normal phenomena encountered during investigation of the vestibular and optokinetic systems: the fact that the 15-second time constant of the vestibulo-ocular reflex is three times that of the cupula, the open- and closed-loop gains of the optokinetic system, and OKAN.²² Other models exist that also explain many of these normal phenomena.²⁵ The model in FIGURE 4 also accounts for repair of spontaneous nystagmus in the dark and reversal phases of postrotary nystagmus and OKAN. Our optokinetic-vestibular model is supported by neurophysiological data; in particular, the notion of a positive feedback "storage" loop has received recent support. As mentioned earlier, Cazin et al. have found evidence to support a pathway from the vestibular nucleus to the nucleus reticularis tegmenti pontis and back again.²¹ The model also satisfactorily describes the features of PAN encountered in our patients while in darkness and the way in which vestibular stimuli affect the oscillations. Of course, the latter findings could be only a coincidence; perhaps there exist other models that would be similarly affected by vestibular stimulation. In any case, our model predicts the PAN responses to velocity steps of various sizes with some accuracy, as was most evident by our success in temporarily stopping the PAN of patient 1.

shown in B. In A, these are represented in a phase plane by the elliptical limit cycle, whose path is determined by nonlinearity $k(\dot{E})$ and the time constants T_c and T_r . Vestibular stimuli will cause the oscillations to be temporarily displaced from the limit cycle, to which they will eventually return. C and D show the effect of a stimulus, applied at the time of reversal of the nystagmus, that causes a phase advance in the cycle. E and F show the effects of a stimulus that causes a phase lag. G and H show the effect of a critically timed stimulus that simultaneously brings cumulative eye position and eye velocity close to zero; the oscillations temporarily cease but then build up again, spiraling out on the phase plane to reach the limit cycle.

This quantitative hypothesis does not, however, attempt to explain the interaction of the pursuit and vestibulo-optokinetic systems either in animals or in our first patient, who was the only one to have clear preservation of some smooth-pursuit function and who was able to halt briefly the nystagmus as it changed direction ("null period"). Our other two patients had no evidence of smooth-pursuit function and showed no "null periods." The problem is that if one simulates the pursuit system as a negative feedback system designed to minimize retinal slip, such a system would stop PAN in the light. (In fact, some patients have PAN only in the dark or after the development of blindness.)^{2,4} There are possible ways around this difficulty, using the corollary discharge scheme of Yasui and Young²⁰ and assuming that this "pursuit" internal positive feedback loop is open in the dark and operates only in the light. With this scheme, we could simulate the fact that patient 1 had some pursuit ability but that her PAN was decreased in amplitude only slightly in the light. Neither does our model give a clear explanation for the short time constant of the vestibulo-ocular reflex, shown by all three patients. The enhanced gain of this reflex, however, is compatible with our hypothesis that there is an inability to use retinal image motion to adjust oculomotor parameters.

Previous attempts to identify the neural lesion responsible for PAN have dwelt on clinicopathological correlation; this has not allowed accurate localization of the site of the disturbance. Both caudal brain-stem and cerebellar abnormalities have been reported.^{5,26-28} PAN also has been accompanied by cerebellar abnormalities resulting from phenytoin intoxication.⁶ Experimental ablation of the flocculus or cerebellum in the primate has not produced PAN, although impaired pursuit, down-beat, gaze-paretic, and rebound nystagmus may occur.^{29,30} The effectiveness of baclofen in treating PAN may suggest the pharmacological nature of the involved neural pathways. Baclofen is a synthetic analogue of γ -aminobutyric acid (gaba). It may exert its inhibitory action by blocking release of excitatory neurotransmitters such as glutamic acid; this effect may be mediated through a gaba receptor.^{31,32} It is known that both cerebellar Purkinje cells and the vestibular commissural system utilize gaba.^{33,34} Consideration of the specific effects of baclofen on the eye movements of our patients gives further evidence of the site of this drug's action. Baclofen completely abolished PAN in both patients 1 and 3 in light and darkness. However smooth-pursuit ability remained absent in patient 3 and appeared worse in patient 1 after treatment with baclofen, indicating that PAN and pursuit deficits did not have a single, common cause. In terms of our model, baclofen seems to have acted upon gain k (lowering it) without improving pursuit or optokinetic performance. This raises the issue, What is the "anatomic" localization of gain k ? FIGURE 4 shows k in the feedback path from the VN to the NRTP, but the model would behave in the same way if k were located in the forward path from the NRTP to the VN, a pathway that involves the commissural system between the two VN. While both pathways primarily are in the pons, the NRTP also projects to the flocculus,³⁵ which in turn projects to the VN, so that the cerebellum also may be involved in determining the value of k . At present the notion of a VN-NRTP-VN pathway depends on studies in the rat. It is possible that species differences exist for the optokinetic-vestibular pathway and that nuclei other than the NRTP are involved in humans; for example, there are reciprocal connections between the VN and perihypoglossal nuclei.³⁶

Another issue is how the normal value of k is maintained: Is this an example of visually mediated parametric control? Both visual inputs and an intact

cerebellum are required for parametric modulation of the vestibulo-ocular reflex.^{37,38} PAN occasionally has been associated with blindness, even when evidence of other neurological dysfunction was lacking.⁴ The eye movements of the blind show other features that suggest disturbed control of parameters of a variety of oculomotor functions; these abnormalities are similar to those resulting from cerebellectomy.³⁹ This evidence suggests that normal visual inputs and normal cerebellar function may be necessary to maintain parameter k at its correct level.

The clinical significance of the successful treatment of PAN with baclofen is discussed elsewhere.⁴⁰ It has raised the possibility of pharmacological treatment of other central disturbances of oculomotor control. Our present study might suggest that use of quantitative hypotheses, based on physiological data, will give insight into the mechanism of action of other drugs given to treat abnormalities of ocular motility.

CONCLUSION

Eye-movement recordings of three patients with periodic alternating nystagmus were analyzed quantitatively. Important findings were as follows:

1. Period length was approximately four minutes and was constant for each patient in light and darkness.
2. Smooth-pursuit function was impaired severely in one patient and absent in the other two. There was no evidence of optokinetic responses in any patient, judged by optokinetic after-nystagmus (OKAN).
3. Rotational vestibular stimuli produced a transient change in PAN amplitude and a permanent change in PAN phase.
4. The gain of the vestibulo-ocular reflex (VOR) was one or greater; the time constant of the VOR was short, typically three seconds.

We used current physiological data to formulate a model that accounted for most normal vestibular and optokinetic functions, including the reversal phase of postrotary nystagmus. Using data from our patients, we made two changes in our model: we denied access of visual signals to the optokinetic-vestibular system and increased the gain of an internal positive optokinetic feedback loop. This caused the system to oscillate with characteristics similar to PAN. We then showed that the model's response to rotational vestibular stimuli was similar to those obtained when we applied such stimuli to our patients, namely, a shift in the phase and a transient change in the amplitude of the oscillations. We used the model to predict successfully a critical vestibular stimulus that would temporarily stop PAN. We treated two of our patients with the drug baclofen, which did not improve smooth pursuit but stopped PAN. Therefore we hypothesized that baclofen decreased the gain of the internal positive feedback loop, a circuit for which there is some anatomic and physiological evidence.

ACKNOWLEDGMENTS

We thank Ms. Vendetta Matthews and Ms. Andrea McCracken for editorial help, Ms. Corena Bridges for technical assistance, and Dr. Thomas Preziosi for referring patient 3.

REFERENCES

1. ROBB, R. M. 1972. Periodic alternation of null point in congenital nystagmus. *Arch. Ophthalmol.* **87**: 169-173.
2. BALOH, R. W., V. HONRUBIA & H. R. KONRAD. 1976. Periodic alternating nystagmus. *Brain* **99**: 11-26.
3. OOSTERVELD, W. J. & W. J. A. C. RADEMAKERS. 1979. Nystagmus alternans. *Acta Otolaryngol.* **87**: 404-409.
4. DAVIS, D. G. & J. L. SMITH. 1971. Periodic alternating nystagmus. A report of eight cases. *Am. J. Ophthalmol.* **72**: 757-762.
5. KEANE, J. R. 1974. Periodic alternating nystagmus with downward beating nystagmus. A clinico-anatomical case study of multiple sclerosis. *Arch. Neurol.* **30**: 399-402.
6. CAMPBELL, W. W., JR. 1980. Periodic alternating nystagmus in phenytoin intoxication. *Arch. Neurol.* **37**: 178-179.
7. RUDGE, P. & J. LEECH. 1976. Analysis of a case of periodic alternating nystagmus. *J. Neurol. Neurosurg. Psychiatry* **39**: 314-319.
8. KORNHUBER, H. H. 1959. Der periodisch alternierende Nystagmus (Nystagmus alternans) und die Enthemmung des vestibulären Systems. *Arch. Ohren Nasen Kehlkopfheilkd.* **174**: 182-209.
9. ZEE, D. S., R. D. YEE & D. A. ROBINSON. 1976. Optokinetic responses in labyrinthine defective human beings. *Brain Res.* **113**: 423-428.
10. YOUNG, L. R. & C. M. OMAN. 1969. Model for vestibular adaptation to horizontal rotation. *Aerosp. Med.* **40**: 1076-1080.
11. MALCOLM, R. & G. MELVILL JONES. 1970. A quantitative study of vestibular adaptation in humans. *Acta Otolaryngol.* **70**: 126-135.
12. WALLACE, M., S. M. BLAIR & G. WESTHEIMER. 1978. Neural pathways common to vestibular and optokinetic eye movements. *Exp. Brain Res.* **33**: 19-25.
13. KOENIG, E., J. H. J. ALLUM & J. DICHGANS. 1978. Visual-vestibular interaction upon nystagmus slow phase velocity in man. *Acta Otolaryngol.* **85**: 397-410.
14. WAESPE, W. & V. HENN. 1977. Neuronal activity in the vestibular nuclei of the alert monkey during vestibular and optokinetic stimulation. *Exp. Brain Res.* **27**: 523-538.
15. ROBINSON, D. A. 1977. Linear addition of optokinetic and vestibular signals in the vestibular nucleus. *Exp. Brain Res.* **30**: 447-450.
16. CAZIN, L., W. PRECHT & J. LANNOU. 1980. Pathways mediating optokinetic responses of vestibular nucleus neurons in the rat. *Pfluegers Arch.* **384**: 19-29.
17. COLLEWIJN, H. 1975. Direction-selective units in the rabbit's nucleus of the optic tract. *Brain Res.* **100**: 489-508.
18. PRECHT, W. & P. STRATA. 1979. Pathways mediating optokinetic responses of cat's vestibular neurons. *Neurosci. Lett. Suppl.* **3**: 351.
19. YOUNG, L. R. 1971. Pursuit eye tracking movements. In *Control of Eye Movements*. P. Bach-y-Rita & C. C. Collins, Eds.: 429-444. Academic Press, Inc. New York, N.Y.
20. YASUI, S. & L. R. YOUNG. 1975. Perceived visual motion as effective stimulus to pursuit eye movement system. *Science* **190**: 906-908.
21. CAZIN, L., W. PRECHT & J. LANNOU. 1980. Firing characteristics of neurons mediating optokinetic responses to rat's vestibular neurons. *Pfluegers Arch.* **386**: 221-230.
22. ROBINSON, D. A. 1977. Vestibular and optokinetic symbiosis: an example of explaining by modeling. *Dev. Neurosci.* **1**: 49-58.
23. COURJON, J. H., M. JEANNEROD, I. OSSUZZIO & R. SCHMID. 1977. The role of vision in compensation of vestibulo-ocular reflex after hemilabyrinthectomy in the cat. *Exp. Brain Res.* **28**: 235-248.
24. GONSHOR, A. & G. MELVILL JONES. 1976. Short term adaptive changes in the human vestibulo-ocular reflex arc. *J. Physiol. London* **258**: 361-379.
25. RAPHAN, T., V. MATSUO & B. COHEN. 1979. Velocity storage in the vestibulo-ocular reflex arc (VOR). *Exp. Brain Res.* **35**: 229-248.
26. TOWLE, P. A. & F. ROMANUL. 1970. Periodic alternating nystagmus: first pathological studied case. (abst.). *Neurology* **20**: 408.

27. SUSAC, J. O. & J. M. HENRY. 1973. Periodic alternating nystagmus: clinico-pathological correlation. In *Neuro-Ophthalmology*. J. S. Glasser & J. L. Smith, Eds. 8: 284-292. C. V. Mosby Co. St. Louis, Mo.
28. GORMAN, W. F. & S. BROCK. 1950. Periodic alternating nystagmus in Friedreich's ataxia. *Am. J. Ophthalmol.* 33: 860-864.
29. ZEE, D. S., A. YAMAZAKI & G. GUCER. 1978. Ocular motor abnormalities in trained monkeys with floccular lesions. *Soc. Neurosci. Abstr.* 4: 168.
30. WESTHEIMER, G. & S. BLAIR. 1973. Oculomotor deficits in cerebellectomized monkeys. *Invest. Ophthalmol.* 12: 618-621.
31. POTASHNER, S. J. 1979. Baclofen: effects of amino-acid release and metabolism in slices of guinea pig cortex. *J. Neurochem.* 32: 103-109.
32. BOWERY, N. G., D. R. HILL, A. L. HUDSON, A. DOBLE, D. N. MIDDLEMISS, J. SHAW & M. TURNBULL. 1980. (-) Baclofen decreases neurotransmitter release in the mammalian CNS by an action at a novel GABA receptor. *Nature* 283: 92-94.
33. SHEPHERD, G. M. 1979. *The Synaptic Organisation of the Brain*. 2nd edit. Oxford University Press. Oxford, England.
34. PRECHT, W., P. C. SCHWINDT & R. BAKER. 1973. Removal of vestibular commissural inhibition by antagonists of GABA and glycine. *Brain Res.* 62: 222-226.
35. BLANKS, R. H. & J. C. BLANKS. 1980. Afferents to the cerebellar flocculus in cat conveying visual input. *Invest. Ophthalmol. Vision Sci.* 19(Suppl. 58).
36. MCCRAE, R. A., R. BAKER & J. DELGADO-CARCIA. 1979. Afferent and efferent organization of the prepositus hypoglossi nucleus. *Prog. Brain Res.* 50: 653-665.
37. MILES, F. A. & B. B. EIGHMY. 1980. Long-term adaptive changes in primate vestibulo-ocular reflex. I. Behavioral observations. *J. Neurophysiol.* 43: 1406-1425.
38. ROBINSON, D. A. 1976. Adaptive gain control of vestibuloocular reflex by the cerebellum. *J. Neurophysiol.* 39: 954-969.
39. LEIGH, R. J. & D. S. ZEE. 1980. Eye movements of the blind. *Invest. Ophthalmol. Vision Sci.* 19: 328-331.
40. HALMAGYI, G. M., P. RUDGE, M. A. GRESTY, R. J. LEIGH & D. S. ZEE. 1980. Treatment of periodic alternating nystagmus. *Ann. Neurol.* (In press.)

POSTURAL IMBALANCE WITH HEAD EXTENSION:
IMPROVEMENT BY TRAINING AS A MODEL
FOR ATAXIA THERAPY*

Th. Brandt, S. Krafczyk, and I. Malsbenden

*Clinical Neurophysiology
Neurological Clinic
Alfried Krupp Hospital
4300 Essen, Federal Republic of Germany*

INTRODUCTION

Head-extension vertigo is not always due to vertebrobasilar insufficiency but sometimes, depending on stimulus conditions, represents a physiological instability of postural balance.¹ An explanation will be presented for physiological ataxia dependent on head position, which is based upon the unadapted combination of multisensory inputs from the stabilizing systems.

Basilar Insufficiency

Vertigo and postural imbalance induced with the head maximally extended while standing and terminated abruptly by returning the head to a neutral upright position are frequently reported experiences. Clinicians usually attribute these symptoms to intermittent basilar insufficiency caused by a functional compression of the vertebral artery, particularly in elderly patients with atheromas or with cervical spondylosis and osteophytes narrowing the transverse foramina.²⁻⁴ Transient attacks of vertigo of central origin are the commonest early symptom of basilar insufficiency because of the steep pressure gradient from the aorta to the terminal pontine arteries, which are long, tenuous, circumferential arteries and therefore provide a most vulnerable blood supply for the vestibular nuclei.³ Also, experimental studies on blood flow in cadavers reveal that extreme head positions may reduce flow through one or another of the vertebral or carotid vessels.⁵ Thus, there is no doubt that vestibular vertigo and ataxia and drop attacks can be precipitated by extreme extension or rotation of the neck, at least when a partial obstruction of the arteries combines with a sudden fall of systemic blood pressure, e.g., in a patient rising from a chair and looking up. An association of dysfunctions that convinces the clinician in his diagnosis is that of vertigo with visual disturbances or diplopia or motor symptoms.

Physiological Head-Extension Vertigo

Apart from the basilar insufficiency, however, symptoms of a to-and-fro vertigo and postural imbalance occur frequently in young and healthy people, e.g., elicited by overhead work while standing on an unstable, wobbling ladder or in situations in which visual cues are conflicting with proprioceptive input

*This research was supported by Deutsche Forschungsgemeinschaft Br 639/3 "Bewegungskrankheit."

(looking up at moving clouds). Such a "normal" instability related to head position can be demonstrated easily by attempting to balance on one foot with the eyes closed and head extended as compared with the normal head position.

Posturographic measurements reveal a significant increase in body-sway amplitudes induced by head extension alone, particularly when the "stabilizing" input of the nonvestibular sensory systems is reduced or eliminated, such as with eye closure and standing on foam rubber. The differential effects of visual conditions upon head-extension body sway provide the validation of our hypothesis that this imbalance is separate and distinct from transient ischemia of the pontomedullary brain stem.

Basically, the following alterations in the reafferent sensory consequences of self-generated body sway may be responsible for the impairment of postural control in the offending (inducing) head position:

1. The utricle otoliths that transduce shear forces are beyond their optimal working range when the plane of the utricular macula (approximately parallel to the horizontal semicircular canal) is elevated relative to its normal horizontal orientation ($\sim 20^\circ$ flexion). With the head maximally extended, the saccular maculae (approximately parallel to the ipsilateral anterior semicircular canal) are rotated predominantly, which causes a rotation of shear forces respectively. The particular saccular contribution to postural control, however, is not known and may be less adapted just as is the case for the semicircular canals.

2. Visual cues that correct posture change their direction in egocentric spatial coordinates. For example, vertical retinal slip of a stationary target viewed with the head elevated indicates fore-aft body sway. Consequently, the compensatory postural adjustments due to otoliths as well as visual signals must be corrected to reflect the change in coordinates.

Posturographic experiments were performed in order to clarify whether physiological head-extension vertigo is a vestibular and/or a visual vertigo. As a second step, healthy subjects were trained in balancing with head extension. This was done in order to determine if imbalance is due to a constant deficiency in the multiloop control of posture or to a lack of practice and lack of sensorimotor calibration. Analysis of the time course of training effects will be discussed mainly in the context of clinical ataxia therapy.

METHODS

Subjects

A total of 13 male and 18 female subjects ranging between 17 and 39 years of age (mean, 26) were employed in three series of experiments and were paid for their participation. All possessed normal sensorimotor function.

Apparatus, Posturography, and Data Analysis

The fore-aft and lateral body sway at free stance were measured separately and simultaneously by use of a stabilometer platform.⁶ This apparatus transduces force moments exerted on foot support (torque about the ankles and reaction forces at the feet), which means that it does not measure simply the "static" net

displacement of the body's center of gravity but also dynamic components due to body inertia. The latter apparently enhance sway amplitudes predominantly at higher frequencies, as Gurfinkel reports that the dynamic component accounts for less than 10% of the force obtained at 0.2 Hz but 50% at 0.5 Hz.⁷

Stabilograms were both stored on FM magnetic tape for further computer analysis and displayed on a strip-chart recorder. Fourier power spectral density and the root-mean-square [$y_i = [n^{-1} \sum_{i=1}^n x_i^2]^{1/2}$] were selected as criteria for evaluation of postural stability. Although Fourier analysis is very common nowadays, it requires stationarity of the stabilogram, which is unlikely to be achieved during a 30-second registration period. If there is no stationarity, then this method is inappropriate because it may introduce frequency components not present in the original recording. The root-mean-square (RMS) represents a suitable measure for average body sway during a certain period and allows for an easy comparison between the effects of different experimental conditions.^{8,9}

A digital computer (Intertechnique IN 110) was used for analysis of 30-second segments of sway measurements (high-pass filter: 0.09 Hz, 60 dB/decade; sample interval: 50 mseconds).

Directional Doppler ultrasonography (Velocimetre D 800 Delalande) having a 4-MHz continuous-wave signal was used to determine possible changes in blood flow of the supratrochlear, carotid, and vertebral arteries when the subjects extended their heads maximally.

Experimental Procedure

Subjects were placed on the force-measuring platform and were tested for body sway with free stance under different conditions of head position with the eyes either open or closed. They were instructed to maintain optimal balance with a fixed, preset foot position. A slab of foam rubber (height, 10 cm; specific weight, 40 g/dm³) was placed on top of the stabilometer platform and covered by a second, rigid foot support. This was to reduce the somatosensory contribution (ankle-joint receptors) to postural control and therefore to enhance disproportionately the sensorial weights of the vestibular and visual systems that were under investigation. The head-extension angles (retroflexion, face up) were measured by means of an inclinometer (mean, 54°).

Experiment 1. Effects of 1 hour of postural balance training under four conditions: eyes open or eyes closed with either head normal upright or maximally extended ($n = 11$). The sequence of conditions was: eyes open, head normal (30 seconds); eyes open, head extension (30 seconds); eyes closed, head normal (30 seconds); eyes closed, head extension (30 seconds). The 2-minute period of balancing was followed by a 2-minute resting phase such that during 1 hour, the total time with head extension was 15 minutes (7.5 minutes, eyes open and 7.5 minutes, eyes closed).

Experiment 2. Effects of 5 days of postural balance training (1 hour per day) with the head either normal and facing straight or toward the right (eyes closed) or with head extension with the eyes either open or closed ($n = 20$). The training again consisted of 2-minute periods and pauses, summing within 1 hour to a total time of 8 minutes of head extension with eyes open, 8 minutes of head extension with eyes closed, and 8 minutes of the head turned toward the right with the eyes closed. The training was interrupted by three measuring phases (duration, 3.5 minutes): at the beginning, after 30 minutes, and the final control after 60 minutes.

Experiment 3. The duration of the effect of postural stabilization of a training

period of 5 days (1 hour per day) with head extension (procedure as in experiment 2) was assessed with weekly measurements of postural sway up to 40 days after termination of training ($n = 10$).

RESULTS AND COMMENT

Blood Flow

In none of the subjects did extension of the head by itself cause any clinical signs that could have been attributed to transient ischemia of the brain stem or cerebellum. Also, cerebral blood flow as measured by directional Doppler

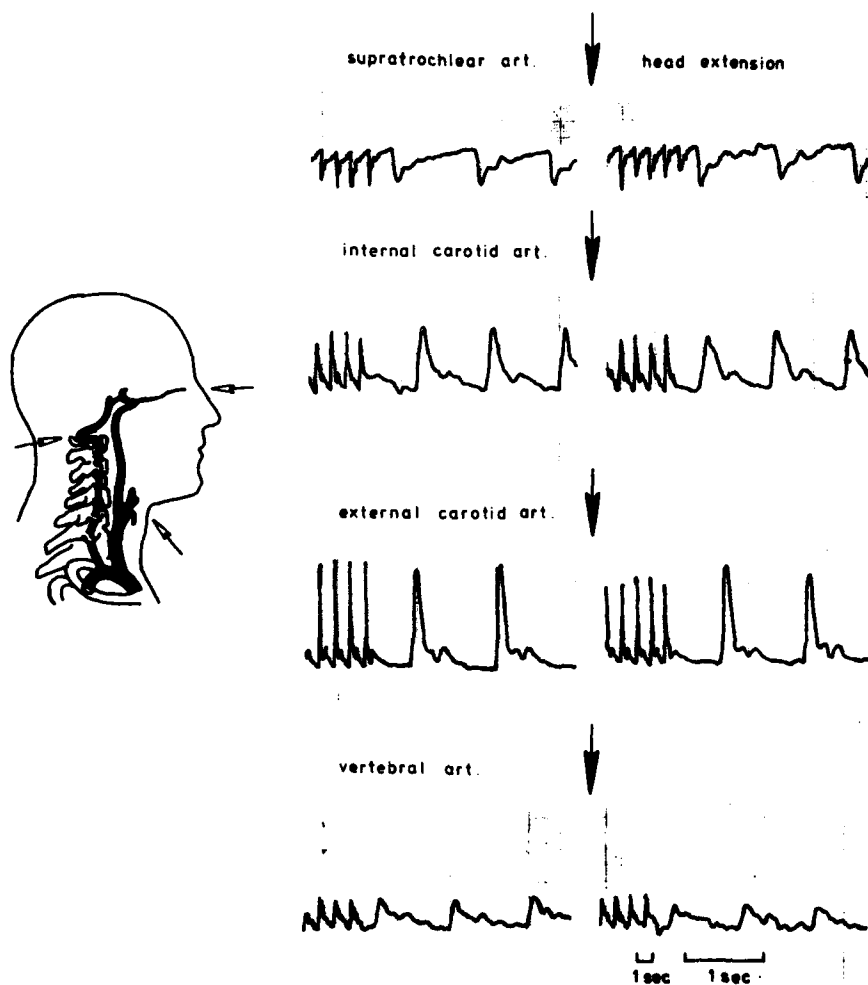


FIGURE 1. Cerebral blood flow as measured by directional Doppler ultrasonography remains unaffected by a change in head position from normal upright to head extension.

ultrasonography remained unaffected by the challenging head position for the supratrochlear as well as for the carotid and vertebral arteries (FIGURE 1).

Posture

When standing on a firm foot support with the eyes and/or the somatosensors widely compensating for the "vestibular deficiency," postural imbalance induced by head extension was comparatively weak or absent (FIGURE 2, top). Postural balance with head extension was impaired significantly, however, with the eyes closed while standing on a slab of foam rubber, which reduces the reliability of the joint receptors (FIGURE 2, middle). The larger amount of forward-backward sway as compared to lateral sway seems to be unspecific since it reflects mechanical joint characteristics and is prominent in most experimental and clinical ataxias. In some subjects the first trial led to an irresistible fall, but most often this was avoided by increased sway amplitudes, particularly in the low-frequency (1-Hz) range which seems to activate postural adjustments. Patients with sensory polyneuropathy who lack accurate positional sense in the legs exhibit an instability with head extension similar to normals standing on foam rubber (FIGURE 2, bottom). With the eyes open there was no significant increase in sway amplitudes, which is indicative of the redundant, multiloop control of posture, with overlapping functional ranges of the stabilizing systems enabling them to compensate partially for each other's deficiencies.

One hour of intermittent practice (total time of head extension, 15 minutes) caused a remarkable improvement of balance. The mean reduction in sway amplitudes for all subjects was 20-30% of the 100% RMS value at the first trial (FIGURES 3 and 4) and represents an exponential short-term training effect. The lower slope of the exponential function for the comparable training effect with normal head position [$y = 63.25 \times e^{-0.0061t}$ versus $y = 97.57 \times e^{-0.0077t}$] may allow the conclusion that head extension ataxia and improvement by training in part are due to vestibulospinal rather than purely somatosensory mechanisms. Determination of the Fourier power spectra reveal that destabilization of postural balance is the most pronounced in the low-frequency body sway (1 Hz) and that training improves sway activity over the whole frequency range below 1 Hz. Within the multiloop control of postural stabilization, each of the visual, vestibular, and somatosensory loops seems to have its own frequency range of optimal function with some overlap between the ranges. A predominant fore-aft body sway around 1 Hz has been described as a typical vestibular oscillation due to the long latency and high threshold of vestibulospinal reflexes, which fits the results by Nashner who determined the latencies for a vestibularly induced discharge in the gastrocnemius muscle to be 200-300 mseconds.^{10,11} In our experiments, however, there was no sharply delineated peak at 1 Hz although postural control was based mainly upon sensory input originating from the vestibular system.

FIGURES 5-7 show that a "short-term daily training effect" and a "long-term training effect" together form a characteristic sawtoothlike curve of sway activity, which within five days reaches an asymptote at 40-50% of the initial sway activity. Again, the exponential functions of percent reduction in mean RMS values of the fore-aft and lateral sway have the greatest slope for the head-extension condition as compared to head normal upright. Since the absolute sway activity is not greater for the head turned toward the right than with the head facing straight ahead, one can conclude that the change in orientation of shear-force vectors on the utricular macula has no significant influence on postural control.

For all head conditions with the eyes open, there was only a slight, short-term

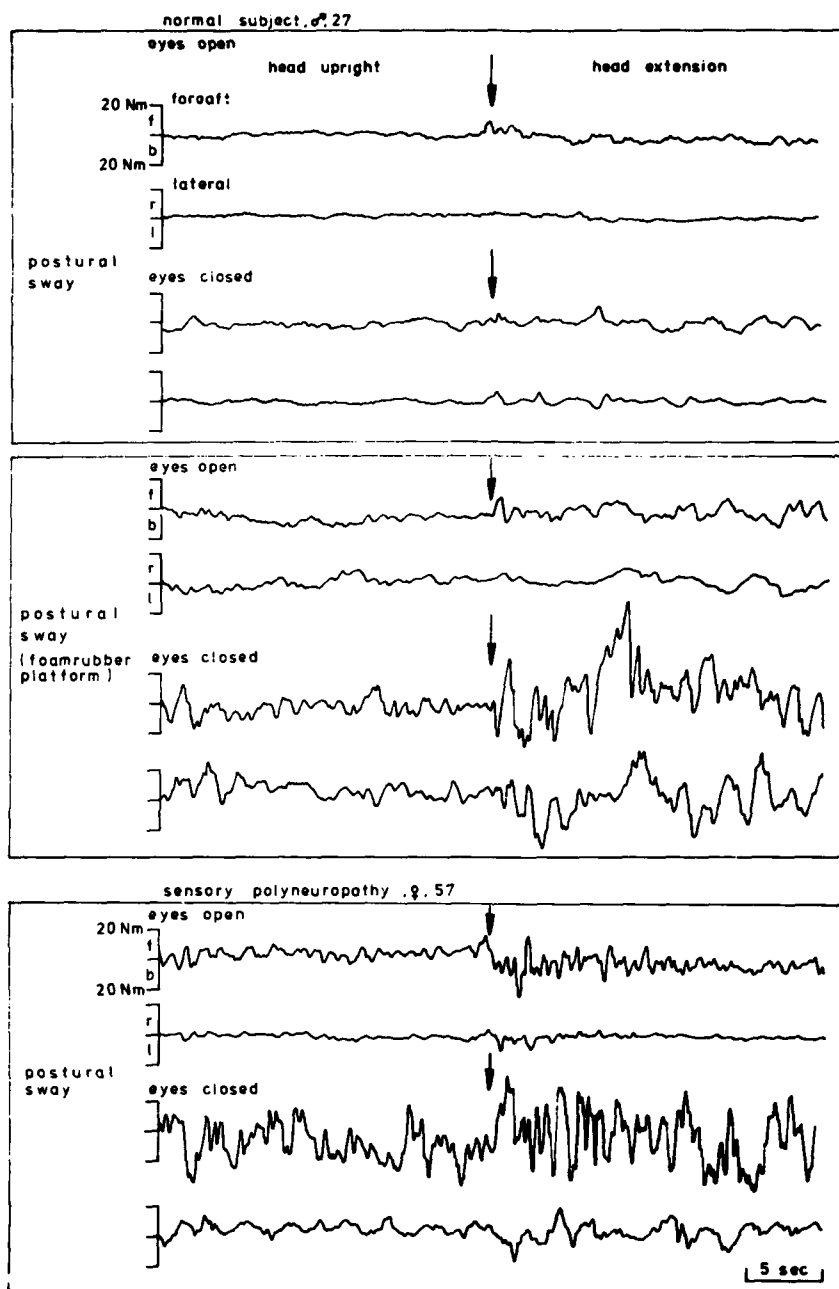


FIGURE 2. Differential effects of head extension and normal head position upon forward-backward and lateral body sway (original recordings) with the eyes open or closed. Normal subjects standing on a firm stabilometer platform (top); normal subjects standing on a slice of foam rubber (middle); and patients with sensory polyneuropathy standing on a firm platform (bottom). Postural imbalance is the most pronounced and similar for the normal standing on foam rubber and the patient during head extension with the eyes closed.

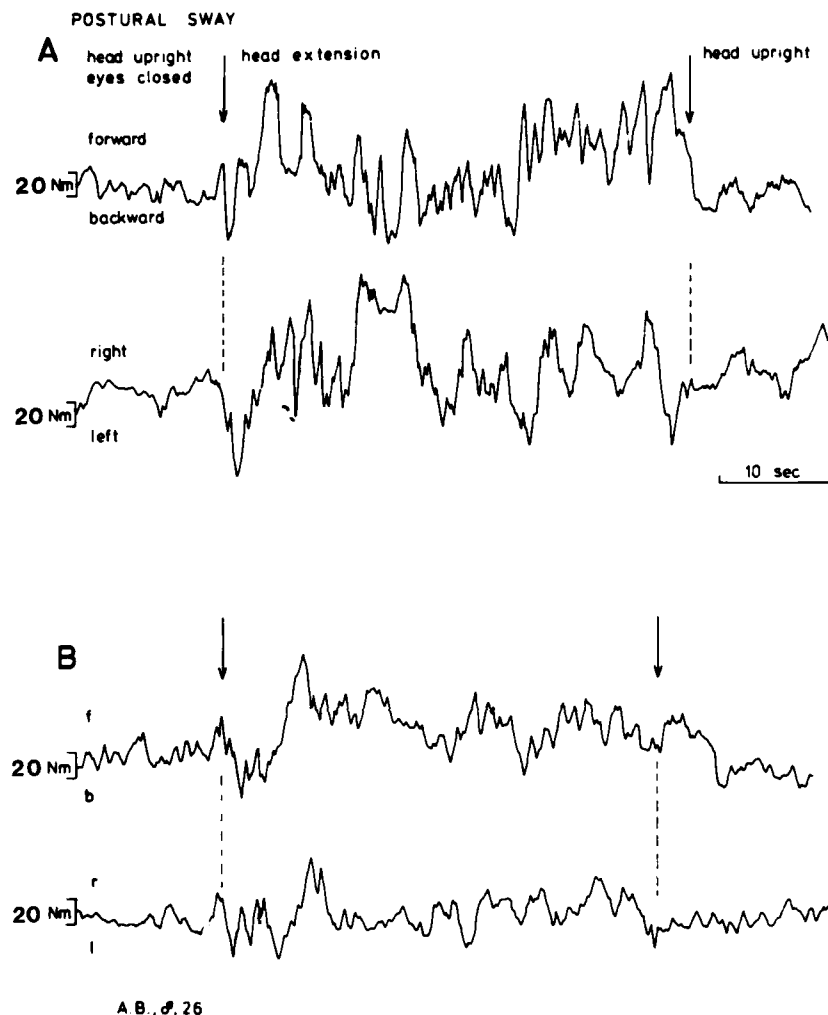


FIGURE 3. Forward-backward and lateral body sway of a normal subject (original recordings) with eyes closed and head extension at the beginning (A) and after one hour of intermittent practice (B) with the offending head position. The short-term training effect is evident for both the fore-aft and the lateral sway.

daily training effect (FIGURES 4-7) but no long-term improvement of balance. This is suggestive of a sufficient visual compensation for the proprioceptive deficiency that makes recalibration of "visuospinal" reflexes by training unnecessary. Vision covers a large frequency range; it not only stabilizes posture in the low-frequency range below 1 Hz but also (with a latency below 150 mseconds) contributes to rapid motor adjustments during postural perturbations or during active movements and concurrent vestibular excitation.¹²⁻¹⁵

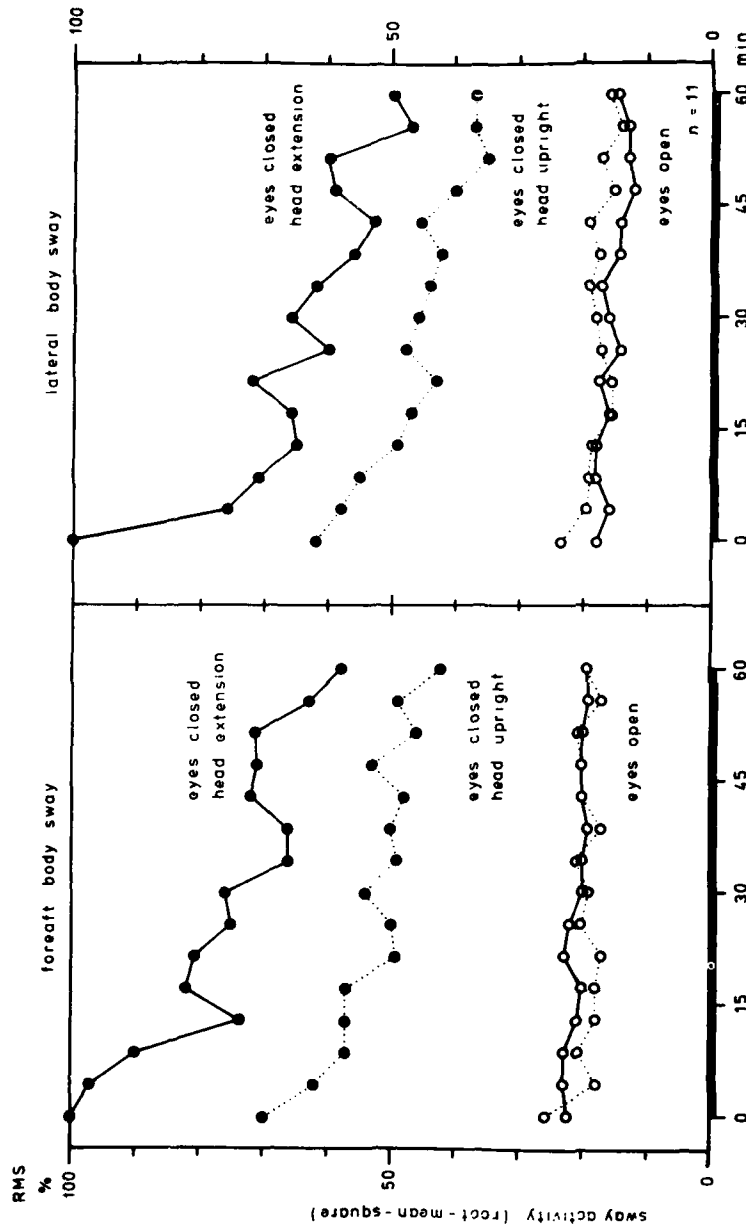


FIGURE 4. Postural balance (effects of training). Percent reduction in mean root-mean-square (RMS) values of fore-aft and lateral body sway for 11 subjects during one hour of postural balance training on foam rubber: head elevation, solid lines; head normal upright, dotted lines. The "exponential" short-term training effect is evident for both head positions with the eyes closed. The greater slope of the function for head elevation (-0.0077 vs. -0.0061), however, allows the conclusion that otolithic mechanisms are involved, rather than purely somatosensory ones. With the eyes open, there is no significant difference for different head positions. This is suggestive of a visual compensation for a proprioceptive deficiency, which makes recalibration or improvement by training unnecessary.

With respect to the hypothesis given in the introduction, our experimental data clearly indicate that there is a physiological postural instability elicited by maximal head extension that is separate and distinct from basilar insufficiency and that may be responsible for the frequent report of vertigo due to unusual head positions. This instability is of particular concern and even may cause an unavoidable fall when the sensory input from other control loops, such as vision and somatosensory joint receptors, largely is eliminated and therefore cannot compensate for the vestibular deficiency. Thus, patients with sensory polyneuropathy have a particularly high risk of succumbing to head-extension vertigo because of the lack of positional sense in the joints.

The experimental posturographic data fit the assumption that postural destabilization mainly is due to reduced accurate head- and body-sway information from the otoliths. Head extension brings the utricular otoliths out of their optimal working range, and obviously the input originating from the saccular otoliths as well as from the semicircular canals is not sufficient to make up for this deficit. On the other hand, the data cannot exclude a major role of somatosensory mechanisms. Visual control of posture seems to be unaffected by a change in coordinates (relative to postural sway) of the retinal slip of stationary targets viewed with head extension as compared to head normal.

Simple training of postural balance on foam rubber improves body-sway activity and therefore postural stability within five days by 30-50%. The time constants of both the development of a long-term training effect and its duration after termination of training (FIGURE 8) must be of particular interest for sports physiologists and clinicians. The rapid improvement is striking in spite of the relatively short training phases, as is the long duration (weeks) of the newly acquired recalibration of sensorimotor control loops. A lack of sensorimotor exercise causes a decrement in balance performance, best known as a transient ataxia after bed rest.^{16,17} This balance impairment, which is improved rapidly within one to three recovery days, is independent of muscle strength because it cannot be avoided by isotonic or isometric exercise in bed.¹⁷ The different effects of our balance training on postural sway with eyes open and eyes closed clearly show that the process of sensorimotor rearrangement and the improvement of balancing are related to the degree of the initial instability. The greater the initial risk of falling, the greater the percent reduction in sway amplitudes by training. Consequently, this should stimulate the clinician to make it a strategy in ataxia therapy to expose the patient increasingly to instable body positions in order to facilitate rearrangement and recruitment of control capacities. Stance and gait aids will alleviate only transiently patients' balance problems, but when used continuously, they will worsen the symptoms because the multiloop control rapidly adapts to the additional feedback and support that they provide.

SUMMARY

Head extension may cause a physiological vertigo and postural imbalance separate and distinct from basilar insufficiency. This physiological imbalance mainly is due to a vestibular sensory deficiency when the utricular otoliths are beyond their working range because of the change in head position. Since the intact visual and somatosensory control loops widely compensate for the vestibular

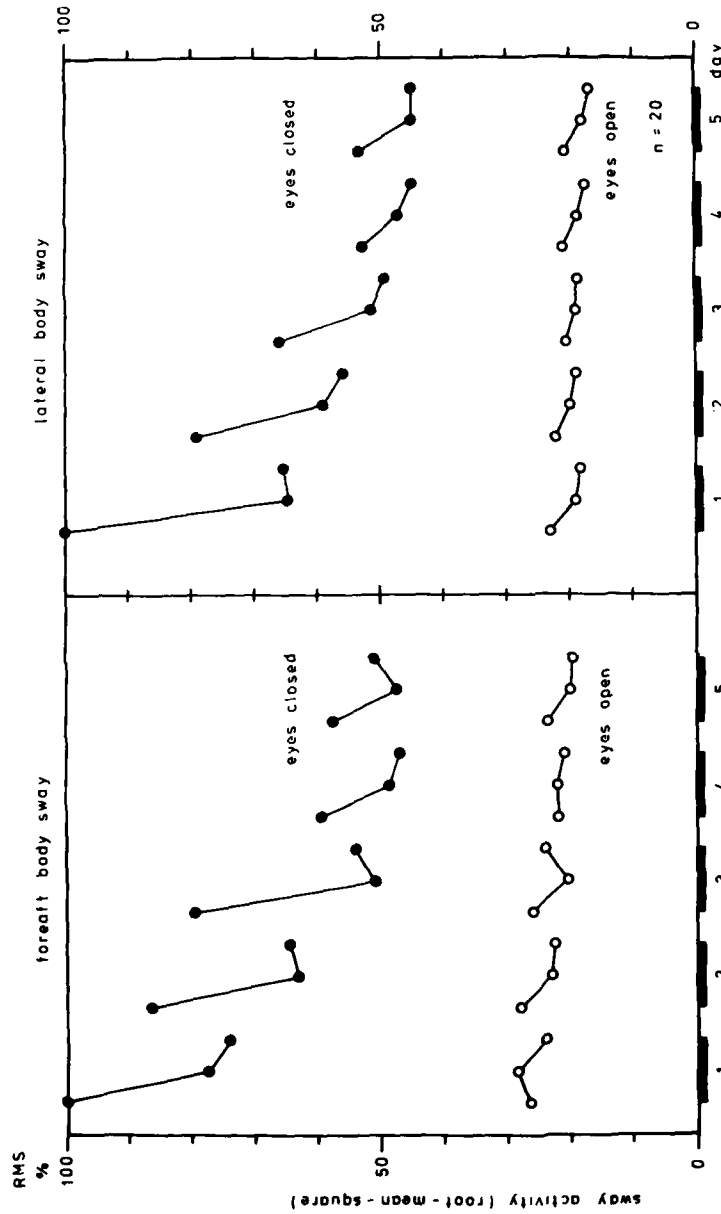


FIGURE 5. Postural balance with head extension (effects of training). Percent reduction in mean RMS values of forward-backward and lateral body sway for 20 subjects during the course of a training period of five days (one hour per day; total time of head elevation with the eyes open, eight minutes; eyes closed, eight minutes). A "short-term daily training effect" (represented by the three measures during one hour) and a "long-term training effect" form a characteristic sawtoothlike curve of sway activity, which reaches an asymptote at 40-50% of the initial sway activity.

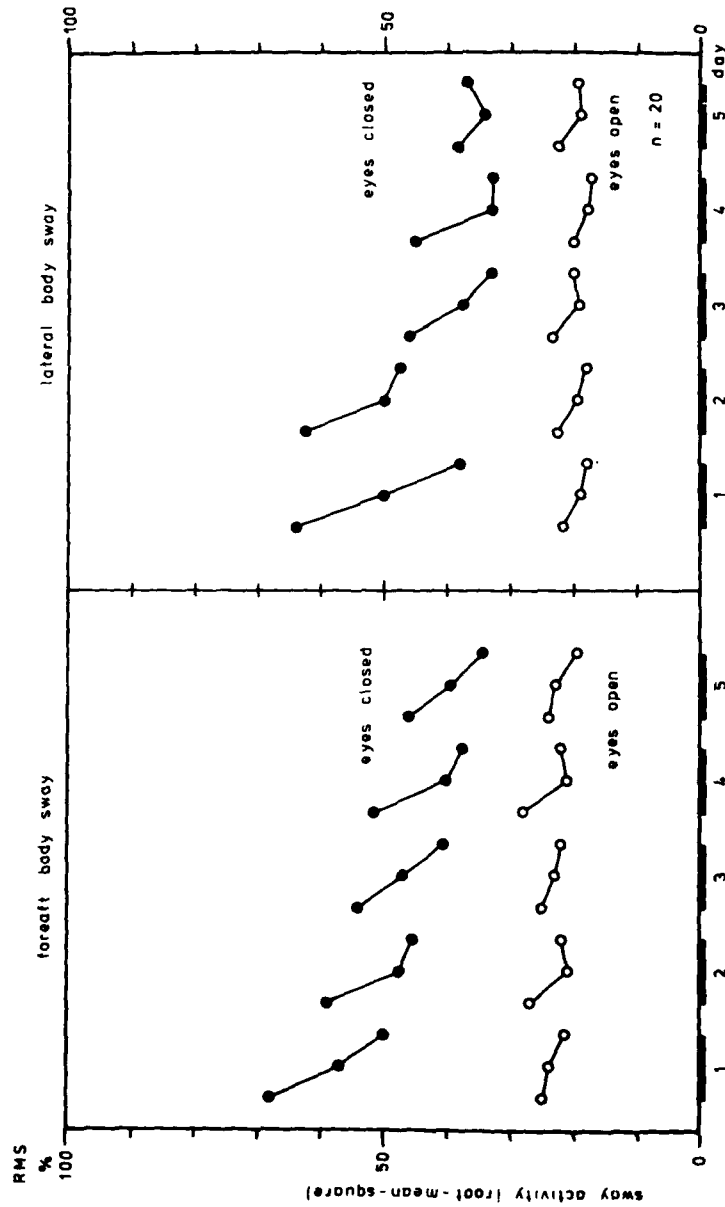


FIGURE 6. Postural balance with head upright (effects of training). Percent RMS values of body sway with the head in the normal upright position relative to the head-elevation condition for 20 subjects during a training period of five days. Again, a sawtooth curve results, but with a lower slope than in the case of head elevation. The daily short-term training effect and the long-term improvement can be attributed to a rearrangement of somatosensory and/or vestibular postural control. With the eyes open, there is only a slight reduction in sway activity during one hour but no long-term improvement of postural stability. This can be interpreted as either that the visual contribution to posture is optimal over a wide range or that postural stability with head elevation and the eyes open is stable enough so that there is no need for a recalibration of sensorimotor control.

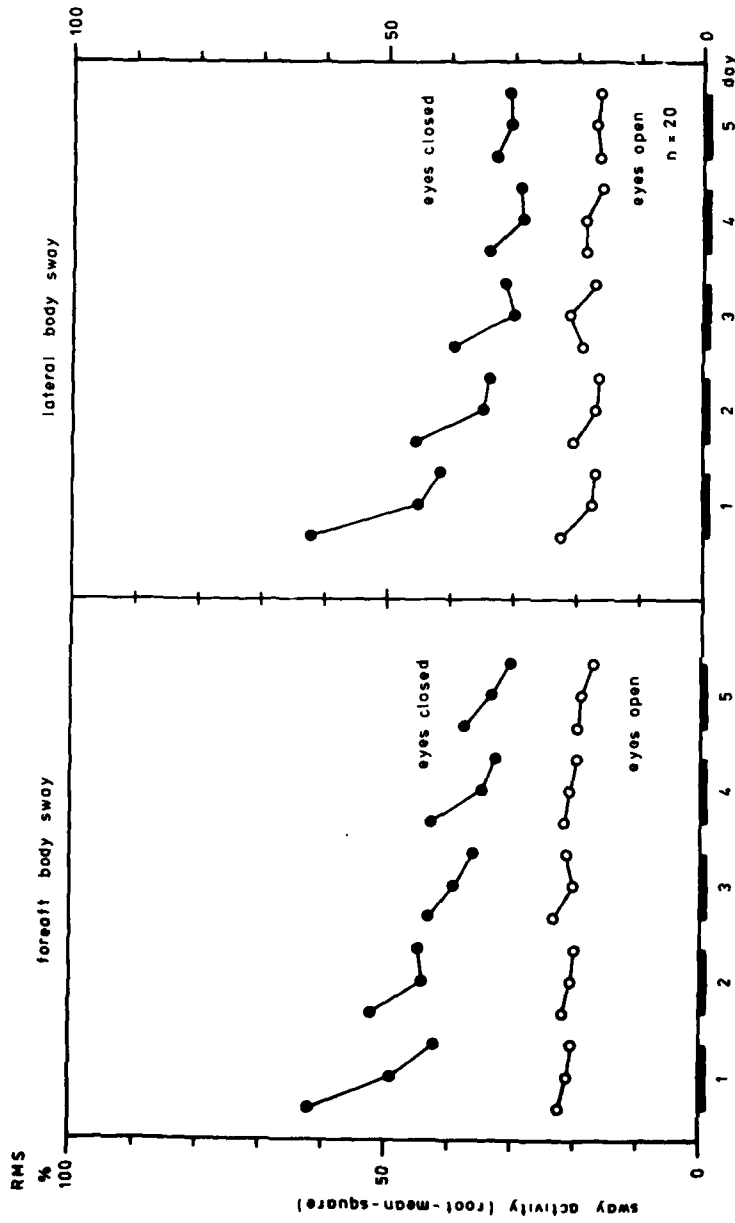


FIGURE 7. Postural balance with head right (effects of training). Percent reduction in RMS values of body sway with the head turned right relative to the head-elevation condition for 20 subjects during a training period of five days. The absolute sway activity is not greater for the head turned toward the right than with the head facing straight ahead, which demonstrates that the change in the orientation of shear-force vectors on the utricular macula has no significant influence on postural control. Short-term and long-term training effects are comparable with those of the normal head-upright condition.

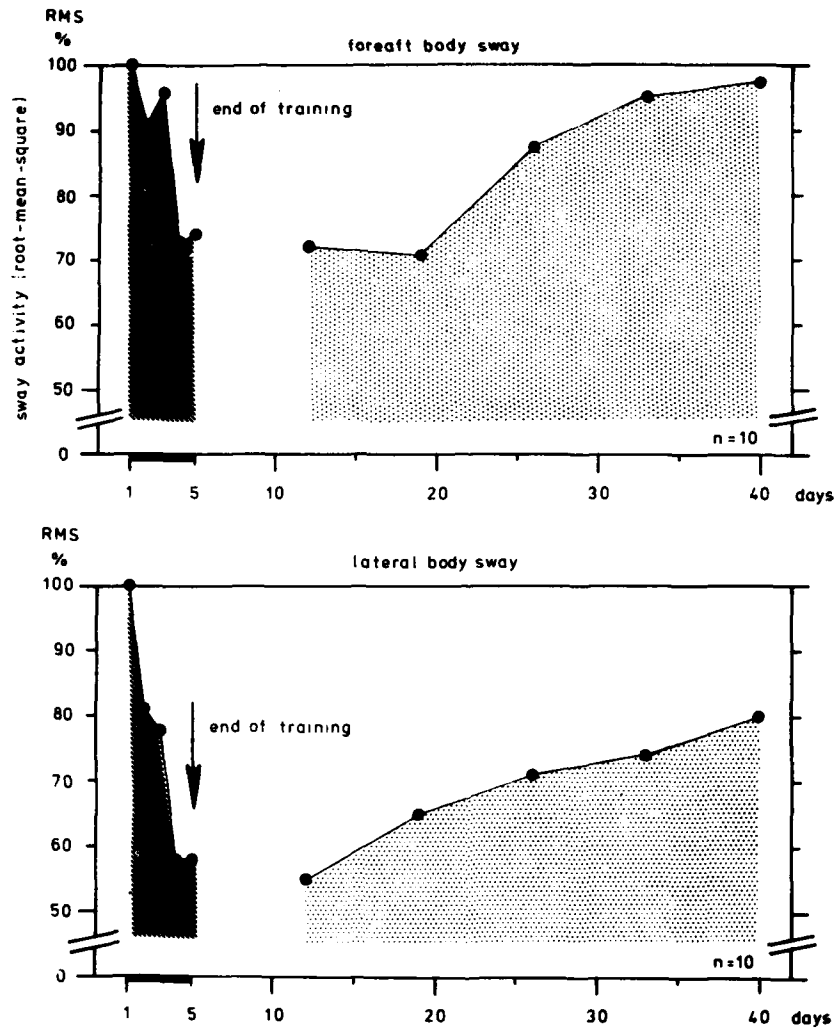


FIGURE 8. Postural balance with head extension (outlasting training effect). The duration of the training effect on postural balance with head extension and eyes closed for 10 subjects. Control measurements of body sway after a training period of five days reveal that without ongoing practice, postural imbalance becomes exponentially worse with a tendency to reach the pretraining values within 40 days (at least for the fore-aft activity).

lar deficiency, head-extension vertigo is of particular concern only in certain stimulus situations or diseases in which the stabilizing input from the eyes or joint receptors is reduced.

Balance training on foam rubber with head extension and closed eyes improved postural-sway activity up to 50% within five days. A daily short-term training effect and a long-term training effect together form a typical exponential

sawtooth curve of postural stability over time. After termination of training, learned balance skill exponentially returns to the pretraining values within weeks. The percentage of improvement through training depends on the amount of initial instability. Clinicians should treat ataxia by exposing patients to stimulus situations producing increasing body instability in order to activate sensorimotor rearrangement.

ACKNOWLEDGMENT

We are grateful to Dr. R. B. Post, Dr. H. W. Leibowitz, and Dr. E. R. Wist for helpful comments.

REFERENCES

1. BRANDT, TH. & R. B. DAROFF. 1980. The multisensory physiological and pathological vertigo syndromes. *Ann. Neurol.* 7: 195-203.
2. DENNY-BROWN, D. 1960. Recurrent cerebrovascular episodes. *Arch. Neurol.* 2: 194-209.
3. WILLIAMS, D. & T. G. WILSON. 1962. The diagnosis of the major and minor syndromes of basilar insufficiency. *Brain* 85: 741-774.
4. SHEEHAN, S., R. B. BAUER & J. S. MEYER. 1960. Vertebral artery compression in cervical spondylosis. *Neurology* 10: 968-986.
5. TOOLE, J. F. & S. H. TUCKER. 1960. Influence of head position upon cerebral circulation. *Arch. Neurol.* 2: 616-623.
6. KAPTEYN, T. S. & G. DE WIT. 1972. Posturography as an auxiliary in vestibular investigation. *Acta Otolaryngol. Stockholm* 73: 101-111.
7. GURFINKEL, E. V. 1973. Physical foundations of the stabilography. *Agressologie* 14: 9-14.
8. KAPTEYN, T. S. & W. BLES. 1976. Effects of optic and vestibular stimuli on stabilograms of patients with dizziness complaints. *Agressologie* 17: 25-31.
9. BLES, W., T. S. KAPTEYN, TH. BRANDT & F. ARNOLD. 1980. The mechanism of physiological height vertigo. II. Posturography. *Acta Otolaryngol. Stockholm* 89: 534-540.
10. MAURITZ, K. H. & V. DIETZ. 1980. Characteristics of postural instability induced by ischemic blocking of leg afferents. *Exp. Brain Res.* 38: 117-119.
11. NASHNER, L. M. 1976. Adapting reflexes controlling the human posture. *Exp. Brain Res.* 26: 59-72.
12. DICHGANS, J., K. H. MAURITZ, J. H. J. ALLUM & TH. BRANDT. 1976. Postural sway in normals and atactic patients: analysis of the stabilizing and destabilizing effects of vision. *Agressologie* 17: 15-24.
13. LESTIENNE, F., J. F. SOECHTING & A. BERTHOZ. 1977. Postural readjustments induced by linear motion of visual scenes. *Exp. Brain Res.* 28: 363-384.
14. NASHNER, L. M. & A. BERTHOZ. 1978. Visual contribution to rapid motor responses during postural control. *Brain Res.* 150: 403-407.
15. BRANDT, TH. & W. BÜCHELE. 1979. Ocular myasthenia: visual disturbance of posture and gait. *Agressologie* 20: 195-196.
16. TAYLOR, H. L., A. HENSCHEL, J. BROZEK & A. KEYS. 1949. Effects of bed rest on cardiovascular function and work performance. *J. Appl. Physiol.* 2: 223-239.
17. HAINES, R. F. 1974. Effect of bed rest and exercise on body balance. *J. Appl. Physiol.* 36: 323-327.

TULLIO PHENOMENON WITH TORSION OF THE EYES AND SUBJECTIVE TILT OF THE VISUAL SURROUND

L. Deecke and T. Mergner

*Department of Neurology
University of Ulm
D-7900 Ulm, Federal Republic of Germany*

D. Plester

*Department of Otolaryngology
University of Tübingen
D-7400 Tübingen, Federal Republic of Germany*

INTRODUCTION

The occurrence of vestibular symptoms such as vertigo and nystagmus upon acoustic stimulation is called the Tullio phenomenon.²⁴ It can be produced experimentally by fenestrating a semicircular canal in animals.^{8,9,24} In man it was observed following canal fenestrations, a now obsolete treatment for otosclerosis, but also can occur in congenital temporal bone abnormalities or infectious diseases including syphilis.¹⁷ In such cases it is believed that high-intensity acoustic stimuli cause endolymph flow in fenestrated or fistulated semicircular canals (cf., Reference 22). Others believe that sound waves themselves or eddy formations cause the phenomenon.^{3,8,9} Similar pathogenetic mechanisms might be involved in most cases of Tullio phenomena reported in the literature. The symptoms of the present case seem to be somewhat different and might suggest that the otolith organs rather than the semicircular canals are involved in the pathogenesis.

CASE REPORT

A 44-year-old male patient consulted the Neurological Department of the University of Ulm because of the complaint of dizzy spells. The exploration revealed that such spells typically occurred on exposure to changes in pressure as produced by loud noise, nose blowing, pressing, obstructing the external meatus with the finger, or altitude changes in a car or airplane. However, most effective was his own speaking, when uttering certain vowels such as e or u. The reported dizziness turned out to be a rather distinct vestibular sensation. In particular he reported the following self-observations: While driving his car and talking he was startled by the appearance of the highway tilting to the right. He learned to produce this effect at will by phonating e or u, which led to an apparent rotation of the surroundings to the right. A similar experience was observed when he was closing the door of his car. The phenomenon also occurred during one of his frequent speeches, which he had to give professionally; with certain words, the audience appeared to tilt in front of him. From his wife he learned that at times he slightly tilted his head toward his left shoulder while speaking.

The history revealed an acoustic trauma three years previously, which was caused by a short circuit in his old domestic stereo set when he was wearing closed earphones.

The bang was reported to be extremely painful and to have caused complete deafness for a couple of minutes, after which reduced audition slowly returned. The right ear was more affected than the left. He did not notice the dizzy spells at first, but half a year after the trauma when he started breathing therapy. It was at that time that phonation of certain vowels, which was part of the therapy, caused these strange sensations.

On examination under Frenzel's glasses in a dark room, a pronounced wheel rotation of the eyes was observed when he uttered u or e. The patient reported that the right illumination lamp of the glasses went down while the left went up. With longer utterances, the eyes maintained their torsional position until the end of the phonation. Eye torsion was accompanied by a slight lateral head tilt to the left. There was no nystagmus either spontaneously or produced by head shaking, position, or positioning. All other neurological examinations, including Unterberger's stepping test, were normal except for a slight and inconsistent deviation to the right in Bárány's pointing test.

Physical ear, nose, and throat examination showed no visible pathology. The tone audiogram was typical for a bang trauma showing a high-frequency hearing loss of 50 dB at 4000 Hz in both ears, without an "air-bone gap." There was hardly any trouble in speech discrimination and no evidence for recruitment in the Békésy audiogram. Cold and warm caloric nystagmus tests showed a somewhat smaller excitability of the right ear as compared to the left. However, brain-stem evoked-response audiograms (BERA) were symmetrical, and radiology and computerized tomography were normal. With Siegle's ear speculum, eardrum mobility was normal.

Documentation of ocular torsion was performed photographically by using special (fiberglass-illuminated) Frenzel's glasses in a dark room and a camera with a highly sensitive film. For quantitative evaluation of the amount of ocular torsion, a line was drawn through a distinct landmark on the iris and the center of the pupil. Its angle to the interpupillary line was measured from photographs taken at rest and during stimulation (cf., FIGURE 1). For this measurement, the photographs were projected onto a screen with angular markings.

Maximal torsion occurred upon shouting e and was 14.6° on the right eye and 12.5° on the left eye. The average of 12 measurements showed no interocular difference: 8.53° (standard deviation = 2.81) for the right eye and 8.57° (SD = 2.0) for the left eye. Positive pressure of the Politzer balloon to the right ear led to a tonic ocular torsion of 3.0° (SD = 0.42) for the right eye and 3.05° (SD = 1.34) for the left eye. Negative pressures were at first ineffective. After sealing the olive of the balloon in the external meatus with Vaseline[®], negative pressure produced a small counterrolling to the opposite side, i.e., the patient's right side. The patient reported that surprisingly, the neon lamp on the ceiling appeared to rotate to the left. Rotation of the surroundings in this direction previously had never been observed by him. Further investigations into the pathogenesis of the phenomenon, such as diagnostic tympanotomy and a glycerol test, were refused by the patient.

DISCUSSION

Rolling (torsion, cyclorotation, wheel rotation) of the eyes physiologically occurs during rotation of the head or the visual surroundings in the frontal plane by the vestibulo-ocular reflex or as optokinetic reaction. As in the other two planes, the ocular movement tends to stabilize the retinal image in space. In animals with lateral eyes, ocular torsion compensates for pitch and may have a considerable amplitude (e.g., rabbit, 30° , cf., Reference 16). In man and in

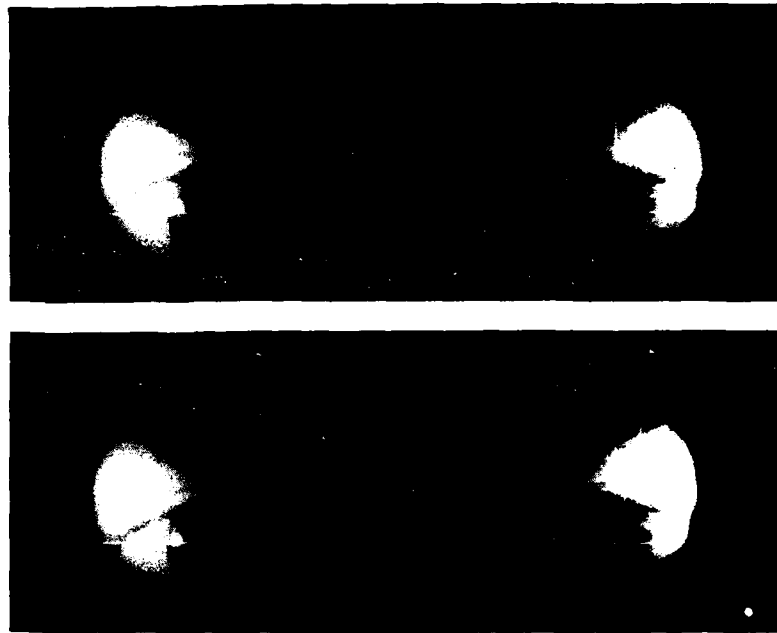


FIGURE 1. Torsional ocular movements in man induced by sound (Tullio phenomenon). Photographs show the patient's eyes through Frenzel's glasses in a dark room at rest (top) and during utterance of *e* (bottom). Angle of ocular torsion was measured by relating landmarks on the iris to the interpupillary line. Here maximal torsion is shown, amounting to 14.6° on the right eye and 12.5° on the left eye. For quantitative measurements, the photographs were projected onto a screen with angular markings.

animals with frontal eyes, ocular torsion compensates for (lateral) tilt and commonly is believed to be smaller in amplitude (ca. 6° ; for exceptions, cf. Reference 1). During head tilt, a dynamic component of ocular torsion can be distinguished from a static component, the latter keeping the eyes in a constant position until the end of the stimulus (cf., for example, Reference 2). Phasic ocular torsion due to dynamic tilt is associated with rotatory nystagmus; it stems from vertical semicircular canal stimulation. Tonic ocular torsion due to static tilt normally is caused by stimulation of otolith receptors and is not associated with nystagmus. Nystagmus of otolith origin seems to be restricted to exceptional cases and complex stimulus conditions.

In man, ocular torsion first was reported by Hunter.¹⁴ Since then it has been produced by various methods, yielding torsions of different amplitudes usually not exceeding 8° . Tilting the head to the shoulder induces a maximum torsion of about 8° ,² while torsion appears to be less when the whole subject is tilted with respect to gravity (5°)¹¹ (for review, see References 6 and 7) or with linear horizontal (lateral) acceleration ($4^\circ/\text{g}$).²⁵ The ocular movement also can be induced visually upon looking into an optokinetic drum from above, as first reported by Fischer (mean torsion of 4°).¹² Using special optokinetic (haploscopic) methods, wheel rotation can be disconjugate, i.e., either convergent or divergent

(about 7°).²¹ The effect of visual-vestibular conflict during static tilt of the visual field alone was first reported to be zero, and later to be small (0.29°).^{5,10,13}

Our torsion amplitudes are surprisingly larger than those cited above, but apparently do not represent the possible maxima. Using afterimages and repeated training, torsion of up to 30° can be achieved voluntarily.¹ Another surprising fact was that despite the large amplitude of the torsion, no nystagmus occurred. Thus the common explanation for the Tullio phenomenon—namely, stimulation of cupular receptors, as suggested for patients with a fenestrated or fistulated semicircular canal²²—is difficult to apply to the present case. Similar cases of sound-evoked tonic ocular torsion appear to be rare in the literature. The case reported by Spitzer and Ritter possibly could resemble the one presented here; their patient showed movement of the head similar to the one in the present case.²³ Unfortunately they did not report examining for ocular torsion with Frenzel's glasses.

Thus far, we could not specify the location and pathogenesis of the Tullio effect in our case since the patient refused invasive diagnostic or therapeutic procedures. However, on the basis of the relevant literature, the following possibilities may be discussed: (1) window ruptures with perilymph fistulae; (2) hydrops of the labyrinth; and (3) luxation or other injuries of the stapes with possible secondary adhesions.

Window ruptures have been observed after acoustic trauma (for case report and short review, cf., Reference 19). Our patient showed no positional fistula symptoms; still his pressure-sensitive Tullio phenomenon possibly could be interpreted as a pressure fistula sign. However, his normal hearing in the low-frequency range and the absence of fluctuating hearing impairments would be against this notion. On the other hand, an endolymphatic hydrops theoretically could be the cause, since in this condition the saccule may come into contact with the stapes footplate.¹⁵ In fact, a Tullio phenomenon can occur at certain periods in the course of Meniere's disease.¹⁸ It is not known whether an acoustic trauma can cause a hydrops, let alone whether such a hydrops would be stable for such a long period of time as observed in our case.

The third possibility, in our opinion, seems the most likely. The acoustic trauma may have caused a luxation of the stapes footplate deep into the vestibule, which was the case in one of Kacker and Hinchcliffe's Tullio patients, caused by a punctate injury to the left ear.¹⁵ Exploration of the left middle ear in their case showed a subluxated hypermobile stapes (the base of which had been pushed into the vestibule) without fistula.¹⁵ A similar lesion may be caused by loud noise and could bring the stapes in close contact to the otolith receptors. According to Miller, both saccule and utricle contribute to ocular counterrolling, the utricular component being larger and the saccular component smaller.²⁰ It would be conceivable that either both or one of the receptor organs is stimulated in a direction-specific way by excursions of the luxated stapes.

Since an elevation of pressure in the external meatus was able to elicit the described tonic ocular torsion, an explanation in terms of either sound waves or eddy formations alone cannot account for the effect observed in our patient.^{3,9} Rather, direct mechanical interaction between the stapes and the maculae is involved.

In future cases of Tullio phenomena, one should always try to differentiate (1) between pure ocular torsion and torsion with additional rotatory nystagmus and (2) between Tullio phenomena induced by sound alone and those also induced by pressure, in order to identify possible differences in the origin of Tullio cases.

SUMMARY

A 44-year-old male patient had an acoustic trauma three years previously, after which he suffered from vertigo and tilting of the environment to the right when uttering the vowels u or e. At such times, a tonic eye torsion to the left, which lasted throughout the utterance, was observed under Frenzel's glasses along with head tilt to the left. The phenomenon could be elicited experimentally by right-ear stimulation with low-frequency noise (mean frequency, 125 Hz; 90 dB), as well as by constant pressure. The patient also reported observing the phenomenon with loud noises, nose blowing, obstruction of his right external meatus with the finger, and with altitude pressure changes in a car. This suggests that the phenomenon is elicited via the eardrum and the ossicular chain.

Since lateral head tilt and counterrolling were tonic and without nystagmus, it is unlikely that one of the semicircular canals is involved as in usual Tullio cases. Rather, the otoliths may play a role in pathogenesis. Possible causative mechanisms are discussed along with the relevant literature.

REFERENCES

1. BALLJET, R. & K. NAKAYAMA. 1978. Training of voluntary torsion. *Invest. Ophthalmol. Vision Sci.* **17**: 303-314.
2. BÁRÁNY, R. 1906. Über die vom Ohrlabrynth ausgelöste Gegenrollung der Augen bei Normalhörenden, Ohrenkranken und Taubstummen. *Arch. Ohren Nasen Kehlkopfheilkd.* **68**: 1-30.
3. VON BÉKÉSY, G. 1935. Über akustische Reizung des Vestibularapparates. *Pfluegers Arch.* **236**: 59-76.
4. BRECHER, G. A. 1934. Die optokinetische Auslösung von Augenrollung und rotatorischem Nystagmus. *Pfluegers Arch.* **234**: 13-17.
5. CRONE, R. A. 1975. Optically induced eye torsion. II. Optostatic and optokinetic cycloverision. *Albrecht von Graefes Arch. Klin. Exp. Ophthalmol.* **196**: 1-7.
6. DIAMOND, S. G., C. H. MARKHAM, N. E. SIMPSON & I. S. CURTHOYS. 1979. Binocular counterrolling in humans during dynamic rotation. *Acta Otolaryngol.* **87**: 490-498.
7. DIAMOND, S. G. & C. H. MARKHAM. 1981. Binocular counterrolling in humans with unilateral labyrinthectomy and in normal controls. *Ann. N.Y. Acad. Sci.* (This volume.)
8. DOHLMAN, G. & K. MONEY. 1963. Experiments on the Tullio vestibular fistula reaction. *Acta Otolaryngol.* **56**: 271-278.
9. VAN EUNEN, A. J. H., H. C. HUIZING & E. HUIZINGA. 1943. Die Tulliosche Reaktion in Zusammenhang mit der Funktion des Mittelohres. *Acta Otolaryngol. Stockholm* **31**: 265-339.
10. GOODENOUGH, D. R., E. SIGMAN, P. K. OLTMAN, J. ROSSO & H. MERTZ. 1979. Eye torsion in response to a tilted visual stimulus. *Vision Res.* **19**: 1177-1179.
11. GRAHE, K. 1933. Eine neue Methode zur Bestimmung der Raddrehung der Augen mit dem Thorner'schen Augenspiegel. *Arch. Ohren Nasen Kehlkopfheilkd.* **134**: 308-313.
12. FISCHER, M. H. 1922. (As cited in Reference 4.)
13. HOWARD, I. P. & W. B. TEMPLETON. 1966. *Human Spatial Orientation*. John Wiley & Sons, Inc. New York, N.Y.
14. HUNTER, J. 1786. *Observations on certain parts of the animal economy*. London, England.
15. KACKER, S. K. & R. HINCHCLIFFE. 1970. Unusual Tullio phenomena. *J. Laryngol. Otol.* **84**: 155-166.
16. KORNHUBER, H. H. 1966. *Physiologie und Klinik des zentralvestibulären Systems*. In

- Hals-Hasen-Ohren-Heilkunde. J. Berendes, R. Link & F. Zöllner, Eds. 3(Part 3): 2150-2351. Thieme. Stuttgart, Federal Republic of Germany.
17. KWEE, H. L. 1972. A case of Tullio phenomenon with congenital middle-ear abnormalities. *ORL Basel* **34**: 145-152.
 18. LANGE, G. 1966. Das Tullio-Phänomen und eine Möglichkeit seiner Behandlung. *Arch. Ohren Nasen Kehlkopfheilkd.* **187**: 643-649.
 19. LYONS, G. D., M. L. DODSON, D. A. CASEY & B. B. MELANCON. 1978. Round window rupture secondary to acoustic trauma. *South. Med. J.* **71**: 71-73.
 20. MILLER, E. F. 1961. Counterrolling of the human eyes produced by head tilt with respect to gravity. *Acta Otolaryngol.* **54**: 479-501.
 21. NAGEL, A. 1868. Über das Vorkommen von wahren Rollungen des Auges um die Gesichtslinie. *Albrecht von Graefes Arch. Ophthalmol.* **14**: 228-246.
 22. SCHUKNECHT, H. F. 1974. *Pathology of the Ear*. Harvard University Press. Cambridge, Mass.
 23. SPITZER, H. & K. RITTER. 1979. Ein Beitrag zum Tullio-Phänomen. *Laryngol. Rhinol.* **58**: 934-936.
 24. TULLIO, P. 1929. *Das Ohr und die Entstehung der Sprache und Schrift*. Urban & Schwarzenberg. München, Germany.
 25. YOUNG, L. R., B. K. LICHTENBERG, A. P. ARROTT, T. A. CRITES, C. M. OMAN & E. R. EDELMAN. 1981. *Ocular torsion on earth and in weightlessness*. *Ann. N.Y. Acad. Sci.* (This volume.)

EFFECT OF FRONTAL-EYE-FIELD LESION ON EYE-HEAD COORDINATION IN SQUIRREL MONKEYS*

Toshiaki O-Uchi, Makoto Igarashi,† and Takeshi Kubo‡

Department of Otorhinolaryngology and
Communicative Sciences
Baylor College of Medicine
Houston, Texas 77030

INTRODUCTION

Electrical stimulation of the human and monkey frontal lobe can elicit the conjugate saccadic eye movements that usually accompany simultaneous head movements.¹⁻⁵ This region of the frontal lobe has been regarded as the "frontal eye field" (FEF). Simultaneous bilateral ablations failed to produce a severe impairment of oculomotor functions, but resulted in a slight inattentiveness and fewer spontaneous eye movements.⁶⁻¹⁰ Optokinetic nystagmus and optokinetic after-nystagmus were unchanged after simultaneous bilateral ablations.^{11,12}

In contrast to this, three striking behavioral changes have been reported consistently after unilateral ablation.^{6,10,13-17} These are (1) eye and head deviation and circling gait directed to the lesion side, (2) neglect of contralateral visual stimuli, and (3) strong preference for the ipsilateral hand.

The FEF classically has been regarded as a cortical motor area responsible for initiating voluntary eye movements. However, single cells whose activities are related to the eye movements were found to discharge not prior to but after the onset of saccades,^{18,19} and effects of lesions, mentioned above, gradually disappear. These two facts have discredited the hypothesis that the FEF is a primary cortical motor area for voluntary eye movement; and recent ablation experiments in rhesus monkeys and cats have suggested that the FEF is involved in the ability of unpracticed visual search and the ability to focus spatial attention.²⁰⁻²²

On the other hand, there is some evidence suggesting that the FEF is involved in eye-head coordination. Bizzi found two types of cells related to eye movements and another type of cell that was related exclusively to head turning in the monkey's (*Macaca mulatta*) FEF.^{18,19} Guitton and Mandl have found three types of cells in the cat's frontal oculomotor area that discharge in relation to eye movements and/or neck-muscle activity.^{23,24} Dubrovsky and Barbas also have found that electrical stimulation of the nerve branch to the dorsal neck muscles and the nerve of the superior rectus muscle elicited field and single-cell activity in the cat's FEF regions.^{25,26} These studies indicated the coexistence of several types of cells related to eye and head movements in the so-called frontal eye field.

In addition to this, King *et al.* recently have shown in the cat the existence of a strong electrophysiological projection from the FEF to cervical motoneurons and

*This study was supported in part by the McFadden Charitable Trust Research Fund, and by NINCDS Grants NS-10940 and NS-07237.

†To whom reprint requests should be addressed.

‡Present affiliation: Department of Otolaryngology, Osaka University Medical School, Fukushima-ku, Osaka 553, Japan.

the vestibular nuclei, through the interstitial nucleus of Cajal.²⁷ All these findings seem to suggest the possibility that the FEF is involved in eye-head coordination.

We previously investigated eye-head coordination during optokinetic and vestibular stimulation in normal squirrel monkeys and in animals with lateral semicircular canal block.²⁸⁻³⁰ A similar experimental paradigm was used in this study to investigate the effect of FEF ablations on eye-head coordination during optokinetic and vestibular stimulation. This study is one of our series on eye-head coordination in squirrel monkeys.

METHODS

Five healthy adult squirrel monkeys (*Saimiri sciureus*) weighing an average of 750 grams were used for this study. First, the monkeys' head movements were screened using a specially built lightweight helmet, which was made from dental cement and had a vertical aluminum shaft that could be connected to the potentiometer.

The methods of head- and eye-movement recordings were described in our previous papers.²⁸⁻³⁰ A pedestal was implanted chronically on top of the monkey's skull, and head turning in the yaw plane was recorded by a lightweight potentiometer, which registered a voltage dependent on head position. Head movements in the roll and pitch planes were restricted. Since the monkey's head was maintained as close as possible to its natural position in daily life, the plane of the lateral semicircular canals was pitched up about 20° to the plane of head turning. Eye movements in the horizontal plane were recorded by d.c. electro-nystagmography using platinum-needle electrodes inserted subcutaneously into the bilateral outer canthi.

The animal was restrained and placed on the rotational table located at the center of the 66-cm diameter white optokinetic drum. The optokinetic drum, which could be rotated separately from the table, had 16 vertical black stripes (1.7 cm wide and equally separated) that covered the entire visual field. All recordings were begun 20 minutes after intramuscular injections of amphetamine sulfate (0.5 mg/kg). Spontaneous nystagmus in the dark was examined after the amphetamine injection. Tonic head deviation, which appeared spontaneously in the dark and in the light, also was investigated after the amphetamine injection.

Eye velocity was calibrated using a 30°/second optokinetic stimulation. Both vestibular and optokinetic responses were investigated in this series. The vestibular test battery (60°/second and 100°/second velocity-step table rotation) and the optokinetic test battery (60°/second and 100°/second constant-speed drum rotation for 50 seconds) were repeated before and after the lesion placement. A five-minute rest was permitted between each recording session. Recording was done twice a week to avoid the habituation effect and the accumulation effect of amphetamine.

After more than five recordings were obtained in each test situation, a cerebral cortical lesion was placed under a sterilized surgical procedure. General anesthesia was induced by intraperitoneal injection of sodium pentobarbital (30 mg/kg). The frontal bone of one side was removed, the dura was opened, the arcuate sulcus and the principal sulcus were identified, and the lesion was made by subpial aspiration using a very-fine-gauge glass suction pipette under the operating microscope. Special care was taken to avoid any injury to the underlying subcortical structures. The contralateral operations were done one to five

months after the first operation in the same way, and recordings were repeated for two to four months. One monkey died accidentally after the second operation; therefore, nine sets of postoperative data were available in this series. All electronystagmographic data were analyzed by manual calculations.

On completion of all postoperative recordings, the monkeys were sacrificed by transcardiac perfusion with 10% neutral buffered formalin under deep general anesthesia with pentobarbital sodium. The brains and temporal bones were processed for microscopic examination.

RESULTS

Spontaneous Eye and Head Nystagmus

Prior to lesion placement, there was no spontaneous head nystagmus in any of the five monkeys, but spontaneous eye nystagmus was found in two monkeys after amphetamine injection. The slow-phase velocity was less than $10^\circ/\text{second}$, with no directional predominance or consistency. Postoperatively, there was spontaneous head and/or eye nystagmus with fast phases directed to the operated side, but not to the intact side.

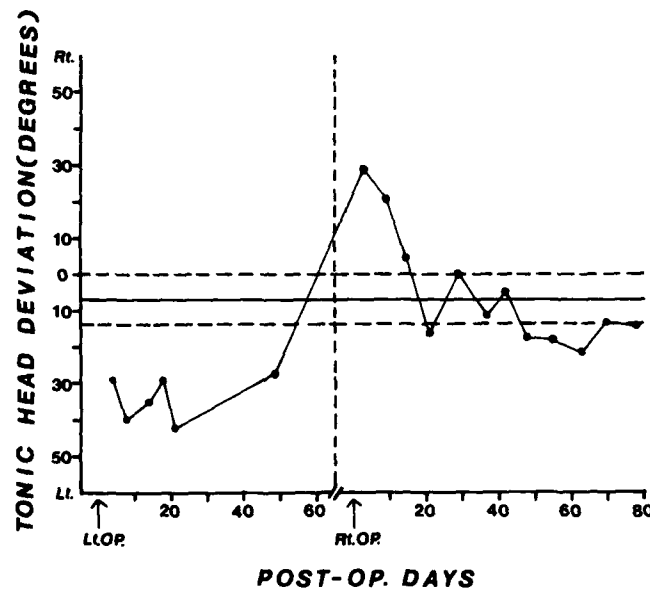


FIGURE 1. Postoperative change of tonic head deviation in the dark (No. 12011). The abscissa indicates postoperative calendar days, and the ordinate indicates tonic head deviation in the dark (degrees). Preoperative mean values and ± 2 standard errors of the mean (SEM) of this monkey are indicated by solid and dashed lines respectively ($n = 6$). Upward arrows on the abscissa indicate the dates of first-stage (left side) and second-stage (right side) FEF operations. Note that dominantly increased tonic head deviation in the dark directed to the operated side was seen after both first- and second-stage operations.

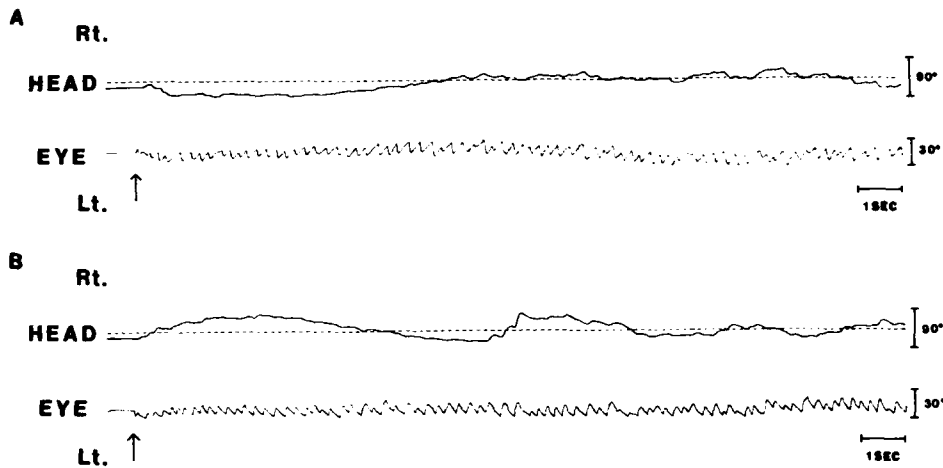


FIGURE 2. Response to optokinetic stimulation at 100°/second in a normal squirrel monkey. The stimulus direction of record A and that of B are opposite. Both records A and B were obtained from the same subject on the same experimental day. Upward arrows indicate the starting point of the stimulus. Upward deflections in head- and eye-movement recordings indicate deviation to the right. Dashed line in head-movement recording shows straight-forward head position. Clear head-and-eye coupled nystagmus is seen, and also a negative correlation between slow-phase velocity of head-and-eye coupled nystagmus. Note that the head deviates toward the side of the fast phases of nystagmus immediately after stimulus onset.

The mean maximum slow-phase velocity of the spontaneous head nystagmus was 9.4°/second in five of the nine postlesion conditions. It was 12.5°/second for the eye nystagmus (found in all nine postlesion conditions) and 17.6°/second for the gaze nystagmus (sum of head and eye movements). The spontaneous nystagmus lasted more than one month in eight out of nine postlesion conditions. Spontaneous head nystagmus disappeared before spontaneous eye nystagmus.

Tonic Head Deviation

Tonic head deviation in the dark usually was less than 6° and was not more than 15°, preoperatively. It was evenly distributed to both sides in all monkeys. Tonic head deviation was more dominant in the light (mean value = 16.2°) and also was distributed evenly to both sides. Interanimal differences were smaller in the light than in the dark.

After operation, tonic head deviation toward the operated side increased in all nine lesion conditions both in the dark and in the light. The mean maximum tonic head deviation to the operated side in the dark was 33.7°. The change in tonic head deviation in the dark was almost similar after the first-stage and second-stage operations. The postoperative increase in tonic head deviation in the dark lasted for an average of 31.8 days. A representative postoperative course of the tonic head deviation in the dark is shown in FIGURE 1.

TABLE 1
PREOPERATIVE MEAN VALUES OF SLOW-PHASE VELOCITY (DEGREES/SECOND) OF HEAD
NYSTAGMUS, EYE NYSTAGMUS, AND GAZE OF FIVE MONKEYS*

	Head	Eye	Gaze
OK 60	24.2	32.3	56.5
OK 100	33.1	57.3	90.4

*OK 60 and OK 100 indicate 60°/second and 100°/second optokinetic stimulation respectively.

Optokinetic Responses

Slow-Phase Velocity of Head, Eye, and Gaze

During optokinetic stimulation, monkeys showed coupled head and eye nystagmus (FIGURE 2). To calculate slow-phase velocity, representative beats of head and eye nystagmus were selected based upon (1) head nystagmus not being interrupted by random head movement, (2) occurrence of head and eye nystagmus being coupled, and (3) slow-phase head and eye velocity being constant for a minimum of three seconds. Preoperative mean values of slow-phase velocity of head nystagmus, eye nystagmus, and gaze of five monkeys are shown in TABLE 1. There was no directional predominance.

Postoperative changes in optokinetic responses are summarized in TABLE 2. Since the general trend was almost the same for optokinetic stimulation at 60°/second (OK 60) and at 100°/second (OK 100), the data are pooled in TABLE 2.

Slow-phase head velocity (SPHV). As shown in TABLE 2, SPHV decreased in 50% of postoperative conditions (after first- and second-stage operations) when the fast phase was directed to the lesion side. The maximum decrease in SPHV produced by OK 60 was 19.7°/second and by OK 100 was 16.9°/second.

TABLE 2
POSTOPERATIVE CHANGES OF OPTOKINETIC RESPONSES*

	Slow-Phase Velocity						Frequency of Nystagmus				Maximum Head Deviation	
	Head		Eye		Gaze		Head		Eye		Ipsi Contra	
	Ipsi	Contra	Ipsi	Contra	Ipsi	Contra	Ipsi	Contra	Ipsi	Contra	Ipsi	Contra
Post First Operation												
Increase	0	2	4	0	3	0	6	0	5	0	6	0
Decrease	4	0	0	3	0	1	0	1	0	8	0	8
No Change	6	8	6	7	7	9	4	9	5	2	4	2
Post Second Operation												
Increase	0	0	3	1	4	0	2	2	2	1	3	0
Decrease	5	0	0	2	0	0	3	4	4	6	0	8
No Change	3	8	5	5	4	8	3	2	2	1	5	0

*Results of stimulation at 60°/second and 100°/second are pooled. Ipsi indicates that the fast phase of nystagmus was directed to the operated side, and contra indicates that the fast phase of nystagmus was directed to the intact side. The numbers in the table show how many times the pooled responses appeared after the FEF operations. Slow-phase gaze velocity was the sum of the slow-phase velocities of head and eye nystagmus.

This change disappeared about two weeks after the operations. Only two postoperative conditions showed an SPHV increase after the first-stage operation when the fast phase was directed to the intact side.

Slow-phase eye velocity (SPEV). There was no change in SPEV in 64% of the postoperative conditions after both first- and second-stage operations (TABLE 2). In the other 36%, SPEV increased when the fast phase was directed to the lesion side and decreased when the fast phase was to the intact side. The maximum increase in SPEV was 48.3°/second and 44.3°/second for OK 60 and OK 100, respectively. The increase disappeared within one month after the first-stage operation, but lasted more than two months after the second-stage operation. On the other hand, the maximum decrease in SPEV was 15.2°/second for OK 60 and 21.3°/second for OK 100. The decrease disappeared about two weeks after the operations.

Slow-phase gaze velocity (SPGV). No change in SPGV was found in 70% of animals after the first-stage operation or in 50% of animals after the second-stage operation. In the remainder, SPGV increased when the fast phase was directed to the lesion side. The maximum gaze error of the SPGV increase was 43.4°/second and 25.9°/second for OK 60 and OK 100 respectively. This gaze error disappeared about two weeks after the first-stage operation, but has lasted more than two months after the second-stage operation. In contrast, when the fast phases were directed to the intact side, there was no clear change in SPGV.

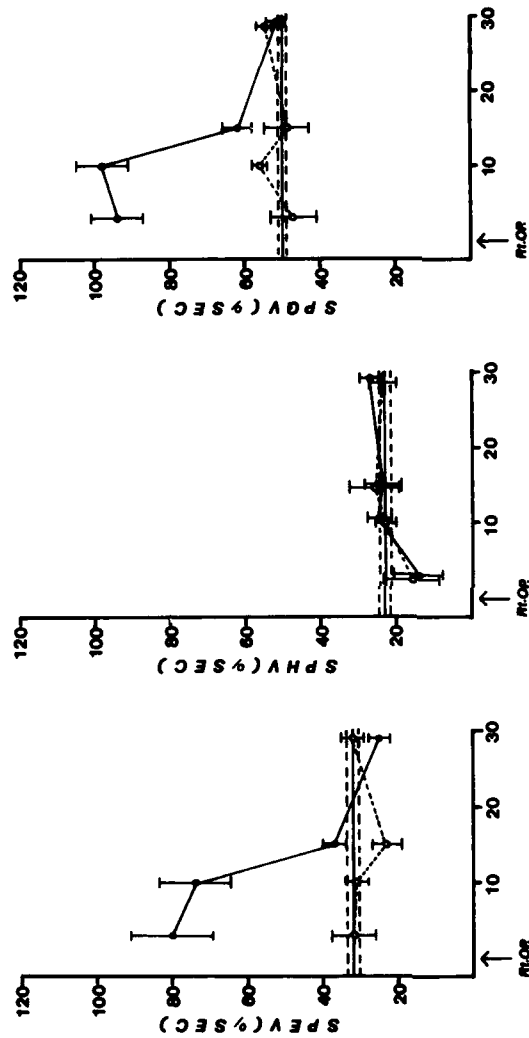
Thus, SPHV decreased and SPEV increased when the fast phases of the nystagmus were directed to the operated side, but since the change in eye velocity was bigger than the change in head velocity, gaze velocity showed an overshoot as a result. The representative postoperative time course of the slow-phase-velocity changes are shown in FIGURE 3.

Frequency of Head and Eye Nystagmus

Preoperatively, the mean frequency of head nystagmus (nystagmic beats during the 30 seconds after stimulus initiation) in five monkeys was 70.4 for OK 60 and 85.0 for OK 100. The mean frequency of eye nystagmus was 108.5 for OK 60 and 122.9 for OK 100. As shown in TABLE 2 and FIGURE 4, after the first-stage lesions, the frequency of both head and eye nystagmus increased in more than half of the total postoperative conditions when the fast phase of the nystagmus was directed to the lesion side. The maximum increase in head nystagmus was 42.4% for OK 60 and 62.2% for OK 100, and in eye nystagmus was 27.6% for OK 60 and 23.2% for OK 100. These changes lasted for more than one month after the operation. Frequency of eye nystagmus decreased when the fast phases were directed to the intact side, but head nystagmus showed no clear change. The maximum change of the decrease in frequency of eye nystagmus was 23.3% for OK 60 and 24.6% for OK 100. After the second lesions were made, there was no clear trend in either eye or head nystagmus as after the first operation.

Head Deviation

When the optokinetic stimulus started, the head immediately deviated to the side contralateral to the stimulus direction. This head deviation was transient and gradually returned toward the center. The first head deviation was anticompen-satory, followed by a compensatory head deviation toward the center (FIG-



POST-OP. DAYS

FIGURE 3. Postoperative changes of slow-phase velocity of eye (SPEV), head (SPHV), and gaze (SPGV) for an optokinetic stimulus of $60^\circ/\text{second}$ (No. 13544). The abscissa indicates the postoperative calendar days, and the ordinates indicate slow-phase eye velocity in the left figure, slow-phase head velocity in the middle figure, and slow-phase gaze velocity in the right figure. Preoperative mean values and ± 2 SEM of this monkey are indicated by solid and dashed lines respectively ($n = 6$). Postoperative changes are shown in solid lines and closed circles when the fast phase was directed to the operated side and are shown in dashed lines and open circles when the fast phase was directed to the intact side. Error bars indicate ± 2 SEM. Note that SPEV increased and SPHV decreased when the fast phase of nystagmus was directed to the operated side, but since the degree of SPEV change was greater than that of SPHV change, SPGV showed overshoot error as a result.

URE 2). All preoperative recordings showed these head deviations. In five normal monkeys, the preoperative mean maximum head deviation was 36.4° for OK 60 and 34.7° for OK 100. There was no directional predominance, preoperatively.

After both the first- and second-stage lesions, maximum head deviation increased in 50% of the postoperative conditions when the head deviation was directed to the lesion side, and decreased in 89% when the head deviation was to the intact side (TABLE 2). This change lasted more than one month after operation. The decrease in head deviation to the intact side was clearer than the increase to the lesion side. These changes in maximum head deviation partly correspond to the tonic head deviation in light. In other words, after each lesion the head

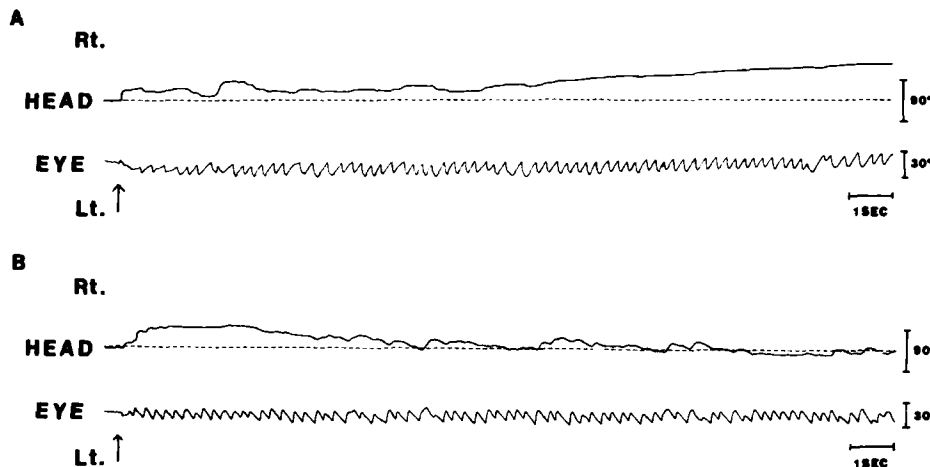


FIGURE 4. Optokinetic responses to a $100^\circ/\text{second}$ stimulus two days after right FEF ablation (No. 13546). Upward arrows indicate the starting point of the stimulus. Upward deflections in head- and eye-movement recordings indicate deviation to the right. Dashed line in head-movement recording shows straight-forward head position. When the fast phase was directed to the intact side (record A), the tonic head deviation did not cross the centerline but was directed to the right side (direction of the slow phase). In contrast to this, when the fast phase was directed to the operated side (record B), frequency of head nystagmus increased and the tonic head deviation was directed to the fast phase of nystagmus. Its maximum value (44.0°) was greater than the preoperative value (30.0°).

deviated to the operated side, both at rest and during active head movements. FIGURE 4 shows the representative postoperative head deviations induced by OK 100.

Negative Correlation Coefficient of Coupled Head and Eye Nystagmus

Slow-phase velocities of head and eye nystagmus are negatively correlated. This means that when head velocity becomes higher, eye velocity becomes lower and vice versa (FIGURE 2). Thus a large negative correlation coefficient indicates good eye-head coordination and vice versa. The preoperative negative correla-

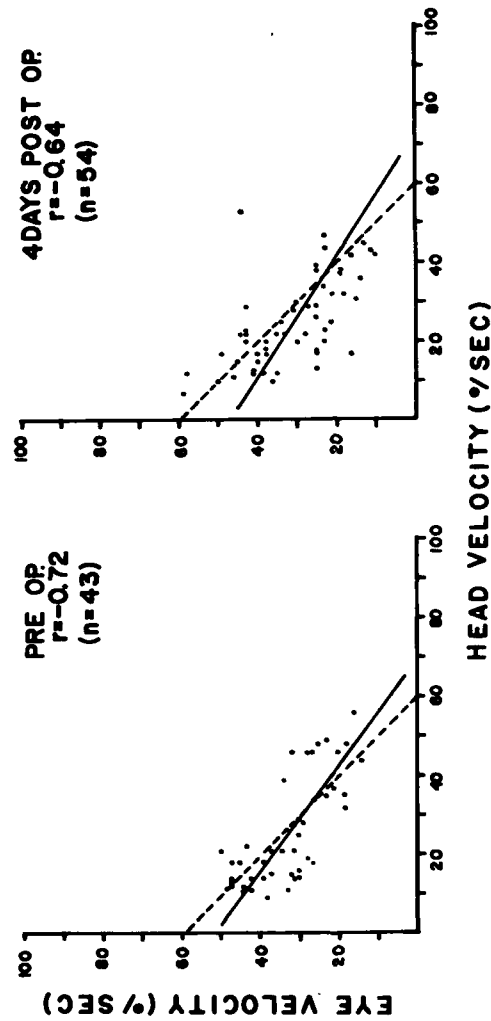


FIGURE 5. Eye-head coordination during optokinetic stimulation (No. 12011). Abscissa and ordinate show slow-phase velocities of head and eye nystagmus respectively. Each dot represents slow-phase velocity of head-and-eye coupled nystagmus induced by OK 60 before (left figure) and four days after left FEF ablation (right figure). Solid and dashed lines in each figure indicate the experimental and -1.0 regression lines, respectively. Postoperative change in the negative correlation coefficient value was not significant statistically [Fisher's Z transformation: $p > 0.05$].

tion coefficients of the five monkeys were about the same as in our previous study.²⁸

No statistically significant change of negative correlation coefficient was found for all five monkeys after both first- and second-stage lesion placements (Fisher's Z transformation:³¹ $p > 0.05$). Preoperative and postoperative slow-phase velocities of coupled head and eye nystagmus of one representative monkey are plotted in FIGURE 5. In this monkey, the correlation was weakened four days after the operation (-0.64) compared to that in the preoperative stage (-0.72), but this change was not significant statistically ($p > 0.05$).

Vestibular Responses to Rotation

When the table was accelerated, maintained at a constant speed, decelerated, and stopped, both head and eye nystagmus were induced (FIGURE 6). SPGV reached its maximum value (maximum SPGV) immediately after the stimulus had reached a constant speed, and at the cessation of stimulation. Head nystag-

TABLE 3
PREOPERATIVE MEAN VALUES OF MAXIMUM SPGV (DEGREES/SECOND) AND THE DURATION (SECONDS) OF EYE NYSTAGMUS EVOKED BY VESTIBULAR STIMULATION*

	Maximum SPGV		Duration	
	PACN	PDCN	PACEN	PDCEN
V 60	51.3	46.8	33.1	30.1
V 100	73.4	64.3	38.0	31.0

*V 60 and V 100 indicate 60°/second and 100°/second vestibular stimulation respectively. PACN, postacceleration nystagmus; PDCN, postdeceleration nystagmus.

mus disappeared earlier than eye nystagmus. Preoperative mean values of maximum SPGV and of eye nystagmus duration in five monkeys are shown in TABLE 3. There was no directional predominance. Postoperative changes of vestibular responses are summarized in TABLE 4. Since the postoperative changes were similar for vestibular stimuli of 60°/second and 100°/second and also for nystagmus in the postacceleration period (PACN) and the postdeceleration period (PDCN), all data are pooled in TABLE 4.

Maximum SPGV

As shown in TABLE 4, maximum SPGV increased by more than one-half after both first- and second-stage operations when the fast phase of the nystagmus was directed to the lesion side. The maximum increase was 35.4% in PACN and 79.5% in PDCN for rotation at 60°/second, and was 44.1% in PACN and 76.3% in PDCN for rotation at 100°/second. The duration of these changes was quite variable among subjects. When the fast phase was to the intact side, maximum SPGV decreased in 40% of animals after the first-stage operation (TABLE 4). On the other hand, maximum SPGV increased in more than half of the animals after the second-stage operation. This result indicates the more complicated status of

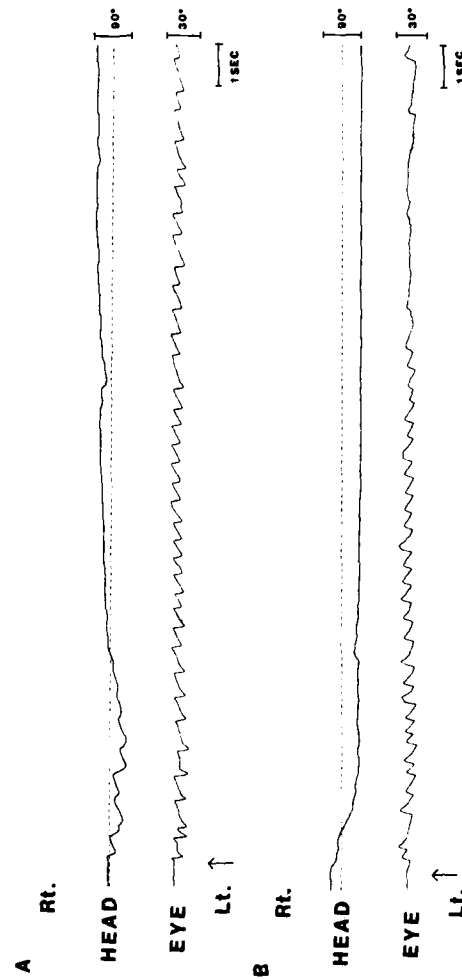


FIGURE 6. Vestibular response of a normal squirrel monkey to rotation at 60°/second. Record A represents postacceleration response and record B indicates postdeceleration response. Upward arrows indicate the start of table rotation (in record A) and cessation of table rotation (in record B), respectively. Dashed line in head-movement recording shows straight-forward head position. Slow-phase gaze velocity showed a maximum value immediately after reaching a constant speed and after cessation. Head nystagmus disappeared before eye nystagmus.

the animals after the second operation. FIGURE 7 (top) shows one example of a postoperative time course of maximum SPGV.

Duration of Vestibular Responses

As shown in TABLE 4, after both first and second lesions, the duration of vestibular eye nystagmus increased in more than half of the tests when the fast phase of nystagmus was directed to the lesion side. The maximum increase was 119.7% in postacceleration eye nystagmus (PACEN) and 205.8% in postdeceleration eye nystagmus (PDCEN) for stimulation at 60°/second. It was 115.4% in PACEN and 117.8% in PDCEN for stimulation at 100°/second. In contrast, the duration of vestibular eye nystagmus decreased in more than half of the tests after both the first and second operations, when the fast phase of the nystagmus was directed to the intact side. The maximum decrease was 49.0% in PACEN

TABLE 4
POSTOPERATIVE CHANGES OF VESTIBULAR RESPONSES*

	Maximum SPGV		Duration	
	Ipsi	Contra	Ipsi	Contra
Post First Operation				
Increase	12	0	11	0
Decrease	0	8	0	13
No Change	8	12	9	7
Post Second Operation				
Increase	13	9	8	2
Decrease	1	3	0	10
No Change	2	4	8	4

*Ipsi and contra as in TABLE 2. The number in the table is the sum of the results of postacceleration and postdeceleration response induced by rotation at 60°/second and 100°/second. Duration represents that of eye nystagmus.

and 64.4% in PDCEN for stimulation at 60°/second, and 61.0% in PACEN and 65.9% in PDCEN for 100°/second. FIGURE 7 (bottom) shows one example of a postoperative time course of the duration of PACEN. When the fast phase of the nystagmus was directed to the operated side, both maximum SPGV and the duration increased, and vice versa.

Morphology

The cortical lesions of five monkeys (nine sides) are shown in FIGURE 8. There was a considerable difference in both the location and size of the lesions. We have examined the brains of over 600 squirrel monkeys and found that there is a large variability of the location, shape, and size of the principal and arcuate sulci. This could be one reason why we experienced difficulty in locating these cortical sulci during the FEF surgery. We did not find a clear relationship between the postoperative functional change and the location and size of the lesions.

On histological sections, the subcortical deep structures were intact in all

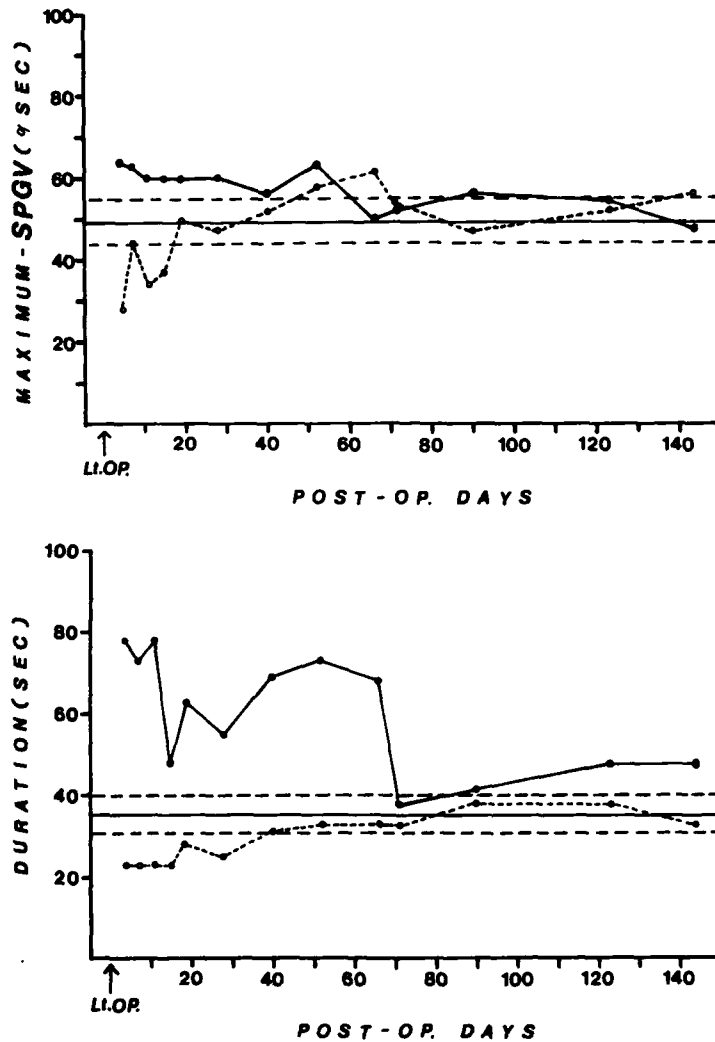


FIGURE 7. Postoperative changes of maximum slow-phase gaze velocity (maximum SPGV) of postacceleration nystagmus (top) and the duration of postacceleration eye nystagmus (PACEN) (bottom) (No. 13543). Stimulus, $60^\circ/\text{second}$. The abscissa indicates postoperative calendar days, and the ordinates represent maximum SPGV (top) and the duration of PACEN (bottom). Preoperative mean values and ± 2 SEM of this monkey are shown in solid and dashed lines, respectively ($n = 6$). Postoperative change is indicated in solid lines and closed circles when the fast phase of the nystagmus was directed to the operated side, and is indicated in dashed lines and open circles when the fast phase was directed to the intact side. Note that both maximum SPGV and the duration of PACEN increased when the fast phase was directed to the operated side and decreased when the direction was opposite. The change of the duration lasted longer than that of maximum SPGV.

animals. Middle and inner ear structures also were normal in all temporal bones.

DISCUSSION

Head Movements

According to Bizzi et al., eye-head coordination is an interaction of central command with peripheral feedback from receptors excited by centrally initiated

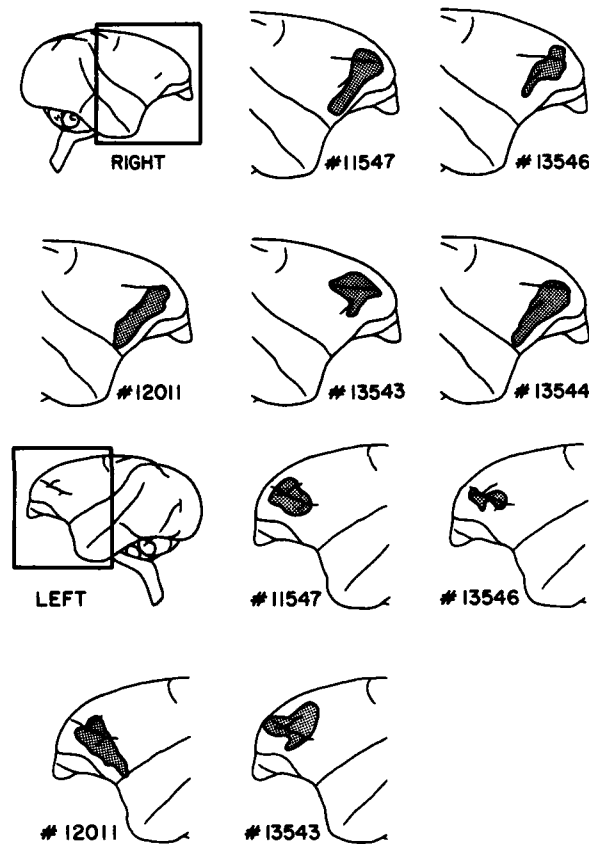


FIGURE 8. Cortical lesions of five monkeys. The top figure shows the right-side lesions, and the bottom figure shows left-side lesions. Lesions are shown as shaded areas. Monkey No. 13544 died accidentally after left-FEF operation.

eye and head movements.³²⁻³⁴ But the most important factor for eye-head coordination is a peripheral vestibular input triggered by centrally initiated head movement in "triggered"- and/or "predictive"-type single coordinated eye and head movements.³⁵ In these authors' experimental paradigms, visual input and

neck proprioceptive input did not play an important role for eye-head coordination compared to that of vestibular input.³⁵ Our previous studies also revealed that vestibular input plays an important role even in repetitive coordinated eye and head movements under optokinetic stimulation.^{28,30} In addition to this, it is reasonable to assume that neck proprioceptive input must play a more important role in repetitive eye and head movements than in single movements of eye-head coordination because multiple neck movements induce the multiple vestibular inputs. Tonic head deviation and change in the frequency of head nystagmus during optokinetic stimulation can be the result of the asymmetry of dorsal-neck-muscle activity induced by unilateral FEF ablation.

Strong afferent and efferent electrophysiological connections with specific directionality between the FEF and dorsal neck muscles have been shown in the cat.²³⁻²⁷ Also, head-turning-related cells were found in *Macaca mulatta*'s FEF.^{18,19} Our present results seem to agree with these previous electrophysiological findings. These changes of neck proprioceptive input can secondarily influence the other central areas that receive an afferent projection from the dorsal neck muscles and seem to be involved in control of coordinated eye-head movements.³⁶⁻⁴¹

Eye Movements

Even though there is no clear evidence of direct morphological projection from the FEF to oculomotor nuclei, electrical stimulation of the FEF can elicit eye movements.^{1-5,42,43} According to Robinson, in *Macaca mulatta*, the great majority of eye movements evoked by FEF stimulation were contralateral conjugate saccades, and the amplitudes ranged from 1° to 70°. From this result, we can expect disturbances of saccades directed to the contralateral side after unilateral FEF ablation.

Since it generally is accepted that the two forms of rapid eye movements, saccades and the fast phase of vestibular nystagmus, are identical,⁴⁴⁻⁴⁷ the same premotor neural circuit probably produces both of them. Then we can expect similar changes in both saccades and the fast phase of vestibular nystagmus after unilateral FEF operation. Spontaneous nystagmus and the change in maximum slow-phase gaze velocity of vestibular responses seemed to agree very well with these expectations. Since the same kind of change was found in optokinetic responses, these changes of eye movements are not affected by the light.

Recently, Marrocco investigated the interaction of the cynomolgous monkey's FEF-evoked saccade with voluntary saccades, pursuit, and vestibular nystagmus and concluded that the FEF appears capable of modulating any ongoing eye movement.⁴⁸ All these findings seem to suggest that the FEF is involved in spatial and/or temporal modulation of eye and head movements.

Eye-Head Coordination

Even when evident changes of eye and head movements were found, the negative correlation coefficient of slow-phase velocity of eye and head nystagmus during optokinetic stimulation did not show significant change after unilateral FEF ablation. Thus the fundamental feedback mechanisms of eye-head coordination did not change regardless of the existence of gaze error. This seems to indicate that the squirrel monkey's FEF could be involved in the spatial and/or

temporal modulation of eye and head movements but is not involved in eye-head coordination under the present experimental conditions.

It is important to consider the interspecies difference. A high degree of convergence has been observed at the single-cell level between dorsal neck muscles and extraocular muscles (or eye movements) in the cat's FEF.^{24,25} Different from this, in the monkey's (*Macaca mulatta*) FEF, eye-movement-related cells discharged irrespectively of head turning.¹⁰ This suggests that the degree of convergence of eye- and neck-muscle activity in FEF cells varies among different species. This interspecies difference of convergence could be due partly to the different relationship between head and body. Also, the relative size of dorsal neck musculature varies considerably in different species because animals hold their heads in different ways.^{49,50} This suggests that the ethological significance of eye-head coordination varies in different species. In addition to this consideration, the monkey's (*Macaca mulatta*) FEF-evoked saccades were quite stereotyped; in other words, they were an all-or-none phenomenon.⁵

It is reasonable to assume that several central-nervous-system structures could be involved in different types of eye-head coordination. Recently, Schiller et al. showed in the monkey that parallel neural pathways are responsible for the control of saccadic eye movements (one mediated through the FEF and the other through the superior colliculus).⁵¹ This work indicated that the FEF works for the control of eye-head movements in combination with other central neural structures.

Through our present study, it was found that FEF ablation in the squirrel monkey produced changes in spatial and/or temporal modulation of head and eye movements, but not in eye-head coordination during optokinetic stimulation.

SUMMARY

The effect of unilateral frontal-eye-field (FEF) ablation on eye-head coordination during optokinetic and vestibular stimulation was investigated in the squirrel monkey (*Saimiri sciureus*). The results suggested that the FEF was involved in spatial and/or temporal modulation of eye and head movements, but not involved in eye-head coordination under the present experimental conditions.

ACKNOWLEDGMENTS

The technical assistance of Mr. M. Simon, Dr. W. B. Kulecz, Mrs. E. Marbley, Mrs. J. Brown, and Mrs. R. Guess is greatly appreciated.

REFERENCES

1. SMITH, W. K. 1949. The frontal eye fields. In *The Precentral Motor Cortex*. P. C. Bucy, Ed.: 307-342. University of Illinois Press. Urbana, Ill.
2. WAGMAN, I. H., R. WERMAN, D. S. FELDMAN, L. SUGARMAN & H. P. KRIEGER. 1957. The oculomotor effects of cortical and subcortical stimulation in the monkey. *J. Neuropathol. Exp. Neurol.* 16: 269-277.
3. WAGMAN, I. H., H. P. KRIEGER, C. A. PAPATHEODORON & M. B. BENDER. 1961. Eye movements elicited by surface and depth stimulation of the frontal lobe of macaque *mulatta*. *J. Comp. Neurol.* 117: 179-188.

4. LEMMEN, L. J., J. S. DAVIS & L. L. RADNOR. 1959. Observations on stimulation of the human frontal eye field. *J. Comp. Neurol.* **112**: 163-168.
5. ROBINSON, D. A. & A. F. FUCHS. 1969. Eye movements evoked by stimulation of frontal eye fields. *J. Neurophysiol.* **32**: 637-648.
6. KENNARD, M. A. & L. ECTORS. 1938. Forced circling in monkeys following lesions of the frontal lobes. *J. Neurophysiol.* **1**: 45-54.
7. METTLER, F. A. 1945. Effects of bilateral simultaneous subcortical lesions in the primate. *J. Neuropathol. Exp. Neurol.* **4**: 99-122.
8. DENNY-BROWN, D. 1951. The frontal lobes and their functions. In *Modern Trends in Neurology*. A. Feiling, Ed.: 13-81. Butterworth. London, England.
9. PRIBRAM, K. H. 1955. Lesions of "frontal eye fields" and delayed response of baboons. *J. Neurophysiol.* **18**: 105-112.
10. BRUCHER, J. M. 1966. The frontal eye field of the monkey. *Int. J. Neurol.* **5**: 262-281.
11. HENDERSON, J. W. & E. C. CROSBY. 1952. An experimental study of optokinetic response. *AMA Arch. Ophthalmol.* **47**: 43-54.
12. PASIK, P. & T. PASIK. 1964. Oculomotor functions in monkeys with lesions of the cerebrum and the superior colliculi. In *The Oculomotor System*. M. B. Bender, Ed.: 40-80. Hoeber. New York, N.Y.
13. KENNARD, M. A. 1939. Alternations in response to visual stimuli following lesions of frontal lobes in monkeys. *Arch. Neurol. Psychiatry* **41**: 1153-1165.
14. CLARK, G. & K. S. LASHLEY. 1947. Visual disturbances following frontal ablations in the monkey. *Anat. Rec.* **97**: 326.
15. DENNY-BROWN, D. 1966. *The Cerebral Control of Movement*. Liverpool University Press. Liverpool, England.
16. LATTO, R. & A. COWEY. 1971. Fixation changes after frontal eye-field lesions in monkeys. *Brain Res.* **30**: 25-36.
17. LATTO, R. & A. COWEY. 1972. Frontal eye-field lesions in monkeys. *Bibl. Ophthalmol.* **82**: 159-168.
18. BIZZI, E. 1968. Discharge of frontal eye field neurons during saccadic and following eye movements in unanesthetized monkeys. *Exp. Brain Res.* **6**: 69-80.
19. BIZZI, E. & P. H. SCHILLER. 1970. Single unit activity in the frontal eye fields of unanesthetized monkeys during eye and head movement. *Exp. Brain Res.* **10**: 151-158.
20. SCHLAG-REY, M. & D. B. LINDSLEY. 1970. Effect of prefrontal lesions on trained anticipatory visual attending in cats. *Physiol. Behav.* **5**: 1033-1041.
21. LATTO, R. 1978. The effects of bilateral frontal eye-field, posterior parietal or superior collicular lesions on visual search in the rhesus monkey. *Brain Res.* **146**: 35-50.
22. LATTO, R. 1978. The effects of bilateral frontal eye-field lesions on the learning of a visual search task by rhesus monkeys. *Brain Res.* **147**: 370-376.
23. GUITTON, D. & G. MANDL. 1978. Frontal 'oculomotor' area in alert cat. I. Eye movements and neck activity evoked by stimulation. *Brain Res.* **149**: 295-312.
24. GUITTON, D. & G. MANDL. 1978. Frontal 'oculomotor' area in alert cat. II. Unit discharges associated with eye movements and neck muscle activity. *Brain Res.* **149**: 313-327.
25. DUBROVSKY, B. O. & H. BARBAS. 1977. Frontal projections of dorsal neck and extraocular muscles. *Exp. Neurol.* **55**: 680-693.
26. BARBAS, H. & B. O. DUBROVSKY. 1980. Characteristics of dorsal neck muscle afferent input to the cat frontal cortex before and after dorsal funiculus section. *Exp. Neurol.* **67**: 35-51.
27. KING, W. M., W. PRECHT & N. DIERINGER. 1980. Synaptic organization of frontal eye field and vestibular afferents to interstitial nucleus of Cajal in the cat. *J. Neurophysiol.* **43**: 912-928.
28. KUBO, T., M. IGARASHI, D. W. JENSEN & J. K. HOMICK. 1981. Eye-head coordination during optokinetic stimulation in squirrel monkeys. *Ann. Otol. Rhinol. Laryngol.* **90**: 85-88.
29. KUBO, T., M. IGARASHI, D. W. JENSEN & W. K. WRIGHT. 1981. Head and eye movements following vestibular stimulus in squirrel monkeys. *ORL* **43**: 26-38.

30. KUBO, T., M. IGARASHI, D. W. JENSEN & W. K. WRIGHT. 1981. Eye-head coordination and lateral canal block in squirrel monkeys. *Ann. Otol. Rhinol. Laryngol.* **90**: 154-157.
31. COHEN, J. & P. COHEN. 1975. *Applied Multiple Regression/Correlation Analysis for the Behavioral Sciences*. Lawrence Erlbaum Associates. Hillsdale, N.J.
32. BIZZI, E., R. E. KALIL, P. MORASSO & V. TAGLIASCO. 1972. Central programming and peripheral feedback during eye-head coordination in monkeys. *Bibl. Ophthalmol.* **82**: 220-232.
33. BIZZI, E., R. E. KALIL & P. MORASSO. 1972. Two modes of active eye-head coordination in monkeys. *Brain Res.* **40**: 45-48.
34. BIZZI, E. 1975. Motor coordination: central and peripheral control during eye-head movement. In *Handbook of Psychobiology*. M. Gazzaniga & C. Blakemore, Eds.: 427-437. Academic Press, Inc. New York, N.Y.
35. MORASSO, P., E. BIZZI & J. DICHGANS. 1973. Adjustment of saccade characteristics during head movements. *Exp. Brain Res.* **18**: 492-500.
36. ABRAHAMS, V. C. 1970. Cervico-lumbar reflex interactions involving a proprioceptive receiving area of the cerebral cortex. *J. Physiol. London* **209**: 45-56.
37. ABRAHAMS, V. C. & P. K. ROSE. 1975. Projections of extraocular, neck muscle, and retinal afferents to superior colliculus in the cat: their connections to cells of origin of tectospinal tract. *J. Neurophysiol.* **38**: 10-18.
38. BERTHOZ, A. & R. LLINÁS. 1974. Afferent neck projections to the cat cerebellar cortex. *Exp. Brain Res.* **20**: 385-401.
39. DUBROVSKY, B. O. & H. BARBAS. 1975. Central projections of dorsal neck muscles. *Neurosci. Abstr.* **1**: 234.
40. WILSON, V. J., M. MAEDA & J. K. FRANK. 1975. Input from neck afferents to the cat flocculus. *Brain Res.* **89**: 133-138.
41. GREYSTY, M. & R. BAKER. 1976. Neurons with visual receptive field, eye movement and neck displacement sensitivity within and around the nucleus prepositus hypoglossi in the alert cat. *Exp. Brain Res.* **24**: 429-433.
42. ASTRUC, J. 1971. Corticofugal connections of area 8 (frontal eye field) in macaca mulatta. *Brain Res.* **33**: 241-256.
43. KÜNZLE, H. & K. AKERT. 1977. Efferent connections of cortical, area 8 (frontal eye field) in macaca fascicularis. A reinvestigation using autoradiographic technique. *J. Comp. Neurol.* **173**: 147-164.
44. COHEN, B. & J. SUZUKI. 1963. Eye movements induced by ampullary nerve stimulation. *Am. J. Physiol.* **204**: 347-351.
45. ROBINSON, D. A. 1968. The oculomotor control system: a review. *Proc. IEEE* **56**: 1032-1049.
46. REINHART, R. J. & B. L. ZUBER. 1969. Cellular activation patterns in the abducens nucleus during horizontal nystagmus in the cat. *Brain Res.* **15**: 284-287.
47. RON, S., D. A. ROBINSON & A. A. SKAVENSKI. 1972. Saccades and the quick phase of nystagmus. *Vision Res.* **12**: 2015-2022.
48. MARROCCO, R. T. 1978. Saccades induced by stimulation of the frontal eye fields: interaction with voluntary and reflexive eye movements. *Brain Res.* **146**: 23-34.
49. NAPIER, J. 1970. *The Roots of Mankind*. Smithsonian Institution Press. Washington, D.C.
50. DE BEER, G. R. 1947. How animals hold their heads. *Proc. Linn. Soc. London* **159**: 125-139.
51. SCHILLER, P. H., S. D. TRUE & J. L. CONWAY. 1979. Effects of frontal eye field and superior colliculus ablations on eye movements. *Science* **206**: 590-592.

ACOUSTIC-INDUCED EYE MOVEMENTS*

K.-P. Schaefer, K.-J. Stüss, and E. Fiebig

Neurobiology Unit
Department of Psychiatry
University of Göttingen
34 Göttingen, Federal Republic of Germany

INTRODUCTION

We close our eyes to block out a sound source in order to enjoy music in its absolute form. On the other hand, we open our eyes to visually perceive a sound source and to better identify it. Acoustically triggered attention-centering reactions allow recognition at times of danger and release defense and protection reflexes, which make the survival of the individual possible. The reflex character of the acoustically induced orientation reaction already has been demonstrated.^{12,17,36} The auditory organ seems to insure an acoustic spatial stability as well, which, due to autonomic and environmental conditions, makes possible the acoustic orientation and the reliable location of sound sources or acoustic targets in the surroundings.^{1,2,18,19,27,35} Hennebert describes acoustically induced tracking eye movements and speaks of a "nystagmus audiocinétique."¹⁵

As a result of these studies, voluntary tracking eye movements in response to moving acoustic signals have been studied more frequently in recent years.^{8,13,14,41-43} The investigations provide a valuable contribution to the understanding of directional hearing in the human being, which before mainly has been the object of psychophysical investigations (cf., References 9 and 16). These studies also offer information on the regulation of oculomotor activities in the open-loop situation and lead to the still unanswered question of whether, in response to acoustic signals, it is possible to differentiate eye movements into voluntary and involuntary categories.

The traditional controversy about the spatial character of the acoustic surroundings also can be proven by experimentation with animals (cf., Reference 9). A very illustrative example can be mentioned: when the optic tectum of the rabbit is stimulated, the immediate reaction is a turning of the ears in that direction of the surrounding field of vision from which the stimulus position is projected.^{22,28,29} With optokinetic and vestibular stimuli, not only does a nystagmus of the eyes occur, but an ear nystagmus also takes place simultaneously. Thereby the discharge patterns of the motor units of the ear muscles correspond to those of the neurons in the vestibular nucleus. These studies suggest that a multimodally organized substrate for the orientation reaction already exists in the brain stem. The ear nystagmus, which is demonstrable only in rudimentary form in human beings, emphatically indicates the maintenance of acoustic spatial stability in individual and environmental movements.

Directly inspired from such experimental studies with animals, we now have started to investigate more closely the influence of moving acoustic signals on the cortical, subcortical, and spinal motor functions in the human being. Thus, not

*This research was supported by the Deutsche Forschungsgemeinschaft (Sonderforschungsbereich 33).

only eye movements but also cortically evoked responses, as well as phase-synchronous body sway during standing, could be demonstrated by means of moving acoustic signals.^{5,8,10,24,30,34} Voluntary and involuntary acoustically induced eye movements, which represent only an exceptional case of general acoustic-motor reactions, will be discussed in more detail in the following.

METHODS

In routine clinical examinations (audiometry, auditory-evoked responses), the acoustic signals generally are applied via earphones. An exact localization of sound in space and the perception of audiokinetic phenomena, however, are possible only under natural conditions involving the effects of the acoustic shadow of the head, the sounding condition of the auricle, the outer acoustic duct, and other factors. The sound source can be moved around the test subject, or the test subject itself can move past the sound source. Moving acoustic signals also may be produced by electronic steering of several stationary loudspeakers (stereophonic listening, movement of a phantom). This method, which we prefer to use, has the advantage that moving acoustic signals may be applied in every imaginable form and at any speed.³⁴ For the release of acoustically evoked potentials, for example, very fast, ramplike sound movements are needed;⁵ whereas for the investigation of body sway, slow movements are essential (circular acoustic movements with periods of 1 to 10 seconds).²⁴ Comparative studies on the influence of actually moving sound sources and stereophonic movement effects are not yet concluded.

Whether in light or in darkness, the test subjects are placed in a screened room with little acoustic reflection and are seated on an electronically controlled swivel chair. Spontaneous head movements are prevented by leaning the head lightly against a headrest with slight fixation. The test subjects are requested either to look straight ahead with their eyes open and, as far as possible, "unpreoccupied" or else to follow the sound movement as closely as possible with their eyes. The test subjects were not informed as to the purpose of the experiment.

Moving acoustic signals are applied by means of 16 loudspeakers, which are arranged at a distance of 2 m around the test subject. The loudspeakers are controlled electronically, which allows the generation of moving pointlike acoustic signals in any form and at any speed in defined directions. The arrangement may be controlled either manually or by means of a laboratory computer (Lab 8/e).³⁴

The direct-current output from the oculogram is conducted by means of bitemporally applied adhesive electrodes. The signals are amplified by means of a high-resistance preamplifier mounted directly on the swivel chair and are conducted via ring contacts to the main amplifier (Tektronix AM 502) and recorded on an eight-channel 1/4-inch FM magnetic tape recorder. An electroencephalograph (EEG) is registered simultaneously to record the momentary state of activity of the subject. Additionally, the eye movements are observed repeatedly during the test with Frenzel glasses, and in some instances kinematographic evaluations are done.

After initial experiments with the application of certain sound qualities of different frequency and intensity, acoustic signals, generally with complex sound patterns, were selected [especially certain pieces of music and sound bursts of

short duration (50 mseconds), defined sound frequency (400 Hz), and random frequency of the sequence of the individual signals]. These allow an easy localization of the sound signals.⁷ The intensity of the signal generally is kept constant at about 70 dB above the sensation threshold. The computer-controlled standard program has a duration of about 30 minutes and provides for the application of square wave and sinusoidal stimuli with amplitudes of $\pm 15^\circ$ to $\pm 90^\circ$ and frequencies between 0.1 Hz and 2 Hz as well as circular sound movements (also with frequencies between 0.1 and 2 Hz). At the end of the test the subjects are questioned as to their subjective impressions.

VOLUNTARY EYE MOVEMENTS

Acoustically stimulated tracking eye movements, analogous to tracking eye movements repending to visual stimuli, can be differentiated into *voluntary* and *involuntary* components. Voluntary movements are described first since they may be performed by everyone.

In this context, it is important that the sound source is audible but remains unseen, i.e., the movement is transmitted solely by directional hearing. For the most part, the volume of the sound signal does not influence substantially the accuracy of the eye movements as long as the sound direction can, on the whole, be distinguished easily. This is parallel to optokinetic nystagmus, which, over large ranges of light intensity, may be observed easily and almost constantly.

In investigations done so far, there is excellent coincidence in that acoustically stimulated tracking eye movements do not consist of "smooth" movements, but rather of a sequence of saccades.^{8,13,14,41,43} They generally occur in steps and

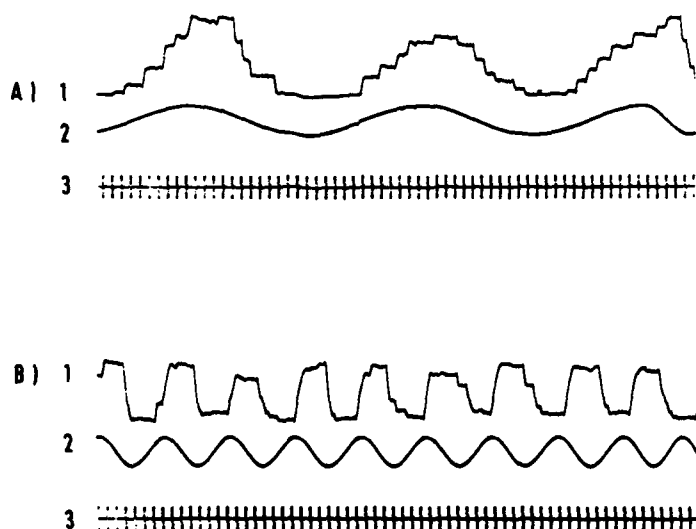


FIGURE 1. The patterns of eye movements depend on frequency of a sinusoidal moving acoustic target. (1) Eye position (calibration as in channel 2). (2) Target position (peak-to-peak, 30°); A - 0.2 Hz, B - 0.75 Hz. (3) Acoustic stimulus (5 Hz).

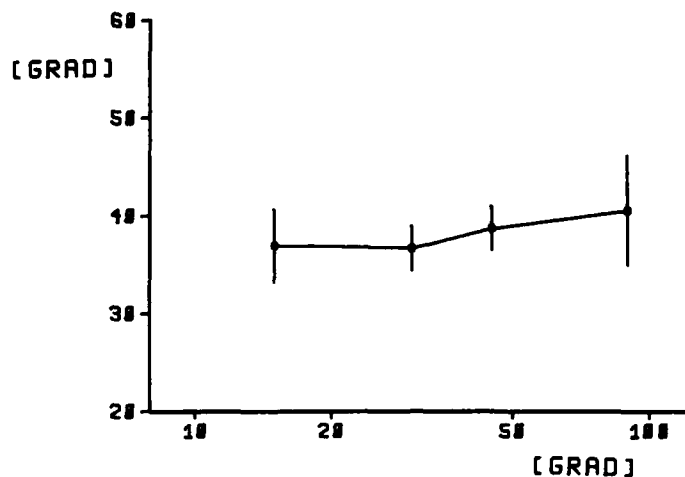


FIGURE 2. The amplitude of the eye movements is not a function of the amplitude of the sinusoidal moving acoustic target (0.1 Hz). Mean of seven subjects with standard deviation. Abscissa, target position; ordinate, eye position.

fail to show the typical form of nystagmus (with rapid and slow phases). However, slight drifting movements frequently may be observed between the individual steps.

The accuracy of the eye movements is poor when the amplitudes of the sound and eye movements are compared. Independent of whether the sound signals arrive at 15° or 90° from the lateral direction, the amplitudes of the eye movements lie at about 35° to 40° (FIGURES 1 and 2). These findings contradict the fact that human directional hearing is considerably more accurate since the localization threshold in the frontal median amounts to 1° to 3°. They agree, however, with other studies, which have demonstrated that voluntary eye movements in darkness also occur with a "preprogrammed amplitude" that almost corresponds to the maximal movement range of the eyes.⁴

On the other hand, the accuracy of the *phase relationship* between sound and eye movement is quite good. Sound and eye movements usually occur synchronously with sinusoidal movements of the signal at frequencies of 0.1 Hz to 1 Hz, which are the only frequencies considered here. Above 0.5 Hz, however, a phase lag of the eyes often may be observed (FIGURE 1). Conformity occurs between the sine movement of the sound and the saccadic eye movement, due to the fact that the characteristic points of the sinusoidal movement of the sound (i.e., the two reversal points and the zero culmination) are reached almost simultaneously. In this case, the eye movements are oriented towards the overall course of the sound movement. The eyes are thus regulated in a predictive manner, i.e., a tracking of the sound movement does not take place. Obviously, there is a prediction system, which is postulated also for visual tracking eye movements.^{32,33,37-40}

If instead of continuous sound (music), single acoustic signals with *stepwise increasing repetition rates* are presented during constant amplitude and frequency of sinusoidal sound-signal movements, then typical changes in the eye movements can be observed.^{10,11}

With individual signals (burst of 50 mseconds duration) presented at rates up to 0.2 Hz, temporary reactions towards the direction of each signal occur. The reaction time varies between 200 and 400 mseconds, while the amplitude is relatively constant at 35° to 40° , independent of the angle from which the sound signal arrives. In visually triggered ocular movements, acoustic-induced reactions frequently consist of two or several saccades.⁹ Following the reaction towards the sound signal, an additional slight drifting in the direction of the zero position often may be noticed. A few seconds later a spontaneous backward motion of the eyes takes place. At sound presentation frequencies of 0.2 Hz to 0.5 Hz, this backward motion no longer occurs and the eyes remain in the new position until the next sound signal becomes audible (FIGURE 3).

At sound presentation frequencies above 0.5 Hz—as well as with music—the eye movements consist of a continuous sequence of saccades. Now the eyes follow the course of motion of the sound signal and a reaction to individual signals no longer is observed. The transition into this stage is marked by a sudden rise in the frequency of the saccades, an increased occurrence of small saccades, and a slightly lowered sum of the amplitudes.

An additional variation of the frequency (between 0.1 Hz and 2 Hz) and amplitude (between $\pm 15^\circ$ and $\pm 90^\circ$) of the given sinusoidal movement of the sound signal demonstrates that the onset of continuous staircase eye movements instead of individual reactions does not depend solely on the repetition rate of transmitted burst signals. If the frequency of the sinusoidal movement is low (0.1 Hz) and the amplitude small ($\pm 15^\circ$), i.e., the sound movement is poorly discernible, more signals per sine period are needed to induce continuous staircase eye movements. The observed minimum number of 4 to 5 impulses may, under the given experimental conditions, increase to 10 signals per period (FIGURE 3).

On the other hand, with a low sine-wave frequency of 0.1 Hz, approximately 15 saccades per period occur. Above 0.5 Hz, however, only 2 to 3 saccades are the rule. Thus the minimum number of saccades that is necessary in order to be able to follow the given sine-wave movement already is attained. Accordingly, with higher movement frequencies, the eyes no longer are able to follow. These studies also reveal that the number of saccades per time unit remains practically constant under the given conditions.^{10,11}

Under the given experimental conditions, *smooth eye movements*, in the sense of visually triggered tracking eye movements, generally cannot be observed. Our own findings in this respect agree with the results of other authors.^{13,43} Only Gottschalk et al. cite the occurrence of smooth eye movements, which occurred only at 10° -per-second movements of the sound.¹⁴ According to Gauthier and Hofferer, these occur only when the moving sound source is made visible or the outstretched hand is made to trace the sound movement.¹³ On close scrutiny, however, slight drifting movements may be observed between the saccades, especially with strong deviation of the eyes. These often are opposed to the sound movement, and the eyes attempt to reach the middle position at a speed of 3° to 12° per second. Obviously, this is a case of drifting movements, which generally are observed in darkness and, according to Robinson, may be the evidence of a leaky integrator.^{4,20,21,25,26,31} Further investigations toward the explanation of this problem are required, especially since individual studies differ considerably in their methods. Zambarbieri et al. also hint at learning processes.⁴³ With the application of acoustic signals, one possibly must take into stronger consideration the characteristics of the acoustic modality as a method of sensory detection at a distance.

In the end, the question arises as to whether voluntary tracking movements

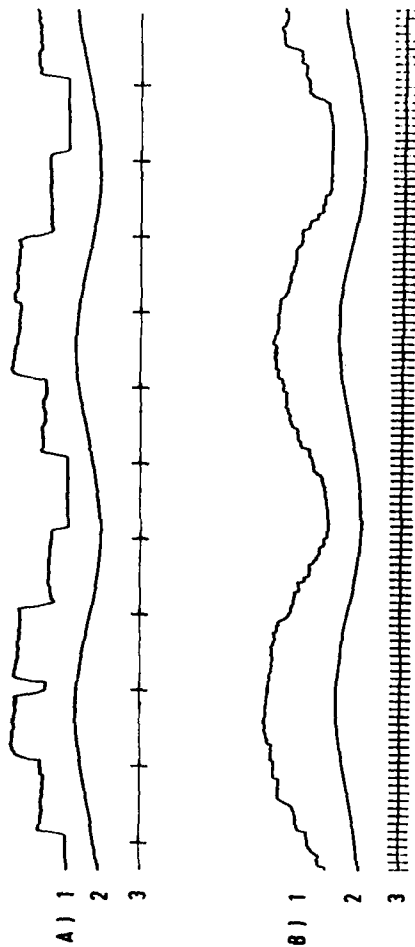


FIGURE 3. The patterns of eye movements depend on the repetition rate of the acoustic stimulus. (1) Eye position (calibration as in channel 2). (2) Acoustic-target position (peak-to-peak, 30°; 0.1 Hz). (3) Acoustic stimulus (A = 0.2 Hz; B = 2 Hz).

with acoustic signals have a *specific character* for this sense modality or if they are to be classified generally as "non-visually directed" eye movements. Voluntary eye movements, either in light or in darkness, that follow neither a visual nor an acoustic signal also lead to staircase saccadic eye movements. This type of eye movement also occurs when the eyes merely follow an imagined target. Comparative studies show that, at the most, changes in the frequency of the saccades and in the sum of the amplitudes may be observed. Moreover, these factors are dependent on the vigilance and concentration capability of the test subjects. Thus it seems more purposeful to ask whether moving acoustic signals are at all able to trigger an optomotor reaction, i.e., involuntary eye movements that render possible an acoustically regulated maintenance of the visual surroundings (FIGURE 4).

INVOLUNTARY EYE MOVEMENTS

In some test subjects, eye movements may be observed even though they do not voluntarily follow the moving sound signal but passively look straight ahead. The test subjects state that they notice these eye movements, but are unable to describe them in more detail. With prolonged exposure to moving acoustic signals, slight vertigo as well as vegetative signs (such as palpitation, dizziness, and outbreak of perspiration) are observable. Music and burstlike stimuli at varying frequencies are perceived as relatively pleasant and sine-wave sounds often are experienced as intolerable.^{8,30,34}

In a larger series of tests, we have, to date, systematically studied about 350

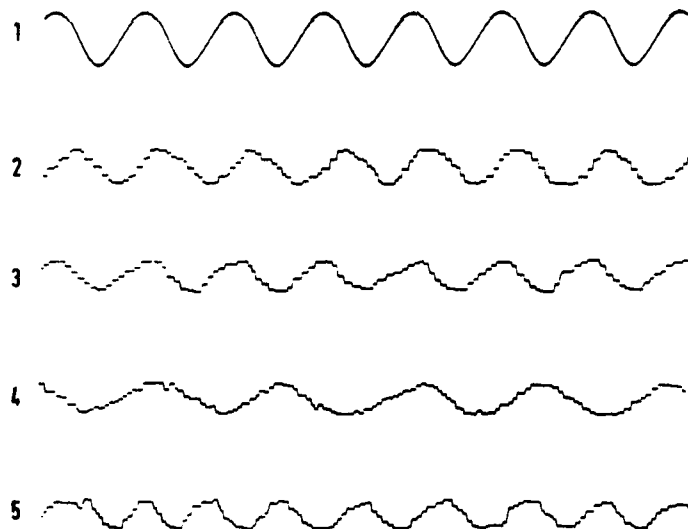


FIGURE 4. There are no differences between voluntary tracking of an acoustic target (2, 3) and the tracking of an imaginary target (4, 5) in light (2, 4) and darkness (3, 5). (1) Acoustic-target position (peak-to-peak, 90°; 0.2 Hz). (2-5) Eye position (calibration as in channel 1).

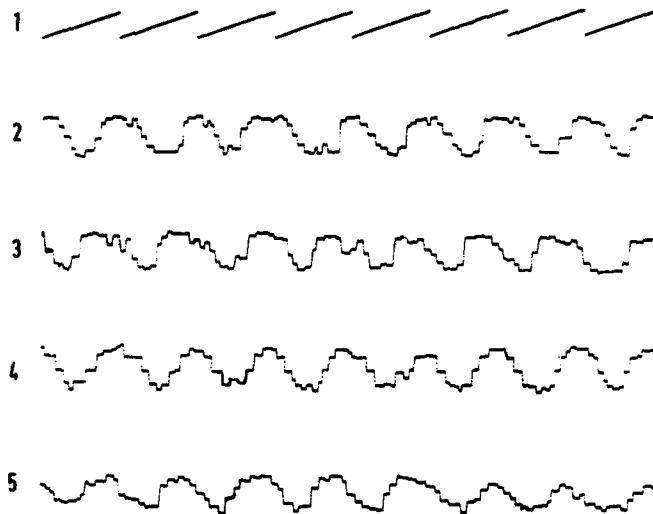


FIGURE 5. There are no differences between voluntary (2, 3) and involuntary (4, 5) tracking of an acoustic target in light (2, 4) and darkness (3, 5). (1) Acoustic-target position (circular movement; period, 5 seconds). (2-5) Eye position (peak-to-peak, 70-80°).

test subjects of different ages and both sexes. In the course of these studies, involuntary eye movements of different intensity could be observed in about 20% of all test subjects. They are more frequent in adolescents than in older persons and slightly more frequent in women than in men. They also could be observed frequently in members of pop music groups. Certain parts of the personality structure (such as immaturity, hysterical structure, and extroversion, among others) seem to play a role, and possibly a minimal cerebral dysfunction comes into consideration as a cause. These factors currently are under investigation.

With few exceptions, acoustically induced eye movements occur only when fixation is impossible, i.e., in darkness or behind Frenzel glasses. Even in darkness, acoustically induced eye movements may be reduced or suppressed by fixation on a point of light or on an imaginary object. Continuous tracking movements, in the sense of smooth movements, generally cannot be observed. Nystagmuslike movement patterns do not occur either, as might be expected by Hennebert or Lackner.^{15,18,19} According to our own observations, it is a question of saccadic movements of the eyes in the direction of the sound movement. Corresponding to voluntary eye movements, the involuntary eye movement may be best characterized as staircase jerks. Slight intersaccadic drifting only occasionally can be observed, either in the direction of the sound movement or, with stronger deviation of the eyes, in the direction of the median plane (FIGURE 5).

Thus, involuntary eye movements in response to moving acoustic signals do not differ (in the form of their oculogram) from the voluntary eye movements described above, or show only minimal gradual differences in regard to the number of saccades and amplitude sum. The speed of the saccades has not yet been studied in detail.^{3,43} Moreover, from the oculogram alone, it often cannot be

decided whether the eye movements are voluntary or involuntary. As already mentioned, the pursuit of an inaudible or merely imaginary moving acoustic signal is accompanied by very similar eye movements. Also with the introduction of sound signals (with increasing frequency of the individual bursts, as described above), no differences result. Involuntary eye movements with a continuous sequence of saccades also occur with a sequence of individual signals presented at a frequency of about 1 Hz. It is not always easy, even for the test subject, to differentiate between passive and active eye movements.

For these reasons it is useful to write a simultaneous EEG as an objective criterion for the momentary condition of the test subject. For this purpose, the *continuous fast Fourier transform* of short individual epochs of 4 to 8 seconds has proven appropriate. Upon being requested to actively follow the moving sound signal, there is an immediate disappearance of the alpha-wave components. As a sign of passive-reflectory activity, it can be demonstrated impressively that the alpha-wave component of the power spectrum does not change when involuntary eye movements are performed at different movement frequencies of the sound (between 0.1 and 2 Hz) (FIGURE 6).

By using a computer-regulated standard program with ramplike, square, sinusoidal, and circular movement around the test subject, involuntary pursuit eye movements could be differentiated in more detail. They may follow the given sound movement in loose or rigid coupling. During the course of the test, they may decrease quickly, become adapted, occur only at certain frequencies of the periodic sound movement in isolated cases, or be present during a prolonged period of time without a relapse until the test subject becomes fatigued.

With *square-wave sound movements* at an amplitude of $\pm 45^\circ$, the eyes generally follow with individual saccadic jerk movements, the amplitude of the eye movements closely corresponding to that of the sound movement. With larger sound movements of $\pm 90^\circ$, the eye-movement amplitudes are only negligibly larger, as they have reached their physiological limit. In some of the test subjects, using careful direct-current recording, a slight drifting of the eyes into the zero position can be observed at low-frequency sound movements of 0.1 Hz. Under the stated conditions, tracking eye movements can be observed up to a sound-movement frequency of close to 1 Hz. Under these experimental conditions, the latency periods of the involuntary eye movements range between 100 and 200 mseconds.

Using *sinusoidal sound movements* with an amplitude of $\pm 45^\circ$ and a frequency of 0.1 Hz, staircase jerks occur in the oculogram, and generally four to six saccades occur with an intersaccadic interval of about 800 mseconds. The amplitudes of these staircase jerks frequently do not surpass 10 to 20°, resulting in a total amplitude of about 60°. With sinusoidal sound movements of $\pm 90^\circ$, a somewhat stronger saccadic response occurs and the total amplitude scarcely surpasses $\pm 45^\circ$. At 0.1 Hz, the saccades in the lateral field of vision decrease, until the eyes are arrested in the lateral position. At a sound-movement frequency of 0.5 Hz and under the same conditions, staircase jerks occur only sporadically and the main characteristics of the oculogram are square-wave movements. At 1 to 2 Hz, the highest tracking frequency is reached (FIGURE 7).

Staircase jerks also can be observed with slow circular movements of 0.1 Hz. In the frontal visual field, the sound movement causes 8 to 10 jerks with amplitudes of between 6 and 10°. Often, the saccadic response occurs with larger amplitudes, and then the total amplitude always amounts to about 80°. When the sound traverses the posterior field, the saccades appear in the visual direction, even though the sound moves behind the test subject. But now the tracking eye

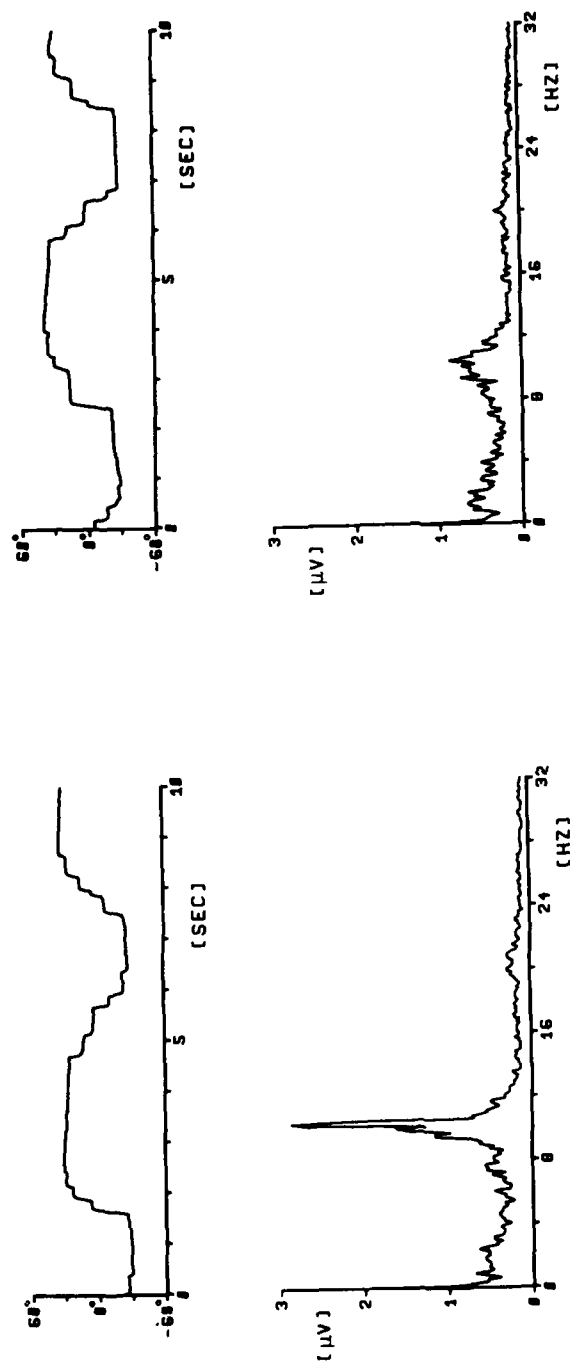


FIGURE 6. In contrast to the eye movements (upper curves), the power spectra of the EEG (lower curves) show a significant difference between involuntary (left curves) and voluntary (right curves) tracking of an acoustic target. During voluntary tracking, the alpha component of the power spectrum is attenuated.

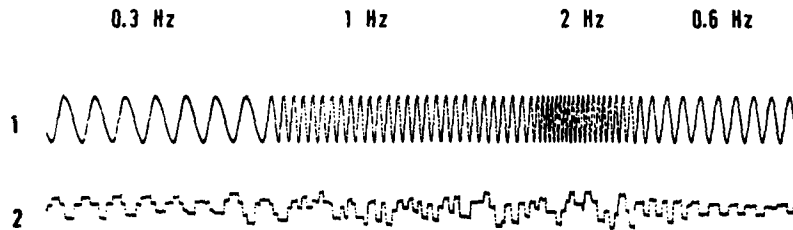


FIGURE 7. Up to target-movement frequencies of 1 Hz, synchronous eye movements are seen. (1) Acoustic-target position (peak-to-peak, 180°). (2) Involuntary eye movement (calibration as in channel 1).

movements are characterized by a few large saccades, generally occurring before the sound reaches the rear median. Higher angular velocities of the sound, i.e., higher rotation frequencies, again lead to the disintegration of the staircase jerks. Large-amplitude saccades of about 70° appear to take their place, which, to a certain extent, can be characterized as genuine counterjerks.

Involuntary eye movements also show relatively constant amplitudes, which almost correspond to the physiological maximum of $\pm 40^\circ$. At larger sound movements of $\pm 90^\circ$, the eyes rest in the end position until the sound movement returns to the beat field (Schlagfeld). This results in a "plateau formation" in the oculogram. The amplitudes of the saccades at low angular velocities (e.g. sound movements of 0.1 Hz) are very small. At larger angular velocities, staircase jerks become more prominent at first; later on, however, they dissolve and turn into pure counterjerks. This phenomenon also is observed with circular movements, although the test subjects no longer are able to locate subjectively the sound during a circulation frequency of 1 Hz. Circular movements also are interesting in respect to the fact that the sound periodically moves behind the test subject and thus is no longer in the area of the field of vision. Even in this phase, lively eye movements occur, as is shown in FIGURE 8. These, however, show a beat direction opposite to that found when the movement is in front. This leads to alternating staircase jerks, which lack a uniform direction of rotation in conformity with the sound movement. After sudden interruption of the sound rotation, there are therefore no postrotatory aftereffects, as with optokinetic and vestibular stimuli.

GENERAL DISCUSSION

The present investigations with moving acoustic signals show that the acoustic system transmits not only directional hearing, but also movement hearing, i.e., besides certain intensity and duration differences, differential effects that result from a change in the position of a sound source also are taken into consideration.

In this context, the investigations with individual sound-signal bursts of increasing repetition rate have not only a neurophysiological but also a psychophysical and a cybernetic aspect. Corresponding to the investigations with individual light stimuli,^{33,37-39} a transition into a continuous answering pattern occurred at approximately 1 Hz. This finding again is in agreement with psychophysical studies, according to which the subjective impression of a moving

continuum (acoustic phi-phenomenon) results from the application of individual acoustic signals at approximately 1 Hz. The dependence of the eye movements on the number of individual impulses per movement period also leads to a cybernetic conclusion: according to this, the repetition rates must be higher than the Nyquist frequency (twice the frequency of the sinusoidal movement of the acoustic target) to avoid aliasing. With repetition rates at least five times higher than the movement frequency, the eye movements correspond to the original target movement. Moreover, according to the present investigations, a predictive system must exist, which already has been postulated in a similar form for visually induced eye movements.^{33,37-39}

Furthermore, it should be stressed that the voluntary tracking eye movements in response to acoustic signals do not correspond to the familiar smooth movements in connection with visual pursuit of a slowly moving point of light. Additionally, the involuntary acoustically induced tracking movements do not

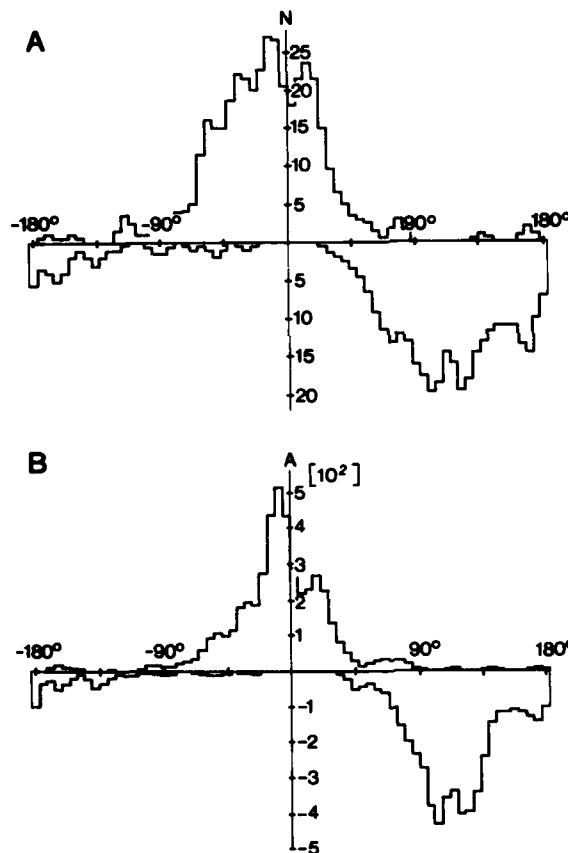


FIGURE 8. Number (A) and amplitude sum (B) of the saccades depend on the position in the circular movement of the acoustic target (average of 100 cycles, $t = 8$ seconds). Frontal median, 0° ; dorsal median, 180° . Number and amplitude sum maxima are seen near the frontal median and near 130° .

resemble the optokinetic nystagmus, as might be expected from Hennebert's term "nystagmus audiokinétique."¹⁵ Voluntary and involuntary acoustically induced eye movements usually consist of single or repeated rapid jerk movements that are carried out in the direction of the sound movement and cannot be considered as correction saccades. Occasional intersaccadic drifting movements resemble neither the actual smooth movements nor the slow nystagmus phases in either form or velocity.

In contrast to visually induced tracking eye movements, voluntary and involuntary acoustically induced tracking eye movements cannot be distinguished in an oculogram. Only in borderline situations, e.g., at high-frequency sinusoidal movements of the sound source, does the dynamic power of the "reflectory" component show an increased accuracy and only a very slight exhaustion of the eye movements. The described movement patterns, as already mentioned, are not to be seen as specific acoustically induced eye movements since they also occur in other voluntary eye movements without visual or acoustic fixation. Obviously, the open-loop situation in the acoustic test must be held responsible for the fact that the voluntary motor functions can make use of a previously developed movement pattern (e.g., from peripheral feedback) without restrictions, so that voluntary and involuntary acoustically induced tracking eye movements are identical.

Under the chosen experimental conditions, however, involuntary acoustically induced eye movements have been observed only in relatively few test subjects. Neither the reasons responsible for this phenomenon nor the physiologically or psychologically accessible individual properties essential for the release of involuntary acoustically induced eye movements could be ascertained. This might be the reason why this very interesting phenomenon of acoustically induced eye movements hitherto has not met with much interest in the clinic. For the present, acoustically induced eye movements render possible the investigation of numerous new problems, such as monaural directional hearing, directional hearing in vertical planes, intermodal interactions involving other sensory systems, and others that hitherto have been accessible only to psychophysical investigation.

SUMMARY

This article reports the influence of moving acoustic signals on eye movements (oculomotor functions) using 350 healthy test subjects. An acoustic test setting developed especially for this purpose has made possible the application of moving acoustic signals of varying frequency and form (square stimuli, sinusoidal stimuli, circular movements), as well as the examination of visual-acoustic and vestibular-acoustic interactions.

It must be stressed that according to these investigations, both voluntary and involuntary eye movements can be demonstrated in response to moving acoustic signals. Involuntary eye movements, however, under the given experimental conditions, only are observed in about 20% of all test subjects and their frequency of occurrence is highest in young female subjects. They are most pronounced in darkness and when there is no fixation, and they can be coupled to varying degrees with the given acoustic signal.

Voluntary and involuntary eye movements do not differ very much from one another. They consist mainly of a series of saccades that form staircase jerks. In both cases, no typical smooth movements or nystagmoid movement forms

occur—which are predominant in tracking eye movements of visual stimuli. Occasionally, slight drifting movements can be demonstrated in the intersaccadic intervals. At a larger movement amplitude and increased movement frequency of the sound signal, pure opposite jerks finally appear, which follow up to a movement frequency of 1 Hz. The eye movements are influenced only slightly by a change in the amplitude of the sound movement ($\pm 15^\circ$ to $\pm 90^\circ$). However, a close phase relationship between eye and sound movement exists. If instead of continuous acoustic signals (music), single burst signals are given at an increasing repetition rate, this results (at low repetition rates of bursts) in orienting reactions upon the individual signals, while at high signal repetition rates (above 0.5 Hz), continuous eye movements in the form of staircase jerks result.

In investigating acoustically induced tracking eye movements, many new questions have arisen that previously have been open only to psychophysical studies.

REFERENCES

1. ARNOULT, M. D. 1950. Post-rotatory localization of sound. *Am. J. Psychol.* **63**: 229-236.
2. ARNOULT, M. D. 1952. Localization of sound during rotation of the visual environment. *Am. J. Psychol.* **65**: 48-58.
3. BECKER, W. & F. FUCHS. 1969. Further properties of the human saccadic system; eye movements and correction saccades with and without visual fixation points. *Vision Res.* **9**: 1247-1259.
4. BECKER, W. & H. M. KLEIN. 1973. Accuracy of saccadic eye movements and maintenance of eccentric eye positions in the dark. *Vision Res.* **13**: 1021-1034.
5. BEMMER, J. 1980. Kortikale evozierte Potentiale auf bewegte akustische Signale. Medical Dissertation. University of Göttingen. Göttingen, Federal Republic of Germany.
6. BUIZZA, A., A. LÉGER, A. BERTHOZ & R. SCHMID. 1979. Otolithic-acoustic interaction in the control of eye movement. *Exp. Brain Res.* **36**: 509-522.
7. CHRISTIAN, W. & D. RÖSER. 1957. Ein Beitrag zum Richtungshören. *Z. Laryngol. Rhinol.* **36**: 431-445.
8. DAUB, W. 1978. Formen und Vorkommen akustisch induzierter Augenbewegungen. Medical Dissertation. University of Göttingen. Göttingen, Federal Republic of Germany.
9. ERULKAR, S. D. 1972. Comparative aspects of spatial localization of sound. *Physiol. Rev.* **52**: 237-360.
10. FIEBIG, E. 1979. Über Form und Genauigkeit willkürlicher Augenfolgebewegungen auf bewegte akustische Signale. Medical Dissertation. University of Göttingen. Göttingen, Federal Republic of Germany.
11. FIEBIG, E., K.-J. SÜSS & K.-P. SCHAEFER. 1979. Ocular movements in response to sinusoidal movements of an intermittently active sound source in humans. *Pfluegers Arch. Suppl.* **379**: R54.
12. FRÖSCHELS, E. 1930. Über einen durch Schallreiz ausgelösten Augenmuskelreflex. *Z. Hals Nasen Ohrenheilkd.* **26**: 511-520.
13. GAUTHIER, G. M. & J. M. HOFFERER. 1976. Eye movements in response to real and apparent motions of acoustic targets. *Percept. Mot. Skills* **42**: 963-971.
14. GOTTSCHALK, C., O. J. GRÜSSER & M. LINDAU. 1978. Tracking movements of the eyes elicited by auditory stimuli at a constant angular velocity. *Pfluegers Arch. Gesamte Physiol. Menschen Tiere* **377**: R46.
15. HENNEBERT, P. E. 1960. Nystagmus audiocinétiq. *Acta Otolaryngol.* **51**: 412-415.
16. HOWARD, J. P. & W. B. TEMPLETON. 1966. Human Spatial Orientation. John Wiley & Sons. London, New York, Sydney & Toronto.
17. JELLINEK, A. 1933. Experimentelle Beiträge zur Lokalisation der akustischen Stellreflexe. *Pfluegers Arch. Gesamte Physiol. Menschen Tiere* **232**: 116-119.

18. LACKNER, J. R. 1974. Influence of visual rearrangement and visual motion on sound localization. *Neuropsychologia* 12: 291-293.
19. LACKNER, J. R. 1977. Induction of illusory self-rotation and nystagmus by a rotating sound field. *Aviat. Space Environ. Med.* 48: 129-131.
20. MATIN, L., E. MATIN & D. G. PEARCE. 1970. Eye movements in the dark during the attempt to maintain a prior fixation position. *Vision Res.* 10: 837-857.
21. MEYER, D. L., D. BONNEMANN & K.-P. SCHAEFER. 1973. Equalization of asymmetries of tonus in the optomotor system of rabbits. A study on oculomotor neurons. *Exp. Brain Res.* 18: 505-511.
22. MEYER, D. L., K.-P. SCHAEFER & A. WINKELMANN. 1972. Single unit response of rabbit ear muscles to postural and accelerative stimulation. *Exp. Brain Res.* 14: 118-126.
23. MILLS, A. W. 1958. On the minimum audible angle. *J. Acoust. Soc. Am.* 30: 237-246.
24. NEETZ, A., K.-J., SÜSS & K.-P. SCHAEFFER. 1980. Influence of moving acoustic sound sources on body balance. *Pfluegers Arch. Suppl.* 384: R24.
25. RASHBASS, C. 1961. The relationship between saccadic and smooth tracking eye movements. *J. Physiol.* 159: 326-338.
26. ROBINSON, D. A. 1964. The mechanics of human saccadic eye movement. *J. Physiol.* 174: 245-264.
27. RYAN, T. A. & P. SCHEHR. 1941. The influence of eye movement and position on auditory localization. *Am. J. Psychol.* 54: 243-252.
28. SCHAEFER, K.-P. 1970. Unit analysis and electrical stimulation in the optic tectum of rabbits and cats. *Brain Behav. Evol.* 3: 222-240.
29. SCHAEFER, K.-P., D. SCHOTT & D. L. MEYER. 1975. On the organization of neuronal circuits involved in the generation of the orientation response [visual grasp reflex]. *Fortschr. Zool.* 23(1): 199-212.
30. SCHAEFER, K.-P. & K.-J. SÜSS. 1977. Eye movements induced by acoustic stimuli. *Electroencephalogr. Electromyogr.* 8: 226.
31. SKAVENSKI, A. A. & R. M. STEINMANN. 1970. Control of eye position in the dark. *Vision Res.* 10: 193-203.
32. STARK, L. 1968. *Neurological Control Systems—Studies in Bioengineering*. Plenum Press. New York, N.Y.
33. STARK, L., G. VOSSIUS & L. R. YOUNG. 1962. Predictive control of eye tracking movements. *IRE Trans. Hum. Factors Electron.* 3: 52-57.
34. SÜSS, K.-J. & K.-P. SCHAEFER. 1979. Moving acoustic sound sources; techniques and applications. *Pfluegers Arch. Suppl.* 382: R49.
35. THOMAS, G. J. 1941. Experimental study of the influence of vision on sound localization. *Am. J. Psychol.* 28: 163-177.
36. TULLIO, D. & S. CANOVA. 1933. Ricerche comparative sopra la stimolazione calorica, elettrica, rotatoria, chimica e sonora del labirinto acustico. *Oto-Rino-Laringol. Ital.* 3: 466-482, 543-576.
37. VOSSIUS, G. 1965. Der kybernetische Aspekt der Willkürbewegung. *Prog. Biocybernetics* 2: 111-140.
38. WESTHEIMER, G. 1954. Eye movements in response to a horizontally moving visual stimulus. *AMA Arch. Ophthalmol.* 52: 932-941.
39. WESTHEIMER, G. & D. W. CONOVER. 1954. Smooth eye movements in the absence of moving visual stimulus. *J. Exp. Psychol.* 47: 283.
40. YOUNG, L. R. 1977. Pursuit eye movement. What is being pursued? *Dev. Neurosci.* 1: 29-36.
41. ZAHN, J. R., L. A. ABEL & L. F. DELL'OSSO. 1978. Audio-ocular response characteristics. *Sensory Processes* 2: 32-37.
42. ZAHN, J. R., L. A. ABEL, L. F. DELL'OSSO & R. B. DAROFF. 1979. The audio-ocular responses: intersensory delay. *Sensory Processes* 3: 60-65.
43. ZAMBARBIERI, D., R. SCHMID, C. PRABLANC & G. MAGENES. Characteristics of eye movements induced by the presentation of acoustic targets. (In press.)

MODIFICATIONS OF VESTIBULAR NYSTAGMUS PRODUCED BY FIXATION OF VISUAL AND NONVISUAL TARGETS*

R. Schmid, D. Zambambieri, and G. Magenes

*Institute of Computer and Systems Science
University of Pavia
27100 Pavia, Italy*

INTRODUCTION

The modifications of vestibular nystagmus due to fixation of visual targets largely have been investigated in both normals and patients. When the subject is presented with a visual target rotating with him, both the slow and fast phases of nystagmus are suppressed and the eyes maintain the central position. In normals, a complete suppression of nystagmus occurs over a range of head angular accelerations up to $50^\circ/\text{second}^2$.¹ When the subject is oscillated in the frequency range around 0.1 Hz in front of a space-stationary visual target, the nystagmoid pattern of eye movement observed in darkness is replaced by a smooth eye movement that fully compensates head rotation in spite of the 0.4 to 0.6 gain of the vestibulo-ocular reflex (VOR) in the dark.^{2,3}

What role does the smooth-pursuit (SP) system play in such modifications of the vestibulo-ocular response?

Conceptually, the following mechanism easily can be imagined. When the subject rotates with a visual target moving with him, the eye deviation induced by the vestibular stimulation produces a retinal slip of target image, and the SP system commands an eye movement that cancels the vestibular component. In contrast, when the subject is made to oscillate in front of a space-stationary visual target, the retinal slip produced by incomplete VOR compensation forces the SP system to cooperate up to a complete visual stabilization. There are at least two arguments that seem to support this point of view. First, the frequency range of optimal fixation suppression is very similar to that of SP.^{4,5} Second, deficits in fixation suppression or in full compensation of head rotation are found only in patients who also present impaired SP and optokinetic nystagmus.^{1,6,7}

The arguments against an exclusive role of SP in fixation suppression are even more numerous. First of all, a complete suppression of nystagmus can be obtained also during vestibular stimulations that would bring about slow-phase velocities far beyond the possibility of the SP system. Second, nystagmus suppression can be produced during the first 100 mseconds of transient responses, when the SP has no time to intervene due to its latency of 130 mseconds.^{2,8} Third, a progressive suppression of nystagmus also can be observed during vestibular habituation produced by repeated step changes in head angular velocity in the dark.^{9,10} Last but not least, significant modifications of rotatory vestibular nystagmus can be produced by fixation of imaginary targets.² If the target is imagined to move with the subject, the gain of the vestibulo-ocular response is reduced to about 0.3. If the target is imagined to remain stationary in space, the fast phase of nystagmus tends to disappear and the gain of the

*Work supported by the Italian National Research Council, CNR, Rome, Italy.

compensatory eye movement becomes close to unity. In spite of the extremely low gain of the otolith-ocular reflex in the dark, significant compensatory eye movements (gain of 0.3 to 0.5) also can be observed during lateral displacements, if the subject is asked to maintain the fixation of a space-stationary imaginary or acoustic target.¹¹

All these latter arguments seem to indicate that nystagmus suppression is obtained through a direct control of VOR gain rather than through a contribution of SP. The possibility of controlling VOR gain and even changing its sign has been proved by experiments on VOR adaptation to reversed-vision conditions.¹²⁻¹⁴ As suggested by Ito and by Robinson, the vestibulocerebellovestibular pathway passing through the Purkinje cells of the flocculus could be the anatomic support for such a VOR-gain control.^{15,16} As a matter of fact, a primary role of the flocculus in fixation suppression has been proved by studies on Purkinje cell activity during combined visual and vestibular stimulations, by the loss of visual suppression of nystagmus after experimental flocculus lesions, and by the clinical observation that deficits in fixation suppression are particularly prominent in patients with cerebellar lesions.^{1,6,7,17-22}

The aim of this paper is to investigate further the modifications of vestibular nystagmus produced by the presentation of nonvisual targets either stationary in space or moving with the subject. Imaginary, proprioceptive, and acoustic targets were used. A quantitative-model interpretation of the experimental results provided useful suggestions on the respective roles of VOR-gain control and SP in adapting the vestibulo-ocular response to the actual oculomotor task.

METHODS

Three different groups of five subjects with normal visual, vestibular, and auditory functions were used for the following experimental situations.

A. Nystagmus Suppression during Sinusoidal Head Oscillations

The subject was seated in a rotatory chair (POLMAN Digital 1) provided with a special arm supporting a loudspeaker and a small lamp (80 cm from the subject's eyes). The subject had his head secured by a restraining device and was made to rotate sinusoidally about the vertical axis with the eyes open in the dark. After 5 cycles of chair oscillation, during which the subject performed mental arithmetic, a click was produced by the loudspeaker, and the subject had to maintain the fixation of an imaginary target placed in front of him and moving with him. When a second click was produced at the end of the 10th cycle, the subject had to fixate at the thumb of his right hand lying on his knee. At the end of the 15th cycle, the loudspeaker was switched on and fed with pulses at 20 Hz. The subject had to maintain the fixation of the sound source. Finally, at the end of the 20th cycle, the sound was replaced by the light of the small lamp.

This testing procedure was repeated twice in different sessions with different parameters of chair oscillation: 0.05 Hz and peak amplitude of 320° (peak angular velocity of 100°/second); 0.1 Hz and peak amplitude of 120° (peak angular velocity of 75°/second). The same peak velocity of 100°/second used at 0.05 Hz could not be maintained at 0.1 Hz due to power limitation of the chair motor. Vestibular habituation during sinusoidal oscillations in this range of frequencies can be excluded.¹²

Calibration of eye movement was made before and after each test.

B. Suppression of Postrotational Nystagmus

The subject was accommodated in the rotatory chair as in situation A. After calibration of eye movement, the chair was accelerated at $1^\circ/\text{second}^2$ to reach a velocity of $120^\circ/\text{second}$. This velocity was maintained for three minutes. Then the chair was stopped (braking time of two seconds).

Four postrotational tests of this type were executed on each subject of this group on different days. In the first test, no fixation task was given to the subject. In the second test, the loudspeaker was switched on 10 seconds after the chair stop and then switched off after 5 seconds. In the third test, the lamp was switched on and off in the same way. In the last test, the room was illuminated for 5 seconds starting 10 seconds after the chair stop.

Since repetition of postrotational stimuli can produce vestibular habituation, suppression of postrotational nystagmus by fixation of imaginary or proprioceptive targets was not examined.^{9,10}

C. Fixation of Space-Stationary Visual and Nonvisual Targets during Sinusoidal Head Oscillations

The subject was accommodated in the rotatory chair as in situations A and B. After calibration of eye movement, the chair was made to rotate sinusoidally at 0.2 Hz with a peak amplitude of 30° . As in situation A, every 10th cycle of chair oscillation, the subject had to perform a new task. The sequence was mental arithmetic in the dark, fixation of an imaginary target, fixation of an acoustic target, and fixation of a visual target, all fixed in space.

The calibration of eye movement was repeated at the end of the test.

Eye-Movement Recording and Data Processing

Eye movements were recorded by d.c. electro-oculography (EOG) through bitemporal leads on the outer canthi. Eye-position and chair-position signals were displayed simultaneously on a polygraph and stored on a magnetic tape. After A/D conversion, EOG data were processed on a digital computer by using a special interactive program.²³ The amplitude, duration, and mean velocity (SPV) of the slow phase of each nystagmus beat were computed. By removing the fast components of nystagmus and fitting together the slow phases,³ the slow cumulative eye position (SCEP) also was reconstructed.

The eye movement recorded in situations A and C during the first cycle following each transition from one experimental condition to the next was not considered in the analysis.

The gain of a response was defined and computed as the ratio between the mean amplitude of SCEP over several cycles and the amplitude of the corresponding chair rotation. This measure of the gain seems to be, a priori, more correct than that given by the ratio between eye and chair peak velocities, except for VOR responses in darkness for which the two measures should be the same. Actually, as far as we know at present, a role of SP cannot be excluded in either nystagmus suppression or full compensation. If SP does play a role, it is likely that its contribution will depend nonlinearly on the value of the ongoing nystagmus SPV. Thus, the gain computed from the response peak velocity will provide a measure of nystagmus suppression or full compensation only in the worst condition concerning SP contribution (maximal difference between SPV

and desired eye velocity). On the contrary, the gain computed from SCEP will provide a more comprehensive measure of the process.

RESULTS

Typical nystagmic responses recorded while the subject was performing mental arithmetic (MA) in the dark during sinusoidal head oscillations at 0.05 and 0.1 Hz are shown in the first records of FIGURES 1 and 2.

In all the subjects examined, the reversal of nystagmus direction occurred almost in phase with the reversal of chair motion, and the compensatory slow-phase eye movement was phase opposite to head movement. The amplitude of nystagmus beats was modulated sinusoidally, with the largest beats occurring when chair velocity reached its maximal values. The number of beats per half a period of chair oscillation was almost the same in the two directions of nystagmus and did not vary significantly among the subjects (mean value of 28 ± 3 at 0.05 Hz and 14 ± 2 at 0.1 Hz). When the subject was presented with a fixation target moving with him, the nystagmic response underwent significant

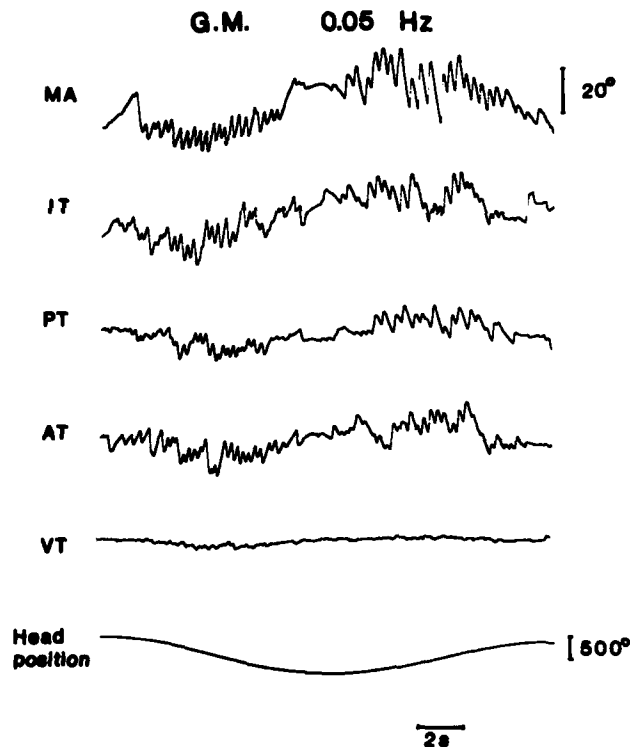


FIGURE 1. Nystagmus suppression during sinusoidal head oscillations at 0.05 Hz with a peak amplitude of 320° . MA, mental arithmetic in the dark; IT, imaginary target; PT, proprioceptive target; AT, acoustic target; VT, visual target. Targets were moving with the subject. The last record gives head angular position.

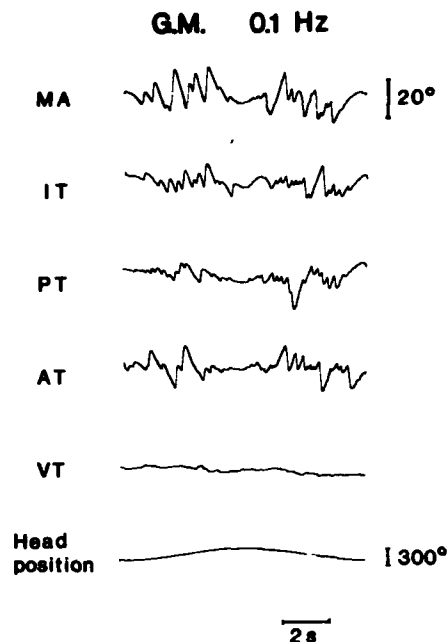


FIGURE 2. Nystagmus suppression during sinusoidal head oscillations at 0.1 Hz with a peak amplitude of 120° . Notations are as in FIGURE 1.

modifications. A complete suppression of nystagmus was observed only when a visual target was presented (records VT in FIGURES 1 and 2). When the subject was asked to maintain the fixation of a nonvisual target—either imaginary (IT), proprioceptive (PT), or acoustic (AT)—the most noticeable modification of nystagmus upon eye inspection of it was a general reduction of nystagmus-beat amplitude. Few beats of large amplitude similar to those recorded in the dark could be observed only during the periods of highest chair velocity, as though the subject were losing temporarily the capability of suppressing nystagmus.

In order to quantify this observation, histograms of beat amplitudes were computed by considering the total number of beats in four periods of chair oscillation for different experimental situations. A typical picture is shown in FIGURE 3, which refers to one subject oscillated at 0.05 Hz. The number of beats per half a period of chair oscillation did not vary significantly from one experimental condition to another (darkness and different fixation conditions). In contrast, remarkable changes were found in the amplitude distribution. A strong concentration toward the small amplitudes could be observed when a fixation target was given to the subject. In the case shown in FIGURE 3, the percentage of beats with amplitude of less than 6° was only 44 when the subject was performing mental arithmetic in the dark, and it doubled when the subject was trying to keep the fixation of a nonvisual target, regardless of the type of target.

Computer analysis of the responses revealed other differences. FIGURE 4 shows the diagrams of the slow cumulative eye position constructed from the responses in FIGURE 1. In the fixation condition, there is a remarkable decrease of

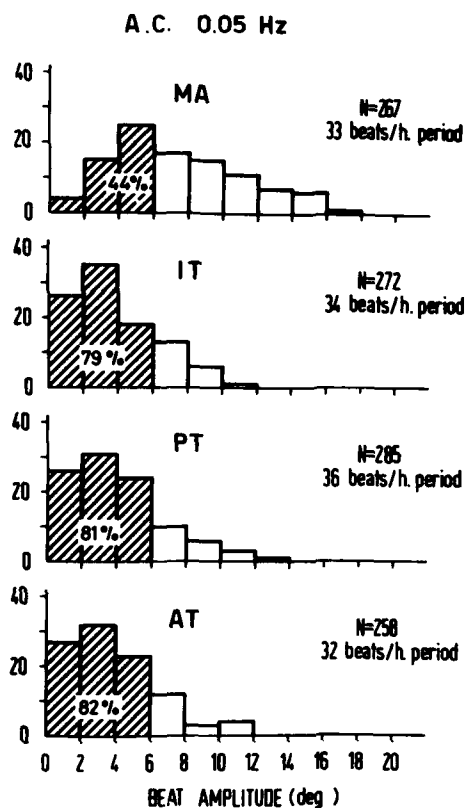


FIGURE 3. Histograms of nystagmus beat amplitude computed from the total number (N) of beats in four periods of chair oscillation for different experimental situations. The frequency of chair oscillation was 0.05 Hz, and the peak amplitude 320° .

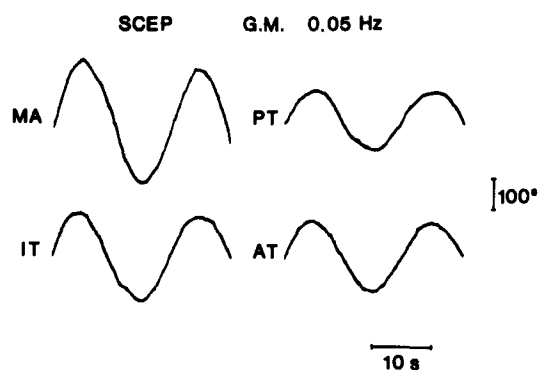


FIGURE 4. Diagrams of the slow cumulative eye position (SCEP) constructed from the responses in FIGURE 1.

SCEP peak amplitude. The decrease was greater when the subject was presented with a real (proprioceptive or acoustic) than with a virtual (imaginary) nonvisual target.

The mean values (five subjects) of the ratio between the average peak amplitude of SCEP over four periods and the peak amplitude of chair rotation (gain) are reported in FIGURE 5 for the two examined frequencies. Standard deviations also are reported. There is a slight decrease of gain from the lower to the upper frequency in all the experimental situations. The mean gains in MA, IT, PT, and AT conditions were 0.54, 0.40, 0.32, and 0.34 at 0.05 Hz and 0.48, 0.34, 0.27, and 0.32 at 0.1 Hz respectively. The difference between the values observed at the two frequencies might depend simply on the fact that the chair movement was programmed for a given amplitude of rotation at the examined frequency,

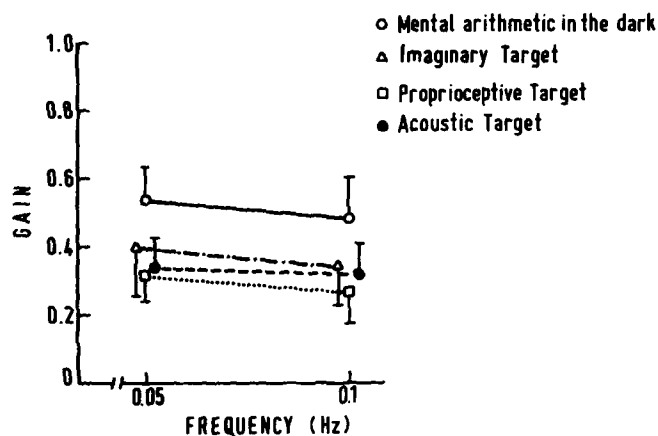


FIGURE 5. Mean values and standard deviations of the gain computed as the ratio between the average peak amplitude of SCEP over four periods and the peak amplitude of chair rotation for the two examined frequencies.

but the real amplitude of chair rotation depended on the subject's weight. The influence of subject's weight obviously is greater, the higher the frequency.

It also is worth reporting that the gains computed from peak SPV in fixation conditions were slightly greater in general than the corresponding gains computed from peak SCEP.

At the end of the sinusoidal suppression tests, the subjects reported the following sensations. When a visual target was presented, a stable vision of it could be maintained almost throughout the cycle of chair oscillation. Only during short periods corresponding to the highest chair velocities did the vision of the lamp become blurred. When a nonvisual target was presented, the subjects felt unable to keep the fixation of it until the chair approached its reversal position. A good fixation was thought to be maintained for a short period during and after chair reversal, and then suddenly was lost. The subjects felt that they had to wait for each new reversal of the chair in order to achieve fixation.

These sensations were perfectly consistent with the characteristics of the recorded responses. Also, because of a previous finding by our group that nystagmus suppression by fixation of an acoustic target was much more effective if the target was presented before the start of chair motion, we wondered whether nystagmus suppression by fixation of nonvisual targets can be initiated only if the target is presented during periods of low eye velocity.

In order to investigate this point, experiments in the form of situation B were conceived. The target (visual or acoustic) was presented 10 seconds after the chair stop in postrotational tests of $120^\circ/\text{second}$. Although postrotational responses are characterized by a great variability concerning both their gain and their time course, a value of SPV ranging from 30 to $50^\circ/\text{second}$ could be assumed present at the time of target presentation. The target was maintained for only 5 seconds, during which the SPV in the dark normally decreases by about 20%. The target then was made to disappear in order to investigate a further point: Does the response immediately return to the normal pattern in the dark or does it remain influenced by the existence of a previous period of suppression?

Typical results are reported in FIGURES 6 and 7. FIGURE 6 shows the eye movements recorded before, during, and after the period of fixation, which corresponds to the interval delimited by the two asterisks. The first four diagrams in FIGURE 7 show the time course of nystagmus SPV computed from the same responses. Each dot gives the mean slow-phase velocity of a nystagmus beat. The first record in FIGURE 6 and diagram 1 in FIGURE 7 refer to the postrotational test performed in the dark without any fixation period. The second record in FIGURE 6 and diagram 2 in FIGURE 7 were obtained from the fixation test performed with

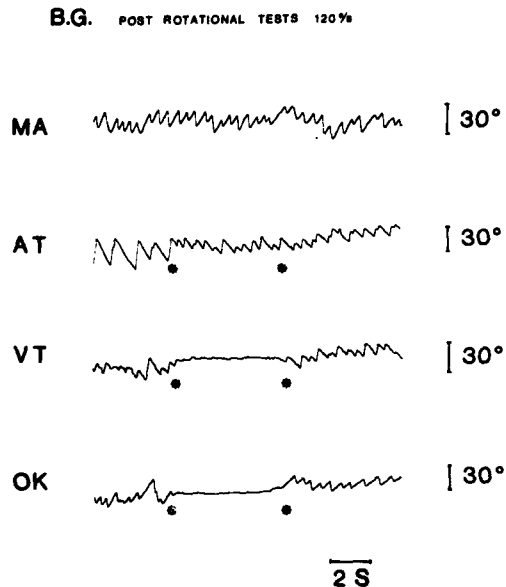


FIGURE 6. Eye movement recorded before, during, and after the period of fixation in the postrotational tests referred to as situation B in the methods section. The period of fixation is delimited by two asterisks.

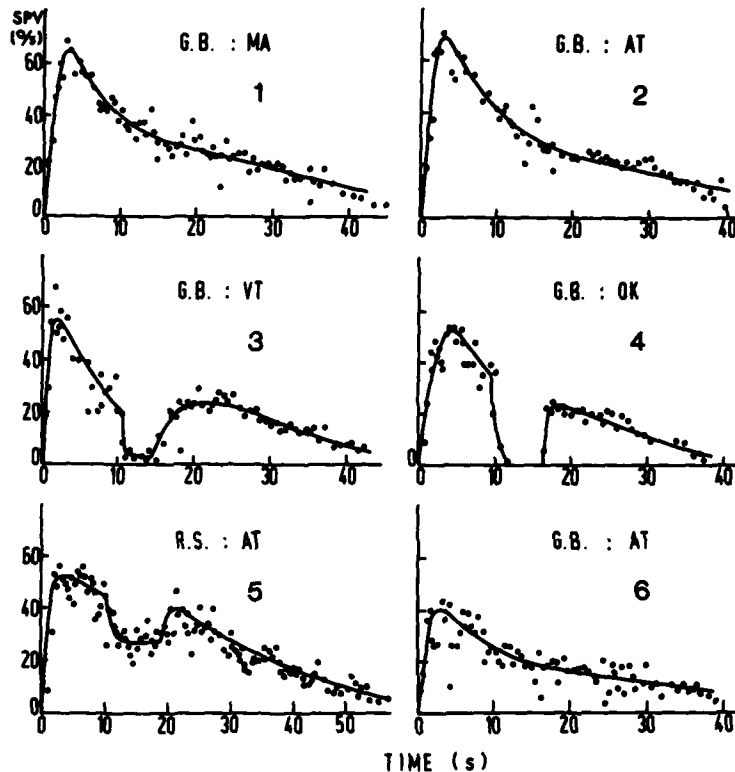


FIGURE 7. Time course of nystagmus slow-phase velocity (SPV) in the postrotational tests. Each dot gives the mean slow-phase velocity of a nystagmus beat. Diagrams 1 to 4 were obtained from the responses in FIGURE 6 (subject G.B.). Diagram 5 was obtained from a different subject, who presented an appreciable nystagmus suppression during the presentation of the acoustic target. Diagram 6 was obtained from the response recorded from subject G.B. during a postrotational test performed with an acoustic target presented 10 seconds before the chair stop and maintained for 25 seconds. Diagram 6 should be compared with diagram 2.

an acoustic target. In this subject and in three other subjects of this group, fixation of an acoustic target presented after the chair stop produced only a change in beat amplitude but no significant variations in nystagmus SPV. In only one subject, AT fixation produced an appreciable depression of nystagmus SPV, but no aftereffect could be observed (diagram 5 in FIGURE 7).

Nystagmus suppression became much more powerful if the acoustic target was presented before the chair stop. Diagram 6 in FIGURE 7 shows the time course of SPV in a postrotational response recorded in this condition. The target was presented 10 seconds before the chair stop and was maintained for 25 seconds. Diagram 6 should be compared with diagram 2 of the same figure. They both were obtained from the same subject.

The fixation of a small lamp produced an almost complete suppression of the postrotational response in all subjects (record 3 in FIGURE 6 and diagram 3 in FIGURE 7). Typically, when the lamp was switched off, the response returned immediately to its normal values of SPV, with a possible small overshoot.

The overshoot disappeared if the light in the room was switched on rather than the small lamp (diagram 4 in FIGURE 7). Except for the response of one subject, which remained clearly depressed after the light was switched off, the responses of the remaining subjects were such as to prevent any definite conclusion about the existence of an aftereffect.

Let us finally consider the results obtained when the subject was made to oscillate at 0.2 Hz in front of a target (visual, imaginary, or acoustic) fixed in space. As shown in FIGURE 8, a full compensation of head rotation could be

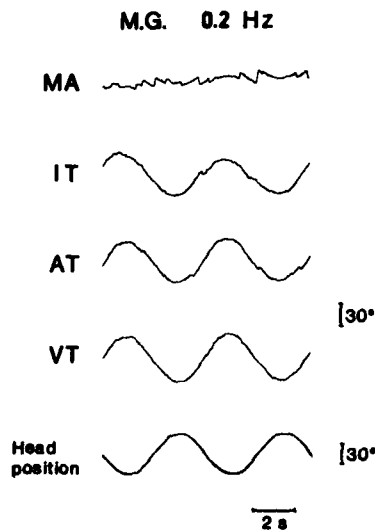


FIGURE 8. Eye movement recorded while the subject was made to oscillate in the dark at 0.2 Hz with no fixation target (record MA) and in front of an imaginary target (record IT), an acoustic target (record AT), or a visual target (record VT) fixed in space. The peak amplitude of chair oscillation was 30°.

obtained only when the subject was presented with a visual target (record VT). The fixation of a nonvisual target (imaginary or acoustic) made the fast phase of nystagmus disappear almost completely, but the gain of the remaining smooth eye movement was slightly less than unity. In some subjects, not as skillful as the one considered in FIGURE 8, compensatory saccades sometimes occurred in the response. In these cases, the gain of the response was computed by combining only the smooth portions of eye movement, as for nystagmus in the dark. The mean values of the gain and its standard deviations (five subjects) were 0.56 ± 0.08 with mental arithmetic in the dark without fixation, 0.84 ± 0.06 with fixation of an imaginary target, 0.88 ± 0.07 with fixation of the acoustic target, and 1.0 with fixation of the visual target.

DISCUSSION

The results reported in this paper confirm a previous finding that vestibular nystagmus can be modified strongly by fixation of nonvisual targets either moving with the subject or fixed in space.^{2,24} Since no smooth pursuit of moving nonvisual targets can be produced by untrained subjects stationary in space,^{25,26} one would be led to conclude that the smooth-pursuit system does not play any significant role in the observed modifications of the vestibulo-ocular response.

As a matter of fact, the results of Lisberger and Fuchs on Purkinje cell (P-cell) activity in the flocculus during nystagmus suppression indicate the existence of a neural circuit different from the SP system and able to control VOR gain.^{17,18} Actually, two components were found in P-cell activity: a head-velocity component and an eye-velocity component, which are linearly additive. The first component is provided by vestibular mossy fibers probably originating from the vestibular nerve or nucleus. The second component, which leads to a modulation of P-cell firing rate that is correlated with eye velocity and uncorrelated with retinal-error velocity, clearly is present during SP eye movements but is not provided by the visual system. It has been suggested that this component reaches the flocculus through a corollary discharge pathway, bringing about an efference copy of eye velocity.^{17,18}

Since the flocculus exerts an inhibitory action on interneurons in the brain-stem VOR pathways, the following mechanism of VOR gain control has been proposed.^{17,18} During head rotation in the dark, the head-velocity and eye-velocity components of P-cell activity are equal and opposite, and they cancel each other; then the inhibition normally exerted by the flocculus on the VOR is not modulated, and the VOR keeps the gain of 0.4 to 0.6 observed in the dark. During nystagmus suppression by fixation of a visual target moving with the subject, the eye-velocity component is zero and the head velocity component passes through the flocculus, reaches the brain-stem interneurons, and inhibits the VOR pathways, the gain of which is maintained equal to zero. During the fixation of a visual target stationary in space, the eye-velocity component of P-cell activity is larger than the head-velocity component. A disinhibition of VOR thus would take place, and VOR gain is increased from 0.4-0.6 to unity.

There is no doubt that such a mechanism of VOR control is able to maintain its gain close to zero or close to unity depending on whether the subject is fixating at a target moving with him or remaining stationary in space during head rotation. The same mechanism also would help the SP system when a stationary subject has to track a moving target. Nevertheless, if the flocculus is able to sustain nystagmus suppression or full compensation, some other system should intervene to initiate this process. In the case of visual target fixation, this role is likely to be played by the SP system.

When the subject is rotated in front of a visual target moving with him, the eye deviation induced by the vestibular stimulation produces a retinal slip, which activates the SP system. The neural command generated by this system then will reduce eye velocity and provoke an imbalance between the head-velocity and eye-velocity components of P-cell activity. The first component would become predominant, and the flocculus inhibition on the VOR would be increased. The eye velocity then will decrease further, and this positive reaction will go on until eye velocity is reduced to zero. Once initiated by the SP system, the same positive reaction will bring the gain of the compensatory eye movement up to unity in the case of fixation on visual targets fixed in space. Does SP merely initiate these

processes or does it also participate in sustaining them? A contribution of SP in steady-state conditions cannot be excluded, as the partial leak of nystagmus suppression at high head angular velocities seems to indicate.

Nevertheless, the major role of SP in steady-state conditions rather would be that of contrasting any deviation of the eyes from the desired position. Due to the adaptation of VOR gain by the flocculus, the SP system is made to work with small retinal-slip velocities and therefore in the range of high gain of its nonlinear characteristic. In this condition, the SP system constitutes an extremely sensitive mechanism that reacts strongly to the occurrence or to any increase of retinal slip.

If it is the SP system that initiates nystagmus suppression or full compensation, how can the results reported in this paper for fixation of nonvisual targets be explained?

Smooth tracking of nonvisual targets is absent almost completely in untrained subjects remaining stationary in space.^{25,26} According to the perceptual feedback hypothesis, smooth-pursuit movements can be produced whenever the central nervous system (CNS) is provided with enough sensory motion information to generate a continuous reference signal to the SP system.^{27,28} It therefore could be concluded that nonvisual systems are unable to provide such an amount of sensory information.

What happens when the CNS receives both proprioceptive and acoustic information about target position and vestibular information about the subject's head rotation? It has been suggested that the motion information provided by the vestibular system can integrate extr vestibular, nonvisual sensory information in such a way as to make a weak SP possible.^{11,29} If this actually is the case, the results reported in this paper can be given a simple interpretation.

To be more specific let us make reference to the block diagram in FIGURE 9, which shows the main pathways involved in oculomotor control. Head angular velocity ($\dot{\theta}_H$) is perceived by the semicircular canals (SCC), which send a measure ($\dot{\theta}_H^*$) of it to the vestibular nuclei (VN) and to the P-cells of the flocculus (Fl). The VOR is completed by the monosynaptic and polysynaptic pathways reaching the oculomotor nuclei through the brain stem, where a neural integrator (I) is located.¹⁶ VOR gain is modulated by the P-cells of the flocculus, which make a linear algebraic addition of the head-velocity signal $\dot{\theta}_H^*$ and the efference copy $\dot{\theta}_E^*$ of eye velocity provided by a corollary discharge pathway.¹⁷ The output of the flocculus is sent to inhibit interneurons in the brain stem VOR pathways. K is a gain factor. Since a vestibular signal still is present in the VN during nystagmus suppression,^{30,31} the inhibitory projections from the flocculus are represented as reaching the brain stem beyond the VN.

A central reconstructor (CR) receives visual information from the retina and nonvisual information from other sensory systems (proprioceptive, acoustic, and vestibular systems). The CR also should receive an efference copy of eye velocity.²⁷ In turn, the CR sends a velocity reference signal $\dot{\theta}_R$ to the smooth-pursuit system (SP Syst.). The output of this system is integrated by the brain-stem integrator I, which is likely to be the same for all the oculomotor pathways.¹⁶ Then the signal reaches the oculomotor nuclei.

Full-field stimulations of the retina also activate the optokinetic system (OK Syst.), which is depicted in FIGURE 9 according to a previous model proposed by Schmid *et al.*^{32,33} One optokinetic pathway reaches the VN and contains a storage mechanism (SM).³⁴⁻³⁷ A second optokinetic pathway reaches the central integrator without passing through the VN.³⁸ This second pathway mainly would be

activated by the stimulation of the central part of the retina and also could be considered as a part of the SP system.³²

How does the system in FIGURE 9 work in the different experimental conditions examined in this paper?

Let us first consider the case of small-visual-target fixation during head rotation. Since the optokinetic system is not involved, the model in FIGURE 9 can be simplified as in FIGURE 10. Retinal-slip velocity, $\dot{\theta}_{RS}$, is obtained as the difference between target velocity, $\dot{\theta}_{VT}$, and absolute eye velocity ($\dot{\theta}_E + \dot{\theta}_H$). K_{SP} represents the open-loop gain of the SP system. In the case of visual-target fixation, a high value of K_{SP} , greater than 10, can be assumed at least for small retinal-slip velocities.

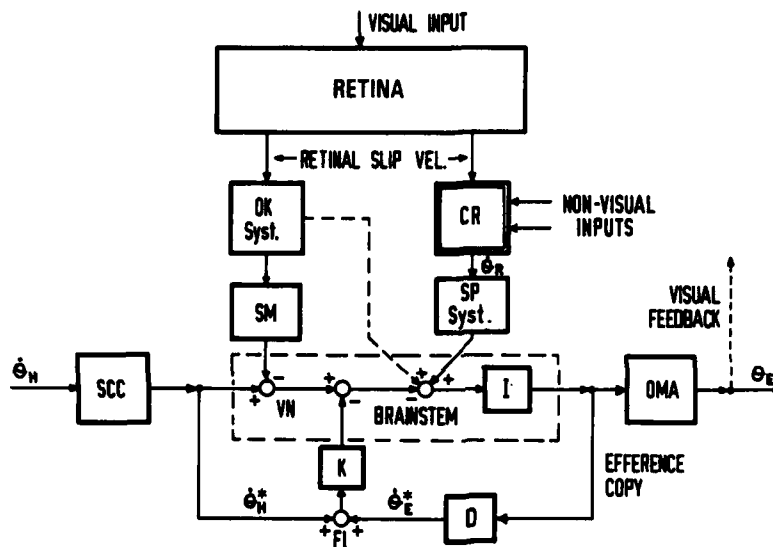


FIGURE 9. Block diagram of the major pathways involved in oculomotor control. CR, central reconstructor of target motion; D, derivator; FI, flocculus; I, central neural integrator; OK Syst., optokinetic system; OMA, oculomotor apparatus; SCC, semicircular canals; SM, storage mechanism; SP Syst., smooth-pursuit system; VN, vestibular nuclei; $\dot{\theta}_E$, eye position in the head; $\dot{\theta}_E$, eye velocity in the head; $\dot{\theta}_E^*$, efference copy of eye velocity; $\dot{\theta}_H$, head angular velocity; $\dot{\theta}_H^*$, head-velocity signal; $\dot{\theta}_R$, reference signal to the SP system; K, gain of the inhibitory cerebellovestibular pathway.

Let $K_V = 0.6$ be the gain of the peripheral vestibular system at the frequencies considered in our sinusoidal tests. In the dark, $\dot{\theta}_{RS} = 0$ and $\dot{\theta}_E = -\dot{\theta}_H$. Then $K_V = 0.6$ also will be the VOR gain in this condition. Conceptually, there is no difference if the gain of 0.6 actually is distributed along the vestibulo-ocular pathways.

When the subject is presented with a visual target moving with him, this results in $\dot{\theta}_{VT} = \dot{\theta}_H$ and $\dot{\theta}_{RS} = -\dot{\theta}_E$. Then the SP system initiates nystagmus suppression. At steady state, the ratio between eye velocity $\dot{\theta}_E$ and head velocity

$\dot{\theta}_H$ (gain of the vestibulo-ocular response) is given by

$$g_s = \frac{K_V}{1 + [K_{SP}/(1 - K)]}$$

where K is the gain of the flocculus inhibitory pathway. By assuming $K_{SP} = 10$ and $K = 0.8$, this results in $g_s = 0.01$. A complete suppression of nystagmus therefore is predicted. At steady state, the SP system would contribute to nystagmus suppression by only 12%.

When the subject is presented with a visual target fixed in space, this results in $\dot{\theta}_{VT} = 0$ and $\dot{\theta}_{RS} = -(\dot{\theta}_H + \dot{\theta}_E)$. If the VOR gain is less than 1, a retinal slip takes place, which forces the SP system to contribute to full compensation of head rotation. At steady state, the gain $g_c = \dot{\theta}_E/\dot{\theta}_H$ is given by

$$g_c = \frac{(1 - K)K_V + K_{SP}}{1 - K + K_{SP}}$$

By giving the parameters the same values as in the preceding case, this results in $g_c = 0.99$. The steady-state SP contribution to full compensation is only 8%.

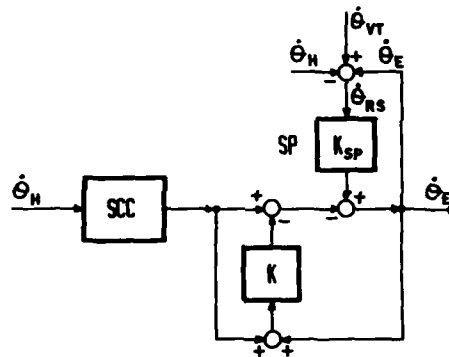


FIGURE 10. Model of visual-vestibular interaction during fixation of small visual targets. SCC, SP, K , $\dot{\theta}_H$, and $\dot{\theta}_E$, as in FIGURE 9. K_{SP} , gain of the smooth-pursuit system; $\dot{\theta}_{RS}$, retinal-slip velocity; $\dot{\theta}_{VT}$, absolute visual-target velocity.

In the case of nonvisual targets, an extremely low value of K_{SP} can be assumed to account for the difficulty of the CR in producing an appropriate signal to the SP system.

By assuming $K_{SP} = 0.2$, this results in $g_s = 0.3$ and $g_c = 0.8$, respectively. These values of the gain are close to those observed experimentally. The steady-state SP contribution is negligible in both conditions of fixation.

Let us finally make a short comment on the results obtained in the postrotational test. Due to the high values of the vestibular component of eye movement during the whole period of target presentation, it reasonably can be expected that the central reconstructor is unable to provide a reference signal to the SP system unless visual information on target motion is provided. The absence of suppression in most of the tests performed with the presentation of an acoustic target after the chair stop thus would be justified.

If the acoustic target is presented before the chair stop, it is likely that a weak reference signal to the SP system can be generated during the first instants of the response, when nystagmus SPV still is small (particularly in our experiments, where the braking time was two seconds). Suppression thus would be triggered, then to be sustained by flocculus inhibition of the VOR. In any case, this important point must be investigated further, probably by using more suitable patterns of stimulation.

The absence of any aftereffect at the end of the presentation of a small target is not surprising, since no storage mechanism is likely to exist in the SP system. On the contrary, when the light was switched on in the room and a full-field optokinetic stimulation was provided to the subject, the storage mechanism in the optokinetic pathway reaching the VN should have been charged. Its later discharge after the return to the dark then would maintain a depressed nystagmus SPV. This fact could not be observed in our results as clearly as in the results of other authors, who used a different profile of chair velocity.³⁶

In conclusion, the results reported in this paper and their quantitative-model interpretation indicate that the main role of the SP system in nystagmus suppression and in full compensation is that of initiating both these processes. At steady state, its contribution is small although not completely absent.

Nystagmus suppression or full head-movement compensation is sustained almost exclusively by an appropriate control of VOR gain through a modulation of the inhibition exerted by the flocculus.

This conclusion is perfectly consistent with the neurophysiological evidence of a participation of flocculus P-cells in nystagmus suppression and with the results of a previous analysis by Barr et al. on voluntary nonvisual control of the human vestibulo-ocular reflex.^{2,17,18} Finally, the model in FIGURE 9 can provide a good reference for the interpretation of SP and nystagmus-suppression deficits in cerebellar and extracerebellar patients.^{1,6,7}

REFERENCES

1. DICHGANS, J., G. M. VON REUTERN & U. RÖMMELT. 1978. Impaired suppression of vestibular nystagmus by fixation in cerebellar and noncerebellar patients. *Arch. Psychiatr. Nervenkr.* **226**: 183-199.
2. BARR, C. C., L. W. SCHULTHEIS & D. A. ROBINSON. 1976. Voluntary, non-visual control of the human vestibulo-ocular reflex. *Acta Otolaryngol.* **81**: 365-375.
3. MEIRY, J. L. 1971. Vestibular and proprioceptive stabilization of eye movements. In *The Control of Eye Movements*. P. Bach-y-Rita & C. C. Collins, Eds.: 483-496. Academic Press, Inc. New York, N.Y.
4. FENDER, D. H. & P. W. NYE. 1961. An investigation of the mechanism of eye movement control. *Kybernetik* **1**: 81-88.
5. SÜNDERHAUF, A. 1960. Untersuchungen über die Regelung der Augenbewegungen. *Klin. Monatsbl. Augenheilkd.* **136**: 837-852.
6. ZEE, D. S., R. D. YEE, D. G. COGAN, D. A. ROBINSON & W. K. ENGEL. 1976. Ocular motor abnormalities in hereditary cerebellar ataxia. *Brain* **99**: 207-234.
7. MIRA, E., E. MEVIO, P. ZANOCCHI & P. CASTELNUOVO. 1981. Impaired suppression of vestibular nystagmus by fixation of visual and acoustic targets in neurological patients. *Ann. N.Y. Acad. Sci.* (This volume.)
8. ROBINSON, D. A. 1965. The mechanics of human smooth pursuit eye movement. *J. Physiol.* **180**: 569-591.
9. JEANNEROD, M., M. MAGNIN, R. SCHMID & M. STEFANELLI. 1976. Vestibular habituation to angular velocity steps in the cat. *Biol. Cybernet.* **22**: 39-48.
10. CLÉMENT, G., J. H. COURJON, M. JEANNEROD & R. SCHMID. 1981. Unidirectional

- habituation of vestibulo-ocular responses by repeated rotational or optokinetic stimulations in the cat. *Exp. Brain Res.* **42**: 34-42.
11. BUIZZA, A., A. LÉGER, A. BERTHOZ & R. SCHMID. 1979. Otolithic-acoustic interaction in the control of eye movement. *Exp. Brain Res.* **36**: 509-522.
 12. GONSHOR, J. H. & G. MELVILL JONES. 1973. Changes of human vestibulo-ocular response induced by vision reversal during head rotation. *J. Physiol.* **234**: 102P.
 13. GONSHOR, A. & G. MELVILL JONES. 1976. Extreme vestibulo-ocular adaptation induced by prolonged optical reversal of vision. *J. Physiol.* **256**: 381-414.
 14. ROBINSON, D. A. 1976. Adaptive gain control of vestibuloocular reflex by the cerebellum. *J. Neurophysiol.* **5**: 954-968.
 15. ITO, M. 1972. Neural design of the cerebellar motor control system. *Brain Res.* **40**: 81-84.
 16. ROBINSON, D. A. 1975. Oculomotor control signals. In *Basic Mechanisms of Ocular Motility and Their Clinical Implications*. G. Lennerstrand & P. Bach-y-Rita, Eds.: 337-374. Pergamon Press, Oxford, England.
 17. LISBERGER, S. G. & A. F. FUCHS. 1977. Role of the primate flocculus in smooth pursuit eye movements and rapid behavioral modifications of the vestibulo-ocular reflex. *Dev. Neurosci.* **1**: 381-389.
 18. LISBERGER, S. G. & A. F. FUCHS. 1978. Role of primate flocculus during rapid behavioral modifications of vestibulo-ocular reflex. I. Purkinje cell activity during visually guided horizontal smooth-pursuit eye movements and passive head rotation. *J. Neurophysiol.* **41**: 733-763.
 19. TAKEMORI, S. & B. COHEN. 1974. Loss of visual suppression of vestibular nystagmus after flocculus lesions. *Brain Res.* **72**: 213-224.
 20. COURJON, J. H. 1978. Role du cervelet dans la compensation visuelle d'un déficit labyrinthique. Doctoral Thesis. Université Claude Bernard, Lyon, France.
 21. HART, C. W. 1967. Ocular fixation and the caloric test. *Laryngoscope* **77**: 2103-2114.
 22. ALPERT, J. N. 1974. Failure of fixation suppression: a pathological effect of vision on caloric nystagmus. *Neurology* **24**: 891-896.
 23. BUIZZA, A., R. SCHMID, A. ZANIBELLI, E. MIRA & P. SEMPLICI. 1978. Quantification of vestibular nystagmus by an interactive program. *ORL* **40**: 147-159.
 24. TAKAHASHI, M., T. UEMURA & T. FUJISHIRO. 1980. Studies of the vestibulo-ocular reflex and visual-vestibular interactions during active head movements. *Acta Otolaryngol.* **90**: 115-124.
 25. GAUTHIER, G. & J. M. HOFFERER. 1976. Eye tracking of self-moved targets in the absence of vision. *Exp. Brain Res.* **26**: 121-139.
 26. ZAMBARBIERI, D., R. SCHMID, C. PRABLANC & G. MACENES. 1980. Characteristics of eye movements induced by the presentation of acoustic targets. *Prog. Oculomotor Res.* (In press.)
 27. YASUI, S. 1974. Nystagmus generation, oculomotor tracking and visual motion perception. Ph.D. Dissertation. Massachusetts Institute of Technology, Cambridge, Mass.
 28. YOUNG, L. R. 1977. Pursuit eye movement—What is being pursued? *Dev. Neurosci.* **1**: 29-36.
 29. BUIZZA, A., R. SCHMID & J. DROULEZ. 1980. Influence of linear acceleration on oculomotor control. *Prog. Oculomotor Res.* (In press.)
 30. KELLER, E. L. & P. D. DANIELS. 1975. Oculomotor related interaction of vestibular and visual stimulation in vestibular nucleus cells in alert monkey. *Exp. Neurol.* **46**: 187-198.
 31. BUETTNER, U. W. & U. BÜTTNER. 1979. Vestibular nuclei activity in the alert monkey during suppression of vestibular and optokinetic nystagmus. *Exp. Brain Res.* **37**: 581-593.
 32. SCHMID, R., D. ZAMBARBIERI & R. SARDI. 1979. A mathematical model of the optokinetic reflex. *Biol. Cybernet.* **34**: 215-225.
 33. SCHMID, R., A. BUIZZA & D. ZAMBARBIERI. 1980. A non-linear model for visual-vestibular interaction during body rotation in man. *Biol. Cybernet.* **36**: 143-151.
 34. ALLUM, J. H. J., W. GRAF, J. DICHGANS & C. L. SCHMIDT. 1976. Visual-vestibular interactions in the vestibular nuclei of the goldfish. *Exp. Brain Res.* **28**: 463-485.

35. ROBINSON, D. A. 1977. Linear addition of optokinetic and vestibular signals in the vestibular nuclei. *Exp. Brain Res.* 30: 447-450.
36. WAESPE, W. & V. HENN. 1979. Motion information in the vestibular nuclei of alert monkeys: visual and vestibular input versus optomotor output. In *Reflex Control of Posture and Movements*. R. Granit & O. Pompeiano, Eds.: 683-693. Elsevier/North-Holland. Amsterdam, the Netherlands.
37. RAPHAN, T., B. COHEN & V. MATSUO. 1977. A velocity-storage mechanism responsible for optokinetic nystagmus (OKN), optokinetic after-nystagmus (OKAN), and vestibular nystagmus. *Dev. Neurosci.* 1: 37-47.
38. KOENIG, E. 1980. Optokinetic and vestibular after effects and their interaction. *Prog. Oculomotor Res.* (In press.)

IMPAIRED SUPPRESSION OF VESTIBULAR NYSTAGMUS BY FIXATION OF VISUAL AND ACOUSTIC TARGETS IN NEUROLOGICAL PATIENTS*

E. Mira, E. Mevio, P. Zanolco, and P. Castelnovo

Otorhinolaryngological Clinic
University of Pavia
27100 Pavia, Italy

It is well known that the magnitude of vestibular-induced nystagmus largely is dependent on the degree of visual fixation permitted during a test procedure.¹⁻³ In normal subjects and in peripheral labyrinthine patients, caloric nystagmus is suppressed markedly by visual fixation, whereas patients with central nervous system (CNS) disorders may show no difference with or without fixation.⁴⁻¹⁰

Experimental evidence that fixation suppression of vestibular nystagmus in monkeys was severely impaired after large flocculus lesions was provided by Takemori and Cohen.¹¹ At present, numerous physiologic and anatomic studies in various animal species prove that the cerebellar flocculus plays an important role in the control of the vestibulo-ocular reflex (VOR) and that it is the center of visual-vestibular interaction.¹²⁻¹⁴

These basic findings suggest that cerebellar patients could be unable to use visual signals to modulate vestibular-induced eye movements. The behavior of visual-vestibular interaction in subjects with cerebellar atrophy seems to support this hypothesis, and its testing could be very useful in topographical diagnosis of cerebellar lesions.^{15,20}

On the other hand, the inability to suppress vestibular nystagmus by visual fixation correlates well with defects in smooth-pursuit (SP) movements and optokinetic nystagmus (OKN). In this case, impaired fixation suppression could be explained by an associated pursuit-system defect, not exclusively of cerebellar origin.^{16,17}

In order to establish whether the failure of fixation suppression of vestibular nystagmus is due entirely to defects in the SP system or to an impaired control of VOR gain by the cerebellum, the relationship between SP eye movements, vestibular nystagmus, and fixation suppression induced by both visual and acoustic targets has been investigated in a group of CNS patients with cerebellar and extracerebellar disorders.

Acoustic targets were adopted on the basis of suggestions given by Schmid et al.:²² retinal-slip velocity induced by slowly moving visual targets represents the natural input of the oculomotor smooth-pursuit system. Other nonvisual stimuli, such as acoustic, proprioceptive, or imaginary targets, can act as sensory input to a central reconstructor of the target velocity relative to the head, which in turn drives the SP system. Pursuit movements generated by these nonvisual stimuli are very poor and largely inadequate.¹⁸⁻²¹ However these inputs are effective in modulating the VOR gain in normal subjects.²² What do they do, in comparison with visual inputs, in CNS patients?

*Work supported by the Italian National Research Council, CNR, Special Project on Biomedical Engineering, Grant No. 80.00342.86, and by the HUSPI Project.

METHODS

Clinical diagnoses and the number of patients examined are reported in TABLE 1. The more homogeneous group, classified as "pure cerebellar," comprises 10 subjects presenting exclusive signs of cerebellar dysfunction due to cortical cerebellar degeneration of various origins. Another group, classified as "associated cerebellar," consists of 9 patients presenting concomitant signs of cerebellar and brain-stem dysfunction due to multiple system degeneration syndromes or to tumors with secondary processes of local edema or vascular disturbances. A third group comprises 12 patients with miscellaneous disorders of the CNS, mainly supratentorial, in whom cerebellar signs definitely were

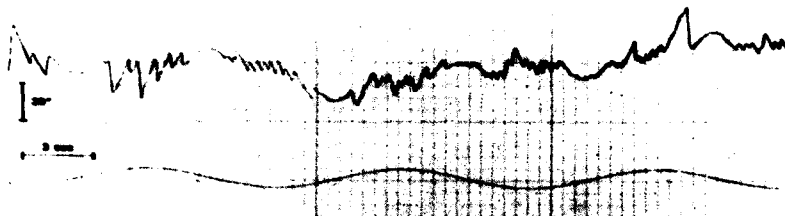
TABLE 1
SUBJECTS

Cerebellar Patients		
Pure Cerebellar Dysfunction		10
Alcoholic degeneration	3	
Toxic degeneration	2	
Degeneration of unknown origin	5	
Associated Cerebellar Dysfunction		9
Spinocerebellar degeneration	2	
Pontocerebellar degeneration	2	
Friedreich's ataxia	3	
Cerebellar glioma (vermis)	1	
Large cerebellar metastasis	1	
TOTAL		19
Extracerebellar Patients		
Multiple sclerosis	2	
Parkinson's disease	2	
Cortical cerebral atrophy	2	
Parasagittal meningioma	1	
Frontoparietal meningioma	1	
Medial cerebral artery thrombosis	2	
Congenital nystagmus	1	
Vascular malformation (occipital lobe)	1	
TOTAL		12

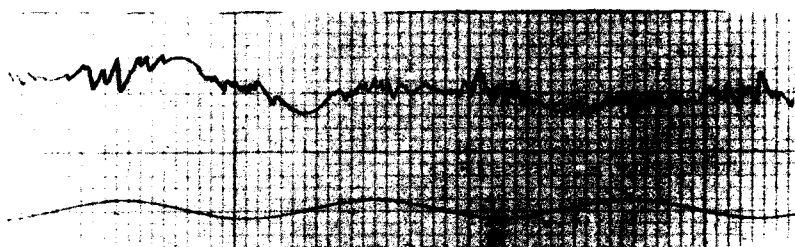
absent. All the patients were submitted to careful and repeated neurological examinations, including pure tone audiometry, caloric tests, electroencephalography (EEG), and computerized tomography (CT). CT results were particularly important in detecting and documenting the location and the size of the lesions. Ten normal subjects, with no signs of otological, vestibular, visual, or neurological dysfunction, were tested as controls. Their age ranged between 18 and 43 years. These subjects were submitted to a more complex series of tests for visual-vestibular and audio-vestibular interaction, the results of which are reported elsewhere.²²

Subjects were seated on a rotatory chair (Polman Digital-1) with the head secured at the center of rotation by a headrest. Saccadic eye movements were

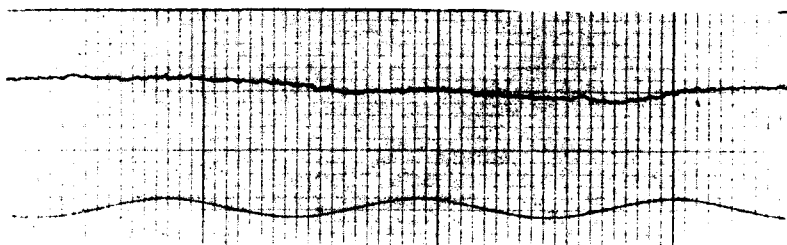
T.M. 26 y. Normal subject



alert in dark



acoustic target



visual target

0.1 Hz Head fixed target

FIGURE 1. EOG records from a normal subject during sinusoidal rotation in darkness with mental arithmetic (frequency, 0.1 Hz; peak-to-peak amplitude, 240°) and during fixation of head-fixed acoustic and visual targets. Lower trace refers to chair velocity (peak velocity, $75^\circ/\text{second}$).

elicited by refixation between visual targets placed in front of the subject at 10°, 20°, and 30° from the primary position, in the horizontal plane. Spontaneous and gaze nystagmuses were tested with eyes open in darkness. Smooth-pursuit movements were elicited by pendular oscillation of a small target, moving at 0.3 Hz and 40° peak-to-peak amplitude.

Vestibulo-ocular responses were assessed during sinusoidal chair rotations at a frequency of 0.1 Hz and peak-to-peak amplitude of 240° (peak velocity, 75°/second). Three different testing conditions were considered: rotation in darkness with eyes open and performing mental arithmetic; rotation in darkness while fixating an acoustic target moving with the head; and rotation in an otherwise dark room while fixating a visual target moving with the head. Each condition was tested during five periods of sinusoidal body oscillation; rotation in darkness was repeated after rotation both with acoustic and with visual targets. Targets were, respectively, a loudspeaker fed with pulses at 20 Hz and providing a signal level of 60 dB and a small red-light-emitting diode, both rigidly attached to the chair and placed 80 cm in front of the subject's head at eye level.

Eye movements in the horizontal plane were recorded by d.c. electro-oculography (EOG); calibration was performed before and after each series of tests. The amplified EOG signal and chair-position or chair-velocity signal were recorded simultaneously on a polygraph and on a magnetic tape. After A/D conversion, EOG data were processed on a digital computer by using a special interactive program.^{23,24} The amplitude, duration, and mean slow-phase velocity of each nystagmus beat were computed. By removing the fast component of nystagmus and fitting together the slow phases, the slow cumulative eye position (SCEP) was reconstructed. The gain of a response was defined and computed as the ratio between the mean amplitude of the SCEP over several cycles and the amplitude of the corresponding chair rotation. The smooth-pursuit gain was computed in the same way, after removing the intermixed saccades. The rationale of the adopted amplitude ratio, in comparison with the more frequently used peak slow-phase velocity/peak velocity of head rotation ratio, has been given by Schmid et al.²²

RESULTS

In normal subjects, the average VOR gain with mental arithmetic in darkness was 0.58 ± 0.12 and smooth-pursuit gain was 0.98 ± 0.06 . Visual fixation suppression always was complete, while fixation of an acoustic target decreased the VOR gain to 0.32 ± 0.09 . Fixation of a proprioceptive or of an imaginary target decreased the gain to 0.27 ± 0.01 and 0.35 ± 0.1 respectively.²² Typical examples of a normal response are reported in FIGURES 1 and 2.

Among pathological subjects, the more homogeneous group was represented by patients with pure cerebellar signs, suggestive of degenerative lesions of the cerebellar cortex. Cerebellar atrophy generally was diffuse. However, in subjects with clinical or neuroradiological signs of prominent localization to single parts of the cerebellum, a closer localization of the defects was omitted, due to the small number of cases examined and to the lack of precision of the diagnostic methods, including computerized tomography.

In this group, vestibular responses in darkness were normal or hyperactive (VOR gain, 0.68 ± 0.15), with mild interindividual variability, and smooth-pursuit eye movements were impaired, with large differences between individuals (SP gain, 0.52 ± 0.23). Visual fixation suppression of vestibular nystagmus always was impaired severely (gain, 0.58 ± 0.20) and acoustic suppression practically was

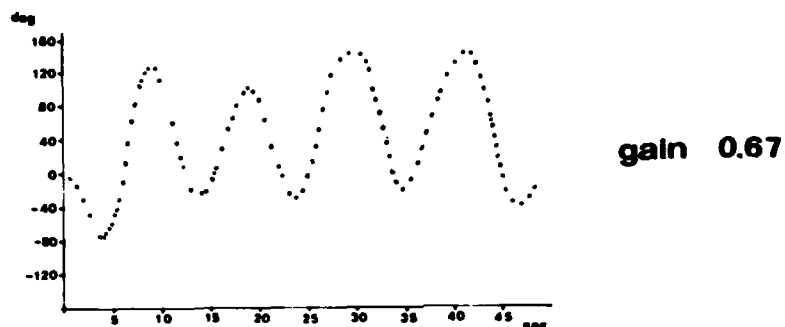
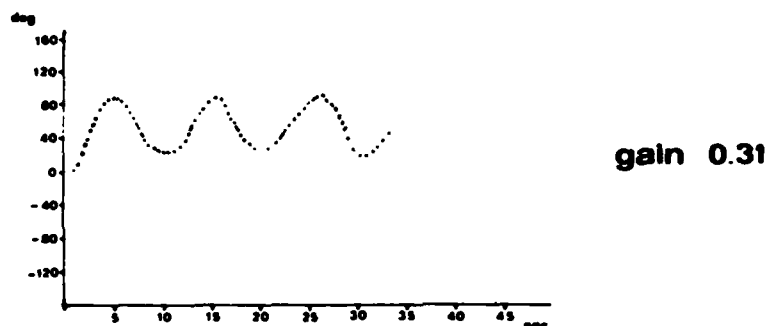
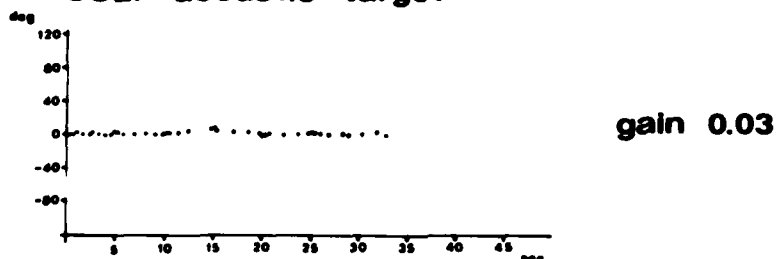
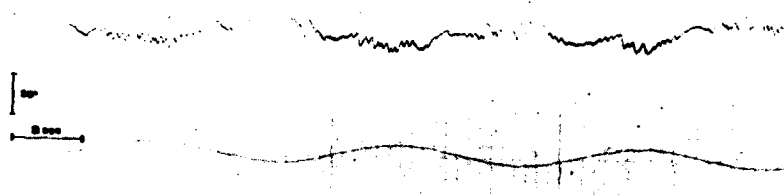
T.M. 26 y. normal subject**SCEP alert in dark****SCEP acoustic target****SCEP visual target**

FIGURE 2. Diagrams of the slow cumulative eye position (SCEP) and values of the VOR gains computed from the records in FIGURE 1.

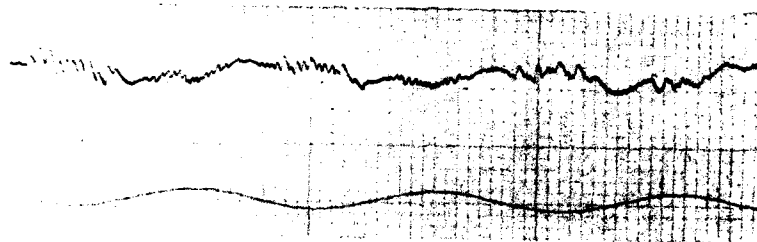
absent (gain 0.60 ± 0.18). Statistically, no significant difference was found among the gains computed in the three different testing conditions ($p > 0.05$) and no correlation could be established between the degree of the smooth-pursuit defect and the failure of fixation suppression.

In the second group of patients, typical cerebellar signs were associated variously with other neurological signs, mainly suggestive of a brain-stem disorder. Smooth-pursuit defects always were evident, with large variation from moderate (SP gain, 0.78) to severe (SP gain, 0.27). In contrast to pure cerebellar

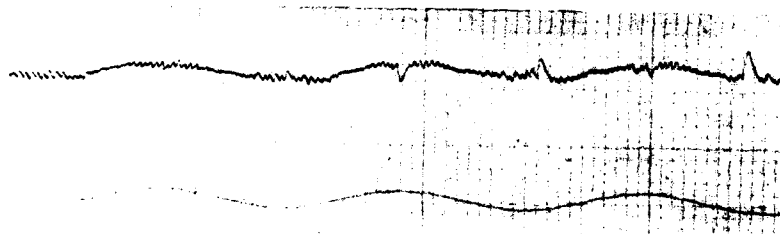
L.B. 66 y. Ponto-cerebellar atrophy



alert in dark



acoustic target



visual target

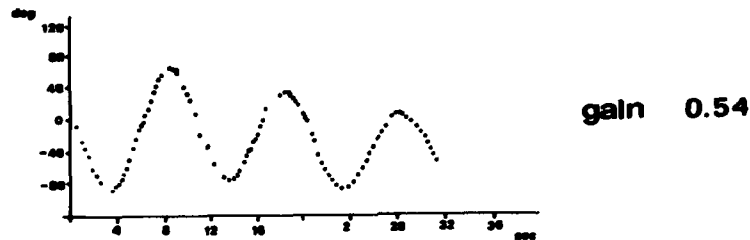
0.1 Hz Head fixed target

FIGURE 3. Impaired visual and acoustic fixation suppression in a patient with pontocerebellar atrophy.

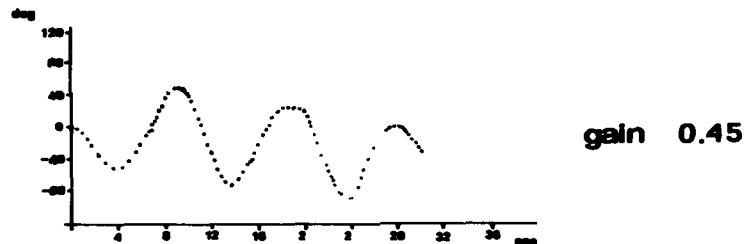
patients, vestibulo-ocular responses in darkness ranged widely from hyperactive (VOR gain, 0.63) to hypoactive (VOR gain, 0.28). Despite these large variations in smooth-pursuit disturbance and vestibular excitability, fixation suppression always was reduced markedly for both visual and acoustic targets. This pattern is similar to that found in pure cerebellar patients, and no correlation exists between VOR gain, SP defect, and fixation-suppression failure.

FIGURES 3 and 4 depict the electronystagmography (ENG) records and the

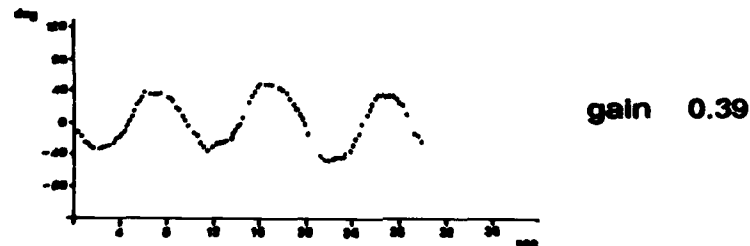
L.B. 66 y. ponto-cerebellar atrophy



SCEP alert in dark



SCEP acoustic target



SCEP visual target

FIGURE 4. Diagrams of the slow cumulative eye position and values of the VOR gains computed from the records in FIGURE 3. SP gain was 0.75.

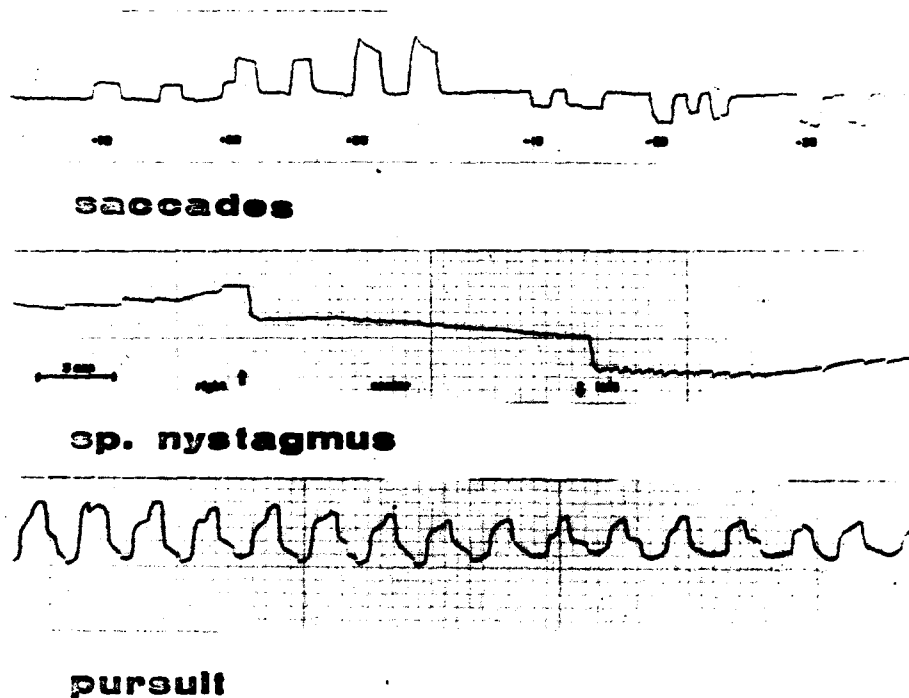
R.C. 44 y. Cortical-cerebral atrophy

FIGURE 5. EOG records of saccadic movements, spontaneous nystagmus (eyes open in darkness), and smooth-pursuit movements in a patient with diffuse cortical cerebral atrophy. SP gain was 0.34.

computed SCEP data of a patient with a pontocerebellar degeneration, mainly affecting the cerebellar cortex. Pursuit movements have slight cogwheelings (SP gain, 0.75), and vestibular response in darkness is enhanced slightly (VOR gain, 0.54); however nystagmus suppression induced by a visual target is weak (VOR gain reduction from 0.54 to 0.39) and that induced by an acoustic target is minimal (VOR gain reduction from 0.54 to 0.45).

In noncerebellar patients, both the nature and the location of the lesions were extremely heterogeneous and neurological features varied greatly. Large variations were found in the intensity of smooth-pursuit impairment and of vestibular response in the dark. In contrast to cerebellar groups, fixation suppression also ranged widely from normal to absent. No correlation was found with the degree of vestibular excitability, while a clear fixation-suppression disturbance consistently was associated with a severe SP defect (SP gain lower than 0.30) and correlated with its severity. Complete failure of visual fixation suppression was observed only in the presence of a total disorganization of smooth-pursuit movements (SP gain not measurable), while mild SP defects usually were associated with a normal ability to suppress vestibular nystagmus. In patients

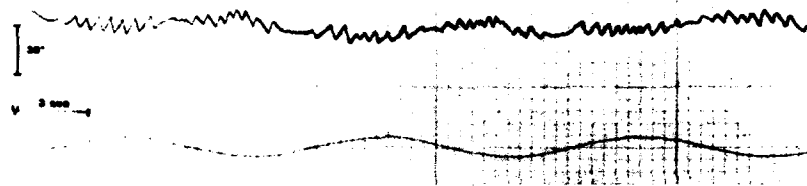
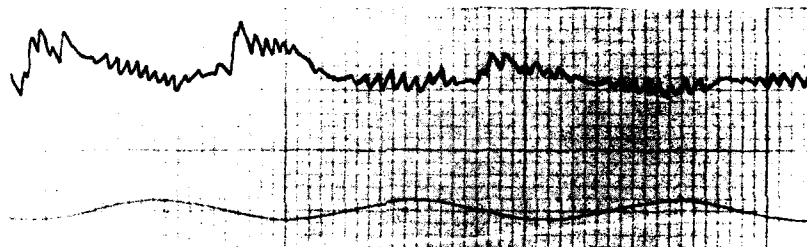
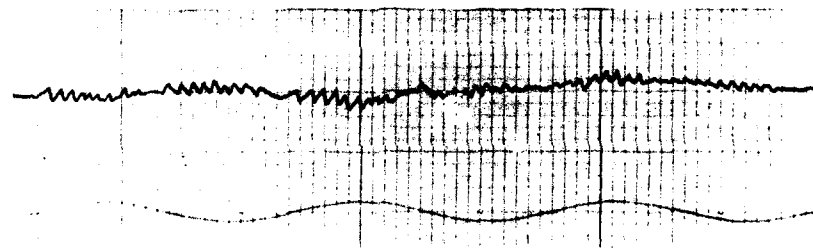
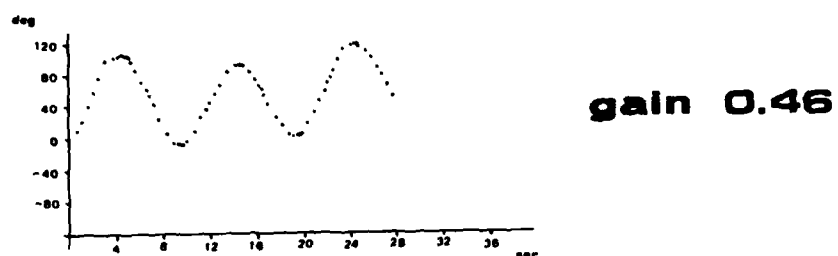
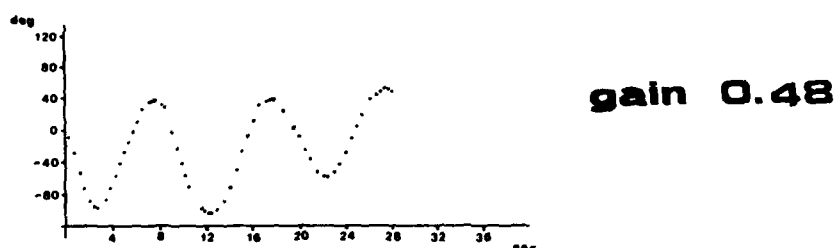
R. C. 44 y. Cortical-cerebral atrophy**alert in dark****acoustic target****visual target****0.1 Hz Head fixed target**

FIGURE 6. Impaired visual and acoustic fixation suppression in the patient of FIGURE 5.

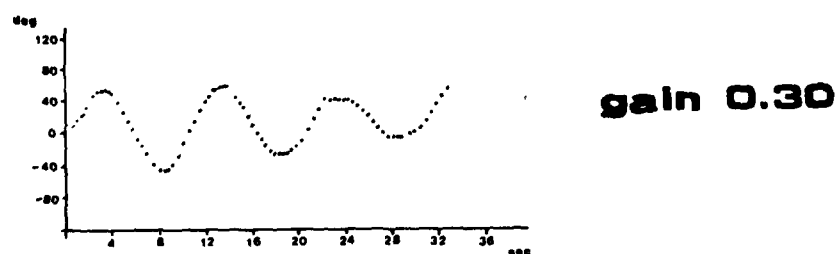
R.C. 44 y. Cortical cerebral atrophy



SCEP alert in dark



SCEP acoustic target



SCEP visual target

FIGURE 7. Diagrams of the slow cumulative eye position and values of the VOR gain computed from the records in FIGURE 6.

with unilateral lesions, impaired fixation suppression always was evident on the side ipsilateral to the SP defect. Acoustic targets generally were less effective than visual targets in inhibiting vestibular nystagmus, but their behavior did not parallel that of visual targets as in cerebellar patients; in two cases (multiple sclerosis and occipital lobe vascular malformation) with complete loss of pursuit movements, acoustic suppression was greater than visual.

FIGURES 5-7 refer to a patient with diffuse cortical cerebral atrophy, showing a severe impairment of smooth-pursuit movements (SP gain, 0.34), diminished but still active visual fixation suppression (VOR gain reduction from 0.46 to 0.30), and absent acoustic fixation suppression (VOR gain variation from 0.46 to 0.48).

FIGURES 8-10 refer to a patient with a large right frontoparietal meningioma. Also in this case, fixation suppression is fairly good in spite of the severe disorganization of smooth-pursuit movements. SP defect mainly to the right (SP gain, 0.23 to the left and 0.12 to the right) fits well with the prominent fixation suppression deficit to the right.

DISCUSSION

Our results substantiate previous observations that failure of fixation suppression is prominent in, but not exclusive to, cerebellar patients.⁴⁻¹⁰ In subjects with pure or associated signs of cerebellar dysfunction, visual fixation suppression generally is absent and its impairment does not correlate with the values of VOR gain in darkness or with those of visual smooth pursuit. Suppression produced by fixation of acoustic targets is equal to or slightly weaker than that produced by visual targets.

In CNS patients with no signs of cerebellar dysfunction, visual fixation suppression ranged widely from normal to absent. Only subjects with severe smooth-pursuit impairment showed an evident failure of the suppression, and in this case a correlation was found with the degree and the side of the SP defect. Acoustic suppression usually was lower than visual, but with a loose quantitative relationship, and in some cases acoustic targets were more effective than visual in inhibiting vestibular nystagmus.

According to the model proposed by Schmid *et al.*,²² these findings support the hypothesis that the cerebellum plays a specific and effective role in the modulation of the vestibulo-ocular reflex and that an impaired fixation suppression is due mainly to a dysfunction of this cerebellar mechanism.

Nystagmus suppression is only triggered and only partially supported by the SP system, which can receive an input either from the retina or from the central reconstructor of nonvisual-target motion.

In the presence of an intact cerebellar mechanism, an impaired fixation can be due only to a nearly complete dysfunction of the smooth-pursuit system. The different pattern of suppression induced by visual and acoustic targets in noncerebellar patients could depend on whether the lesion affects the visual or nonvisual parts of the SP system.

Our conclusions differ slightly from those of Dichgans *et al.*,¹⁶ and suggest that the cerebellum adds a direct and important component to fixation suppression of the VOR, probably by way of its inhibitory connections to the vestibular nuclei.

Some collateral observations in our patients are worth noting. These refer to the vestibulo-ocular response in the cerebellar group and to the impairment of optokinetic nystagmus.

Vestibular hyperexcitability in cerebellar patients has been observed by

E.P. 35 year Right frontal meningioma

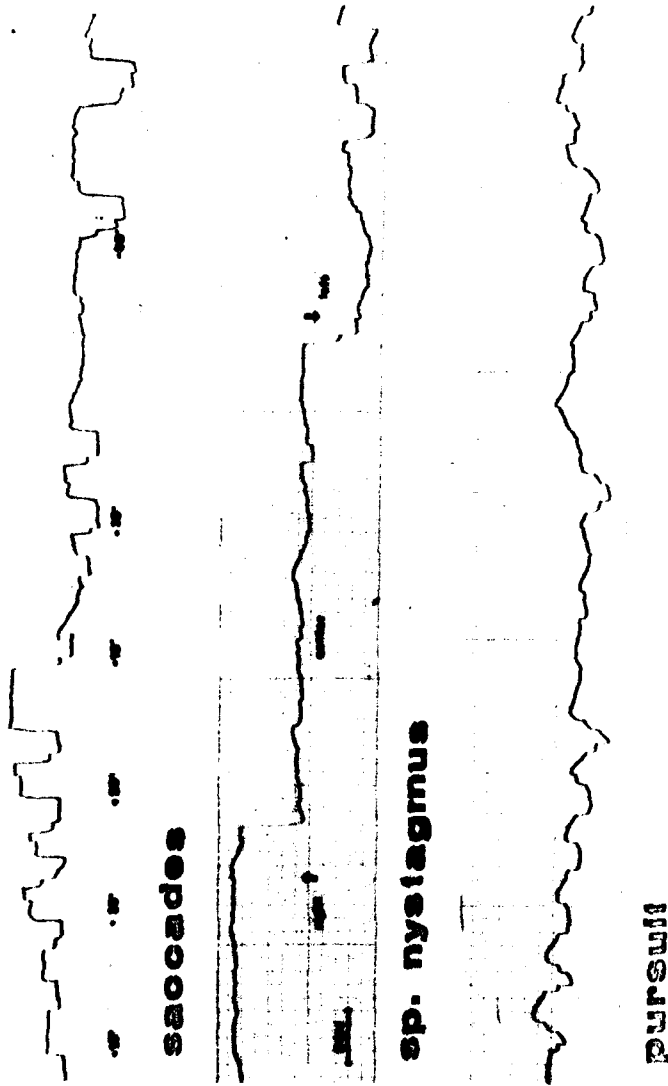
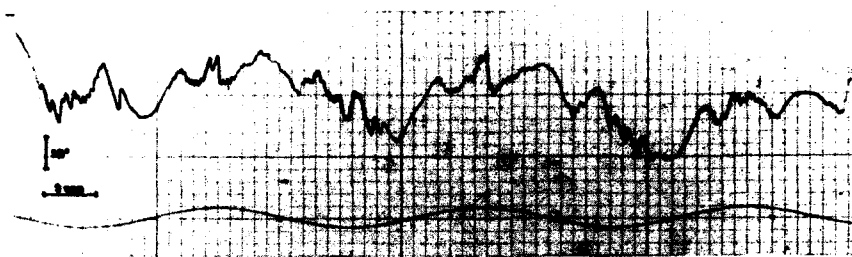


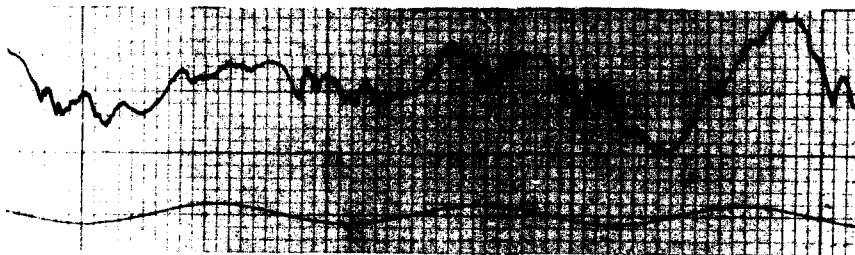
FIGURE 8. EOG records of saccadic movements, spontaneous nystagmus, and smooth-pursuit movements in a patient with right frontoparietal meningioma. Pursuit deficit is mainly to the right (SP gain, 0.23 to the left and 0.12 to the right).

several authors.^{16,25,26} In our group, it was found mainly in pure cerebellar cases; while in subjects with signs of concomitant brain-stem involvement, VOR gain largely varies from hyperactive to hypoactive, as reported by Baloh *et al.*¹⁵ In both groups, no correlation exists between the magnitude of the vestibulo-ocular response in darkness and the failure of fixation suppression.

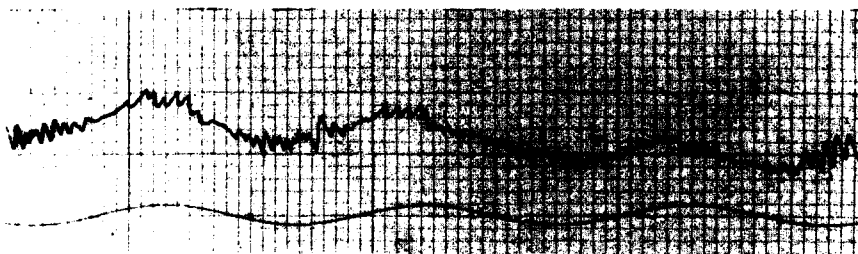
E.P. 35 year Right frontal meningioma



alert in dark



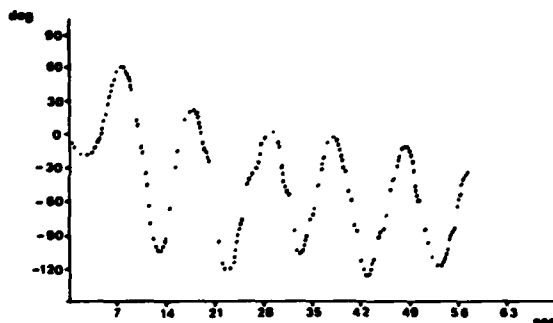
acoustic target



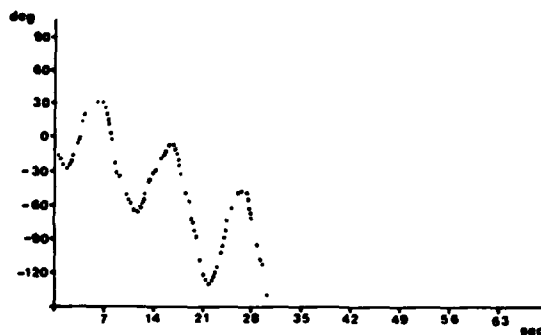
visual target

0.1 Hz Head fixed target

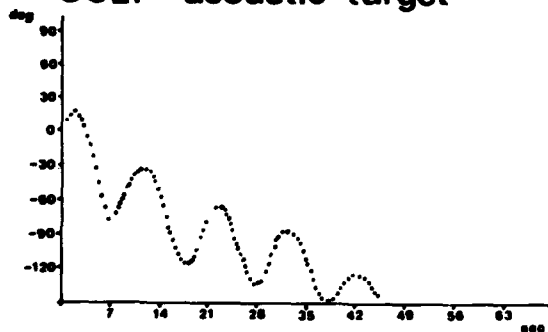
FIGURE 9. Impaired visual and acoustic suppression in the patient of FIGURE 8. Fixation suppression deficit is mainly to the right.

E.P. 35 y. right frontal meningioma

gain 0.72 R
0.78 L

SCEP alert in dark

gain 0.45 R
0.59 L

SCEP acoustic target

gain 0.30 R
0.50 L

SCEP visual target

FIGURE 10. Diagrams of the slow cumulative eye position and values of the VOR gain computed from the records in FIGURE 9.

Optokinetic nystagmus induced by a large-field visual stimulation (stripe velocity, 60°/second) was recorded in some of our patients; all the examined cases, both in the cerebellar and noncerebellar groups, showed an OKN reduction well correlated with the smooth-pursuit impairment, as reported by several authors.^{16,17,25} According to Dichgans *et al.* and Sato *et al.*, in unilateral lesions, a unidirectional fixation-suppression defect corresponds to the unidirectional impairment of SP and OKN.^{16,17} In our group this correlation was found only in noncerebellar patients, but this fact could be due to the bilateral location of the lesions in the majority of our cerebellar cases.

For clinical examination, we confirm the value of testing visual-vestibular and, more generally, sensory-vestibular interaction for diagnosing central vestibular disorders. With the exception of the simpler tests of suppression of caloric nystagmus or of the bedside method proposed by Dichgans *et al.*,¹⁶ if one has gone to the trouble of measuring accurately head and eye position or velocity during rotation, it would be useful to consider different testing conditions in order to provide a great deal more information about the function of central vestibular pathways.²⁷ As a rule, all the tests showing an impaired modulation of the vestibulo-ocular reflex are indicative of a cerebellar dysfunction, even if they give positive responses also in the presence of severe disorders of other parts of the CNS that largely affect the SP system.

SUMMARY

Suppression of vestibular nystagmus induced by fixation of visual and acoustic targets moving with the head during sinusoidal rotation (0.1 Hz, 75°/second peak velocity) was tested in cerebellar and noncerebellar patients. Visual suppression was impaired greatly in cerebellar patients, without correlation with visual smooth-pursuit defects. Acoustic suppression was equal to or slightly weaker than visual suppression. In noncerebellar patients, a disturbance of visual suppression was found only in the presence of a severe impairment of pursuit eye movements. Acoustic suppression did not parallel the visual-suppression pattern.

In clinical vestibular examination, an impaired modulation of the vestibulo-ocular reflex suggests a cerebellar dysfunction, but also can occur in the presence of disorders of other parts of the CNS severely affecting the SP system.

REFERENCES

1. OHM, J. 1926. Über den Einfluss des Sehen auf den vestibulären Drehnystagmus und Nachnystagmus. *Z. Hals Nasen Ohrenheilkd.* **16**: 521-540.
2. FRENZEL, H. 1955. Spontan- und Provocations-Nystagmus als Krankheitssymptom: ein Leitfaden für seine Beobachtung, Aufzeichnung und Formanalyse. Springer Verlag, Berlin, Federal Republic of Germany.
3. BALOH, R. W., L. SOLINGEN, A. W. SILLS & V. HONRUBIA. 1977. Caloric testing. I. Effect of different conditions of ocular fixation. *Ann. Otol. Rhinol. Laryngol.* **86**(Suppl. 43): 1-6.
4. COATS, A. C. 1970. Central electronystagmographic abnormalities. *Arch. Otolaryngol.* **92**: 43-53.
5. DEMANEZ, J. P. 1968. L'influence de la fixation oculaire sur le nystagmus postcalorique. *Acta Oto-Rhino-Laryngol. Belg.* **22**: 749-754.

6. MACCARIO, M., J. R. BACKMAN & J. KOREIN. 1972. Paradoxical caloric response in altered states of consciousness. *Neurology* 22: 739-754.
7. HART, C. W. 1973. The ocular fixation index. *Ann. Otol. Rhinol. Laryngol.* 82: 848-851.
8. ALPERT, J. N. 1974. Failure of fixation suppression: a pathologic effect of vision on caloric nystagmus. *Neurology* 24: 891-896.
9. KATO, I., Y. KIMURA, M. AOYAGI, K. MIZUKOSHI & T. KAWASAKI. 1977. Visual suppression of caloric nystagmus in normal individuals. *Acta Otolaryngol.* 83: 245-251.
10. TAKEMORI, S. 1977. Visual suppression test. *Ann. Otol. Rhinol. Laryngol.* 86: 80-85.
11. TAKEMORI, S. & B. COHEN. 1974. Loss of visual suppression of vestibular nystagmus after flocculus lesions. *Brain Res.* 72: 213-224.
12. ITO, M. 1972. Neural design of the cerebellar motor control system. *Brain Res.* 40: 81-84.
13. ROBINSON, D. A. 1976. Adaptive gain control of vestibuloocular reflex by the cerebellum. *J. Neurophysiol.* 39: 954-969.
14. KIMM, J., J. A. WINFIELD & A. E. HENDRICKSON. 1979. Visual-vestibular interactions and the role of the flocculus in the vestibulo-ocular reflex. *Prog. Brain Res.* 50: 703-713.
15. BALOH, R. W., H. A. JENKINS, V. HONRUBIA, R. D. YEE & C. G. Y. LAU. 1979. Visual-vestibular interaction and cerebellar atrophy. *Neurology* 29: 116-119.
16. DICHGANS, J., G. M. VON REUTERN & U. RÖMMELT. 1978. Impaired suppression of vestibular nystagmus by fixation in cerebellar and noncerebellar patients. *Arch. Psychiatr. Nervenkr.* 226: 183-199.
17. SATO, Y., I. KATO, T. KAWASAKI, K. MIZUKOSHI & M. HAYANO. 1980. Failure of fixation suppression of caloric nystagmus and ocular motor abnormalities. *Arch. Neurol.* 37: 35-38.
18. YASUI, S. 1974. Nystagmus generation, oculomotor tracking and visual motion perception. Ph.D. Dissertation. Massachusetts Institute of Technology. Cambridge, Mass.
19. GAUTHIER, G. & J. M. HOFFERER. 1976. Eye-tracking of self-moved targets in the absence of vision. *Exp. Brain Res.* 26: 121-139.
20. YOUNG, L. R. 1977. Pursuit eye movement. What is being pursued? *Dev. Neurosci.* 1: 29-36.
21. ZAMBARBIERI, D., R. SCHMID, C. PRABLANC & G. MAGENES. Characteristics of eye movements induced by the presentation of acoustic targets. *Prog. Oculomotor Res.* (In press.)
22. SCHMID, R., D. ZAMBARBIERI & G. MAGENES. 1981. Modifications of vestibular nystagmus produced by fixation of visual and nonvisual targets. *Ann. N.Y. Acad. Sci.* (This volume.)
23. ANZALDI, E. & E. MIRA. 1975. An interactive program for the analysis of ENG tracings. *Acta Otolaryngol.* 80: 120-127.
24. BUIZZA, A., R. SCHMID, A. ZANIBELLI, E. MIRA & P. SEMPLICI. 1978. Quantification of vestibular nystagmus by an interactive computer program. *ORL* 40: 147-159.
25. BALOH, R. W., H. R. KONRAD & V. HONRUBIA. 1975. Vestibuloocular function in patients with cerebellar atrophy. *Neurology* 25: 160-168.
26. ZEE, D. S., R. D. YEE, D. G. COGAN, D. A. ROBINSON & W. K. ENGEL. 1976. Ocular motor abnormalities in hereditary cerebellar ataxia. *Brain* 99: 207-234.
27. BARR, C. C., L. W. SCHULTHEIS & D. A. ROBINSON. 1976. Voluntary, non-visual control of the human vestibulo-ocular reflex. *Acta Otolaryngol.* 81: 365-375.

A PHYSICAL MODEL OF HUMAN POSTURAL DYNAMICS*

C. W. Stockwell,† S. H. Koozekanani,‡ and K. Barin‡

†Department of Otolaryngology

‡Department of Electrical Engineering

Ohio State University

Columbus, Ohio 43210

For more than a century, persistent efforts have been made to develop a test of vestibulospinal function. However, these efforts largely have been frustrated by the fact that the vestibulospinal system is imbedded in a postural-control system that also receives inputs from visual, proprioceptive, and perhaps other sensory modalities, each with its own complex dynamics, and that controls a musculoskeletal system with over 200 degrees of freedom. In the face of such complexity, the chance of finding a set of response variables that optimally characterizes a specific dysfunction is remote unless a systematic analysis is carried out. Control engineers have developed powerful methods for analyzing complex control systems, but even these methods are overwhelmed by the complexity of human postural control. Obviously some simplifications are necessary.

The simplest physical model of human postural sway is a single-link inverted pendulum, capable of rotating only about the ankle joints. Using such a physical model, Nashner developed a detailed control model of the sensory systems involved in postural control.¹ Gurfinkel subsequently described the dynamics of a one-link inverted pendulum atop a triangle-shaped foot.² Unfortunately, while the single-link inverted-pendulum model reduces the analysis of postural control to manageable proportions, it does not describe adequately human postural dynamics. Virtually every investigator who has been able to measure relative movement between the various body segments reports that significant movement occurs at all joints, not only at the ankle.³⁻⁷

Hemami and his associates have studied the stability of two-link and three-link models.^{5,8-10} Recently we developed a four-link model by adding Hemami and Jaswa's three-link model to Gurfinkel's triangular foot. The method of free-body analysis was employed to yield equations in a form better suited for digital computation.¹¹ Our model is elaborated fully by Koozekanani et al.¹² This paper briefly reviews and extends the model and describes our attempts thus far to validate it.

THE PHYSICAL MODEL

The model describes the human body in the sagittal plane with arms folded across the chest. It assumes that the body segments rotate about simple pin joints and that the spine is rigid. It further assumes that the left and right ankle joints rotate about the same axis and that the feet do not move.

The body is modeled as a system composed of five homogeneous rigid

*This work was supported by National Institutes of Health Grant NS13903.

segments—a triangular foot (link₁); a shank (link₁); a thigh (link₂); a torso, including arms folded at the waist (link₃); and a head (link₄)—as shown in FIGURE 1. This system possesses four degrees of freedom: θ_1 about the ankle (X_1Y_1), θ_2 about the knee (X_2Y_2), θ_3 about the hip (X_3Y_3), and θ_4 about the neck (X_4Y_4). Note that a distinction is made between θ_i , the inertial angle of a link, and θ'_i , the anatomical angle between a link and the one immediately below it.

FIGURE 2a shows the free-body diagram for link_i, where link_i can be any body link except the foot, which is a special case that is considered separately below.

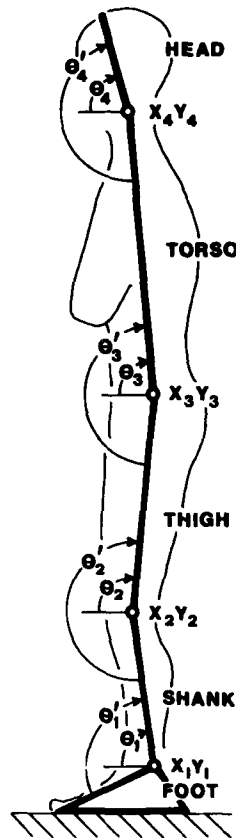


FIGURE 1. Five-link sagittal-plane model of the human body.

The model is generalizable to any number of links, but it is sufficient for our purpose to consider only four links—shank, thigh, torso, and head.

For link_i:

$$\ddot{x}_i = \left[\sum_{k=1}^{i-1} l_k (\ddot{\theta}_k \sin \theta_k + \dot{\theta}_k^2 \cos \theta_k) \right] + d_i (\ddot{\theta}_i \sin \theta_i + \dot{\theta}_i^2 \cos \theta_i) \quad (1)$$

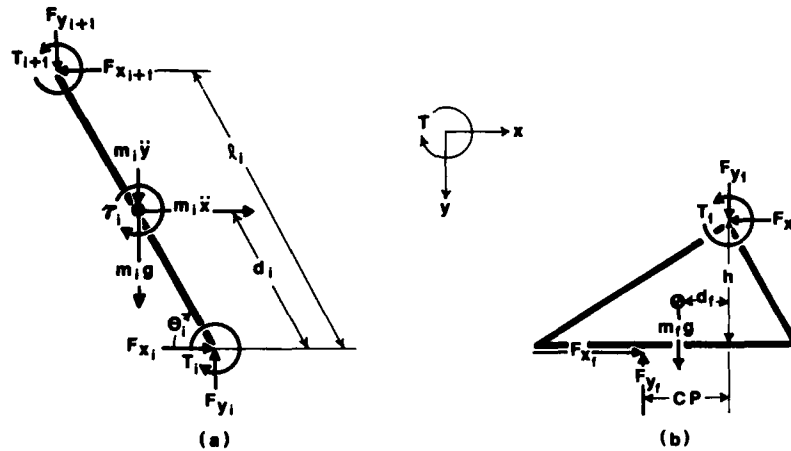


FIGURE 2. Free-body diagram of the body links. (a) link_i free-body diagram, (b) foot free-body diagram.

$$\ddot{y}_i = \left[\sum_{k=1}^{i-1} l_k (-\ddot{\theta}_k \cos \theta_k + \dot{\theta}_k^2 \sin \theta_k) \right] + d_i (-\ddot{\theta}_i \cos \theta_i + \dot{\theta}_i^2 \sin \theta_i) \quad (2)$$

$$F_{x_i} = F_{x_{i+1}} + m_i \ddot{x}_i \quad (3)$$

$$F_{y_i} = F_{y_{i+1}} + m_i g - m_i \ddot{y}_i \quad (4)$$

$$\tau_i = J_i \ddot{\theta}_i + [F_{x_i} d_i + F_{x_{i+1}} (l_i - d_i)] \sin \theta_i + [F_{y_i} d_i + F_{y_{i+1}} (l_i - d_i)] \cos \theta_i \quad (5)$$

The variables used in these equations are defined in FIGURE 2a and the Appendix. Note that

$$F_{x_{N+1}} = F_{y_{N+1}} = 0$$

Also note that

$$T_i = \sum_{k=i}^N \tau_k \quad (6)$$

That is, the torque at any joint is the sum of the link torques that occur above that joint. The ankle-joint torque, T_1 , is the sum of all the link torques of the body.

FIGURE 2b shows the free-body diagram for link_t, the triangular foot.

For link_t:

$$F_{x_t} = F_{x_1} \quad (7)$$

$$F_{y_t} = F_{y_1} + m_t g \quad (8)$$

$$CP = (T_1 + m_t g d_t + F_{x_1} h) / F_{y_t} \quad (9)$$

The variables used in these equations are defined in FIGURE 2b and the Appendix. Note that, for a given individual,

$$F_{y_t} \approx w = \left(\sum_{k=1}^N m_k + m_t \right) g$$

If, further, we let $h \approx 0$, then

$$\begin{aligned} \text{CP} &= w^{-1} T_1 + w^{-1} m_l g d_l + 0 \\ \text{CP} &= aT_1 + c \end{aligned} \quad (10)$$

that is, for a given individual, the body's center of pressure is proportional to ankle torque plus a constant.

METHOD

We have developed a method for estimating θ_i , $\dot{\theta}_i$, and $\ddot{\theta}_i$. Pin lights are attached to a human subject at the knee (X_2Y_2), hip (X_3Y_3), and mastoid (X_4Y_4) and atop a rigid bar about 30 cm above the subject's forehead, as shown in FIGURE 3. Position of the lights is monitored at 1/30-second intervals by a pair of ordinary video cameras connected by a special interface to a DEC 11/34 computer. Camera 1 detects the forehead and mastoid lights, and camera 2 detects the hip and knee lights. The position of the ankle (X_1Y_1) is not monitored; its position is measured at the beginning of the observation period and entered into the computer as a constant. This monitoring system is an improved version of one developed by Cheng.¹³

Following data collection, values of θ_i and $\dot{\theta}_i$ are computed. θ_i values then are smoothed by a digital filtering method. Numerical differentiation of the smoothed θ_i data yields the values for $\dot{\theta}_i$ and $\ddot{\theta}_i$ needed to evaluate the equations.

The other variables in the equations— l_i , m_i , d_i , J_i , d_l , and h —are estimated on the basis of standardized coefficients derived from cadaver studies and anthropometric measurements.¹⁴

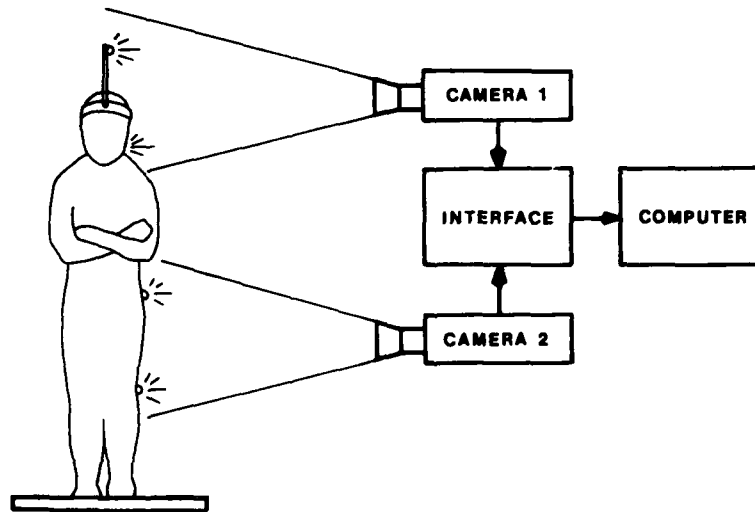


FIGURE 3. Schematic diagram of the video-computer system.

RESULTS

Using our video-computer monitoring system, we attempted to determine whether a four-degrees-of-freedom model really was necessary or whether perhaps a simpler model would be adequate to describe human postural sway. The answer to this question is given by FIGURE 4, which shows the amplitude spectra of the measured joint angles of 10 normal subjects during three minutes of quiet standing. Note that θ'_i (anatomical angles), and not θ_i (inertial angles), are shown. If a single-link model were adequate, significant movement would be present in only one joint, the ankle joint, θ'_1 . A two-link model would imply movement in only two joints, probably the ankle, θ'_1 , and the hip, θ'_3 . Instead,

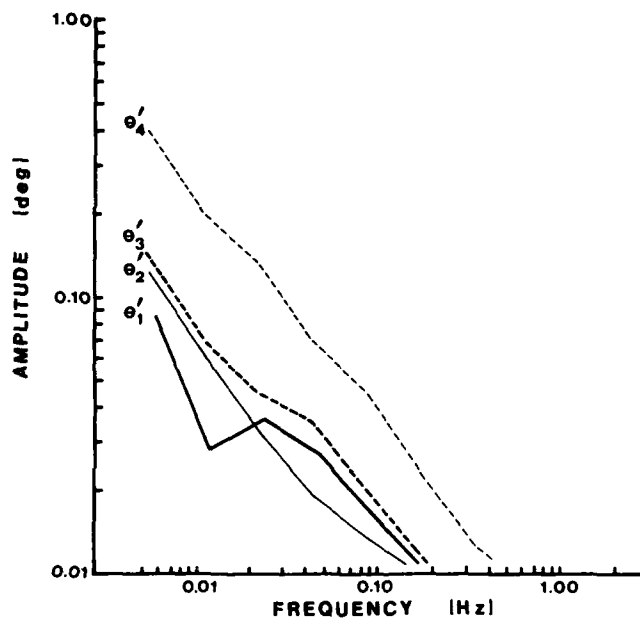


FIGURE 4. Fourier coefficients of θ'_i for 10 subjects standing quietly for three minutes with eyes open. θ'_i is defined in FIGURE 1.

significant movement is seen in all body joints measured, indicating that a model with at least four degrees of freedom is required to describe adequately human body sway.

An example of the complexity of body-joint movements is shown in FIGURE 5. Two major shifts in CP are seen, one backward (arrow 1) and the other forward (arrow 2). The backward shift is accompanied by an increase in θ'_1 and θ'_2 and a decrease in θ'_3 . The same pattern is seen in the lesser postural shifts. Some motions appear to be anticomensatory (arrows 3 and 4); they throw CP off the apparent control point and are followed quickly by a movement in the opposite direction that returns CP approximately to its previous position. Other motions appear to be irrelevant to postural control (arrows 5 and 6), since they produce virtually no change in CP.

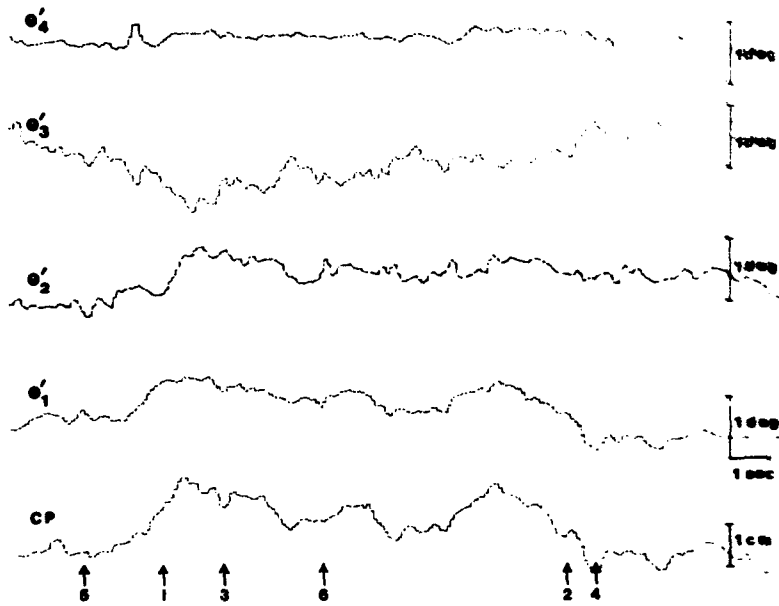


FIGURE 5. Graphic plot of θ'_i and CP during quiet standing with eyes open. θ'_i and CP are defined in FIGURES 1 and 2. Arrows indicate features of the record that are described in the text.

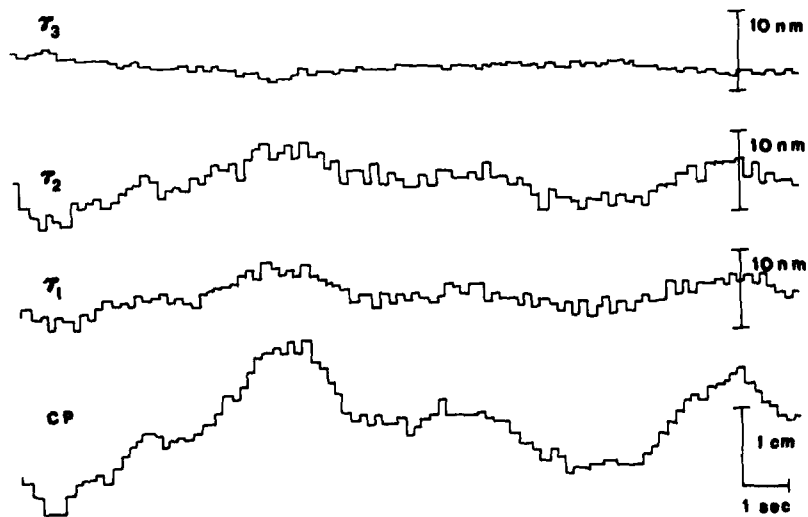


FIGURE 6. Graphic plot of τ_i and CP during quiet standing with eyes open. τ_i and CP are defined in FIGURE 2.

An example of the relation between τ_i and CP is shown in FIGURE 6. Recall from Equations 6 and 10 that

$$\sum_{k=1}^N \tau_k = T_1 - (CP - c)/a$$

(τ_4 is not shown in FIGURE 6, but its contribution to CP is small.) Most of the change in CP is associated with changes in τ_1 and τ_2 . τ_3 is virtually constant, which indicates that the torso must be rotating opposite to the direction of thigh and shank rotation, that is, that the motion of the torso is decoupled with respect to leg motion. This appears to be a characteristic mode of human postural control. It is apparent in the example shown in FIGURE 5, and has been noted by others.⁴⁻⁶

We also have attempted to determine whether the model is sufficient, that is, whether it is adequate to describe human body sway or whether an even more complex model is required. While we are not able to obtain independent measures of joint torques with which to compare the model's predictions, we have made comparisons between measured and predicted CP by having several subjects stand on a force plate while joint position was being monitored. These experiments showed that measured CP was matched closely by CP predicted by the model.¹² Further validation of the model is under way, including an examination of the effects of errors in estimating body-link parameters. Results thus far indicate that 95% of the time, CP predicted by the model is within ± 0.3 cm of CP measured by a force plate.

DISCUSSION

Our results thus far indicate that a four-degrees-of-freedom physical model of human postural sway is necessary and probably sufficient. The model is complex, but the governing equations are written in a form that makes evaluation feasible with a digital computer.

There are several advantages to an explicit and well-developed model of postural sway. First, the model dictates the method of response measurement. Most studies of postural control have utilized methods—such as force plate, displacement transducer, or video camera—that measure one variable and thus have employed a one-degree-of-freedom model, even though the choice of physical model was not always explicit.^{1,15-17} Relatively few studies have been based on multilink models.³⁻⁶ Our results suggest that a reasonably adequate description of postural sway must be based on no less than four variables. Second, the model specifies the relationship between the state variables, θ_i and $\dot{\theta}_i$, and τ_i and thus simplifies the task of testing hypotheses about the form of the feedback laws that govern postural control. The model offers no clues as to what forms these feedback laws might take, but since they can be written in terms of θ_i , $\dot{\theta}_i$, and τ_i , the possibility arises that linear approximations will be adequate, which is a decided advantage since linear hypotheses are easier to evaluate.

REFERENCES

1. NASHNER, L. M. 1970. Sensory feedback in human posture control. Sc.D. Thesis. Massachusetts Institute of Technology, Cambridge, Mass.
2. GURFINKEL, E. V. 1973. Physical foundations of stabilography. *Agressologie* 14(C): 9-14.

3. VALK-FAL, T. 1973. Analysis of the dynamical behavior of the body whilst "standing still." *Agressologie* 14(C): 21-25.
4. ROBERTS, T. D. M. & G. STENHOUSE. 1976. The nature of postural sway. *Agressologie* 17(A): 11-14.
5. CAMANA, P. C., H. HEMAMI & C. W. STOCKWELL. 1977. Determination of feedback for human posture control without physical intervention. *J. Cybern.* 7: 199-226.
6. ANDRES, R. O. 1979. A postural measurement system for induced body sway assessment. Ph.D. Thesis. University of Michigan. Ann Arbor, Mich.
7. BARIN, K. 1980. An empirical evaluation of the one-link pendulum model of human postural dynamics. M.S. Thesis. Ohio State University. Columbus, Ohio.
8. GOLLIDAY, C. L. & H. HEMAMI. 1978. Postural stability of a two-degree-of-freedom biped by general linear feedback. *IEEE Trans. Autom. Control* AC-22: 74-79.
9. HEMAMI, H., F. C. WEIMER, C. S. ROBINSON, et al. 1978. Biped stability considerations with vestibular models. *IEEE Trans. Autom. Control* AC-23: 1074-1079.
10. HEMAMI, H. & V. C. JASWA. 1978. On a three-link model of the dynamics of standing up and sitting down. *IEEE Trans. Syst. Man Cybern.* SMC-8: 115-120.
11. MCGHEE, R. B., S. H. KOOZEKANANI, F. C. WEIMER, et al. 1979. Dynamic modelling of human locomotion. In *Proceedings, 1979 Joint Automatic Control Conference*, Denver, Colo.: 405-413. American Institute of Chemical Engineers. New York, N.Y.
12. KOOZEKANANI, S. H., C. W. STOCKWELL, R. B. MCGHEE, et al. 1980. On the role of dynamic models in quantitative posturography. *IEEE Trans. Biomed. Eng.* BME-27: 605-609.
13. CHENG, I. S. 1974. Computer-television analysis of biped locomotion. Ph.D. Thesis. Ohio State University. Columbus, Ohio.
14. MILLER, D. I. & R. C. NELSON. 1973. *Biomechanics of Sport*: 88-118. Lea & Febiger. Philadelphia, Pa.
15. COATS, A. C. & M. S. STOLTZ. 1969. The recorded body-sway response to galvanic stimulation of the labyrinth: a preliminary study. *Laryngoscope* 79: 85-103.
16. BLACK, F. O., D. P. O'LEARY, C. WALL, et al. 1977. The vestibulo-spinal stability test: normal limits. *Trans. Am. Acad. Ophthalmol. Otolaryngol.* 84: 549-560.
17. BERTHOZ, A., M. LACOUR, J. F. SOECHTING, et al. 1979. The role of vision on the control of posture during linear motion. *Prog. Brain Res.* 50: 197-209.

APPENDIX
NOTATION USED IN EQUATIONS

Subscript f	refers to foot link
Subscript i, k	refers to any body link, excluding foot
N	total number of body links, excluding foot
\ddot{x}	horizontal acceleration
\ddot{y}	vertical acceleration
θ	angular position
$\dot{\theta}$	angular velocity
$\ddot{\theta}$	angular acceleration
m	mass
I	moment of inertia
F_x	horizontal reaction force

(continued)

APPENDIX (continued)

F_y	vertical reaction force
T	joint torque
τ	link torque
g	gravitational acceleration
CP	position of center of pressure re ankle joint
w	total weight
X	measured horizontal joint position
Y	measured vertical joint position
d_l	distance of center of mass from lower joint (see FIGURE 2a)
d_t	distance of center of mass from vertical projection of ankle joint (see FIGURE 2b)
h, l	length of link (see FIGURE 2)
a, c	constants

DISSOCIATION OF THE EYES IN SACCADIC MOVEMENT

T. Miyoshi, S. Hiwatashi, S. Kishimoto, and A. Tamada

*Department of Otolaryngology
Kyoto University
Kyoto 606, Japan*

Eye movements have been investigated since the end of the nineteenth century in the fields of physiology and experimental psychology. Dodge classified eye movements into five types: saccadic, slow continuous, coordinate compensatory, reactive compensatory, and convergence or divergence.¹ Saccadic eye movements, in which the point of fixation moves from one object to another in the visual field with a quick jump, doubtless are the most common of the five fundamental types of eye movements, as Dodge pointed out. They can be seen in routine behavior, such as reading or looking around. On the other hand, the characteristics of saccades seem to be similar to those of quick phases of optokinetic or caloric nystagmus. Because of this similarity, the characteristics of saccadic eye movements have attracted the interest of various researchers. Thus the latency, duration, velocity, and amplitude of saccadic eye movements have been studied by several investigators.¹⁻¹⁰ They have reported that the latency was distributed between 120 and 300 mseconds but was relatively fixed in each investigation. The duration of saccadic eye movement ranged from 40 to 250 mseconds and was closely related to the amplitude of the saccade. The velocity also was relatively constant for a given amplitude and was not much influenced by practice. In most of these reports, a saccade was treated as a synchronized movement of both eyes and was regarded generally as a conjugate movement.^{10,11} However, some authors described the duration or latency as differing according to the direction of movement.^{2,4,6,11} Other papers mentioned the disconjugation of both eyes in saccadic eye movement. White reported that in many cases, the time of initiation and maximum velocity of saccades varied slightly from one eye to the other.⁴ Typically, the left eye began its motion a short time before the right eye when the stimulus was to the left, and vice versa. Robinson revealed that nasal saccades had, on the average, durations about 5 mseconds longer than those of temporal saccades.⁶ White also reported a difference in duration of saccade between both eyes according to direction of movement. Hyde stated that the velocity of the eye was greater when returning from lateral to center than when traveling to the periphery.¹¹

Because of the anatomical and physiological differences between abduction and adduction in the oculomotor system, it is quite possible that the eyes move disconjugately during horizontal saccades. Simultaneous monocular d.c. recordings of both eyes are necessary to determine whether this dissociation of eye movements really exists or not. In order to compare the movements of both eyes, rather fine analyzing methods must be used. The pen-writing system is not adequate for this purpose, because the time between initiation and cessation of saccade may be as short as a few milliseconds. Therefore, a signal processor was used for fine analysis in this investigation.

MATERIALS AND METHOD

Subjects

The test subjects were 10 healthy adults, 27 to 53 years old. All of them had sufficiently good vision to see the target and were free from oculomotor impairments.

Apparatus

The apparatus consisted of a target-presenting system for saccadic eye movement, a projection-type optokinetic stimulator, a six-channel d.c. electro-

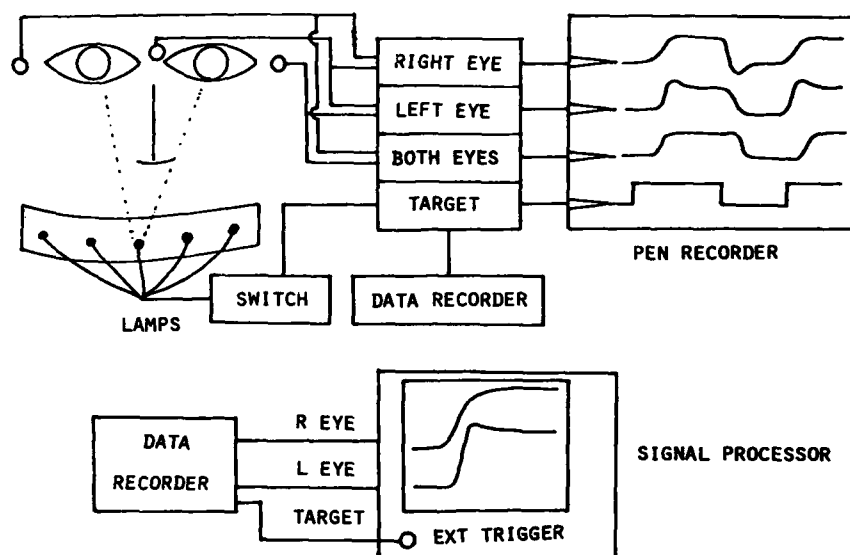


FIGURE 1. Block diagram of the experimental apparatus.

nystagmograph (ENG), a four-channel cassette-type FM data recorder, and a two-channel signal processor, or "memory-scope" (FIGURE 1). The target-presenting system had five red-light-emitting diodes (LED), each 2 mm in diameter. They were mounted on a half-cylindrical screen 100 cm in radius. They were arranged in a horizontal arc with a uniform visual angle of 10° to either side from the center. These LEDs were lighted randomly one after another by a push-button system. The target positions emerged from this stimulator as electrical potentials. In most cases, optokinetic nystagmus also was investigated. The optokinetic stimulator consisted of a projector and the same half-cylindrical screen used with the saccade stimulator. The projector was focused on the center of the screen and projected 12 stripes onto it. The projected stripes moved with various velocities and accelerations. The screen—along with both stimulators,

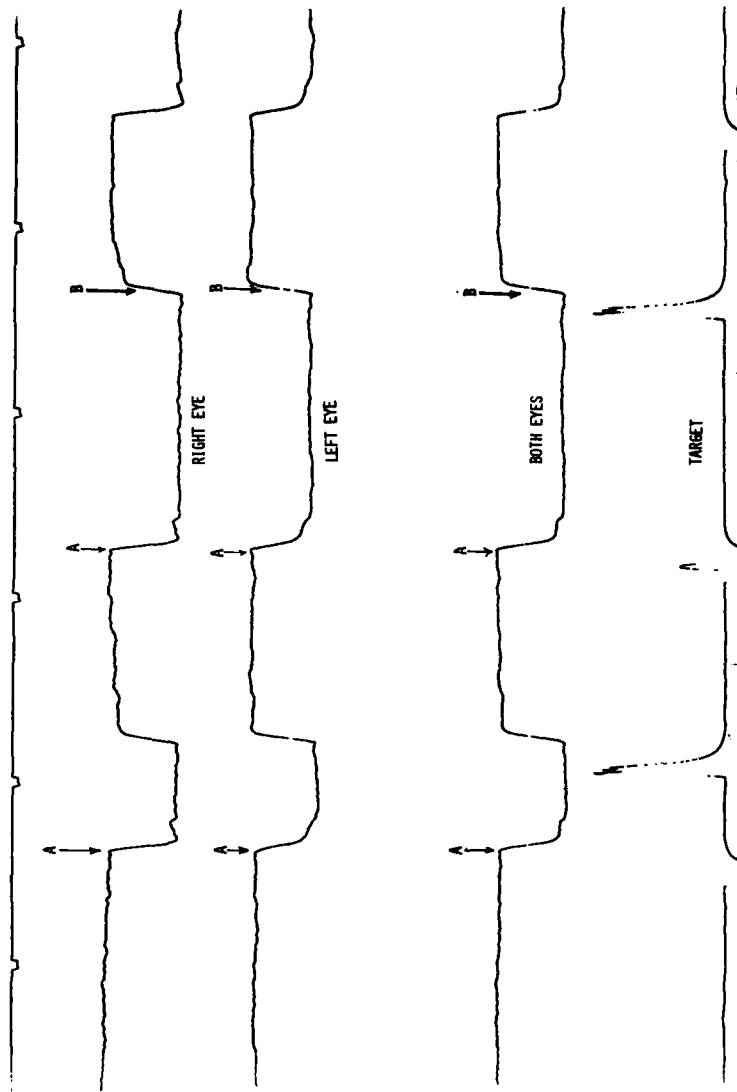


FIGURE 2. EOG of monocular and binocular recordings of horizontal saccade. The top curve is a monocular recording of the right eye, the next curve is a monocular recording of the left eye, the third curve is a binocular recording, and the bottom curve is a derivative of the target position.

saccadic and optokinetic—could be turned to any angle and could be moved so that its arc was vertical in front of the subject. The subject sat in a chair facing the center of the arc with his chin fixed on a chin rest and was asked to move his head as little as possible. He also was asked to fixate each of the lighted LEDs one after the other or to follow the passing stripes successively.

Recording Eye Movement

The monocular electro-oculograms (EOG) of the movements of each eye were recorded with a pen-writing d.c. ENG. Eight paste-type Zn-ZnSO₄ electrodes—which had been devised and patented by the author¹²—were attached on both outer canthi, midway between both eyebrows, near the upper and lower margins of both orbits, and on the forehead as a reference point. The ENG had six channels for monocular recording of the right eye and the left eye, for binocular recording, for target position, and for two other reference phenomena. The first four phenomena were recorded simultaneously in a cassette-type data recorder, which was connected with the ENG. The paper speed for recording was 60 mm/second. Consequently, the resolving power in the time dimension was about 2 mseconds.

Data Analysis

The resolving power was adequate to describe such characteristics of saccadic eye movement as latency, duration, velocity, and trace of the eyes (FIGURE 2). However, the time differences between initiation of movement of the eyes in saccades scarcely could be recognized on the EOG. For the purpose of

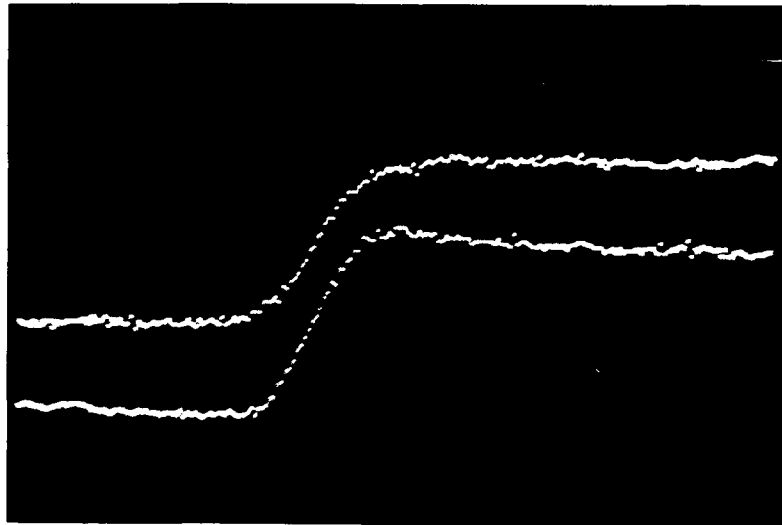


FIGURE 3. The relationship of the eyes in saccade to the right. Upper curve is movement of the right eye, and lower curve is movement of the left eye.

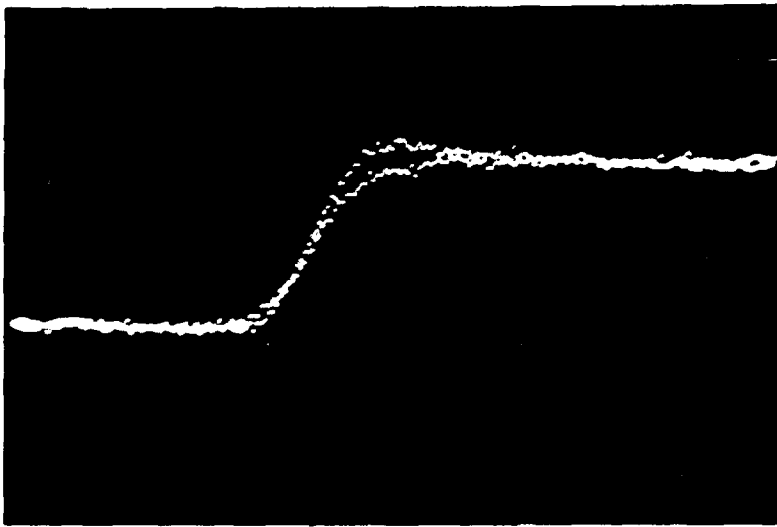


FIGURE 4. The superimposition of the curves in FIGURE 3.

detailed investigation, the raw data on tape were displayed on the cathode ray tube (CRT) of the processor. The potential jump of eye position was used as a trigger for processing the phenomena. By means of suitable delay and sweep times, the desired portion of the curve of saccade could be expanded along the

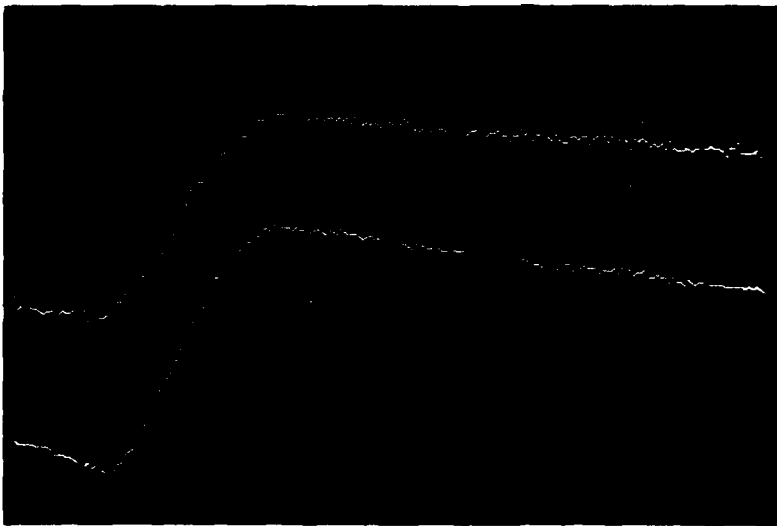


FIGURE 5. The relationship of the eyes in the quick phase of horizontal optokinetic nystagmus to the right. The upper curve is optokinetic nystagmus of the right eye, and the lower curve is that of the left eye.

time direction and be brought onto the CRT. The delay time was chosen so as to bring the beginning and end of a saccade onto the CRT. The curves displayed on the CRT were photographed. Monocular recordings of the saccade of each eye were computed, displayed, and inspected for the relationship between the movements of each eye (FIGURE 3). By means of vertical-position regulators, both curves were shifted and overlapped on the CRT (FIGURE 4); thus the relationship between the curves could be seen more clearly. The quick phases of optokinetic nystagmus were analyzed by the same procedure as were saccadic eye movements. A photodiode was set just in front of the projector so as to catch a light stripe; it emitted an electrical spike as a trigger that indicated the moment when that stripe passed through the center of the visual field. Two monocular recordings of quick phases were displayed on the CRT in the same manner as saccade (FIGURES 5 and 6). Thus the latency, duration, and velocity of saccades and quick

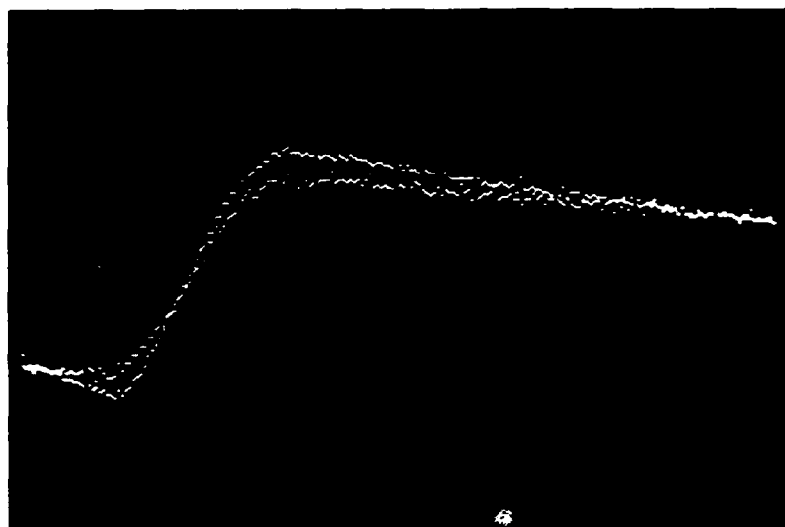


FIGURE 6. The superimposition of the two curves in FIGURE 5.

phases of optokinetic nystagmus were computed. In this report, however, we mainly consider the relationship between both eyes during horizontal or vertical saccades and quick phases of optokinetic nystagmus.

RESULTS

FIGURES 3 and 4 illustrate the typical relationship between both eyes during a saccadic eye movement to the right. The upper curve of FIGURE 3 is a saccade of the right eye to the right, i.e., abduction of the right eye, and the lower curve is a saccade of the left eye to the right, i.e., adduction of the left eye. FIGURE 4 shows the superimposition of the same two curves. FIGURES 7 and 8 show leftward saccades of both eyes. The upper curve of FIGURE 7 is a saccade of the right eye to

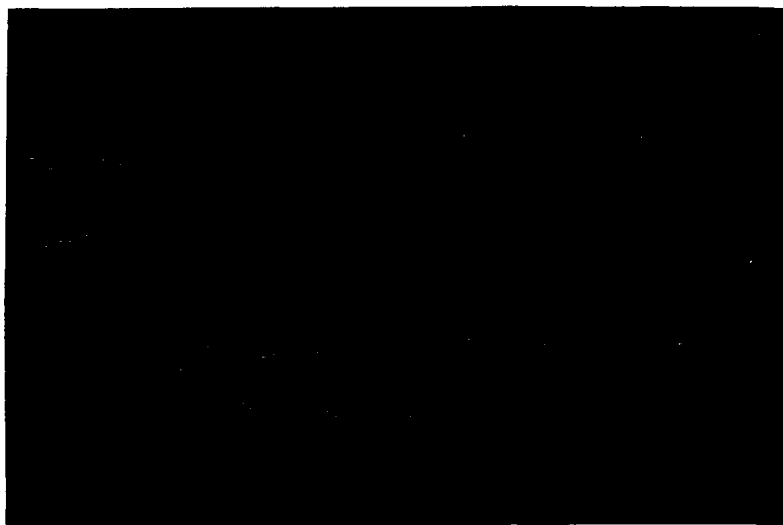


FIGURE 7. The relationship of the eyes in saccade to the left. Curves as in FIGURE 3.

the left, i.e., adduction, and the lower curve is the left eye to the left, i.e., abduction. FIGURE 8 is the superimposition of these two curves. Most saccades to either direction show the same relationship between the eyes. The abducting eye starts a few milliseconds earlier than the adducting eye. The adducting eye, however, moves faster than the abducting eye and reaches the target a few



FIGURE 8. The superimposition of the two curves in FIGURE 7.

milliseconds earlier (FIGURES 3, 4, 7, and 8). The adducting eye has a tendency to overshoot the new target at the end of saccade. The abducting eye has, in contrast, a tendency to creep up on the new target. As a consequence, both eyes converge at the turning point of the saccade and then diverge to fixate the new target. These characteristics can be seen in most horizontal saccadic eye movements. FIGURE 9 illustrates this and shows the distributions of time differences at the beginning and end of the saccade. The time delay of adduction to abduction at the beginning of saccade shows a normal distribution, ranging from -4 mseconds to 30 mseconds. The mode is 6 mseconds, the mean is 7.4 mseconds, and the standard deviation is 5.0 mseconds. The time precedence of adduction at the turning point is distributed from -20 mseconds to 40 mseconds. The mode is 10 mseconds, the mean is 7.6 mseconds, and the standard deviation is 8.6 mseconds. These facts indicate that during horizontal saccades, both eyes jump to the new target not only asynchronously but also disconjugately, with a complicated disparity. These characteristics and relationships can be seen even when

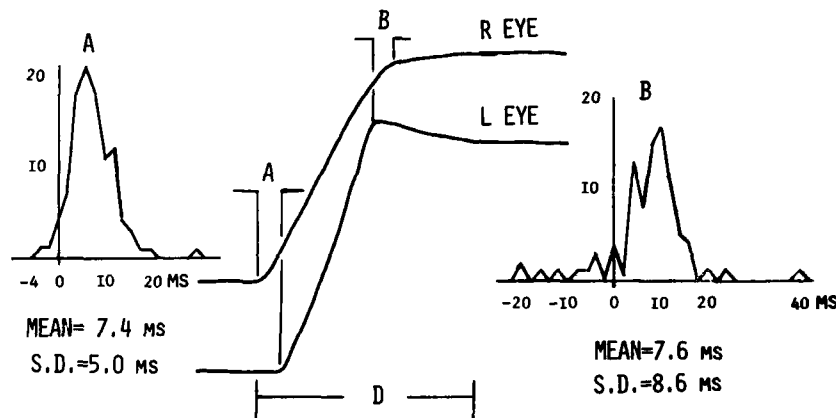


FIGURE 9. The schema of the relationship between movements of both eyes and distribution of time differences in horizontal saccade. A: Time difference at beginning of saccade. B: Time difference at turning point. D: Duration of saccade.

one eye is covered and the other moves consensually. In vertical saccades, on the other hand, the beginning and end of movement of both eyes are fairly synchronous. The velocities of both eyes in vertical saccades are identical. There is a tendency to overshoot the target in upward saccades. In downward saccades, in contrast, the eyes tend to reach the new target gradually. These tendencies are seen in both eye movements equally and are conjugate (FIGURES 10 and 11). Accordingly, there is no difference between two monocular recordings and a binocular recording. This synchrony of conjugate movement in vertical saccades is in contrast to the asynchrony and disconjugate movements of the eyes in horizontal saccades.

A similar tendency can be seen in optokinetic nystagmus. During quick phases of optokinetic nystagmus toward the right, the abducting right eye starts to move a few milliseconds earlier than the adducting left eye. The shift from quick

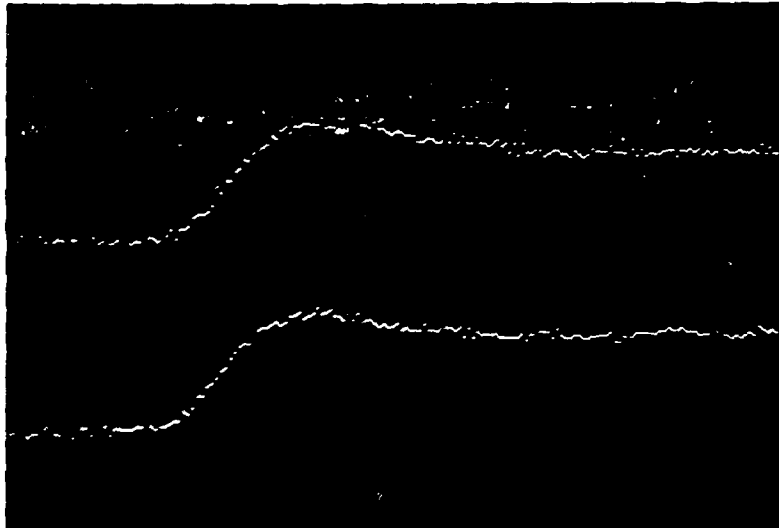


FIGURE 10. The movement of both eyes in upward saccade. The upper curve is right-eye movement, and the lower curve is left-eye movement. There is no disparity between the two movements. There is a tendency to overshoot.

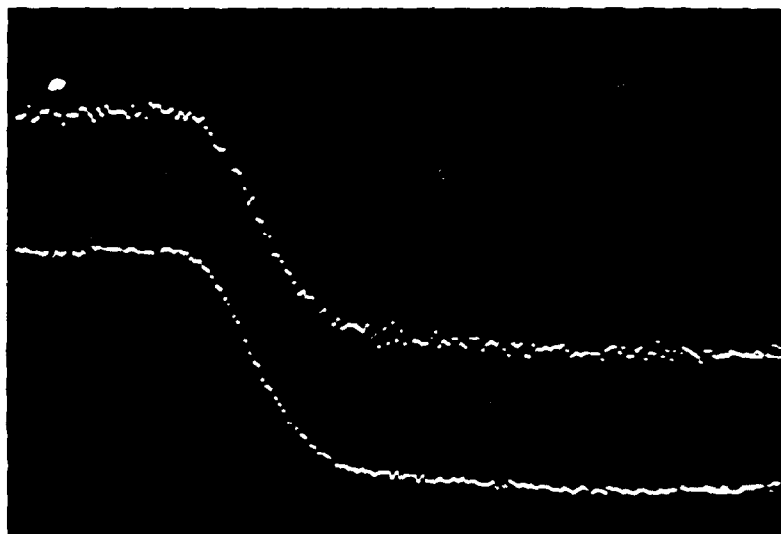


FIGURE 11. The movement of both eyes in downward saccade. Both eyes conjugate well and have a tendency to creep.

phases to slow phases is gradual in the abducting eye. In contrast the shift is more sudden in the adducting eye (FIGURE 5). FIGURE 6 shows the superimposition of the curves from FIGURE 5; the time difference at the beginning of quick phases and the shape of the curve at the turn from quick to slow phases can be seen clearly. The quick-phase velocity of the adducting left eye is greater than that of the adducting right eye.

These facts correspond to the overshoot and undershoot in horizontal saccadic eye movements. In quick phases of optokinetic nystagmus toward the left, the time differences at the beginning, the velocities, and the curves of the turning of the eyes are the reverse of those toward the right.

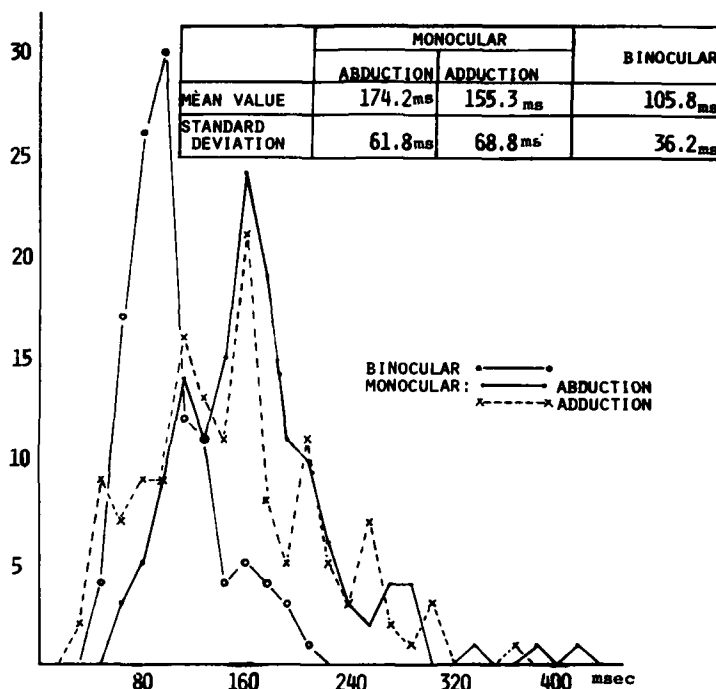


FIGURE 12. The distribution of duration in monocular and binocular recordings of horizontal saccade. The duration in the binocular recording is remarkably shorter than that in the monocular recordings.

The latency and duration of saccade in monocular recordings of each eye and in a binocular recording were measured on the EOG. The durations of horizontal saccades in both monocular and binocular recordings can be seen in FIGURE 12. Their amplitude is 10° of arc, and they seem to distribute normally. The mean duration is 174.2 mseconds in the recording of the abducting eye, 153.3 mseconds in the recording of the adducting eye, and 105.8 mseconds in the binocular recording; the standard deviations are 61.8 mseconds, 68.8 mseconds, and 36.2 mseconds respectively. The duration of horizontal saccades in the binocular

recording is remarkably shorter than that of both monocular recordings. This time difference seems to correspond to the period from the turning point to the concurrence of the two monocular curves. This fact suggests that the speed of both eyes in approaching from both sides after the turning point must be approximately the same.

DISCUSSION

The latency, duration, and velocity of saccadic eye movement have been studied by various researchers. Most of them have treated the saccade as a conjugate movement. Therefore, binocular recordings or monocular recordings of only one eye were used. The results were not always consistent. However, these researchers used different methods of investigation. Dodge and Westheimer used an optical method.^{1,3} Robinson used a search coil mounted on a contact lens.⁶ Hyde employed high-speed photography.¹¹ Brockhurst, White, Saslow, Becker, and Baloh utilized electrical methods.^{2,4,7-9} Some of these investigators reported that duration, velocity, and latency differed with the direction of saccades: temporal and nasal, right and left, or lateral and central.^{4,6,11} The methods of registration with which they found these differences were monocular. All except Robinson concluded that the velocity of eye movements to the center was higher than of lateral eye movements. Robinson stated that in most subjects, temporal saccades had a higher velocity than did nasal saccades.⁶ Most of these researchers used monocular observation of only one eye and therefore did not mention the relationship between the eyes. White and Westheimer used monocular registration of both eyes simultaneously.^{3,4} Westheimer, however, had no interest in the correlation between both eyes.³ White reported that in the initiation of saccades, the left eye began its motion a short time before the right eye when the stimulus was to the left and vice versa.⁴ These facts can be expressed in another way: the abducting eye begins to move shortly before the adducting eye in horizontal saccades. It is a well-known fact that adduction and abduction of the eye are controlled by different nerves—the oculomotor and abducens nerves. In horizontal eye movement, the abducens nucleus is fired first, and then the oculomotor nerve is stimulated by impulses from the abducens nucleus through the medial longitudinal fasciculus (MLF).¹³ Based on the similarity of the time order in the firing of nuclei and in the action of external eye muscles as reported in this study, we propose the following hypothesis. The main cause of the time difference between the eyes in horizontal saccade must be the difference in the neural mechanism of abduction and adduction of the eye. In horizontal optokinetic nystagmus, where the same neural pathway is utilized, the relationship between both eyes in quick phase is very similar to that of horizontal saccade, as demonstrated in the present study. This fact also supports our hypothesis. Caloric nystagmus was analyzed in the same way in a few cases, and similar results were observed. Caloric nystagmus also is induced through this common neural path.

This neural system does not participate in vertical eye movement. This coincides well with the fact that disconjugate movements of both eyes have not been seen in vertical saccades. Hyde reported that at the end of abduction, the eye creeps onto the new target.¹¹ This evidence is the same as our results in the present study. On the other hand, Hyde stated that adduction ceased abruptly. This result also resembles ours in that the adducting eye has a tendency to overshoot the new target. As to eye velocity in saccades, the most consistent result

is that the nasal, or left-eye-to-right, saccade is faster than the temporal, or left-eye-to-left, saccade. This result can be expressed in other terms: the eye velocity of adduction is faster than that of abduction. These facts suggest the following hypothesis: horizontal saccades are initiated by the abducens system, and adduction is a reflexive movement triggered by abduction. In saccadic eye movements, the gaze angle jumps from the point of regard to a new target that has imaged on the peripheral retina. This eye movement is thought to be predictive and is controlled by a feed-forward system through the cerebellum. The visual angle between the fixation point and the new target is calculated from the position of the target's image on the peripheral retina. The amplitude of movement is preset according to the results of calculation before the saccade and jumps to the approximate position of the new target. In this jump, visual perception is suppressed by the efferent copy of the eye movement. The period from initiation to turning point in saccades may correspond to this period of suppression. After the turning point, however, as the velocity decreases, perception possibly recovers. Then the error in the angle can be detected by an image position on the retina that is perceived by the recovered visual acuity and is corrected with creeping of both eyes from both sides by vergence or with small saccades, namely, corrective saccades.

The characteristics of horizontal saccades induced by monocular stimulation were not different from those of horizontal saccades induced by binocular stimulation. This fact suggests that in the case of monocular vision, horizontal saccades also may be initiated by the abducens system. Contraction of the lateral rectus of the covered eye and relaxation of the lateral rectus of the uncovered eye are programmed and executed in accordance with the image position on the retina of the uncovered eye. Then the nuclei of the medial rectus of both eyes are stimulated by impulses from both abducens, and the muscles relax or contract respectively. Surely the error of the new point of regard is detected by the uncovered eye. However, the correction, again, may be initiated by the abducens system.

The quick phase of horizontal optokinetic nystagmus must be controlled by the same mechanism because the characteristics of quick phase bear a striking resemblance to those of saccadic eye movement.

Vertical eye movement is controlled by a quite different system, mainly by the oculomotor nerve. The oculomotor nuclei are fired directly by impulses from the higher central nervous system. These impulses are supposed to be given bilaterally. Therefore, vertical saccades of both eyes start synchronously and jump to the new target conjugately with the same velocity of excursion. In consequence, a remarkable contrast between vertical and horizontal saccade can be seen.

SUMMARY

In horizontal saccades, abduction and adduction are not conjugate. Abduction starts shortly before adduction and reaches the turning point shortly after adduction. The duration in binocular recording is much shorter than in monocular recordings. The abducting eye has a tendency to move gradually on the new target. The adducting eye has, on the contrary, a tendency to overshoot. The characteristics of quick phases of horizontal optokinetic nystagmus, in which both eyes jump disconjugately to the new target, are similar to those of horizontal

saccades. The main cause of this disparity may be a difference in neural mechanisms between abduction and adduction. Vertical saccades are not conjugate.

REFERENCES

1. DODGE, R. 1903. Five types of eye movement in the horizontal meridian plane of the field of regard. *Am. J. Physiol.* **8**: 307-329.
2. BROCKHURST, R. J. & K. S. LION. 1951. Analysis of ocular movements by means of an electrical method. *Arch. Ophthalmol.* **46**: 311-314.
3. WESTHEIMER, G. 1974. Mechanism of saccadic eye movements. *Arch. Ophthalmol.* **52**: 710-724.
4. WHITE, C. & R. EASON. 1962. Latency and duration of eye movements in the horizontal plane. *J. Opt. Soc. Am.* **52**: 210-213.
5. BARTZ, A. 1962. Eye-movement latency, duration and response time as a function of angular displacement. *J. Exp. Psychol.* **64**: 318-324.
6. ROBINSON, D. 1964. The mechanics of human saccadic eye movement. *J. Physiol.* **174**: 245-264.
7. SASLOW, M. 1967. Latency for saccadic eye movement. *J. Opt. Soc. Am.* **57**: 1030-1033.
8. BECKER, W. & A. FUCHS. 1969. Further properties of the human saccadic system: eye movements and correlation saccades with and without visual fixation points. *Vision Res.* **9**: 1247-1258.
9. BALOH, R., A. SILLS, W. KUMLEY & V. HONRUBIA. 1975. Quantitative measurement of saccade amplitude, duration and velocity. *Neurology* **12**: 1065-1070.
10. BALOH, R., W. KUMLEY & V. HONRUBIA. 1976. Algorithm for analyses of saccadic eye movements using a digital computer. *Aviat. Space Environ. Med.* **47**: 523-527.
11. HYDE, J. 1959. Some characteristics of voluntary human ocular movements in the horizontal plane. *Am. J. Ophthalmol.* **48**: 85-94.
12. MIYOSHI, T. 1977. Foveal and peripheral nystagmus. In *Proceedings of the Fifth Barany Society Meeting*: 171-174. Japan Society for Equilibrium Research. Kyoto, Japan.
13. BENDER, M. & E. WEINSTEIN. 1944. Effects of stimulation and lesion of the median longitudinal fasciculus in the monkey. *Arch. Neurol. Psychiatry* **52**: 105-113.

DIFFERENT EFFECTS INVOLVED IN THE INTERACTION OF SACCADDES AND THE VESTIBULO-OCULAR REFLEX*

Reinhart Jürgens, Wolfgang Becker, and Peter Rieger

*Neurophysiology Section
University of Ulm
D-7900 Ulm, Federal Republic of Germany*

INTRODUCTION

The vestibulo-ocular reflex (VOR) stabilizes the direction of gaze in space, whereas a quick eye movement rapidly shifts it into a new position. Both types of eye movements interact in many natural situations. In darkness, for example, the slow phases (i.e., the VOR) of vestibular nystagmus (VN) frequently are interrupted by involuntary quick eye movements, the quick phases, which always counteract the slow phases. Voluntary saccades, on the other hand, may interact with the VOR in any direction.

Both voluntary saccades and quick phases of nystagmus seem to stem from the same neuronal circuitry.¹ It therefore might be expected that their interaction with the VOR also would be the same. In a previous study we have, by contrast, demonstrated that the interaction between goal-directed saccades and the VOR is different from the interaction between quick phases of VN and the VOR² (see also below), and we speculated that our results were related to the different purposes that saccades and quick phases subserve: whereas quick phases only roughly reorient eye position when the eyes are displaced somewhat in the orbit by the slow phase, it is the purpose of saccades to acquire visual targets with high precision. Thus, it seems conceivable that the mechanism responsible for the particular type of interaction that occurs between saccades and the VOR is related to the mechanism by which goal-directed saccades achieve their accuracy. In order to pursue this idea, the present study investigated the accuracy of goal-directed saccades during sinusoidal head rotation. It could be demonstrated that saccades under such conditions have an even better accuracy than would be expected from our previous "interaction results."²

METHODS

Ten healthy subjects sat on a hydraulically driven chair with their heads stabilized on the chair frame. The chair was rotated sinusoidally around the vertical axis at 1.0 Hz and 120°/second peak velocity. The subjects were instructed to fixate on visual targets (red-light-emitting diodes) that were mounted on two horizontal bars, one fixed in space and the other rotating with the subjects. Each bar had five targets, with an angular separation of 11.4° between each target. All targets were switched on sequentially in random order. When one of the stationary targets was shown, the VOR gain, aided by visual fixation, reached almost 1.0; when the target was rotating with the subjects, there

*This work was supported by the Deutsche Forschungsgemeinschaft (SFB 70/U3).

was a residual VOR with an average gain of 0.3. Only saccades made either between two stationary targets or between two rotating targets were considered. Horizontal eye movements were recorded electro-oculographically and analyzed by a computer.³

Test for Linear Summation of Quick and Slow Eye Movements

FIGURE 1, left, schematically shows eye position and eye velocity of saccades embedded in a sinusoidal smooth eye movement. It illustrates that saccades could be in the same ("ipsi") or in the opposite ("contra") direction as the slow movement, or somewhere between the two extremes (upper trace). It assumes a linear summation of quick and smooth eye-velocity commands (lower trace). FIGURE 1, right, describes the procedure used to test whether or not such embedded saccades do, in fact, add linearly with the smooth component. First, the amplitude-duration (A-D) relation for the subjects' normal saccades between stationary targets with the head still was established. Given the measured parameters ϕ and T of embedded saccades as defined in FIGURE 1, left, linear summation predicts that their mean-velocity deviation, $\Delta\bar{v}$ ($\Delta\bar{v} = \Delta\phi/T$, see FIGURE 1), from normal saccades with the same duration, T , should equal the smooth-component velocity. As a measure of this velocity, one can consider the velocity just before (v_b) or just after (v_a) the saccade. Thus, a plot of $\Delta\bar{v}$ against v_b or v_a should be a straight line of slope +1, as in FIGURE 1, lower right, if linear summation takes place.

RESULTS

Previous Experiments

In a number of different experiments with humans, it could be demonstrated that goal-directed saccades add partially with smooth eye movements of various origins whereas quick phases of nystagmus do not. These results are summarized in FIGURE 2. Consider, for example, the center left panel labeled "VOR + fixation." It depicts how the characteristics of visually guided saccades change if they are embedded in the smooth eye movements that result from the combined action of the VOR and the visual fixation system during rotation in the light. The figure shows the velocity deviation, $\Delta\bar{v}$, of these saccades from normal saccades as a function of the smooth velocity after each saccade. The upper of the two curves (open circles) was obtained with a peak head velocity of $\dot{\psi} = 125^\circ/\text{second}$. It has a clear positive slope, indicating a linear summation of saccades with the smooth movement. However, the curve differs from the theoretical line for linear summation in two ways: (1) its average slope is less than 1.0, suggesting an *incomplete* summation of saccades with the VOR, and (2) it has an unexpected offset of about $+70^\circ/\text{second}$, which indicates that the embedded saccades were faster than normal even if there was transiently no smooth movement (saccade occurring during turnaround of head position); we termed this phenomenon "activation effect." The lower curve in the same panel corresponds to a peak head velocity of $\dot{\psi} = 75^\circ/\text{second}$. It has the same slope, but only a $15^\circ/\text{second}$ activation. The same phenomena were observed also when acoustically evoked saccades were embedded in a pure VOR during rotation in the dark (upper left

Test for "Linear Summation"

Definition of Parameters

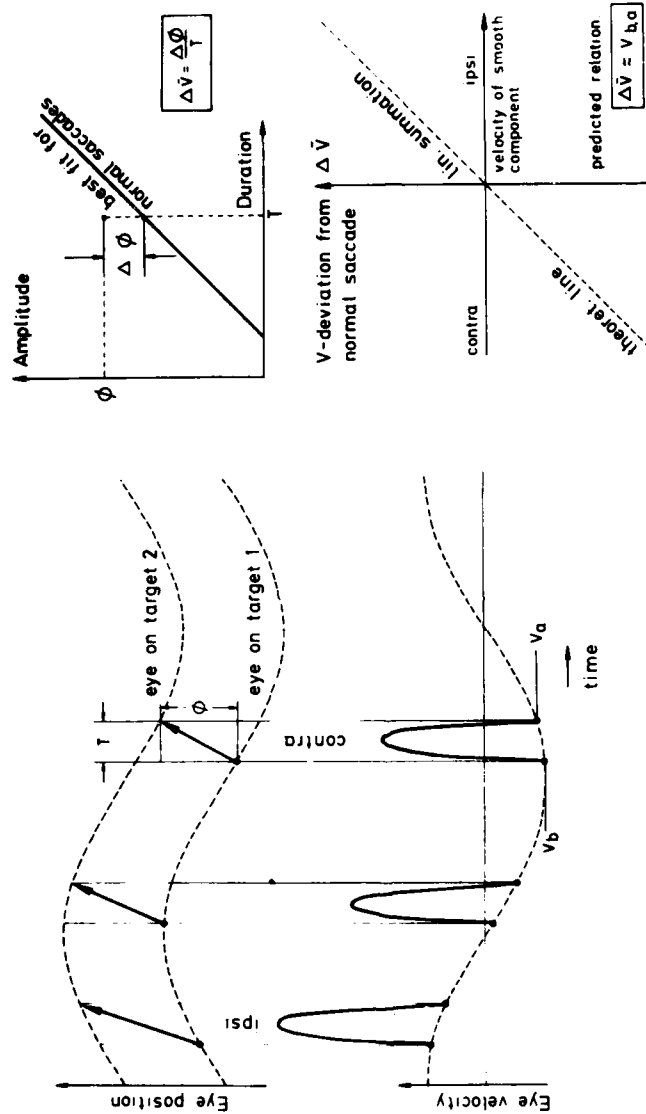


FIGURE 1. Left: schematized time courses of eye position (upper trace) and eye velocity (lower trace) of saccades (solid lines and arrows) embedded in a sinusoidal smooth eye movement (broken line). Right: test for linear summation of saccade and smooth-movement velocities. Linear summation predicts $\Delta \dot{V}$ (defined in the upper right panel) to equal the smooth-component velocity v_b (before the saccade) or v_a (after the saccade). v_b and v_a are defined in the lower left panel.

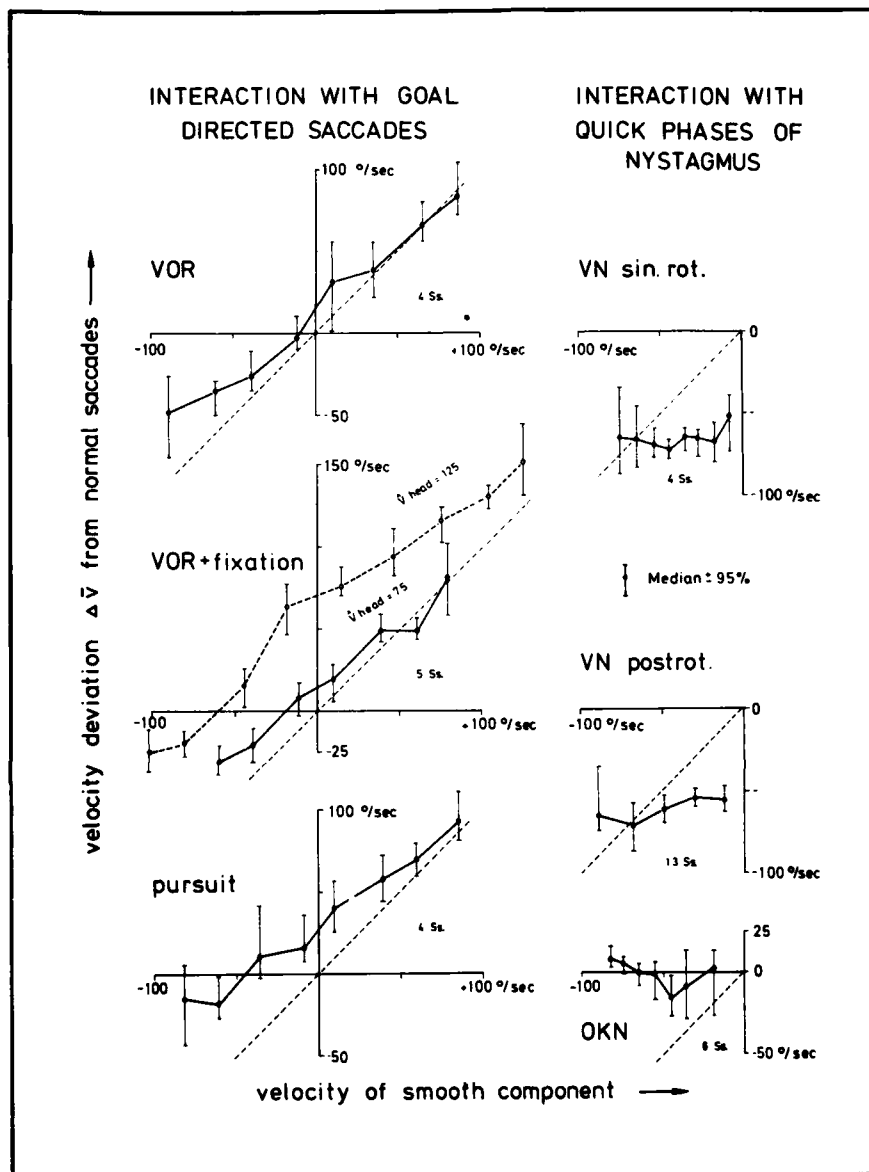


FIGURE 2. Comparison of the interaction of goal-directed saccades (left) and of quick phases of nystagmus (right) with smooth eye movements generated in different ways. The velocity deviation of goal-directed saccades exhibits a similar correlation with smooth-component velocity whether the latter is generated by VOR alone (saccades to acoustic stimuli in dark), by a combination of VOR and fixation (saccades to lit targets), or by pursuit (head stationary but target moving). The velocity deviation of quick phases of vestibular and optokinetic nystagmus is uncorrelated with smooth-component velocity whether the latter is generated during sinusoidal rotation in dark (VN sin. rot.), during postrotatory nystagmus (VN postrot.), or during optokinetic nystagmus (OKN). Median values of pooled data from several subjects; number of subjects indicated in each panel.

panel) or when goal-directed saccades occurred during pure visual pursuit movements (lower left panel).

By contrast, quick and slow phases of VN and optokinetic nystagmus (OKN) interacted in a quite different way. FIGURE 2, right, compares the velocity of quick phases of VN (produced during sinusoidal rotation and during postrotatory nystagmus in the dark) to saccades made in the dark while there was no rotation. The figure shows the velocity difference between quick phases and dark saccades as a function of the slow-phase velocity. For both situations, the slope of this relation is almost horizontal, and the relation has a negative offset. This indicates that (1) quick- and slow-phase velocities of VN do not add and (2) quick phases of VN are slower than saccades in darkness. Preliminary results with OKN suggest that quick and slow phases of OKN do not add either, but that OKN quick phases are about as fast as normal saccades (FIGURE 2, lower right).

Metrics of Saccades during Visual Suppression of VOR

The first aim of the present study was to investigate whether the occurrence of the unexpected activation effect depends on the saccades being embedded into smooth eye movements. The previous experiments showed that saccades could be faster than normal even if there was momentarily no smooth movement (cf., previous section). This suggested that the activation effect depends on stimulation of the vestibular system rather than on the presence of a smooth-pursuit movement. To this end, saccades during VOR (targets stationary in space) and during VOR suppression (targets rotating with the subjects) were compared. In the latter case, there were almost no smooth eye movements, but the input vestibular command still was present. The velocity characteristics of the saccades in the two situations were assessed by evaluating their A-D slopes. In order to isolate the activation effect, first the "net saccade amplitudes," A , were calculated by removing the VOR contribution, assuming a partial summation of 70% (cf., previous section), from the measured amplitudes, ϕ (see inset in FIGURE 3).

As displayed in FIGURE 3, the A-D slopes of saccades made during VOR and during suppression of VOR appeared almost exactly the same, but both were about 10% steeper than for normal saccades. These findings suggest that the saccadic system is, in fact, activated by the vestibular stimulation per se. The mechanism by which this stimulation leads to the activation is not clear at present.

Does the Activation Effect Influence the Accuracy of Goal-Directed Saccades?

Human saccades frequently undershoot their target. The average size of saccades responding to target steps of more than 10° of amplitude is roughly 90% of the target amplitude. One may ask whether activated saccades, due to their higher velocity, have a different accuracy. To answer this question, we measured the net amplitude of saccadic responses to target steps of 11.4° , 22.8° , 34.2° , and 45.6° amplitude during VOR (target stationary in space) and during VOR suppression (target rotating with the subject).

As can be seen from FIGURE 3, both types of saccades have essentially the same amplitude as normal saccades. Those during head rotation, however, reach

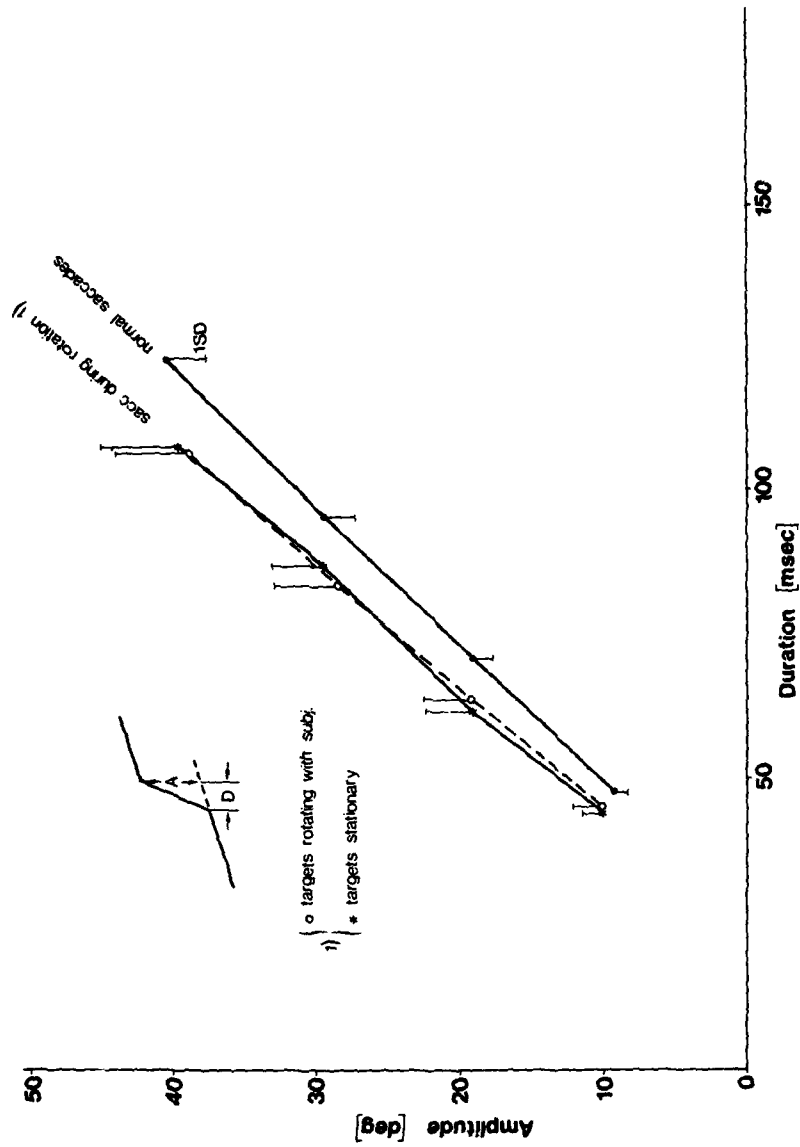


FIGURE 3. Family of amplitude-duration (A-D) relations of goal-directed saccades under different experimental conditions. Note that the amplitudes, A, have been measured as indicated in the inset and do not include contributions caused by an ongoing smooth component (see text for details).

their targets with shorter durations. Saccades of about 40° amplitude, for example, needed only 108 mseconds or so during head rotation but about 122 mseconds without head rotation. The described constancy of saccade amplitudes conflicts with the idea of a rigid preprogramming of the saccade amplitude by means of a predetermined duration. With preprogramming, activated saccades would have the same duration as normal ones but, being faster, would achieve a larger amplitude during this time. Rather, our findings are in agreement with the idea that the saccade is controlled by nonvisual feedback during its execution.⁵

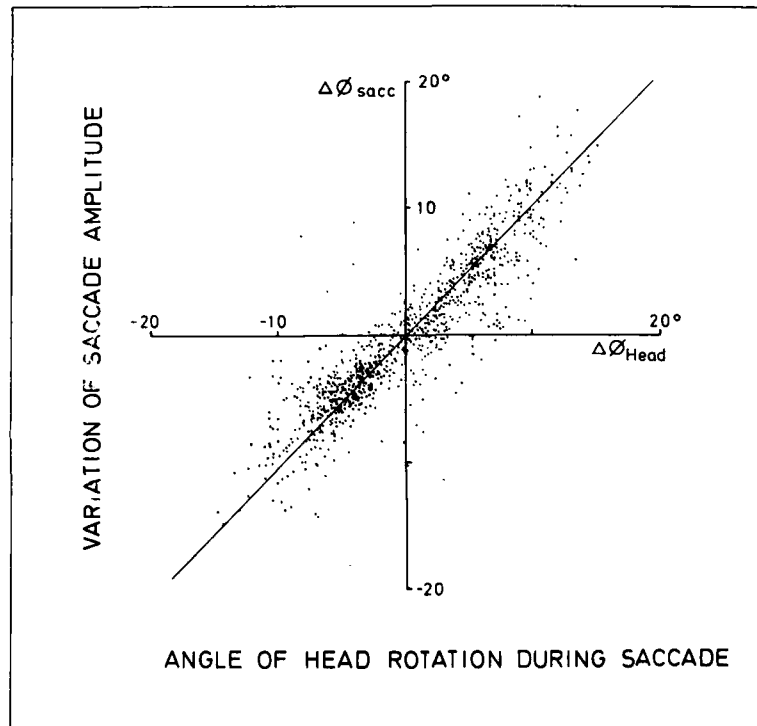


FIGURE 4. Variation of saccade amplitude ($\Delta\phi_{\text{sacc}}$, defined as the amplitude deviation of goal-directed saccades in the VOR + fixation condition from normal saccades elicited by the same target displacement) as a function of the angle of head rotation, $\Delta\phi_{\text{Head}}$, during each embedded saccade. Pooled data from all subjects and all target amplitudes.

Does the Incomplete Summation Influence the Accuracy of Goal-Directed Saccades?

During sinusoidal head rotation, saccades aimed at stationary targets in space (VOR + fixation) must account for the angle $\Delta\phi_{\text{Head}}$ through which the head is turned during their execution, in order to achieve normal accuracy. Assuming,

for instance, a head-rotation velocity of $100^\circ/\text{second}$ and a saccade duration of 50 mseconds, an ipsi-saccade must have a 5° larger (and a contra-saccade, a 5° smaller) amplitude than a normal saccade elicited by the same target amplitude. If there were a full linear summation of saccade velocity and VOR velocity, the necessary $\Delta\phi_{\text{Head}}$ values would ensue automatically. But, since the summation effect amounted to only about 70%, an actual $\Delta\phi_{\text{sacc}}$ of only $70\% \cdot 100^\circ/\text{second} \cdot 50 \text{ mseconds} = 3.5^\circ$ can be expected in the given example ($\Delta\phi_{\text{sacc}}$ denotes the amplitude deviation of an embedded saccade from a normal saccade). This prediction was tested.

FIGURE 4 relates $\Delta\phi_{\text{sacc}}$ to $\Delta\phi_{\text{Head}}$ (pooled data from all subjects). Interestingly, the relation has a slope of almost 1.0. This indicates that the angle of head rotation during the saccade is 100% accounted for, and not only 70% as expected. Therefore it can be concluded that the eyes reach their target with exactly the same accuracy as normal saccades.

This unexpected constancy of the saccade accuracy is analyzed in more detail in FIGURE 5, which represents saccadic responses to target steps of 11.4° in the VOR + fixation condition. In FIGURE 5A, the amplitudes of embedded saccades are plotted as a function of $\Delta\phi_{\text{Head}}$. The relationship has a slope of close to 1.0, in accordance with FIGURE 4, and an intercept of 10° . The intercept indicates an accuracy of 88% for these saccades, which is fairly normal. In FIGURE 5B, the variation of saccade velocity (defined as the difference of individual peak velocities from the average peak velocity) is plotted as a function of the head velocity measured during the saccade. This relation has a slope of 0.7, in agreement with the notion that only 70% of VOR velocity is added to the velocity of the embedded saccade. As outlined above, this incomplete addition of the VOR velocity will account for about 70% of the head displacement during the saccade. In order to compensate for the remaining 30%, the duration of the saccade is varied. This is shown in FIGURE 5C.

It will be noted that ipsi-saccades have, on the average, longer durations than contra-saccades. Ipsi-saccades that occur at $100^\circ/\text{second}$ head velocity, for example, have a duration about 4 mseconds longer as compared with those at zero head velocity. Given the A-D slope of these saccades ($450^\circ/\text{second}$, see FIGURE 3), such a lengthening increases the saccade amplitude by 1.8° . The average duration of saccades aimed at 11.4° was about 50 mseconds. Thus, with a head velocity of $100^\circ/\text{second}$, 30% of head displacement during such a saccade corresponds to $30\% \cdot 100^\circ/\text{second} \cdot 50 \text{ mseconds} = 1.5^\circ$, which is in fairly good agreement with the value of 1.8° derived from FIGURE 5C. Similar results were obtained with target steps of 22.8° .

These data therefore suggest that an adjustment of the saccade duration helps to achieve the desired accuracy of gaze in our experiment.

MODEL IMPLICATIONS

Recent human experiments support the concept that saccades are not "ballistic" in nature, but rather seem to be controlled by a "local feedback," which helps the saccade to reach its desired position despite variations of velocity from one saccade to another.^{4,5} The "local feedback" hypothesis offers a basis for the interpretation of the present experimental results.

The relevant section of a model of the oculomotor system based on this hypothesis is given in FIGURE 6. It assumes that during goal-directed saccades, a

signal representing 70% of head velocity ($g = 0.7$) is added to the neural activity that determines saccade velocity (i.e., the saccadic pulse). The summated velocity signal is integrated, thereby yielding "eye position in head." A copy of this internal eye position representation is then fed back locally and compared to the "desired eye position in head." A saccade, once initiated, will continue as long as the difference of these two signals exceeds a given threshold.

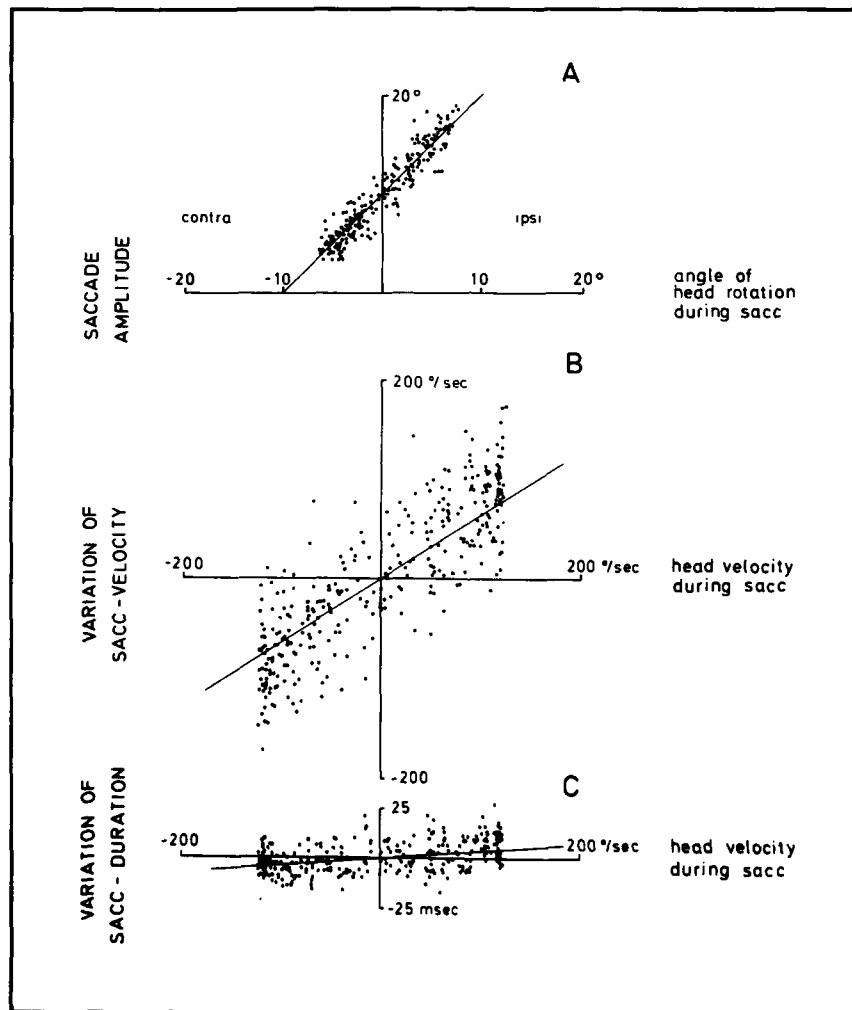


FIGURE 5. Parameters of saccadic reactions to target steps of 11.4° in the VOR + fixation condition. A: amplitude of embedded saccades as a function of the angle of head rotation, $\Delta\phi_{\text{Head}}$, during each saccade. B: variation of saccade peak velocity as a function of head velocity during each saccade. C: variation of saccade duration as a function of head velocity during each saccade.

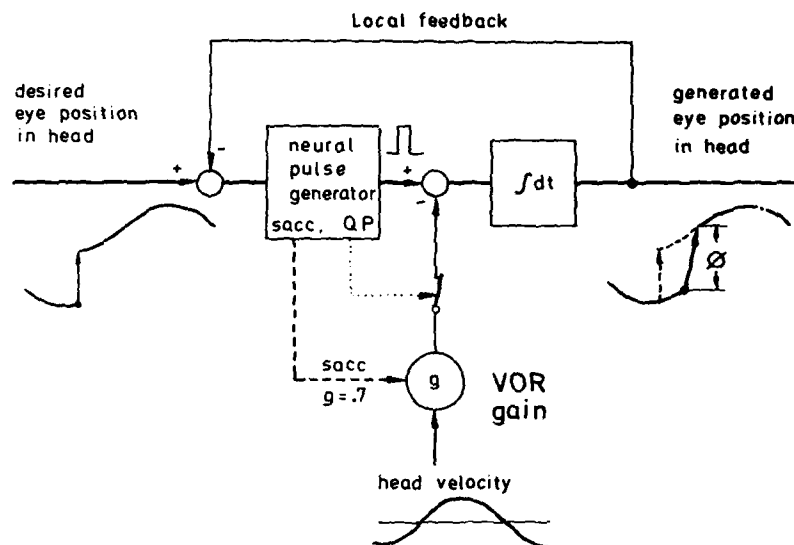


FIGURE 6. Simplified part of an oculomotor model that contains a "local feedback" controlling the saccades. Outside of saccades, the VOR gain is allowed to reach 1.0. During voluntary saccades, the VOR is assumed to have a gain of 0.7; and during quick phases of nystagmus, the VOR is thought to be switched off completely. Voluntary responses to target steps in the VOR + fixation condition require a combination of a smooth compensatory movement and a rapid gaze step. A typical time course of the desired eye-position signal in this condition is given in the left graph; and a typical response to this pattern is schematized by the solid lines in the right graph; dashed arrow and curve indicate desired time course. Note that the generated saccade amplitude, ϕ , differs from the amplitude of the desired gaze step (dashed arrow). At the end of a saccade, generated and desired eye positions match. This match is ensured by the local feedback mechanism and depends neither on variation of saccade velocity (e.g., caused by an activation of the saccade) nor on the lack of a full VOR while the saccade is executed (due to incomplete summation of VOR and saccade velocities).

Such a scheme could therefore explain the normal accuracy of activated saccades as well as the normal accuracy of saccades that are embedded in the VOR. Whatever momentary intensity the saccade pulse assumes, the feedback mechanism ensures a constant accuracy by shortening or lengthening the saccade duration accordingly. The proposed model also corrects the incomplete summation of VOR and saccadic commands automatically since it compares "generated eye-in-head position" with "desired eye-in-head position" and ensures the match of these two signals at the end of each saccade.

In summary, the model would explain our observations on voluntary, goal-directed saccades that are embedded in the VOR. It was not possible, however, to decide in the present study to what extent the quick phases of nystagmus (which interact with the VOR in a different way) share the postulated feedback circuitry. Although it has been shown that quick phases "reorient" eye position in the direction of head turning,⁶ their performance is too variable to allow enough insight into their intrinsic goals by means of studying behavioral data. Which neuronal structures are common to quick phases and voluntary saccades and which are not therefore is a question that remains to be elucidated further.

SUMMARY

The accuracy of human goal-directed saccades during passive sinusoidal whole-body rotation is the same as that of normal saccades with the head still. Two mechanisms contribute to this accuracy:

1. There is an incomplete summation (70% on the average) of saccade and VOR velocities.
2. The duration of saccades during head rotation is lengthened if VOR and saccade velocities have the same direction, and is shortened if their direction is opposite.

The latter finding supports the hypothesis that saccades are controlled by local feedback.

ACKNOWLEDGMENTS

We are indebted to Miss H. Kohler for her help with the illustrations and to Mr. A. Renner for his technical support.

REFERENCES

1. COHEN, B. & V. HENN. 1972. The origin of quick phases of nystagmus in the horizontal plane. *Bibl. Ophthalmol.* **82**: 36-55.
2. JÜRGENS, R., W. BECKER, P. RIEGER & A. WIDDERICH. 1981. Interaction between goal directed saccades and VOR is different from interaction between quick phases and VOR. In *Progress in Oculomotor Research*. A. Fuchs & W. Becker, Eds.: 11-18. Elsevier, New York, N.Y.
3. JÜRGENS, R. & W. BECKER. 1978. A computer program library for detecting and analyzing eye movements. In *Biosigma* 78, 2: 187-193. Committee for International Conferences on Signals and Images in Biology and Medicine. Paris, France.
4. JÜRGENS, R., W. BECKER & H. H. KORNHUBER. 1981. Natural and drug-induced variations of velocity and duration of human saccadic eye movements: evidence for a control of the neural pulse generator by local feedback. *Biol. Cybern.* **39**: 87-96.
5. ZEE, D. S., L. M. OPTICAN, J. D. COOK, D. A. ROBINSON & W. KING ENGEL. 1976. Slow saccades in spinocerebellar degeneration. *Arch. Neurol.* **33**: 243-251.
6. CHUN, K. S. & D. A. ROBINSON. 1978. A model of quick phase generation in the vestibuloocular reflex. *Biol. Cybern.* **28**: 209-221.

MODIFICATION OF SACCADIC EYE MOVEMENTS BY VARIOUS CENTRAL NERVOUS SYSTEM DYSFUNCTIONS*

Yo Kimura and Isao Kato

*Department of Otolaryngology
Yamagata University School of Medicine
990-23 Yamagata, Japan*

Yukio Watanabe and Kanemasa Mizukoshi

*Department of Otolaryngology
Toyama Medical and Pharmaceutical University
930-01 Toyama, Japan*

INTRODUCTION

Slow saccadic eye movements are observed in some patients with neurological diseases such as Huntington's chorea, Wilson's disease, progressive supranuclear palsy, and various types of spinocerebellar degeneration.¹⁻⁹ Routine electronystagmography (ENG) equipment, however, cannot detect slowing of saccades until the velocity decreases severalfold, and the mechanism of saccade slowing remains unknown. Recently, quantitative measurements of saccades with a laboratory digital computer have been used to accurately assess saccades.¹⁰⁻¹²

The present experiments are concerned on the one hand with investigating saccade abnormalities and on the other hand with defining the differences between two types of tracking eye movements and assessing the differential diagnosis of patients with central nervous system (CNS) dysfunction.

METHOD AND MATERIALS

Thirty-two normal subjects were studied to determine the reliability and usefulness of a clinical test for accurate measurement of saccadic eye movements.

Recording of Eye Movements

Electrodes were placed laterally to both outer canthi to record horizontal eye movements, and a ground electrode was located on the forehead. The binocular horizontal direct-current ENG was recorded with a rectilinear pen linkage. All eye movements were stored on magnetic tape for later digital-computer analysis.

*Supported by the Ministry of Education of Japan (Grants No. 477659 and 577620).

Saccadic Eye Movement

Target Generation

The subject was seated in a chair with his head fixed mechanically. He was asked to follow a small lamp that was moved horizontally using a manual drive. The lamp was turned on randomly, giving stepwise jumps of random amplitude from 10 to 60° with random intervals between jumps. A standard tracking sequence is (1) calibration, (2) a series of 90 stepwise jumps, and (3) recalibration.

Data Analysis

Parameters of each saccade in analyzing data with a digital computer (PDP-11/40) are as follows: (1) latency, (2) maximum velocity, and (3) amplitude. A computer program also was developed to measure the slow-phase-component velocity for induced optokinetic nystagmus (OKN).¹³

Normal Data

FIGURE 1a illustrates a saccade sequence in a normal subject.

1. Coefficients between maximum velocity and logarithmic transformation

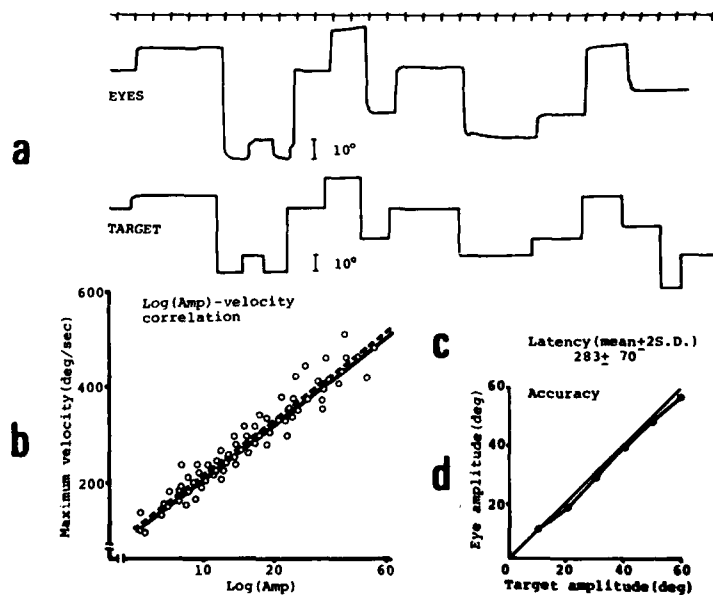


FIGURE 1. Horizontal saccadic eye movements in a normal subject. a: saccade sequence. b: coefficients between maximum velocity and logarithmic transformation of amplitude. c: latency. d: relationship between saccade amplitude and target amplitude.

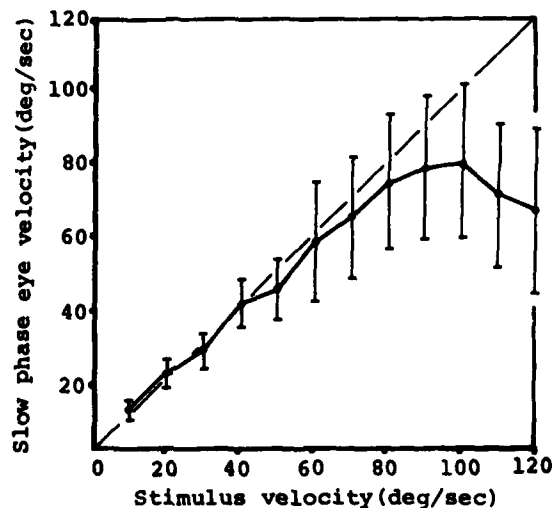


FIGURE 2. The mean value of slow-phase OKN averaged in 10 normal subjects.

of amplitude [$\log(\text{Amp})$] were adopted. The relationship between normal saccade velocity and $\log(\text{Amp})$ was fitted to a straight line; the average slope was $377^\circ/\text{second}$ (FIGURE 1b).

$$Y = 377X - 157 \text{ (degrees/second)} \quad (r = 0.959)$$

2. The latency (reaction time) of saccades was nearly constant, about 283 ± 70 mseconds, regardless of target-jump interval and target-jump amplitude (FIGURE 1c), but the initial saccade occurred within about 410 ± 141 mseconds after the target jump for each saccade.

3. Eye amplitude was nearly equal to target amplitude (FIGURE 1d).

Smooth pursuit and OKN also were tested to define differences between saccade and the pursuit system.

Optokinetic Nystagmus

The subject sat surrounded by a large screen on which black and white stripes were projected. The stripes were rotated with an acceleration rate of $1.2^\circ/\text{second}^2$ for 100 seconds and a peak stimulus velocity of $120^\circ/\text{second}$ in clockwise and counterclockwise directions.¹⁴ To define abnormal OKN, slow-phase velocity was adopted as a measure (FIGURE 2).

Pursuit Eye Tracking Test

The subject was asked to follow a small target moving sinusoidally with a frequency of 0.3 Hz and an amplitude of 20° . Under these conditions, the peak

velocity of the target was $18.8^\circ/\text{second}$. Abnormalities in pursuit eye movements were established by irregularities in the smooth sinusoidal curve of the eyes.¹⁵

Materials

Based on these normal data, saccade abnormalities together with abnormalities in pursuit eye movements were studied in 55 patients with various CNS dysfunctions as listed in TABLE 1. The clinical diagnoses were confirmed by operation, computerized tomography, angiography, and other neurological examinations.

RESULTS

Unilateral Cerebral Lesions

Subjects with unilateral lesions of the cerebrum included 6 patients who had had cerebrovascular accidents and 11 patients with brain tumors: 5 with frontal lobe lesions, 3 with temporal lobe lesions, 4 with occipital lobe lesions, and 5 with frontoparietal lesions.

In 10 patients, saccades were normal. In 7 patients, saccades toward the side contralateral to the lesion had the following characteristics (FIGURE 3A): (1) hypometric and multiple saccades, (2) prolongation of latency and duration, and (3) normal velocity in each saccade. All 7 patients who had saccade abnormalities showed slow-phase OKN abnormalities toward the lesion side. Smooth pursuit toward the lesion side also was impaired.

Basal Ganglia Diseases

Patients with basal ganglia diseases included three with Parkinson's disease, two with Huntington's chorea, one with striatonigra degeneration, and one with Wilson's disease. Three of the patients had impairments of smooth pursuit and OKN. Four patients had a long latency of saccade onset, and one patient had a

TABLE 1
LOCATIONS OF LESIONS IN 55 PATIENTS

Cerebrum	Tumor	11
	Vascular	7
Cerebellum	Tumor	1
	Vascular	6
Mesencephalon	Vascular	1
Pons	Vascular	3
CP angle	Tumor	6
Basal ganglia	Parkinson's disease	3
	Huntington's chorea	2
	Wilson's disease	1
	Striatonigra degeneration	1
Others	Spinocerebellar degeneration	13

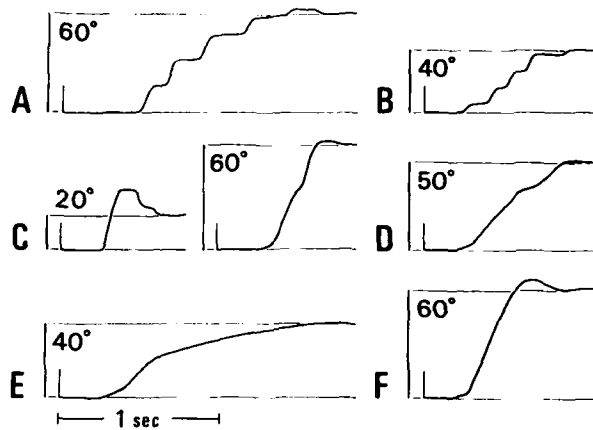


FIGURE 3. The types of saccades. Vertical lines indicate target displacement. A: multiple-step and hypometric saccades (MSHS) with long latency. B: MSHS with normal latency. C: overshoots at small target amplitude and dual-step saccades with short intersaccadic latency at large target amplitude. D: MSHS with slow-velocity segments. E: prominent slow saccades. F: slow-velocity and long-duration saccades.

prominent slowing of saccades (FIGURE 3F). Saccade accuracy was not impaired in any of the patients.

Cerebellar Lesions

The seven patients with cerebellar lesions included three with cerebellar vermal infarction, two with cerebellar vermal hemorrhages, one with hemispheric infarction, and one with hemispheric metastatic tumor.

In the two patients with hemispheric lesions, hypometric and multiple-step saccades were present toward the side ipsilateral to the lesion (FIGURE 3B). Two patients with cerebellar vermal lesions had hypermetria toward both sides at small target amplitudes, while, in contrast, hypometric and dual-step saccades with short intersaccadic latencies were detected at large target amplitudes (FIGURE 3C). In all patients with cerebellar lesions, however, the amplitude-velocity relationships were unaffected. These patients also had normal reaction times.

In the patient with a unilateral cerebellar tumor, both smooth pursuit and slow-phase OKN toward the side of the lesion were impaired. In three patients with cerebellar vermal lesions, OKN slow phases were normal at stimulus velocities lower than 40°/second, but were reduced greatly at stimulus velocities higher than 60°/second.

Upper-Brain-Stem Lesions

Four patients with vascular disorders in the upper brain stem were tested in this series: two patients with pontine hemorrhage, one patient with midbrain infarction, and one patient with aneurysm of the basilar artery.

The two patients with pontine hemorrhages had a total defect of smooth pursuit, OKN, and saccades. In the remaining two patients, saccade velocity was impaired prominently (FIGURE 3D and E). From a detailed analysis, saccade velocity toward the contralateral side of the lesion was rather slower than that toward the lesion side in the patient with mesencephalic infarction. In the patient with aneurysm of the basilar artery near the pontine base, in contrast, saccade velocity toward the side of the lesion was slower than that toward the contralateral side.

Both smooth pursuit and OKN slow phases were unaffected in the patient with mesencephalic infarction. In the patient with aneurysm of the basilar artery, smooth pursuit was not impaired, but slow-phase OKN was reduced prominently.

Lower-Brain-Stem Lesions

Six patients with cerebellopontine (CP) angle tumors were tested. In one patient who had brain-stem compression, overshooting of saccades was observed, but the maximum velocity of each saccade was nearly normal. The other patients had no saccade abnormalities. Pursuit and slow-phase OKN impairments in patients with CP angle tumors most often were ipsilateral but sometimes were bilateral.

Spinocerebellar Ataxia

Thirteen patients with spinocerebellar ataxia were investigated—3 with ataxia of the spinal form, such as Friedreich's ataxia; 5 with ataxia of the spinocerebellar form; and 5 with ataxia of the cerebellar form. Of the 13 patients with spinocerebellar ataxia, 5 patients showed shorter latency than did normal subjects. Patients with ataxia of the spinocerebellar form had the strongest impairment of saccade velocity. Furthermore, slowing of saccades in patients with ataxia of the cerebellar form was stronger than in patients with ataxia of the spinal form. Both smooth pursuit and OKN were impaired bilaterally in all 13 patients.

DISCUSSION

TABLE 2 summarizes saccade abnormalities together with other oculomotor abnormalities, based on the results described above. In this report, we should like to make some comments on the unidirectional abnormalities of saccade and pursuit in patients with unilateral CNS lesions.

FIGURE 3 shows typical types of saccadic refixations observed in our patients. Saccadic refixations are classified into normometric or dysmetric types.¹⁶ The dysmetric movements are either hypermetric or hypometric, to be designated as either overshooting or undershooting, respectively. The most common type of hypometria is the dual step of a physiologic undershoot manifested by normal subjects. Multiple-step hypometric saccades (MSHS) can be divided into two types, normal and slow, based upon the peak angular velocity of each segment of the eye movement.¹⁶ Normal-velocity MSHS can be regarded as abnormal eye

movements only if they occur predominantly in one direction or with excessive frequency.^{18,17} In the present study, in patients with unilateral cerebral or cerebellar lesions, MSHS with excessive frequency occurred predominantly in one direction. These MSHS commonly were seen toward the side contralateral to the lesion in patients with unilateral cerebral disease, while in contrast this pattern frequently was observed toward the lesion side in patients with unilateral cerebellar lesions. The velocity of MSHS, however, was not reduced. The impairments of smooth pursuit and slow-phase OKN in the patients with either cerebral or cerebellar lesions occurred toward the ipsilateral side of the lesion.

Robinson reported that horizontal saccades can be induced by stimulation of the contralateral cerebral cortex.^{18,19} Kornhuber suggested that in patients with unilateral cerebellar lesions, the dysmetria occurred ipsilaterally to the lesion and that the velocity of hypometric saccades might be normal.^{20,21} Furthermore, Aschoff and Cohen demonstrated hypometric saccades in animal experiments.²²

TABLE 2
SUMMARY OF SACCADIC, SMOOTH-PURSUIT, AND OKN ABNORMALITIES IN UNILATERAL
CNS DISORDERS AT DIFFERENT LOCATIONS

Unilateral Lesions	Saccade Velocity	Saccade Accuracy	Saccade Latency	Smooth Pursuit	Slow-Phase OKN
Cerebrum	—*	MSHS† (Contra)‡	Increased (Contra)	Impaired (Ipsi)	Impaired (Ipsi)
Cerebellum	—	MSHS (Ipsi)§	—	Impaired (Ipsi)	Impaired (Ipsi)
Mesencephalon	Impaired (Blt)¶	—	—	—	—
Pons	Impaired (Blt)	—	—	—	Impaired (Blt)
CP angle	—	—	—	Impaired (Ipsi)	Impaired (Ipsi)

*—: normal.

†MSHS: multiple-step hypometric saccades.

‡Contra: contralateral.

§Ipsi: ipsilateral.

¶Blt: bilateral.

The amplitude-velocity relationship, however, was unaffected by cerebellar cortical lesions. Therefore, it is suggested that the amplitude of saccades is modulated by the contralateral cerebrum and ipsilateral cerebellum, and that the velocity of MSHS is unaffected by either type of lesion.

Slowing of saccades occurred bilaterally in patients with mesencephalic and pontine vascular disorders. From detailed analysis of each parameter, however, saccades toward the side contralateral to the lesion were decreased further in a patient with mesencephalic disorder, while saccades toward the side of the lesion were decreased rather prominently in a patient with pontine lesion. Smooth pursuit, in contrast, was not impaired in either mesencephalic or pontine disorders.

Furthermore, in the patients with spinocerebellar ataxia, saccades were slow. This might be caused by transneuronal atrophy of oculomotor neurons in the

brain stem, as Kornhuber has suggested.^{20,21} The slowing of saccades observed in these patients also is compatible with physiological evidence that the paramedian pontine reticular formation (PPRF) is essential for the production of horizontal rapid eye movements.²³ Hence, it follows that the pontine and/or the mesencephalic paramedian reticular formation mainly govern saccade velocity, and that the pathway responsible for saccades might cross between the mesencephalon and the pons.

Another point of interest is that in a patient with mesencephalic infarction, prominent saccade slowing was observed with well-preserved smooth pursuit and OKN. This suggests that the saccadic system may have important differences from the system producing quick phases of OKN. This is a matter to be investigated in the future.

CONCLUSION

From the analysis of quantitative eye-movement recordings in patients with neurologic diseases, several types of saccade dysfunctions could be discriminated. Observations of these saccade abnormalities are of diagnostic importance. Together with other ENG findings, measurements of saccadic eye movements may provide a differential diagnosis among patients with CNS disorders.

ACKNOWLEDGMENTS

The authors are indebted to Dr. Susumu Sato, Department of Neurosurgery, Yamagata Prefectural Hospital, and Prof. Osamu Nakai, Department of Neurosurgery, Yamagata University, for permitting us to study their patients.

REFERENCES

1. STARR, A. 1967. A disorder of rapid eye movements in Huntington's chorea. *Brain* **90**: 545-564.
2. KIRKHAM, T. H. & D. F. KAMIN. 1974. Slow saccadic eye movements in Wilson's disease. *J. Neurol. Neurosurg. Psychiatry* **37**: 191-194.
3. NEWMAN, N., A. J. GAY, M. H. STROUD & J. BROOKS. 1970. Defective rapid eye movements in progressive supranuclear palsy: an ocular electromyographic study. *Brain* **93**: 775-784.
4. DIX, M. R., M. J. G. HARRISON & P. D. LEWIS. 1971. Progressive supranuclear palsy. *J. Neurol. Sci.* **13**: 237-256.
5. WADIA, N. H. 1971. A new form of hereditary familial spinocerebellar degeneration with slow eye movements. *Brain* **94**: 359-374.
6. WADIA, N. H. 1973. An indigenous form of hereditary familial spinocerebellar degeneration with slow eye movement. *Neurology India* **21** (Suppl.): 561-580.
7. STARKMAN, S., S. KAUL, J. FRIED & M. BEHERENS. 1972. Unusual abnormal eye movements in a family with hereditary spinocerebellar degeneration. *Neurology* **22**: 402.
8. SINGH, B., H. IVAMOTO & R. J. STROBOS. 1973. Slow eye movements in spinocerebellar degeneration. *Am. J. Ophthalmol.* **76**: 237-240.
9. ZEE, D. S., L. M. OPTICAN, J. D. COOK, D. A. ROBINSON & W. K. ENGEL. 1976. Slow saccade in spinocerebellar degeneration. *Arch. Neurol.* **33**: 243-251.
10. BALOH, R. W., A. W. SILLS, W. E. KUMLEY & V. HONRUBIA. 1975. Quantitative

- measurement of saccade amplitude, duration, and velocity. *Neurology* **25**: 1065-1070.
11. BALOH, R. W., H. R. KONRAD, A. W. SILLS & V. HONRUBIA. 1975. The saccade velocity test. *Neurology* **25**: 1071-1076.
 12. BALOH, R. W., W. E. KUMLEY & V. HONRUBIA. 1976. Algorithm for the quantitative analyses of saccade accuracy, reaction time and velocity. *Aviat. Space Environ. Med.* **47**: 523-527.
 13. WATANABE, Y. 1979. Computer analysis of ENG recordings in routine equilibrium examination. *J. Otolaryngol. Jpn.* **82**: 1553-1575. (In Japanese.)
 14. MIZUKOSHI, K., M. NACABA, Y. OHNO, K. ISHIKAWA, M. AOYAGI, Y. WATANABE, I. KATO, & H. INO. 1975. Neurological studies upon intoxication by organic mercury compounds. *ORL* **37**: 74-87.
 15. BENITEZ, J. T. 1970. Eye-tracking and optokinetic test: diagnostic significance in peripheral and central vestibular disorders. *Laryngoscope* **80**: 834-848.
 16. TROOST, B. T., R. B. WEBER & R. B. DAROFF. 1974. Hypometric saccades. *Am. J. Ophthalmol.* **78**: 1002-1005.
 17. BAHILL, A. T. & B. T. TROOST. 1979. Types of saccadic eye movements. *Neurology* **29**: 1150-1152.
 18. ROBINSON, D. A. 1964. The mechanism of human saccadic eye movement. *J. Physiol.* **174**: 245-264.
 19. ROBINSON, D. A. 1968. Eye movement control in primates: the oculomotor system contains specialized subsystem for acquiring and tracking visual targets. *Science* **161**: 1219-1224.
 20. KORNHUBER, H. H. 1969. Physiologie und Klinik vestibulären systems. *Arch. Klin. Exp. Ohren Nasen Kehlkopfheilkd.* **194**: 111-148.
 21. KORNHUBER, H. H. 1974. The vestibular system and the general motor system. In *Handbook of Sensory Physiology*. H. H. Kornhuber, Ed. **6**(2): 581-620. Springer-Verlag, Berlin, Federal Republic of Germany.
 22. ASCHOFF, J. C. & B. COHEN. 1971. Changes in saccadic eye movements produced by cerebellar cortical lesions. *Exp. Neurol.* **32**: 123-133.
 23. COHEN, B., A. KOMATSUZAKI & M. B. BENDER. 1968. Electrooculographic syndrome in monkeys after pontine reticular formation lesions. *Arch. Neurol.* **18**: 78-92.

VISUAL-VESTIBULAR INTERACTION IN CENTRAL NERVOUS SYSTEM DISORDERS

Isao Kato, Tadashi Nakamura, Yo Kimura, Yoshio Koike,
and Kanemasa Mizukoshi*

*Department of Otolaryngology
Yamagata University School of Medicine
990-23 Yamagata, Japan*

INTRODUCTION

The function of the vestibulo-ocular reflex (VOR) is to keep an image stable on the retina.¹ Recent investigations of eye movements in human subjects, monkeys, cats, and rabbits have revealed striking modification of VOR gain (maximum slow-phase velocity/maximum head velocity) by vision, which tends to stabilize retinal images of the visual surround.¹⁻⁵ This modulation of VOR gain by vision was abolished effectively by total cerebelloflocculectomy.^{1,4,5} As a result, VOR gain was increased by 30% in cats.⁵ Based on these experimental data, visual-vestibular interaction now has been used as a diagnostic tool to assess cerebellar dysfunctions.^{6,7} The diagnostic value, however, has not yet been established for examination of disturbances of the brain stem. In order to achieve this goal, visual-vestibular interaction was measured and compared between normal individuals and patients who showed failure of fixation suppression of caloric nystagmus.⁸

METHODS

Subjects

Sixteen normal adults between the age of 20 and 44 years, who had neither auditory nor vestibular abnormalities, were subjects for the present study. They were instructed not to take drugs or drink alcohol for 24 hours before the test. Twenty-seven patients with central nervous system (CNS) disorders were studied. All the patients showed failure of fixation suppression. Nine out of 27 patients were excluded because they were postoperative cases, because of incomplete clinical or electro-oculographic (EOG) data, or because they were taking either diphenylhydantoin or barbiturates. The remaining 18 patients, whose lesions were documented by clinical and/or objective evidence, were classified into three groups as follows:

Group A included eight patients with pure cerebellar atrophy. Neurologic examination revealed signs of cerebellar dysfunction only. Two of these cerebellar-atrophy patients were documented by pneumoencephalography.

Group B consisted of six patients, one with pinealoma and one with glomus jugular tumor, which subsequently were documented by surgical procedures.

*Department of Otolaryngology, School of Medicine, Toyama Medical and Pharmaceutical University, 930-01 Toyama, Japan.

The remaining four patients had had vascular accidents, which were confirmed by history, clinical symptoms, laboratory findings, angiography, and computer tomography (CT) scanning.

In group C, two out of four patients had brain-stem encephalitis and/or degenerative diseases, as evidenced by history and laboratory findings. One patient had a cerebellar hemorrhage, which was corrected by a surgical procedure. Ten days after the EOG test was performed, this patient came to autopsy after a heart attack. The remaining patient had an acoustic neurinoma at the fourth stage, which was removed by a surgical procedure. The lesion sites of these 18 patients are summarized in TABLE 1.

Methods

A newly devised rotatory chair, which could be controlled automatically, was used for measurements of VOR gain and effects of visual fixation on perrotatory nystagmus. The subjects were rotated about the chair's vertical axis with head fixed 30° forward. Two types of angular acceleration, sinusoidal and constant,

TABLE 1
LESION SITES OF PATIENTS WITH CNS DISORDERS

Group	Site/Type	Number of Patients
A	Cerebellar Atrophy	8
B	Brain Stem	
	Vascular	4
	Tumor	2
C	Cerebellum & Brain Stem	
	Vascular	1
	Acoustic Tumor	1
	Degenerative or Inflammatory	2

were applied. The sinusoidal stimulus was composed of frequencies over the range of 0.125–0.25 Hz and amplitudes over the range of 20°, 30°, and 60° respectively. VOR gain was established by the ratio of 10 successive peak-to-peak eye velocities to head velocities. VOR gain was measured both in total darkness and with eyes fixed on a spot moving with the head. The constant-acceleration stimulus of 5°/second² for 20 seconds was followed by 100°/second constant velocity for 40 seconds, and the chair then was decelerated to zero velocity at an angular acceleration of –5°/second². The subject fixed his gaze on a spot moving with his head for 5 seconds during the period of constant velocity and then while the rotation chair was at a standstill. The fixation-suppression-induced slow-phase velocity was compared with that during the control period. Thus, the percentage reduction of slow-phase velocity was established.

Recording

Electrodes (Ag-AgCl) were attached laterally to the outer canthus of each eye, and horizontal eye movements were recorded with direct-current electro-

oculography. Eye movements and slow-phase velocity were recorded simultaneously with a polygraph and stored on an FM magnetic tape. The EOG was calibrated by making subjects look at a target moving with a sinusoidal waveform (frequency, 0.3 Hz; amplitude, 20°) before and after each test procedure.

RESULTS

FIGURE 1 shows a typical recording of head and eye position in a normal subject. The VOR gain in total darkness was about 0.6 (FIGURE 1A) and was nearly zero with eyes fixed (FIGURE 1B). When the chair was rotated with constant acceleration, the slow-phase velocity of nystagmus increased gradually. Perrotatory nystagmus during the period of constant velocity was suppressed

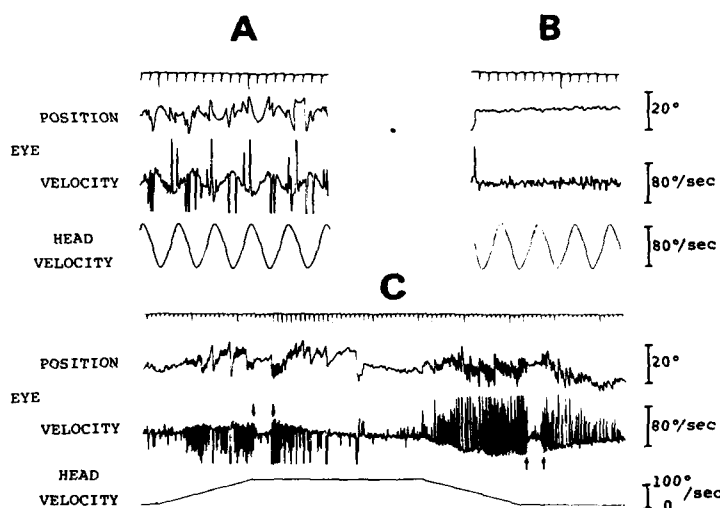


FIGURE 1. Typical recording of head and eye position in a normal subject. VOR gain in the dark (A) and in the light (B). Perrotatory nystagmus during the period of constant velocity is suppressed completely with eyes fixed (black arrows) (C).

completely with eyes fixed on a spot. During the period of deceleration of the chair, a nystagmus contralateral to the direction of that during acceleration was present, and postrotatory nystagmus was suppressed adequately with eyes fixed on a spot when the chair stopped rotating (FIGURE 1C).

In order to find the best test condition for sinusoidal stimulation in normal subjects, the test was performed over the frequency range of 0.125–0.25 Hz and an amplitude range of 20°, 30°, and 60° respectively. The average VOR gain in darkness was nearly 0.6 and did not depend on frequency or amplitude. Standard deviations (SD) did not depend on frequency at each amplitude, but did increase at the lower amplitudes (TABLE 2A). Of these conditions, 0.25-Hz frequency and 60° amplitude were selected as the best condition (TABLE 2A). The mean VOR gain was 0.67 ± 0.07 at 0.25 Hz (from 0.54 to 0.76). The VOR gain with eyes fixed was less than 0.2 regardless of amplitude or frequency (TABLE 2B).

TABLE 2
NORMAL LIMITS OF VOR GAIN AT EACH FREQUENCY AND AMPLITUDE

Amplitude	A*			B†		
	Frequency	Mean	SD	Frequency	Mean	SD
60°	0.25	0.67	0.07	0.25	0.09	0.08
	0.165	0.68	0.10	0.165	0.05	0.06
	0.125	0.63	0.08	0.125	0.02	0.04
30°	0.40	0.61	0.16	0.40	0	0
	0.33	0.57	0.13	0.33	0	0
	0.25	0.65	0.15	0.25	0	0
20°	0.40	0.65	0.18	0.40	0	0
	0.33	0.56	0.20	0.33	0	0
	0.25	0.54	0.21	0.25	0	0

*VOR gain in the dark.

†VOR gain in the light.

The left illustration of FIGURE 2 compares the VOR gain in the dark between normal subjects and patients of each group. N on the abscissa indicates normal subjects. A, B, and C refer to patients belonging to the respective groups. As shown in this figure, the VOR gain of seven patients in group A (cerebellar atrophy) increased toward 1.0 but did not exceed it, and the two lower values overlap partly with the upper normal limits. The remaining one patient had a striking increase in VOR gain. In group A, the average VOR gain was 0.85 ± 0.11 in the dark. In group B (upper-brain-stem lesions), the VOR gain was increased

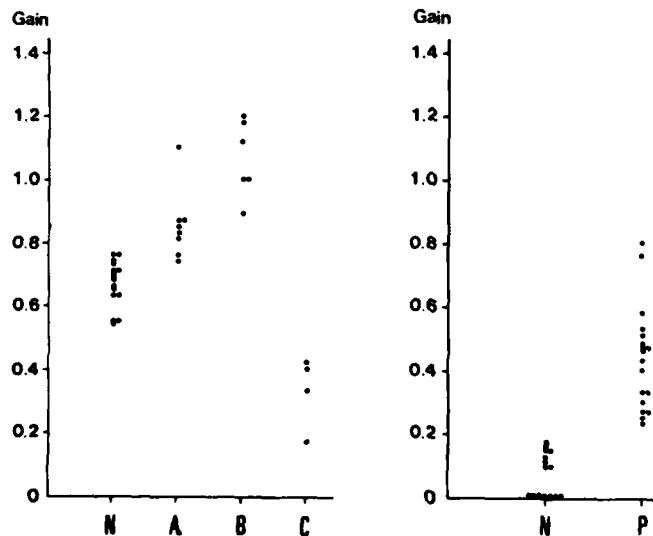


FIGURE 2. Left illustration shows VOR gain in the dark for normal subjects and all patients. N: normal subjects. A, B, and C: patients belonging to respective groups. Right illustration indicates VOR gain in the light for normal subjects (N) and all patients (P).

strongly and exceeded 1.0 except for one patient. The average VOR gain in this group was 1.06 ± 0.12 in the dark. In group C (brain-stem and cerebellar lesions), VOR gain decreased markedly in the dark. The mean VOR gain was 0.33 ± 0.11 .

The right illustration of FIGURE 2 compares VOR gain of normal subjects and patients with eyes fixed on a spot. N on the abscissa indicates normal subjects, and P indicates the patients. The VOR gain was less than 0.2 in normal subjects but more than 0.2 in patients (from 0.2 to 0.8). Thus, in these patients, visual fixation failed to suppress vestibular responses.

FIGURE 3 demonstrates a representative case in group A. This patient had a pure cerebellar atrophy. The VOR gain in darkness was 0.86 (FIGURE 3A), and the VOR gain with eyes fixed was 0.5 (FIGURE 3B). As shown in FIGURE 3C, there were almost no effects of visual fixation on perrotatory nystagmus.

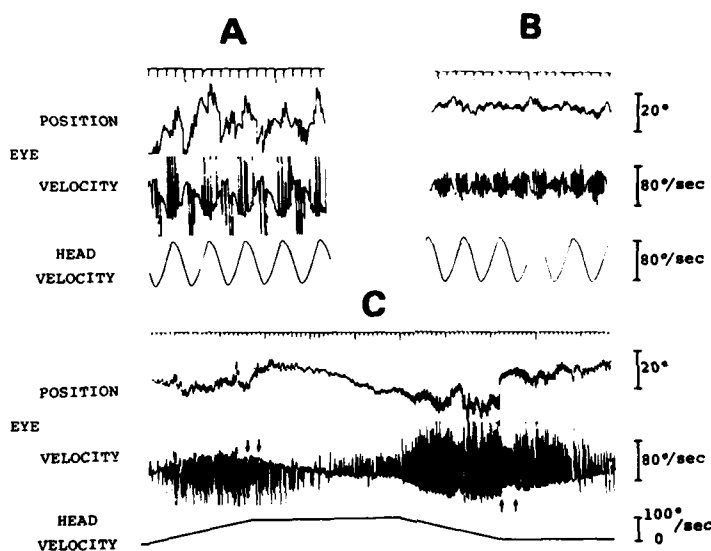


FIGURE 3. VOR gain in a patient with pure cerebellar atrophy. VOR gain in the dark is 0.86 (A) and in the light is 0.5 (B). Effects of visual fixation during perrotatory nystagmus are reduced (C).

FIGURE 4 shows a typical record of group B. In this patient, VOR gain was 1.12 in the dark (FIGURE 4A) and VOR gain with eyes fixed was 0.43 (FIGURE 4B). As shown in FIGURE 4C, effects of visual fixation were reduced for perrotatory nystagmus in both directions. This patient showed paralysis of upward gaze with full eye movements in the horizontal axis. A CT scan revealed a high-density area in the midbrain (FIGURE 5).

A typical case from group C is demonstrated in FIGURE 6. In this patient, caloric nystagmus was not elicited in the dark but was enhanced during attempted fixation. As shown in FIGURE 6A, VOR gain in darkness decreased markedly (0.33), and VOR gain with eyes fixed was 0.4. Perrotatory nystagmus was not elicited in the dark but was activated with eyes fixed (FIGURE 6C). This patient had a cerebellar hemorrhage, disclosed by CT scanning. Gross sections of the cerebellum and brain stem in this patient revealed the hematoma cavity in

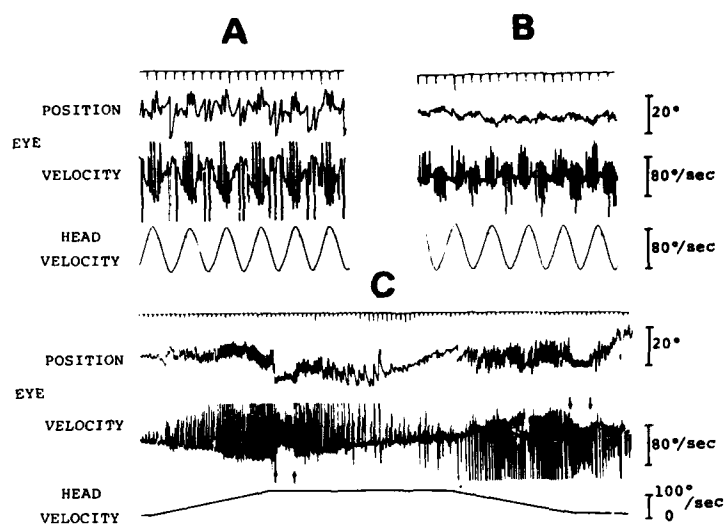


FIGURE 4. VOR gain in a patient with brain-stem lesion. VOR gain in the dark is 1.12 (A) and in the light is 0.43 (B). Effects of visual fixation during perrotatory nystagmus are reduced (C).

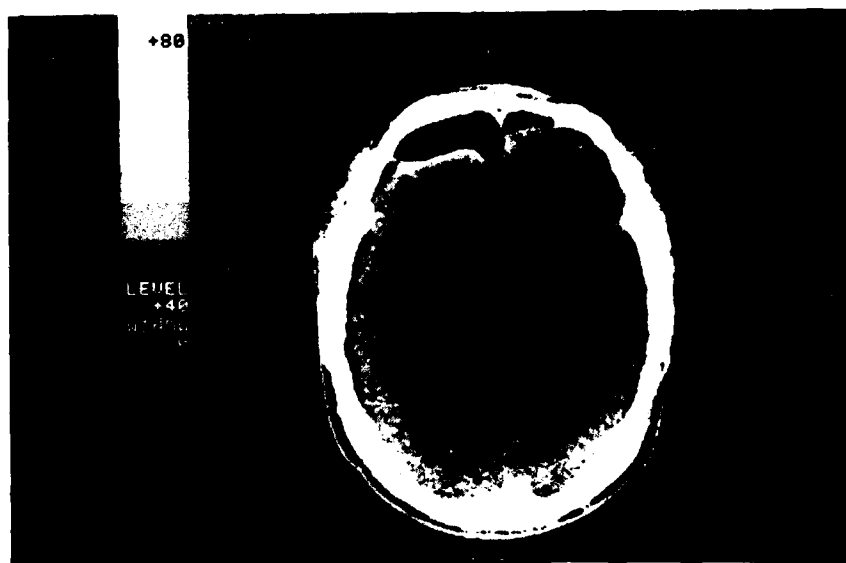


FIGURE 5. CT scanning in the same patient as illustrated in FIGURE 4. In this section through the third ventricle, a rounded high-density area is seen in the area corresponding to the pineal body.

and around the right dentate nucleus. The brain stem had an unusual brown-colored plaque almost in the center of the pons at the level of the trigeminal nerve roots, corresponding to the site of the paramedian pontine reticular formation (PPRF). The flocculus and the area of the vestibular nuclei apparently were spared.

These results made it possible to classify the cases into the following four types:

Type 1: VOR gain and visual fixation during perrotatory nystagmus were normal.

Type 2: VOR gain approached 1.0, but did not exceed it. Visual fixation of perrotatory nystagmus was reduced or abolished.

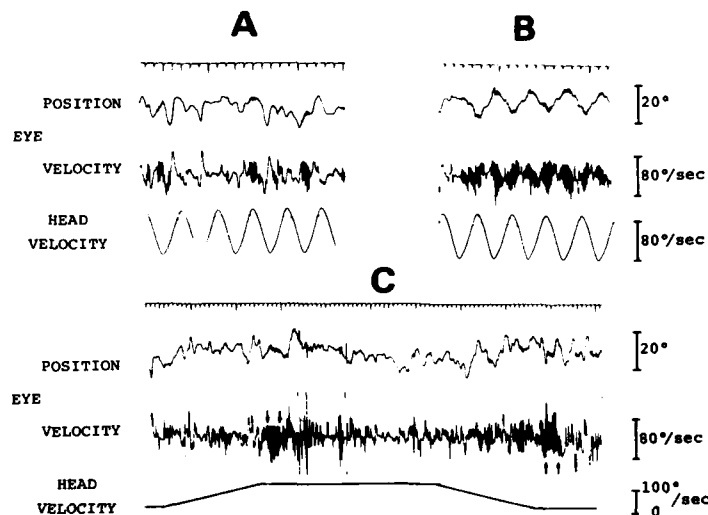


FIGURE 6. VOR gain in a patient with cerebellar and brain-stem lesion. VOR gain in the dark is 0.33 (A) and in the light is 0.4 (B). Effects of visual fixation during perrotatory nystagmus are enhanced (C).

Type 3: VOR gain increased beyond 1.0 and visual fixation of nystagmus was reduced or abolished.

Type 4: VOR gain was decreased and perrotatory nystagmus was not elicited.

Type 2 was seen frequently in group A patients, i.e., those with cerebellar atrophy. Type 3 commonly was observed in group B patients, i.e., those with upper and lower brain-stem lesions, and type 4 changes were found in group C patients, those with pontine lesions.

DISCUSSION

When the head is rotated, if eye movements are equal but opposite to head movements, the VOR gain is defined as 1.0. Thus, retinal images are kept still during head movements. Recent physiological data indicate that this gain control

is executed by the flocculus, i.e., that the flocculus receives primary vestibular signals as well as visual signals from the retina, and sends inhibitory outputs to second-order vestibular neurons, which modulate the VOR in either an excitatory or inhibitory manner.^{1,9,10} In rabbits, it was reported that the VOR gain increased with fixed slit light, and dropped with slit light moving in phase with the turntable. This modulation by visual stimulation was abolished effectively after total flocculectomy.¹ A similar light-guided modulation of VOR gain also was lost after ablation of the flocculus in both cats and monkeys.^{4,5} Thus it is conceivable that the flocculus is a medium through which the visual system can alter or modify VOR gain.

Based on these data, measurement of VOR gain prevails now as a test battery to detect cerebellar dysfunction.^{6,7} In patients with cerebellar atrophy (group A), VOR gain in darkness rose as a whole but overlapped slightly with the upper normal limits. All the patients in group A showed an increase in VOR gain ($p < 0.01$) with eyes fixed, i.e., effects of visual fixation on VOR were reduced markedly (FIGURE 2, right, P column). In 10 patients with cerebellar atrophy, the average VOR gain was within normal limits. In 3 patients with clinically pure cerebellar disease, VOR responses increased.⁷ In 5 patients with hereditary cerebellar ataxia, VOR gain in darkness increased nearly to 1.0, and VOR gain with eyes fixed also was increased.⁶ Since great differences exist between reports of values of VOR gain, it remains unclear whether these differences are attributable solely to the involvement of the vestibulocerebellum.

The present experiment in patients with cerebellar lesions did not support the results obtained from cats, but did support those from experiments with cerebellectomized monkeys, which revealed little or no change of VOR gain on the basis of qualitative observations.^{5,11}

In patients with upper-brain-stem lesions, on the contrary, VOR gain increased dramatically (FIGURE 2, left, B column). Effects of visual fixation on nystagmus also were reduced (FIGURE 4C). In this patient, however, the smooth-pursuit system was well preserved. This patient showed a typical pretectal syndrome, but no other symptoms. Zee et al. reported that an increased VOR gain could be interpreted as a compensatory response to a pursuit-system defect.⁶ In fact, degrees of inability to suppress caloric nystagmus were well correlated with such oculomotor dysfunctions as smooth-pursuit failure, gaze-holding failure, and impaired optokinetic nystagmus.¹² As seen in this patient as well as several others, the ability to modulate VOR gain did not depend solely on the pursuit system.¹³

The major point of interest to be discussed is that VOR gain increased remarkably in group B, but slightly in group A (FIGURE 2, left, A and B columns). The underlying neuronal mechanisms are not yet clear, but some explanations seem possible. It is suggested that the flocculus has a function to adjust VOR gain by referring information about eye movements obtained through the visual pathways.¹ If the visual pathways were disrupted in the brain stem, VOR gain could not be increased to 1.0 in the light; but in fact some functions would work to compensate for insufficient VOR gain. The flocculus presumably may exert this compensatory function. This idea is based on the following studies.

Gonshor and Melvill Jones and Gauthier and Robinson showed that subjects wearing a reversing prism or magnifying glasses could compensate for the retinal image slip by decrease or increase of VOR gain respectively.^{2,14} This modification was abolished completely with total flocculectomy in cats.⁵ These experimental data strongly support the view that the flocculus plays an essential role in the modification of VOR gain.

It therefore follows that if the visual pathway were damaged in the brain

stem, VOR gain would increase to 1.0 by means of some compensatory mechanism executed by the flocculus, while if the flocculus were damaged, the modification of VOR gain as a compensatory response would not be executed and VOR gain probably could not be increased. Another hypothesis assumes that some other structure within other parts of the brain also might monitor and modify VOR gain, based on the idea that the known examples of visual-vestibular interaction in the cerebellum only are fragments of the puzzle.^{6,13} In group C, patients with pontine and/or cerebellar lesions, the VOR gain in darkness was reduced markedly and this decrease was significant in comparison with normal subjects (FIGURE 2, left, C column; FIGURE 6A). In these patients, perrotatory nystagmus and caloric nystagmus were not elicited in the dark, but characteristically were enhanced during the period with eyes fixed (FIGURE 6C).

A meticulous microscopic survey has not been performed yet in the patient represented in FIGURE 6. Gross pathology, however, revealed an unusual brown-colored plaque almost in the center of the pons, corresponding to the site of the original PPRF, while the flocculus and the area of the vestibular nuclei apparently were spared. These pathological findings might be a clue to the EOG findings for group C. This is a matter to be investigated in the future. As shown in the left illustration of FIGURE 2, patients with CNS disorders can be classified into three groups. Hence, measurement of VOR gain in combination with effects of visual fixation on perrotatory nystagmus may provide a valid indication of some lesions in the central nervous system.

ACKNOWLEDGMENTS

The authors thank Prof. O. Nakai, Department of Neurosurgery, Yamagata University, and also Dr. S. Sato, Department of Neurosurgery, Yamagata Prefectural Hospital, for allowing us to study their patients and for use of the clinical records.

REFERENCES

1. ITO, M., T. SHIIDA, N. YAGI & M. YAMAMOTO. 1974. Visual influence on rabbit horizontal vestibulo-ocular reflexes presumably effected via the cerebellar flocculus. *Brain Res.* **65**: 170-174.
2. GONSHOR, A. & G. MELVILL JONES. 1973. Changes of human vestibulo-ocular response induced by vision-reversal during head rotation. *J. Physiol.* **234**: 102-103.
3. MILES, F. A. & J. H. FULLER. 1974. Adaptive plasticity in the vestibulo-ocular responses of the rhesus monkey. *Brain Res.* **80**: 512-516.
4. TAKEMORI, S. & B. COHEN. 1974. Loss of visual suppression of vestibular nystagmus after flocculus lesions. *Brain Res.* **72**: 213-224.
5. ROBINSON, D. A. 1976. Adaptive gain control of vestibulo-ocular reflex by the cerebellum. *J. Neurophysiol.* **39**(5): 954-969.
6. ZEE, D. S., R. D. YEE, D. G. COGAN, D. A. ROBINSON & W. K. ENGEL. 1976. Ocular motor abnormalities in hereditary cerebellar ataxia. *Brain* **99**: 207-234.
7. BALOH, R. W., H. J. JENKINS, V. HONRUBIA, R. D. YEE & C. G. Y. LAU. 1979. Vestibular-visual interaction and cerebellar atrophy. *Neurology* **29**: 116-119.
8. COATS, A. C. 1970. Central electronystagmographic abnormalities. *Arch. Otolaryngol.* **92**: 43-53.
9. BRODAL, A. & B. HØIVIK. 1962. Site and mode of termination of primary vestibulocerebellar fibres in the cat. An experimental study with silver impregnation methods. *Arch. Ital. Biol.* **102**: 1-64.

10. MAEKAWA, K. & J. I. SIMPSON. 1973. Climbing fiber responses evoked in the vestibulo-cerebellum of rabbit from the visual system. *J. Neurophysiol.* **36**: 649-665.
11. WESTHEIMER, G. & S. M. BLAIR. 1974. Functional organization of primate oculomotor system revealed by cerebellectomy. *Exp. Brain Res.* **21**: 463-472.
12. SATO, Y., I. KATO, T. KAWASAKI, K. MIZUKOSHI & M. HAYANO. 1980. Failure of fixation suppression of caloric nystagmus and ocular motor abnormalities. *Arch. Neurol.* **37**: 35-38.
13. BARR, C. C., L. W. SCHULTHEIS & D. A. ROBINSON. 1976. Voluntary, non-visual control of the human vestibulo-ocular reflex. *Acta Otolaryngol.* **81**: 365-375.
14. GAUTHIER, G. M. & D. A. ROBINSON. 1975. Adaptation of the human vestibuloocular reflex to magnifying lenses. *Brain Res.* **92**: 331-335.

EYE-VELOCITY PROGRAMMING IN BRAIN-STEM DISORDERS

Carsten Wennmo, Nils G. Henriksson, Illmari Pyykkö,
and Lucyna Schalén

*Department of Otorhinolaryngology
University Hospital of Lund
S-221 85 Lund, Sweden*

INTRODUCTION

Visual illusions and vertigo are common symptoms in patients with brain-stem disorders.¹ Although many patients with brain-stem disorders do not have the above-described symptoms, an analysis of visually or vestibularly evoked eye movements may provide important information.²⁻⁴

There is experimental and clinical evidence that the immediate supranuclear center for upward gaze is located in the pretectum while the corresponding center for downward gaze is located more ventrally in the mesencephalic tegmentum.⁵⁻⁷ This suggests two separate areas for upward and downward gaze.

The corresponding centers for horizontal eye movements are located in the pons, in the paramedian pontine reticular formation (PPRF). Units for rapid eye movements are located in the rostral parts, while units for slow eye movements are located more caudally.⁸⁻¹⁰ These findings suggest separate mechanisms for rapid and slow eye movements.

In a previous study in patients with brain-stem lesions we found that saccades and smooth pursuit generally are more vulnerable than the quick and slow phases of nystagmus.⁴ The above-described observations suggest separate mechanisms for voluntary eye movements and nystagmus.

Hence it can be expected that patients with disorders at different sites in the brain stem may present various patterns in their eye-movement disturbances.

The purpose of this paper is to find out how lesions at different levels in the brain stem affect eye-velocity programming.

MATERIAL

Thirty patients with lesions in the brain stem were referred to us by the Department of Neurology for electro-oculographical analysis. In the workup were included otoneurological and neuro-ophthalmological examination and axial computerized tomography. Mean age of the patients was 63 years (range, 17-81). The duration of the symptoms averaged 13 months with a wide range of 1 week to 12 years.

Twenty normal subjects with no history of vestibular or central nervous disease were used as controls. No drugs were allowed before the testing. Mean age of the controls was 48 years (range, 23-72).

In order to interpret the results, the patients were divided into three different groups according to the clinical findings, indicating at which level of the brain stem the lesions were located. (1) Five patients with progressive supranuclear palsy (PSP)—a degenerative disease with maximum pathological abnormality in

the rostral parts of the brain stem. This group consisted of patients at different stages of the disease. (2) Fifteen patients with pontine disorders. This group consisted of 11 cases with infarctions, 3 cases with tumors, and 1 case with encephalitis. (3) Ten patients with lesions in the medulla oblongata. Eight of these cases had infarctions in the lateral medullary area, and 2 had medullary infarctions.

TEST PROCEDURE

The testing procedures were similar to those reported in earlier studies.^{4,11,12}

The subjects were placed in a chair with occipital support for head stabilization. The eye movements were recorded by direct-current (d.c.) electro-oculography in a manner previously described for this laboratory.^{11,12} To avoid errors due to filter effects, an analysis was made of the influence of different filters on the velocity patterns of different eye movements before the selection of the low-pass filter of 15 Hz was made.¹¹ Calibrations were checked twice, once before and once in the middle of the test.

Our interest was directed toward the velocity patterns of eye movements and, to a lesser degree, the accuracy of voluntary saccades and the number of superimposed saccades in the smooth pursuit.

The following eye movements were analyzed:

Smooth pursuit was induced by telling the patient to watch a light spot, 30 mm in diameter, projected on a screen 160 cm in front of the subject. The target was driven in predictable ramps of 60° amplitude at six different target velocities from 10° to 60°.

Voluntary saccades were induced by asking the patients to make rapid refixations between two targets, 5°, 10°, 20°, 40°, and 60° apart.

Rotatory responses were produced by rotating the subjects in a revolving chair at a rate of 120° for 60 seconds, following which the chair was decelerated within 1 second. The nystagmus was recorded in darkness.

Optokinetic responses (OKN) were induced by rotating a striped cylinder around the subjects with a speed of 90°/second.

Optovestibular responses were produced by rotating the patient as in the rotation test but now inside the striped cylinder with open eyes in light.

RESULTS

Smooth Pursuit

All patients but two showed severe impairments in the maximum velocities of the smooth pursuit. In FIGURE 1 is depicted the mean of the maximum smooth-pursuit velocities in the three groups of patients. There was no significant difference between the pontine and the medullary group. The PSP group, however, had significantly slower smooth pursuit than did the pontine and medullary patients ($p < 0.05$, Student's *t*-test).

A reduced velocity in smooth pursuit frequently, but not always, was accompanied by an increased number of superimposed saccades. An increased number of superimposed saccades (above mean + 2 standard deviation in normal

subjects) were found in all the patients with PSP, in 9 of the 15 patients with pontine lesions, and in 8 of the 10 patients in the medullary group.

Voluntary Saccades

All patients with PSP and pontine disorders had a significantly reduced velocity in the voluntary saccades (below mean - 2 SD in normal subjects). In the medullary group, however, this was found in 6 of the 10 patients. FIGURE 2 shows the mean values of the saccadic velocity at different amplitudes in the three groups of patients. There were significant differences in the velocities between

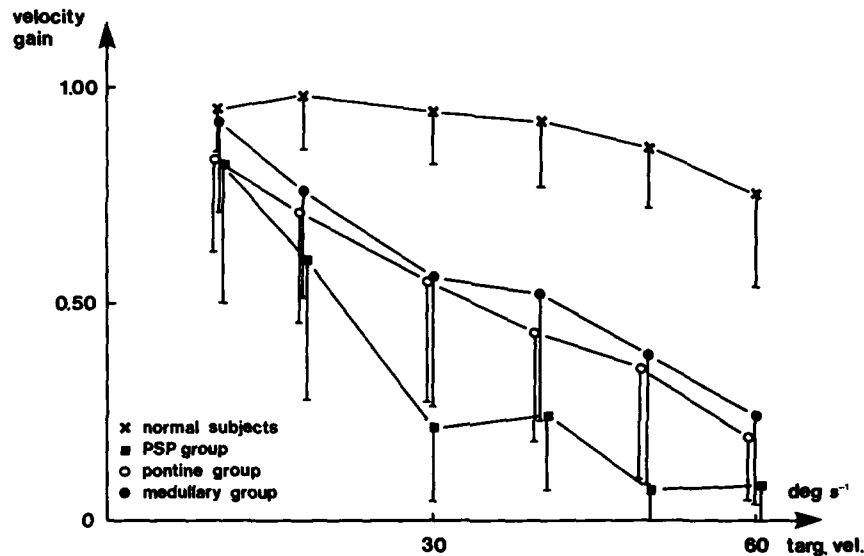


FIGURE 1. Curves of maximum velocity gain in smooth pursuit of 20 normal subjects and of three groups of patients at different target velocities. The mean values with spreads (1 SD) of each group and at each velocity of the target are depicted.

the groups and also between each of the different groups and the normals ($p < 0.05$).

The accuracy of voluntary saccades, expressed as the amplitude of the initial saccade, was impaired significantly in all patients with PSP, in 10 of the 15 patients with pontine lesions, and in 3 of the 10 patients with medullary lesions.

Nystagmus Responses in the Rotation Test

The fast-phase velocity was reduced significantly in 1 patient of the 4 PSP patients tested, in 7 of the 15 patients with pontine disorders, but in only 1 of the 10 medullary patients tested. One patient with a medullary lesion even had a

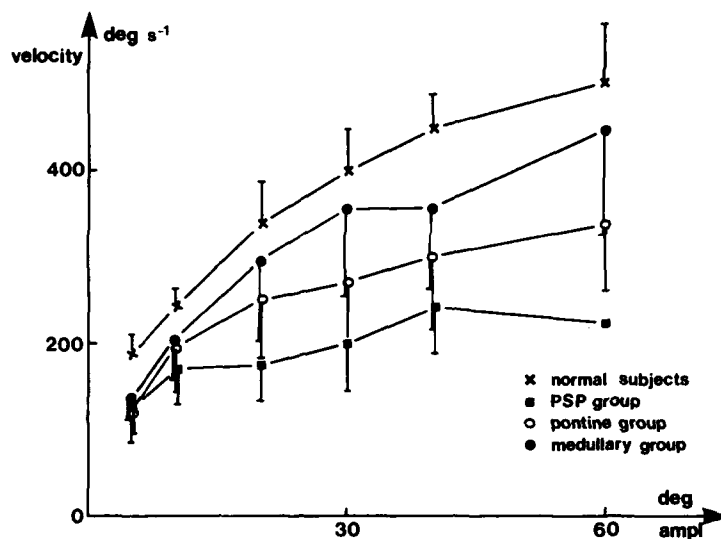


FIGURE 2. Peak velocity-amplitude relationship of voluntary saccades in three groups of patients and in normal subjects. The mean values in each group at different amplitudes with 1 SD are depicted.

significantly increased velocity. In FIGURE 3 is depicted the mean of the fast-phase velocities in patients and normal subjects. The means of the fast-phase velocities in medullary patients at amplitudes of 30° and 40° were increased significantly compared to normal subjects ($p < 0.05$).

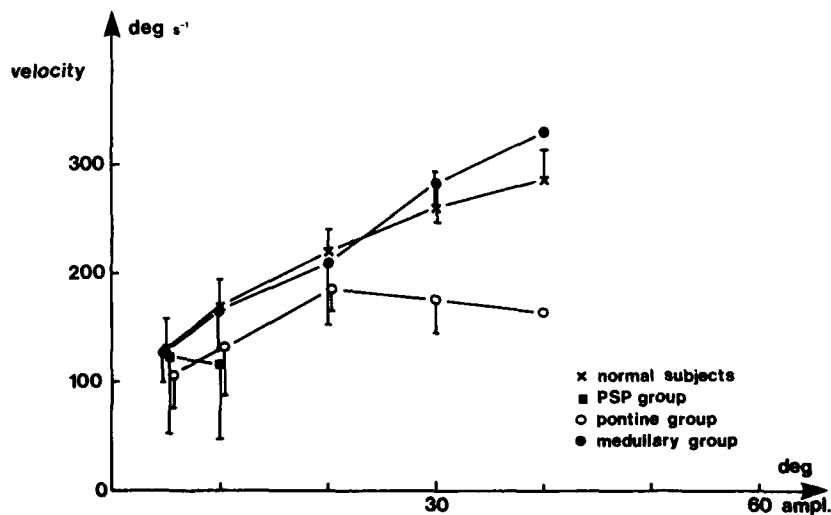


FIGURE 3. Velocity patterns of fast phases of nystagmus in the rotatory test in normal subjects and the three groups of patients. Mean and spreads as in FIGURE 2.

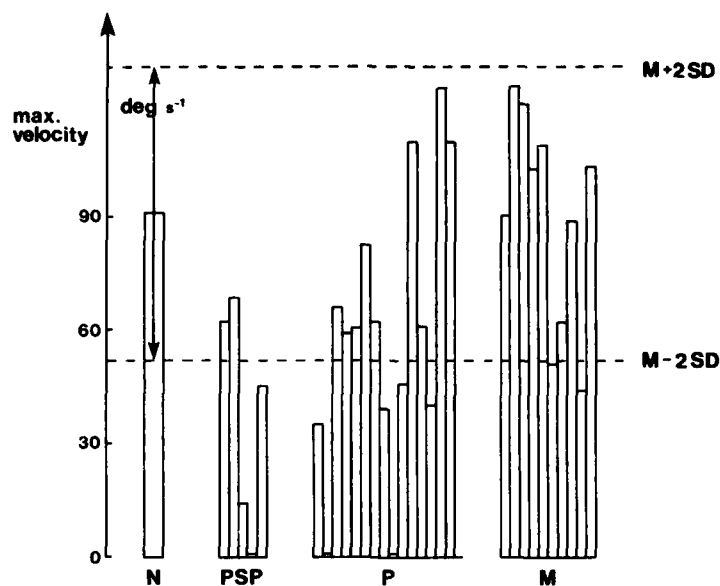


FIGURE 4. Maximum slow-phase velocities in the three groups of patients are compared with the mean of the maximum slow-phase velocities in 20 normal subjects. Each patient is represented individually. Dashed lines indicate 2 SD above and below the mean values in normal subjects. N: mean values in 20 normal subjects. PSP: patients with progressive supranuclear palsy. P: patients with pontine disorders. M: patients with medullary and lateral medullary disorders.

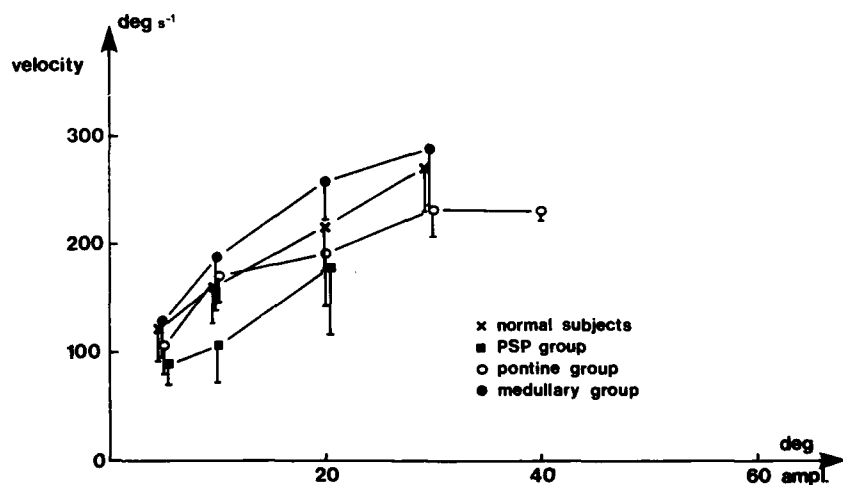


FIGURE 5. Velocity patterns of the fast phases of OKN in normal subjects and in patients. Means and spreads as in FIGURE 2.

The maximum velocity in the slow component was reduced significantly in 3 of the 5 PSP patients, in 6 of the 15 patients with pontine lesions, and in 2 of the 10 patients with medullary lesions (FIGURE 4).

Nystagmus Responses in the Optokinetic Test

The velocity of the fast component was reduced significantly in 1 of the 5 patients in the PSP group and in 2 of the 15 patients with pontine disorders, but was normal in all medullary patients except 3, who even had significantly increased velocities. In FIGURE 5 is shown the mean of the velocities of the fast component in patients and normal subjects. The medullary group had significantly increased velocities compared to normal subjects ($p < 0.01$), while the PSP group had significantly reduced velocities ($p < 0.05$).

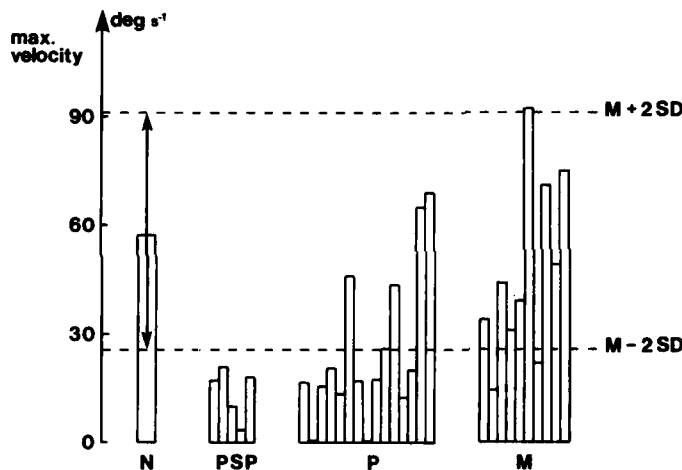


FIGURE 6. Maximum slow-phase velocities in the OKN test. Abbreviations as in FIGURE 4.

The maximum slow-phase velocity was reduced in all PSP patients, in 10 of the 15 patients with pontine lesions, and in 2 of the 10 patients with medullary lesions (FIGURE 6).

Nystagmus Responses in the Optovestibular Test

The velocity of the fast component was reduced significantly in 3 of the 4 patients with PSP, in 8 of the 12 (3 were not tested) patients with pontine lesions, and in 2 of the 9 patients with medullary lesions. In FIGURE 7 is depicted the mean of the fast-phase velocities in patients and normal subjects. All groups except the medullary group differ significantly from normal subjects ($p < 0.001$).

The slow-phase velocity was below the normal in 4 out of 4 (1 was not tested) patients with PSP, in 9 out of 12 patients with pontine lesions, and in 3 out of 9 patients with medullary lesions (FIGURE 8).

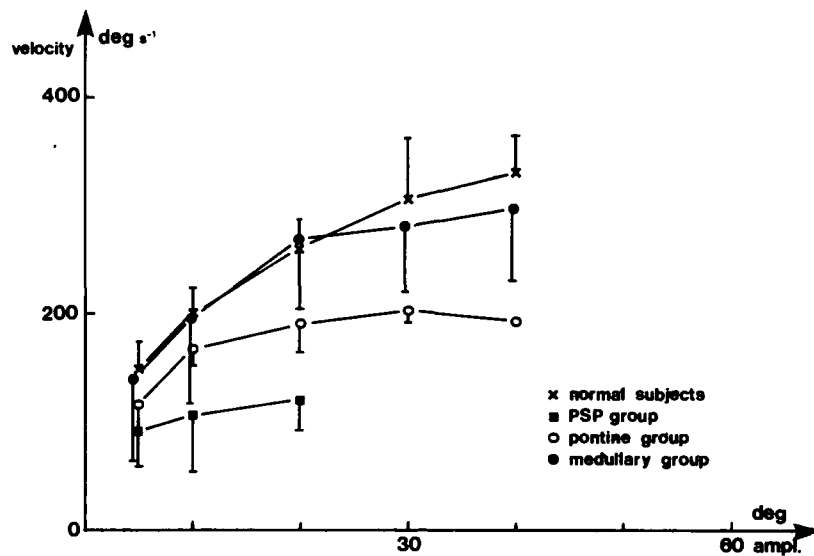


FIGURE 7. Velocity patterns of the fast phases in the optovestibular test. Means and spreads as in FIGURE 2.

DISCUSSION

The electro-oculographic findings described in the present series of 30 patients with brain-stem lesions have confirmed the results of previous studies and have added to our knowledge of the characteristics of lesions at different sites in the brain stem.²⁻⁴

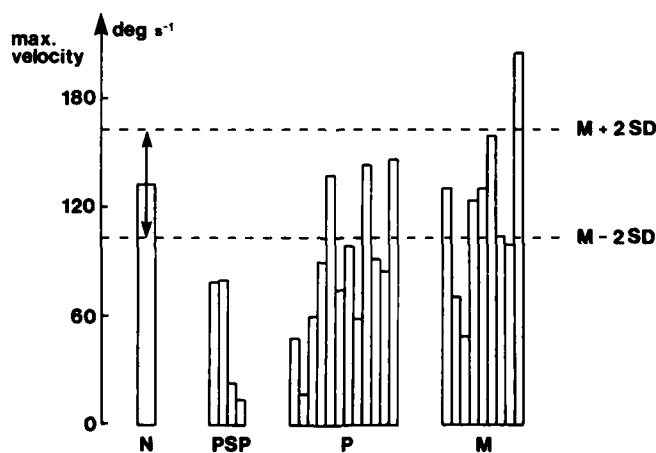


FIGURE 8. Maximum slow-phase velocities in the optovestibular test. Abbreviations as in FIGURE 4.

The maximum smooth-pursuit velocity was reduced uniformly in all cases but two, independent of the site of the lesion. Defective smooth pursuit in cases with lateral medullary lesions, as we have shown in the present paper, had been reported earlier by Hörnsten, Kommerell and Hoyt, and Pyykkö and Wennmo.¹³⁻¹⁵ It is, however, not immediately obvious why patients with infarctions in the medulla should have disturbances of smooth pursuit, since the site of the lesion in many of our cases might be below the level of the PPRF. Nevertheless experiments on rabbits may be of relevance to the present findings because they support the assumption that afferent cerebellar visual fibers via the inferior olive are of importance in performing smooth pursuit.¹⁶ Hence it is reasonable to assume that malfunctioning of these fibers may be a contributory factor to the abnormal smooth pursuit in cases of medullary lesions.

All cases with lesions in the rostral and intermediate parts of the brain stem had reduced velocities of voluntary saccades, while patients with lesions in the medulla frequently had normal saccadic velocities. Our findings are consistent with the notion that rapid eye movements, such as voluntary saccades, are integrated more rostrally in the brain stem than are slow eye movements.⁹⁻¹⁰ Our results, however, somewhat contradict the results of Baker et al., who found units in the medulla with activity correlated not only to eye position but also to saccadic velocity.¹⁷

Both components in any type of nystagmus were preserved more frequently than were the voluntary saccades and the smooth pursuit, as pointed out in a previous study.⁴

Among the various types of nystagmus studied, the optovestibular type most frequently was liable to functional decline, possibly because of the need for two different sources of impulses.

The findings of preserved optokinetic slow phases in medullary and lateral medullary lesions in contrast to highly impaired smooth pursuit indicate that these two types of visually induced eye movements use different mechanisms. In testing OKN, we rotated the drum at a rather high speed (90°/second) and the patient had no possibility of fixating. Hence it was mainly the reflexive type of OKN that was tested.¹⁸ Pathways relaying this type of OKN may reach directly the phasic units in the rostral parts of the pons from subcortical areas.^{19,20} As patients with medullary disorders have their lesion below the level of the PPRF, this neuronal organization can explain why the OKN slow phases are preserved more commonly in medullary lesions than in pontine disorders and in patients with progressive supranuclear palsy.

In contrast to the optovestibular nystagmus, where both components were disturbed to about the same extent, the slow-phase velocity in OKN was reduced much more often than was the fast-phase velocity. This preservation and even enhancement of the fast-phase velocity in OKN as well as in postrotatory nystagmus, particularly in medullary lesions, may be due to the interruption of the cerebellar control of the PPRF, where all fast phases are supposed to be triggered.^{10,21} This is in agreement with earlier observations of enhancement of the fast-phase velocity in patients with cerebellar lesions.¹⁸

Our findings indicate that an analysis of eye-movement velocities may provide important information on the localization of a brain-stem disorder. As computerized axial tomography of lesions in the posterior fossa has a high incidence of false-negative answers, the results of this type of electro-oculographical analysis may supplement radiological diagnosis of lesions in this area.

The relation between the site of a lesion and the preservation of some eye movements and disturbance of others also may be used for completing our understanding of normal eye motor processing.

SUMMARY

Eye movements in 30 patients with brain-stem lesions were evaluated with electro-oculography, and the findings were analyzed with regard to the site of the lesion in the brain stem. Eye velocities generally were reduced more severely in pontine than in medullary lesions. In medullary lesions, there even was a slight enhancement of the velocities in the fast component of optokinetic and postrotatory nystagmus. In contrast to the slow-phase velocity of OKN, which often was preserved in medullary lesions, the smooth-pursuit velocity was reduced in lesions at all levels in the brain stem. This indicates that these two types of visually induced eye movements use different mechanisms.

REFERENCES

1. HAGSTRÖM, L., G. HÖRNSTEN & B. P. SILVERSKIÖLD. 1969. Oculostatic and visual phenomena occurring in association with Wallenberg's syndrome. *Acta Neurol. Scand.* **45**: 568-582.
2. BALOH, R. W., H. R. KONRAD, A. W. SILLS & V. HONRUBIA. 1975. The saccade velocity test. *Neurology* **25**: 1071-1076.
3. BALOH, R., V. HONRUBIA & A. W. SILLS. 1977. Eye tracking and optokinetic nystagmus. *Ann. Otol. Rhinol. Laryngol.* **86**: 108-114.
4. WENNMO, C. & B. HINDFELT. 1980. Eye movements in brainstem lesions. *Acta Otolaryngol. Stockholm* **90**: 230-236.
5. PASIK, P., T. PASIK & M. B. BENDER. 1969. The pretectal syndrome in monkeys. I. Disturbances of gaze and body posture. *Brain* **92**: 521-534.
6. JAKOBS, L., P. J. ANDERSON & M. B. BENDER. 1973. The lesions producing paralysis of downward but not upward gaze. *Arch. Neurol.* **28**: 319-323.
7. COGAN, D. C. 1974. Paralysis of down-gaze. *Arch. Ophthalmol.* **91**: 192-199.
8. LUSCHEI, E. S. & A. F. FUCHS. 1972. Activity of brainstem neurons during eye movements of alert monkeys. *J. Neurophysiol.* **35**: 445-461.
9. KELLER, E. L. 1974. Participation of medial pontine reticular formation in eye movement generation in monkey. *J. Neurophysiol.* **37**: 316-332.
10. HENN, V. & B. COHEN. 1976. Coding of information about rapid eye movements in the pontine reticular formation of alert monkeys. *Brain Res.* **108**: 307-325.
11. HENRIKSSON, N. G., I. PYYKKÖ, L. SCHALÉN & C. WENNMO. 1980. Velocity patterns of rapid eye movements. *Acta Otolaryngol. Stockholm* **89**: 504-512.
12. SCHALÉN, L. 1980. Quantification of smooth pursuit eye movements. *Acta Otolaryngol. Stockholm* **90**: 404-413.
13. HÖRNSTEN, G. 1974. Wallenberg's syndrome. II. Oculomotor and oculostatic disturbances. *Acta Neurol. Scand.* **50**: 447-468.
14. KOMMERELL, G. & W. F. HOYT. 1973. Lateropulsion of saccadic eye movements. *Arch. Neurol.* **28**: 313-318.
15. PYYKKÖ, I. & C. WENNMO. 1980. Dissociation in the eye motor function in brainstem lesions. *Pract. Otolaryngol. Kyoto* **73**(5): 857-863.
16. MAEKAWA, K. & J. I. SIMPSON. 1973. Climbing fiber responses evoked in vestibulo cerebellum of rabbit from visual system. *J. Neurophysiol.* **36**: 649-666.
17. BAKER, R., M. GREY & A. BERTHOZ. 1975. Neuronal activity in the prepositus hypoglossi nucleus correlated with vertical and horizontal eye movements in the cat. *Brain Res.* **101**: 366-371.

18. WENNMO, C., B. HINDFELT & I. PYYKKÖ. Eye movements in cerebellar and cerebello-pontine disease. (To be published.)
19. KUBO, T., T. MATSUNAGA & Y. HAYASHI. 1978. Convergence of visual and vestibular inputs on pontine reticular formation of the rabbit. *Brain Res.* **147**: 177-182.
20. MIYOSHI, T., M. SHIRATO & S. HIWATASHI. 1978. Foveal and peripheral vision in optokinetic nystagmus. In *Vestibular Mechanisms in Health and Disease*. J. D. Hood, Ed: 294-301. Academic Press. London, England.
21. RAPHAN, T. & B. COHEN. 1978. Brainstem mechanisms for rapid and slow eye movements. *Ann. Rev. Physiol.* **40**: 527-552.

COMPENSATION OF UNILATERAL VESTIBULAR LOSS IN VESTIBULAR NEURONITIS*

A. Katsarkas

McGill University
and
Department of Otolaryngology
Royal Victoria Hospital
Montreal, Quebec, Canada H3A 1A1

J. S. Outerbridge

Biomedical Engineering Unit
McGill University
Montreal, Quebec, Canada H3G 1Y6

INTRODUCTION

The dramatic behavioral manifestations of acute unilateral vestibular sensory loss have been described by a number of authors both in animals and humans.¹⁻³ In humans the early clinical findings are severe disorientation and postural disturbance, nausea and vomiting, marked spontaneous nystagmus with the fast phase toward the healthy side, and reduced ipsilateral caloric response. Most of these symptoms subside markedly in a few days or weeks, but the spontaneous nystagmus persists longer, occasionally changing direction after a substantial period of time.⁴ Residual disorientation after rapid head movements also may persist, sometimes for years.

Since the turn of the century,⁵ attempts have been made to explain the compensation process after unilateral vestibular loss, using available neurophysiologic data. There have been suggestions from clinicians that the degree of compensation was correlated best with the postural improvement, with the decrease in intensity of the spontaneous nystagmus, or with the rotational or the caloric response of the nonaffected site.^{3,5-7}

Neurophysiologic data from experimental animals submitted to a unilateral labyrinthectomy made clear that a vestibular sensory rearrangement proximal to the first-order neuron takes place during the compensation process.^{8,9} In cats immediately after a unilateral ablation of the labyrinth, the resting discharge of the secondary vestibular neurons is shut off on both the operated and the healthy side. Interestingly, cerebellectomy releases the shutdown of the resting discharge of the healthy side but has no effect on the resting discharge of the operated side. The latter discharge reappears in a few days, regardless of the presence or absence of the cerebellum, and reaches almost normal levels in about one month after the labyrinthectomy.^{10,11} Following unilateral labyrinthectomy in frogs, there is a gradual increase in the efficacy of excitatory commissural inputs to ipsilateral central vestibular neurons and of their inhibitory cerebellar and brain-stem inputs.^{12,13}

It is possible therefore that the compensation process after unilateral labyrinth-

*This work was supported in part by the Canadian Medical Research Council and the Macdonald Stewart Foundation.

thectomy is due mainly to a rearrangement of excitatory and inhibitory signals at the level of the secondary vestibular neurons. At this point, the contribution of the cerebellum is not understood completely; "rebalancing" of the vestibulo-ocular reflex (VOR) occurs regardless of whether the cerebellum has been ablated previously or not.¹⁴ Other sensory modalities also play a role in this process, but the neurophysiologic mechanism is not well defined either.^{15,16} Recently, rotational tests have been used to measure the degree of compensation in unilateral vestibular loss in humans and experimental animals.¹⁷⁻¹⁹

The clinical paradigms suitable for the study of the brain-stem compensation process after unilateral loss of vestibular function are rather limited in number. Obviously Menière's disease with its recurrent attacks and fluctuating vestibular function does not allow any compensation process to progress smoothly. If the compensation process is studied in patients after unilateral labyrinthectomy or vestibular nerve section, it may be argued that compensation already has taken place, at least in part, before the operation, as these operations are performed for recurrent vestibular problems. Finally one is left with groups of patients who suddenly lose their vestibular function on one side from causes such as vascular accidents, head injuries, infections, etc. There are three main disadvantages in studying the compensation process in these groups. First, there usually are no objective data prior to onset of the disease. Second, the loss of unilateral vestibular function frequently is partial. Third, there exists the possibility of partial recovery of primary neuron function, masking the effects of central compensation processes. These disadvantages appear to be less severe than those inherent in Menière's disease or postlabyrinthectomy patients. We therefore have chosen to examine a particular set of patients from this group, namely, those with vestibular neuronitis. This disorder is characterized by an acute onset of vertigo, with all the manifestations of unilateral vestibular loss, which frequently is compensated after a long period of time. It is thought to be a viral infection affecting the neurons of Scarpa's ganglion.²⁰⁻²²

Eleven patients with typical manifestations of this disease were tested repeatedly by caloric and/or sinusoidal stimuli during a period of time varying from a few months to four years from onset of the disease. The results are presented and discussed in this paper.

METHODS AND CASES

Eleven patients, eight men and three women, aged 38 to 65 and without previous history of vertigo, were included in this study. They all presented with a typical history of unilateral vestibular loss without concomitant symptoms. They all were examined by one of us (A.K.), six of them a few days after and the remaining five a few months after the onset of the disease. They all had a neurologic evaluation that showed no abnormalities other than those related to unilateral vestibular loss. They all had audiograms that showed either normal hearing or mild bilateral sensorineural loss, which was interpreted as presbycusis. Eight were in good health otherwise; three had unrelated medical problems. All patients who were seen early in their disease came either by wheelchair or helped by relatives for the initial examination. They all improved subsequently. All patients reported in three months to one year either that they felt perfectly back to normal or that they experienced mild lightheadedness when they were tired or when they turned the head fast, especially toward the affected side.

Spontaneous and positional nystagmus and the responses to bithermal caloric stimuli were recorded, with eyes closed, at irregular intervals using a.c. electro-oculography with a time constant of three seconds. Details have been published elsewhere.²³ Patients also were exposed repeatedly to a sinusoidal stimulus of 1/6 Hz and a peak velocity of 60°/second; prior to each rotation, which lasted for two minutes, the patients were tested for possible spontaneous nystagmus. Eye movements were recorded by d.c. electro-oculography, head fixed to the chair and eyes open behind frosted goggles that provided an illuminated but featureless visual input. Mental alertness was maintained by an interesting discussion. No patients were taking any centrally acting drugs at the time of testing.

All rotational test results were analyzed off-line by a computer program that extracted the slow-phase eye velocity of the response; the peak amplitude ratio (eye velocity/head velocity) was measured for each cycle of the response, and the average peak amplitude ratio was computed for rotation to the right (PARR) and to the left (PARL). The peak amplitude preponderance with (CPAP) and without (PAP) correction for spontaneous nystagmus was computed as the ratio of the difference of the absolute peak amplitude ratios to their sum.

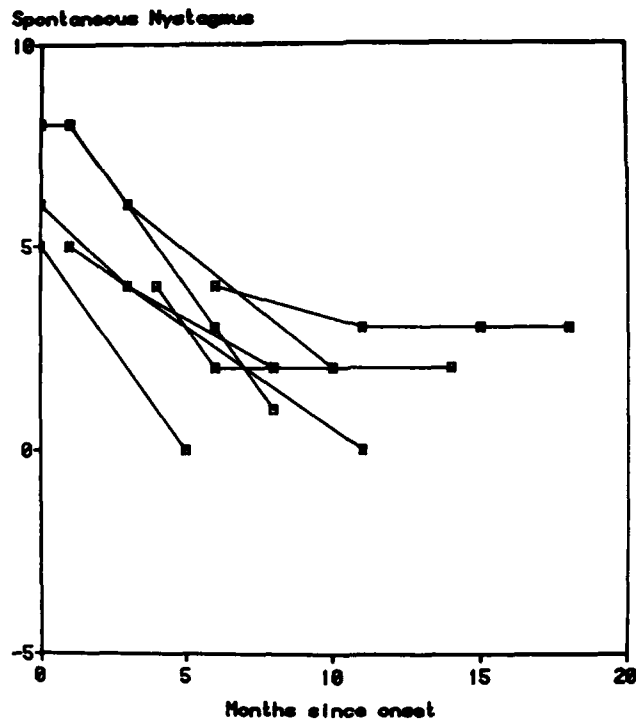


FIGURE 1. Spontaneous nystagmus velocity (slow-phase degrees/second in rotational test position) versus time since onset of symptoms. Positive velocity indicates quick phase toward the healthy side. Here and in FIGURES 2, 3, 5, and 6, lines connect measurements (squares) on individual patients; measurements within the first month are plotted at zero.

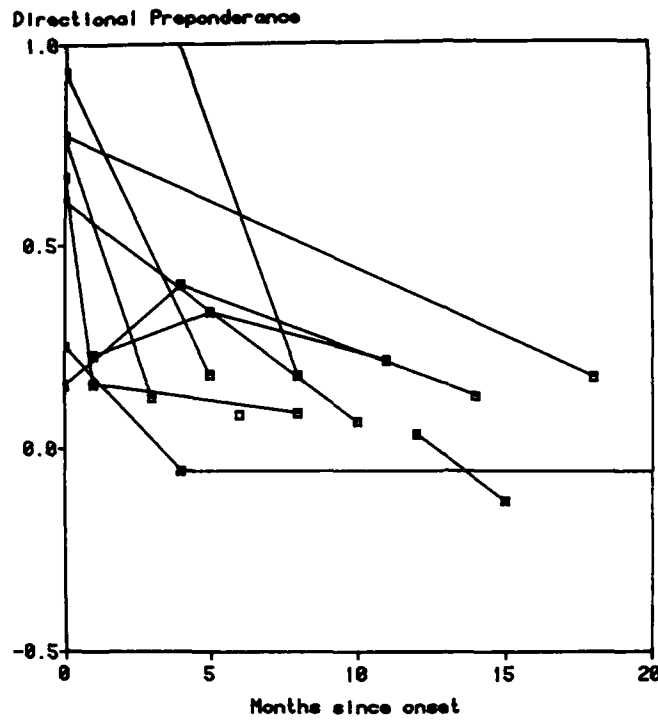


FIGURE 2. Directional preponderance ratio of bithermal caloric test versus time since onset of symptoms. Positive ratio indicates preponderance toward healthy side.

RESULTS

Spontaneous Nystagmus

Initially all patients showed spontaneous nystagmus with the fast phase toward the healthy side. The velocity of this nystagmus decreased with time (FIGURE 1). Three patients showed no spontaneous nystagmus 44, 11, and 5 months respectively after the onset of their disease. Two patients showed a direction reversal of their spontaneous nystagmus in the caloric test position at 15 and 8 months after disease onset. The remaining six patients showed low-amplitude spontaneous nystagmus during the last test, the longest period since disease onset being 18 months for one of the patients.

Directional Preponderance (Bithermal Caloric)

The directional preponderance of the bithermal caloric response decreased with time, following the same trend as the spontaneous nystagmus (FIGURE 2).

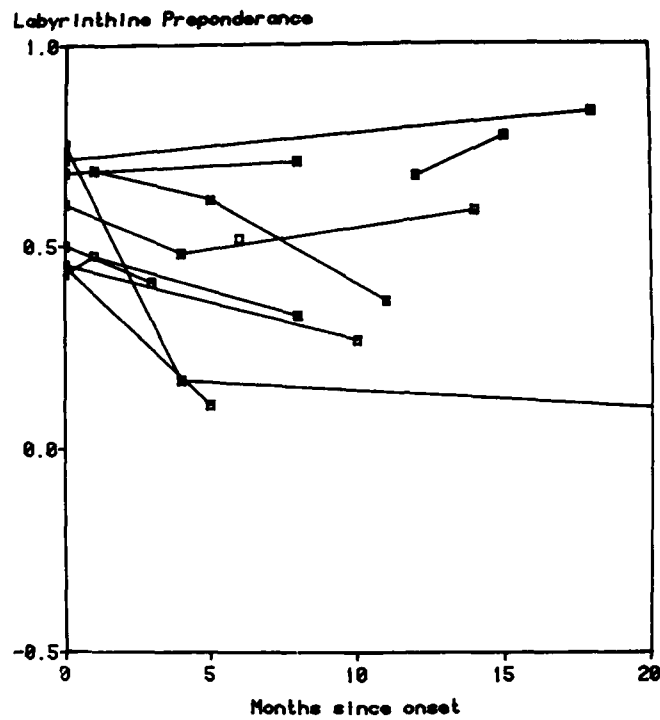


FIGURE 3. Labyrinthine preponderance ratio of bithermal caloric test versus time since onset of symptoms. Positive ratio indicates preponderance toward healthy side.



FIGURE 4. Computed slow-phase eye velocity during sinusoidal rotation at 1/6 Hz in a patient with vestibular neuronitis, tested 10 days after disease onset.

Labyrinthine Preponderance (Bithermal Caloric)

All patients initially showed weaker bithermal caloric responses on the affected side. The initial labyrinthine preponderance varied from patient to patient between 77% and 43%. This value decreased with time in six patients. In four of these six patients, all four caloric responses increased with time, but the responses on the affected side increased more than those on the healthy side. In the remaining two patients, the cold caloric responses on the healthy side remained unchanged with time, while the other three caloric responses increased. The labyrinthine preponderance remained unchanged in two and increased with time in two patients; in the latter two cases, there was an increase of caloric responses on the healthy side, while the responses on the affected side remained unchanged in a period of 18 and 8 months respectively. One patient was tested only once (FIGURE 3).

Peak Amplitude Ratio (Sinusoidal Rotation)

The average PAR varied from patient to patient, ranging from 0.88 to 0.31 on the healthy side and from 0.82 to 0.17 on the affected side. In seven patients, the PAR was measured more than once. In six out of these seven patients, PAR values on the affected side showed a clear tendency to approach the values of the healthy side with time. In one patient, first tested 10 days after the onset of the disease, a number of cycles showed a "clipping" of the eye response during rotation toward the affected side (FIGURE 4). Unfortunately no other cases underwent rotational testing less than 10 days from disease onset.

Peak Amplitude Preponderance (Sinusoidal Rotation)

PAP generally decreased with time from onset of symptoms, showing the same general trend as the spontaneous nystagmus and caloric directional preponderance (FIGURE 5). However when PAP was computed after correction for spontaneous nystagmus (FIGURE 6), the values were small in all cases and showed no significant change with time. A scatter diagram of (uncorrected) PAP versus labyrinthine preponderance (FIGURE 7, left) suggests some positive correlation, but there clearly is no correlation when corrected PAP values (CPAP) are used (FIGURE 7, right).

DISCUSSION

In all patients there was a progressive decrease in spontaneous nystagmus velocity and in the directional preponderance of the bithermal caloric response, and the peak amplitude preponderance showed the same trend. Similar observations have been reported by several authors.^{7,17,18} However, the corrected peak amplitude preponderance always remains close to zero, showing that the occurrence of PAP is due primarily to the presence of spontaneous nystagmus. Labyrinthine preponderance, on the other hand, appeared to be quite unrelated in some cases. This parameter decreased in almost half of our cases, coming close to zero in two patients, while it increased or remained unchanged in the rest of the patients. Since the magnitude of the labyrinthine preponderance presumably

is related closely to the extent of damage to the first-order vestibular neurons during the disease process, it would appear that this process was reversible—totally or partially—in some cases but not in others. The fact that the decreases in spontaneous nystagmus, directional preponderance, and PAP occur regardless of the trend in the magnitude of labyrinthine preponderance suggests that these three parameters reflect the degree of static and dynamic restoration of the central vestibular neuron, while the magnitude and the trend of labyrinthine preponderance shows the extent of damage and restoration of the primary vestibular neuron in disease processes such as vestibular neuronitis. However,

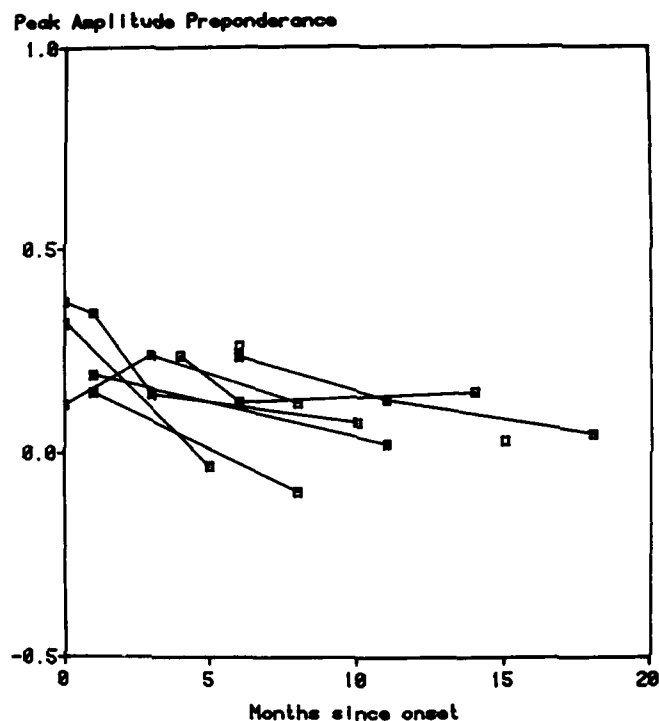


FIGURE 5. Peak amplitude preponderance ratio of rotational test versus time since onset of symptoms. Positive ratio indicates higher slow-phase velocity during rotation toward the healthy side.

the increase in labyrinthine preponderance in some patients might be interpreted as a reflection of central compensation also.

Corrected peak amplitude preponderance was close to zero in all cases, regardless of the magnitude of labyrinthine preponderance. Therefore it is possible for a patient with vestibular neuronitis to have substantial labyrinthine preponderance of the bithermal caloric response toward the healthy side but to have rotational responses that are symmetrical after correction for spontaneous nystagmus. However, presence of spontaneous nystagmus is only one of several

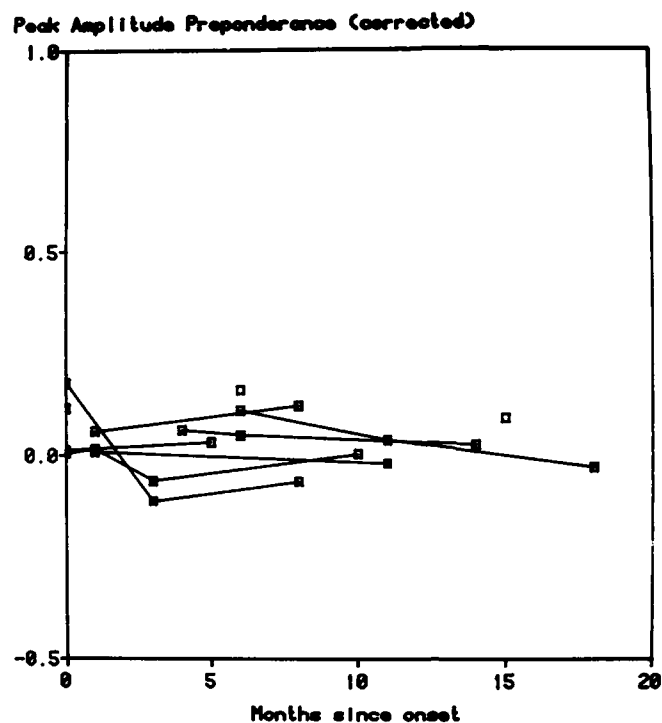


FIGURE 6. Corrected peak amplitude preponderance ratio of rotational test (corrected for spontaneous nystagmus) versus time since onset of symptoms. Positive ratio indicates higher slow-phase velocity during rotation toward the healthy side.

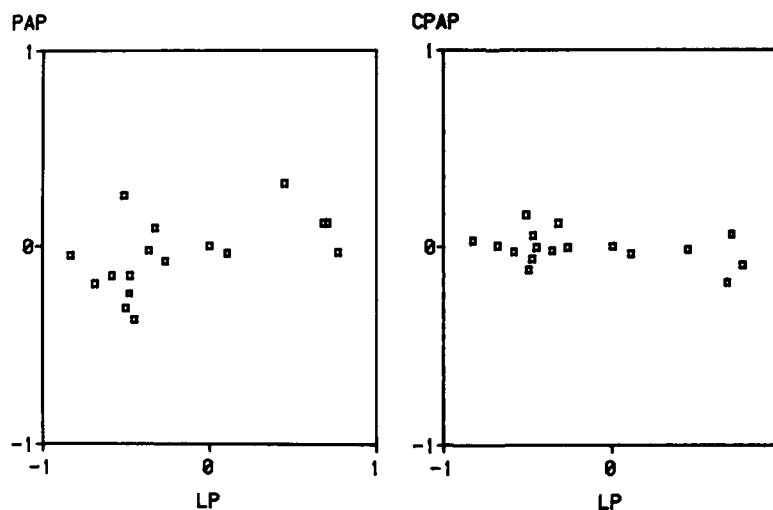


FIGURE 7. Raw (PAP, left) and corrected (CPAP, right) peak amplitude preponderance versus labyrinthine preponderance (LP). Caloric and rotational tests were performed within one week, usually the same day, except for two cases in which tests were performed within three weeks. Two results are plotted for some patients.

possible causes of asymmetry in rotational responses. Another, which was seen clearly in only one case, is "clipping" or flattening of the sinusoidal response on one side. The possibility that nonlinear responses of this kind are characteristic of the early, relatively uncompensated stage of the disorder is an interesting one, which will be pursued. At present, however, it can be concluded that there is little, if any, nonlinearity of rotational response in cases of vestibular neuronitis after the acute stage. This finding, if confirmed, may be useful in differential diagnosis of central versus peripheral vestibular lesions.

ACKNOWLEDGMENTS

We would like to thank Dr. G. Melvill Jones for suggestions and helpful discussions, and Mrs. M. Mai and Mrs. H. L. Galiana for help in collecting and processing the data.

REFERENCES

1. FLOURENS, P. 1842. Recherches experimentales sur les propriétés et fonctions du système nerveux dans les animaux vertébrés. Chez J.-B. Baillière. Paris, France.
2. PURKINJE, J. 1820. Beytrage zur naheren Kenntniss des Schwindels aus heautognostischen Daten. (As cited in KRUTA, V. 1965. M.J.P. Flourens—J.E. Purkinje. University of Paris. Paris, France.)
3. BARANY, R. 1906. Untersuchungen über den vom Vestibularapparat des Ohres reflektorisch ausgelosten rhythmischen Nystagmus und seine Begleiterscheinungen. *Monatschr. Ohrenheilkd.* **40**: 193-297.
4. JUNG, R. & H. H. KORNUBER. 1964. Results of electronystagmography in man: the value of optokinetic, vestibular, and spontaneous nystagmus for neurologic diagnosis and research. In *The Oculomotor System*. M. B. Bender, Ed.: 428-488. Harper and Row. New York, N.Y.
5. STENGER, H. H. 1959. "Erholungsnystagmus" nach einseitigem Vestibularisausfall, ein dem Bechterew-Nystagmus verwandter Vorgang. *Arch. Ohren Nasen Kehlkopfheilkd.* **175**: 545-549.
6. FLUUR, E. 1960. Vestibular compensation after labyrinthine destruction. *Acta Otolaryngol.* **52**: 367-375.
7. FISCH, U. 1973. The vestibular response following unilateral vestibular neurectomy. *Acta Otolaryngol.* **76**: 229-238.
8. PRECHT, W. 1974. Characteristics of vestibular neurons after acute and chronic labyrinthine destruction. In *Handbook of Sensory Physiology. Vestibular System*. H. H. Kornhuber, Ed. **6/2** (Part 2): 451-462. Springer-Verlag. New York, N.Y.
9. SCHAEFER, K. P. & D. C. MEYER. 1974. Compensation for vestibular lesions. In *Handbook of Sensory Physiology. Vestibular System*. H. H. Kornhuber, Ed. **6/2** (Part 2): 463-492. Springer-Verlag. New York, N.Y.
10. MCCABE, B. F. & I. H. RYU. 1969. Experiments on vestibular compensation. *Laryngoscope* **79**: 1728-1736.
11. MCCABE, B. F., I. H. RYU & T. SEKITANI. 1972. Further experiments on vestibular compensation. *Laryngoscope* **82**: 381-396.
12. DIERINGER, N. & W. PRECHT. 1979. Mechanisms of compensation for vestibular deficits in the frog. I. Modification of the excitatory commissural system. *Exp. Brain Res.* **36**: 311-328.
13. DIERINGER, N. & W. PRECHT. 1979. Mechanisms of compensation for vestibular deficits in the frog. II. Modification of the inhibitory pathways. *Exp. Brain Res.* **36**: 329-341.
14. HADDAD, G. M., A. R. FRIENDLICH & D. A. ROBINSON. 1977. Compensation of nystagmus after VIIIth nerve lesions in vestibulo-cerebellectomized cats. *Brain Res.* **135**: 192-196.

15. COURJON, J. H., M. JEANNEROD, I. OSSUZIO & R. SCHMID. 1977. The role of vision in compensation of vestibulo ocular reflex after hemilabyrinthectomy in the cat. *Exp. Brain Res.* **28**: 235-248.
16. PUTKONEN, P. T. S., J. H. COURJON & M. JEANNEROD. 1977. Compensation of postural effects of hemilabyrinthectomy in the cat. A sensory substitution process? *Exp. Brain Res.* **28**: 249-257.
17. STEFANELLI, M., E. MIRA, R. SCHMID & R. LOMBARDI. 1978. Quantification of vestibular compensation in unilateral Menière's disease. *Acta Otolaryngol.* **85**: 411-419.
18. WOLFE, J. W. & C. M. KOS. 1976. Nystagmic responses of the rhesus monkey to rotational stimulation following unilateral labyrinthectomy: a preliminary report. *Trans. Am. Acad. Ophthalmol. Otolaryngol.* **82**: 60-69.
19. WOLFE, J. W. & C. M. KOS. 1977. Nystagmic responses of the rhesus monkey to rotational stimulation following unilateral labyrinthectomy: final report. *Trans. Am. Acad. Ophthalmol. Otolaryngol.* **84**: 38-45.
20. DIX, M. R. & C. S. HALLPIKE. 1952. The pathology, symptomatology and diagnosis of certain common disorders of the vestibular system. *Proc. R. Soc. Med.* **45**: 341-354.
21. MORGENSTEIN, K. M. & H. I. SEUNG. 1971. Vestibular neuronitis. *Laryngoscope* **81**: 131-139.
22. BALOH, R. W. & V. HONRUBIA. 1979. *Clinical Neurophysiology of the Vestibular System*: 206-207. F.A. Davis Co. Philadelphia, Pa.
23. KIRKHAM, T. H. & A. KATSARKAS. 1977. An electrooculographic study of internuclear ophthalmoplegia. *Ann. Neurol.* **2**: 385-392.

TEMPORAL BONE CHARACTERISTICS IN MENIERE'S DISEASE*

Jan Stahle, Hermann F. Wilbrand,† and Helge Rask-Andersen

*Department of Otolaryngology
University Hospital
University of Uppsala
S-750 14 Uppsala, Sweden*

INTRODUCTION

Reports on perisaccular fibrosis, reduced visibility of the vestibular aqueduct (VA) on tomograms, and bony obstruction of the VA in occasional cases gave us the incentive for experimental and clinical studies of the temporal bone in patients with Meniere's disease.¹⁻¹¹ We previously have described several morphologic characteristics, and as a result of new findings, both the medical and surgical treatments of this disease have been modified.^{11,12}

The extent of the problem of Meniere's disease is reflected by the incidence figures.¹³ In Sweden, the yearly incidence has been calculated as 1 case in a population of 2,163. This gives an overall incidence of 46/100,000. If one assumes that the incidence of Meniere's disease is the same in the United States population, then there will be approximately 100,000 patients per year. A conservative estimate of the prevalence of affected persons in the United States is about two million.

The present study was undertaken in an attempt to obtain some additional information about any gross morphologic factors that could predispose to the development of Meniere's disease or be characteristic of this disorder.

MATERIAL

The material comprised 50 healthy individuals, designated the control group, and 63 patients with Meniere's disease. Both ears were examined in all cases. The mean age in both groups was 46 years.

The control group included no patients, but was made up of members of the hospital staff and persons not connected with the hospital. All individuals in the control group underwent otologic examination, including pure-tone audiometry. No persons with symptoms of chronic otitis or a history of disease of the inner ear were accepted for the control group.

In the group of patients with Meniere's disease, the average duration of the disease was 9.7 years (range 0.3-54.0 years). In 29 patients the right side was affected; in 27, the left side was affected; and in 7, the disease was bilateral. The patients were highly select. Most of them represented a category of cases in whom the vertigo was judged to be intractable to medical therapy. For this reason they were referred to the University Hospital in Uppsala—a center in Sweden specializing in treatment of Meniere's disease—for special care and a decision

*This work was supported by the Swedish Medical Research Council (Project No. 3908).

†Department of Diagnostic Radiology.

about surgery. Twenty-three of these 63 patients were operated on following the examinations.

Besides the findings in the controls and patients, some information from earlier studies on 58 temporal bones obtained at autopsy will be included in this presentation.

METHODS

Plain radiography, tomography, microdissection, plastic molding, and measurements at surgery were the principal methods used.

Radiography

The temporal bones in both patients and controls were examined under standardized conditions. Plain radiography was performed on an Orbix (Siemens-Elcoma) apparatus, with use of the Dulac system modified by Rådberg et al.¹⁴ Both temporal bones were reproduced for comparison between the two sides in transorbital, semiaxial, and axial projections. Every individual temporal bone then was examined on highly coned radiographs in the Stenvers and lateral (Runström II) projections.

Tomography

Only one off-lateral projection for tomographic reproduction of the VA was used in this study, in spite of our previous finding that complementary positioning may be needed in some cases for optimal visualization of the aqueduct's entire length. The applied technique was judged sufficiently adequate to get a clear idea of the relation between the degree of periaqueductal pneumatization and visualization of the aqueduct.

Planimetry

Planimetry of the mastoid air-cell system was carried out on films of each temporal bone in the Runström II projection, thus adopting the method used by Diamant.^{15,16} The middle ear space was not included in the area. Because of the magnification inherent in the radiographic reproducing system, the planimetric values from measurements on the films were reduced to natural size.

Plastic Molding

Macerated temporal bone specimens were filled with a mixture of unsaturated polyesters (Akemi) through the internal acoustic meatus and the oval and round windows. A cast of the labyrinthine hollow and adjacent channels remained after breakdown of the skeletal parts by 5 M hydrochloric acid. The molds (FIGURES 3, 4, and 5) allowed three-dimensional visualization of the topographic relationship of the VA and its accessory canal to the vestibular labyrinth, especially the posterior semicircular canal, the facial canal, the

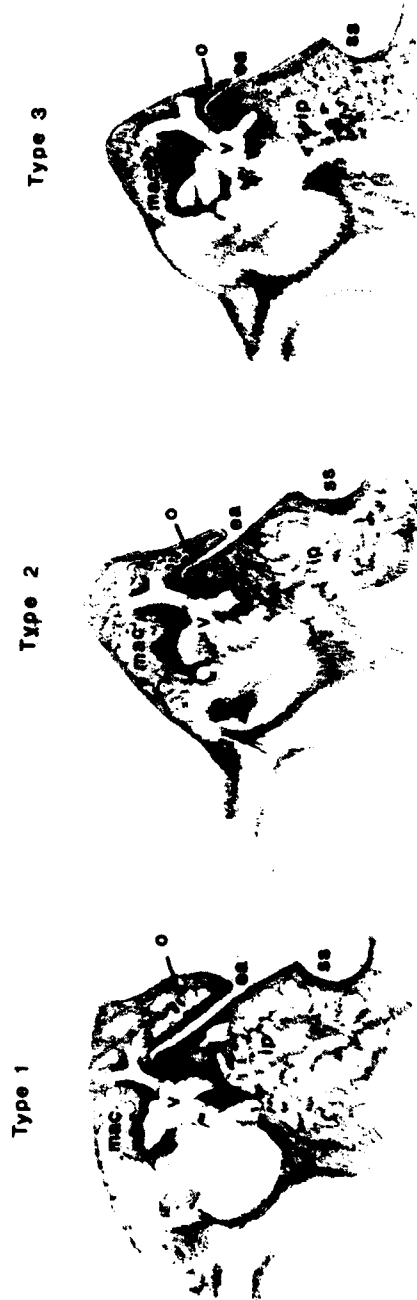


FIGURE 1. Schematic drawings illustrating the three types of periaqueductal pneumatization. The operculum (o) is the bony roof covering the vestibular aqueduct. Type 1: large-cell, rich pneumatization. Type 2: small-cell, sparse pneumatization or bone marrow spaces. Type 3: absence of air cells and marrow spaces (concrete petrous bone). ea, external aperture of the vestibular aqueduct; ip, infralabyrinthine pneumatization; ss, sigmoid sinus; mac, mastoid air cells; v, vestibule.

TABLE 1
DISTRIBUTION OF THE THREE TYPES OF PERIAQUEDUCTAL PNEUMATIZATION (DETERMINED WITH TOMOGRAPHY)

Material	Type of Periaque ductal Pneumatization (%)			Total Number of Ears
	1	2	3	
Controls	39.0	26.0	45.0	100
Meniere Patients	10.6	15.4	74.0	123

internal acoustic meatus, the jugular fossa, and the bony plate of the posterior face of the pyramid.

OBSERVATIONS AND COMMENTS

Periaque ductal Pneumatization

With tomography, variations in periaque ductal pneumatization were observed. Three different types were identified (FIGURE 1): type 1—large cell rich pneumatization; type 2—small air cells and sparse pneumatization or bone marrow spaces (which cannot be differentiated from each other with tomography); and type 3—a complete absence of air cells. Types 1 and 2 were more common in the control group than among Meniere patients. Type 3 dominated in the Meniere group (TABLE 1).

TABLE 2
DISTRIBUTION OF CONTROL GROUP (n = 100 EARS) AND PATIENTS WITH MENIERE'S DISEASE (n = 125 EARS) BY TYPE OF PNEUMATIZATION OF THE PETROUS PYRAMID

		Periaqueductal Pneumatization Type			
		1 (n = 29)	2 (n = 26)	3 (n = 45)	
Controls					Significance
Pneumatization medial to the arcuate eminence	yes	27	15	14	p < 0.001
	no	2	11	31	
Infralabyrinthine pneumatization	yes	27	17	24	p < 0.001
	no	2	9	21	
		Periaqueductal Pneumatization Type			
		1 (n = 13)	2 (n = 19)	3 (n = 93)	
Meniere Patients					Significance
Pneumatization medial to the arcuate eminence	yes	13	15	32	p < 0.001
	no	0	4	61	
Infralabyrinthine pneumatization	yes	12	18	54	p < 0.001
	no	1	1	39	

Structure of the Petrous Pyramid

Reduced periaqueductal pneumatization was correlated to sparse pneumatization medial to the arcuate eminence, as well as below the labyrinth (TABLE 2). In cases with no periaqueductal pneumatization (type 3), air cells medial to the

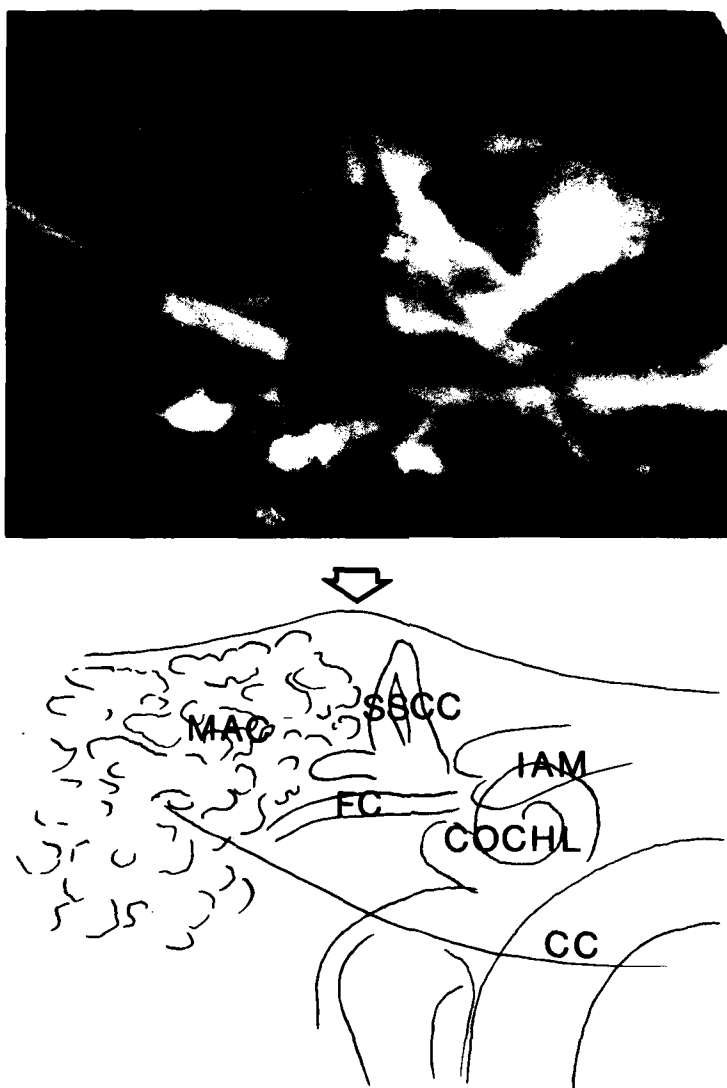


FIGURE 2. Radiograph of a right temporal bone in the Stenvers projection (top) with a corresponding drawing (bottom) for orientation. There is no pneumatization medial to the arcuate eminence (large arrow). MAC, mastoid air cells; SSCC, superior semicircular canal; IAM, internal acoustic meatus; FC, facial canal; COCHL, cochlea; CC, carotid canal.

TABLE 3
INFLUENCE OF PERIAQUEDUCTAL PNEUMATIZATION ON SOME MORPHOLOGIC FACTORS IN
THE TEMPORAL BONE (CONTROL GROUP, $n = 100$ EARS)*

		Periaqueductal Pneumatization			Significance
		Type 1 ($n = 29$)	Type 2 ($n = 26$)	Type 3 ($n = 45$)	
Total length of vestibular aqueduct (mm)	M	14.9	13.0	9.3	$p < 0.01$
	SD	3.58	2.13	2.46	
Width of the external aperture of the vestibular aqueduct (mm)	M	6.4	4.8	3.5	$p < 0.01$
	SD	2.34	1.52	1.10	
Mastoid air cells area (cm^2)	M	15.0	11.3	9.6	$p < 0.01$
	SD	4.10	2.80	2.87	

*Means (M) and standard deviations (SD).

arcuate eminence rarely were found, nor was there infralabyrinthine pneumatization ($p < 0.001$). A typical case is presented in FIGURE 2.

Visibility of the Vestibular Aqueduct

The visibility of the VA in its entire length on tomograms appears to be influenced by the degree of periaqueductal pneumatization. In the control group, the aqueduct was visible in 81% and not visible in 19%. In Meniere patients, the corresponding figures were 73 and 27%, respectively. In the diseased ears alone in the Meniere group ($n = 69$), 65% of the aqueducts were visible and 35% were not visible.

In all 29 controls with type 1 pneumatization, the VA was visible in its entire length, while among controls with type 3, the aqueduct was visible in only 35% of the ears. In the ears of the Meniere patients, 74% of which showed type 3 periaqueductal pneumatization (TABLE 1), most nonvisible aqueducts belonged to the type 3 category. We therefore believe that nonvisibility of the VA on tomograms in Meniere patients does not necessarily indicate nonpatency or aqueductal stenosis. Rather it may reflect a structural feature of the temporal bone that is observed more often in Meniere patients. When noticed, however, drainage operations upon the endolymphatic sac are not advised.¹⁷

It should be pointed out that only one off-lateral projection for tomographic reproduction of the VA was used in this study. From our previous investigations, it is clear that repositioning to other tomographic angles increases the number of fully reproduced aqueducts.⁵

Vestibular Aqueduct and Mastoid Area

Positive correlation was found between the mastoid air-cell area and the development of periaqueductal pneumatization (TABLE 3). Those ears displaying a well-developed mastoid air-cell area more often were of type 1 (large-cell, rich periaqueductal pneumatization). In addition, the mean area of the mastoid air cells in Meniere patients was smaller than in controls (TABLE 4). This confirms

TABLE 4
SOME MORPHOLOGIC CHARACTERISTICS OF THE TEMPORAL BONE AS MEASURED ON
TOMOGRAPHS AND RADIOGRAPHS

	Patients with Meniere's Disease					
	Control Group (n = 100 Ears)		Nondiseased Ears (n = 55)		Diseased Ears (n = 69)	
			Mean	SD	Mean	SD
Total length of the vestibular aqueduct (mm)	11.86	3.67	9.25	2.33	8.49	2.75
Width of the external aperture of the vestibular aqueduct (mm)	4.69	2.08	4.19	1.30	3.56	1.75
Area of mastoid air cells (cm ²)	11.59	3.95	8.22	3.74	7.93	4.08

observations made by Ganz and Eichel-Streiber, but is contrary to recent findings by Oku *et al.*^{18,19}

The importance of pneumatization for the topographic anatomy of the internal ear is exemplified in FIGURES 3, 4, and 5. Large-cell, rich pneumatization (FIGURE 4) is associated with a broad operculum and a long VA ending with a

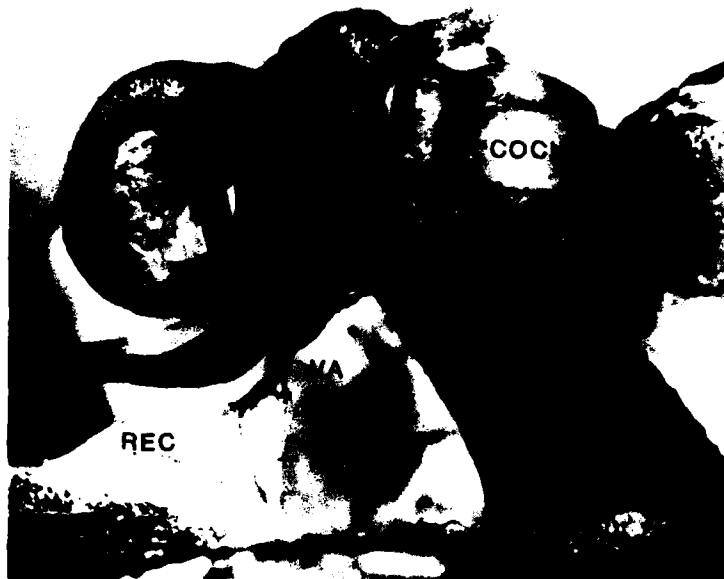


FIGURE 3. Plastic mold of a left human internal ear seen from above. The vestibular aqueduct (VA) ends in a fan-shaped recess, which houses the endolymphatic sac. The paravestibular canaliculus (PVC) is seen distinctly. The star indicates part of the facial canal. JAM, internal acoustic meatus; VA, vestibular aqueduct; LSCC, SSCC, and PSCC, lateral, superior, and posterior semicircular canals; REC, recess of the vestibular aqueduct; CC, carotid canal; UFK, upper facial knee.

recesslike widening (FIGURE 3). Absence of air cells around the aqueduct (FIGURE 5) implies a small operculum and a short and narrow aqueduct.

The Paravestibular Canaliculus (PVC)

This minute structure—also named the accessory canal of the VA²⁰—regularly can be found at microdissection. It runs through the petrous pyramid



FIGURE 4. Plastic mold of a left human internal ear seen from behind in the pyramidal-axial view. This is an example of type 1 periaqueductal pneumatization. The distance between the vestibular aqueduct (VA) and the posterior cranial fossa, which corresponds to the operculum (O), is quite long. ELS, endolymphatic sac; FC, facial canal; RW, round window; OW, oval window. For other abbreviations, see FIGURE 3.

from the vestibule to the posterior cranial fossa in close proximity to the vestibular aqueduct (FIGURE 6). It houses mainly veins representing the main venous drainage system from the vestibule.^{21,22} Minute arteries branching from the labyrinthine artery and the posterior meningeal artery have been described.²²⁻²⁴

The PVC has been demonstrated tomographically in 10 out of 35 ears in a series of healthy subjects and in 10 out of 86 ears in patients with long-standing Meniere's disease.⁶



FIGURE 5. Plastic mold of a left human internal ear seen from behind in the pyramidal-axial view, conforming with the surgeon's transmastoid view. This is an example of type 3 periaqueductal pneumatization. The opercular volume (O) is quite small and consistent with the absence of periaqueductal air cells. The VA is short compared with the corresponding aqueduct in FIGURE 4. LFK, lateral facial knee; UFK, upper facial knee; CT, chorda tympani; JF, jugular fossa. The star indicates a vascular canal passing along the vertical portion of the facial canal. For other abbreviations, see FIGURE 3.

Besides blood vessels, the canaliculus is filled with loosely textured connective tissue similar to that typical of the VA. Numerous minute vascular channels connect the PVC with the VA. Apart from its drainage functions, it is postulated that the canaliculus is of nutritional importance for the endolymphatic duct and the proximal portion of the sac. The common finding of concrete, nonpneumatized bone around the VA in Meniere patients could correspond to absence or malformation of the PVC.

Position of the Endolymphatic Sac

As a consequence of reduced periaqueductal pneumatization in Meniere patients, the greater part of the endolymphatic sac (ELS) might be positioned outside the vestibular aqueduct on the posterior slope of the pyramid (FIGURE 7).

Normally the proximal part of the sac, containing the *pars rugosa*, lies within the aqueduct enclosed by well-pneumatized bone and loose, highly vascular connective tissue.² The operculum that covers the peripheral portion of the VA normally contains air cells and marrow spaces. Between the membranous walls of the duct and sac, on the one hand, and the bony walls of the aqueduct, on the other, normally there are well-developed vascular communications.²⁵ Anastomoses between periaqueductal bone marrow sinusoids and perisaccular vessels also have been described.²¹

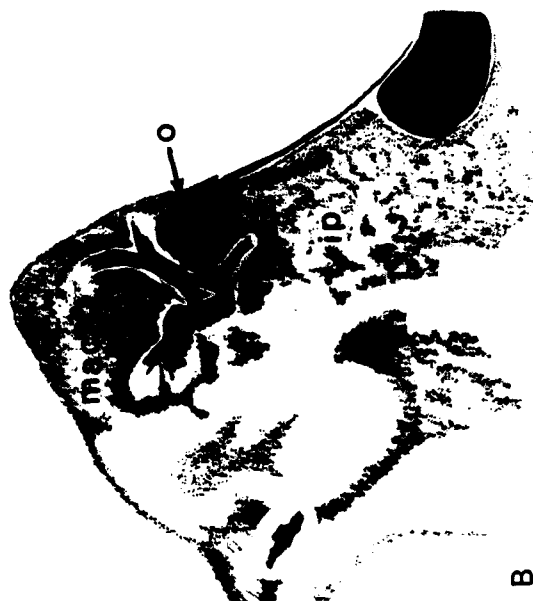
In addition to its resorptive function, morphologic characteristics may indicate that the sac plays an immunodefensive role. In the epithelium in the intermediate part of the sac, morphologic signs influencing the incoming substances are present. A vigorous interaction between lymphocytes and macrophages, similar to that observed in antigen-activated lymphoid tissue, may be seen.²⁶

There appears to be some evidence that the size of the VA is reduced in patients with Meniere's disease. In consequence, there is reason to believe that the ELS also will be diminished. This is manifested in the fact that the external aperture of the VA is smaller in Meniere patients than in normal individuals. This is confirmed by the finding of Egami *et al.* of hypoplasia of the VA and ELS in endolymphatic hydrops.²⁷ These authors concluded that the changes were the result of a congenital hypoplasia, since no evidence of acquired bony pathology was found.



FIGURE 6. Plastic mold of a right human internal ear. Several vascular branches of the accessory canal, which is also called the paravestibular canaliculus (PVC), merge in a main canal whose course is medial to the vestibular aqueduct. The cerebral portion of the vestibular aqueduct ends in a triangular recess (REC), which houses the endolymphatic sac. FC, facial canal; GG, geniculate ganglion.

Type 3



B

Type 1



A

FIGURE 7. Variations in the location of the endolymphatic sac due to differences in periaqueductal pneumatization. A (left): In a healthy person with well-developed periaqueductal pneumatization (type 1), the pars rugosa of the endolymphatic sac lies within the aqueduct and has rich vascular communications with the surrounding bone and its marrow spaces. B (right): In a patient with Meniere's disease, on the other hand, the aqueduct is short and narrow and has solid walls (type 3). In this case, the sac is hypoplastic and the pars rugosa probably lies partly outside the aqueduct. o, operculum; ip, infralabyrinthine pneumatization; mac, mastoid air cells; v, vestibule.

We consider that owing to this aberrant position and smaller size, a sac that lies mainly outside the aqueduct may have a reduced vascular and metabolic supply. It thus may be presumed to be far more vulnerable functionally than a sac situated within the aqueduct in the normal way. An unprotected sac might constitute the Achilles' heel of the internal ear. If the position and the size of the sac are decisive in some way for maintenance of a normal function, as we have suggested, no medicine will be able to produce a change. A definite cure can never be expected under such circumstances. Medicines, diets, and other regimes can affect only the secondary manifestations of an irreversible morphologic abnormality. Such general disorders as diabetes mellitus, hypothyroidism, hyperlipoproteinemia, food sensitivity, and different forms of stress might give rise to the extra burden on the internal ear leading to transformation of the endolymphatic sac from a state of only just balanced function to one of intermittent or constant resorptive failure.

CONCLUSIONS

1. The temporal bone in Meniere patients differs in several respects from that in normal individuals.
2. Three types of periaqueductal pneumatization have been defined from tomograms: type 1, large cells and rich pneumatization; type 2, small air cells and sparse pneumatization; and type 3, complete absence of air cells. Type 1 is seen mostly in normal individuals, and type 3 predominates in Meniere patients.
3. In consequence of reduced periaqueductal pneumatization, the vestibular aqueduct is shorter and its external aperture narrower in Meniere patients than in normal subjects. The mean length measured on tomograms was 11.86 mm in the controls and 8.49 mm on the diseased side in Meniere patients.
4. The mean area of mastoidal air cells in the control group was 11.59 cm², which corresponds with other reports. In Meniere patients this figure was 7.93 cm².
5. Pneumatization medial to the arcuate eminence and below the labyrinth rarely is seen on radiographs in Meniere patients.
6. The vestibular aqueduct was visible in its entire length in 81% of the ears of the controls and in 65% of the diseased ears in patients with Meniere's disease. Repositioning to other tomographic angles increases the number of fully reproduced aqueducts. Nonvisibility thus is not pathognomonic for Meniere's disease and does not necessarily correspond to nonpatency.
7. From the observed skeletal characteristics of the petrous pyramid in Meniere patients, it is supposed that the membranous content also might be afflicted. The reduced size of the endolymphatic sac and its presumed aberrant position might indicate hypoactivity. This could interfere with its probable resorptive and immunodefensive functions.

SUMMARY

The petrous portion of the temporal bone in patients with Meniere's disease differs from that of healthy individuals mainly in its lack of periaqueductal pneumatization and its consequently short and narrow vestibular aqueduct. Diminished pneumatization may have an impact upon the tomographic reproducibility of the aqueduct. A total lack of periaqueductal pneumatization is

prevalent in long-standing Meniere's disease. Tomography may serve as a tool by providing a basis for the choice of surgical procedure. Roentgenologic and histologic studies have indicated that the *pars rugosa* of the endolymphatic sac in normals mainly is housed inside the distal part of the vestibular aqueduct. In patients with Meniere's disease, the sac might be located outside the aqueduct and therefore deprived of the functions of the loose and highly vascular tissue normally surrounding it within the aqueduct. This might influence the total vascular supply of the sac, thereby interfering with its resorptive and immunodefensive functions.

REFERENCES

1. HALLPIKE, C. S. & H. CAIRNS. 1938. Observations on the pathology of Meniere's syndrome. *J. Laryngol.* **53**: 625-655.
2. ZECHNER, G. & E. ALTMANN. 1969. Histological studies on the human endolymphatic duct and sac. *Pract. Oto-Rhino-Laryngol.* **31**: 65-83.
3. CLEMIS, J. D. & G. E. VALVASSORI. 1968. Recent radiographic and clinical observations on the vestibular aqueducts. *Otolaryngol. Clin. North Am.* **1**: 339-346.
4. GUSSEN, R. 1971. Meniere's disease: new temporal bone findings in two cases. *Laryngoscope* **81**: 1695-1707.
5. STAHL, J. & H. F. WILBRAND. 1974. The vestibular aqueduct in patients with Meniere's disease. *Acta Otolaryngol.* **78**: 36-48.
6. STAHL, J. & H. F. WILBRAND. 1974. The para-vestibular canaliculus. *Can. J. Otolaryngol.* **3**: 262-270.
7. WILBRAND, H. F., H. RASK-ANDERSEN & D. GILSTRING. 1974. The vestibular aqueduct and the para-vestibular canal. *Acta Radiol. Diagn.* **15**: 337-355.
8. WILBRAND, H. F., J. STAHL & H. RASK-ANDERSEN. 1977. Tomography in Meniere's disease—why and how. *Adv. Oto-Rhino-Laryngol.* **24**: 71-93.
9. WILBRAND, H. F. 1976. Meniere's disease—roentgenologic diagnosis. *Arch. Oto-Rhino-Laryngol.* **212**: 331-337.
10. WILBRAND, H. F. 1980. Tomography of the temporal bone in patients with Meniere's disease. In *Proceedings, Sixth Shambaugh International Workshop on Otomicrosurgery and Third Shea Fluctuant Hearing Loss Symposium*. Chicago, Ill. (In press.)
11. ARENBERG, I. K., H. RASK-ANDERSEN, H. F. WILBRAND & J. STAHL. 1977. The surgical anatomy of the endolymphatic sac. *Arch. Otolaryngol.* **103**: 1-11.
12. STAHL, J. 1980. Allergic, diuretic and metabolic treatment of fluctuant hearing loss. In *Proceedings, Sixth Shambaugh International Workshop on Otomicrosurgery and Third Shea Fluctuant Hearing Loss Symposium*. Chicago, Ill. (In press.)
13. STAHL, J., C. STAHL & I. K. ARENBERG. 1978. Incidence of Meniere's disease. *Arch. Otolaryngol.* **104**: 99-102.
14. RÄDBERG, C., A. THIBAUT & G. DELVAUX. 1971. Skull radiography with Orbix. Siemens Elema AB. Solna, Sweden.
15. RUNSTRÖM, G. 1933. A roentgenological study of acute and chronic otitis media. *Acta Radiol. Suppl.* **17**: 1-88.
16. DIAMANT, M. 1940. Otitis and pneumatization of the mastoid bone. *Acta Otolaryngol. Suppl.* **41**: 1-149.
17. AUSTIN, D. F. 1980. Use of polytomography in Meniere's disease. *Arch. Otolaryngol.* **106**: 377-382.
18. GANZ, H. & F. VON EICHEL-STREIBER. 1973. Menieresche Erkrankung und Schläfenbeinpneumatisation; planimetrische Untersuchungen. *Arch. Klin. Exp. Ohren Nasen Kehlkopfheilkd.* **205**(2): 171-174.
19. OKU, T., M. HASEGAWA & I. WATANABE. 1980. Meniere's disease and the mastoid pneumatization. *Acta Otolaryngol.* **89**: 118-120.
20. SIEBENMANN, F. 1894. Die Blutgefäße im Labyrinth des menschlichen Ohres. J. F. Berkmann. Wiesbaden, Germany.

21. RASK-ANDERSEN, H. 1979. The vascular supply of the endolymphatic sac. *Acta Otolaryngol.* **88**: 315-327.
22. SANDO, J., T. EGAMI & T. HARADA. 1980. Course and contents of the paravestibular canaliculus. *Ann. Otol. Rhinol. Laryngol.* **89**: 147-156.
23. OGURA, Y. & J. D. CLEMIS. 1971. A study of the gross anatomy of the human vestibular aqueduct. *Ann. Otol. Rhinol. Laryngol.* **80**: 813-825.
24. BAST, T. H. & J. B. ANSON. 1949. *The Temporal Bone and the Ear*. Charles C. Thomas, Publishers. Springfield, Ill.
25. ANSON, J. B. & J. A. DONALDSON. 1973. *Surgical Anatomy of the Temporal Bone and Ear*. 2nd edit. W. B. Saunders Co. Philadelphia, London & Toronto.
26. RASK-ANDERSEN, H. & J. STAHLE. 1980. Immunodefence of the inner ear? Lymphocyte-macrophage interaction in the endolymphatic sac. *Acta Otolaryngol.* **89**: 283-294.
27. EGAMI, T., I. SANDO & F. O. BLACK. 1978. Hypoplasia of the vestibular aqueduct and the endolymphatic sac in endolymphatic hydrops. *Adv. Otorhinolaryngol.* **26**: 339-344.

MICRODISC GEL ELECTROPHORESIS IN SODIUM DODECYL SULFATE OF ORGANIC MATERIAL FROM RAT OTOCONIAL COMPLEXES*

M. D. Ross, K. G. Pote, K. E. Rarey, and L. M. Verma

Department of Anatomy
University of Michigan
Ann Arbor, Michigan 48109

INTRODUCTION

The gravity receptors of all vertebrates utilize a "test mass" consisting of a complex arrangement of mineral and organic substance that lies over the sensory receptor areas (maculas).²³ Carlström has shown that in most vertebrates, the mineral is a polymorph of calcium carbonate (vaterite, aragonite, calcite) in the form of minute, single crystals called otoconia ("ear dust").² The otoconia contain a small amount of organic material that is continuous with intervening and underlying organic substance of the otoconial membrane, the organic and inorganic complements being referred to here collectively as an otoconial complex. In contrast, in certain fishes, a solitary otolith ("ear stone") occurs or mixtures of otoliths and otoconia are present.² The Agnatha, which otherwise lack mineralized tissue, have otoconia that, surprisingly, contain calcium phosphate (amorphous apatite, Reference 2).

In the gravity receptors of man and other warm-blooded animals, only calcite is present and the otoconia have a basically similar morphology regardless of the species studied (FIGURES 1-3). They exhibit the characteristic threefold symmetry of calcite, and the rhombohedron is the basic structural unit. Moreover, the mammalian otoconia have the crystallographic properties of single crystals of calcite including the appropriate Miller indices ($\bar{1}011$) (determined for human otoconia, see Reference 16).^{2,16} Thus, the otoconia of man and other mammals take their shape largely from the mineral they contain rather than from their organic fractions (FIGURE 4), even though both materials may be essential to their existence.

It is unclear why individual crystals of mineral substance occur in an overwhelming number of vertebrate inner ears when other mineral deposits in the body are polycrystalline, or why one polymorph of calcium carbonate is used preferentially instead of another in particular classes of animals. From a chemical viewpoint, however, the fact that calcium ions combine with anions to form a mineral deposit in all normal vertebrate inner ears implies that phylogenetically there was a need to store calcium against periods of short supply. The fact that a well-ordered array of mineral material and organic substance has endured throughout the long evolutionary history of the vertebrate gravity receptors demonstrates that perfection of function was approached by this union. Required ions were stored in their ground-energy state (or entatic state)²¹ through the participation of an appropriate "capture" protein material (see Reference 24). The end result was a reservoir of ions to buffer the surrounding fluid

*This work was conducted with the support of National Aeronautics and Space Administration Grant NSG 9047 and National Institutes of Health Grant AG00767.

(endolymph) against periods of calcium ion deficiency and against shifts in pH while, simultaneously, providing needed mass to make the detection of the direction of gravitational force easier.

This viewpoint of otoconial complexes leads naturally to the question of the chemical nature of the organic material that is found within and outside of the otoconial crystals. Organic substance appears to be essential to calcite seeding and crystal growth of otoconia in the fetus and to the rapid accumulation of calcium ions observed under certain *in vivo* and *in vitro* experimental conditions.^{12,14,17-19,22} New calcite cannot form with the rapidity encountered in these experiments under purely inorganic mechanisms of crystal growth.

Organic substance also apparently protects otoconia against dissolution. Mathematical calculations of coefficients of activities of the ions in artificial endolymph (and perilymph) used in *in vitro* studies have demonstrated that pure calcite would have dissolved in the fluids, but otoconia did not.¹⁷ Little is known with certainty about the chemical nature of the organic material inside and outside otoconia (the material at the two sites may not be identical), except that it is PAS-positive† and that it is, or contains, glycoprotein.²⁵

Detailed chemical analysis of the organic substance would appear to be a formidable task. A pair of saccular complexes of the rat weighs only about 9.5 μg , and a pair of utricular complexes about 14.5 μg .¹⁸ As much of this mass consists of the heavier calcite, it would seem at first glance that the amount of organic material would be too small to allow meaningful analyses, even through heroic efforts of pooling of samples. However, new and extremely sensitive microanalytical methods for separating proteins out of mixtures according to their molecular weights are appearing constantly in the literature, and ever more exquisitely sensitive amino acid analyzers are coming on the market. Thus, analysis of at least the protein constituents of otoconial organic substance appears possible.

In this article we describe some of the results of our efforts to determine the number of proteins in otoconial complexes and their molecular weights using a microdisc gel electrophoresis method presented by Gainer.⁶ Although we began this research by pooling 60 complexes per sample, we have learned that pooling of only 4 to 10 complexes is necessary for a single analysis, and the prospect of analyzing a sample consisting of only one pair of saccular or utricular complexes is bright. The work is, nevertheless, complicated in that several technical modifications, solubility tests, and staining procedures should be employed before results can be considered to be definitive and the proteins can be said to be well characterized. Early indications are, however, that the proteins of saccular and of utricular complexes are identical and that one of the major proteins has a relatively low molecular weight, ~17,000 daltons. This is within the range of molecular weights of other known calcium-binding proteins, such as calmodulin and troponin-C. The exciting possibility exists that this peptide will prove to be the calcium-fixing protein in otoconial complexes.

MATERIAL AND METHODS

Sprague-Dawley rats were used throughout. Except for initial studies in which large numbers of otoconial complexes were pooled (up to 60) from discard rats of various weights, animals 250–325 g have been used. The method of protein separation we have employed routinely is microdisc gel electrophoresis and

†PAS is periodic acid-Schiff.



FIGURE 1. Human utricular otoconia have a configuration typical of mammals (compare with FIGURES 2 and 3). The majority of the otoconia have rounded body surfaces and pointed ends. The three terminal faces are typical of calcite crystals (see FIGURE 4). Organic material is present in the otoconia (not seen) and is continuous with organic substance intervening between the crystals (arrows). A few otoconia in the rhombohedral form occur in human utricular complexes (arrowhead, upper right). $\times 6,630$.



FIGURE 2. Otoconia typical of the monkey utricle are illustrated. Compare with FIGURES 1, 3, and 4. $\times 5,100$.



FIGURE 3. Rat saccular otoconia have slightly more irregular body surfaces than do either monkey or human otoconia, but the basic configuration is the same. Crossed otoconia like the one near the center of the electron micrograph are found in other species and may be a form of crystal twinning. $\times 2,550$.



FIGURE 4. Inorganic calcite sometimes has a configuration similar to that of otoconia, as this photomicrograph demonstrates. This specimen is from a collection at the Department of Geology and Mineralogy, University of Michigan, origin unknown. $\times 2.21$.

Coomassie blue staining of the gels as described by Gainer.⁸ This method is capable of detecting 5×10^{-10} g protein.

Microdissection and Sample Collection

Animals were decapitated, and the bullas were removed quickly to small dishes for microdissection. Initially, microdissections of otoconial complexes were carried out in distilled water (double distilled, deionized) under the assumption that the organic material of the otoconial membrane most likely was insoluble in water. However, all recent experiments have been carried out in artificial endolymph (AE) to better match ionic conditions normally present around the tissues being dissected and to minimize cell lysis and protein contamination of our samples. Artificial endolymph was prepared according to the following formula.^{15,1}

AE: 1.0 mM NaCl; 148 mM KCl; 10 mM KHCO₃;

1 mM MgCl₂; 1.5 mM CaCl₂, pH 7.4-7.8

The tissue was removed to fresh fluid several times as the otoconial complexes were dissected rapidly, and the complexes always were moved to fresh fluid immediately before they were picked up with the aid of a micropipette. This served to wash away possible contaminating proteins. The sample then was placed in a 1.5-ml centrifuge tube with $\sim 3 \mu\text{l}$ of fluid. Saccular and utricular complexes were kept separate. Otoconial complexes from 2-6 animals were pooled, and the supernatant fluid was removed carefully. Otoconial samples were utilized immediately or were stored (covered) at -42°C until used.

EDTA Chelation

Our early work was carried out by collecting 30-60 otoconial samples in small foil cups to which a drop or two of 0.1 M (ethylenedinitrilo)-tetraacetic acid (EDTA) was added. The cups were supported in wells in staining dishes, and chelation was carried out in the cold. The EDTA was withdrawn carefully every other day, and after a week, when it appeared that only a gel-like residue was left, the samples were dried over silica gel. The residue was solubilized in sodium dodecyl sulfate (SDS) and prepared for gel electrophoresis. This method led to some variation in results, and therefore direct solubilization in SDS was attempted (see below). EDTA also has been used in combination with trichloroacetic acid (TCA) for comparison with non-EDTA-treated material, to examine the question of solubility of some otoconial complex protein in EDTA.

Solubilization and Denaturation

Two different methods of denaturation and solubilization have proved successful.

1. The first of these involved direct solubilization and denaturation of the pooled complexes in a mixture of $3 \mu\text{l}$ SDS and $3 \mu\text{l}$ β -mercaptoethanol in an oven at 100°C for three-five minutes. The mixture next was cooled and then doubled with $2\times$ concentrated upper buffer, which contained dithiothreitol and bromo-

phenol blue. Approximately 6 microliters of this fluid served as the sample that was placed on the gel. When saccular and utricular samples were combined for comparison purposes, ~3 μ l of each sample were combined (6 μ l total) for analysis.

2. The second method was more complicated, and some sample loss may have occurred because of the washes involved. Otoconial complexes were dissolved in TCA at 90°C for 15 minutes. The residue was cooled on ice for 5 minutes and then centrifuged in a cold room (Eppendorf centrifuge, ~15,000g force) for about 45 minutes. The supernatant was withdrawn carefully, and the residue was washed twice in cold acetone, with the supernatant carefully wicked away. After the last wash, the residual acetone was evaporated in an oven at 37°C. This left a very small, whitish mass (assumedly protein), which then was solubilized in SDS at 90°C for 5 minutes. The solution was cooled to room temperature, and β -mercaptoethanol was added according to Gainer's recipe. After the volume was doubled with 2 \times concentrated upper buffer, procedures outlined under method 1 were followed.

Gels

The gels were made according to the recipe provided by Gainer except for addition of 0.1% SDS.* The stacking gel in initial studies was 3% polyacrylamide (pH 6.1), and the running gel was 7.5% (pH 9.2). In order to achieve better separation of some of our bands, we recently have used a 3.0% (pH 6.1) stacking gel and a 12.5% (pH 9.2) running gel. The gels were cast in hematocrit tubes 7 cm long and having a uniform internal bore of 1.1 mm.

Conditions of Electrophoresis and Staining

Upper and lower buffers have been prepared following Gainer's methodology. In order to sharpen our bands, we added 1 mM ethyleneglycol-bis-(β -aminoethyl ether) *N,N'*-tetraacetic acid (EGTA) to the upper buffer (the EGTA chelates any calcium ions present). The 7.5% gels were run at constant voltage (120 V) at 5 mA (0.5 mA/gel) in a Model 1400 Ames gel bath with a Miles RP500 power supply. The 12.5% gels were run with a constant current of 0.5 mA/gel, with voltage between 120 and 450.

Routinely, the electrophoresis was continued until the bromophenol blue reached within 1 cm of the bottom of the gels; but on some occasions the electrophoresis was stopped when the tracking dye had traveled only about halfway down the gels. This was done to determine whether one or more peptides were running ahead of the dye. The gels were removed from the tubes and placed in test tubes with 0.25% Coomassie blue stain for 2-16 hours. The gels were destained in a solution of acetic acid and methanol, as described by Gainer.

Standards

Standards were run simultaneously with the unknowns (otoconial complex samples) to make molecular-weight determinations possible. We have employed

Dalton Mark VI, bovine hemoglobin, chymotrypsinogen, β -galactosidase, and lysozyme (obtained from Sigma Chemical Co., St. Louis, Mo., USA).

Molecular-Weight Determination

The gels were read on a Quantimet 720 image-analyzing computer using a software computer program written for the purpose by Thomas J. Williams. Relative mobility of each protein peak was calculated as

$$\text{Relative mobility} = \left(\frac{\text{distance of protein migration}}{\text{length of the running gel after destaining}} \right) \times \left(\frac{\text{length of the running gel before destaining}}{\text{distance of bromophenol blue migration}} \right)$$

A standard curve was obtained by plotting the relative mobilities of the standard proteins against the log of their molecular weights. The molecular weights of the unknown sample proteins were extrapolated from this standard curve.

Scanning Electron Microscopy

Otoconial complexes were exposed to artificial endolymph for 15 or 30 minutes, removed, coated with gold, and examined in a JEOL JSM U-3 scanning electron microscope at 15 kV. This was done to determine the effect (if any) of the fluid on otoconial complex integrity and to ascertain the relative cleanness of the samples we were analyzing.

RESULTS

The initial electrophoretic results obtained with residues derived through chelation of otoconial complexes prior to solubilization and denaturation in SDS- β -mercaptoethanol were encouraging because bands of protein separated out on the gels and their molecular weights could be assessed on the basis of the weights of the standards run simultaneously. The range of molecular weights of the bands produced usually was similar (~15,000 to ~55,000 daltons) from one experiment to another, but the number of bands often was different. These experiments indicated either that the chelation process had some unknown effect on the proteins or that (more likely) withdrawal of the supernatant fluid, which was changed periodically, resulted in loss of soluble proteins.

Direct solubilization in SDS yielded more promising results. Two major protein bands were evident in both saccular and utricular complexes by this method. The lower-molecular-weight material was in the range of 16,800–18,000 daltons, and the higher-molecular-weight protein was ~51,000 daltons. Several minor bands were present in between the major bands but often were not identical from one trial to the next. During the period when these experiments were conducted, using the combination of 3% and 7.5% gels, we learned that as few as four pooled complexes provided sufficient protein to serve as samples for two gels. We also began to carry out microdissections in artificial endolymph, and scanning electron microscopy of otoconial complexes prepared in this fluid

demonstrated that the complexes were in superior condition even after one-half hour or more exposure to the fluid (FIGURE 5). Such periods of time are far in excess of those required for microdissection of our samples (5-10 minutes).

In order to determine if low-molecular-weight peptides were running ahead of the bromophenol blue, the electrophoresis sometimes was terminated when the dye had reached the midpoint of the gels. Subsequent staining of the gels failed to demonstrate the presence of bands below the tracking dye.

The matter of variability in minor protein bands observed from one experiment to the next had to be resolved. We therefore attempted to obtain a more pure protein sample by employing the TCA method of protein precipitation. The precipitate produced always was exceedingly small and was lost completely on

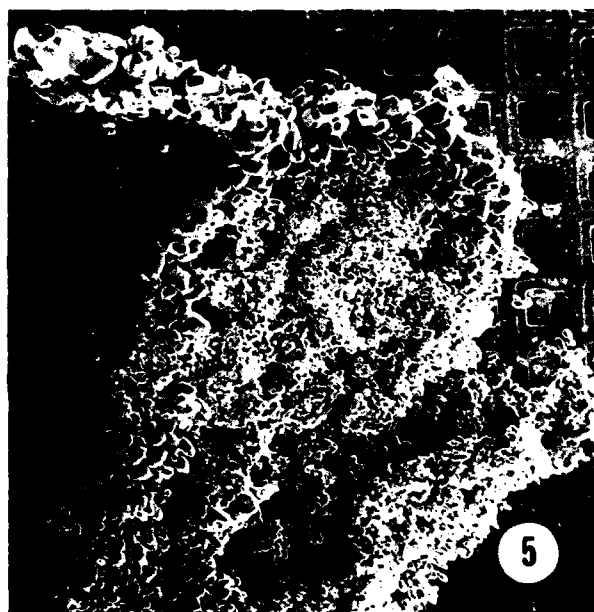


FIGURE 5. The typical appearance of a utricular otoconial complex microdissected in artificial endolymph is demonstrated here. The sample is free of debris, and otoconial integrity has been maintained. This complex was exposed to artificial endolymph for 30 minutes, but collection of the sample ordinarily requires only 5-10 minutes. $\times 100$.

more than one occasion during the washing procedures when the sample inadvertently was wicked away with the acetone wash. Nevertheless, several experiments were successful and provided further evidence that there were two major proteins in the organic substance in the saccular and utricular complexes. The proteins apparently were identical, for the two kinds of complexes and their molecular weights corresponded in general to those observed in our previous experiments. Minor bands still differed in number and in molecular weight from one experiment to the next. The problem of possible loss of some protein during the TCA preparative procedures became worrisome.

In order to avoid this possibility, direct solubilization and denaturation in SDS and β -mercaptoethanol were reinstated. In addition, the running gel concentra-

tion was increased to 12.5%. This was done to slow the migration of the lower-molecular-weight peptides. The results of experiments run under these conditions were consistent from one day to the next. The bands were sharply defined in the gels, and the pattern of banding appeared to be identical for both major and minor bands of the complexes (FIGURE 6).

Several major protein bands were apparent in gels run under these improved experimental conditions. Two of the most prominent occurred at ~16,500 and

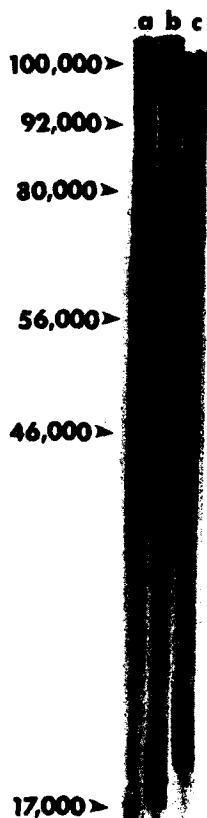


FIGURE 6. A typical set of 12.5% gels containing proteins obtained from saccular (a), combined saccular and utricular (b), and utricular (c) complexes is illustrated here. The apparent molecular weights are indicated to the left of the figure and are the same for each sample, based on calculations of the relative mobilities of the proteins compared to standards, with the distance of the bands from the tracking dye taken into account.

~46,000 daltons, and further significant proteins were at ~56,000, ~80,000, and >100,000 molecular weight (MW). Several minor bands were present between 56,000 and 80,000 daltons. It was noteworthy that the protein banding pattern of the combined utricular and saccular proteins was identical to the patterns observed in either single sample (FIGURE 6).

DISCUSSION

The most important finding of this research is that analysis of the proteins of the organic material of the otoconial complexes is possible when sensitive microanalytical methods are employed. The present research has taken only the first step in this direction, but further modification of the basic technique used here and inclusion of other sensitive staining methods should mean that, in the future, protein separation by molecular weight will be possible in sample pools containing only two otoconial masses. This would make the analysis of normal and defective or nonmineralized human otoconial complexes practical, permitting us to ascertain whether one or more proteins are missing in abnormal complexes.

On the basis of our present results, it appears that the proteins present in saccular and utricular otoconial complexes are identical. This is a matter of some importance to determine, because previous investigations have shown that saccular otoconia are more prone than the utricular to degenerate with age and disease, or after administration of certain drugs.^{7-9,11,16} It was demonstrated also that *in vivo* uptake and/or exchange of $^{45}\text{Ca}^{++}$ occurs more rapidly and in greater quantities in saccular otoconia.¹⁸ These findings could indicate that some inherent chemical and structural difference existed between otoconia from the two sites, but our results indicate that some other explanation must be sought.

It is of interest that a major protein band in the range of ~17,000 daltons separated out consistently in the gels. This apparent molecular weight is within the range of other known calcium-fixing proteins. For example, the MW of calmodulin has been reported to be ~15,000-19,000 daltons under various experimental conditions, and 16,790 MW by amino acid sequencing.¹⁰ Troponin-C has a calculated MW of 17,846 and has been reported to weigh between ~17,000 and 22,000 when differing analytical methods were employed.³ It is possible that the low-molecular-weight protein we have identified in otoconial complexes is an analogous calcium-binding agent, especially in light of the fact that the calcium-fixing proteins show remarkable stability in evolution with respect to their amino acid content and sequencing.

In this same context it is relevant to note that Degens and his colleagues found that the protein of fish otolith, which they named otolin, is a highly acidic, fibrous protein with a molecular weight of >150,000.^{4,5} Cleavage with urea/hydroxylamine produced units of ~70,000-80,000 MW. Fish otoliths contain the aragonite polymorph of calcium carbonate. In the case of mollusc shells containing the calcite polymorph, cleavage with hydroxylamine yielded proteins ranging between 20,000 and 80,000 daltons.⁴ The range in otoconial complex protein material is ~17,000 to >100,000. Further tests and the use of additional standard will be required to define the upper limit of the high-molecular-weight proteins present. It is worthwhile emphasizing, however, that the molecular weights of the proteins of fish otoliths, mollusc shells, and otoconial complexes, insofar as these have been determined, are more alike than dissimilar even though different methods of protein analysis were used. The extent of agreement is remarkable considering that the biosystems investigated had little more in common than their

ability to store a polymorph of calcium carbonate. On the other hand, the organic material of the otoconial complexes seems to be entirely different from that of a related inner ear membrane, the tectorial. Steel carried out SDS gel electrophoresis of the tectorial membranes of normal and abnormal mice and found (in both cases) a range of ~62,000-180,000 MW, with a major band at 140,000 daltons.²⁰

It is important to note that Degens reported that water-soluble proteins account for between 0.1 and 2% of the total organic material in shells. Meenakshi *et al.* discussed their own findings as well as those of other investigators, which indicate that it is the intracrystalline part of shell protein that is particularly water- and EDTA-soluble.¹³ Thus, pretreatment with EDTA, such as we carried out in our first experiments, is to be avoided unless the purpose is to analyze the fluid for soluble proteins. We have not yet fully characterized the EDTA-soluble (or water-soluble) protein(s) of otoconial complexes.

The reliability of the findings we have made in these initial studies will depend upon the cleanness of the samples we have analyzed. Scanning electron microscopy of some of the samples that we have microdissected demonstrates that our specimens are free of debris (FIGURE 5). It is impossible to know that every sample is equally clean, however. The reproducibility of protein banding from one experiment to another under our improved experimental conditions leads us to believe that contamination is not a significant factor in our results. However, further experiments in which otoconia are separated from otoconial membrane material by centrifugation or sedimentation procedures, then washed and analyzed, will be required before this question can be answered entirely.

ACKNOWLEDGMENTS

We thank Dr. Babu Vadlamudi and Mr. Charles Daniels of the Department of Biological Chemistry for their technical assistance during this research, and Dr. Dale Oxender of the Department of Biological Chemistry for use of equipment essential to the investigation.

REFERENCES

1. BOSHER, S. K. & R. L. WARREN. 1978. Very low calcium content of cochlear endolymph, an extracellular fluid. *Nature* **273**: 377-378.
2. CARLSTRÖM, D. 1963. A crystallographic study of vertebrate otoliths. *Biol. Bull.* **125**: 441-463.
3. COLLINS, J. H., J. D. POTTER, M. J. HORN, G. WILSHIRE & N. JACKMAN. 1973. The amino acid sequence of rabbit skeletal muscle troponin-C: gene replication and homology with calcium-binding proteins from carp and hake muscle. *FEBS Lett.* **36**: 268-272.
4. DEGENS, E. T. 1976. Molecular mechanisms on carbonate, phosphate, and silica deposition in the living cell. *Top. Curr. Chem.* **64**: 1-112.
5. DEGENS, E. T., W. G. DEUSER & R. L. HAEDRICH. 1969. Molecular structure and composition of fish otoliths. *Marine Biol.* **2**: 105-113.
6. GAINER, H. 1971. Micro disc electrophoresis in sodium dodecyl sulfate. An application to the study of protein synthesis in individual identified neurons. *Anal. Biochem.* **44**: 589-605.
7. HARADA, Y. & Y. SUGIOMOTO. 1977. Metabolic disorder of otoconia after streptomycin intoxication. *Acta Otolaryngol.* **84**: 65-71.
8. JOHNSON, L.-G. 1971. Degenerative changes and anomalies of the vestibular system in man. *Laryngoscope* **81**: 1682-1694.

9. JOHANSSON, L.-G. & J. E. HAWKINS, JR. 1972. Sensory and neural degeneration with aging, as seen in microdissections of the human inner ear. *Ann. Otol.* **81**: 179-193.
10. KLEE, C. B., T. H. CROUCH & P. G. RICHMAN. 1980. Calmodulin. *Ann. Rev. Biochem.* **49**: 489-515.
11. LIM, D. J. 1973. Formation and fate of the otoconia. *Ann. Otol. Rhinol. Laryngol.* **82**: 23-35.
12. LYON, M. F. 1955. The development of the otoliths of the mouse. *J. Embryol. Exp. Morphol.* **3**: 213-229.
13. MEENAKSHI, V. T., P. E. HARE & K. M. WILBUR. 1971. Amino acids of the organic matrix of neogastropod shells. *Comp. Biochem. Physiol.* **40B**: 1037-1043.
14. NAKAHARA, H. & G. BEVELANDER. 1979. An electron microscope study of crystal calcium carbonate formation in the mouse otolith. *Anat. Rec.* **193**: 233-241.
15. RAUCH, S. 1964. *Biochemie des Hörorgans*. Georg Thieme Verlag. Stuttgart, Federal Republic of Germany.
16. ROSS, M. D., L.-G. JOHANSSON, D. PEACOR & L. ALLARD. 1976. Observations on normal and degenerating human otoconia. *Ann. Otol.* **85**: 310-326.
17. ROSS, M. D., K. G. POTE, P. L. CLOKE & C. CORSON. 1980. In vitro $^{45}\text{Ca}^{++}$ uptake and exchange by otoconial complexes in high and low K^+/Na^+ fluids. *The Physiologist* **23**: S129-S130.
18. ROSS, M. D. & T. J. WILLIAMS. 1979. Otoconial complexes as ion reservoirs in endolymph. *The Physiologist* **22**: S63-S64.
19. SALAMAT, M. S., M. D. ROSS & D. R. PEACOR. 1980. Otoconial formation in the fetal rat. *Ann. Otol.* **89**: 229-238.
20. STEEL, K. 1980. The proteins of normal and abnormal tectorial membranes. *Acta Otolaryngol.* **89**: 27-32.
21. VALLEE, B. L. & R. J. P. WILLIAMS. 1968. Metalloenzymes: the entatic nature of their active sites. *Proc. Nat. Acad. Sci.* **59**: 498-505.
22. VEENHOF, V. B. 1969. The development of statoconia in mice. Thesis. University of Amsterdam. Amsterdam, the Netherlands.
23. VINNIKOV, YA. A. 1974. Evolution of the gravity receptor. *Minerva Otorinolaringol.* **24**: 1-48.
24. WILLIAMS, R. J. P. 1979. Inorganic elements in biology and medicine. *Chem. Br.* **15**: 506-512.
25. WISLOCKI, G. B. & A. J. LADMAN. 1955. Selective and histochemical staining of the otolithic membranes, cupulae and tectorial membrane of the inner ear. *J. Anat.* **89**: 3-12.

MÉNIÈRE'S DISEASE: ENDOLYMPHATIC SAC
DECOMPRESSION COMPARED WITH SHAM (PLACEBO)
DECOMPRESSION

J. Thomsen,* P. Bretlau, M. Tos, and N. J. Johnsen*

*University Ear, Nose, and Throat Department
Gentofte Hospital
DK-2900 Hellerup, Denmark*

and

*University Ear, Nose, and Throat Department
Rigshospitalet
DK-2100 Copenhagen, Denmark*

Since the establishment of an ear, nose, and throat (ENT) department in 1910, affiliated with the University of Copenhagen, there has been a tradition of treating patients with Ménière's disease at the university department. In the beginning, both mild and severe cases were treated; but after the establishment of several other ENT departments in Denmark, and the increase in the number of otologists in private practice, only the very severe cases were referred to the university ENT departments. These were patients who had been given up on by private otologists as well as by provincial ENT departments and who were referred to the university departments as a last resort.

Based on the personal experiences of Dida Dederding, an otologist suffering from Ménière's disease herself, Mygind and Dederding put forward the hypothesis that Ménière's disease is caused by a hydroelectrolytic disturbance of the inner ear.^{1,2} They demonstrated the possibility of aggravating the cochlear/ vestibular symptoms with water load and of alleviating the symptoms with water and salt restrictions. This also added to the referral of "impossible" Ménière patients.

Because of an urgent need for satisfactory means of treatment, we began in 1970 out of sheer desperation, though based on some pathophysiological thinking, to treat patients with Ménière's disease with lithium carbonate. It was believed that lithium had the property of influencing the transport of water and ions into and out of special biological compartments, such as the endolymphatic space.

It was shown in an open study that in 70%, the effect of treatment with lithium was excellent, as judged by the patients' own statements concerning the reduction in frequency and severity of the attacks. Although a placebo effect could not be ruled out in this open trial, the high (70%) and persistent (17 months) effect did justify continued investigations on the effect of lithium on Ménière's disease.

In two subsequent, controlled series of investigations on the effect of lithium upon the symptoms in Ménière's disease, however, it was demonstrated that the effect of lithium could be maintained at 70% but that the effect of a placebo equaled the effect of the active medication.^{3,4}

*At the time this research was begun, Drs. Thomsen and Johnsen were affiliated with Rigshospitalet. Gentofte Hospital is the current affiliation of all authors. Both hospitals are part of the University of Copenhagen.

In an evaluation of the glycerol test, which has been used by some authors to select patients suitable for endolymphatic shunt surgery, it was demonstrated that evaluation of the results is difficult and the value of the test questionable, but at the same time it was demonstrated that patients with Ménière's disease were indeed very good placebo responders.^{5,6}

In a review of the world literature on Ménière's disease, Torok found that almost without exception, advocates of either medical or surgical treatment claimed success in 60-80% of patients.⁷ Torok indicated that because so many diverse therapies were proclaimed to be successful, it would seem appropriate to consider the influence of some factor common to all, i.e., the placebo effect.⁷

This idea is very similar to our concept of the treatment of Ménière's disease, and we agreed to the idea put forward by Shambaugh that Ménière's disease might call for a controlled double-blind study on the effect of surgery.⁸ The present study report is such a controlled study of the effect of an endolymphatic sac shunt operation (Silastic sheet mastoid shunt) versus the effect of a placebo operation (regular mastoidectomy).

METHOD

In order to participate in the trial, the patients had to fulfill the following criteria: presence of typical attacks of fluctuating hearing loss, tinnitus, and vertigo; often accompanied by nausea, vomiting, and pressure in the ear; with at least one attack every two weeks; a history not less than six months but no longer than five years; normal renal, cardiac, and thyroid function; and no obvious allergies. The patients had to be considered psychologically normal and willing to participate in the trial for the entire 12 months. Furthermore, they were examined in detail to exclude tumors or other pathology of the cerebellopontine angle.

During a period of three months before surgery, the patients filled in a dizziness questionnaire daily while continuing the medical treatment initiated by their own otologist, in order to ensure a reasonable number of attacks to allow a statistical evaluation and to exclude placebo responders in the pretest evaluation.

Patients were informed that they would participate in a trial testing the efficacy of two different surgical procedures for the treatment of their disease. They were not informed that half of the patients would be submitted to a purely placebo operation. The patients were assigned randomly for each treatment group.

The active treatment consisted of a regular endolymphatic sac shunt operation with insertion of Silastic into the sac, draining out into the mastoid cavity.

The placebo treatment consisted of a regular mastoidectomy, at which much care was taken not to remove the bone over the endolymphatic sac, in order to avoid a decompression.

The patients were operated on in two university ENT departments in Copenhagen, the Rigshospital and Gentofte hospital, and the patients operated on at the Rigshospital were controlled every month at Gentofte hospital and vice versa in order to deprive the investigator of any information about the operative procedure employed. A standardized operation description was written in the patients' charts in order to deprive the nursing staff at the hospital of information on the character of the operation. Each day all the patients filled in the dizziness questionnaire, stating the frequency of attacks as well as the duration and

severity of individual attacks. All symptoms within the Ménière syndrome (hearing loss, tinnitus, dizziness, nausea, vomiting, pressure in the ears) were recorded, and the patients classified their symptoms according to a 0-3 scale.

Each month the investigators evaluated the patients' present state of disease by giving scores from 0-10 depending on the severity of the disease. After termination of the 12-month trial period, the investigators evaluated the overall effect of the operation on each patient, and the patients also were asked to give their opinion about the effect of the operation. In addition, pure-tone audiograms were taken. The pre- and postoperative results were classified according to the American Academy of Ophthalmology and Otolaryngology (AAOO) classification.⁹ A thorough statistical analysis of the median values of the patients' total scores for all five parameters was carried out using the Mann-Whitney U test, the Friedmann test, and the Kolmogorov-Smirnov two-sample test. The postoperative follow-up was 100%. All patients were followed monthly for a minimum of 12 months, and the code was broken 12 months after operation on the last patients.

PATIENTS

Thirty patients with typical Ménière's disease were selected for surgery because of unsuccessful medical treatment. No patient fulfilling the criteria refused to participate in the trial. Fifteen patients received the active operation, and 15 the placebo operation. Six patients in each group were females, 9 were males. In the active group, the age ranged from 25 to 63 years, an average of 49.9; in the placebo group, the average age was 53.9 years, ranging from 28 to 69 years.

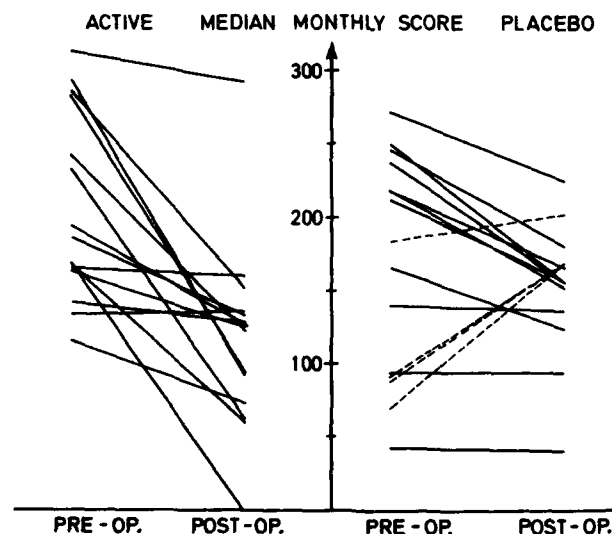


FIGURE 1. Total pre- and postoperative scores in both groups for all parameters. Broken lines indicate patients with higher scores postoperatively compared with preoperatively. No significant difference between active and placebo.

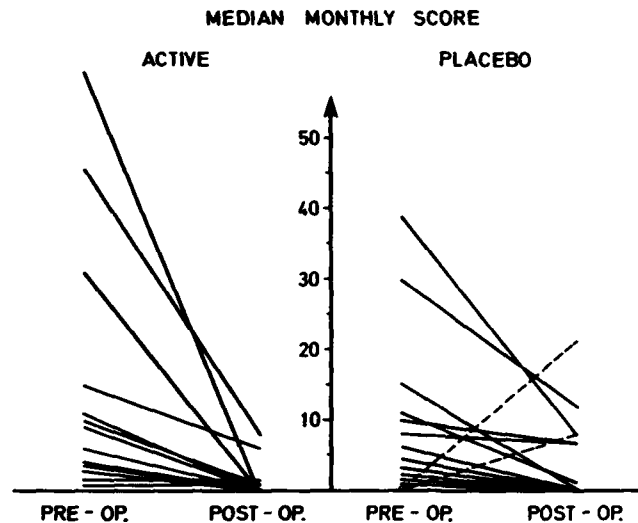


FIGURE 2. Pre- and postoperative scores for nausea and vomiting. Broken lines indicate patients with higher scores postoperatively. No significant difference between active and placebo.

In 5 patients (16.6%), Ménière's disease was bilateral—2 in the active group and 3 in the placebo group.

Medians of total scores for *all parameters* added together are shown for both the active and the placebo group in FIGURE 1. There was a significant ($p < 0.01$) lower score postoperatively compared with preoperatively for both groups, while no significant difference could be demonstrated between the two groups. All patients in the active group had lower scores postoperatively compared with preoperatively, while four patients in the placebo group had higher scores postoperatively. However, as will be seen below, this was due to a high score for hearing loss and tinnitus. The total score therefore must be broken down into the individual scores for nausea and vomiting, vertigo or dizziness, pressure in the ear, tinnitus, and subjective hearing impairment.

For *nausea and vomiting*, both groups scored lower postoperatively compared with preoperatively ($p < 0.01$) while no significant difference could be registered between the active and the placebo group. It is seen that in the active group, all patients had lower scores after the operation, while 13 out of 15 patients in the placebo group had lower scores postoperatively. This difference is not significant (FIGURE 2).

For the parameter *dizziness or vertigo*, the same pattern appears (FIGURE 3). For both groups, a significant ($p < 0.01$) reduction in the scores is registered after the operation, but also a slightly significantly ($p < 0.05$) higher score postoperatively in the placebo group compared with the active group. This higher score is due to only two patients (the same two patients who scored high with regard to vomiting); but if this is looked upon as a reduction of the scores in all patients in the active group and 13 out of 15 in the placebo group, this statistical difference disappears.

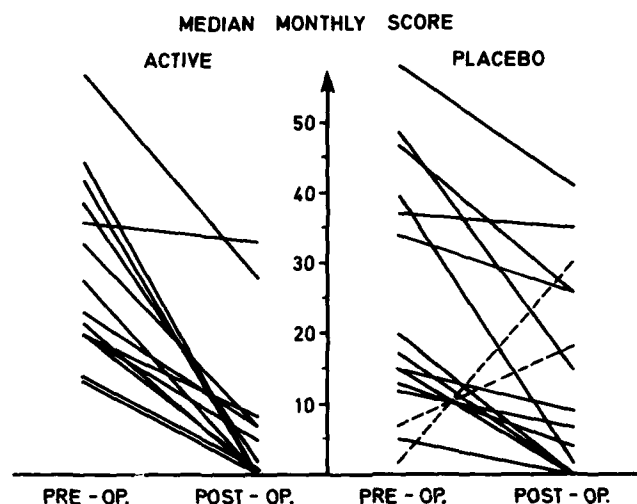


FIGURE 3. Pre- and postoperative scores for dizziness and vertigo. Broken lines indicate patients with higher scores postoperatively. Slightly significantly ($p < 0.05$) lower scores in the active group compared with the placebo group.

Concerning tinnitus and subjective hearing impairment, no difference could be demonstrated between the active and placebo groups.

With regard to pressure in the ear (FIGURE 4), both groups had a significant ($p < 0.01$) reduction in the scores, but no difference could be demonstrated between the two groups.

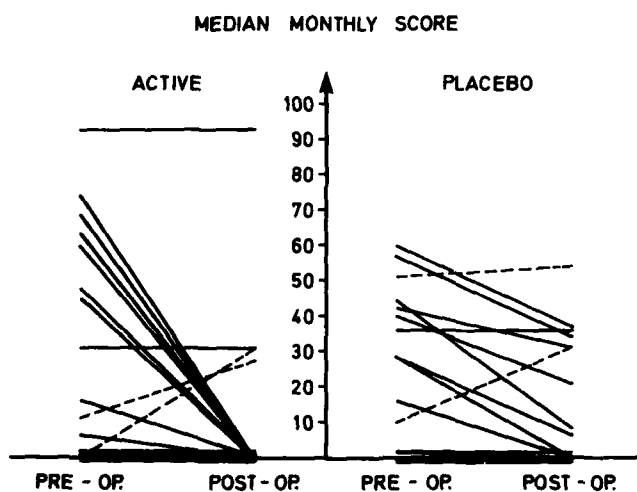


FIGURE 4. Pre- and postoperative scores for pressure in the ear. Broken lines indicate patients with higher scores postoperatively. No significant difference between active and placebo.

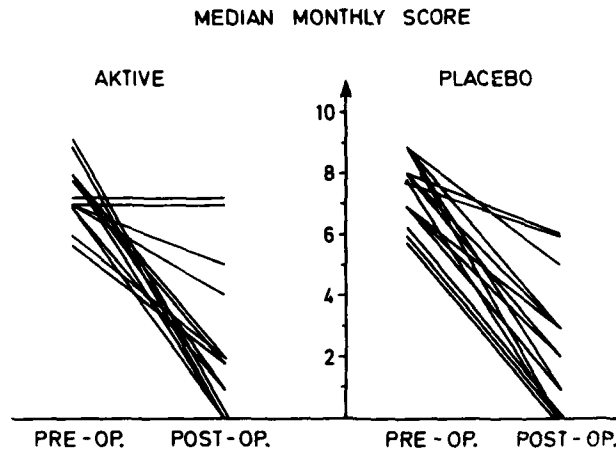


FIGURE 5. Pre- and postoperative values for the investigators' global scores. No significant differences between active and placebo, but a highly significant ($p < 0.005$) reduction in scores postoperatively for both groups.

Each month the investigators had given a global score for each patient's present state of disease. The median monthly score for both the active and the placebo group showed a highly significant reduction postoperatively compared with preoperatively ($p < 0.005$), while no differences could be demonstrated between the active and the placebo group (FIGURE 5).

At the termination of the trial, the investigators attempted—based on conversations with the patients—to assess the total value of the operation for each patient. The physician judged the operation to be very beneficial to 73% of the patients in the active group and 80% in the placebo group; fairly beneficial to 14.5% in the active group and 20% in the placebo group; while 2 patients (13.5%) in the active group were evaluated as having had no effect from surgery. There thus was no difference between the two groups in the evaluation by the investigators at a time when they were unaware of which group the patients belonged to.

TABLE 1
CLASSIFICATION OF TEST PARAMETERS

AAOO Class	Treatment			
	Active		Placebo	
	n	%	n	%
A	1	7	1	7
B	12	80*	6	40*
C	0	0	4	20
D	2	13*	5	33*
Total	15	100	15	100

*Chi² test, not significant.

At the termination of the 12-month observation period, each patient had a pure-tone audiogram taken; the average mean values for 250, 500, and 1,000 Hz showed no difference between the active and the placebo group.

The various subjective and objective parameters were classified according to the AAOO posttreatment reporting criteria, and the results are shown in TABLE 1. There was a larger number of patients in the active group belonging to class A and B compared with the placebo group, but this difference is not significant. If class C is also included in the success group (since this class includes patients with absence of definitive attacks but deterioration of hearing), the tendency toward a better result disappears in the actively operated patients.

At the final visit, the patients were asked whether they thought the operation had been of benefit to them. As shown in TABLE 2, 73% in the active group and 67% in the placebo group found the value of the operation was good. Three patients in the active group (20%) and five patients (33%) in the placebo group thought the result was reasonable, and only one patient indicated that the operation had no effect whatsoever; this patient belonged to the actively operated group. Thus, regarding the patients' opinion of the value of the operation, there was no significant difference between the active endolymphatic shunt operation and the placebo operation.

DISCUSSION

Clinical and laboratory studies indicate that Ménière's disease is the clinical manifestation of inner ear changes caused by dysfunction of the endolymphatic sac.¹⁰ This dysfunction is believed to cause a progressive accumulation of endolymph, which in turn results in distension, herniation, and ruptures of the endolymphatic system. Dida Dederding, who suffered from all the symptoms included in the Ménière's complex, died in 1955 and donated her temporal bone to the otopathological laboratory at the Rigshospital. Her right temporal bone is shown in FIGURE 6, and it did indeed display a severe hydrops. However, the fact that the histological features of hydrops are present in a multitude of conditions indicates that these features do not represent a specific pathological picture of any particular disease—Ménière's disease being no exception. It is possible, and even plausible, that this is the way in which the inner ear reacts nonspecifically to various pathological conditions.¹¹ It also is possible that hydrops manifests itself as a postmortem change, i.e., a histological artefact.¹² Kimura concluded that hydrops can develop from almost any kind of insult or injury to the ear.¹³

Jongkees, citing Hymans van den Bergh, states that the existence of a

TABLE 2
PATIENTS' EVALUATION OF THE VALUE OF THE OPERATION

Operation	Good		Reasonable		Poor		Total	
	n	%	n	%	n	%	n	%
Active	11	73	3	20	1	7	15	100
Placebo	10	67	5	33	0	0	15	100
Total	21		8		1		30	

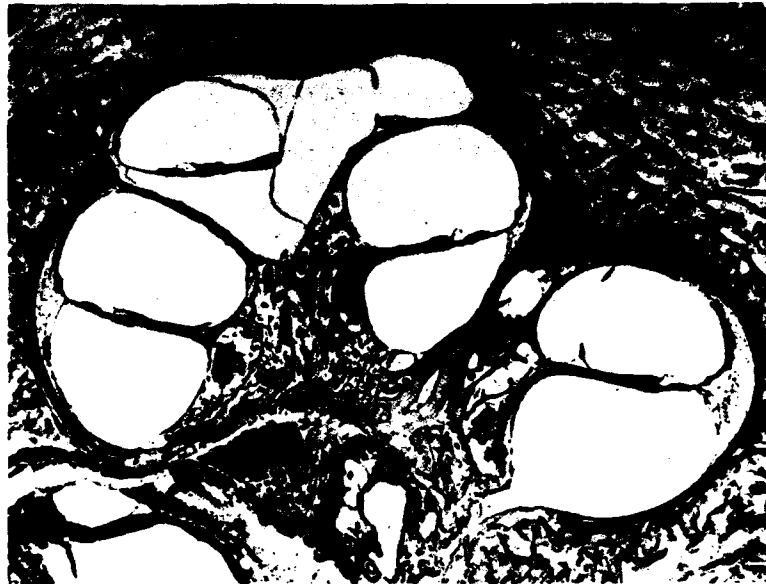


FIGURE 6. The right temporal bone of Dida Dederding, showing severe hydrops in all coils of the cochlea.

multitude of therapies—with enthusiastic defenders of their efficacy—is the best proof of the lack of good therapy.¹⁴ Since the original description by Prosper Ménière, dozens of treatments have been proposed to cure, control, or alleviate Ménière's disease. Some of these have been popular for a short time, others for longer periods, but none has withstood the test of time. Exclusive of symptomatic treatment of vertigo, most medical therapies have no logical therapeutic basis. All treatments having an assumed palliative or curative effect are based on some notion of etiology, among which are metabolic disorders, sympathetic vasomotor disturbances, endocrine diseases, allergies, avitaminoses, and psychogenic problems.

In general, the explanations as to how these conditions affect inner ear physiology are hypothetical and lack supporting data.¹⁰

With regard to surgical procedures for treatment of Ménière's disease, it remains to be shown that it is the specific surgical procedure of whatever kind that is responsible for the claimed effect on the symptoms, and not just a mere unspecific influence on the inner ear or even a placebo effect.

In the present study, we have demonstrated that a purely placebo operation (a mastoidectomy) is as effective to all symptoms in Ménière's disease as is an active regular endolymphatic shunt operation. Minor differences could be demonstrated, but the major difference in symptoms was between pre- and postoperative symptoms rather than between postoperative symptoms in the active compared with the placebo group. This alleviation of the symptoms was especially pronounced with regard to nausea, vomiting, and dizzy spells. Our results with the placebo operation are as good as those obtained by Brackmann and Anderson with the shunt procedure.⁵ Also with regard to classification

according to AAOO, the results are similar: in our series of placebo operations, 33% were classified as failures (class D) compared with 29% in the series of Brackmann and Anderson.¹⁵

When the investigator was unaware of the surgical procedure performed on the patient, his evaluation was as good in the placebo group as in the active group, 80% compared with 73%. The patients themselves made similar evaluations.

Brackmann and Anderson have related their postoperative results to various parameters.¹⁵ They found that neither preoperative hearing level, preoperative vestibular function, nor duration of symptoms and age at surgery had any influence on the postoperative results. The results in cases of fair flow and fair or poor sac were comparable with results in cases in which these factors were judged to be good. Others, e.g., Schindler,¹⁶ have reported a poor correlation between the surgeon's ability to identify the sac and its actual presence in histological material. Plantenga and Browning noted that in 80% of their samples, the sac "was not a sac or baglike structure."¹⁷ In temporal bones with idiopathic endolymphatic hydrops, their Ménière cases showed no objective pathological features in the endolymphatic sac, or in the vestibular aqueduct when compared with normals.

We therefore are of the opinion that the impact of surgery upon the symptoms of Ménière's disease is completely unspecific and unrelated to the actual shunt procedure. We furthermore believe that our success is based mainly on a pure placebo effect obtained through the surgical procedure and quite similar to the effect previously obtained by giving the patients placebo tablets.⁴

In dealing with a disease or a syndrome like Ménière's disease with its fluctuations in intensity of symptoms, spontaneous remission of symptoms, etc., open, uncontrolled studies are without any value in testing a treatment modality, be it medical or surgical. The investigation must be conducted double blindly (i.e., both investigator and patient are ignorant of which group the patient belongs to). Probably, the bias effect of the investigator on the patient is particularly pronounced in the dizzy patient. The double-blind technique therefore is an absolute necessity in such investigations, and any leak in the blind must be considered disastrous. This was the reason why we gave a standardized description of the operation in the charts irregardless of the operative procedure. It served to deprive the nursing personnel of information about the procedure and prevented them from dropping hints, knowingly or unknowingly, about the type of operation the patient had undergone.

The conducting of a double-blind trial raises many ethical questions. While it is accepted that controlled studies may be feasible in medicine (e.g., comparing results from experimental drugs and placebos), they are "impossible" in surgery. Some surgeons even have argued that it is unethical to withhold a treatment one believes to be beneficial even though it has not yet been proven. On the other hand, it can of course be argued that it is unethical not to perform these studies before a large number of people are subjected to a procedure that might be proven to be of no value. It even has been suggested that there should be a surgical equivalent of the Food and Drug Administration to scientifically test new surgical procedures before they are used widely.¹⁸

Another question is how to design future trials, and in what way and to what extent the patients should be informed about the trial. To compare a surgical treatment with a simultaneous medical treatment of a controlled group might result in a higher success rate in the group exposed to surgery, but it actually tells nothing about the mechanism behind the efficacy, and it only may be an

indication that surgery is a better placebo treatment than is medical treatment; such trials will therefore be of no value.

A trial exposing one group of patients to surgery and keeping a similar group, maybe randomly, on the waiting list for surgery gives rise to the same dilemma when evaluating the results. In all probability, the outcome will be in favor of surgery, because of the strain and dissatisfaction involved in waiting for a treatment that might relieve unpleasant symptoms. Double-blind prospective studies are the only trials that may give some information about the efficacy of the surgical procedure. But here the patient's knowledge about the procedure plays an important part. If the patients are informed that they may be subjected to a purely placebo operation, many patients will withdraw from the trial, leaving a selected control group and a test result that no longer would be representative of the remainder of the patients suffering from the same complaints. Furthermore, knowledge of the possibility of having a purely placebo operation probably reduces the efficacy also in the actively treated group, and the outcome of the trial will be equivocal. These were some of the considerations behind our decision not to tell the patients that they might receive a purely placebo operation, but merely that we were testing two different, but probably equally effective, operations.

Our investigations were initiated before the Helsinki Declaration on Medical Ethics was made effective in Denmark, and they therefore were not subject to the demand of full patient information and informed consent on the part of the patient. We believe that the Helsinki Declaration in the future, unfortunately, will prevent us from performing similar studies.

SUMMARY

The placebo effect in surgery for Ménière's disease was investigated in a double-blind, controlled surgery by comparing the effect of a regular endolymphatic shunt with the effect of a purely placebo operation (regular mastoidectomy).

Thirty patients with typical Ménière's disease participated in the study. They were selected for surgery because of unsuccessful medical treatment and were chosen randomly for each treatment group. The patients filled in daily dizziness questionnaires for 3 months before and 12 months after surgery, registering nausea, vomiting, vertigo, tinnitus, hearing impairment, and pressure in the ears.

The patients were operated on in two university ENT departments. Those operated on in one department were controlled each month at the other department, and vice versa. At the termination of the trial, the investigators as well as the patients gave their overall opinion of the efficacy of the operation.

Minor differences could be demonstrated between the active and the placebo group, but the greatest difference in symptoms was found when comparing pre- and postoperative scores, in which both groups improved significantly.

REFERENCES

1. MYGIND, S. H. & D. DEDERDING. 1932. The significance of water metabolism in general pathology as demonstrated by experiments on the ear. *Acta Oto-Laryngol.* 17: 424-458.
2. MYGIND, S. H. & D. DEDERDING. 1938. Clinical experiments with reference to the

- influence of the water metabolism on the ear. *Ann. Otol. Rhinol. Laryngol.* **47**: 360-369.
3. THOMSEN, J., P. BECH, A. GEISLER, S. PRYTZ, O. J. RAFAELSEN, P. VENDBORG & K. ZILSTORFF. 1976. Lithium treatment of Ménière's disease. *Acta Oto-Laryngol.* **82**: 294-296.
 4. THOMSEN, J., P. BECH, S. PRYTZ, P. VENDBORG & K. ZILSTORFF. 1979. Ménière's disease: lithium treatment (demonstration of placebo-effect in a double-blind cross-over trial). *Clin. Otolaryngol.* **4**: 119-123.
 5. THOMSEN, J. & S. VESTERHAUGE. 1979. A critical evaluation of the glycerol test in Ménière's disease. *J. Otolaryngol.* **8**: 145-150.
 6. ARENBERG, I. K. & G. J. SPECTOR. 1977. Endolymphatic sac surgery for conservation of hearing. *Arch. Otolaryngol.* **103**: 268-270.
 7. TOROK, N. 1977. Old and new in Ménière's disease. *Laryngoscope* **87**: 1870-1877.
 8. SHAMBAUGH, G. E. 1964. Double-blind surgery. *Arch. Otolaryngol.* **79**: 435-436.
 9. ALFORD, B. R. 1972. Ménière's disease: criteria for diagnosis and evaluation of therapy for reporting. *Trans. Am. Acad. Ophthalmol. Otolaryngol.* **76**: 1462.
 10. SCHUKNECHT, H. F. 1978. A critical evaluation of treatments for Meniere's disease. *JCEORL & Allergy* **38**: 15-30.
 11. SADÉ, J. 1981. Menière's disease. *J. Laryngol.* **95**: 261-271.
 12. KELEMAN, G. 1980. Personal communication to J. Sadé. (As cited in Reference 11.)
 13. KIMURA, R. S. 1976. Experimental pathogenesis of hydrops. *Arch. Otol. Rhinol. Laryngol.* **212**: 263-275.
 14. JONGKEES, L. B. W. 1980. Some remarks on Ménière's disease. *ORL* **42**: 1-9.
 15. BRACKMAN, D. E. & R. G. ANDERSON. 1980. Ménière's disease: results of treatment with the endolymphatic subarachnoid shunt. *ORL* **42**: 101-118.
 16. SCHINDLER, R. A. 1979. The ultrastructure of the endolymphatic sac in Ménière's disease. *Adv. Oto-Rhino-Laryngol.* **25**: 127-133.
 17. PLANTENGA, K. F. & G. BROWNING. 1979. The vestibular aqueduct and endolymphatic sac and duct in endolymphatic hydrops. *Arch. Otolaryngol.* **105**: 546-552.
 18. MILLMAN, M. 1978. Coronary artery bypass surgery: Who profits? *Nord. Med.* **93**: 5-8.

CRANIAL COMPUTERIZED TOMOGRAPHY IN SPINOCEREBELLAR ATROPHIES

D. Claus and J. C. Aschoff

*Department of Neurology
University of Ulm*

D-7900 Ulm, Federal Republic of Germany

Spinocerebellar heredoataxias include more than 50 different types of atrophic processes with differences in clinical appearance, pathology, heredity, age of onset, and course of the disease. The literature of the past years reports computer tomography (CT) examinations of only 10 patients with Friedreich's disease, and the results were inhomogeneous.^{1,2} We therefore examined different types of atrophies in the posterior fossa in more than 100 patients.

Sixty-nine men and 41 women either with spinocerebellar heredoataxias or with cerebellar atrophies (average age, 42 years) were examined. Fifty-three patients suffered from Friedreich's ataxia corresponding to the clinical criteria of Barbeau et al.³⁻⁵ Four patients had Marie's spastic ataxia; 51 patients, late cerebellar atrophies of different etiology; and 2 patients, olivopontocerebellar atrophy.

A complete computerized tomography was carried out in all patients. For analysis, we focused on pathological widening of cerebral and cerebellar cortical sulci in relation to a vast amount of normal and age-matched values, derived from our experience with nearly 30,000 patients.

Furthermore, we measured the distances of internal cerebrospinal fluid spaces, and vermal and other infratentorial cisterns (FIGURE 1). Normal values for these are third ventricle, up to 8 mm; fourth ventricle, 20 mm; Evans index, up to 0.275; and cella media index, up to 0.240.

According to Haubek, an atrophy of vermal structures is diagnosed when four or more cross furrows are clearly visible in a single CT slice, and an atrophy of the cerebellar hemispheres if more than two furrows are to be seen.⁶

RESULTS

Ten of the 53 patients (19%) with Friedreich's ataxia showed an additional atrophy of the cerebral cortex. A clearly marked atrophy of the upper vermis (culmen and declive) or of the paravermis could be seen in the CT's of 33 patients (62%) of the Friedreich group. The median width of the ventricles and the indices were in the normal range (TABLE 1); the diameter of the fourth ventricle was more than 20 mm in four cases.

When comparing the 41 patients who had a more than 10 years course of the disease with the 12 patients who had a more recent onset of their symptoms, an atrophy of the cerebral cortex was found only in the first group. Atrophies of the vermis and paravermis clearly are more frequent in the longer-affected group, i.e., 76% versus 17% (TABLE 2).

When the patients were compared according to degree of disability (patients who needed a wheelchair versus those who could walk), a difference was seen in the occurrence of cerebral atrophies; atrophies of the vermis and paravermis

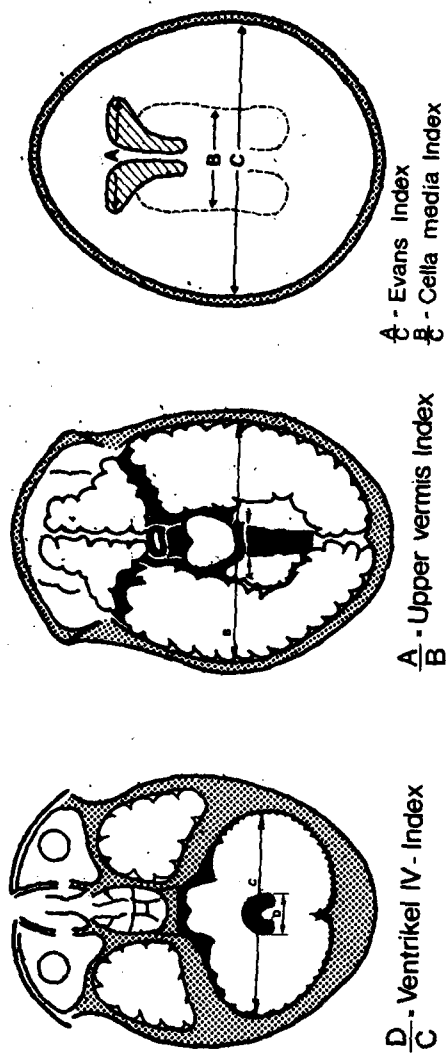
FIGURE 1. Applied indices.⁹

TABLE 1
DISTRIBUTION AND FREQUENCY OF ATROPHIES IN PATIENTS
WITH FRIEDREICH'S ATAXIA (n = 53)

	Cerebellum			Enlarged Cisterns		
	Cerebral Cortex	Vermis and Paravermis	Dorsal and Lateral Hemispheres	Cerebellopontine Angle Cistern	Cisterna Pontis	Cisterna Ambiens
n	10 (19%)	33 (62%)	4 (8%)	0	1 (2%)	0

TABLE 2
DISTRIBUTION AND FREQUENCY OF ATROPHIES IN TWO GROUPS OF PATIENTS WITH
FRIEDREICH'S ATAXIA OF DIFFERENT DURATION

	Cerebellum			Enlarged Cisterns		
	Cerebral Cortex	Vermis and Paravermis	Dorsal and Lateral Hemispheres	Cerebellopontine Angle Cistern	Cisterna Pontis	Cisterna Ambiens
Group 1* (n)	10 (24%)	31 (76%)	4 (10%)	0	1 (2%)	0
Group 2† (n)	0	2 (17%)	0	0	0	0

*Group 1: duration > 10 years (n = 41; average age, 35 years).

†Group 2: duration < 10 years (n = 12; average age, 18 years).

TABLE 3
DISTRIBUTION AND FREQUENCY OF ATROPHIES IN TWO GROUPS OF PATIENTS WITH
DIFFERENT DISABILITY AS A RESULT OF FRIEDREICH'S ATAXIA

	Cerebellum			Enlarged Cisterns		
	Cerebral Cortex	Vermis and Paravermis	Dorsal and Lateral Hemispheres	Cerebellopontine Angle Cistern	Cisterna Pontis	Cisterna Ambiens
Group 1* (n)	8 (22%)	27 (73%)	3 (8%)	0	1 (3%)	0
Group 2† (n)	2 (13%)	6 (38%)	1 (6%)	0	0	0

*Group 1: wheelchair (n = 37; average age, 35 years).

†Group 2: without wheelchair (n = 16; average age, 24 years).

increased from 38% in the less disabled to 73% in the more disabled patients (TABLE 3).

Atrophies of the vermis and paravermis were prominent in all four cases suffering from Marie's syndrome and included the dorsal and lateral parts of the upper cerebellar hemispheres. The cerebral cortex was not involved in these four patients; the fourth ventricle was enlarged in one case.

As far as late cerebellar atrophies are concerned (17 alcoholic, 3 paraneoplastic, 5 diphenylhydantoin, 16 idiopathic, and 10 different other origins), 25 of these 51 patients (TABLE 4) exhibited an atrophy of the cerebral cortex in addition to the cerebellar process. The atrophic process of the posterior fossa showed a clear accentuation of the paleocerebellum in the alcoholic cases. In all the other cases, it involved the vermis and paravermis as well as the dorsal and lateral parts of the upper cerebellar hemispheres. Basal cisterns were enlarged more often than

TABLE 4
DISTRIBUTION AND FREQUENCY OF ATROPHIES IN TWO GROUPS OF PATIENTS WITH
CEREBELLAR ATROPHIES (n = 51)

	n	Cerebellum			Enlarged Cisterns		
		Cerebral Cortex	Vermis and Paravermis	Dorsal and Lateral Hemispheres	Cerebello-pontine Angle Cistern	Cisterna Pontis	Cisterna Ambiens
Group 1*	17	15 (88%)	16 (94%)	7 (41%)	4 (24%)	3 (18%)	3 (18%)
Group 2†	34	10 (29%)	32 (94%)	27 (79%)	4 (12%)	4 (12%)	1 (3%)
Group 1 + Group 2	51	25 (49%)	48 (94%)	34 (67%)	8 (16%)	7 (14%)	4 (8%)

*Group 1: alcoholic.

†Group 2: others.

in the other (Friedreich's or Marie's spastic disease) groups. The median values of the measured indices were higher, and the width of the third ventricle averaged up to 5.5 mm—in 3 cases, it was over 8 mm. The width of the fourth ventricle was more than 20 mm in 7 cases.

DISCUSSION

Greenfield, Oppenheimer, and other authors repeatedly have claimed that at necropsy, the cerebellum in Friedreich's ataxia often is inconspicuous macroscopically, whereas degenerative changes of Purkinje cells can be seen microscopically.^{7,8} Contrary to the above-mentioned macroscopic data of autopsy cases, computed tomography *in situ* can prove a marked enlargement of the outer cerebrospinal fluid spaces, and in cases of Friedreich's ataxia, especially over the paleocerebellum.

CT, therefore, enables us to differentiate different and partially characteristic types of atrophic processes in the posterior fossa, as shown for three different

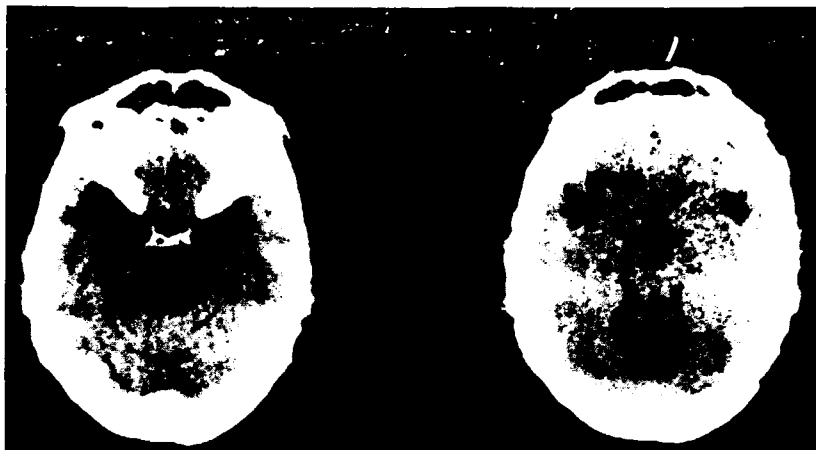


FIGURE 2. CT of a case with Friedreich's ataxia.

groups:

1. In Friedreich's ataxia (FIGURE 2), enlargements of the subarachnoid space over the paleocerebellum are seen. Lateral parts of the cerebellar hemispheres are not involved. Widenings of basal cisterns are rare and not typical. Atrophies over the cerebral cortex may appear after longer duration of the disease.

2. Symptomatic and late cerebellar atrophies (FIGURE 3) are characterized by a ubiquitous loss of substance of all structures in the posterior fossa, primarily of the paleocerebellum, but the brain stem and cerebellar hemispheres are



FIGURE 3. CT in late cerebellar ataxia.

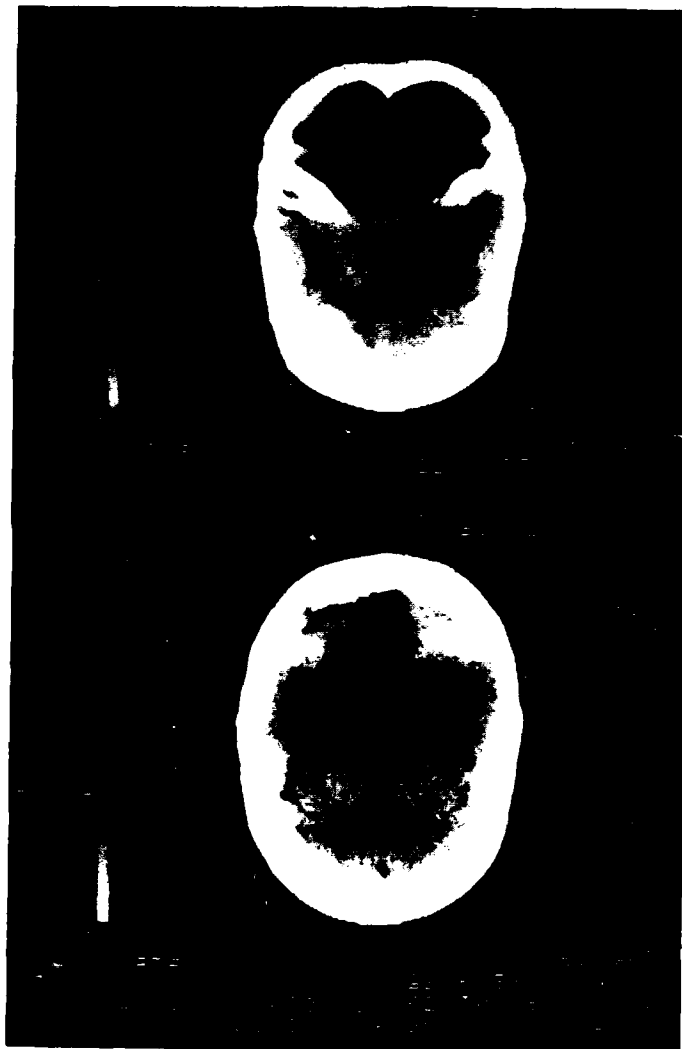


FIGURE 4. CT in a case suffering from Marie's spastic ataxia.

involved as well. In alcoholic cases, the atrophy is more accentuated over the vermis and paravermis, whereas there is no special difference between the other types of atrophy.

3. Four patients with Marie's spastic ataxia (FIGURE 4) were examined and could be differentiated easily from the above-mentioned Friedreich's group. In these patients with Marie's spastic ataxia, the atrophy involved not only vermal and paravermal structures but spread out to dorsal and lateral parts of the upper cerebellar hemispheres as well, corresponding to the Holmes type of cerebellar cortical atrophy.

CT has finally proved to be very helpful in the difficult differentiation between cerebellar cortical atrophy of the Holmes type and olivopontocerebellar atrophy of the Menzel type (FIGURE 5). The entire cerebellar hemispheres are atrophic, with accentuation of the laterodorsal neocerebellar parts. The pons is



FIGURE 5. CT in olivopontocerebellar atrophy.

narrowed, the fourth ventricle enlarged. In deep slices, the cerebellar tonsils diverge. In contrast to the other types of atrophy, the vermis scarcely is affected.

The values of the indices did not provide new or different information, so they are not discussed here.

SUMMARY

Cranial computerized tomography was carried out in 110 patients with cerebellar ataxia (53 with Friedreich's ataxia, 4 with Marie's spastic ataxia, 51 with cerebellar atrophy, and 2 patients with olivopontocerebellar atrophy).

In CT scans, cerebellar atrophies are found to be of various localization and partially of characteristic distribution. CT, therefore, greatly helps to distinguish

different types of cerebellar and spinocerebellar atrophies and allows the differentiation of cerebellar atrophies of various origins from other diseases, such as multiple sclerosis.

REFERENCES

1. LANGELIER, R., J. P. BOUCHARD & R. BOUCHARD. 1979. Computed tomography of posterior fossa in hereditary ataxias. *J. Can. Sci. Neurol.* **6**: 195-198.
2. MARUYAMA, S. 1977. Examination of spinocerebellar degenerative patients by computerized tomography. In Report No. 1: 119-129. Research Group on Spinocerebellar Degeneration. Tokyo, Japan.
3. BARBEAU, A. 1976. Friedreich's ataxia 1976—an overview. *J. Can. Sci. Neurol.* **3**: 389-397.
4. BODECHTEL, G. & A. SCHRADER. 1953. Die Erkrankungen des Rückenmarks. In *Handbuch der inneren Medizin* 2/5: 512-520. Springer Verlag. Berlin, Göttingen & Heidelberg.
5. SKRE, H. 1975. Friedreich's ataxia in western Norway. *Clin. Genet.* **7**: 287-298.
6. HAUBEK, A. & K. LEE. 1979. Computed tomography in alcoholic cerebellar atrophy. *Neuroradiology* **18**: 77-79.
7. GREENFIELD, J. G. 1954. *The Spino-Cerebellar Degenerations*: 64. Blackwell Scientific Publications. Oxford, England.
8. OPPENHEIMER, D. R. 1979. Brain lesions in Friedreich's ataxia. *J. Can. Sci. Neurol.* **6**: 173-176.
9. CLAUS, D. & J. C. ASCHOFF. 1980. Computer-Tomographie bei Atrophien im Bereich der hinteren Schädelgrube. *Arch. Psychiatr. Nervenkr.* **229**: 179-187.

VESTIBULAR AND NEUROLOGICAL DISORDERS IN DIVING COMPETITORS

H. Krejcova, L. Krejci,* J. Jirout, B. Stracarova, and P. Rezek*

Department of Neurology
Charles University
Prague, Czechoslovakia

INTRODUCTION

High diving from a board or tower is an exhausting sporting event that has important psychic and physical effects. Most dives are performed in an upside-down head and body position combined often with somersaults, loops, or rotation around the person's axis. The orientation of the speeding, falling subject above and under water places very high demands on the central nervous system and particularly on the vestibular apparatus. The water-body collision is a crucial point of stress, leading to repeated head blows and vertebral column compressions.

The combination of factors that can influence function of the central nervous system, spine, and vestibular apparatus seems to be unique, and has not been studied before. It differs from the mechanism of other, at-first-sight similar sports or professional activities, such as aerobatics, trapeze acrobatics, skydiving, figure skating, skateboarding, wind skating, surfboarding, wind surfing, ballet, boxing, or jumps on the trampoline.

The purpose of our study was to investigate possible negative influences of board and tower diving on the central nervous system, vertebral column, and vestibular apparatus. Owing to the lack of space, ophthalmological findings—including detailed tear examination/secretion, pH level, sodium and potassium distribution/slit lamp, ophthalmoscopic and visual-field controls, and electroretinography as well as otolaryngological results including bacteriological and audiological controls, audiometry, and tympanometry—are not incorporated in this study and will be published elsewhere.

SUBJECTS AND METHODS

Forty divers were examined, who had performed thousands of dives into water from different heights ranging from 1 to 10 meters. They were divided into three groups according to the intensity of training, total number of dives, and length of the active diving period (TABLE 1). Divers were studied with neurologic and vestibular examinations, including electroencephalography (EEG), electro-nystagmography (ENG), radiology (x-ray), and otolaryngologic and ophthalmologic examination. The battery of tests was carried out during the period of most intensive training. Controls were performed pre- and posttraining at half-year intervals.

Neurologic examination included investigation of vertebral motility especially in the cervical and lumbosacral regions. EEG examinations were

*Department of Ophthalmology.

TABLE 1
SURVEY OF EXAMINED DIVERS ACCORDING TO GROUPS, AGE, SEX,
INTENSITY OF TRAINING, TOTAL NUMBER OF PERFORMED DIVES,
AND LENGTH OF THE ACTIVE DIVING PERIOD

Group*	Divers	Age (years)	Monthly		Dives
			Training (hours)	Dives	
1	24	7-16	12-32	200-700	in 1 to 6 years 2,000-34,000
2	10	13-19	25-50	600-1,100	in 6 to 13 years 60,000-120,000
3	6	20-68	18-50	500-1,000	in 6 to 30 years 56,000-245,000

*Group 1, children and teenagers (5 male, 19 female). Group 2, representative group (1 male, 9 female). Group 3, trainers (2 male, 4 female).

performed on an eight-channel electroencephalograph (GRD) by the ten-twenty system.

Vestibular examination consisted of Hautant's arm deviation, and stance and gait deviation. ENG recordings were made by means of horizontal and vertical leads on a four-channel Beckmann Dynograph. Spontaneous and gaze nystagmus were registered, and positional and positioning tests were performed. Each position was maintained for 60 seconds. Recordings were done with eyes closed in semidarkness and also with eyes open in bright light with optic fixation. Thermal tests were applied according to Hallpike and Stahle.^{1,2} The investigation was performed with eyes open in a dark room. If subjects became drowsy, they were alerted with mental arithmetic. The results were evaluated according to Claussen's butterfly vestibulometry.³

Optokinetic nystagmus (OKN) was elicited in both horizontal and vertical directions by projecting a black and white striped pattern rotating at 75° and 100° per second on a half-cylinder screen. Bárány's rotational test was applied and postrotational nystagmus was recorded.⁴ An eye tracking test (ETT) was performed using a moving pendulum to elicit continuous pursuit. On being set in motion, the pendulum's period was 0.5 cycles per second. The amplitude in the frontal plane did not surpass 25°.

Biomechanics of Forces Acting on the Head and Spine in Board and Tower Diving^{5,6}

The greatest overload force is produced when the falling body decelerates in about the upper one meter of water. If a dive is performed correctly, water is struck by the stretched arms and the head, and flows smoothly around the penetrating body. The force that then acts on the head, for example, can be expressed by a simple equation $F = m \cdot g \cdot h$, in which m stands for the weight of the head, g for the overload force, and h for the height of the dive (in meters). If, however, the dive is performed incorrectly and the main collision lands on the face or occiput, the pressure dynamics change according to the equation $F = m \cdot g \cdot h - c \cdot v^2$, in which c is the constant of resistance offered by water to the penetrating body. This force acts in a counter direction to the movement of the body. It depends on the landing velocity v and increases proportionately to its

square. It acts upon the individual body organs only partially—by a force corresponding to the proportion of the organ surface to the total collision-damping surface. Even if the dive is perfect, the striking force on the head and the cervical spine of a person of 50 kg body weight diving from a 10-m tower reaches a value of up to 5,000 newtons.

RESULTS

Neurological Findings

Twenty-four divers—children and teenagers—in the first group admitted that they try to suppress their subjective complaints, such as lightheadedness, headache, instability, blurring of vision, or giddiness, following intensive training. The majority of divers of the second and third groups suffered from pain in the cervicocranial as well as the lumbosacral region or in the shoulders. On neurological examination there was reduced motility of the cervical spine in 27 out of the total of 40 divers (67.5%). In 13 of these 27, there was reduced ability to incline the head to both sides; and in 4 of them, this was only unilateral. Rotation blockade was present in 19 of the examined subjects: it was unilateral in 7 of them and bilateral in 12. Reduced motility in the lumbosacral region was present in 9 divers. Eight of these suffered simultaneously from cervical blockade. Three divers had reduced motility of the humeroscapular joint. Scoliosis was present in 19 out of the 40 divers (47.5%).

Vestibulo-Ocular Findings

Spontaneous nystagmus with eyes open and closed was found in 4 divers (TABLE 2); in another 8 subjects, it was present only with closed eyes. Gaze

TABLE 2
SURVEY OF INCIDENCE OF VESTIBULO-OCULAR ABNORMALITIES

	Group 1	Group 2	Group 3
Nystagmus			
a. spontaneous	4	6	2
b. gaze	9	6	1
c. positional	15	3	6
Caloric			
a. hyperreflexia	9	6	2
b. hyporeflexia	5	1	2
c. directional preponderance	1	2	2
Rotational			
a. hyperreflexia	9	6	2
b. hyporeflexia	2	1	1
OKN	4	6	4
Tracking Eye Movements	3	1	—
Other Abnormalities	5	1	—

nystagmus was found in 16 divers (40%), and *positional* nystagmus in 24 (60%). Of these 24, both *positional* and *positioning* nystagmus were present in 14 cases, *positional* nystagmus alone in 6 cases, and *positioning* nystagmus alone in 4 cases.

Caloric and rotational hyperresponsiveness appeared in 17 (42.5%); in 11, it was symmetrical; and in 6, asymmetrical. In 4 of these 17, the response was dysrhythmic during alertness. Hypoexcitability was found in 8 cases; it was bilateral in 4 of them. In only 4 cases was there a hypoexcitable response during the rotational test. Directional preponderance was present in 5 examined divers: it was of the peripheral type in 3, and of central origin in 2.

An impaired optokinetic response was present in 14 cases (35%). In 9 divers, we found irregular OKN: it was irregular and asymmetrical in 4, and irregular and symmetrical in 5. In 5 other divers, OKN was regular but asymmetrical, because of the influence of directional preponderance. Eye tracking was

TABLE 3
SURVEY OF EEG FINDINGS IN ALL THREE GROUPS OF EXAMINED DIVERS

Group	Divers	Normal	Atypical	General	Abnormal	
					Focal Irritation	
					Yes	No
1	24	12	4	1	6	1
2	10	4	2	1	1	2
3	6	1	2	2	—	1
Total	40	17	8	4	7	4

impaired in 5 subjects, in that smooth eye movements were interrupted by nystagmic jerks.

Summarizing the vestibular findings, we found evidence for peripheral vestibular disease in 11 (27.5%) and central vestibular disease in 19 (47.5%) of the examined divers.

EEG Findings

Atypical changes in the EEG records consisted of low-voltage theta waves distributed irregularly over the brain surface (see TABLE 3). The generalized abnormality consisted of theta waves or of paroxysmal bursts of alpha or theta waves. In focally abnormal EEG records, foci of sharp alpha waves or spikes were present, localized in the majority of cases in the temporal or parieto-occipital region. Most of the focal EEG abnormalities were found in children.

X-Ray Findings

In the first group, we found functional vertebral changes in 79% of the divers, whereas disc lesions or spondylotic deformities were not seen in any of them (see TABLE 4). In the second group, functional vertebral involvement was present in

TABLE 4
SURVEY OF X-RAY FINDINGS IN ALL THREE GROUPS OF EXAMINED DIVERS

	Group 1	Group 2	Group 3
Discopathy	—	7	5
Spondylosis	—	6	5
Deformans	—	7	4
Scoliosis	5	—	—
Occiput-Atlas	—	—	—
Dislocation	2	3	2
Atlas-Axis	—	—	—
Dislocation	6	3	2
Anteflexion	—	—	—
Irregularities	4	4	3
Rotational	—	—	—
Synkinesis	—	—	—
Irregularities	19	9	5

90%; and in the third group, in 50%. Simultaneously with the above-described functional involvement, discogenic and spondylotic changes were present in 70% of high divers and in 83% of examined trainers. Functional vertebral involvement following repeated injuries led to structural changes of the cervical spine.

A survey of the incidence of EEG, x-ray, and vestibulo-ocular abnormalities of the examined divers can be found in TABLE 5. The combination of EEG and x-ray abnormalities was present only in 3 cases in the first group. The combined occurrence of x-ray and vestibulo-ocular abnormalities was observed in 17 subjects. The combination of EEG, x-ray, and vestibulo-ocular abnormalities was found in 17 examined divers (first group, in 33.2%; second group, in 50%; third group, in 66.4%). An increasing number of abnormalities is dependent on increased demands on the divers.

DISCUSSION

Board and tower dives can be divided into five different phases: concentration, jump, water-body collision, diving, and relaxation. The divers' concentration comprises increased muscle tension, decreased intrathoracic pressure due to hyperventilation, and increased vertebral column motility due to prejump training. During the jump, muscle tension together with the vertebral column motility

TABLE 5
SURVEY OF INCIDENCE OF EEG, X-RAY, AND VESTIBULO-OCULAR ABNORMALITIES
IN ALL THREE GROUPS OF EXAMINED DIVERS

	Group 1	Group 2	Group 3
EEG & X-Ray	3	—	—
Vestibulo-Ocular & X-Ray	10	5	2
EEG, X-Ray & Vestibulo-Ocular	8	5	4
Normal	3	—	—
Total	24	10	6

is increased greatly. Intrathoracic pressure is elevated because of breath holding. Congestion of the cerebral vessels follows immediately, influenced by gravity, overload of the falling body, and upside-down head and body position. *Water-body collision* is accompanied in addition by water-head blows and vertebral column compression. *Diving* is followed either by decreasing muscle tension and vertebral column decompression or by continuous muscle spasms if the jump was not performed correctly. *Relaxation* includes decreased intrathoracic pressure because of hyperventilation above water level as well as cerebral vessel decongestion due to erect head and body position.

The third phase—water-body collision—seems to be the most important from the point of view of development of postjump vestibular, central nervous system, and spinal disorders.

Subjective complaints and objective findings in divers are directly dependent on the training intensity and on the total number and quality of the performed dives. Incorrect dives are followed by increased frequency of the subjects' complaints as well as by early functional and organic disorders.

The etiopathogenic factors are numerous: upside-down head and body position in diving, acceleration due to gravity and to high overload of the falling body, which is directly proportional to the depth of the board or tower dive, repeated changes in linear acceleration and rotational stimuli elicited by somersaults and loops, the water-body collision, the rapid body deceleration due to water-column resistance, fluctuation of the intrathoracic pressure due to hyperventilation and breath holding, irritation of cervical sympathetics due to movements of the cervical spine caused either by correct or incorrect dives. All these factors necessitate rapid fluctuations of the blood supply in the central nervous system—congestion, decongestion, or even spasm—which are responsible for reversible or irreversible changes. Even motility involvement in the lumbosacral region and scoliosis may contribute to the impairment of vestibular functions.^{7,8}

The high incidence of vestibular abnormalities in divers of all three groups is striking (75% !) and could be explained as a real sequel of repeated injuries to the central nervous system and the cervical spine, and to disorders of blood supply in vertebral vessels influenced by the autonomous nervous system.

Peripheral vestibular syndromes were found mostly after water-head blows due to incorrectly performed dives. Central vestibular syndromes were observed mainly in divers who had experienced strong water-head blows several months or years before.

Vestibular pathologies never were accompanied by vertigo. Frequent subjective complaints about headache and blurring of vision and alteration of the optokinetic response and eye tracking movements together with numerous EEG abnormalities suggest the presence of brain *microinjuries*, the prestate of brain concussions.⁹⁻¹¹ It is evident that the repeated water-body collisions are responsible also for cervical and lumbosacral functional or later structural pathologies. We did not prove any topical neurologic findings or loss of consciousness after performed dives. None of the subjects suffered from brain concussion, acute prolapse of the intervertebral disc, or bone fracture.

CONCLUSION

Because of the complicated mechanism of board and tower diving, the vestibular apparatus, central nervous system, and vertebral column particularly are prone to be affected most frequently.

1. Vestibular lesions—some peripheral, but most central—were the first symptoms indicating pathological response of the central nervous system to a high intensity of training.

2. Beside the peripheral and central vestibular pathologies, EEG abnormalities and alteration of OKN response and ETT as well as such subjective complaints as headache, lightheadedness, giddiness, and blurring of vision are sequels of repeated diving probably due to mild brain microinjuries.

3. Irregularities of mutual occiput-atlas and atlas-axis relations, anteflexion irregularities, and rotational synkinesis involvements could be explained as functional disorders of the cervical spine preceding organic vertebral changes.

These changes appear to be dependent on the rapid and repeated falls into water, water-head and water-body collisions, vertebral-column compressions and decompressions, muscle spasms, and irregularities in the blood supply of the central nervous system.

REFERENCES

1. HALLPIKE, C. S. 1955. The caloric tests. *Pract. Oto-Rhino-Laryngol.* 17: 173-178.
2. STAHL, J. 1958. Electro-nystagmography in the caloric and rotatory tests. A clinical study. *Acta Oto-Laryngol. Suppl.* 137.
3. CLAUSSEN, D. F. 1973. Butterfly vestibulometry, a practical evaluation scheme. *Equilibrium Res.* 3(1): 80-85.
4. BÁRÁNY, R., Ed. 1907. *Physiologie und Pathologie des Bogengangsapparates beim Menschen.* Franz Deuticke. Leipzig and Wien.
5. ILJIN, S. V. 1979. Metodika razčetov gidrodinamičeskich soprotivlenij v sportivnom plavanii. In *Teorija i Praktika Fizičeskoj Kultury: 9. Fizkultura i Sport.* Moscow, Russia.
6. ONOPRIENKO, B. I. 1979. Ispolzovanije Medžirovanija dlja Isledovanija Soprotivlenija vody Dviženiju tela Plovca: 8. *Fizkultura i Sport.* Moscow, Russia.
7. HINOKU, M. & N. USHIO. 1975. Lumbosacral proprioceptive reflexes in body equilibrium. *Acta Otolaryngol. Suppl.* 330: 197-210.
8. YAMAMOTO, H. & K. YAMADA. 1975. Equilibrium function in scoliosis. In *Proceedings, Fifth Extraordinary Meeting of the Bárány Society.* M. Morimoto, Ed.: 253-257. Bárány Society and Japan Society for Equilibrium Research. Kyoto, Japan.
9. GILBERT, M. M. 1971. The neurophysiological basis for post-concussional headaches. In *Proceedings, International Headache Symposium.* D. J. Dalessio, T. Dalsgaard-Nielsen & S. Diamond, Eds.: 75-78. Sandoz, Ltd. Basel, Switzerland.
10. WOLFF, H. G. 1963. *Headache and Other Head Pain.* Oxford University Press. New York, N.Y.
11. JUNG, R. & H. H. KORNHUBER. 1964. Results of electronystagmography in man: the value of optokinetic, vestibular and spontaneous nystagmus for neurologic diagnosis and research. In *The Oculomotor System.* M. B. Bender, Ed.: 428-488. Hoeber Medical Division. New York, N.Y.

VISUAL SUPPRESSION OF CALORIC NYSTAGMUS IN BRAIN-STEM LESIONS

Setsuko Takemori,* Tadashi Aiba,† and Ryoichi Shizawa‡

*Toranomon Hospital
Okinaka Memorial Institute for Medical Research
Tokyo, Japan 107*

INTRODUCTION

The ability to fix the eyes on a target, visual fixation, is important for the maintenance of equilibrium. Gaze nystagmus and saccadic pursuit eye movements are seen often in clinical cases with disturbance of visual fixation. Measurement of visual suppression is one technique to examine visual fixation.¹ Demanez *et al.* and Hart measured visual fixation by comparing the amplitude and frequency of caloric nystagmus with eyes closed and with eyes open.^{2,3} They called this measure the "ocular fixation index."

Lesions that affect visual fixation are of theoretical and clinical interest. Alpert reported that a failure of fixation is highly correlated with posterior fossa lesions.⁴ In accord with this, visual suppression of caloric nystagmus was reduced or abolished by cerebellar lesions.^{1,5} In contrast, visual suppression of caloric nystagmus was altered after brain-stem lesions, especially after pontine lesions.⁵ In these cases, there was augmentation rather than reduction of caloric nystagmus in light. The purpose of this paper is to illustrate visual suppression of caloric nystagmus after brain-stem lesions and to clarify the mechanism of loss of visual suppression and augmentation of caloric nystagmus in light.

METHODS

Thirty-nine patients with brain-stem lesions were studied (TABLE 1, left side). Horizontal and vertical eye movements were recorded by electro-oculography (EOG) using Ag-AgCl electrodes. The time constant for eye-movement recordings was 3.0 seconds and for eye-velocity recordings, 0.03 seconds. Direct-current recordings were used in some cases to study the relationship between eye position and nystagmus. Eye movements were differentiated to obtain eye velocity, and quick-phase velocity was rectified to obtain slow-phase velocity. Upward pen deflections in the figures indicate eye movements to the right and upward.

During testing, subjects lay on a bed with their heads raised 30°. The examiner's index finger was held 50 cm above the subjects as the point on which they were to fix their eyes. Twenty milliliters of water, generally at 20°C, were

*Neurotology.

†Neurosurgery.

‡Neurology.

TABLE 1
BRAIN-STEM LESIONS AND VISUAL SUPPRESSION

	Ipsilateral Nystagmus			Contralateral Nystagmus		
	Augmented Nystagmus in Light*	Reduced Visual Sup- pression	Normal Visual Sup- pression	Augmented Nystagmus in Light*	Reduced Visual Sup- pression	Normal Visual Sup- pression
I. Midbrain Lesions (9 cases)						
Pinealoma			9			9
II. Pontine Lesions (22 cases)						
a. Glioma (6 cases)						
1. Unilateral (PPRF lesion, etc.) (4 cases)	4				2	2
2. Bilateral (2 cases)	2			2		
b. Vascular le- sions (13 cases)						
1. MLF syn- drome (5 cases)	2	1	2	1	2	2
2. Millard- Gubler syndrome (3 cases)	3				3	
3. Others (5 cases)	4	1		1	1	3
c. Multiple sclerosis (2 cases)	2	1	—	—	2	1
Pontine le- sions total	17	3	2	4	10	8
III. Medullary Lesions (8 cases)						
a. Wallenberg syndrome (4 cases)		2	2		1	3
b. Syringobulbia (1 case)			1			1
c. Others (3 cases)		—	3		—	3
Medullary le- sions total		2	6		1	7

*Altered visual suppression.

used to irrigate the external auditory canal during a 20-second period in light with eyes covered. The room lights were turned off for 30–45 seconds. During this time, slow-phase velocity of caloric nystagmus reached a maximum. The lights then were turned on for 5–10 seconds with eyes open, and the subject watched the examiner's index finger. In normal individuals, this causes immediate

suppression of nystagmus, and slow-phase eye velocity drops. At the end of this period, the room lights were turned off again and the eyes were covered until the end of caloric nystagmus (FIGURE 1).

Visual suppression of caloric nystagmus was determined by measuring mean slow-phase velocity during the last 10 seconds in darkness (a) and comparing it to slow-phase velocity in light with eyes open (b).

$$\text{Visual Suppression (\%)} = [(a - b)/a] \times 100$$

RESULTS

The results are summarized in TABLE 1. Illustrative cases will be presented.

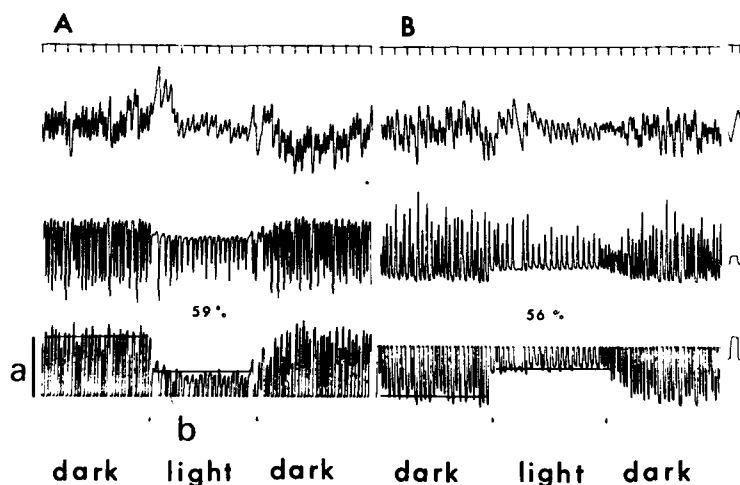


FIGURE 1. Visual suppression in normal adult. A: caloric nystagmus to the left. B: caloric nystagmus to the right. The top traces show the time base at 1 mark/second. The second traces are eye-movement recordings; time constant, 3.0 seconds; calibration, 10°. The third traces are eye-velocity recordings; time constant, 0.03 second; calibration, 20°/second. The fourth traces are slow-phase-velocity recordings; calibration, 20°/second. a: mean slow-phase velocity of caloric nystagmus in darkness. b: mean slow-phase velocity of caloric nystagmus in light with eyes fixed on a target. Visual suppression is normal.

Case 1

A 33-year-old male complained of tinnitus of both ears and numbness of the left extremities, which gradually increased over 10 days. There was gaze nystagmus to the right and horizontal positional and positioning nystagmus to the right on first examination (March 22, 1980). On March 27, an abducens palsy of the right eye was noted. On March 31, conjugate gaze paralysis to the right was seen. A right paramedian pontine reticular formation (PPRF) lesion was suspected. Computerized tomography suggested that the lesion was a pontine glioma. After radiotherapy, the gaze paralysis disappeared gradually.

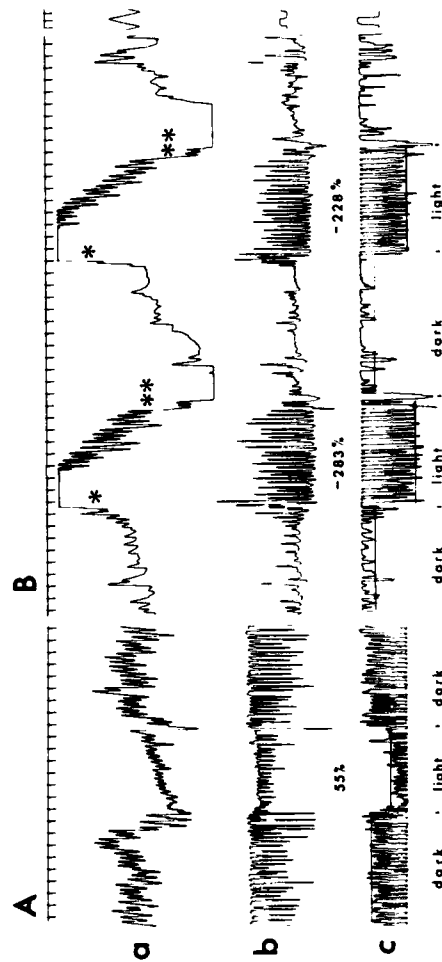


FIGURE 2. Case 1. Right pontine glioma (right PPRF lesion). A and B as in FIGURE 1. a: eye-movement recordings; time constant, 3.0 seconds, calibration, 10°. b: eye-velocity recordings; time constant, 0.03 second, calibration, 20°/second. c: slow-phase-velocity recordings; calibration, 20°/second. Visual suppression of caloric nystagmus to the left is normal. Visual suppression of caloric nystagmus to the right is abolished, and caloric nystagmus is augmented in light.

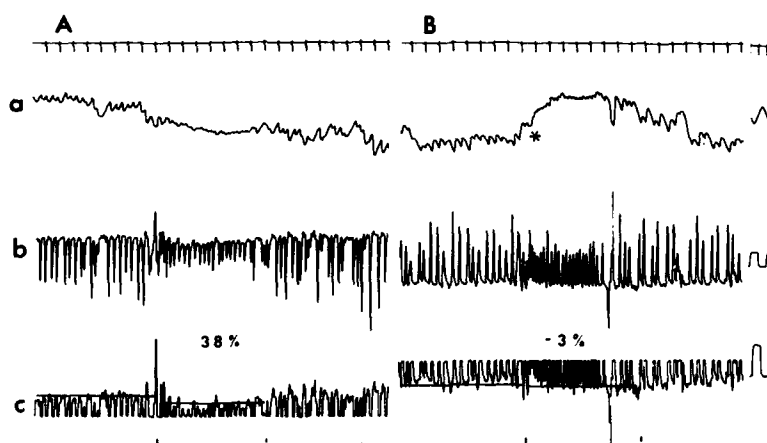


FIGURE 3. Case 2. A, B, a, b, and c as in FIGURES 1 and 2. Right Millard-Gubler syndrome. Visual suppression of caloric nystagmus to the left is reduced (38%). Visual suppression of caloric nystagmus to the right is abolished (-3%), and caloric nystagmus is augmented in light.

Initially, visual suppression of caloric nystagmus to the right was altered in this patient, in that caloric nystagmus was augmented in light (FIGURE 2B). Visual suppression of caloric nystagmus to the left was normal (FIGURE 2A). Visual suppression became normal with the improvement of the gaze paralysis.

Case 2

A 48-year-old male was giving a lecture in a university in Tokyo on May 20, 1980, when he suddenly felt sick and had a severe headache. He had instability of the left side when he moved his left hand and leg. On examination, he had a right facial palsy and a contralateral (left) hemiplegia. A vascular lesion of the right pons was suspected (Millard-Gubler syndrome).

Visual suppression of caloric nystagmus to the right was abolished, and caloric nystagmus was augmented slightly in light (FIGURE 3B). Visual suppression of leftward caloric nystagmus was reduced somewhat (FIGURE 3A).

Case 3

A 17-year-old girl complained of hypesthesia of the right side of the face, double vision, and a gait disturbance that appeared gradually over one month. On examination, there was an abducens palsy in the right eye, right facial palsy, impairment of facial sensation on the right, and hemiplegia on the left. These symptoms disappeared gradually while the patient was receiving steroid hormonal therapy. The numbness of the contralateral extremities reappeared three months later. Again, the numbness disappeared while she was receiving steroids. Multiple sclerosis was suspected.

Visual suppression of caloric nystagmus to the right was altered, and caloric

nystagmus was augmented in light (FIGURE 4B). There also was less visual suppression of caloric nystagmus to the left than in normals (FIGURE 4A). (The right eye had paralysis of abduction due to the abducens palsy; therefore, visual suppression was tested by recording the left eye.)

DISCUSSION

Caloric nystagmus is almost the same in light as in darkness in patients with diffuse cerebellar lesions, e.g., spinocerebellar degeneration. After unilateral flocculus lesions in rhesus monkeys, visual suppression of caloric nystagmus to the ipsilateral side was reduced and visual suppression of caloric nystagmus to the contralateral side was normal.⁶ After bilateral flocculus lesions, visual suppression of caloric nystagmus was abolished bilaterally.⁷ Visual suppression was reduced bilaterally after nodulus lesions.⁷ Lesions of other parts of the cerebellum did not affect visual suppression of caloric nystagmus in rhesus monkeys.⁷ Thus, after cerebellar lesions, visual suppression either was not affected or was reduced or abolished, and caloric nystagmus never showed augmentation in light.⁵

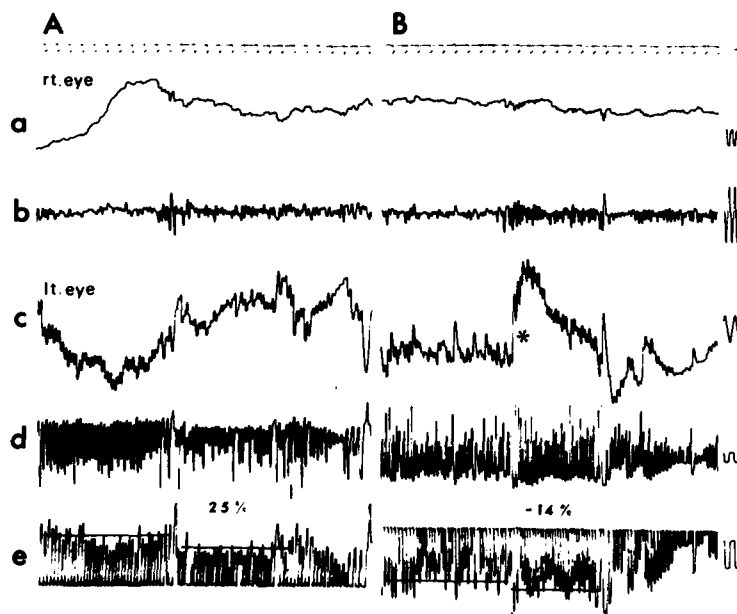


FIGURE 4. Case 3. Multiple sclerosis (right pontine lesion). A and B as in FIGURE 1. a: eye-movement recordings of the right eye; time constant, 3.0 seconds; calibration, 100 μ V. b: eye-velocity recordings of the right eye; time constant, 0.03 second; calibration, 100 μ V. c: eye-movement recordings of the left eye; time constant, 3.0 seconds; calibration, 10°. d: eye-velocity recordings of the left eye; time constant, 0.03 second; calibration, 20°/second. e: slow-phase-velocity recordings of caloric nystagmus to the left; calibration, 20°/second. The right eye has the abducens palsy. Visual suppression of caloric nystagmus to the left is reduced (25%). Visual suppression of caloric nystagmus to the right is abolished, and there is augmentation of caloric nystagmus in light (-14%).

Visual suppression was normal in the patients after midbrain lesions (TABLE 1). After medullary lesions, two cases of Wallenberg syndrome showed reduced visual suppression of caloric nystagmus to the ipsilateral side. This might be caused by an influence of the lesions on the pons in the acute stage of the illness.

On the other hand, after pontine lesions, augmentation of caloric nystagmus to the ipsilateral side with reduced visual suppression was common, being present in 19 of 22 cases. Augmentation of caloric nystagmus to the contralateral side in light also was present in 4 cases. It was milder than augmentation of ipsilateral caloric nystagmus and disappeared gradually with improvement of symptoms as visual suppression of contralateral caloric nystagmus became normal. Thus, lesions of the pons have a different effect on visual suppression than do cerebellar, midbrain, or medullary lesions.

Alertness and eye position are very important in evoking nystagmus, and they were studied to clarify the phenomenon of augmentation of caloric nystagmus in light in pontine lesions. To maintain alertness, subjects counted numbers backward from 100 to 0 during the test. The left side of FIGURE 5 shows typical augmentation of caloric nystagmus in light as described previously (dark 1, light 1, visual suppression -41%). However when counting backward (right side of FIGURE 5), the slow-phase velocity of caloric nystagmus in darkness became larger (99, 98, 98, . . . , dark 2). In this condition, there was a reduction of 25% when the subject attempted to fix the target (compare dark 2 with light 2). Thus, after correcting for alertness, 25% might be the correct percent of visual suppression. In this case, a lower level of alertness in darkness probably was responsible for the augmentation of caloric nystagmus in light.

Eye position also is known to have an effect on slow-phase velocity of nystagmus. Fourteen normal adults were tested to examine the influences of eye position on caloric nystagmus. When the eyes were deviated 10° in the quick-phase direction, the slow-phase velocity of caloric nystagmus increased by $1.4^\circ \pm 1.3^\circ/\text{second}$. When the eyes were deviated 10° in the slow-phase direction, the

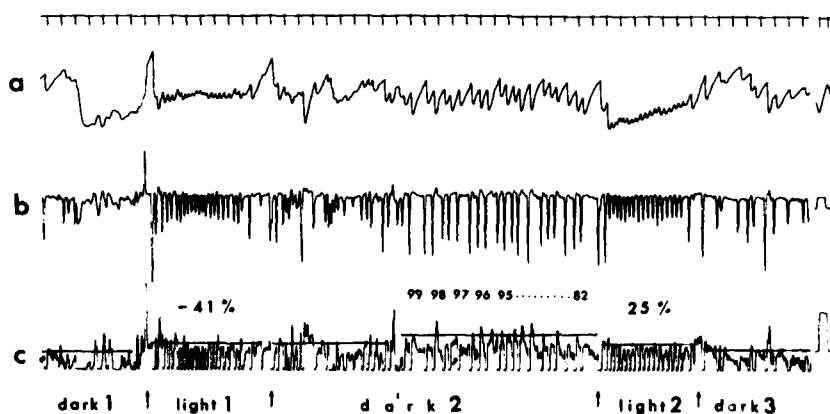


FIGURE 5. Alertness and caloric nystagmus (right pontine glioma). a, b, and c as in FIGURE 2. Visual suppression of caloric nystagmus to the left was -41% (dark 1, light 1). When the subject was told to count numbers from 100 to 0, the caloric nystagmus became stronger (dark 2), and the visual suppression was 25% (dark 2, light 2). (See text for details.)

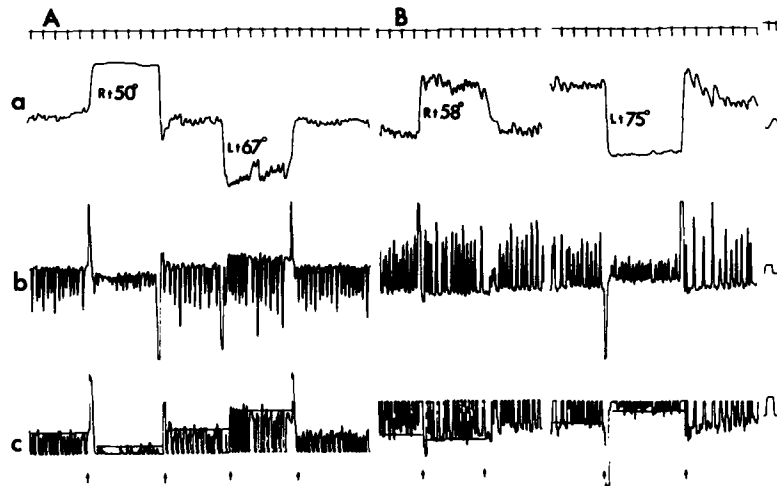


FIGURE 6. Eye position and caloric nystagmus. A, B, a, b, and c as in FIGURES 1 and 2. When the eyes deviated to the direction of the slow phase, caloric nystagmus was strongly inhibited. Caloric nystagmus was augmented with eye deviation to the direction of the quick phase. In trace a, Rt 50° and Lt 67° indicate that the eyes deviated 50° to the right and 67° to the left. The traces in a are d.c. recordings of eye movements.

velocity of the slow phases of caloric nystagmus was reduced by $4.1^\circ \pm 2.0^\circ/\text{second}$. Thus, there was a reduction in the slow-phase velocity of caloric nystagmus caused by eye deviation in the slow-phase direction, and eye velocity was larger when the eyes were deviated in the quick-phase direction. This is more apparent with larger deviations of the eyes (FIGURE 6).

The paramedian zone of the pontine reticular formation (PPRF) is known to be important for horizontal eye movements and gaze deviations. PPRF lesions cause ipsilateral paralysis of gaze and an absence of quick phases to the ipsilateral side.⁸⁻¹⁰ Therefore, the eyes are held constantly to the contralateral side after this lesion.

As shown in FIGURE 1, there was no eye deviation in darkness in normal subjects. The patient of FIGURE 2 had a small lesion of the right PPRF. Quick phases were impaired to the right side after the right PPRF lesion, and the eyes deviated to the contralateral (left) side in darkness. This is shown in FIGURE 2B. The eyes deviated to the left, i.e., to the contralateral side, in darkness (**), and they moved to the midposition when the subject attempted to fixate on the examiner's index finger when the lights were turned on (*). Although the EOG recordings in FIGURE 2 were not d.c. coupled, the initial movement of the eyes in light can be seen. In darkness, the eye deviation to the contralateral side caused strong suppression of caloric nystagmus. When the lights were turned on to test visual suppression, however, the eyes moved to the center to enable the patient to fix his eyes on the examiner's index finger. This movement was in the quick-phase direction. It enabled the patient to have larger nystagmus, leading to augmentation of slow-phase eye velocity in light. Similar augmentation of caloric nystagmus in light also was seen with eyes deviated to the side contralateral to the lesion in FIGURES 2-4 (*). Thus, in pontine lesions, both alertness and eye

position seem to be very important in causing augmentation of caloric nystagmus in light.

CONCLUSION

Caloric nystagmus to the side ipsilateral to the lesion was augmented in light after pontine lesions. The augmentation of caloric nystagmus in light seemed to be caused by two factors, an enhancement of the level of alertness and a change in eye position that reduced the paresis of quick phases. Visual suppression of caloric nystagmus was normal after midbrain lesions and was affected only minimally after medullary lesions.

REFERENCES

1. TAKEMORI, S. 1977. Visual suppression test. *Ann. Otol. Rhinol. Laryngol.* **86**: 80-85.
2. DEMANEZ, J. P. & A. LEDOUX. 1970. Automatic fixation mechanisms and vestibular stimulation. Their study in central pathology with ocular fixation index during caloric test. *Adv. Oto-Rhino-Laryngol.* **17**: 90-98.
3. HART, C. W. 1973. The ocular fixation index. *Ann. Otol. Rhinol. Laryngol.* **82**: 848-851.
4. ALPERT, J. N. 1974. Failure of fixation suppression: a pathologic effect of vision on caloric nystagmus. *Neurology* **24**: 891-896.
5. TAKEMORI, S. 1978. Visual suppression test. *Clin. Otolaryngol.* **3**: 145-153.
6. TAKEMORI, S. & B. COHEN. 1974. Loss of visual suppression of vestibular nystagmus after flocculus lesions. *Brain Res.* **72**: 213-224.
7. TAKEMORI, S. 1975. Visual suppression of vestibular nystagmus after cerebellar lesions. *Ann. Otol. Rhinol. Laryngol.* **84**: 318-326.
8. COHEN, B., A. KOMATSUZAKI & M. B. BENDER. 1968. Electro-oculographic syndrome in monkeys after pontine reticular formation lesions. *Arch. Neurol.* **18**: 78-92.
9. GOEBEL, H. H., A. KOMATSUZAKI, M. B. BENDER & B. COHEN. 1971. Lesions of the pontine tegmentum and conjugate gaze paralysis. *Arch. Neurol.* **24**: 431-440.
10. KOMATSUZAKI, A. & K. KITAMURA. 1975. Nystagmus and abnormal eye movement in lesions of the brain stem and the cerebellum. *Adv. Neurological Sci.* **18**: 979-999.

THE ROLE OF THE PLANTAR MECHANORECEPTOR IN EQUILIBRIUM CONTROL

Isamu Watanabe and Jin Okubo

Department of Otolaryngology
Tokyo Medical and Dental University
Tokyo 113, Japan

Several methods for observing body equilibrium or postural reflexes have been developed recently: the statokinesimeter, three-point suspension, the pedoscope, and gravigonometry of the sway of the center of gravity.¹⁻⁴ Studies utilizing these methods are now actively under way. In the past several years, we have engaged in studies of body sway in order to determine how it is controlled. We have reported that body sway in a dark field is different from that in a bright field with eyes open and eyes closed. It is more valuable to observe labyrinth disturbances in a dark field.⁵ It also has been reported that breathing and position of the feet have considerable influence on the test results.⁶ Many other factors besides these control body sway.

When a person stands on two feet, he feels weight resistance on the plantar surface, but little is known yet about how plantar mechanoreceptors influence body sway. Adrian stated on the basis of his electrophysiological experimentation that the plantar and palmar sensory receptors have slower adaptation than do other sensory organs.^{7,8} This agrees well with the idea that the plantar and palmar sensory receptors should be slow in adapting.¹⁴⁻¹⁶

We developed a method for adding weight resistance to the plantar mechanoreceptors, and have studied body-sway control mechanisms. These findings are reported in this paper.

METHODS

FIGURE 1 shows the device developed for measurement of the sway of the center of gravity. The block diagram shows that differences in orbits caused by differences in weight, as well as differences in the area of the center of gravity caused by height differences, could be adjusted automatically or manually at each measuring meter. For plantar-mechanoreceptor stimulation, we prepared three transparent plates overlaid with shotgun balls 2 mm in diameter placed at distances of 1, 1.5, or 2 cm. The shotgun balls protrude about 1 mm from the surface of the plate, which was placed on a goniometer. The subjects stood on the plate for measurement of body sway. The transparent plate eliminated foot position as a stimulation load on the plate, so that the same position of the foot would be maintained in all the repeated tests (FIGURE 2).

Twenty subjects having no past history of labyrinth disturbances or head injuries (male; average age, 24.5 years) were used in the experiments. Of these, 16 were chosen for plantar-mechanoreceptor stimulation. The order of use of the three plates was chosen by random allocation. For comparison with the results, 10 subjects were given a breath-holding test. It is well known that respiration influences body sway; our reason for using breath holding was that we already knew from our past research that this would reduce body sway.⁹

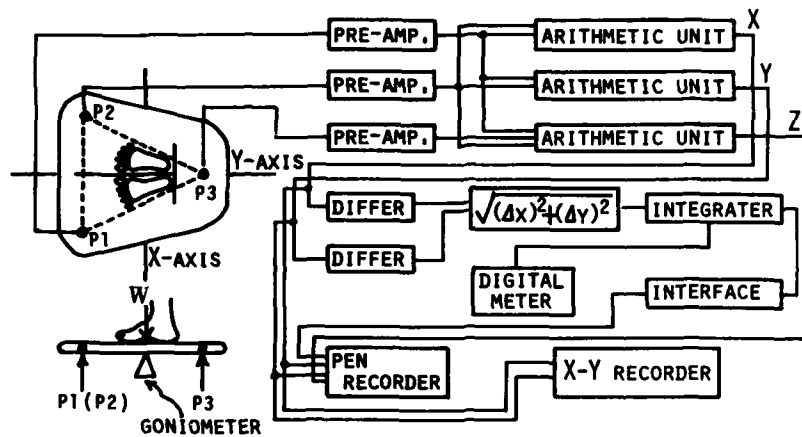


FIGURE 1. Block diagram of the data processing system.

Two subjects were tested for neuronal discharge in the tibial nerve. Needle electrodes were used to record action potentials of plantar-mechanoreceptor neurons while subjects were standing on each of the plates.

RESULTS

The discharge that takes place in tibial nerve fibers when the plantar surface is stimulated by the stimulus plate is shown in FIGURE 3. We confirmed that the neurons were innervated from the plantar surface by tapping and showing that the frequency increased when the subject bent forward or backward. The frequency also increased or decreased in response to greater or smaller loading respectively.

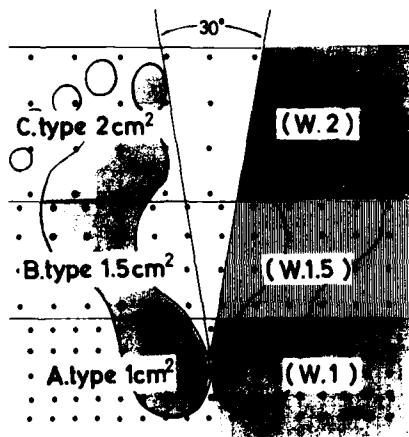


FIGURE 2. Method of plantar-mechanoreceptor stimulation by three types of shot-gun-ball plates.

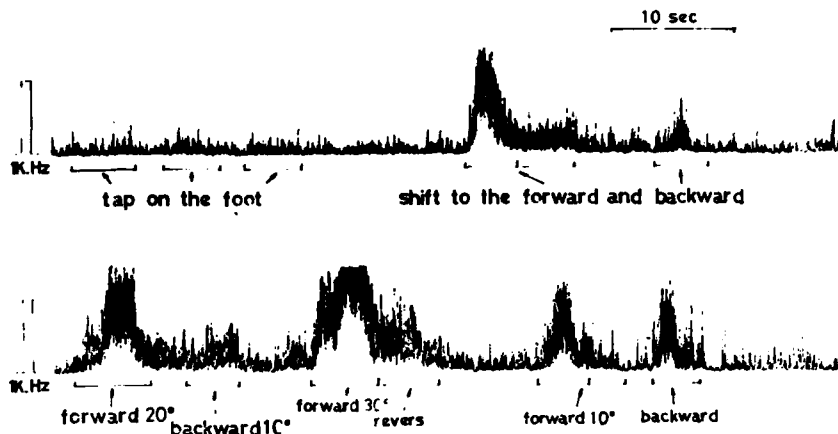


FIGURE 3. Neuron discharge of n. tibialis unit in response to body movement and tap on the foot.

FIGURE 4 is a comparison of the neuronal discharges on the different plates. W0 represents no stimulation; W1, on the plate of shotgun balls arranged at 1-cm distances; W1.5, balls at 1.5-cm distances; and W2, at 2-cm distances. Discharges were recognized on plates W1 and W1.5, showing a distinct difference from W2. When the Jendrassik maneuver was done, an increase of discharge occurred even on plate W2. This is an interesting finding and suggests that the increase of the discharge here is the result of the external disturbance of the cerebellum connections that control the arms and feet.¹⁰

FIGURE 5 (TABLE 1) is a comparison of the sway areas and the sway-shifting

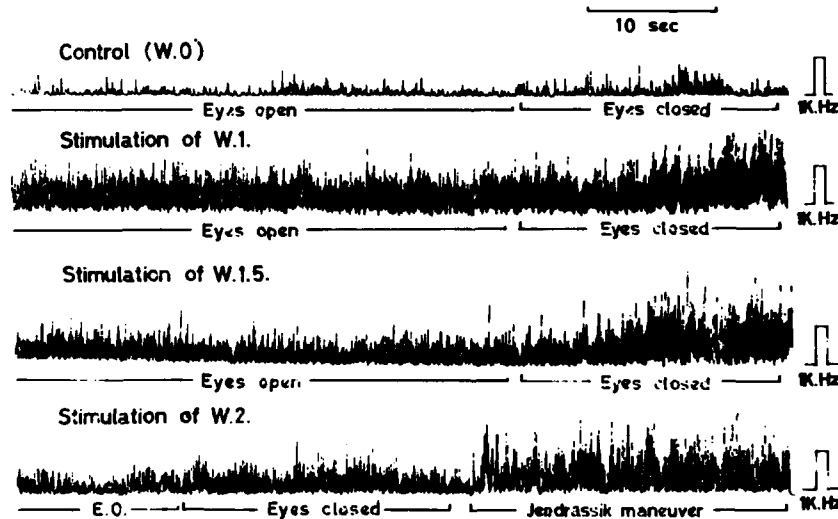


FIGURE 4. Neuron discharge of n. tibialis unit in response to mechanical plantar stimulation by shotgun-ball plates.

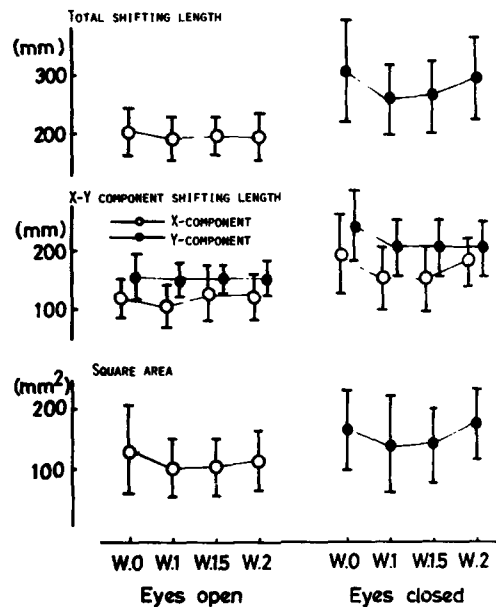


FIGURE 5. Shifting length and square area of the center of gravity under various conditions (20 seconds).

TABLE 1

COMPARISON OF SQUARE AREA AND TOTAL SHIFTING LENGTH OF SWAY FOR EACH STIMULATION OF THE PLANTAR PRESSURE RECEPTOR WITH EYES OPEN AND CLOSED

	without		Square Area (mm ²) (n = 16)				with 2 cm	
	EO	EC	with 1 cm	with 1.5 cm	EO	EC	EO	EC
Mean	129	169	100	144	106	140	114	179
(±) SD	83	77	57	84	49	64	53	66
	without		Shifting Length (mm) (n = 16)				with 2 cm	
	EO	EC	with 1 cm	with 1.5 cm	EO	EC	EO	EC
Total Shifting Length								
Mean	201.4	309.3	195.4	262.5	199.5	264.3	196.4	288.3
(±) SD	42.3	110.6	34.4	79.7	34.7	68.8	38.8	75.6
X-Component Shifting Length								
Mean	125.3	199.3	122.4	164.6	126.0	164.3	124.2	181.8
(±) SD	38.5	82.8	33.0	54.2	38.1	60.9	35.6	50.3
Y-Component Shifting Length								
Mean	153.6	241.1	153.4	212.4	156.6	212.9	153.8	214.6
(±) SD	30.3	85.1	26.3	68.5	18.0	49.2	26.3	46.6

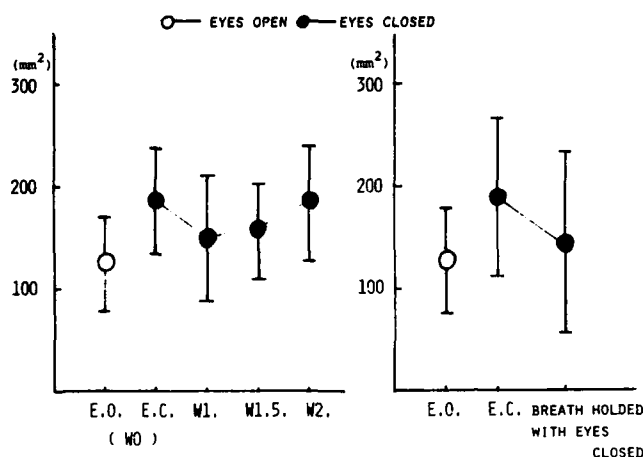


FIGURE 6. Square area of the center of gravity under various conditions (20 seconds).

lengths when the plantar mechanoreceptors were stimulated. With eyes open, there was no significant difference except for a change of sway area. With eyes closed, there were differences in the sway area and the sway-shifting length in W1 and W1.5 compared with those of W0, but almost no difference in W2. Apparently, the input information from the plantar mechanoreceptors on plates W1 and W1.5 was effective enough to guide the righting reflex when the eyes were closed. However, in view of the change in the sway area in W2 in the eyes-open situation where visual stimulation was available, changes in the input information could have an effect on the righting reflex.

Next, a comparison was made between the change of body sway caused by plantar-mechanoreceptor stimulation and that caused by breath holding (FIGURE 6). On the left are the values measured during mechanoreceptor stimulation with eyes open (EO) and eyes closed (EC), and on the right are the values with breath held (TABLE 2); breath holding resulted in a decrease in values.⁹ In order to analyze these phenomena, the body sway recorded on each of the plates was compared by power spectrum (FIGURE 7). The ordinate is a logarithmic scale showing power, and the abscissa is an integral scale of the recorded analysis by ratio up to 10 Hz. The range of the control values (W0) is shown by the shaded area, and the spectrum for body sway on each of the plates is represented by a different line (see key in figure). Most of the subjects showed a power spread of the X-component as far as 4 to 5 Hz, while the Y-component spectrum spread as far as 7 to 10 Hz. High-frequency power appeared in the Y-component. The

TABLE 2

STATISTICAL DATA ON THE EFFECT OF BREATH HOLDING (BH) ON THE AREA OF BODY SWAY AND THE TOTAL SHIFTING LENGTH OF THE CENTER OF GRAVITY (n = 10)

	Square Area of Sway		Total Shifting Length	
	before BH	during BH	before BH	during BH
Mean Value	172 mm ²	146 mm ²	308 mm	218 mm
Standard Deviation	±68	±76	±84	±96

power spectrum of body sway on these stimulation plates at these power levels showed differences over 3 Hz, up to 5 Hz. There was a strong effect of W1 on both the X- and Y-components, particularly when the eyes were closed. In the body-sway control system when visual information was cut off, the afferent information from labyrinth and deep sensation summated so that the body sway was controlled efficiently. Considering the fact that the sway control is centered at 4 to 5 Hz, presumably the control mechanism should have a summing junction higher in the central nervous system than the spinal level.

FIGURE 8 is power-spectral analysis of the influence of breath holding on body sway. There was not much difference between breathing and breath holding. Especially when the eyes were open, no difference was seen, as with plantar stimulation. With breath held when the eyes were closed, power became smaller

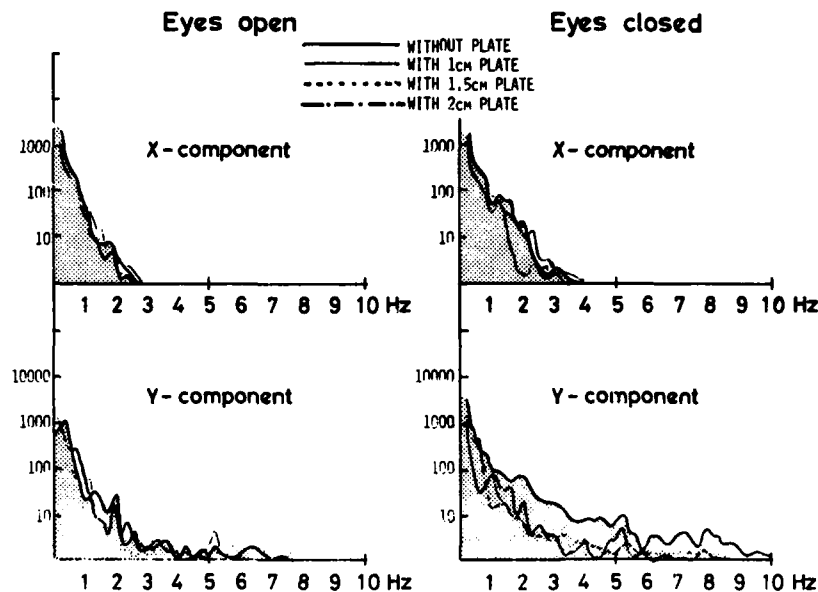


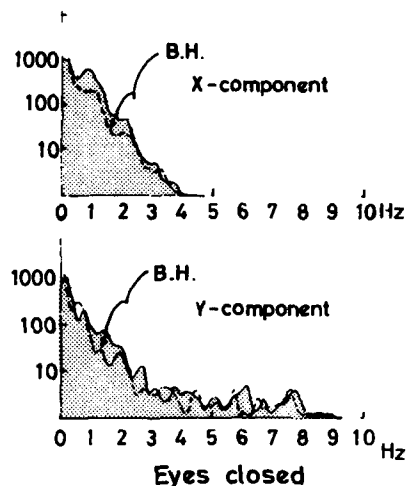
FIGURE 7. Change of power spectrums due to influence of plantar stimulations. Subject N.K., age 25, male (normal).

in 6 cases out of 10 at the low frequencies of 1 to 2 Hz, as shown by the dotted line in the figure. This phenomenon was present in both the X- and Y-components.

DISCUSSION AND CONCLUSION

Ever since Magnus,¹⁰ the labyrinth, proprioceptive, visual, and touch receptors have been considered to be important factors for the control of body equilibrium. The objective of gravimetric analysis is to observe these control mechanisms as a whole, expressed as the center-of-gravity sway. However, the factors that rule body sway are not limited to those mentioned above; psychologi-

FIGURE 8. Change of power spectrum due to influence of breath holding. Same subject as in FIGURE 7.



cal factors also are involved, which makes the analysis more complicated. Of all these factors, the plantar pressure receptor's role in the control of sway is not yet well known. Empirically, neurological patients with equilibrium disturbances often assume a legs-open posture, and some cases of spinocerebellar degeneration can be diagnosed from some fine movements of the instep or toes. By observing these movements when the plantar surface touched the ground, some fine movements could be observed, reflecting constant efforts to central swaying. This means that the plantar mechanoreceptors maintain the center-of-gravity resistance while they forward this pressure information to the central nervous system for equilibrium control.

In order to cope with these delicate pressure changes, we used mechanical stimulation to study the influence of the information on recovery. At the same time, the characteristics of the mechanoreceptor were studied in comparison with the changes in body sway under the influence of breathing conditions. The

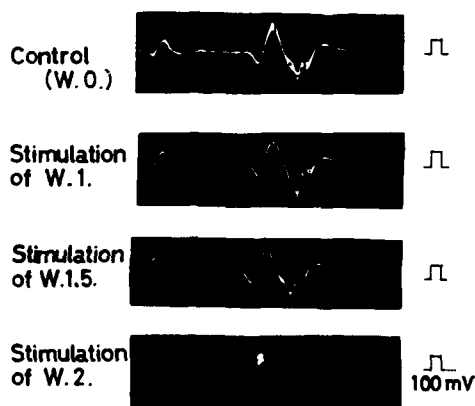


FIGURE 9. M-wave and H (Hoffmann) response to mechanical plantar stimulation by shotgun-ball plates.

characteristics of the receptors are summarized as follows: W1 and W1.5 stimulus plates were effective in changing body-sway area and sway-shift length. The results of the tibial-nerve neuron discharge showed an evident increase on the W1 and W1.5 plates. It will be interesting to find out through what process these increased discharges are contributing to control.

We recorded Hoffmann's reflex simultaneously with this experiment (FIGURE 9). The result was that there was no change of M and H waves when subjects were on the different stimulus plates. From this fact, we are obliged to think that the stimulation of plantar mechanoreceptors under the experimental conditions did not produce its influence only at the spinal level but was input to a higher level of the nervous system.

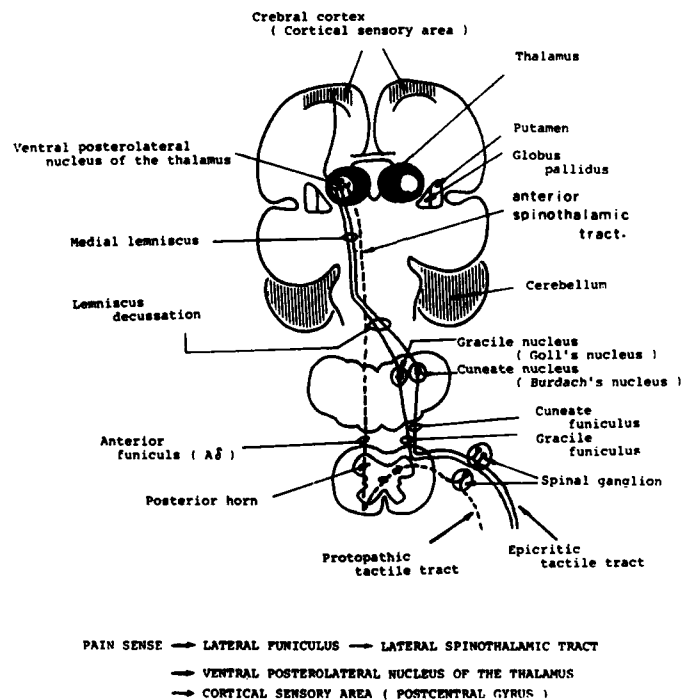


FIGURE 10. Schema of the lemniscal system (by Bowsher and Albe-Fessard).¹²

The anterior spinothalamic pathway reacts to touch and pressure sensation. Bowsher and Albe-Fessard report that the anterior spinothalamic tract is well developed in human beings and monkeys, which stand on two feet, and emphasize its importance.¹² This system is made of relatively large fibers of the Aδ type. In another of our experiments on patients with spinocerebellar degeneration, where the plantar mechanoreceptors were stimulated with wire net, sway-speed control was "slow."¹³ These results agree with Marseden et al.'s experiment on the arms, where they demonstrated an effect of motor receptors from the skin sensory systems.¹¹ We believe there is an important neural pathway

from the palms and the plantar surface of the foot. In our experiments, where the sole surface is evenly and totally stimulated, the W1 stimulation condition evidently was more effective than was W2 stimulation.

For the transmittance of this information, the systems illustrated in FIGURE 10 are known to be involved; of these, the posterior column tract and the anterior spinothalamic tract have been identified. Particularly, the epicritic pathway in the medial lemnisci of the posterior column participates in identification of species and has a role in the integral circuit.

Also, while treating a patient with Parkinson's disease, we found that when the plantar-stimulation test was done, at the stage when the tremor disappeared, recurrence of tremor occurred in combination with body sway. We now are inclined to think from these factors that the plantar-input information either directly or indirectly influences muscle-rhythm control at the cerebral-basal-ganglia level. In addition, we studied the mechanoreceptor stimulation's influence on the electroencephalograph, but there was no change.

The influences of breath holding on body sway tended to decrease the sway area and the shift length from those with plantar-mechanoreceptor stimulation. Actually the mean values are smaller while the standard deviations (SD) are large. These decreases in area and shift length must be reflecting the influence of chest and abdominal breathing. But, as McCaffrey and Kern advocate,^{17,18} autonomic-nervous-system reaction should be taken into consideration in view of the change in CO₂ concentration in various types of respiration, which affects the influence of the nasal mucous membrane on the autonomic nervous system. This will be a study for the future.

At any rate, the power-spectrum analysis of the factors controlling body sway revealed the power response to be at about 1-2 Hz when the breath was held, while in the case of plantar-mechanoreceptor stimulation, the power response was seen at 3-5 Hz. As these two sway-control factors had different response frequencies, involvement of different control systems is suggested. In breath holding, influence of chest and abdomen movements may be considered; but with mechanoreceptor stimulation, the system that may be involved in the motor control must be at the basal-ganglia level, in view of the relatively fast frequency at 3-5 Hz.

REFERENCES

1. BARON, J. B. 1964. Présentation d'un appareil pour mettre en évidence les déplacements du centre de gravité du corps dans le polygone de sustentation. *Arch. Mal. Prof.* 25: 41-49.
2. SUGANO, T., et al. 1970. Measurement of body movement and its clinical applications. *Jpn. J. Physiol.* 20: 296-308.
3. HIRASAWA, Y. 1973. Study of human standing ability. *Agressologie* 14c: 37-44.
4. WATANABE, I., et al. 1978. Sway of the center of gravity by gravigonimetric test. 1. Fundamental study. *Equilibrium Res.* 37: 228-238. (Japanese.)
5. OKUBO, J. & I. WATANABE. 1979. Influence of foot position and visual field condition in the examination for equilibrium function and sway of the center of gravity in normal persons. *Agressologie* 20: 127-132.
6. OKU, T., et al. 1979. The influence of foot posture and visual input on swaying of the center of gravity. In *Symposium on Posturography*: 115-122. Nara Prefectural Medical College Press. Nara City, Japan.
7. ADRIAN, E. D. 1947. *The Physical Background of Perception*. Oxford Clarendon Press. Oxford, England.
8. ADRIAN, E. D. 1928. *The Basis of Sensation*. Christophers. London, England.

9. WATANABE, I., *et al.* 1976. Postural equilibrium and respiratory rhythm. *Agressologie* 17A: 45-50.
10. OSCCARSON, O. 1973. Functional organization of spinocerebellar paths. In *Handbook of Sensory Physiology*. A. Iggo, Ed. 2: 339-380. Springer Verlag. Berlin, Heidelberg & New York.
11. MARSDEN, C. D., P. A. MERTON & H. B. MOTON. 1976. Servo action in the human thumb. *J. Physiol.* 257: 1-44.
12. BOWSER, D. & J. C. ALBE-FESSARD. 1965. The anatomophysiological basis of somato-sensory discrimination. *Int. Rev. Neurobiol.* 8: 35-75.
13. OKUBO, J., *et al.* 1979. Plantar pressure receptors and body sway in cases of spinocerebellar degeneration. *Equilibrium Res.* 38: 207-215. (Japanese.)
14. HAGEBARTH, K. E. 1960. Spinal withdrawal reflexes in the human lower limbs. *J. Neurol. Neurosurg. Psychiatry* 23: 222-227.
15. HAGEBARTH, K. E. & A. B. VALLBO. 1968. Discharge characteristic of human muscle afferents during muscle stretch and contraction. *Exp. Neurol.* 22: 674-694.
16. VALLBO, A. B. 1971. Muscle spindle at the onset of isometric voluntary contractions in man. Time difference between fusimotor and skeletomotor effects. *J. Physiol.* 318: 405-431.
17. MCCAFFREY, T. V. & E. B. KERN. 1979. Response of nasal airway resistance to hypercapnia and hypoxia in the dog. *Acta Otolaryngol.* 87: 545-553.
18. MCCAFFREY, T. V. & E. B. KERN. 1979. Response of nasal airway resistance to hypercapnia and hypoxia in man. *Ann. Oto-Laryngol.* 88: 247-252.
19. MAGNUS, R. 1924. *Korperstellung*. Julius Springer. Berlin, Germany.

OCULAR TORSION IN THE CAT AFTER LESIONS OF THE INTERSTITIAL NUCLEUS OF CAJAL*

John H. Anderson†

Departments of Otolaryngology and Physiology
University of Minnesota Medical School
Minneapolis, Minnesota 55455

INTRODUCTION

Sensory inputs from the vertical semicircular canals and otolith organs help to maintain gaze during changes in head posture relative to gravity. It is known that both the canal and otolith inputs can contribute to this vestibulo-ocular reflex (VOR).¹ However, the way in which these inputs interact, vis-à-vis the VOR, and the central nervous system (CNS) structures and pathways that are important for this are not well delineated. One aspect of this problem is to quantitate the responses to each input when it is present alone, such as has been done with pure vertical canal and otolith stimulation.¹⁻⁴ Regarding the CNS structures, considerable evidence based on lesion studies, single-unit recording, and clinical case reports suggests that the interstitial nucleus of Cajal (INC) and certain other areas of the midbrain are important for controlling vertical gaze.⁵⁻¹⁶ In this regard it has been found that lesions of the INC significantly change the characteristics of the VOR during pure vertical canal stimulation.²

The present work further examines the VOR: the response to stimulation of the otolith organs during static lateral tilt. In this case, the response is a rotation of the eyes opposite to the head tilt and is assumed not to be influenced by the semicircular canals. The objective of the study was to compare the amount of ocular counterrolling in normal and INC-lesioned cats and thereby to provide some evidence that might suggest whether or not the INC plays a role in the canal-otolith interactions vis-à-vis the vertical VOR.

METHODS

Alert, restrained cats were used. To allow for tilting, a given animal was placed in a box to which the animal's head was attached firmly by means of bolts chronically implanted into the skull. The animal box was fixed to a small gimbal structure, which permitted the entire cat to be tilted onto its side. During the tilt, the otolith organs were stimulated by changes in the components of gravity along the animal's coordinate axes.¹⁸ In particular, the component along the cat's transverse (interaural) axis is assumed to have been the effective stimulus. It is proportional to $\sin \theta$, where θ is the angle of head tilt.

The eyes of the cat were photographed with a 35-mm camera, which was positioned directly in front of the animal and focused on the midpoint between

*This work was supported by grants from the North Atlantic Treaty Organization, the National Institute of Neurological and Communicative Disorders and Stroke (RO1-NS 16567; P50-NS12125), and the University of Minnesota Graduate School.

†Supported by a Research Career Development Award (K04-NS00395).

the eyes. To discount possible transient responses due to head movement, photographs were not taken until 60 seconds after the cat had been positioned. The negatives of the film were projected onto a flat surface with a print enlarger so that the eyes could be seen easily and direct measurements made on the orientation of the animal's pupils. The direction of orientation is that of the upper edge of the pupil: nasally directed is referred to as inward, and temporally directed as outward. In order to facilitate the measuring, three drops of a 3% ophthalmic solution of carbachol chloride were put on the surface of each eye, one-half hour before photographing. This had the effect of constricting the pupils into a slit, so that the orientation of the pupils could in fact be measured. An example of one normal cat is shown in FIGURE 1 (top).

Although this technique is straightforward, there are several sources of measurement error that should be noted. Among these are the alignment of the camera relative to the cat, the position of the film within the camera, and the



FIGURE 1. The pupil orientation is shown for a normal cat (top) and a cat with a kainic acid lesion of the left INC (bottom). Note that the pupils were constricted by carbachol chloride.

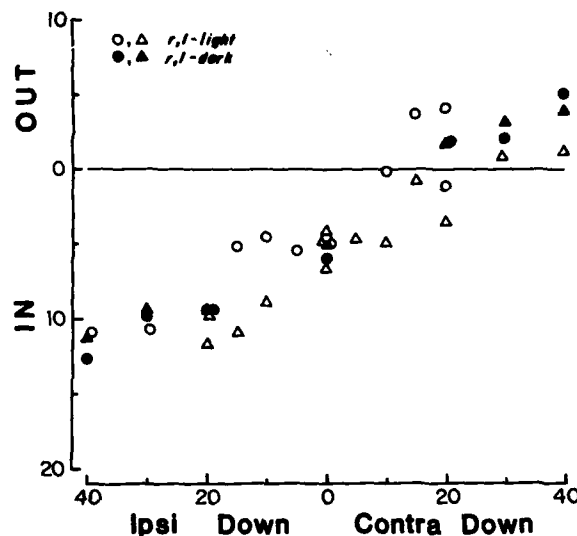


FIGURE 2. Measurements of the pupil orientation for one normal cat during static lateral tilt with the side ipsi or contra to the eye being down. The upper edge of the pupil defines its orientation: IN for nasally directed; OUT for temporally directed. Each data point is the mean of five measurements from photographs taken in the light [O, right (r); Δ , left (l)] or dark [● (r); \blacktriangle (l)].

position of the film negative within the print enlarger. Another source of error is the pupil itself. During the course of one photographing session ($\frac{1}{2}$ to $1\frac{1}{2}$ hours), the shape of the pupil sometimes would change, likely due to changes in local carbachol chloride concentration, which would affect the pupillary muscle contraction. It is estimated that all together these errors give a measurement accuracy of about $\pm 1.0^\circ$. The resolution of the measurement itself is about $\pm 0.3^\circ$.

Kainic acid lesions of the interstitial nucleus of Cajal were made by stereotaxically injecting $0.75 \mu\text{l}$ of a phosphate buffer containing $0.75 \mu\text{g}$ of kainic acid. The lesion, as judged by glial proliferation and the loss of INC neurons, typically extended from A4.5 to A6.5 (Horsley-Clark coordinates), about 2 mm in diameter.

RESULTS

Normal Animals

The counterrotation of the eyes was determined by measuring the pupil orientation in four normal cats. For two of the animals, two situations were used: (a) with the room lights on, and (b) in complete darkness. In the latter case, a strobed flash—synchronized to the shutter opening (duration of approximately 8 msec)—was used to photograph the pupils. Comparing the data from the two situations, no significant differences were found. It therefore will be assumed

that visual inputs were not affecting the eye position significantly in the present experimental situation.

Measurements of pupil orientation for one animal are plotted in FIGURE 2. In the absence of any head tilt, the upper edge of both pupils was directed inward by about 4-6°. While the animal was tilted, there was a change as the eyes counterrotated: for the eye ipsilateral to the side that was tilted down, the pupil

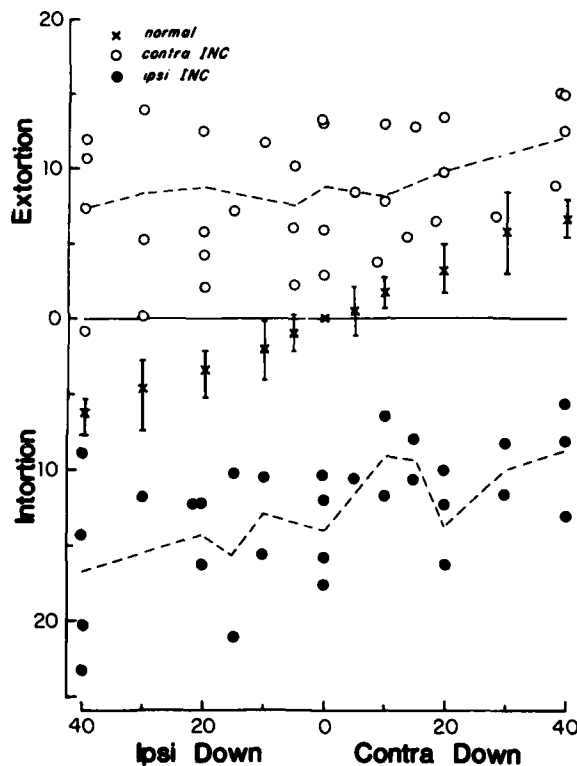


FIGURE 3. Ocular counterrolling during static lateral tilt. \times : mean (\pm standard error) of pupil orientations, normalized to 0° for no tilt, for four normal cats. Circles are data from three cats with unilateral kainic acid lesions of the INC, each point being the mean value for 10 measurements (from one animal) of pupil orientation for the eye ipsi- (●) or contralateral (○) to the lesion. Dashed lines are mean values of the circles. Note: 5.5° have been added to each point for the lesioned animals. Ipsi- and contralateral side down are in reference to the eye.

was more inward directed; for the other, contralateral eye, it was less inward or was outward directed. To emphasize the eye movements, the pupil orientations were normalized to 0° for the case of no head tilt. Changes due to a tilt then are referred to as intortion-extortion. This was done for data (obtained from photographs taken in the light) from the four normal cats and is shown in FIGURE 3. The mean values (\times) show changes of about 5-6° for 40° of head tilt to either side.

INC-Lesioned Animals

In three cats, kainic acid was used to make a unilateral lesion of the INC. In these animals, an asymmetry in pupil orientation was present. This was observed within 24 hours of the injection and still was present three months later. An example of the asymmetry is shown in FIGURE 1 (bottom). In this animal, the left INC had been lesioned. Note that the left pupil is rotated inward and the right pupil is rotated slightly outward, in marked contrast to a normal cat, such as shown in FIGURE 1 (top). FIGURE 3 shows the amount of asymmetry and counterroll for the three unilateral INC cats. The eye contralateral to the lesion (O) was extorted throughout most of the range of tilting, the amount varying from 0-12°. In contrast, the eye ipsilateral to the lesion (●) was intorted from 5-15° throughout. Note that 5.5° were added to all data points for the INC cats in order to facilitate a comparison with the normal data (x).

In two cats, bilateral lesions of the INC were made. For these animals there was no asymmetry in pupil orientation when the head was in the normal upright position. Over the range of tilting used, 40°, the amount of ocular counterroll was not significantly different from that of normal cats (cf. FIGURE 3).

DISCUSSION

In the present experiments, ocular counterroll was measured. For static tilts of $\pm 40^\circ$, the eyes rotated 5-6° in normal cats. For this range of tilt and within the limitations of the measurement techniques used, no significant difference was found with the animals in the dark compared to in the light. Under other stimulus conditions, however, visual inputs may have a significant effect. It is known that optokinetic stimuli, such as a rotating disc with alternate black and white sectors, can cause torsional eye movements.¹⁷ Also, in man, tilting head movements performed by the subject himself in the light cause slow eye movements that are interrupted frequently by torsional saccades.¹⁸ Regarding the latter, Petrov and Zenkin reported that between the rapid changes in eye orientation due to the saccades, the slow-phase eye movements did compensate for the head tilt.¹⁸ In contrast, the slow-phase eye movements observed in the dark compensated less well for the head movements, and there were fewer saccades. This suggests that in man, when both visual and vestibular inputs are present, ocular counterroll may be able to stabilize gaze for small transient changes in head position relative to gravity.

This behavior is in contrast to what was found in the present experiments, wherein only static tilts were used: the amount of counterroll was much less than the amount of head tilt, on the order of 10-20%. This low gain is in agreement with the results of other investigators who used lateral tilt,¹⁹⁻²¹ and also is similar to what has been found during dynamic vestibular (i.e., otolith) stimulation in the dark.^{4,21} Otolith inputs by themselves seem to have a relatively small effect on compensatory eye movements, although they do make significant contributions when other sensory inputs, e.g., semicircular canal and visual, are present.^{1,22}

The results from the animals with lesions of the interstitial nucleus of Cajal suggest that the INC can influence the torsional position of the eyes. Unilateral lesions caused an asymmetrical positioning of both eyes, which was present during head tilt as well as in the absence of any head tilt, indicating an imbalance in tonic inputs to the extraocular muscles. This behavior seems to be different in one respect from that described by Hassler and Hess and Szentágothai.^{5,23} They

made electrolytic lesions of the INC and described an abnormal torsion of the eyes if the head was held in a normal, upright position or rotated to one side.^{24,6} One possible reason for the difference is that in the earlier experiments electrolytic lesions were made, while for the present kainic acid was used. The former would have destroyed not only the neurons but also the fibers traversing the region of the INC, among which are fibers from the contralateral INC and projections to the rostral interstitial nucleus of the medial longitudinal fasciculus.^{7,25,26}

Compared to normals, the unilateral INC-lesioned animals tended to show less of a change in the amount of counterroll when comparing ipsi- and contralateral side down, although there was considerable scatter in the data. The decreased response during tilt might have been due to the tonic bias to the motoneurons and asymmetry in muscle activation or, alternatively, to a decreased otolith input to the motoneurons. Pertinent to the latter possibility are the results from the bilateral INC-lesioned animals. In these there was no significant asymmetry in eye position. Comparing ipsi- and contralateral side down, the changes in counterroll were similar to those in the normal cats. This suggests that the ocular response to static otolith stimulation, per se, is not directly under the influence of the INC and that the decreased response in the unilateral INC animals may have been due to a tonic bias. It should be noted, however, that dynamic ocular responses to pure otolith stimulation might be affected differently.

In contrast to the present results, bilateral INC lesions do change the VOR responses during stimulation of the vertical semicircular canals,² suggesting that the INC is necessary for the integration of an eye-velocity signal (due to the canal inputs) into an eye-position signal.²⁷ The effect of INC lesions on the vertical VOR during pitch rotations,²² wherein both canal and otolith inputs are present, thus would seem to be due in large part to effects on the canal contribution to the VOR. Whether or not the dynamic otolith contribution is affected remains to be determined.

REFERENCES

1. PETTOROSI, V. E. & N. H. BARMACK. 1978. The influence of bilateral plugging of the anterior or lateral semicircular canals on vertical and horizontal vestibulo-ocular reflexes in the rabbit. *Soc. Neurosci. Abstr.* 4: No. 1956.
2. ANDERSON, J. H. 1981. Behavior of the vertical canal VOR in normal and midbrain lesioned cats. *Prog. Oculomotor Res.* (In press.)
3. DARLOT, C., J. LÓPEZ-BARNEO & D. TRACEY. 1981. Asymmetries of vertical vestibular nystagmus in the cat. *Exp. Brain Res.* 41: 420-426.
4. BAARSMA, E. A. & H. COLLEWIJN. 1975. Eye movements due to linear accelerations in the rabbit. *J. Physiol.* 245: 227-247.
5. SZENTÁGOTHAÏ, J. 1943. Die zentrale innervation der Augenbewegungen. *Arch. Psychiatr. Nervenkr.* 116: 721-760.
6. HESS, W. R. 1948. Zwischenhirn und Motorik. *Helv. Physiol. Pharmacol. Acta. Suppl.* 5.
7. CARPENTER, M. B., J. W. HARBISON & P. PETER. 1970. Accessory oculomotor nuclei in the monkey: projections and effects of discrete lesions. *J. Comp. Neurol.* 140: 131-154.
8. PASIK, P., T. PASIK & M. B. BENDER. 1969. The pretectal syndrome in monkeys. I. Disturbances of gaze and body posture. *Brain* 92: 521-534.
9. KÖMPF, D., T. PASIK, P. PASIK & M. B. BENDER. 1979. Downward gaze in monkeys: stimulation and lesion studies. *Brain* 102: 527-558.
10. BÜTTNER, U., J. A. BÜTTNER-ENNEVER & V. HENN. 1977. Vertical eye movement related

- unit activity in the rostral mesencephalic reticular formation of the alert monkey. *Brain Res.* **130**: 239-252.
11. KING, W. M. & A. F. FUCHS. 1979. Reticular control vertical saccadic eye movements by mesencephalic burst neurons. *J. Neurophysiol.* **42**: 861-876.
 12. KING, W. M., W. PRECHT & N. DIERINGER. 1980. Synaptic organization of frontal eye field and vestibular afferents to the interstitial nucleus of Cajal in cat. *J. Neurophysiol.* **43**: 912-928.
 13. HALMACYI, G. M., W. A. EVANS & J. M. HALLINAN. 1978. Failure of downward gaze: the site and nature of the lesion. *Arch. Neurol.* **35**: 22-26.
 14. CHRISTOFF, N. 1974. A clinicopathologic study of vertical eye movements. *Arch. Neurol.* **31**: 1-8.
 15. TROJANOWSKI, J. Q. & S. H. WRAY. 1980. Vertical gaze ophthalmoplegia: selective paralysis of downgaze. *Neurology* **30**: 605-610.
 16. SOECHTING, J. F., J. H. ANDERSON & A. BERTHOZ. 1977. Dynamic relations between natural vestibular inputs and activity of forelimb extensor muscles in the decerebrate cat. III. Motor output during rotations in the vertical plane. *Brain Res.* **120**: 35-47.
 17. BRECHER, G. A. 1934. Die optokinetische Auslösung von Augenrollung und rotatorischem Nystagmus. *Pfluegers Arch. Gesamte Physiol. Menschen Tiere* **234**: 13-28.
 18. PETROV, A. P. & G. M. ZENKIN. 1973. Torsional eye movements and constancy of the visual field. *Vision Res.* **13**: 2465-2477.
 19. HANNEN, R. A., M. KABRISKY, C. R. REPLOGLE, V. L. HARTZLER & P. A. ROCCAFORTE. 1966. Experimental determination of a portion of the human vestibular system response through measurement of eyeball counterroll. *IEEE Trans. Biomed Eng.* **13**(2): 65-70.
 20. DIAMOND, S. G., C. H. MARKHAM, N. E. SIMPSON & I. S. CURTHOYS. 1979. Binocular counterrolling in humans during dynamic rotation. *Acta Otolaryngol.* **87**: 490-498.
 21. WOELLNER, R. C. & A. GRAYBIEL. 1959. Counterrolling of the eyes and its dependence on the magnitude of gravitational or inertial force acting laterally on the body. *J. Appl. Physiol.* **14**(4): 632-634.
 22. ANDERSON, J. H., W. PRECHT & C. PAPPAS. 1979. Changes in the vertical vestibulo-ocular reflex due to kainic acid lesions of the interstitial nucleus of Cajal. *Neurosci. Lett.* **14**: 259-264.
 23. HASSLER, R. & W. R. HESS. 1954. Experimentelle und anatomische Befunde über die Drehbewegungen und ihre nervösen Apparate. *Arch. Psychiatr. Nervenkr.* **192**: 488-526.
 24. HASSLER, R. 1972. Supranuclear structures regulating binocular eye and head movements. *Bibl. Ophthalmol.* **82**: 207-219.
 25. BÜTTNER-ENNEVER, J. A. & U. BÜTTNER. 1978. A cell group associated with vertical eye movements in the rostral mesencephalic reticular formation of the monkey. *Brain Res.* **151**: 31-47.
 26. GRAYBIEL, A. M. 1977. Organization of oculomotor pathways in the cat and rhesus monkey. *Dev. Neurosci.* **1**: 79-88.
 27. ROBINSON, D. A. 1975. Oculomotor control signals. In *Basic Mechanisms of Ocular Motility and Their Clinical Implications*. P. Bach-y-Rita & G. Lennerstrand, Eds.: 337-374. Pergamon Press, Elmsford, N.Y.

Index of Contributors

A
 Adler, B. 284-302
 Aiba, T. 846-854
 Akert, K. 157-170
 Anderson, J. H. 865-871
 Arai, Y. 571-578
 Arrott, A. P. 80-92
 Aschoff, J. C. 831-838

B
 Babin, R. W. 112-129
 Baker, R. 171-188
 Baloh, R. W. 600-613
 Barin, K. 722-730
 Barnes, G. R. 560-570
 Becker, W. 361-372, 744-754
 Bender, M. B. xiii
 Berthoz, A. 144-156
 Bilotto, G. 395-402
 Bizzini, B. 157-170
 Bles, W. 590-599
 Bock, O. L. 352-360
 Bovenkerk, G. 590-599
 Boyle, R. 373-394
 Brandt, Th. 636-649
 Brecha, N. C. 215-229
 Bredberg, G. 11-19
 Bretlau, P. 820-830
 Büttner, U. 274-283, 491-503
 Büttner-Ennever, J. A. 157-170

C
 Castelnuovo, P. 706-721
 Chubb, M. C. 446-454
 Claus, D. 831-838
 Clement, G. 340-351
 Cohen, B. xi, 44-55, 421-433
 Collewijn, H. 284-302, 312-329
 Courjon, J. H. 340-351
 Crandall, W. F. 249-261
 Crites, T. A. 80-92
 Curio, G. 284-302
 Curthoys, I. S. 189-209

D
 Deecke, L. 361-372, 650-655
 de Jong, J. M. B. V. 590-599
 Dennett, D. 421-433
 Diamond, S. G. 69-79
 Dichgans, J. 434-445

E
 Edelman, E. R. 80-92
 Evinger, C. 171-188

F
 Fernández, C. 40-43
 Fiebig, E. 674-688
 Fuchs, A. F. 446-454

G
 Goldberg, J. 395-402
 Goldberg, J. M. 40-43
 Graf, W. 20-30
 Gresty, M. 614-618
 Grob, P. 157-170
 Grüsser, O.-J. 284-302

H
 Halmagyi, G. M. 614-618
 Harada, Y. 31-39
 Henn, V. 44-55, 274-283, 330-339, 421-433, 491-503
 Henriksson, N. G. 774-783
 Highstein, S. M. 102-111, 210-214
 Hirata, K. 31-39
 Hiwatashi, S. 731-743
 Honrubia, V. 600-613
 Hood, J. D. 532-539
 Hudspeth, A. J. 1-10

I
 Igarashi, M. 656-673
 Ikeda, S. 56-68
 Ito, J. 93-101

J
 Jacobs, R. 1-10
 Jäger, J. 330-339
 Jeannerod, M. 340-351
 Jirout, J. 839-845
 Johnsen, N. J. 820-830
 Jürgens, R. 744-754

K
 Kaga, K. 412-420
 Kamio, T. 526-531
 Karten, H. J. 215-229
 Kato, I. 455-464, 755-763, 764-773
 Katsarkas, A. 784-793
 Kawasaki, T. 455-464
 Keller, E. L. 249-261
 Kimura, M. 476-490
 Kimura, Y. 755-763, 764-773
 Kishimoto, S. 731-743
 Koenig, E. 434-445
 Koike, Y. 764-773
 Koozekanani, S. H. 722-730
 Krafczyk, S. 636-649
 Krejci, L. 839-845
 Krejcova, H. 839-845
 Kubo, T. 656-673

L
 Lacour, M. 403-411
 Lahue, R. H., Jr. 262-273
 Landolt, J. P. 262-273
 Leigh, R. J. 619-635
 Lichtenberg, B. K. 80-92

Lisberger, S. G. 513-525

Löf, G. 11-19

Lyttkens, L. 11-19

MMaekawa, K. 476-490

Magenes, G. 689-705

Malsbenden, I. 636-649

Mandl, G. 303-311

Markham, C. H. 69-79, 189-209

Marsh, R. R. 412-420

Martins, A. J. 312-329

Masaki, M. 56-68

Matsuoka, I. 93-101

McCabe, B. F. 112-129

McCrea, R. A. 171-188

Melville Jones, G. 303-311

Mergner, T. 361-372, 650-655

Mevio, E. 706-721

Miles, F. A. 513-525

Mira, E. 706-721

Miyata, H. 56-68

Miyoshi, T. 731-743

Mizukoshi, K. 455-464, 755-763, 764-773

Mizuno, M. 579-589

Money, K. E. 262-273

Morimoto, M. 93-101

NNaito, M. 579-589

Nakamura, T. 764-773

Nakao, S. 189-209

Noda, H. 465-475

OOkubo, J. 855-864

Oman, C. M. 80-92, 352-360

O-Uchi, T. 656-673

Outerbridge, J. S. 784-793

PPause, M. 284-302

Peterson, B. W. 395-402

Plester, D. 650-655

Pompeiano, O. 373-394

Pote, K. G. 808-819

Precht, W. 230-248

Prosser, A. J. 560-570

Pyykkö, I. 774-783

RRaphan, T. 44-55, 421-433

Rarey, K. E. 808-819

Rask-Andersen, H. 11-19, 794-807

Reinis, S. 262-273

Reisine, H. 102-111

Rezek, P. 839-845

Rieger, P. 744-754

Robinson, D. A. 504-512, 619-635

Ross, M. D. 808-819

Ryu, J. H. 112-129

SSasa, M. 93-101

Sasaki, S. 130-143

Sato, Y. 455-464

Schaefer, K.-P. 674-688

Schalén, L. 774-783

Schessel, D. A. 210-214

Schmid, R. 340-351, 689-705

Schreiter, U. 284-302

Schultheis, L. W. 504-512

Sekine, S. 526-531

Shimazaki, C. 571-578

Shimazu, H. 130-143

Shimizu, M. 526-531

Shimizu, N. 579-589

Shizawa, R. 846-854

Shotwell, S. L. 1-10

Simpson, J. I. 20-30

Stahle, J. 794-807

Stark, L. 540-559

Steinman, R. M. 312-329

Stockwell, C. W. 722-730

Stracarova, B. 839-845

Stüss, K.-J. 674-688

Suzuki, J.-I. 412-420, 526-531

TTakaori, S. 93-101

Takeda, T. 476-490

Takemori, S. 846-854

Tamada, A. 731-743

Tanaka, Y. 412-420

Thomsen, J. 820-830

Tokita, T. 56-68

Tos, M. 820-830

UUemura, T. 571-578

Verma, L. M. 808-819

Vidal, P. P. 144-156, 403-411

Waespe, W. 491-503

Watanabe, I. 855-864

Watanabe, Y. 755-763

Weiss, L. 284-302

Wennmo, C. 774-783

Wilbrand, H. F. 794-807

Wilson, V. J. 395-402

Xerri, C. 403-411

Yagi, T. 526-531

Yee, R. D. 600-613

Yoshida, K. 144-156

Yoshida, M. 579-589

Young, L. R. 80-92

Zambarbieri, D. 689-705

Zangemeister, W. H. 540-559

Zanocco, P. 706-721

Zee, D. S. 619-635

Subject Index

- A**ccessory optic system (AOS), 215-229
 functional organization of, 225-228
 retinal projections, 216-218
- Accuracy of gaze, 579-589
 apparatus, 581
 data analysis, 581-582
 discussion, 588
 dysmetric versus gain of VOR, 587-588
 experimental procedures, 581
 head movements and, 582-587
 introduction, 579
 methods, 579-582
 neuro-otological findings, 582
 results, 582-588
 subjects, 579-581
- Acoustic-induced eye movements, 674-688
 discussion, 684-686
 introduction, 674-675
 involuntary, 680-684
 methods, 675-676
 summary, 686-687
 voluntary, 676-680
- Acoustic trauma, 650-654
- Activation of the flocculus, 476-490
 comments, 488
 horseradish peroxidase (HRP) injections, 477-479, 484
 introduction, 476
 latency distribution, 483-484
 mossy fiber potentials and NRTP stimulation, 479-480
 neuronal activity of NRTP neurons, 480-484
 neuronal recording sites, histological examination, 484
 NOT and, 476, 478, 484, 485, 486, 487, 488
 orthodromic and antidromic activation, 480-483
 pretectal region, 484-488
 pretectal relay neurons, 484-488
 Purkinje cells, 476-477
 visual mossy fiber afferents, 477-484
- Active body movement, sigma-movement, 293
- Active head rotations, 540-559
 coordinated gaze types, 541, 551-554
 gaze-plane analysis, 554-556
 gaze types, 548-551
 influences on frequency of gaze types, 558
 instantaneous change of CEM gain, 556-557
- introduction, 540
 latency in coordinated gaze, 547-548
 main sequence, 541-542
 neck muscle EMG, 542-545
 results and discussion, 541-557
 types of head model accelerations, 545-547
 variability, 557
- Activity of the flocculus, 491-503
 conflicting visual-vestibular stimulation, 494
 discussion, 497-502
 input activity, 492-497
 introduction, 491
 methods, 491-492
 optokinetic nystagmus, 491, 492
 optokinetic stimulation, 492, 497
 output activity, 497
 Purkinje cells, 492, 497, 499
 results, 492-497
 simple spike (SS) activity, 496, 497, 498
- Adaptive gain control in the primate VOR, hypothesis, 521-524
- Aftereffects, vestibular and optokinetic stimulation and interaction, 434-445
 apparatus, 435
 discussion, 442-444
 experimental procedure, 435-437
 introduction, 434-435
 methods, 435-437
 OKAN and, 441
 pure vestibular stimulation, 437, 438
 results, 437-442
 subjects, 435
 summary, 444
 vestibular, despite prior fixation suppression, 437-441
 visual-vestibular interaction, 442
- Aftereffects of sigma-movements, 296
- Anterior suprasylvian (ASS) cortex (cat), 366, 369, 370-371, 372
 neuronal responses 361-363
- Antidromic activation, see Orthodromic and antidromic activation
- Antidromic spike, 481, 482-483
- Ascending tract of Deiters' (ATD), 102-111
 abducens nucleus, 103-106
 coronal sections, 104
 eye position, 102
 morphology of ATD neurons, 106
 pause signals and phases of nystagmus, 102-103

Ascending tract of Deiter's (Cont'd)

- unitary discharge rate, 108
- ventral lateral vestibular, 103, 106, 107, 109

Ataxia therapy, postural imbalance and, 636-649

- apparatus, posturography, and data analysis, 637-638
- basilar insufficiency, 636, 644
- blood flow, 639-640
- experimental procedure, 638-639
- head-extension vertigo, 636-637, 644
- introduction, 636
- methods, 637-639
- posture, 640-644
- results and comment, 639-644
- subjects, 637
- summary, 644-649

Avian accessory optic system, 215-229

- accessory optic nuclei, 215
- inferior olivary complex, 220-222
- introduction, 215-216
- nBOR complex, 218-220, 220-222, 223-224
- oculomotor complex, 223-224, 225
- retinal projections, 216-218
- second-order connections of, 215-216
- vestibulocerebellum, 219-220, 222

Basal ganglia diseases, saccades and, 758-759

- Basilar insufficiency, 636, 644
- Binocular counterrolling, 69-79
 - characteristics, 73, 74, 75
 - discussion, 77-78
 - introduction, 69-71
 - loss of labyrinthine function, 71
 - magnitude of (patients with unilateral inner ear disease), 72
 - methods, 71-72
 - results, 72-77
 - role of vision in OCR response, 77
 - utricle, 70, 77, 78

Body sway, 675**Brachium conjunctivum (BC), 103****Brain-stem disorders, eye-velocity programming, 774-783**

- discussion, 780-782
- introduction, 774
- material, 774-775
- medullary disorder, 779
- optokinetic nystagmus, 775, 779
- optovestibular nystagmus, 775, 779
- pontine disorder, 774
- progressive supranuclear palsy (PSP), 774
- results, 775-779
- rotation test, 776-779

smooth pursuit, 775-776

- summary, 782
- test procedure, 775
- voluntary saccades, 775, 776

Brain-stem lesions, saccades and, 759-760**Brain-stem lesions, visual suppression of nystagmus, 846-854**

- augmentation of caloric nystagmus in light, 847, 851
- discussion, 851-854
- introduction, 846
- methods, 846-851

Brain-stem projection, 455-464

- discussion, 460-463
- effect of NRTP lesion on optokinetic responses, 459-460
- field potentials in flocculus, 458-459
- to flocculus, 456-457
- introduction, 455
- methods, 455-456
- from NRTP to flocculus, 460-462
- precerebellar nucleus relevant to optokinetic responses, 463
- projection from caudal part of DNR to flocculus, 462
- results, 456-460
- role of NRTP in OKN, 462-463

Cat cortical cells (visual-vestibular interactions), 262-273

- animal preparation and data collection, 262-263
- calculation of receptive field characteristics, 263-264
- discussion, 271-272
- head-tilt, 262, 263-264, 265-269
- introduction, 262
- methods, 262-264
- receptive field characteristics, changes in following heavy water, 269-270
- receptive field characteristics, changes in following tilting, 265-269
- receptive field plots, 264-265
- results, 264-271

Cat medial pontine neurons, 189-209

- burst-tonic units, 194-196
- comparison of firing patterns of PRF units and identified premotor neurons, 196
- discussion, 206-207
- introduction, 189
- long-lead burst units, 194
- medium-lead burst units, 191-194
- methods, 190-191
- miscellaneous units, 196
- pause units, 196

- projection to the flocculus, 200-201
- projection of inhibitory pause neurons to burst inhibitory neurons, 201-206
- projection of PRF neurons to abducens nucleus, 196-200
- results, 191-206
- Central nervous system (CNS) disorders, 764-773
 - CT scanning, 769
 - introduction, 764
 - lesion sites of patients, 765
 - methods, 764-765
 - recording, 765-766
 - results, 766-770
 - subjects, 764-765
 - VOR gain, 765, 766, 767, 768, 769, 770-772
- Central nervous system (CNS) dysfunctions, *modifications of saccade*, 755-763
 - basal ganglia lesions, 758-759
 - brain-stem lesions, 759-760
 - cerebellar lesions, 759
 - conclusion, 762
 - data analysis, 756
 - discussion, 760-762
 - introduction, 755
 - method and material, 755-758
 - normal data, 756-757
 - optokinetic nystagmus, 757
 - pursuit eye tracking test, 757-758
 - recording eye movements, 755
 - results, 758-760
 - spinocerebellar ataxia, 760
 - target generation, 756
 - unilateral cerebral lesions, 758
- Cerebellar ataxia, accuracy of gaze, 579-589
 - apparatus, 581
 - data analysis, 581-582
 - discussion, 588
 - dysmetric gaze versus gain of VOR, 587-588
 - experimental procedures, 581
 - gaze with and without head movements, 582-587
 - introduction, 579
 - methods, 579-582
 - neuro-otological findings, 582
 - results, 582-588
 - subjects, 579-581
- Cerebellar dysfunction test, 528-531
 - clinical application, 528-529
 - discussion, 529-531
 - experiment sequence, 527
 - means and standard deviations, 527
 - methods, 528-527
 - phase changes of VOR, 529, 530
 - results, 527-528
- summary, 531
- VOR gains, 528, 529
- Cerebellar lesions, saccades and, 759
- Cervicocollic reflex, 398-400
 - interaction of, 400-401
- Chemical transmission, vestibular type I
 - hair cell and, 210-214
 - calyx or nerve chalice, 210, 211-212, 213
 - conclusions based on, 213
 - irregular fibers, morphophysiology of, 211-212
 - regular and irregular units, 211, 213
 - subthreshold activity, frequency and pattern, 212
- Circularvection (CV), 274-283
 - discussion, 278-282
 - introduction, 274
 - methods, 274-275
 - neurophysiology, 275, 277-278, 281-282
 - psychophysics, 274-275, 275-277, 278-281
 - results, 275-278
 - sinusoidal rotation, 274, 275, 276, 277, 278, 279, 280, 281, 282
 - summary, 282
- Circularvection (CV) adaptation, time course of, 355-356, 357
- Compensatory eye movements, combined muscular actions for, 27
- Computerized tomography, 831-838
 - cerebellar atrophies, 835
 - discussion, 834-837
 - Friedreich's ataxia, 831, 833, 834-835
 - introduction, 831
 - Marie's syndrome, 833, 834, 835, 836, 837
 - results, 831-834
 - summary, 837
- Contralateral labyrinth, second-order vestibular neurons activated from, 147-151
- Counterrolling, binocular, 69-79
 - characteristics, 73, 74, 75
 - discussion, 77-78
 - introduction, 69-71
 - loss of labyrinthine function, 71
 - magnitude of (patients with unilateral inner ear disease), 72
 - methods, 71-72
 - results, 72-77
 - role of vision in OCR response, 77
 - utricle, 70, 77, 78
- D**entate nucleus and y-group, 446-454
 - conclusions, 453
 - electrical stimulation, 452
 - introduction, 446
 - methods, 446-448
 - non-UHEV units, 451-452

- Dentate nucleus and y-group (Cont'd)
 results, 448-452
 upward head and eye velocity (UHEV)
 units, 448-450
- Directional hearing, 674, 676
- Directional plasticity, 504-512
 cross-axis ratio, 508, 509, 510
 discussion, 511
 introduction, 504-506
 methods, 507-508
 neural connections, 505
 results, 508-511
 vestibulocerebellum (nodulus and flocculi), 508
- Directional sensitivity, vertebrate hair cells, 1-10
 displacement-response curves, 8
 intracellular recordings, 2, 5, 6
 introduction to, 1-2
 kinocilium, 1, 3, 4
 materials and methods, 2-5
 receptor potentials, 6-7
 relationship between displacement of tip of hair bundle and cellular receptor potential, 8-9
 results, 5-8
 scanning electron microscopy, 3, 4
 symmetry, 1, 3
- Direction- and velocity-related visual mossy fibers, 468-473
- Direction-only visual mossy fibers, 466-468
- Discrete-visual-target motion, units responding to, 256-257
- Dissociation of the eyes, 731-743
 apparatus, 732-734
 data analysis, 734-736
 discussion, 741-742
 introduction, 731
 materials and methods, 732-736
 recording movement, 734
 results, 736-741
 subjects, 732
 summary, 742-743
- Disturbances during lateral gaze, 571-578
 bilateral lesions, 575-576
 comments and conclusions, 576-577
 electro-oculography, 571
 gaze overshoots, 577
 introduction, 571
 methods, 571-572
 results, 572-576
 terrestrial magnetic sensor, 571
 unilateral lesions, 572-575
 VOR gain, 572-573
- Diving competitors, vestibular and neurological disorders, 839-845
 biomechanics (board and tower diving), 840-841
- caloric and rotational tests, 842
 conclusion, 844-845
 discussion, 843-844
 EEG findings, 842
 eye tracking test (ETT), 840
 introduction, 839
 neurological findings, 841
 optokinetic nystagmus, 840
 positional nystagmus, 842
 subjects and methods, 839-840
 vestibulo-ocular findings, 841-842, 843
 x-ray findings, 842-843
- Dorsal nucleus of the raphe (DNR), caudal part of, 456, 457, 458-459, 460, 462, 463
 projection to flocculus, 462
- DNR stimulation, field potentials in flocculus following, 458-459
- Dysmetric gaze versus the gain of the VOR, frequency of occurrence, 587-588
- E**fference copy, 284, 285, 290, 299-301
- Electro-oculography (EOG), 45
- Endolymphatic duct, 11-19
 discussion, 16-18
 future experiments and, 17
 in a guinea pig, 12, 17
 introduction, 11
 materials and methods, 11-13
 resorption of endolymph, 17-18
 results, 13-15
- Endolymphatic sac (ELS), 802-805
- Equilibrium control, plantar mechanoreceptor, 855-864
 anterior spinothalamic pathway, 862-863
 data processing system, 856
 discussion and conclusion, 860-863
 introduction, 855
 methods, 855-856
 results, 856-860
 schema of lemniscal system, 862
- (Ethylenedinitrilo)-tetraacetic acid (EDTA), 812
- Extraocular muscles, oculomotor complex projections, 225
- Eye-head coordination, 540-578
 active head rotations, 540-554
 disturbances during lateral gaze, 571-578
 vestibular influence, 560-570
- Eye-head coordination, frontal-eye-field (FEF) lesion, 656-673
 discussion, 669-671
 duration of vestibular responses, 667
 eye-head coordination, 670-671
 eye movements, 670
 frequency of head and eye nystagmus, 661
 head deviation, 661-663

- head movements, 669-670
- introduction, 656-657
- methods, 657-658
- morphology, 667-669
- negative correlation of head and eye nystagmus, 663-665
- optokinetic responses, 660-669
- results, 658-669
- slow-phase eye velocity (SPEV), 660-661, 662
- slow-phase gaze velocity (SPGV), 660-661, 662, 665-667, 668
- slow-phase head velocity (SPHV), 660-661, 662
- spontaneous eye and head nystagmus, 658-659
- summary, 671
- tonic head deviation, 658, 659
- vestibular responses to rotation, 665-667
- Eye-movement recordings, EHA nystagmus and, 41
- Eye movements, acoustic-induced, 674-688
- Eye-muscle geometry, 20-30
 - compensatory eye movements, 27
 - discussion, 25-28
 - insertion points and lines of action, 24
 - introduction to, 20-21
 - kinematic characteristics, 21, 28
 - in man and rabbit, 25, 26
 - methods, 21-22
 - optic axis, 23
 - results, 22-24
 - spatial relations, 23
 - vestibulo-ocular reflexes, 21, 22
- Eye-velocity programming, 774-783
 - discussion, 780-782
 - introduction, 774
 - materials, 774-775
 - medullary disorder, 779
 - optokinetic nystagmus, 775, 779
 - optovestibular nystagmus, 775, 779
 - pontine disorder, 774
 - progressive supranuclear palsy (PSP), 774
 - results, 775-779
 - rotation test, 776-779
 - smooth pursuit, 775-776
 - summary, 782
 - test procedure, 775
 - voluntary saccades, 775, 776
- F**alling monkey, visual motion cues, 403-411
 - data processing, 405-406
 - discussion, 408-410
 - electromyographic (EMG) responses, 403
 - with enhanced (EV) or reduced (RV) visual input, 407-408
 - free-fall device, 404-405
 - introduction, 403
 - methods, 403
 - muscle responses, normal vision, 406-407
 - muscle responses, visual manipulations, 407-408
 - preparation, 403-404
 - in total darkness, 407
 - visual environment during falls, 405
 - with visual stabilization, 407
- Fixation of visual and acoustic targets, impaired suppression of nystagmus, 706-721
 - discussion, 716-720
 - fixation suppression, 706, 709-710, 712, 713-716, 718, 720
 - introduction, 706
 - methods, 707-709
 - results, 709-716
 - summary, 720
- Fixation of visual and nonvisual targets, modifications of nystagmus, 689-705
 - discussion, 699-703
 - eye-movement recording and data processing, 691-692
 - introduction, 689-690
 - methods, 690-692
 - nystagmus suppression, postrotational, 691
 - nystagmus suppression during sinusoidal head oscillations, 690
 - results, 692-698
 - smooth-pursuit (SP) system, 689-690, 691-692, 699-703
 - target fixation during sinusoidal head oscillations, 691
- Fixation suppression, 706, 709-710, 712, 713-716, 718, 720
 - aftereffects and, 437-441
- Flash frequency f_{σ} , sigma-movement and, 286-290
- Flash sequence, 293-294
- Flocculus, activation, 476-490
 - comments, 488
 - horseradish peroxidase (HRP) injections, 477-479, 484
 - introduction, 476
 - latency distribution, 483-484
 - mossy fiber potentials and NRTP stimulation, 479-480
 - neuronal activity of NRTP neurons, 489-484
 - neuronal recording sites, histological examination of, 484
 - NOT and, 476, 478, 484, 485, 486, 487, 488
 - orthodromic and antidromic activation, 480-483
 - pretectal region, 484-488
 - pretectal relay neurons, 484-488

Flocculus (Cont'd)

- Purkinje cells, 476-477
- visual mossy fiber afferents, 477-484
- Flocculus, activity of, 491-503
 - conflicting visual-vestibular stimulation, 494
 - discussion, 497-502
 - input activity, 492-497
 - introduction, 491
 - methods, 491-492
 - optokinetic nystagmus, 491, 492
 - optokinetic stimulation, 492, 497
 - output activity, 497
 - Purkinje cells, 492, 497, 499
 - results, 492-497
 - simple spike (SS) activity, 496, 497, 498
- Flocculus, cerebellar, optokinetic responses and, 455-464
 - brain-stem projection, 456-457
 - discussion, 460-463
 - effect of NRTP lesion on optokinetic responses, 459-460
 - field potentials, 458-459
 - introduction, 455
 - methods, 455-456
 - precerebellar nucleus relevant to optokinetic responses, 463
 - projection of caudal part of DNR, 462
 - projection from NRTP, 460-462
 - results, 456-460
 - role of NRTP in OKN, 462-463
- Flocculus, visual mossy fiber inputs, 465-475
 - direction-only, 466-468
 - direction- and velocity-related, 468-473
 - discussion, 473-474
 - introduction, 465
 - methods, 465-466
 - results, 466-473
 - smooth-pursuit eye movement, 465, 468-469, 474
- Frog semicircular canal, phasic components, 31-39
 - bubble displacement and coil voltage, 32
 - discussion, 37-39
 - introduction, 31
 - materials and methods, 31-32
 - results, 32-37
 - schematic representation, 32
 - semicircular canal, 31
- Frontal-eye-field (FEF) lesion, 656-673
 - discussion, 669-671
 - duration of vestibular responses, 667
 - eye-head coordination, 670-671
 - eye movements, 670
 - head deviation, 661-663
 - head and eye nystagmus, frequency of, 661

- head and eye nystagmus, negative correlation of, 663-665
- head movements, 669-670
- introduction, 656-657
- methods, 657-658
- morphology, 667-669
- optokinetic responses, 660-669
- results, 658-669
- slow-phase eye velocity (SPEV), 660-661, 662
- slow-phase gaze velocity (SPGV), 660-661, 662, 665-667, 668
- slow-phase head velocity (SPHV), 660-661, 662
- spontaneous eye and head nystagmus, 658-659
- summary, 671
- tonic head deviation, 658, 659
- vestibular responses to rotation, 665-667

- G**oal-directed saccades, 744, 745, 747, 751-753, 754
- accuracy of, 748-751
- Gravity and rotatory nystagmus, 44-55
- discussion, 52-54
 - eye movements, 45
 - introduction, 44
 - methods, 44-45
 - off-vertical axis rotation, 49-50, 52
 - optokinetic stimulator, 45
 - peak eye velocity, 47
 - results, 46-52
 - semicircular canals, 52
 - slow-phase eye velocity, 48-49
 - vestibulo-ocular reflex (VOR), 54

- H**ead extension, postural balance, 645, 648
- Head extension and normal head position, differential effects of, 640, 641
 - Head-extension vertigo, 636-637, 644
 - Head movements, gaze with and without, 582-587
 - Head nodding, 614-618
 - compensating for nystagmus, 615-616
 - introduction, 614-615
 - as involuntary movement (tremor), 615
 - switching off nystagmus, 616-618
 - Head tilt, 262, 263-264, 271
 - Head tilting, changes in receptive field characteristics following, 265-269
 - Heavy water, 262, 272
 - changes in receptive field characteristics following, 269-270
 - Helsinki Declaration on Medical Ethics, 629
 - Horizontal conjugate gaze, 102-111

- Horizontal eye movement signals (in second-order vestibular nuclei neurons in the cat), 144-156
 abducens nucleus, 146
 activated from contralateral labyrinth, 147-151
 activated from ipsilateral labyrinth, 151-153
 data processing, 147
 discussion, 153-155
 eye movement recording, 145
 identification of vestibular nucleus neurons, 145-146
 introduction, 144-145
 methods, 145-147
 nystagmus, 144
 recording of neuronal activity, 146
 results, 147-153
 saccades, 152
 vestibular stimulation, 146
- Horizontal fast eye movement, 130-143
 collateral projection of EBN axons in brain stem, 136-138
 discharge pattern of EBNs, 132-133
 discussion, 140-142
 dorsomedial reticular formation, 132
 introduction, 130-131
 location of EBNs, 135-136
 long-lead burst neurons, 132, 135
 methods, 131-132
 nystagmic cycle, 132
 results, 132-140
 reticulospinal neurons, 137-138
 target neurons of EBN axons, 138-140
 termination of EBN axons in ipsilateral abducens nucleus, 133-135
 type I and II vestibular nuclei neurons, 128, 139-140, 141
- Horizontal linear acceleration, ocular torsion during, 84-87
- Horizontal optokinetic eye nystagmus (OKN), 230-231
- Horseradish peroxidase (HRP) injections, 477-479, 484
- Human postural dynamics, 722-730
 discussion, 728
 introduction, 722
 method, 725
 notations for equations, 730
 physical model, 722-725
 postural control, 722, 726, 728
 results, 726-728
- Hypometric and multiple saccades, 758, 759, 760-761
- I**diopathic childhood nystagmus, head nodding, 614-618
 compensating for nystagmus, 615-616
 introduction, 614-615
 as involuntary movement (tremor), 615
 switching off nystagmus, 616-618
- Image motion, *see* Natural retinal image motion
- Impaired suppression of nystagmus, 706-721
 discussion, 716-720
 fixation suppression, 706, 709-710, 712, 713-716, 718, 720
 introduction, 706
 methods, 707-709
 results, 709-716
 summary, 720
- Infants, labyrinthine hypoactivity on gross motor development, 412-420
 bilateral dysfunction, 412
 congenitally hearing-impaired group, 416-417
 control group, 415-416
 discussion, 417-419
 gross motor development, 412
 introduction, 412
 methods, 413
 perrotatory and postrotatory nystagmus, 413
 procedure, 413-414
 results, 414-415
 rotation tests, 412, 414-415
 subjects, 413
- Inferior olivary complex, nBOR complex projections upon, 220-222
- Inferior olivary projections upon the vestibulocerebellum, 222
- Input activity, primate flocculus, 492-497
- Instability in the optokinetic-vestibular system, periodic alternating nystagmus and, 619-635
 characteristics, 620-623
 clinical material, 620-622
 conclusion, 633
 discussion, 631-633
 effects of drug treatment, 625-626
 hypothesis for, 626-631
 introduction, 619
 methods, 619-620
 model to simulate, 628-631
 optokinetic responses, 625
 results, 622-626
 smooth ocular pursuit, 625
 vestibulo-ocular responses, 623-625
- Interaction, neuronal, *see* Neuronal interaction
- Interstitial nucleus of Cajal (INC), ocular torsion in the cat and, 865-871
 counterrolling during static lateral tilt, 868
 discussion, 869-870

Interstitial nucleus of Cajal (Cont'd)

- INC-lesioned animals, 869
- introduction, 865
- methods, 865-867
- normal animals, 865-868
- pupil orientation, normal cat, 866-867
- results, 867
- VOR responses, 870

Ionic lanthanum as a tracer, endolymphatic duct and, 11-19

- discussion, 16-18
- future experiments, 17
- in a guinea pig, 12, 17
- introduction, 11
- materials and methods, 11-13
- resorption of endolymph, 17-18
- results, 13-15

Ipsilateral labyrinth, second-order neurons activated from, 151-153**Ipsilateral medial and lateral vestibular nuclei, neuronal interaction and, 93-101**

- discussion, 99-100
- HRP studies, 99
- introduction, 93
- LVN stimulation on MVN neurons, 97-98
- materials and methods, 93-94
- MVN stimulation on LVN neurons, 94-96
- results, 94-98

Kinetic neurons, 118**Kinocilium, axonemal, 1, 3, 4****Labyrinthine and neck stimulation, combined neuronal responses, 367-370**

- turning sensations, 370

Labyrinthine disease, disturbances during

- lateral gaze, 571-578
- bilateral lesions, 575-576
- comments and conclusions, 576-577
- electro-oculography, 571
- gaze overshoots, 577
- introduction, 571
- methods, 571-572
- results, 572-576
- terrestrial magnetic sensor, 571
- unilateral lesions, 572-575
- VOR gain, 572-573

Labyrinthine hypoactivity, 412-420

- bilateral dysfunction, 412
- congenitally hearing-impaired group, 416-417
- control group, 415-416
- discussion, 417-419

gross motor development, 412

- introduction, 412
- methods, 413
- perrotatory and postrotatory nystagmus, 413
- procedure, 413-414
- results, 414-415
- rotation tests, 412, 414-415
- subjects, 413

Lanthanum, see Ionic lanthanum**Lateral-eyed and frontal-eyed animals, eye-muscle geometry, 20-30**

- compensatory eye movements, 27
- discussion, 25-28
- insertion points and lines of action, 24
- introduction, 20-21
- kinematic characteristics, 21, 28
- in man and rabbit, 25, 26
- methods, 21-22
- optic axis, 23
- results, 22-24
- spatial relations, 23
- vestibulo-ocular reflexes, 21, 22

Lateral gaze disturbance, 571-578

- bilateral lesions, 575-576
- comments and conclusions, 576-577
- electro-oculography, 571
- gaze overshoots, 577
- introduction, 571
- methods, 571-572
- results, 572-576
- terrestrial magnetic sensor, 571
- unilateral lesions, 572-575
- VOR gain, 572-573

Lateropulsion, 600, 601**Left-right vision reversal, self-motion sensation and, 352-360**

- conclusions, 359-360
- discussion, 358-359
- Experiment I, 354-355
- Experiment II, 355-356, 357
- Experiment III, 356
- introduction, 352
- methods, 352-354
- results, 354-358
- reversed circularvection (RCV), 352, 354-355, 356, 358, 359
- summary, 360
- vestibulo-ocular reflex tests, 358

Macular and neck stimulation: phase relation of LVN unit responses to, 390-391

- response characteristics of LVN neurons to, 375-379
- sensitivity of LVN unit responses to, 389-390

- Mastoid air-cell area, vestibular aqueduct and, 799-801
- Mechanisms of nystagmus, *see* Physiological mechanisms of nystagmus
- Medial longitudinal fasciculus (MLF), 102, 103
- Medial longitudinal fasciculus, vestibulocollic reflex and, 397-398
- Ménière's disease, 820-830
 discussion, 826-829
 endolymphatic hydrops, 826
 endolymphatic sac, 821, 826
 Helsinki Declaration and, 829
 introduction, 820-821
 method, 821-822
 patients, 822-826
 placebo effect, 825-826, 827, 828, 829
 summary, 829
 temporal bone characteristics, 794-807
- Modification of nystagmus, 689-705
 discussion, 699-703
 eye-movement recording and data processing, 691-692
 introduction, 689-690
 methods, 690-692
 nystagmus suppression, postrotational, 691
 nystagmus suppression during sinusoidal head oscillation, 690
 results, 692-698
 smooth-pursuit (SP) system, 689-690, 691-692, 699-703
 target fixation during sinusoidal head oscillations, 691
- Modification of saccade, 755-763
 basal ganglia lesions, 758-759
 brain-stem lesions, 759-760
 cerebellar lesions, 759
 conclusion, 762
 data analysis, 756
 discussion, 760-762
 introduction, 755
 method and material, 755-758
 normal data, 756-757
 optokinetic nystagmus, 757
 pursuit eye tracking test, 757-758
 recording eye movements, 755
 results, 758-760
 spinocerebellar ataxia, 760
 target generation, 756
 unilateral cerebral lesions, 758
- Mossy fiber potentials, evoked by NRTP stimulation, 479-480
- Mossy fibers, 465-475
- Motion sickness, 303-311
 discussion, 308-310
- introduction, 303
 methods, 303-305
 results, 305-308
 symptoms, 308
 vision reversal in normal light, 305-307
 vision reversal in stroboscopic light (low- and high-frequency tests), 307-308
- Moving acoustic signals, influence on eye movements, 674-688
- N**atural retinal image motion, 312-329
 data acquisition and analysis, 314-315
 discussion, 327-329
 introduction, 312-313
 methods, 313-316
 recording, 313-314
 results, 316-327
 revolving magnetic-field monitor, 313-314
 stimulation, 314
 subjects, 315-316
- Neck afferents, stimulation of, 365
- Neck responses, vestibular and, 361-372
 ASS cortex (cat), 361-363, 366, 369, 370-371, 372
 discussion, 370-371
 horizontal canal stimulation, 361-363
 introduction, 361
 methods and results, 361-370
 neck afferents stimulation, 365
 neuronal responses, 365-366, 367-370
 summary, 372
 turning sensations, 364-365, 367, 370
- Neck stimulation, response characteristics of LVN units to, 379-382
- Neural activity in the NRTP, 249-261
 discrete-visual-target motion, 256-257
 discussion, 257-260
 introduction, 249
 methods, 250-251
 optokinetic-related cells, 251-253
 results, 251-257
 saccade-related neurons, 253-256
- Neuronal interaction, 93-101
 discussion, 99-100
 HRP studies, 99
 introduction, 93
 LVN stimulation on MVN neurons, 97-98
 materials and methods, 93-94
 MVN stimulation on LVN and neurons, 94-96
 results, 94-98
- Neuronitis, *see* Vestibular neuronitis
- Neurons, nonlinear characteristics, 112-124
 discussion, 118-128
 experimental results, 113-118

Neurons (Cont'd)

- histological procedures, 113
- introduction, 112
- kinetic neurons, 118
- materials and methods, 112-118
- neuron discharge rate, 114, 115
- recording procedures, 113
- relationship between response and magnitude of stimulus, 116, 117
- semicircular canals, 120-125
- stimulating procedures, 113
- summary, 128
- surgical procedures, 112-113
- vestibular nuclei, 113, 127-128

Neurological test, cerebellar dysfunction, 526-531

- clinical application, 528-529
- discussion, 529-531
- experiment sequence, 527
- means and standard deviations, 527
- methods, 526-527
- phase changes of VOR, 529, 530
- results, 527-528
- summary, 531
- VOR gains, 528, 529

Nonlinear characteristics of neurons, 112-129

- discussion, 118-128
- experimental results, 113-118
- histological procedures, 113
- introduction, 112
- kinetic neurons, 118
- materials and methods, 112-118
- neuron discharge rate, 114, 115
- recording procedures, 113
- relationship between response and magnitude of stimulus, 116, 117
- semicircular canals, 120-125
- stimulating procedures, 113
- summary, 128
- surgical procedures, 112-113
- vestibular nuclei, 113, 127-128

Non-UHEV units, 451-452

Normal light, vision reversal:

- high-frequency tests, 305-307
- low-frequency tests, 305

Nucleus of the basal optic root (nBOR) complex:

- organization of, 218-219
- projections upon inferior olivary complex, 220-222
- projections upon oculomotor complex, 223-224
- projections upon vestibulocerebellum, 219-220

Nucleus of the optic tract (NOT), 476, 478, 484, 485, 486, 487, 488

Nucleus reticularis tegmenti pontis (NRTP), 455, 456-457, 458-463, 479-484, 485-488

- HRP injections into, 484
- lesion of, 236-237
- projection to flocculus, 460-462
- role in OKN, 462-463

Nucleus reticularis tegmenti pontis, neural activity in, 249-261

- discrete-visual-target motion, 256-257
- discussion, 257-260
- introduction, 249
- methods, 250-251
- optokinetic-related cells, 251-253
- results, 251-257
- saccade-related neurons, 253-256

NRTP lesion, effect on optokinetic responses, 459-460

NRTP neurons, neuronal activity of, 480-484

NRTP stimulation:

- field potentials in flocculus following, 458-459
- mossy fiber potentials evoked by, 479-480

Ocular counterrolling (OCR), 69-79

- characteristics, 73, 74, 75
- discussion, 77-78
- introduction, 69-71
- loss of labyrinthine function, 71
- magnitude of (patients with unilateral inner ear disease), 72
- methods, 71-72
- results, 72-77
- role of vision in OCR response, 77
- utricle, 70, 77, 78

Ocular torsion, 80-92

- acceleration from weightlessness, 87-88
- conclusion and summary, 90-91
- horizontal linear acceleration, 84-87
- introduction, 80
- methods, 80-90
- photographic analysis, 80-82
- roll vection (supine and weightlessness), 89-90
- video measurement, 82-84

Ocular torsion in the cat, 865-871

- counterrolling during static lateral tilt, 868
- discussion, 869-870
- INC-lesioned animals, 869
- introduction, 865
- methods, 865-867
- normal animals, 865-868
- pupil orientation, normal cat, 866-867
- results, 867

- tilt, 868
- VOR responses, 870
- Oculomotor complex:
 - nBOR complex projections upon, 223-224
 - projections upon the extraocular muscles, 225
- Optokinetic after-nystagmus (OKAN), 421-422, 423, 424, 425, 426, 427, 428, 429-430, 431
- Optokinetic after-nystagmus (OKAN I), 434, 443-444
 - aftereffects and, 441
- Optokinetic and vestibular stimuli, responses of units in the pretectum and NRTP to, 241-244
- Optokinetic nystagmus (OKN), 44, 455, 456, 459, 461
 - role of NRTP in, 462-463
- Optokinetic pathways, 230-248
 - circuitry of, to Vn, 245-246
 - comparison of optokinetic responses, 245
 - effects of lesions on OKN, 241
 - effects of lesions on Vn responses, 234-240
 - introduction, 230-231
 - lesion of the NRTP, 236-237
 - lesions of the pretectum, 234-236
 - lesion of the vestibular commissure, 237-238
 - material and methods, 231
 - optokinetic responses of vestibular neurons, 231-233
 - other lesions, 238
 - responses to optokinetic and vestibular stimuli, 241-244
 - results and discussion, 231-246
- Optokinetic reaction, 651
- Optokinetic responses, comparison between pretectal, NRTP, and vestibular neurons, 245
- Optokinetic responses of vestibular neurons, 231-233
 - time course of, 232
- Orientation reaction, acoustically induced, 674
- Orthodromic and antidromic activation, 480-483
- Otolithic oculomotor system, 56-68
 - data processing, 57-58
 - discussion, 66-67
 - introduction, 56
 - methods, 56-58
 - results, 58-67
 - running test, 57, 61-62
 - summary, 67-68
 - up-down test, 56-57, 58-61
 - vertical eye tracking test, 56, 58-61
- Otosclerosis, 650
- Output activity, primate flocculus, 497
- P**aravestibular canaliculus (PVC), 801-802
- Periaqueductal pneumatization, 797
- Periodic alternating nystagmus (PAN), 619-635
 - characteristics, 622-623
 - clinical material, 620-622
 - conclusion, 633
 - discussion, 631-633
 - effects of drug treatment, 625-626
 - hypothesis for, 626-631
 - introduction, 619
 - methods, 619-620
 - model to simulate, 628-631
 - optokinetic responses, 625
 - results, 622-626
 - smooth ocular pursuit, 625
 - vestibulo-ocular responses, 623-625
- Phasic components, frog semicircular canal, 31-39
 - bubble displacement and coil voltage, 32
 - discussion, 37-39
 - introduction, 31
 - materials and methods, 31-32
 - results, 32-37
 - schematic representation, 32
 - semicircular canal, 31
- Physiological mechanisms of nystagmus, 40-43
 - eye-movement recordings, 41
 - semicircular-canal and otolith afferents, 41-42
 - squirrel monkeys, 41
 - vestibular-nerve recordings, 41
- Plantar mechanoreceptor, 855-864
 - anterior spinothalamic pathway, 862-863
 - data processing system, 856
 - discussion and conclusion, 860-863
 - introduction, 855
 - methods, 855-856
 - results, 856-860
 - schema of lemniscal system, 862
- Plasticity, directional, see Directional plasticity
- Postural control, 722, 726, 728
- Postural imbalance, 636-649
 - apparatus, posturography, and data analysis, 637-638
 - basilar insufficiency, 636, 644
 - blood flow, 639-640
 - experimental procedure, 638-639
 - head-extension vertigo, 636-637, 644
 - introduction, 636
 - methods, 637-639
 - posture, 640-644

- Postural imbalance (Cont'd)
 results and comment, 639-644
 subjects, 637
 summary, 644-649
- Posturography, 637-638
- Precerebellar nucleus relevant to
 optokinetic responses, 463
- Pretecal region:
 neuronal activity, 485-488
 stimulation threshold mapping in, 484-485
- Pretecal relay neurons, 484-488
- Pretecal, lesions of, 234-236
- Primate flocculus, input-output activity, 491-503
 conflicting visual-vestibular stimulation, 494
 discussion, 497-502
 input activity, 492-497
 introduction, 491
 methods, 491-492
 optokinetic nystagmus, 491, 492
 optokinetic stimulation, 492, 497
 output activity, 497
 Purkinje cells, 492, 497, 499
 results, 492-497
 simple spike (SS) activity, 496, 497, 498
- Primate VOR, "error" signals subserving
 adaptive gain control, 513-525
 gain changes from foveal pursuit tracking, 519-521
 hypothesis (adaptive gain control in primate VOR), 521-524
 introduction, 513
 primate flocculus, 518-519
 substitutes for retinal slip signals, 517-518
 substitutes for vestibular (head-velocity) signals, 513-517
- Pure vestibular stimulation, aftereffects of, 437, 438
- Purkinje cells, mossy fiber activation of, 476-477
- R**andom dot patterns, sigma-movement of, 294-295
- Rat otoconial complexes, 808-819
 conditions of electrophoresis and staining, 813
 discussion, 817-818
 EDTA chelation, 812
 gels, 813
 introduction, 808-811
 material and methods, 811-814
 microdissection and sample collection, 812
 molecular-weight determination, 814
 results, 814-817
 scanning electron microscopy, 814
 solubilization and denaturation, 812-813
 standards, 813
- Rebound nystagmus, 532-539
 caloric stimulus, 532, 537
 direction of gaze, 537
 discussion, 537-539
 electronystagmography, 532
 rotational tests, 537
 slow-component velocities, 535, 536, 538
 spontaneous nystagmus, 533-535
- Reflex dynamics, 395-402
 functional roles of CCR and VCR, 401-402
 medial longitudinal fasciculus, 397-398
 vestibulocollic, 395-398
- Reticulovestibular organization, 130-143
 collateral projection of EBN axons in brain stem, 136-138
 discharge pattern of EBNs, 132-133
 discussion, 140-142
 dorsomedial reticular formation, 132
 introduction, 130-131
 location of EBNs, 135-136
 long-lead burst neurons, 132, 135
 methods, 131-132
 nystagmic cycle, 132
 results, 132-140
 reticulospinal neurons, 137-138
 target neurons of EBN axons, 138-140
 termination of EBN axons in ipsilateral abducens nucleus, 133-135
 type I and II vestibular nucleus neurons, 138, 139-140, 141
- Retinal image motion, 312-329
 data acquisition and analysis, 314-315
 discussion, 327-329
 introduction, 312-313
 methods, 313-316
 recording, 313-314
 results, 316-327
 revolving magnetic-field monitor, 313-314
 stimulation, 314
 subjects, 315-316
- Reversed circularvection (RCV), self-motion sensation and, 352, 354-355, 356, 358, 359
- Revolving magnetic-field monitor, 313-314
- Rolling (torsion, cyclorotation, wheel rotation) of the eyes, 651-652
- Roll vection, ocular torsion during, 89-90
- Rotatory nystagmus, gravity effects, 44-55
 discussion, 52-54
 eye movements, 45
 introduction, 44

- methods, 44-45
- off-vertical axis rotation, 49-50, 52
- optokinetic stimulator, 55
- peak eye velocity, 47
- results of, 46-52
- semicircular canals, 52
- slow-phase eye velocity, 48-49
- vestibulo-ocular reflex (VOR), 54
- Running test (otolith oculomotor system), 57
 - in healthy adults, 61-62
 - in patients with bilateral loss of labyrinthine excitability, 63-66
- S**accade, modification, 755-763
 - basal ganglia lesions, 758-759
 - brain-stem lesions, 759-760
 - cerebellar lesions, 759
 - conclusion, 762
 - data analysis, 756
 - discussion, 760-762
 - introduction, 755
 - method and material, 755-758
 - normal data, 756-757
 - optokinetic nystagmus, 757
 - pursuit eye tracking test, 757-758
 - recording eye movements, 755
 - results, 758-760
 - spinocerebellar ataxia, 760
 - target generation, 756
 - unilateral cerebral lesions, 758
- Saccade, onset of, 566-567
- Saccade-related neurons, 253-256
- Saccades and the vestibulo-ocular reflex (VOR), 744-754
 - activation effect and goal-directed saccades, 748-750
 - incomplete summation and goal-directed saccades, 750-751
 - introduction, 744
 - methods, 744-745
 - model implications, 751-753
 - results, 745-751
 - saccades during visual suppression of VOR, 748
 - summary, 754
 - test for quick and slow eye movements, 745
- Saccadic eye movements:
 - characteristics of, 731
 - duration of, 565-566
 - typical relationship between eyes, 734, 736-738, 739, 741
- Saccadic movement, dissociation of the eyes in, 731-743
 - apparatus, 732-734
 - data analysis, 734-736
 - discussion, 741-742
 - introduction, 731
 - materials and methods, 732-736
 - recording eye movement, 734
 - results, 736-741
 - subjects, 732
 - summary, 742-743
- Scanning electron microscopy, 3, 4
- Secondary optokinetic after-nystagmus (OKAN II), 434, 441, 443, 444
- Secondary vestibular after-nystagmus (VAN II), 434, 437, 439, 440-441, 442, 443-444
- Self-motion sensation, 352-360
 - conclusions, 359-360
 - discussion, 358-359
 - Experiment I, 354-355
 - Experiment II, 355-356, 357
 - Experiment III, 356
 - introduction, 352
 - methods, 352-354
 - results, 354-358
 - reversed circularvection (RCV), 352, 354-355, 356, 358, 359
 - summary, 360
 - vestibulo-ocular reflex tests, 358
- Semicircular canal afferents, velocity storage and, 421, 431
- Semicircular canals, Steinhausen model, 112
- Sigma-movement, 284-302
 - during active body movements, 293
 - aftereffects, 296
 - discussion, 299-301
 - elicited by stationary stereopatterns, 290-291
 - flash sequence and, 293-294
 - interaction of vestibulo-ocular reflex and Sigma-OKN, 296-299
 - of random dot patterns, 294-295
 - Sigma paradigms and, 293-295
 - spatial period P_s and flash frequency f_s and, 286-290
 - of three-dimensional objects, 291-293
 - visual movement perceived with stabilized retinal stimuli, 284-286
- Sigma paradigm:
 - experiments designed to refute, 293-294
 - modification of, 294-295
- Sinusoidal rotation, 274, 275, 276, 277, 278, 279, 280, 281, 282
 - gaze shift, 594
 - nystagmus, 594-595
- Sinusoidal rotation, vestibular habituation, 330-339
 - conclusions, 337-338
 - in humans, 336-337

- Sinusoidal rotation, vestibular habituation (Cont'd)
 introduction, 330
 methods, 330-331
 in the monkey, 331-333
 in neuronal activity along the VOR pathway, 333-336
 results, 331-337
 summary, 338
 of vestibular nystagmus and motion sensation, 335
- Sinusoidal stimuli responses, 590-599
 discussion, 598
 gaze shift, 594
 horizontal circularvection, 596-597
 introduction, 590
 methods, 590-594
 nystagmus, 594-596
 results, 594-597
 summary, 598-599
- Slow cumulative eye position (SCEP), 691-692, 693-695
- Smooth-pursuit eye movement, 465, 468-469, 474
- Smooth-pursuit (SP) system, 689-690, 691-692, 699-703
- Spatial period P_s , sigma-movement and, 286-290
- Spinocerebellar ataxia, saccades and, 760
- Spinocerebellar atrophies, cranial computerized tomography in, 831-838
- Spontaneous nystagmus, unilateral habituation and, 342, 345-346, 349-350
- Squirrel monkey, EHA nystagmus and, 41
- Stabilized retinal stimuli, visual movement perceived with, 284-286
- Stereopatterns, stationary, sigma-movement elicited by, 290-291
- Stored activity, manifestations of, 421
- Stroboscopic light, absence of motion sickness, 303-311
 discussion, 308-310
 introduction, 303
 methods, 303-305
 results, 305-308
 visual reversal in normal light, 305-307
 vision reversal in stroboscopic light (low- and high-frequency tests), 307-308
- Syphilis, 850
- T**emporal bone characteristics, 794-807
 conclusions, 805
 endolymphatic sac, 802-805
 introduction, 794
 material, 794-795
 methods, 795-797
 observations and comments, 797-805
 paravestibular canaliculus (PVC), 801-802
 periaqueductal pneumatization, 797
 planimetry, 795
 plastic molding, 795-797
 radiography, 795
 structure of petrous pyramid, 798-799
 summary, 805-806
 tomography, 795
 vestibular aqueduct and mastoid area, 799-801
- Three-dimensional objects, sigma-movement of, 291-293
- Three-neuron arc, 171-188
 eye position and eye velocity, 172
 integrator, 183-184
 introduction, 171
 motoneurons and motor units, 174-177
 primary afferent vestibular neurons, 177-178
 rate position and velocity diagrams, 175
 secondary vestibular neurons, 178-183
 VOR in operation, 171-174
- Tomography, computerized, *see* Computerized tomography
- Torsion, ocular, 80-92
 acceleration from weightlessness, 87-88
 conclusion and summary, 90-91
 horizontal linear acceleration, 84-87
 introduction, 80
 methods, 80-90
 photographic analysis, 80-82
 roll vection, 89-90
 video measurement, 82-84
- Torsional ocular movements in man induced by sound, *see* Tullio phenomenon
- Tracer, ionic lanthanum, 11-19
 discussion, 16-18
 future experiments and, 17
 in a guinea pig, 12, 17
 introduction, 11
 materials and methods, 11-13
 resorption of endolymph, 17-18
 results, 13-15
- Transsynaptic study, 157-170
 abducens internuclear pathway, 166
 diffuse patterns of silver grain, 166-167
 discussion, 163-167
 distribution of silver grains, 160
 experimental details, 158
 grain densities in structures, 159
 introduction, 157
 labeling of cell bodies, 164
 methods, 157-158

- motoneurons from internuclear cells, 165
- results, 158-163
- retrograde tracer substance, 157
- Tullio phenomenon, 650-655
 - case report, 650-651
 - differentiation, 653-654
 - discussion, 651-653
 - introduction, 650
 - rolling (torsion, cyclorotation, wheel rotation), 651-652
 - summary, 654
- Turning sensation (human), concurrent indication of, 364-365
- U**nilateral cerebral lesions, saccade and, 758
- Unilateral habituation, 340-351
 - data processing, 342
 - introduction, 340
 - methods, 340-342
 - optokinetic training, 341, 342, 346-350
 - postexposure testing, 342
 - preexposure testing, 341
 - results and comments, 342-350
 - spontaneous nystagmus, 342, 345-356, 349-350
 - unidirectional optokinetic training, 341
 - unidirectional vestibular training, 341
 - vestibular training, 341, 342-346
- Unilateral vestibular loss, compensation of (in vestibular neuronitis), 784-793
 - computed slow-phase eye velocity, 788
 - directional preponderance (bithermal caloric), 787
 - discussion, 789-792
 - introduction, 784-785
 - labyrinthine preponderance (bithermal caloric), 789
 - methods and cases, 785-786
 - peak amplitude preponderance (sinusoidal rotation), 789
 - peak amplitude ratio (sinusoidal rotation), 789
 - results, 787
 - spontaneous nystagmus, 784, 786, 787
- Up-down test, 56-57
 - in healthy adults, 58-59
 - in patients with bilateral loss of labyrinthine excitability, 60-61
- Upward head and eye velocity (UHEV)
 - units, 448-450
 - discharge characteristics, 449
- V**elocity storage, 421-433
 - discussion, 430-431
 - introduction, 421-422
 - methods, 422
- OKAN and, 421-422, 423, 424, 425, 426, 427, 428, 429-430, 431
 - results, 422-430
 - semicircular canal afferents, 421, 431
 - storage integrator and, 429, 430, 431
- Vertebrate hair cells, 1-10
 - displacement-response curves, 8
 - intracellular recordings, 2, 5, 6
 - introduction, 1-2
 - kinocilium, 1, 3, 4
 - materials and methods, 2-5
 - receptor potentials, 6-7
 - relationship between displacement of tip of hair bundle and cellular receptor potential, 8-9
 - results, 5-8
 - scanning electron microscopy, 3, 4
- Vertical eye tracking:
 - in healthy adults, 58-59
 - patients with bilateral loss of labyrinthine excitability, 60-61
- Vertical eye tracking test, 56
- Vertical smooth eye movements, dentate nucleus and y-group in generation of, 446-454
 - conclusions, 453
 - electrical stimulation, 452
 - introduction, 446
 - methods, 446-448
 - non-UHEV units, 451-452
 - results, 448-452
 - upward head and eye velocity (UHEV) units, 448-450
- Vestibular after-nystagmus (VAN I), 434, 437, 438, 439, 442-443
- Vestibular after-nystagmus I after fixation (VANF I), 439, 442-443
- Vestibular after-nystagmus II after fixation (VANF II), 439, 440-441, 442
- Vestibular and neck responses, 361-372
 - ASS cortex (cat), 361-363, 366, 369, 370-371, 372
 - discussion, 370-371
 - horizontal canal stimulation, 361-363
 - introduction, 361
 - methods and results, 361-370
 - neuronal responses, 365-366, 367-370
 - stimulation of neck afferents, 365
 - summary, 372
 - turning sensations, 364-365, 367, 370
- Vestibular and oculomotor physiology:
 - accuracy of gaze, 579-589
 - acoustic-induced eye movements, 674-688
 - activation of the flocculus, 476-490
 - active head rotations, 540-559
 - activity of the flocculus, 491-503

Vestibular and oculomotor physiology

(Cont'd)

aftereffects, 434-445
 ascending tract of Deiters', 102-111
 avian accessory optic system, 215-229
 binocular counterrolling, 69-79
 brain-stem projection, 455-464
 cat medial pontine neurons, 189-209
 central nervous system (CNS) disorders, 764-773
 chemical transmission, 210-214
 circularvection, 274-283
 computerized tomography, 831-838
 dentate nucleus and y-group, 446-454
 directional plasticity, 504-512
 directional sensitivity, 1-10
 dissociation of the eyes, 731-743
 disturbances during lateral gaze, 571-578
 diving competitors, 839-845
 endolymphatic duct, 11-19
 eye-muscle geometry, 20-30
 eye-velocity programming, 774-783
 frontal-eye-field lesion, 656-673
 habituation, 330-339
 habituation, unilateral, 340-351
 head nodding, 614-618
 horizontal eye movement signals, 144-156
 human postural dynamics, 722-730
 impaired suppression of nystagmus, 706-721
 labyrinthine hypoactivity, 412-420
 mechanisms of nystagmus, 40-43
 Ménière's disease, 820-830
 modification of saccade, 755-763
 modification of nystagmus, 689-705
 motion sickness, 303-311
 natural retinal image motion, 312-329
 neck responses, 361-372
 neural activity in NRTP, 249-261
 neuronal interaction, 93-101
 nonlinear characteristics of neurons, 112-129
 ocular torsion, 80-92
 ocular torsion in the cat, 865-871
 optokinetic pathways, 230-248
 otolithic oculomotor system, 56-68
 periodic alternating nystagmus, 619-635
 phasic components, 31-39
 plantar mechanoreceptor, 855-864
 postural imbalance, 636-649
 rat otoconial complexes, 808-819
 rebound nystagmus, 532-539
 reflex dynamics, 395-402
 responses to sinusoidal stimuli, 590-599
 reticulovestibular organization, 130-143
 rotatory nystagmus, 44-55
 saccades and the VOR, 744-754

self-motion sensation, 352-360
 sigma-movement, 284-302
 temporal bone characteristics, 794-807
 test for cerebellar dysfunction, 526-531
 three-neuron arc, 171-188
 transsynaptic study, 157-160
 Tullio phenomenon, 650-655
 unilateral habituation, 340-351
 velocity storage, 421-433
 vestibular influence on head-eye coordination, 560-570
 vestibular neuronitis, 784-793
 vestibulospinal neurons, 373-394
 visual mossy fiber inputs, 465-475
 visual motion cues, 403-411
 visual suppression of nystagmus, 846-854
 visual-vestibular interactions, 262-273
 VOR plasticity, 513-525
 Wallenberg's syndrome, 600-613
 Vestibular and optokinetic stimulation and interaction, aftereffects of, 434-445
 apparatus, 435
 discussion, 442-444
 experimental procedure, 435-437
 introduction, 434-435
 methods, 435-437
 OKAN and, 441
 pure vestibular stimulation, 437, 438
 results, 437-442
 subjects, 435
 summary, 444
 vestibular, despite prior fixation suppression, 437-441
 visual-vestibular interaction, 442
 Vestibular commissure, lesion of, 237-238
 Vestibular habituation, 330-339
 conclusions, 337-338
 in humans, 336-337
 introduction, 330
 methods, 330-331
 in the monkey, 331-333
 in neuronal activity along the VOR pathway, 333-336
 results, 331-337
 summary, 338
 of vestibular nystagmus and motion sensation, 335
 Vestibular influence, upon head-eye coordination, 560-578
 apparatus, 560-561
 data reduction, 562-564
 discussion, 568-569
 duration of saccadic eye movement, 565-566
 experimental procedure, 561
 introduction, 560
 latency of eye movement, 564-565
 methods, 560-562

- postrotational nystagmus, 562
- qualitative features, 562
- quantitative features, 562-563
- results, 562-567
- saccades, 562
- target flash presentation (TF condition), 561-562
- velocity of head movement, 566-567
- voluntary head rotation in the dark (VR condition), 562
- Vestibular-nerve recordings, EHA nystagmus and, 41
- Vestibular neuronitis, 784-793
 - computed slow-phase eye velocity, 788
 - directional preponderance (bithermal caloric), 787
 - discussion, 789-792
 - introduction, 784-785
 - labyrinthine preponderance (bithermal caloric), 789
 - methods and cases, 785-786
 - peak amplitude preponderance (sinusoidal rotation), 789
 - peak amplitude ratio (sinusoidal rotation), 789
 - results, 787
 - spontaneous nystagmus, 784, 786, 787
- Vestibular nuclear neurons (Vn), 231-232, 241
 - circuitry of the optokinetic path to, 245-246
 - effects of lesions on, 234-241
- Vestibular type I hair cell, chemical transmission, 210-214
 - calyx or nerve calice, 210, 211-212, 213
 - conclusions, 213
 - morphophysiology of irregular fibers, 211-212
 - regular and irregular units, 211, 213
 - subthreshold activity, frequency and pattern, 212
- Vestibulocerebellum:
 - inferior olivary projections upon, 222
 - nBOR complex projections upon, 219-220
- Vestibulocollic reflex, 395-398
 - interaction of, 400-401
 - role of the medial longitudinal fasciculus in, 397-398
- Vestibulo-ocular reflex, 651
- Vestibulo-ocular reflex and Sigma-OKN, interaction of, 296-299
- Vestibulo-ocular reflex (VOR) plasticity, 513-525
 - gain changes from foveal pursuit tracking, 519-521
 - hypothesis (adaptive gain control in primate VOR), 521-524
 - introduction, 513
 - primate flocculus, 518-519
 - substitutes for retinal slip signals, 517-518
 - substitutes for vestibular (head-velocity) signals, 513-517
- Vestibulo-ocular responses, unilateral habituation, 340-351
 - data processing, 342
 - introduction, 340
 - methods, 340-342
 - optokinetic training, 341, 342, 346-350
 - postexposure testing, 342
 - preexposure testing, 341
 - results and comments, 342-350
 - spontaneous nystagmus, 342, 345-346, 349-350
 - unidirectional optokinetic training, 341
 - unidirectional vestibular training, 341
 - vestibular training, 341, 342-346
- Vestibulospinal neurons, 373-394
 - convergence of macular and neck inputs on LVN neurons, 382
 - discussion, 389-391
 - Fourier analysis of unit responses, 374-375
 - introduction, 373-374
 - macular and neck responses during head rotation, 382-389
 - methods, 374-375
 - phase relation of LVN unit responses, 390-391
 - response of LVN units to neck stimulation, 379-382
 - response to macular vestibular stimulation, 375-379
 - results, 375-389
 - sensitivity of LVN unit responses, 389-390
 - summary, 391-392
- Video measurement, ocular torsion, 82-84
- Vision reversal, motion sickness due to, 303-311
- Vision reversal, self-motion sensation and, 352-360
- Visual mossy fiber afferents to the flocculus, 477-484
- Visual mossy fiber inputs, 465-475
 - direction-only visual mossy fibers, 466-468
 - direction- and velocity-related visual mossy fibers, 468-473
 - discussion, 473-474
 - introduction, 465
 - methods, 465-466
 - results, 466-473
 - smooth-pursuit eye movements, 465, 468-469, 474

- Visual motion cues, 403-411
 data processing, 405-406
 discussion, 408-410
 electromyographic (EMG) responses, 403
 with enhanced (EV) or reduced (RV)
 visual input, 407-408
 free-fall device, 404-405
 introduction, 403
 methods, 403
 muscle responses, normal vision, 406-407
 muscle responses, visual manipulations,
 407-408
 preparation, 403-404
 in total darkness, 407
 visual environment during falls, 405
 with visual stabilization, 407
- Visual suppression of nystagmus, 846-854
 augmentation of caloric nystagmus in
 light, 847, 851
 discussion, 851-854
 introduction, 846
 methods, 846-851
- Visual-vestibular interaction, aftereffects
 of, 442
- Visual-vestibular interaction in vestibular
 neurons, 230-248
- Visual-vestibular interactions, velocity
 storage and, 421-433
- Visual-vestibular interactions (in cortical
 cells in the cat), 262-273
 animal preparation and data collection,
 262-263
 calculation of receptive field
 characteristics, 263-264
 discussion, 271-272
 head tilt, 262, 263-264, 265-269
- introduction, 262
 methods, 262-264
 receptive field characteristics, changes in
 following heavy water, 269-270
 receptive field characteristics, changes in
 following tilting, 265-269
 receptive field plots, 264-265
 results, 264-271
- W**allenberg's syndrome, 600-613
 case material, 601-602
 discussion, 610-612
 eye deviation with and without fixation,
 603-605
 introduction, 600-601
 methods, 603
 results, 603-610
 saccadic eye movements, 605, 606
 smooth pursuit and optokinetic
 nystagmus, 606-609
 summary, 612
 vestibulo-ocular reflex, 609
 visual-vestibular interaction, 609-610
- Weightlessness, ocular torsion and, 80-92
 acceleration from weightlessness, 87-88
 conclusion and summary, 90-91
 horizontal linear acceleration, 84-87
 introduction, 80
 methods, 80-90
 photographic analysis, 80-82
 roll vection, 89-90
 video measurement, 82-84
- Y**-group, see Dentate nucleus and y-
 group